NASA SP-321

FREE TURBULENT SHEAR FLOWS

Volume I—Conference Proceedings

A conference held at
LANGLEY RESEARCH CENTER
Hampton, Virginia
July 20–21, 1972

NATIONAL AERONAUTICS AND SPACE ADMINISTRATION

NASA SP-321

FREE TURBULENT SHEAR FLOWS

Volume I—Conference Proceedings

Proceedings of a conference held at
NASA Langley Research Center, Hampton, Virginia, July 20-21, 1972

Prepared by NASA Langley Research Center

Scientific and Technical Information Office 1973
NATIONAL AERONAUTICS AND SPACE ADMINISTRATION
Washington, D.C.

THE PROCEEDINGS OF THIS CONFERENCE ARE DEDICATED TO

MITCHEL H. BERTRAM

1924 – 1972

Head, Hypersonic Aircraft Fluid Mechanics Branch
Hypersonic Vehicles Division
NASA Langley Research Center
Hampton, Virginia

PREFACE

The Langley Working Conference on Free Turbulent Shear Flows was held at NASA Langley Research Center July 20-21, 1972. The general format for this conference was based on the 1968 AFOSR-IFP-Stanford Conference on the "Computation of Turbulent Boundary Layers." There were, however, some major differences, primarily in the range and quality of the data used. The objectives of the Langley conference were

(1) To collect and process a set of reliable data for a variety of free mixing problems

(2) To assess the present theoretical capability for predicting mean velocity, concentration, and temperature distributions in free turbulent flows and to identify those methods which hold the most promise for future development

(3) To identify and recommend future experimental studies which might significantly advance the knowledge of free shear flows and, if possible, to assign a priority to these experiments

(4) To increase the understanding of the basic turbulent mixing process for application to free shear flows

In order to accomplish these objectives, the available prediction methods for free shear flows were confronted with a set of standardized data. The resulting computations together with the discussions and the reports of the conference committees constitute Volume I of these proceedings. The standardized data, which were used as test cases, are given in Volume II. A short introductory paper by James M. Eggers and Stanley F. Birch which summarizes the data and outlines the selection procedure used is also included in Volume II.

Virtually all the discussion which followed the papers has been retained with minimal editing. Transcripts of the discussions were sent to the speakers only when the session chairmen or the conference committee believed that this was desirable to improve clarity. The Langley personnel responsible for editing the discussion and prediction papers in Volume I for technical clarity were Stanley F. Birch, David H. Rudy, and Dennis M. Bushnell. Those responsible for compiling the data of Volume II were Stanley F. Birch and James M. Eggers.

COMMITTEES

CONFERENCE CHAIRMAN:

Mark V. Morkovin (Illinois Institute of Technology)

NASA LANGLEY CONFERENCE COMMITTEE:

Dennis M. Bushnell, Chairman
Stanley F. Birch, Coordinator
James M. Eggers
William L. Grose
J. Wayne Keyes
Edward P. McDaid
Lucio Maestrello
Joe J. Mathis, Jr.
R. Clayton Rogers

DATA SELECTION COMMITTEE:

R. H. Page (Rutgers University)
C. E. Peters (ARO, Inc.)
I. Wygnanski (Tel Aviv University)

COMMITTEE TO RECOMMEND CRITICAL EXPERIMENTS:

S. J. Kline, Chairman (Stanford University)
D. E. Coles (California Institute of Technology)
James M. Eggers (NASA Langley Research Center)
Philip T. Harsha (ARO, Inc.)

CONFERENCE EVALUATION COMMITTEE:

Mark V. Morkovin, Chairman (Illinois Institute of Technology)
Dennis M. Bushnell (NASA Langley Research Center)
R. B. Edelman (General Applied Science Laboratories, Inc.)
Paul A. Libby (University of California at San Diego)

CONTENTS

MORNING SESSION – July 21, 1972

Chairman: Mitchel H. Bertram*

Cochairman: Aubrey M. Cary, Jr.

*Robert L. Trimpi served as chairman in the absence of Mitchel H. Bertram.

AFTERNOON SESSION – July 21, 1972

Chairman: H. H. Korst
Cochairman: Joe J. Mathis, Jr.

CALCULATION OF TURBULENT FREE MIXING

STATUS AND PROBLEMS

By Dennis M. Bushnell
NASA Langley Research Center

INTRODUCTION

The first impulse when compiling an introductory paper to a conference such as the present one is to provide a review or overview of the research in the subject area. However, since several fairly recent reviews are already available (refs. 1 to 4), some background on the motivation in organizing this conference and one view of the status and problems of turbulent free mixing calculations will be presented. The other attendees at the conference have their own views of the present status in this area, and indeed, the major purpose of this conference is to ascertain the present capability to predict several of the simpler turbulent free mixing flows. It is hoped that each attendee will air his views in the papers to be presented and in the discussions which follow – both formal and informal.

The motivation behind much of the turbulent shear layer research is one or more of the large number of possible applications. Some of these applications are given in the following list, which is obviously biased toward aerospace:

Propulsion
Shock interference heating
Noise
Tangential slot injection (film cooling)
Pollution
Wakes
Augmenters and ejectors
Separated flows
Nuclear rockets
V/STOL high-lift devices

At the Langley Research Center (LaRC) free mixing in practically all the areas shown has been an important concern, with the most effort involved in slot injection, V/STOL, noise, and propulsion. In other industrial fields there are many more applications of turbulent free mixing research which could be listed. Therefore, even in the present climate of applied technology over basic research there is still a strong mandate to develop accurate calculation schemes for free mixing.

In the present conference only the basic mixing problems of free shear layers, jets, and wakes are considered. However, within these basic flows there is included a considerable range of conditions including nonsimilarity, compressibility, and secondary and heterogeneous flows. A brief outline of the various combinations included in the present conference is given in the following list:

Free shear layers:

- Similar
  Nonsimilar
- Incompressible
  Compressible

Jets:

- Similar
  Nonsimilar
- Incompressible
  Compressible
- Single
  Coaxial
- Axisymmetric
  Two dimensional
- Homogeneous
  Heterogeneous

Wakes:

- Similar
  Nonsimilar
- Incompressible
  Compressible
- Axisymmetric
  Two dimensional

Paper no. 2 by Stanley F. Birch and James M. Eggers will discuss further details concerning the data chosen as test cases. This is a formidable set of conditions with which to confront a calculation method. Most of the published procedures were generally applie to only a few of the test cases to be considered by the predictors at this conference.

This fairly complete confrontation of turbulence closure method with basic data should give a clearer picture of which method works where and which approaches deserve further development. By "further development" is meant application to some of the important "real life" effects which are not specifically included in the basic data considered for this conference. Several of these effects will be briefly discussed.

FREE MIXING PHENOMENA NOT CONSIDERED IN PRESENT CONFERENCE

Transverse Pressure Gradients

Several authors (e.g., refs. 5 and 6) have indicated that the common assumption of constant static pressure across a free mixing layer is not borne out by the available data. This assumption becomes increasingly suspect as Mach number increases (ref. 5), and the fact that the static pressure is variable may have a profound effect on turbulence spreading rates. The probable cause of this static pressure variation is the $\overline{\rho v'^2}$ ($\overline{\rho}$ is density, $\overline{v'^2}$ is mean-square transverse turbulence velocity) term in the normal momentum equation (ref. 7). There are also more complicated flows where a static-pressure variation occurs because of outside influences (such as shock interactions). In paper no. 4 David H. Rudy and Dennis M. Bushnell discuss transverse pressure gradients in free turbulent flows in more detail.

Longitudinal Pressure Gradients

Longitudinal pressure gradients can occur quite often, especially in combustors, interactions between shock waves and shear layers, and separated flows. Very little is presently known, either experimentally or theoretically, concerning the influence of longitudinal pressure gradients on turbulent free mixing. Ferri (ref. 8) indicates a large effect on wake mixing due to the passage of a weak shock. Detailed data are necessary in this case before the turbulence closure models can be adequately tested for application to combustor design and so forth.

Transitional and Low Reynolds Number Turbulence

Transitional and low Reynolds number turbulence can be quite important in many applications, especially at low unit Reynolds numbers. Recent experience in calculations of turbulent boundary layer (refs. 9 to 12) indicates a pronounced increase in turbulent shear stress near the end of transition and beginning of turbulent flow. This high shear condition is aggravated at high Mach number and can occur for quite large Reynolds numbers ($R_{e,\theta} \rightarrow 10^4$ at high Mach number ($R_{e,\theta}$ is momentum-thickness Reynolds number)). This low Reynolds number effect may also occur in free shear flows (ref. 13) and indeed may account for some of the anomalies present in the available data for these flows. In any event, a viable calculation method should have the capability of computing through transition. Again, further detailed experimental data are necessary to calibrate the calculation methods for this effect.

Longitudinal Curvature

It is well known in boundary-layer flows that concave longitudinal curvature can significantly increase the level of turbulent shear stress (e.g., ref. 14). In addition, concave curvature can trigger embedded longitudinal Görtler vortices, even in nominally two-dimensional flows (refs. 15 and 16). Free mixing flows with longitudinal curvature occur in actual applications (e.g., Coanda effect, shear layer near attachment), and several investigators have considered this problem (e.g., refs. 17, 18, and 19), but further detailed data are needed, especially in the compressible case, before the turbulence closure models can be seriously confronted with the influences of longitudinal curvature.

Chemical Reactions

The possibility of an increase in turbulent shear due to density and pressure fluctuation terms associated with chemical reactions has been postulated by several authors (e.g., refs. 20 and 21) and is currently under investigation theoretically (ref. 22). However, for a low speed combusting boundary-layer flow (ref. 23), calculations using a "conventional" eddy viscosity model were found to provide good prediction of the data when the temperature dependence of the mean properties was taken into account. The possibility of using "conventional" turbulence closure techniques in combusting flows must be investigated further.

Nonparallel Flows and Confined Mixing

For the general case of nonparallel flows or confined mixing, the problem is no longer parabolic and the formation of regions of separated and secondary flow is certainl a possibility. Efficient numerical methods are becoming available to handle these cases (using the two-dimensional Navier-Stokes equations, refs. 24 to 27). The problem is one of developing adequate turbulence models to handle the three-dimensional nature of the shear flow (refs. 28, 29, and 30). Again, further detailed data are necessary.

There is also the possible effect of acoustical feedback; the paper of Glass (ref. 31) is a very chastising experience and is a warning of the sensitivity of free turbulence spreading rate not only to outside influences but to self-induced effects as well.

MOTIVATION FOR PRESENT CONFERENCE

The motivation for holding the present conference stems from recent work at LaRC on free shear layers and jets by members of the LaRC conference committee. In the course of their research several anomalies appeared, which are included in the following list:

1. Nonunique variation of σ (spreading rate) with Mach number for shear layers
2. Question of density difference versus density level viscosity models
3. Appearance in the literature of different predictions from the same turbulence model
4. Apparent nonuniversality of many of the available methods
5. Available turbulent boundary-layer expertise (nonsimilar scale adjustments, low Reynolds number effects) should be applied to the free-mixing problem
6. Comprehensive review and comparisons with data needed for latest models – particularly to indicate the efficacy of turbulent kinetic energy approaches

The σ (spreading rate) variations and the problems associated therewith are discussed in paper no. 2 and also in paper no. 4. The question of density difference versus density level models is an old problem in that a model which relies on an eddy viscosity proportional to the mass flow difference across the mixing zone does not predict the correct behavior when the velocity and density are not equal across the layer, but the mass flow is (ref. 32). Therefore, the use of this model is questionable when compared with the extrapolation of boundary-layer viscosity models which are proportional to the local density.

Another problem was the appearance of different predictions in the literature where supposedly the same viscosity model was employed. Was this due to a difference in numerical techniques? If so, which result was correct? Also, several of the models (and numerical methods) were developed for a particular class of flows (e.g., coaxial jets, wakes), and the range of application of several of the available closure assumptions was therefore in some doubt.

It was felt that a confrontation of as many of the methods as possible with a broad data base would tend to resolve some of these questions. This approach is similar to that employed by Harsha (ref. 4).

HEIRARCHY OF CLOSURE SCHEMES

A brief sketch of the various computational (closure) techniques is given below, along with their approximate representation at the present conference:

Method	Approximate representation	Prime usage
Integral	1	Equilibrium flows
Differential-mean field	6	Near-equilibrium, nonequilibrium flows
Differential-mean turbulence field without length-scale equation	6	
Differential-mean turbulence field with length-scale equation	1	Nonequilibrium flows, especially mixing of flows with differing scales
Statistical fluid mechanical approaches		To be determined; should be more accurate for a wider range of turbulent shear flows

At the Stanford Conference (ref. 33), the integral methods outnumbered the differential approaches more than 2 to 1, whereas in the present conference practically all the methods are numerical (differential). This is probably due in part to a bias on the part of the conference committee, but it also indicates a continuing shift in the last 4 years toward more fundamental closure techniques. This was, of course, made possible by large digital computers and numerical solutions to highly nonlinear partial differential equations (ref. 34).

In the near future, for nonequilibrium and general turbulent flows the most promising methods (based on the author's experience) are probably those which include some length-scale equation in a so-called mean turbulent field approach. Several investigators are developing this type of method (refs. 35 to 39). Of these approaches, reference 39 presents the most complete study of free-mixing applications.

The last category in the heirarchy of closure methods is the possibility of applying statistical fluid mechanical approaches to the calculation of "practical" shear flows. J. R. Herring comments on this in paper no. 3, but mention should be made of recent unpublished work by Dr. A. B. Huang at Georgia Institute of Technology. His distribution function approach is essentially that of Lundgren (ref. 40) and seems to hold some promise of significantly reducing the empirical input generally involved in the development of a closure model. In this regard a quote from Kraichnan (ref. 41) seems appropriate: ". . . the variables in the direct-interaction equations are statistical averages. They can be expected to vary smoothly with their arguments and therefore can be adequately represented by relatively few numbers. At turbulent Reynolds numbers, the individual

velocity fields vary jaggedly and unpredictably with distance and time and require relatively many numbers for a good description."

For compressible applications eddy-viscosity models may be the only viable methods until several questions are settled. Some of these are indicated in the following list:

1. Additional input (kinetic energy or Reynolds stress) is required (ref. 4).

2. Highly nonequilibrium flows require a length-scale equation; approximately six "constants" must be evaluated and optimized (functions of Reynolds number ?).

3. Rigorous application to compressible cases is difficult because of lack of detailed turbulence data, especially for p' (pressure fluctuation) terms (which could be large).

4. Compressible application also entails additional equations for second-order correlations involving temperature fluctuations with more constants.

The most serious problem is probably the question of just what influence do the p' terms (which can be quite large) have on the shear stress in compressible flows. Recent work (ref. 9) indicates that for boundary-layer flows with quite large density ratios (up to 140) the Reynolds stress can be modeled with low speed eddy-viscosity approaches once the low Reynolds number effect is recognized. Does this mean that the p' terms are small even though p' itself is quite large $\left(\sqrt{\overline{p'^2_w}}/\overline{p}\right.$ up to 20 percent $\left(\sqrt{\overline{p'^2_w}}\right.$ is root-mean-square wall pressure fluctuation, $\overline{p}$ is mean static pressure$\left.\right)\left.\right)$? This question requires considerable research including very difficult p' correlation measurements before compressible flows can be confidently modeled by using mean turbulent field approaches.

REFERENCES

1. Halleen, R. M.: A Literature Review on Subsonic Free Turbulent Shear Flow. AFOSR-TN-5444, U.S. Air Force, Apr. 1964. (Available from DDC as AD 606 758.)

2. Sforza, P. M.; Trentacoste, N. P.; and Mons, R. F.: Turbulent Mixing: A Review, Revaluation, and Extension. AIAA Paper No. 69-31, Jan. 1969.

3. Azzouz, D.; and Pratt, N. H.: Supersonic Turbulent Mixing. I – Literature Survey and Assessment of the State-of-the-Art. A.A.S.U. Rep. No. 281, Univ. of Southampton, May 1968.

4. Harsha, Philip Thomas: Free Turbulent Mixing: A Critical Evaluation of Theory and Experiment. AEDC-TR-71-36, U.S. Air Force, 1971. (Available from DDC as AD 718 956.)

5. Warren, Walter R., Jr.: An Analytical and Experimental Study of Compressible Free Jets. Ph. D. Dissertation, Princeton Univ., 1957.

6. Lee, Shen Ching: A Study of the Two-Dimensional Free Turbulent Mixing Between Converging Streams With Initial Boundary Layers. Ph. D. Dissertation, Univ. of Washington, 1966.

7. Hinze, J. O.: Turbulence. McGraw-Hill Book Co., Inc., 1959.

8. Ferri, Antonio: A Critical Review of Heterogeneous Mixing Problems. Astronaut. Acta., vol. 13, nos. 5 & 6, Aug. 1968, pp. 453-465.

9. Bushnell, Dennis M.; and Morris, Dana J.: Shear-Stress, Eddy-Viscosity, and Mixing-Length Distributions in Hypersonic Turbulent Boundary Layers. NASA TM X-2310, 1971.

10. McDonald, H.: Mixing Length and Kinematic Eddy Viscosity in a Low Reynolds Number Boundary Layer. Rep. J214453-1, Res. Lab., United Aircraft Corp., Sept. 1970.

11. Cebeci, Tuncer: A Model for Eddy-Conductivity and Turbulent Prandtl Number. Rep. No. MDC-J0747/01, McDonnell Douglas Corp., May 1970.

12. Simpson, Roger L.: Characteristics of Turbulent Boundary Layers at Low Reynolds Numbers With and Without Transpiration. J. Fluid Mech., vol. 42, pt. 4, 1970, pp. 769-802.

13. Sato, Hiroshi: The Stability and Transition of a Two-Dimensional Jet. J. Fluid Mech., vol. 7, pt. 1, Jan. 1960, pp. 53-80.

14. Wilcken, H.: Effect of Curved Surfaces on Turbulent Boundary Layers. NASA TT-F-11,421, 1967.

15. Bushnell, D. M.; and Alston, D. W.: Calculation of Compressible Adverse Pressure Gradient Turbulent Boundary Layers. AIAA J., vol. 10, no. 2, Feb. 1972, pp. 229-230.

16. Tani, Itiro: Production of Longitudinal Vortices in the Boundary Layer Along a Concave Wall. J. Geophys. Res., vol. 67, no. 8, July 1962, pp. 3075-3080.

17. Wyngaard, J. C.; Tennekes, H.; Lumley, J. L.; and Margolis, D. P.: Structure of Turbulence in a Curved Mixing Layer. Phys. Fluids, vol. 11, no. 6, June 1968, pp. 1251-1253.

18. Sawyer, R. A.: Two-Dimensional Reattaching Jet Flows Including the Effects of Curvature on Entrainment. J. Fluid Mech., vol. 17, pt. 4, Dec. 1963, pp. 481-498.

19. Schwartzbach, C.: An Experimental Investigation of Curved Two-Dimensional Turbulent Jets. Turbulent Shear Flows, AGARD-CP-93, Jan. 1972, pp. 16-1 – 16-12.

20. Eschenroeder, Alan Q.: Intensification of Turbulence by Chemical Heat Release. Phys. Fluids, vol. 7, no. 11, Nov. 1964, pp. 1735-1743.

21. Malte, P. C.: Turbulent Transport in a Combusting Shear Flow. Paper 68-27, Combustion Inst., Oct. 1968.

22. Donaldson, Coleman duP.: A Progress Report on an Attempt To Construct an Invariant Model of Turbulent Shear Flows. Turbulent Shear Flows, AGARD-CP-93, Jan. 1972, pp. B-1 – B-24.

23. Jones, J. W.; and Isaacson, L. K.: A Turbulent Boundary Layer With Mass Addition, Combustion, and Pressure Gradients. AFOSR 70-1428TR, U.S. Air Force, May 1970. (Available from DDC as AD 710 308.)

24. Boerner, C. J.: Numerical Solution of Turbulent Annular Swirl Flows. HTL TR No. 93 (Contract No. DAHC04-67-C-0021), Univ. of Minnesota, July 1970. (Available from DDC as AD 716 450.)

25. Richards, C. G.; and Chavez, S. P.: Numerical Study of the Coanda Effect. AFWL-TR-69-141, U.S. Air Force, Dec. 1969. (Available from DDC as AD 865 080.)

26. Shavit, G.; and Lavan, Z.: Analytical and Experimental Investigation of Laminar Mixing of Confined Heterogeneous Jets. AIAA Paper No. 71-601, June 1971.

27. Tatom, F. B.; and Kezios, S. P.: Interaction of a Turbulent Compressible Underexpanded Two-Dimensional Jet With a Crossflowing Free Stream. AIAA Paper No. 71-611, June 1971.

28. Bradshaw, Peter: Variations on a Theme of Prandtl. Turbulent Shear Flows, AGARD-CP-93, Jan. 1972, pp. C-1 – C-10.

29. Hunt, James L.; Bushnell, Dennis M.; and Beckwith, Ivan E.: The Compressible Turbulent Boundary Layer on a Blunt Swept Slab With and Without Leading-Edge Blowing. NASA TN D-6203, 1971.

30. Bradshaw, P.: Calculation of Boundary-Layer Development Using the Turbulent Energy Equation. VII: Three-Dimensional Flow. NPL Aero Rep. 1286, Brit. A.R.C., Jan. 30, 1969.

31. Glass, David R.: Effects of Acoustic Feedback on the Spread and Decay of Supersonic Jets. AIAA J., vol. 6, no. 10, Oct. 1968, pp. 1890-1897.

32. Alpinieri, Louis J.: Turbulent Mixing of Coaxial Jets. AIAA J., vol. 2, no. 9, Sept. 1964, pp. 1560-1567.

33. Kline, S. J.; Morkovin, M. V.; Sovran, G.; and Cockrell, D. J., eds.: Computation of Turbulent Boundary Layers – 1968 AFOSR-IFP-Stanford Conference. Vol. I – Methods, Predictions, Evaluation and Flow Structure. Stanford Univ., c.1969.

34. Donaldson, Coleman duP.: Calculation of Turbulent Shear Flows for Atmospheric and Vortex Motions. AIAA J., vol. 10, no. 1, Jan. 1972, pp. 4-12.

35. Glushko, G. S.: The Differential Equation for the Turbulence Scale and Calculation of the Turbulent Boundary Layer on a Flat Plate. Turbulent Flows: All-Union Symposium on Problems of Turbulent Flows, Including Geophysical Applications, Iu. G. Gurevich, ed., Izdatel'stvo Nauka (Moscow), 1970, pp. 37-44.

36. Rotta, J. C.: Recent Attempts To Develop a Generally Applicable Calculation Method for Turbulent Shear Flow Layers. Turbulent Shear Flows, AGARD-CP-93, Jan. 1972, pp. A-1 – A-11.

37. Daly, Bart J.; and Harlow, Francis H.: Transport Equations in Turbulence. Phys. Fluids, vol. 13, no. 11, Nov. 1970, pp. 2634-2649.

38. Wolfshtein, M.: On the Length-Scale-of-Turbulence Equation. Israel J. Technol., vol. 8, nos. 1-2, 1970, pp. 87-99.

39. Spalding, Dudley Brian: A Two-Equation Model of Turbulence. VDI-Forsch., Heft 549, 1972, pp. 5-16.

40. Lundgren, T. S.: Distribution Functions in the Statistical Theory of Turbulence. Phys. Fluids, vol. 10, no. 5, May 1967, pp. 969-975.

41. Kraichnan, Robert H.: Direct-Interaction Approximation for Shear and Thermally Driven Turbulence. Phys. Fluids, vol. 7, no. 7, July 1964, pp. 1048-1062.

A CRITICAL REVIEW OF THE EXPERIMENTAL DATA FOR DEVELOPED FREE TURBULENT SHEAR LAYERS

By Stanley F. Birch* and James M. Eggers
NASA Langley Research Center

2

INTRODUCTION

In selecting test cases for use in this conference, both the Langley Conference Committee and the Data Selection Committee recognized the need to include shear layers among the selected test cases. However, because of the confusion and apparent contradictions which existed in the interpretation of the experimental data, three of the five shear-layer test cases were specified without reference to any particular data. The primary purpose of this paper is to review the relevant data and to present the results in a convenient form for comparison with the numerical predictions for these three test cases (test cases 1, 2, and 3). Since these flows were specified to be developed turbulent flows, this will be the primary concern of the present paper. Some mention will be made of transitional flow, but only to differentiate it from developed turbulent flow. This is not intended to be a detailed study of the transition process itself.

SYMBOLS

b	width of shear layer
b^o	spreading rate of shear layer
$c = \frac{b}{x}$	
d,k	constants
ℓ_1,ℓ_2	lengths
m	density ratio, ρ_2/ρ_1
R	Reynolds number
$R_x = \frac{u_1 x}{\nu}$, where x	is the farthest downstream station surveyed

*NRC-NASA Resident Research Associate.

r velocity ratio, u_2/u_1

u velocity

x,y Cartesian coordinates

ϵ eddy viscosity

θ momentum thickness

$\lambda = \dfrac{u_1 - u_2}{u_1 + u_2}$

ν kinematic viscosity

ξ similarity parameter, $\sigma y/x$

ρ density

σ constant in similarity parameter ξ, also called spreading parameter

Subscripts:

o value when $u_2 = 0$

$1,2$ conditions on high- and low-velocity side of shear layer, respectively

Primes denote fluctuating quantities.

ANALYTIC SOLUTIONS

The analytic solution of the boundary-layer equations generally used to compare with experimental data for the two-dimensional shear layer (fig. 1) was first derived by Görtler in 1942 (ref. 1). This solution is well known and, since details of its derivation are readily available (ref. 2, pp. 689-690), the results will only be briefly summarized here.

It is assumed that the effective kinematic viscosity is given by

$$\epsilon = kb(u_1 - u_2) \tag{1}$$

where k is a constant, b is the width of the shear layer, and u_1 and u_2 are the velocities on both sides of the shear layer. The adoption of a stream function and the assumption of similarity automatically satisfy the continuity equation and reduce the boundary-layer equations to a simple third-order differential equation

$$F'''(\xi) + 2\sigma^2 F(\xi)F''(\xi) = 0 \tag{2}$$

where $\xi = \frac{\sigma y}{x}$ with boundary conditions $F'(\xi) = 1 \pm \lambda$ at $\xi = \pm\infty$ where

$$\lambda = \frac{u_1 - u_2}{u_1 + u_2}$$

This leads to the general series solution in powers of λ

$$u = \frac{u_1 + u_2}{2}\left[1 + \lambda\, \mathrm{erf}(\xi + d) + \ldots\right] \tag{3}$$

leaving two constants, σ and d, to be determined. The constant σ, which is a measure of the spreading rate of the shear layer, depends on the magnitude of the eddy viscosity and must be determined experimentally. The second constant d appears because only two of the three required boundary conditions have been specified. Note that this constant merely deflects the mixing region and has no direct influence on σ.

There has been considerable discussion in the literature on the correct third boundary condition (refs. 3, 4, and 5), but this relates primarily to the theoretical problem of semi-infinite streams. In practice the flow is always bounded. Experimentally and numerically the shear layer is generally approximated by the near field of a jet, and the requirement that $\partial u/\partial y$ be zero, on the line or plane of symmetry, is employed as the third boundary condition; thus the problem of indeterminancy is eliminated.

EFFECTS OF LOW REYNOLDS NUMBER

Before discussing the spreading rate in a developed turbulent shear layer, it is important to define what is meant by the term "developed." From an experimental point of view, it is seldom sufficient to require simply that the mean flow be self-similar, since it is often extremely difficult to establish when this has been achieved. This is especially true if only mean velocity measurements are available. The turbulence components are a much more sensitive indication of similarity, and it is strongly recommended that they be measured whenever possible. For present purposes the term "developed" will be used to refer to shear layers for which the data indicate that the turbulent and mean velocity components have achieved self-similarity and the maximum shear stress

has reached a constant value. However, it should be emphasized that this is no guarantee that the flow is truly developed. Some examples will be given of flows which appear to be self-similar, on the basis of mean and fluctuating velocity data, but which still do not seem to have reached their asymptotic spreading rate.

The variation of the center-line shear stress with downstream distance in a subsonic shear layer with zero velocity ratio is show schematically in figure 2. When the boundary layer is laminar at the point of separation, the near field can be divided into two more or less distinct regions. The first region ℓ_1 is shown here as the distance from the point of separation to the point of maximum shear stress. This region is sometimes defined as the distance to the point at which the fluctuating velocity component is a maximum (ref. 6) or as the distance to transition (ref. 7). The second region ℓ_2 is the subsequent distance to developed flow. The distance ℓ_1 has been reported to be virtually independent of Reynolds number (refs. 6 and 7), depending only on the initial boundary-layer thickness, but it is important to remember that ℓ_1 is a strong function of the initial disturbance level. This disturbance level will, in general, be different for different apparatuses and may also vary with Reynolds number for the same apparatus.

The second region ℓ_2 is much less sensitive to initial conditions, and at least for the range $500 < \frac{u_1\theta}{\nu} < 1000$, Bradshaw (ref. 6) found that the Reynolds number based on ℓ_2 was nearly constant. Since for a typical laboratory experiment ℓ_2 is 5 or 10 times ℓ_1, it is generally sufficiently accurate to quote a combined length

$$\ell_1 + \ell_2 \approx 7.0 \times 10^5 \frac{\nu}{u_1} \tag{4}$$

as the length required for both the mean and the fluctuating velocity components to become similar, while the mean velocity profiles alone appear to be similar at about

$$\ell_1 + \ell_2 \approx 4.0 \times 10^5 \frac{\nu}{u_1} \tag{5}$$

Recent results by Spencer (ref. 8) indicate that if the fluctuating pressures are considered, true similarity may require a Reynolds number, based on shear layer length, of about 1.3×10^6. When the boundary layer is turbulent at the point of separation, the shear stress rises slowly and the maximum again becomes approximately constant at $x \approx 7.0 \times 10^5 \frac{\nu}{u_1}$. However, its value is higher than that produced by a laminar boundary layer (refs. 6, 9, and 10). This suggests that one or perhaps both of these flows are not truly fully developed and that a constant value of the peak shear stress, independent of initial conditions, is only achieved far downstream. At present there are no experimental results to confirm this conclusion. The available results all show that the shear stress

in a shear layer depends on initial conditions, even in regions of the flow which otherwise appear to be developed. (See table 1, refs. 8 to 18.)

For velocity ratios u_2/u_1 greater than zero, the situation becomes very complex. The flow now develops from two boundary layers which will in general have different momentum thicknesses. Both boundary layers may be laminar or turbulent or one may be laminar and the other turbulent. It seems very unlikely that the developing region of such flows can be accurately characterized by any simple criteria, but, in general, the length required for the flow to become fully developed will increase with velocity ratio.

These results are based on a fairly limited range of conditions, but they do give a simple and useful guide for the design of experiments and provide an excellent first check on experimental data for which no turbulence measurements are available. To put it another way, failure to satisfy Bradshaw's criteria (eq. (4)) may not prove that a flow is transitional but it does place a burden on the experimenter to demonstrate that his flow is developed. Simply showing that the mean velocity data can be collapsed on a similarity plot is not good enough.

Data taken in low Reynolds number shear layers generally yield low values of σ, if the boundary layer was laminar before separation. This effect is believed to be similar to that described in references 19, 20, 21, and 22 for low Reynolds number boundary layers. The difference between the values of σ computed over the developing region of the flow and in the developed region is seldom more than 20 to 30 percent in subsonic flows with low velocity ratios. However, the peak shear stress can reach twice its developed value (ref. 6) and the difference does appear to increase with Mach number in supersonic flows.

VARIATION OF σ WITH u_2/u_1

So far discussion has been restricted mainly to shear layers with a velocity ratio $\frac{u_2}{u_1} = 0$. In 1962 Golik (ref. 23) proposed the relation

$$\frac{\sigma_o}{\sigma} = \frac{u_1 - u_2}{u_1} \tag{6}$$

based on data by Szablewski (ref. 24), for the variation of σ with u_2/u_1. The following year Sabin (refs. 25 and 26) and Abramovich (ref. 27, pp. 36-42) independently published the relation

$$\frac{\sigma_o}{\sigma} = \frac{u_1 - u_2}{u_1 + u_2} = \frac{1 - r}{1 + r} = \lambda \tag{7}$$

and supported their theoretical arguments with new experimental data. In 1968 Miles and Shih (ref. 28) proposed the relation

$$\frac{\sigma_o}{\sigma} = \frac{1}{1 + 5r^2} \tag{8}$$

and in 1972 Yule (refs. 29 and 30) proposed

$$\frac{\sigma_o}{\sigma} = \frac{1 - r}{(1 + r)^{1/2}} \tag{9}$$

All these relations were supported by experimental data. These four relations are shown in figure 3, and obviously predict different variations of σ_o/σ with r. However, the situation is not as bad as it might seem at first sight. Golik's result can probably be discounted since it was based on very limited data which were not supported by later experimental results. Yule's relation appears to be based on only two new data points, and this does not seem to be sufficient to establish any relation between σ and r. In any case, these new data by Yule differ only slightly from the data obtained by Miles and Shih. However, equations (8) and (9) do differ significantly. In particular, note that equation (9) unlike equation (8) predicts that $\frac{1}{\sigma} \to 0$ as $r \to 1.0$, which seems to be required theoretically.

Before discussing the experimental data in detail, it is important to emphasize that the expression for eddy viscosity and the variation of σ and r are directly related and cannot be specified independently. Sabin characterized equation (7) as "a plausible functional relation between these two quantities." This statement is certainly true, but it has led to some confusion since it seems to imply that the result cannot be formally derived from Görtler's theory.

Consider Görtler's expression for ϵ

$$\epsilon = kcx(u_1 - u_2) \tag{10}$$

where c is a constant defined by

$$b = cx$$

and

$$\sigma = \frac{1}{2}(kc\lambda)^{-1/2} \tag{11}$$

or

$$\sigma^2 = \frac{1}{4kc\lambda}$$

If the width of the mixing layer is defined as

$$b = y_a - y_b = cx \tag{12}$$

where y_a is the value of y where $\xi = 1$ and y_b is the value of y where $\xi = 0$, it follows since

$$\xi = \frac{\sigma y}{x}$$

or

$$\frac{\sigma b}{x} = 1$$

then

$$c = \frac{1}{\sigma}$$

In general, for any consistent definition of b, $c \propto \frac{1}{\sigma}$.

Inserting this into equation (11) gives

$$\sigma 2 = \frac{\sigma}{4k\lambda}$$

or

$$\frac{\sigma_o}{\sigma} = \lambda \tag{13}$$

Therefore, if Prandtl's hypothesis is used in the form

$$\epsilon = kb(u_1 - u_2)$$

where the viscosity is based on the actual width of the mixing region, as is usual in numerical solutions, it is not necessary to use equation (13) explicitly. If the resulting solution is self-similar, it will automatically satisfy equation (13).

The available experimental values of σ are shown in figure 3 as a function of the velocity ratio r. The data from reference 27 (pp. 36-42) were given in nondimensional form, and other values of σ (refs. 9, 12 to 14, 17, and 25 to 33) have been normalized by using a value of $\sigma_o = 11$. Although this is common practice, it is an unsatisfactory method of illustrating the variation of σ with r for a number of reasons. First, it gives equal weight to all data points (some of which were measured in transitional flows). Second, the variation in σ_o mentioned earlier tends to exaggerate the scatter in the data. (See tables 1 and 2.) It is not possible to establish the variation of σ with r by comparing values of σ taken in different apparatuses at different velocity ratios unless the corresponding values of σ_o are known and in many experiments σ_o was not measured. If the variation in σ is to be determined separately from each set of experiments, then it is suggested that σ be measured for at least four different values of r. Of the six sets of data which satisfy this requirement, one (ref. 31) must be discarded because of low

Reynolds number effects. Of the remaining five sets of data (fig. 4), three include determinations of σ_0, but in only one case (ref. 34)* is the numerical value of σ_0 given; in the other two cases, the data are given in nondimensional form (ref. 27, pp. 36-42). This leaves two sets of data for which no values of σ_0 are given. For these data a value of σ_0 was chosen which best collapsed the data. A value of $\sigma_0 = 11$ was used to normalize Sabin's data, which is the value originally used in references 25 and 26, while $\sigma_0 = 9.3$ was found to be best for the data published by Miles and Shih, compared with $\sigma_0 = 12$ which they used in reference 28. This last set of data was also modified slightly. As originally reported (ref. 35), mean velocity profiles were taken at five x stations for each value of r. The spreading parameter σ was then computed for each velocity profile, and the resulting five values of σ were averaged. The value of x used in the calculations was the actual distance from the end of the splitter plate rather than the distance from the virtual origin of mixing. This led to some error in the calculated values of σ which increased with velocity ratio r and with initial boundary-layer thickness but decreased with increasing x. Since two sets of data were given for different initial boundary-layer thicknesses, it was possible to partially compensate for these errors without repeating the calculations. First, the values of σ computed for the two stations closest to the origin were dropped, and a new average was calculated. Then, a linear extrapolation through these two sets of data was used to estimate the values of σ which would correspond to a flow with zero initial boundary-layer thickness. This resulted in no change in σ for velocity ratios less than 0.3, but the correction increased for higher velocity ratios, resulting in a maximum increase in σ of about 20 percent for a velocity ratio of 0.83. The resulting data were then normalized by using a value of $\sigma_0 = 9.3$. It is not clear why these data required a lower value of σ_0 to bring them into correspondence with the data from the other experiments, but it seems possible that the boundary layers may have been turbulent before separation. The agreement between these data and those reported in reference 29 seems to support this conclusion, since the boundary layers in the latter experiment were turbulent.

As can be seen in figure 4, the data from the five experiments, normalized as described previously, are all in good agreement with the prediction of equation (7). Note that the data points corresponding to the highest velocity ratio for each of the two experiments reported in reference 27 (pp. 36-42) have been omitted from figure 4. These data points deviate significantly from the rest of the data and obviously do not correspond to the mixing rates in fully developed shear layers. This deviation is discussed in reference 27 (pp. 36-42) and is attributed to the increased influence of free-stream turbulence on mixing rate at high velocity ratios.

---

* The authors would like to thank B. G. Jones for pointing out that the σ_0 given in reference 34 was a measured value.

It is perhaps worth emphasizing at this point that while the data in figure 4 seem to confirm the predictions of Görtler's simple theory, the result is, for many practical problems, rather academic. Görtler's theory is only valid for regions of the flow which are sufficiently far downstream that the effects of initial conditions can be ignored and the flow has become self-similar. This distance increases quickly with velocity ratio, and much of the available experimental data and many practical problems do not satisfy these criteria. For such flows the mixing rates will be affected by the initial conditions and may differ significantly from the prediction of equation (7).

Stephen J. Kline of Stanford University recently suggested a new method of plotting the data shown in figure 4. If σ_0/σ is plotted against λ, the result is a straight line passing through the origin and the point (1,1). This method of plotting the data seems to offer some advantages over other methods: It simplifies the selection of a σ_0 to optimize the fit between theory and experiment, and it may also be very useful for studying flows in which the velocity ratio r is varying. The data plotted in this form are shown in figure 5.

VARIATION OF σ WITH MACH NUMBER

Figure 6 shows experimental values of σ for zero-velocity-ratio shear layers as a function of Mach number. This includes a determination of σ at a Mach number of 5 recently obtained at the NASA Langley Research Center (LaRC). The total temperature in each of these flows was approximately constant. Again some selection was involved in the presentation of these data in that not all the available data listed in table 3 (refs. 16, 36 to 44) are shown in figure 6. To present all the available results would lead to a scatter of data, matched only by the attempts to correlate them (refs. 27 (pp. 293-302), 45 to 53), and would tend to mask any real experimental trend which may be indicated. It seems reasonable to discount Johannesen's early results (ref. 39) since the author himself suggested that the mixing rate was affected by shock waves in the nozzle, and he later repeated the experiment with a new nozzle (ref. 40). The discrepancy between Cary's data (ref. 38) and those obtained by other workers over the same Mach number range is not as easy to explain. It is pointed out in reference 16 that the data, which were obtained by using an interferometer, would have limited accuracy especially for the lower Mach number flows. Although this is true, the discrepancy appears to be larger than can be explained as a simple experimental error and probably indicates some difference in the actual flows. While the present authors can offer no clear explanation for the difference, it does seem that the preponderance of data, which indicate lower values of σ for this Mach number range, is more representative of the mixing in a developed shear layer. Therefore, to illustrate the general experimental trend more clearly, Cary's data have been omitted from figure 6.

The remaining data seem to follow two more or less distinct curves. For clarity, these two sets of data have been marked by open and solid symbols in the supersonic region. One set of data, marked by open symbols, indicates a sharp increase in σ with Mach number as the flow becomes supersonic with a tendency to level out again for hypersonic velocities. The second set of data, marked by solid symbols, shows little or no variation with Mach number. At a Mach number of 5 the two sets of data differ by about a factor of 3, and this difference appears to be increasing with further increases in Mach number. The only obvious significant difference between these two sets of data is in the Reynolds number, the data marked by solid symbols generally having a lower value of R_x. Note that the Reynolds number for the Mach 4 and the Mach 8 data (ref. 41) is considerably lower than the R_x of at least 4×10^6 required to achieve fully developed mean profiles for the Langley Mach 5 shear layer. The data from reference 44 refer specifically to the developing region of a shear layer and extend only about 10 to 15 initial boundary-layer thicknesses downstream from the separation point. There is no reason to believe that the mixing rates calculated for these flows will equal the mixing rates in developed turbulent flows. It is therefore suggested that on the basis of the data available at present, the faired line shown in figure 6 best represents the variation of σ with Mach number for developed shear layers. However, because of the limited data available at present and because effects of initial conditions are still poorly understood, some uncertainty must exist as to the absolute accuracy of these data, and further high Reynolds number data for supersonic and hypersonic shear layers are very desirable.

Interest in the effects of Reynolds number on the turbulence levels in supersonic and hypersonic free shear flows has been heightened by a recent paper by Finson (ref. 54). In this paper Finson draws attention to the significant differences between the turbulence levels in high and low Reynolds number hypersonic wakes. While the flow in a hypersonic wake is considerably more complex than the mixing in a simple shear layer, the Reynolds number effects described in reference 54 seem to be at least qualitatively similar to those discussed previously in this paper.

VARIATION OF σ WITH DENSITY RATIO

Although a number of correlations of the variation of σ with Mach number have been proposed, the authors know of no published eddy viscosity model, applicable to a wide range of free turbulent flows, which includes a specific Mach number effect. Most models assume that the change in σ is due to the associated change in density ratio across the shear layer and that for a given velocity and density distribution, the mixing rate is independent of whether the density distribution is due to changes in temperature, composition, or Mach number. This conclusion has recently been challenged by Brown

and Roshko (ref. 32), who claim that density differences in subsonic flows have relatively small effect on the turbulent mixing rate.

The spreading rate in a developed turbulent shear layer appears to be linear with x for both homogeneous and heterogeneous flows at all velocity ratios, and conditions on both sides of the mixing layer do not change with distance downstream. This would seem to make the shear layer an ideal flow in which to study the effects of density ratio on the turbulent mixing rate. Although this is probably true, the design of a suitable apparatus poses a number of serious problems. It is no coincidence that most of the detailed studies of the mixing in homogeneous shear layers employed rather large apparatuses (refs. 8, 9, and 14). This may have been due in part to a desire to generate a shear layer which was large enough to allow detailed measurements to be made, but more important, it was necessary to employ a large apparatus or a high unit Reynolds number (ref. 6) to insure that the flow would be developed. To achieve suitably high Reynolds numbers in a heterogeneous experiment can be quite difficult. The experimenter finds that in selecting a suitable gas combination which will give the required large density difference, he often must season his selection with considerations of expense and danger. As a result of these difficulties there are little data available for the mixing in heterogeneous shear layers, and in none of these experiments is the flow clearly developed.

Of the four available experimental studies, three list values of σ (table 4). Values of σ are not available for the fourth (ref. 55), but the variation in spreading rate with density ratio m is given. These experiments cover approximately the same density ratio and Reynolds number range as those described in reference 32. Although there are insufficient data at any one velocity ratio for a meaningful plot of the variation of σ with m, it is obvious that there is considerable disagreement between the four sets of experimental results. There is good agreement between the measured values of σ in references 18 and 33 for a density ratio of 4.0 and a velocity ratio of about 0.25, but the results differ by nearly a factor of 2 at a velocity ratio of approximately 0.5. At a velocity ratio of 0.377 Brown and Roshko found that σ varied by only about 60 percent when the density ratio was changed by a factor of 49; Abramovich et al. found that the spreading rate changed by nearly a factor of 4 over the same range of density ratios. In all these experiments R_x was less than that generally required to give developed flow in a homogeneous shear layer. It is difficult to draw any definite conclusion from these results except that most of the data are probably influenced by low Reynolds number effects. A comparison of the measured values of σ in the homogeneous mixing experiments from references 18, 30, and 33 with those from references 8 and 25, tends to support this conclusion. (See fig. 3.)

The turbulent mixing in heterogeneous shear flows has been studied for more than years, and it is surprising and disappointing to find that one of the most fundamental

questions still remains unanswered: Does density ratio have any significant effect on the mixing rate? This question is important and must be answered before we can claim any real understanding of the turbulent mixing in supersonic or variable-density free shear flows.

Although the absolute values of σ from these heterogeneous mixing experiments are of questionable value for determining the effect of density ratio on mixing rate, the reported variation of σ with velocity ratio is still of some interest. This is due to the widely different predictions of available eddy viscosity models. These data plotted as a function of velocity ratio r are shown in figure 7. Except for the experiments from reference 55, where the spreading rates at $r = 0$ are given, the data have been normalized by using a value of σ_o, which fits the points corresponding to the lowest velocity ratios to the curve $\frac{\sigma_o}{\sigma} = \lambda$. Note that in spite of the expected scatter most of the data fall close to the curve. This suggests that the variation of σ_o/σ with r is not strongly dependent on the density ratio across the shear layer. In contrast to this, many eddy viscosity models show a strong dependence on density ratio. For example, a simple mass flow difference model of the form

$$\epsilon = kb\left|(\rho u)_1 - (\rho u)_2\right| \tag{14}$$

predicts a variation given by

$$\frac{\sigma_o}{\sigma} = \left|\frac{1 - mr}{1 + r}\right| \tag{15}$$

Equation (15) is plotted in figure 8, and it can be seen that it predicts a strong dependence on m. For values of $m > 5.0$ and $r > 0.2$, σ_o/σ increased with r, and in some cases, values of σ_o/σ were nearly an order of magnitude greater than those found experimentally. It should also be noted that equation (14), unlike Prandtl's constant exchange hypothesis, is not invariant with respect to a Galilean transformation.

CONCLUSIONS

One of the most important conclusions of this study must be that many, if not most, of the apparent inconsistencies which exist in the interpretation of the experimental data for free shear layers result from confusing data taken in developed turbulent flows with those taken in transitional or developing flows. Only a small fraction of the flows studied thus far appear to be developed, and many workers are apparently unaware that the effects of the initial conditions can persist far downstream. The present authors are not suggesting that experimental studies of developing flows are unimportant. On the contrary

many flows of practical importance are not developed, and one of the major advantages of the better turbulence models is their potential ability to predict such flows. However, as the authors have attempted to show in this review, experimental studies in developing flows can lead to erroneous conclusions if the mixing rates in the corresponding developed flows are not known.

The conclusions of this study as they relate to the first three conference test cases are as follows:

1. The variation of σ_o/σ with r in a developed subsonic homogeneous shear layer is best represented by

$$\frac{\sigma_o}{\sigma} = \frac{1 - r}{1 + r}$$

where $r = \frac{u_2}{u_1}$, σ is the spreading parameter, σ_o is the spreading parameter at $u_2 = 0$, and u_1 and u_2 are velocities on high- and low-velocity side of shear layer, respectively. Although some of the data do not support this relation, the discrepancies appear to be satisfactorily explained as low Reynolds number effects or the effects of initial conditions.

2. The effects of Mach number are more uncertain primarily because of limited data and the absence of any turbulence measurements for supersonic shear layers. On the basis of the data available at present, the faired line shown in figure 6 seems to best represent the variation of the spreading parameter with Mach number for a developed supersonic shear layer.

3. The data available for heterogeneous shear layers are not sufficient to clearly establish the effect of density ratio on mixing rate. Although there is little experimental evidence to suggest that variations in the density ratio across a shear layer will greatly change its mixing rate, it appears to the present authors to be more appropriate at this time to emphasize the need for better data at high Reynolds number than to speculate on the absolute accuracy of the available data.

REFERENCES

1. Görtler, H.: Berechnung von Aufgaben der freien Turbulenz auf Grund eines neuen Näherungsansatzes. Z. Angew. Math. Mech., Bd. 22, Nr. 5, Oct. 1942, pp. 244-254.

2. Schlichting, Hermann (J. Kestin, transl.): Boundary-Layer Theory. Sixth ed., McGraw-Hill Book Co., Inc., 1968.

3. Yen, K. T.: On the Indeterminateness of the Boundary Conditions for the Mixing of Two Parallel Streams. Trans. ASME, Ser. E: J. Appl. Mech., vol. 27, no. 3, Sept. 1960, pp. 390-392.

4. Ting, Lu.: On the Mixing of Two Parallel Streams. J. Math. & Phys., vol. XXXVIII, no. 3, Oct. 1959, pp. 153-165.

5. Klemp, J. B.; and Acrivos, Andreas: A Note on the Laminar Mixing of Two Uniform Parallel Semi-Infinite Streams. J. Fluid Mech., vol. 55, pt. 1, Sept. 12, 1972, pp. 25-30.

6. Bradshaw, P.: The Effect of Initial Conditions on the Development of a Free Shear Layer. J. Fluid Mech., vol. 26, pt. 2, Oct. 1966, pp. 225-236.

7. Sato, Hiroshi: Experimental Investigation on the Transition of Laminar Separated Layer. J. Phys. Soc. Jap., vol. 11, no. 6, June 1956, pp. 702-709.

8. Spencer, Bruce Walton: Statistical Investigation of Turbulent Velocity and Pressure Fields in a Two-Stream Mixing Layer. Ph. D. Thesis, Univ. of Illinois, 1970.

9. Wygnanski, I.; and Fiedler, H. E.: The Two-Dimensional Mixing Region. J. Fluid Mech., vol. 41, pt. 2, Apr. 13, 1970, pp. 327-361.

10. Batt, R. G.; Kubota, T.; and Laufer, J.: Experimental Investigation of the Effect of Shear-Flow Turbulence on a Chemical Reaction. AIAA Paper No. 70-721, June 1970.

11. Cordes, G.: Untersuchungen zur statischen Druckmessung in turbulenter Strömung. Ing.-Arch., Bd. VIII, Heft 4, Aug. 1937, pp. 245-270.

12. Tollmien, Walter: Berechnung turbulenter Ausbreitungsvorgänge. Z. Angew. Math. Mech., Bd. 6, Heft 6, Dec. 1926, pp. 468-478. (Available in English translation as NACA TM 1085, 1945.)

13. Reichardt, Hans: Gesetzmässigkeiten der freien Turbulenz. VDI-Forschungsh. 414, 1942.

14. Liepmann, Hans Wolfgang; and Laufer, John: Investigations of Free Turbulent Mixing. NACA TN 1257, 1947.

15. Crane, L. J.: The Laminar and Turbulent Mixing of Jets of Compressible Fluid. Pt. II – The Mixing of Two Semi-Infinite Streams. J. Fluid Mech., vol. 3, pt. I, Oct. 1957, pp. 81-92.

16. Maydew, R. C.; and Reed, J. F.: Turbulent Mixing of Axisymmetric Compressible Jets (in the Half-Jet Region) With Quiescent Air. SC-4764(RR), Sandia Corp. (Albuquerque, N. Mex.), Mar. 1963.

17. Mills, R. D.: Numerical and Experimental Investigations of the Shear Layer Between Two Parallel Streams. J. Fluid Mech., vol. 33, pt. 3, Sept. 2, 1968, pp. 591-616.

18. Johnson, Dennis Alan: An Investigation of the Turbulent Mixing Between Two Parallel Gas Streams of Different Composition and Density With a Laser Doppler Velocimeter. Ph. D. Diss., Univ. of Missouri, 1971.

19. Simpson, Roger L.: Characteristics of Turbulent Boundary Layers at Low Reynolds Numbers With and Without Transpiration. J. Fluid Mech., vol. 42, pt. 4, 1970, pp. 769-802.

20. McDonald, H.: Mixing Length and Kinematic Eddy Viscosity in a Low Reynolds Number Boundary Layer. Rep. J214453-1, Res. Lab., United Aircraft Corp., Sept. 1970.

21. Cebeci, Tuncer: A Model for Eddy-Conductivity and Turbulent Prandtl Number. Rep. No. MDC-J0747/01, McDonnell Douglas Corp., May 1970.

22. Bushnell, Dennis M.; and Morris, Dana J.: Shear-Stress, Eddy-Viscosity, and Mixing-Length Distributions in Hypersonic Turbulent Boundary Layers. NASA TM X-2310, 1971.

23. Golik, Raymond John: On Dissipative Mechanisms Within Separated Flow Regions (With Special Consideration to Energy Transfer Across Turbulent, Compressible, Pr = 1, Mixing Regions). Ph. D. Thesis, Univ. of Illinois, 1962.

24. Szablewski, W.: Turbulente Vermischung ebener Heissluftstrahlen. Ing.-Arch., Bd. XXV, Heft 1, Jan. 1957, pp. 10-25.

25. Sabin, C. M.: An Analytical and Experimental Study of the Plane, Incompressible, Turbulent Free Shear Layer With Arbitrary Velocity Ratio and Pressure Gradient. AFOSR-TN-5443, U.S. Air Force, Oct. 1963. (Available from DDC as AD 430 120.)

26. Sabin, C. M.: An Analytical and Experimental Study of the Plane, Incompressible, Turbulent Free-Shear Layer With Arbitrary Velocity Ratio and Pressure Gradient. Trans. ASME, Ser. D: J. Basic Eng., vol. 87, no. 2, June 1965, pp. 421-428.

27. Abramovich, G. N.: The Theory of Turbulent Jets. M.I.T. Press, c.1963.

28. Miles, John B.; and Shih, Jing-shihong: Similarity Parameter for Two-Stream Turbulent Jet-Mixing Region. AIAA J., vol. 6, no. 7, July 1968, pp. 1429-1430.

29. Yule, A. J.: Two-Dimensional Self-Preserving Turbulent Mixing Layers at Different Free Stream Velocity Ratios. R. & M. No. 3683, Brit. A.R.C., 1972.

30. Yule, Andrew J.: Spreading of Turbulent Mixing Layers. AIAA J., vol. 10, no. 5, May 1972, pp. 686-687.

31. Seban, R. A.; and Back, L. H.: Velocity and Temperature Profiles in Turbulent Boundary Layers With Tangential Injection. Trans. ASME, Ser. C: J. Heat Transfer, vol. 84, no. 1, Feb. 1962, pp. 45-54.

32. Brown, Garry; and Roshko, Anatol: The Effect of Density Difference on the Turbulent Mixing Layer. Turbulent Shear Flows, AGARD-CP-93, Jan. 1972, pp. 23-1 – 23-12.

33. Baker, Richard L.; and Weinstein, Herbert: Experimental Investigation of the Mixing of Two Parallel Streams of Dissimilar Fluids. NASA CR-957, 1968.

34. Spencer, B. W.; and Jones, B. G.: Statistical Investigation of Pressure and Velocity Fields in the Turbulent Two-Stream Mixing Layer. AIAA Paper No. 71-613, June 1971.

35. Shih, Jing-shihong: Similarity Parameter for Two-Stream Turbulent Jet-Mixing Region. M.S. Thesis, Univ. of Missouri, 1968.

36. Gooderum, Paul B.; Wood, George P.; and Brevoort, Maurice J.: Investigation With an Interferometer of the Turbulent Mixing of a Free Supersonic Jet. NACA Rep. 963, 1950.

37. Bershader, D.; and Pai, S. I.: On Turbulent Jet Mixing in Two-Dimensional Supersonic Flow. J. Appl. Phys., vol. 21, no. 6, June 1950, p. 616.

38. Cary, Boyd Balford, Jr.: An Optical Study of Two-Dimensional Jet Mixing. Ph. D. Thesis, Univ. of Maryland, 1954.

39. Johannesen, N. H.: The Mixing of Free Axially-Symmetrical Jets of Mach Number 1.40. R. & M. No. 3291, Brit. A.R.C., 1957.

40. Johannesen, N. H.: Further Results on the Mixing of Free Axially-Symmetrical Jets of Mach Number 1.40. R. & M. No. 3292, Brit. A.R.C., 1959.

41. Rhudy, J. P.; and Magnan, J. D., Jr.: Turbulent Cavity Flow Investigation at Mach Numbers 4 and 8. AEDC-TR-66-73, U.S. Air Force, June 1966. (Available from DDC as AD 483 748.)

42. Sirieix, M.; and Solignac, J. L.: Contribution a l'Etude Experimentalè de la Couche de Melange Turbulent Isobare d'un Ecoulement Supersonique. Separated Flows, Pt. I, AGARD CP No. 4, May 1966, pp. 241-270.

43. Eggers, James M.: Velocity Profiles and Eddy Viscosity Distributions Downstream of a Mach 2.22 Nozzle Exhausting to Quiescent Air. NASA TN D-3601, 1966.

44. Hill, W. G., Jr.; and Page, R. H.: Initial Development of Turbulent, Compressible, Free Shear Layers. Trans. ASME, Ser. D: J. Basic Eng., vol. 91, no. 1, Mar. 1969, pp. 67-73.

45. Tripp, Wilson: The Base Pressure Behind a Blunt Trailing Edge for Supersonic Two-Dimensional Flow, Approaching Streams Having the Same Stagnation Temperature but Dissimilar Mach Numbers and Stagnation Pressures. Ph. D. Diss., Univ. of Illinois, 1956.

46. Korst, H. H.; and Tripp, Wilson: The Pressure on a Blunt Trailing Edge Separating Two Supersonic Two-Dimensional Air Streams of Different Mach Number and Stagnation Pressure but Identical Stagnation Temperature. Proceedings of the Fifth Midwestern Conference on Fluid Mechanics, Univ. of Michigan Press, 1957, pp. 187-199.

47. Alber, Irwin E.; and Lees, Lester: Integral Theory for Supersonic Turbulent Base Flows. AIAA Paper No. 68-101, Jan. 1968.

48. Channapragada, R. S.; and Woolley, J. P.: Turbulent Mixing of Parallel Compressible Free Jets. AIAA Paper No. 65-606, June 1965.

49. Vasiliu, John.: Pressure Distribution in Regions of Step-Induced Turbulent Separation. J. Aerosp. Sci., vol. 29, no. 5, May 1962, pp. 596-601, 631.

50. Bauer, R. C.: An Analysis of Two-Dimensional Laminar and Turbulent Compressible Mixing. AEDC-TR-65-84, U.S. Air Force, May 1965. (Available from DDC as AD 462 202.)

51. Hill, Jacques A. F.; and Nicholson, James E.: Compressibility Effects on Fluid Entrainment by Turbulent Mixing Layers. NASA CR-131, 1964.

52. McDonald, H.: The Turbulent Supersonic Base Pressure Problem: A Comparison Between a Theory and Some Experimental Evidence. Aeronaut. Quart., vol. XXVII, pt. 2, May 1966, pp. 105-126.

53. Donaldson, Coleman duP.; and Gray, K. Evan: Theoretical and Experimental Investigation of the Compressible Free Mixing of Two Dissimilar Gases. AIAA J., vol. 4, no. 11, Nov. 1966, pp. 2017-2025.

54. Finson, Michael L.: Hypersonic Wake Aerodynamics at High Reynolds Numbers. AIAA Paper No. 72-701, June 1972.

55. Abramovich, G. N.; Yakovlevsky, O. V.; Smirnova, I. P.; Secundov, A. N.; and Krasheninnikov, S. Yu.: An Investigation of the Turbulent Jets of Different Gases in a General Stream. Astronaut. Acta, vol. 14, no. 3, Mar. 1969, pp. 229-240.

TABLE 1.- EXPERIMENTAL DETERMINATIONS OF σ_o IN SUBSONIC SHEAR LAYERS

Reference	Investigator	Date	Nozzle shape and dimensions (a)	Initial conditions (a)	Theory used	R, per meter	[b] R_x	σ_o	Comments
12	Tollmien	1926	A; 224 cm		Tollmien	20.5×10^5	2.3×10^6	11.8	Only one profile used to compute σ_o
11	Cordes	1937	R; 25 by 65 cm		Tollmien	10.2×10^5	6.0×10^5	12.0	
13	Reichardt	1942	R; 32 by 32 cm		Görtler	2×10^5	2.8×10^6	13.5	Very high value of σ_o
14	Liepmann and Laufer	1947	R; 152 by 19 cm (60 by 7.5 in.)	S.P. (laminar)	Görtler and Tollmien	12.1×10^5	1.1×10^6	11.0	Note change in σ_o
						12.1×10^5	1.1×10^6	12.0	
15	Crane	1957	A; 8.9 cm (3.5 in.)	Nozzle	Crane	14.4×10^6	3.3×10^6	12.7	Based on rather limited data by Lawrence
16	Maydew and Reed	1963	A; 7.6 cm (3.0 in.)	Nozzle	Crane	15.7×10^6	4.6×10^6	10.5	No information given about boundary layer
			A; 7.6 cm (3.0 in.)		Crane	19.0×10^6	5.6×10^6	10.8	before separation (probably turbulent)
			A; 7.6 cm (3.0 in.)		Crane	21.3×10^6	6.3×10^6	11.0	
17	Mills	1968	R; 20 by 5 cm (8 by 2 in.)	S.P.	Numerical solution	11.2×10^5	2.6×10^5	10.0	No information given about boundary layer
						8.5×10^5	1.75×10^5	10.4	before separation (probably turbulent)
9	Wygnanski and Fiedler	1970	R; 50.8 by 17.8 cm (20 by 7 in.)	St., T.W.	Comparison with reference 14	7.9×10^5	4.7×10^5	9.0	T.W. just upstream of separation
8	Spencer	1970	R; 38 by 17.8 cm (15 by 7 in.)	S.P. (laminar)	Korst	20.7×10^5	2.6×10^6	11.0	Appears to be best data available at present
10	Batt, Kubota, and Laufer	1970	R; 63.5 by 12.7 cm (25 by 5 in.)	S.P. (laminar)	Profiles were compared with those in references 14 and 9	10.2×10^5	6.6×10^5	12.0	Turbulence measurements tend to confirm
				St. (laminar)		10.2×10^5	6.6×10^5	12.0	effect of trip wire on σ_o
				St., T.W.		10.2×10^5	6.6×10^5	9.0	
18	Johnson	1971	R; 2.5 by 2.5 cm (1.0 by 1.0 in.)	S.P.	Görtler	12.5×10^5	1.3×10^5	9.0	Very low R_x

[a] Abbreviations used are

A	Axisymmetric
R	Rectangular
S.P.	Splitter plate
St.	Backward-facing step
T.W.	Trip wire

[b] $R_x = \frac{u_1 x}{\nu}$ where x is the farthest downstream station surveyed.

TABLE 2.- EXPERIMENTAL VALUES OF σ FOR VARIOUS VALUES OF u_2/u_1 IN SUBSONIC SHEAR LAYERS

Reference	Investigator	Date	u_2/u_1	σ	σ_o/σ	R_x
25, 26	Sabin	1963	0.36	25		2.3×10^5
			.46	32		
			.62	47		
			.66	54		
27 (pp. 36-42)	Yakovlevskiy	1963	0		1.0	
			.1		.83	
			.12		.76	
			.235		.615	
			.40		.52	
			.58		.51	
27 (pp. 36-42)	Zhestkov	1963	0		1.0	
			.17		.67	
			.22		.585	
			.28		.52	
			.465		.34	
			.52		.32	
			.70		.29	
31	Seban and Back	1962	.2	14.7		
			.36	16.4		
			.6	27.9		9×10^4
17	Mills	1968	0	10.4		1.75×10^5
			.3	18.3		
			.6	25.0		2.6×10^5
			0	10.0		
			.3	16.4		
			.6	26.0		
33	Baker and Weinstein	1968	.111	12.1		8×10^4
			.25	13.75		
			.43	16.01		
			.666	37.5		
28	Miles and Shih	1968	.15	12.6		1.9×10^6
			.225	15.0		
			.36	21.6		
			.475	28.2		
			.55	34.8		
			.65	43.2		
			.755	54.6		
			.83	66.6		
8, 34	Spencer and Jones	1971	0	11		2.6×10^6
			.15	13.3		
			.22	15.7		
			.305	20.4		
			.54	41.4		
			.61	50.4		
			.76	77.0		
32	Brown and Roshko	1972	.143	12.8		5×10^5
			.377	18.5		
18	Johnson	1971	0	9		1.3×10^5
			.3	14.85		
			.6	25.2		
29, 30	Yule	1972	.3	19		8×10^5
			.6	36		

TABLE 3.- EXPERIMENTAL DETERMINATIONS OF σ_0 IN SUPERSONIC SHEAR LAYERS

Reference	Investigator	Date	Mach number	R, per meter	R_x	σ_0
36	Gooderum, Wood, and Brevoort	1950	1.6	6.2×10^7	1.2×10^7	15.0
37	Bershader and Pai	1950	1.7	6.9×10^7	4.8×10^5	17.0
38	Cary	1954	1.0	28.2×10^6	9.5×10^5	16.0
			1.33	4.3×10^7	8.9×10^5	17.0
			1.59	6.2×10^7	1.7×10^6	33.0
39	Johannesen	1957	1.4	4.9×10^7	1.3×10^6	21.9
					3.1×10^6	11.9
40	Johannesen	1959	1.4	4.9×10^7	3.1×10^6	13.2 & 13.7
16	Maydew and Reed	1963	1.49	4.3×10^7	1.1×10^7	15.0
			1.96	7.5×10^7	2.2×10^7	20.0
41	Rhudy and Magnan	1966	3.99	7.5×10^6	7.67×10^5	12.4
			7.53	8.5×10^6	1.03×10^6	14.0
42	Sirieix and Solignac	1966	3.0			29.0
			4.0			34.0
43	Eggers	1966	2.22	10.8×10^7	1.6×10^7	22.0
44	Hill and Page	1969	2.1	4.9×10^7	1.1×10^7	16.0
			2.5	4.6×10^7	1.0×10^7	16.0
			3.2	4.2×10^7	6.4×10^6	16.0
			3.5	4.2×10^7	6.4×10^6	16.0
			3.7	4.2×10^7	4.8×10^6	16.0
[a] Unpublished	Morrisette and Birch	1972	5.0	31.5×10^6	8×10^6	37.0

[a] Data obtained at NASA Langley Research Center by E. Leon Morrisette.

TABLE 4.- EXPERIMENTAL VALUES OF σ IN HETEROGENEOUS SHEAR LAYERS

Reference	Investigator	Date	ρ_2/ρ_1	u_2/u_1	σ	[a] σ_o/σ	R_x
33	Baker and Weinstein	1968	4.0	0.5	36.9		
				.25	15.4		
				.111	14.6		$\approx 6 \times 10^4$
			↓	.143	10.5		
55	Abramovich et al.	1969	.27	0		0.22	10^5 to 10^6
			.27	.5		.1	
			1.3	0		.32	
				.22		.20	
				.5		.12	
			↓	.75		.08	
			7.0	0		.9	
				.2		.27	10^4 to 10^5
			↓	.7		.115	
32	Brown and Roshko	1972	.143	.377	23		
			7.0	.143	9		
			7.0	.377	15		7×10^4 to 5×10^5
18	Johnson	1971	4.0	.28	15.9		
				.45	19.8		$\approx 6 \times 10^4$

[a] The spreading rate b^o of the shear layer is not defined in reference 55, but it is assumed that $\frac{b^o}{b_o^o} \approx \frac{\sigma_o}{\sigma}$.

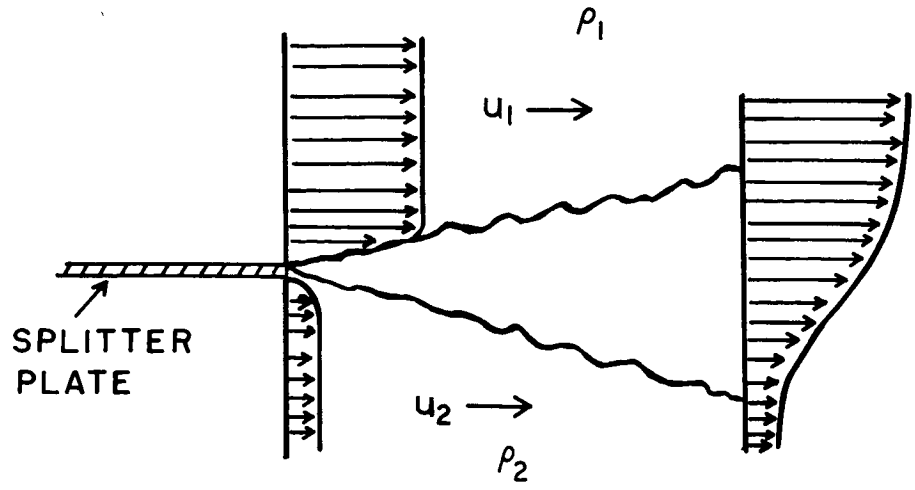

Figure 1.- Free shear layer.

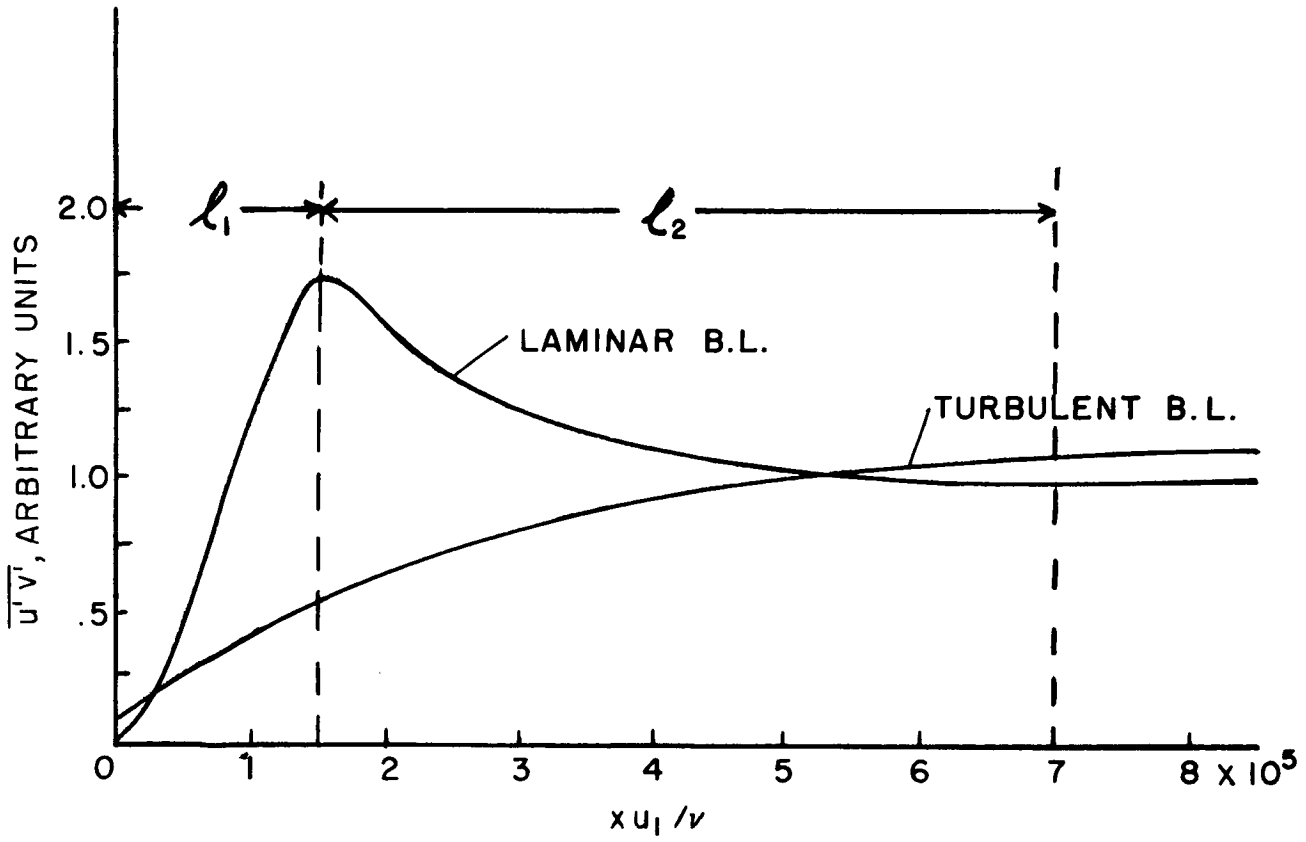

Figure 2.- Variation of shear stress $\overline{u'v'}$ in near field of a shear layer.

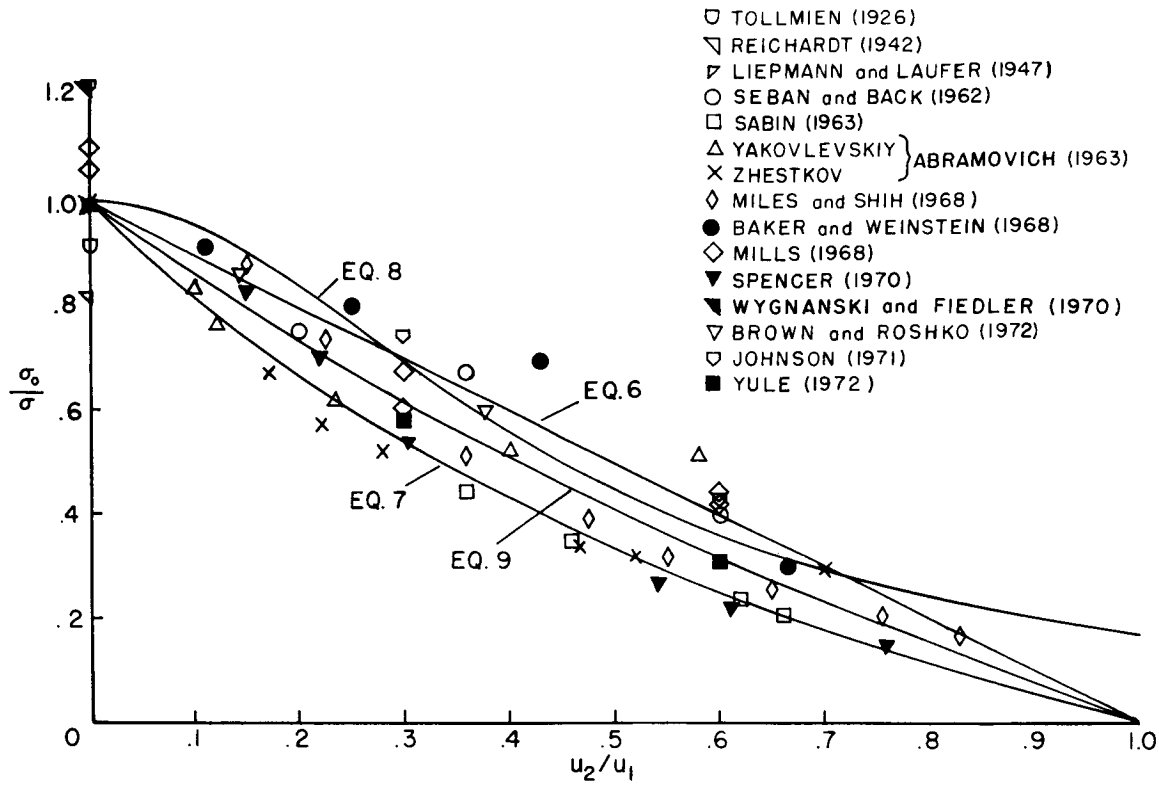

Figure 3.- Variation of spreading parameter σ_o/σ with velocity ratio u_2/u_1.

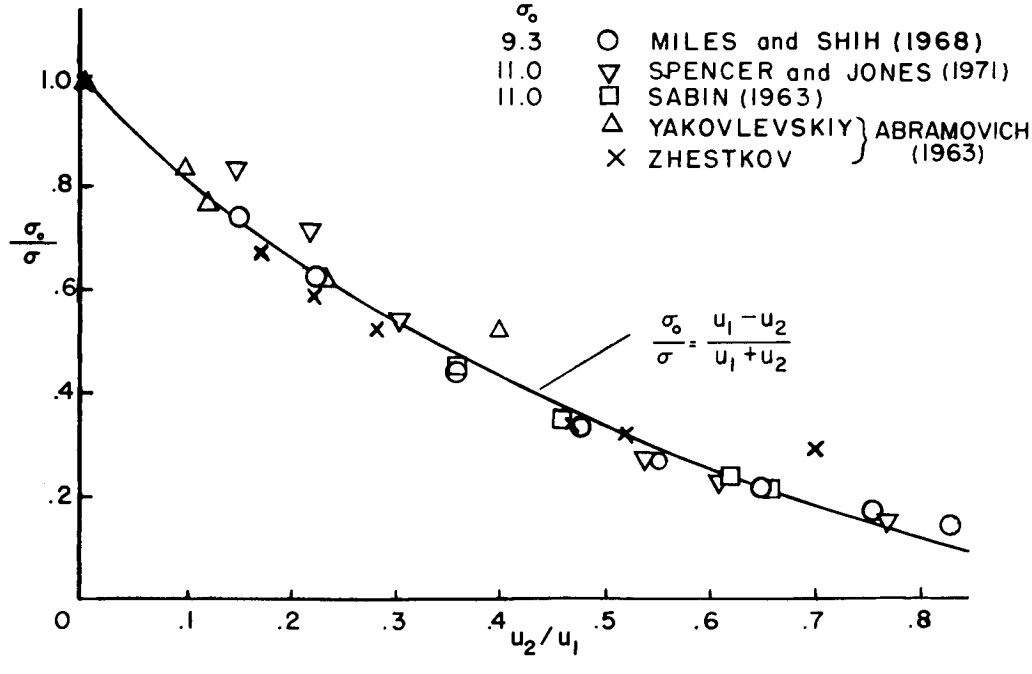

Figure 4.- Variation of σ_o/σ with velocity ratio u_2/u_1.

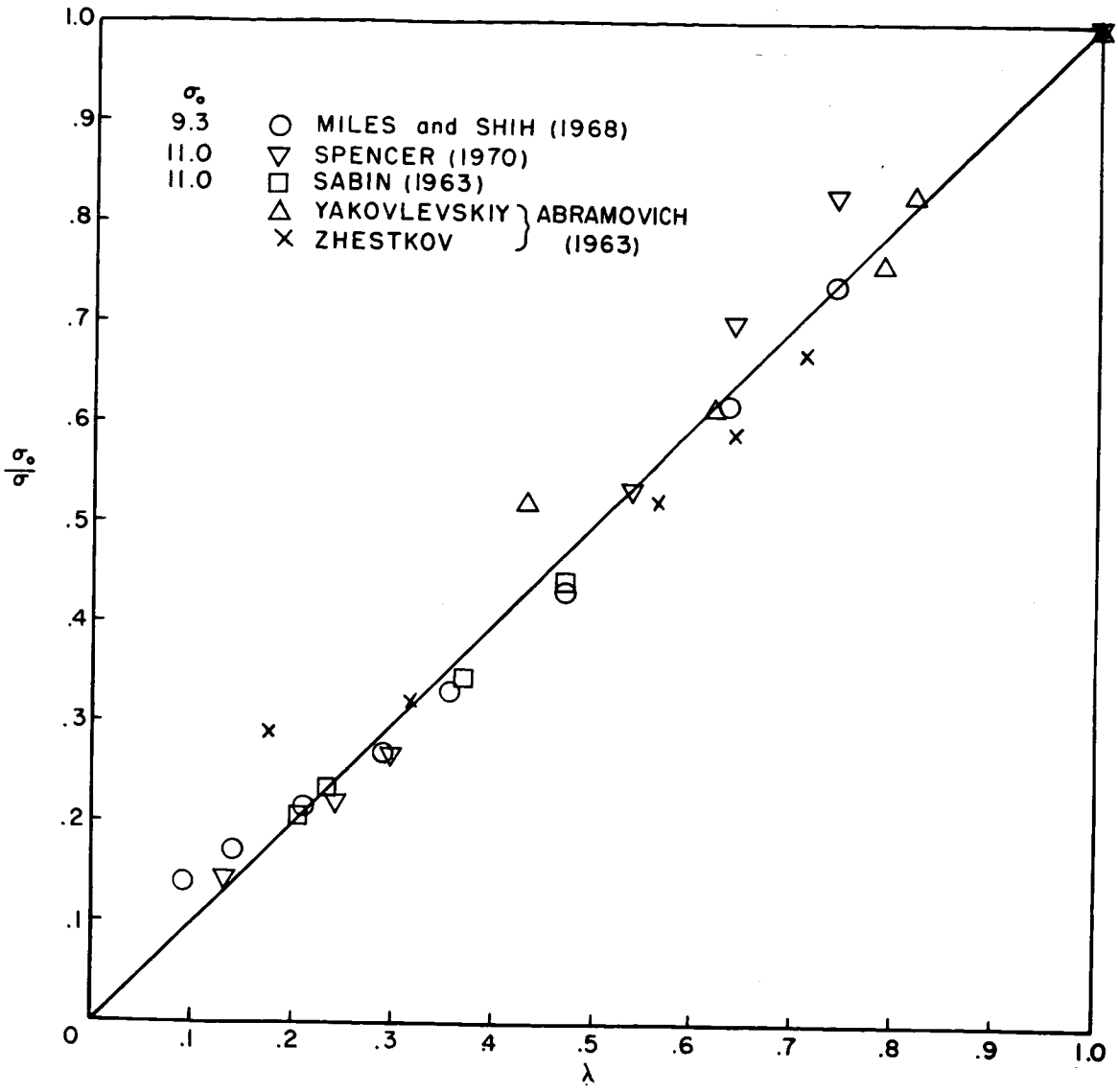

Figure 5.- Variation of σ_o/σ with λ.

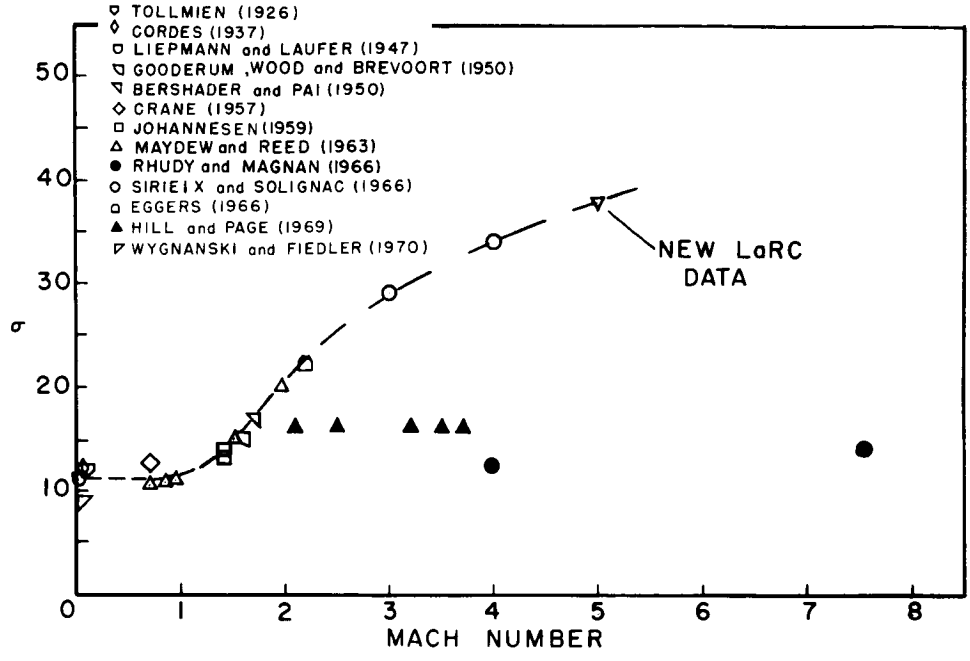

Figure 6.- Variation of σ with Mach number.

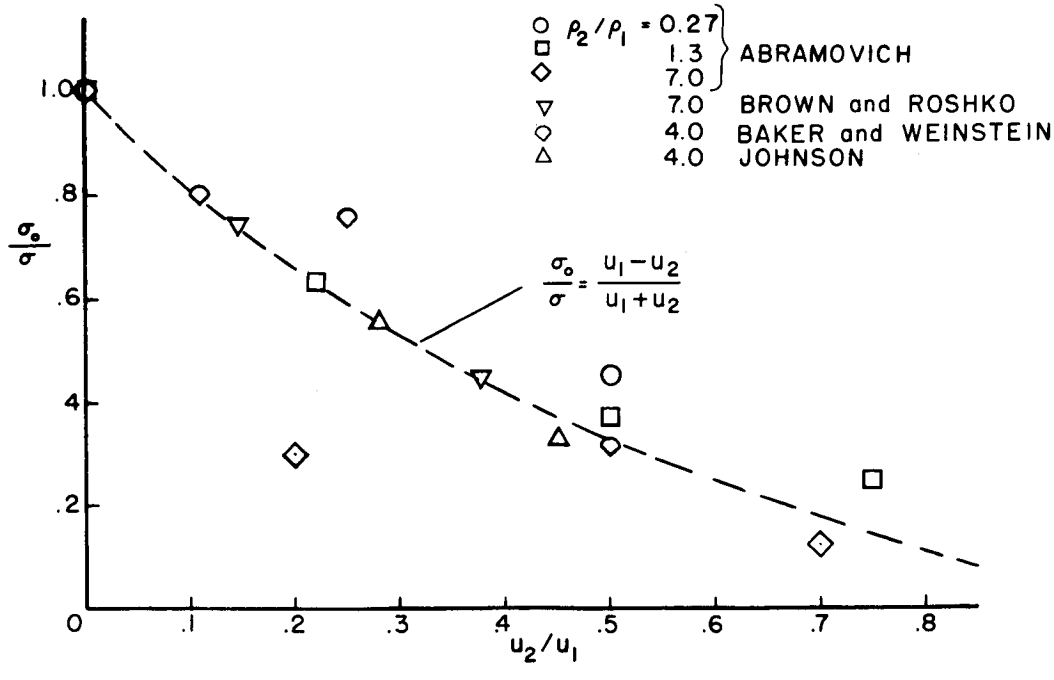

Figure 7.- Variation of σ_o/σ with velocity ratio u_2/u_1 for heterogeneous shear layers.

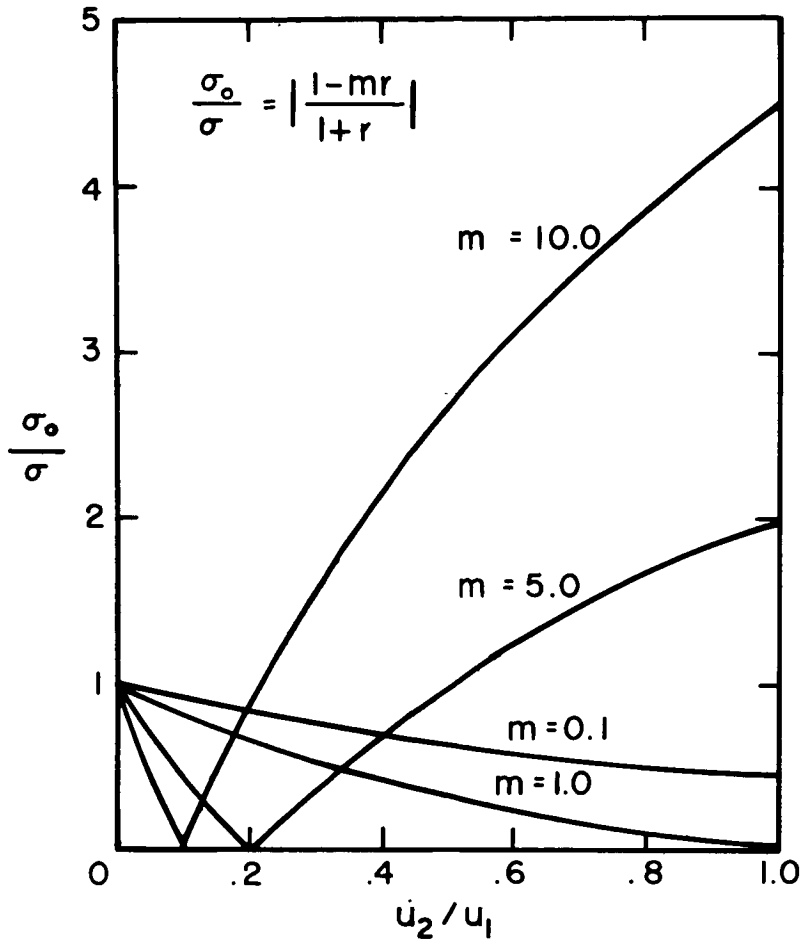

Figure 8.- Variation of spreading parameter σ_o/σ with velocity ratio for different values of density ratio $m = \frac{\rho_2}{\rho_1}$.

DISCUSSION

S. J. Kline: I merely want to comment in respect to Sabin's theory that the curve of σ_o/σ versus velocity ratio was not fitted. It was derived before there were any data, and he derived it in a different way than you suggested – he derived it on the basis of the assumption that the transverse velocity component is a function of velocity ratio only. It does not require anything but that, and the answer pops out and then the data were subsequently plotted on, so the theory was never fitted to the data.

S. F. Birch: No, the point I was trying to make was that in his paper he was somewhat modest on this point. He characterized it as a plausible functional relation between the two quantities. I believe this has been confusing to a number of people, in the sense that he did not emphasize the fact that this was derived directly from Prandtl's constant exchange hypothesis. It does follow directly. One method has been indicated by Professor Kline, and there is a second way of doing it, described in my paper. We have also checked the result numerically.

M. V. Morkovin: What flows do you feel are good touchstones for the theories that we are going to hear, and will the audience know "what flow is what number" when they are discussed?

S. F. Birch: Everyone was sent a list of the test cases with the letter of invitation. Is this what you are referring to?

M. V. Morkovin: Everyone in the audience or just the predictors?

S. F. Birch: No, everyone who received an invitation got a list of the test cases. If they have not brought them with them, we can supply some extra copies.

M. V. Morkovin: The question was also which are good touchstones?

S. F. Birch: Well, we believe that the shear layers (or near field region of jets) are more sensitive than some of the coaxial downstream mixing regions to such things as density ratio and Mach number ratio. This was the reason they were included in the flow test cases. To a certain extent it will be up to the committees, in general, to decide whether or not this is correct.

A. Roshko: I have a comment on a remark made toward the end of your talk. I am not sure I understood you correctly – did you say, or imply, that you would want Galilean invariance for an eddy-viscosity model?

S. F. Birch: I think it is possible to model some flows with a model which is not invariant. However, if it is not invariant, you do restrict yourself in its application or range of application.

A. Roshko: But, if you require Galilean invariance, then you are immediately requiring that the effect of ρ_2/ρ_1 be the same as that of ρ_1/ρ_2.

S. F. Birch: The ratio ρ_1/ρ_2 is not changed by Galilean transformation.

A. Roshko: Well, that is what I mean. For example, let us say you have the low density on the high-speed side, that will have one effect on the spreading rate, but if you require that the model be Galilean invariant, then you could reverse the velocities without reversing the densities. Then you ought to expect the same spreading rate on the requirement that it be Galilean invariant. I do not think that for the steady flows you can require them to be Galilean invariant, or equivalent to a nonsteady flow, say an infinite sheet spreading simply in a transverse direction.

S. F. Birch: I am not sure that I really follow your remarks. It seems to me that the shear stress must be invariant with respect to Galilean transformation in the full equations. Perhaps, I do not understand your point.

A. Roshko: Possibly we could take it up separately.

S. F. Birch: Yes, certainly.

I. E. Alber: I do not know if you have considered the parameter which describes the effect of the initial turbulent boundary layer or whether you have reached a similarity state or not, but some earlier calculations show that you have to go a distance of at least about 100 initial momentum thicknesses before you have essentially washed out the character of the initial boundary layer, at least in terms of its scale and this increase significantly with Mach number as well, so that, in fact, many of these cases at higher Mach numbers may not really be similar.

S. F. Birch: Yes, this is a point which perhaps I did not emphasize enough in my talk. In the experiments which were run here at Langley at Mach 5, we found that the Reynolds number required to get what looked like fully developed flow was 5 to 10 times higher than would have been required for a subsonic flow. Therefore, apparently this distance does increase with Mach number. I am not absolutely certain that our Reynolds numbers were high enough, in spite of the fact that we did get good similarity behavior for the mean profiles. The data reported here were for the highest Reynolds number test run so far, so presumably it best represents the fully developed spreading rate.

The following comments were submitted in writing before the conference and are included here because of their relevance to the discussion:

P. Bradshaw: It seems just possible that Brown and Roshko's [1] "two-dimensional large eddies" are the same as the posttransitional disturbances that delayed the onset of self-preservation in my experiments.[2] However, I am not confident about the use of my sim-

---

[1] Brown, Garry; and Roshko, Anatol: The Effect of Density Difference on the Turbulent Mixing Layer. Turbulent Shear Flows, AGARD-CP-93, Jan. 1972, pp. 23-1 – 23-12.

[2] Bradshaw, P.: The Effect of Initial Conditions on the Development of a Free Shear Layer. J. Fluid Mech., vol. 26, pt. 2, Oct. 1966, pp. 225-236.

ple Reynolds number criterion for self-preservation $\left(u_1 \frac{x}{\nu} > 7 \times 10^5\right)$ at exit boundary-layer Reynolds numbers very different from the range I used. Certainly my results indicated a Reynolds number criterion rather than an x/θ_o criterion but it is not obvious physically why the viscosity should matter to the posttransitional decay. As usual we need more data. It would be very helpful to have measurements of velocity or density fluctuations in Brown and Roshko's rig to see if rms values (ρ' or u') are self-preserving.

I don't think the uncertainties about self-preservation are strong enough to invalidate the conclusion that density ratio has little effect on spreading rate. We can take Brown and Roshko's order-of-magnitude arguments a little further and examine the Mach number fluctuation, which Morkovin's hypothesis requires to be small. For simplicity look at $M_\tau = \frac{\sqrt{|\overline{uv}|}}{a}$: in a mixing layer at $M = 1$ (about the Mach number at which the spreading rate starts to change significantly) we have $M_{\tau,max} \approx 0.1$. In a boundary layer at $M_1 = 4$ with $c_f = 0.001$, we again have $M_{\tau,max} = M_1\sqrt{\frac{c_f}{2}} \approx 0.1$. Therefore, if the Morkovin limit is roughly $M_1 = 4$ in a boundary layer, it is plausible that it should be only $M_1 \approx 1$ in a jet. Of course, the insensitivity to density ratio implies that Morkovin's hypothesis breaks down because of the effect of <u>pressure</u> fluctuations on the turbulence $\left(\text{if } \text{rms } p \propto \rho\overline{uv}, \text{ rms } \frac{p}{p_{abs}} \propto \gamma M_\tau^2\right)$. This deserves further thought, but will cheer the people who are interested in large density ratios at low speeds.

STATISTICAL TURBULENCE THEORY AND TURBULENCE PHENOMENOLOGY

By J. R. Herring
National Center for Atmospheric Research*

SUMMARY

The question considered here is how deductive turbulence theory can shed light on the validity of turbulence phenomenology at the level of second-order, single-point moments. Chosen for particular consideration are the phenomenological formula relating the dissipation to the turbulence energy and the Rotta-type formula for the return to isotropy. First, methods which deal directly with most or all of the scales of motion explicitly are reviewed briefly. The two discussed here are the spectral technique of Orszag and Patterson (ref. 1) and the subgrid scale parameterization of Smagorinsky (ref. 2) and Lilly (ref. 3). It appears that, at present, the spectral technique can deal with homogeneous turbulence with satisfactory accuracy up to a (micro) Reynolds number of 45. The virtues and faults of the subgrid scale method are briefly pointed out.

The statistical theory of turbulence is presented here as an expansion about randomness. Two concepts are involved: (1) a modeling of the turbulence as nearly multipoint Gaussian and (2) a simultaneous introduction of a generalized eddy viscosity operator. In this context, the direct interaction approximation (DIA) of Kraichnan (ref. 4) and a more recent theory, the test field model (TFM) of Kraichnan (ref. 5), are discussed briefly.

Some results obtained by using the DIA and TFM to predict the energy dissipation relation and the return to isotropy are next presented. For self-similar free decay, the theory gives an energy-dissipation relationship in qualitative agreement with the phenomenology; but the numerical coefficient appears, at large Reynolds numbers, to be about 40 percent smaller than that used, for example, by Donaldson (ref. 6). This result is considered an indication of a lack of universality of the phenomenological formula in question. For the return to isotropy, the results are in satisfactory accord with the phenomenology, but here again there are symptoms of lack of universality of the phenomenology.

Finally, it is observed that the structure of the phenomenology closely resembles, in some respects, the large Reynolds number limiting form of the DIA equations.

*The National Center for Atmospheric Research is sponsored by the National Science Foundation.

This observation is illustrated by the form of the triple moment used by Hanjalić and Launder (ref. 7), which may be obtained as a limiting form of the DIA equation for the same third-order moment.

INTRODUCTION

The past few years have seen great advances in numerical computations of turbulent flows around a variety of complicated geometrical shapes. One has to be impressed by the volume of these calculations and by their success in predicting mean velocity profiles, etc., as witnessed, for example, by the compilation of comparisons of test calculations with experiments by Reynolds (ref. 8), and as will undoubtedly be demonstrated again at the present conference. Although the general outlook engendered by these calculations is optimistic, the flourishing of empirical constants, which must be determined by appeals to experiments, is somewhat disturbing. This state of affairs should not be indefinitely tolerated; somehow, a "deductive turbulence theory," free of empiricism, can be brought to bear on these problems, and at the very least can determine the phenomenological constants for the present models. Of course, a deductive theory probably will determine much more than is now contained in the phenomenology – for example, the two-point correlation functions.

This paper will describe how statistical turbulence theory can be brought to bear on the problem of determining the parameters of turbulent flow models and how such a theory could help evaluate several of the phenomenological constants entering the treatment of homogeneous flows. The basic philosophy here is that an understanding of turbulence for relatively simple geometries will shed light on the correctness of the phenomenological equations used in the more interesting and complicated flow geometries. In developing such an approach it may be appropriate to alter (or even give up part of) the empiricism.

The word statistical is used here in the sense of statistical mechanics. Several such theories have been offered, most notably Kraichnan's direct interaction approximation (ref. 9) which will be discussed in more detail later. These theories offer closed deductive equations for the statistical parameters of the flow field (that is, the mean value of the velocity field, and the covariance). Alternatively, some procedures employ the distribution function of the velocity (Lundgren, ref. 10) or the distribution for its Fourier transform (Herring, refs. 11 and 12). The theories may be described as expansions about a type of randomness, which in some sense is supposed to be close to turbulence. Most are free of empirical parameters but make somewhat arbitrary assumptions about the statistics of the flow.

Consider some of the equations used to treat turbulent flows. (Symbols are defined in the appendix of this paper.) The equation for the mean Reynolds stress, $R_{ij} = \langle v_i v_j \rangle$, is

$$\left(\partial R_{ij}/\partial t\right) + \left(U_k \partial R_{ij}/\partial x_k\right) = -\left(R_{ik}\partial U_j/\partial x_k\right) - \left(R_{jk}\partial U_i/\partial x_k\right) - \left(\partial\langle v_i v_j v_k\rangle/\partial x_k\right)$$

$$- \left[\left(\partial\langle v_i p\rangle/\partial x_j\right) + \left(\partial\langle v_j p\rangle/\partial x_k\right)\right]$$

$$+ \underline{\left\langle p\left[\left(\partial v_i/\partial x_j\right) + \left(\partial v_j/\partial x_i\right)\right]\right\rangle}$$

$$+ \left(\partial^2 R_{ij}/\partial x_k \partial x_k\right) - \underline{2\nu\left\langle\left(\partial v_i/\partial x_k\right)\left(\partial v_j/\partial x_k\right)\right\rangle} \qquad (1)$$

Here U_i is the mean velocity field and p is the pressure field. The (constant) ambient fluid density ρ_o has been set at 1, restricting the discussion to incompressible flows. The angle brackets denote an average about the instantaneous velocity field, $\underline{v}$. Equation (1) is needed to "close" the equation for the mean velocity field U_i, which is not given here (see, for example, Reynolds, ref. 8, p. 9). Before closed equations for $\underline{U}$ and $\underline{\underline{R}}$ can be written, the third, fourth, and sixth terms on the right-hand side of equation (1) must be related back to $\underline{U}$ and $\underline{\underline{R}}$. Here attention will be restricted to the fifth and seventh terms (underlined), which alone survive for homogeneous flows. The fifth term is responsible for the return of an initially nonisotropic flow field to isotropy. It is usually modeled by an equation of the form (Rotta, ref. 13):

$$\left\langle p\left[\left(\partial v_i/\partial x_j\right) + \left(\partial v_j/\partial x_i\right)\right]\right\rangle = -C\,\frac{\epsilon}{E}\left(\langle v_i v_j\rangle - \frac{2}{3}\,\delta_{ij}E\right) \qquad (2)$$

Here $E = \frac{1}{2}R_{ii}$ is the total turbulent kinetic energy and ϵ is the energy dissipated by viscosity:

$$\epsilon = 2\nu\left\langle\left(\partial v_i/\partial x_k\right)\left(\partial v_i/\partial x_k\right)\right\rangle$$

For ϵ it is customary to take

$$\epsilon = AE^{3/2}/L \qquad (3)$$

The seventh term on the right-hand side of equation (1) is usually modeled in either of two ways:

$$2\nu\left\langle\left(\partial v_i/\partial x_k\right)\left(\partial v_j/\partial x_k\right)\right\rangle = \frac{1}{3}\,\delta_{ij}\epsilon$$

or

$$\left\langle\left(\partial v_i'/\partial x_k\right)\left(\partial v_j'/\partial x_k\right)\right\rangle \approx R_{ij}/\lambda^2$$

The first, which seems more appropriate for large Reynolds number flow, will be used here. In equation (3), L is a length scale associated with the large-scale part of the turbulence. In the following discussion, L is taken to be the longitudinal integral scale, following Batchelor (ref. 14, p. 105, Eq. 6.1.2). The quantity A is supposed to be a constant of order unity; $A = 0.707$ according to Donaldson (ref. 6). Note that equation (2) in conjunction with equation (1) (suppressing temporarily the viscous term) states that R_{ij} relaxes to its isotropic value $\frac{2}{3}\,\delta_{ij}E$ exponentially if C and the turbulence decay rate ϵ/E are constants.

The immediate goal is to see what statistical turbulence theory can reveal about the universality (or, indeed, validity) of equations (2) and (3). This question is explored for the restricted case of homogeneous flows. It is admittedly a very restricted context, but by no means an empty question, as shall be demonstrated.

The most direct method of assessing equations (2) and (3) by a turbulence theory is to set up a decay calculation to be done by the particular theory in question, march the theory's covariance equations forward in time, and compare the results of the calculation with equations (2) and (3). The generality of equation (3) could be tested by varying the initial energy spectral shape (or equivalently, the initial shape of $\left\langle \underline{v}(\underline{x},0)\,\underline{v}(\underline{x}',0)\right\rangle$), and perhaps by driving the system at low wave number to simulate the destabilizing effects of shear instability. The same procedure could be used to test equation (3), with the additional freedom of varying the degree and spectral shape of the initial anisotropy. At best, a reliable statistical theory would pin down universal values for A and C; at worst, it would reveal that A and C as defined by equations (2) and (3) are time and context dependent, so that the equations are useless as universal closure prescriptions. Even if these equations are found to be justified for homogeneous flows, there remains the problem of explaining how they could be valid (with the same values of A and C) for nonhomogeneous flows. The success of the models may be taken as some indication of the universality of the equations.

Before proceeding with this task, two methods which are capable (with a large enough computer) of answering these questions directly will be reviewed briefly. These are methods which directly integrate the Navier-Stokes equations. They will have an important role in the next few years in understanding turbulence. A comparison of their predictions at low Reynolds numbers for good statistical initial data will help select the correct statistical theory. Wind-tunnel data is not very helpful here because of the lack of statistical initial data at $t = 0$ (just after the grid bars have generated the turbulence). Moreover, the statistical theories are most easily studied if the initial state of the velocity field is random; this "statistical aspect" of the initial data cannot be matched by wind-tunnel experiments. As these methods are improved, they will replace wind-tunnel data as reliable data for low Reynolds number flow. In addition, they provide much more detail than wind-tunnel data; the numerical integrations have enormous amounts of data concerning the flow. These data can be stored on tapes, and interrogated as desired.

DIRECT INTEGRATION OF NAVIER-STOKES EQUATIONS

The simplest turbulence theory is just the Navier-Stokes equations; since most turbulence calculations are numerical anyway, no insight is lost by considering direct integration of the Navier-Stokes equations forward in time, starting from some suitable initial data (for example, data generated by random numbers). Several years ago, this approach appeared much too time consuming to be feasible. It still is not feasible for the sort of problems considered at this conference. However, for simple boundaries and for moderate Reynolds numbers $\left(R_\lambda = 30 \text{ or } 40\right)$, it is now possible to do a creditable job of treating turbulence, including all relevant scales of motion, directly by computer. Orszag and Patterson (ref. 1), using the spectral technique, have succeeded in simulating homogeneous turbulence in a periodic cubical box, with good numerical accuracy, up to a Reynolds number R_λ of 45. Their results, I believe, will soon replace wind-tunnel data in accuracy for the case of homogeneous turbulence. As mentioned, this method employed a spectral technique; the velocity field was Fourier analyzed and each Fourier mode was assigned an initial value according to a set of Gaussian random numbers. These were generated so as to yield a statistically Gaussian, homogeneous, isotropic initial spatial velocity field. They then integrated the equations of motion forward in time, allowing the dynamics to build up correlations out of the initial state of chaos. Of course, the realization of complete initial chaos (and isotropy) is limited by the finite number of degrees of freedom that can be handled by a computer. At present, Orszag and Patterson treat one time step of a $(32)^3$-mode decay calculation in 7.5 sec of CDC 7600 time, and about 100 time steps are required to evolve the system significantly.

It may appear somewhat surprising that Orszag and Patterson resort to Fourier modes in a day when finite mesh methods have all but taken over as a rapid numerical

integration technique for the Navier-Stokes equations. There are three points, however, which make their method competitive with the grid-point method, especially for problems with simple geometry. First, the estimates of derivatives made by the Fourier transform method are much superior to those made by the finite spatial grid method. Second, the finite trigonometric series approximation to the velocity field (sometimes called an infinite order approximation) converges uniformly and very rapidly to the exact solution as the order of the approximation is increased. Such convergence is not obtained for an arbitrary polynomial or piecewise-polynomial approximation to the flow field, as is, for example, used in ordinary finite mesh or finite element schemes. The third point is that the fast Fourier transform technique can be successfully implemented for this problem so as to greatly speed up the calculation (the evaluation of convolution sums). Orszag estimates that for the same given accuracy, the "Galerkin-Fourier" method is faster by a factor of 3 (for a three-dimensional cubic box of turbulence) than the Arakawa staggered mesh differencing scheme.

So far, the main use of these simulations has been to develop insight into the nature of the turbulence and to check the statistical approximations, such as the direct interaction approximation of Kraichnan, which will be discussed subsequently. One simple turbulence parameter pinned down by these calculations is the (differential) skewness, defined by

$$S = \frac{\left\langle \left(\partial v_1 / \partial x_1\right)^3 \right\rangle}{\left\langle \left(\partial v_1 / \partial x_1\right)^2 \right\rangle^{3/2}}$$

It measures the strength of nonlinear transfer in the turbulence microscale region. The simulations give a value for S of ≈ 0.47 $\left(\text{for } 20 \lessapprox R_\lambda \lessapprox 50\right)$, whereas the experimental value in this range is more nearly 0.43 (Frenkiel and Klebanoff, ref. 15).

One present problem with the wave-number spectral technique lies in the difficulty of obtaining good statistical information at low wave numbers without using a formidable number of wave-number points. The method uses a grid of equally spaced points, and in three dimensions the density of such points is proportional to k^2, so there are problems in accurately representing the large-scale features of the flow. At present, this causes difficulties in simulating free, moderate R_λ, turbulence decay if the initial energy spectrum to be simulated has too much energy at small k (that is, $E(k) \propto k$, $k \to 0$). The problem is that as the spectrum decays, the larger k regions decay out faster because

viscosity acts on them more strongly, leaving only the low k region excited at later times, and this region has poor statistics. At present no self-similar calculations (which are necessary to obtain eqs. (1) and (2)) have been done because of the problem at low wave numbers. According to Leith (ref. 16), a self-similar spectrum whose decay law is $E \propto t^{-1}$ requires $E(k) \propto k$ at small k.

Another method which should be mentioned at this point is the "subgrid scale closure approximation," to which Smagorinsky (ref. 2), Lilly (ref. 3), and Deardorff (refs. 17 and 18) have made substantial contributions. The method is really a phenomenological closure scheme, but the logistics of the approximation is such that as computers become larger the phenomenology can be phased out, leaving in the limit only the exact numerical procedure. The procedure is, very briefly, to average the Navier-Stokes equations over a cubical box of dimensions δ (δ is actually the grid size of the calculation). The dimensions of this box determine the "subgrid scale." Roughly speaking, any scale larger than δ is treated explicitly, and any scale of motion smaller than δ is not treated explicitly but is represented in the averaged equations of motion by mixing-length-type terms. More precisely, the averages of products of fluctuating terms are approximated by suitable functions of average field quantities. The particular functional forms are chosen in accordance with eddy viscosity ideas and are consistent with Kolmogoroff's inertial range assumption (the eddy coefficients are proportional to a scale length δ and to the dissipation rate only). The logic of the procedure implies that the scale size δ is at least as small as the scale sizes in the inertial range. Hence, in using this method, one must be prepared to treat explicitly all scale sizes larger than the scales in the inertial range. As mentioned, the method does contain an empirical constant, but Lilly has shown how it is related in a simple way to Kolmogoroff's constant. The procedure has been applied successfully to thermal convection and shear flow by Deardorff (refs. 17 and 18).

More recently, Lilly (ref. 3) has made an analogous closure for third-order moments. The idea here is to again form averages of the equations of motion over the grid size δ. Now, however, instead of relating the averaged Reynolds stresses to mean gradients, equations of motion for the Reynolds stresses themselves are sought by suitable manipulation of the equations of motion. In this way a relationship is obtained between the time derivatives of the Reynolds stresses and their local sources and sinks which include the averaged triple moments. The latter are then "approximated" by mixing-length-like terms involving the mean gradients of the velocity field and the Reynolds stresses themselves.

The equations obtained this way for the subgrid scale parameterization are very similar to those obtained from other closure procedures (cf. Hanjalić and Launder, ref. 7) with the obvious difference in interpreting and computing the mean fields.

One virtue of the subgrid scale method not possessed by methods parameterizing all scales of motion is that a parameterization of only those scales much smaller than the energy-containing range give the theory a universality not possessed by the other methods. For example, it is hard to accept that $L\epsilon/E^{3/2}$ is the same for any type of flow, regardless of how the turbulence is generated, if E and L pertain to the energy-containing region. One has much less difficulty here if the scales and energy involved are in the inertial range.

Another virtue of the method is its ability to assess its own accuracy. If the actual explicitly treated flux of momentum, for example, turns out to be much larger than that estimated by the subgrid scale closure procedure, the total flux calculation may safely be considered accurate, regardless of the accuracy of the subgrid scale procedure. Deardorff (ref. 18) has found this to be essentially the case for a calculation of a buoyantly active shear layer at heights greater than one or two δ.

One difficulty with this approach, appreciated by Fox and Lilly (ref. 19), is that there appears to be no strictly deductive way whereby scales of motion less than a certain scale size may be treated as statistical and scales larger than this size may be treated deterministically. Because of the nonlinearity of the Navier-Stokes equations, small-scale uncertainties will in time penetrate the large-scale region, thereby contradicting the logical framework of the theory. This difficulty may be cast in terms of statistical turbulence theory by considering a statistical initial value problem in which scales larger than δ are identical from ensemble member to ensemble member but scale sizes less than δ are known only statistically (varying in amplitude and phase from ensemble member to ensemble member). This initial specification corresponds to the logical framework of the "subgrid scale" closure approximation. As time passes, however, destabilizing nonlinear terms in the equations of motion cause the scale sizes larger than δ to be contaminated with that uncertainty initially residing at scale less than δ. This mixing transforms the initial "mean" (or certain) field into an eventual "fluctuation" (or uncertain) field. Of course, the closure procedure takes no cognizance of this fact, and therein lies a problem in calculations of the evolution of a flow. As long as the errors do not penetrate the large-scale energy-containing region, it may safely be assumed that the predicted values of these large scales are correct. However, once the errors penetrate the large-scale region, the solutions of the subgrid scale procedure must be interpreted as a "typical" flow field, and the logical connection with the initial flow field is obscure. It is of some interest in this connection to have estimates of error-growth time scales.

A theory for error growth has recently been developed by Leith and Kraichnan (ref. 20). These investigators use the "test-field approximation," which is a type of statistical approximation that will be discussed subsequently. Their conclusion is that

errors initially confined to infinitely small scales grow and saturate a region of scale sizes δ within a time $\approx 9.5\epsilon^{-1/3}\delta^{2/3}$, which is 11 times the eddy circulation time for length scales δ. Their analysis was limited to the limit of infinite Reynolds number and to δ in the inertial range. Whether or not the errors grow until they penetrate the energy-containing range is not yet known, although if δ is initially sufficiently large, there seems little doubt that the energy region would be contaminated by error.

STATISTICAL TURBULENCE THEORY

The original objective of applying statistical turbulence theory to the practical problems of determining turbulence parameters is pursued next. The physical content of several of the theories is discussed briefly, but the equations are not derived. As mentioned in the introduction, these theories are pivoted on the idea that turbulence is, in some sense, close to a state of randomness. "Completely random" would mean, here, that the averages of products of the velocity field at different space-time points $y = (\tilde{y},t)$ are joint normal. (A space-time point is indicated by y, the spatial components by $\tilde{y}$, and the time component by t.) For the third- and fourth-order moments, in particular,

$$\left.\begin{aligned}
\left\langle v_i(y_1)v_j(y_2)v_k(y_3)\right\rangle &= \left\langle v_i(y_1)\right\rangle\left\langle v_j(y_2)v_k(y_3)\right\rangle + \left\langle v_i(y_1)v_j(y_2)\right\rangle\left\langle v_k(y_3)\right\rangle \\
&\quad + \left\langle v_i(y_1)v_k(y_3)\right\rangle\left\langle v_j(y_2)\right\rangle \\
\left\langle v_i(y_1)v_j(y_2)v_k(y_3)v_\ell(y_4)\right\rangle &= \left\langle v_i(y_1)v_j(y_2)\right\rangle\left\langle v_k(y_3)v_\ell(y_4)\right\rangle + \cdots \\
&\quad + \left\langle v_i(y_1)\right\rangle\left\langle v_j(y_2)v_k(y_3)v_\ell(y_4)\right\rangle + \cdots
\end{aligned}\right\} \tag{4}$$

where the dots indicate omitted terms in which the indices 1, 2, 3, and 4 are permuted. Here the property of randomness is expressed in terms of two-point (and three-point) functions like $\langle v_i(y)v_j(y')\rangle$, which are more general covariances than those used in equation (1). For deductive turbulence theories the two-point correlation functions are indispensable. It is noted, in this connection, that the problem of viscous decay (flow at very low Reynolds number) is closed with respect to the two-point functions $R_{ij}(x,x',t) = \langle v_i(\underline{x},t)v_j(\underline{x}',t)\rangle$ but not with respect to the single-point function $R_{ij}(x,x,t)$; hence the need for the two-point functions at the very least.

The hypothetical consequences of complete randomness for the Navier-Stokes equations are examined now. These equations are written in a compact notation (summation convention understood):

$$\mathcal{L}^{o}_{in}(y)u_n(y) = P_{ij}\left(\tilde{y}\right)\frac{\partial}{\partial \tilde{y}_l}\left(u_l u_j - \left\langle u_l u_j \right\rangle\right) \tag{5}$$

where the operator $\mathcal{L}^{o}$ is

$$\mathcal{L}^{o}_{in} \equiv \delta_{in}\left(\frac{\partial}{\partial t} - \nu\nabla^2_{\tilde{y}}\right) - P_{in}\left(\tilde{y}\right)U_l(y)\frac{\partial}{\partial \tilde{y}_l} - P_{ij}\left(\tilde{y}\right)\frac{\partial}{\partial \tilde{y}_n}U_j$$

and the operator $P_{ij}\left(\tilde{y}\right)$ is specified by

$$\nabla^2_{\tilde{y}}P_{ij}\left(\tilde{y}\right) = \delta_{ij} - \frac{\partial^2}{\partial \tilde{y}_i \partial \tilde{y}_j}$$

Here, $\underline{u}$ is the departure of $\underline{v}$ from its ensemble mean, $\underline{U} = \langle \underline{v} \rangle$. To obtain P_{ij} Poisson's equation must be inverted for the boundary conditions appropriate to the problem at hand (a cubic box of homogeneous turbulence). The operator $P\left(\tilde{y}\right)$ simply suppresses the compressible part of $\left(\underline{v} \cdot \nabla\right)\underline{v}$, so that $\nabla \cdot \underline{v}\left(\underline{x},t\right) = 0$, and results from an elimination of the pressure term from the equations of motion.

In equation (5) the terms which give rise to the closure problem are isolated on the right-hand side. These are the terms that may build up multipoint non-joint-normal correlations out of multipoint normal initial data. That is to say, relations (4) are consistent with the Navier-Stokes equations if the right-hand side of equation (5) is suppressed. The simplest nontrivial closure procedure is to discard the right-hand side of equation (5) entirely. Such a theory, sometimes called the quasi-linear or mean-field theory (also called by Deissler "weak turbulence" approximation in ref. 21), has met with some success for thermal convection (Herring, refs. 22 and 23). It has also been applied to shear flows by Deissler (ref. 21).

First the assumption of complete randomness, as embodied by equations (4), is tried on equation (5). Closed equations for $\left\langle u_i(y)u_j(y')\right\rangle$ are then obtained simply by multiplying equation (5) evaluated at y by itself at y'. The result is

$$\mathcal{L}^{o}_{in}(y)\mathcal{L}^{o}_{i'n'}(y')\left\langle u_n(y)u_{n'}(y')\right\rangle = P_{ij}\left(\tilde{y}\right)P_{i'j'}\left(\tilde{y}'\right)\frac{\partial^2}{\partial\tilde{y}_l\partial\tilde{y}'_{l'}}\left[\left\langle u_l(y)u_{l'}(y')\right\rangle\left\langle u_j(y)u_{j'}(y')\right\rangle\right.$$

$$\left. + \left\langle u_l(y)u_{j'}(y')\right\rangle\left\langle u_j(y)u_{l'}(y')\right\rangle\right]$$

$$\equiv F_{ii'}(y,y') \tag{6a}$$

It is convenient to rewrite equation (6a) as a first-order equation in time by multiplying it by $\left(\mathcal{L}^{o}\right)^{-1}(y)$, with the result

$$\mathcal{L}^{o}_{in}(y)\left\langle u_n(y)u_{n'}(y)\right\rangle = \int G^{o}_{n'i'}(y',z)dz\, F_{ii'}(y,z) \tag{6b}$$

where

$$\tilde{\mathcal{L}}^{o}_{in}(y)G^{o}_{np}(y,y') = P_{ip}\left(\tilde{y}\right)\delta(y - y')$$

Here, $\tilde{\mathcal{L}}$ is the adjoint of $\mathcal{L}$.

The dz-integration here is over all the spatial part of z, but the time integration extends only over the past up to the time argument of y',t'. It is recalled here that basic interest is in the simultaneous moments, $\left\langle v_i(y)v_j(y)\right\rangle$. An equation of motion for these may be obtained from equation (6b) by forming the limit,

$$\lim_{y\to y'}\left[\mathcal{L}^{o}_{in}(y)\left\langle u_n(y')u_i(y)\right\rangle + \mathcal{L}^{o}_{in}(y')\left\langle u_n(y')u_i(y)\right\rangle\right] \equiv N(y) \tag{7}$$

There is a fundamental difficulty with equations (6a) and (6b); namely, they do not conserve kinetic energy (for closed systems $N \neq 0$). This difficulty stems from the fact that the "turbulence force" $P\left(\underline{v}\cdot\nabla\right)\underline{v}$ has been assumed to be a completely random stirring force, and random forces are known to increase the kinetic energy of systems to which they are applied. Hence, the assumption of complete randomness must be abandoned.

The statistical theories modify $\mathcal{L}^o(y)$ used in equations (6a) and (6b) to a new operator $\mathcal{L}(y)$ so as to restore energy conservation. The modification consists of including on the left-hand side of equations (6) a generalized eddy viscosity term so as to make $N = 0$ for closed systems. Formally, $\mathcal{L}^o(y)$ is replaced by $\mathcal{L}(y)$, and $G^o(y,z)$ $\left(\equiv(\mathcal{L}^o)^{-1}\right)$ by $G(y,z)$ $\left(\equiv\mathcal{L}^{-1}\right)$. The modified equations are

$$\mathcal{L} = \mathcal{L}^o + \eta$$

$$\mathcal{L}^o_{in}(y)\left\langle u_n(y)u_{n'}(y')\right\rangle + \int \eta_{in}(y,z)dz\left\langle u_n(z)u_{n'}(y')\right\rangle = \int G_{n'j}(y',z)dz\, F_{ij}(y,z) \qquad (8a)$$

where $F_{ij}(y,z)$ is defined by equation (6a). The operator $\eta(y,z)$ is defined by

$$\frac{1}{2}\eta_{in}(y,z) = -P_{ij}(y)\frac{\partial}{\partial\tilde{y}_l}P_{pn}(z)\frac{\partial}{\partial\tilde{z}_s}G_{lp}(y,z)\left\langle u_s(z)u_j(y)\right\rangle$$

$$- P_{ij}(y)\frac{\partial}{\partial\tilde{y}_l}P_{ps}(z)\frac{\partial}{\partial\tilde{z}_n}G_{lp}(y,z)\left\langle u_s(z)u_j(y)\right\rangle \qquad (8b)$$

The new term on the left-hand side of equation (8a) cancels the right-hand side upon forming the equation for the total energy, $N = 0$.

Equations (8a) and (8b) constitute a complete statistical theory for the two-point convariances $\left\langle \underline{v}(y)\underline{v}(y')\right\rangle$. The ingredients embodied in it are: (1) the modeling of the turbulence force $P(\tilde{y})(\underline{v}\cdot\nabla)\underline{v}$ as Gaussian-multivariate and (2) the simultaneous introduction of a generalized eddy viscosity operator $\eta(y,z)$, so that energy is conserved within the context of the Gaussian assumption. The type of "modeling" done here involves a qualitative characterization of the statistics of the flow rather than any explicit quantitative assumption about relationships between the various terms in the theory.

Still to be specified is $G(y,z)$. On this point the theories differ. Generally $G(y,z)$ specifies the mechanisms whereby the flow at different space-time points becomes decorrelated and decays away under the joint action of viscosity and turbulence. At very low Reynolds numbers G is expected to be entirely viscous, so that

$$\mathcal{L}^o_{in}(y)G_{nj}(y,y') = P_{ij}(\tilde{y})\delta(y - y') \qquad \left(R_\lambda \to 0\right) \qquad (9a)$$

At larger Reynolds numbers the turbulence itself contributes an eddy viscosity, so that in the determination of $G(y,z)$ the generalized eddy viscosity operator $\eta(y,z)$ is included:

$$\tilde{\mathcal{L}}^{o}_{in}(y)G_{nj}(y,y') + \int \eta_{in}(y,z)dz\, G_{nj}(z,y') = P_{ij}(\tilde{y})\delta(y - y') \tag{9b}$$

The choice of equation (9a) is sometimes called the "two-time quasi-normal approximation," and is sensible only at very small Reynolds numbers $(R_\lambda \leqq 10)$. The choice of equation (9b) together with equation (8a) constitutes the direct interaction approximation (Kraichnan, ref. 4). Note that equation (9b) lapses over into equation (9a) for small Reynolds number flow.

Another approach in determining $G(y,y')$ is to select the most appropriate physical mechanism responsible for producing decorrelation, work out the corresponding G-function, and use it in equations (8a) and (8b). Such a procedure was used by Kraichnan (ref. 5) in deriving the test-field model, a theory which uses a G-function that incorporates "pressure scrambling" and viscous effects alone. The test-field model also makes the more severe approximation of modeling the turbulence force on white noise, which is a simplification introduced to avoid the time-history integrals in equations (8a) and (8b). Yet another method (to my knowledge yet untried) is to base G on the evolution of a pair of particles whose relative position at $t = t'$ is $\tilde{y} - \tilde{y}'$.

At this point the objection may be raised that the comments of the last paragraph have introduced an arbitrariness into the theory, which was to be avoided. Expressed differently, why worry about specific physical mechanisms for decorrelating the flow, if the DIA is a complete theory. The answer is that the DIA, though complete, cannot be correct at large Reynolds numbers because it does not behave properly under <u>random</u> uniform velocity translation (Kraichnan, ref. 24). As a consequence, it does not have a proper inertial range $\left(E(k) \propto k^{-3/2}\right.$ instead of $\left.E(k) \propto k^{-5/3}\right)$. On the other hand, the two mechanisms mentioned above do produce a properly invariant theory.

The arbitrariness alluded to in discussing the test-field model is just the (arbitrarily assumed) strength parameter which couples the "test field" to the actual velocity field. The (statistical) deviation of this (compressive) test field from the actual velocity field measures the decorrelation effects expressed by g. This theory, with a single adjustable parameter, is capable of treating nonisotropic and nonhomogeneous flows.

The accuracy of the direct interaction and test-field models has recently been assessed by comparing their predictions with the Orszag-Patterson type of simulations at low to moderate Reynolds numbers (Herring and Kraichnan, ref. 25). These comparisons were made for homogeneous and isotropic flow fields with $R_\lambda \leqq 50$. A detailed

comparison was made for the Fourier transform of the two-point function $R_{ij}(\underline{x},\underline{x}',t)$, as well as for the total energy decay and skewness. The direct interaction approximation gave entirely satisfactory results for all the above spectra, including the dissipation and energy transfer spectra. The test-field model gave satisfactory results for all the above spectra if the parameter mentioned previously was adjusted so that the predicted and simulated skewness agreed. At much larger R the test-field model with the same parameter gave the Kolmogoroff spectrum, with the Kolmogoroff constant $C = 1.8$.

COMPARISON OF STATISTICAL THEORY WITH PARAMETERIZED EQUATIONS

Assuming that they are valid, what do these theories indicate about the universality of equations (2) and (3)? Consider first equation (3), which may be examined within the context of homogeneous, isotropic flows. On general grounds, an equation like (3) can be expected if the decay is self-similar; that is, if

$$\left\langle v_i(\underline{x}',t)v_j(\underline{x}'-\underline{x},t)\right\rangle \equiv R_{ij}(\underline{x},t) = \text{Function of } (x/\lambda, x'/\lambda, t)$$

where λ is the Taylor microscale. Equivalently, the energy spectrum $E(k)$, defined to be the Fourier transform of R_{ii} with respect to $\underline{x} - \underline{x}'$, should be of the form $F(k\lambda,t)$ for k in both the energy containing range and the dissipation range. Figure 1 shows $\epsilon L/E^{3/2}$ as a function of t for such a self-similar calculation. Here the initial energy spectrum is that found experimentally by Ling and Huang (ref. 26). The theory, incidentally, does not confirm that this initial spectrum is self-similar during the decay; the spectrum predicted by the theory is a good deal more peaked (especially at large R_λ) than this. The final asymptotic values of R_λ label the curves. In all cases studied, it was found that $R_\lambda(t)$ became independent of t for $t \geqq 1$ and that the $E(k)$, $k^2E(k)$, and energy transfer spectrum became self-similar. (Note that $E(k\lambda(t))/E_0\lambda(t)$ is a universal function of R_λ and $k\lambda$.) For a given initial R_λ, $A = \epsilon L/E^{3/2}$ becomes very nearly constant at large t, but the value of A appears to be a function of R_λ. At the larger values of R_λ, $A \leqq 0.5$ is indicated. This may be compared to the value $A = 0.7$ (Donaldson, ref. 6), used in the phenomenological approach.

The difference ($\approx$40 percent) between the computed value of A and the phenomenological value of $\approx$0.7 probably indicates the kind of departure from universality to be expected in using the phenomenological approach. The lack of universality in the value of A probably is due to the lack of universality in the spectral shape of $E(k)$ in the energy containing region.

Consider next equation (2) for the deviation of R_{ij} from its isotropic value, $2E\delta_{ij}/3$. The statistical theories may also be applied to this case. To solve this problem requires an order of magnitude more work than the homogeneous isotropic problem, even for the homogeneous case. This is because the energy-correlation function must be specified at all angles. The simplest way to do this is to assume that departures from isotropy may be parameterized by $E_1(k)$ and $E_2(k)$, where E_1 and E_2 are the energy perpendicular and parallel to the axis of symmetry. The departure from isotropy is then represented simply by $\Delta = E_1 - E_2$, and the phenomenology of equation (2) is

$$d\Delta/dt = -C(E/\epsilon)\Delta$$

where

$$\Delta = \int_0^\infty \Delta(k)dk$$

An application of the DIA theory to homogeneous, axisymmetric turbulence has been completed, the details of which will be published elsewhere. Only those points bearing on the phenomenology (that is, eq. (2)) are reported here.

In general, the DIA theory gives equations for $d\Delta(k)/dt$ and $dE(k)/dt \equiv \frac{d}{dt}\left(E_1(k) + E_2(k)\right)$, which quadratically couple $\Delta(k)$ and $E(k)$ for all wave numbers k with the corresponding G-functions. A careful examination of these equations, which are similar to the Fourier transform of equations (7) and (8), shows that the equation for $\Delta(k)$ is nearly linear. This result is, a priori, somewhat surprising since terms contributing to $d\Delta(k)/dt$ proportional to $\Delta(p)\Delta\left(\underline{k}-\underline{p}\right)$ are not easily seen to be small. This result tends to lend credence to equation (2). A particularly simple equation results if the energy and $\Delta(k)$ spectrum may be regarded as very sharp $\left(E(k)\right.$ and $\left.\Delta(k) \propto \delta\left(k - k_0\right)\right)$ and if "memory effects" are neglected. In this case,

$$d\Delta(k,t)/dt = -2\eta(k)\Delta(k)$$

For the case in which $E(k)$ is sharply peaked about k_0, it may be shown, under the restrictions stated above, that

$$L = \frac{3\pi}{4k_0} \qquad \eta\left(k_0\right) = \frac{0.858E_0{}^{1/2}}{L}$$

which gives

$$d\Delta/dt = \frac{-1.71E^{1/2}\Delta}{L} \tag{10}$$

where η is the eddy viscosity coefficient, which is just the "Fourier representative" of the operator $\eta(y,z)$ as given by equation (8b).

Equation (10) should not be taken too seriously, especially in view of the rather restrictive assumptions involved in its derivation. It is, nevertheless, an equation agreeing with the phenomenology as to type and order of magnitude and originating in a deductive theory.

Of course, for a particular initial value problem it is possible to do much better than equation (10) by constructing numerical solutions for the direct interaction approximation. Such results are presented in figure 2. This shows $C = (E/\epsilon)\left(d \ln|E_1 - E_2|/dt\right)$ as a function of t for the case $E_1(k) = \frac{2\pi k^2 \exp(-2k)}{k + 0.5}$, $E_2(k) = 0$, initially, and $R_\lambda(0) = 47.6$. It can be seen that C levels off for the later stages of decay, and then begins to decrease slowly. The initial value of this spectrum was chosen because for isotropic turbulence at the same value of R_λ, the decay of $E(k)$ appeared to be self-similar. The values of $C(t)$ appear consistent with Rotta's suggested value (ref. 27). This comparison should not, however, lead to any generalizations since different initial spectral shapes give somewhat different values for C and since the computed values here are not strictly constant. For example, if the deviation of E_1 from E_2 is made more pronounced at larger k than in the above example, larger values of C result.

So far in confronting statistical theory with phenomenology, certain terms contributing to the evolution of the Reynolds stress have been dealt with in isolation, and only for homogeneous flows. Although such calculations are instructive, they can hardly be thought adequate to deal with shear flow in which mean fields $\underline{U}$ as well as boundaries are present. In my opinion, it will be a few (2 or 3) years before direct computation using the DIA on simple geometries at very large Reynolds numbers will be done. David Leslie, in his forthcoming book "Developments in the Theory of Turbulence," estimates that it would take about 10 man-years to program DIA equations like equations (8a) and (8b) to deal realistically with large R_λ shear flows. I think this estimate is a bit pessimistic, but of the correct order of magnitude.

An alternate to a frontal attack is to try to simplify the DIA equations analytically, using asymptotic functional forms appropriate to large Reynolds numbers, and perhaps large distances from boundaries. Some progress that has already been made in this direction by Leslie (ref. 28) is described in detail in Chapter 15 of his book cited above. Perhaps the severe analytic complexities of the DIA can be in some sense reduced so as to approach the complication level of phenomenological theories discussed at this conference. Consider, for example, the triple moment term in equation (2). Hanjalić and Launder (ref. 7) approximate this term by

$$\left\langle u_m(y)u_l(y)u_j(y)\right\rangle = c_s \frac{E}{\epsilon}\left(R_{js}\frac{\partial}{\partial \tilde{y}_s}R_{lm} + R_{ls}\frac{\partial}{\partial \tilde{y}_s}R_{jm} + R_{ms}\frac{\partial}{\partial \tilde{y}_s}R_{lj}\right) \tag{11}$$

where

$$R_{ij} = \left\langle u_i(y)u_j(y)\right\rangle$$

The DIA equation for equation (11) is

$$\begin{aligned}\left\langle u_m(y)u_l(y)u_j(y)\right\rangle = \lim_{y'\to y}\int dz\Bigg\{ & G_{mp}(y',z)P_{pr}(z)\frac{\partial}{\partial z_s}\left[R_{lr}(y,z)R_{js}(y,z) + R_{ls}(y,z)R_{js}(y,z)\right] \\ & + G_{lp}(y,z)P_{pr}(z)\frac{\partial}{\partial z_s}\left[R_{ms}(y,z)R_{rj}(z,y) + R_{mr}(y,z)R_{sj}(z,y)\right] \\ & + G_{jp}(y,z)P_{pr}(z)\frac{\partial}{\partial z_s}\left[R_{mr}(y',z)R_{ls}(y',z) + R_{ms}(y',z)R_{lr}(y,z)\right]\Bigg\}\end{aligned} \tag{12}$$

Equation (12) reduces to equation (11) if (arbitrarily)

$$G_{ij}(y,y') = \frac{1}{2}c_s\frac{E}{\epsilon}\delta(t-t')\delta\left(\tilde{y}-\tilde{y}'\right)\delta_{ij}$$

$$P_{ij} = \delta_{ij}$$

No claim is made here that these expressions for G and P become valid at very large Reynolds numbers and far from boundaries. In fact, quite the contrary is suggested by

an examination of the G-equation. However, perhaps an examination of the complete equations (8a) and (8b), along lines begun by Leslie (ref. 28), will show whether anything close to these can be valid or, better yet, will suggest how to improve equation (11), especially near boundaries and at moderate Reynolds numbers. One point that is clear from even a cursory examination of equations (11) and (12) is that equation (12) is nonlocal in both space and time, whereas equation (11) is not.

Of course the preceding discussion presumes that the statistical theory discussed here is valid. On this point, the reader may examine the comparison of theory with simulation (for isotropic flow) by Herring and Kraichnan (ref. 25) and judge for himself. It is hoped that a more detailed comparison of theory with computer experiment for more general types of flow will soon tell whether this type of theory is on the right track.

LIMITATIONS OF THEORY

In closing, some of the limitations and defects of the statistical moment theory discussed here will be pointed out. First, there are limitations connected with the fact that the theory is statistical. In comparing theory with experiment, this leads to problems of how to specify initial data. Suppose, for example, the decay of turbulence generated by a wind-tunnel grid is to be predicted. The two-point velocity correlation just behind the grid bars can be measured, and from this data an energy spectrum can be obtained which the statistical theory uses as $E(k,0)$. However, the use of this spectrum alone as initial data in the statistical theory cannot produce the observed subsequent decay even if the theory used is exact. This is because the experiment (or, ideally, an ensemble of experiments) has higher order (statistical) correlations built up at the initial time, whereas the theory presumes these to be zero. Therefore, if only the energy spectrum can be specified initially, the theory can be expected to deviate from experiment while the higher order moments in the statistical theory are being built up from zero. The theory could be worked out for specified initial values for higher order moments, but I do not know that these are measurable. The same dilemma may also afflict the phenomenological theories also in connecting the mean velocity and Reynolds stresses to the "preturbulent state."

That the DIA does not give the proper inertial range has already been mentioned. It is not known, however, how serious this is with regard to the behavior of the single-point Reynolds stresses, even at large Reynolds numbers. In this connection, it may be shown – under rather weak assumptions – that an equation like equation (3) is obtained for the DIA at large R_λ. The value of A has, however, not been computed. In any case the test-field model could be used, but it is a less complete theory than the DIA. Alternatively, there is the Lagrangian history direct interaction theory (Kraichnan, ref. 9), which com-

pares very well indeed with large Reynolds number flows; but this is a very complicated theory, whose logical foundations, in my opinion, are not as secure as those of the DIA.

Finally, there are problems for which the statistical-moment approach discussed here is not very profitable; that is, extremely intermittent flows consisting of very small regions of intense shear separated by quiescent volumes. In this case, the statistical moment theory requires a specification of very high order moments to adequately describe the physics of the problem. Hence, closure at low order moments would be inappropriate.

APPENDIX

DEFINITIONS OF SYMBOLS

A	empirical constant relating energy integral scale and energy dissipation (see eq. (3))
C	constant
c_s	triple moment constant introduced by Hanjalić and Launder (ref. 7, eq. (2.3))
E	total turbulent kinetic energy, $\frac{1}{2}\langle u^2 \rangle$
F_{ij}	turbulent functional defined in equation (6a)
G	Green's function which includes eddy viscosity effects (see eq. (9b))
G^o	Green's function which does not include eddy viscosity effects (see eq. (6b))
g	dimensionless scaling parameter entering test field model (see ref. 25 for further details)
k	wave number
L	longitudinal integral scale
$\mathcal{L} = \mathcal{L}^o + \eta$	
$\mathcal{L}^o$	operator (see eq. (5))
N	defined by equation (7)
P	pressure "projection" operator, defined just after equation (5)
p	pressure field
$\underline{\underline{R}}$	ensemble mean Reynolds stress tensor
R_{ij}	ensemble mean Reynolds stress tensor components

R_λ Taylor microscale Reynolds number

s differential skewness, $\dfrac{\left\langle \left(\partial v_1/\partial x_1\right)^3 \right\rangle}{\left\langle \left(\partial v_1/\partial x_1\right)^2 \right\rangle^{3/2}}$

t time

U_i ith component of ensemble mean velocity field $\underline{U}$

$\underline{U}$ ensemble mean velocity field

$\underline{u}$ deviation of velocity field from its ensemble mean

$\underline{v}$ instantaneous velocity field vector

$\underline{x}$ vector coordinate

y space-time point $(\tilde{y},t)$

$\tilde{y}$ three-vector part of space-time point y

z space-time point $(\tilde{z},t)$

$\tilde{z}$ three-vector part of space-time point z

$\Delta(k)$ deviation from isotropy spectrum, $\equiv 2\pi k^2 \left\langle \left|u_3(\underline{k},t)\right|^2 - \left|u_1(\underline{k},t)\right|^2 \right\rangle$

$\Delta = \int_0^\infty \Delta(k)dk$

δ grid-scale length in subgrid-scale method

δ_{ij} Kronecker delta (= 0 if $i \neq j$; = 1 if $i = j$)

$\delta(y - y')$ Dirac δ-function

ϵ energy dissipation rate, $\equiv -2\nu \left\langle v_i \nabla^2 v_i \right\rangle$

η	eddy viscosity operator (see eq. (8b))
λ	Taylor microscale
ν	kinematic viscosity coefficient
ρ_o	constant fluid density, set equal to 1
'	used to distinguish one space point from another
$\langle\ \rangle$	indicates ensemble mean

Subscripts:

i,j,k,l, m,n,p,s	vector indices (= 1, 2, 3); summation convention holds, unless otherwise stated

REFERENCES

1. Orszag, Steven A.; and Patterson, G. S., Jr.: Numerical Simulation of Turbulence. Statistical Models and Turbulence, Vol. 12 of Lecture Notes in Physics, M. Rosenblatt and C. Van Atta, eds., Springer-Verlag, 1972, pp. 127-147.

2. Smagorinsky, J.: General Circulation Experiments With the Primitive Equations, Pt. 1, The Basic Experiment. Mon. Weather Rev., vol. 91, no. 3, Mar. 1963, pp. 99-164.

3. Lilly, D. K.: The Representation of Small-Scale Turbulence in Numerical Simulation Experiments. Proceedings of the IBM Scientific Computing Symposium on Environmental Sciences, Nov. 1967, pp. 195-210.

4. Kraichnan, Robert H.: The Structure of Isotropic Turbulence at Very High Reynolds Numbers. J. Fluid Mech., vol. 5, pt. 4, May 1959, pp. 497-543.

5. Kraichnan, Robert H.: An Almost-Markovian Galilean-Invariant Turbulence Model. J. Fluid Mech., vol. 47, pt. 3, June 14, 1971, pp. 513-524.

6. Donaldson, Coleman duP.: Calculation of Turbulent Shear Flows for Atmospheric and Vortex Motions. AIAA J., vol. 10, no. 1, Jan. 1972, pp. 4-12.

7. Hanjalić, K.; and Launder, B. E.: A Reynolds Stress Model of Turbulence and Its Application to Thin Shear Flows. J. Fluid Mech., vol. 52, pt. 4, Apr. 25, 1972, pp. 609-638.

8. Reynolds, W. C.: Computation of Turbulent Flows – State-of-the-Art, 1970. Rep. MD-27 (Grants NSF-GK-10034 and NASA NgR-05-020-420), Dep. Mech. Eng., Stanford Univ., Oct. 1970. (Available as NASA CR-128372.)

9. Kraichnan, Robert H.: Direct-Interaction Approximation for Shear and Thermally Driven Turbulence. Phys. Fluids, vol. 7, no. 7, July 1964, pp. 1048-1062.

10. Lundgren, T. S.: A Closure Hypothesis for the Hierarchy of Equations for Turbulent Probability Distribution Functions. Statistical Models and Turbulence, Vol. 12 of Lecture Notes in Physics, M. Rosenblatt and C. Van Atta, eds., Springer-Verlag, 1972, pp. 70-100.

11. Herring, J. R.: Self-Consistent-Field Approach to Turbulence Theory. Phys. Fluids, vol. 8, no. 12, Dec. 1965, pp. 2219-2225.

12. Herring, J. R.: Self-Consistent-Field Approach to Nonstationary Turbulence. Phys. Fluids, vol. 9, no. 11, Nov. 1966, pp. 2106-2110.

13. Rotta, J.: Statistische Theorie nichthomogener Turbulenz. 1. Mitteilung. Z. Phys., Bd. 129, 1951, pp. 547-572.

14. Batchelor, G. K.: The Theory of Homogeneous Turbulence. Cambridge Univ. Press, 1959.

15. Frenkiel, François N.; and Klebanoff, Philip S.: Statistical Properties of Velocity Derivatives in a Turbulent Field. J. Fluid Mech., vol. 48, pt. 1, July 13, 1971, pp. 183-208.

16. Leith, C. E.: Diffusion Approximation to Inertial Energy Transfer in Isotropic Turbulence. Phys. Fluids, vol. 10, no. 7, July 1967, pp. 1409-1416.

17. Deardorff, James W.: A Numerical Study of Three-Dimensional Turbulent Channel Flow at Large Reynolds Numbers. J. Fluid Mech., vol. 41, pt. 2, Apr. 1970, pp. 453-480.

18. Deardorff, J. W.: A Three-Dimensional Numerical Investigation of the Idealized Planetary Boundary Layer. Geophys. Fluid Dyn., vol. I, no. 4, Nov. 1970, pp. 377-410.

19. Fox, Douglas G.; and Lilly, Douglas K.: Numerical Simulation of Turbulent Flows. Rev. Geophys. & Space Phys., vol. 10, no. 1, Feb. 1972, pp. 51-72.

20. Leith, C. E.; and Kraichnan, R. H.: Predictability of Turbulent Flows. J. Atmos. Sci., vol. 29, no. 6, Sept. 1972, pp. 1041-1058.

21. Deissler, Robert G.: Problem of Steady-State Shear-Flow Turbulence. Phys. Fluids, vol. 8, no. 3, Mar. 1965, pp. 391-398.

22. Herring, J. R.: Investigation of Problems in Thermal Convection. J. Atmos. Sci., vol. 20, no. 4, July 1963, pp. 325-338.

23. Herring, J. R.: Investigation of Problems in Thermal Convection: Rigid Boundaries. J. Atmos. Sci., vol. 21, no. 3, May 1964, pp. 277-290.

24. Kraichnan, Robert H.: Lagrangian-History Closure Approximation for Turbulence. Phys. Fluids, vol. 8, no. 4, Apr. 1965, pp. 575-598.

25. Herring, Jackson R.; and Kraichnan, Robert H.: Comparison of Some Approximations for Isotropic Turbulence. Statistical Models and Turbulence, Vol. 12 of Lecture Notes in Physics, M. Rosenblatt and C. Van Atta, eds., Springer-Verlag, 1972, pp. 148-194.

26. Ling, S. C.; and Huang, T. T.: Decay of Weak Turbulence. Phys. Fluids, vol. 13, no. 12, Dec. 1970, pp. 2912-2924.

27. Rotta, J. C.: Turbulent Boundary Layers in Incompressible Flow. Boundary Layer Problems. Vol. 2 of Progress in Aeronautical Sciences, Antonio Ferri, D. Küchemann, and L. H. G. Sterne, eds., Macmillan Co., c.1962, pp. 1-219.

28. Leslie, D. C.: Simplification of the Direct Interaction Equations for Turbulent Shear Flow. J. Phys. A: Gen. Phys., vol. 3, no. 3, May 1970, pp. L16-L18.

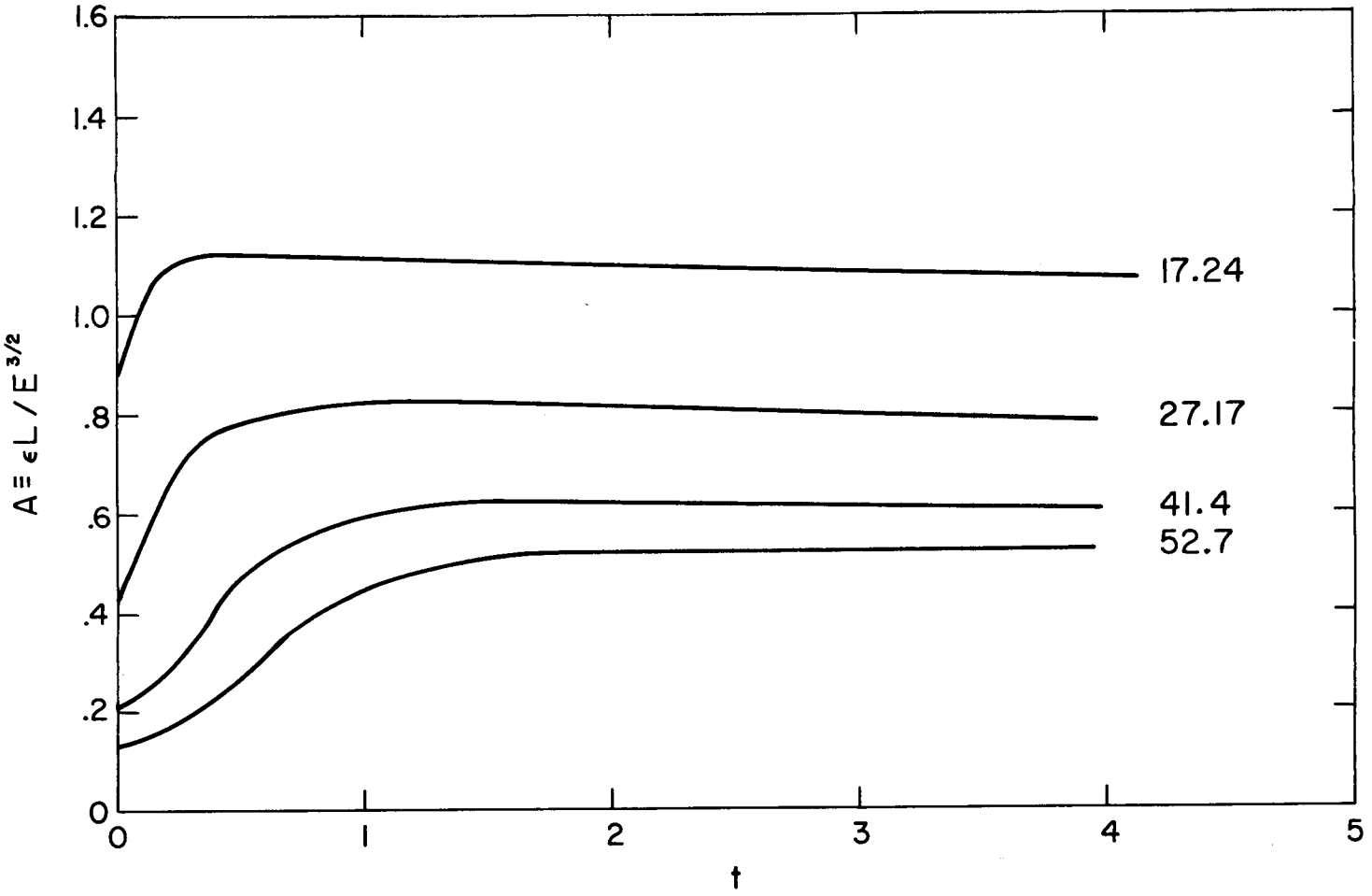

Figure 1.- Curves of $A \equiv \epsilon L / E^{3/2}$ as a function of time t for initial value problem, $E(k,0) = \lambda^2\left(1 + \sqrt{2}k\lambda\right)k \exp\left(-\sqrt{2}k\lambda\right)$. $\lambda = 0.1$, 0.2, 0.3, and 0.8, corresponding to $R_\lambda(0) = 20$, 40, 60, and 80. Curves are labeled by final asymptotic value of R_λ. Theory used is TFM; $g = 1.5$.

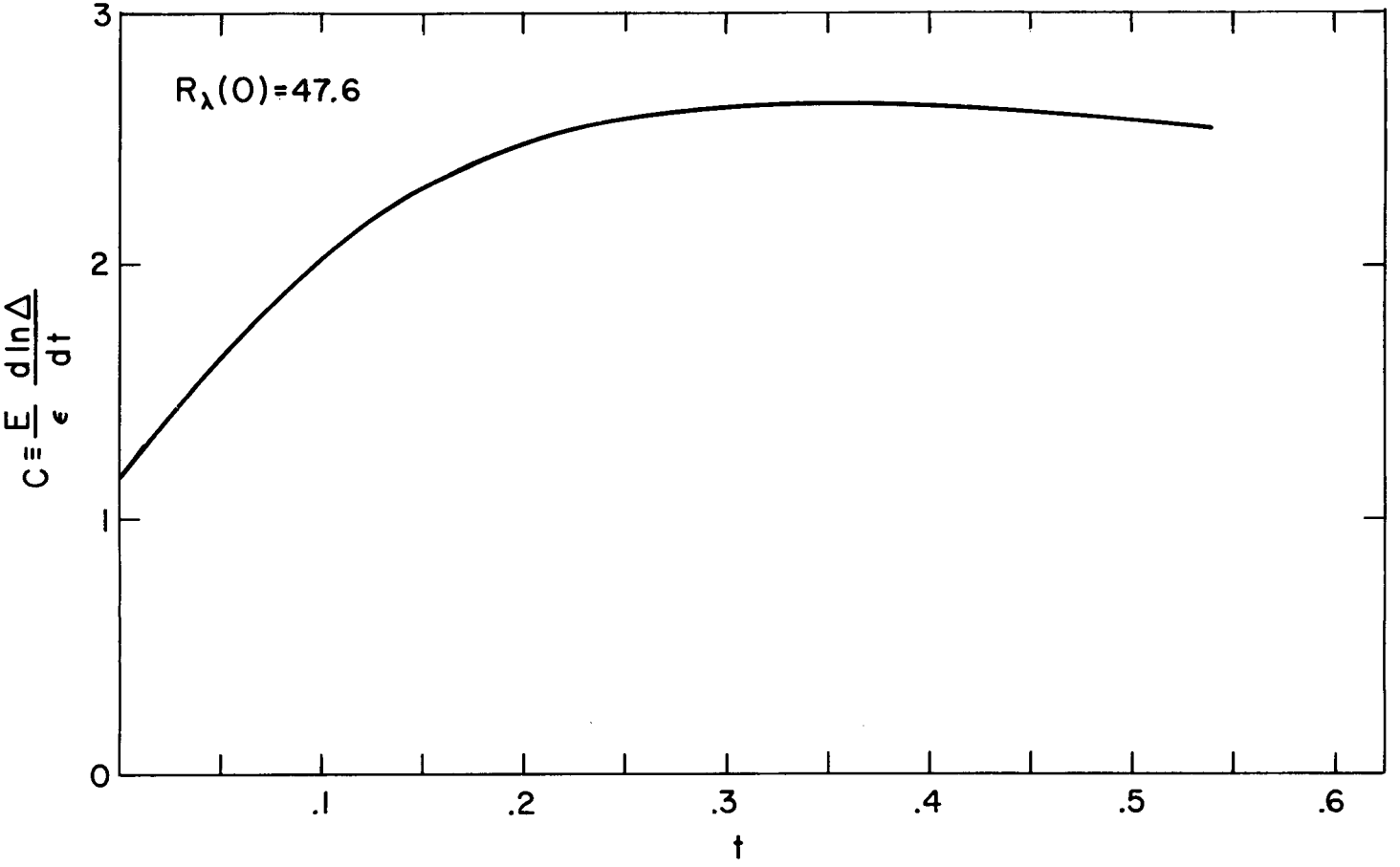

Figure 2.- Return-to-isotropy coefficient C (eq. (2)) as a function of time, according to the DIA theory. Curve depicts $\frac{E}{\epsilon} \frac{d \ln \Delta}{dt}$ for initial spectrum $E_1(k,0) = \frac{2\pi k^2 \exp(-2k)}{k + 0.5}$, $E_2(k,0) = 0$, where $E_1(k,0) = 2\pi k^2 \left\langle \left| u_1(\underline{k},t) \right|^2 + \left| u_2(\underline{k},t) \right|^2 \right\rangle$ and $E_2(k,0) = 2\pi k^2 \left\langle \left| u_3(\underline{k},t) \right| \right\rangle^2$.

A RATIONAL APPROACH TO THE USE OF PRANDTL'S MIXING LENGTH MODEL IN FREE TURBULENT SHEAR FLOW CALCULATIONS

By David H. Rudy and Dennis M. Bushnell
NASA Langley Research Center

SUMMARY

Prandtl's basic mixing length model was used to compute 22 of the 24 test cases for the Langley Working Conference on Free Turbulent Shear Flows. The calculations employed appropriate algebraic length scale equations and single values of mixing length constant for planar and axisymmetric flows, respectively. Good agreement with data was obtained except for flows, such as supersonic free shear layers, where large sustained density changes occur. The inability to predict the more gradual mixing in these flows is tentatively ascribed to the presence of a significant turbulence-induced transverse static-pressure gradient which is neglected in conventional solution procedures. Some type of an equation for length scale development was found to be necessary for successful computation of highly nonsimilar flow regions such as jet or wake development from thick wall flows.

4

SYMBOLS

c_p specific heat at constant pressure

$\overline{c_p} = \frac{c_p}{c_{p,e}}$

D nozzle diameter

j geometry parameter, 0 or 1 for two-dimensional or axisymmetric flow, respectively

k thermal conductivity

l mixing length

l_{sd} mixing length associated with second-derivative term in equation (5)

l/δ	mixing length constant
M	Mach number
N_{Pr}	Prandtl number, $\mu c_p/k$
N_{Sc}	Schmidt number
p	static pressure
Δp	static-pressure difference across shear layer
R	constant in equation of state for a perfect gas
R_b	Reynolds number based on characteristic body dimension, $\mu_e u_e r_b/\rho_e$
r	radial coordinate
$\bar{r} = \frac{r}{r_b}$	
r_b	characteristic body dimension
T	static temperature
$\overline{T} = \frac{T}{T_e}$	
u	mean velocity in streamwise direction
$\bar{u} = \frac{u}{u_e}$	
$\overline{u'v'}$	turbulent shear stress
v	mean velocity in transverse direction
$\overline{v'}$	fluctuating velocity in transverse direction
$w = 1 - \frac{u}{u_e}$	

x streamwise coordinate in physical plane

$\bar{x} = \frac{x}{r_b}$

y transverse coordinate in physical plane

$\bar{y} = \frac{y}{r_b}$

$\left.\begin{matrix} \bar{y}_{.01}, \bar{y}_{.05}, \bar{y}_{.95} \\ \bar{y}_{.99}, \bar{y}_{.995} \end{matrix}\right\}$ value of $\bar{y}$ where $\frac{u - u_{\ell}}{u_e - u_{\ell}} = 0.01, 0.05, 0.95, 0.99, 0.995$, respectively

α concentration

β mixing angle in wake flows

γ ratio of specific heats

δ width of mixing region

$\bar{\delta} = \frac{\delta}{r_b}$

ϵ eddy kinematic viscosity

ζ streamwise Von Mises coordinate

$\bar{\zeta} = \frac{\zeta}{r_b}$

θ momentum thickness

μ dynamic viscosity

$\bar{\mu} = \frac{\mu}{\mu_e}$

ρ density

$\bar{\rho} = \frac{\rho}{\rho_e}$

σ spreading parameter

σ_o	spreading parameter when $\frac{u_2}{u_1} = 0$ and $M \to 0$
τ	transverse Von Mises coordinate; or shear stress
$\bar{\tau}$	nondimensional transverse Von Mises coordinate, $\frac{\tau}{(\rho_e u_e)^{1/1+j} r_b}$
ϕ	mixing angle for jet flows

Subscripts:

c	end of potential core
ℓ	center line
e	external stream
i	initial
ip	inflection point
j	jet exit plane
l	laminar
n	nth species
p	primary flow
s	secondary flow
t	turbulent
1	high-velocity side of shear layer
2	low-velocity side of shear layer
I,II	regions I and II in jet flows (figs. 2 and 4) and wake flows (fig. 3)
III	region III in jet flows (figs. 2 and 4)

Superscript:

j geometry parameter where $j = 0$ in two-dimensional flows and $j = 1$ in axisymmetric flows

THE MIXING LENGTH CONCEPT

The classic phenomenological model for the turbulent shear stress is the mixing length theory (refs. 1 and 2) developed by L. Prandtl in 1925. Although the model lacks a rigorous physical basis, it has nonetheless proved to be quite successful in both boundary-layer and free shear flow calculations.

In formulating his model, Prandtl assumed that the Reynolds stress is produced by momentum transfer normal to the mean flow direction from regions of high momentum to regions of low momentum. The mixing length l is then defined (in rough analogy to the mean free path of a molecule) to be the average distance over which a fluid element transfers momentum. A detailed description of the model's theoretical development is available in many texts (e.g., ref. 3, p. 277 and ref. 4, p. 545).

Mathematically, for quasi-parallel shear flows the eddy viscosity is expressed as the product of the square of the mixing length and the absolute value of the local mean velocity gradient, that is,

$$\epsilon = l^2 \left| \frac{\partial u}{\partial y} \right| \tag{1}$$

Therefore, the turbulent shear stress for two-dimensional or axisymmetric flow becomes

$$\tau_t = -\rho \overline{u'v'} = \rho \epsilon \frac{\partial u}{\partial y} = \rho l^2 \left| \frac{\partial u}{\partial y} \right| \frac{\partial u}{\partial y} \tag{2}$$

where the mixing length is generally taken to be the product of an empirically determined constant and some characteristic scale of the mixing region, that is,

$$l = \text{Constant} \times \delta$$

or

$$\text{Constant} = \frac{l}{\delta} \tag{3}$$

Thus,

$$\tau_t = \rho\left(\frac{l}{\delta}\right)^2 \delta 2\left|\frac{\partial u}{\partial y}\right|\frac{\partial u}{\partial y} \tag{4}$$

Equation (4) has been widely used in the calculation of a variety of flows with both analytical and numerical solution methods. After early use in pipe flow and flat-plate boundary-layer analytical solutions, the mixing length model has been particularly successful in the numerical computations of both incompressible (e.g., refs. 5 and 6) and compressible (e.g., refs. 7 and 8) turbulent boundary-layer flows with appropriate definitions of the mixing length specified for the "wall" and "wake" regions. For example, Patankar and Spalding (ref. 7) defined the mixing length as a numerical function of the distance from the wall and the boundary-layer thickness. Bushnell and Beckwith (ref. 9) then extended the use of the mixing length model to include the compressible nonequilibrium case.

A number of well-known approximate analytic solutions were developed for low-speed free flows by using Prandtl's mixing length model. Prandtl studied the smoothing of a velocity discontinuity (ref. 4, p. 687) and assumed similar velocity profiles. Tollmien assumed similarity and presented solutions for both the circular jet (ref. 4, p. 699) and the two-dimensional jet (ref. 4, p. 696) issuing into still surroundings as well as the two-dimensional two-stream mixing layer (ref. 4, p. 689). Schlichting (ref. 4, p. 691) in his thesis first examined the two-dimensional wake. Using measurements in the wake of a circular cylinder, he found l/δ to be 0.18. Kuethe (ref. 10) extended Tollmien's solution for the mixing region of a plane jet to the general case of the mixing of two parallel streams with different velocities. Kuethe also solved the problem of the mixing region surrounding an axisymmetric jet issuing into still surroundings by assuming local similarity. Using experimental measurements and taking the mixing length to be proportional to the width of the mixing region, he obtained $l/\delta = 0.0705$. Squire and Trouncer (ref. 11) considered axisymmetric coaxial jets and used $l/\delta = 0.082$.

Several objections to the mixing length concept have been raised. For instance, according to equation (2) the eddy kinematic viscosity ϵ always vanishes at points of zero velocity gradient, a condition which is physically unrealistic (e.g., the center line of a jet or wake). Prandtl (ref. 1) recognized this difficulty and proposed that ϵ be considered proportional to a statistical mean of $\partial u/\partial y$ in the vicinity of a velocity maximum. The mixing length model for shear stress thus becomes

$$\tau_t = \rho l^2 \frac{\partial u}{\partial y}\left[\left(\frac{\partial u}{\partial y}\right)^2 + l_{sd}^2\left(\frac{\partial^2 u}{\partial y^2}\right)^2\right]^{1/2} \tag{5}$$

where l_{sd} is an additional length which must be determined experimentally. Equation (5) has seldom been used in analytical solutions because of the mathematical difficulties of including its more complex form. (There is no such problem if numerical solutions are employed.)

Another deficiency of the model given by equation (4) becomes evident in the study of the two-stream mixing layers. In this case the analytic solution exhibits a discontinuity in $\partial^2 u/\partial y^2$ at the mixing region boundaries instead of predicting the expected asymptotic approach of the mixing region velocity to the two free-stream values. Equation (5) is free of this problem.

In addition, the original assumption of constant mixing length across the mixing region has led to inaccurate predictions of the fluctuating components, according to Liepmann and Laufer (ref. 12), despite generally good agreement of the mean velocity profiles with experimental data.

Later Alexander, Baron, and Comings (ref. 13) demonstrated that Prandtl's original development required the assumption that the turbulence intensity and mixing length be isotropic. They concluded, however, that this first-order assumption did not seriously limit the application of the model. The original physical concept of a mixing length seemingly requires that its magnitude be small in comparison with mean flow dimensions. However, the fact that it has been found experimentally (ref. 14) that the mixing length is not small in comparison with mean flow dimensions is often considered a basic defect of the mixing length theory.

Recently several authors (e.g., ref. 15) have shown, by means of the turbulent kinetic energy approach, that the mixing length hypothesis implies that production equals dissipation of turbulence energy. Comparison of figures 6-9 and 7-44 in Hinze (ref. 3) shows that this assumption is much more defensible in boundary layers than in free shear flows.

Most investigators abandoned the mixing length in favor of Prandtl's later constant exchange coefficient eddy viscosity model (ref. 16), whose mathematical definition was more easily incorporated into analytical solutions. This "new" model overcame some of the difficulties of the mixing length model and gave slightly better agreement with experimental data. It has become historically the most widely used incompressible model.

Recently Elassar and Pandolfini (ref. 17) numerically investigated the compressible free shear layer in a backstep region and concluded that l/δ must have different values in the similar and nonsimilar regions. Wagner (ref. 18) used the mixing length model with the second-derivative term (eq. (5)) and $\frac{l}{\delta} = \frac{l_{sd}}{\delta} = 0.08$ to correctly predict the development of the hypersonic turbulent wake produced by a wedge.

The first attempt to systematically apply the mixing length model to a significant range of free turbulent flows was Harsha's study (ref. 19) of eddy viscosity models.

Harsha applied a single mixing length constant, 0.082 (the value used by Squire and Trouncer (ref. 11)), to both compressible and incompressible flows. Apparently, for all regions except the potential core of a jet, he defined the width parameter to be twice the half-velocity radius $\left(\text{the radius for which } u = \left(u_{\text{℄}} + u_e\right)/2\right)$. In the shear-layer region of jets he used the width of the mixing region. This approach led to poor overall agreement with the selected experimental data although he obtained good prediction of the velocity potential core length for the subsonic circular jet and the subsonic coaxial air-air mixing cases. His predicted potential core was too short for the compressible jet issuing into still air and too long for hydrogen-air coaxial mixing flows with mass flow ratio $\rho_e u_e/\rho_j u_j$ greater than 2.0. For all these calculations, the asymptotic slope and the center-line velocity decay curve was underpredicted. However, the mixing length model did predict the early center-line velocity increase for both an axisymmetric and a two-dimensional subsonic wake very satisfactorily, although the downstream values were underpredicted in both cases.

THE "RATIONAL" APPROACH

The present effort was the result of a desire on the part of the conference organizers to have the mixing length eddy viscosity model compared with newer formulations. Recent success (refs. 9, 20, and 21) at Langley in the use of Prandtl's model in high-speed boundary layers indicated that the model should be given further consideration in free shear flows as well. Rather than repeat the Harsha approach (ref. 19) with the 24 conference test cases, an approach which might be termed a more "rational" approach was selected in which each class of flows would be given individual consideration. The designation "rational" merely indicates that the approach was designed to better represent the actual physics of free mixing than can be accomplished by conventional use of the basic model.

On the basis of boundary-layer experience, the so-called "rational" approach was, at the beginning of the investigation, visualized as the inclusion of the following modifications in the basic mixing length model (eq. (2)):

(1) A consistent set of values for the proportionality constant l/δ were to be used. Originally it seemed that this might involve a different constant for each region of a jet or wake. However, the results to be presented in this paper indicate a single value of l/δ for all two-dimensional flows and a single value for all axisymmetric flows, a conclusion in agreement with the experience of Spalding's group at Imperial College (refs. 15 and 22 and paper 11 of this compilation).

(2) Most importantly, a simple length scale equation would be included to provide a reasonable transition from the relatively small scale of turbulent motion in the shear layer of a jet to the larger scales of turbulence in the far field. Similar consideration would be given to wake and coaxial flows developing from wall flows. This approach had been successfully used in the slot injection studies of references 20 and 21.

(3) Recent experience (ref. 23) in turbulent-boundary-layer calculations has shown a pronounced increase in turbulent shear stress near the end of transition and the beginning of turbulent flow. This "low Reynolds number effect" was to be investigated for any relevant free shear flow test cases. However, for the test cases considered herein this effect was not included due to the lack of information concerning possible magnitudes and variations of the "low Reynolds number effect" in free turbulent flows.

(4) The use of an intermittency factor in the calculation procedure was to be explored. Wagner (ref. 18) had previously used intermittency in his hypersonic wake calculations.

(5) The effect of including the second-derivative term in the mixing length model (i.e., eq. (5)) would be studied for some of the test cases.

SOLUTION PROCEDURE AND TURBULENCE MODELS

Basic Equations

Solutions were obtained by using a computer code developed by Sinha, Fox, and Weinberger (refs. 24 and 25) for chemically nonreacting, quasi-parallel shear flows.

The boundary-layer equations with suitable boundary conditions are assumed to describe the motion of free shear flows. Only quasi-parallel flows are considered. Effects of longitudinal curvature and transverse pressure gradient are not included. For the mixing of dissimilar ideal gases the governing equations are as follows:

Conservation of mass

$$\frac{\partial}{\partial x}\left(\rho u y^j\right) + \frac{\partial}{\partial y}\left(\rho v y^j\right) = 0 \tag{6a}$$

Conservation of streamwise momentum

$$\rho u \frac{\partial u}{\partial x} + \rho v \frac{\partial u}{\partial y} = -\frac{\partial p_e}{\partial x} + \frac{1}{y^j}\frac{\partial}{\partial y}\left(\mu y^j \frac{\partial u}{\partial y}\right) \tag{6b}$$

Conservation of energy

$$\rho u c_p \frac{\partial T}{\partial x} + \rho v c_p \frac{\partial T}{\partial y} = u \frac{\partial p_e}{\partial x} + \frac{1}{y^j} \frac{\partial}{\partial y}\left(k y^j \frac{\partial T}{\partial y}\right) + \mu\left(\frac{\partial u}{\partial y}\right)^2 + \frac{\mu}{N_{Sc}} \sum_n \left(c_{p,n} \frac{\partial \alpha_n}{\partial y} \frac{\partial T}{\partial y}\right) \tag{6c}$$

Conservation of nth species

$$\rho u \frac{\partial \alpha_n}{\partial x} + \rho v \frac{\partial \alpha_n}{\partial y} = \frac{1}{y^j} \frac{\partial}{\partial y}\left(\frac{\mu}{N_{Sc}} y^j \frac{\partial \alpha_n}{\partial y}\right) \tag{6d}$$

where $j = 0$ or 1 for two-dimensional or axisymmetric flow, respectively. The associated boundary conditions are as follows:

At the center line ($y = 0$),

$$\frac{\partial u}{\partial y} = \frac{\partial T}{\partial y} = \frac{\partial \alpha_n}{\partial y} = 0 \tag{6e}$$

for all values of x.

At the edge of the mixing region,

$$\left.\begin{aligned} \lim_{y \to \infty} u(x,y) &= u_e \\ \lim_{y \to \infty} T(x,y) &= T_e \\ \lim_{y \to \infty} \alpha_n(x,y) &= \alpha_{n,e} \end{aligned}\right\} \tag{6f}$$

Equations (6a) to (6f) are solved in the modified Von Mises plane defined by the following transformation:

$$(1 + j)\tau^j \frac{\partial \tau}{\partial y} = \rho u y^j \tag{7a}$$

$$(1 + j)\tau^j \frac{\partial \tau}{\partial x} = -\rho v y^j \tag{7b}$$

and

$$\zeta = (1 + j)^{-2} \int_{x_i}^{x} \frac{dx}{R_b} \tag{8}$$

In the transformed plane only the momentum, energy, and species equations are needed since the continuity equation is inherently satisfied in the definition of the transformation. The transformed equations are then nondimensionalized with respect to external stream conditions and r_b, a characteristic length. It should be noted that Wagner (ref. 18) has shown the analysis of references 24 and 25 to be incorrect for longitudinal pressure gradient flows since the continuity equation was not satisfied by the nondimensional Von Mises transformation used in that analysis. The correctly transformed equations of motion are as follows:

Momentum

$$\frac{\partial \bar{u}}{\partial \bar{\zeta}} = \frac{\bar{\tau}}{1 + j}\left(1 + M_e^2\right)\frac{d\left(\ln u_e\right)}{d\bar{\zeta}}\frac{\partial \bar{u}}{\partial \bar{\tau}} + \left(\frac{1}{\bar{\rho}\bar{u}} - \bar{u}\right)\frac{d\left(\ln u_e\right)}{d\bar{\zeta}} + \frac{1}{\bar{\tau}^j}\frac{\partial}{\partial \bar{\tau}}\left(\bar{\rho}\bar{\mu}\bar{u}\,\frac{\bar{y}^{2j}}{\bar{\tau}^j}\frac{\partial \bar{u}}{\partial \bar{\tau}}\right) \tag{9a}$$

Energy

$$\frac{\partial \overline{T}}{\partial \bar{\zeta}} = \frac{\bar{\tau}}{1 + j}\left(1 - M_e^2\right)\frac{d\left(\ln u_e\right)}{d\bar{\zeta}}\frac{\partial \overline{T}}{\partial \bar{\tau}} + \frac{\bar{\tau}^{-j}}{\overline{c_p}}\frac{\partial}{\partial \bar{\tau}}\left(\frac{\bar{\rho}\bar{\mu}}{N_{Pr}}\bar{u}\,\frac{\bar{y}^{2j}}{\bar{\tau}^j}\overline{c_p}\frac{\partial \overline{T}}{\partial \bar{\tau}}\right) + \left(\gamma_e - 1\right)M_e^2\frac{d\left(\ln u_e\right)}{d\bar{\zeta}}\left(\overline{T} - \frac{1}{\bar{\rho}\overline{c_p}}\right)$$

$$+ \frac{\bar{\rho}\bar{\mu}\bar{u}}{\overline{c_p}}\left(\frac{\bar{y}}{\bar{\tau}}\right)^{2j}\left(\frac{\partial \bar{u}}{\partial \bar{\tau}}\right)^2 + \left(\frac{\bar{\rho}\bar{\mu}}{N_{Sc}\overline{c_p}}\right)\left(\frac{\bar{y}}{\bar{\tau}}\right)^{2j}\bar{u}\frac{\partial \overline{T}}{\partial \bar{\tau}}\sum_n \overline{c_{p,n}}\frac{\partial \alpha_n}{\partial \bar{\tau}} \tag{9b}$$

Species

$$\frac{\partial \alpha_n}{\partial \bar{\zeta}} = \frac{\bar{\tau}}{1 + j}\left(1 - M_e^2\right)\frac{d\left(\ln u_e\right)}{d\bar{\zeta}}\frac{\partial \alpha_n}{\partial \bar{\tau}} + \bar{\tau}^{-j}\frac{\partial}{\partial \bar{\tau}}\left(\frac{\bar{\rho}\bar{\mu}\bar{u}}{N_{Sc}}\frac{\bar{y}^{2j}}{\bar{\tau}^j}\frac{\partial \alpha_n}{\partial \bar{\tau}}\right) \tag{9c}$$

Equations (9a) to (9c) were applied to turbulent flow by assuming that

$$\bar{\mu} = \bar{\mu}_l + \bar{\mu}_t \tag{10}$$

and by using turbulent Schmidt and Prandtl numbers. Suitable expressions were used for the laminar viscosity of the various gases used.

The flow was computed by using an implicit finite-difference technique (which is described in detail in refs. 24 and 25) to march downstream from the initial input profile.

Use of Von Mises Transformation

Apparently, most of the available computer codes for quasi-parallel free viscous flow solutions (e.g., refs. 7, 24, and 26) solve the boundary-layer equations in a Von Mises plane rather than the physical plane. For programing simplicity, a constant step size in the direction normal to the flow is usually assumed as in the procedure of reference 24. From equation (7a) this radial coordinate $\bar{\tau}$ in the method of reference 24 is defined by

$$\bar{\tau} = \left(\int_0^{\bar{y}} \bar{\rho} \bar{u} \bar{y}^j d\bar{y} \right)^{1/1+j} \tag{11}$$

Equation (11) shows that specifying equal $\Delta\bar{\tau}$ steps implies specifying equal increments of axial-direction mass flow across the computed region. Thus, larger steps (in terms of the physical plane) are located in regions of relatively low velocity (with respect to the free-stream or jet center-line velocity); this significantly reduces the accuracy in the crucial mixing regions. This problem is particularly evident in the calculation of compressible flows, especially the shear-layer calculations. As an example, in a typical Mach 5 two-dimensional shear-layer calculation with $u_2/u_1 = 0.05$, 49 of the 90 points across the mixing region profile are located in the region where u is approximately constant $\left(u/u_1 \geqq 0.90\right)$.

Turbulence Models

In accordance with the "rational approach" previously outlined, a conceptually simple (i.e., first order) model for the length scale variation in the streamwise direction was formulated for each of the major classes of flows. Thermal transport and mass transport were related to the momentum transport through the use of constant values of the turbulent Prandtl number and Schmidt number, respectively.

Two-dimensional shear layers.- Figure 1 shows the initial velocity profile used to generate the two-dimensional shear layers of test cases 1, 2, and 3. The same type of step profile was used for both the initial temperature and initial concentration profiles. Because of the inaccuracies introduced by the Von Mises transformation at the edge of the mixing region, the following definition for the width $\bar{\delta}$ of the region was necessary:

$$\bar{\delta} = (\text{Scaling factor})\left(\bar{y}_{.95} - \bar{y}_{.05}\right) \tag{12}$$

where $\bar{y}_{.95}$ indicates the point in the mixing layer where $(u - u_{\ell})/(u_e - u_{\ell}) = 0.95$. The scaling factor is necessary to obtain the "true" value of δ $(\text{i.e., } \bar{y}_{.99} - \bar{y}_{.01})$ and was taken to be 1.425 from the mean fit curve to the experimental data for two-stream mixing given by Halleen (ref. 27). This definition of width was used also for test case 5 and in the potential core region of all jet flows.

Since the initial boundary-layer profiles were given for test case 4, the two-dimensional version of the "coaxial jet length scale model" was applied to that case.

Jets into still air.- Figure 2 shows the length scale model developed for jets issuing into still air. The nondimensional mixing region width $\bar{\delta}$ is partially defined by the mixing angle ϕ. This definition allows a smooth transition between the relatively small mixing scale at the end of the potential core (which is designated region I) and the large scale turbulence downstream (region III).

For region I, $\bar{\delta}_I$ is given by equation (12); for region II,

$$\bar{\delta}_{II} = (\text{Scaling factor})(\bar{y}_{.95} - \bar{y}_{\ell}) + (\bar{x} - \bar{x}_c)\tan\phi \tag{13}$$

where $\bar{x}_c$ is the location of the end of the potential core. Region II extends to the point downstream at which $\bar{\delta}_{II}$ becomes $2(\text{Scaling factor})(\bar{y}_{.95} - \bar{y}_{\ell})$. Finally, in region III,

$$\bar{\delta}_{III} = 2(\text{Scaling factor})(\bar{y}_{.95} - \bar{y}_{\ell}) \tag{14}$$

The scaling factor for regions II and III was taken to be 1.2 from the similarity profile for a self-preserving jet given by Wygnanski and Fiedler (ref. 28).

Since the governing equations were nondimensionalized with respect to the external streams, some small arbitrary edge velocity was necessary. However, the velocity ratio u_{ℓ}/u_e at the initial profile had to be large enough to reasonably represent the physical problem being studied but not so large that the accuracy on the low-velocity site would be limited by the peculiarities of the Von Mises transformation discussed previously. The values of u_{ℓ}/u_e used in the initial profiles for the jets issuing into still air are listed in the following table:

Test case	Initial u_{ℓ}/u_e
6	34.65
7	35.37
8	41.80
18	70.0
19	55.30

This length scale model was also used to compute test case 13, a two-dimensional jet in a moving stream.

Wakes.- Figure 3 shows the length scale model employed in wake flows. Again, a linear variation defined by the angle β is assumed to approximate the increased scale of turbulent motion when the boundary layers on the wake-generating body mix in the initial wake region. For region I in figure 3, the width $\bar{\delta}$ is given by

$$\bar{\delta}_I = (\text{Scaling factor})\left(\bar{y}_{.95} - \bar{y}_{\ell}\right) + \left(\bar{x} - \bar{x}_i\right)\tan\beta \tag{15}$$

where $\bar{x}_i$ is the location of the start of region I which is usually the trailing edge of the body. Region I terminates when the two terms in equation (15) are of equal magnitude. The width $\bar{\delta}$ in region II is then given by

$$\bar{\delta}_{II} = 2(\text{Scaling factor})\left(\bar{y}_{.95} - \bar{y}_{\ell}\right) \tag{16}$$

The same scaling factor, 1.2, utilized in the jet flows downstream of the potential core was also used for wake flows.

Coaxial jets.- The model shown in figure 4(a) was employed for coaxial jet flows. The primary jet flow is assumed to mix with the initial boundary-layer flow in a region whose growth is characterized by mixing angles ϕ_1, ϕ_2, and ϕ_3. In all calculations these angles were assumed to be equal. This model results in a radial distribution of $\bar{\delta}$, such as the one shown in figure 4(b), and features two overlapping scales of turbulent motion, $\bar{\delta}_{Outer}$ and $\bar{\delta}_{Inner}$, given by

$$\bar{\delta}_{Inner} = \bar{\delta}_{p,i} + 2\left(\bar{x} - \bar{x}_i\right)\tan\phi \tag{17}$$

$$\bar{\delta}_{Outer} = \left(\bar{y}_{.995} - \bar{r}_j\right) + \left(\bar{x} - \bar{x}_i\right)\tan\phi \tag{18}$$

where $\bar{x}_i$ is measured from the exit plane of the primary jet nozzle. In the calculations, $\bar{\delta}$ is $\bar{\delta}_{Inner}$ for $\bar{y} < \bar{r}_p$ and $\bar{\delta}_{Outer}$ for $\bar{y} > \bar{r}_s$. Between $\bar{r}_p$ and $\bar{r}_s$, $\bar{\delta}$ is found by a linear interpolation between $\bar{\delta}_{Inner}$ and $\bar{\delta}_{Outer}$. The nondimensional radii $\bar{r}_p$ and $\bar{r}_s$ are defined by

$$\bar{r}_p = \frac{1}{2}\left[\bar{r}_j + \left(\bar{x} - \bar{x}_i\right)\tan\phi\right] \tag{19}$$

and

$$\bar{r}_s = \begin{cases} \bar{r}_j + \frac{1}{2}\bar{\delta}_{s,i} & \text{for } \bar{x} \leq \bar{x}_c \\ \frac{1}{2}\left[\bar{r}_j + \bar{\delta}_{s,i} + \left(\bar{x} - \bar{x}_i\right)\tan\phi\right] & \text{for } \bar{x} > \bar{x}_c \end{cases} \tag{20}$$

where $\bar{r}_j$ is the inner nozzle radius, $\bar{x}_c$ is the location of the end of the core region, and $\bar{\delta}_{s,i}$ is the initial thickness of the external boundary layer. This length scale modeling allows (to zeroth order) for the orderly growth of the initial boundary layer (or shear layer) scales. Far downstream the more conventional approach of a single large scale for the entire flow is recovered.

A differential equation for the local length scale would obviously be better than the present approach just outlined. The purpose here is simply to point out that if the physics of scale development is taken into account, predictions are considerably improved. In the present approach, this scale development is handled in the simplest manner possible.

POSSIBLE INFLUENCE OF TRANSVERSE STATIC-PRESSURE GRADIENT ON TURBULENT FREE MIXING

The conventional approach to turbulent free mixing calculations (the approach used in the present paper) involves solving the boundary-layer equations with some turbulence closure model. On the basis of an order of magnitude analysis, the normal (or transverse) static-pressure gradient is assumed to be quite small in the basic boundary-layer equations. By assuming constant static pressure in the transverse direction, the solution of the normal momentum equation is unnecessary. Recent studies (refs. 29 and 30) indicate that this assumption of constant static pressure is not correct in boundary layers where there are large density changes across the layer. Changes in static pressure of 10 to 30 percent have been observed in nominally two-dimensional, high Mach number ($M > 6$) boundary layers.

The normal momentum equation for two-dimensional turbulent quasi-parallel shear flows takes the form

$$\frac{\partial p}{\partial y} = -\frac{\partial\left(\overline{\rho v'^2}\right)}{\partial y} \tag{21}$$

where density fluctuations have been neglected in an order of magnitude analysis. Hinze (ref. 3) notes that for low-speed flows the normal static-pressure changes induced by the turbulence (from eq. (21)) were 2 orders of magnitude larger than the static-pressure changes induced by the mean flow. The basic question is whether or not the normal static-pressure gradient induced by the turbulence (eq. (21)) can become sufficiently large to affect the spreading rate and turbulence structure of a free turbulent mixing flow. The success of various calculation methods (turbulence closure models) in low-speed flows indicates that the influence is most likely negligible in these flows. However, large density changes would presumably increase the magnitude of the turbulence-induced normal static-pressure gradient (from eq. (21)); therefore, the answer to the basic question may well be that the spreading rate and turbulence structure are in fact affected where large density changes occur.

Estimates were made of the probable static-pressure change for an $M_1 = 5$ free shear layer obtained recently in the nozzle test apparatus at the Langley Research Center. (These data are discussed in paper 2 by Birch and Eggers.) By using the integrated form of equation (21) and estimates of $\overline{v'^2}$ from the subsonic shear layer of Liepmann and Laufer (ref. 12), the change in static pressure for this flow would be of the order of a 100-percent decrease near the maximum shear region. Obviously $\overline{v'^2}$ and perhaps the Reynolds stress must be lower than the normalized values of reference 12 for this $M_1 = 5$ case, since such a transverse static-pressure gradient would not be tolerated by the flow.

There are at least two possible mechanisms connected with a turbulence-induced $\partial p/\partial y$ which could affect the spreading rate of a free turbulent shear flow:

(1) Direct influence of turbulence-induced $\partial p/\partial y$ upon the normal mean velocity v and hence directly upon the spreading rate (refs. 31 and 32). A pressure gradient dp/dx is imposed within the shear flow.

(2) Indirect influence of turbulence-induced $\partial p/\partial y$ upon $\overline{v'^2}$ and $\overline{u'v'}$ by means of a turbulence field adjustment to decrease $\partial p/\partial y$ until a balance is achieved.

Obviously both of these mechanisms as well as others could be operating simultaneously. The important point is that as the density change across a turbulent free mixing region increases, the influence of the turbulence-induced $\partial p/\partial y$ may become increasingly more important, especially in determining the absolute physical dimensions of the flow field (i.e., the entrainment rate).

Transverse static-pressure data for free shear layers are available in references 32 to 34. For low-speed flows the data indicate a minimum pressure of the order of 2 percent near the inflection point in the velocity profile. The low-speed data of Lee (ref. 35) and Jones and Spencer (ref. 36) indicate small static-pressure changes (less than 1 per-

cent) for shear layers with $\frac{u_2}{u_1} = 0.35$ and 0.30, respectively. Further data for the transverse static-pressure distribution in jets are available in references 31 and 37 and some data for wakes are found in reference 38. The available data do seem to indicate an increase of transverse static-pressure gradient with increasing Mach number across the shear layer.

It is interesting to note that the integrated form of equation (21) is

$$\left|\frac{\Delta p}{p_{\text{¢}}}\right| \approx \left(\frac{\overline{\rho v'^2}}{p_{\text{¢}}}\right)_{ip}$$

or

$$\left|\frac{\Delta p}{p_{\text{¢}}}\right| \approx \frac{\overline{v'^2}}{u_{\text{¢}}^2} \frac{\gamma_{\text{¢}}}{\gamma_{ip}} M_{\text{¢}}^2 \frac{R_{\text{¢}}}{R_{ip}} \frac{T_{\text{¢}}}{T_{ip}} \tag{22}$$

where the subscript ip indicates the inflection point in the shear-layer profile. Therefore, Mach number may well have an effect greater than simple density changes (caused by gas composition) upon possible changes in entrainment rate due to $\partial p/\partial y$.

The possibility that static-pressure variation may be responsible for the rather large changes in spreading rate with Mach number noted in connection with test case 2 in the present paper is entirely speculative at this point. There are several possible approaches that could be used to investigate this possibility. One such method would be to incorporate the complete normal momentum equation in a method such as Donaldson's (ref. 39) where $\overline{v'^2}$ is directly computed. If an equation for $\overline{v'^2}$ is lacking, it could be related to the Reynolds stress by some constant or function. Again, it would be necessary to solve the normal momentum equation (including the convective terms). The best method (i.e., most correct) of including the normal momentum equation would be a full field Navier-Stokes solution with turbulence terms included. However, if molecular diffusion of momentum is neglected in the normal momentum equation, a first-order solution may be obtained numerically by including the equation in a streamwise iteration loop with the usual boundary-layer equations.

There are, of course, other mechanisms which could also account for the disagreement between experiment and theory for case 2. These possibilities include the increased influence of $\overline{p'v'}$ and other terms in the second-order correlation equations. These

terms are usually negligible at low speeds but presumably become more important at high speeds. Currently there are no available models or data for these terms in high-speed flows which could be used to check this hypothesis.

RESULTS AND DISCUSSION

Solutions were obtained for all 17 of the primary test cases and for five of the seven optional cases. The two cases omitted were case 22, a hydrogen-air coaxial jet flow, and case 23, a subsonic compound coaxial air jet. These cases were omitted because of numerical and programing difficulties encountered rather than failure of the basic turbulence models being used.

During the investigation it was found that l/δ could be considered a function only of flow geometry. A value of 0.07 was used in all two-dimensional flows and 0.05 was used in all axisymmetric flows including the shear-layer region of jets.

In general, for constant density subsonic flows the turbulent Prandtl and Schmidt numbers were taken to be 1.0. For variable-density flows either 0.7 or 0.8 was used, with the Prandtl number assumed equal to the Schmidt number in all cases.

Two-Dimensional Shear Layers

Test case 1.- Two-dimensional subsonic constant-density free shear layers were computed for velocity ratios u_2/u_1 of 0.05, 0.2, 0.4, 0.6, and 0.8 by using "step" input profiles for velocity and temperature as previously described. Since the equations were normalized with respect to the secondary stream, a nominally zero value of u_2 was not possible in the present program; $\frac{u_2}{u_1} = 0.05$ was used in both test cases 1 and 2. The results from the computations of test case 1 are shown in figure 5. The spreading parameter σ is defined by the following relationship:

$$\sigma = \frac{1.855\left(X_B - X_A\right)}{Y_B - Y_A} \tag{23}$$

where Y_A and Y_B are the lateral distances between points at which $\frac{u - u_2}{u_1 - u_2}$ is 0.1 and 0.9 at longitudinal stations X_A and X_B, respectively. The spreading parameter σ is thus the reciprocal of the spreading rate of the shear layer.

Equation (12) was used to define the width $\bar{\delta}$, and l/δ was taken to be 0.07. By extrapolating the computed values of σ to the case where u_2/u_1 is zero, σ_o was

found to be 11.4. This value was used to normalize the computed values of σ. As shown in figure 6, the results agree with the well-known relationship (from ref. 40)

$$\frac{\sigma_o}{\sigma} = \frac{u - u_2}{u_1 + u_2}$$

Test case 2.- Two-dimensional shear layers were computed for five values of M_1 to determine the effect of Mach number on the spreading rate (test case 2). The results are shown in figure 6 along with experimental data from references 12, 28, 31, 34, and 41 to 50 as well as the unpublished data recently obtained at the Langley Research Center at $M_1 = 5.0$. These shear-layer data have been adjudged the most reliable by Birch and Eggers in paper 2 of this compilation.

Equation (12) was used to define the width $\bar{\delta}$. With an l/δ of 0.07, only a slight increase in σ is predicted for increasing values of M_1 in striking contrast to much of the available data. At $M_1 = 5.0$, the effect of decreasing the mixing rate by lowering l/δ is shown. The cause underlying the inability of the mixing length model to predict the spreading rate of supersonic shear layers is perhaps directly related to the validity of the fundamental assumptions inherent in the boundary-layer approach to free mixing problems. One possible explanation is the existence of a transverse static-pressure gradient which could affect the turbulence spreading rate. The effect of such a pressure gradient was previously discussed in detail in this paper. There is also the possible influence of "low Reynolds number effects" as discussed by Birch and Eggers in paper 2. The data that may be influenced by such effects are indicated in figure 6. It should also be noted that the values of σ computed with $\frac{u_2}{u_1} = 0.05$ were scaled to correspond to $\frac{u_2}{u_1} = 0$ (using fig. 5).

Test case 3.- Test case 3 was designed to determine the effect of density ratio on the growth of fully developed two-dimensional shear layers. With $\frac{u_2}{u_1} = 0.2$, calculations were made for shear layers with density ratio ρ_1/ρ_2 of approximately 1/14, 2, 7, and 14. For all but the $\frac{\rho_1}{\rho_2} = \frac{1}{14}$ shear layer, the density difference was accounted for in the program by two methods: the subsonic mixing of gases with different molecular weights, and the mixing of two air streams with supersonic or hypersonic velocity in the primary stream. The $\frac{\rho_1}{\rho_2} = \frac{1}{14}$ shear layer was obtained by mixing hydrogen in the primary stream with air in the secondary stream. The $\frac{\rho_1}{\rho_2} = 2$, 7, and 14 shear layers were the result of mixing hydrogen and helium, helium and air, and air and hydrogen; the corre-

sponding air into air equivalent density ratios were computed by using $M_1 = 2.24$, 5.48, and 8.06, respectively. Turbulent Prandtl numbers of 0.7 and 0.8 were used for the dissimilar gas and supersonic flows, respectively; the turbulent Schmidt numbers were also 0.7 and 0.8, respectively. Appropriate input profiles of the type shown in figure 1 were used in each instance. The results, shown in figure 7, indicate that σ is a similar function of density differences irrespective of the mechanism producing that difference. However, it should be remembered that in test case 2 the supersonic results were greatly in error when compared with the data.

Test case 4.- Test case 4 considers the subsonic mixing of two streams initially developed on a symmetric airfoil with a 10° trailing edge. The coaxial jet length scale model was used for this calculation. A representative small angle of 8° (the value used in the slot injection studies of refs. 20 and 21) was used. The predicted profiles at two locations, $x = 12.7$ cm and $x = 76.2$ cm, are compared with Lee's experimental measurements (ref. 35) in figures 8(a) and 8(b), respectively. For this test case and test case 5, the computed profiles are matched with the experimental profiles at the point where $u = (u_1 - u_2)/2$ since the numerical calculation does not satisfy the proper boundary conditions (ref. 51). The predicted profile at $x = 12.7$ cm indicates only slightly more mixing than the experimental data. Much farther downstream at 76.2 cm the prediction indicates significantly more mixing. Better agreement could have been achieved by adjusting the angles ϕ_1, ϕ_2, and ϕ_3 but such manipulation was beyond the intent of the current investigation. It should be noted that the streams mix with a fairly large initial angle (10°).

Test case 5.- The Hill and Page (ref. 50) supersonic $(M_1 = 2.09)$ shear layer (test case 5) was computed with $l/\delta = 0.07$, where $\bar{\delta}$ was defined by equation (12). Computed profiles at two stations are shown in figure 9. The effect of the different boundary conditions used in the computations is evident on the low-velocity side of the shear layer. The data were obtained in a cavity-type flow and may be influenced by the "low Reynolds number effects." Both calculated profiles indicate more rapid mixing than the experimental data, which is the expected behavior from the results of test case 2. (See section entitled "Possible Influence of Transverse Static-Pressure Gradient on Turbulent Free Mixing.")

Jets Issuing Into Still Air

For all flows of this type the length scale model of figure 2 was employed. An l/δ of 0.05 was used in all three regions of the axisymmetric jets including region I. The value of l/δ should actually be varied from 0.07 at the nozzle exit where the shear layer is thin and essentially two-dimensional to 0.05 at the end of the core where the flow is fully axisymmetric. Hence, for flows with relatively short potential cores (e.g., test cases 6 and 8) the use of a single value lower than the average value through the core

results in less mixing and hence too long a potential case. The present model predicted the decay of the center-line velocity remarkably well by using an angle ϕ of 8°.

Test case 6.- Figure 10 shows the results of the computation of the Maestrello and McDaid subsonic jet (ref. 52). The potential core is longer than indicated by the experimental data but the decay rate of the center-line velocity in regions II and III is well predicted. Test case 6 is an example of a jet for which l/δ must have a value near 0.07 in the shear-layer region to correctly predict the core length.

Test case 7.- For the Eggers Mach 2.22 jet (ref. 49), the potential core length is well predicted, but the agreement with the center-line velocity decay curve using $\phi = 8^{\circ}$ is not as good as the corresponding comparison in the previous subsonic jet flow in test case 6. The prediction for test case 7 is shown in figure 11(a) with a $\phi = 89^{\circ}$ calculation which corresponds to an immediate jump in length scale at the end of the core to the region III value. This represents the usual method of applying the mixing length model to jet flows (e.g., Harsha, ref. 19). Obviously the prediction of the center-line velocity decay as the far field is approached is significantly improved by using a "length scale equation" between the near field and far field. A prediction with $\phi = 0^{\circ}$ is also shown. Velocity profiles at three locations are shown in figures 11(b) and 11(c). These results indicate that the correct profile is obtained when the center-line value is correctly predicted.

Test case 8.- A value of l/δ of 0.05 and mixing angle of 8° were used to predict the high-temperature subsonic data of Heck (ref. 53). The center-line distributions of velocity and temperature for test case 8 are given in figures 12(a) and 12(b), respectively. As shown in these figures, the velocity potential core length is again incorrect although the velocity decay rate outside the core is well matched. A turbulent Prandtl number of 0.7 predicts the temperature decay rate correctly.

Test case 18.- The fully developed axisymmetric jet data of Wygnanski and Fiedler (ref. 28) provided a test of the far field length scale model in a subsonic flow (test case 18). Starting with the given similarity profile at $x/D = 60$, a location in the self-preserving region, the solution was obtained with $l/\delta = 0.05$. With an initial velocity ratio $u_{\text{¢}}/u_e$ of 70, the computed spreading rate of the jet was found to be linear and in excellent agreement with the data. Figure 13(a) shows the center-line velocity prediction over the range of the data. The similarity of the data was retained in the calculations as shown in figure 13(b) where x_{vo} indicates the streamwise distance from the virtual origin of the jet. Equation (14) was used to define δ.

Test case 19.- Test case 19 is a supersonic high-temperature jet (ref. 53) similar to the subsonic jet of test case 8. The turbulent Prandtl number was assumed to be 0.7 and $l/\delta = 0.05$ and $\phi = 8^{\circ}$. Figure 14(a) shows that the predicted potential core is too long; however, the correct velocity decay rate is predicted as the far field is approached.

Figure 14(b) indicates that similar conclusions apply to the center-line temperature distribution. If the core length problem could be remedied for compressible shear-layer mixing, the center-line variation would then probably be correctly predicted for the entire flow field.

In all the compressible jet cases it should be noted that the near field (where the present calculations give least accurate agreement with data) is the only region where large density gradients occur. It is speculated that the mechanism responsible for the disagreement in this region is the same mechanism operative in the supersonic free shear layers. In the present paper it is suggested that this mechanism is related to turbulence-induced static-pressure gradients. Other possible mechanisms operable in this region are the "low Reynolds number effect" discussed by Birch and Eggers in paper 2 and the l/δ adjustment from two-dimensional to axisymmetric.

Plane Jet in a Moving Stream

Test case 13.- The length scale model shown in figure 2 was used to predict subsonic test case 13. No initial profile data were available other than the experimentally determined momentum thickness and u_j/u_e. A step velocity profile was selected so that u_j/u_e was matched. Value of l/δ of 0.07 and a mixing angle of 8^o gave an excellent prediction of the center-line velocity distribution as shown in figure 15. Since the external stream had a constant nonzero velocity, the experimental velocity ratio u_{ℓ}/u_e could be accurately represented numerically, unlike the previously discussed jets issuing into still air.

Coaxial Jet Flows

The length scale model shown in figure 4 was used for all flows of this type. A value of l/δ of 0.05 was used in regions I and II. All solutions were started at the nozzle exit with the initial boundary-layer profiles. For the AEDC experimental data (test cases 10, 20, and 21) these profiles were approximated by using the estimates of boundary-layer thicknesses given in reference 54. The mixing angles ϕ_1, ϕ_2, and ϕ_3 were taken to be equal in all cases.

Test case 9.- Test case 9 represents the data of Forstall and Shapiro (ref. 55). The suggested initial profile, which was adjusted to account for probable pitot probe positioning errors, was used to start the solution. The results of the computation using $l/\delta = 0.05$ and all mixing angles equal to 8^o are shown in figure 16. The experimental center-line velocity decay in region II is well predicted by using angles of 8^o although the potential core length is unpredicted. However, it should be noted that the core length is a function of ϕ_3 for a given l/δ. As discussed previously, a larger average l/δ is needed in the core.

Test case 10.- Figure 17 shows the results of applying the coaxial jet length scale model to the subsonic hydrogen-air data of Chriss (ref. 56). Both the center-line velocity and center-line hydrogen concentration variations for test case 10 are well predicted with $l/\delta = 0.05$ and mixing angles of 8°.

Test case 11.- Figure 18 shows the computational results for test case 11 which represents an inner subsonic air jet mixing with an outer Mach 1.30 air jet studied by Eggers and Torrence (ref. 57). Mixing angles of 2° gave better predictions of the center-line velocity variation than did angles of 8°. However, neither calculation predicted as large a drop in center-line velocity as the data indicate and neither calculation correctly predicted the rate of velocity increase as the far field is approached.

Test case 12.- Good prediction of the center-line velocity decrease for the hydrogen-air data of Eggers (ref. 58) was obtained for test case 12 with $l/\delta = 0.05$ and mixing angles of 8° even though this choice of angle resulted in an underprediction of the potential core length. The center-line velocity distribution is shown in figure 19(a). The same prediction trend is also observed in the center-line hydrogen concentration variation as shown in figure 19(b). The turbulent Schmidt and Prandtl numbers were both 0.8.

Test case 20.- Test case 20 represents the mixing of subsonic coaxial jets as measured by Chriss and Paulk (ref. 54). The best overall prediction with the coaxial length scale model was achieved with mixing angles of 6° as shown in figure 20. The calculations with angles of 6° and 8° are shown for comparison; however, as discussed previously, l/δ should actually have had a larger average value through the core region.

Test case 21.- As shown in figure 21(a) the coaxial model again predicted the correct center-line velocity decay rate for the subsonic hydrogen-air data of Chriss (ref. 56). However, a value of l/δ of 0.05 gave an overprediction of the potential core length for a mixing angle of 8°. An l/δ of 0.07 with all angles ϕ $(\text{i.e., } \phi_1, \phi_2, \phi_3)$ equal to 8° gives a better core length prediction. The concentration profile prediction for test case 21 is given in figure 21(b).

Wake Flows

The length scale model shown in figure 3 was used in computing all wake flows. In addition, the effect of including the second-derivative term (eq. (5)) was investigated for some of these wakes.

Test case 14.- The predicted center-line velocity distribution is shown in figure 22 for the two-dimensional wake data (test case 14) of Chevray and Kovasznay (ref. 59). By using a value of l/δ of 0.07 and a mixing angle β of 8°, a reasonably accurate overall prediction is obtained. As expected, addition of the second-derivative term $\left(\text{with } \frac{l_{sd}}{\delta} = \frac{l}{\delta}\right)$

results in an increase in the mixing rate, the increase giving a more accurate velocity rise in the near wake region while overpredicting the data as the far field is approached. A calculation with $\phi = 89^{\circ}$, which corresponds to using no linear variation in length scale downstream of the body, is shown to demonstrate the improved prediction in the near wake region with the present linear variation. The effect of the angle disappears as the asymptotic region is approached. A calculation with $\beta = 4^{\circ}$ and no second-derivative term is also shown for comparison.

The deviation between prediction and experiment in the far field is emphasized when the data is plotted in terms of $1/w_{\ell}^2$ where w_{ℓ} is the center-line velocity defect.

Test case 15.- Computations of Chevray's axisymmetric wake (ref. 60) with $\frac{l}{\delta} = 0.05$ and $\beta = 8^{\circ}$ are shown in figure 23. The initial rapid increase of the center-line velocity (due in part to the pressure gradient just behind the body) is not predicted even when the second-derivative term $\left(\text{with } \frac{l_{sd}}{\delta} = \frac{l}{\delta}\right)$ is included. The second-derivative model, however, gives better downstream agreement than the basic model. Test case 15 is an example of a flow in which the value of β probably should be high initially and lowered to 8° a few diameters downstream (as is done automatically by the method of ref. 20), but such optimization was beyond the present intent.

Test case 16.- The asymptotic region of the plane supersonic wake of Demetriades (ref. 61) is well predicted with $\frac{l}{\delta} = 0.07$ and $\beta = 8^{\circ}$. (See fig. 24.) The second derivative increases the mixing rate only slightly for test case 16.

Test case 17.- The supersonic (M = 3.0) axisymmetric wake data of Demetriades (ref. 62) is underpredicted for test case 17 with $\frac{l}{\delta} = 0.05$ and $\beta = 8^{\circ}$ even though the second-derivative term is included. (See fig. 25.) The calculation was started at $\frac{x}{D} = 17$, a location actually near the end of the transition region; hence these data may be influenced by the "low Reynolds number effects." Assuming turbulent flow at $\frac{x}{D} = 17$ results in an underprediction of the data in the turbulent region $\left(\frac{x}{D} > 20\right)$.

Test case 24.- The two-dimensional supersonic wake data of Demetriades (ref. 63) include data in the transition region $\left(602.9 \leqq \frac{x}{D} \leqq 938.4\right)$. The wake-generating wedge was heated so that transition would occur far downstream of the model. The calculation for test case 24 was started in the laminar region at $\frac{x}{D} = 183.7$. In reference 64 Demetriades

gives the experimental streamwise distribution of the intermittency factor on the wake center line for the corresponding unheated flow. This distribution was used to compute through the given region of transitional flow. Such an approach had previously been employed by Harris (ref. 65) who used the streamwise intermittency function of Dhawan and Narasimha (ref. 66) in the computation of compressible boundary layers. The results shown in figure 26 indicate that the data were slightly underpredicted in the laminar and transitional regions with improved agreement in the fully turbulent region. A wake flow mixing angle of 8° was used.

CONCLUDING REMARKS

Prandtl's mixing length model has been applied in a consistent manner to compute the wide range of free turbulent mixing flows selected as test cases in this compilation. On the basis of these computations, the following concluding remarks can be made.

The mixing length constant l/δ was found to be lower in axisymmetric flows than in planar flows. With $l/\delta = 0.05$ in axisymmetric flows and 0.07 in two-dimensional flows, the calculations compare very favorably with the data for jets downstream of the core, wake flows, and low-speed shear layers.

For the mixing of flows with differing or developing turbulent length scales (such as near field to far field transition region in a jet and wake flows developing from boundary layers), some method of correctly determining the local length scale should be used. In the present paper, a linear algebraic function based on modeling the physical spreading of the turbulence was used. Perhaps a more satisfactory approach would be the use of one of the various "two-equation" turbulence models of Spalding's group (paper 11 of this compilation) where a differential length scale equation is solved.

The mixing length model was unable to successfully compute the spreading rates of free shear layers with large sustained density differences. This inability is tentatively ascribed to the assumption of constant static pressure in the transverse direction (the conventional quasi-parallel flow assumption). Therefore, a successful calculation method for this class of flows (free turbulent mixing flows with sustained large density changes or differences) may necessitate including equations for the mean normal momentum and $\overline{v'^2}$.

As discussed by Birch and Eggers in paper 2 of this compilation, there seems to be an important "low Reynolds number effect" in some of the available data. However, further analysis of the data is needed before this effect can be incorporated into prediction methods.

REFERENCES

1. Prandtl, L.: Bericht über Untersuchungen zur ausgebildeten Turbulenz. Z. Angew. Math. Mech., Bd. 5, Heft 2, Apr. 1925, pp. 136-139. (Available in English translation as NACA TM 1231, 1949.)

2. Prandtl, L.: Ueber die ausgebildete Turbulenz. Lecture presented at International Congress for Applied Mechanics (Zurich), Sept. 1926. (Available in English translation as NACA TM 435, 1927.)

3. Hinze, J. O.: Turbulence. McGraw-Hill Book Co., Inc., 1959.

4. Schlichting, Hermann (J. Kestin, transl.): Boundary-Layer Theory. Sixth ed., McGraw-Hill Book Co., 1968.

5. Pletcher, Richard H.: On a Finite-Difference Solution for the Constant-Property Turbulent Boundary Layer. AIAA J., vol. 7, no. 2, Feb. 1969, pp. 305-311.

6. Ng, K. H.; Patankar, S. V.; and Spalding, D. B.: The Hydrodynamic Turbulent Boundary Layer on a Smooth Wall, Calculated by a Finite-Difference Method. Computation of Turbulent Boundary Layers – 1968 AFOSR-IFP-Stanford Conference, Vol. I, S. J. Kline, M. V. Morkovin, G. Sovran, and D. J. Cockrell, eds., Stanford Univ., c.1969, pp. 356-365.

7. Patankar, S. V.; and Spalding, D. B.: Heat and Mass Transfer in Boundary Layers. Second ed., Int. Textbook Co. Ltd. (London), c.1970.

8. Adams, John C., Jr.: Eddy Viscosity-Intermittency Factor Approach to Numerical Calculation of Transitional Heating on Sharp Cones in Hypersonic Flow. AEDC-TR-70-210, U.S. Air Force, Nov. 1970.

9. Bushnell, Dennis M.; and Beckwith, Ivan E.: Calculation of Nonequilibrium Hypersonic Turbulent Boundary Layers and Comparisons With Experimental Data. AIAA J., vol. 8, no. 8, Aug. 1970, pp. 1462-1469.

10. Kuethe, Arnold M.: Investigations of the Turbulent Mixing Regions Formed by Jets. J. Appl. Mech., vol. 2, no. 3, Sept. 1935, pp. A-87 – A-95.

11. Squire, H. B.; and Trouncer, J.: Round Jets in a General Stream. R. & M. No. 1974, Brit. A.R.C., 1944.

12. Liepmann, Hans Wolfgang; and Laufer, John: Investigations of Free Turbulent Mixing. NACA TN 1257, 1947.

13. Alexander, Lloyd G.; Baron, Thomas; and Comings, Edward W.: Transport of Momentum, Mass, and Heat in Turbulent Jets. Bull. Ser. No. 413, Univ. of Illinois, May 1953.

14. Batchelor, G. K.: Note on Free Turbulent Flows, With Special Reference to the Two-Dimensional Wake. J. Aeronaut. Sci., vol. 17, no. 7, July 1950, pp. 441-445.

15. Rodi, W.; and Spalding, D. B.: A Two-Parameter Model of Turbulence, and Its Application to Free Jets. Wärme- und Stoffübertragung, vol. 3, no. 2, 1970, pp. 85-95.

16. Prandtl, L.: Bemerkungen zur Theorie der freien Turbulenz. Z. Angew. Math. & Mech., Bd. 22, Heft 5, Oct. 1942, pp. 241-243.

17. Elassar, R. J.; and Pandolfini, P. P.: An Examination of Eddy Viscosity Models for Turbulent Free Shear Flows. Paper No. 71-FE-17, Amer. Soc. Mech. Eng., May 9-12, 1971.

18. Wagner, Richard D.: Measured and Calculated Mean-Flow Properties of a Two-Dimensional, Hypersonic, Turbulent Wake. NASA TN D-6927, 1972.

19. Harsha, Philip Thomas: Free Turbulent Mixing: A Critical Evaluation of Theory and Experiment. AEDC-TR-71-36, U.S. Air Force, Feb. 1971. (Available from DDC as AD 718 956.)

20. Beckwith, Ivan E.; and Bushnell, Dennis M.: Calculation by a Finite-Difference Method of Supersonic Turbulent Boundary Layers With Tangential Slot Injection. NASA TN D-6221, 1971.

21. Bushnell, Dennis M.: Calculation of Relaxing Turbulent Boundary Layers Downstream of Tangential Slot Injection. J. Spacecraft & Rockets, vol. 8, no. 5, May 1971, pp. 550-551.

22. Spalding, Dudley Brian: A Two-Equation Model of Turbulence. VDI-Forsch., Heft 549, 1972, pp. 5-16.

23. Bushnell, Dennis M.; and Morris, Dana J.: Shear-Stress, Eddy-Viscosity, and Mixing-Length Distributions in Hypersonic Turbulent Boundary Layers. NASA TM X-2310, 1971.

24. Sinha, Ram; Fox, Herbert; and Weinberger, Lawrence: An Implicit Finite Difference Solution for Jet and Wake Problems. Pt. I: Analysis and Test Cases. ARL 70-0025, U.S. Air Force, Feb. 1970. (Available from DDC as AD 707 865.)

25. Sinha, Ram; Fox, Herbert; and Weinberger, Lawrence: An Implicit Finite Difference Solution for Jet and Wake Problems. Pt. II: Program Manual. ARL 70-0024, U.S. Air Force, Feb. 1970. (Available from DDC as AD 707 866.)

26. Hopf, H.; and Fortune, O.: Diffusion Controlled Combustion for Scramjet Application. Pt. II – Programmer's Manual. Tech. Rep. 569 (Contract No. NAS 1-5117), Gen. Appl. Sci. Lab., Inc., Dec. 1965.

27. Halleen, R. M.: A Literature Review on Subsonic Free Turbulent Shear Flow. AFOSR-TN-5444, U.S. Air Force, Apr. 1964. (Available from DDC as AD 606 758.)

28. Wygnanski, I.; and Fiedler, H.: Some Measurements in the Self-Preserving Jet. J. Fluid Mech., vol. 38, pt. 3, Sept. 18, 1969, pp. 577-612.

29. Laderman, A. J.; and Demetriades, A.: Measurements of the Mean and Turbulent Flow in a Cooled-Wall Boundary Layer at Mach 9.37. AIAA Paper No. 72-73, Jan. 1972.

30. Fischer, M. C.; Maddalon, D. V.; Weinstein, L. M.; and Wagner, R. D., Jr.: Boundary-Layer Pitot and Hot-Wire Surveys at $M_\infty \approx 20$. AIAA J., vol. 9, no. 5, May 1971, pp. 826-834.

31. Johannesen, N. H.: Further Results on the Mixing of Free Axially-Symmetrical Jets of Mach Number 1.40. R. & M. No. 3292, Brit. A.R.C., 1962.

32. Warren, Walter R., Jr.: The Static Pressure Variation in Compressible Free Jets. J. Aeronaut. Sci., vol. 22, no. 3, Mar. 1955, pp. 205-207.

33. Pitkin, Edward T.; and Glassman, Irvin: Experimental Mixing Profiles of a Mach 2.6 Free Jet. J. Aerosp. Sci., vol. 25, no. 12, Dec. 1958, pp. 791-793.

34. Maydew, R. C.; and Reed, J. F.: Turbulent Mixing of Axisymmetric Compressible Jets (in the Half-Jet Region) With Quiescent Air. SC-4764(RR), Sandia Corp. (Albuquerque, N. Mex.), Mar. 1963.

35. Lee, Shen Ching: A Study of the Two-Dimensional Free Turbulent Mixing Between Converging Streams With Initial Boundary Layers. Ph. D. Diss., Univ. of Washington, 1966.

36. Jones, Barclay G.; and Spencer, Bruce W.: A Study of the Local Pressure Field in Turbulent Shear Flow and Its Relation to Aerodynamic Noise Generation. SR-2 (Grant No. NASA NGR 14-005-149), Univ. of Illinois, Jan. 31, 1971. (Available as NASA CR-119339.)

37. Miller, David R.; and Comings, Edward W.: Static Pressure Distribution in the Free Turbulent Jet. J. Fluid Mech., vol. 3, pt. 1, Oct. 1957, pp. 1-16.

38. Schetz, Joseph A.: Some Studies of the Turbulent Wake Problem. Astronaut. Acta, vol. 16, no. 2, Feb. 1971, pp. 107-117.

39. Donaldson, Coleman duP.: Calculation of Turbulent Shear Flows for Atmospheric and Vortex Motions. AIAA J., vol. 10, no. 1, Jan. 1972, pp. 4-12.

40. Sabin, C. M.: An Analytical and Experimental Study of the Plane, Incompressible, Turbulent Free Shear Layer With Arbitrary Velocity Ratio and Pressure Gradient. AFOSR-TN-5443, U.S. Air Force, Oct. 1963. (Available from DDC as AD 430 120.)

41. Tollmien, Walter: Berechnung turbulenter Ausbreitungsvorgänge. Z. Angew. Math. Mech., Bd. 6, Heft 6, Dec. 1926, pp. 468-478. (Available in English translation as NACA TM 1085, 1945.)

42. Cordes, G.: Untersuchungen zur statischen Druckmessung in turbulenter Strömung. Ing.-Arch., Bd. VIII, Heft 4, Aug. 1937, pp. 245-270.

43. Reichardt, Hans: Gesetzmässigkeiten der freien Turbulenz. VDI-Forschungsh. 414, 1942.

44. Gooderum, Paul B.; Wood, George P.; and Brevoort, Maurice J.: Investigation With an Interferometer of the Turbulent Mixing of a Free Supersonic Jet. NACA Rep. 963, 1950. (Supersedes NACA TN 1857.)

45. Bershader, D.; and Pai, S. I.: On Turbulent Jet Mixing in Two-Dimensional Supersonic Flow. J. Appl. Phys., vol. 21, no. 6, June 1950, p. 616.

46. Crane, L. J.: The Laminar and Turbulent Mixing of Jets of Compressible Fluid. Pt. II – The Mixing of Two Semi-Infinite Streams. J. Fluid Mech., vol. 3, pt. I, Oct. 1957, pp. 81-92.

47. Rhudy, J. P.; and Magnan, J. D., Jr.: Turbulent Cavity Flow Investigation at Mach Numbers 4 and 8. AEDC-TR-66-73, U.S. Air Force, June 1966. (Available from DDC as AD 483 748.)

48. Sirieix, M.; and Solignac, J. L.: Contribution a l'Etude Experimentale de la Couche de Melange Turbulent Isobare d'un Ecoulement Supersonique. Separated Flows, Pt. I, AGARD CP No. 4, May 1966, pp. 241-270.

49. Eggers, James M.: Velocity Profiles and Eddy Viscosity Distributions Downstream of a Mach 2.22 Nozzle Exhausting to Quiescent Air. NASA TN D-3601, 1966.

50. Hill, W. G., Jr.; and Page, R. H.: Initial Development of Turbulent, Compressible, Free Shear Layers. Trans. ASME, Ser. D: J. Basic Eng., vol. 91, no. 1, Mar. 1969, pp. 67-73.

51. Lock, R. C.: The Velocity Distribution in the Laminar Boundary Layer Between Parallel Streams. Quart. J. Mech. & Appl. Math., vol. IV, pt. 1, 1951, pp. 42-63.

52. Maestrello, L.; and McDaid, E.: Acoustic Characteristics of a High-Subsonic Jet. AIAA J., vol. 9, no. 6, June 1971, pp. 1058-1066.

53. Heck, P. H.: Jet Plume Characteristics of 72-Tube and 72-Hole Primary Suppressor Nozzles. T.M. No. 69-457 (FAA Contract FA-SS-67-7), Flight Propulsion Div., Gen. Elec. Co., July 1969.

54. Chriss, D. E.; and Paulk, R. A.: An Experimental Investigation of Subsonic Coaxial Free Turbulent Mixing. AEDC-TR-71-236, AFOSR-72-0237TR, U.S. Air Force, Feb. 1972. (Available from DDC as AD 737 098.)

55. Forstall, Walton, Jr.; and Shapiro, Ascher H.: Momentum and Mass Transfer in Coaxial Gas Jets. J. Appl. Mech., vol. 17, no. 4, Dec. 1950, pp. 399-408.

56. Chriss, D. E.: Experimental Study of the Turbulent Mixing of Subsonic Axisymmetric Gas Streams. AEDC-TR-68-133, U.S. Air Force, Aug. 1968. (Available from DDC as AD 672 975.)

57. Eggers, James M.; and Torrence, Marvin G.: An Experimental Investigation of the Mixing of Compressible-Air Jets in a Coaxial Configuration. NASA TN D-5315, 1969.

58. Eggers, James M.: Turbulent Mixing of Coaxial Compressible Hydrogen-Air Jets. NASA TN D-6487, 1971.

59. Chevray, Renè; and Kovasznay, Leslie S. G.: Turbulence Measurements in the Wake of a Thin Flat Plate. AIAA J., vol. 7, no. 8, Aug. 1969, pp. 1641-1643.

60. Chevray, R.: The Turbulent Wake of a Body of Revolution. Trans. ASME, Ser. D: J. Basic Eng., vol. 90, no. 2, June 1968, pp. 275-284.

61. Demetriades, Anthony: Turbulent Mean-Flow Measurements in a Two-Dimensional Supersonic Wake. Phys. Fluids, vol. 12, no. 1, Jan. 1969, pp. 24-32.

62. Demetriades, Anthony: Mean-Flow Measurements in an Axisymmetric Compressible Turbulent Wake. AIAA J., vol. 6, no. 3, Mar. 1968, pp. 432-439.

63. Demetriades, Anthony: Observations on the Transition Process of Two-Dimensional Supersonic Wakes. AIAA J., vol. 9, no. 11, Nov. 1971, pp. 2128-2134.

64. Demetriades, Anthony: Observations on the Transition Process of Two-Dimensional Supersonic Wakes. AIAA Paper No. 70-793, June-July 1970.

65. Harris, Julius E.: Numerical Solution of the Equations for Compressible Laminar, Transitional, and Turbulent Boundary Layers and Comparisons With Experimental Data. NASA TR R-368, 1971.

66. Dhawan, S.; and Narasimha, R.: Some Properties of Boundary Layer Flow During the Transition From Laminar to Turbulent Motion. J. Fluid Mech., vol. 3, pt. 4, Jan. 1958, pp. 418-436.

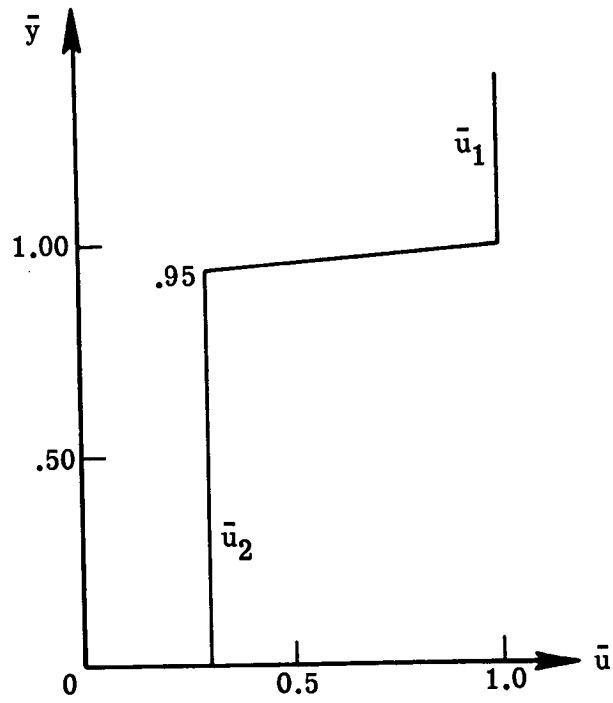

Figure 1.- Initial velocity profile used in two-dimensional shear-layer calculations. Test cases 1 to 3.

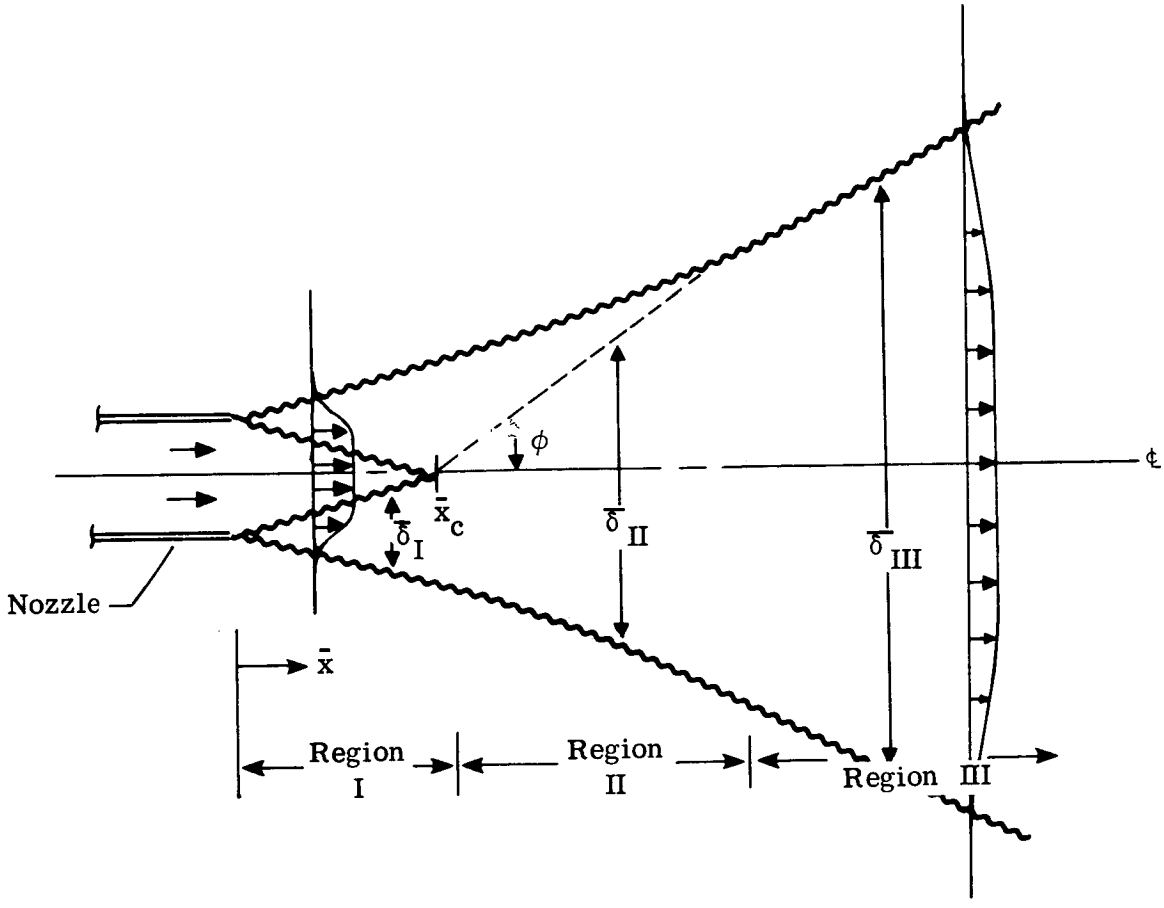

Figure 2.- Definition of mixing region width for jets issuing into still air.

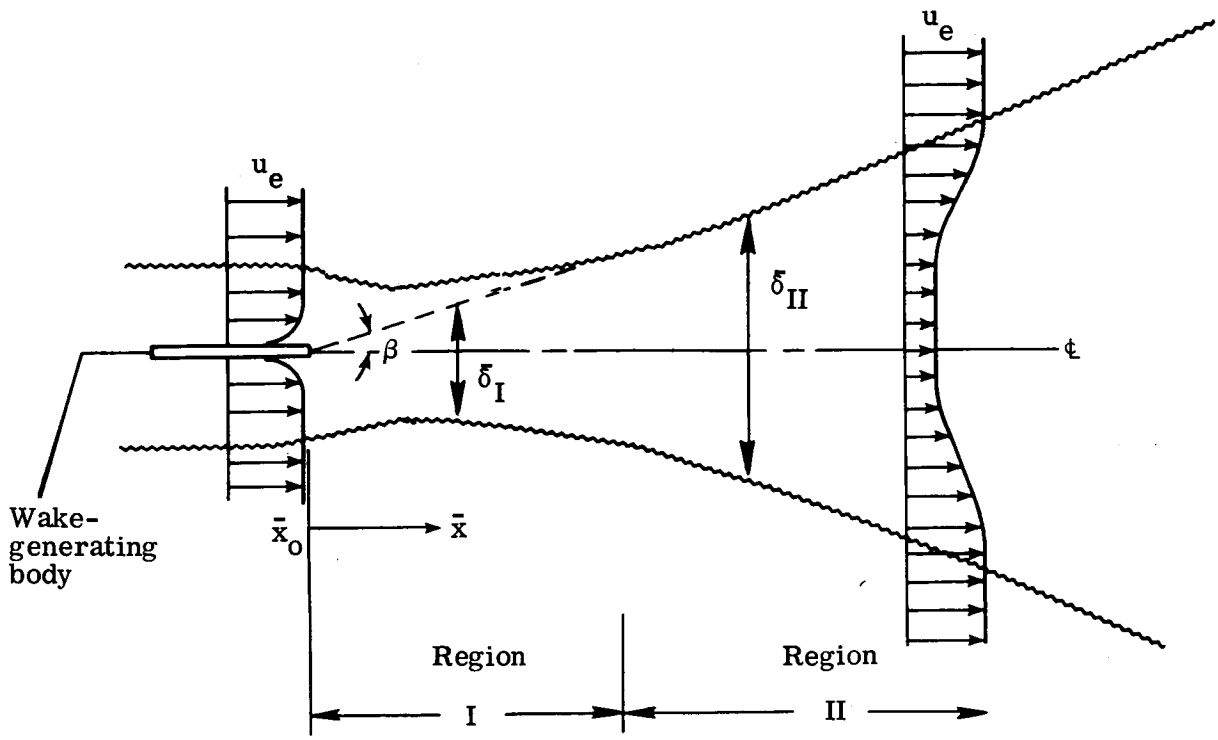

Figure 3.- Definition of mixing region width for wake flows.

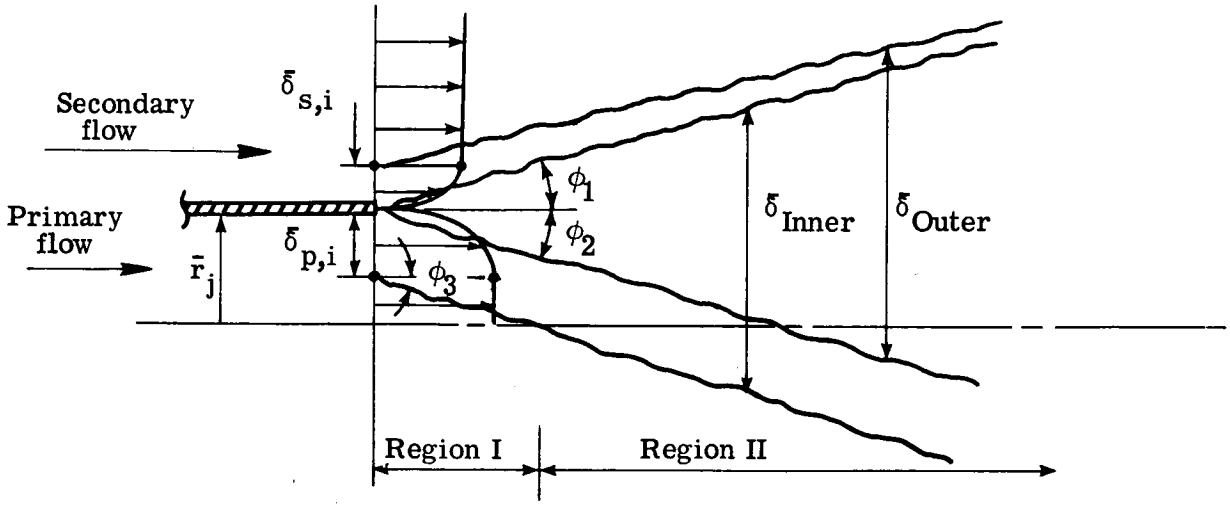

(a) Sketch of idealized flow field.

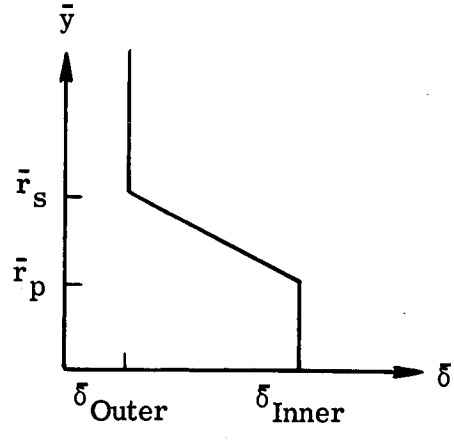

(b) Variation of $\bar{\delta}$ with $\bar{y}$.

Figure 4.- Definition of mixing region width for coaxial jet flows.

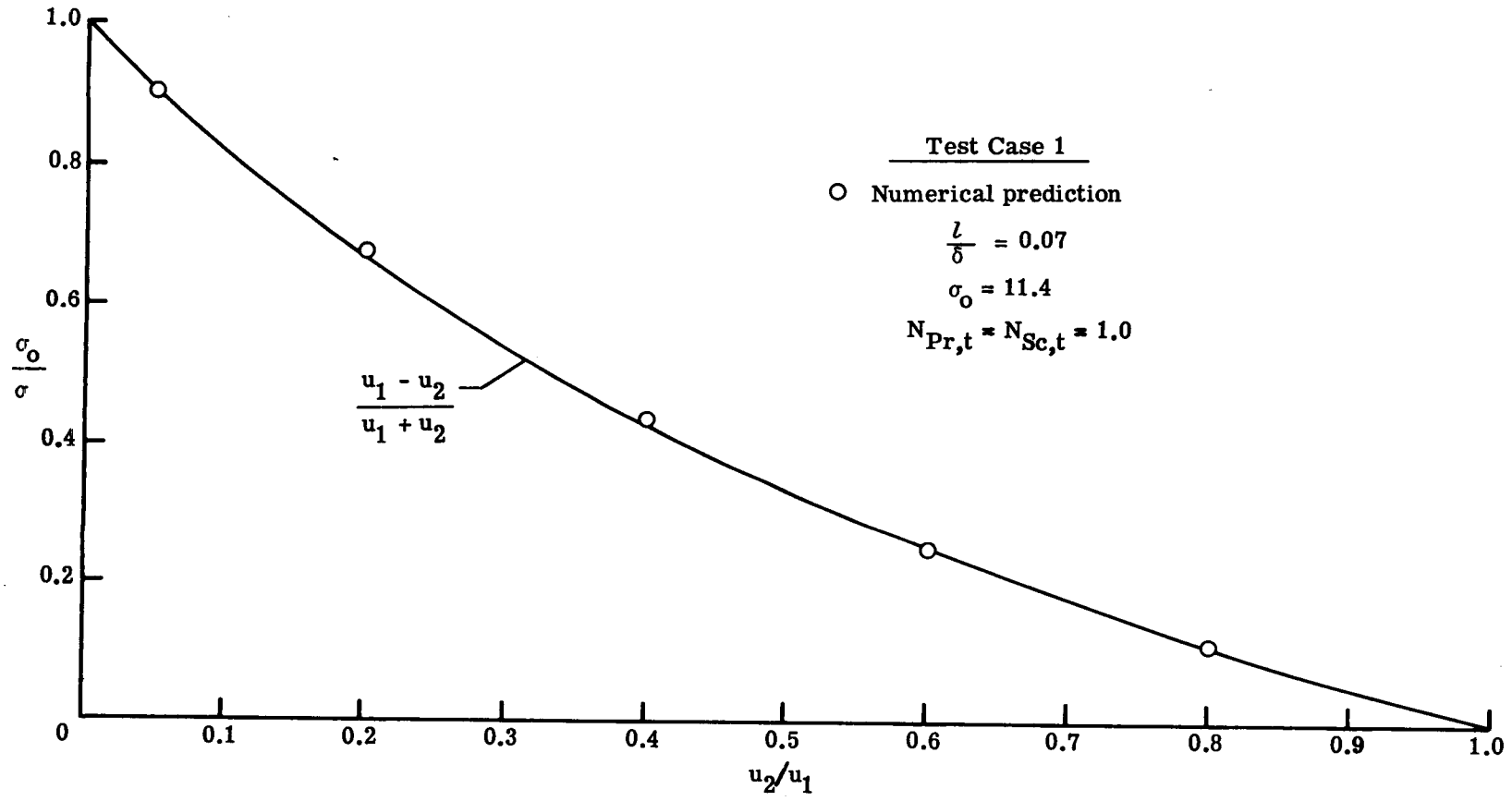

Figure 5.- Variation of spreading parameter with velocity ratio for two-dimensional subsonic constant-density free shear layers. Test case 1.

Symbol	Author	Date	Reference
▽	Tollmien	1926	41
◇	Cordes	1937	42
○	Reichardt	1942	43
▱	Liepmann and Laufer	1947	12
◸	Gooderum, Wood, and Brevoort	1949	44
◸	Bershader and Pai	1950	45
◇	Crane	1957	46
□	Johannesen	1959	31
△	Maydew and Reed	1963	34
◇	Rhudy and Magnan	1966	47
○	Sirieix and Solignac	1966	48
▱	Eggers	1966	49
▽	Hill and Page	1969	50
◸	Wygnanski and Fiedler	1969	28
▷	Morrisette and Birch	1972	Unpublished

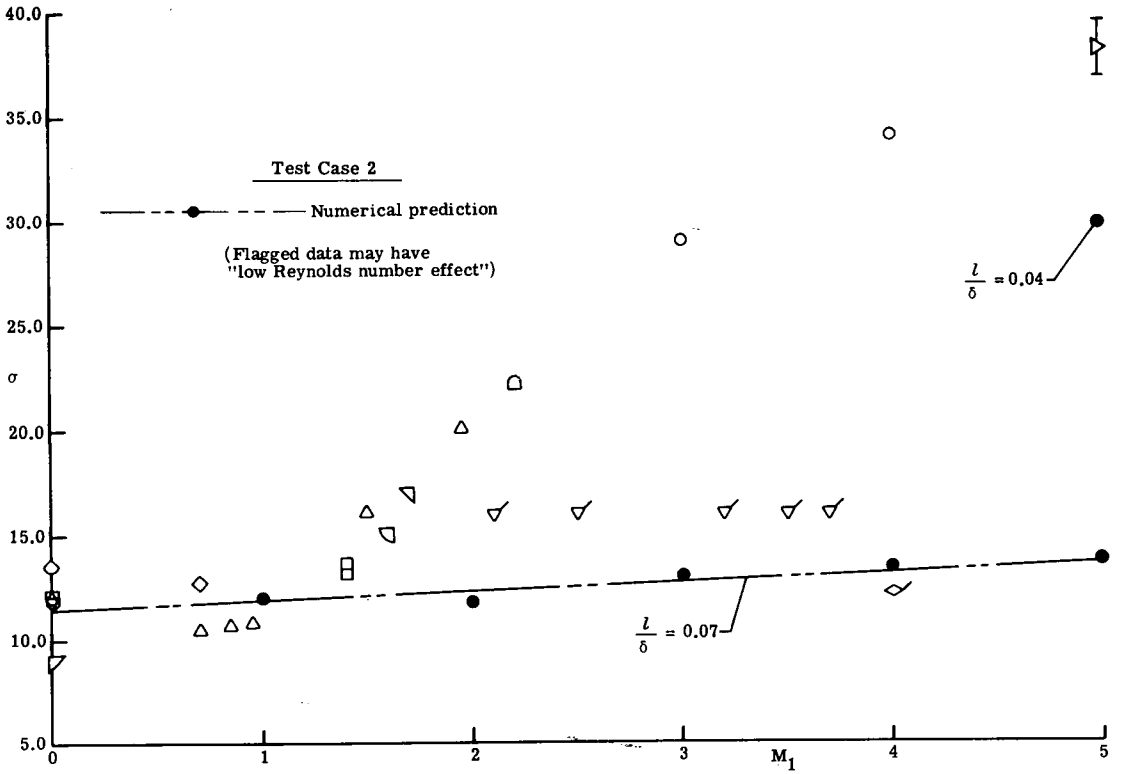

Figure 6.- Effect of Mach number on spreading parameter for two-dimensional free shear layers. Test case 2.

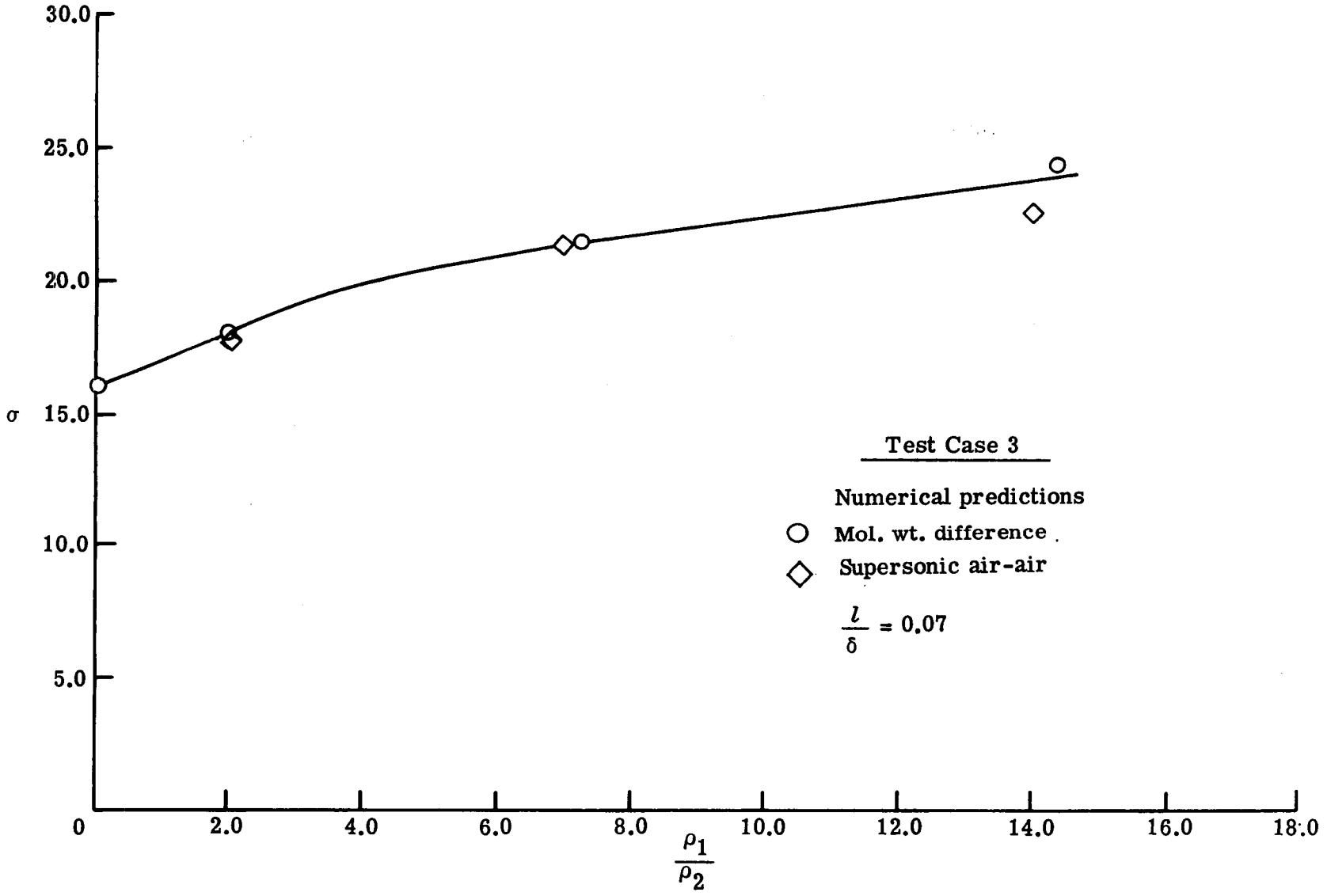

Figure 7.- Prediction of spreading parameter for two-dimensional variable-density free shear layers. Test case 3.

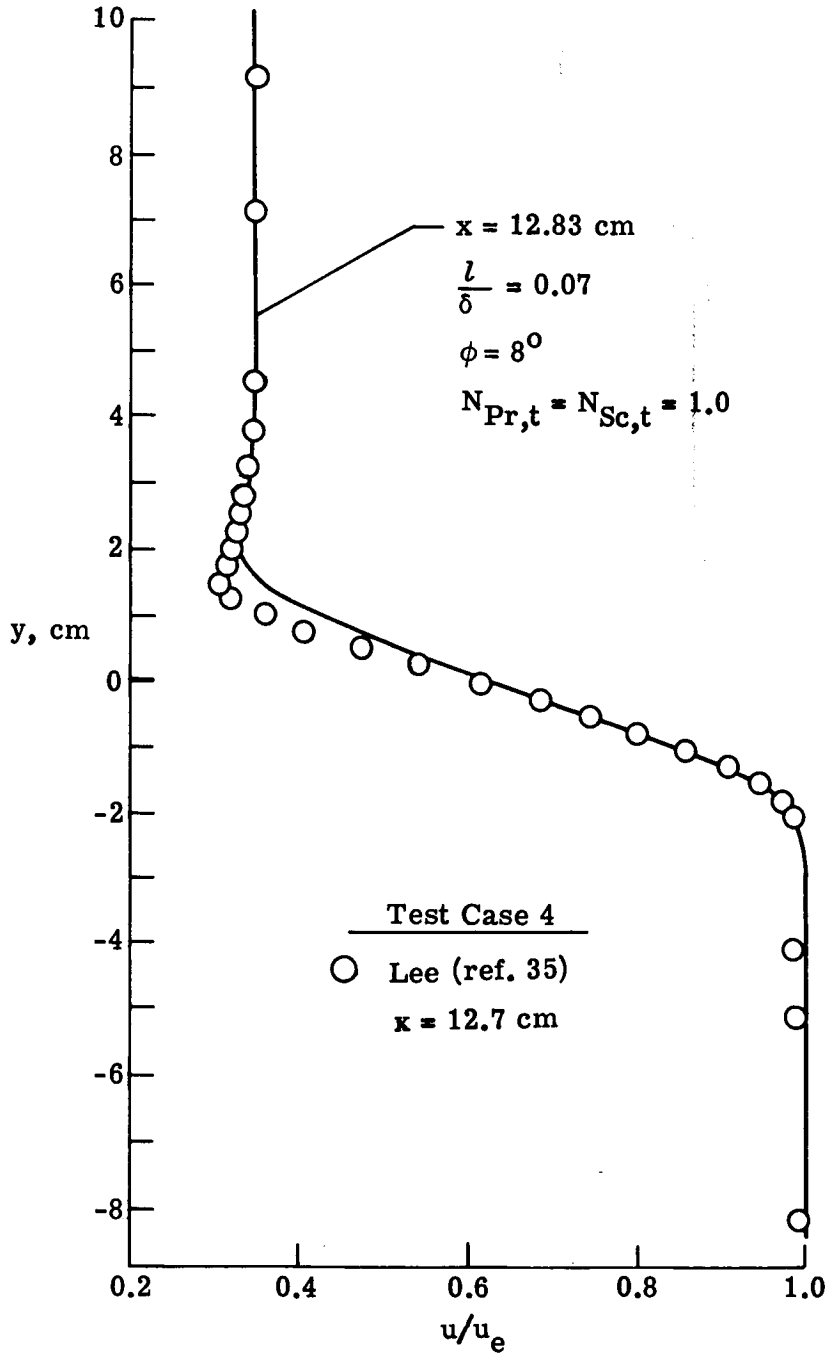

(a) x = 12.7 cm.

Figure 8.- Predicted and experimental velocity profiles. Test case 4.

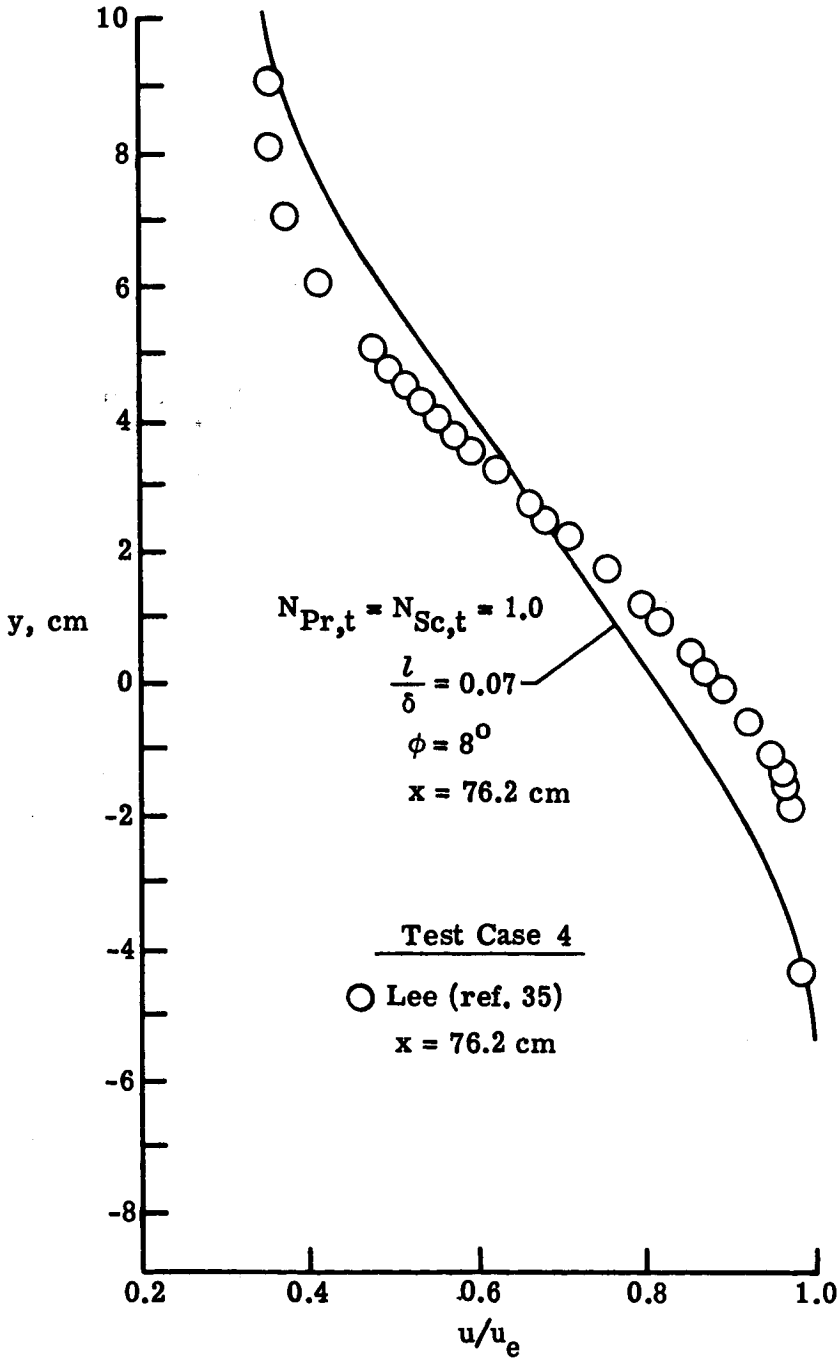

(b) x = 76.2 cm.

Figure 8.- Concluded.

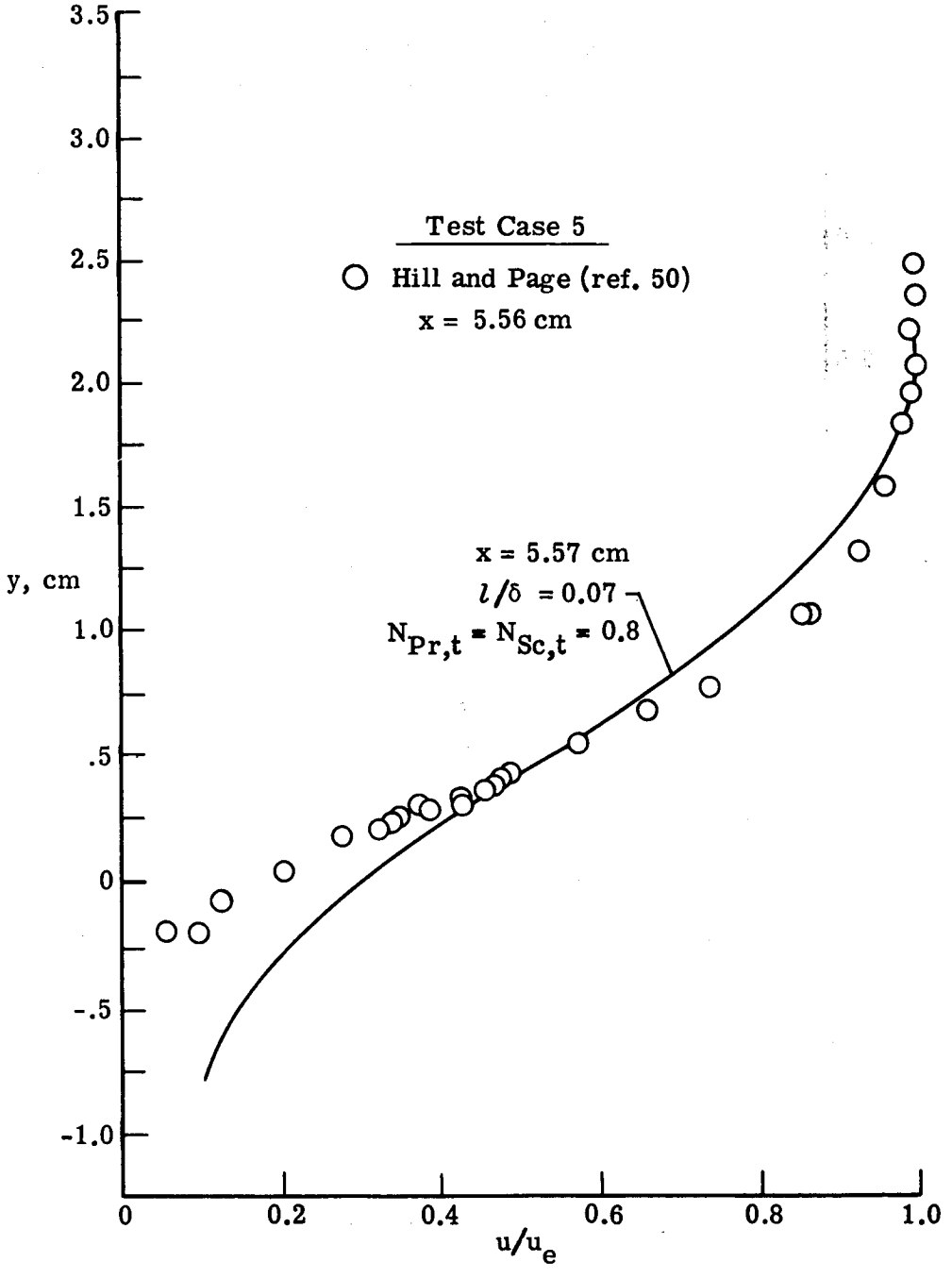

(a) x = 5.57 cm.

Figure 9.- Predicted and experimental velocity profiles. Test case 5.

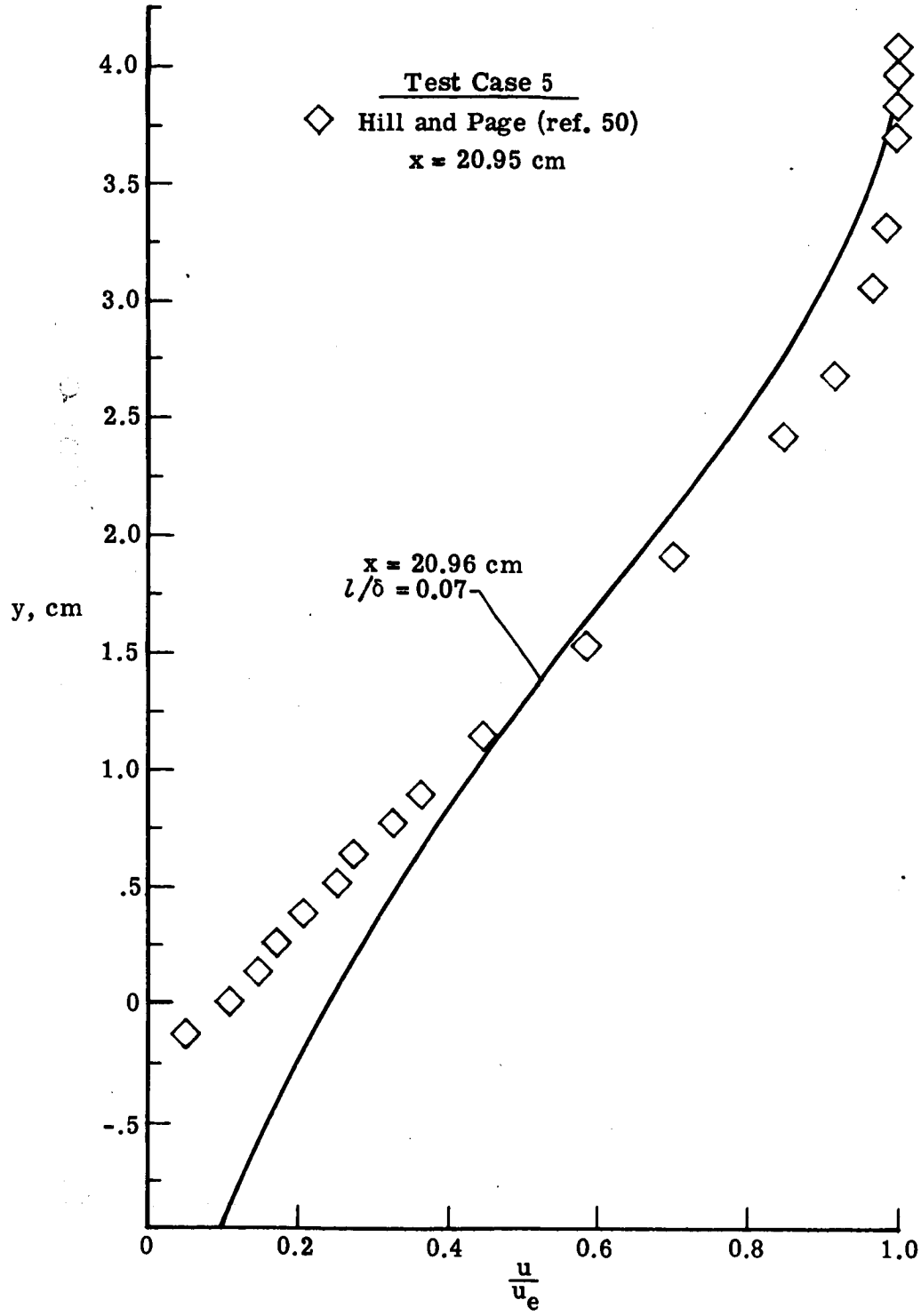

(b) x = 20.95 cm.

Figure 9.- Concluded.

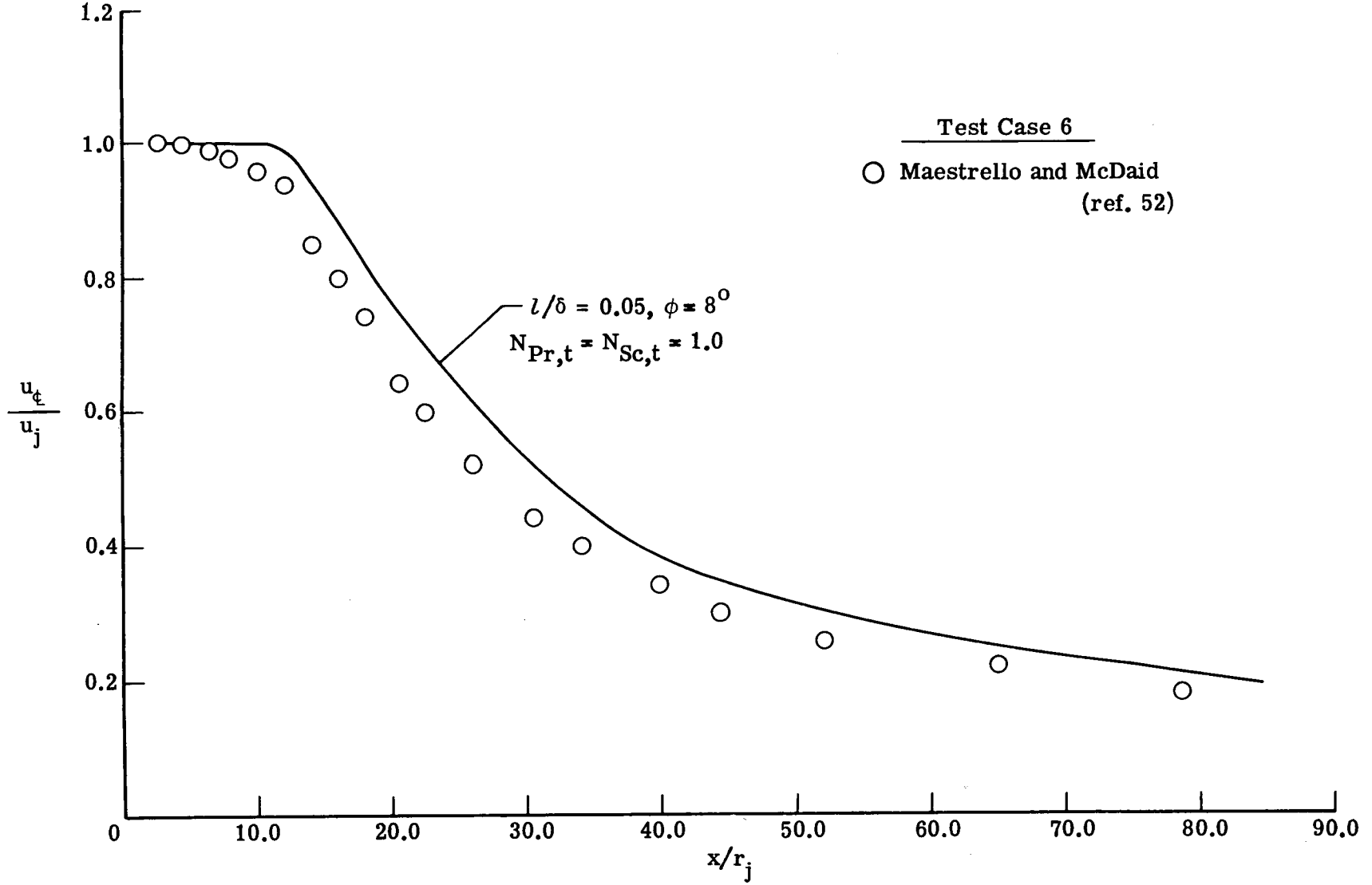

Figure 10.- Predicted and experimental center-line velocity distribution for a subsonic axisymmetric jet issuing into still air. Test case 6.

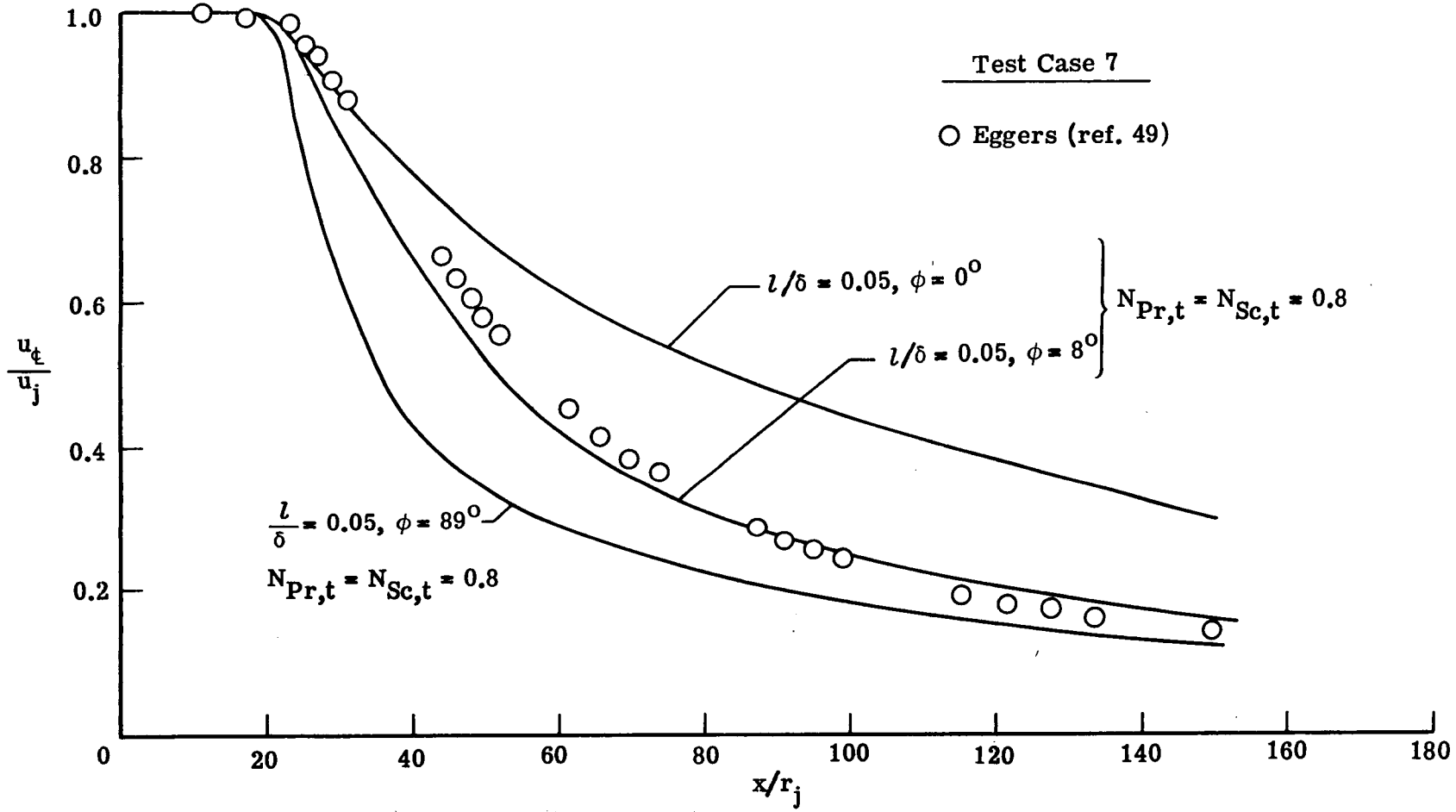

(a) Center-line distribution.

Figure 11.- Predicted and experimental velocity for a supersonic axisymmetric jet issuing into still air. Test case 7.

Test Case 7

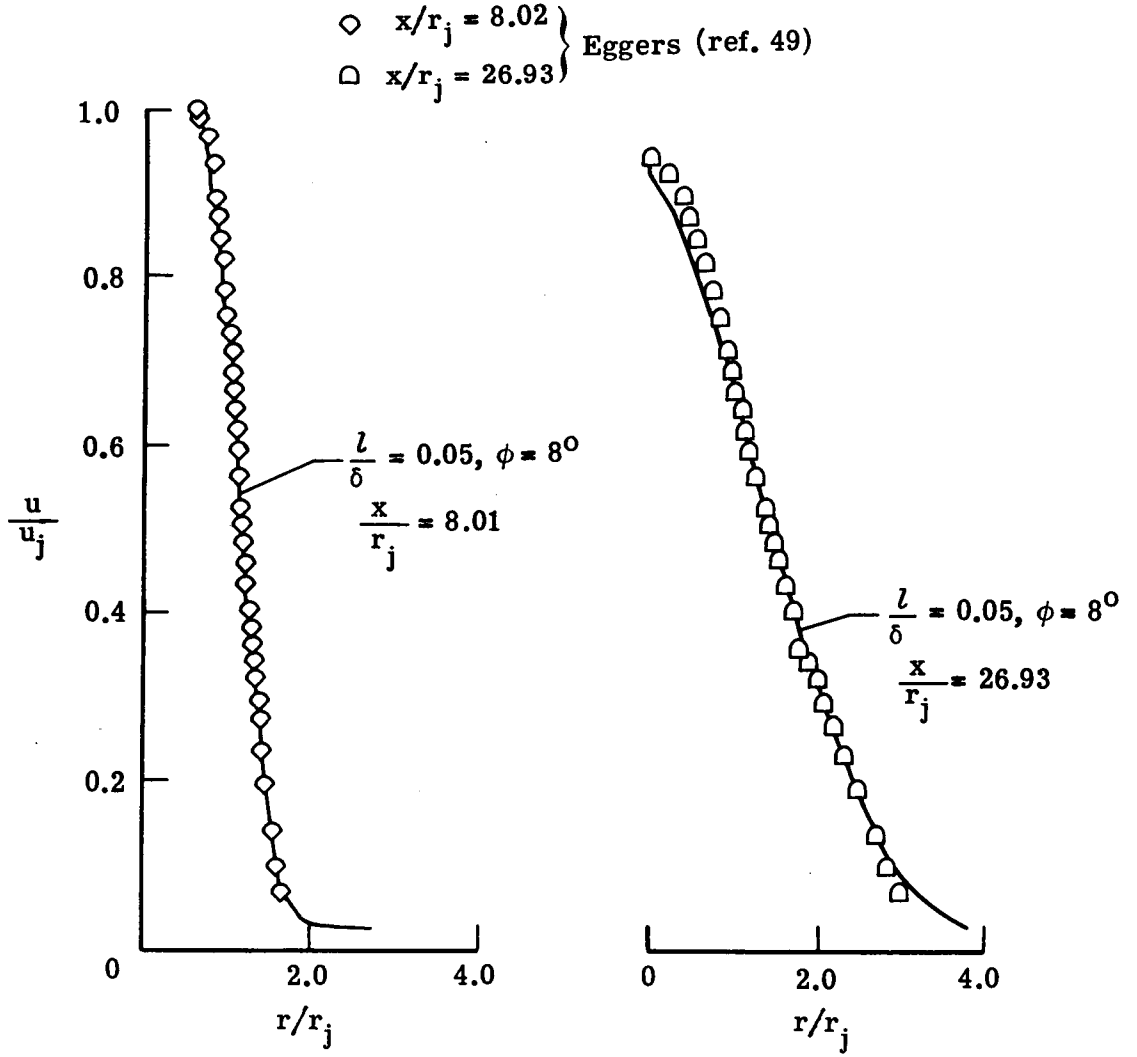

(b) Profiles at $x/r_j \approx 8$.

(c) Profiles at $x/r_j \approx 27$.

Figure 11.- Continued.

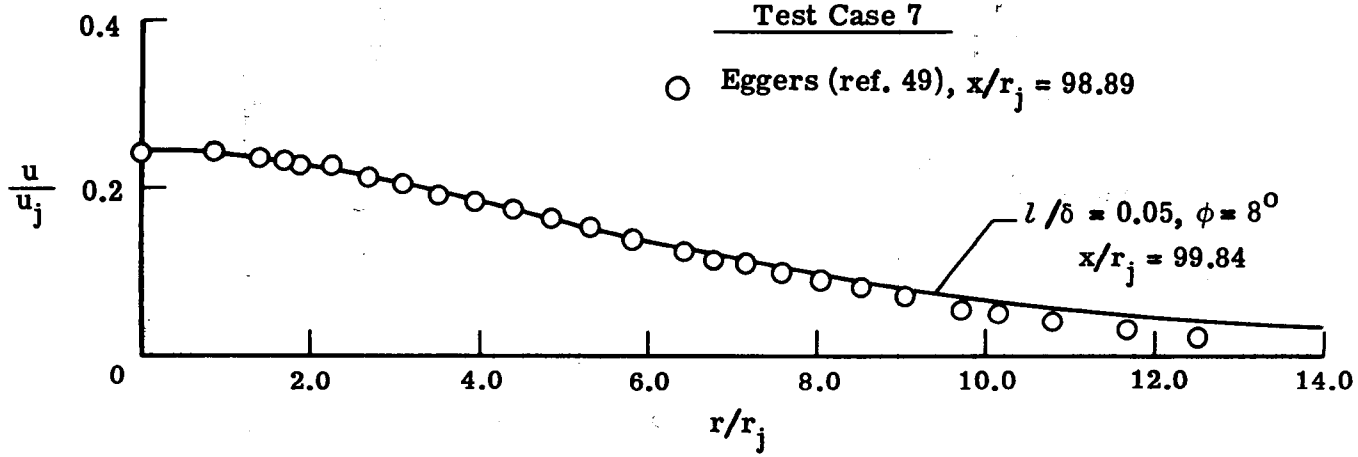

(d) Profiles at $x/r_j \approx 99$.

Figure 11.- Concluded.

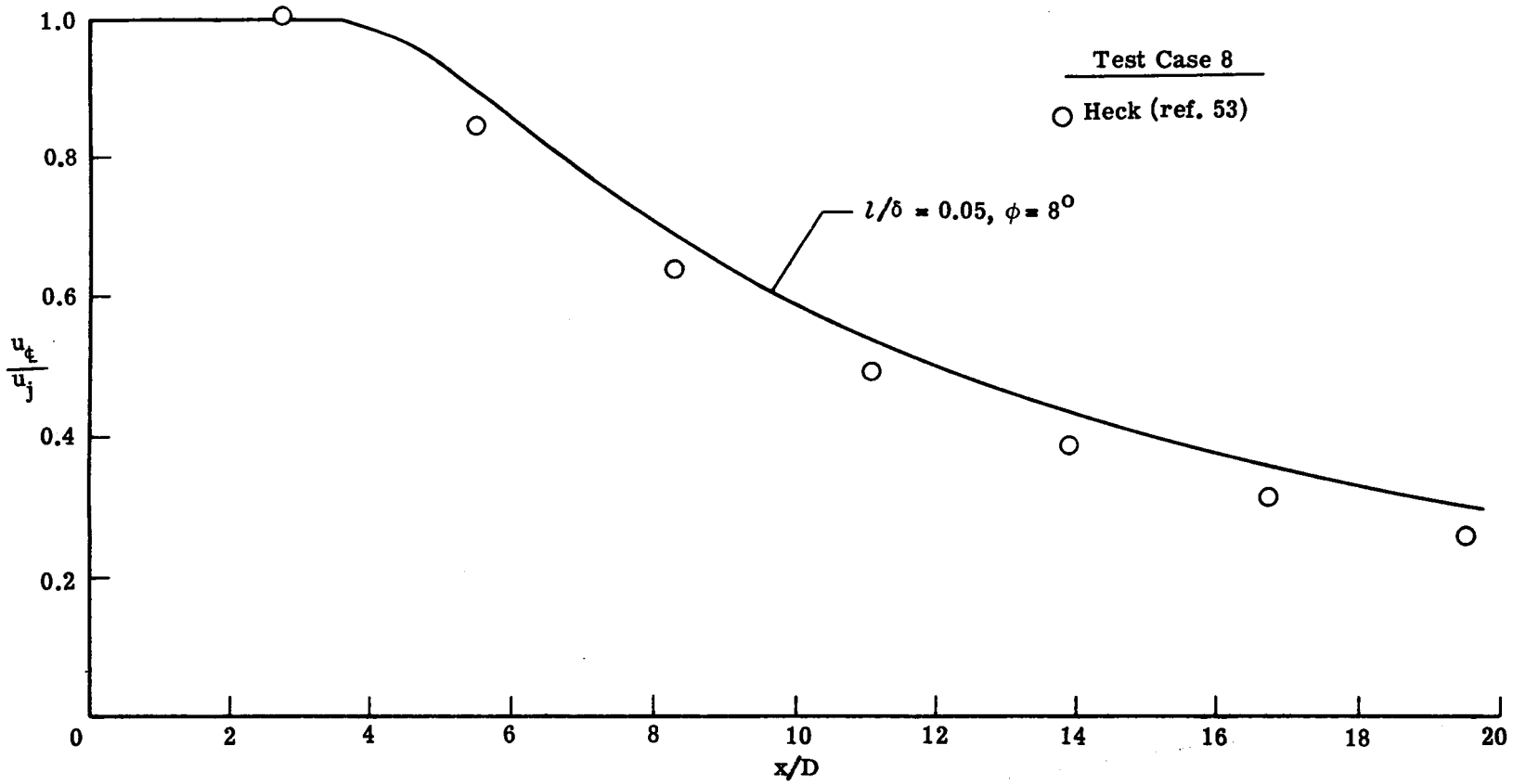

(a) Velocity.

Figure 12.- Predicted and experimental center-line distribution for high-temperature axisymmetric jet issuing into still air. Test case 8.

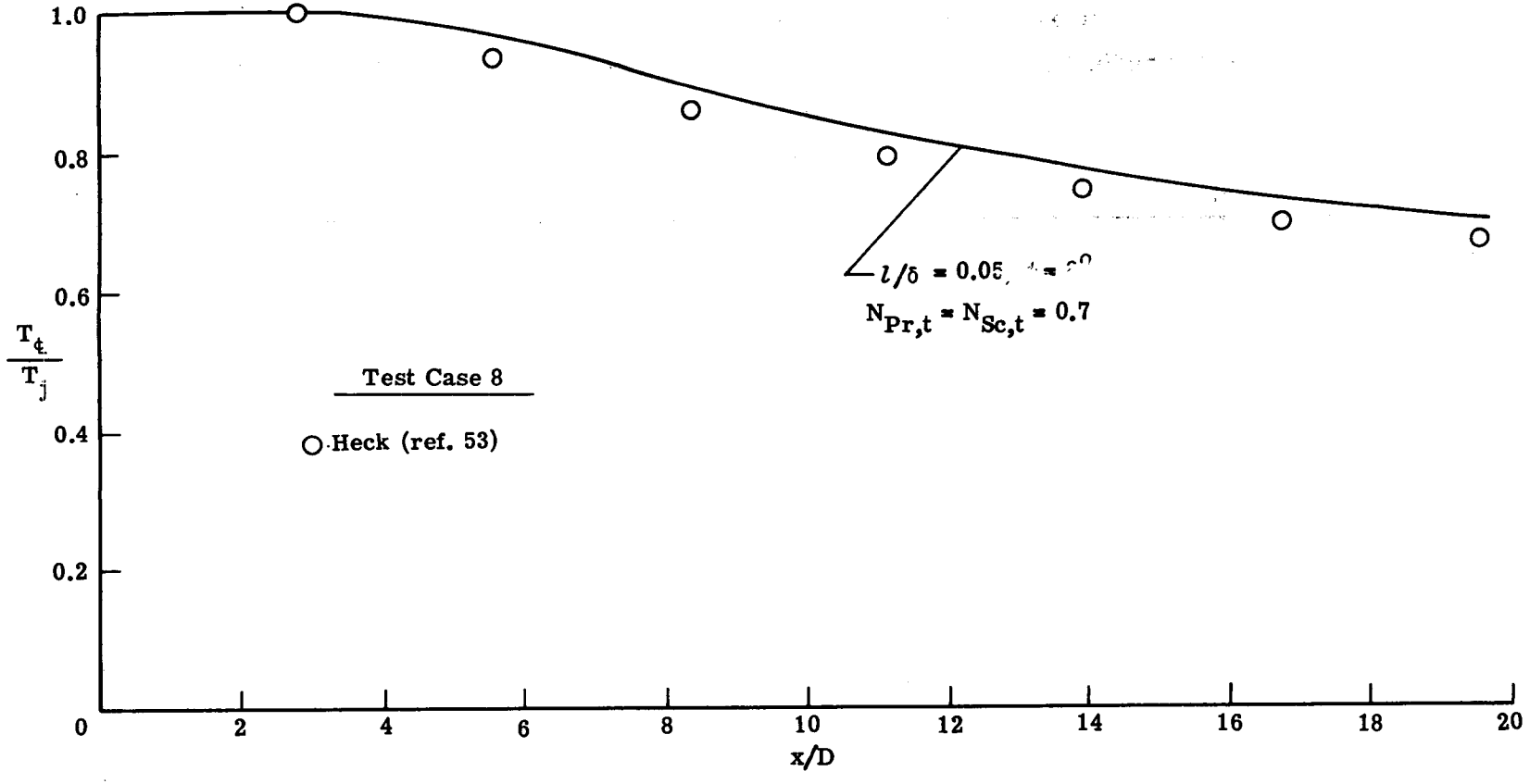

(b) Static temperature.

Figure 12.- Concluded.

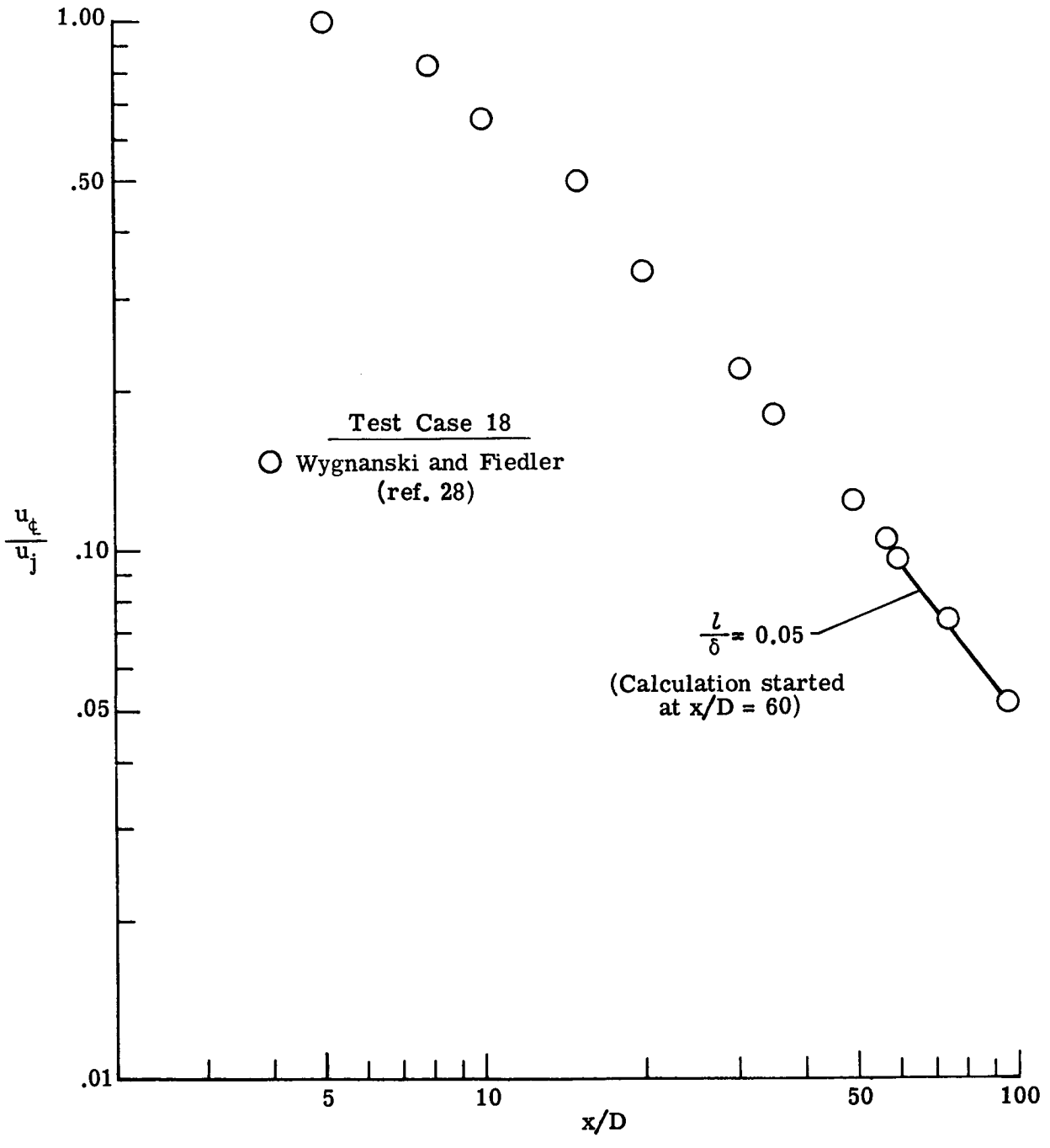

(a) Center-line distribution.

Figure 13.- Predicted and experimental velocity for the far field of an axisymmetric jet issuing into still air. Test case 18.

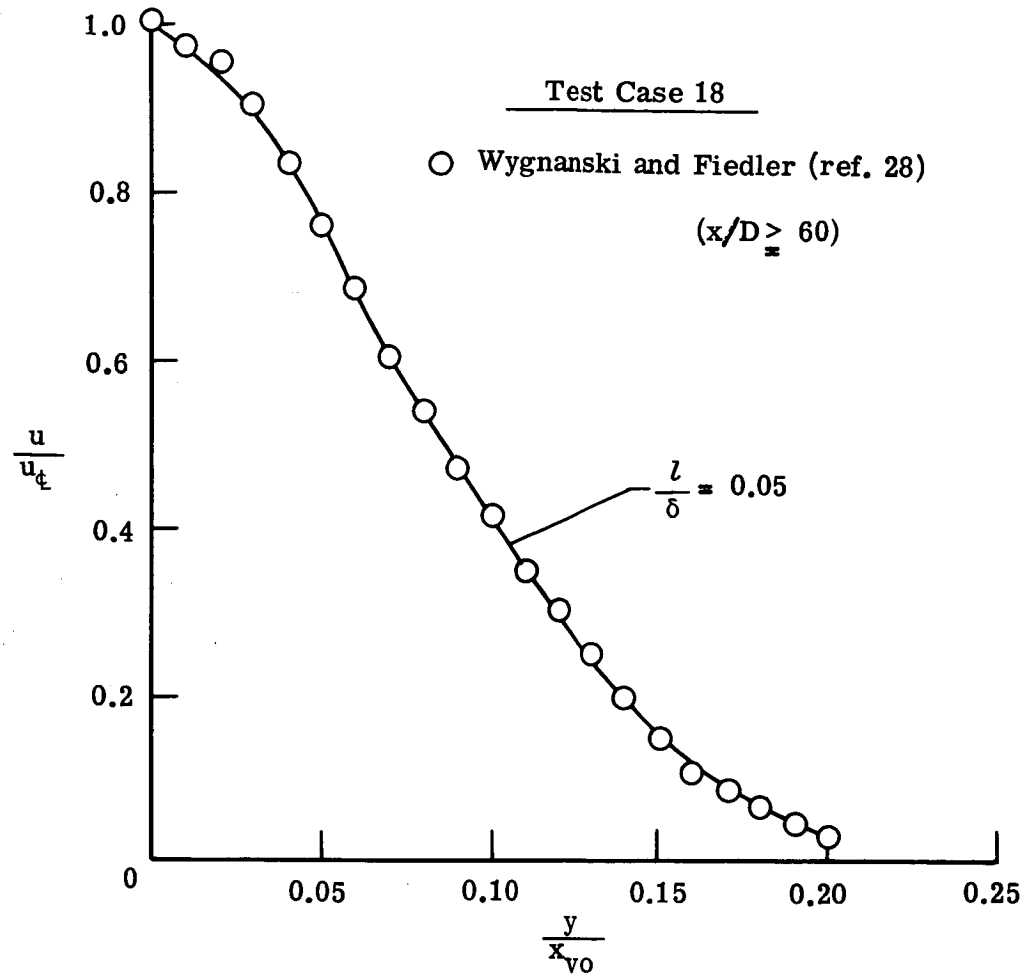

(b) Similarity profiles.

Figure 13.- Concluded.

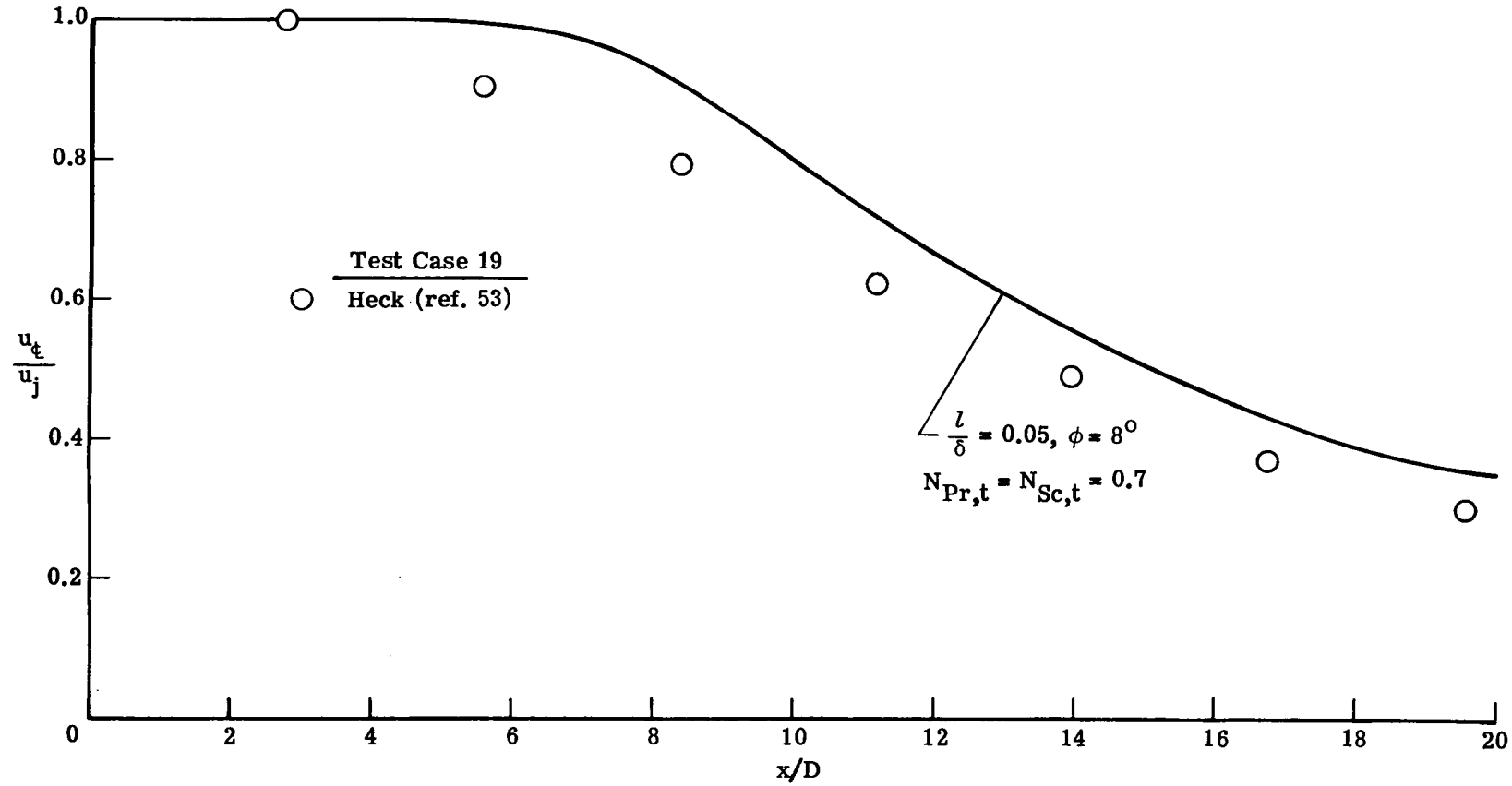

(a) Velocity.

Figure 14.- Predicted and experimental center-line distribution for high-temperature supersonic axisymmetric jet issuing into still air. Test case 19.

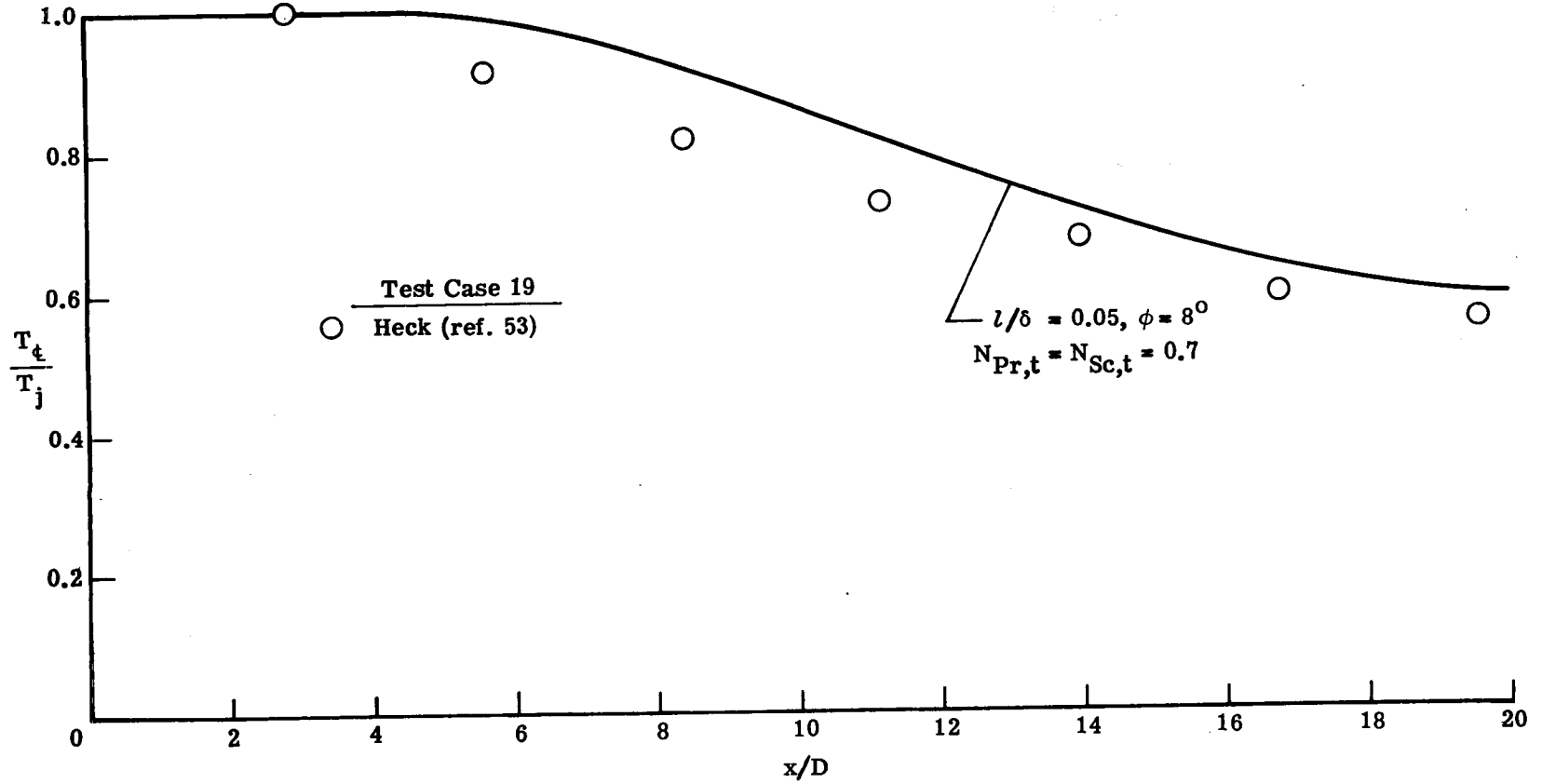

(b) Static temperature.

Figure 14.- Concluded.

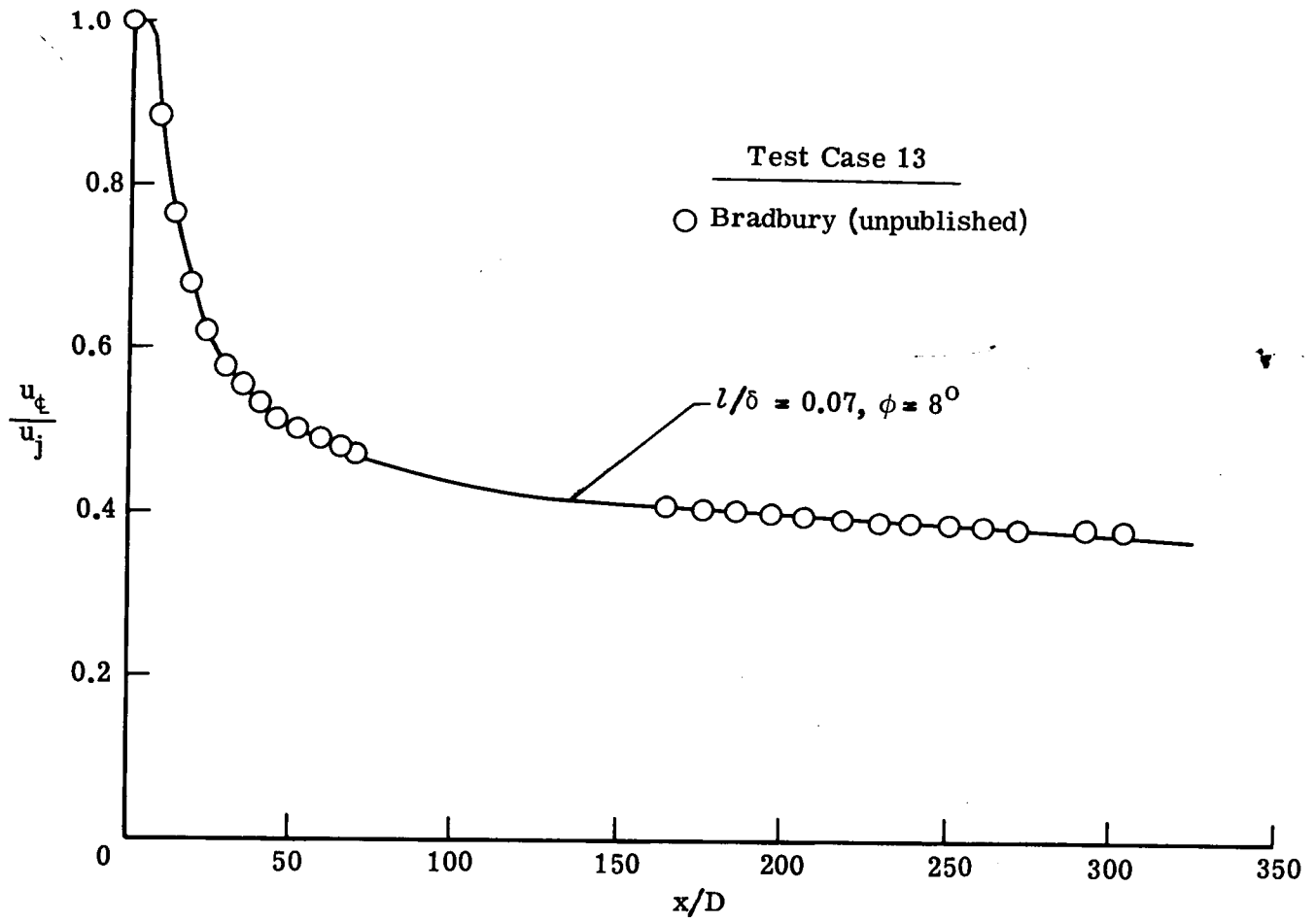

Figure 15.- Predicted and experimental center-line velocity for two-dimensional jet in a moving stream. Test case 13.

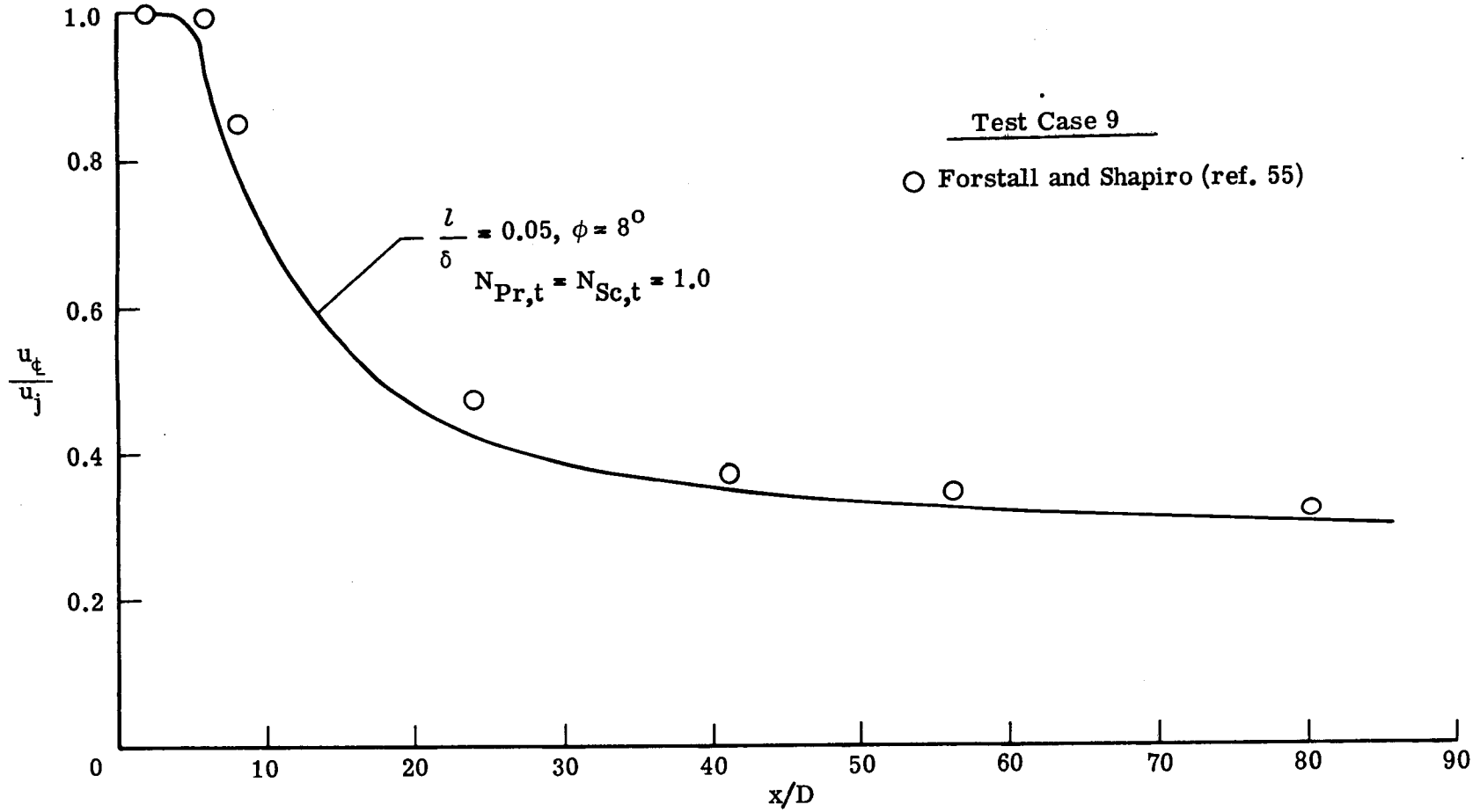

Figure 16.- Predicted and experimental center-line velocity for coaxial air jets. Test case 9.

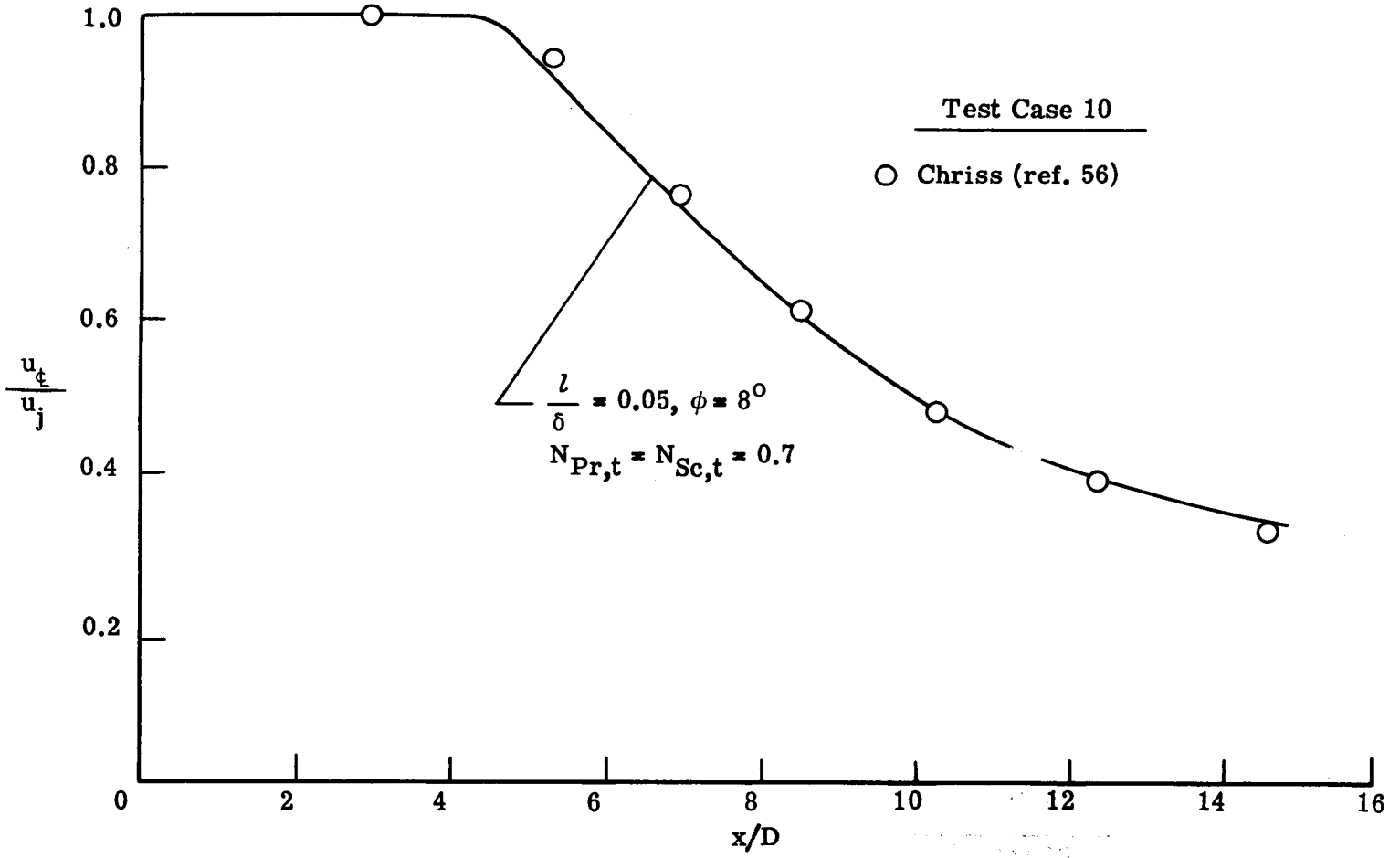

(a) Velocity.

Figure 17.- Predicted and experimental center-line distribution for subsonic hydrogen-air coaxial flow. Test case 10.

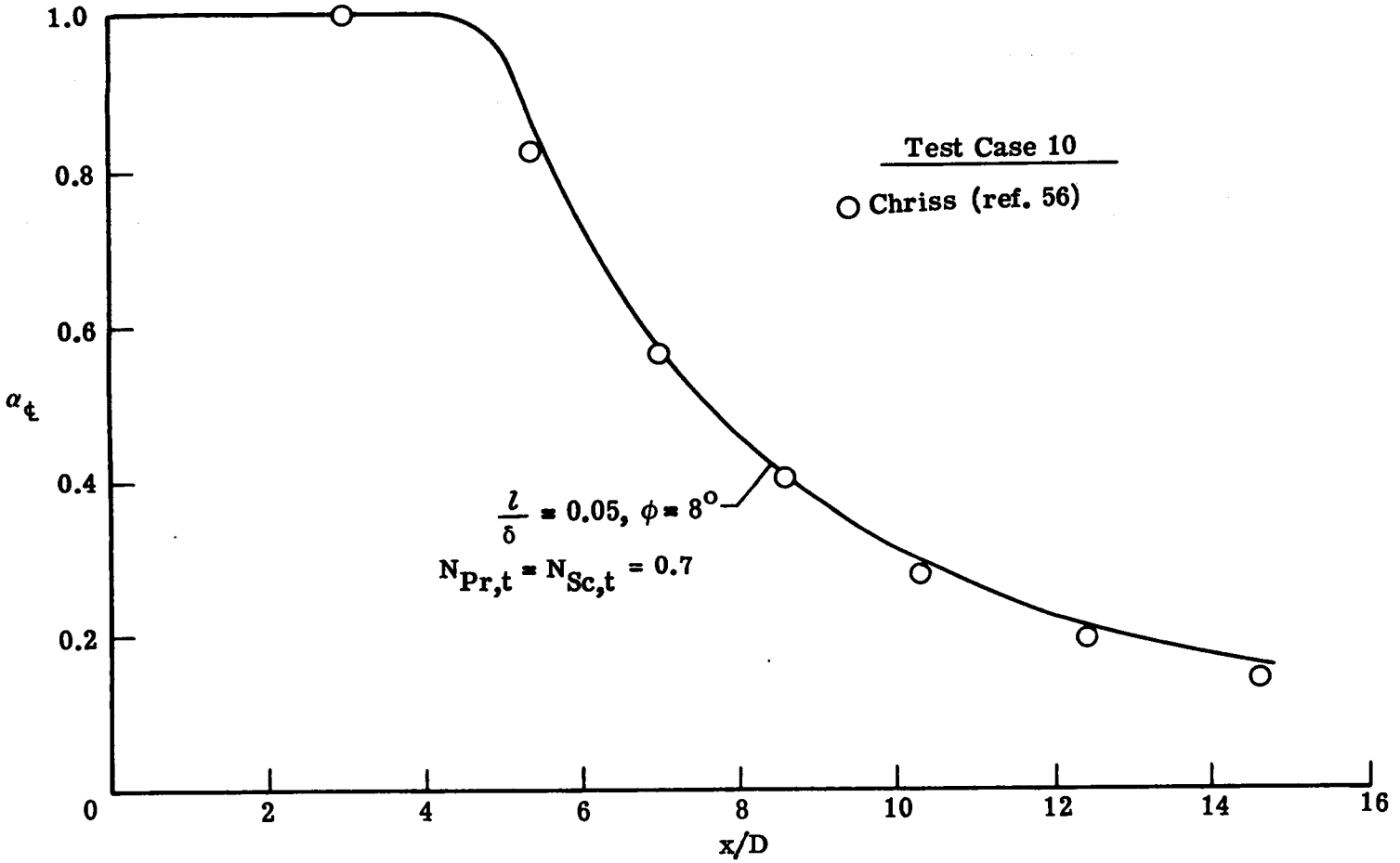

(b) Mass fraction of hydrogen.

Figure 17.- Concluded.

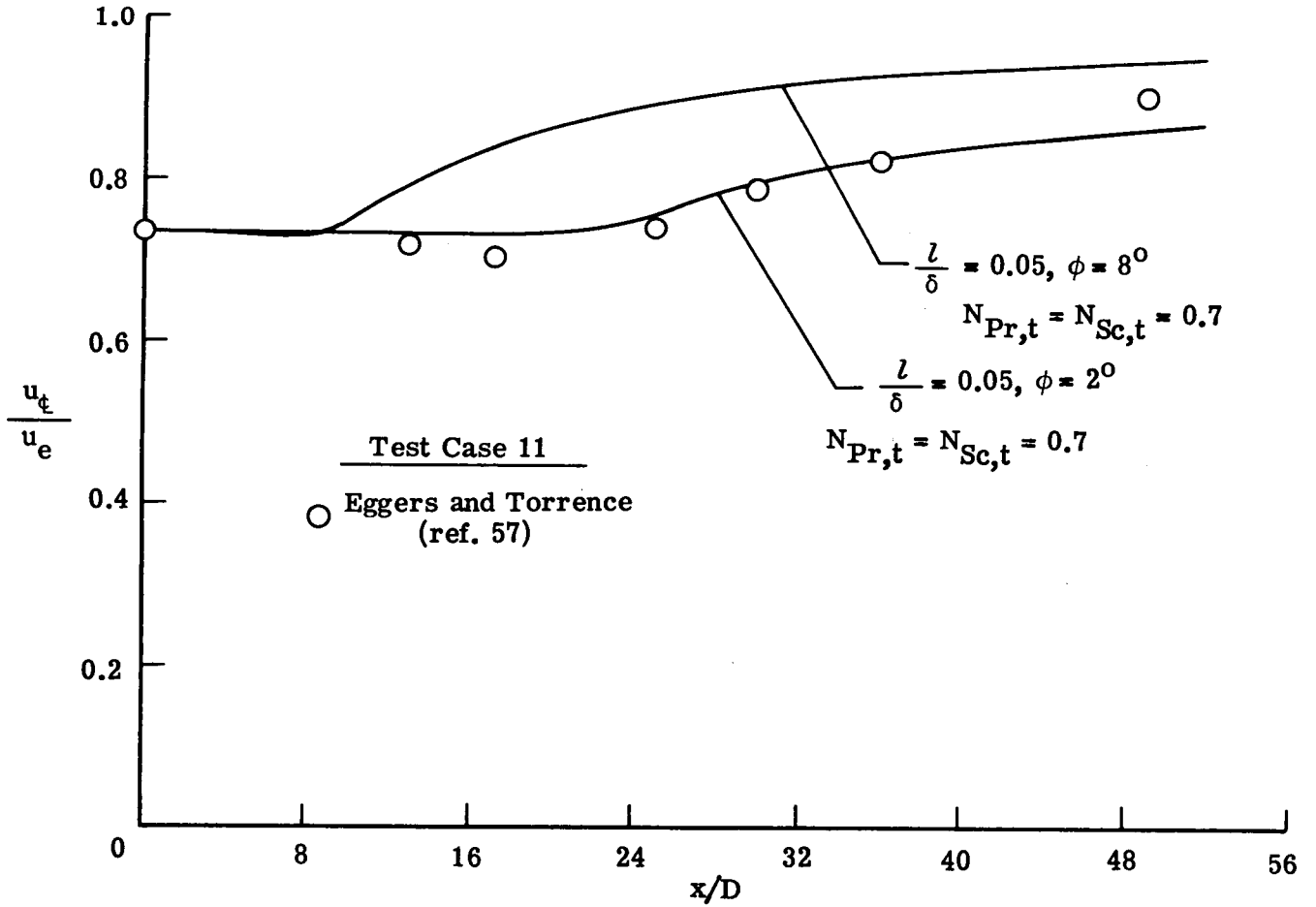

Figure 18.- Predicted and experimental center-line velocity for air-air coaxial jets. Test case 11.

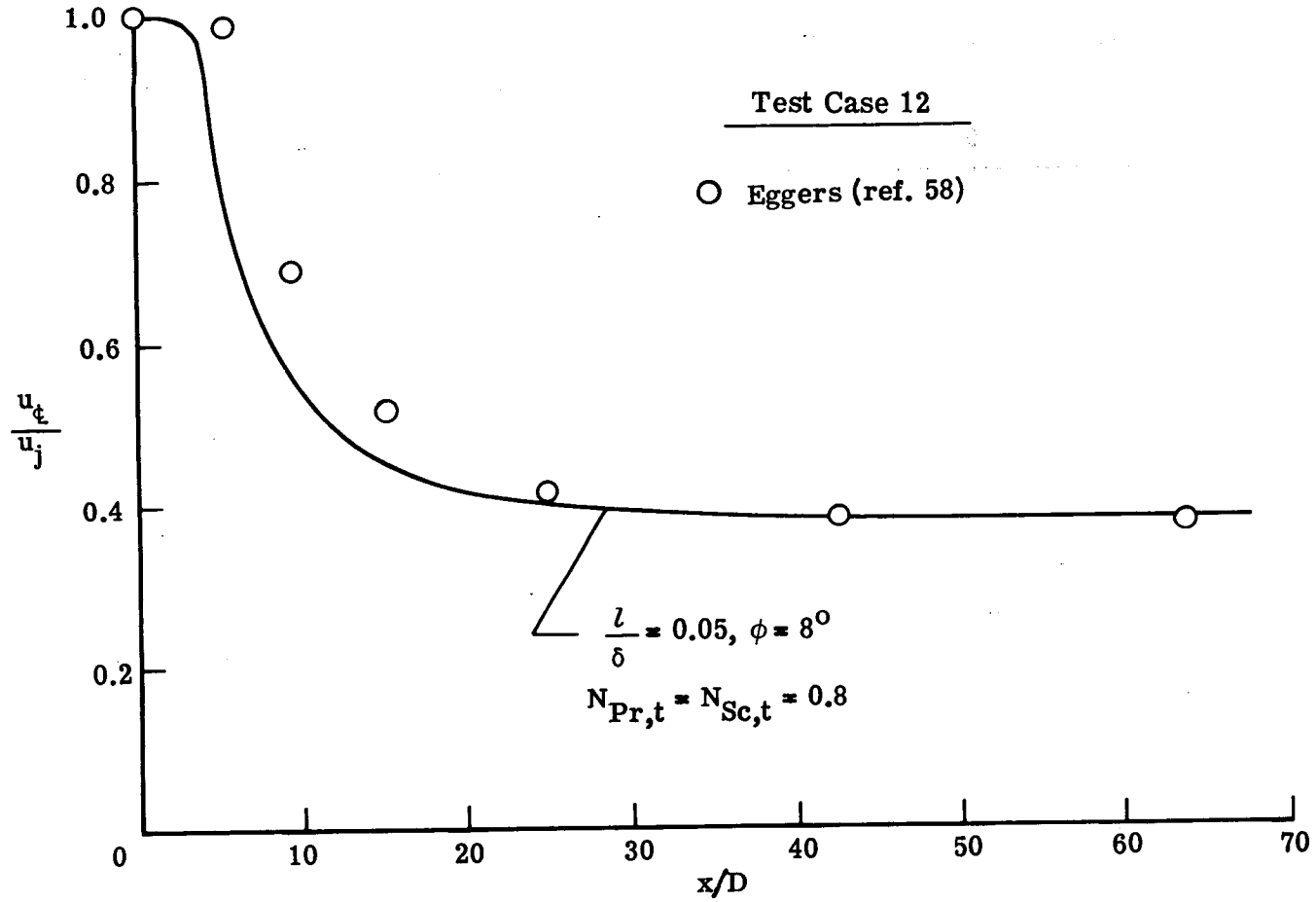

(a) Velocity.

Figure 19.- Predicted and experimental center-line distribution for hydrogen-air coaxial jets. Test case 12.

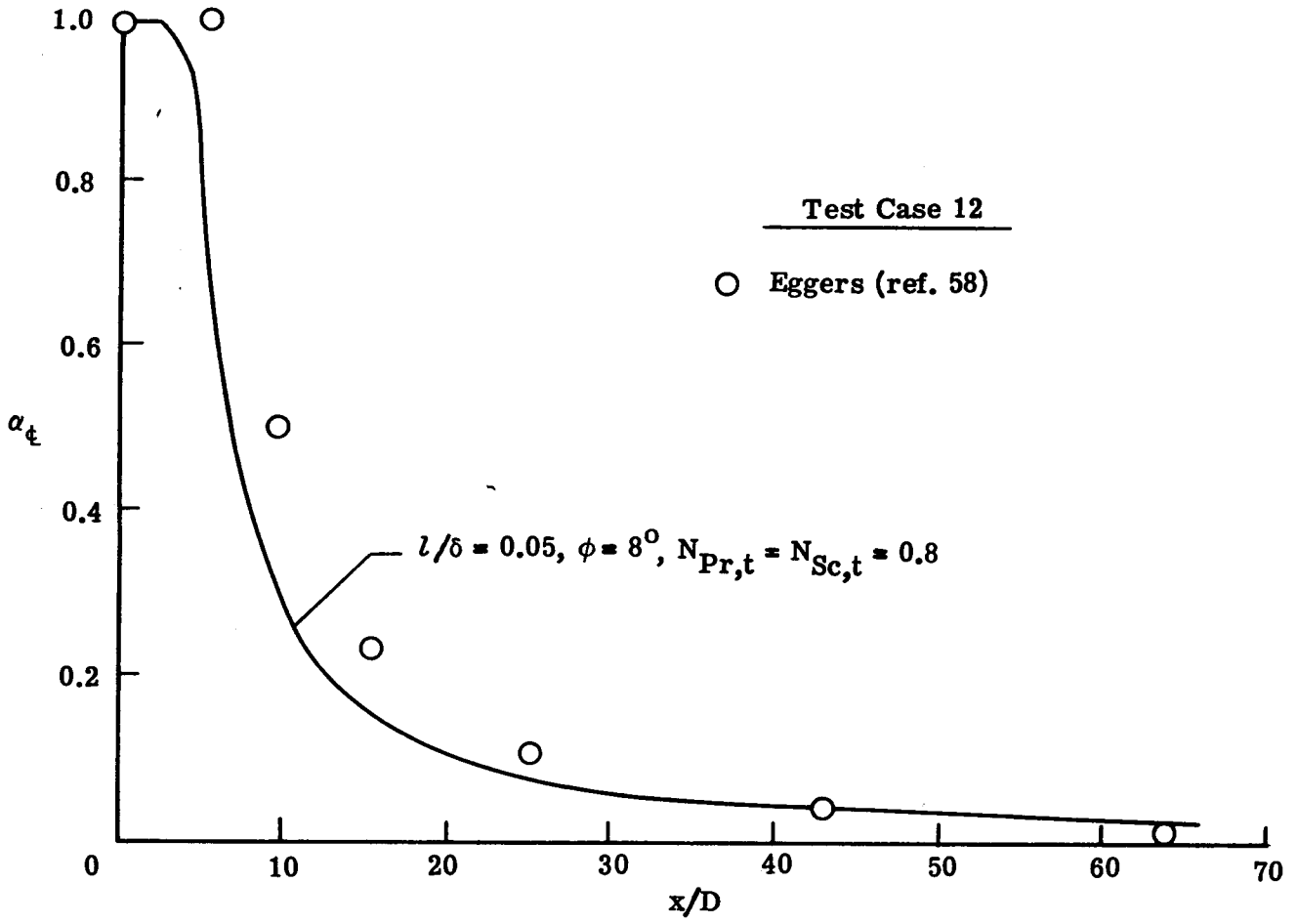

(b) Mass fraction of hydrogen.

Figure 19.- Concluded.

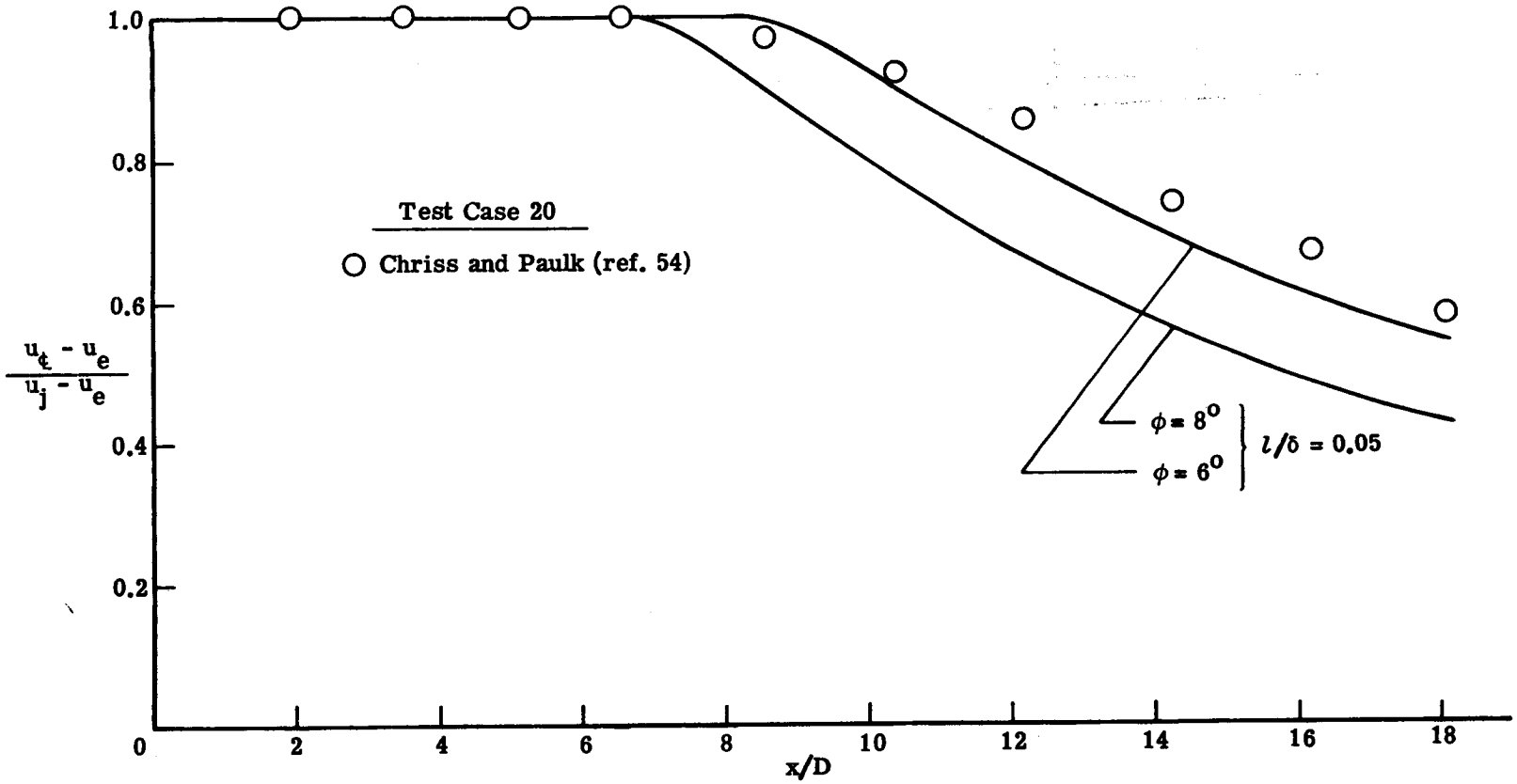

Figure 20.- Predicted and experimental center-line velocity for subsonic coaxial air jets. Test case 20.

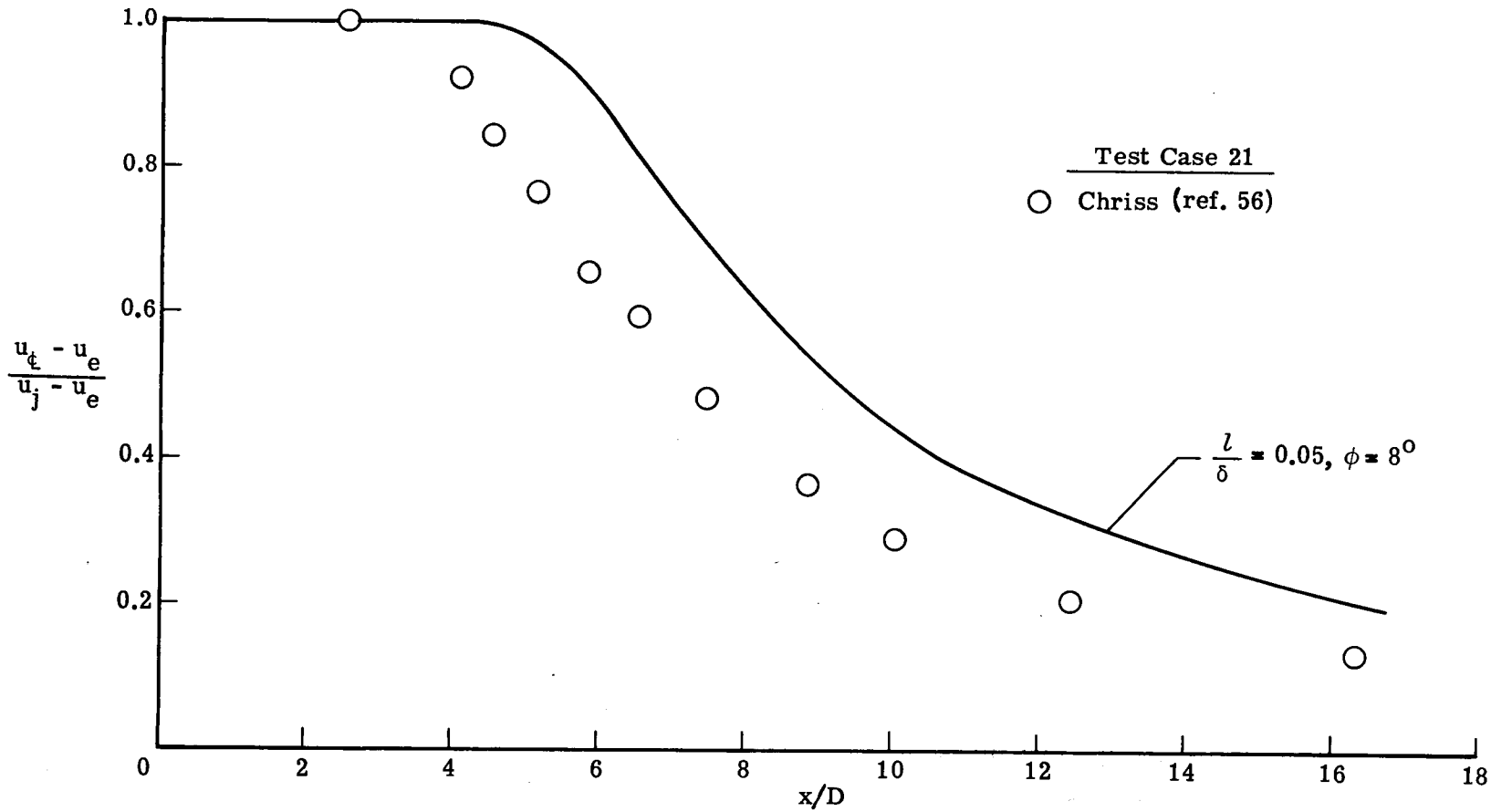

(a) Velocity.

Figure 21.- Predicted and experimental center-line distribution for subsonic hydrogen-air coaxial mixing. Test case 21.

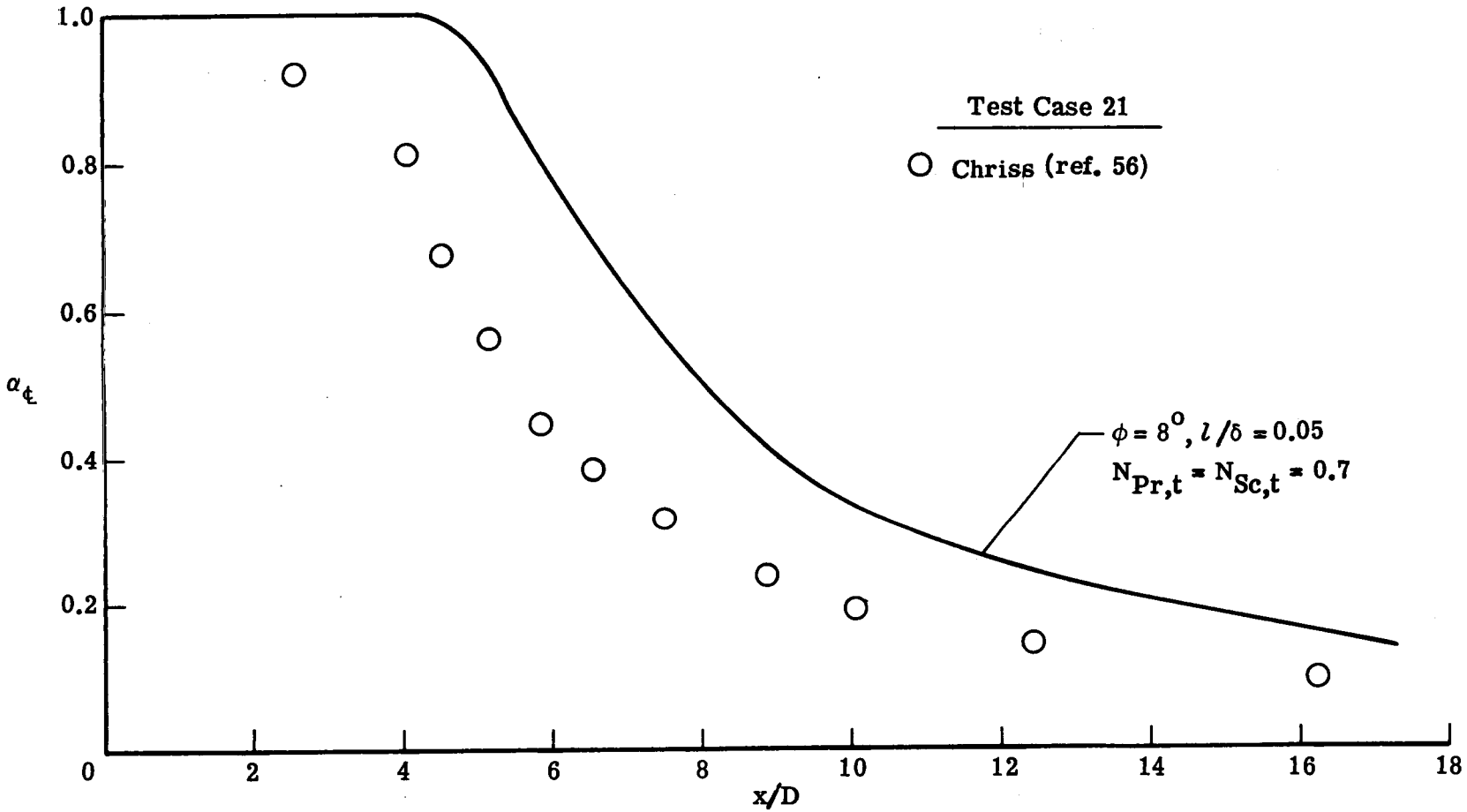

(b) Mass fraction of hydrogen.

Figure 21.- Concluded.

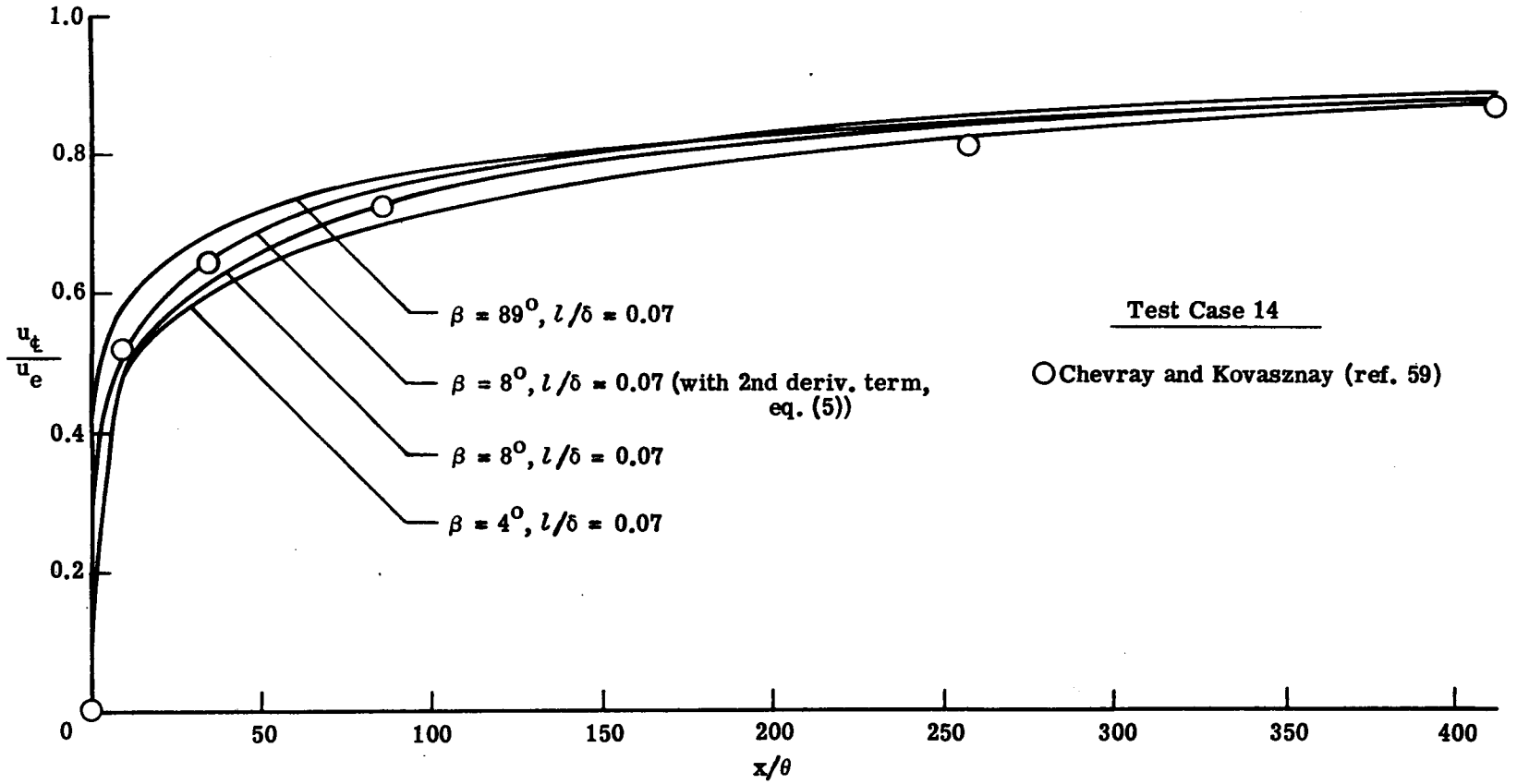

Figure 22.- Predicted and experimental center-line velocity for a two-dimensional subsonic wake. Test case 14.

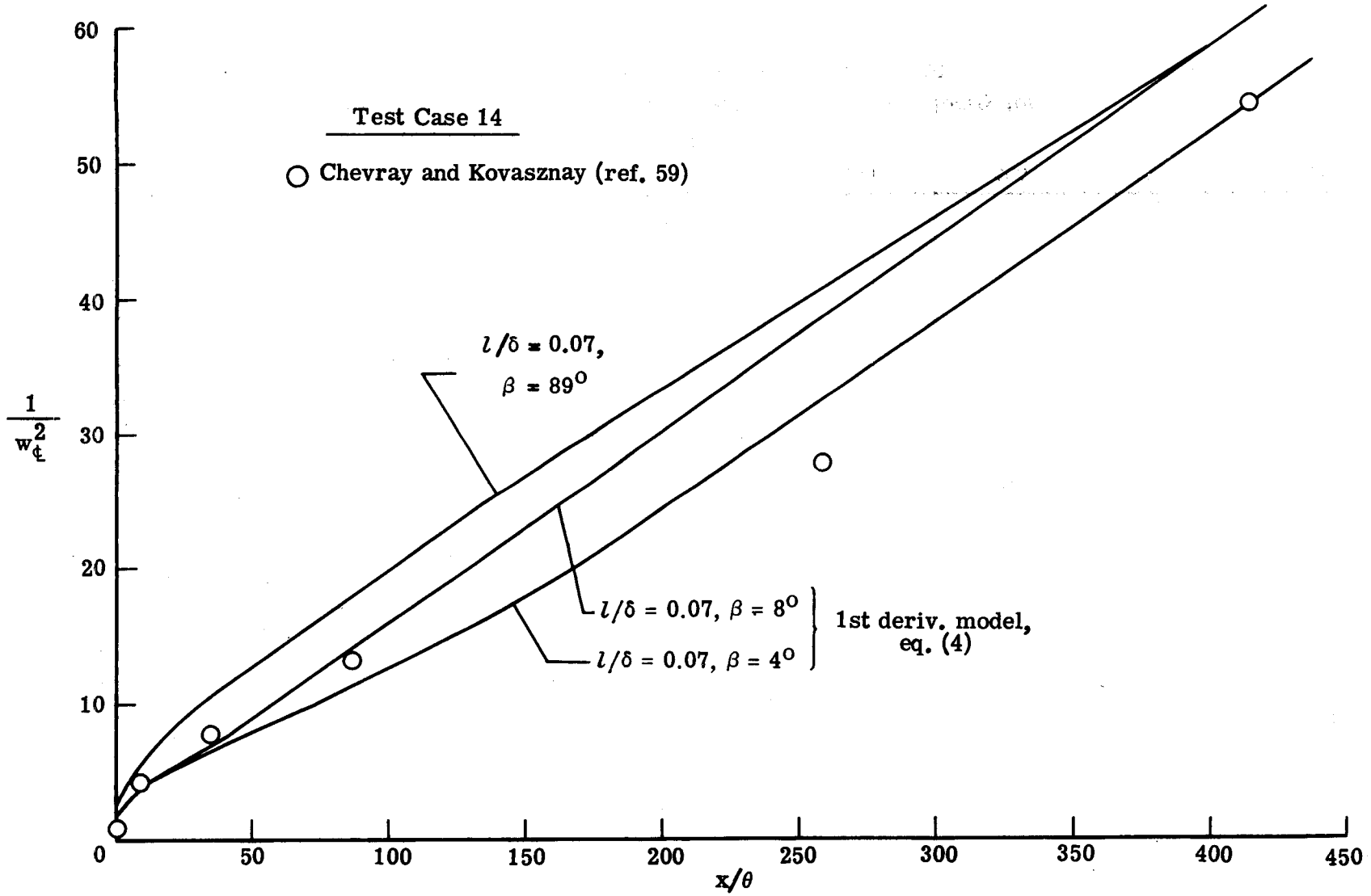

Figure 22.- Concluded.

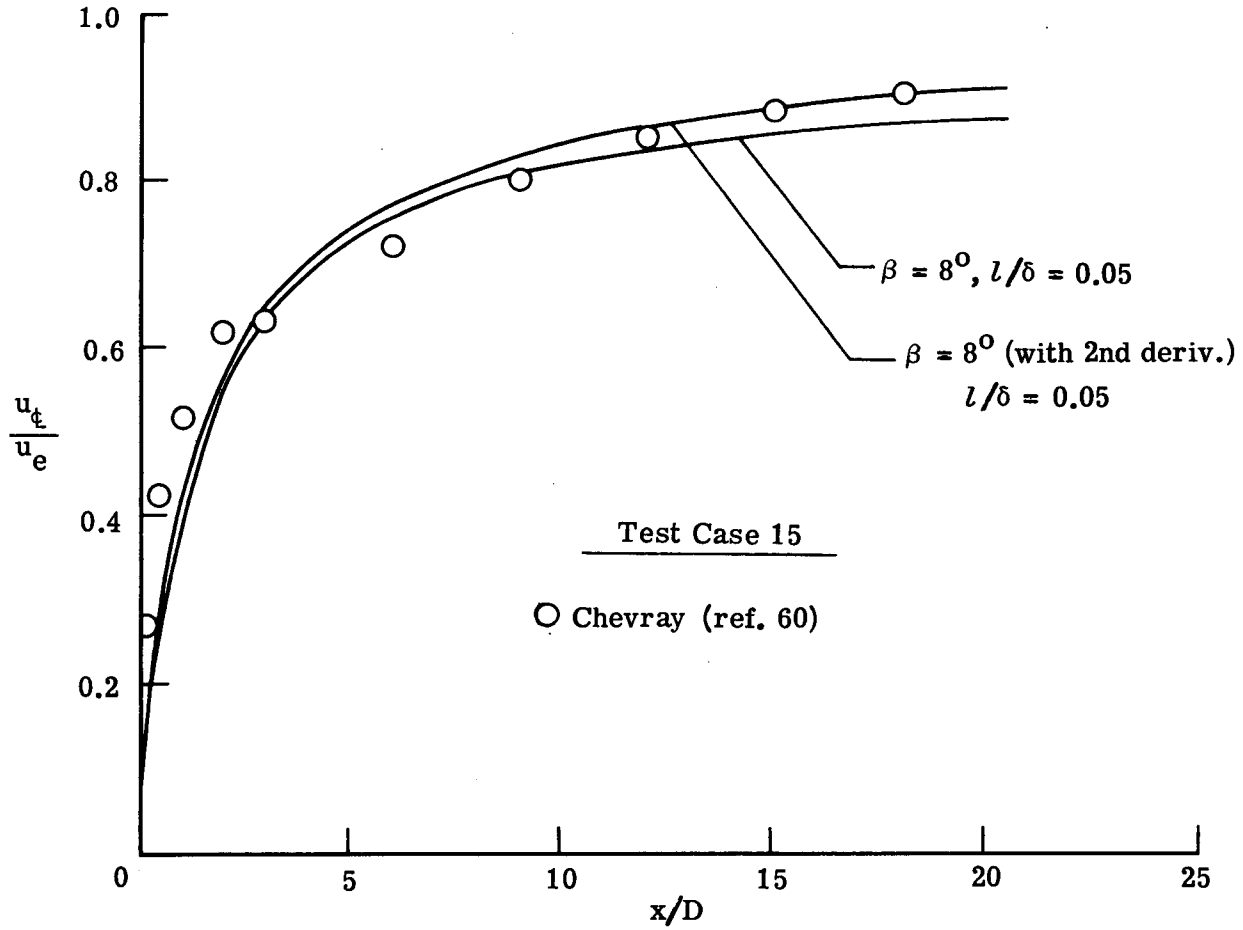

Figure 23.- Predicted and experimental center-line velocity for a subsonic axisymmetric wake. Test case 15.

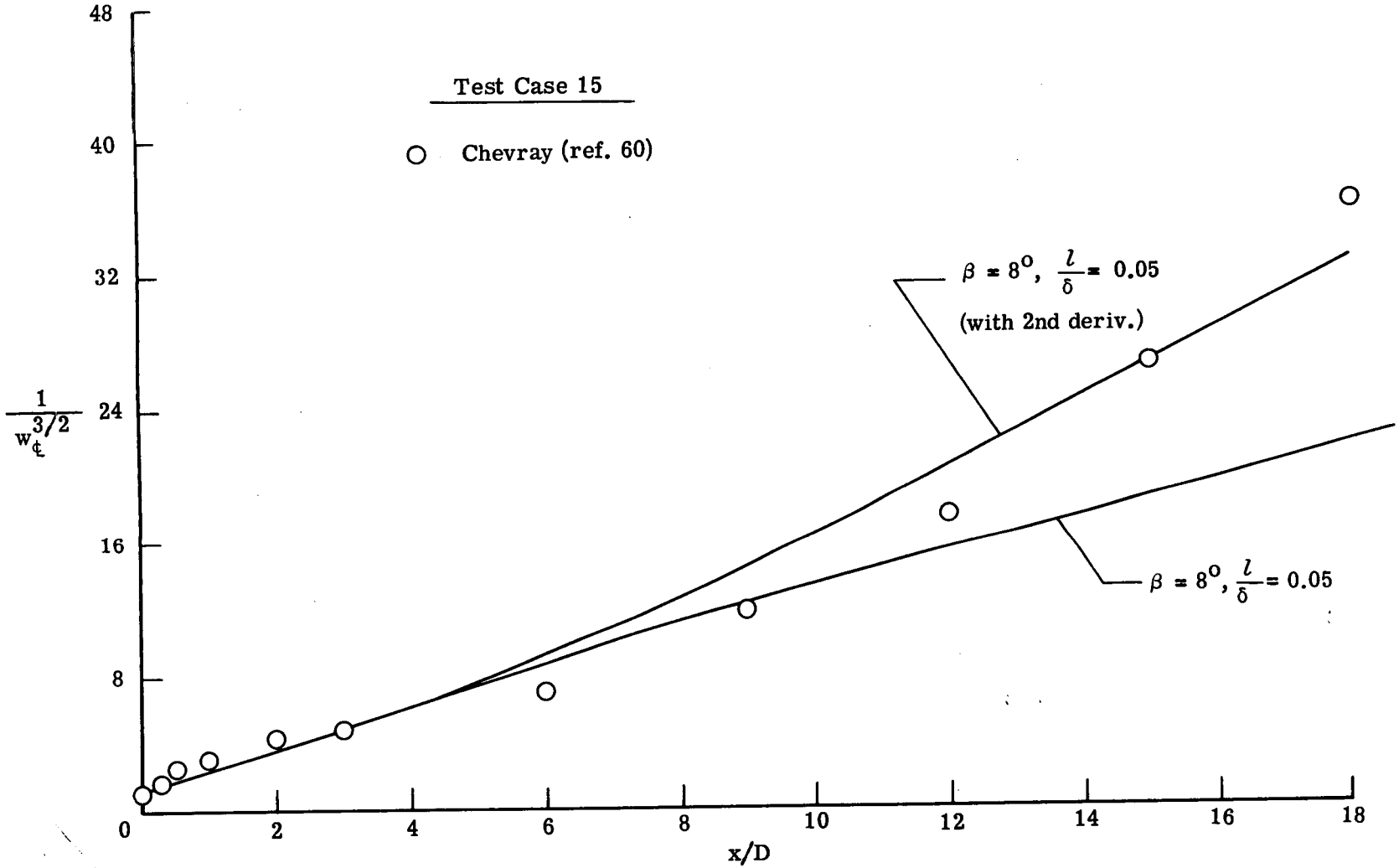

Figure 23.- Concluded.

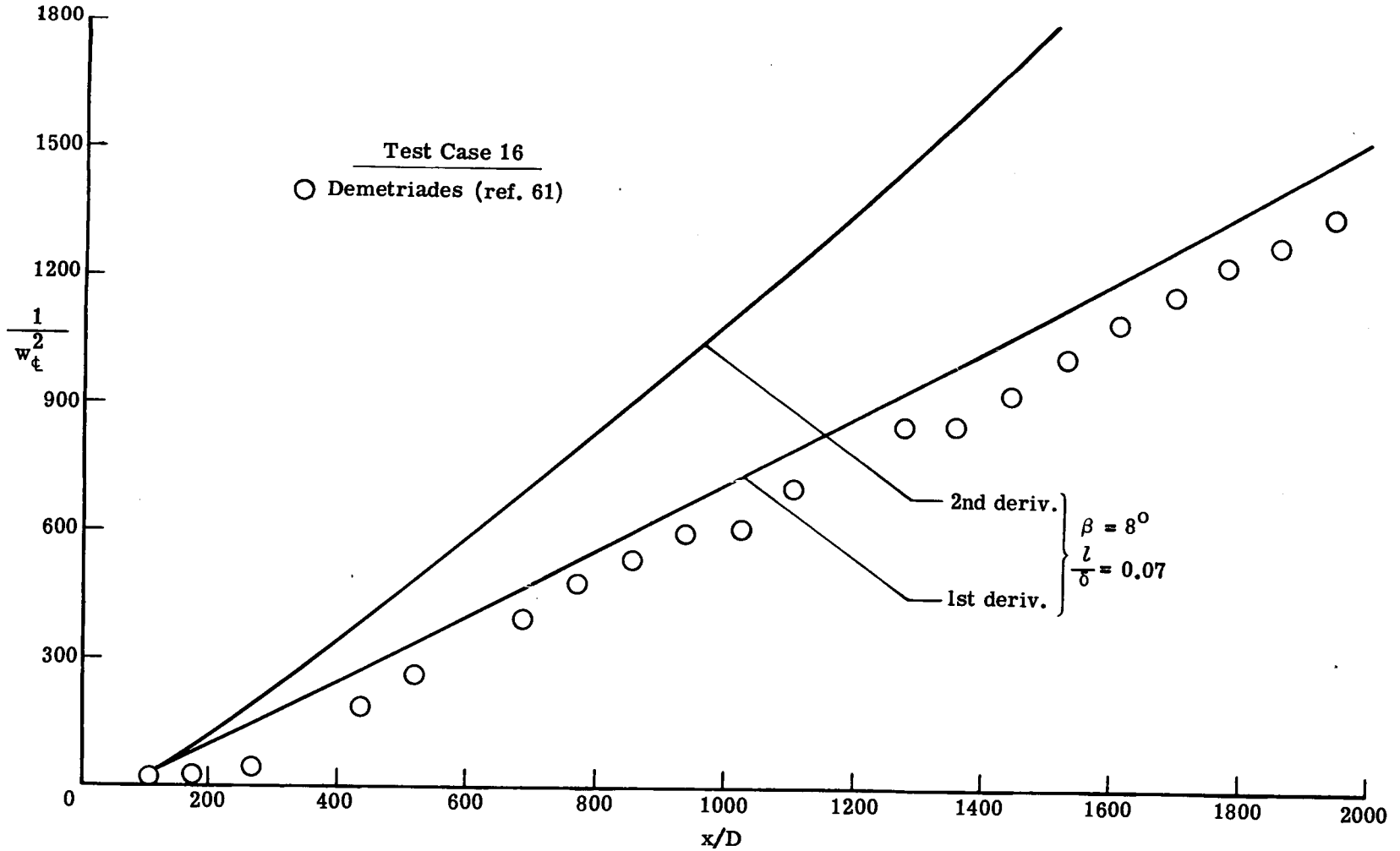

Figure 24.- Predicted and experimental center-line velocity for a two-dimensional supersonic wake. Test case 16.

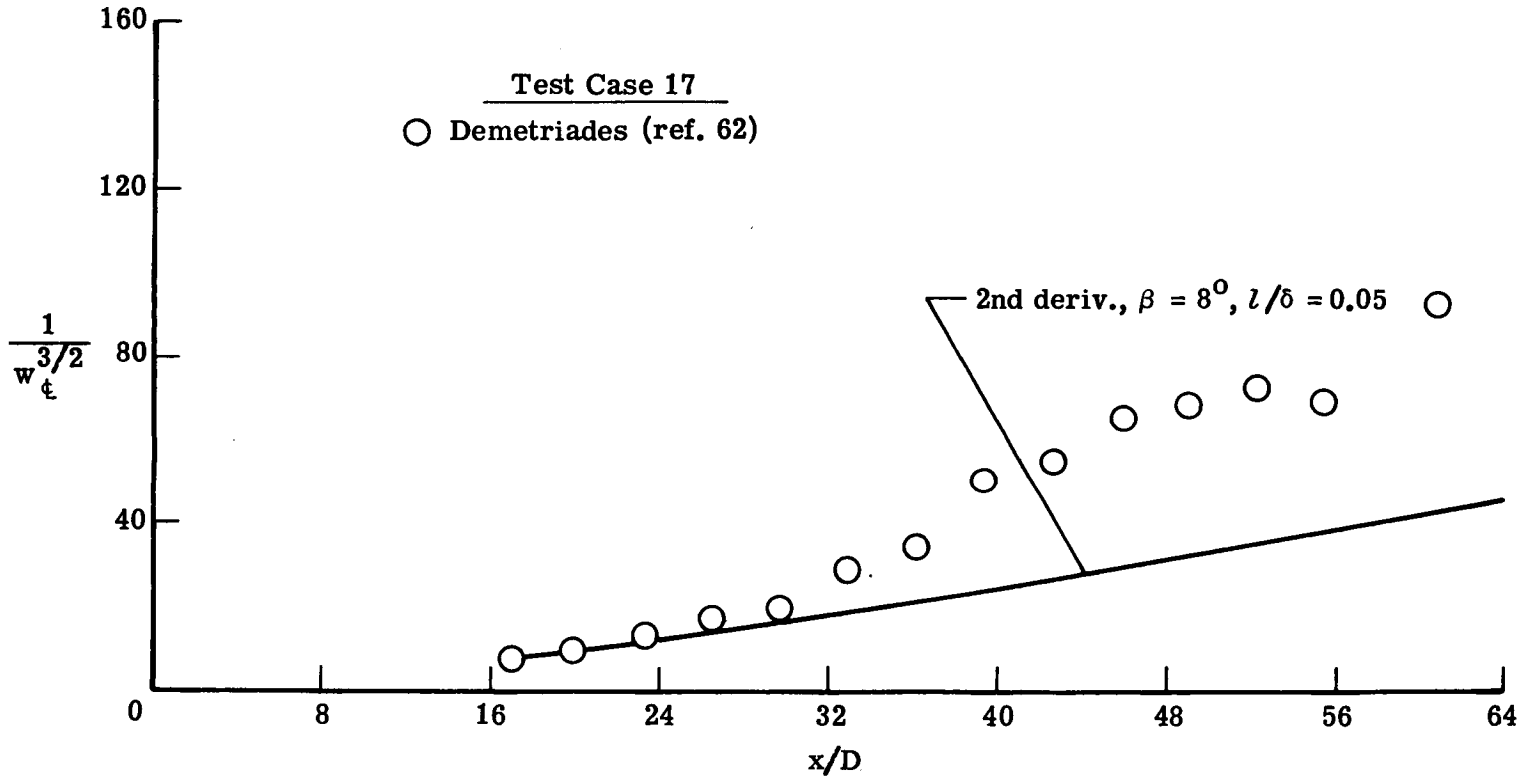

Figure 25.- Predicted and experimental center-line velocity for an axisymmetric supersonic wake. Test case 17.

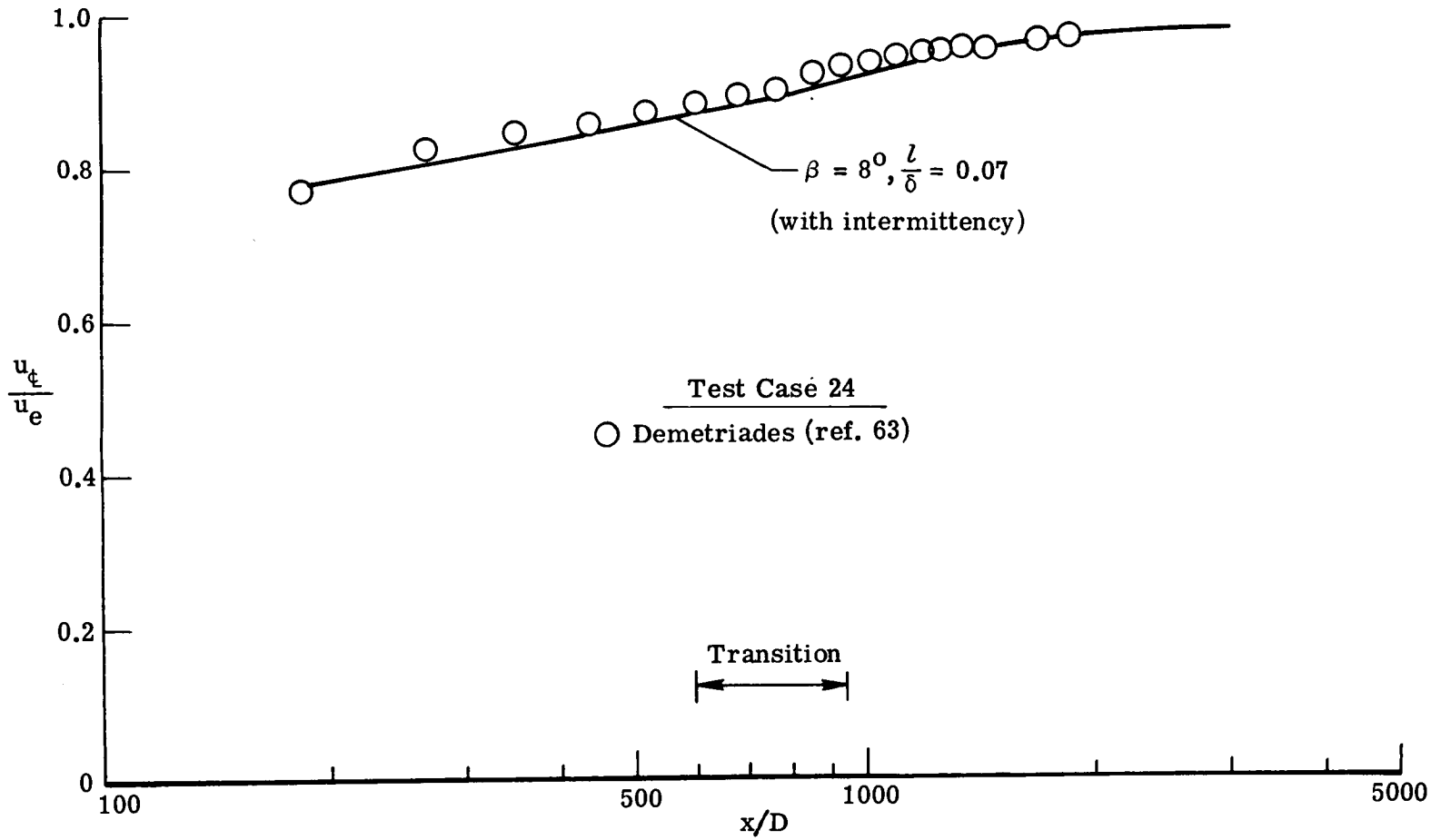

Figure 26.- Predicted and experimental center-line velocity for a two-dimensional supersonic wake. Test case 24.

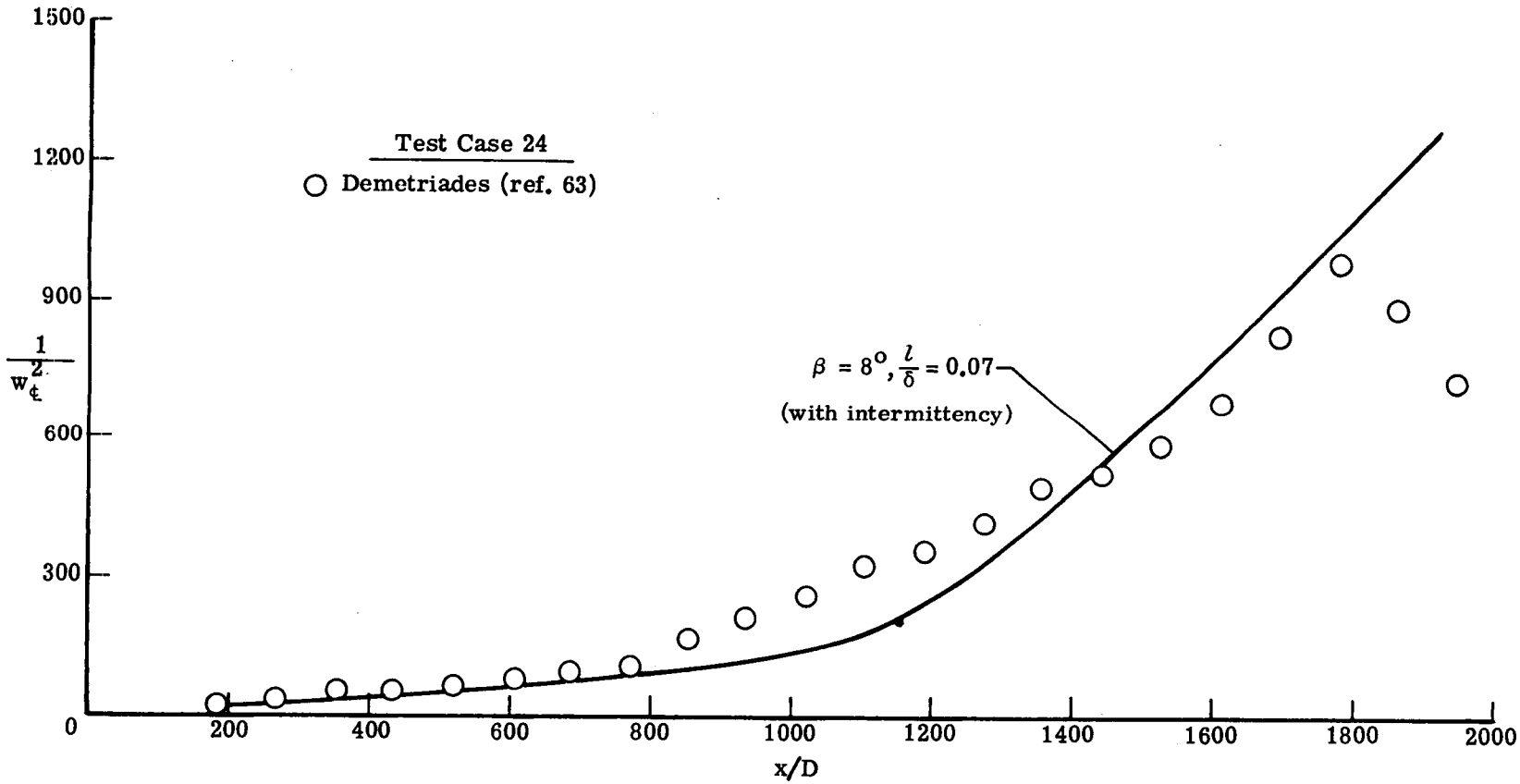

Figure 26.- Concluded.

DISCUSSION

H. McDonald: Can we regard this paper as a yardstick by which to judge the other predictions; in other words, if you cannot do any better than Prandtl's mixing length, then why bother? That is the first question I would like for you to try and answer. The second one is, are you advocating a development of Prandtl's mixing length and should this work be pursued, or do you think that this is the point at which to abandon the specific concept of mean field-direct relation with the turbulence and go on perhaps to the turbulence kinetic energy equation and multiequation models of turbulence?

D. H. Rudy: Since a length scale equation has been added to the basic mixing length model, the calculations cannot be regarded as baseline calculations in the classical sense. The Imperial College paper has that type of mixing length calculation. Our use of the mixing length is merely an attempt to better represent the physics of turbulent mixing in nonequilibrium flows. The Conference Evaluation Committee is of course best qualified to determine what this approach means in terms of other prediction methods. Personally, I think that approaches like the various "two-equation" models which incorporate a length scale equation appear promising.

D. M. Bushnell: We use this thing just as a tool to analyze the flows. We've used other tools before and the mixing length is a convenient handle to put on the flow to find out if it is doing anything surprising. I think it is obvious that you want to continue development and each method in the hierarchy has its own application, and I think I'll leave it at that.

V. W. Goldschmidt: I guess I have a similar question: What is the basis for determining whether the model works or not? Is it strictly a comparison with mean velocity or are we going to try to look at turbulence stresses as well? I think if we take that daring step your conclusions would have to be rephrased a little bit differently. Am I correct?

D. H. Rudy: Yes, we have examined only mean flow quantities and not the details of the turbulence which are of course more sensitive to modeling. Perhaps the Evaluation Committee will comment on this but I do agree with your observation.

H. McDonald: I'm sorry our time doesn't permit any more questions. I'd like to proceed if I may.

Written Comments

S. J. Kline: For many decades most workers, including the discussor, have had the idea that the mixing length and eddy viscosity were fundamentally different assumptions. However, recent developments suggest this is not so; there are two points. First, both are closures which depend only on the local mean strain and scaling on the layer width. Second, it follows from this that whenever one is used, there exists an equivalent formulation

which is wholly consistent and equivalent within the accuracy of this level of approximation. In the case of Rudy and Bushnell's formulation, for example, one can write

$$\tau = \frac{\rho l^2}{\delta^2}\,\delta^2 \left|\frac{\partial \bar{u}}{\partial y}\right| \frac{\partial \bar{u}}{\partial y} \tag{1}$$

If we also write

$$\tau = \rho \epsilon \frac{\partial \bar{u}}{\partial y} \tag{2}$$

and equate τ in equation (1) and equation (2), we have

$$\epsilon = l^2 \frac{\partial u}{\partial y} \simeq l^2 \frac{\Delta U}{\delta}$$

and, since l is scaled on δ (l/δ = Constant), this is equivalent to $\epsilon = k\delta\,\Delta U$. Thus, the differences observed in the two cases should arise from the forms and values taken for the constants, and not from a fundamental difference between mixing length and eddy viscosity formulations.

P. J. Ortwerth: The measured static-pressure defects which concern the authors have been analyzed by myself prior to the formulation of my model. An order of magnitude analysis shows that to first order the proper integration of the radial momentum equation becomes

$$\bar{p} + \overline{(\rho v)' v'} = p_e \tag{1}$$

and the normal velocity component remains a second-order term – that is,

$$\rho \bar{v}^2 << \overline{(\rho v)' v'} \tag{2}$$

Further, equation (1) has been subsequently verified by Roger Craig in our laboratory by comparing $\rho \overline{v'^2}$ measured with a hot wire anemometer, Thermo Systems model 1100, and measured static pressure on jets.

A KINEMATIC EDDY VISCOSITY MODEL INCLUDING THE INFLUENCE OF DENSITY VARIATIONS AND PRETURBULENCE

By Leonard S. Cohen
United Aircraft Research Laboratories

SUMMARY

A model for the kinematic eddy viscosity has been developed which accounts for the turbulence produced as a result of jet interactions between adjacent streams as well as the turbulence initially present in the streams. In order to describe the turbulence contribution from jet interaction, the eddy viscosity suggested by Prandtl has been adopted, and a modification has been introduced to account for the effect of density variation through the mixing layer. The form of the modification was ascertained from a study of the compressible turbulent boundary layer on a flat plate. A kinematic eddy viscosity relation which corresponds to the initial turbulence contribution has been derived by employing arguments used by Prandtl in his mixing length hypothesis. The resulting expression for self-preserving flow is similar to that which describes the mixing of a submerged jet.

Application of the model has led to analytical predictions which are in good agreement with available turbulent mixing experimental data.

INTRODUCTION

In the analytical treatment of turbulent shear flows, the local shear stress may be expressed as the product of an eddy viscosity and the local velocity gradient by analogy with the laminar flow representation. However, while the molecular viscosity for laminar flow depends only on the fluid properties, the eddy viscosity is related to the structure of the turbulence in the shear flow. At present, turbulent flow phenomena are not well understood, so that empirical hypotheses are utilized to create a mathematical basis for the investigation of turbulent motion. These phenomenological theories lead to a formulation of the kinematic eddy viscosity (eddy viscosity divided by local density) which may be used with the equations of motion and a suitable equation of state to determine the local time-average conditions throughout a flow field.

The constant exchange coefficient hypothesis for the kinematic eddy viscosity suggested by Prandtl is widely used in analytical studies of the mixing layer formed at the boundary between adjacent fluid streams. In this hypothesis the kinematic eddy viscosity is taken to be proportional to the product of the mixing-layer width and the difference between the velocities at the edges of the mixing layer. Application of this formulation

to the investigation of the mixing of incompressible streams of the same fluid, for example, the classical analysis conducted by Görtler (ref. 1), has yielded results which have been verified experimentally. Recent studies of compressible jet mixing (refs. 2 and 3), however, have shown that Prandtl's relationship is not valid when the fluid density varies through the mixing layer. Moreover, the prediction that turbulent transport will cease when there is no velocity gradient in the flow is inconsistent with the experimental evidence (refs. 4 and 5). In this case, it appears that the initial turbulence of the fluid streams plays an important role in jet mixing. As a result of these findings several new formulations of the kinematic eddy viscosity or equivalent mixing parameter have been recommended (refs. 5 to 9). Unfortunately, the general validity of these new expressions has not been satisfactorily demonstrated.

The present investigation was performed to resolve the discrepancies regarding the effect of density on the kinematic eddy viscosity and the influence of initial jet turbulence. Prandtl's hypothesis is adopted to describe the mixing of isothermal, incompressible streams of the same fluid which results from the turbulence produced by interactions between the streams. The hypothesis is modified to account for density variations through the mixing layer by making use of flat-plate, compressible turbulent boundary-layer information. The contribution of initial stream turbulence to the kinematic eddy viscosity is investigated for a constant turbulent intensity and an intensity which decays in the flow direction. In the latter case, use is made of the initial period decay law which characterizes turbulent flow downstream of grids.

SYMBOLS

a	constant
b	transverse extent of mixing layer, m (ft)
C_1, C_2, C_3	constants
C_D	drag coefficient
D	diameter, m (ft)
d	characteristic dimension of jet nozzle, m (ft)
e	exponent for two-dimensional ($e = 0$) or axisymmetric ($e = 1$) flow
g_c	conversion factor, 32.2 lbm-ft/lbf-sec^2

I	intensity of turbulence defined by equation (33)
ℓ	mixing length, m (ft) (see eq. (2))
ℓ'	fluctuating mean free path of fluid particles, m (ft)
M	Mach number
m	ratio of external stream velocity to centerline velocity
m_1	velocity ratio fixed by turbulence level
N	characteristic dimension of grid, m (ft)
n	ratio of external stream density to centerline density
n_1	density ratio fixed by turbulence level
R_θ	Reynolds number
r	distance from tube centerline, m (ft) (except where indicated)
$r_{1/2}$	half thickness of jet, m (ft)
T	temperature, K (degree R)
U	velocity of stream approaching grid, m/sec (ft/sec)
u	velocity in longitudinal direction, m/sec (ft/sec)
u'	longitudinal velocity fluctuation, m/sec (ft/sec)
u_τ	friction velocity, m/sec (ft/sec) (see eq. (7))
$\bar{u}$	average velocity defined in equation (24), m/sec (ft/sec)
v'	transverse velocity fluctuation, m/sec (ft/sec)
x	axial distance, m (ft)

x_c length of core region, m (ft)

x_1 axial distance at which $m = m_1$, m (ft)

y transverse distance, m (ft) (except where indicated)

$\bar{y}$ transverse distance from centerline to inner boundary of mixing layer, m (ft)

z distance from wall, m (ft) (except where indicated)

α_1, α_2 constants in equations (15) and (16)

β constant in equation (41)

γ ratio of specific heats

δ boundary-layer thickness, m (ft)

ϵ kinematic eddy viscosity, m^2/sec (ft^2/sec)

η_j mass fraction of species j

θ centerline decay exponent

κ constant in equation (3)

ξ parameter defined by equation (13)

ρ density, kg/m^3 (lbm/ft^3)

σ spreading parameter (see eq. (22))

τ shear stress, N/m^2 (lbf/ft^2)

Subscripts:

$\mathfrak{c}$ centerline

e external stream

j	jet stream
o	denotes value for incompressible submerged jet
r	reference
τ	total condition
w	wall
∞	asymptotic value

KINEMATIC EDDY VISCOSITY MODEL

When a jet discharges into a quiescent or flowing external stream, a distinctive flow field develops which may be divided into two principal regions. (See fig. 1.) In the initial region or "core" region, a mixing layer of finite thickness with a continuous distribution of velocity, temperature, and species concentration forms at the boundary between the two streams. For the idealized system shown in figure 1, the velocities of the jet and external streams u_j and u_e are uniform, the jet nozzle with characteristic dimension d has infinitesimally thin walls, and the pressure is constant throughout the flow. The mixing layer gradually broadens in the direction of flow and ultimately extends to the centerline of the jet at $x = x_c$, which marks the end of the initial region. In the developed region, the velocity on the centerline $u_{\text{℄}}$ decreases while the width of the layer continues to increase.

The equations of motion, modified according to the usual boundary-layer assumptions (ref. 10), are used in the analytical treatment of jet mixing. For turbulent jets, the local shear stress is related to a kinematic eddy viscosity ϵ according to the Boussinesq hypothesis

$$g_c \tau = \rho \epsilon \frac{\partial u}{\partial y} \tag{1}$$

Thus, once the kinematic eddy viscosity is specified, all local conditions throughout the flow field may be determined for selected boundary conditions.

Prandtl proposed two formulations to characterize the rate of mixing resulting from jet-induced turbulence. In the earlier mixing-length hypothesis, Prandtl suggested the relation

$$\epsilon = \ell^2 \left| \frac{\partial u}{\partial y} \right| \tag{2}$$

in which the mixing length ℓ may be thought of as the transverse extent of an identifiable lump of fluid (i.e., an eddy). In Prandtl's new theory, referred to as the constant exchange coefficient hypothesis, it is assumed that the kinematic eddy viscosity varies in the axial direction only. From considerations of flow similarity, for example, that the ratio of the mixing length to the transverse extent of the mixing layer b is constant throughout the flow, it can be shown that

$$\epsilon = \epsilon(x) = \kappa b \left| u_{\ell} - u_e \right| \tag{3}$$

where κ is a universal constant in each region of the jet for a given geometry. Analytical studies conducted by Tollmien (ref. 11) with equation (2) and Görtler (ref. 1) with equation (3) produced the velocity distributions through a mixing layer presented in figure 2. As very little difference between the profiles can be discerned, the formulations of equations (2) and (3) can be considered to be equivalent for practical purposes, and hence the ratio of ℓ/b may be considered to be a constant in an incompressible free jet mixing layer. Equation (3) is simpler to use, however, and for this reason it is adopted as the basic relation in the present model.

In any general formulation of the kinematic eddy viscosity it is necessary to consider the turbulence initially present in the streams, that is, the "preturbulence," as well as the turbulence produced as a result of the interactions between the streams. When the velocity ratio $m \equiv \frac{u_e}{u_{\ell}}$ differs significantly from unity, the growth of the mixing layer is controlled by jet interaction since shearing stresses of large magnitude occur, which induce high-intensity turbulent activity. As m approaches unity, however, the preturbulence contribution may become the dominant factor. Thus, in a jet mixing situation where $m_{x=0} \ll 1$, the initial spread of the mixing layer depends on jet-induced turbulence, while far downstream, after appreciable decay of the centerline velocity, the effect of preturbulence may become important. It should be noted, however, that when mixing aids such as vortex generators or mixing "fingers" are present in the nozzle supplying the fluids or when the fluids to be mixed are introduced into the main flow through angled injectors, the preturbulence contribution to the eddy diffusivity might predominate even for $m \ll 1$. Two classes of mixing phenomena may therefore be considered to stem from the two sources of turbulence identified above: (1) The turbulence level is initially set by the jet turbulence and then gradually decays to the background or "preturbulence" level; (2) the jet turbulence level is below the background level at $x = 0$ and the "preturbulence" is the controlling parameter over the full extent of the mixing region.

Effect of Density Variation

As noted in the introduction, the results presented in references 2 and 3 indicate that equation (3) is not suitable when there is a significant density variation in the mixing

layer. Unfortunately, the available compressible mixing layer data are not sufficiently extensive or reliable to indicate how equation (3) should be modified for this effect. However, since the free-shear mixing layer and the wake or outer region of the turbulent boundary layer are described by the same system of equations, it is suggested that the influence of compressibility for zero pressure gradient can be ascertained by examining the behavior of the compressible boundary layer on a flat plate for which comprehensive information exists. In order to implement this approach, an expression must be obtained which relates ϵ to parameters which characterize the boundary layer. Thus, if equations (1) and (2) are combined to eliminate the velocity gradient, the result is

$$\epsilon = \ell\left(\frac{g_c \tau}{\rho}\right)^{1/2} \tag{4}$$

which may be written in the expanded form

$$\epsilon = \delta\left(\frac{\ell}{\delta}\right)\left(\frac{\tau}{\tau_w}\right)^{1/2}\left(\frac{g_c \tau_w}{\rho_w}\right)^{1/2}\left(\frac{\rho_w}{\rho}\right)^{1/2} \tag{5}$$

In equation (5) δ is the boundary-layer thickness and the subscript w denotes conditions at the plate surface. It was shown in reference 12 that neither the ratio of the local shear stress to wall shear stress nor the parameter ℓ/δ displays a great sensitivity to either the Mach number or the Reynolds number. Therefore, it may be concluded that

$$\frac{\epsilon}{\delta u_\tau \left(\rho_w/\rho\right)^{1/2}} = f(y/\delta) \tag{6}$$

where the friction velocity u_τ is given by

$$u_\tau = \left(\frac{g_c \tau_w}{\rho_w}\right)^{1/2} \tag{7}$$

Equation (6) implies that the normalization of the kinematic eddy viscosity with the product $\delta u_\tau (\rho_w/\rho)^{1/2}$ results in a universal parameter, which is a function of only the dimensionless transverse distance through the boundary layer. This has been verified by using the calculation procedure described in reference 12, with the exception that a value for the exponent on the density ratio ρ_w/ρ of 0.4 fits the data better than the derived value of 0.50. Results of the calculation are given in figure 3 for Mach numbers of 0, 2.0, and 5.0.

By applying the analogy between the wake region of the turbulent boundary layer and the turbulent mixing layer, it is assumed that equation (6) may be rewritten for the mixing layer in the following form:

$$\frac{\epsilon}{b u_{\tau,r}\left(\rho_r/\rho\right)^{0.4}} = f_1(y/b)$$

where ρ_r and $u_{\tau,r}$ are jet reference conditions and b is the extent of the mixing layer in the direction normal to the jet axis. Furthermore, since the kinematic eddy viscosity is independent of y for an incompressible jet, or shear layer, the form of f_1 is then known and the relation may be written as

$$\frac{\epsilon}{b u_{\tau,r}\left(\rho_r/\rho\right)^{0.4}} = \text{Constant} \tag{8}$$

for both compressible and incompressible mixing layers. Assuming the existence of velocity and temperature profile similarity, it may be deduced that

$$u_{\tau,r}^2 = \frac{g_c \tau_r}{\rho_r} = \epsilon \left.\frac{\partial u}{\partial y}\right|_r \sim \epsilon \frac{\left|u_{\ell} - u_e\right|}{b} \tag{9}$$

Thus,

$$\epsilon = \kappa\left(\frac{\rho_r}{\rho}\right)^{0.8} b\left|u_{\ell} - u_e\right| \tag{10}$$

which generalizes equation (3) to include density variations. It still remains, however, to specify the ratio ρ_r/ρ. It should be noted that this ratio must reduce to unity when there is no density variation through the mixing layer and that it must reflect the experimentally observed decrease in the mixing rate when the Mach number of a supersonic, submerged jet is increased at constant static temperature (refs. 13 and 14). A possible representation is

$$\frac{\rho_r}{\rho} = f^* \frac{\rho_{\ell} + \rho_e}{2\rho_{\ell}} \tag{11}$$

where f^* is an empirical parameter equal to unity for incompressible jet mixing, which may vary with Mach number for example (ref. 15). Introducing equation (11) into equation (10) leads to

$$\epsilon = \kappa\left(f^* \frac{\rho_{\ell} + \rho_e}{2\rho_{\ell}}\right)^{0.8} b\left|u_{\ell} - u_e\right| \tag{12}$$

Comparison of Modified Formulation With Experimental Jet Spreading Data

The spreading parameter σ is usually reported in the results of jet mixing studies. This parameter may be thought of as a scaling factor in the transformation from the x-y physical coordinate system into a system with the single independent variable ξ defined as

$$\xi \equiv \sigma \frac{y - \bar{y}}{x} \tag{13}$$

Under conditions of profile similarity, there is a value of σ that will allow all velocity profiles

$$\frac{u - u_e}{u_{\ell} - u_e} = F(\xi) \tag{14}$$

to be collapsed to a single curve.

Another consequence of profile similarity is the existence of a unique relationship between the spreading parameter σ and the extent of the mixing region b for a given flow situation. The extent of the mixing region may be defined as the transverse distance between the points at which

$$u - u_e = \alpha_1(u_{\ell} - u_e) = u_1 - u_e \tag{15}$$

and

$$u - u_e = \alpha_2(u_{\ell} - u_e) = u_2 - u_e \tag{16}$$

where α_1 and α_2 are arbitrary but universal constants and U_1 and U_2 are the velocities at the extrema of the mixing region located at y_1 and y_2, respectively. From equation (14) (the similarity law) it follows that

$$\alpha_1 = F(\xi_1) = F\left(\sigma \frac{y_1 - \bar{y}}{x}\right) \tag{17}$$

and

$$\alpha_2 = F(\xi_2) = F\left(\sigma \frac{y_2 - \bar{y}}{x}\right) \tag{18}$$

From the definition of the extent of the mixing region,

$$b = y_1 - y_2 = (y_1 - \bar{y}) - (y_2 - \bar{y}) \tag{19}$$

and hence

$$\frac{\sigma b}{x} = \sigma \frac{y_1 - \bar{y}}{x} - \sigma \frac{y_2 - \bar{y}}{x} = \xi_1 - \xi_2 \tag{20}$$

Therefore, for any arbitrary nondimensional profile function F, it is seen that

$$\frac{\sigma b}{x} = F^{-1}(\alpha_1) - F^{-1}(\alpha_2) = \text{Constant} \tag{21}$$

where F^{-1} is the inverse of the profile function of equation (14) and the constant depends only on the form of the profile function once the values of α_1 and α_2 have been chosen. Hence, it is seen that the spreading parameter is proportional to the cotangent of the spreading angle of the mixing region, and if σ is a constant, then b must vary linearly with x.

Investigations of incompressible jet mixing systems have shown that the lateral extent of the mixing region b does vary linearly with x, for example, in the core region, or in a fully developed region, where the external stream is quiescent. It may be further shown that in this case the kinematic eddy viscosity is related to the spreading parameter by the equation

$$\sigma = \sqrt{\frac{2\bar{u}x}{4^{(1-e)}\epsilon}} \tag{22}$$

and hence the spreading parameter is proportional to the square root of the turbulent Reynolds number of the jet, which is also a constant. In equation (22) $e = 0$ for a two-dimensional jet, $e = 1$ for an axisymmetric jet, and $\bar{u}$ is the characteristic velocity given as

$$\bar{u} = \frac{u_{\text{¢}} + u_e}{2} \tag{23}$$

For the present consideration of density variation through the mixing layer, it is reasonable to extend the validity of equation (22), at least for moderate variations in density, by employing a suitable definition of the characteristic velocity, and the kinematic eddy viscosity determined in equation (12). The following expression for the characteristic velocity proposed by Yakovlevskiy (ref. 16) for the range of $0.3 \leqq \frac{\rho_e}{\rho_{\text{¢}}} \leqq 2$ will be adopted:

$$\bar{u} = \frac{\rho_e u_e + \rho_{\text{¢}} u_{\text{¢}}}{\rho_e + \rho_{\text{¢}}} \tag{24}$$

Then, introducing equations (12) and (24) into equation (22) and defining $m \equiv \frac{u_e}{u_{\ell}}$ and $n \equiv \frac{\rho_e}{\rho_{\ell}}$, result in

$$\sigma = \left[\frac{(1 + mn)\left(\frac{1 + n}{2}\right)^{-1.8}}{4(1-e)_{\kappa} f^{*0.8}\left(\frac{b}{x}\right)|1 - m|} \right]^{1/2} \tag{25}$$

which pertains to compressible jet mixing flows in which b/x is constant.

Typical experimental velocity profiles for incompressible and compressible jets mixing with quiescent and moving external stream are plotted from references 13, 17, and 18 in figure 4. The values of σ used in figure 4 were determined by matching the slopes of the experimental velocity profiles with the slope of the profile for the incompressible submerged jet at $\frac{u - u_e}{u_{\ell} - u_e} = 0.5$. As can be seen, the choice of a suitable value of σ for each mixing flow system results in essentially exact coincidence of all velocity profiles, thus lending validity to the similarity assumption of equation (14) upon which the validity of equation (25) rests. Equation (25) may be put into a more useful form by forming the ratio σ/σ_o, where σ_o is the spreading parameter for an incompressible, submerged jet (i.e., $m = 0$, $n = 1$) having a value of approximately 11.0 in the core region (ref. 17). This results in the expression

$$\frac{\sigma}{\sigma_o} = \frac{(1 + mn)}{\left(\frac{1 + n}{2}\right)^{1.8} |1 - m| f^{*0.8}} \tag{26}$$

For an incompressible jet discharging into a moving external stream, $n = 1$ and $f^* = 1$, and hence equation (26) reduces to

$$\frac{\sigma}{\sigma_o} = \frac{1 + m}{|1 - m|} \tag{27}$$

which is in general agreement with experimental measurements taken from references 16, 17, 19, and 20. (See fig. 5.) For compressible submerged jets (i.e., $m = 0$),

$$\frac{\sigma}{\sigma_o} = \left(\frac{1 + n}{2}\right)^{-1.8} (f^*)^{-0.8} \tag{28}$$

which may be written as

$$\frac{\sigma}{\sigma_o} = (f^*)^{-0.8}\left(\frac{1 + \frac{\gamma_\ell - 1}{2} M_\ell^2}{1 + \frac{\gamma_\ell - 1}{4} M_\ell^2}\right)^{1.8} \tag{29}$$

for constant static pressure and molecular weight throughout the mixing layer. Equation (29) is compared with data from references 11, 13, 14, 17, and 21 to 27 in figure 6 for various assumed variations of f^* with jet Mach number. A value of unity for f^* over the Mach number range 0 to 3.0 appears to result in fair agreement with most of the data points. In particular, the choice of $f^* = 1$ is predictive of the comprehensive experimental studies of Maydew and Reed (ref. 13) and Olson and Miller (ref. 14). Accordingly, the parameter f^* will be taken as unity in the remainder of this work.

Experimental data from two-stream mixing studies in which there exists a density variation through the mixing layer provide the most important test of equation (26). Such data, obtained from references 28 and 29, are compared with equation (26) in figure 7. The agreement between measured and calculated values is very satisfactory except for velocity ratios greater than about 0.50. This discrepancy will be investigated in some detail in subsequent sections. A listing of the test conditions and jet widths from references 29 and 30 as well as the calculated results from equation (26) is also given in table I.

Effect of Initial Turbulence

As a result of recent experimental studies, it has been suggested (ref. 5) that initial turbulence becomes the controlling factor in jet mixing at values of the velocity ratio m near unity. This breakdown of the jet interaction mechanism, exemplified by equation (12), is also apparent from some of the data presented in figures 5 and 7 for $m \geq 0.4$, which deviate from the analytical result (eq. (26)). When preturbulence controls, it appears that the spreading parameter becomes independent of m, at least for $n = 1.0$, so that equation (26) is no longer valid.

For the purpose of developing a formulation of the kinematic eddy viscosity for the preturbulence mechanism, it is convenient to begin with the basic expression (ref. 30)

$$\epsilon = -\overline{v'\ell'} \tag{30}$$

Equation (30) relates the kinematic eddy viscosity to a parameter associated with the eddy size of the turbulence field ℓ' and the transverse velocity fluctuation v'. In the spirit

of Prandtl's mixing length hypothesis (ref. 20), it is assumed that the mean of the product of fluctuating quantities is proportional to the product of the means of the absolute values of these quantities, that is,

$$\epsilon = -a\left|\overline{v'}\right| \cdot \left|\overline{\ell'}\right| \tag{31}$$

with $0 < a \leqq 1$ $(a \neq 0)$. Although nothing is known about the numerical parameter a, it may be inferred that it is related to a correlation factor which is descriptive of the turbulent field. As shown in reference 30, $\left|\overline{\ell'}\right|$ may be taken to be proportional to the mixing length, which for similar flows is also proportional to the width of the mixing region. Hence,

$$e \sim bI\bar{u} \tag{32}$$

in which the turbulent intensity I is defined as

$$I \equiv \frac{\left|\overline{v'}\right|}{\bar{u}} \tag{33}$$

which for situations involving isotropic turbulence is identical with the conventional definition of intensity and where $\bar{u}$ is given by equation (23). Noting that the longitudinal gradient of the mixing layer width varies directly with the turbulent intensity (ref. 20), as in the case of jet-induced turbulence, then,

$$b = b_i + C_1 \int_{x_i}^{x} I \, dx \tag{34}$$

It follows from equation (32) that

$$\epsilon = C_2 I \bar{u} \left(b_i + C_1 \int_{x_i}^{x} I \, dx \right) \tag{35}$$

where C_2 is a constant.

In general, the turbulence will decay from some initial value starting a small distance downstream from $x = 0$. The decay will continue with distance in the flow direction until a value of intensity commensurate with the background turbulence level is attained.

An interesting special case of equation (35) results if it is assumed that the mean absolute value of the transverse velocity fluctuation always varies in direct proportion to the average flow velocity. In this event, that is,

$$|\overline{v'}| \sim \bar{u}$$

it follows that

$$I = I_{x=0}$$

and

$$b \sim x$$

for $b_i = 0$ at $x = 0$. Introduction of this assumption implies that the shear flow induced by the preturbulence is self-preserving, in that the distribution of the nondimensional turbulent shear stress across the shear region is similar at any cross section. The turbulent (Reynolds) stress is given by

$$\frac{g_c \tau}{\rho \bar{u}^2} = -\frac{\overline{u'v'}}{\bar{u}^2} \sim \frac{|\overline{u'}| \cdot |\overline{v'}|}{\bar{u}^2}$$

but

$$|\overline{u'}| \sim |\overline{v'}|$$

following Prandtl (ref. 31). Therefore,

$$\frac{g_c \tau}{\rho \bar{u}^2} \sim I_{x=0}^2$$

as required. Verification of this behavior for plane jets in most of the developed region is provided by measurements presented in reference 32.

The spreading parameter for a constant turbulent intensity is obtained by taking $I = I_{x=0}$ and combining equations (22) and (35) with the result

$$\sigma = \left\{(0.5)4^{(1-e)} C_2 I_{x=0} \left[\frac{b_i}{x} + C_1 I_{x=0}\left(1 - \frac{x_i}{x}\right)\right]\right\}^{-1/2} \tag{36}$$

which is independent of the local velocity ratio. For a free jet where the mixing is initially controlled by jet-induced turbulence, there must exist some distance $x = x_1$, at which the velocity ratio attains a value m_1 and the spreading parameters given by equations (25) and (36) must coincide. Thus,

$$C_2 I_{x=0} = \kappa \frac{|1 - m_1|(1 + n_1)}{1 + m_1 n_1} \left(\frac{1 + n_1}{2}\right)^{0.8} \tag{37}$$

so that the appropriate value of the velocity ratio m_1 at which the mixing becomes controlled by the preturbulence mechanism may be obtained, in principle, from the mainstream turbulence level. The mixing downstream of the position x_1 is controlled by the preturbulence mechanism, and the appropriate kinematic eddy viscosity relation is obtained by combining equations (35) and (37), that is,

$$\epsilon = \kappa \left(\frac{1 + n_1}{2}\right)^{0.8} b|1 - m_1| u_{\ell} \left[\left(\frac{1 + n_1}{1 + n}\right)\left(\frac{1 + mn}{1 + m_1 n_1}\right)\right] \tag{38}$$

It is interesting to note that equation (38) corresponds to the expression describing the mixing of an incompressible submerged jet since the factor in the brackets is only a slowly varying function of m and n.

Far downstream from the origin of jet mixing, m and n approach unity and the asymptotic kinematic eddy viscosity for the turbulent jet becomes

$$\epsilon_{n=m=1} = \epsilon_{\infty} = \kappa b|1 - m_1| u_{\ell} \left(\frac{1 + n_1}{1 + m_1 n_1}\right)\left(\frac{1 + n_1}{2}\right)^{0.8} \tag{39}$$

This expression may be compared with the asymptotic relation given in reference 2, that is,

$$\epsilon_{\infty} = 0.04 r_{1/2} u_{\ell} \tag{40}$$

which was used to correlate data from a study involving the mixing of coflowing hydrogen and air at nearly equal stream velocities. In equation (40) $r_{1/2}$ is the distance between the jet centerline and the transverse position at which $u - u_e = 0.5(u_{\ell} - u_e)$. Since $b \approx 2r_{1/2}$, equation (40) may be rewritten as

$$\epsilon_{\infty} \approx 0.02 b u_{\ell}$$

which is identical in form to equation (39).

Initial turbulence levels are generally low in jets which are produced by expanding a gas through a nozzle. However, if there are blockages in the flow as in the case of a ducted fan engine or if mixing aids such as vortex generators are deliberately introduced into the flow, high levels of turbulence can result. In these cases, the initial turbulence

level cannot be sustained in the jet flow, and it is expected that $|\overline{v'}|$ will decay with distance downstream. Although the nature of this decay is not known, it is of interest to apply the initial period decay law found for isotropic turbulence downstream of grids to the present problem. The decay law

$$\frac{U^2}{v'^2} = \frac{\beta}{C_D}\left(\frac{x}{N} - \frac{x_o}{N}\right) \tag{41}$$

has been verified by a number of authors including Batchelor and Townsend (ref. 33) for grid Reynolds numbers from 640 to 5600, Webb (ref. 34) for grid Reynolds numbers from 2000 to 12 000 at various pressures with argon, helium, and air, and Kistler (ref. 35) for high Reynolds numbers. In equation (41) β is an absolute constant, $\frac{1}{2}\rho U^2 C_D$ is the drag of unit cross-sectional area of the grid, and N is an effective unit of length, which depends on the spacing of the grid elements. The ratio x_o/N, which has a value between 5 and 15, corresponds to the station at which the decay begins.

In order to adapt the decay law for use in equation (35), it is convenient to use the following modified form of equation (41):

$$\frac{1}{v'^2} - \frac{1}{v'^2_{x=0}} = \frac{\beta x}{U^2 C_D N} \tag{42}$$

or

$$\frac{v'^2}{v'^2_{x=0}} = \left(1 + \frac{\beta x v'^2_{x=0}}{U^2 C_D N}\right)^{-1} \tag{43}$$

Furthermore, by assuming that

$$\frac{v'^2}{v'^2_{x=0}} \sim \frac{|\overline{v'}|^2}{|\overline{v'}|^2_{x=0}} \tag{44}$$

the eddy diffusivity for the preturbulence mechanism following the decay law of equation (42) takes the form

$$\epsilon = C_4\left(\frac{NU^2C_D}{\beta}\right)\frac{\int_0^\theta \frac{d\theta}{\overline{u}(1+\theta)^{1/2}}}{(1+\theta)^{1/2}} \tag{45}$$

where b_i has been taken to be equal to zero, and

$$\theta \equiv \frac{\beta x v'^2_{x=0}}{U^2 C_D N} \tag{46}$$

The integral in equation (45) may be evaluated immediately to yield

$$\epsilon = 2C_4\left(\frac{NU^2C_D}{\beta\bar{u}}\right)\left[1 - (1+\theta)^{-1/2}\right] \tag{47}$$

for the core and asymptotic regions, as $\bar{u}$ is constant for these cases. Moreover, since $\beta \approx 100$ and $C_D \approx 1$ (ref. 33) and expected turbulence levels are such that $0.05 \leqq \frac{v'^2}{U^2} \leqq 1.0$, θ becomes large relative to unity a small number of grid spacings downstream of the initial station. In this event,

$$\epsilon = 2C_3\left(\frac{NU^2C_D}{\beta\bar{u}}\right) = \text{Constant} \tag{48}$$

in the core region, while far downstream of the initial station

$$\epsilon \rightarrow \epsilon_\infty = 2C_3\left(\frac{NU^2C_D}{\beta u_{\text{¢}}}\right) \tag{49}$$

The kinematic eddy viscosity formulations derived above cannot be verified at this time since pertinent experimental information does not exist. It is interesting to note with respect to equation (48), however, that a constant kinematic eddy viscosity often successfully correlates experimental mixing data (ref. 4).

Application of the Model

The principal results of the preceding analysis are embodied in the three expressions for the kinematic eddy viscosity, equations (12), (38), and (47). The choice of which form to use in a particular mixing study depends on the expected value of m_1 and whether the turbulent intensity in the jet streams decays or remains approximately constant with distance downstream. While a value of m_1 close to unity may be obtained, in theory, in a very carefully designed experiment, values of m_1 between 0.4 and 0.5 are found to be representative of a major portion of the existing mixing data (ref. 20, also figs. 5 and 7).

Some caution should be exercised in the application of the model to flows in which the ratio of external to centerline density is very large compared with unity, for example, the mixing of a central hydrogen jet with an outer air stream when the static temperatures of the two streams are not too different. As the density ratio increases and/or the velocity ratio increases above unity, the rate of mixing increases and ultimately leads to the generation of a significant positive pressure gradient in the initial mixing region and flow reversal of the inner jet (refs. 36 and 37). According to the data presented in reference 38, a back-flow vortex is formed at a momentum flux ratio nm^2 of 169. Furthermore, characteristics of wakelike flow, for example, centerline velocity initially decreasing, then increasing, are observed for momentum flux ratios greater than about 4. Use of the models for momentum flux ratios much in excess of 4, therefore, is not recommended.

In summary, when the ratio of velocities at the edges of the mixing layer is less than m_1, equation (12) is used; otherwise, equation (38) or (47) is used. It is recommended that equation (47) be used only in studies in which artificially high levels of turbulence are present because of the introduction of mixing aids into the flow field.

DISCUSSION OF RESULTS – COMPARISON OF THEORY WITH EXPERIMENTAL DATA

The kinematic eddy viscosity model developed in the preceding sections was used with the United Aircraft Research Laboratories mixing-combustion computer program (ref. 38) to generate flow-field information which could be compared with available measurements. A value of m_1, treated as a program input, indicated that the kinematic eddy viscosity was to be calculated from equation (12) for $m \leqq m_1$ and from equation (38) for $m > m_1$. The value of n_1 was calculated in the program at the longitudinal station where $m = m_1$. If the initial velocity ratio exceeded m_1, n_1 was taken as the ratio of the external stream density to the initial jet density. For the results discussed below, m_1 was taken to be equal to 0.40. The transverse extent of the mixing zone b was calculated according to the method discussed earlier (eqs. (15) and (16)) with $\alpha_1 = 0.95$ and $\alpha_2 = 0.05$ in the core region. Values of κ which were employed are given in table II (refs. 39 and 40).

The Two-Dimensional Shear Layer

Computed velocity profiles at two axial stations for $m = 0.01$ and $m = 0.10$ are compared with Görtler's theoretical profile (ref. 1) in figure 8. The excellent agreement obtained is an indication that the computer program is operating properly.

Mixing of Coaxial Incompressible Jets

Landis (ref. 28) investigated the mixing of a 0.64-cm-diameter (0.25-in.) heated air jet with a coflowing annular air stream at room temperature. In certain tests, small amounts of helium or carbon dioxide were also metered into the central jet. The velocity of the central jet was about 60 m/sec (200 ft/sec) while the velocity of the external stream was varied from 15 to 41 m/sec (50 to 135 ft/sec) to change m. The largest temperature difference between the streams was 180 K (325° R).

Measurements of the longitudinal variation of the centerline velocity ratio for various tests are compared with calculated results in figures 9 and 10. For the data presented in figures 9(a) and (b), the initial velocity ratio is 0.25 and the eddy diffusivity is calculated from equation (12) until $m \cong 0.4$. In figure 9(c) and figures 10(a) and (b), the initial velocity ratio exceeds m_1, and equation (38) of the model is employed throughout. Although the initial values of m and n are identical for both parts of figure 10, the nonunity value of n for figure 10(a) resulted from a temperature difference of 58 K (105° R) between the jet and external streams, while that in figure 10(b) was caused principally by the addition of helium to the jet. Thus, the use of a density correction to account for temperature and/or concentration variations through the mixing layer appears to be justified.

Subsonic Mixing in a 53-cm-Diameter (21-in.) Tube

In the experiments of reference 41, a Mach 0.3 jet at 733 K (1320° R) was brought into contact with a cold, Mach 0.1 external stream in a duct. The measure of agreement between calculated and experimental velocity and temperature profiles at two axial stations is shown in figures 11 and 12. Both magnitudes and trends are seen to be reproduced accurately.

Mixing of a Submerged Supersonic Free Jet

Eggers (ref. 42) conducted an analytical and experimental study of the mixing of a Mach 2.22 air jet with quiescent air. The axisymmetric jet which issued from a 2.56-cm-diameter (1.007-in.) nozzle was probed at seven axial stations in the core region and 23 axial stations in the developed region.

Predicted and experimental profiles at three stations are shown in figure 13. In order to treat this problem with the existing mixing analysis, it was necessary to assume that the external stream had some velocity. The chosen value of $u_e = 30$ m/sec (100 ft/sec) is thought to be sufficiently small relative to the jet velocity so as not to invalidate the comparison. The predicted mixing region is seen to spread somewhat more rapidly than is indicated by the measurements but the agreement is still considered to be good.

Ducted Mixing of a Supersonic Jet With an Annular Subsonic Jet

Isoenergetic mixing of a central Mach 2.6 air jet with a low-velocity external air stream was investigated in reference 43. Mach number profiles from the cited reference are shown with the computed results in figures 14 and 15. The effect of a shock system on the profile at $x/D = 2.5$ should be noted. Good agreement is obtained at the four axial locations shown over most of the duct cross section. The lower predicted values in the vicinity of the pipe centerline in the downstream profiles are to be expected inasmuch as the wall boundary layer was not accounted for. The analytical results and the data show the interesting phenomenon of the acceleration of the subsonic external stream to supersonic Mach numbers.

Other Examples

The models presented in this paper have been applied extensively so that numerous other comparisons with data are available in the literature. Groves (ref. 44) and Cohen and Guile (ref. 45) have utilized the recommended kinematic eddy viscosity formulations in a treatment of the mixing and combustion of a supersonic central hydrogen jet with an outer supersonic vitiated air stream. The momentum flux ratio of the jet mixing system studied was approximately 1.5. Eggers (ref. 46) studied supersonic hydrogen-air mixing $\left(nm^2 \approx 2.2 \text{ and } 7.7\right)$ and found that a kinematic eddy viscosity of the form given by equation (12) satisfactorily correlated his data.

CORRELATION OF EXPERIMENTAL CENTERLINE DECAY RATES

The decay of centerline concentration is generally presented in the form

$$\eta_{j,\ell} = \left(\frac{x}{x_c}\right)^{-\theta}$$

where x_c is the core length. A correlation of existing data (including that from refs. 47, 48, and 49) emerges within the framework of the ideas presented in this paper, when the observed values of θ are plotted against the initial jet velocity ratio $m_{x=0}$. It is found from figure 16 that θ is approximately unity over the range of velocity ratios where preturbulence predominates independent of density ratio. Over the range of velocity ratios where jet interactions constitute the dominant turbulence producing mechanism, θ is larger than unity and depends on both m and n. These findings are consistent with the jet spreading data of reference 50.

CONCLUSIONS

On the basis of the analysis presented herein and comparison between the analysis and existing data, it may be stated that

1. The proposed model for the kinematic eddy viscosity, involving an extension of Prandtl's constant exchange coefficient hypothesis to account for the effect of density variation through the mixing layer, yields good agreement with measured jet spreading parameters.

2. Transport of heat and mass can occur when the velocities of the jet and external streams are equal as a result of initial turbulence.

3. Additional mixing data are required to provide verification of the kinematic eddy viscosity model. In particular, information concerning the rate of mixing of jets at several different initial turbulence levels would be of value.

REFERENCES

1. Görtler, H.: Berechnung von Aufgaben der freien Turbulenz auf Grund eines neuen Näherungsansatzes. Z. Angew. Math. Mech., Bd. 22, Nr. 5, Oct. 1942, pp. 244-254.

2. Zakkay, Victor; Krause, Egon; and Woo, Stephen D. L.: Turbulent Transport Properties for Axisymmetric Heterogeneous Mixing. AIAA J., vol. 2, no. 11, Nov. 1964, pp. 1939-1947.

3. Ferri, A.; Libby, P. A.; and Zakkay, V.: Theoretical and Experimental Investigation of Supersonic Combustion. High Temperatures in Aeronautics, Carlo Ferrari, ed., Pergamon Press, 1964, pp. 55-118.

4. Ragsdale, Robert G.; and Edwards, Oliver J.: Data Comparisons and Photographic Observations of Coaxial Mixing of Dissimilar Gases at Nearly Equal Stream Velocities. NASA TN D-3131, 1965.

5. Alpinieri, Louis J.: An Experimental Investigation of the Turbulent Mixing on Non-Homogeneous Coaxial Jets. PIBAL Rep. No. 789 (Contract No. AF 49(638)-217), Polytech. Inst. Brooklyn, Aug. 1963.

6. Ferri, Antonio; Libby, Paul A.; and Zakkay, Victor: Theoretical and Experimental Investigation of Supersonic Combustion. ARL 62-467, U.S. Air Force, Sept. 1962.

7. Peters, C. E.: A Model for the Free Turbulent Eddy Viscosity. AEDC-TR-65-209, U.S. Air Force, Nov. 1965. (Available from DDC as AD 473663.)

8. Hill, Jacques A. F.; and Nicholson, James E.: Compressibility Effects on Fluid Entrainment by Turbulent Mixing Layers. NASA CR-131, 1964.

9. Channapragada, R. S.; and Woolley, J. P.: Turbulent Mixing of Parallel Compressible Free Jets. AIAA Paper No. 65-606, June 1965.

10. Van Driest, E. R.: Turbulent Boundary Layer in Compressible Fluids. J. Aeronaut. Sci., vol. 18, no. 3, Mar. 1951, pp. 145-160, 216.

11. Tollmien, Walter: Berechnung Turbulenter Ausbreitungsvorgänge. Z. Angew. Math. Mech., Bd. 6, Heft 6, Dec. 1926, pp. 468-478. (Available in English translation as NACA TM 1085, 1945.)

12. Maise, George; and McDonald Henry: Mixing Length and Kinematic Eddy Viscosity in a Compressible Boundary Layer. AIAA J., vol. 6, no. 1, Jan. 1968, pp. 73-80.

13. Maydew, R. C.; and Reed, J. F.: Turbulent Mixing of Axisymmetric Compressible Jets (in the Half-Jet Region) With Quiescent Air. SC-4764(RR), Sandia Corp. (Albuquerque, N. Mex.), Mar. 1963.

14. Olson, Robert E.; and Miller, David P.: Fluid Application. 6. Aerodynamic Studies of Free and Attached Jets. Rep. A-1771-24 (Contract DA-49-186-ORD-912), Res. Lab., United Aircraft Corp., Oct. 14, 1963. (Available from DDC as AD 427 335.)

15. Channapragada, Rao, S.: Compressible Jet Spread Parameter for Mixing Zone Analyses. AIAA J., vol. 1, no. 9, Sept. 1963, pp. 2188-2189.

16. Yakovlevskiy, O. V.: Thickness of the Turbulent Mixing Zone on the Boundary of Two Streams of Gases of Different Velocity and Density. FTD-TT-65-1928, U.S. Air Force, Feb. 18, 1966. (Available from DDC as AD 630 411.)

17. Liepmann, Hans Wolfgang; and Laufer, John: Investigations of Free Turbulent Mixing. NACA TN 1257, 1947.

18. Weinstein, Alvin S.: Diffusion of Momentum From Free and Confined Slot Jets Into Moving Secondary Streams. AFCRC-TN-55-476, U.S. Air Force, May 4, 1955.

19. Sabin, C. M.: An Analytical and Experimental Study of the Plane, Incompressible, Turbulent Free-Shear Layer With Arbitrary Velocity Ratio and Pressure Gradient. Trans. ASME, Ser. D: J. Basic Eng., vol. 87, no. 2, June 1965, pp. 421-428.

20. Abramovich, G. N.: The Theory of Turbulent Jets. M.I.T. Press, c.1963.

21. Cordes, G.: Untersuchungen zur statischen Druckmessung in turbulenter Strömung. Ing.-Arch., Bd. VIII, Heft 4, Aug. 1937, pp. 245-270.

22. Gooderum, Paul B.; Wood, George P.; and Brevoort, Maurice J.: Investigation With an Interferometer of the Turbulent Mixing of a Free Supersonic Jet. NACA TR 963, 1950. (Supersedes NACA TN 1857.)

23. Bershader, D.; and Pai, S. I.: On Turbulent Jet Mixing in Two-Dimensional Supersonic Flow. J. Appl. Phys., vol. 21, no. 6, June 1950, p. 616.

24. Cary, Boyd Balford, Jr.: An Optical Study of Two-Dimensional Jet Mixing. Ph. D. Thesis, Univ. of Maryland, 1954.

25. Crane, L. J.: The Laminar and Turbulent Mixing of Jets of Compressible Fluid. Pt. II – The Mixing of Two Semi-Infinite Streams. J. Fluid Mech., vol. 3, pt. I, Oct. 1957, pp. 81-92.

26. Johannesen, N. H.: The Mixing of Free Axially-Symmetrical Jets of Mach Number 1.40. R. & M. No. 3291, Brit. A.R.C., 1957.

27. Johannesen, N. H.: Further Results on the Mixing of Free Axially-Symmetrical Jets of Mach Number 1.40. R. & M. No. 3292, Brit. A.R.C., 1959.

28. Landis, Fred: The Turbulent Mixing of Co-Axial Gas Jets. Sc. D. Thesis, Massachusetts Inst. Technol., 1950.

29. Willis, D. Roger; and Glassman, Irvin: The Mixing of Unbounded Coaxial Compressible Streams. Jet Propulsion, vol. 27, no. 12, Dec. 1957, pp. 1241-1252.

30. Shigemitsu, Yutaka: Statistical Theory of Turbulence. USAAVLABS Tech. Rep. 66-25, U.S. Army, June 1966. (Available from DDC as AD 635 654.)

31. Schlichting, Hermann (J. Kestin, transl.): Boundary Layer Theory. Fourth ed., McGraw-Hill Book Co., Inc., c.1960.

32. Bradbury, L. J. S.: The Structure of a Self-Preserving Turbulent Plane Jet. J. Fluid Mech., vol. 23, pt. 1, Sept. 1965, pp. 31-64.

33. Batchelor, G. K.; and Townsend, A. A.: Decay of Isotropic Turbulence in the Initial Period. Proc. Roy. Soc., ser. A, vol. 193, no. 1032, Apr. 22, 1948, pp. 539-558.

34. Webb, W. H.: An Experimental Study of the Decay of Turbulent Energy in Several Gases and at High and Low Density. AFOSR 2302, U.S. Air Force, Jan. 1962.

35. Kistler, A. L.; and Vrebalovich, T.: Grid Turbulence at Large Reynolds Numbers. J. Fluid Mech., vol. 26, pt. 1, Sept. 1966, pp. 37-47.

36. Ghia, Kirti N.; Torda, T. Paul; and Lavan, Zalman: Turbulent Mixing in the Initial Region of Heterogeneous Axisymmetric Coaxial Confined Jets. NASA CR-1615, 1970.

37. Rozenman, Tzvi; and Weinstein, Herbert: Recirculation Patterns in the Initial Region of Coaxial Jets. NASA CR-1595, 1970.

38. Cohen, Leonard S.: An Analytical Study of the Mixing and Nonequilibrium Chemical Reaction of Ducted Compressible Streams. AIAA Paper No. 66-617, June 1966.

39. Hinze, J. O.; and Van der Hegge Zijnen, B. G.: Transfer of Heat and Matter in the Turbulent Mixing Zone of an Axially Symmetric Jet. Appl. Sci. Res., vol. A1, no. 5-6, 1949, pp. 435-461.

40. Forthmann, E.: Turbulent Jet Expansion. NACA TM 789, 1936.

41. Burley, Richard R.; and Bryant, Lively: Experimental Investigation of Coaxial Jet Mixing of Two Subsonic Streams at Various Temperature, Mach Number, and Diameter Ratios for Three Configurations. NASA MEMO 12-21-58E, 1959.

42. Eggers, James M.: Velocity Profiles and Eddy Viscosity Distributions Downstream of a Mach 2.22 Nozzle Exhausting to Quiescent Air. NASA TN D-3601, 1966.

43. John, James E. A.: An Experimental Investigation of the Bounded Mixing of Two Compressible Axially Symmetric Jet Streams. Rep. No. 399 (Contract N6-ori-105), Aeronaut. Eng. Lab., Princeton Univ., 1957.

44. Groves, Frank R., Jr.: Practical Application of Computer Programs for Supersonic Combustion. Contract No. NAS1-10341, Louisiana State Univ., June 1972. (Available as NASA CR-112029.)

45. Cohen, Leonard S.; and Guile, Roy N.: Investigation of the Mixing and Combustion of Turbulent, Compressible Free Jets. NASA CR-1473, 1969.

46. Eggers, James M.: Turbulent Mixing of Coaxial Compressible Hydrogen-Air Jets. NASA TN D-6487, 1971.

47. Chriss, D. E.: An Experimental Study of the Turbulent Mixing of Subsonic Axisymmetric Gas Streams. AEDC-TR-68-133, U.S. Air Force, Aug. 1968. (Available from DDC as AD 672 975.)

48. Eggers, James M.; and Torrence, Marvin G.: An Experimental Investigation of the Mixing of Compressible-Air Jets in a Coaxial Configuration. NASA TN D-5315, 1969.

49. Fejer, A. A., Hermann, W. G.; and Torda, T. P.: Factors That Enhance Jet Mixing. ARL 69-0175, U.S. Air Force, Oct. 1969. (Available from DDC as AD 700 761.)

50. Abramovich, G. N.; Yakovlevsky, O. V.; Smirnova, I. P.; Secundov, A. N.; and Krasheninnikov, S. Yu.: An Investigation of the Turbulent Jets of Different Gases in a General Stream. Astronaut. Acta, vol. 14, no. 3, Mar. 1969, pp. 229-240.

TABLE I.- COMPARISON OF EXPERIMENTAL AND PREDICTED SPREADING PARAMETERS

m	n	[a] $(b/x)_{experimental}$	$(\sigma/\sigma_o)_{experimental}$	$(\sigma/\sigma_o)_{calculated}$
Landis (ref. 28)				
0.25	1.300	0.185	1.372	1.37
.25	1.087	.165	1.540	1.57
.46	1.087	.095	2.680	2.57
.50	1.300	.106	2.40	2.57
Willis and Glassman (ref. 29)				
0	0.915	0.216	1.18	1.08
.382	.927	.1298	1.96	2.34
.678	.952	.0759	3.35	5.30
0	.842	.1968	1.29	1.16
.279	.852	.1421	1.79	1.97
.496	.876	.0986	2.57	3.20
.319	1.324	.1403	1.81	1.60
.567	1.361	.0836	3.04	3.04
.234	1.218	.1655	1.53	1.394
.415	1.251	.1266	2.00	2.10

[a] $(b/x)_o$ determined to be 0.254 from data. Value suggested by Abramovich (ref. 20) is 0.270.

TABLE II.- SPREADING PARAMETERS FOR CONSTANT DENSITY JET MIXING

	σ	a_K
Core region (e = 0)	11.0 (ref. 17)	0.00764
Developed region:		
Axisymmetric (e = 1.0)	22.6 (ref. 39)	0.0089
Two-dimensional (e = 0)	9.1 (ref. 40)	0.0136

[a] Calculated from equations (3) and (22) with $(b/x)_0 = 0.27$ in the core region and $(b/x)_0 = 0.22$ in the developed region as suggested in reference 20.

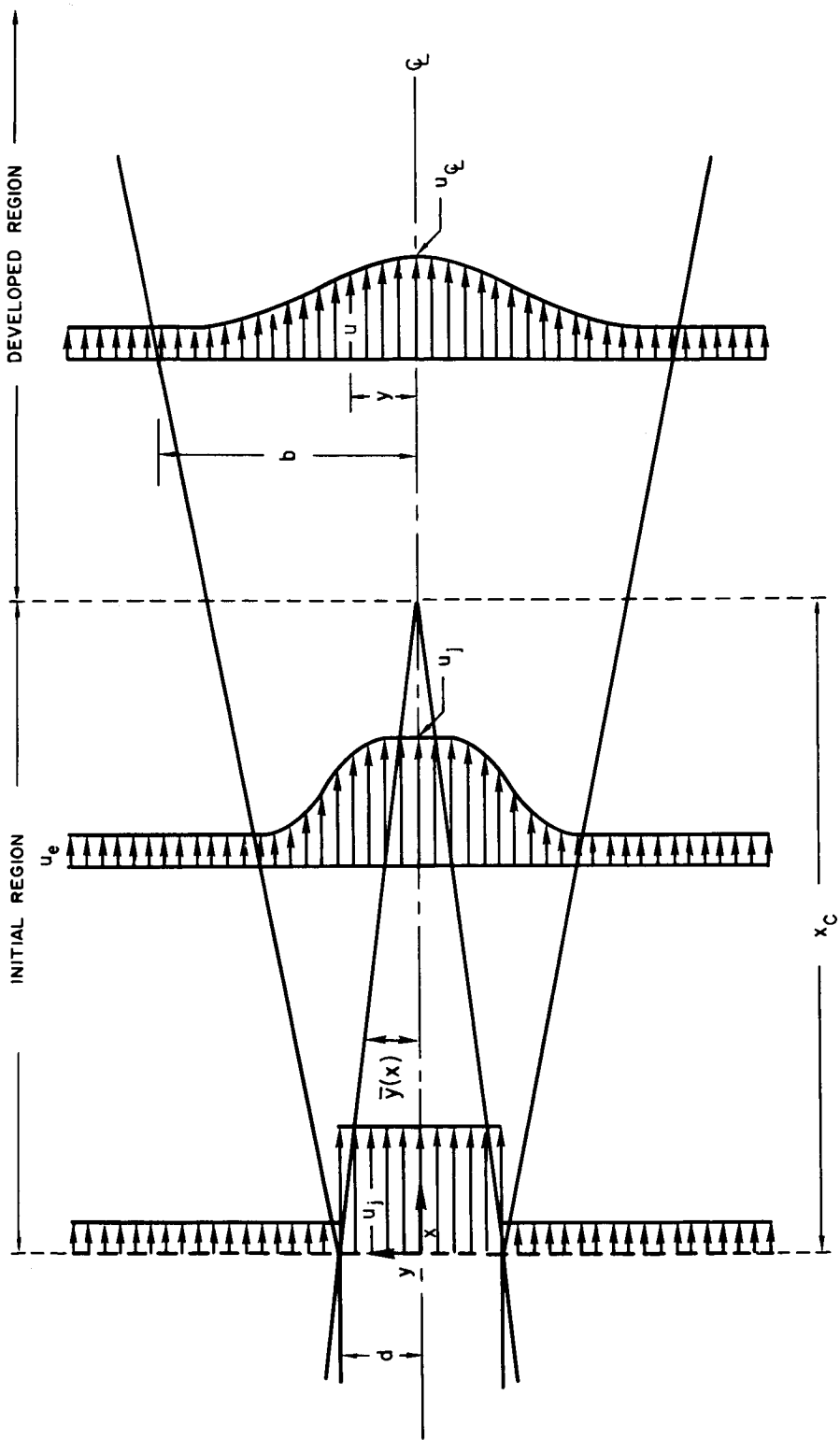

Figure 1.- Schematic of mixing of coflowing streams.

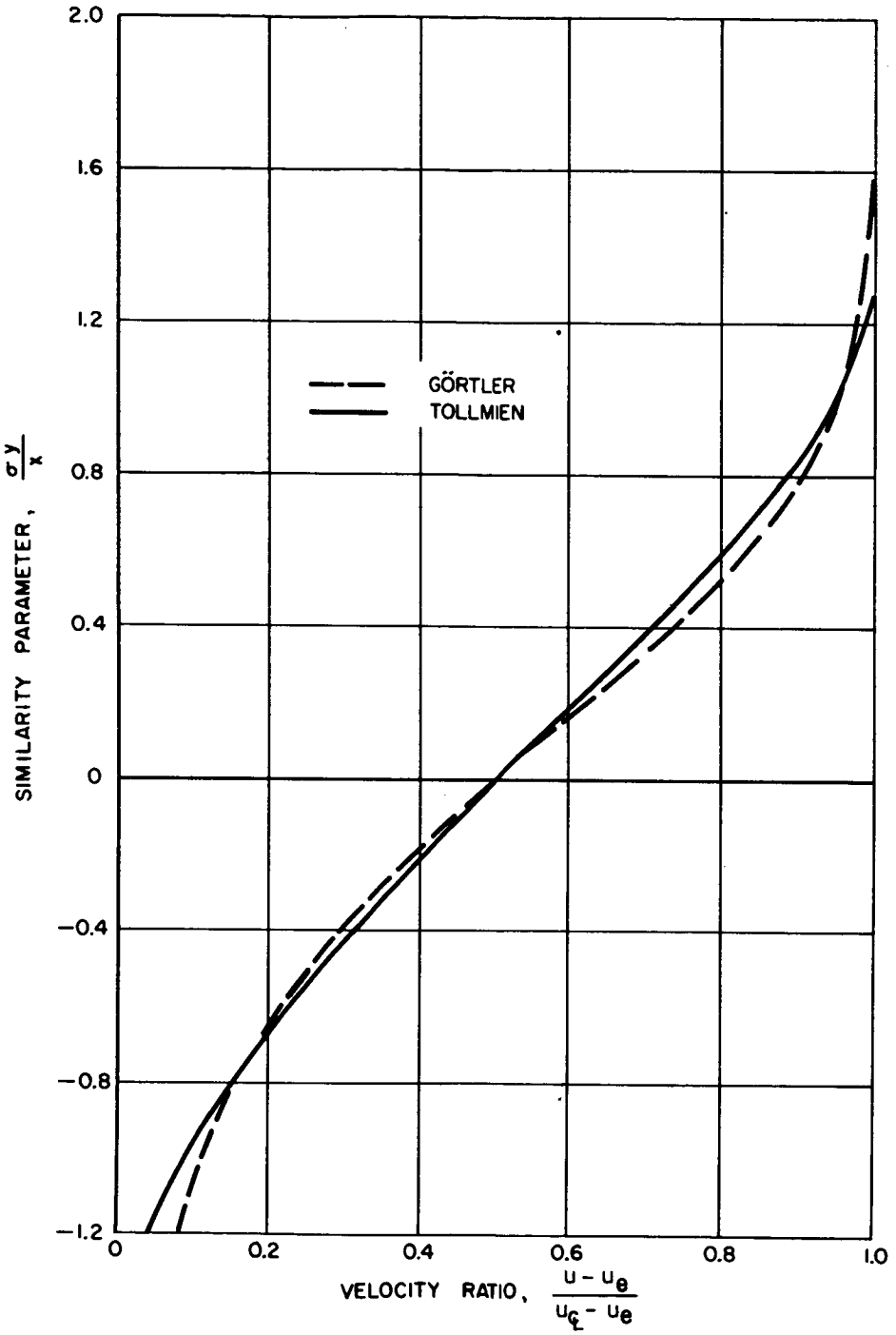

Figure 2.- Theoretical velocity profiles.

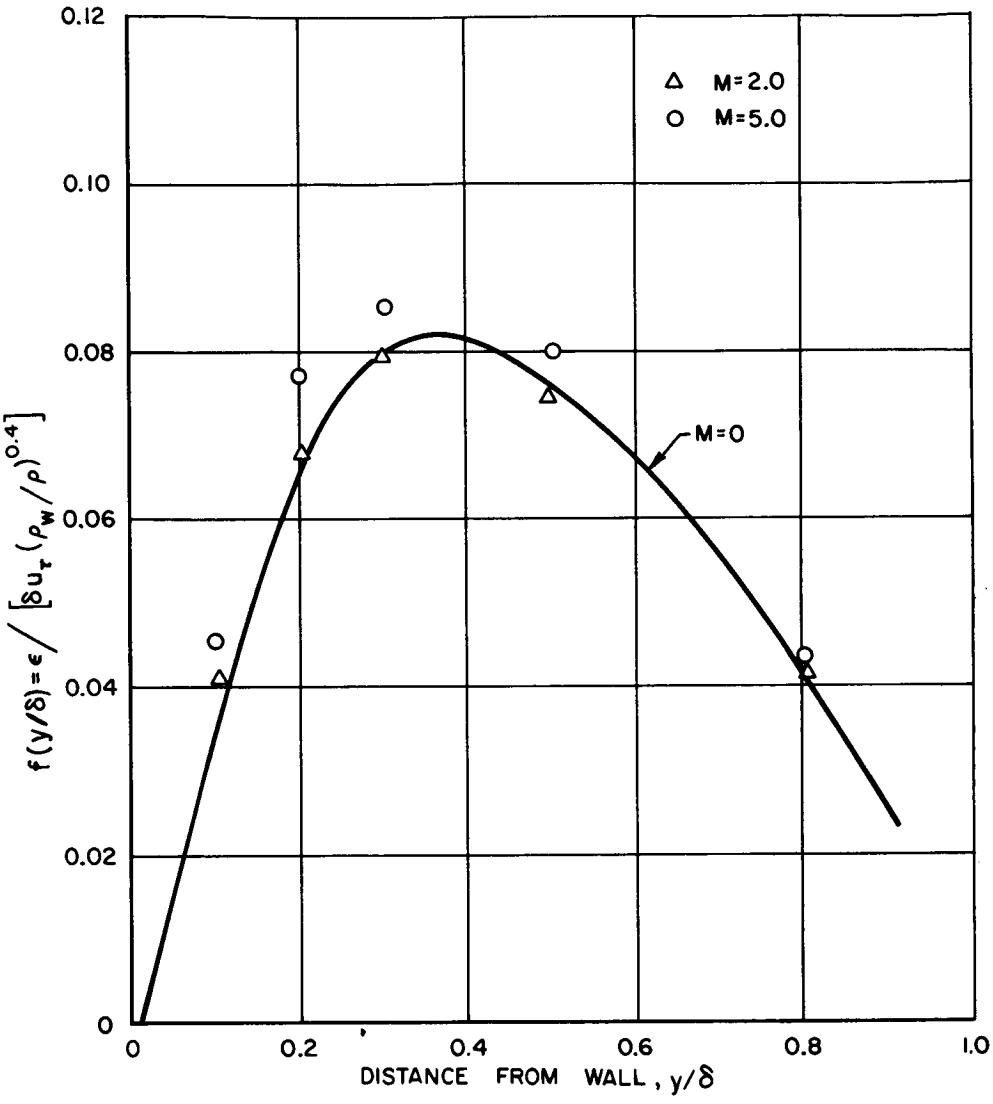

Figure 3.- Correlation of kinematic eddy viscosity for flat-plate, turbulent, compressible, boundary layers. $R_\theta = 10^5$.

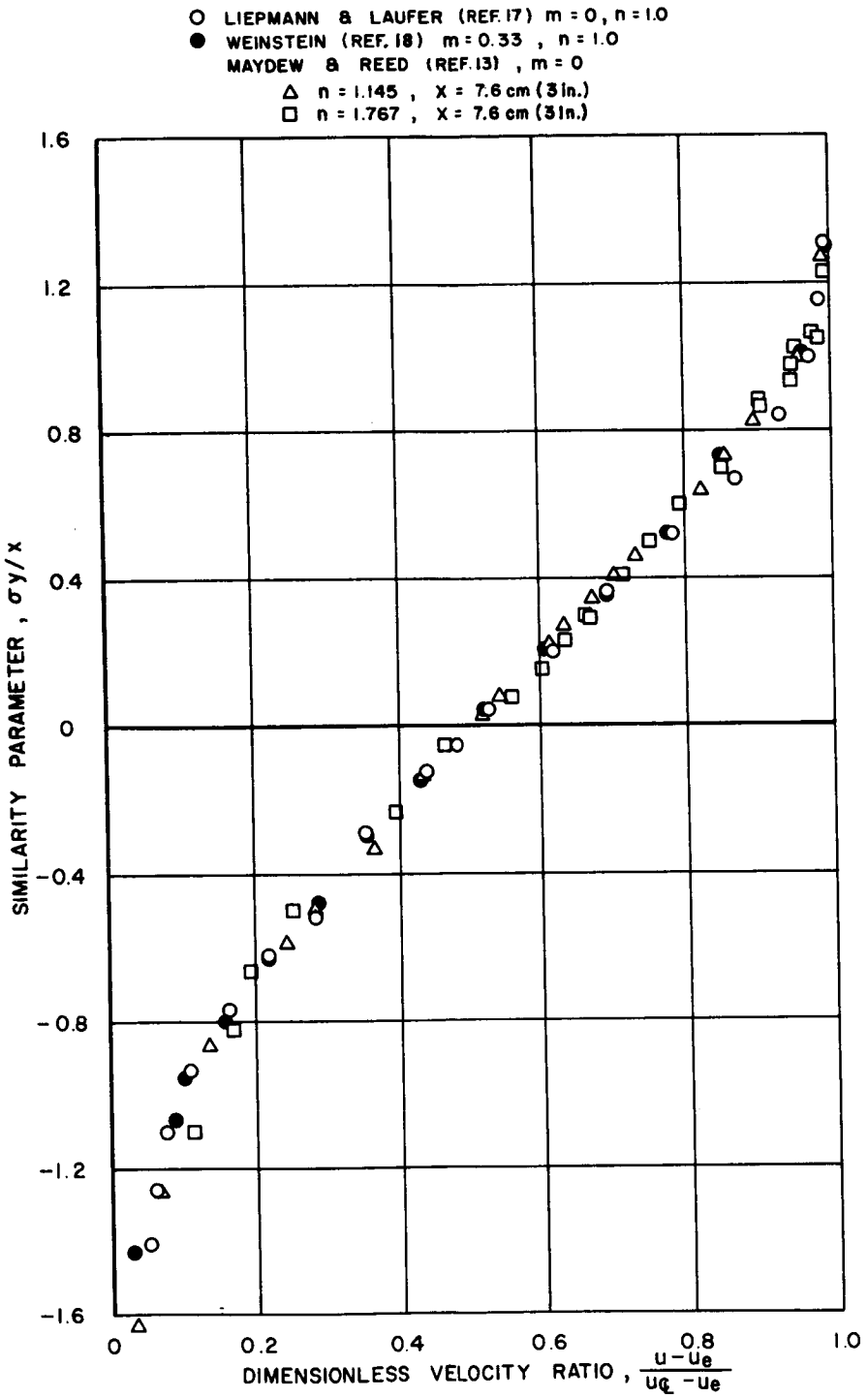

Figure 4.- Correlation of experimental mixing data in core region.

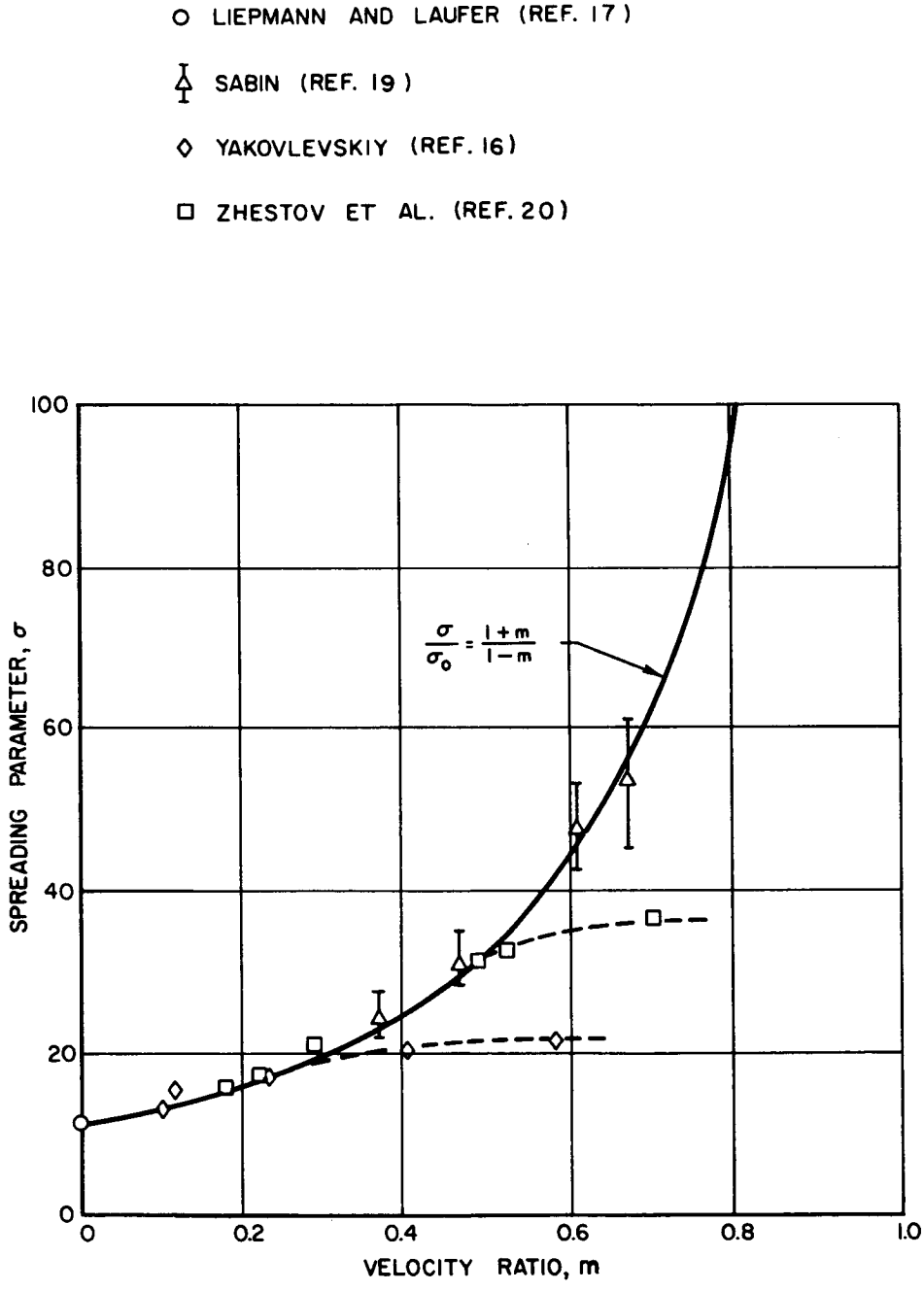

Figure 5.- Effect of velocity ratio on the spreading parameter.

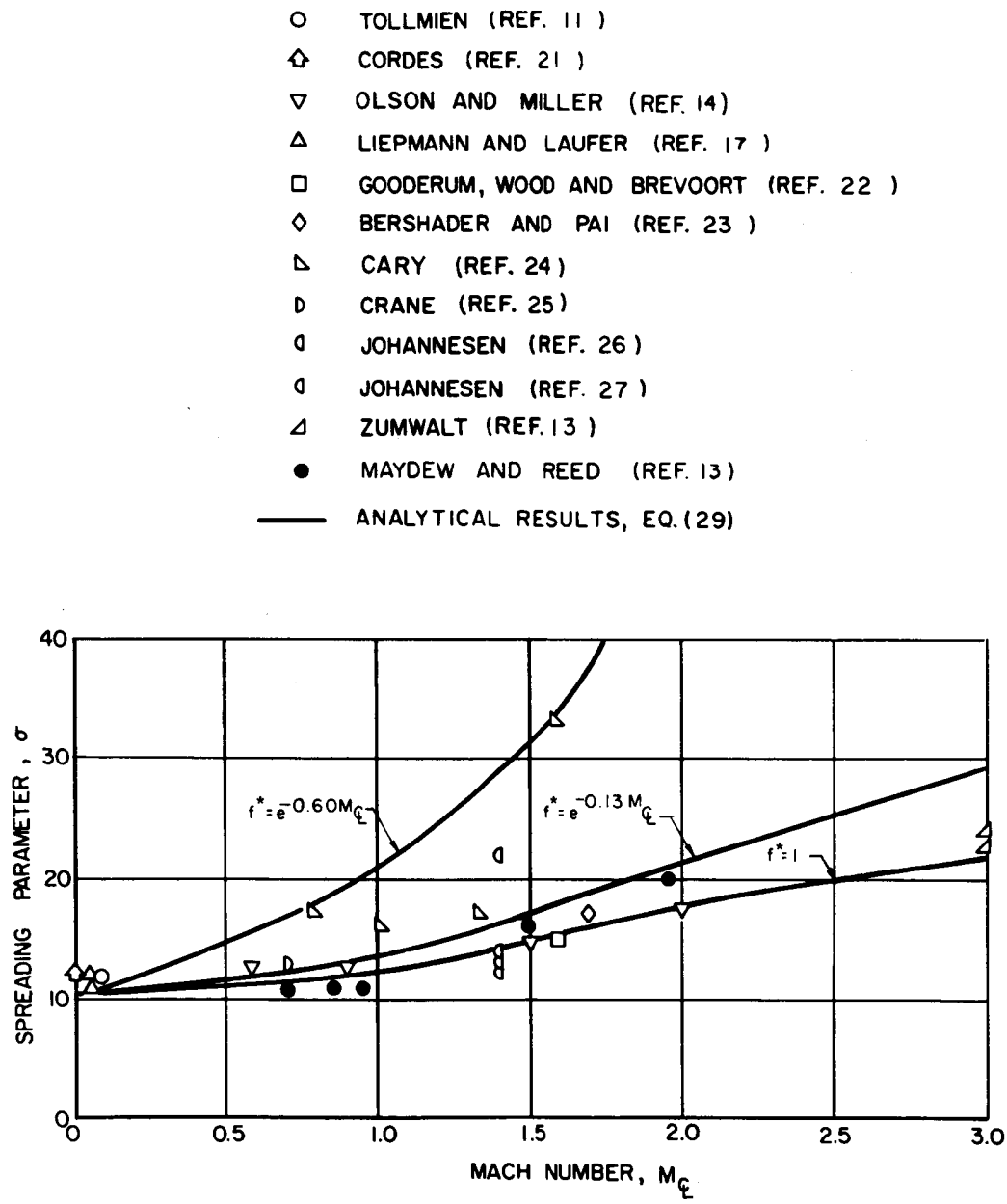

Figure 6.- Effect of Mach number on spreading of turbulent half jets.

LANDIS (REF. 28)

SYM	□	▽	◇	◺
m	0.25	0.25	0.46	0.50
n	1.300	1.087	1.087	1.300

WILLIS & GLASSMAN (REF. 29)

SYM	○	◌	⊖	△	⟑	⟒	●	⊖	▲	⟑
m	0	0.382	0.678	0	0.279	0.496	0.319	0.567	0.234	0.415
n	0.915	0.927	0.952	0.842	0.852	0.876	1.324	1.361	1.218	1.251

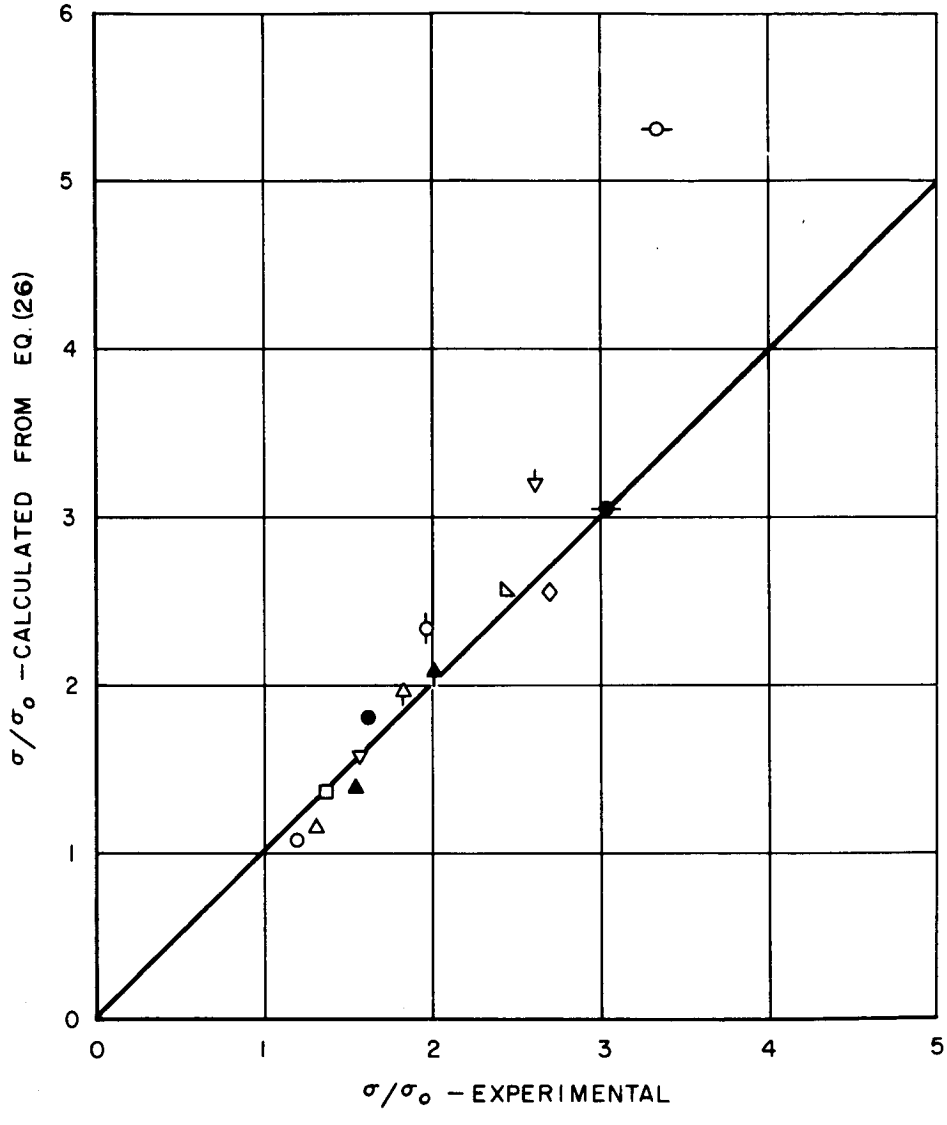

Figure 7.- Comparison of theoretical and experimental spreading parameters in core region.

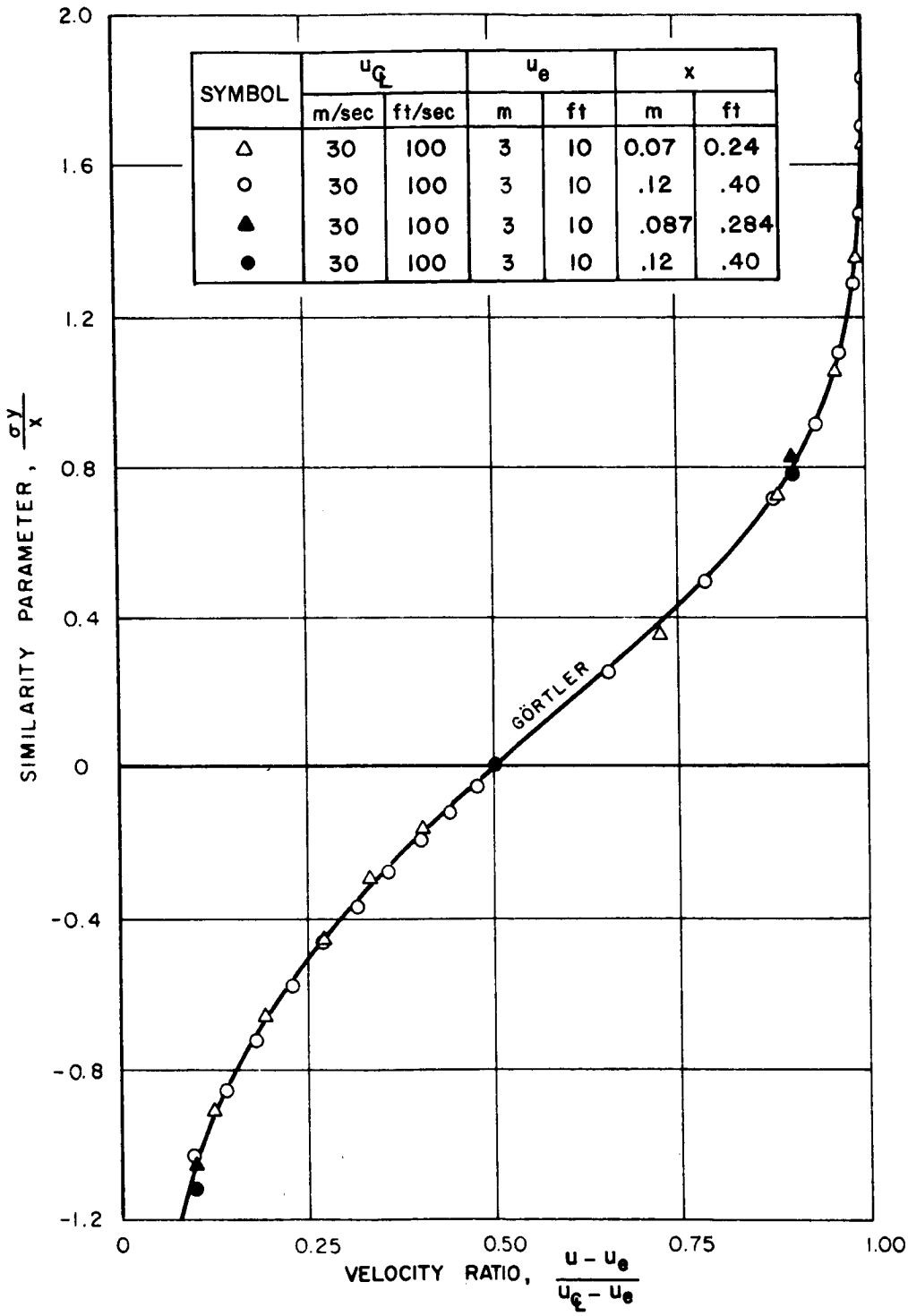

Figure 8.- Comparison of computed results with Görtler profile.

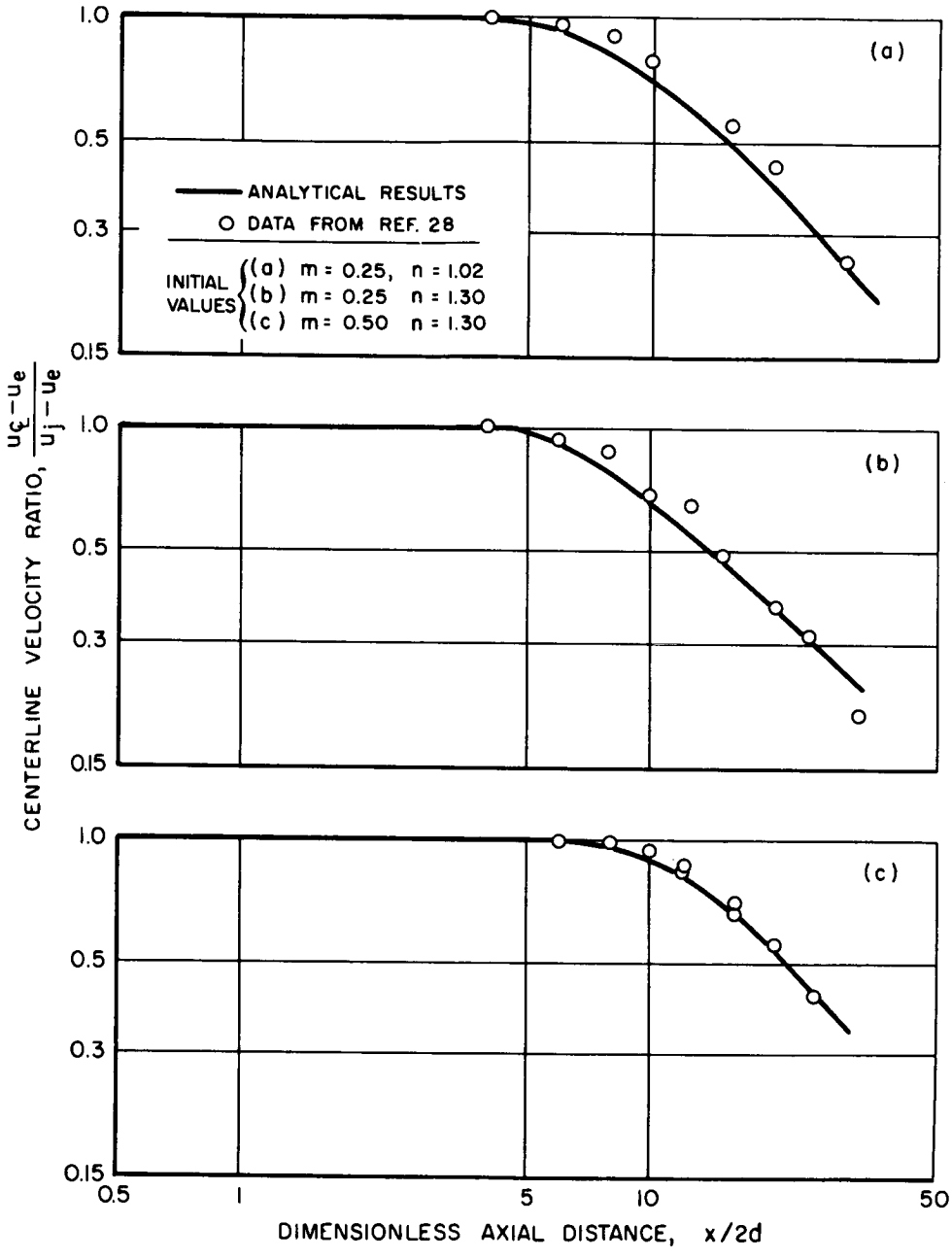

Figure 9.- Centerline velocity distributions for mixing of coaxial incompressible jets.

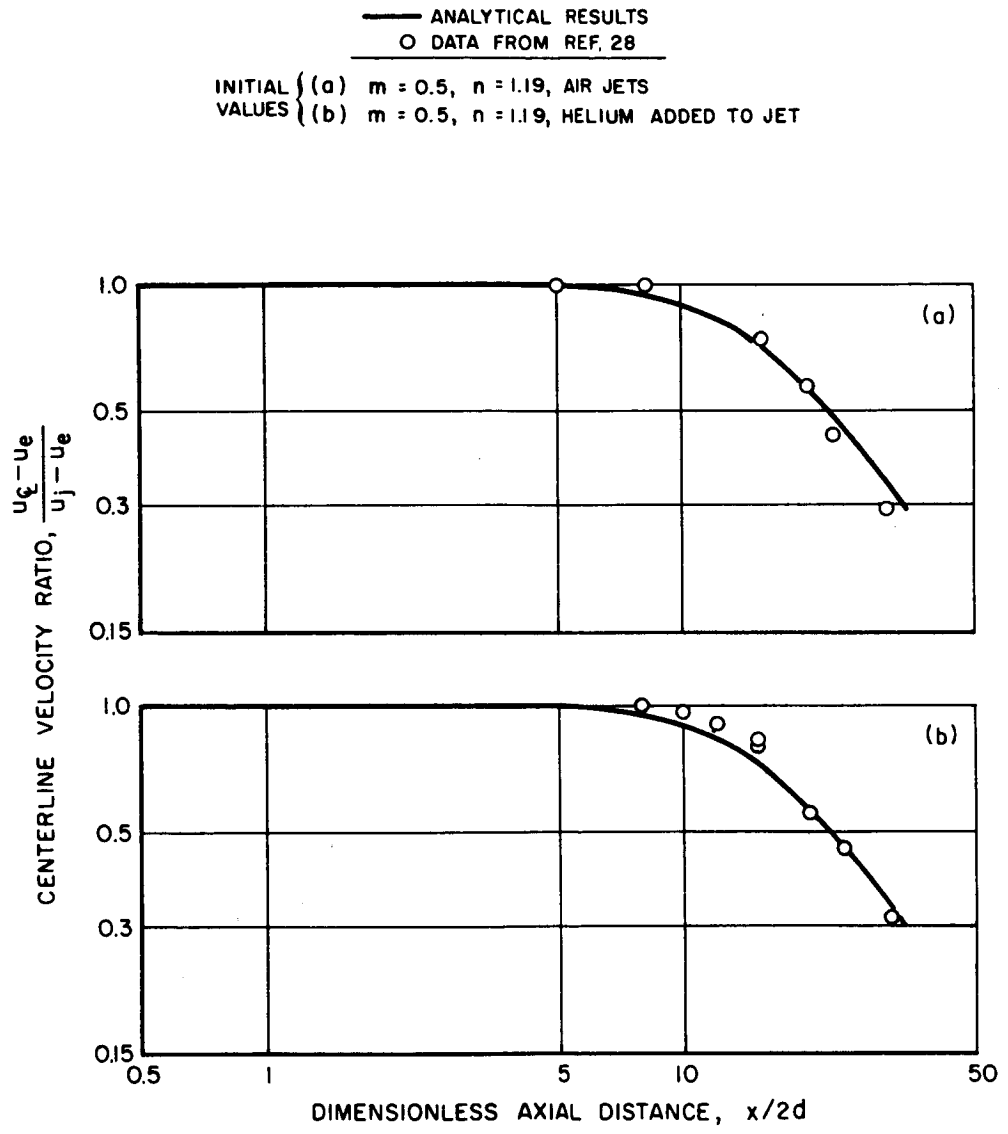

Figure 10.- Centerline velocity distributions for mixing of coaxial incompressible jets.

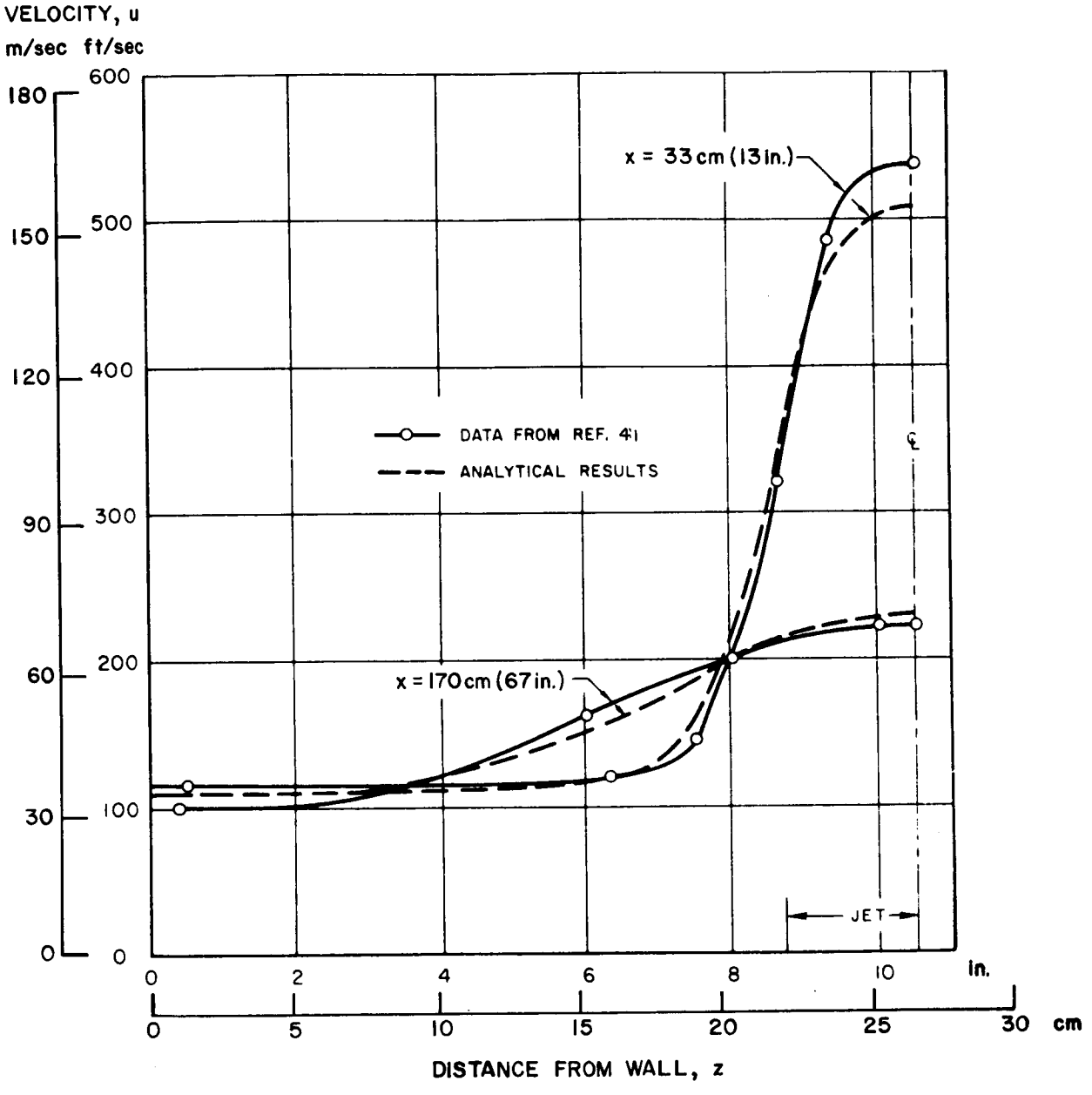

Figure 11.- Radial velocity profiles for subsonic mixing in a 53-cm-diameter (21-in.) tube.

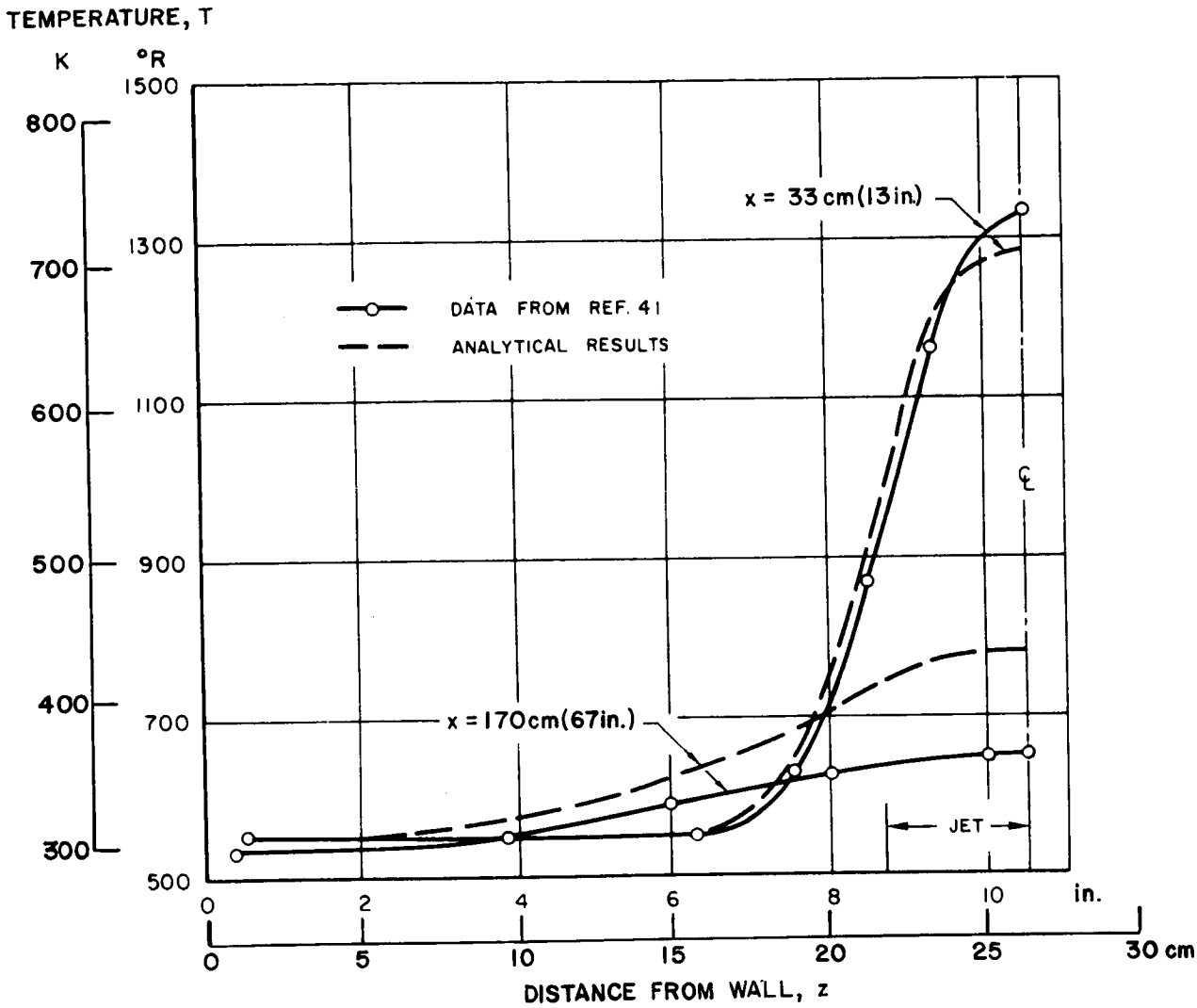

Figure 12.- Radial temperature profiles for subsonic mixing in a 53-cm-diameter (21-in.) tube.

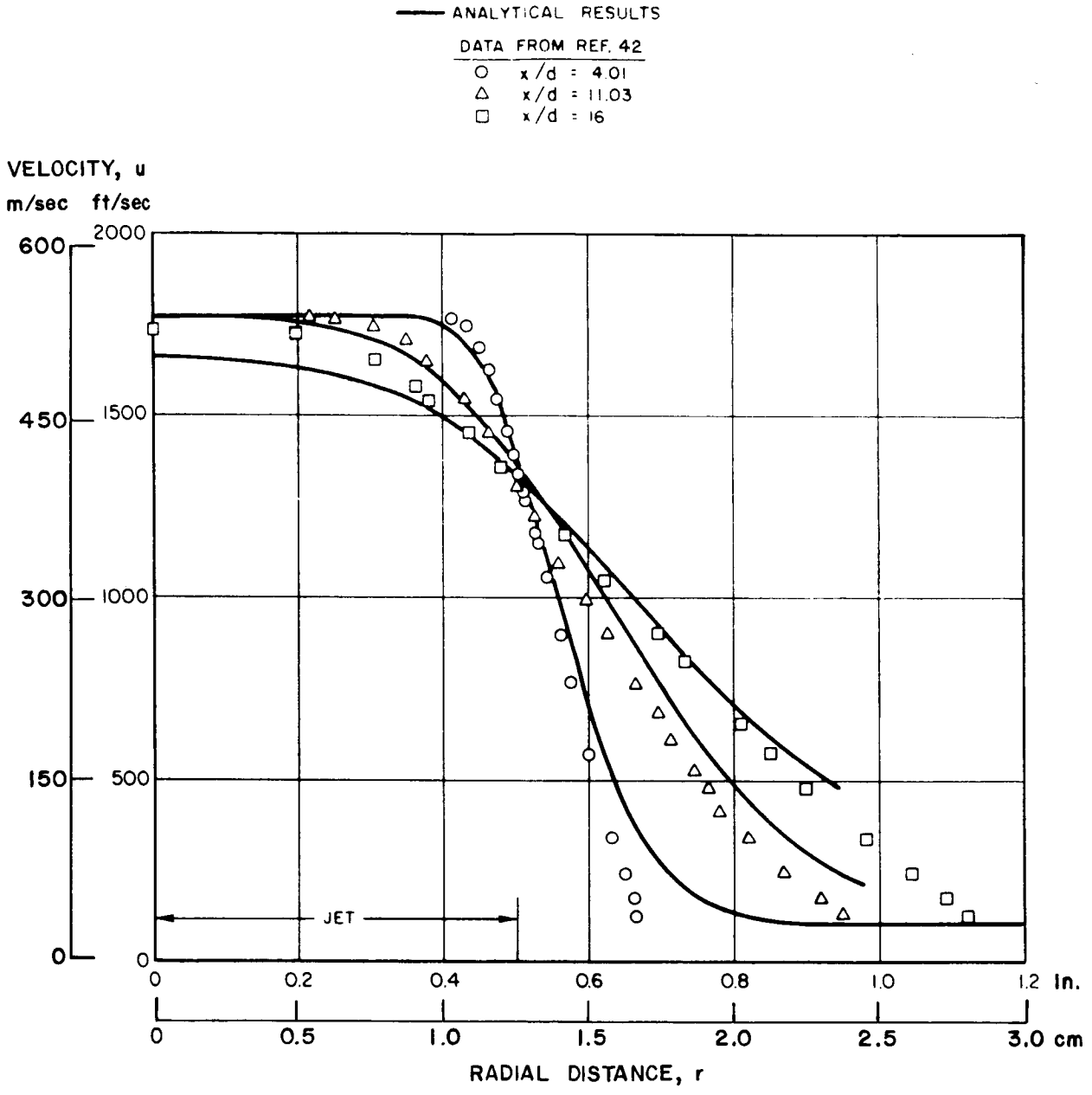

Figure 13.- Mixing of a submerged Mach 2.22 air jet.

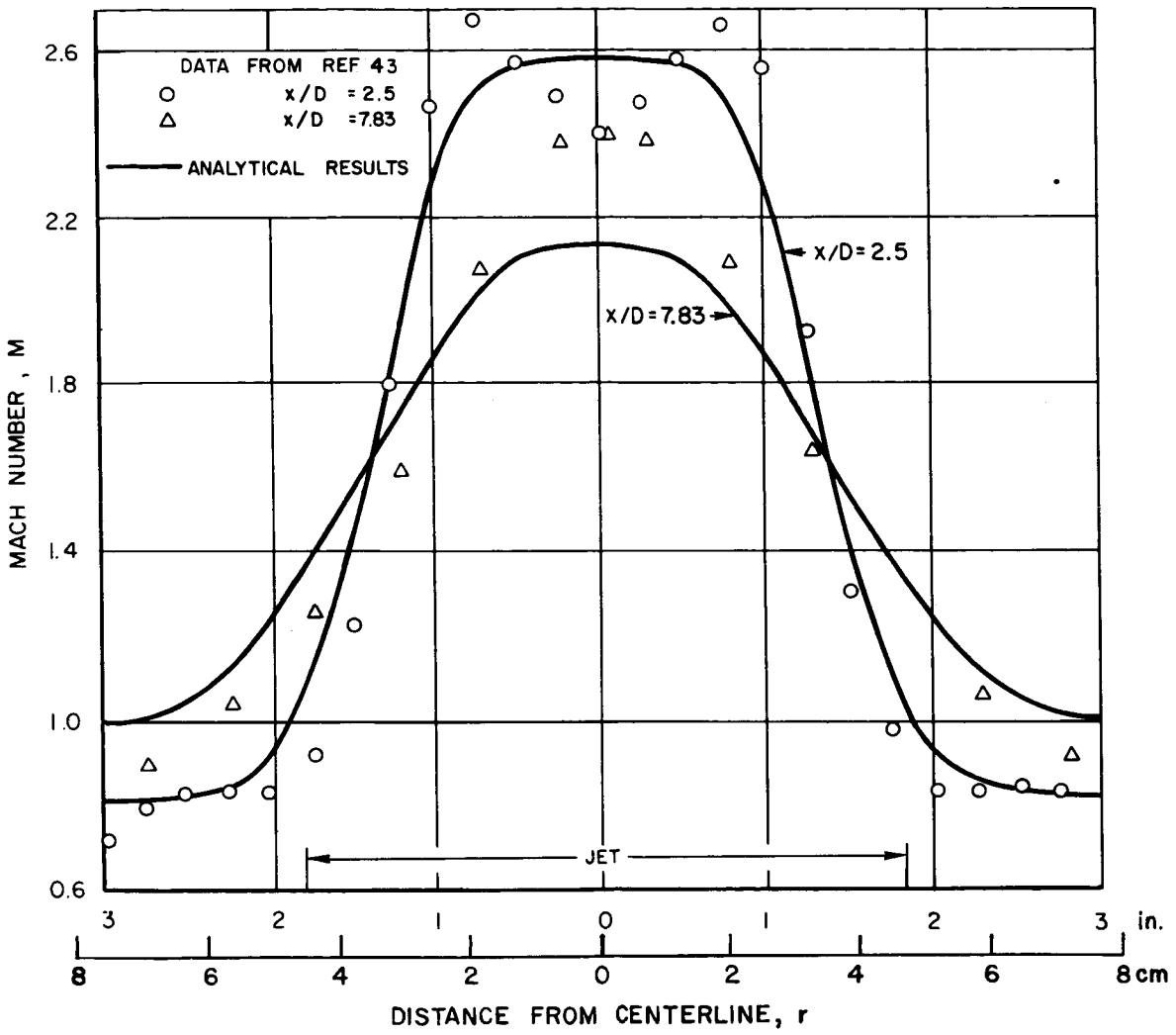

Figure 14.- Mixing of a Mach 2.6 jet with a subsonic external stream in a 15-cm-diameter (6-in.) tube.

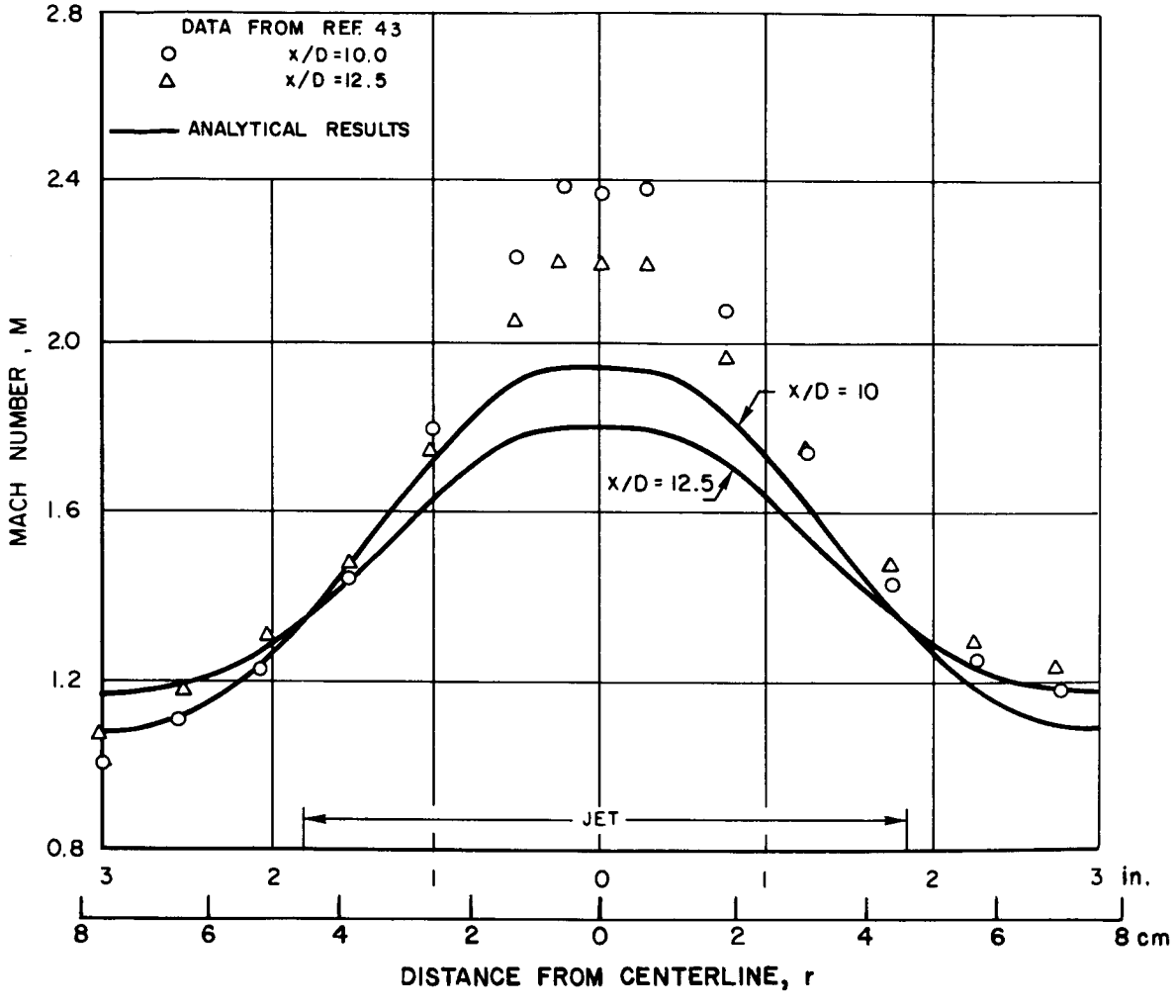

Figure 15.- Mixing of a Mach 2.6 jet with a subsonic external stream in a 15-cm-diameter (6-in.) tube.

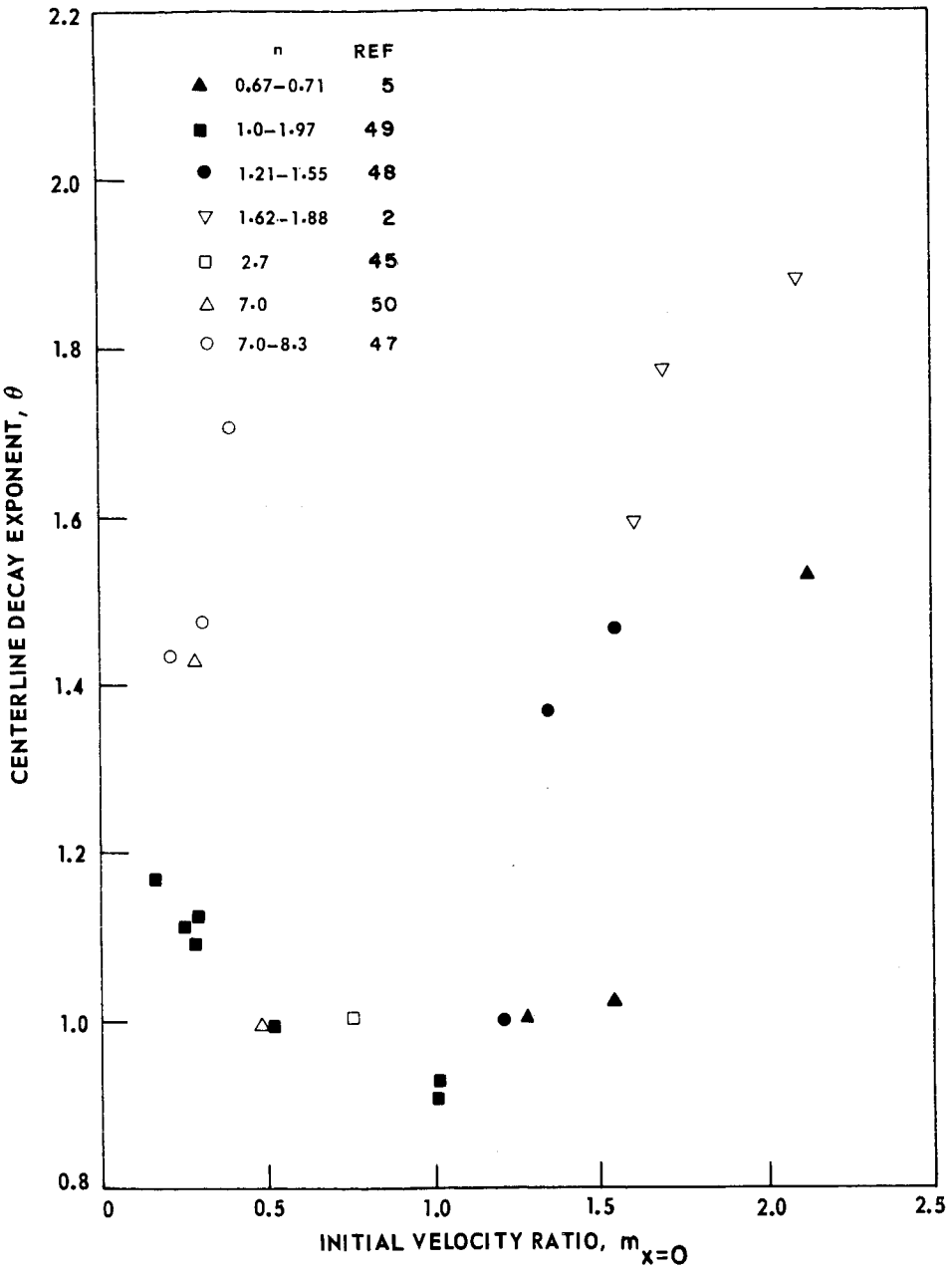

Figure 16.- Correlation of centerline decay exponent.

M. V. Morkovin: Will you ask the awkward question or will I?

H. McDonald: I think Dr. Cohen made it quite clear as to how he viewed the present procedure, that is a pragmatic industrial procedure which is designed to effect some calculations, and as he points out, that any developed turbulence model, I don't want to put words in Dr. Cohen's mouth – any developed turbulence model will have to take certain effects into account before they can be of use to people like the propulsion group at United Aircraft Corporation and in addition will have to explain certain things which the present model does in an albeit empirical manner. Is that correct, Dr. Cohen?

L. S. Cohen: Yes.

M. V. Morkovin: You talk about these preturbulent mechanisms. Well, how many parameters do you really have for the preturbulent mechanism – how do you choose for a given situation? What is the upstream boundary-layer effect or what? I mean, is it just because you have seen it before and you know you are a good cook, or do you have some real mechanisms in mind?

L. S. Cohen: Well I think your comment about being a good cook is part of it, certainly. As I mentioned, it turns out accidently the only thing you really have to select in the model is the m_1 parameter.

M. V. Morkovin: Look, what is the mechanism – you said the mechanism?

L. S. Cohen: I am sorry, I did not mean to imply that what I am calling preturbulence is just a pot into which I am throwing all of my ignorance. What I am saying is, there is some initial turbulence level which, I suppose if we were wise enough, we would go in and measure in all of these difficult cases. In deriving this model, we simply assumed that this initial turbulence level could be sustained somehow in the flow and that this m_1 parameter is directly relatable to this initial turbulence level. The mechanism by which this initial turbulence is produced, I have no idea how it is produced initially. I just think we do not know what the causes are but the effect is a particular initial turbulence level so that no mechanism is put forth for the production of this initial turbulence level.

S. W. Zelazny: I have a comment concerning your second slide and that was the mass fraction decay exponent. You had shown a plot and the plot showed a definite dip in that decay exponent for velocity ratios near unity. I think maybe you might be putting a little bit more into the data interpretation than we have a right to expect, primarily because if you look at the data that are available that enable us to calculate that decay exponent, you will find that most of the data are restricted to about 20 diameters downstream. Some of the data that you used, for example Alpineri's data, did show a decay exponent in the

ballpark of unity. I do not think 20 diameters is sufficiently far downstream to really call it an asymptotic decay and that is what we are looking for.

L. S. Cohen: I guess I agree with what you are saying, but I really do not have any comment on it, I think that your point is well taken.

ANALYSIS OF FREE TURBULENT SHEAR FLOWS BY NUMERICAL METHODS*

By H. H. Korst, W. L. Chow,
University of Illinois at Urbana-Champaign

R. F. Hurt,
Bradley University

R. A. White, and A. L. Addy
University of Illinois at Urbana-Champaign

SUMMARY

Analysis of free turbulent shear flows inherently requires the utilization of conceptual and quantitative formulations concerning the exchange mechanisms. The effort has essentially been directed to classes of problems where the phenomenologically interpreted effective transport coefficients could be absorbed by, and subsequently extracted from (by comparison with experimental data), appropriate coordinate transformations. The transformed system of differential equations could then be solved without further specifications or assumptions by numerical integration procedures.

An attempt has been made to delineate different regimes for which specific eddy viscosity models can be formulated. In particular, this will account for the carryover of turbulence from attached boundary layers, the transitory adjustment, and the asymptotic behavior of initially disturbed mixing regions. Such models have subsequently been used in seeking solutions for the prescribed two-dimensional test cases yielding apparently a better insight into overall aspects of the exchange mechanisms.

Considerable difficulty has been encountered in the utilization of computer programs dealing with axially symmetric geometry as they presently exist at the University of Illinois at Urbana-Champaign. Consequently, only a brief account of these methods and programs has been included – mainly in the form of references.

INTRODUCTION

Much progress in understanding flow separation, separated flows, and wakes has been made since the mutual dependence between viscid and inviscid flow regions has been properly recognized. Development of an attached boundary layer, its separation from solid boundaries forming a free shear layer capable of mass entrainment

*This work was partially supported by NASA through Research Grant No. NsG-13-59 and subsequently through NGL-14-005-140.

from the wake, and energy transfer to and across individual streamlines have been related to the recompression process at the end of the wake and thus have allowed the analysis of previously not understood flow problems of practical importance.

Over more than a decade, work at the University of Illinois at Urbana-Champaign has been focused on propulsion problems relating to base pressure, base heating, and ejector nozzles for thrust augmentation, and so forth. In support of a comprehensive systems approach (based on the understanding of constituent flow components) much attention had to be given to free shear layers which has resulted in both analytical and experimental programs. These efforts have, however, been clearly guided by, and subordinated to, practical objectives.

When called to the task of participating in the present effort, the authors were restricted, naturally, to what had already been developed for serving their own programs. The response is, therefore, selective inasmuch as some of their computer programs have not been found flexible enough to handle all the cases submitted to the predictors.

SYMBOLS

c	concentration of species
c_p	specific heat at constant pressure
C	Crocco number
d	viscosity index
D	energy defect thickness
f	dimensionless stream function (similarity solution)
g	function of transformed x-coordinate
h	enthalpy
I	integrals defined in reference 6
k	thermal conductivity
L	reference length

M	molecular weight or Mach number
Pr_t	turbulent Prandtl number
r	radius
R	gas constant
Re_x	Reynolds number based on x, $u_a x/\nu_a$
Sc_t	turbulent Schmidt number
T	temperature
u	longitudinal velocity component
v	transverse velocity component
W	dimensionless center-line velocity defect
x	longitudinal coordinate
x_o	shifted origin position
y	transverse coordinate
δ	boundary-layer thickness
δ^{**}	momentum thickness of boundary layer
δ^{***}	energy thickness of boundary layer
ϵ	eddy diffusivity
$\zeta = \frac{r}{r_a}$	where r_a is the radius of the central jet
η	similarity variable
θ	static temperature ratio

Λ	stagnation temperature ratio
μ	dynamic viscosity
ν	laminar kinematic viscosity
ξ	dimensionless x-coordinate
$\overline{\xi}$	transformed coordinate
ρ	density
σ	spread rate parameter
σ_o	spread rate parameter for incompressible flow
ϕ	dimensionless velocity
ψ	stream function
$\overline{\psi}$	dimensionless stream function

Subscripts:

a	faster free stream
asy	asymptotic condition
b	slower free stream
c	center-line value
d	particular viscosity index value, or the dividing streamline
e	error function
ℓ	laminar state
o	stagnation state

RA large value of η

t turbulent or transitional state

1,2,4 integrals in reference 6

ANALYSIS

This analysis is restricted at the outset to constant-pressure mixing. Any additional assumptions, as they will affect the mathematical rigor or impose physical restrictions on the solution, will be discussed as they are introduced.

It will be useful to differentiate between kinematic and dynamic similarity when single-independent-variable solutions are utilized. The former refers to nonasymptotic mixing profiles which can be related to similarity profiles by accounting for initial disturbances through appropriate coordinate shifts. Normally, such profiles will not exhibit dynamic similarity as the initial exchange mechanism is not consistent with that of the "matched" solution. On the other hand, when the initial profile of the mixing region results from a strong expansion of an attached boundary layer, there may be nearly dynamic similarity within a newly started shear region at the very edge of the expanded profile, while the growth of the dissipative shear regions occurs within a vortex layer and thus does not exhibit kinematic similarity.

TWO-DIMENSIONAL MIXING

Fundamental Equations

The conservation equations for a pure substance[1] are

$$\frac{\partial}{\partial x}(\rho u) + \frac{\partial}{\partial y}(\rho v) = 0 \tag{1}$$

$$\rho u \frac{\partial u}{\partial x} + \rho v \frac{\partial u}{\partial y} = \frac{\partial}{\partial y}\left(\epsilon_t \rho \frac{\partial u}{\partial y}\right) \tag{2}$$

$$\rho u c_p \frac{\partial T}{\partial x} + \rho v c_p \frac{\partial T}{\partial y} = \frac{\partial}{\partial y}\left(k_t \frac{\partial T}{\partial y}\right) + \rho \epsilon_t \left(\frac{\partial u}{\partial y}\right)^2 \tag{3}$$

The stream function is now introduced

$$\frac{\partial \psi}{\partial y} = + \frac{\rho}{\rho_a} u \qquad \frac{\partial \psi}{\partial x} = - \frac{\rho}{\rho_a} v$$

[1] An extension for gas mixtures is discussed subsequently. For a more detailed account, see Hurt (ref. 1).

and new dimensionless variables defined

$$\phi = \frac{u}{u_a} \qquad \xi = \frac{x}{L} \qquad \overline{\psi} = \frac{\psi}{u_a L} \qquad \theta = \frac{T}{T_a} = \frac{\rho_a}{\rho} \tag{4}$$

where $\overline{\psi}$, related to the stream function ψ, is to be used as an independent variable in the Von Mises plane. Accordingly, after introducing the free-stream Crocco number,

$$C_a{}^2 = \frac{u_a{}^2}{2c_p T_{o_a}} \tag{5}$$

and accounting for the transport mechanisms by the kinematic viscosity $\epsilon_t = \frac{\mu_t}{\rho}$ and the effective Prandtl number Pr_t, the following equations are obtained:

$$\left.\frac{\partial \phi}{\partial \xi}\right|_{\overline{\psi}} = \frac{\partial}{\partial \overline{\psi}}\left|_{\xi}\left[\frac{\epsilon_t}{Lu_a}\frac{\phi}{\theta^2}\left.\frac{\partial \phi}{\partial \overline{\psi}}\right|_{\xi}\right]\right. \tag{6}$$

$$\left.\frac{\partial \theta}{\partial \xi}\right|_{\overline{\psi}} = \frac{\partial}{\partial \overline{\psi}}\left[\frac{1}{Pr_t}\frac{\epsilon_t}{Lu_a}\frac{\phi}{\theta^2}\left.\frac{\partial \theta}{\partial \overline{\psi}}\right|_{\xi}\right] + \frac{\epsilon_t}{Lu_a}\frac{2C_a{}^2}{1 - C_a{}^2}\frac{\phi}{\theta^2}\left(\frac{\partial \phi}{\partial \overline{\psi}}\right)^2 \tag{7}$$

A far reaching simplification of the analysis can be achieved by setting (ref. 2)

$$\mu_t \rho^{(1-d)} = f(\xi) \tag{8}$$

where $d = 1 - \omega$ (ω being the exponent of the Sutherland equation for the dynamic viscosity of a gas) corresponds to the laminar mixing problem.

The transformation

$$d\overline{\xi} = \frac{1}{Re_L}\frac{\epsilon_t}{\nu_\ell \theta^{2-d}}\, d\xi \tag{9}$$

then produces a pair of parabolic simultaneous partial differential equations which can be solved without reference to any specific assumption concerning exchange mechanisms (except d and Pr_t). These equations are

$$\frac{\partial \phi}{\partial \overline{\xi}} = \frac{\partial}{\partial \overline{\psi}}\left(\frac{\phi}{\theta^d}\frac{\partial \phi}{\partial \overline{\psi}}\right) \tag{10}$$

$$\frac{\partial \theta}{\partial \overline{\xi}} = \frac{1}{Pr_t}\frac{\partial}{\partial \overline{\psi}}\left(\frac{\phi}{\theta^d}\frac{\partial \theta}{\partial \overline{\psi}}\right) + \frac{2C_a{}^2}{1 - C_a{}^2}\frac{\phi}{\theta^d}\left(\frac{\partial \phi}{\partial \overline{\psi}}\right)^2 \tag{11}$$

For given initial conditions, step-by-step integrations using implicit iterative procedures for better convergence (see ref. 3) can be carried out with the help of high-speed digital computers.

Results appear in the form of $\phi\left(\bar{\xi},\bar{\psi}\right)$ and $\theta\left(\bar{\xi},\bar{\psi}\right)$ and the coordinate y/L is found from

$$\psi = \int_0^{y/L} \frac{\phi}{\theta}\, d\left(\frac{y}{L}\right) \tag{12}$$

Similarity Solutions

"Exact solutions".- By starting with equation (10) and following the development for nonisoenergetic mixing of two uniform streams having identical compositions (ref. 4), an effective Prandtl number of unity, and satisfying the boundary conditions

$$y \to -\infty, \quad u \to u_b, \quad T_o \to T_{o_b}$$

$$y \to +\infty, \quad u \to u_a, \quad T_o \to T_{o_a}$$

leads to

$$f''' + \left[\frac{\Lambda - C_a{}^2 f'^2}{1 - C_a{}^2}\right]^d ff'' - d\left(\Lambda' - 2C_a{}^2 f' f''\right)\frac{f''}{\Lambda - C_a{}^2 f'^2} = 0 \tag{13}$$

where $f(\eta) = \dfrac{\bar{\psi}}{g\left(\bar{\xi}\right)}$, $f'(\eta) = \phi$, η is the independent similarity variable defined by

$$\left.\frac{\partial \eta}{\partial \bar{\xi}}\right|_{\bar{\psi}} = -\frac{fg'}{f'g} \tag{14}$$

$$\left.\frac{\partial \eta}{\partial \bar{\psi}}\right|_{\bar{\xi}} = \frac{1}{gf'} \tag{15}$$

and primes indicate differentiation with respect to the respective independent variable. From the assumption of similarity, it follows that one may set

$$gg' = 1$$

so that

$$g\left(\bar{\xi}\right) = \sqrt{2\bar{\xi}} \tag{16}$$

and the transformation to physical coordinates can be accomplished with

$$\int \theta \, d\eta = \int \frac{1}{\sqrt{2\xi}} d\left(\frac{y}{L}\right) \tag{17}$$

By adopting Göertler's formulation (ref. 5) of σ,

$$\frac{\epsilon_t}{\nu\theta^{2-d}} = \frac{1}{4\sigma_d{}^2} Re_L \frac{x}{L} \tag{18}$$

one obtains

$$2\sigma_d \frac{y}{x} = \int_{\eta_j}^{\eta} \theta \, d\eta \tag{19}$$

where the origin of y is placed at the zero streamline where $f(\eta_j) = 0$. The notation σ_d has been introduced to stress the fact that the similarity parameter σ depends not only on the procedure of matching between an experimental and an analytical profile but also on the choice (if one is needed or indicated) of the analytical formulation (ref. 4).

An extension to analyze the mixing of two streams having different gas constants R_a and R_b is easily accomplished for Prandtl and Lewis numbers of unity by the expression

$$\frac{\rho_a}{\rho} = \frac{1}{1 - C_a{}^2} \left\{ \frac{\left[\phi\left(1 - \frac{R_b}{R_a}\right) + \frac{R_b}{R_a} - \phi_b\right]\left[\phi - \phi_b + \frac{T_{o_b}}{T_{o_a}}(1 - \phi)\right]}{(1 - \phi_b)^2} - \phi^2 C_a{}^2 \right\} \tag{20}$$

(See discussion of test case 3, also.)

Error function solution.- Proposed as a first-order approximation for solving equation (10) under the conditions of incompressible flow with $d = 0$ by Göertler (ref. 5), the error function distribution for the velocity profile is

$$\phi = \frac{1}{2}(1 + \phi_b) + \frac{1 - \phi_b}{2} \operatorname{erf} \eta \tag{21}$$

where $\eta = \sigma_e\left(\frac{y}{x}\right)$. The error function solution has been widely used for momentum integral methods devised to deal with compressible, diabatic (ref. 6), and even reactive (ref. 7) free shear layers. Auxiliary integrals for determining mass, momentum, and energy transfer, as well as shear stress, dissipation rates, and property distributions, have been tabulated (ref. 6) or made subroutines of more comprehensive programs dealing with propulsion problems (ref. 8). A discussion of differences between spread rate parameters $(\sigma_e, \sigma_d, \text{etc.})$ has been included in reference 4.

Initially Disturbed Mixing Region

Similarity solutions are reached asymptotically as the influence of initial disturbances (in velocity and property profiles and in the exchange mechanism) decreases. The gradual approach to similarity profiles can be represented in its latest stages by a lateral shift of mixing profiles, that is, by satisfying the momentum integrals. This still leaves open the question of how to interpret properly similarity parameters such as σ when the exchange mechanism is to be evaluated at other than far-downstream locations. Attention will be given to the latter problem in the section on "Eddy Viscosity Concepts."

Origin-shift methods.- Utilization of similarity solutions for initially disturbed profiles by origin-shift methods has been suggested in different forms by various authors, and the work of Hill and Page (ref. 9) and Kessler (ref. 10) may be consulted for further details. Use of the momentum integral for determining lateral and longitudinal coordinate shifts will, however, become unfeasible when wakes or mixing between streams of nearly equal velocity in the presence of relatively large initial disturbances have to be considered. It should be noted that virtual origins for exchange coefficient growth have been found useful in connection with eddy viscosity models employed in finite-difference integrations of the fundamental equations (see the section "Eddy Viscosity Concepts").

Local similarity.- The restriction on the type of viscosity models consistent with the longitudinal coordinate transformation expressed by equation (9) will be found most unrealistic for cases where a relatively thick boundary layer undergoes a rapid expansion (such as in base flows) before the onset of constant-pressure mixing. This can lead to effective quenching of the turbulence level in the expanded profile (which is then rotational but not strongly dissipative) while the dissipative exchange mechanism remains confined to a much narrower shear region (refs. 11 and 12). This shear region exhibits features of local similarity and is initially laminar before undergoing transition. Growth of such transitional shear regions, for single-stream mixing, has been analyzed in some detail by Gerhart (ref. 13), and there seems to be confirmation that the similarity parameter σ retains its qualitative relevance and quantitative value. Since turbulent mixing now appears to originate well downstream of the "expansion corner," agreement with origin-shift methods concerning the energy levels of the dividing streamline is surprising but can be supported by detailed calculations.

Numerical integrations.- Computer programs have been developed to perform the step-by-step numerical integration of the system of equations (refs. 1 and 2), and an implicit iterative method of integration is utilized which improves the economy of the calculations while retaining accuracy and assuring numerical stability.

The integration uses initial and boundary conditions given in physical coordinates x and y but proceeds with calculations in the transformed $\bar{\xi}\bar{\psi}$-plane. Dimensionless velocity $\left(\phi = \frac{u}{u_a}\right)$, temperature $\left(\theta = \frac{T}{T_a}\right)$, or density $\left(\rho/\rho_a\right)$ distributions are then found as

functions of $\bar{\psi}$ (or y/L) for parametric values of the variable $\bar{\xi}$. Location of the $\bar{\xi}$ value with the x-scale depends upon the viscosity law as contained in the transforming equation (eq. (9)) which can be written

$$\bar{\xi} = \frac{1}{Re_L} \int \frac{\epsilon}{\nu_\ell \theta^{2-d}} d\,\frac{x}{L}$$

Attempts have been made to gain information on the integrand by matching of calculated and experimentally determined profiles, for example, by the dissipation integral (ref. 2) or other unique features (such as minimum velocity in wakes). (See section concerned with determination of the eddy viscosity.)

For the problems at hand, however, one needs this information as input, and certain speculative assumptions on the behavior of the turbulent eddy viscosity still are to be specified in the section "Eddy Viscosity Concepts" in order to explain their use for obtaining solutions to the test cases.

AXIALLY SYMMETRIC MIXING REGIONS

An extension of the theoretical analysis and the resulting computer program for jet mixing dealing with axisymmetric geometries and nonhomogeneous gases has been made by Hurt (ref. 1). Like many others (e.g., refs. 14 and 15), he utilizes the system of global conservation equations as well as conservation of species without chemical reactions. The simplifying assumptions are consistent with boundary-layer approximations but, in addition, he assumes a turbulent Lewis number of unity which implies that the turbulent Schmidt and Prandtl numbers are equal to each other yet not necessarily equal to unity individually. Also, specific heats at constant pressures are assumed to be functions of concentrations but not of temperature, which limits his analysis to moderate temperature variations even though it attempts to cope with compressibility. In this sense, and with regard to improved numerical integration procedures, Hurt's work is an extension of that by Donovan and Todd (ref. 15). The resulting set of equations is in analogy with those of the preceding sections except for the accounting for species and the use of a dimensionless enthalpy rather than temperature in the energy equations:

$$\left.\begin{aligned}
\frac{\partial \phi}{\partial \xi} &= \frac{\partial}{\partial \bar{\psi}}\left[\bar{\epsilon}\bar{\rho}^2\zeta^2\phi\,\frac{\partial \phi}{\partial \bar{\psi}}\right] \\
\frac{\partial c_i}{\partial \xi} &= \frac{\partial}{\partial \bar{\psi}}\left[\frac{\bar{\epsilon}}{Sc_t}\,\bar{\rho}^2\zeta^2\phi\,\frac{\partial c_i}{\partial \bar{\psi}}\right]_{i=1,N} \\
\frac{\partial \bar{h}}{\partial \xi} &= \frac{\partial}{\partial \bar{\psi}}\left[\frac{\bar{\epsilon}}{Pr_t}\,\bar{\rho}^2\zeta\phi\,\frac{\partial \bar{h}}{\partial \bar{\psi}}\right] + \frac{2Ca^2}{1 - Ca^2}\,\bar{\epsilon}\bar{\rho}^2\zeta^2\phi\left(\frac{\partial \phi}{\partial \bar{\psi}}\right)^2
\end{aligned}\right\} \qquad (22)$$

Here,

$$\bar{\rho}\frac{u}{u_a} = \frac{1}{\zeta}\frac{\partial\bar{\psi}}{\partial\zeta} \qquad \bar{\rho}\frac{v}{u_a} = -\frac{1}{\zeta}\frac{\partial\bar{\psi}}{\partial\xi}$$

C_a is the Crocco number of the internal stream, and $\bar{\epsilon} = \frac{\epsilon}{u_a r_a}$ were r_a is a reference radius of the coaxial stream, $\bar{\rho} = \frac{\rho}{\rho_a}$, and $\bar{h} = \frac{h}{h_a}$.

In addition, the perfect gas law for isobaric mixing of a multispecies mixture

$$\bar{\rho} = \frac{1}{\gamma\bar{T}} \tag{23}$$

was utilized, where

$$\gamma = \frac{\sum_{i=1}^{N} \frac{c_i}{\bar{M}_i}}{\sum_{i=1}^{N} \frac{c_{a_i}}{\bar{M}_i}} \tag{24}$$

$\bar{M}_i$ is the molecular weight of the ith species, and $\bar{T} = \frac{T}{T_a}$. The static temperature ratio $\bar{T}$ was evaluated from the energy equation and then the stagnation temperature ratio was found by using the following formulation developed from the relationship between stagnation and static enthalpy:

$$\Lambda = \bar{T}\left(1 - C_a{}^2\right) + \left(\frac{\phi^2 C_a{}^2}{\alpha}\right) \tag{25}$$

where

$$\alpha = \frac{\sum_{i=1}^{N} c_i c_{p_i}}{\sum_{i=1}^{N} c_{a_i} c_{p_{a_i}}} \tag{26}$$

and Λ is the local stagnation temperature ratio. In contrast to the two-dimensional case, the transformation of the streamwise coordinate ξ (to eliminate the eddy viscosity from the equation) was not included in Hurt's analysis. This was due to evidence that the effective turbulent exchange coefficient could not be considered, with sufficient accuracy, to be a function of the streamwise coordinate only. His program, thus, can accommodate as input suitable eddy viscosity models. At this stage, however, there do not appear to be

sufficient experimental data and insight into controlling mechanisms to expect a simple yet universal formulation for a phenomenological eddy viscosity model.

It is of interest to note the efforts of Spalding and his coworkers at Imperial College (e.g., ref. 16) and others to gain a better insight into turbulent exchange mechanisms by use of multiparameter models involving the kinetic energy of turbulent motion.

EDDY VISCOSITY CONCEPTS

Within the restrictions imposed by the coordinate transformation (eq. (9)) and the resulting coupling of the viscosity to the density for two-dimensional mixing problems, there is still the possibility of coping with fully laminar, fully turbulent, and transitional cases. The initial conditions have first to be examined.

INITIAL CONDITIONS RELATED TO APPROACHING BOUNDARY LAYER

A mixing region can be the result of flow separation associated with

(i) Constant pressure (wake behind a flat plate)

(ii) An acceleration (as in the supersonic base pressure problem)

(iii) A pressure rise (due to an adverse pressure gradient)

In any one of these cases, the attached boundary layer will cause an initial disturbance for the mixing region. Each case, however, will be different in its kinematic and dynamic effects.

The constant-pressure case appears to be the simplest. One would expect that both the flow profile and the viscous structure remain virtually unchanged. The acceleration causes a change in the velocity profile (which could possibly be accounted for by a streamline expansion method), but it also tends to quench the turbulent mechanism (refs. 11 and 12). This can lead to the situation discussed in the section "Local Similarity" which produces a transitional problem in a "mixing sublayer" imbedded in a vortex layer.

Separation associated with a pressure rise presents the most complicated problem and points to the need for a momentum integral approach (ref. 17) and origin-shift treatment of the mixing zone (e.g., ref. 10).

INITIAL EXCHANGE MECHANISMS

It is evident that a mere description of velocity, temperature, and concentration profiles will, in the turbulent case, generally not be sufficient to solve the problem of computing the development of the mixing region. What is missing could be most important – at

least for the early stages of the mixing process – namely, its initial mechanisms. Only case (i) does provide such information if one uses the work of Maise and McDonald (ref. 18). Case (ii), on the other hand, generates local similarity – provided the expansion is sufficiently "strong" – first in the laminar (or "laminarized") mixing sublayer and then in its turbulent continuation where one depends on information on transition Reynolds numbers, such as given by Chapman, Kuehn, and Larson (ref. 19). Case (iii), because of its complexity, raises special interest for exploring how quickly initial conditions become submerged in the mechanisms generated by the mixing process itself. In the next section a tentative model for developing turbulent shear layers is projected.

FULLY TURBULENT MIXING BETWEEN TWO STREAMS ORIGINALLY SEPARATED BY A FLAT PLATE

As each stream approaches the trailing edge of the plate, it possesses its individual boundary layers having thickness, momentum thickness, and energy thickness, the corresponding shape factors, and an eddy viscosity distribution as given by Maise and McDonald (ref. 18) or determined with more precision by extensions of their method (e.g., to account for heat transfer).

Initial Level of Eddy Viscosity

If conditions in the two streams are very dissimilar, the eddy viscosity level in one of them may be dominating at the point of confluence. As the restraint on fluctuations imposed by the wall is removed, it seems logical to assume that the peak value of the eddy viscosity will originally prevail. It is of interest to note that such peak values can be correlated, for a wide range of Mach numbers, by the simple relation

$$\left.\frac{\epsilon_t}{\nu}\right|_{peak} = \frac{Re_\delta^{0.896}}{120} \tag{27}$$

Filling of the Wake

Breakup of the laminar sublayer and the large velocity gradient generated in the attached boundary layer control the next phase. If this process can be considered (at least for that portion of the profile where the mixing mechanism is most effective) to be reasonably close to the asymptotic single-stream jet mixing condition,

$$\frac{\epsilon}{\nu} = \frac{1}{4\sigma^2} Re_L \frac{x}{L} \tag{28}$$

may be selected where σ is related to the flow conditions in the faster stream, and the origin for x is at the point of confluence. (This scheme is akin to the concept of local similarity.)

Approaching the Asymptotic Solution

With the jet mixing mechanism thus building up, it will eventually approach the asymptotic case for both the kinematic and dynamic aspects.

At the matching conditions, after selecting an appropriate similarity profile, one has to account for both the momentum and energy defects at $x = 0$.

This can be achieved by applying an origin shift x_o and by utilizing the concept of equivalent bleed (ref. 6). By using the integrals defined and tabulated in reference 6 for the error function profile, one relates the mechanical energy defect in the approaching streams at $x = 0$, $D = \dfrac{\delta_a^{***} + \phi_b^3 \delta_b^{***}}{2}$ through

$$\frac{2\sigma D}{(-x_o) u_a^3 \rho_a} = \left[I_1(\eta_{RA}) - I_1(\eta_d)\right](1 - \phi_b^2) - I_4(\eta_{RA}) \tag{29}$$

while the momentum defect is accommodated through the concept of equivalent bleed which determines

$$I_1(\eta_d) = \frac{1}{1 - \phi_b}\left[I_1(\eta_{RA}) - I_2(\eta_{RA}) - \sigma(\Delta a + \Delta b)\right] \tag{30}$$

where

$$\Delta a = \frac{\delta_a^{**}}{(-x_o)}$$

$$\Delta b = \frac{\rho_b}{\rho_a} \phi_b^2 \frac{\delta_b^{**}}{(-x_o)}$$

and

$$\phi_b \neq 1$$

Combining equations (29) and (30) yields, for the origin shift,

$$x_o = \sigma \frac{(1 + \phi_b)\left[\delta_a^{**} + \dfrac{\rho_b}{\rho_a} \phi_b^2 \delta_b^{**}\right] - \left(\delta_a^{***} + \phi_b^3 \delta_b^{***}\right)}{I_1(\eta_{RA})(1 - \phi_b^2) - I_4(\eta_{RA}) - (1 + \phi_b)\left[I_1(\eta_{RA}) - I_2(\eta_{RA})\right]} \tag{31}$$

The similarity parameter σ refers here to the two-stream case (ref. 6).

It is necessary to comment on the manner in which the asymptotic case is "approached." If the "filling of the wake" (in the sense of the preceding section) becomes pronounced due to $\phi_b > 0$, the increase in eddy viscosity described by equation (28) will initially prevail over that related to the asymptotic solution. Hence, an overshoot will be

experienced so that the approach to the asymptotic profile occurs in the sense of relaxation rather than amplification of the mixing mechanism.

For the case where $\phi_b = 0$, such an overshoot should be less pronounced. The energy defect integral, as utilized for determining the origin shift x_o, differs from the dissipation integrals defined in reference 2)

$$DI = \int_{-\infty}^{+\infty} \frac{\phi}{\theta}(1 - \phi)\left(\phi - \phi_b\right)\frac{dy}{L} \tag{32}$$

or

$$DI = \int_{-\infty}^{+\infty} (1 - \phi)\left(\phi - \phi_b\right)d\overline{\psi} \tag{33}$$

only by a constant value (due to the fact that the momentum of the mixing streams is preserved once external forces such as wall shear friction are not present). The dissipation integral has been evaluated and presented in graphical form as shown in figure 1 for a variety of flow conditions.

Use of both forms (eq. (32) for the experimental profile and eq. (33) for the analytical solution) is then convenient for establishing the relation between x/L and $\overline{\xi}$ and $\epsilon/\nu(x/L)$.

Wake Problem – Both Streams Having Identical Velocities and Initial Boundary Layers

For wake flows, the asymptotic solution shall be represented by a constant level of the eddy viscosity (Schlichting (ref. 5)) so that, with reference to the momentum thickness of one approaching boundary layer,

$$\frac{\epsilon}{\nu} = 0.0888 Re_L \frac{\delta_a^{**}}{L} \tag{34}$$

Proposed Models for Turbulent Eddy Diffusivity

A schematic presentation of eddy viscosity models as used in the present study is shown in figure 2.

RELATION BETWEEN THE STREAMWISE COORDINATES x AND $\overline{\xi}$

The proposed eddy viscosity model establishes a relation between the transformed coordinate $\overline{\xi}$ and the physical coordinate x, and thus allows identification and location of the calculated mixing profiles

$$\bar{\xi} = \int \frac{\epsilon}{\nu_\theta^{2-d}} \frac{1}{Re_L} d\left(\frac{x}{L}\right) + \text{Constant} \tag{35}$$

DETERMINATION OF THE EDDY VISCOSITY FROM MATCHING OF EXPERIMENTAL AND ANALYTICAL PROFILES

The concepts developed for ϵ/ν in the preceding sections are essentially conjectures. Indeed, the analytical model and the calculation procedures have been worked out in such a way as to remove the need for depending on a specific viscosity law. Actually, one can utilize equation (9) for determining the viscosity law.

To accomplish this, it is necessary to define the matching of profiles for value pairs of x and $\bar{\xi}$, which leads to a unique $\bar{\xi} = \bar{\xi}(x)$ relationship which then can yield, for $d = 2$

$$\frac{\epsilon}{\nu} = \left.\frac{d\bar{\xi}}{d\left(\frac{x}{L}\right)}\right|_x Re_L \tag{36}$$

Obviously, only single parameters can be matched for both the calculated and the experimental profiles.

Two possible choices are

(i) The minimum velocity, as it is well defined in wake problems

(ii) The dissipation integral given by equations (29), (32), and (33)

An illustration of this procedure is given in the section "Test Case – Solutions."

EDDY VISCOSITY IN AXIALLY SYMMETRIC MIXING REGIONS

Much uncertainty exists concerning suitable turbulent exchange coefficient formulations for axially symmetric flow. The appearance of the transverse coordinate r in the conservation equations also complicates the situation since it would restrict the possibilities of a transformation (e.g., eq. (9) for the two-dimensional case) to the unattractive form where a singularity in the exchange coefficient could occur as $r \to 0$. Empirical relations, therefore, still are favored in dealing with individual cases (ref. 1) but apparently cannot be expected to give satisfactory results when applied to widely different flow conditions. (See discussion of test case 11.)

TEST CASE – SOLUTIONS[2]

TEST CASE 1: TWO-DIMENSIONAL SHEAR LAYER

Spreading Parameter for a Fully Developed Incompressible Free Shear Layer (Influence of ϕ_b)

The effect of the free-stream velocity ratio $\frac{u_b}{u_a} = \phi_b$ on the spreading parameter σ for similarity mixing profiles has recently been reviewed by Yule (ref. 20). Shown in figure 3 is the relation

$$\frac{\sigma_o}{\sigma} = \frac{1 - \phi_b}{1 + \phi_b}$$

as presently used in computer programs at the University of Illinois and which also has been utilized for calculations of asymptotic mixing regions in the discussion of test case 4.

TEST CASE 2: TWO-DIMENSIONAL SHEAR LAYER

Spreading Parameters for a Fully Developed Turbulent Free Shear Layer With Zero Velocity Ratio (Influence of Mach Number)

Much uncertainty exists as to the effects of Mach number on the mixing mechanism, as can be illustrated by the large discrepancies for observed or predicted values for σ (ref. 9). Shown in figure 4 is the simple linear relationship

$$\sigma = 12 + 2.76M_a$$

as proposed for use in the lower Mach number range $M_a < 3$ (ref. 6).

TEST CASE 3: TWO-DIMENSIONAL SHEAR LAYER

Spreading Parameter for a Fully Developed Low-Speed Free Shear Layer With a Velocity Ratio of 0.2 and Density ratios ρ_b/ρ_a of 14, 1/2, 1/7, and 1/14

It is the judgment of the authors that conclusions concerning spread parameters must be based on more extensive and reliable experimental data than appears to be presently available. Evaluation of earlier experiments by Pabst (ref. 21) conducted for a single temperature ratio of 2.3 did not show an appreciable effect on σ. To facilitate future correlations, theoretical calculations for $\sigma_d(\Delta y/x)$ based on the procedure outlined in the section "Similarity Solutions" with a selected value for $d = 2$ are presented in figure 5. The abscissa in figure 5 represents either the ratio of T_b/T_a or ρ_a/ρ_b since

[2] $d = 2$ for all calculations presented.

low-speed flows are being considered. According to equation (20), the effects of the stagnation temperature ratio and gas constant ratio should be equivalent.

TEST CASE 4: TWO-DIMENSIONAL SHEAR LAYER

Influence of Initial Boundary Layers, Incompressible Flow, $\phi_b = 0.35$

As requested, results of theoretical calculations for the velocity profiles are shown in figure 6. The corresponding shear stress distributions are given in figure 7. The correlation procedure between the physical and transformed dimensionless streamwise coordinates x/L and $\bar{\xi}$ is illustrated by the use of the dissipation integrals according to equations (32) and (33) in figures 8 and 9. The extracted information on the effective turbulent eddy viscosity ϵ/ν is shown in figure 10.

This figure also compares these viscosity coefficients with those resulting from the concepts developed in the section "Eddy Viscosity Concepts." A strong overshoot as a continuation of the wake-filling mechanism over the asymptotic solution is clearly evidenced.

TEST CASE 5: TWO-DIMENSIONAL SHEAR LAYER

Initial Development of a Turbulent Compressible Free Shear Layer

The requested theoretically calculated velocity profiles are shown in figure 11. One must note that the y-scale in figure 11 reflects conservation of momentum, while the experimental data require a translation to satisfy this physical constraint. Figures 12 and 13 have been added to show the degree of agreement between the eddy viscosity distributions based on the dissipation integral correlation and the concepts proposed in the section "Eddy Viscosity Concepts." Again, an overshoot is noted, but it is rather moderate since no wakelike contribution exists for $\phi_b = 0$.

TEST CASES 6 TO 13, 15, AND 17 TO 23: AXIALLY SYMMETRIC FLOW CASES

Considerable difficulty has been encountered in attempts to obtain numerical computer solutions by using the approach and programs of reference 1. This situation has been caused primarily by communication problems (Dr. Hurt had left the University of Illinois) and by difficulties encountered in switching to a different computer system with limited storage capacity. Consequently, attention is directed to reference 1 as containing specific examples for program capabilities. In addition, calculated center-line velocity distributions as they apply to test case 11 are shown in figure 14.

TEST CASE 14: TWO-DIMENSIONAL WAKE – LOW SPEED

Shown in figure 15 is the center-line velocity development as a function of the transformed coordinate $\bar{\xi}$. Figure 16 illustrates the use of the presently proposed viscosity model for the three regimes described previously. This produces the plot of $1/W^2$ as a function of $x/\delta_a{}^{**}$ (fig. 17), which is the required answer to this test case. Agreement with experimental data was found to be reasonably good.

TEST CASE 16: TWO-DIMENSIONAL WAKE – SUPERSONIC ADIABATIC FLOW

With transition at station 1, the present viscosity model assumes the form shown in figure 18 with experimental ϵ/ν values (obtained with the help of dissipation function correlation) also presented. A strong overshoot along the trough-concept-rise is noticed with subsequent relaxation towards the asymptotic (constant ϵ) solution. It must be noted that the theoretical calculations for $1/W^2$ as a function of x/D (fig. 19 (required)) and T_c/T_a as a function of x (fig. 20) have been obtained by following the trough-rise portion. The difference between the "relaxing" and the "rising" ϵ/ν branch should, however, not produce significant differences, especially in view of the rather large scatter of experimental data. Overshoot and subsequent relaxation of ϵ/ν is experimentally – albeit indirectly – evidenced by figure 1 of reference 22. Computer results $\left(\phi_c \text{ and } T_c/T_a \text{ as a function of } \bar{\xi}\right)$ are presented in figure 21.

TEST CASE 24: TWO-DIMENSIONAL WAKE – COMPRESSIBLE DIABATIC FLOW (TRANSITIONAL)

Prandtl number for this case has been selected as 0.72 throughout. This is consistent with the expectation of a significantly long laminar mixing region followed by transition and turbulent mixing for which $Pr_t = 0.72$ is incidentally a reasonable approximation. Based on theoretical calculations, and with the use of information on transition in free shear layers (ref. 19), one arrives at a transition location of 7.01 cm (2.76 in.) corresponding to $Re_x = 180\,000$ where

$$Re_x = \frac{Re_L\left(x_t/L\right)_t}{\left(T_c/T_a\right)_i^2}$$

The resulting relation between ϵ/ν and x/L is shown in figure 22. Correlation between $\bar{\xi}$ and x/L by the integration of equation (9) and the finite-difference calculations $\left(\phi_c,\ T_c/T_a \text{ as a function of } \bar{\xi} \text{ in fig. 23}\right)$ then produce figure 24 which shows

$1/W^2$ as a function of x/D and figure 25 which is a comparison of calculated and measured center-line temperature ratios. It is of interest to note the effects of transition as they appear in both the calculated and experimentally determined data.

REFERENCES

1. Hurt, Robert Frank: A Theoretical and Experimental Investigation of Axisymmetric, Non-Homogeneous, Compressible Turbulent Mixing. Ph. D. Thesis, Univ. of Illinois at Urbana-Champaign, 1970.

2. Lilienthal, Peter Frederick, II: Development of Viscous Free Shear Layers Between Two Compressible Constant Pressure Isoenergetic Streams With Special Considerations of Its Dissipative Mechanisms. Ph. D. Thesis, Univ. of Illinois, 1970.

3. Grabow, Richard M.: Finite Difference Methods. Laminar Separated Flows, VKI CN 66a, Von Karman Inst. Fluid Dyn., Apr. 1967.

4. Korst, H. H.; and Chow, W. L.: On the Correlation of Analytical and Experimental Free Shear Layer Similarity Profiles by Spread Rate Parameters. Trans. ASME, Ser. D: J. Basic Eng., vol. 93, no. 3, Sept. 1971, pp. 377-382.

5. Schlichting, Hermann (J. Kestin, transl.): Boundary Layer Theory. Fourth ed., McGraw-Hill Book Co., Inc., c.1960.

6. Korst, H. H.; and Chow, W. L.: Non-Isoenergetic Turbulent $(Pr_t = 1)$ Jet Mixing Between Two Compressible Streams at Constant Pressure. NACA CR-419, 1966.

7. Davis, Lorin R.: Experimental and Theoretical Determination of Flow Properties in a Reacting Near Wake. AIAA J., vol. 6, no. 5, May 1968, pp. 843-847.

8. Addy, A. L.: Thrust-Minus-Drag Optimization by Base Bleed and/or Boattailing. J. Spacecraft & Rockets, vol. 7, no. 11, Nov. 1970, pp. 1360-1362.

9. Hill W. G., Jr.; and Page, R. H.: Initial Development of Turbulent, Compressible, Free Shear Layers. Trans. ASME, Ser. D: J. Basic Eng., vol. 91, no. 1, Mar. 1969, pp. 67-73.

10. Kessler, Thomas J.: Two-Stream Mixing With Finite Initial Boundary Layers. AIAA J., vol. 5, no. 2, Feb. 1967, pp. 363-364.

11. Page, R. H.; and Sernas, V.: Apparent Reverse Transition in an Expansion Fan. AIAA J., vol. 8, no. 1, Jan. 1970, pp. 189-190.

12. Korst, H. H.: Dynamics and Thermodynamics of Separated Flows. Review Lecture presented at 1969 International Seminar on Heat and Mass Transfer in Flows With Separated Regions and Measurement Techniques (Herceg-Novi, Yugoslavia), Sept. 1969.

13. Gerhart, P. M.: A Study of the Reattachment of a Turbulent Supersonic Shear Layer With the Closure Condition Provided by a Control Volume Analysis. Ph. D. Thesis, Univ. of Illinois, 1971.

14. Libby, Paul A.: Theoretical Analysis of Turbulent Mixing of Reactive Gases With Application to Supersonic Combustion of Hydrogen. ARS J., vol. 32, no. 3, Mar. 1962, pp. 388-396.

15. Donovan, Leo F.; and Todd, Carroll A.: Computer Program for Calculating Isothermal, Turbulent Jet Mixing of Two Gases. NASA TN D-4378, 1968.

16. Rodi, W.; and Spalding, D. B.: A Two-Parameter Model Turbulence, and Its Application to Free Jets. Wärme-und Stoffüberstragung, vol. 3, no. 2, 1970, pp. 85-95.

17. White, Robert A.: Effect of Sudden Expansions or Compressions on the Turbulent Boundary Layer. AIAA J., vol. 4, no. 12, Dec. 1966, pp. 2232-2234.

18. Maise, George; and McDonald, Henry: Mixing Length and Kinematic Eddy Viscosity in a Compressible Boundary Layer. AIAA J., vol. 6, no. 1, Jan. 1968, pp. 73-80.

19. Chapman, Dean R.; Kuehn, Donald M.; and Larson, Howard K.: Investigation of Separated Flows in Supersonic and Subsonic Streams With Emphasis on the Effect of Transition. NACA Rep. 1356, 1958.

20. Yule, Andrew J.: Spreading of Turbulent Mixing Layers. AIAA J., vol. 10, no. 5, May 1972, pp. 686-687.

21. Szablewski, W.: Turbulente Vermischung ebener Heissluftstrahlen. Ing.-Arch., Bd. XXV, Heft 1, Jan. 1957, pp. 10-25.

22. Demetriades, Anthony: Observations on the Transition Process of Two-Dimensional Supersonic Wakes. AIAA Paper No. 70-793, June-July 1970.

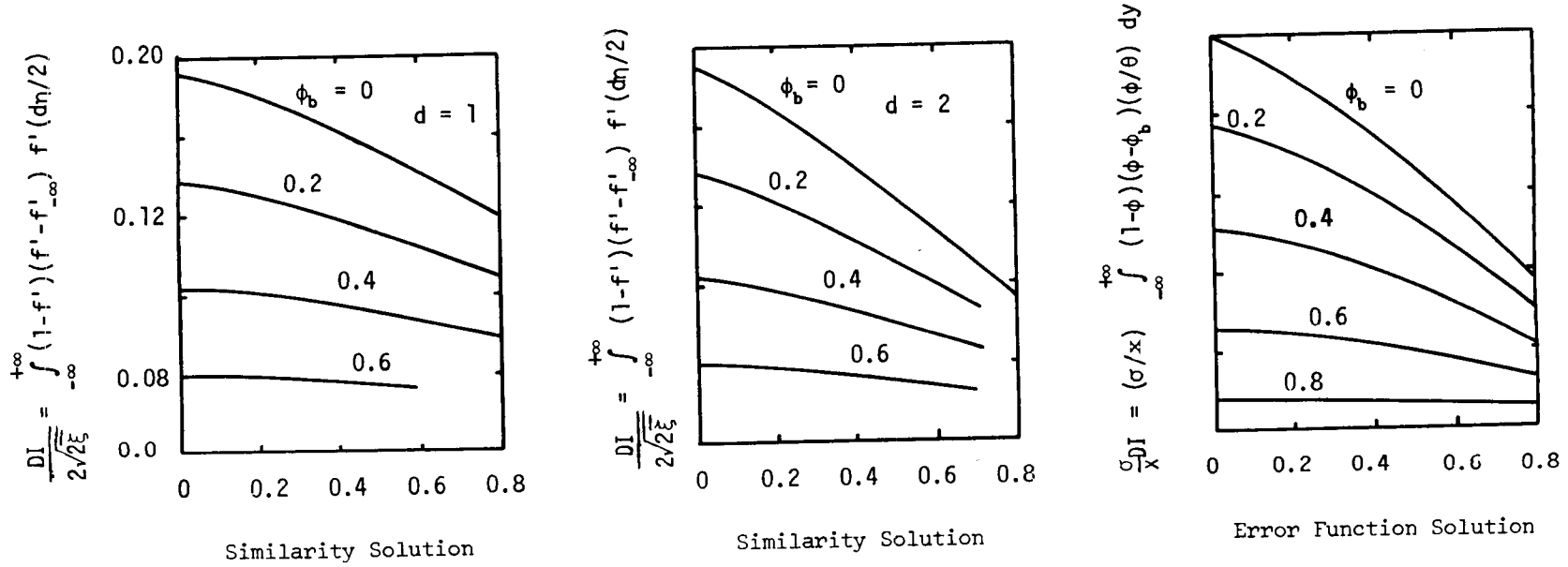

Figure 1.- Total dissipation of mechanical energy as a function of C_a^2 and velocity ratio ϕ_b for $T_{o_a} = T_{o_b}$. (Adapted from ref. 2.)

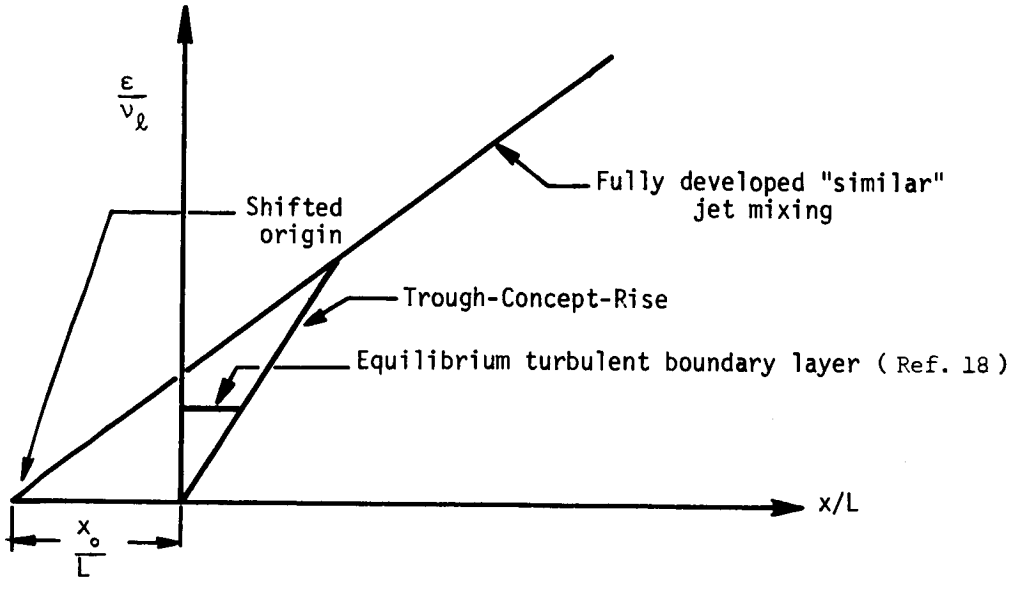

(a) Turbulent free jet mixing.

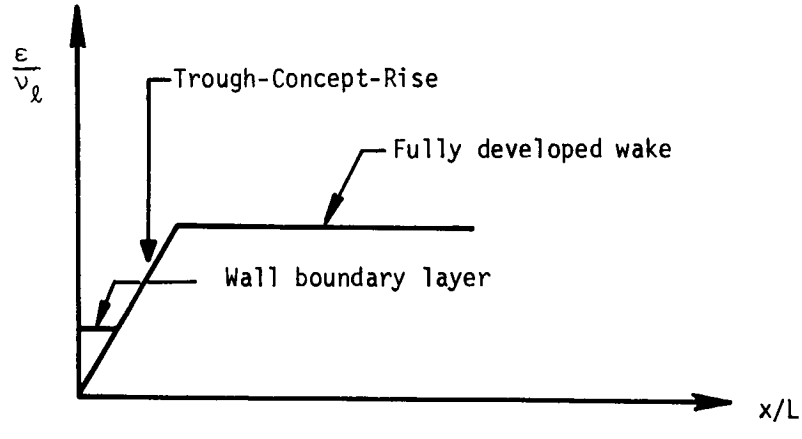

(b) Turbulent wake flow.

Figure 2.- Viscosity model.

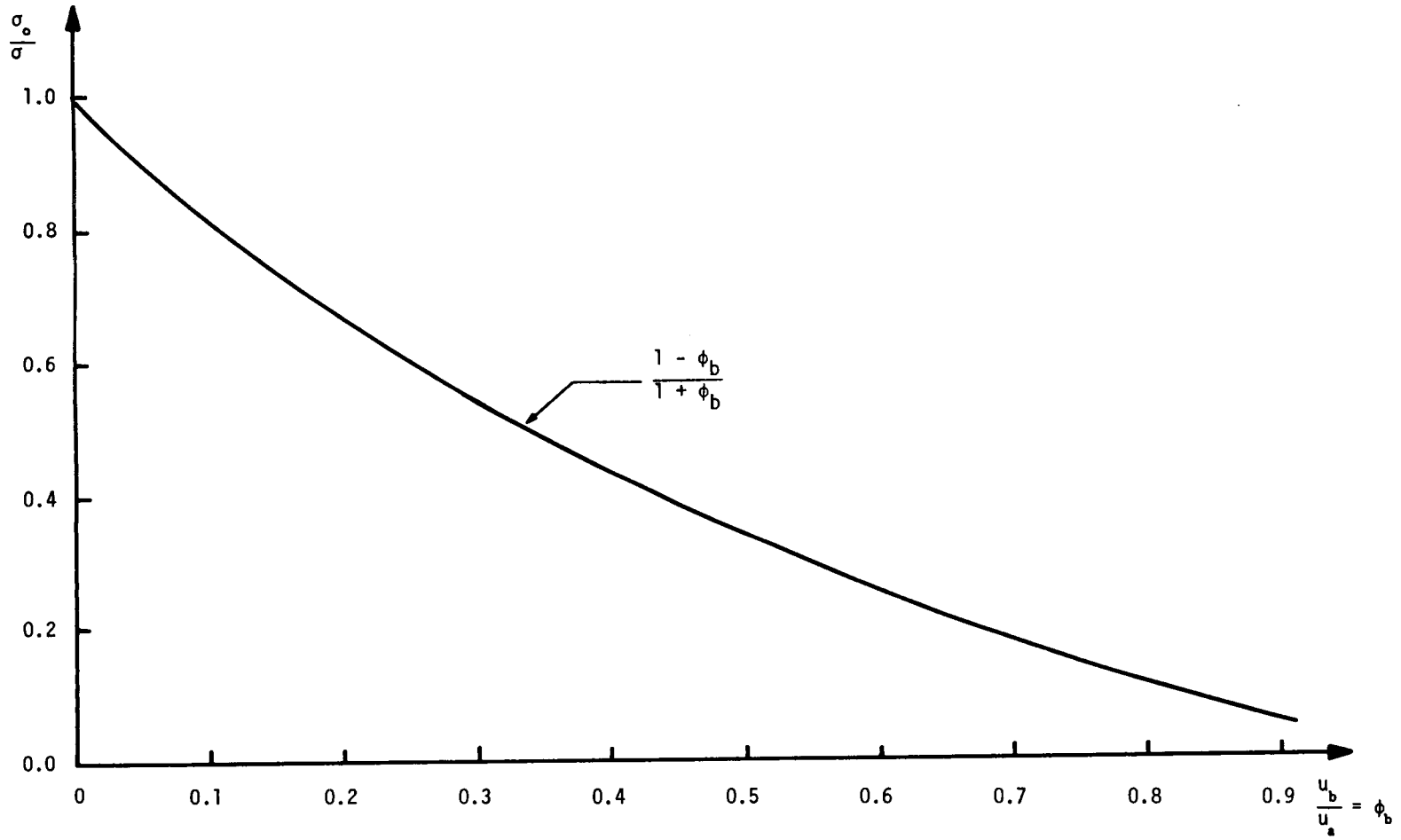

Figure 3.- Influence of velocity ratio ϕ_b on similarity parameter σ.

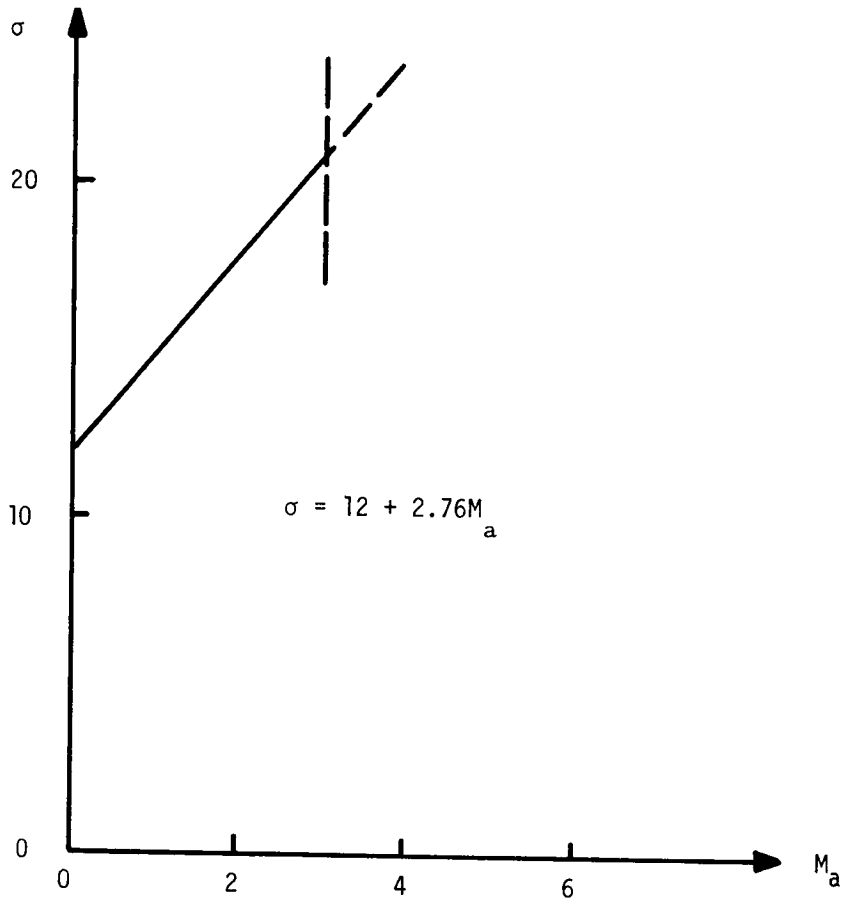

Figure 4.- Influence of free-stream Mach number on similarity parameter σ.

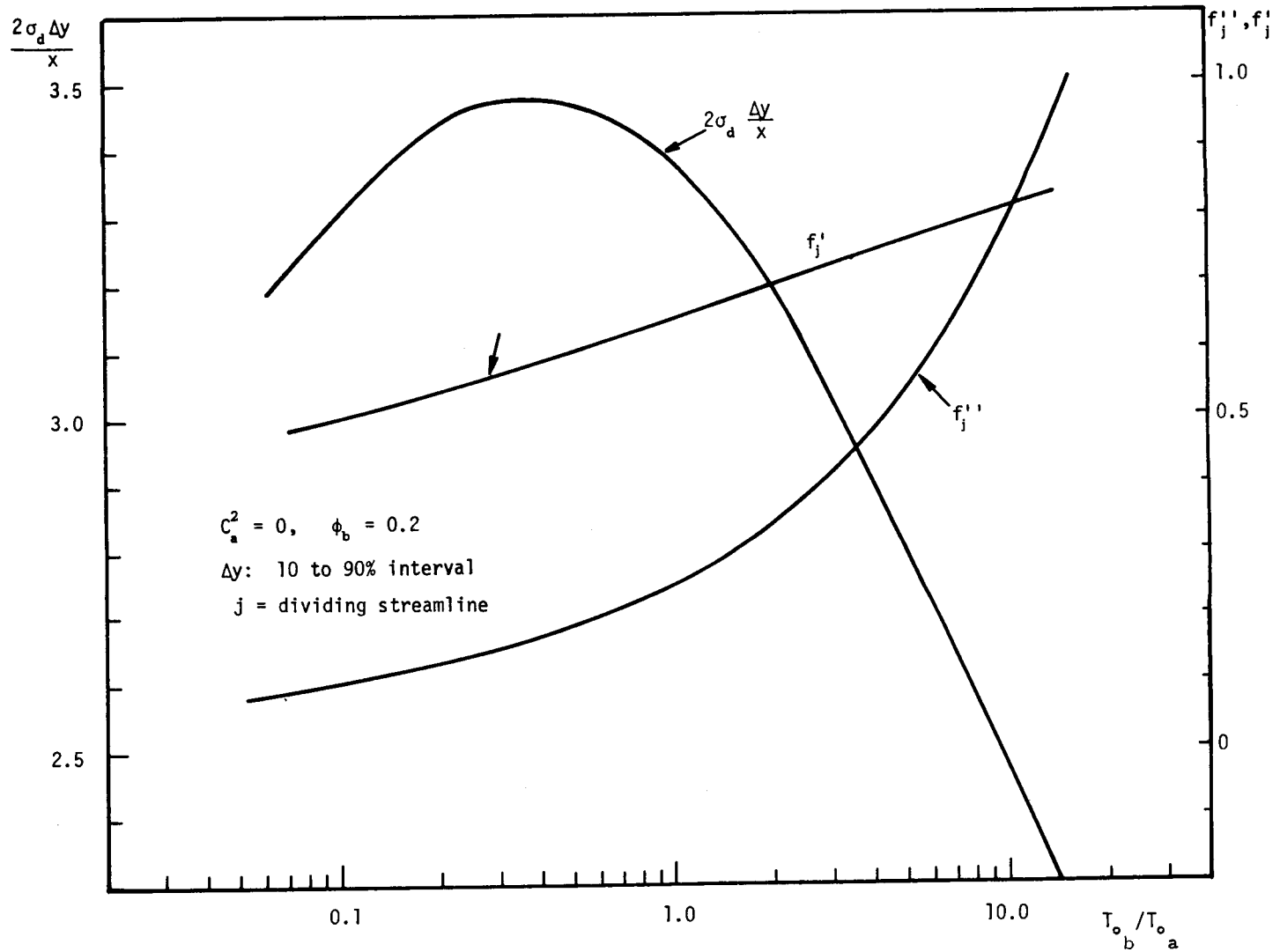

Figure 5.- Influence of density ratio (or temperature ratio) on similarity solution for two-stream mixing (d = 2).

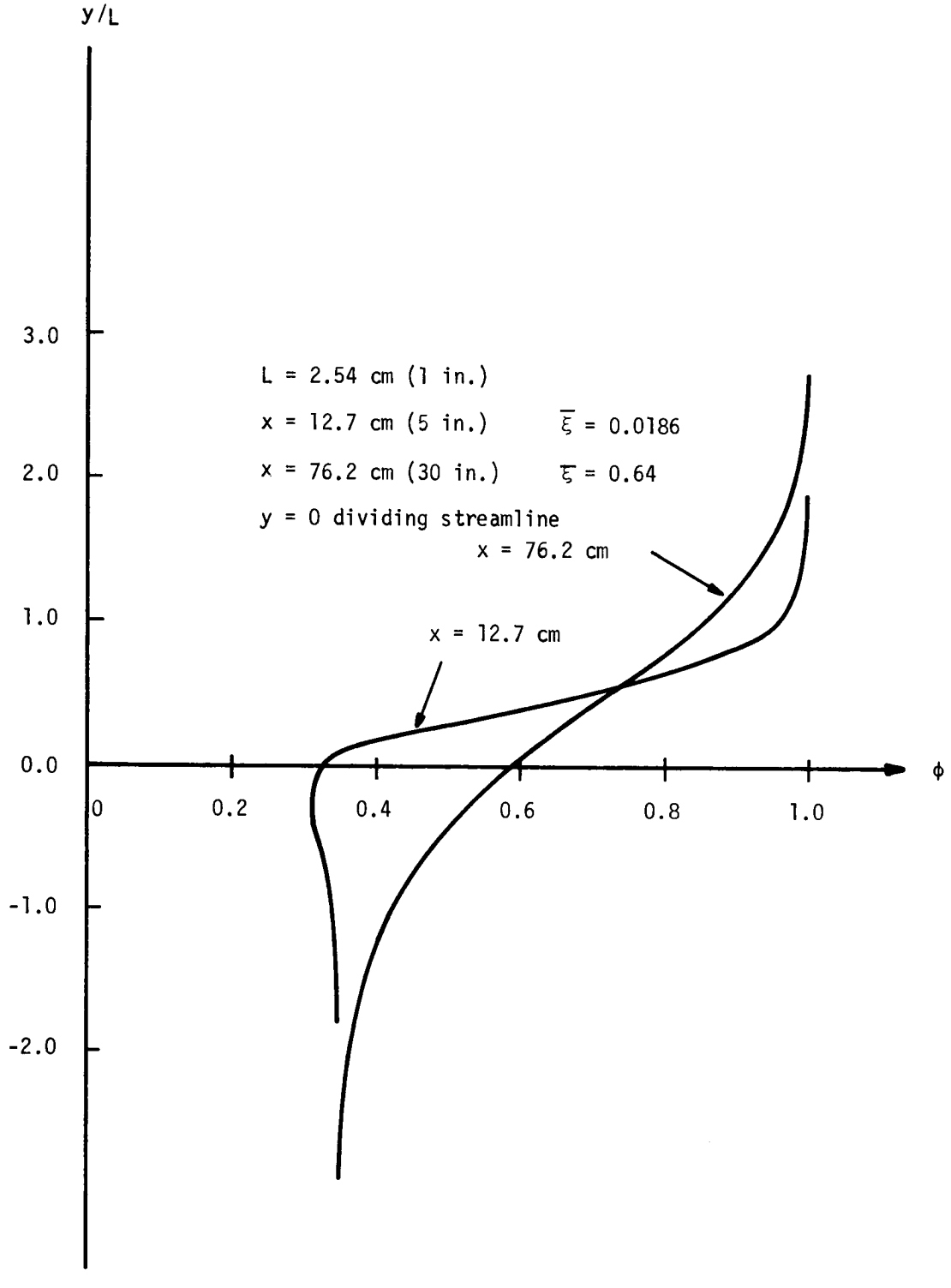

Figure 6.- Calculated velocity profiles at specified downstream locations for test case 4.

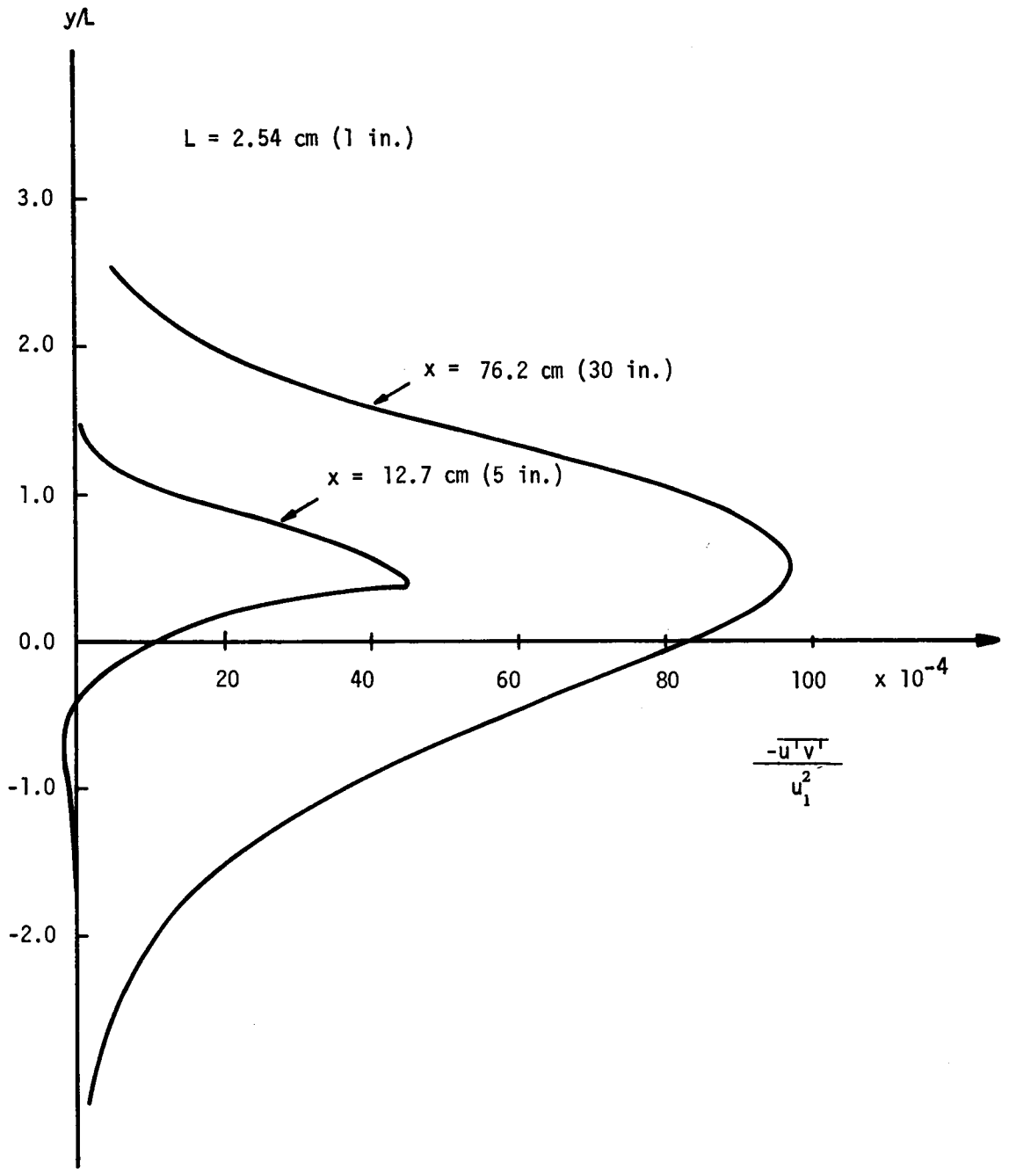

Figure 7.- Calculated shear stress profiles at specified downstream locations for test case 4.

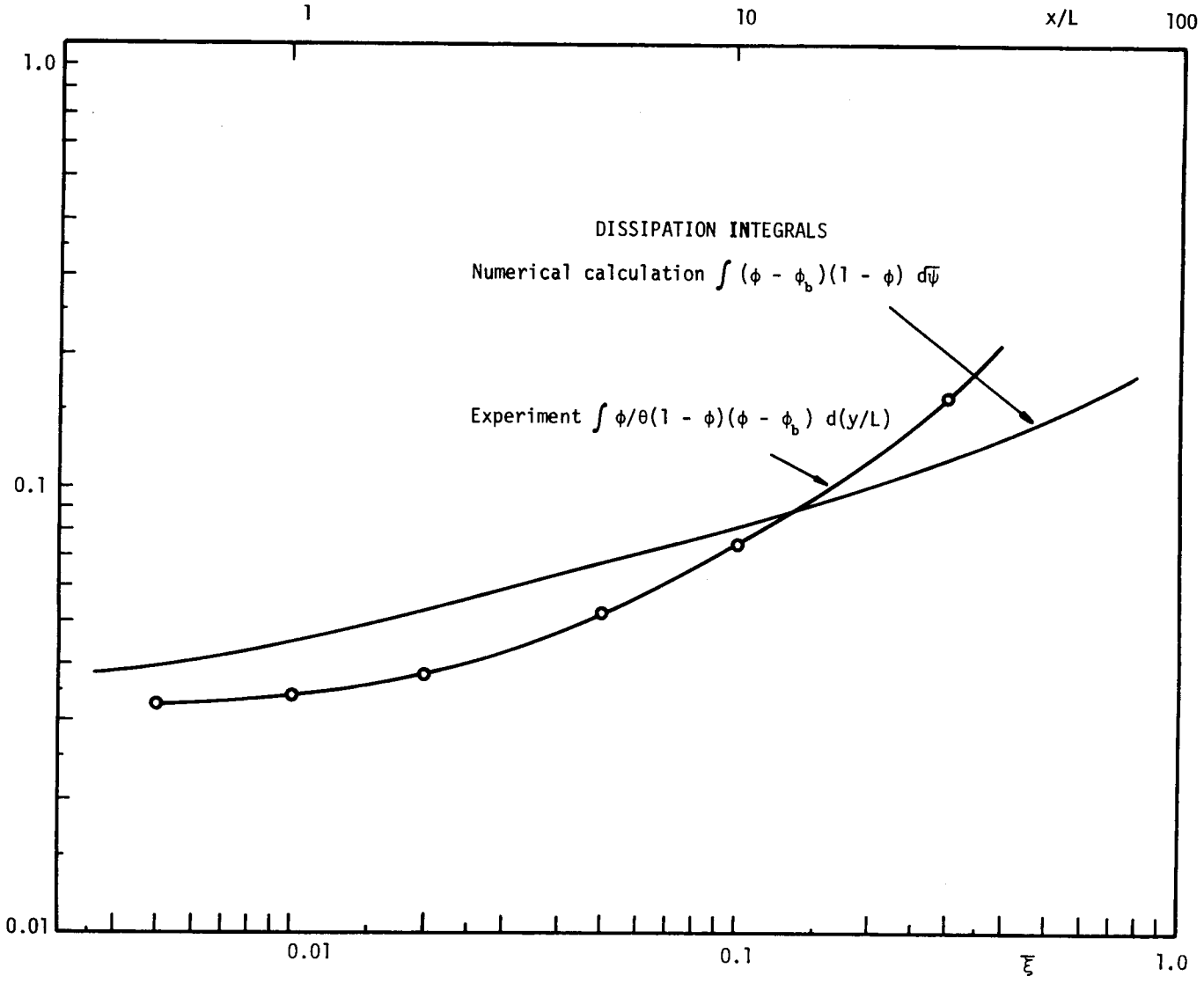

Figure 8.- Dissipation integrals as obtained by theoretical calculations and from experimental data for test case 4.

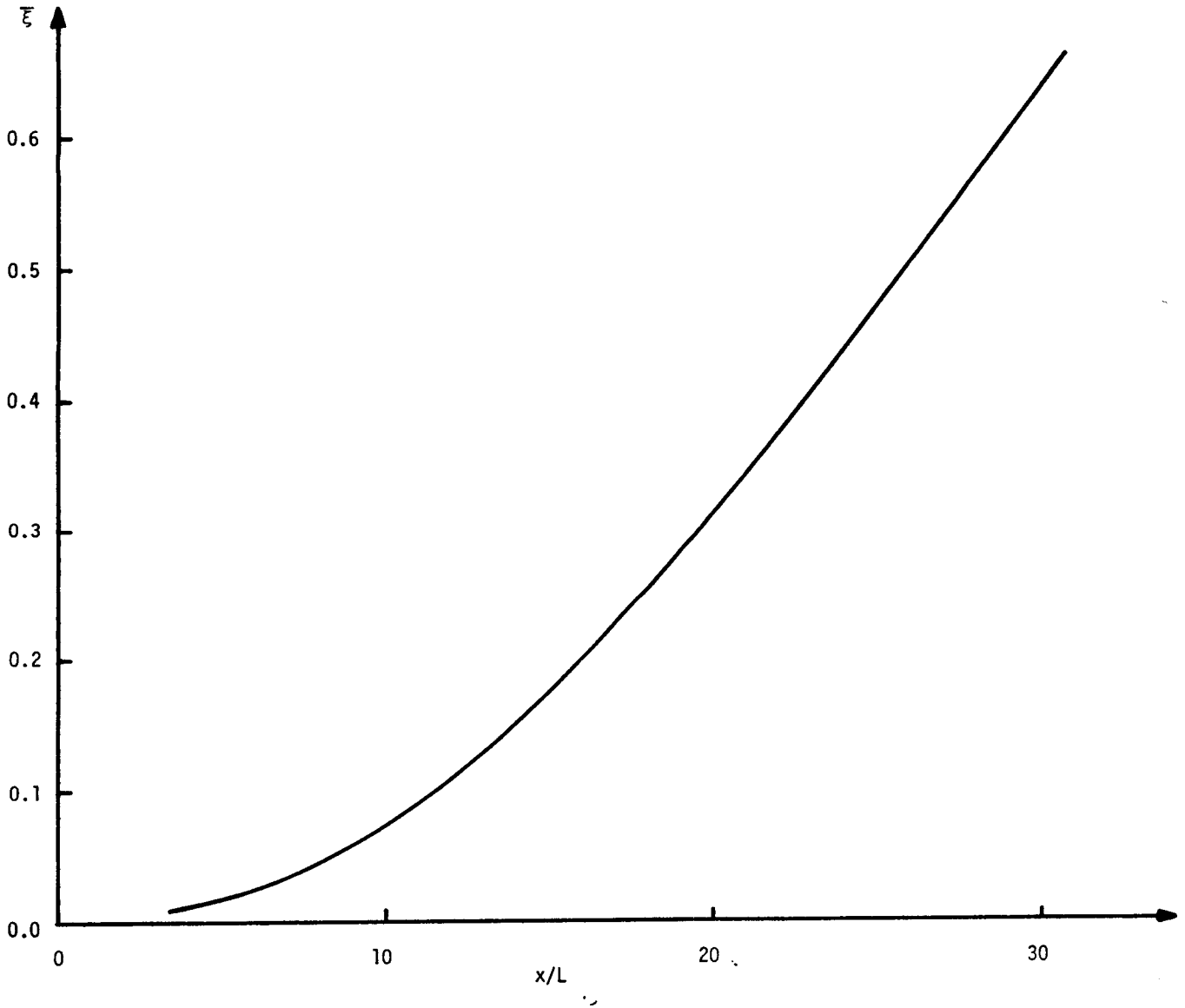

Figure 9.- Correlation of $\bar{\xi}$ and x/L by utilization of dissipation integrals for test case 4.

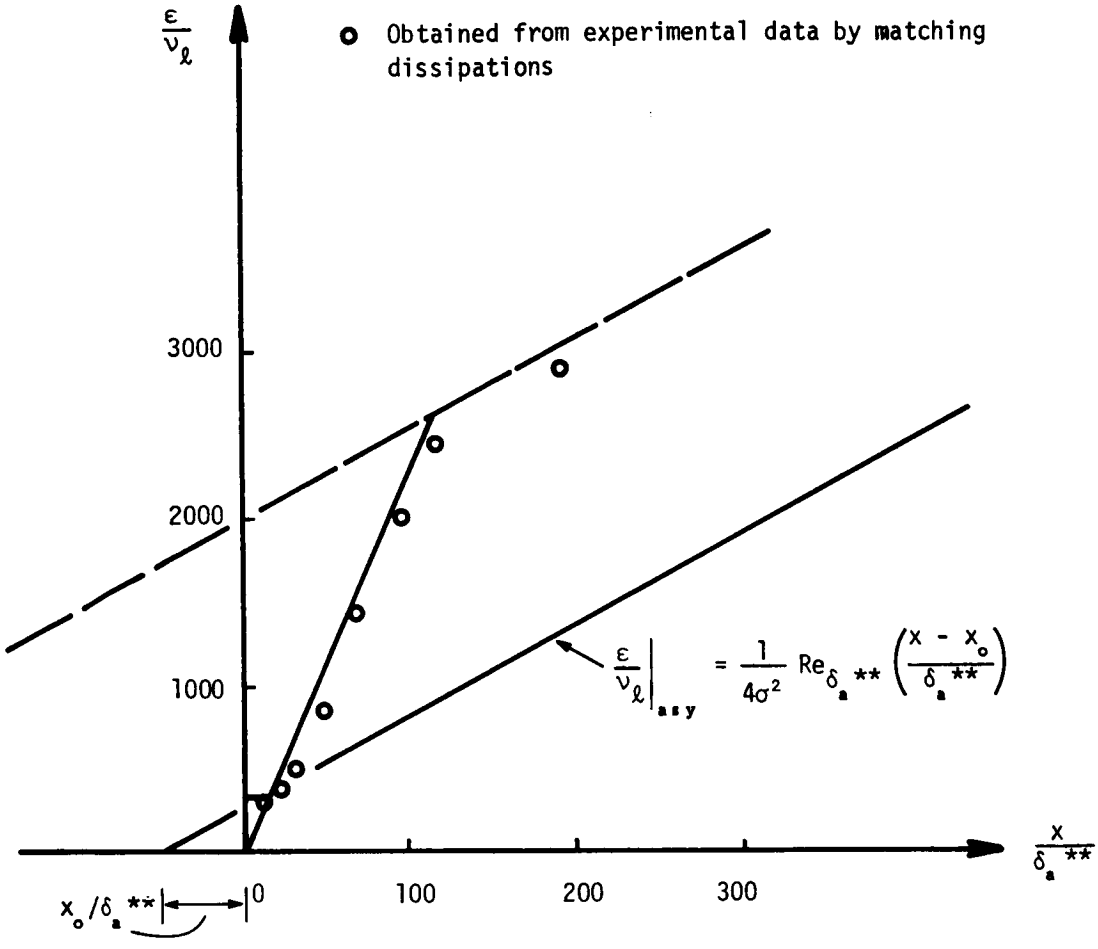

Figure 10.- Presentations of ϵ/ν for test case 4.

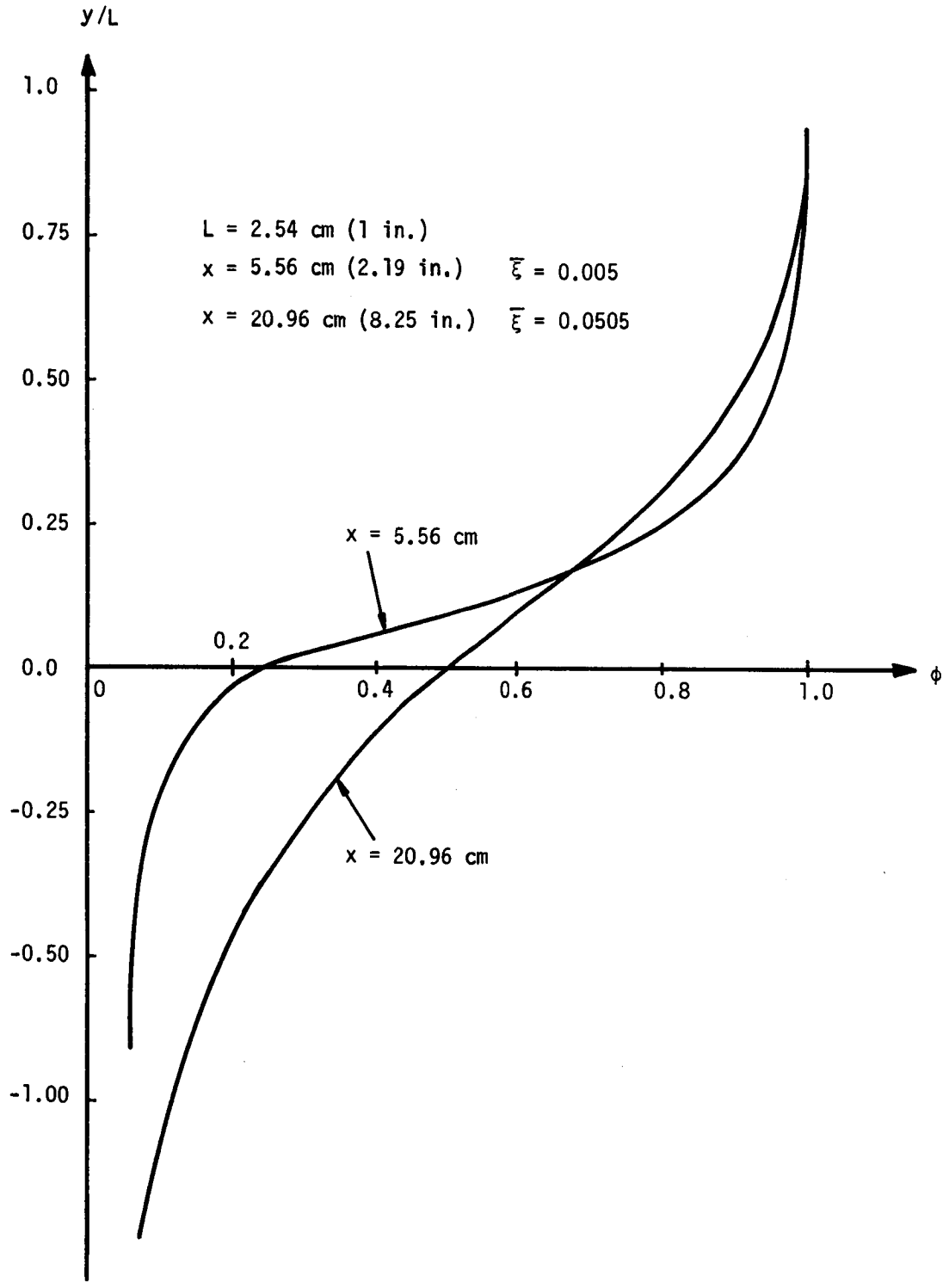

Figure 11.- Calculated velocity profiles at specified downstream locations for test case 5.

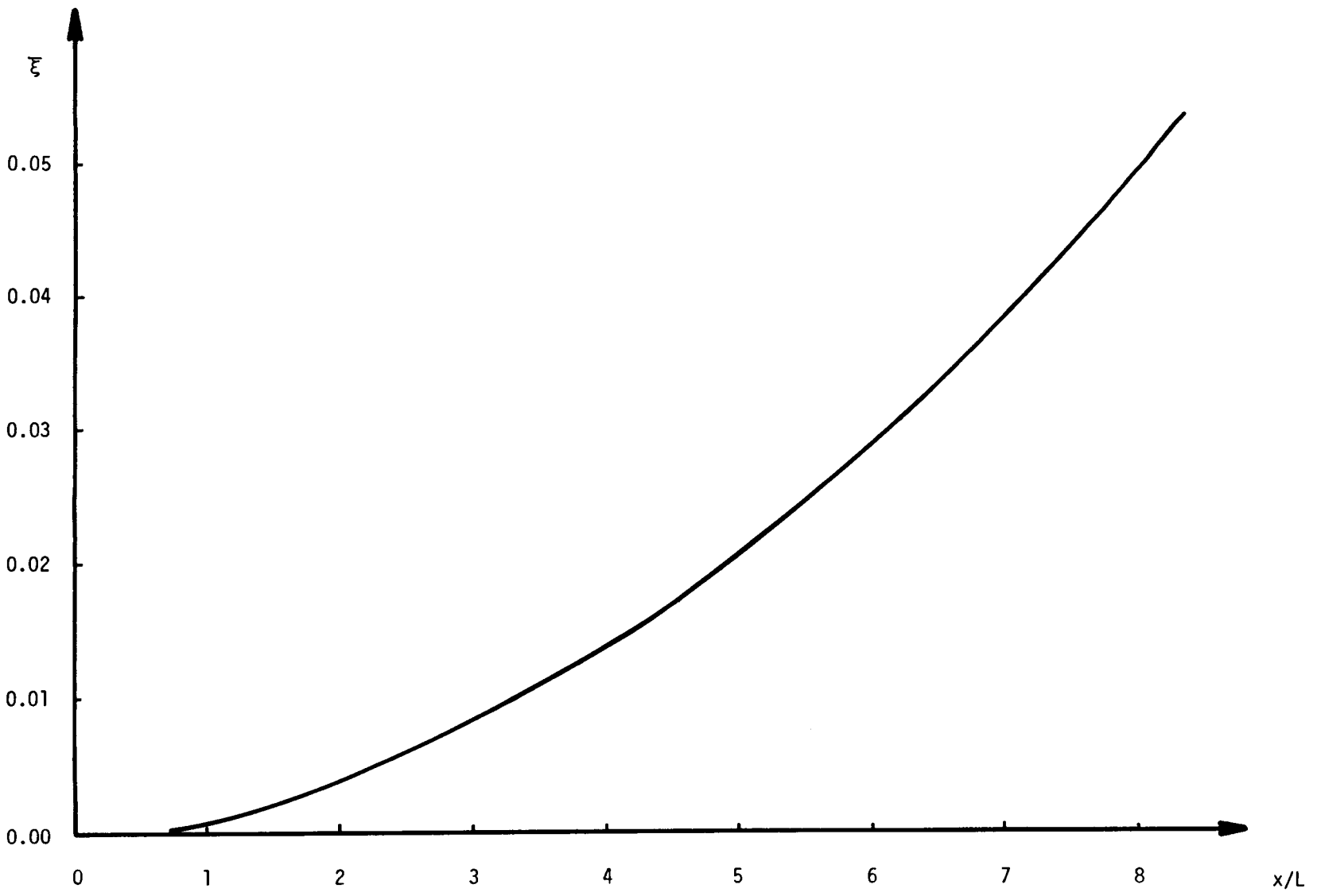

Figure 12.- Correlation of $\bar{\xi}$ and x/L by utilization of dissipation integrals for test case 5.

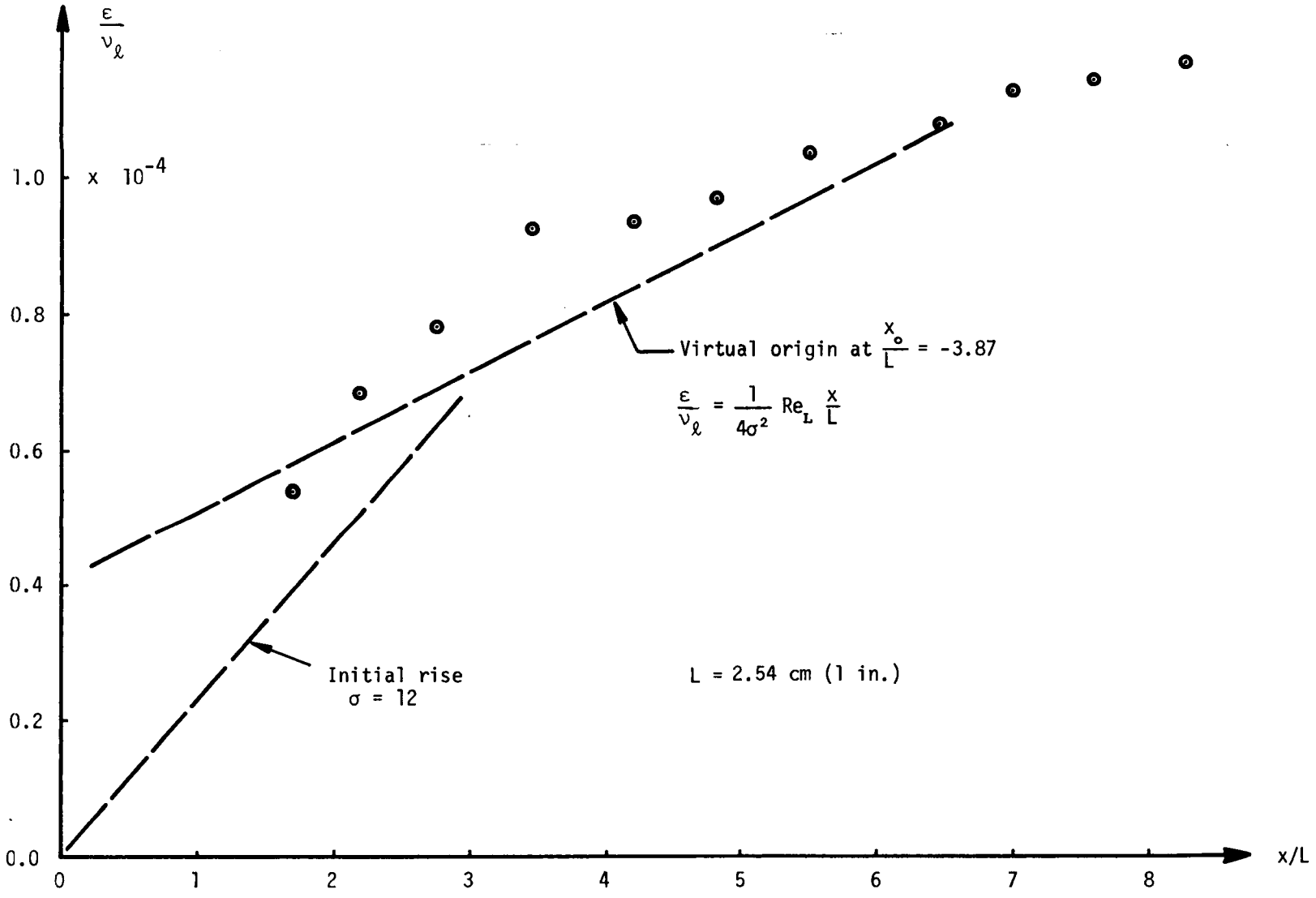

Figure 13.- Presentation of ϵ/ν for test case 5.

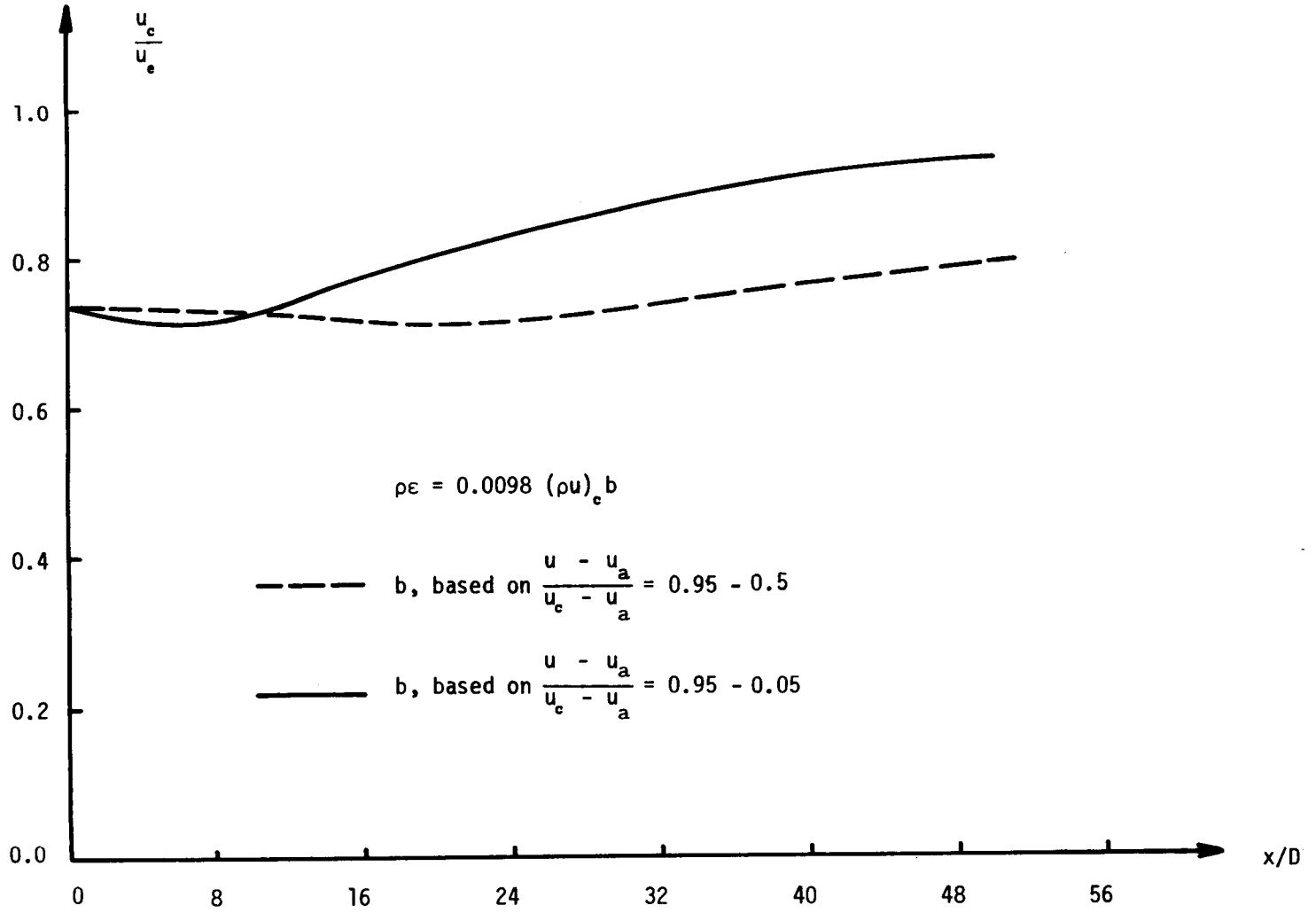

Figure 14.- Calculated center-line velocities for test case 11.

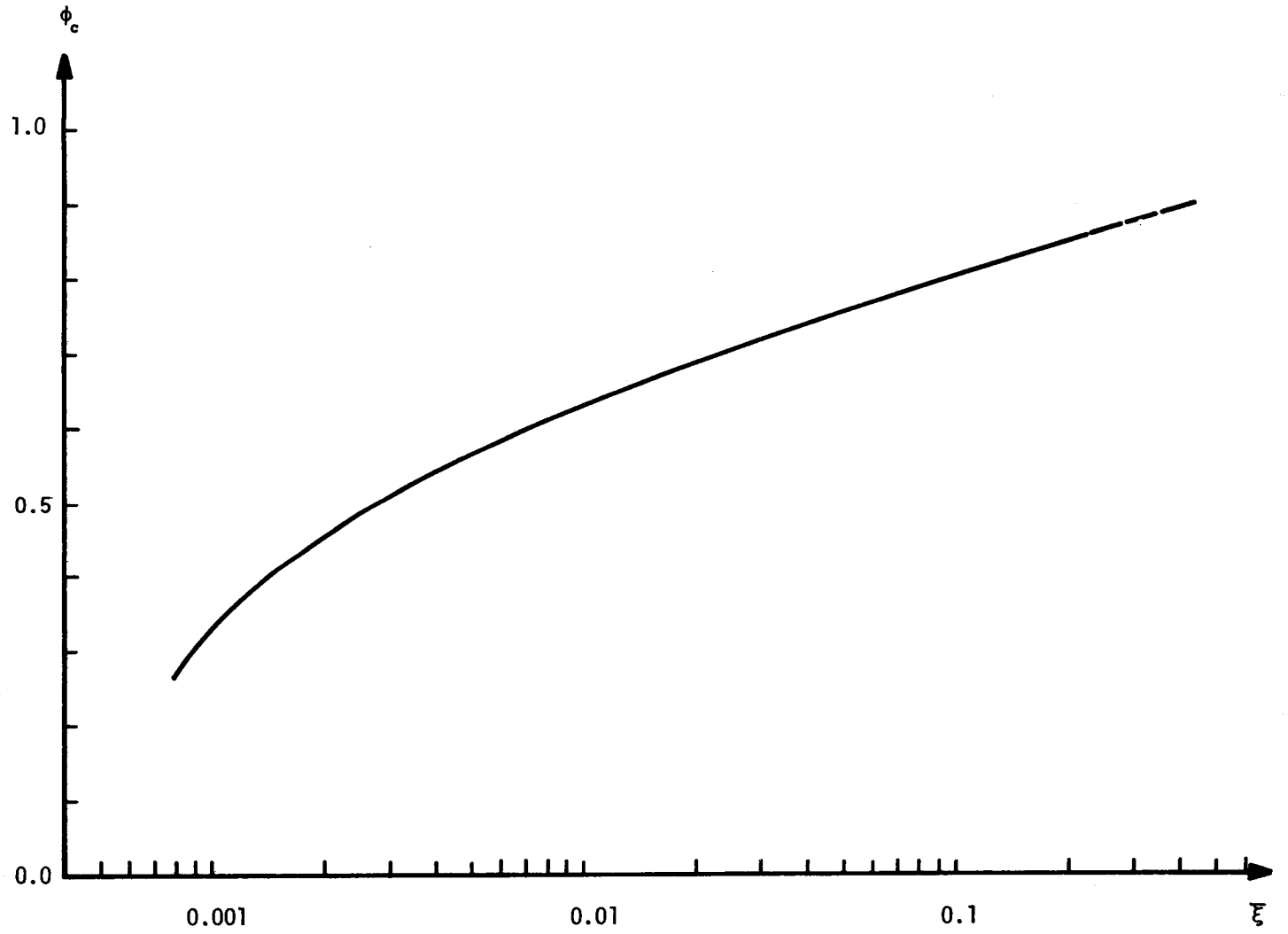

Figure 15.- Calculated center-line velocity as function of $\bar{\xi}$ for test case 14.

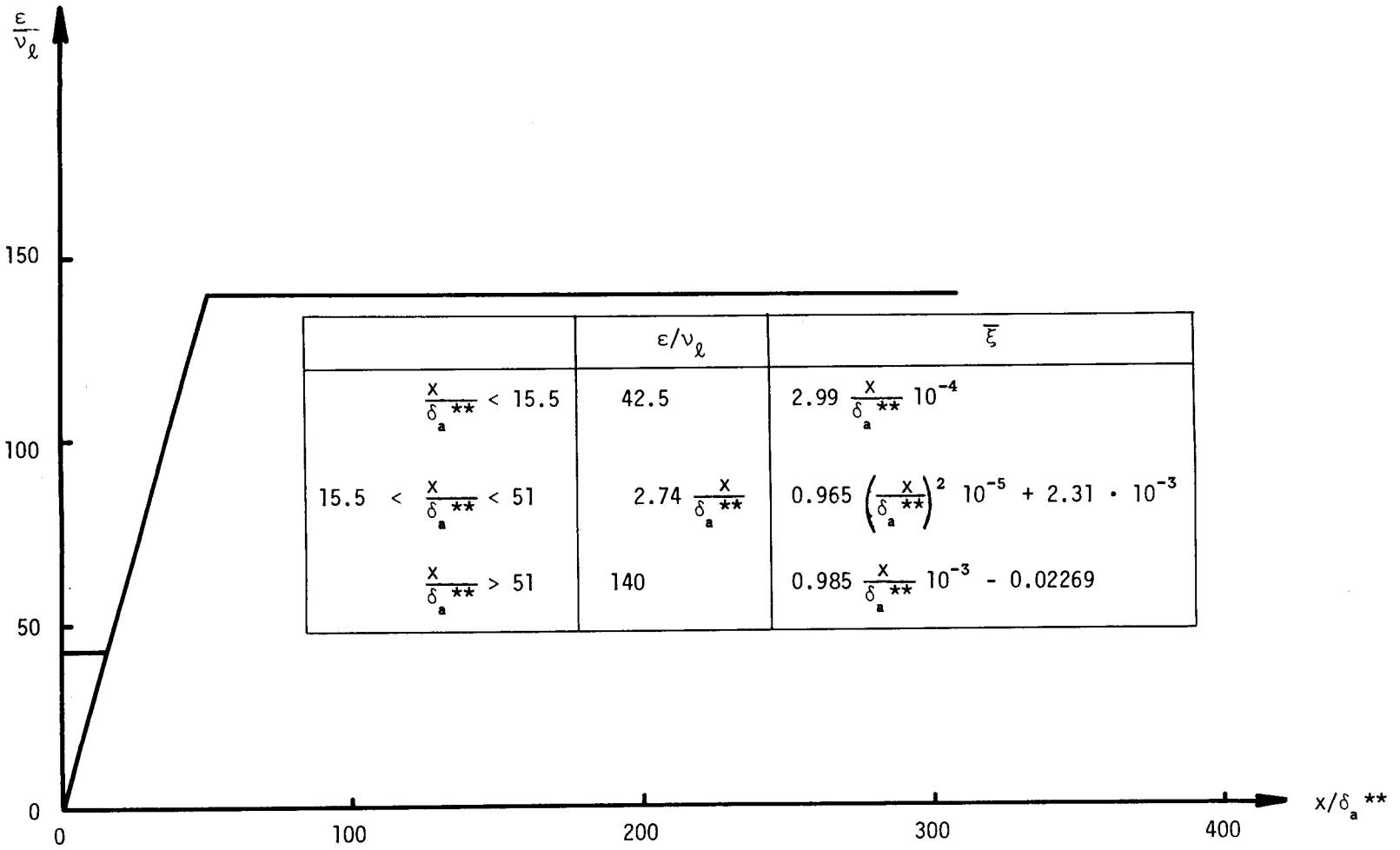

	ε/ν_ℓ	$\overline{\xi}$
$\frac{x}{\delta_a^{**}} < 15.5$	42.5	$2.99 \frac{x}{\delta_a^{**}} 10^{-4}$
$15.5 < \frac{x}{\delta_a^{**}} < 51$	$2.74 \frac{x}{\delta_a^{**}}$	$0.965 \left(\frac{x}{\delta_a^{**}}\right)^2 10^{-5} + 2.31 \cdot 10^{-3}$
$\frac{x}{\delta_a^{**}} > 51$	140	$0.985 \frac{x}{\delta_a^{**}} 10^{-3} - 0.02269$

Figure 16.- Viscosity model for test case 14.

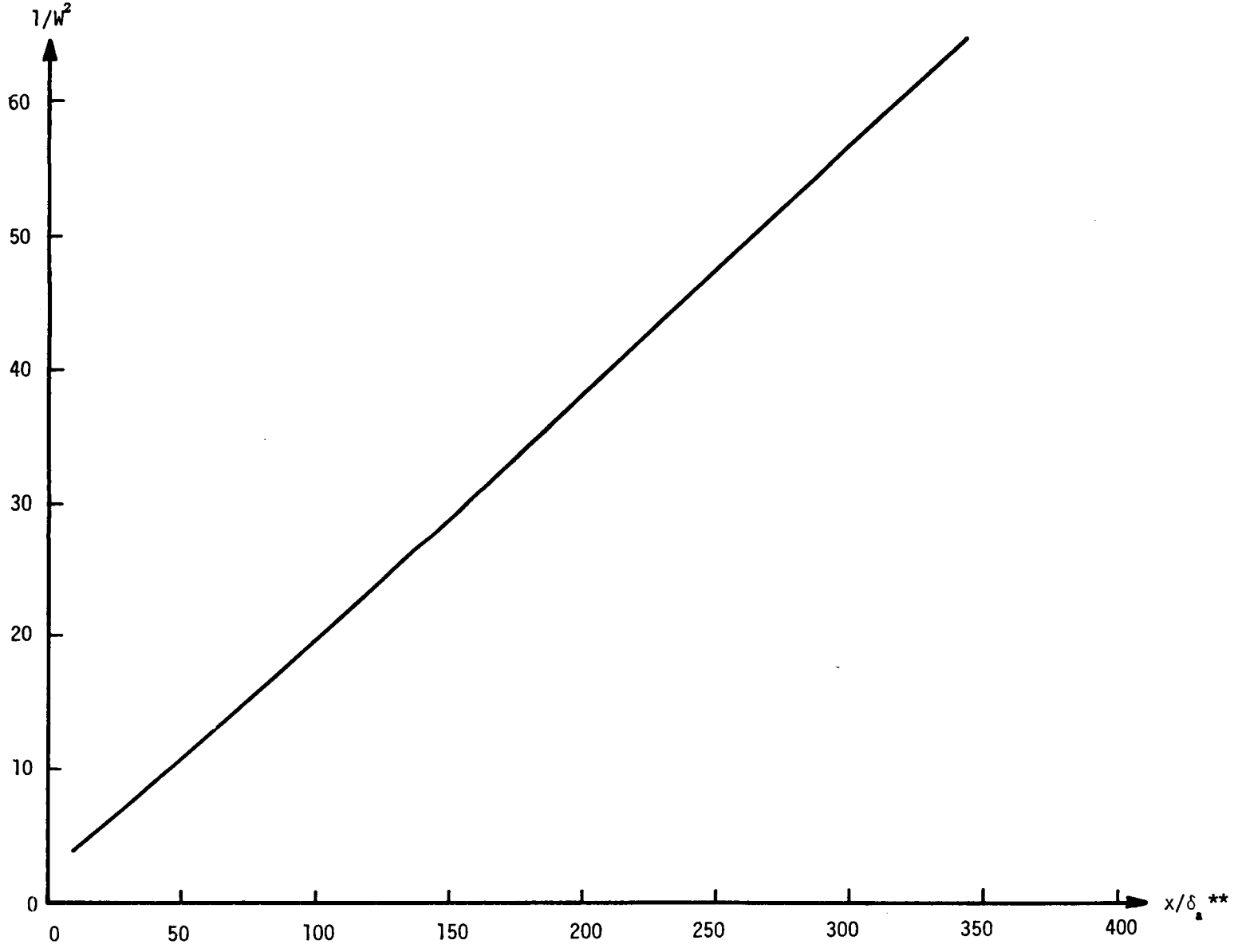

Figure 17.- Predicted center-line velocity defect for test case 14.

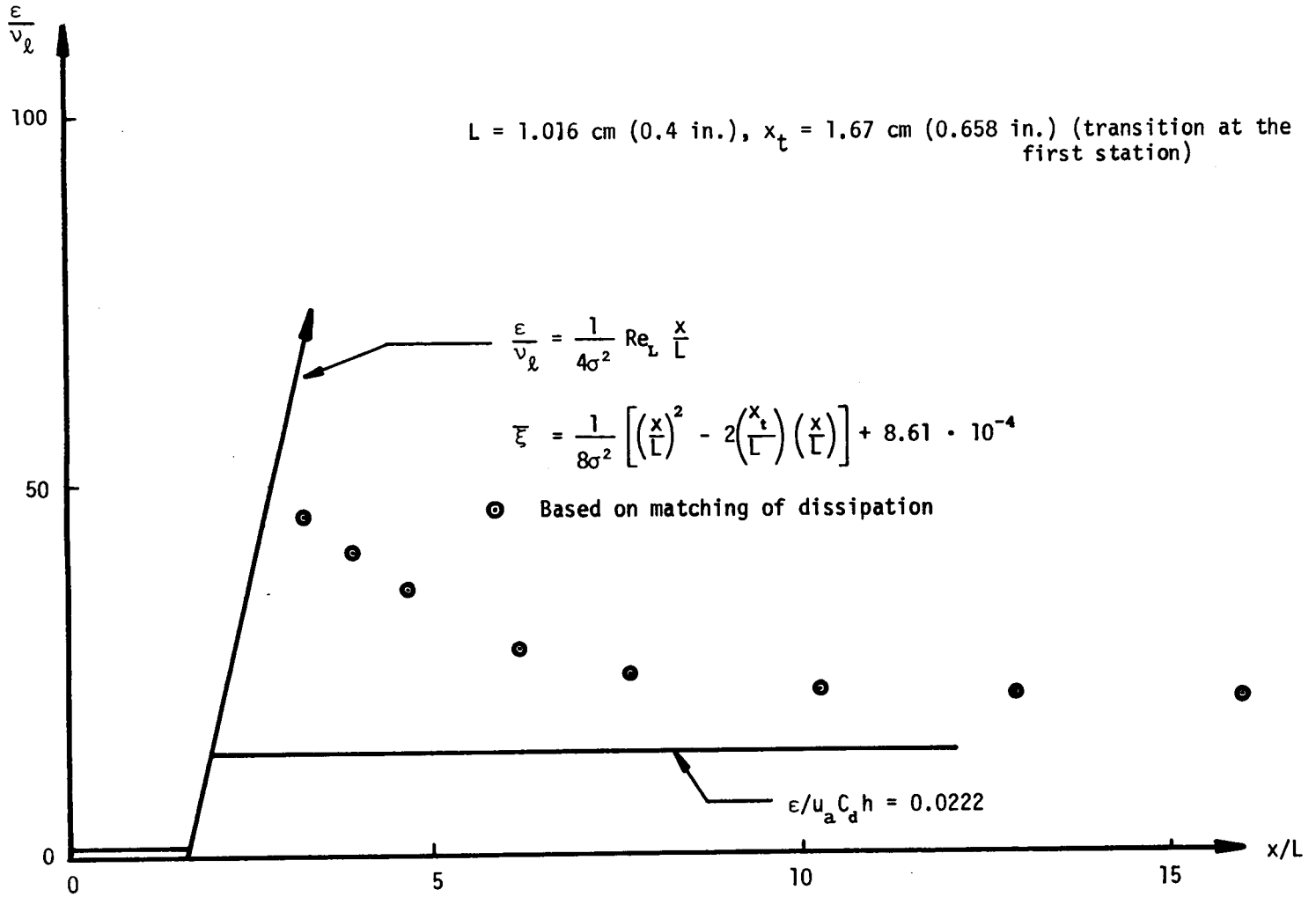

Figure 18.- Conceptual and experimentally determined eddy viscosity for test case 16.

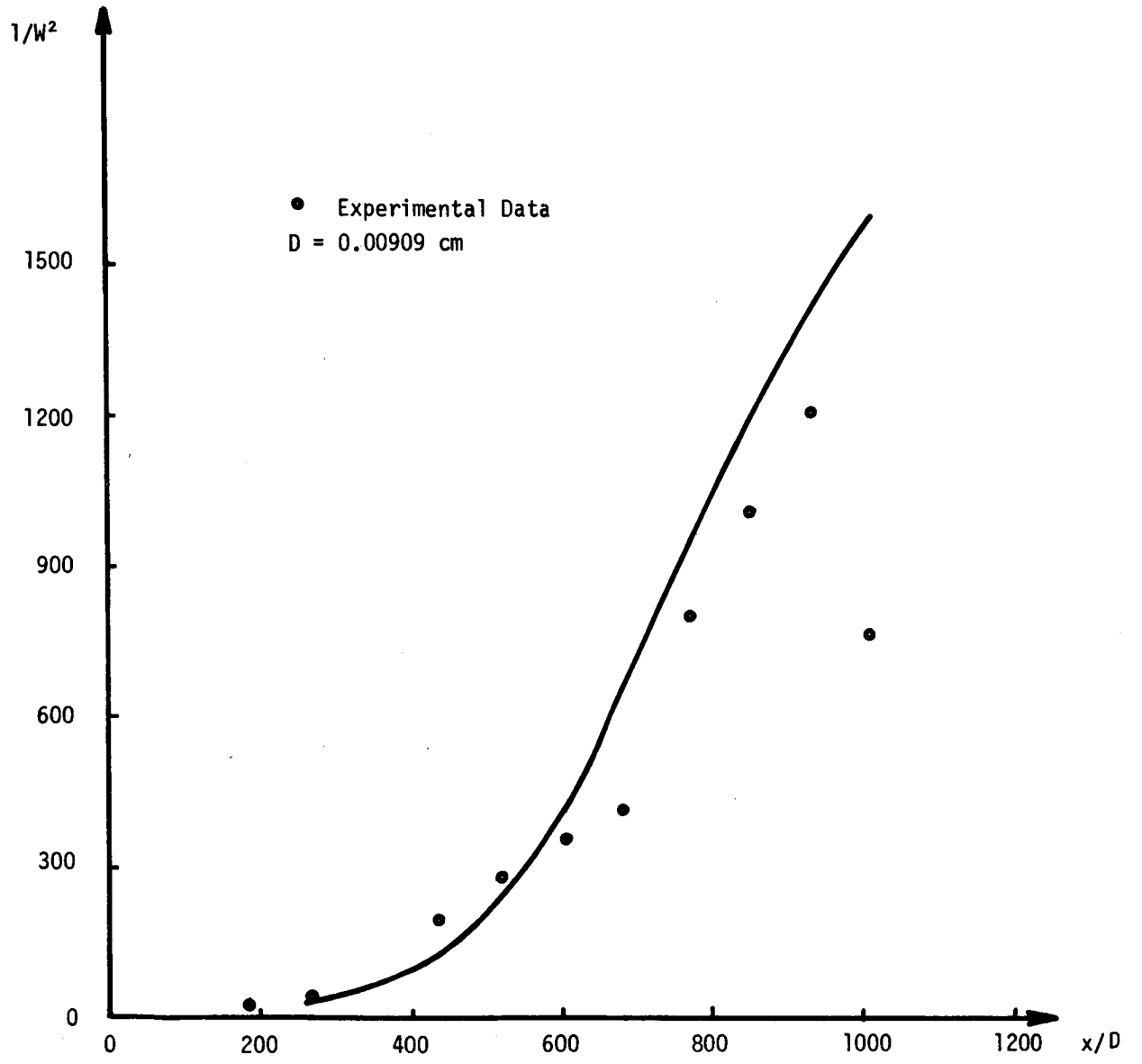

Figure 19.- Predicted and experimental center-line velocity defect for test case 16.

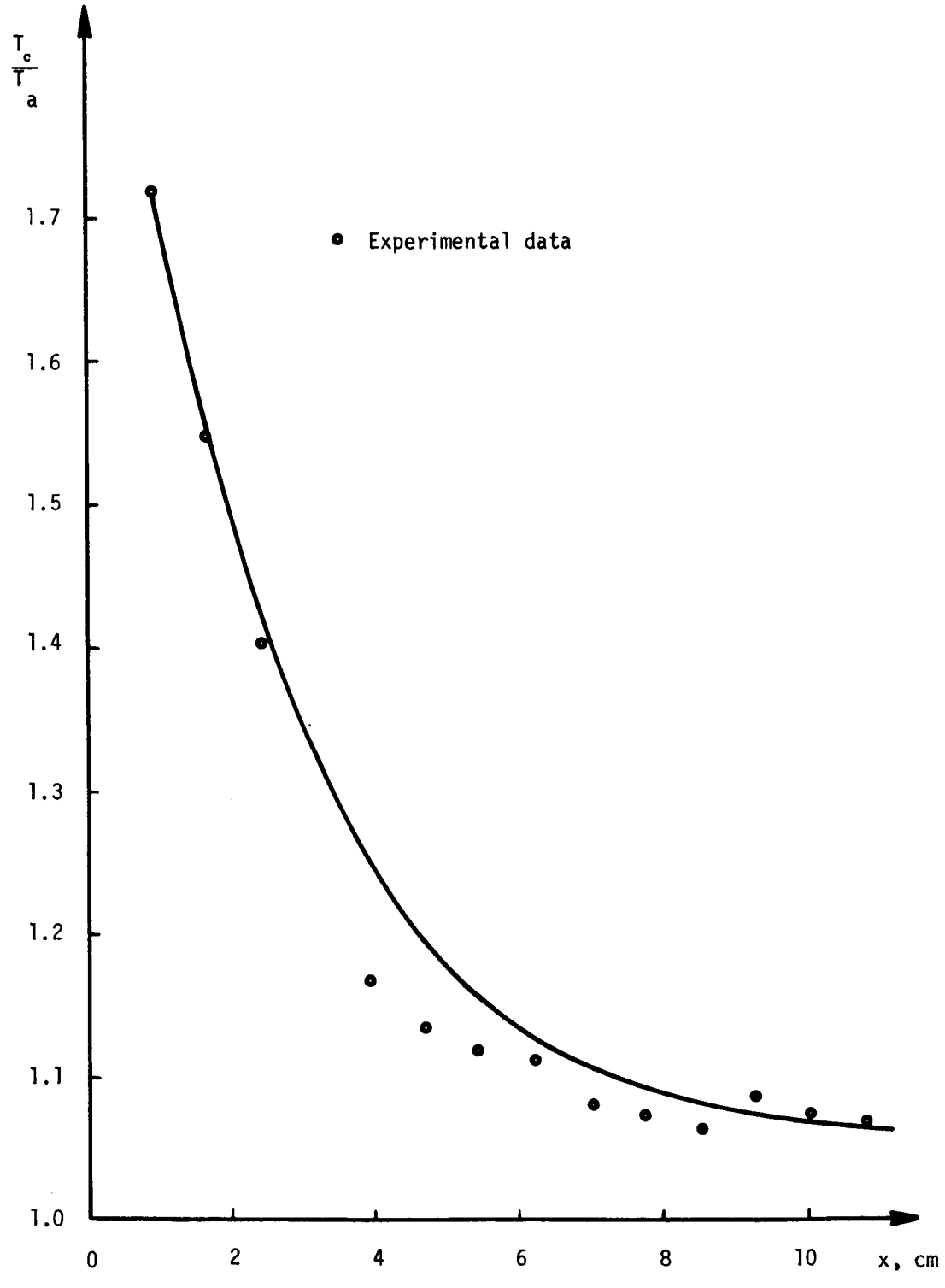

Figure 20.- Predicted and experimental center-line temperature ratio for test case 16.

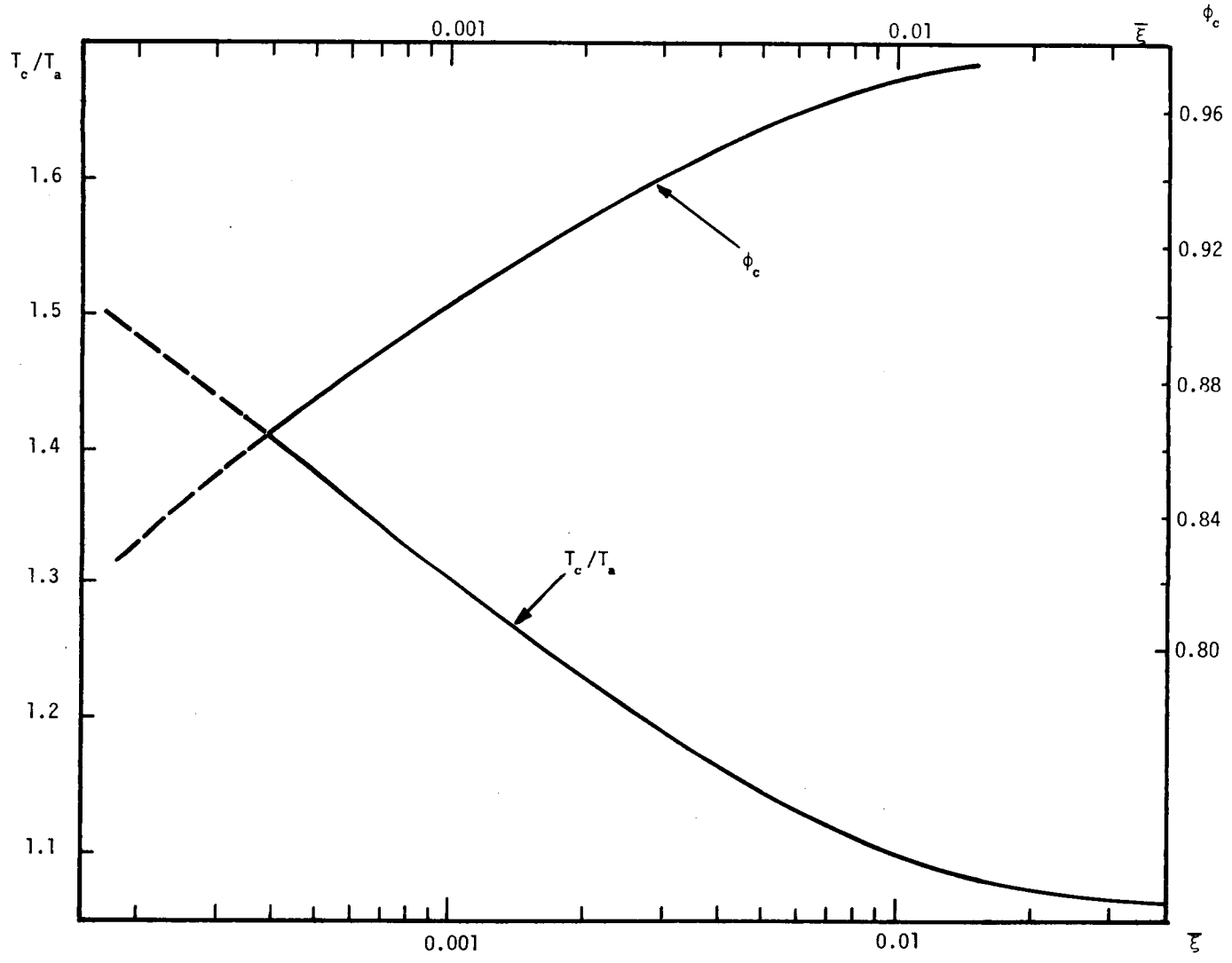

Figure 21.- Calculated center-line velocity and temperature ratios as functions of $\bar{\xi}$ for test case 16.

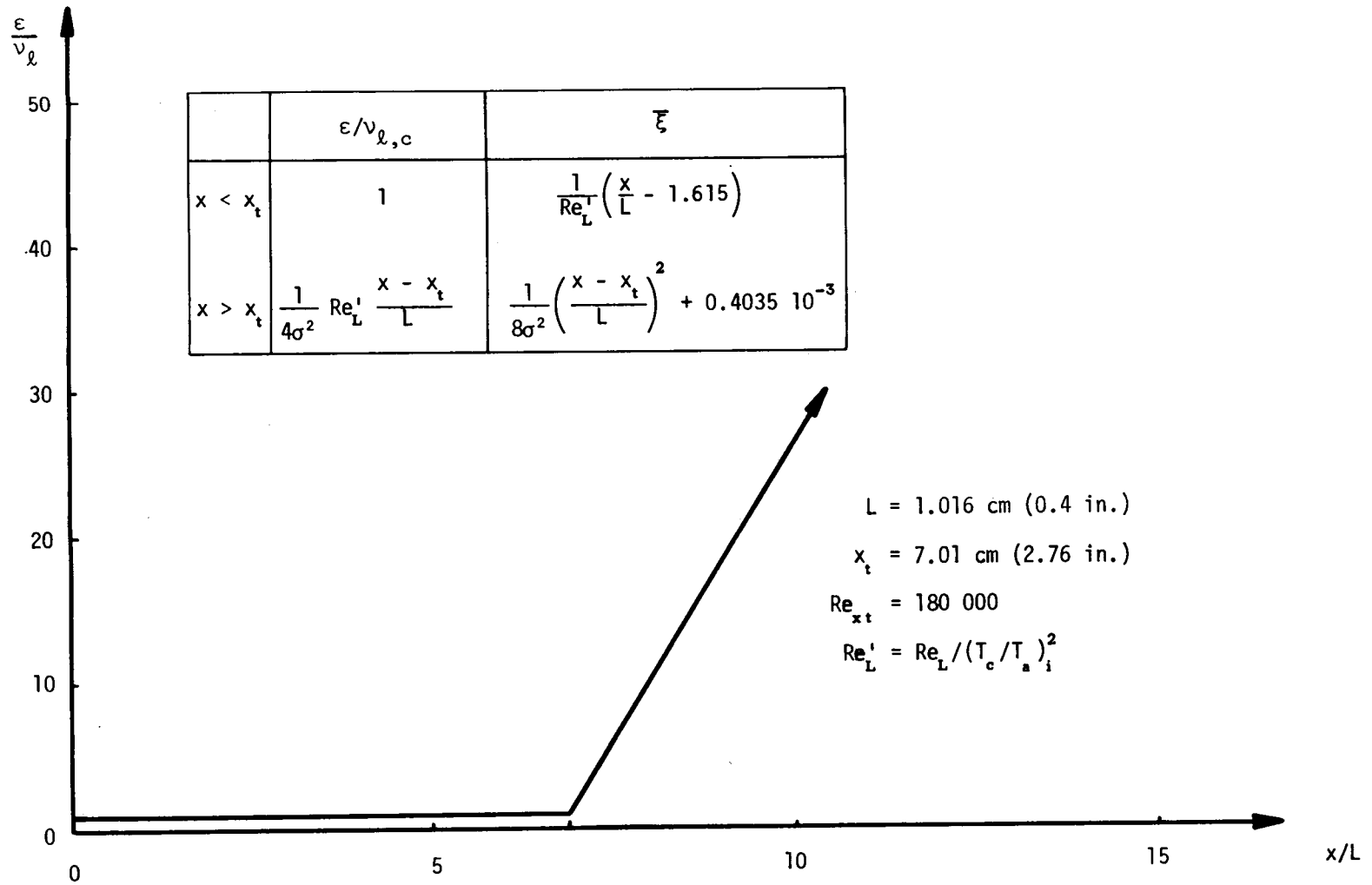

Figure 22.- Conceptual eddy viscosity for test case 24.

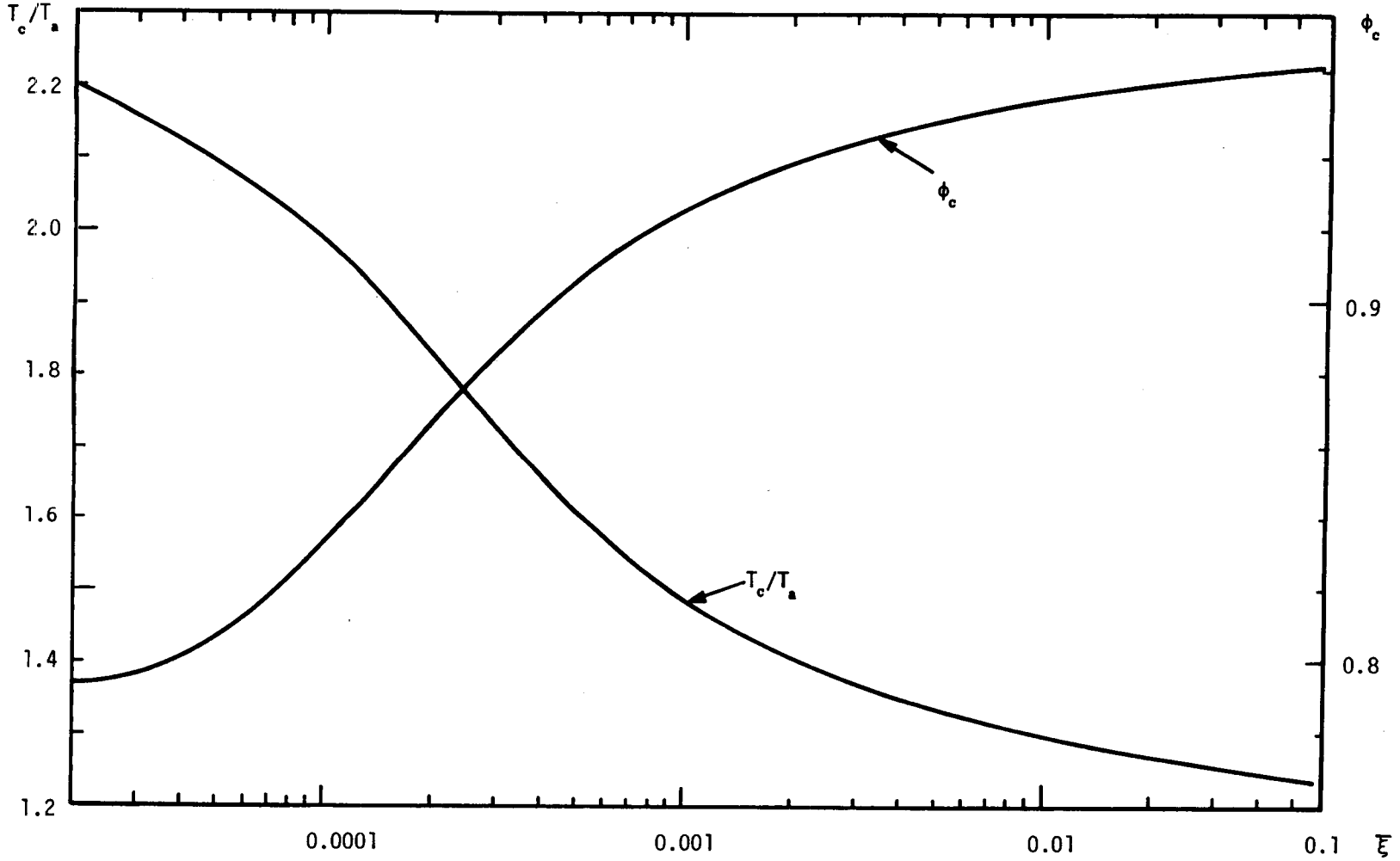

Figure 23.- Calculated center-line velocity and temperature ratios as functions of $\bar{\xi}$ for test case 24.

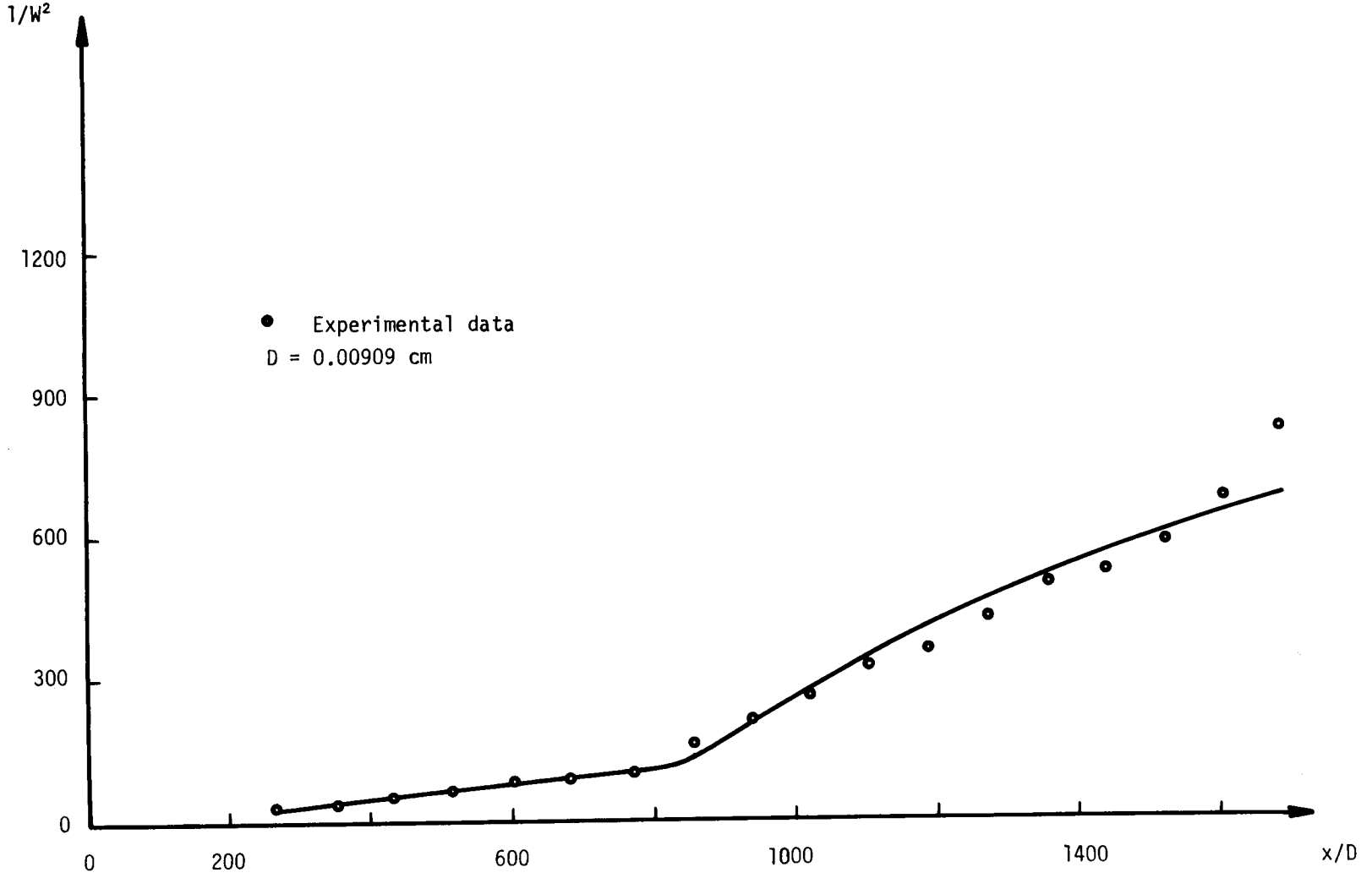

Figure 24.- Predicted and experimental center-line velocity defect for test case 24.

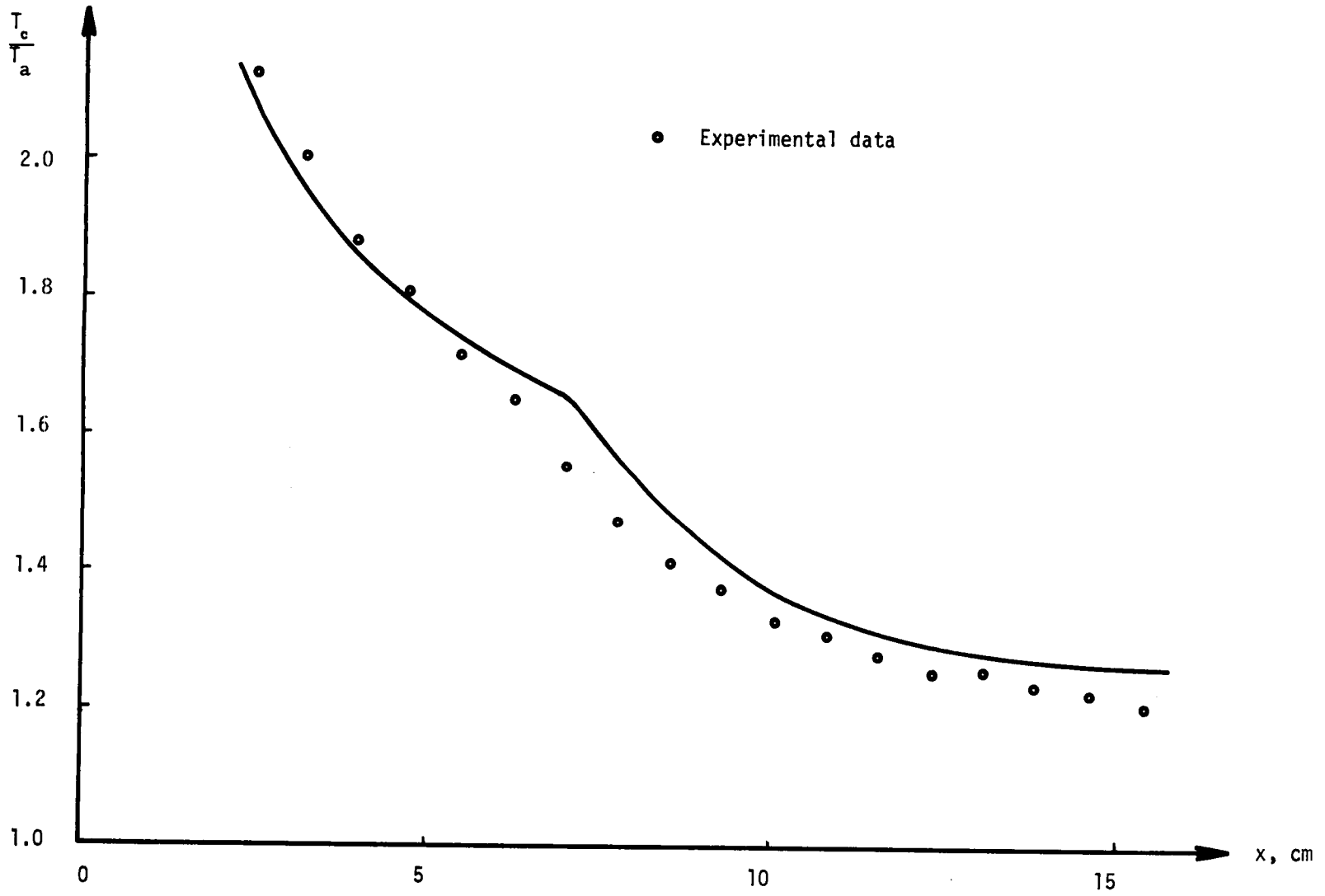

Figure 25.- Predicted and experimental center-line temperature ratios for test case 24.

Professor Goldschmidt: I am sorry, I must not have understood very well. How did you define your shift in the origin – this x_o – is it completely arbitrary or is it computed somehow?

W. L. Chow: No, first I said it is a matching of energy defect of the mean flow of the actual mixing profile to a fictitious one with a shifted origin, and meanwhile we have to also apply an equivalent bleed concept. In other words, if we have an initial boundary-layer flow, we always have a developing flow even far downstream. The flow looks similar, still shifted somewhat, so we have to use the initial boundary-layer effect to correlate it and we call that an equivalent bleed concept. It is described in the paper and it is long so I would rather not go into it at this time. If you would like to discuss anything else I would be glad to answer your question in detail, in private.

THE RELATIONSHIP BETWEEN EDDY-TRANSPORT AND SECOND-ORDER CLOSURE MODELS FOR STRATIFIED MEDIA AND FOR VORTICES*

By Coleman duP. Donaldson
Aeronautical Research Associates of Princeton, Inc.

INTRODUCTION

A question which invariably arises when one considers the calculation of turbulent shear flows is, "How complex a model should be used to calculate such motions?" Available at the present time are models varying in complexity from very simple eddy-transport models to models in which all the equations for the nonzero second-order correlations are solved simultaneously with the equations for the mean variables. For this reason, it might be instructive to present a discussion of the relationship between these two models of turbulent shear flow. Two types of motion will be discussed: first, turbulent shear flow in a stratified medium and, second, the motion in a turbulent line vortex. These two cases are instructive because in the first example eddy-transport methods have proven reasonably effective, whereas in the second, they have led to erroneous conclusions.

It is not generally appreciated that the simplest form of eddy-transport theory can be derived from second-order closure models of turbulent flow by a suitably limiting process. This paper will discuss this limiting process and the suitability of eddy-transport modeling for stratified media and line vortices.

SYMBOLS

a,b	model parameters
c_p	specific heat at constant pressure
D	operator
g	gravitational acceleration
g_i, g_k	general acceleration vectors

*This work was supported in part by the Air Force Office of Scientific Research (AFSC), under Contract F44620-69-C-0089; and in part by NASA, under Contract NASw-1868.

i,j,k	indices
m,n	proportionality constants
N	stability parameter (eq. (90))
N_{Ri}	Richardson number
P	parameter (eq. (49))
p	pressure
Q	turbulent energy, $(UU + VV + WW)^{1/2}$
q	scalar velocity, $\left[(u^i)'u_i'\right]^{1/2}$
r,ϕ,z	cylindrical coordinates
r_c	vortex core radius (fig. 7)
T	temperature
t	time
U,V,W	nondimensional second-order velocity correlations
$\overline{u},\overline{v},\overline{w}$	mean velocity in r-, ϕ-, z-direction, respectively, for two-dimensional line vortex; mean velocity in x-, y-, z-direction, respectively, for atmospheric motion
x,y,z	Cartesian coordinates
α	length scale proportionality constant
Γ	vortex strength
Δ	difference
δ	breadth of layer under consideration

δ_{ik}	Kronecker delta
ϵ	local deformation in vortex
κ	Von Kármán's constant
$\Lambda_1, \Lambda_2, \Lambda_3$	length scales
λ	dissipative scale
μ	viscosity
ν	kinematic viscosity
ρ	density
τ_{ij}	stress tensor
τ_t	turbulent shear stress

Subscripts:

char	characteristic
crit	critical
max	maximum
o	undisturbed, adiabatic atmosphere

Bars over a quantity indicate mean values. Primes indicate the instantaneous fluctuation of the quantity from its mean value.

A SECOND-ORDER CLOSURE MODEL FOR TURBULENT SHEAR FLOW

In reference 1 the author presented a discussion of the development of an invariant second-order closure model for turbulent shear flow in an incompressible medium. The basic equations of this model are

$$\frac{\partial \bar{u}_j}{\partial x_j} = 0 \tag{1}$$

$$\frac{\partial \bar{u}_i}{\partial t} + \bar{u}^j \bar{u}_{i,j} = -\frac{1}{\rho}\bar{p}_{,i} + \left[\bar{\tau}_i{}^j - \overline{\left(u^j\right)' u_i'}\right]_{,j} \tag{2}$$

$$\frac{\partial \overline{u_i' u_k'}}{\partial t} + \bar{u}^j \left[\overline{u_i' \left(u^j\right)'}\right]_{,j} = -\overline{u_j' u_k'} \frac{\partial \bar{u}_i}{\partial x_j} - \overline{u_j' u_i'} \frac{\partial \bar{u}_k}{\partial x_j} + \frac{\partial}{\partial x_j}\left[\Lambda_2 q \left(\frac{\partial}{\partial x_j}\overline{u_i' u_k'} + \frac{\partial}{\partial x_i}\overline{u_j' u_k'} + \frac{\partial}{\partial x_k}\overline{u_j' u_i'}\right)\right] + \frac{\partial}{\partial x_k}\left(\Lambda_3 q \frac{\partial \overline{u_j' u_i'}}{\partial x_j}\right) + \frac{\partial}{\partial x_i}\left(\Lambda_3 q \frac{\partial \overline{u_j' u_k'}}{\partial x_j}\right) - \frac{q}{\Lambda_1}\left(\overline{u_i' u_k'} - \delta_{ik}\frac{q^2}{3}\right) + \nu \frac{\partial^2}{\partial x_j^2}\overline{u_i' u_k'} - 2\nu \frac{\overline{u_i' u_k'}}{\lambda^2} \tag{3}$$

with

$$\bar{\tau}_{ij} = \mu\left(\bar{u}_{i,j} + \bar{u}_{j,i}\right) \tag{4}$$

and

$$q = \left[\overline{\left(u^i\right)' u_i'}\right]^{1/2} \tag{5}$$

In this model, the length scales Λ_1, Λ_2, and Λ_3 are assumed to be proportional to one another. The dissipative scale λ is given by

$$\lambda^2 = \frac{\Lambda_1{}^2}{a + \left(b\rho q \Lambda_1/\mu\right)} \tag{6}$$

From a rather lengthy parameter search to determine the values of the quantities a, b, Λ_1, Λ_2, and Λ_3 that are to be used in the calculations, it was found that good results were obtained by using

$$\left.\begin{aligned} a &= 2.5 \\ b &= 0.125 \\ \frac{\Lambda_2}{\Lambda_1} &= 0.1 \\ \frac{\Lambda_3}{\Lambda_1} &= 0.1 \end{aligned}\right\} \tag{7}$$

It was further found that the remaining free parameter Λ_1 was approximately equal to 0.6 times the longitudinal integral scale of the motions studied in the parameter search.

In reference 2, this model was extended to the case of turbulent motion and transport in the earth's boundary layer. The case considered is that when the scales of the mean distributions of velocity and temperature are not greatly different and the Prandtl and Schmidt numbers are 1. The resulting equations, written in Cartesian tensor notation, are

$$\frac{\partial \overline{u}_i}{\partial x_i} = 0 \tag{8}$$

$$\frac{D\overline{u}_i}{Dt} = -\frac{\partial \overline{p}}{\partial x_i} + \nu_o \frac{\partial}{\partial x_j}\left(\frac{\partial \overline{u}_i}{\partial x_j} + \frac{\partial \overline{u}_j}{\partial x_i}\right) - \frac{\partial \overline{u_i' u_j'}}{\partial x_j} + \frac{1}{T_o} g_i \overline{T} \tag{9}$$

$$\frac{D\overline{T}}{Dt} = \nu_o \frac{\partial^2 \overline{T}}{\partial x_j^2} - \frac{\partial \overline{u_j' T'}}{\partial x_j} \tag{10}$$

$$\frac{D\overline{u_i' u_k'}}{Dt} = -\overline{u_j' u_k'} \frac{\partial \overline{u}_i}{\partial x_j} - \overline{u_j' u_i'} \frac{\partial \overline{u}_k}{\partial x_j} + \frac{1}{T_o}\left(g_i \overline{u_k' T'} + g_k \overline{u_i' T'}\right) + \frac{\partial}{\partial x_j}\left[\Lambda_2 q\left(\frac{\partial \overline{u_i' u_j'}}{\partial x_k} + \frac{\partial \overline{u_j' u_k'}}{\partial x_i} + \frac{\partial \overline{u_k' u_i'}}{\partial x_j}\right)\right] + \frac{\partial}{\partial x_i}\left(\Lambda_3 q \frac{\partial \overline{u_j' u_k'}}{\partial x_j}\right) + \frac{\partial}{\partial x_k}\left(\Lambda_3 q \frac{\partial \overline{u_j' u_i'}}{\partial x_j}\right) - \frac{q}{\Lambda_1}\left(\overline{u_i' u_k'} - \frac{\delta_{ik}}{3} q^2\right) + \nu_o \frac{\partial^2 \overline{u_i' u_k'}}{\partial x_j^2} - 2\nu_o \frac{\overline{u_i' u_k'}}{\lambda^2} \tag{11}$$

$$\frac{D\overline{u_k' T'}}{Dt} = -\overline{u_j' u_k'} \frac{\partial \overline{T}}{\partial x_j} - \overline{u_j' T'} \frac{\partial \overline{u}_k}{\partial x_j} + \frac{1}{T_o} g_k \overline{(T')^2} + \frac{\partial}{\partial x_j}\left[\Lambda_2 q\left(\frac{\partial \overline{u_j' T'}}{\partial x_k} + \frac{\partial \overline{u_k' T'}}{\partial x_j}\right)\right] + \frac{\partial}{\partial x_k}\left(\Lambda_3 q \frac{\partial \overline{u_j' T'}}{\partial x_j}\right) - \frac{q}{\Lambda_1} \overline{u_k' T'} + \nu_o \frac{\partial^2 \overline{u_k' T'}}{\partial x_j^2} - 2\nu_o \frac{\overline{u_k' T'}}{\lambda^2} \tag{12}$$

$$\frac{D\overline{(T')^2}}{Dt} = -2\overline{u_j' T'} \frac{\partial \overline{T}}{\partial x_j} + \frac{\partial}{\partial x_j}\left[\Lambda_2 q \frac{\partial \overline{(T')^2}}{\partial x_j}\right] + \nu_o \frac{\partial^2 \overline{(T')^2}}{\partial x_j^2} - 2\nu_o \frac{\overline{(T')^2}}{\lambda^2} \tag{13}$$

In these equations,

$$\frac{D}{Dt} = \frac{\partial}{\partial t} + \bar{u}_j \frac{\partial}{\partial x_j} \tag{14}$$

T_o and ν_o are the local temperature and kinematic viscosity, respectively, in an undisturbed adiabatic atmosphere; $\overline{T}$ is the departure of the mean temperature from the adiabatic temperature T_o; and T' is the instantaneous fluctuation of the temperature about its mean.

For the two cases of motion considered herein, equations (1) to (14) reduce to the following:

For the case of a two-dimensional line vortex in cylindrical coordinates r,ϕ,z with velocities $\bar{u},\bar{v},\bar{w}$, equations (2) and (3) result in

$$\frac{\partial \bar{v}}{\partial t} = -\frac{\partial \overline{u'v'}}{\partial r} - \frac{2}{r}\overline{u'v'} + \nu\left(\frac{\partial^2 \bar{v}}{\partial r^2} + \frac{1}{r}\frac{\partial \bar{v}}{\partial r} - \frac{\bar{v}}{r}\right) \tag{15}$$

$$\begin{aligned}\frac{\partial \overline{u'u'}}{\partial t} = {} & \frac{4\bar{v}}{r}\overline{u'v'} + 3\frac{\partial}{\partial r}\left(\Lambda_2 q \frac{\partial \overline{u'u'}}{\partial r}\right) - \frac{2\Lambda_2 q}{r}\frac{\partial \overline{v'v'}}{\partial r} + \frac{3\Lambda_2 q}{r}\frac{\partial \overline{u'u'}}{\partial r} + \frac{4\Lambda_2 q}{r^2}\left(\overline{v'v'} - \overline{u'u'}\right) \\ & + 2\frac{\partial}{\partial r}\left(\Lambda_3 q \frac{\partial \overline{u'u'}}{\partial r}\right) - \frac{2}{r}\frac{\partial\left(\Lambda_3 q \overline{v'v'}\right)}{\partial r} + \frac{2}{r}\frac{\partial\left(\Lambda_3 q \overline{u'u'}\right)}{\partial r} + \frac{2}{r^2}\Lambda_3 q\left(\overline{v'v'} - \overline{u'u'}\right) \\ & - \frac{q}{\Lambda_1}\left(\overline{u'u'} - \frac{q^2}{3}\right) + \nu\left[\frac{\partial^2 \overline{u'u'}}{\partial r^2} + \frac{1}{r}\frac{\partial \overline{u'u'}}{\partial r} + \frac{2}{r^2}\left(\overline{v'v'} - \overline{u'u'}\right) - \frac{2}{\lambda^2}\overline{u'u'}\right]\end{aligned} \tag{16}$$

$$\begin{aligned}\frac{\partial \overline{v'v'}}{\partial t} = {} & -\left(\frac{2\bar{v}}{r} + \frac{\partial \bar{v}}{\partial r}\right)\overline{u'v'} + \frac{\partial}{\partial r}\left(\Lambda_2 q \frac{\partial \overline{v'v'}}{\partial r}\right) + \frac{3\Lambda_2 q}{r}\frac{\partial \overline{v'v'}}{\partial r} - \frac{2}{r}\frac{\partial\left(\Lambda_2 q \overline{v'v'}\right)}{\partial r} \\ & + \frac{2}{r}\frac{\partial\left(\Lambda_2 q \overline{u'u'}\right)}{\partial r} + \frac{4\Lambda_2 q}{r^2}\left(\overline{u'u'} - \overline{v'v'}\right) + \frac{2\Lambda_3 q}{r}\frac{\partial \overline{u'u'}}{\partial r} + \frac{2\Lambda_3 q}{r^2}\left(\overline{u'u'} - \overline{v'v'}\right) \\ & - \frac{q}{\Lambda_1}\left(\overline{v'v'} - \frac{q^2}{3}\right) + \nu\left[\frac{\partial^2 \overline{v'v'}}{\partial r^2} + \frac{1}{r}\frac{\partial \overline{v'v'}}{\partial r} + \frac{2}{r^2}\left(\overline{u'u'} - \overline{v'v'}\right) - \frac{2\overline{v'v'}}{\lambda^2}\right]\end{aligned} \tag{17}$$

$$\frac{\partial\overline{w'w'}}{\partial t} = \frac{\partial}{\partial r}\left(\Lambda_2 q \frac{\partial\overline{w'w'}}{\partial r}\right) + \frac{\Lambda_2 q}{r}\frac{\partial\overline{w'w'}}{\partial r} - \frac{q}{\Lambda_1}\left(\overline{w'w'} - \frac{q^2}{3}\right)$$

$$+ \nu\left(\frac{\partial^2\overline{w'w'}}{\partial r^2} + \frac{1}{r}\frac{\partial\overline{w'w'}}{\partial r} - \frac{2\overline{w'w'}}{\lambda^2}\right) \tag{18}$$

$$\frac{\partial\overline{u'v'}}{\partial t} = \frac{\overline{v}}{r}\left(2\overline{v'v'} - \overline{u'u'}\right) - \frac{\partial\overline{v}}{\partial r}\overline{u'u'} + 2\frac{\partial}{\partial r}\left(\Lambda_2 q \frac{\partial\overline{u'v'}}{\partial r}\right) - \frac{2}{r}\frac{\partial\left(\Lambda_2 q\overline{u'w'}\right)}{\partial r} + \frac{4\Lambda_2 q}{r}\frac{\partial\overline{u'v'}}{\partial r}$$

$$- \frac{8\Lambda_2 q}{r^2}\overline{u'v'} + \frac{\partial}{\partial r}\left(\Lambda_3 q \frac{\partial\overline{u'v'}}{\partial r}\right) + \frac{2}{r}\frac{\partial\left(\Lambda_3 q\overline{u'v'}\right)}{\partial r} - \frac{\Lambda_3 q}{r}\frac{\partial\overline{u'v'}}{\partial r} - \frac{4\Lambda_3 q\overline{u'v'}}{r^2}$$

$$- \frac{q}{\Lambda_1}\overline{u'v'} + \nu\left(\frac{\partial^2\overline{u'v'}}{\partial r^2} + \frac{1}{r}\frac{\partial\overline{u'v'}}{\partial r} - \frac{4\overline{u'v'}}{r^2} - \frac{2\overline{u'v'}}{\lambda^2}\right) \tag{19}$$

For the atmospheric motion considered herein, in which only a mean velocity $\overline{u}$ in the horizontal direction x exists and in which the mean lateral and vertical velocities $\overline{v}$ and $\overline{w}$ in the directions y and z, respectively, are zero, the appropriate equations derived from equations (8) to (13) are

$$\frac{\partial\overline{u}}{\partial t} = -\frac{\partial\overline{p}}{\partial x} + \nu_o\frac{\partial^2\overline{u}}{\partial z^2} - \frac{\partial\overline{u'w'}}{\partial z} \tag{20}$$

$$\frac{\partial\overline{T}}{\partial t} = \nu_o\frac{\partial^2\overline{T}}{\partial z^2} - \frac{\partial\overline{T'w'}}{\partial z} \tag{21}$$

$$\frac{\partial\overline{u'u'}}{\partial t} = -2\overline{u'w'}\frac{\partial\overline{u}}{\partial z} + \frac{\partial}{\partial z}\left(\Lambda_2 q\frac{\partial\overline{u'u'}}{\partial z}\right) - \frac{q}{\Lambda_1}\left(\overline{u'u'} - \frac{q^2}{3}\right) + \nu_o\frac{\partial^2\overline{u'u'}}{\partial z^2} - 2\nu_o\frac{\overline{u'u'}}{\lambda^2} \tag{22}$$

$$\frac{\partial\overline{v'v'}}{\partial t} = \frac{\partial}{\partial z}\left(\Lambda_2 q\frac{\partial\overline{v'v'}}{\partial z}\right) - \frac{q}{\Lambda_1}\left(\overline{v'v'} - \frac{q^2}{3}\right) + \nu_o\frac{\partial^2\overline{v'v'}}{\partial z^2} - 2\nu_o\frac{\overline{v'v'}}{\lambda^2} \tag{23}$$

$$\frac{\partial\overline{w'w'}}{\partial t} = \frac{2g}{T_o}\overline{w'T'} + 3\frac{\partial}{\partial z}\left(\Lambda_2 q\frac{\partial\overline{w'w'}}{\partial z}\right) + \frac{2}{\rho_o}\frac{\partial}{\partial z}\left(\rho_o\Lambda_3 q\frac{\partial\overline{w'w'}}{\partial z}\right)$$

$$- \frac{q}{\Lambda_1}\left(\overline{w'w'} - \frac{q^2}{3}\right) + \nu_o\frac{\partial^2\overline{w'w'}}{\partial z^2} - 2\nu_o\frac{\overline{w'w'}}{\lambda^2} \tag{24}$$

$$\frac{\partial \overline{u'w'}}{\partial t} = -\overline{w'w'}\,\frac{\partial \bar{u}}{\partial z} + \frac{g}{T_o}\,\overline{u'T'} + 2\,\frac{\partial}{\partial z}\left(\Lambda_2 q\,\frac{\partial \overline{u'w'}}{\partial z}\right) + \frac{1}{\rho_o}\,\frac{\partial}{\partial z}\left(\rho_o \Lambda_3 q\,\frac{\partial \overline{u'w'}}{\partial z}\right)$$

$$- \frac{q}{\Lambda_1}\,\overline{u'w'} + \nu_o\,\frac{\partial^2 \overline{u'w'}}{\partial z^2} - 2\nu_o\,\frac{\overline{u'w'}}{\lambda^2} \qquad (25)$$

$$\frac{\partial \overline{u'T'}}{\partial t} = -\overline{u'w'}\,\frac{\partial \bar{T}}{\partial z} - \overline{w'T'}\,\frac{\partial \bar{u}}{\partial z} + \frac{\partial}{\partial z}\left(\Lambda_2 q\,\frac{\partial \overline{u'T'}}{\partial z}\right) - \frac{q}{\Lambda_1}\,\overline{u'T'} + \nu_o\,\frac{\partial^2 \overline{u'T'}}{\partial z^2} - 2\nu_o\,\frac{\overline{u'T'}}{\lambda^2} \qquad (26)$$

$$\frac{\partial \overline{w'T'}}{\partial t} = -\overline{w'w'}\,\frac{\partial \bar{T}}{\partial z} + \frac{g}{T_o}\,\overline{(T')^2} + 2\,\frac{\partial}{\partial z}\left(\Lambda_2 q\,\frac{\partial \overline{w'T'}}{\partial z}\right) + \frac{1}{\rho_o}\,\frac{\partial}{\partial z}\left(\rho_o \Lambda_3 q\,\frac{\partial \overline{w'T'}}{\partial z}\right)$$

$$- \frac{q}{\Lambda_1}\,\overline{w'T'} + \nu_o\,\frac{\partial^2 \overline{w'T'}}{\partial z^2} - 2\nu_o\,\frac{\overline{w'T'}}{\lambda^2} \qquad (27)$$

$$\frac{\partial \overline{(T')^2}}{\partial t} = -2\overline{w'T'}\,\frac{\partial \bar{T}}{\partial z} + \frac{\partial}{\partial z}\left[\Lambda_2 q\,\frac{\partial \overline{(T')^2}}{\partial z}\right] + \nu_o\,\frac{\partial^2 \overline{(T')^2}}{\partial z^2} - 2\nu_o\,\frac{\overline{(T')^2}}{\lambda^2} \qquad (28)$$

For most people who practice the art of predicting turbulent flows, the equations for the line vortex (eqs. (15) to (19)) and for the flow in the atmospheric boundary layer (eqs. (20) to (28)) are of a familiar form. If distributions on the dependent variables are given at time $t = 0$, the development of the motion at subsequent times can be computed by simultaneous solution of the appropriate coupled sets of partial differential equations. This is the general approach of second-order modeling.

The older and still widely used method of treating these problems is to consider only the equations for the mean variables and to assume that the second-order correlations which appear in them might be represented by empirically determined eddy-transport models patterned after the transport of the appropriate quantity by molecular means. The section which follows will examine what information can be gleaned from the equations for the second-order correlations about the nature of such eddy-transport models.

SUPEREQUILIBRIUM MODELS

To determine how to obtain information about the nature of eddy-transport models from the model or rate equations for the appropriate second-order correlations, one must consider what is implied when it is assumed that a turbulent flow can exhibit an eddy viscosity or an eddy diffusivity.

First, it is apparent that if the turbulent transport of a quantity depends only on the local gradient of that quantity and a scale length associated with the mean flows at the location under consideration, the turbulent transport cannot have a "memory" of its past history along the streamline. This is tantamount to the assumption that at each point in the flow the turbulent-transport correlations can track their local equilibrium values. These local equilibrium values can be obtained from the rate equations for the correlations by setting the left-hand sides of the equations, as they are given in the preceding section, equal to zero. Thus it is assumed that the rate of change of a transport correlation as it follows the mean motion is small compared with the production, dissipation, and diffusion terms which occur at the point in question.

Second, the notion of an eddy-transport coefficient is one which does not allow the behavior of the turbulent transport at one point in the flow to affect directly the turbulent transport at another point. This notion is equivalent to the neglect of the diffusion terms in the equations for the second-order correlations, for it is these terms which link the generation of transport correlations at one point in the flow to the transport correlations at another point.

Finally, the use of an eddy-transport model is a practice generally restricted to flows with high Reynolds numbers. Therefore, the high Reynolds number limit of the equations for the second-order correlations can be taken if it is desired to derive a simple form of eddy-transport model from these equations.

If the three rules set forth above are followed, it should be possible to derive from the equations for the second-order correlations a simple theory of eddy transport. As discussed above, this theory represents the equilibrium, nondiffusive, high Reynolds number limit of a second-order closure model. For reasons of brevity, this limit has for some time been referred to by the author as the "superequilibrium" limit.

By following the three rules set forth, the following equations are found to be the superequilibrium equations for a line vortex:

$$0 = \frac{4\bar{v}}{r}\overline{u'v'} - (1 + 2b)\frac{q}{\Lambda}\overline{u'u'} + \frac{q^3}{3\Lambda} \tag{29}$$

$$0 = -2\left(\frac{\partial \bar{v}}{\partial r} + \frac{\bar{v}}{rz}\right)\overline{u'v'} - (1 + 2b)\frac{q}{\Lambda}\overline{v'v'} + \frac{q^3}{3} \tag{30}$$

$$0 = -(1 + 2b)\frac{q}{\Lambda}\overline{w'w'} + \frac{q^3}{3} \tag{31}$$

$$0 = -\left(\frac{\partial \bar{v}}{\partial r} + \frac{\bar{v}}{r}\right)\overline{u'u'} + \frac{2\bar{v}}{r}\overline{v'v'} - (1 + 2b)\frac{q}{\Lambda}\overline{u'v'} \tag{32}$$

For atmospheric motion, one finds

$$0 = -2\overline{u'w'}\,\frac{\partial\bar{u}}{\partial z} - \frac{q}{\Lambda}(1 + 2b)\overline{u'u'} + \frac{q^3}{\Lambda} \tag{33}$$

$$0 = -\frac{q}{\Lambda}(1 + 2b)\overline{v'v'} + \frac{q^3}{\Lambda} \tag{34}$$

$$0 = \frac{2g}{T_o}\,\overline{w'T'} - \frac{q}{\Lambda}(1 + 2b)\overline{w'w'} + \frac{q^3}{\Lambda} \tag{35}$$

$$0 = -\overline{w'w'}\,\frac{\partial\bar{u}}{\partial z} + \frac{g}{T_o}\,\overline{u'T'} - \frac{q}{\Lambda}(1 + 2b)\overline{u'w'} \tag{36}$$

$$0 = -\overline{u'w'}\,\frac{\partial\bar{T}}{\partial z} - \overline{w'T'}\,\frac{\partial\bar{u}}{\partial z} - \frac{q}{\Lambda}(1 + 2b)\overline{u'T'} \tag{37}$$

$$0 = -\overline{w'w'}\,\frac{\partial\bar{T}}{\partial z} + \frac{g}{T_o}\overline{(T')^2} - \frac{q}{\Lambda}(1 + 2b)\overline{w'T'} \tag{38}$$

$$0 = -2\overline{w'T'}\,\frac{\partial\bar{T}}{\partial z} - 2b\,\frac{q}{\Lambda}\overline{(T')^2} \tag{39}$$

In writing these equations, Λ_1 was taken equal to Λ.

EDDY TRANSPORT IN THE ATMOSPHERE

It is instructive to carry out the solution of equations (33) to (39). These equations are algebraic for all the nonzero correlations. The solution of equations (33) to (39) can be obtained if the following definitions are introduced: Let (for $\partial\bar{u}/\partial z > 0$)

$$\left.\begin{aligned}
\overline{u'u'} &= UU\Lambda_1^2\left(\frac{\partial\bar{u}}{\partial z}\right)^2 & \overline{u'T'} &= UT\Lambda_1^2\,\frac{\partial\bar{u}}{\partial z}\,\frac{\partial\bar{T}}{\partial z}\\
\overline{v'v'} &= VV\Lambda_1^2\left(\frac{\partial\bar{u}}{\partial z}\right)^2 & \overline{w'T'} &= WT\Lambda_1^2\,\frac{\partial\bar{u}}{\partial z}\,\frac{\partial\bar{T}}{\partial z}\\
\overline{w'w'} &= WW\Lambda_1^2\left(\frac{\partial\bar{u}}{\partial z}\right)^2 & \overline{(T')^2} &= TT\Lambda_1^2\left(\frac{\partial\bar{T}}{\partial z}\right)^2\\
\overline{u'w'} &= UW\Lambda_1^2\left(\frac{\partial\bar{u}}{\partial z}\right)^2 & q^2 &= QQ\Lambda_1^2\left(\frac{\partial\bar{u}}{\partial z}\right)^2
\end{aligned}\right\} \tag{40}$$

and note that

$$QQ = Q^2 = UU + VV + WW \tag{41}$$

Substitution of the definitions given in equations (40) and (41) into equations (33) to (39) results in

$$Q(1 + 2b)UU = \frac{Q^3}{3} - 2UW \tag{42}$$

$$Q(1 + 2b)VV = \frac{Q^3}{3} \tag{43}$$

$$Q(1 + 2b)UW = -WW + N_{Ri}UT \tag{44}$$

$$Q(1 + 2b)UT = -UW - WT \tag{45}$$

$$Q(1 + 2b)WT = -WW + N_{Ri}TT \tag{46}$$

$$Q(2b)TT = -WT \tag{47}$$

In these equations, N_{Ri} is the Richardson number given by

$$N_{Ri} = \frac{\frac{g}{T_o}\frac{\partial \overline{T}}{\partial z}}{\left(\frac{\partial \overline{u}}{\partial z}\right)^2} \tag{48}$$

It is immediately obvious from equations (42) to (47) that all the nondimensional second-order correlations are a function only of the Richardson number and the parameter b from the second-order closure model. It will be remembered that the value of b determined in the parameter search reported previously is 0.125.

It is convenient to express the solution of equations (42) to (47) in terms of the parameter

$$P = \frac{1 - (4 + 15b)N_{Ri} + \left[1 + 2(2 - 9b)N_{Ri} + (4 + 9b)^2\left(N_{Ri}\right)^2\right]^{1/2}}{6} \tag{49}$$

In terms of this parameter, the various correlations may be written

$$Q^2 = \frac{1}{b(1 + 2b)^2} P \tag{50}$$

$$UU = \frac{\left(P + bN_{Ri}\right)\left[P + (1 + 4b)N_{Ri}\right] + 2b\left[P + (1 + b)N_{Ri}\right]}{3(1 + 2b)\left(P + bN_{Ri}\right)\left[P + (1 + 4b)N_{Ri}\right]} Q^2 \tag{51}$$

$$VV = \frac{1}{3(1 + 2b)} Q^2 \tag{52}$$

$$WW = \frac{P + (1 + 2b)N_{Ri}}{3(1 + 2b)\left[P + (1 + 4b)N_{Ri}\right]} Q^2 \tag{53}$$

$$UW = -\frac{b}{3} \frac{P + (1 + b)N_{Ri}}{\left(P + bN_{Ri}\right)\left[P + (1 + 4b)N_{Ri}\right]} Q^3 \tag{54}$$

$$UT = \frac{b}{3(1 + 2b)} \frac{2P + (1 + 2b)N_{Ri}}{\left(P + bN_{Ri}\right)\left[P + (1 + 4b)N_{Ri}\right]} Q^2 \tag{55}$$

$$WT = -\frac{b}{3\left[P + (1 + 4b)N_{Ri}\right]} Q^3 \tag{56}$$

$$TT = \frac{1}{3\left[P + (1 + 4b)N_{Ri}\right]} Q^2 \tag{57}$$

It is clear from these equations that when the parameter $P = 0$, there is no turbulence $\left(Q^2 = 0\right)$ and all the second-order correlations vanish. The critical value of the Richardson number for which this occurs is a function of b and is given by

$$\left(N_{Ri}\right)_{crit} = \frac{1 + b}{4b(1 + 3b)} \tag{58}$$

For $b = 0.125$, the critical Richardson number is

$$\left(N_{Ri}\right)_{crit} = 1.636 \tag{59}$$

All the nondimensional second-order correlations as functions of the Richardson number are plotted in figures 1 to 5. From these figures, the profound difference between turbulence and turbulent transport in stable and unstable atmospheres is obvious. Note particularly that the nondimensional vertical transport of matter and heat falls off far more rapidly than do the nondimensional turbulent energy components when a stable atmospheric situation is approached. In fact, above a Richardson number of 1, vertical turbulent transport has almost ceased to exist although there is still some atmospheric turbulence.

It should be noted that the superequilibrium results just obtained specify the non-dimensional values of second-order correlations. For example, if the value of $b = 0.125$ is assumed to be correct, a Richardson number of 0.10 would give

$$UW = -0.2712 \tag{60}$$

$$WT = -0.2631 \tag{61}$$

The transports of momentum and heat would then be given by (for $\partial\bar{u}/\partial z > 0$)

$$-\rho_o\overline{u'w'} = 0.2712\rho_o\Lambda^2\left(\frac{\partial\bar{u}}{\partial z}\right)^2 \tag{62}$$

$$-\rho_o(c_p)_o\overline{w'T'} = 0.2631\rho_o\Lambda^2\frac{\partial\bar{u}}{\partial z}\frac{\partial\overline{T}}{\partial z} \tag{63}$$

It is clear from these expressions that the actual transport is not defined until the length scale Λ is known. This is a difficulty with atmospheric flows, for unless Λ is determined at a given altitude and the local Richardson number specified there, the transports are not known. In general, Λ will depend at a given altitude on the Richardson number but can assume a range of values depending on the past history of the motion. Although this range of values is limited so that the order of magnitude of the transport might be determined, there will always be a variation in transport proportional to the square of the variation in Λ at any fixed Richardson number.

For classical laboratory flows, this problem does not exist. In this case, it is generally found that Λ is proportional to the characteristic breadth of the layer under consideration while the gradients are proportional to a characteristic velocity, temperature, or concentration difference divided by this characteristic breadth. Thus, for the classical shear flows,

$$\Lambda_1^2\left(\frac{\partial\bar{u}}{\partial z}\right)^2 = \delta_{char}^2\left(\frac{\Delta\bar{u}_{char}}{\delta_{char}}\right)^2 = \text{Const}\left(\Delta\bar{u}_{char}\right)^2 \tag{64}$$

and, likewise,

$$\Lambda_1^2\frac{\partial\bar{u}}{\partial z}\frac{\partial\overline{T}}{\partial z} = \text{Const}\ \Delta\bar{u}_{char}\ \Delta\overline{T}_{char} \tag{65}$$

For each type of flow, these constants are well defined. This type of simplicity is, alas, not true of the atmosphere.

It is instructive to compare the results of superequilibrium theory with certain well-known results from classical turbulent-transport theory for the case when no gravitational effects are involved. To do this, the Richardson number is placed equal to zero in the expressions given in equations (49) to (57), and for $b = 0.125$, the following expressions are obtained:

$$P = 0.3333 \tag{66}$$

$$Q^2 = \frac{1}{3b(1 + 2b)^2} = 1.7066 \tag{67}$$

$$UU = \frac{1 + 6b}{9b(1 + 2b)^3} = 0.7964 \tag{68}$$

$$VV = WW = \frac{1}{9b(1 + 2b)^3} = 0.4551 \tag{69}$$

$$UW = TW = -\frac{\sqrt{3/b}}{9(1 + 2b)^3} = -0.2786 \tag{70}$$

$$UT = \frac{2}{3(1 + 2b)^3} = 0.3413 \tag{71}$$

$$TT = \frac{1}{3b(1 + 2b)^2} = 1.7066 \tag{72}$$

Some interesting results are noted from the above comparison. First, superequilibrium theory indicates that $\overline{v'v'} = \overline{w'w'}$ and, further, that

$$\frac{\overline{u'u'}}{\overline{v'v'}} = \frac{\overline{u'u'}}{\overline{w'w'}} = \frac{UU}{VV} = \frac{UU}{WW} = 1 + 6b = 1.75 \tag{73}$$

Second, the value of $-\overline{u'w'}/q^2$, which Bradshaw, Ferriss, and Atwell (ref. 3) assume to be a constant equal to 0.15, is defined by superequilibrium theory to be

$$-\frac{UW}{q^2} = \frac{1}{1 + 2b}\sqrt{b/3} = 0.163 \tag{74}$$

This is a rather surprisingly accurate result in view of the fact that the value of b was determined from very different considerations in the development of the second-order closure model.

The value of Von Kármán's constant κ in his expression for the turbulent shear near a surface may also be derived from superequilibrium theory:

$$\tau_t = -\rho\overline{u'w'} = \rho\kappa^2 z^2\left(\frac{\partial\overline{u}}{\partial z}\right)^2 \tag{75}$$

From the present results,

$$\tau_t = -\rho UW\Lambda_1^2\left(\frac{\partial\overline{u}}{\partial z}\right)^2 = \frac{\sqrt{3/b}}{9(1+2b)^3}\rho\Lambda_1^2\left(\frac{\partial\overline{u}}{\partial z}\right)^2 \tag{76}$$

In reference 1 it was found that near a surface, Λ is of the form $\Lambda = \alpha z$, where α in the parameter search is found to be 0.7. Letting

$$\Lambda = 0.7z \tag{77}$$

equation (76) gives

$$\tau_t = \frac{0.49\sqrt{3/b}}{9(1+2b)^3}\rho z^2\left(\frac{\partial\overline{u}}{\partial z}\right)^2 \tag{78}$$

Comparison of equations (75) and (78) reveals that

$$\kappa^2 = \frac{0.49\sqrt{3/b}}{9(1+2b)^3} = 0.137 \tag{79}$$

or

$$\kappa = 0.37 \tag{80}$$

The value of Von Kármán's constant is actually 0.4. Again, the agreement between results obtained by taking the equilibrium, nondiffusive limit of the present second-order closure model of turbulent shear flow and the classical mixing-length theory is rather remarkable.

EDDY TRANSPORT IN A VORTEX?

If a scheme such as that pursued in the previous section for the superequilibrium equation for a line vortex is followed, the following definitions are introduced into equations (29) to (32):

$$\overline{u'w'} = UU\Lambda^2\left(\frac{\partial\overline{v}}{\partial r} - \frac{\overline{v}}{r}\right)^2 \tag{81}$$

$$\overline{v'v'} = VV\Lambda^2\left(\frac{\partial\overline{v}}{\partial r} - \frac{\overline{v}}{r}\right)^2 \tag{82}$$

$$\overline{w'w'} = WW\Lambda^2\left(\frac{\partial\overline{v}}{\partial r} - \frac{\overline{v}}{r}\right)^2 \tag{83}$$

$$\overline{u'v'} = UV\Lambda^2\left|\frac{\partial\overline{v}}{\partial r} - \frac{\overline{v}}{r}\right|\left(\frac{\partial\overline{v}}{\partial r} - \frac{\overline{v}}{r}\right) \tag{84}$$

$$q = Q\Lambda\left|\frac{\partial\overline{v}}{\partial r} - \frac{\overline{v}}{r}\right| \tag{85}$$

From this substitution, the following equations are obtained:

$$Q(1 + 2b)UU = \frac{Q^3}{3} + 4UVN \tag{86}$$

$$Q(1 + 2b)VV = \frac{Q^3}{3} - 2UV - 4UVN \tag{87}$$

$$Q(1 + 2b)WW = \frac{Q^3}{3} \tag{88}$$

$$Q(1 + 2b)UV = -UU + 2(VV - UU)N \tag{89}$$

In these equations N is a stability number defined as

$$N = \frac{\overline{v}/r}{\frac{\partial\overline{v}}{\partial r} - \frac{\overline{v}}{r}} \tag{90}$$

The solution of equations (86) to (89) in terms of the parameters b and N is

$$UU = \frac{Q^2}{1 + 2b}\left(\frac{1}{3} - 4bN\right) \tag{91}$$

$$VV = \frac{Q^2}{1 + 2b}\left(\frac{1}{3} + 2b + 4bN\right) \tag{92}$$

$$WW = \frac{Q^2}{3(1 + 2b)} \tag{93}$$

$$UV = -bQ^3 \tag{94}$$

with

$$Q^2 = UU + VV + WW = \frac{1}{b(1+2b)^2}\left(\frac{1}{3} - 8bN - 16bN^2\right) \tag{95}$$

It is clear, since Q^2 is positive definite, that under the assumptions made here turbulence is impossible if

$$N < -\frac{1}{4}\left(1 + \sqrt{1 + \frac{1}{3b}}\right) \tag{96}$$

or if

$$N > \frac{1}{4}\left(\sqrt{1 + \frac{1}{3b}} - 1\right) \tag{97}$$

For the value of b used herein (0.125), these limits become $N < -0.729$ and $N > 0.229$.

Figure 6 shows the behavior of the quantities UU, VV, WW, UV, and Q^2 with variations of the stability parameter N for $b = 0.125$. The results are plotted in terms of the ratios of the quantities to their values for $N = 0$, namely, $(UU)_O$, $(VV)_O$, and so forth. Thus, figure 6 shows the ratios of $\overline{u'u'}$, $\overline{v'v'}$, $\overline{w'w'}$, $\overline{u'v'}$, and q^2 in a vortex to these quantities in a parallel shearing motion having the same mean deformation rate and scale.

It may be seen from figure 6 that the turbulent energy and shear have the same value for $N = -1/2$ as they do for $N = 0$. Between $N = -1/2$ and $N = 0$, the turbulent energy and shear are larger than they are in a parallel shearing motion. For $N < -0.729$ and $N > 0.229$, as mentioned previously, no locally sustained turbulent flow is possible. Thus, for $-0.729 < N < -0.5$, locally self-sustained turbulence is possible, although the turbulence is damped by centrifugal effects. For $0 < N < 0.229$, turbulence is also possible, but here again it is damped by the action of centrifugal forces.

What sort of flows does each of these regions represent? First, note that when $\partial\overline{v}/\partial r = 0$, $N = -1$. Thus at the core radius of a vortex (defined here as the radius where $\partial\overline{v}/\partial r = 0$), a turbulent vortex is stable. Near the center of a free vortex, the tangential velocity $\overline{v}$ is of the form $\overline{v} = mr - 2nr^2$ so that as $r \to 0$, $N \to -\infty$. Also, for a free vortex, $\overline{v} \to \Gamma/2\pi r$ as $r \to \infty$ and one finds then that as $r \to \infty$, $N \to -1/2$. Thus for the classical vortex distribution,

$$\overline{v} = \frac{\Gamma}{2\pi r}\left(1 - e^{-r^2/4\nu t}\right) \tag{98}$$

The flow in the outer regions of the vortex exhibits an eddy diffusivity similar to a parallel flow. As the core of the vortex is approached, the flow becomes more and more stable. It becomes completely stable somewhat outside the core of the vortex. Indeed, the flow is stable at the point of maximum deformation $\frac{\partial \overline{v}}{\partial r} - \frac{\overline{v}}{r}$. This behavior of the stability parameter N for the classical vortex is shown in figure 7.

The region of increased turbulence and shear between $N = -1/2$ and $N = 0$ can be understood if it is noted that the stability parameter may be written

$$N = \frac{\overline{v}/r}{\frac{1}{2\pi}\frac{\partial \Gamma}{\partial r} - \frac{2\overline{v}}{r}} \tag{99}$$

Thus the region $-1/2 < N < 0$ represents flows for which $d\Gamma/dr$ is negative. These are, of course, flows which exhibit the well-known Taylor instability (ref. 4).

The region $0 < N < 0.229$ is representative of flows occurring between two cylinders rotating in the same direction, so that Γ at the outer cylinder is larger than Γ at the inner cylinder when the centrifugal forces due to the general level rotation cannot completely stabilize the flow.

For a free vortex, it may be surmised from this analysis that the core regions of vortices are locally stable. Regions outside the core are unstable and can generate turbulence. If the core regions of vortices are to exhibit a turbulent shear, this must be caused by turbulence which has diffused into the core region from outer regions which are unstable or by turbulence which has been generated by a shear in the axial direction that is not considered in this analysis. This fact, namely, that the turbulent shear $-\rho\overline{u'v}$ in a vortex is not directly related to the local deformation $\frac{\partial \overline{v}}{\partial r} - \frac{\overline{v}}{r}$, would lead one to believe that it would be impossible to establish any general rules for determining an eddy viscosity for a vortex. To calculate such flows reliably, it will probably be necessary to use the full power of second-order closure methods.

It might be noted, in this connection, that if one were to use an energy method on such flows, much of the physics of the problem would be lost. This may be seen by considering the sum of equations (86) to (89) with $UU = VV$ as the governing equation of the flow. In this case, the parameter N disappears from the equations and the essential physics of the problem have been lost.

CONCLUDING REMARKS

This short paper has tried to exhibit the relationship between a full second-order closure model for turbulent flow and the older eddy-viscosity models of such flows. It has been shown that classical eddy-transport theory can be obtained from a consideration of the equilibrium, nondiffusive, high Reynolds number limit of the equations of a second-order closure model.

The nature of such limits has been discussed for the flow in sheared stratified media and for a line vortex. The limitations of an eddy-transport model of turbulence in a line vortex have been discussed through the use of the equations derived by the limiting process described herein.

REFERENCES

1. Donaldson, Coleman duP.: A Progress Report on an Attempt To Construct an Invariant Model of Turbulent Shear Flows. Turbulent Shear Flows, AGARD-CP-93, Jan. 1972, pp. B-1 – B-24.

2. Donaldson, Coleman duP.: Construction of a Dynamic Model of the Production of Atmospheric Turbulence and the Dispersal of Atmospheric Pollutants. Rep. No. 175, Aeronaut. Res. Assoc. Princeton, Inc., June 1972.

3. Bradshaw, P.; Ferriss, D. H.; and Atwell, N. P.: Calculation of Boundary-Layer Development Using the Turbulent Energy Equation. J. Fluid Mech., vol. 28, pt. 3, May 26, 1967, pp. 593-616.

4. Taylor, G. I.: Stability of Viscous Liquid Contained Between Two Rotating Cylinders. Phil. Trans. Roy. Soc. (London), vol. 223, Feb. 8, 1923, pp. 289-343.

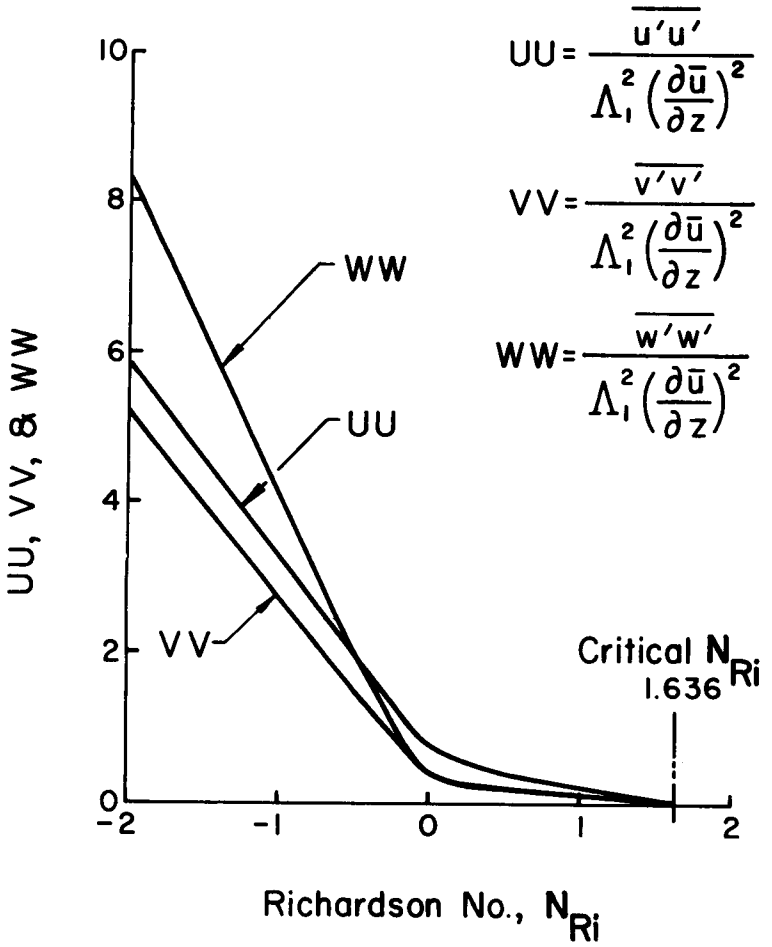

Figure 1.- Superequilibrium values of the turbulence components as a function of the Richardson number for b = 0.125.

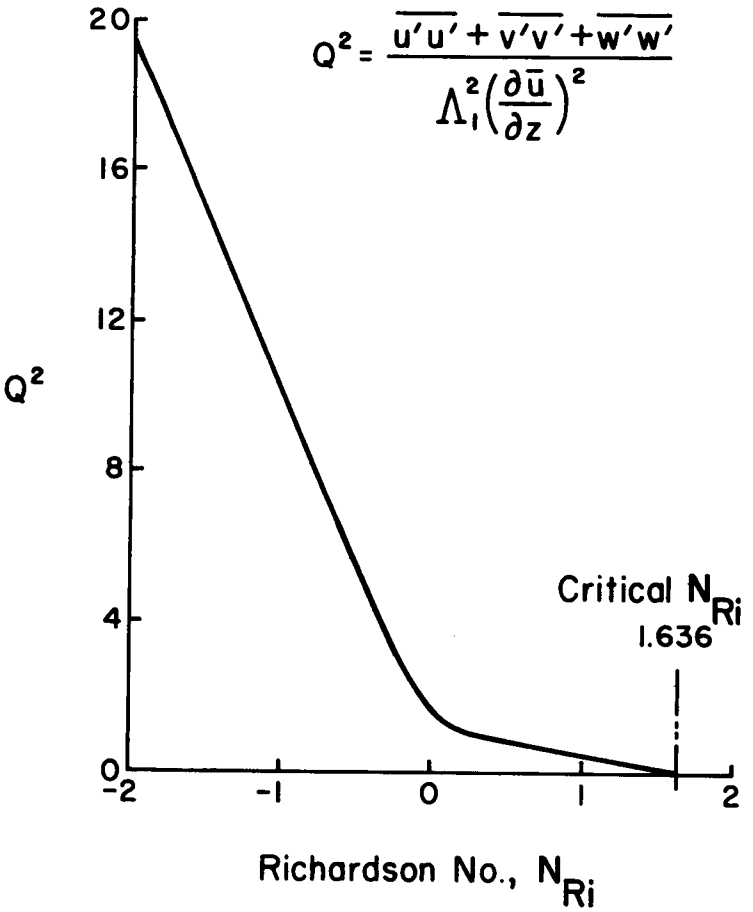

Figure 2.- Superequilibrium value of the sum of the squares of the turbulent velocity fluctuations as a function of the Richardson number for b = 0.125.

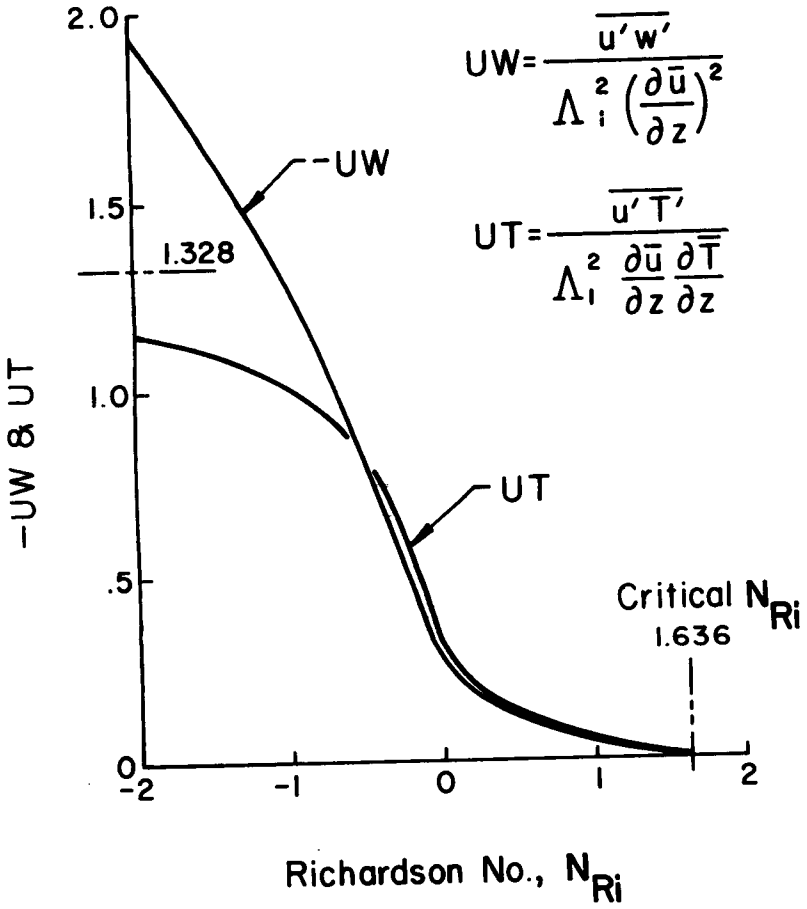

Figure 3.- Superequilibrium values for shear and longitudinal heat- and mass-transfer correlations as functions of the Richardson number for b = 0.125. Note that UT approaches the value 1.328 for $N_{Ri} = -\infty$.

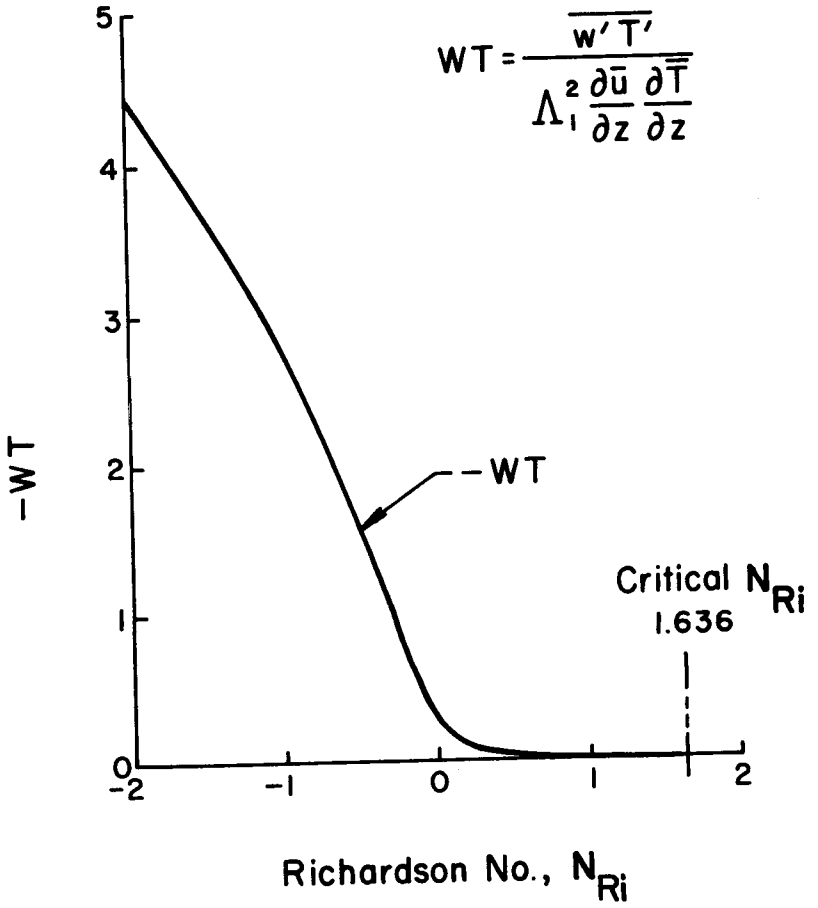

Figure 4.- Superequilibrium values for vertical heat-transfer correlation as a function of the Richardson number for b = 0.125.

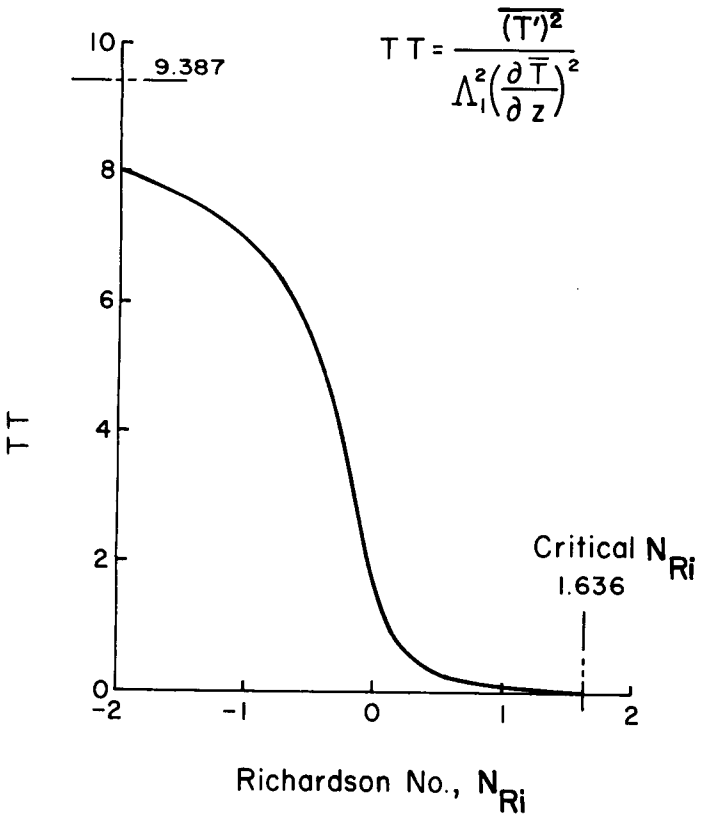

Figure 5.- Superequilibrium values for TT as a function of the Richardson number for b = 0.125. Note that this function approaches the limit 9.387 for $N_{Ri} = -\infty$.

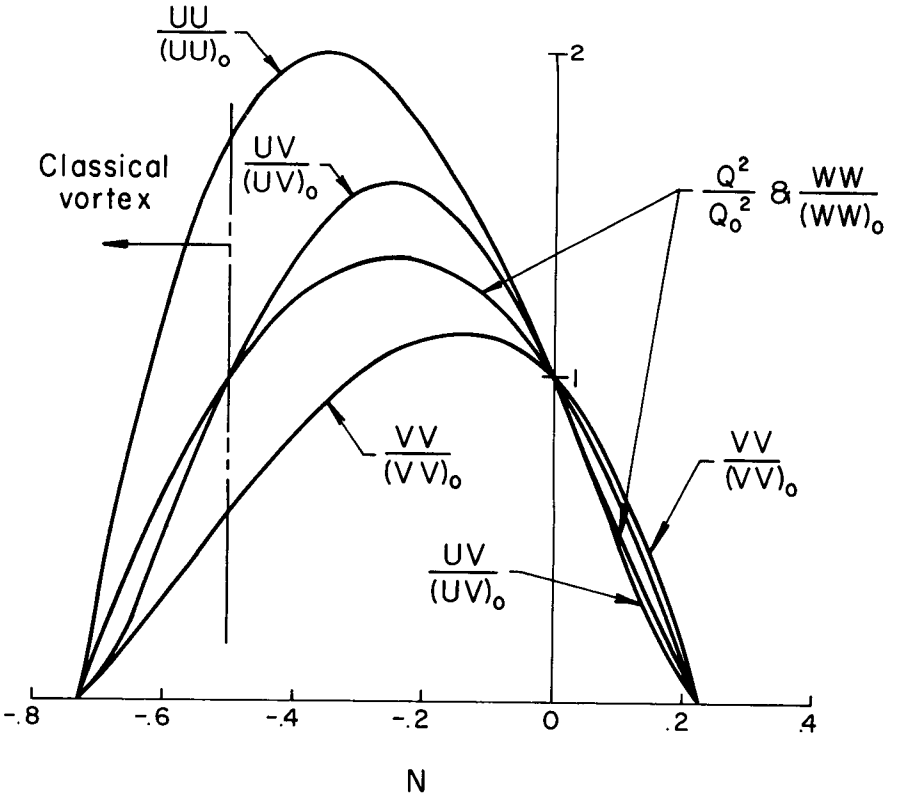

Figure 6.- Behavior of UU, VV, WW, Q^2, and UV as functions of the stability parameter N for b = 0.125.

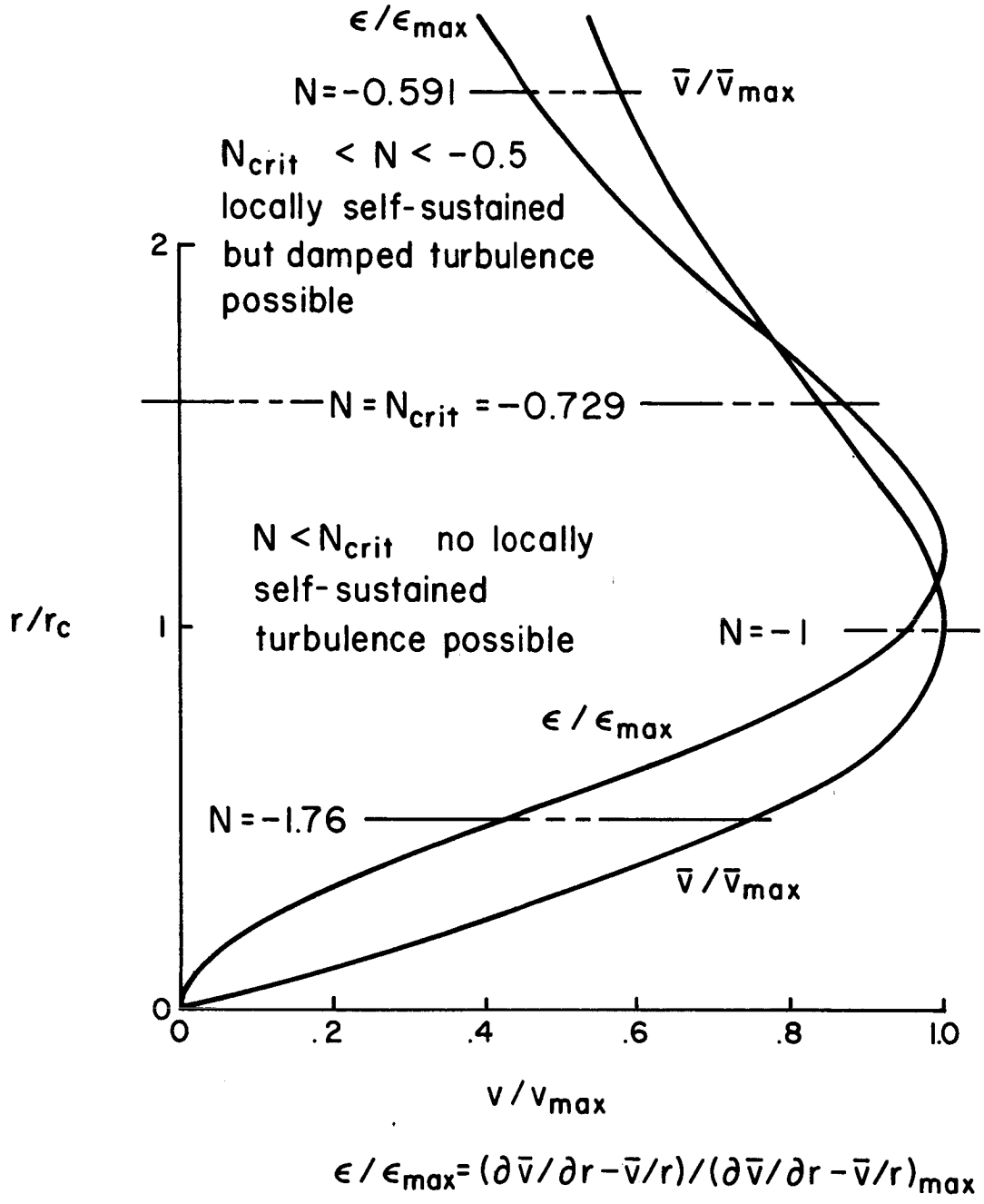

Figure 7.- Behavior of the stability parameter N for a classical line vortex (see eq. (98)).

DISCUSSION

G. L. Mellor: We just finished an experiment at Princeton a year or so ago which is a boundary layer on a flat wall followed by a curved wall and we did a complete set of turbulent measurements. It was very dramatic indeed; we could see the turbulence nearly shut off on the convex side of the wall. And then we did try to develop an expression for the eddy viscosity by balancing production with dissipation using these equations. You can, as you did, find a correction for the eddy viscosity in terms of the proper curvature parameter and it works very well. So I'll just put in two cents here that it seems to work well and it seems to compare with the rather dramatic measurements that we've developed in the last couple of years.

C. duP. Donaldson: One of the points to be made here is that if you are going to do some trick flow like this, it is best not to shortcut and just use, say, the energy and stress equations with some trick for guessing what is missing because you may overlook the physics of the problem. If you use all the equations, you get the physics right.

S. I. Pai: I notice that you assume the mixing lengths for velocity and for temperature are the same. My questions are (1) Do you make this assumption to simplify the analysis and to obtain some essential features of this problem? and (2) If these mixing lengths are different, would you expect that your results would be modified considerably?

C. duP. Donaldson: Yes, the same lengths were chosen to simplify the analysis. In this case, which is the superequilibrium limit, you will begin to see the nature of the problem. No matter what you choose for your eddy-viscosity model, if you want to see whether you should really use such a model or not, you can make this kind of limiting argument. It is true that if you have vastly different scales of the temperature and velocity fields, you are going to have to do something different. As an example, take a large turbulent pipe flow in which you know all the pertinent mean quantities, and with the turbulence model you have, compute all the turbulent characteristics in this flow. Then, if you assume a tiny pencil of heated air is placed in the center of the tube so as to form a very thin hot jet in that region and you use the same scale in the $\overline{u_i'T'}$ and $\overline{(T')^2}$ equations as you use in the $\overline{u_i'u_k'}$ equation, you will find a remarkable result. The general spread of the hot material is about as it should be, but a hot spot stays near the center of the tube. This is a result of using the wrong scale in the $\overline{u'T'}$ and $\overline{(T')^2}$ equations. When the scales of the mean temperature and mean velocity fields are so disparate, one may not use the same scales in the equations for the various second-order correlations.

S. C. Lee: I have two questions. First, I haven't seen any of your models compared with the suggested cases. My question is, have you compared any, and if you did, would we be able to see any of your comparisons?

C. duP. Donaldson: The only comparisons made to date were for the cases which were used to construct the model. In these cases, model parameter searches were made to try to obtain a best fit to the existing data for a free jet, a two-dimensional shear layer, and a flat-plate boundary layer. The model was determined to be that one that gave the best fit to all three cases.

I think I should point out here something that I've said ever since I started making such calculations; namely, it's pretty hard to calculate better at first blush something that somebody has been calculating empirically for the last 20 years. That really wasn't my reason for getting into these second-order closure methods – my real reason was to get at the calculation of some problem which just can't be done by conventional methods and for which you just don't known what the answer is at all, such as the vortex and the behavior of turbulence in stratified media.

S. C. Lee: My second question is related to your particular model with which you are interested in atmospheric conditions for stable and unstable atmospheric conditions. Have you calculated any of those?

C. duP. Donaldson: Yes.

S. C. Lee: Would those be in the paper?

C. duP. Donaldson: Not in the paper to be published in these proceedings. Some results have been published elsewhere. I have just finished writing a paper which is to be mailed out soon to many of the people at this meeting. I think you are on the list.

S. Corrsin: You have identified one necessary condition for the use of an eddy-viscosity model and you of course know that also there is another kind of necessary condition; that is, the characteristics length of the mechanism transporting the property you are interested in must be very small compared with any distance over which the mean property changes appreciably and this is violated by almost all flows that we ever talk about. So there is quite a different class of reasons why eddy-viscosity models may be wrong in principle but work in practice.

C. duP. Donaldson: I understand – valid comment.

G. L. Mellor: I ask Stan, who states this necessary condition – I know it has something to do with kinetic theory but who states it for turbulent?

S. Corrsin: Well as far as ordinary transport models go there's a book on Transport by a fellow named Bosworth[1] that was published in the 1940's which is the only textbook I have seen that actually mentions it. But as far as turbulence phenomena go, in general the gradient transport term is the first term in an infinite-series approximation and this is

[1] Bosworth, Richard Charles Leslie: Heat Transfer Phenomena – The Flow of Heat in Physical Systems. John Wiley & Sons, Inc., [1952].

why, for instance, the Prandtl modified-mixing-length theory with the second-order term could be better. In fact, if your computers get big enough, it may be better to just put on higher and higher derivatives in an attempt to make something which is physically meaningful as well as computable.

C. duP. Donaldson: Yes, that's certainly true for those cases that you can do like that. When, indeed, the flow is completely stable in the superequilibrium sense in the region where the deformations are largest, you can't do that.

FREE TURBULENT MIXING IN A COFLOWING STREAM*

By Joseph A. Schetz
Virginia Polytechnic Institute and State University

DEVELOPMENT OF THE MODEL

The turbulent transport model used here is of the classical, gradient transport, eddy viscosity type; that is, it is based upon

$$\tau = \rho\epsilon \frac{\partial U}{\partial y} \tag{1}$$

where ϵ is to be expressed in terms of mean flow quantities. (Symbols are defined at the end of the text.) Thus, no turbulence information is used in the functional expression for the eddy viscosity; however, recent work in extending the model has employed turbulence information in the proportionality constant. This work will be discussed further in a later section. The development of the model is described in references 1 to 4, but a short summary of the major points is included here for convenience.

This work grew out of an inquiry into the relation, if any, between various more or less successful eddy viscosity models, each developed for a different flow situation. Consider the following three planar examples:

Prandtl (jet mixing) model (ref. 5)

$$\epsilon_1 = 0.037 b_{1/2} \left| U_{max} - U_{min} \right| \tag{2}$$

Schlichting (wake) model (ref. 6)

$$\epsilon_2 = 0.022 C_D D U_e \tag{3}$$

Clauser (boundary-layer) model (ref. 7)

$$\epsilon_3 = 0.018 U_e \delta^* \tag{4}$$

These apparently bear no direct relation to each other, even though they are all intended to model rather similar flow problems. It is very useful to examine the Schlichting wake model more closely. First,

$$C_D D \equiv 2\theta \tag{5}$$

*This work was supported in part by the Hypersonic Propulsion Branch, Langley Research Center, NASA.

so that equation (3) becomes

$$\epsilon_2 = 0.044 U_e \theta \tag{6}$$

Now, equations (4) and (6) appear in actual contradiction, but this discrepancy quickly vanishes when it is observed that Schlichting used a linearized "far wake" analysis in developing his model, where the integrand in the momentum thickness θ was approximated as

$$\frac{U}{U_e}\left(1 - \frac{U}{U_e}\right) \approx 1 - \frac{U}{U_e} \tag{7}$$

which makes it the same as that for the displacement thickness δ^*. Thus, the Clauser boundary-layer model and the Schlichting wake model, in reality, differ only in the value of the proportionality constant. This too can be explained, as will be shown later.

A study of the Prandtl jet model in relation to the Clauser model showed that they could not be reduced to the same functional form. However, a simple numerical exercise demonstrates that the actual values of ϵ predicted by each model for a series of reasonable profile shapes (variation of U with y) are virtually identical. This comparison requires a generalization of the Clauser model to let the displacement thickness measure a mass-flow excess with respect to the free stream as well as the more usual mass-flow defect. Also, since a wake or jet has two sides to the mixing layer as opposed to a one-sided boundary layer, the Clauser model must be written as

$$\epsilon_3 = 0.036 U_e \int_0^\infty \left| 1 - \frac{U}{U_e} \right| dy \tag{8}$$

This model will provide good predictions of the development of planar, constant-density flows of either the wake type (see test case 14 below) or jet type (see ref. 4).

At this early point in the development, it remained to extend the model in equation (8) to axisymmetric and/or variable-density cases. The constant-density axisymmetric case was considered first. The model for this geometry was obtained by introducing a new, physical interpretation of the Clauser model (applicable to either its original form, eq. (4), or its extended form, eq. (8)). This interpretation is stated, "The turbulent viscosity $\rho\epsilon$ is proportional to the mass flow defect (or excess) per unit width of the mixing region." This can be carried over to the axisymmetric situation as

$$\rho\epsilon_4 = \frac{K\rho_e U_e}{L} \int_0^\infty \left| 1 - \frac{U}{U_e} \right| 2\pi r \, dr \tag{9}$$

where L is some characteristic width required to be dimensionally correct. Note that the unit width of the planar case does not appear here. Some studies were made to determine a suitable width for this use. The obvious choice of the local half-radius $r_{1/2}$ was

found to be unsuitable for all but jet cases with $U_j/U_e \gg 1$. Since such cases are of marginal practical interest, this choice was rejected, and the simple choice of the initial radius a was made. For wakes, $r_{1/2}(0)$, the half-radius at the "initial" station at the end of the "near wake," is used.

It was still necessary to determine the constant K for use in equation (9). It should be emphasized here that a useful turbulent exchange model must contain fixed empirical constants that are determined once and then are not changed from problem to problem! In the present case, this was accomplished by considering the experimental case of Forstall and Shapiro (ref. 8) with $U_j/U_e = 2.0$. The prediction using $K\pi = 0.018$ (the apparent correspondence to Clauser's constant in eq. (4) is pure coincidence) is compared with experiment in figure 1, where the excellent agreement can be noted. This constant has been adopted as universal for use with this model and has not been changed for comparisons with any other experimental case. Two points are worth noting from figure 1. First, a variation in the constant does not change the slope of the predicted velocity decay, it merely moves the curve up and down on the paper. Thus, the correct decay rate predicted is due solely to the functional form of the model. Second, the straightforward extension of Prandtl's planar model, equation (2), to the axisymmetric case

$$\epsilon_5 = 0.025 r_{1/2} \left| U_{max} - U_{min} \right| \tag{10}$$

gives a poor prediction.

The extension of the unified model, equation (8) for planar and equation (9) for axisymmetric cases, to variable-density situations was accomplished by simply using the appropriate definition for the mass-flow defect (or excess). Thus, the final model is:

Planar

$$\rho\epsilon = 0.036\rho_e U_e \int_0^\infty \left| 1 - \frac{\rho U}{\rho_e U_e} \right| dy \tag{11}$$

Axisymmetric

$$\rho\epsilon = \frac{0.018\rho_e U_e}{a} \int_0^\infty \left| 1 - \frac{\rho U}{\rho_e U_e} \right| 2r\, dr \tag{12}$$

This is at variance with the suggestions of some workers in the boundary-layer field, who have used a "kinematic displacement thickness" based on $1 - \frac{U}{U_e}$ for variable-density cases in trying to extend Clauser's basic model to such situations. It will be shown below that such a choice is clearly inappropriate for at least free-mixing problems.

TEST CASES

Calculations were run for test cases 9, 10, 11, 12, 14, 15, 16, and 17, using equation (11) or (12) as appropriate to the particular problem. The equations of motion were solved numerically by using an explicit finite-difference scheme in von Mises (x,ψ) coordinates. The actual computer routine used is a modification of that developed in reference 9. The program is written in FORTRAN II, and the total execution time on an IBM 370/155 for the compressible, two-dimensional wake case (test case 16) was 1 minute, 8 seconds, as an example. Two-dimensional shear layers (test cases 1 to 5) and jets in still air (test cases 6 to 8) were excluded since the concept of a mass-flow defect (or excess) with respect to some "free stream" is unclear for such situations.

The results for the Forstall and Shapiro jet with $U_j/U_e = 4.0$ (test case 9) are shown in figure 2. The rate of decay of the center-line velocity is not as accurately predicted here as for the same experiment with $U_j/U_e = 2.0$ shown in figure 1. The agreement is greatly improved for this case, as well as for all cases with $U_j/U_e \gg 1$, by using $L = r_{1/2}$ in equation (9), but the predictions at the lower, more useful, values of U_j/U_e are worsened.

The hydrogen-air jet of Chriss (test case 10) is considered in figures 3, 4, and 5. The predictions of center-line values of the velocity and hydrogen concentration are quite good, and the predicted profile shape is in good agreement with the data. This is strong support for the utility of the functional form of $\epsilon(y)$ as modeled in equation (12). It is also interesting to consider the use of δ_K^* rather than δ^* $\left(\text{that is, } 1 - \frac{U}{U_e} \text{ rather than } 1 - \frac{\rho U}{\rho_e U_e} \text{ in eq. (12)}\right)$ for this highly variable density problem. The results are shown as dashed curves in figures 3 and 4, where the use of δ_K^* gives much poorer agreement with the data.

The results for the air-air, compressible jet experiment of Eggers and Torrence (test case 11) are shown in figure 6. The calculations are started beyond the end of the "potential core," and the agreement with the data is good.

Results obtained from equation (12) by Eggers for his hydrogen-air jet problem (test case 12) are shown in figure 7. The decay rate of center-line quantities for this low mass-flux ratio $\left(\rho_j U_j/\rho_e U_e = 0.16\right)$ is considerably overestimated.

The low-speed wake cases of Chevray and Kovasznay (test case 14) and Chevray (test case 15) are plotted in figures 8 and 9. The adequacy of the model for such cases is clearly demonstrated by these results. Note that the same constants previously determined for a boundary layer in the planar model and for a jet in the axisymmetric model have been successfully used here for wakes.

The supersonic wake cases of Demetriades (test cases 16 and 17) are given in figures 10, 11, and 12. The planar wake case appears to be rather poorly predicted in figure 10, but it should be noted that the method of presenting the comparison, as dictated by the meeting organizers, is very sensitive to small inaccuracies in either the data or the prediction. A more conventional plot of the same results is shown in figure 11.

The agreement between prediction and data for the axisymmetric wake is good. The prediction in terms of W is given in figure 12. A conventional plot of these results is given in reference 4.

LIMITATIONS OF THE MODEL

It is worthwhile to summarize the limitations of this model as they can be discerned either from the derivation or from the results for the test cases and other experimental cases that have been considered in references 1 to 4.

First, the model makes no attempt to describe flows either in the "near wake" or in the potential core of a jet. Thus, it is always strictly necessary to start with some "initial" profile that is downstream of these regions. If the region of primary interest is long as measured in diameters, however, one can simply assume that the model applies in the potential core and accept the attendant inaccuracy in the near field.

Second, the results show that the accuracy of the predictions obtained, as compared with experimental data, deteriorates for $\left(\rho_j U_j/\rho_e U_e\right) \to \infty$ and $\left(\rho_j U_j/\rho_e U_e\right) \to 0$. The best results are obtained in the range $0.4 \leqq \left(\rho_j U_j/\rho_e U_e\right) \leqq 3.0$. Fortunately, essentially all wakes and most jets of practical interest fall in this range.

Finally, in all cases, even those where the overall prediction is good, the area of poorest agreement is in the near field downstream of the "initial" station. It is believed that this is due to the fact that the Clauser model, from which the models presented here are directly descended, was developed for a flow in dynamic "equilibrium." Clearly, the rapidly relaxing flows in the near field are not in such a state.

IMPORTANT PHENOMENA NOT COVERED BY THE TEST CASES

It is unfortunate that none of the wake cases selected as test cases were for the wake behind a bluff body such as a circular cylinder, since it has been known for some time that the proportionality constant in any eddy viscosity model must be increased above a value appropriate for jets or the wake behind a streamline body in order to obtain comparable agreement with the data. This question was examined in detail in reference 4, where it was found that the proportionality constant must be made a function of

the turbulence field in order to make a rational choice of an appropriate value. In the constant-density planar case, for example, it was shown that the proportionality constant in the extended Clauser model, equation (8), should be taken as

$$K \propto \frac{\overline{(U')^2}}{|U_c - U_e|^2} \tag{13}$$

A further interesting case which is not adequately handled by conventional eddy viscosity models is the wake behind a self-propelled body where the net momentum defect is zero.

SYMBOLS

a	initial jet radius
$b_{1/2}$	half-width
C_D	drag coefficient
D	diameter
K	constant
L	characteristic length
r	radial coordinate
$r_{1/2}$	half-radius
U	axial velocity
$\overline{(U')^2}$	time average of square of axial-velocity fluctuation
$W = 1 - \frac{U_c}{U_e}$	
X	axial coordinate
y	normal coordinate
α	mass fraction of hydrogen

δ^*	displacement thickness of boundary layer
δ^*_K	kinematic displacement thickness
ϵ	eddy viscosity
θ	momentum thickness of boundary layer
ρ	density
τ	shear stress

Subscripts:

c	center line
e	free stream
j	initial jet condition
max	maximum
min	minimum
1,2,3,4,5	different eddy viscosity models

REFERENCES

1. Schetz, J. A.; and Jannone, J.: Planar Free Turbulent Mixing With an Axial Pressure Gradient. Trans. ASME, Ser. D: J. Basic Eng., vol. 89, no. 4, Dec. 1967, pp. 707-714.

2. Schetz, Joseph A.: Turbulent Mixing of a Jet in a Coflowing Stream. AIAA J., vol. 6, no. 10, Oct. 1968, pp. 2008-2010.

3. Schetz, Joseph A.: Analysis of the Mixing and Combustion of Gaseous and Particle-Laden Jets in an Air Stream. AIAA Paper No. 69-33, Jan. 1969.

4. Schetz, Joseph A.: Some Studies of the Turbulent Wake Problem. Astronaut. Acta, vol. 16, no. 2, Feb. 1971, pp. 107-117.

5. Prandtl, L.: Notes on the Theory of Free Turbulence. Z. Angew. Math. Mech., Bd. 22, Nr. 5, Oct. 1942, pp. 241-243.

6. Schlichting, H.: Über das ebene Windschattenproblem. Ing.-Arch., Bd. 1, 1930, p. 567.

7. Clauser, Francis H.: The Turbulent Boundary Layer. Vol. IV of Advances in Applied Mechanics, H. L. Dryden and Th. von Kármán, eds., Academic Press, Inc., 1956, pp. 1-51.

8. Forstall, Walton, Jr.; and Shapiro Ascher H.: Momentum and Mass Transfer in Coaxial Gas Jets. J. Appl. Mech., vol. 17, no. 4, Dec. 1950, pp. 399-408.

9. Zeiberg, Seymour; and Bleich, Gary D.: Finite-Difference Calculation of Hypersonic Wakes. AIAA J., vol. 2, no. 8, Aug. 1964, pp. 1396-1402.

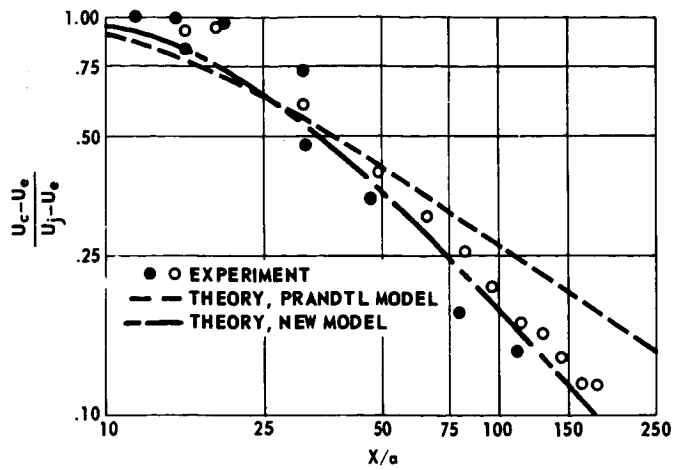

Figure 1.- Prediction and experiment for air-air jet of Forstall and Shapiro (ref. 8). $U_j/U_e = 2.0$.

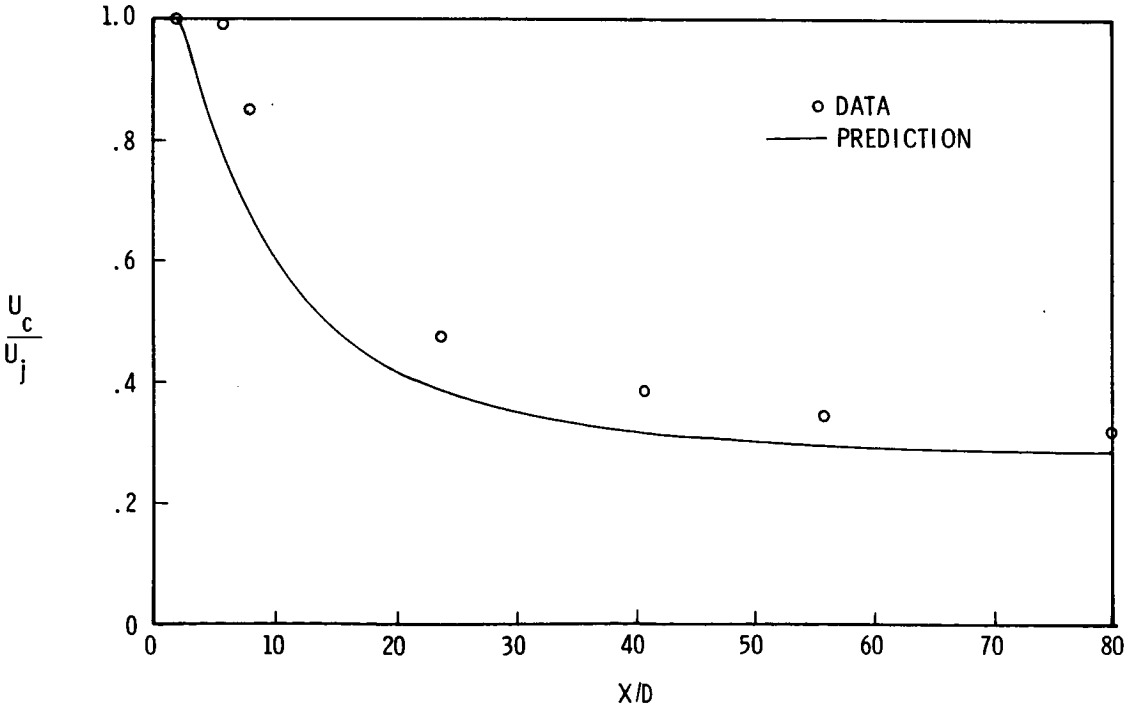

Figure 2.- Prediction and experiment for test case 9 (Forstall and Shapiro jet, $U_j/U_e = 4.0$).

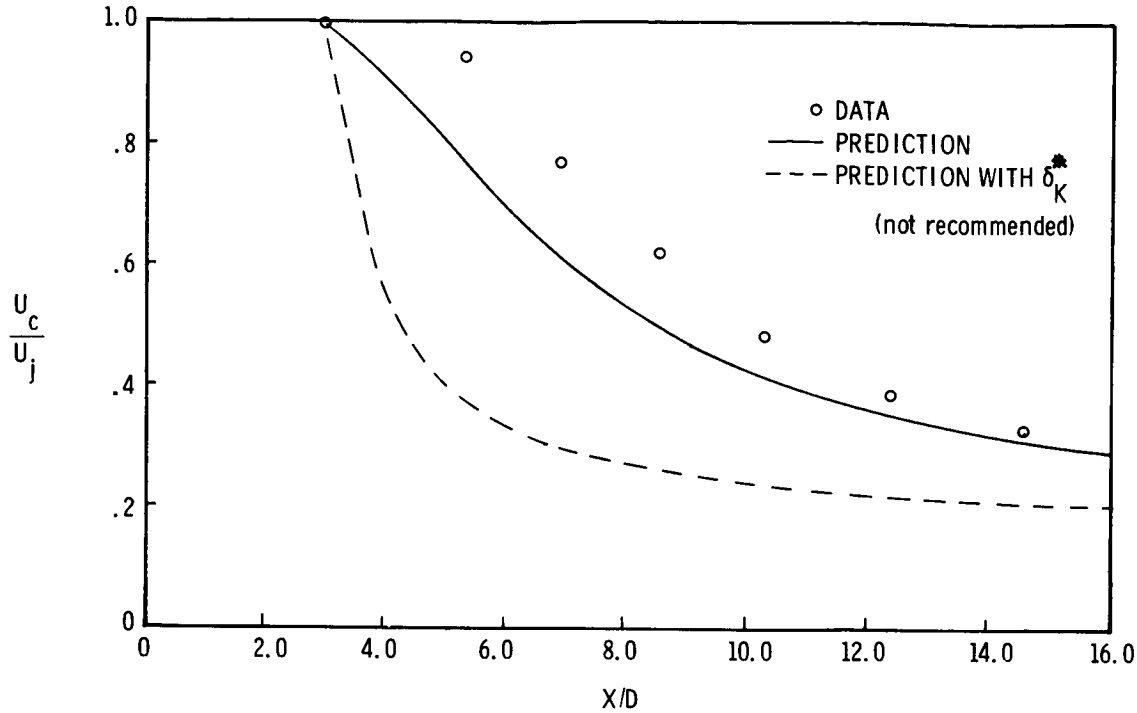

Figure 3.- Predicted and experimental center-line velocity for test case 10 (Chriss hydrogen-air jet, $\rho_j U_j / \rho_e U_e = 0.56$).

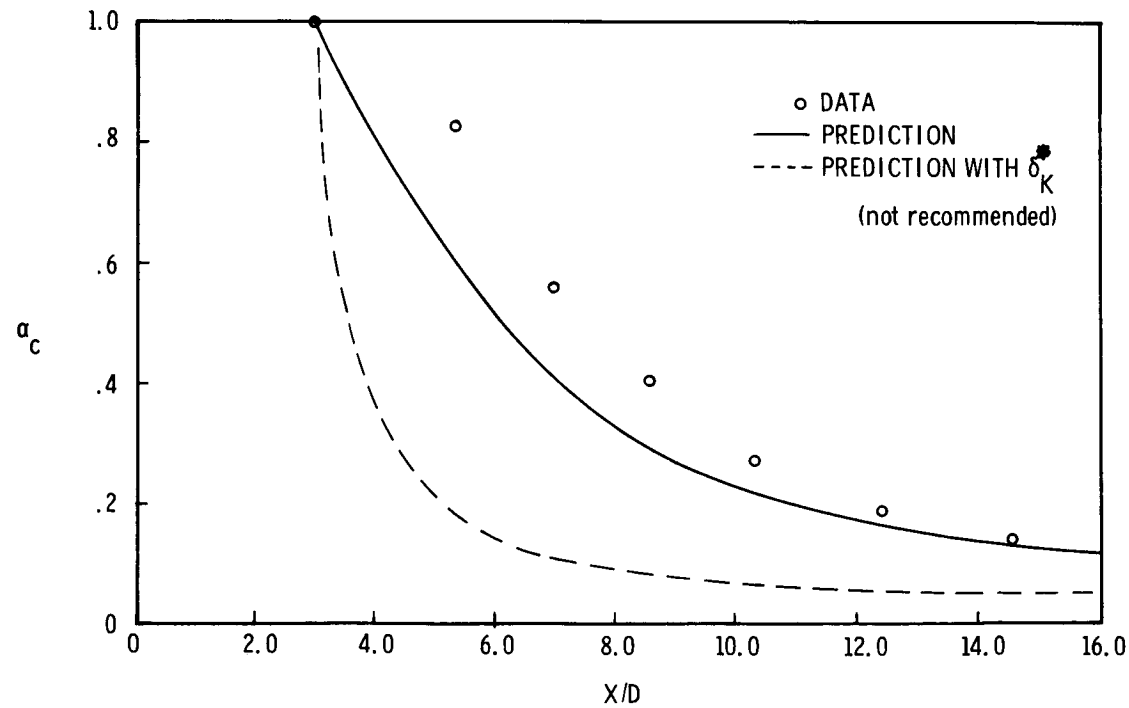

Figure 4.- Predicted and experimental center-line mass fraction of hydrogen for test case 10 (Chriss hydrogen-air jet, $\rho_j U_j / \rho_e U_e = 0.56$).

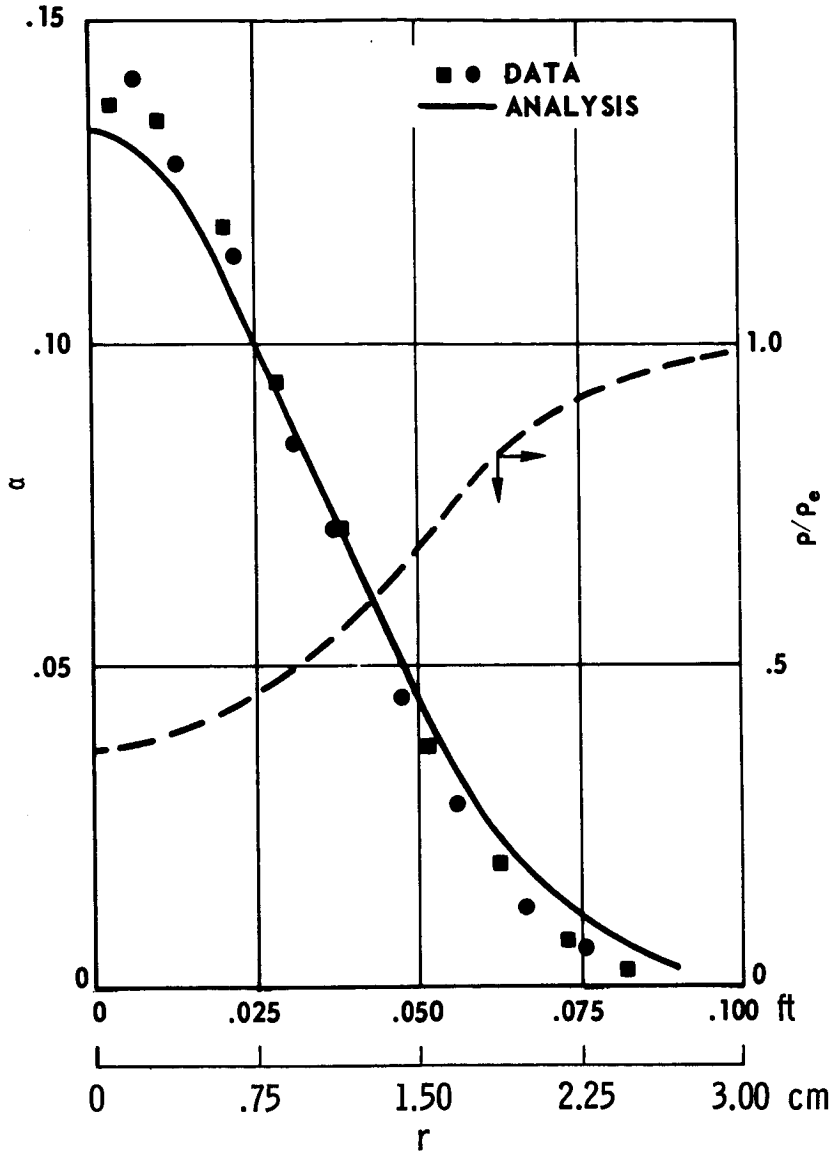

Figure 5.- Radial profiles at X/D = 14.6 for test case 10 (Chriss hydrogen-air jet, $\rho_j U_j / \rho_e U_e = 0.56$).

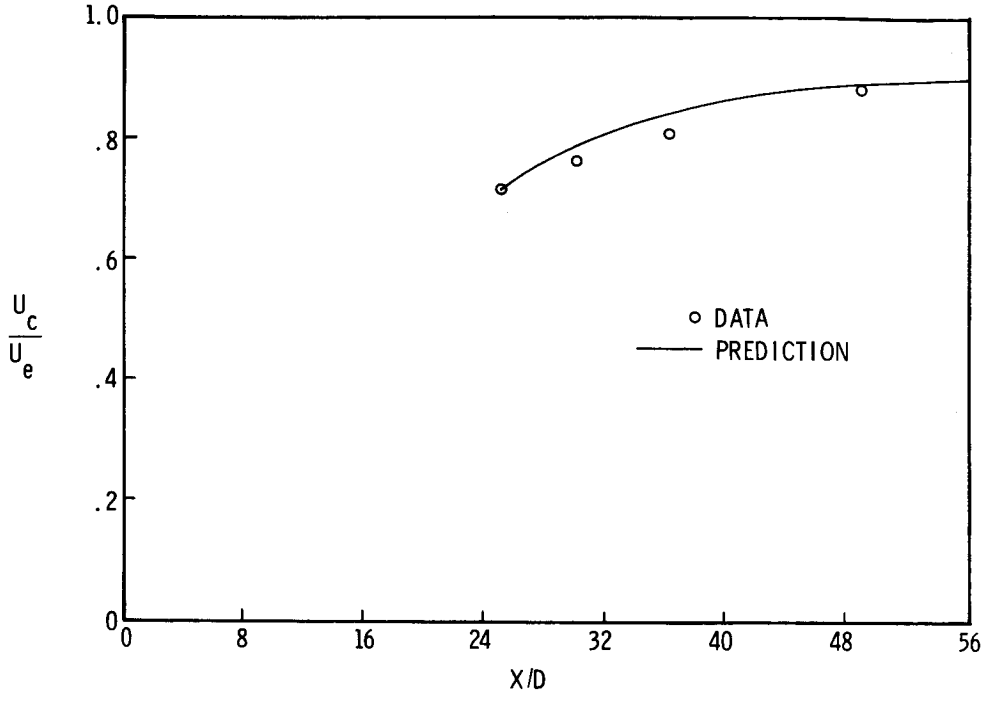

Figure 6.- Prediction and experiment for test case 11 (Eggers and Torrence jet).

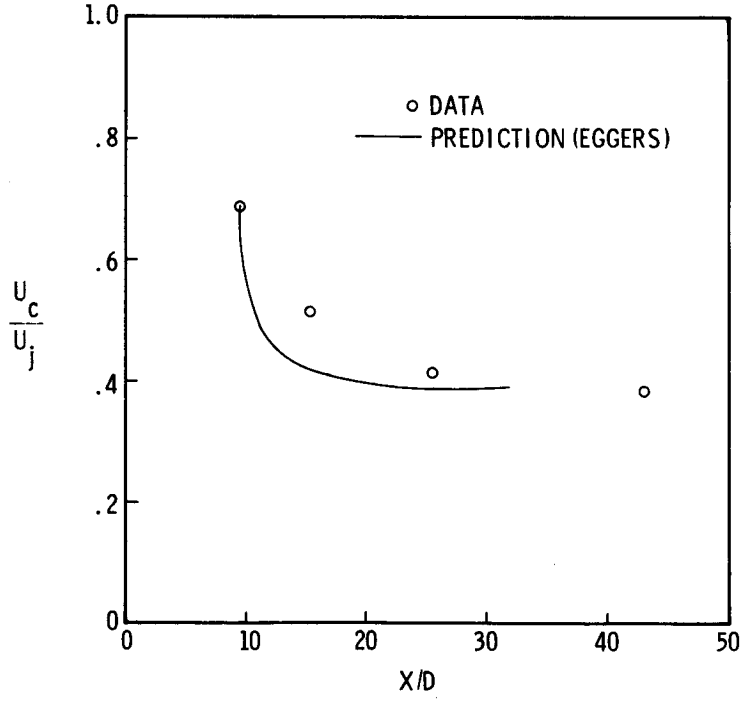

Figure 7.- Prediction and experiment for test case 12 (Eggers hydrogen-air jet, $\rho_j U_j / \rho_e U_e = 0.16$).

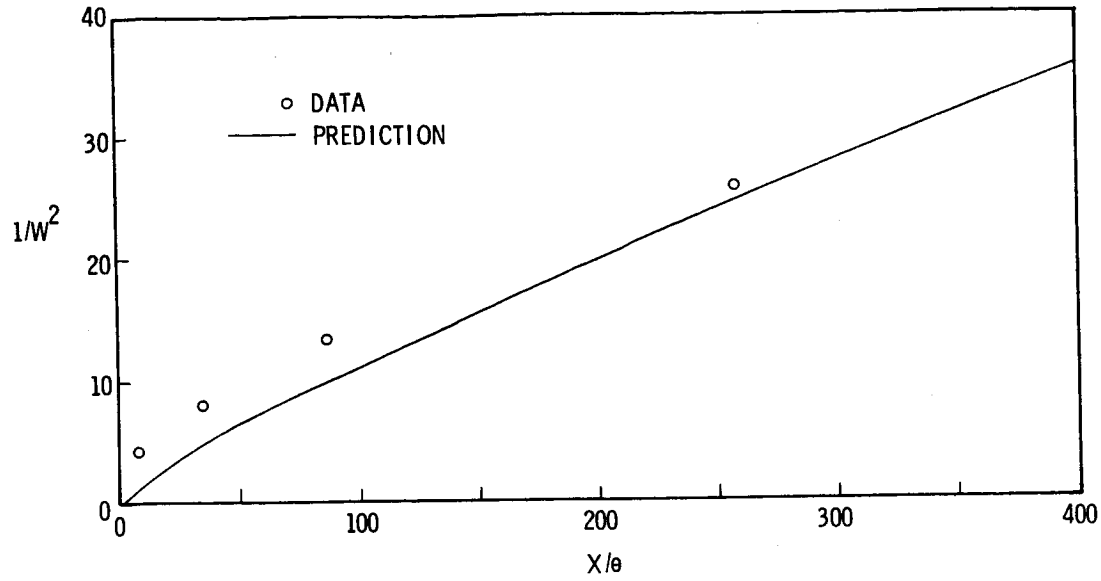

Figure 8.- Prediction and experiment for test case 14 (Chevray and Kovasznay, two-dimensional wake).

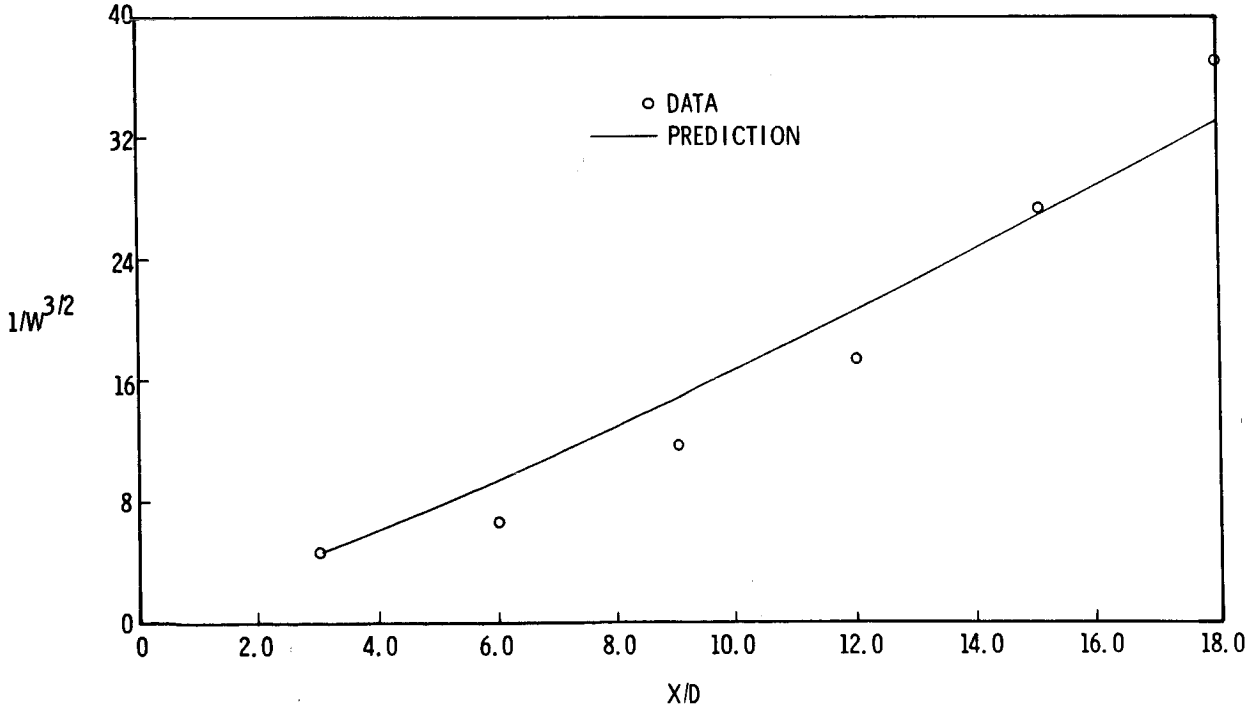

Figure 9.- Prediction and experiment for test case 15 (Chevray axisymmetric wake).

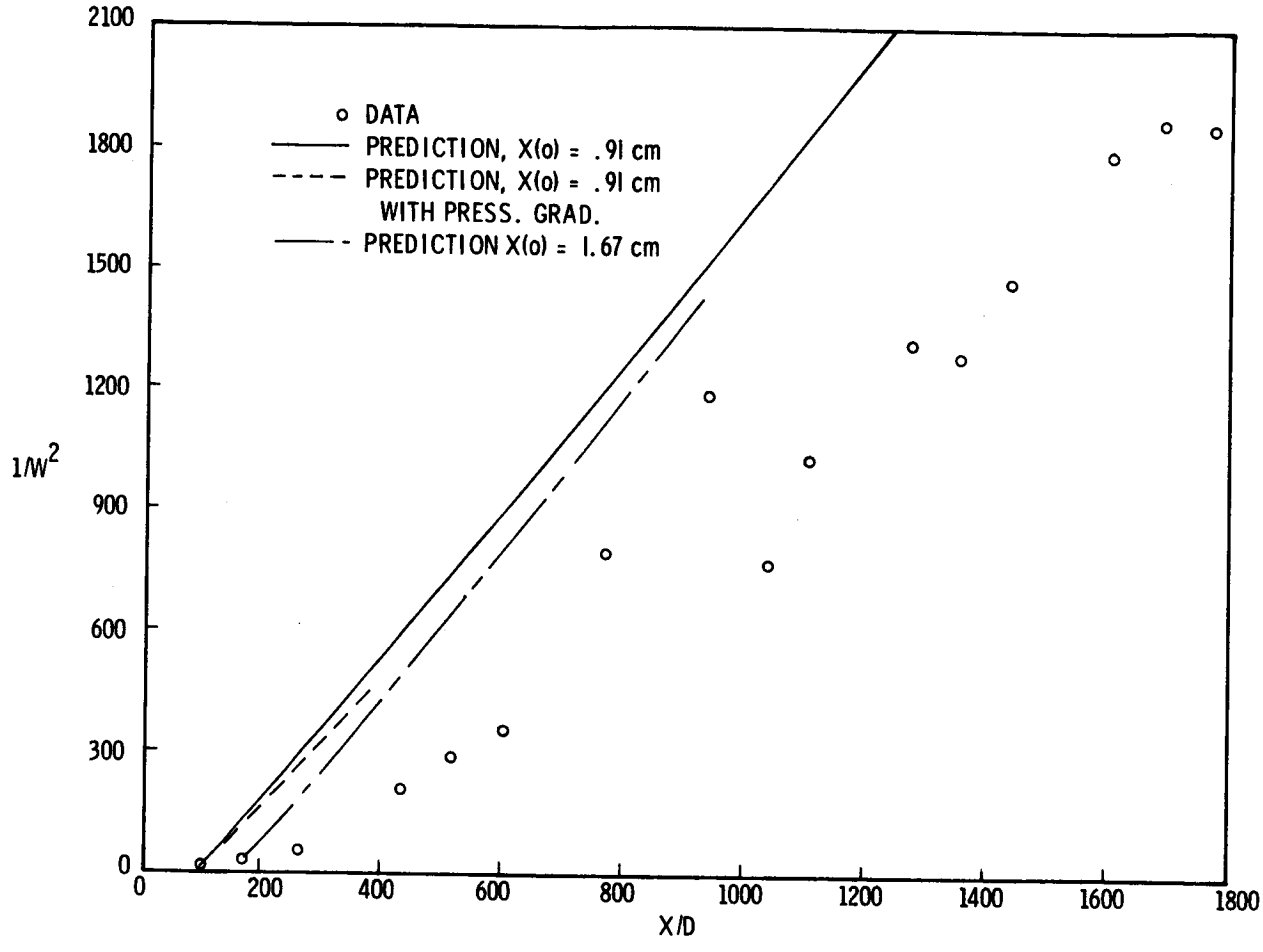

Figure 10.- Prediction and experiment for test case 16 (Demetriades two-dimensional wake).

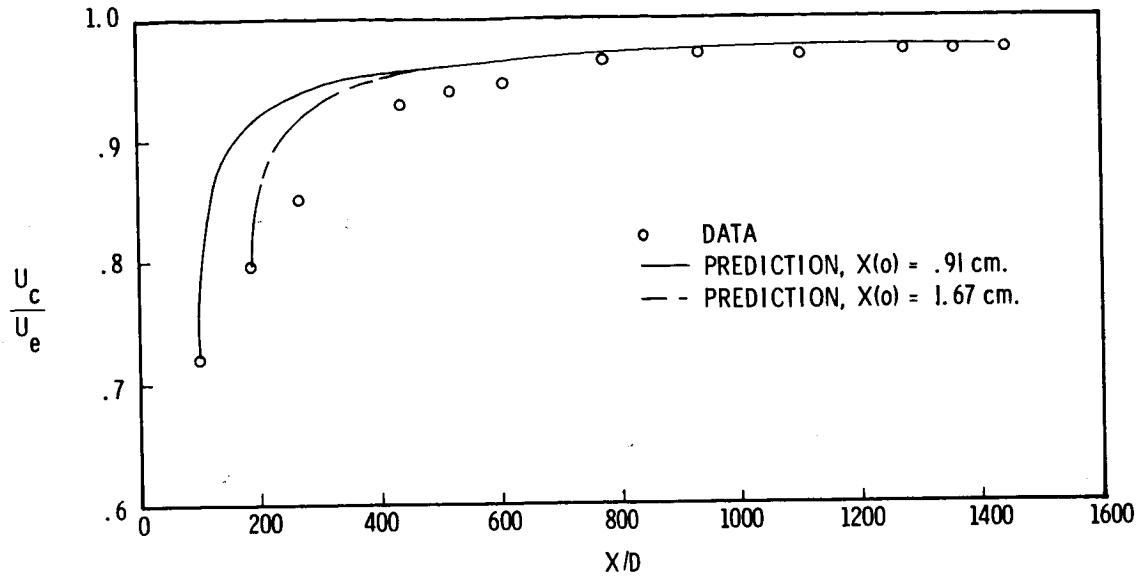

Figure 11.- Center-line velocity plot for test case 16 (Demetriades two-dimensional wake).

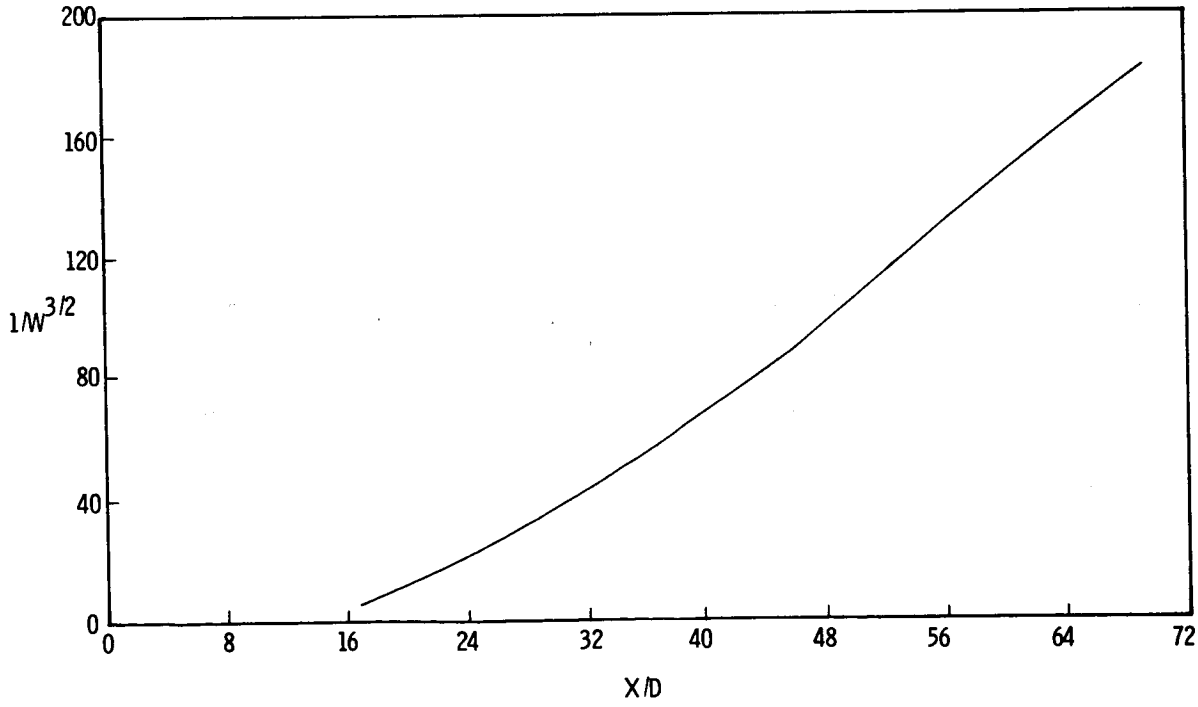

Figure 12.- Prediction for test case 17 (Demetriades axisymmetric wake).

DISCUSSION

S. W. Zelazny: Your model as applied to axisymmetric free layers uses the initial jet radius a as the characteristic length. I have shown* that using the velocity half-radius $r_{1/2}$ rather than the initial jet radius results in an eddy viscosity model that accurately models quiescent jets, which your model cannot. Comparisons between predictions and experiment using both $r_{1/2}$ and a for coflowing streams showed that the two models give about the same results. Where have you shown that using $r_{1/2}$ "was found to be unsuitable for all but jet cases with $U_j/U_e \gg 1$"?

J. A. Schetz: If you experiment with the choice of this length scale which must be introduced, you can improve the comparison in different regimes of the data. It is true that an improvement is obtained by using the half-radius in the region of high mass-flux ratios which corresponds to a jet in a quiescent medium. One could adopt that choice if he were interested in problems mostly in that regime. However, considering comparisons with data in the regime of greatest practical interest, the use of the initial radius is definitely superior.

H. McDonald: I don't know if there is that much controversy over the selection of the kinematic displacement thickness as far as boundary-layer methods are going. I think that Cebeci and Mellor both used the kinematic definition and both achieved very good agreement in their predictions. We are then faced with the dilemma that in boundary layer one uses the kinematic displacement thickness, and manifestly from your results, we have to use the normal definition. It would seem to me, in light of Rudy and Bushnell's paper (paper no. 4), one should use mixing-length formulation.

J. A. Schetz: No, there is not much of a controversy. The situation is that, I think, in boundary layers you don't usually get the tremendous density variations that we have in a hydrogen jet into an air free stream. We have made calculations for boundary layers using a kinematic or the real displacement thickness and the effect is generally not very large.

J. Laufer: I noticed in your axisymmetric formulation, when you take the formulation for the limiting case of constant density, and very far downstream where you assume similarity, that you end up with an ϵ that varies as the square of the width of your shear region rather than the usual function of linear variation. Have you worried about that situation?

---

*Zelazny, Stephen W.: Eddy Viscosity in Quiescent and Coflowing Axisymmetric Jets. AIAA J., vol. 9, no. 11, Nov. 1971, pp. 2292-2294.

J. A. Schetz: Not directly. I think it is well to recall that in the case of a moving external stream, the exact equations do not admit a similar solution of the classical type. Only the linearized equations accept such a solution.

M. V. Morkovin: I noticed that you avoided the first three test cases.

J. A. Schetz: Yes, the shear-layer cases. I'm talking about a mass-flow defect or excess with respect to some main stream, and if you have two streams in which +y has one velocity and -y has another, that does not make much sense.

B. J. Audeh: You said that this model is not to be used in the potential core, but we have a problem of where to use it. You have shown concentration profiles, and did an excellent job, but if I missed starting at the right place would my concentrations be off considerably?

J. A. Schetz: Calculations can be started at any station beyond the potential core. You could patch in a potential-core prediction, but it is insensitive to where you start as long as you are beyond the potential core. You either have to have a prediction model which you believe in for the potential core and start at the end of that, or start at some measured profile which is clearly beyond the potential core.

PREDICTIONS OF AXISYMMETRIC FREE TURBULENT SHEAR FLOWS USING A GENERALIZED EDDY-VISCOSITY APPROACH*

By J. H. Morgenthaler and S. W. Zelazny
Bell Aerospace Company, Division of Textron

SUMMARY

The lack of a general theory for predicting turbulent flows has resulted in the development of various empirical techniques applicable to specific classes of these flows. One class of flows of considerable interest for many years, because of the various engineering applications, is designated as free turbulent shear flows. A generalized eddy-viscosity approach has been successfully applied to these flows and is reported. Results presented herein for the test cases selected for evaluation by the Data Selection Committee of the NASA Working Conference on Free Turbulent Shear Flows show that predictions were obtained which are adequate for most engineering applications.

Because of the importance of starting computations from the injection station where experimentally determined mean and turbulence parameters are rarely available, a very simple core model applicable to simple step-type (slug) profiles was developed. Agreement between predicted and experimental mean profiles was generally almost as good for calculations made by using this model throughout the core region and the transition model for all subsequent regions as predictions made by starting from experimental profiles in the transition region.

The generalized eddy-viscosity model, which was developed in part through correlation of turbulence parameters, successfully predicted turbulent shear stress, turbulent intensity, and mean velocity profiles for a 0.040-inch-diameter microjet. Therefore, successful scaling by the model was demonstrated since data used in its development was for jet areas up to 90 000 times as large as the microjet and velocities only 1/20th as high.

INTRODUCTION

There has been considerable interest for many years in turbulence, since most flow fields of practical importance are turbulent. Unfortunately, there is no general analytical technique available for their prediction. In fact, a group of French scientists (ref. 1) has objected to the use of a set of partial differential equations, such as

*Work supported in part by the Air Force Office of Scientific Research under Contract F44620-70-C-0016, with technical monitoring by Dr. Bernard T. Wolfson.

the equations of change, for application to turbulent flows; they feel that since a turbulent flow field is in "pure chaos," the instantaneous velocity of a particle of fluid cannot be sufficiently regular to satisfy the constraints of partial differential equations such as the Navier-Stokes equations. Unfortunately, no substitute for the equations of change has been proposed.

Therefore, the current approach in analysis of turbulent flows is to assume that the laminar form of the equations of change apply to instantaneous values of the velocity, density, enthalpy, and concentration. These equations are then time-averaged, such that cross correlations, that is, Reynolds transport terms, occur in addition to the original "laminar-type" terms. Evaluation of these terms requires experimental information concerning the nature of turbulence, since there are insufficient independent equations to specify a given turbulent flow uniquely. The fact that experimental data are required for specification of the Reynolds transport terms is the reason that analyses of turbulent flows, whatever the approach, must be considered semiempirical.

Two general techniques that have been used extensively to provide the needed turbulence input are the eddy-viscosity and the turbulence kinetic energy (TKE) approaches. (See refs. 2 to 4.) Both were developed primarily for the prediction of momentum transport (for example, mean velocity fields) because the velocity field was frequently of primary interest. However, as more complex applications arise such as supersonic combustors and chemical lasers, prediction of mass and energy transport becomes more important than momentum transport. At present, the assumption generally made is that turbulent Prandtl and Schmidt numbers are constant (generally less than unity, the value specified being rather arbitrary) so that the identical approach used for predicting momentum transport can be used for predicting mass and energy transport as well.

Unfortunately, the assumption of constant turbulent Prandtl and Schmidt numbers has been shown in a number of investigations to be only a rough approximation (for example, refs. 5 to 7) so that not until adequate mixing models for mass and energy transport also are devised can solution of practical problems involving multispecies turbulent flows be obtained with confidence. Of course, generality of an analysis is desirable; however, from a practical standpoint, it is not necessary (nor very likely) that all turbulent flows will be correlated with a single semiempirical mixing model. As long as flows of a given class can be predicted over the complete range of practical interest, useful computations can be made.

Several years ago, the eddy-viscosity approach was selected for further development at Bell Aerospace Company, because it appeared to have a number of advantages over the newer TKE approach (refs. 8 to 11) for application to practical combustor problems:

(1) Successful modeling techniques established for momentum transport could be applied directly to the modeling of mass and energy transport, and thereby would make the assumption of constant turbulent Schmidt, Prandtl, and Lewis numbers unnecessary.

(2) Compressible multispecie free shear layer flows were of greatest interest; such flows were not successfully treated prior to 1971 by use of the TKE approach. The simplicity and flexibility of the eddy-viscosity approach for application to practical systems such as combustors were judged to be significant.

(3) Profiles computed downstream of the injection station were less sensitive to precise initial conditions. In fact, as demonstrated, the eddy-viscosity approach permits calculations to be begun from the injector face by assuming simple (and obviously very approximate) step functions for mean velocity, mass faction, and stagnation temperature; whereas, the TKE approach requires detailed initial shear stress profiles.

(4) The eddy-viscosity approach does not require an explicit relationship between the shear stress and the TKE. At present there is a controversy as to whether the shear stress is directly proportional to the TKE or the square root of the TKE and thus its general applicability is somewhat uncertain.

(5) Empirical relationships are required for the second and higher order correlations in the TKE equation. The data used to develop these empirical relationships is limited to simple flow conditions, that is, low-speed constant-density flows. Quite possibly these relations will not apply in general to more complex practical flow systems.

(6) The TKE approach had not been demonstrated to predict successfully the details of mixing and reacting jet flow.

(7) Both the TKE and eddy-viscosity techniques use phenomenological approaches, and therefore, neither can be expected to describe the detailed physics of the flow. The success of predictions and the ease of their use are principal factors to consider in judging the relative merits of the approaches.

SYMBOLS

D	jet diameter
f	ratio of transverse to longitudinal root-mean-square values of velocity fluctuations (eq. (2))
G	radial variation function for eddy viscosity (eq. (9)); also gas
L	characteristic length (eq. (7))

M	Mach number
$N_{Pr,T}$	turbulent Prandtl number
$N_{Sc,T}$	turbulent Schmidt number
R_{uv}	shear correlation coefficient (eq. (1))
r	radial coordinate (fig. 1)
r_1	value of r where $\frac{U - U_e}{U_j - U_e} = 0.99$
r_2	value of r where $\frac{U - U_e}{U_j - U_e} = 0.01$
T	total temperature
U	mean velocity in z-direction
u	fluctuating velocity in text and mean axial velocity in figures
u'	root-mean-square value of fluctuating axial velocity, $\sqrt{\overline{u^2}}$
v	fluctuating velocity in r-direction
v'	root-mean-square value of fluctuating radial velocity, $\sqrt{\overline{v^2}}$
w	fluctuating tangential velocity component or $\frac{1 - u}{u_e}$
w'	root-mean-square value of fluctuating tangential velocity, $\sqrt{\overline{w^2}}$
x,z	axial coordinates
z_c	velocity core length (fig. 1)
$\bar{z} = \frac{z}{D}$	
α	mass fraction

ϵ eddy viscosity

ρ mean density

τ_ϵ Reynolds momentum flux (shear stress)

Subscripts:

c evaluated at center line

e evaluated at $r = \infty$

j evaluated at $r = 0$, $z = 0$

max maximum value at a given z

o evaluated at $r = o$

u evaluated at velocity half-width

A bar over a symbol denotes a time-averaged quantity.

GENERALIZED EDDY-VISCOSITY MODEL FOR COFLOWING STREAMS

Background

When the decision was made to pursue an eddy-viscosity approach for turbulent mixing analyses, a procedure was selected which, if successful, would circumvent many of the shortcomings of previous eddy-viscosity models. Perhaps, most important was the decision to model transport of mass, momentum, and energy separately and to consider the wide range of flow conditions for the model development (refs. 5 and 12) presented in table 1. Previous investigators had demonstrated that any select set of data could be successfully correlated (refs. 13 to 19) by using various types of models and assuming the turbulent Prandtl and Schmidt numbers to be constant. Unfortunately, most of these models had rather limited application (refs. 5 and 20).

The data in table 1 include both very low-speed single-component free jets as well as supersonic compressible multispecies coflowing streams for the configuration shown in figure 1. Because of the wide range of conditions, it was apparent that some of the assumptions made by previous investigators for mathematical simplicity could not be valid. For example, the assumption that has been most frequently made for this reason

is that no variation in the transverse (radial) direction exists in either the eddy viscosity, or alternatively the eddy diffusivity of momentum. (See refs. 13 to 19.) Unfortunately, this assumption has no valid basis (ref. 12) so that a general model must be a function of radial as well as axial position.

Another important decision was to apply the computational technique for the numerical differentiation of experimental mixing data previously developed (refs. 21 to 23) prior to initiating model development. By using this procedure, designated the inverse solution technique, mean velocity and concentration profiles are differentiated once in the radial direction, each of the remaining terms in an integral form of the shear-layer equations evaluated, and the appropriate turbulent transport coefficients solved for as a function of position in the flow field. Such information was considered to be essential for successful model development. Overall mass and momentum balances were evaluated for consistency; only high quality data which yielded species mass and momentum balances to within 20 percent of their average value at each axial station were used for the modeling.

General guidelines were established for the model development which, if successfully followed, almost certainly would lead to more general eddy-viscosity-type mixing models than those previously reported:

(1) Attempt to model the structure of the turbulence, for example, shear stress and turbulent intensities, not merely mean quantities.

(2) Predictions should exhibit self-preservation in region IV (fig. 1) which are independent of jet initial conditions.

(3) Consider the lack of attainment of equilibrium of the mean and turbulence param eters upstream of the self-preservation region by using anemometry data in the model development. Failure to follow this guideline which permits consideration of flow "history" was considered an important reason for lack of generality of previous eddy-viscosity models.

(4) Use of the strong points of past models, for example, the eddy-viscosity model should yield predictions in agreement with the successful Prandtl-type model for incompressible free jet flows in the similarity region.

(5) Judge the merit of the model by comparison of predicted and experimental profiles at each axial station for which data are available. The ability to predict proper profile shapes was considered to be more important than merely obtaining agreement with experimental data along the center line.

By using these guidelines and the results obtained from the inverse solution technique, models for the maximum values of the turbulent shear stress and eddy viscosity were devised as well as their variation in the direction transverse to the flow (radial

direction). Details of this development were presented in references 5 and 12; a summary is presented herein.

Model Development

For coflowing streams, in which there is a predominant flow direction, the shear-layer equations apply; they are the same as the boundary-layer equations except for initial and boundary conditions. The classical definitions of the turbulent shear stress applicable to incompressible flows

$$\tau_\epsilon = \rho\overline{uv} = -\rho R_{uv} u'v' = \epsilon \frac{\partial U}{\partial r} \tag{1}$$

Equation (1) was used together with the assumption that the effects of density fluctuations are negligible, as is usually done in the analysis of free turbulent shear flows. This assumption has been shown to be valid for compressible flows (up to Mach 3) in which molecular weight is constant. (See ref. 24.) Empirical relations were developed for various parameters in equation (1), that is, for u', v', and R_{uv}, which permitted prediction of turbulence quantities such as τ_ϵ and u'^2, as well as mean profiles.

The data of references 25 to 30 suggested that the ratio of axial to radial turbulent intensity, as a first approximation, may be expressed only as a function of axial position, and that the ratio of radial to tangential turbulent intensity is essentially unity.

$$\frac{v'}{u'} = f^{1/2} \quad \text{and} \quad \frac{v'}{w'} \approx 1 \tag{2}$$

where

$$f = \begin{cases} 0.5 + 0.005\bar{z} & (\bar{z} \leq 100) \\ 1.0 & (\bar{z} > 100) \end{cases}$$

and

$$\bar{z} = \frac{z}{D}$$

The empirical relationship between turbulent kinetic energy and the shear stress suggested in reference 11 was used to relate the eddy viscosity to u'^2

$$\tau_\epsilon = 0.15\rho\left(u'^2 + v'^2 + w'^2\right)\frac{\partial U/\partial r}{(\partial U/\partial r)_{max}} \tag{3}$$

Therefore, by using equations (2) and (3) and assuming that the region of maximum shear occurs at the half-width of the jet r_u

$$\frac{\tau_\epsilon}{(\tau_\epsilon)_u} = \frac{\rho u'^2}{(\rho u'^2)_u} \frac{\partial U/\partial r}{(\partial U/\partial r)_u} \tag{4}$$

and

$$\frac{\epsilon}{\epsilon_u} = \frac{\rho u'^2}{(\rho u'^2)_u} \tag{5}$$

Applying equations (1), (2), and (3) at the jet half-width r_u resulted in an expression for the maximum value of the correlation coefficient

$$(R_{uv})_u = -0.15 \frac{1 + 2f}{f^{1/2}} \tag{6}$$

The empirical relation for the maximum value of $(u'^2)_u$ that followed the general guidelines and correlated hot-wire anemometry data was (refs. 5 and 12)

$$(u'^2)_u = 0.12 \frac{\int_0^\infty |\rho U - \rho_e U_e| r \, dr}{\rho_u L} \left(\frac{\partial U}{\partial r}\right)_u \left(1 + e^{-4.6 U_j/U_e}\right) \tag{7}$$

where

$$L = r_u + (D - r_u) e^{-0.115\bar{z}}$$

Substituting equations (2), (6), and (7) into equation (1) yields an expression for the maximum value of the eddy viscosity[1]

$$\epsilon_u = \frac{0.018(1 + 2f)\left(1 + e^{-4.6 U_j/U_e}\right) \int_0^\infty |\rho U - \rho_e U_e| r \, dr}{L} \tag{8}$$

---

[1] The original model developed in reference 12 included an empirical function of density ratio. Subsequent analysis suggested that, in general, this function was not necessary and has been excluded from the model. Interestingly, Brown and Roshko (ref. 34) have shown that the mixing rate of planar shear layers also exhibits an independence of density ratio.

Variation of the eddy viscosity in the transverse (radial) direction was evaluated by using equation (5). The empirical expression $G\left(r/r_u\right)$ used to represent this radial variation was

$$\frac{\epsilon}{\epsilon_u} = \frac{\rho u'^2}{\left(\rho u'^2\right)_u} = \frac{1.05 - 0.15e^{-4.6r/r_u}}{1.0 + 0.05\left(r/r_u\right)^7} \equiv G\left(r/r_u\right) \tag{9}$$

Equations (8) and (9) define the generalized eddy-viscosity model developed for the transition region. This model, together with the assumption that $N_{Sc,T}$ and $N_{Pr,T}$ were constant, was used for predicting the mixing of the free turbulent shear flows selected by the conference data selection committee.

Discussion of Model

The eddy-viscosity model successfully followed all the general guidelines at least partially, and therefore it is unique. Several of its features deserve comment:

(1) Radial variation of ϵ and $\rho u'^2$ are included in the empirical function $\epsilon/\epsilon_u \equiv G\left(r/r_u\right)$ defined in equation (9). This function is plotted in figure 2 along with constant and variable density data of references 25 to 28 and 31 to 33 which were used for its determination. There are several reasons for the scatter of the data: (a) turbulence quantities have not become self-preserving at the axial stations for which they were available and (b) data obtained by using the inverse solution technique scatter even more than the anemometry data since numerical differentiation of experimental data is utilized in this technique. Consistency of the injected mass and momentum integral balances to better than ±10 percent (rather than ±20 percent) is required to reduce the scatter.

Nevertheless, the composite results in figure 2 strongly indicate that the eddy viscosity reaches a maximum at some distance from the center line and that it exhibits an intermittent-type behavior at the outer edge of the mixing region analogous to the behavior of boundary layers (ref. 2). The data also indicate that ϵ/ϵ_u is monotonically decreasing for $r/r_u > 1$ and that it reaches a maximum at about $r/r_u \approx 0.6$, that is, in the vicinity of half-width of the jet. The exact location of the maximum is difficult to pinpoint because of the data scatter; however, the maximum of the function defined by equation (9) occurs at $r/r_u = 0.66$. No consistent trend was apparent which correlated with density variation across the mixing region. Therefore, as a first approximation, the solid curve represented by equation (9) was used to represent the average variation of eddy viscosity in the transverse direction. This approximation is obviously superior to the assumption that ϵ/ϵ_u is constant which was frequently made by previous investigators; however, it is apparent from figure 2 that a correlation which includes other parameters than r/r_u is needed to reduce the scatter.

(2) Both the eddy viscosity and turbulent intensity u'/U_j are proportional to the mass defect. The mass defect has been successfully used by a number of investigators to model the turbulent shear stress over a wide range of flow conditions and test geometries. It was shown by Clauser (ref. 35) to correlate the eddy viscosity in the outer region of a two-dimensional turbulent incompressible boundary layer in the absence of pressure gradients. Schetz (refs. 18 and 19) extended the mass defect concept to model axisymmetric coflowing streams in the transition region. Zelazny (ref. 36) further generalized this concept to apply to both jets in a quiescent atmosphere and coflowing streams. It should also be noted that the generalized eddy-viscosity model predicts the same center-line velocity decay rate in the similarity region as the Prandtl model.

(3) Recognition was given the fact that turbulent shear stress is not determined exclusively by local mean flow properties at a particular location; that is, until the flow is in the self-preservation region (fig. 1), prior development or "history" of the flow must be considered, for example, initial conditions and wall effects. An attempt was made to include this effect in the model empirically by defining a characteristic length L (eq. (7)) and a function f (eq. (2)), both of which varied significantly with axial location in the near region up to about 100 diameters downstream ($\bar{z} = 100$).

The fact that $L = r_u$ (a function of axial position) was a more appropriate characteristic length than $L = D/2$ (a constant) was discussed in reference 36. The more sophisticated relation of equation (7) was demonstrated to yield superior predictions for the data of table 1. Figure 3 is a plot of L for several of the test cases, and shows this parameter reaches a minimum value for $\bar{z}$ ranging from 6 to 10. Since this parameter is empirical, and somewhat arbitrarily defined, its further modification may well lead to improved results.

The function f defined in equation (2) varies linearly from 0.5 at $\bar{z} = 0$ to 1.0 at $\bar{z} = 100$. It accounts empirically for the fact that u' and v' are not in equilibrium in the near region of a free shear flow. The additional refinement of considering f a function of radial position was deemed unnecessary in light of the spread of the data for u'^2 shown in figure 2.[2]

The relations L and f both attempt to allow for the fact that the free turbulent shear flows do not attain self-preserving profiles for much of the region of practical interest. (See fig. 1.) Obviously, these relations are only rough approximations for this effect since free turbulent flows do not exhibit a "universal" law by which turbulence parameters and mean properties attain self-preserving profiles. Preturbulence levels such as those caused by screens and initial profile shapes caused by splitter plates may play a significant role in determining the axial location at which this condition is achieved.

---

[2]For constant-density flows, $\frac{\epsilon}{\epsilon_u} = \frac{u'^2}{u_u'^2}$ (eq. (6)).

(4) An empirical function, $1 + \exp\left(-4.6U_j/U_e\right)$ which yields better correlation when $U_e >> U_j$ was introduced to broaden the range of applicability. However when $U_j > U_e$, this function has a negligible effect on the eddy-viscosity model, for example, for the axisymmetric test cases the relation ranged from 1.00 to 1.04. On the other hand, a significant improvement in predictions was obtained for jets where $U_j << U_e$ such as those reported by Zawacki and Weinstein (ref. 25). The amplification provided by this function, which reaches a maximum value of 2, may account for the increase in the turbulent momentum transfer caused by the recirculation regions that occur in these "wake-like" flows.

Core Model

The generalized eddy-viscosity model was developed by using published data for coflowing streams. Unfortunately, there were few data available for the core region because of the difficulty in obtaining valid measurements in this region prior to the recent development of the laser-Doppler technique. Of course, a model applicable to the core is of great practical importance since in practical combustors and chemical lasers, for example, the ignition and most of the combustion occur within this region. Unfortunately, generally neither initial mean profiles nor shear stress profiles are known. The simplest type of initial condition for starting calculations would be a "step-type" or "slug" profile in which bulk mean quantities were simply used to characterize each stream. Naturally, a core mixing model appropriate to step-type initial profiles might not apply when used with experimental profiles. However, such a deficiency would not be important for modeling the transition and similarity regions as long as realistic profiles were generated prior to reaching the end of the core. An effort to develop a core model is one task of the current Bell Aerospace AFOSR contract.

As demonstrated in this paper the generalized eddy-viscosity model was quite successful in the transition region for which it was developed. The simplest possible approach was to assume a core model with the same functional form; therefore, as a first approximation, the transition model was multiplied by a constant factor (less than unity) to correct for the overmixing predicted using it in the core. The constant 0.4 proved to be satisfactory, and the "core model" which resulted, that is, $\epsilon_{core} = 0.4\epsilon_{transition}$, was far more successful than anticipated. Of course, when applying the transition model to the core region, the limits of the integral for the mass defect (eq. (8)) were changed from 0 to ∞ (the extent of the mixing zone in the transition region) to r_1 and r_2 (the extent of the mixing zone in the core). Success of this model was demonstrated by the very reasonable predictions attained when using either experimental or slug profiles at the injection station. It suggests that the general functional form of the transition model may be appropriate for the core as well; however, further work on core modeling is required before any conclusions can be drawn.

Additional efforts to model the core region are in progress at Bell Aerospace with recent results reported in reference 37. Also reported in reference 37 is a review of methods used in the modeling of turbulent axisymmetric coflowing streams and quiescent jets. Concepts such as a universal center-line mass fraction decay exponent, the Reichardt hypothesis, and a virtual origin were demonstrated generally to be inadequate for characterization of these flows.

COMPARISON OF PREDICTIONS WITH EXPERIMENTAL DATA

The generalized mixing model was used to predict the flow fields for the twelve axisymmetric jet cases and the two axisymmetric wake cases listed in table 2. The governing shear layer equations were solved numerically in the Von Mises coordinates by using an explicit finite-difference method. Three types of predictions were made: (1) Step-type (slug) initial profiles were assumed at the injection station (x = 0) and the core model used until the velocity on the center line of the jet was less than its initial (core) value; the transition model was used thereafter. (2) The first experimental profiles reported downstream of the core were used for the initial profiles (x/D designated on curve) and the transition model used exclusively. (3) The first experimental core profile was used for those cases in which the boundary-layer effects on the splitter plate were not pronounced (x/D designated on curve). (Initial velocity profiles that exhibited pronounced boundary-layer effects required a programing change to define the extent of the mixing region; this change was not deemed to be warranted in the light of the success obtained by using the slug profile.) Generally, three sets of curves are presented in each figure and correspond to each of these types of predictions. Figures are plotted in the manner specified by the data selection committee.

Test Case 6 (Maestrello and McDaid)

Predictions of the mean velocity for the high-speed quiescent jet are compared with the experimental data in figure 4 for test case 6 (ref. 38), results showed good agreement. Since no transition region profiles were available, only predictions from the injection station were possible. The predicted center-line velocities were at most 14 percent greater than the experimental velocities. This good agreement indicates that the initial slug velocity profile was adequate. However, as expected even better agreement was obtained when the actual experimental core profile (x/D = 1.0) was used. This result tends to validate the simple core model for use with realistic initial profiles.

Test Case 7 (Eggers)

Velocity data for the supersonic (Mach 2.22) quiescent jet are compared with the predictions in figure 5(a) for test case 7 (ref. 32). The agreement achieved appears to be

adequate for most engineering applications; however, the model overestimated the mixing rate (maximum error was 24 percent). Note, however, that it had underestimated the mixing rate in the previous case with a maximum error of 14 percent. Again little difference in predictions was observed when experimental core profiles were used and thus the results of the previous case were confirmed. Comparison of predicted axial velocity profiles with the data are shown in figure 5(b) for both the slug and experimental initial profiles. Good agreement was obtained at $x/r_0 = 8.0$ and adequate agreement at $x/r_0 = 27$ and 99 for each type of prediction.

Test Case 8 (Heck)

Predictions of the center-line velocity and total temperature for the high-temperature quiescent jet are shown in figures 6(a) and 6(b) for test case 8 (ref. 39). Since both momentum and thermal energy transport are significant in this case, it was necessary to specify a turbulent Prandtl number. A constant $N_{Pr,T} = 0.70$ was assumed, since this value appears to be representative of values reported in the literature. Calculations were started from the point of injection using the slug and experimental initial profiles. The former overestimated the mixing rate for both velocity and total temperature with a maximum error of 20 percent; the latter resulted in somewhat better agreement. In addition, when calculations were started from the transition region predictions of both velocity and temperature were in excellent agreement with data (maximum error was only 8 percent).

Test Case 9 (Forstall)

Predictions of the center-line velocity decay for the coflowing air (with 10 percent He tracer) mixing with airstreams are shown in figure 7(a) for test case 9 (ref. 40). The model underestimates the mixing rate with differences between prediction and experiment less than 14 percent. Examination of the initial experimental profile and the assumed initial slug profile shown in figure 7(b) suggests one reason for the disagreement. The assumed momentum flux at the injection station is considerably larger than the actual momentum flux because of significant momentum loss to the splitter plate. Therefore, mixing was predicted to be slower than actually observed. As a test of the importance of this effect, predictions also were made with a slug profile adjusted so that the momentum flux obtained from both the experimental and slug profiles would be equal (fig. 7(b)). Predicted center-line velocity decay for this case which is also presented in figure 7(a) is in excellent agreement with experimental values. In addition, calculations made by starting from the transition region show that good agreement was attained between the data and the predictions (within 10 percent).

Test Case 10 (Chriss)

Results for the high-speed, subsonic, coflowing streams of hydrogen mixing with air are shown in figure 8 for test case 10 (ref. 31). The center-line predictions obtained by using both an initial slug profile and experimental core profiles underestimated the mixing (29 percent difference for velocity and 57 percent difference for mass fraction). No significant difference was observed between these cases. Calculations started from the transition region show that slightly better agreement was obtained for the hydrogen mass fraction (within 55 percent) but poorer agreement was obtained for the center-line velocity (within 45 percent). The first experimental transition velocity profile, obtained at $x/D = 5.34$, is presented in figure 8(c). Good agreement at this station demonstrated again the adequacy of the simple core model. However, these results demonstrate that the eddy-viscosity model does not include all the complexities required for exact predictions. The predictions for this case and that of Eggers (test case 12 (ref. 41)) are the poorest of the entire set. Nevertheless, results probably still are adequate for many engineering purposes.

Test Case 11 (Eggers and Torrence)

Predictions for coflowing air (with 1 percent ethylene tracer) and airstreams are presented in figure 9 for test case 11 (ref. 7). These results show good agreement between predicted and experimental velocities and are obtained by using the initial slug profile (within 8 percent) even though data taken at the injector face exhibited boundary-layer effects at the splitter plate. Predictions also were made by starting from the transition region for this case, and they showed better agreement (within 5.5 percent).

Test Case 12 (Eggers)

Results for the Mach 0.89 inner hydrogen jet mixing with a Mach 1.32 outer airstream are presented in figure 10 for test case 12 (ref. 41). A turbulent Prandtl number of 0.9 was used in the calculations as suggested in reference 36. Predictions for velocity obtained starting both from the core and transition regions (fig. 10(a)) are somewhat low; predictions initially were 40 percent too low, but agreement was considerably better at downstream stations. The center-line hydrogen mass fraction decay (fig. 10(b)) was greatly overestimated (nearly 75 percent too low at $x/D = 6$). This overmixing is surprising, since for the similar conditions of Chriss (test case 10) the model predicted undermixing, although it gave reasonable agreement overall. Examination of the schlieren photographs of these tests suggest that pressure gradients exist in the near region (ref. 41). Of course, since the shear layer equations are used in the analysis, transverse pressure gradients could not be considered. The omission of pressure-gradient effects may, at least in part, account for the poor agreement in figure 10.

Test Case 15 (Chevray)

Predictions for an axisymmetric wake are shown in figure 11(a) for test case 15 (ref. 42). The model underestimated the mixing rate for this wake. Note, however, that the scale $w^{-3/2}$ is somewhat misleading since it amplifies small discrepancies. For example, at $x/D = 18.0$, the difference between predicted and experimental velocity is 15 percent; whereas, with respect to the $w^{-3/2}$ scale, the difference is 70 percent. Chevray also has measured the turbulent shear stress and a comparison between data and predictions is shown in figure 11(b) at $x/D = 12.0$. The predicted and experimental shear are in reasonably good agreement at this station; however, comparisons at other axial stations were not consistently this good. The ability of the model to predict turbulence quantities is discussed in the next section.

Test Case 17 (Demetriades)

Good agreement between experimental and predicted velocities was obtained for the compressible wake data presented in figure 12 for test case 17 (ref. 43). The maximum disagreement was only 8.0 percent. This result suggests that the model developed by use of jet data exclusively is reasonably valid for wake data as well.

The predictions for the wake flows were made by omitting the term $1.0 + \exp\left(-4.6U_j/U_e\right)$, from the model since actual wake data were not used in the development of this expression (for which $U_j = 0$). Calculations made by including this term improved agreement with the Chevray data but agreement between predictions and the Demetriades data became poorer. Additional wake data must be evaluated before an empirical velocity ratio expression can be validated.

Optional Test Cases

Predictions also were made for the five optional test cases (figs. 13 to 17) which utilized axisymmetric geometry. Since the previous cases showed that valid results were obtained by starting with the initial slug profile, and since such profiles are the simplest to use, predictions were made only with these profiles.

The agreement obtained between the predictions and the experimental data for test case 18 (Wygnanski and Fiedler, refs. 29 and 30) was outstanding; that is, similar (region III, fig. 1) velocity profiles were predicted. Agreement for test case 19 (Heck, ref. 39) was also quite good (within 20 percent) as it had been for the earlier test case 8 (Heck, ref. 38). The velocity agreement is not very good (within 33 percent) for test case 20 (Chriss, ref. 44); however, the hydrogen concentration for this case was somewhat better (about 29 percent). As before, agreement was not good for either velocity or concentration for test case 21 (Chriss, ref. 31) (nearly 16 percent for velocity and 100 percent for concentration). Agreement for test case 22 (Eggers, ref. 41) also was not good; the

model drastically overestimated the mixing rate as it had for test case 12 (Eggers, ref. 41). Lack of agreement is not surprising since the data exhibits an anomalous behavior in which the center-line jet velocity becomes less than the free-stream velocity, evidence that severe pressure gradients may have occurred. For this reason, an analysis using shear-layer equations may not be appropriate.

PREDICTION OF TURBULENCE PARAMETERS

In the development of the generalized eddy-viscosity model, an effort was made to correlate both turbulence and mean quantities. Recently purchased hot wire and laser-Doppler anemometers are being used to characterize the flow from small jets in an effort to obtain empirical correlations for jet noise. Such data present an excellent opportunity to compare turbulence parameters predicted by using the model directly with experimental parameters. If successful in these predictions, the model might be used with some confidence in the development of an empirical correlation for noise.

Results of hot-wire measurements made for a 1.02-mm-diameter (0.040-in.) free jet by Baker, Moon et al. (ref. 45) are presented in figures 18 to 21; initial jet velocity was 213.4 m/sec (700 ft/sec). The data are very consistent since variation in momentum balances was less than 2.5 percent from the mean value, that is, $\int_0^\infty \rho U^2 r \, dr$ ranged from 0.0512 to 0.0533 N (0.01152 to 0.01198 lbf). Predictions were made by using the initial slug profile and the core model in the near region followed by the transition model as previously described. Agreement is seen to be very adequate for turbulent shear stress τ_ϵ, axial turbulent intensity u'/U_j, and mean velocity U_j. In the case of τ_ϵ and u'/U_j, agreement was poorest at the initial station (x = 30.48 mm (1.2 in.)) where the x-wire is long (1.27 mm (0.050 in.)) relative to the jet diameter. For this reason, characterization of the near region, that is, core and transition, are in progress using the laser-Doppler technique. The agreement between experimental and predicted velocities using the model (fig. 20) is outstanding, even at the initial station. The accuracy of predictions of mean values (within 2 percent) is significantly better than the shear stress (within 20 percent). This result demonstrates that predicted mean values exhibit a degree of insensitivity to the inaccuracies introduced in predicting the shear stress. That is, the eddy viscosity is used directly for computation of shear stress, but it merely influences a coefficient used in the numerical integration procedure to obtain mean velocity. The center-line velocity is plotted as a function of axial position in figure 21. The decay exponent is correctly given by -1 for both experimental and predicted results as is appropriate for flow in the similarity region.

Additional experiments were made for a sonic free jet; although exact static pressure matching was not attained at the nozzle exit agreement between predicted and experimental parameters, it was essentially as good as that shown in figures 18 to 20.

These results enhance our confidence in the applicability of the model for engineering calculations. They also showed the model was useful for scaling since data used for its development (table 1) were for jet areas up to 90 000 times as large as the 1.02-mm (0.040-in.) microjet and velocities 1/20th as high. No modification of the model was made for the microjet predictions.

CONCLUSIONS AND RECOMMENDATIONS

Generalized eddy-viscosity models developed for the similarity, transition, and core regions were presented which did creditable jobs of predicting mean velocity profiles (and reasonably well for concentration and temperature profiles when appropriate) for most of the 14 axisymmetric free turbulent shear flows selected by the data selection committee. The core model was demonstrated to be reasonably valid even when slug (step-type) profiles were assumed at the injector. Results established the validity of the eddy-viscosity approach for engineering predictions including practical hardware design and its optimization. (For example, see ref. 46.)

The model also was shown to predict turbulence shear stress and axial turbulence intensity as well as mean velocity for jets varying in area by a factor of 90 000 and velocities varying twentyfold. Its applicability over a wide range of jet geometries as well as flow conditions was thereby established.

The model has several important features; it includes (1) a transverse (radial) variation of the eddy viscosity, (2) the mass defect, (3) allowance for the fact that turbulent shear is not dependent exclusively on local mean flow properties (by defining an empirical characteristic length, and a function allowing for axial variation in the ratio of the axial to radial turbulence intensities), and (4) allowance for the variation in the ratio of jet velocity to external stream velocity.

The assumption of constant turbulent Schmidt and Prandtl numbers was made in order to predict flow fields in which mass and energy transport occurred in addition to momentum transport. In order to obtain satisfactory predictions, these parameters were varied from 0.6 to 0.9. These results clearly demonstrate the need for separate models for mass and energy if realistic predictions are to be made without the benefit of prior experimental data.

The critical guideline used in the development of the generalized eddy-viscosity model was application of the inverse solution technique to a wide range of valid experimental data so that quantitative results were available for determination of the various func-

tional relations and constants. The same technique should be applied for the development of turbulent mixing models for mass and energy transport, so that the unacceptable assumption that the turbulent Schmidt and Prandtl numbers are constant can be relaxed.

Examination of those workshop cases in which poorest predictions were obtained indicates that the ratio $(\rho U)_j / (\rho U_e)_e \leqq 0.6$. This result suggests that further improvement of the eddy-viscosity model may be possible by including an appropriate relation containing this ratio.

Examination of available free turbulent shear flow data suggests that more detailed experimental investigations be conducted. These investigations should include the following effects: (1) pressure gradients and pressure levels other than atmospheric, (2) initial conditions at the injection station, (3) heavy gas jets exhausting into light gases, for example, oxygen into hydrogen, and (4) jet to free-stream velocity ratios near unity.

REFERENCES

1. Pai, Shih-I: Viscous Flow Theory. II – Turbulent Flow. D. Van Nostrand Co., Inc., c.1957.

2. Hinze, J. O.: Turbulence. McGraw-Hill Book Co., Inc., 1959.

3. Kline, S. J.; Morkovin, M. V.; Sovran, G.; and Cockrell, D. J., eds.: Computation of Turbulent Boundary Layers – 1968 AFOSR-IFP-Stanford Conference. Vol. I – Methods, Predictions, Evaluation and Flow Structure. Stanford Univ., c.1969.

4. Nash, John F.; and Patel, Virendra C.: Three-Dimensional Turbulent Boundary Layers. SBC Technical Books, 1972.

5. Zelazny, S. W.; Morgenthaler, J. H.; and Herendeen, D. L.: Reynolds Momentum and Mass Transport in Axisymmetric Coflowing Streams. Proceedings of the 1970 Heat Transfer and Fluid Mechanics Institute, Turbot Sarpkaya, ed., c.1970, pp. 135-152.

6. Peters, C. E.; Chriss, D. E.; and Paulk, R. A.: Turbulent Transport Properties in Subsonic Coaxial Free Mixing Systems. AIAA Paper 69-681, June 1969.

7. Eggers, James M.; and Torrence, Marvin G.: An Experimental Investigation of the Mixing of Compressible-Air Jets in a Coaxial Configuration. NASA TN D-5315, 1969.

8. Glushko, G. S.: Turbulent Boundary Layer on a Flat Plate in an Incompressible Fluid. Bull. Acad. Sci. USSR, Mech. Ser., no. 4, 1965, pp. 13-23. (Available in English translation from DDC as AD 638 204, May 1966.)

9. Patankar, S. V.; and Spalding, D. B.: A Finite-Difference Procedure for Solving the Equations of the Two-Dimensional Boundary Layer. Int. J. Heat & Mass Transfer, vol. 10, no. 10, Oct. 1967, pp. 1389-1411.

10. Bradshaw, P.;Ferriss, D. H.; and Atwell, N. P.: Calculation of Boundary-Layer Development Using the Turbulent Energy Equation. J. Fluid Mech., vol. 28, pt. 3, May 26, 1967, pp. 593-616.

11. Lee, S. C.; and Harsha, P. T.: Use of Turbulent Kinetic Energy in Free Mixing Studies. AIAA J., vol. 8, no. 6, June 1970, pp. 1026-1032.

12. Zelazny, S. W.; Morgenthaler, J. H.; and Herendeen, D. L.: Shear Stress and Turbulent Intensity Models for Coflowing Axisymmetric Streams. AIAA Paper 72-47, Jan. 1972.

13. Zakkay, Victor; Krause, Egon; and Woo, Stephen D. L.: Turbulent Transport Properties for Axisymmetric Heterogeneous Mixing. PIBAL Rep. No. 813 (Contract AF 33(616)-7661), Polytech. Inst. Brooklyn, Mar. 1964. (Available from DDC as AD 460 970.)

14. Ferri, Antonio; Libby, Paul A.; and Zakkay, Victor: Theoretical and Experimental Investigation of Supersonic Combustion. ARL 62-467, U.S. Air Force, Sept. 1962.

15. Ferri, Antonio; Libby, Paul A.; and Zakkay, Victor: Theoretical and Experimental Investigation of Supersonic Combustion. PIBAL-713 (Contract AF 49(638)-217), Polytech. Inst. Brooklyn, Sept. 1962.

16. Donaldson, Coleman duP.; and Gray, K. Evan: Theoretical and Experimental Investigation of the Compressible Free Mixing of Two Dissimilar Gases. AIAA J., vol. 4, no. 11, Nov. 1966, pp. 2017-2025.

17. Cohen, L. S.: A New Kinematic Eddy Viscosity Model. Rep. G211709-1, United Aircraft Corp., Jan. 1968.

18. Schetz, Joseph A.: Turbulent Mixing of a Jet in a Coflowing Stream. AIAA J., vol. 6, no. 10, Oct. 1968, pp. 2008-2010.

19. Schetz, Joseph A.: Unified Analysis of Turbulent Jet Mixing. NASA CR-1382, 1969.

20. Harsha, Philip Thomas: Free Turbulent Mixing: A Critical Evaluation of Theory and Experiment. AEDC-TR-71-36, U.S. Air Force, Feb. 1971. (Available from DDC as AD 718 956.)

21. Morgenthaler, John H.: Supersonic Mixing of Hydrogen and Air. NASA CR-747, 1967.

22. Morgenthaler, John H.; and Marchello, Joseph M.: Turbulent Transport Coefficients in Supersonic Flow. Int. J. Heat & Mass Transfer, vol. 9, no. 12, Dec. 1966, pp. 1401-1418.

23. Morgenthaler, J. H.: Mixing in High Speed Flow. Rep. No. 9500-920143, Bell Aerosystems Co., Oct. 1968.

24. Bradshaw, P.; and Ferriss, D. H.: Calculation of Boundary-Layer Development Using the Turbulent Energy Equation. II – Compressible Flow on Adiabatic Walls. NPL Aero Rep. 1217, Brit. A.R.C., Nov. 24, 1966.

25. Zawacki, Thomas S.; and Weinstein, Herbert: Experimental Investigation of Turbulence in the Mixing Region Between Coaxial Streams. NASA CR-959, 1968.

26. Sami, Sedat: Velocity and Pressure Fields of a Diffusing Jet. Ph. D. Diss., Univ. of Iowa, 1966.

27. Sami, Sedat: Balance of Turbulence Energy in the Region of Jet-Flow Establishment. J. Fluid Mech., vol. 29, pt. 1, July 18, 1967, pp. 81-92.

28. Sami, Sedat; Carmody, Thomas; and Rouse, Hunter: Jet Diffusion in the Region of Flow Establishment. J. Fluid Mech., vol. 27, pt. 2, Feb. 2, 1967, pp. 231-252.

29. Wygnanski, I.; and Fiedler, H.: Some Measurements in the Self Preserving Jet. D1-82-0712, Flight Sci. Lab., Boeing Sci. Res. Lab., Apr. 1968.

30. Wygnanski, I.; and Fiedler, H.: Some Measurements in the Self-Preserving Jet. J. Fluid Mech., vol. 38, pt. 3, Sept. 18, 1969, pp. 577-612.

31. Chriss, D. E.: Experimental Study of the Turbulent Mixing of Subsonic Axisymmetric Gas Streams. AEDC-TR-68-133, U.S. Air Force, Aug. 1968. (Available from DDC as AD 672 975.)

32. Eggers, James M.: Velocity Profiles and Eddy Viscosity Distributions Downstream of a Mach 2.22 Nozzle Exhausting to Quiescent Air. NASA TN D-3601, 1966.

33. Gibson, M. M.: Spectra of Turbulence in a Round Jet. J. Fluid Mech., vol. 15, pt. 2, Feb. 1963, pp. 161-173.

34. Brown, Garry; and Roshko, Anatol: The Effect of Density Difference on the Turbulent Mixing Layer. Turbulent Shear Flows, AGARD-CP-93, Jan. 1972, pp. 23-1 – 23-12.

35. Clauser, Francis H.: The Turbulent Boundary Layer. Vol. IV of Advances in Applied Mechanics, H. L. Dryden and Th. von Kármán, eds., Academic Press, Inc., 1956, pp. 1-51.

36. Zelazny, Stephen W.: Eddy Viscosity in Quiescent and Coflowing Axisymmetric Jets. AIAA J., vol. 9, no. 11, Nov. 1971, pp. 2292-2294.

37. Zelazny, Stephen William: Modeling of Turbulent Axisymmetric Coflowing Streams and Quiescent Jets: A Review and Extension. Ph. D. Diss., State Univ. of New York at Buffalo, Sept. 1972.

38. Maestrello, L.; and McDaid, E.: Acoustic Characteristics of a High-Subsonic Jet. AIAA J., vol. 9, no. 6, June 1971, pp. 1058-1066.

39. Heck, P. H.: Jet Plume Characteristics of 72-Tube and 72-Hole Primary Suppressor Nozzles. T.M. No. 69-457 (FAA Contract FA-SS-67-7), Flight Propulsion Div., Gen. Elec. Co., July 1969.

40. Forstall, Walton, Jr.; and Shapiro, Ascher H.: Momentum and Mass Transfer in Coaxial Gas Jets. J. Appl. Mech., vol. 17, no. 4, Dec. 1950, pp. 399-408.

41. Eggers, James M.: Turbulent Mixing of Coaxial Compressible Hydrogen-Air Jets. NASA TN D-6487, 1971.

42. Chevray, R.: The Turbulent Wake of a Body of Revolution. Trans. ASME, Ser. D: J. Basic Eng., vol. 90, no. 2, June 1968, pp. 275-284.

43. Demetriades, Anthony: Mean-Flow Measurements in an Axisymmetric Compressible Turbulent Wake. AIAA J., vol. 6, no. 3, Mar. 1968, pp. 432-439.

44. Chriss, D. E.; and Paulk, R. A.: An Experimental Investigation of Subsonic Coaxial Free Turbulent Mixing. AEDC-TR-71-236 (AFOSR-72-0237TR), U.S. Air Force, Feb. 1972. (Available from DDC as AD 737 098.)

45. Baker, A. J.; Moon, L. F.; Morgenthaler, J. H.; and Peschke, W. T.: Project 8(R) Fluid Mechanics and Combustion Technology. Rep. No. 9500-920246, Bell Aerospace Co., Jan. 1972.

46. Morgenthaler, J. H.; Zelazny, S. W.; and Herendeen, D. L.: Combustor Correlation Technique. AIAA Paper No. 72-1074, Nov.-Dec. 1972.

47. Alpinieri, Louis J.: Turbulent Mixing of Coaxial Jets. AIAA J., vol. 2, no. 9, Sept. 1964, pp. 1560-1567.

TABLE 1.- COAXIAL JET MIXING DATA USED IN MODEL DEVELOPMENT

[External gas stream was air in all cases]

Investigator	Case number	Jet gas	D, mm	D, in.	ρ_j, kg/m^3	ρ_j, lbm/ft^3	U_j, m/sec	U_j, ft/sec	$(z/D_j)_{min}$	$(z/D_j)_{max}$	$\frac{(U)_j}{(U)_e}$	$\frac{(\rho u)_j}{(\rho u)_e}$	$\frac{(\rho u^2)_j}{(\rho u^2)_e}$	M_j	M_e
Chriss (ref. 31)	*1	H_2	12.7	0.5	87.6	5.47×10^{-3}	1005.8	3300	2.95	14.55	6.300	0.560	3.520	0.79	0.42
	*2	H_2	12.7	.5	92.7	5.79	975.4	3200	.49	14.50	4.400	.390	1.710	.79	.60
	*3	H_2	12.7	.5	87.8	5.48	929.6	3050	.42	20.80	3.800	.320	1.210	.73	.66
	*4	H_2	12.7	.5	85.7	5.35	731.5	2400	.50	20.80	3.000	.240	.720	.57	.67
	*5	H_2	12.7	.5	82.7	5.16	579.1	1900	.41	12.70	2.400	.190	.460	.44	.65
	6	H_2	12.7	.5	80.7	5.04	944.9	3100	.50	19.20	4.600	.620	2.850	.71	.42
	7	H_2	12.7	.5	79.3	4.95	746.8	2450	.50	16.30	3.200	.410	1.310	.56	.49
	8	H_2	12.7	.5	74.0	4.62	594.4	1950	.51	12.40	2.500	.300	.750	.43	.50
	9	Air	12.7	.5	1322.4	82.56	286.5	940	.50	14.30	2.400	3.600	8.650	.87	.71
Zakkay (ref. 13)	*1	H_2	7.6	.3	48.2	3.01	603.5	1980	10.0	30.00	1.460	.047	.069	.51	1.6
	2	H_2	7.6	.3	64.1	4.00	701.0	2300	13.3	30.00	1.690	.072	.122	.60	1.6
	3	H_2	7.6	.3	76.9	4.80	1002.8	3290	13.3	30.00	2.420	.124	.300	.89	1.6
	*4	He	7.6	.3	141.0	8.80	454.2	1490	13.3	30.00	1.100	.103	.113	.51	1.6
	5	He	7.6	.3	163.4	10.2	691.9	2270	13.3	26.70	1.670	.185	.309	.82	1.6
	6	Ar	7.6	.3	1633.8	102.0	219.5	720	13.3	30.00	.530	.590	.312	.82	1.6
	7	Ar	7.6	.3	2066.3	129.0	231.6	760	13.3	26.70	.560	.790	.442	.89	1.6
	8	Ar	7.6	.3	2354.6	147.0	256.0	840	16.7	30.00	.620	.976	.605	1.00	1.6
Eggers (ref. 32)	*1	Air	25.4	1.0	2402.7	150.0	539.2	1769	.0	75.00				2.22	.0
Eggers and Torrence (ref. 7)	*1	Air/ethylene	24.4	.96	1457.6	91.0	289.6	950	.0	49.00	.740	.640	.447	.90	1.3
Alpinieri (ref. 47)	1	CO_2	50.8	2.0	2162.4	135.0	95.1	312	5.25	12.50	.470	.660	.310		
	*2	CO_2	50.8	2.0	2226.5	139.0	128.6	422	5.25	12.50	.650	.950	.617		
	3	CO_2	50.8	2.0	2114.4	132.0	154.2	506	5.25	12.50	.780	1.170	.912		
Zawacki and Weinstein (ref. 25)	*1	Air	18.14	.714	1217.4	76.0	.366	1.20	.0	11.30	.025	.025	.001		
	*2	Air	18.14	.714	1217.4	76.0	.503	1.65	.0	11.30	.035	.036	.001		
	3	Air	18.14	.714	1217.4	76.0	.920	3.02	.0	14.00	.063	.063	.004		
	*4	Air	18.14	.714	1217.4	76.0	1.829	6.00	.0	14.00	.125	.125	.063		
	*5	Air	18.14	.714	1217.4	76.0	4.328	14.2	.0	21.00	.294	.294	.089		
	6	Air	18.14	.714	1217.4	76.0	14.630	48.0	1.40	14.00	1.000	1.000	1.000		
	7	Freon 12	18.14	.714	4869.5	304.0	1.207	3.96	.35	14.00	.086	.344	.030		
	*8	Freon 12	18.14	.714	4837.4	302.0	2.621	8.60	.35	21.60	.179	.714	.127		
	*9	Freon 12	18.14	.714	4869.5	304.0	1.341	4.4	.35	14.00	.185	.740	.137		
	*10	Freon 12	18.14	.714	4837.4	302.0	.564	1.85	.35	14.00	.132	.526	.070		
Sami (refs. 26 to 28)	*1	Air	304.8	12.0	1217.4	76.0	10.668	35.0	1.00	10.00					
Wygnanski (refs. 29 and 30)	†1	Air	25.5	1.004	1217.4	76.0	57.912	190.0	5.00	100.00					

*(1) Momentum integral balances were within 4 percent of their average value at any axial station.
(2) Injected mass integral balances were within 20 percent of their average value at any axial station and were within 13 percent of their average value at 80 percent of the axial stations.

†Detailed profiles not available.

TABLE 2.- AXISYMMETRIC FREE TURBULENT SHEAR LAYER DATA FOR NASA LANGLEY WORKSHOP TEST CASES

Investigator	Test case	Jet gas	D, mm	D, in.	ρ_j, kg/m^3	ρ_j, lbm/ft^3	U_j, m/sec	U_j, ft/sec	U_e, m/sec	U_e, ft/sec	$(z/D_j)_{min}$	$(z/D_j)_{max}$	$\frac{(U)_j}{(U)_e}$	$\frac{(\rho U)_j}{(\rho U)_e}$	$\frac{(\rho U^2)_j}{(\rho U^2)_e}$	M_j	M_e
Maestrello and McDaid (ref. 38)	6	Air	61.98	2.44	1.310	0.0818	211.2	693.0	0	0.0	1.0	39.6	∞	∞	∞	0.65	0.0
Eggers (ref. 32)	7	Air	25.578	1.007	2.404	.1501	539.19	1769.0	0	.0	.0	74.7	∞	∞	∞	2.22	.0
Heck (ref. 39)	8	Air	109.22	4.30	.532	.0332	318.52	1045.0	0	.0	2.79	19.53	∞	∞	∞	.70	.0
Forstall (ref. 40)	9	[a]Air	6.35	.25	1.113	.0695	36.58	120.0	9.144	30.0	.0	80.0	4.0	3.7	14.8	.10	.03
Chriss (ref. 31)	10	H_2	12.7	.50	.088	.0055	1005.84	3300.0	157.58	517.0	2.97	14.55	6.3	.56	3.52	.79	.421
Eggers and Torrence (ref. 7)	11	[b]Air	24.384	.96	1.458	.091	289.56	950.0	390.14	1280.0	.0	49.0	.74	.64	.47	.9	1.3
Eggers (ref. 41)	12	H_2	11.608	.457	.096	.00601	1074.12	3524.0	394.11	1293.0	.0	63.0	2.72	.163	.443	.89	1.32
Chevray (ref. 42)	15	Air	254.00	[c]10.0	1.217	.0760	-------	------	27.43	90.0	.0	18.0	----	-----	------	----	.09
Demetriades (ref. 43)	17	Air	3.962	[d].156	-----	-------	-------	------	679.09	2228.0	17.0	58.7	----	-----	------	----	2.94
Wygnanski and Fiedler (refs. 29 and 30)	18	Air	26.416	1.04	1.217	.0760	58.52	192.0	0	.0	5.0	100.0	----	-----	------	.18	.0
Heck (ref. 39)	19	Air	109.22	4.3	.392	.0245	841.86	2762.0	0	.0	2.79	19.53	----	-----	------	1.41	.0
Chriss and Paulk (ref. 44)	20	[e]Air	12.7	.5	.625	.0390	121.92	400.0	58.52	192.0	1.92	18.10	2.08	1.98	4.13	.26	.13
Chriss (ref. 31)	21	H_2	12.7	.5	.086	.0054	746.76	2450.0	233.48	766.0	2.58	16.32	3.20	.44	1.40	.55	.49
Eggers (ref. 41)	22	H_2	11.608	.457	.096	.0060	1109.47	3640.0	606.55	1990.0	.0	58.0	1.83	.06	.11	.91	2.50

[a] 10 percent helium tracer by volume.
[b] 1 percent ethylene tracer by volume.
[c] Six to one prolate spheroid, 5 ft long.
[d] Base diameter of a suspended rod.
[e] 2 percent hydrogen tracer by volume.

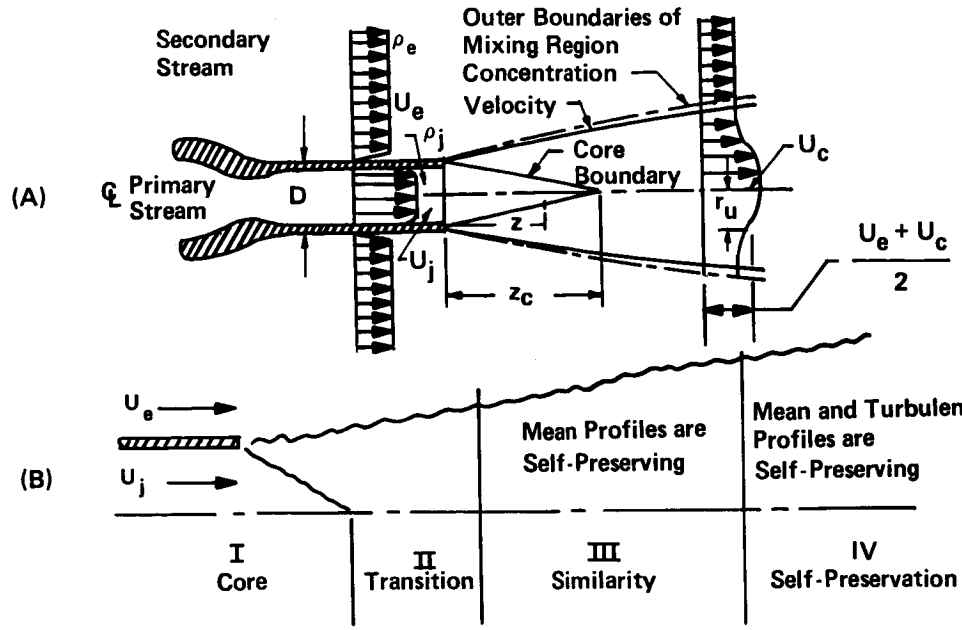

Figure 1.- Schematic of coaxial turbulent jet and definition of mixing regions.

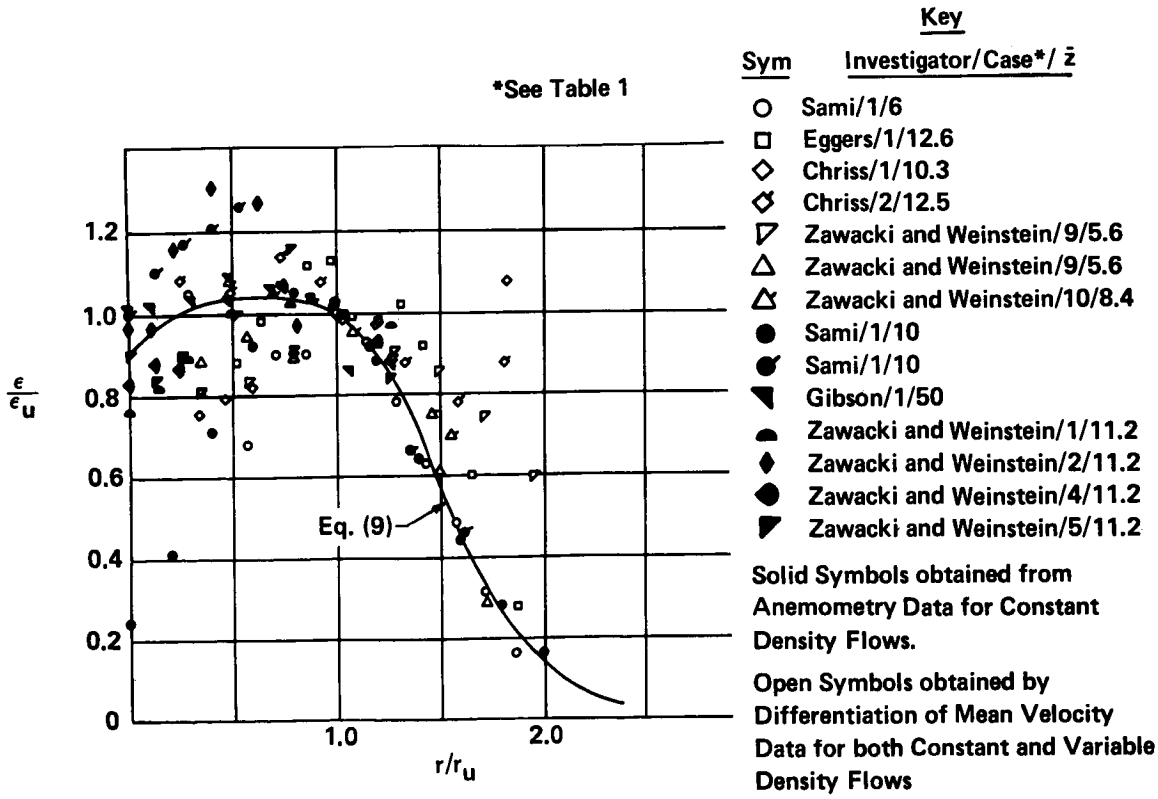

Figure 2.- Radial variation of ϵ/ϵ_u.

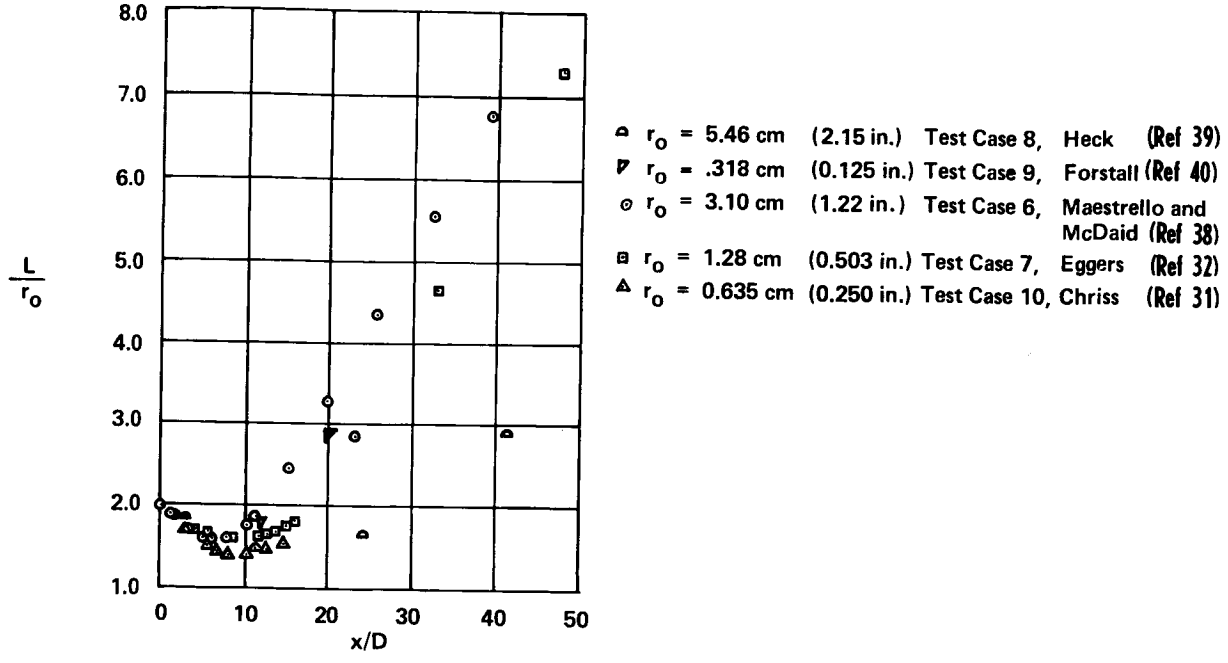

Figure 3.- Predicted characteristic length (eq. (7)).

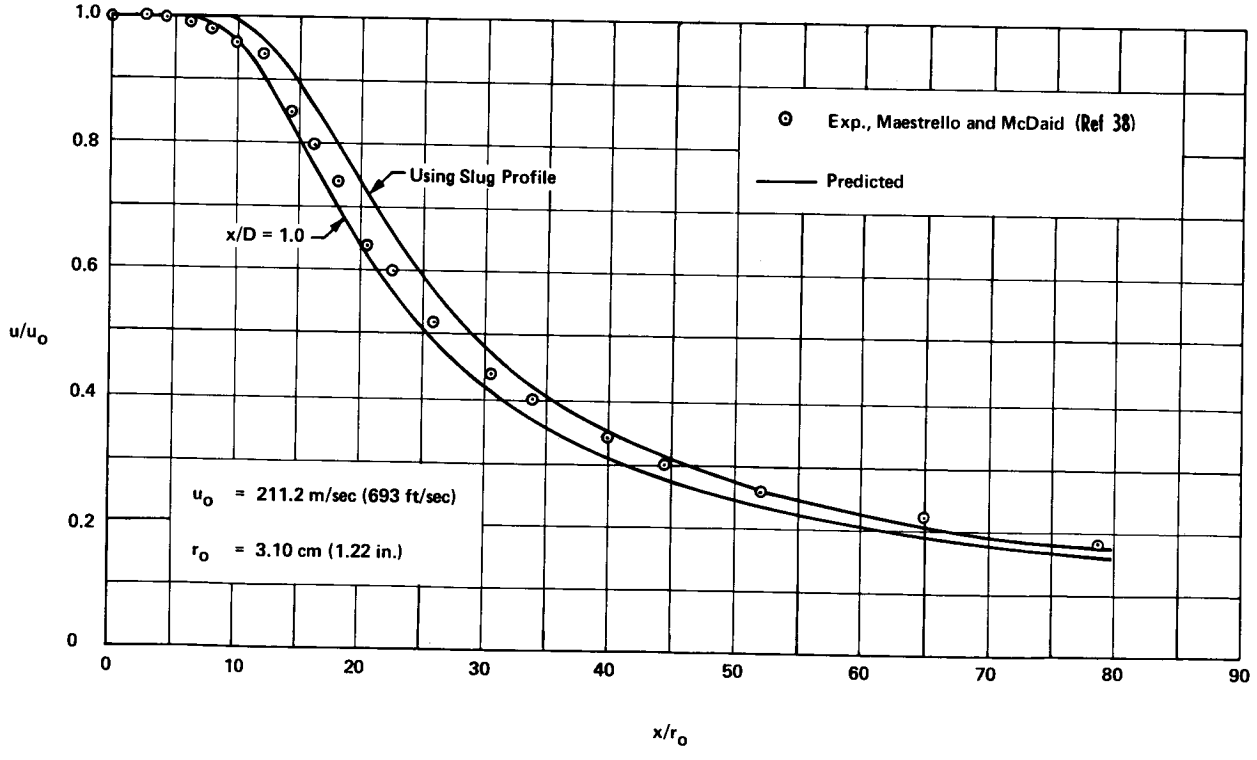

Figure 4.- Predicted and experimental center-line velocity for test case 6 (Maestrello and McDaid (ref. 38)).

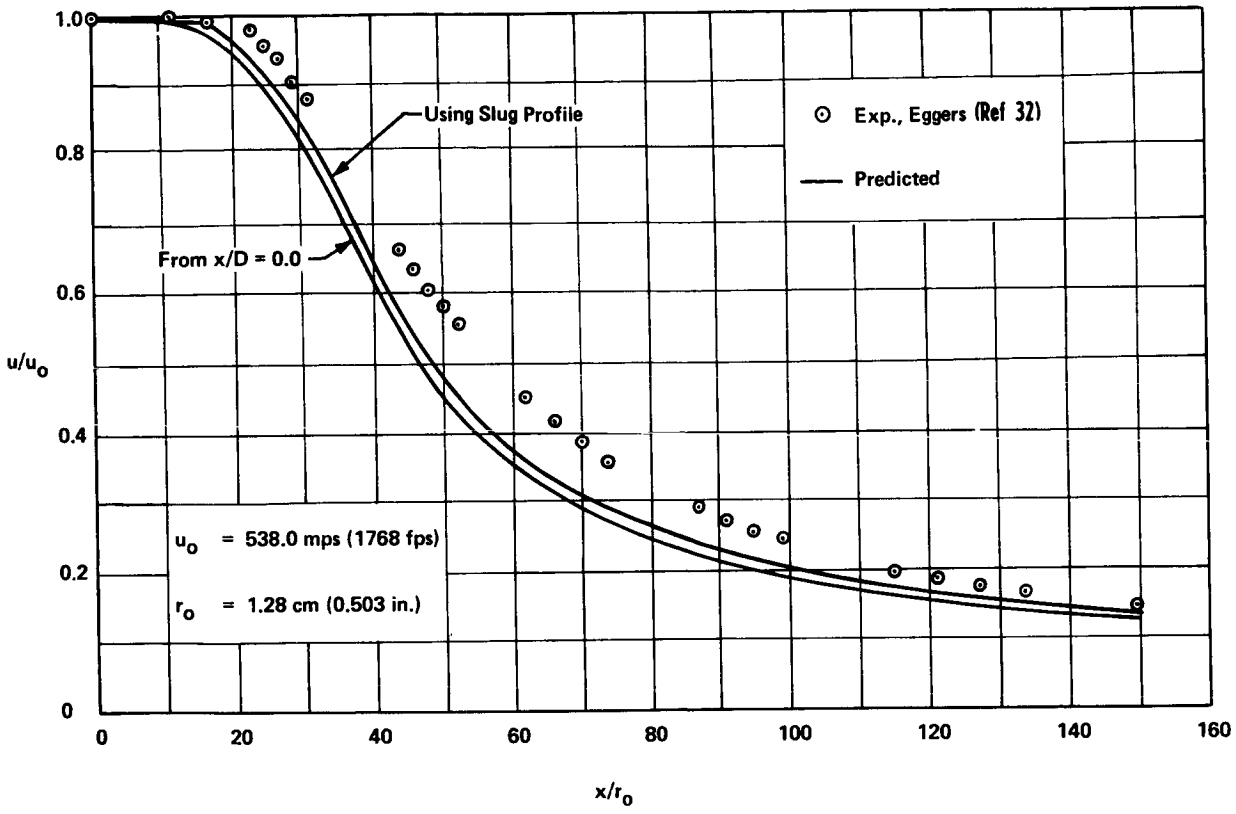

(a) Center-line velocity.

Figure 5.- Comparison of predicted and experimental velocities for test case 7 (Eggers (ref. 32)).

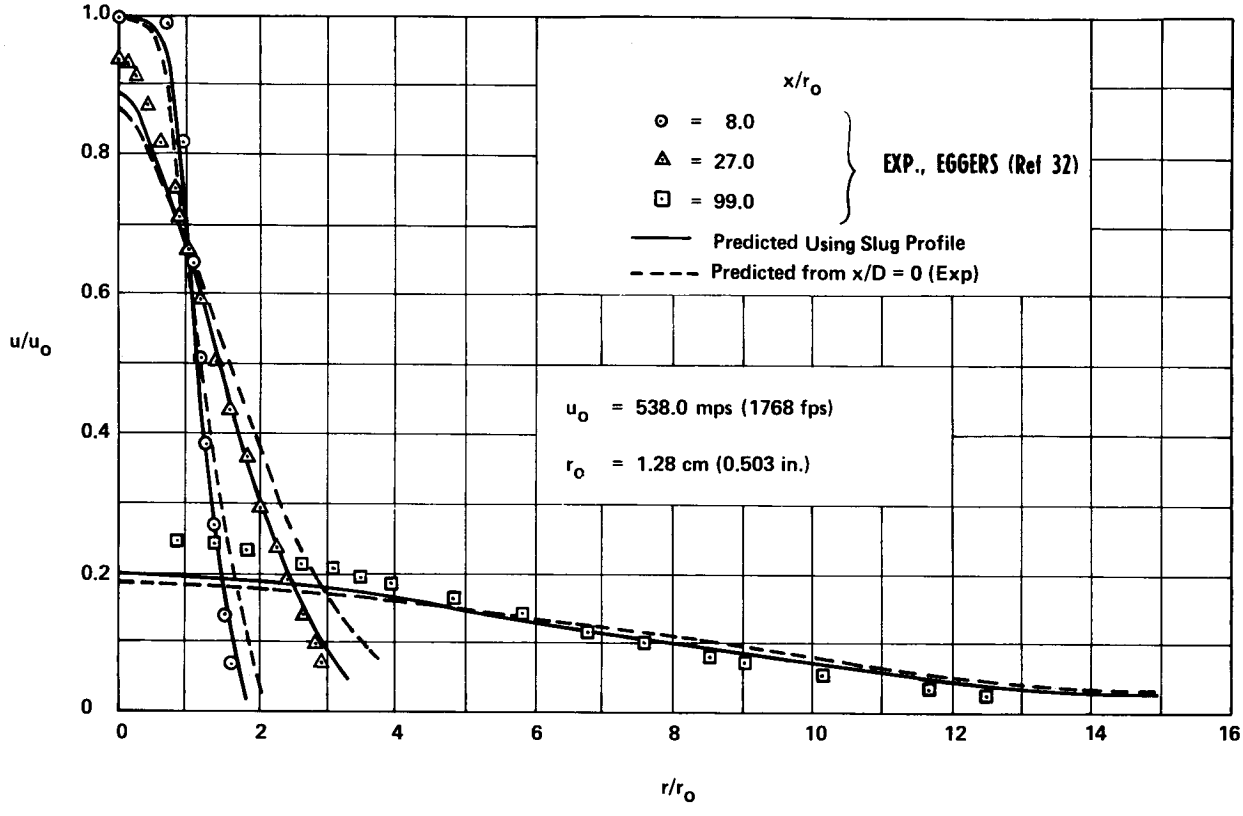

(b) Axial velocity against distance from center line.

Figure 5.- Concluded.

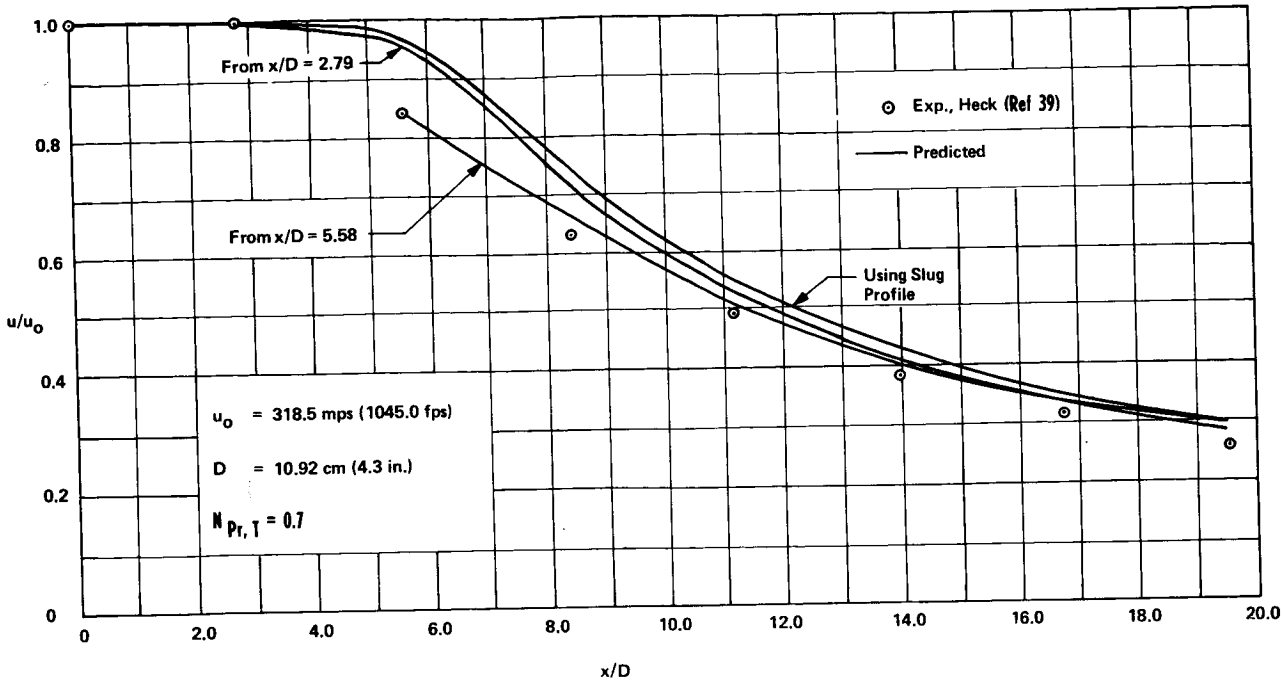

(a) Center-line velocity.

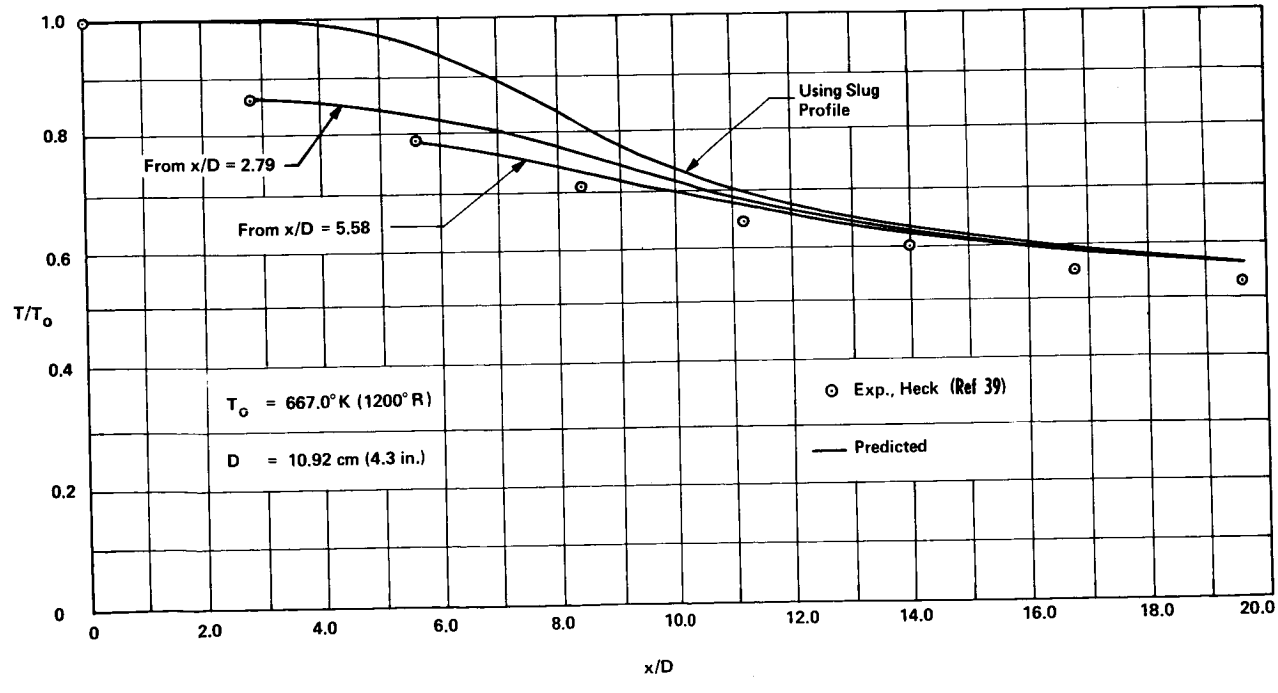

(b) Center-line total temperature.

Figure 6.- Comparison of predicted and experimental velocities and total temperatures for test case 8 (Heck (ref. 39)).

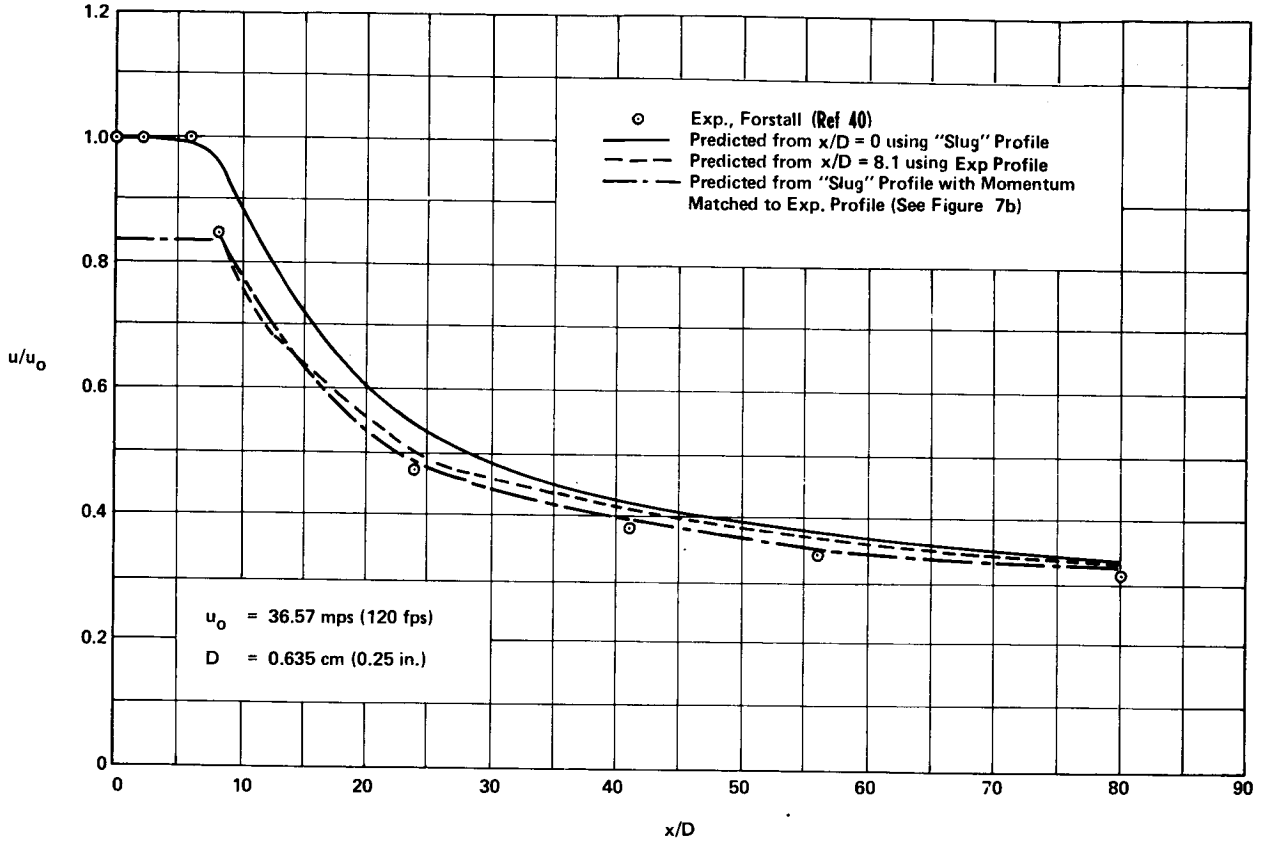

(a) Predicted and experimental center-line velocity

Figure 7.- Velocity and slug profiles for test case 9 (Forstall (ref. 40)).

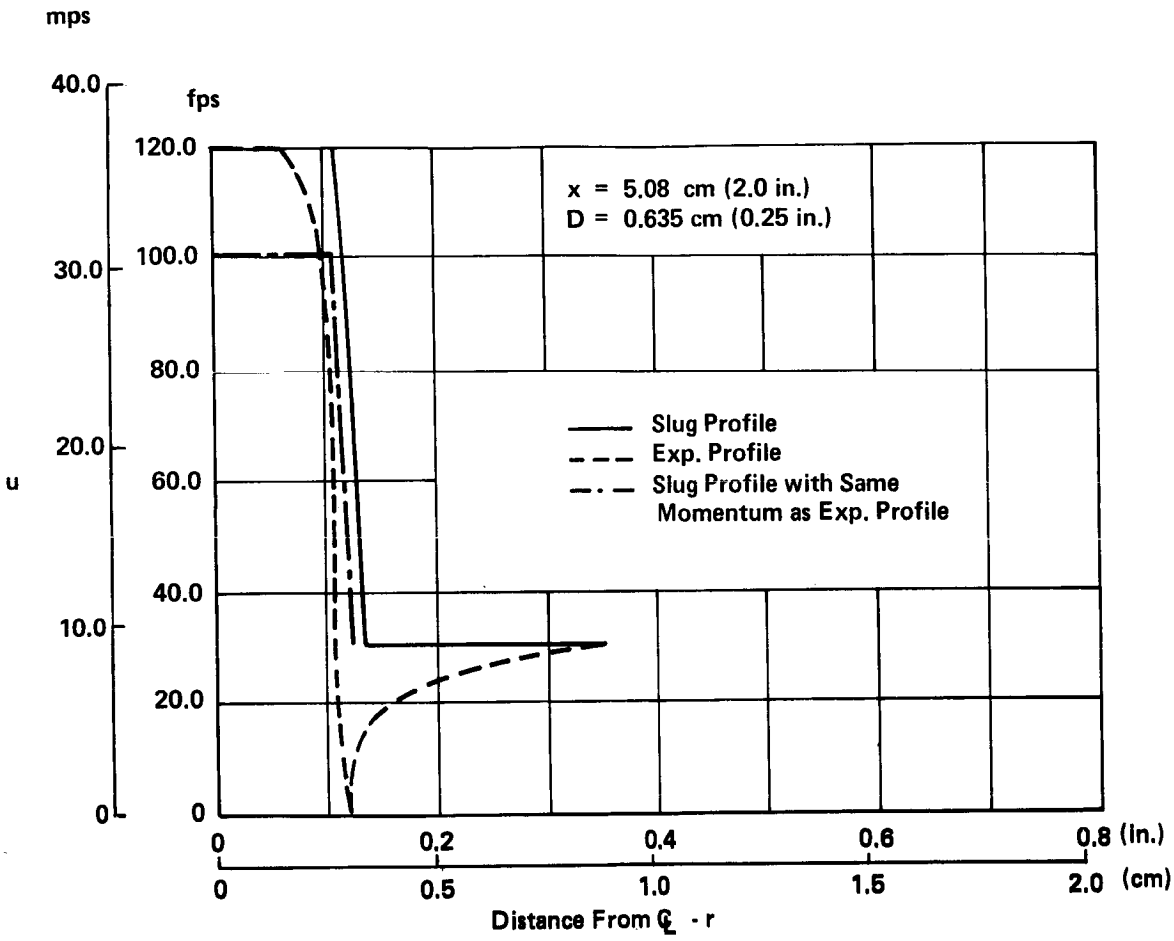

(b) Experimental and assumed slug profile at $x/D = 0$.

Figure 7.- Concluded.

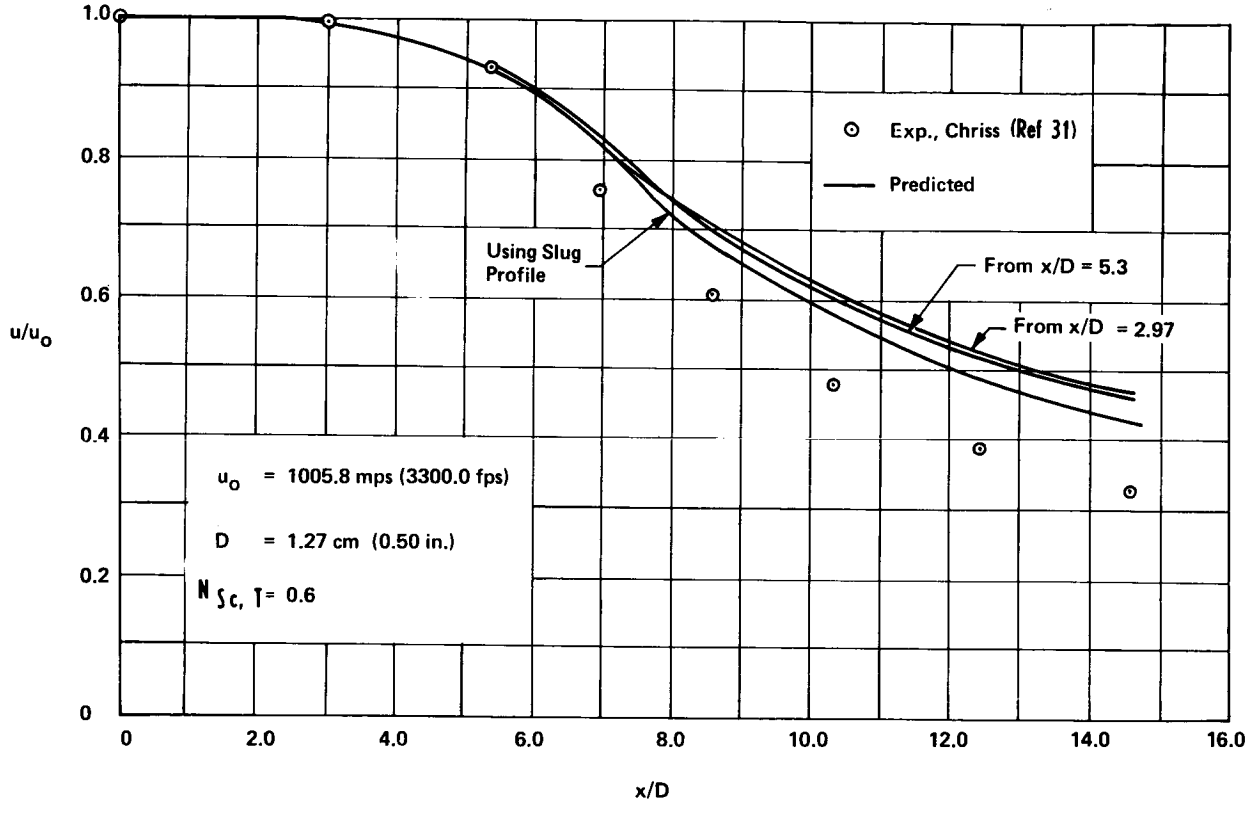

(a) Predicted and experimental center-line velocity.

Figure 8.- Velocities and H_2 mass fraction for test case 10 (Chriss (ref. 31)).

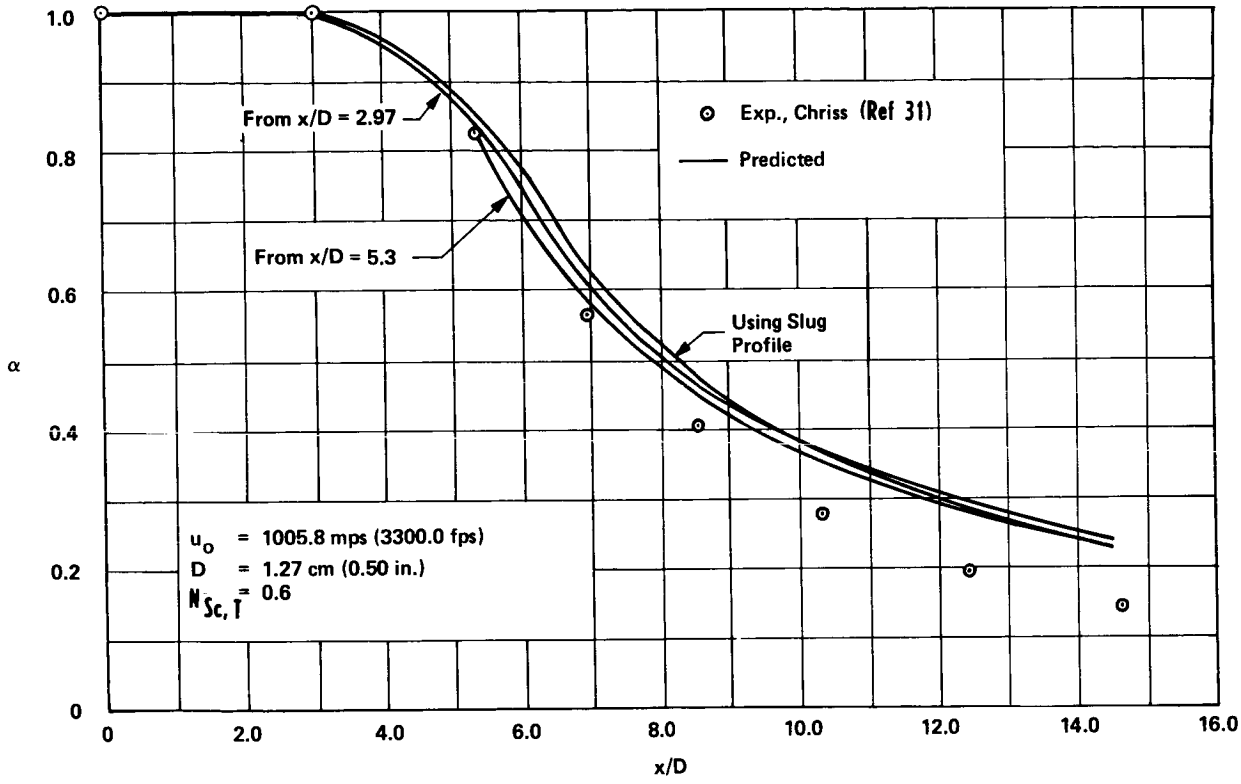

(b) Predicted and experimental center-line H_2 mass fraction.

Figure 8.- Continued.

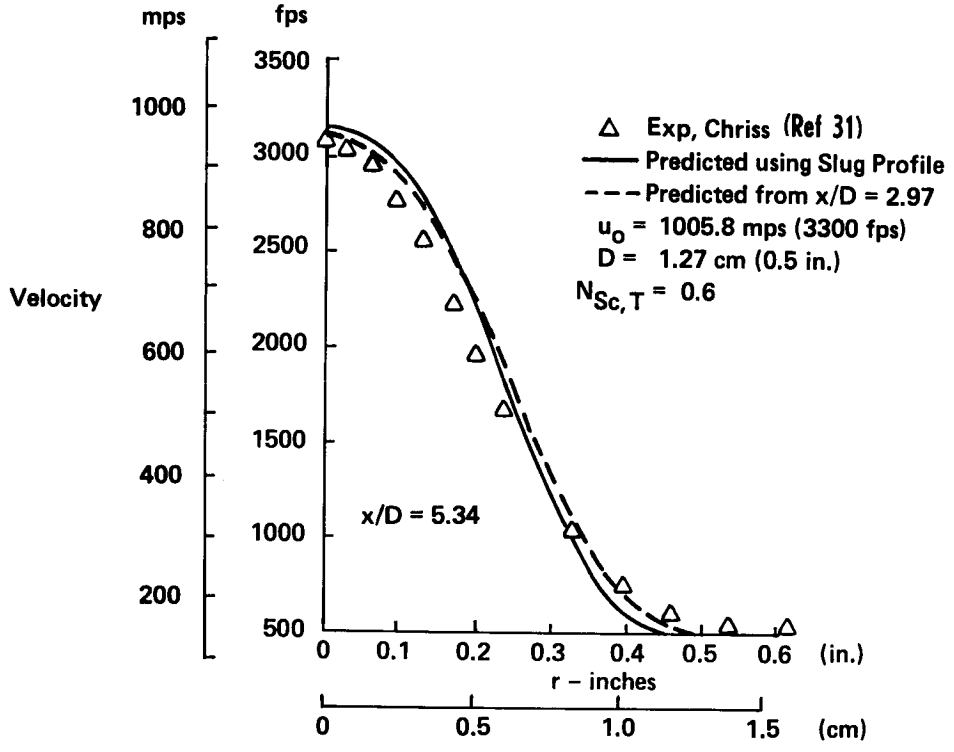

(c) Predicted and experimental axial velocity as a function of distance from center line at x/D = 5.34.

Figure 8.- Concluded.

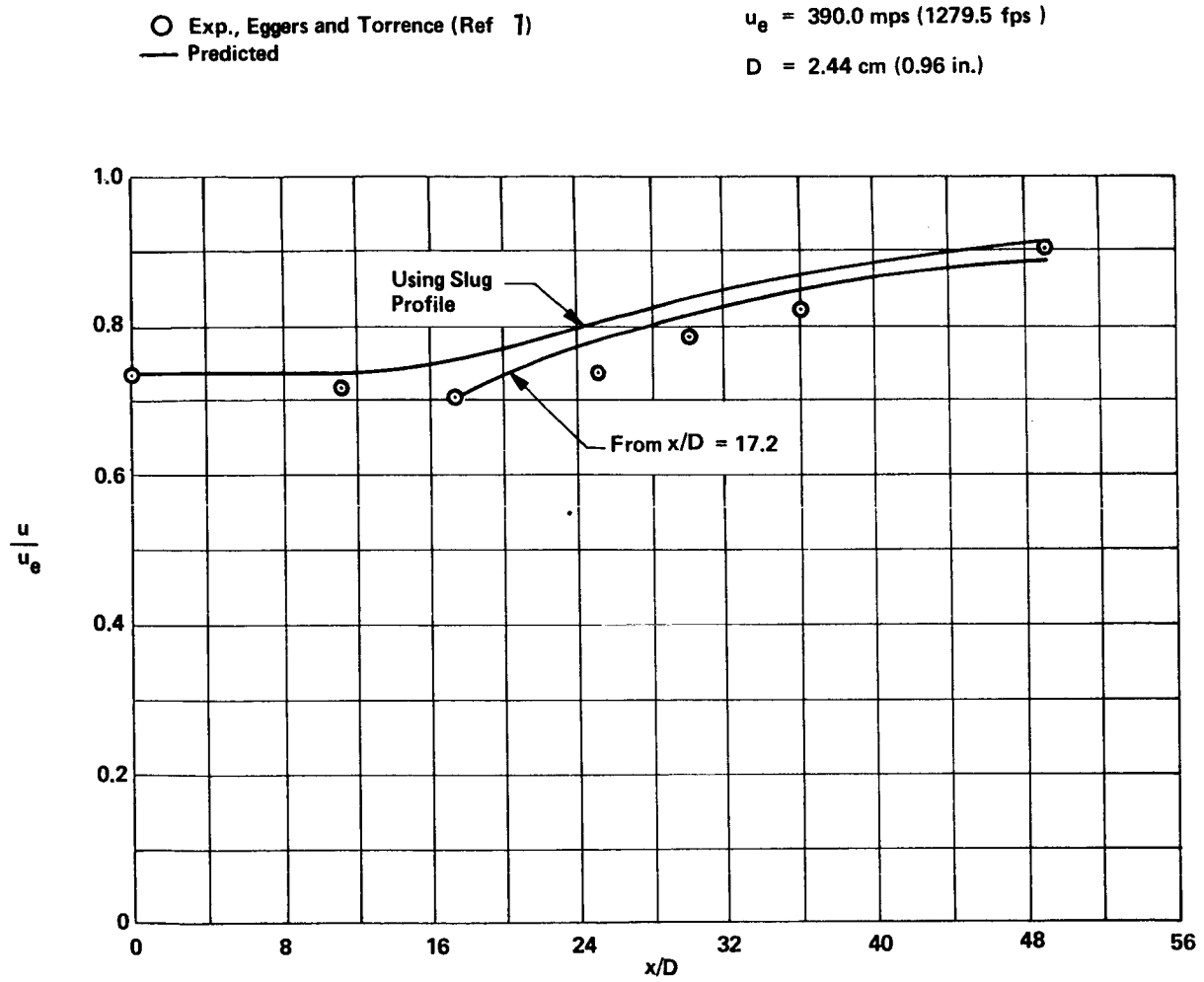

Figure 9.- Predicted and experimental center-line velocity for test case 11 (Eggers and Torrence (ref. 7)).

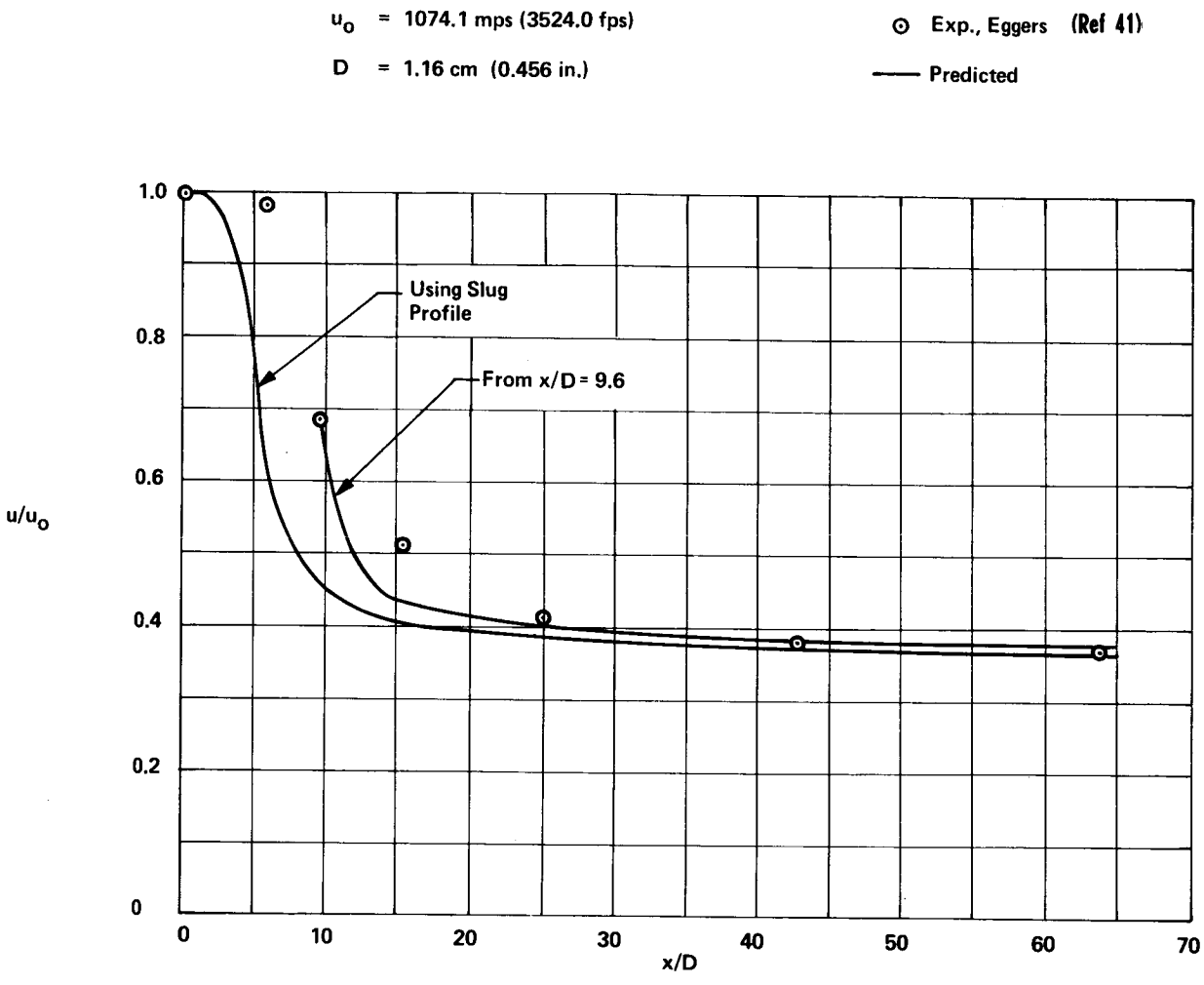

(a) Predicted and experimental center-line velocity.

Figure 10.- Velocities and H_2 mass fraction for test case 12 (Eggers (ref. 41)).

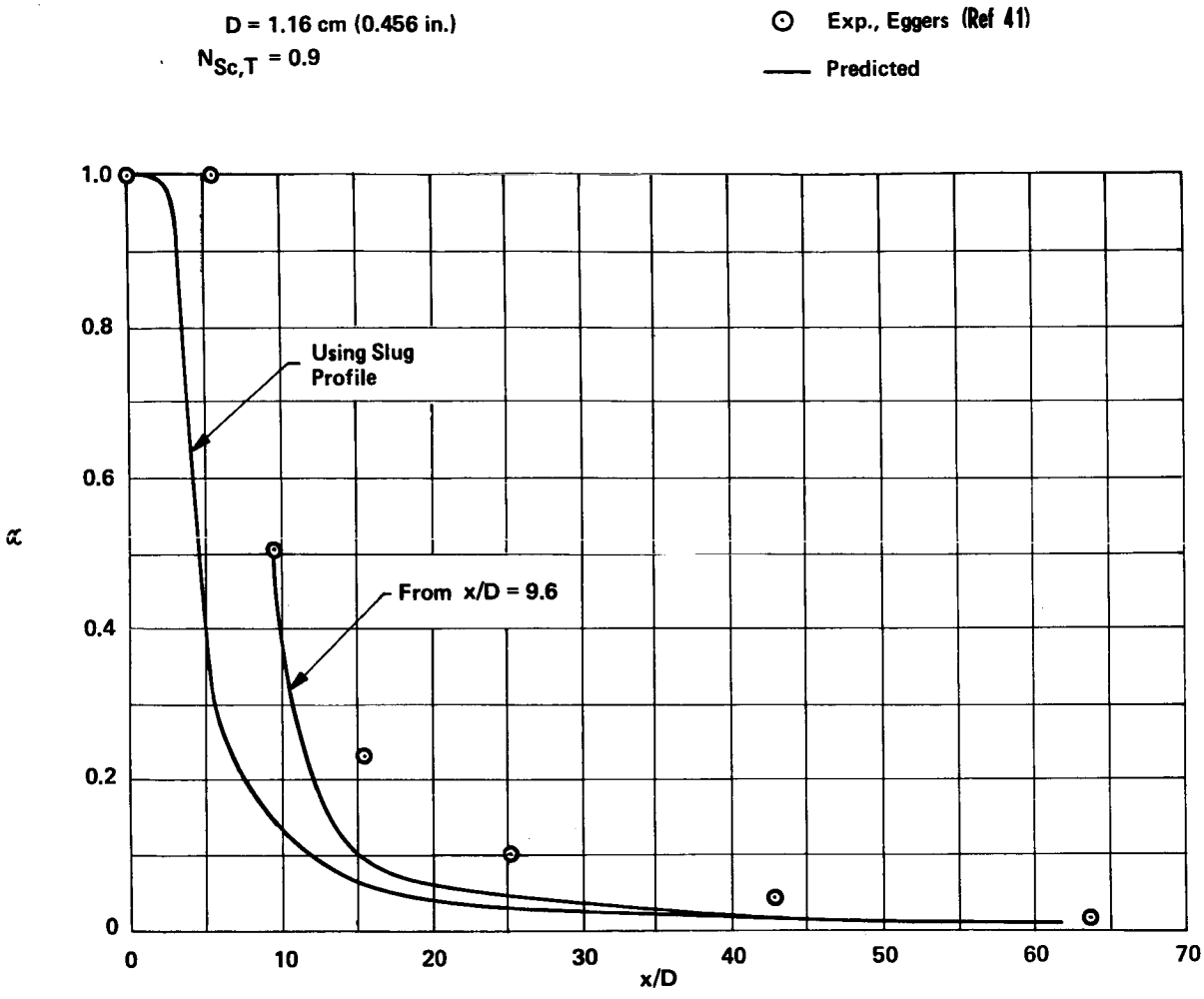

(b) Predicted and experimental center-line H_2 mass fraction.

Figure 10.- Concluded.

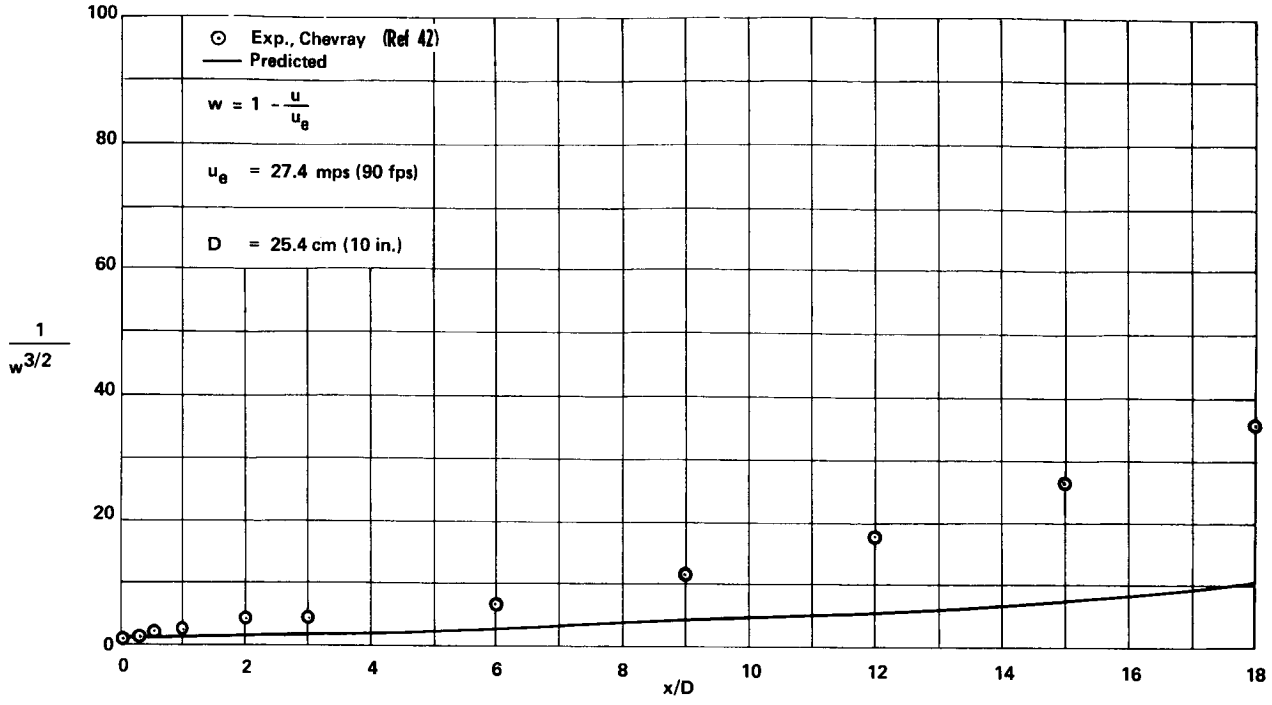

(a) Predicted and experimental center-line velocity. $(1 - u/u_e)^{-3/2}$ as a function of x/D.

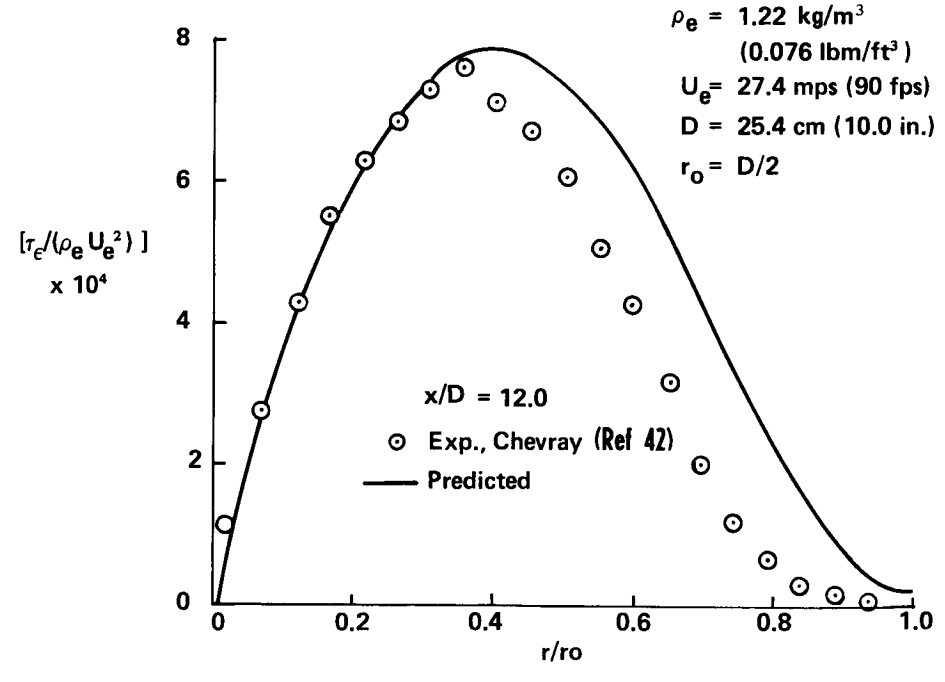

(b) Predicted and experimental shear stress profile at x/D = 12.0.

Figure 11.- Velocities and shear stress profiles for test case 15 (Chevray (ref. 42)).

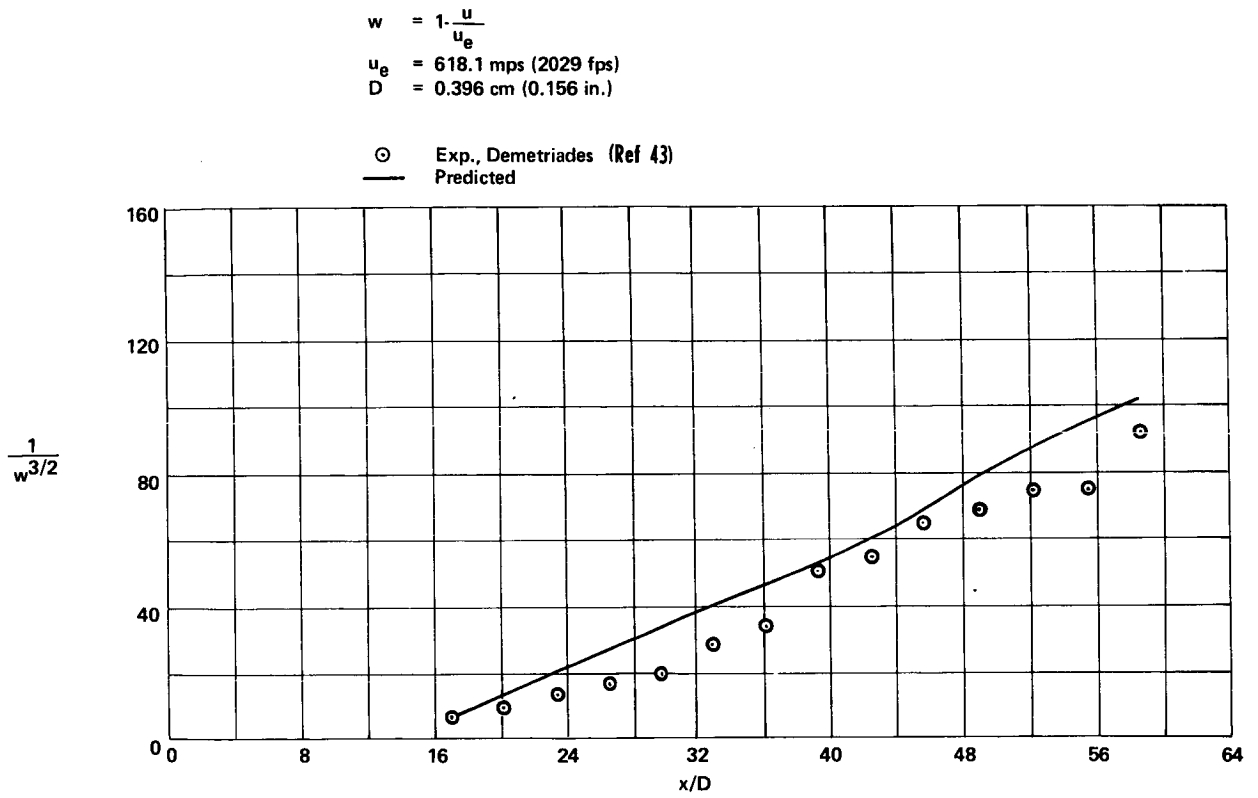

Figure 12.- Predicted and experimental center-line velocity for test case 17 (Demetriades (ref. 43)).

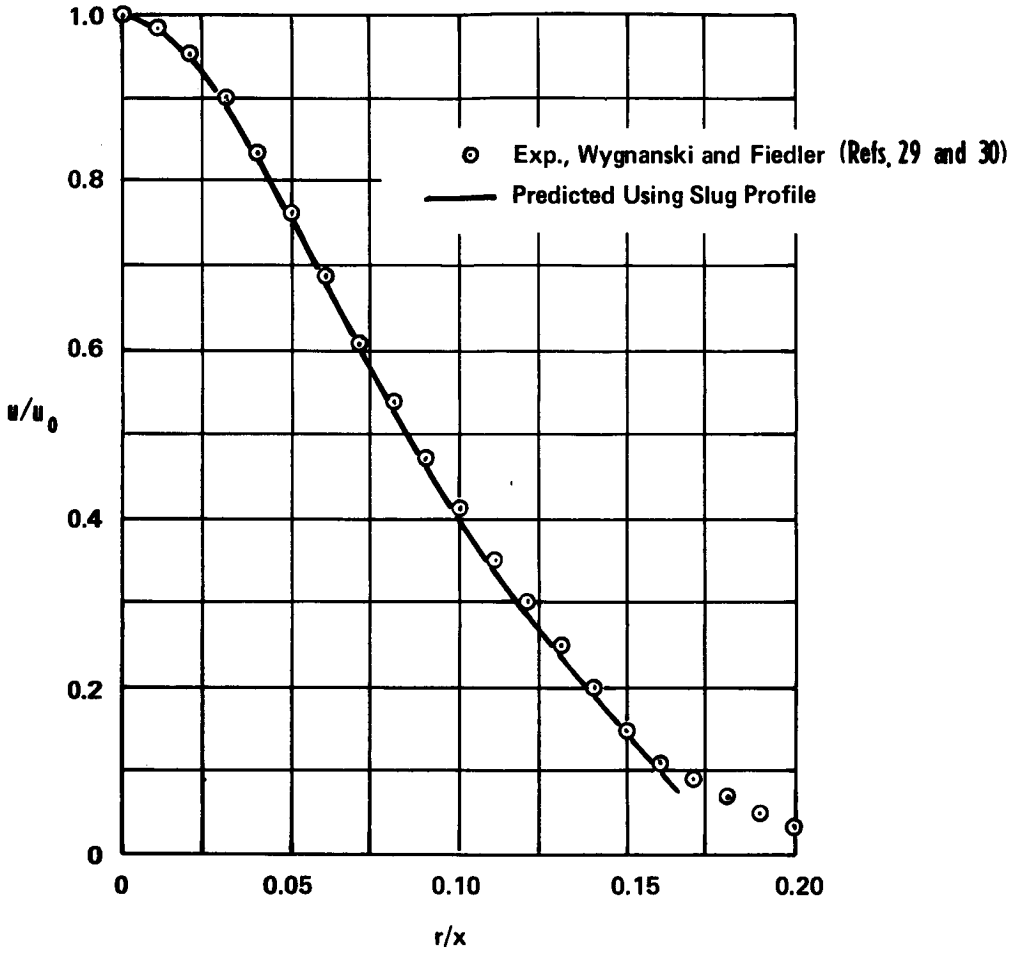

Figure 13.- Velocity profile in similarity coordinates for test case 18 (Wygnanski and Fiedler (refs. 29 and 30)).

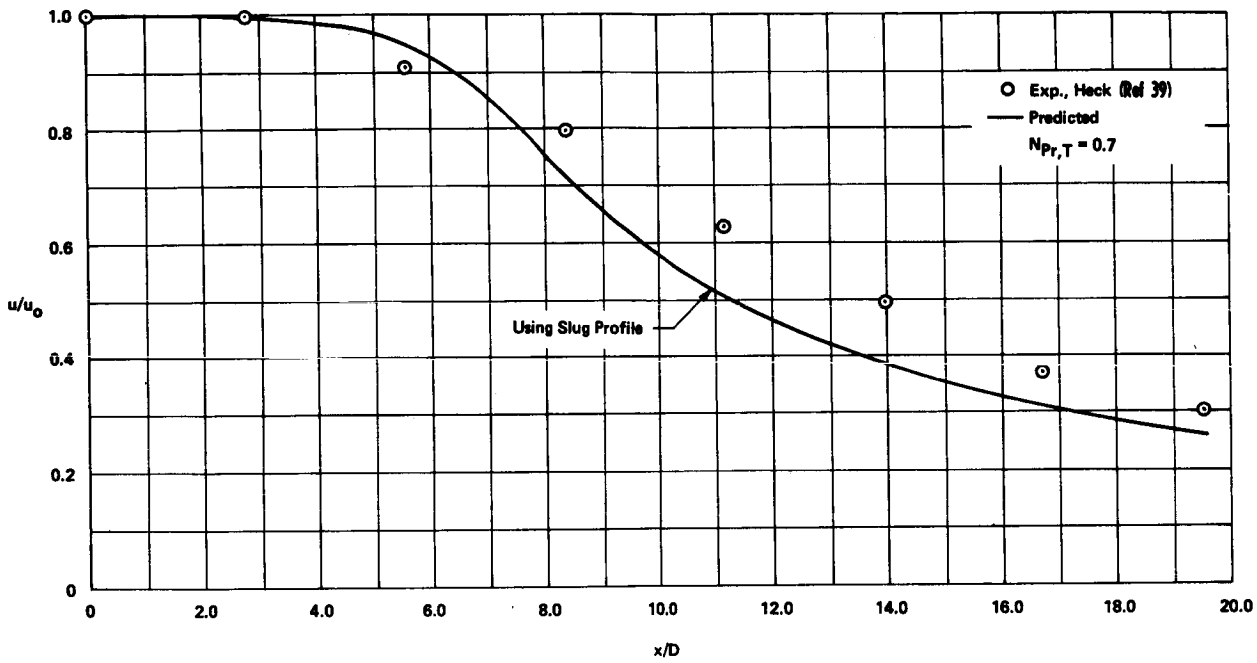

Figure 14.- Predicted and experimental center-line velocity for test case 19 (Heck (ref. 39)).

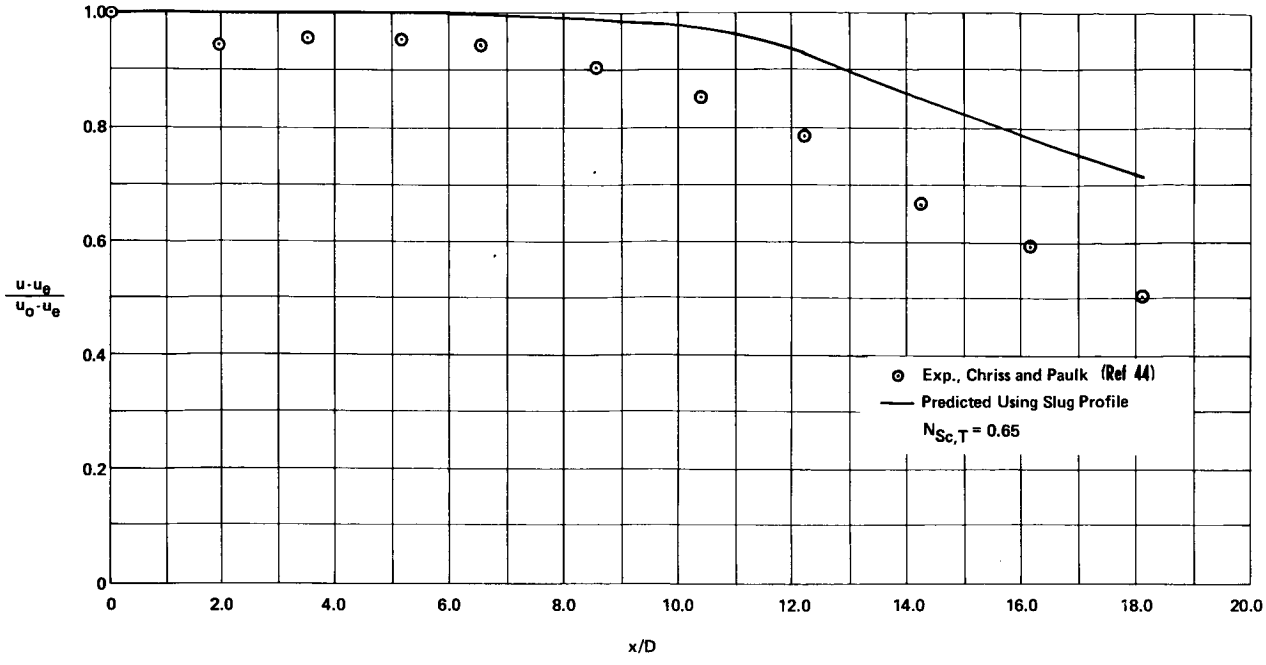

(a) Predicted and experimental center-line velocity.

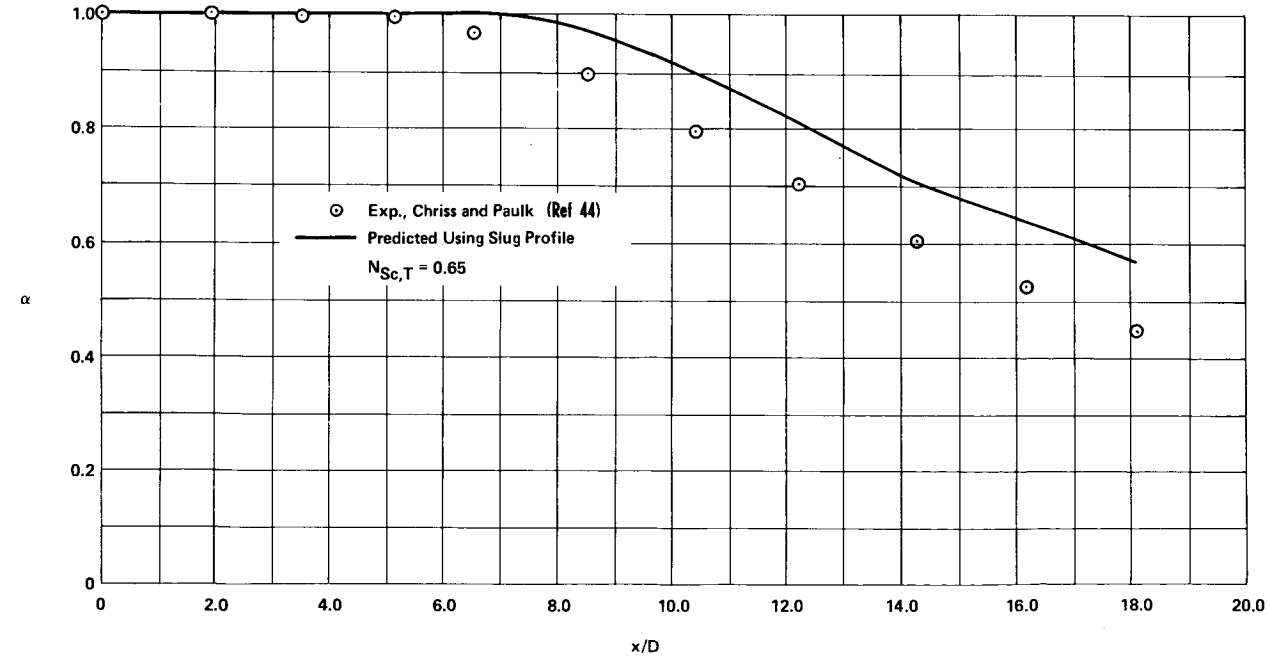

(b) Predicted and experimental center-line H_2 mass fraction.

Figure 15.- Velocities and mass fraction for test case 20 (Chriss and Paulk (ref. 44)).

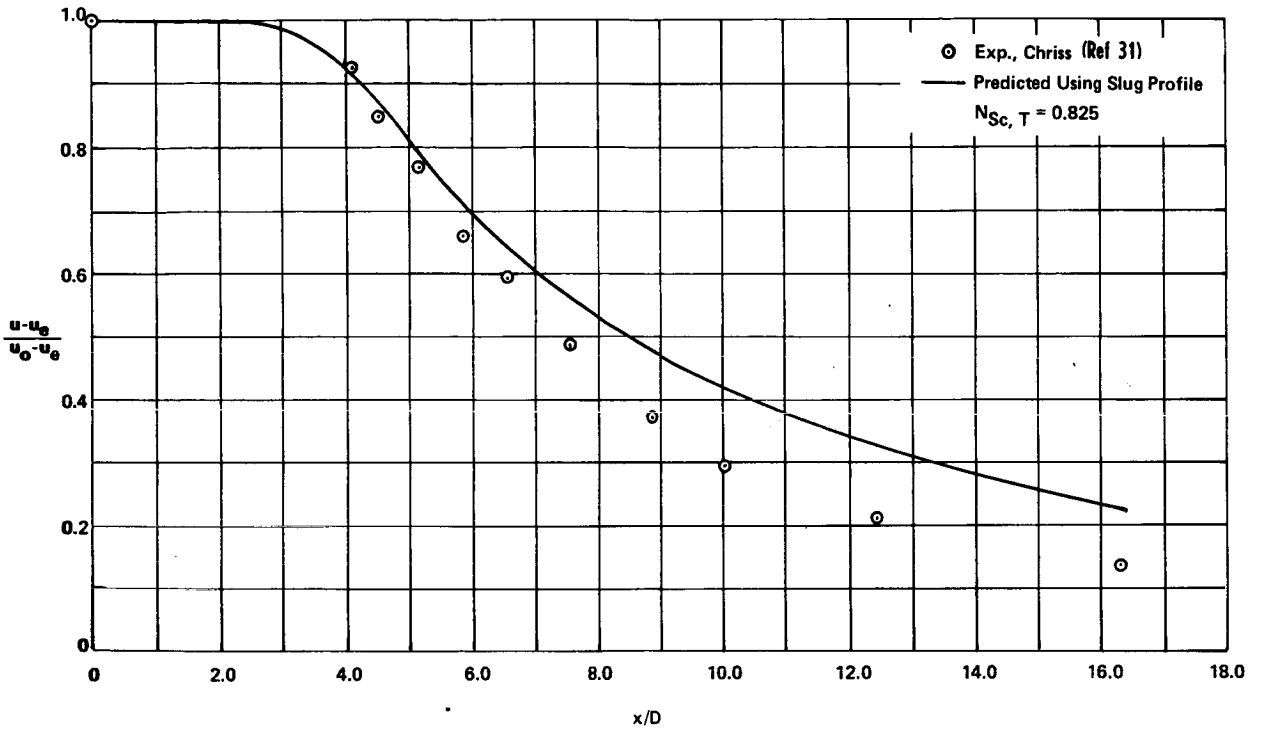

(a) Predicted and experimental center-line velocity.

Figure 16.- Velocities and mass fraction for test case 21 (Chriss (ref. 31)).

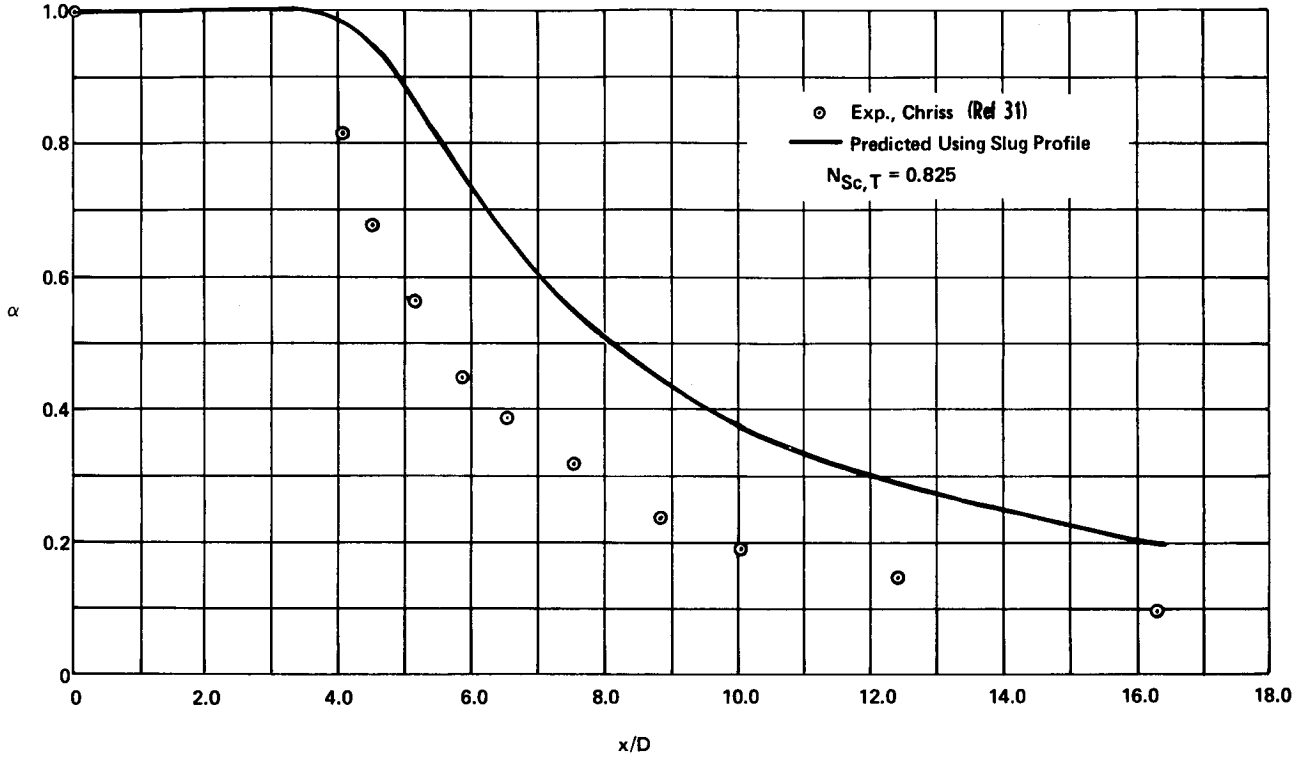

(b) Predicted and experimental center-line H_2 mass fraction.

Figure 16.- Concluded.

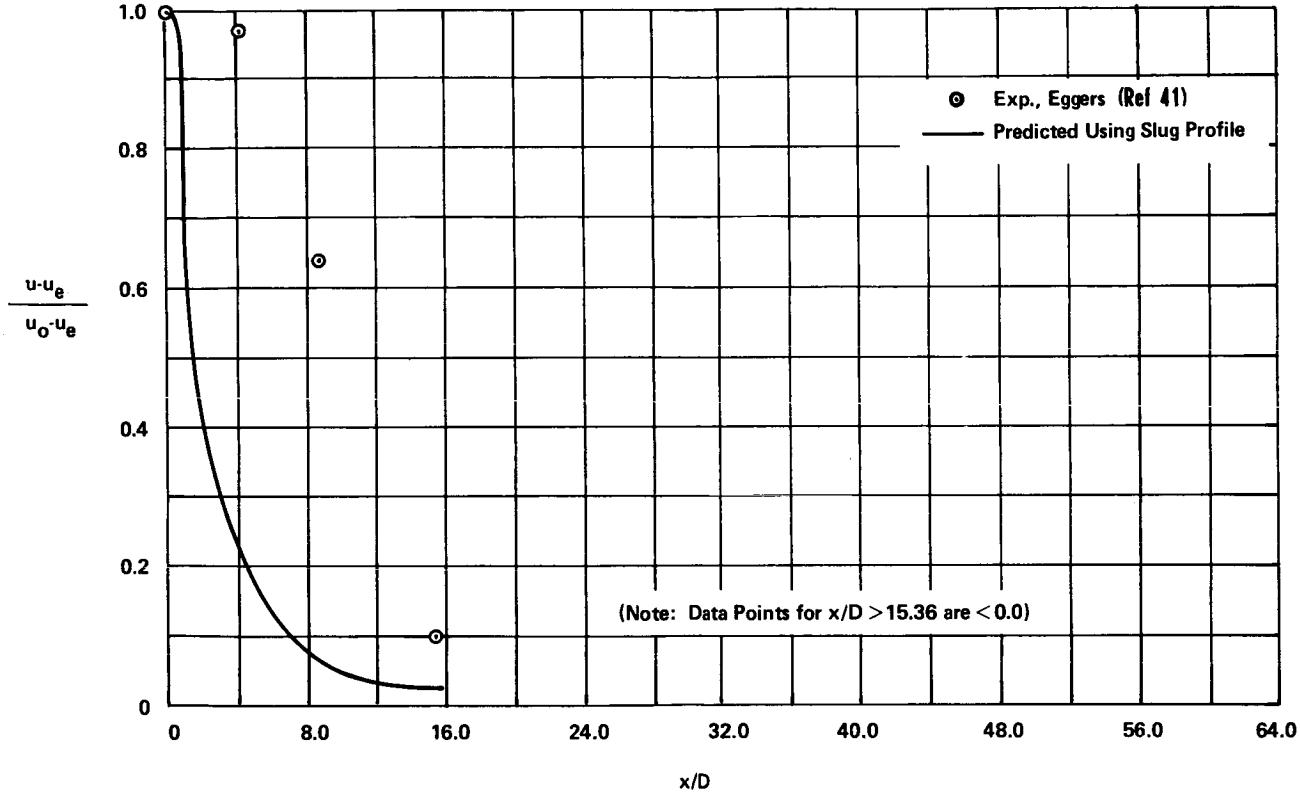

Figure 17.- Predicted and experimental center-line velocity for test case 22 (Eggers (ref. 41)).

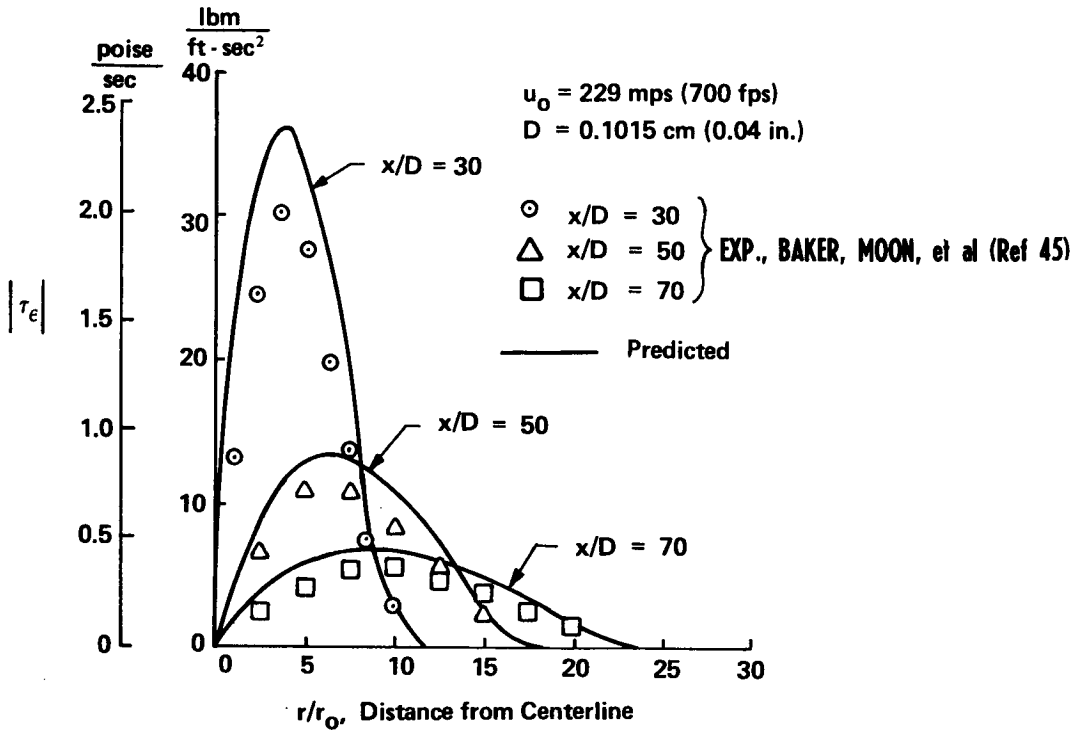

Figure 18.- Shear stress profiles at x/D = 30, 50, and 70 for data of Baker, Moon, et al. (ref. 45).

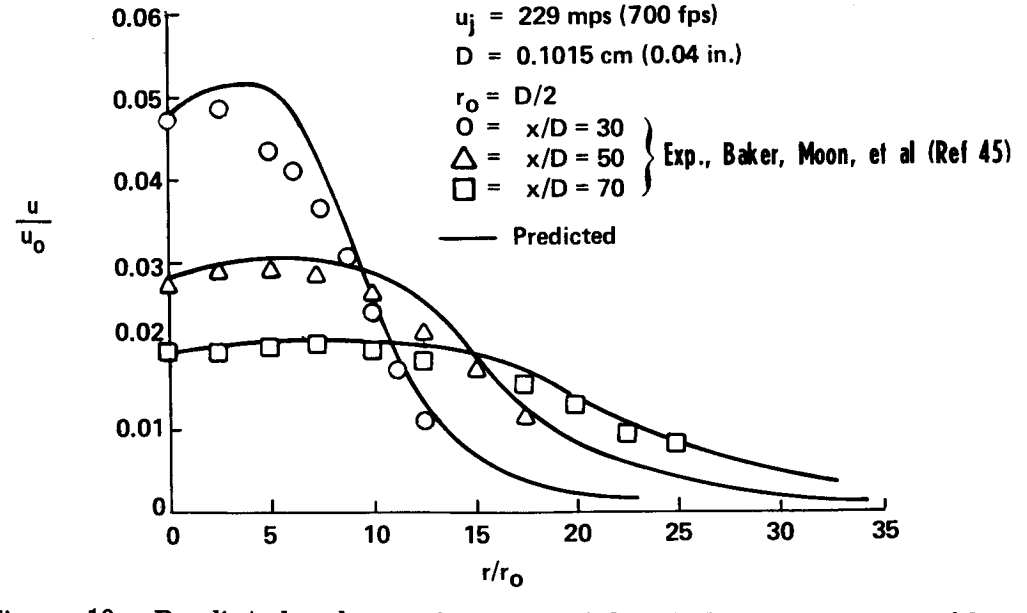

Figure 19.- Predicted and experimental axial turbulent intensity profiles at x/D = 30, 50, and 70.

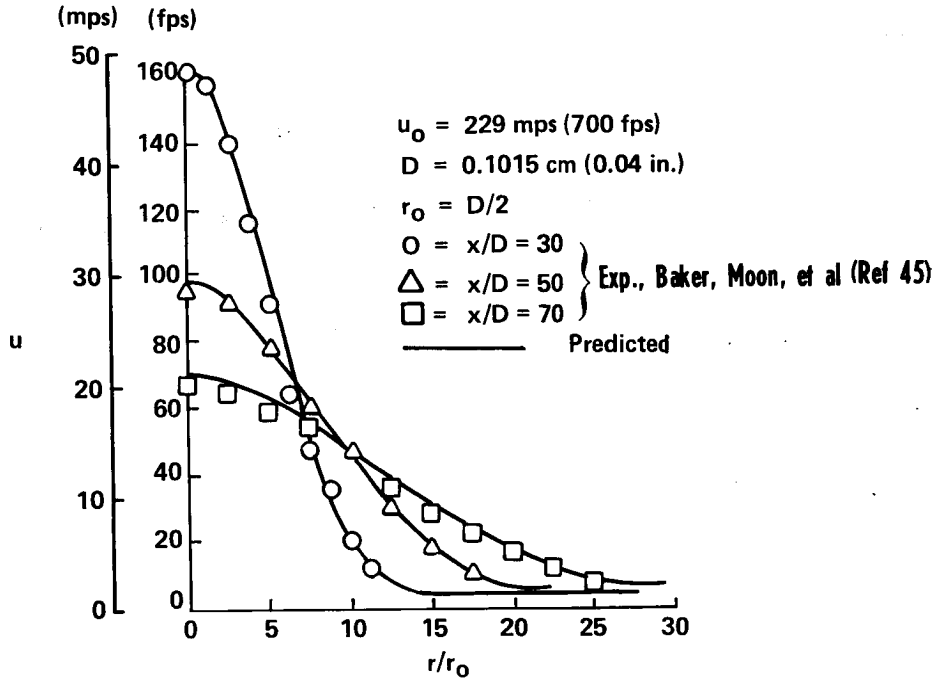

Figure 20.- Predicted and experimental axial velocity profiles at x/D = 30, 50, and 70.

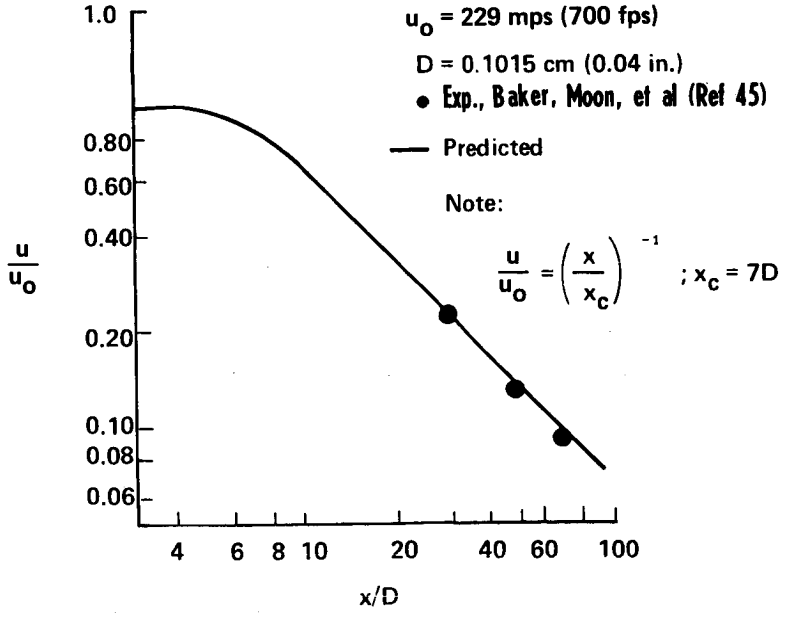

Figure 21.- Predicted and experimental center-line velocity.

DISCUSSION

S. Corrsin: This is a trivial remark, but on the figure showing eddy viscosity ϵ versus radial distance r you have a finite slope of ϵ at the center line of the axis of the jet. I wonder whether it would be better to have a horizontal slope there.

J. H. Morgenthaler: Of course, the center line is an axis of symmetry; however, because $(\partial u/\partial r)_{\text{¢}} = 0$, it is not possible (or necessary) to define $(\partial \epsilon/\partial r)_{\text{¢}}$.

I. E. Alber: Also, with respect to your eddy viscosity model, I noticed that you had the eddy viscosity ϵ proportional to u'^2. Nominally, from dimensional analysis, one would take ϵ proportional to u'. Is there any reason that you chose that over the more conventional scheme?

J. H. Morgenthaler: Steve, would you like to answer that one?

S. W. Zelazny: The proportionality you are referring to (eq. (5)) was obtained by assuming (1) the shear stress is directly proportional to the turbulence kinetic energy, an assumption used in a number of the Workshop papers using the turbulence kinetic energy approach, (2) the ratio of the transverse turbulence intensity to the axial turbulence intensity is independent of radial position, and (3) the shear correlation coefficient is directly proportional to the partial derivative of the axial velocity with respect to the radial coordinate, that is, $\partial U/\partial r$. The relation, ϵ proportional to u'^2, also may be obtained from dimensional analysis if it is assumed that the eddy viscosity is functionally dependent on density u'^2 and the maximum value of $\partial U/\partial r$ at a given axial station.

J. H. Morgenthaler: In other words, we did not pull the relation out of our hat.

M. V. Morkovin: Concerning the same point, how do you use equation (5)? Do you use ϵ just to evaluate u'^2? It is not used in the development of other relationships, is it?

S. W. Zelazny: Equation (5) was used to develop the empirical expression, $G(r/r_u)$ of equation (9) describing the radial variation of eddy viscosity and turbulence intensity. It showed that both eddy viscosity "data" and turbulence intensity data could be used to obtain an approximation for ϵ/ϵ_u and $(\rho u'^2)/(\rho u'^2)_u$ consistent with the assumptions listed in my reply to Dr. Alber. It is not true that ϵ is just used to evaluate u'^2 since ϵ is essential for prediction of the mean values.

J. H. Morgenthaler: In figure 2 of the paper, there are open symbols and closed symbols which didn't show up very well on the slide, but as you can see, some points were obtained by direct differentiation of the mean data, and some were obtained directly from hot-wire turbulence measurements.

M. V. Morkovin: But I'm saying, that all you are trying to do is to fit some transverse variation of ϵ. In your computations as you are marching in the axial direction, the effect of transverse variation does not influence predictions since the function $G(r/r_u)$ is independent of z. That is, the transverse variation only affects prediction of the turbulence quantities, doesn't it?

J. H. Morgenthaler: The transverse variation of ϵ has a great influence on predictions, as is illustrated in the figure. The local value of ϵ greatly influences the rate of momentum transport as minor perturbations in ϵ have demonstrated during the development of the model. It is true, however, that the computation of mean quantities is not influenced by the prediction of turbulence intensity. In other words, the model may predict valid mean profiles but be considerably poorer in its predictions of turbulence quantities.

T. Cebeci: Well, let us have one more question before we take our coffee break.

S. C. Lee: I am looking at your figure 2 right now. I have a question related to this figure. It looks from the figure that the function $G(r/r_u)$ might be considered to be constant between $r/r_u = 0$ and $r/r_u = 1.5$. What effect would this assumption have on the predictions?

J. H. Morgenthaler: We believe the radial variation to be important based on our modeling experience. We have run a case which shows that the length of the transition region is significantly influenced as are mean quantities (see the figure). For example, the velocity at the ℓ at $z = 50\ D$ (2.0 in.) was 92.0 ft/sec for $G(r/r_u)$ defined by equation (9), but was 64.3 ft/sec when the assumption was made that $G \equiv 1$.

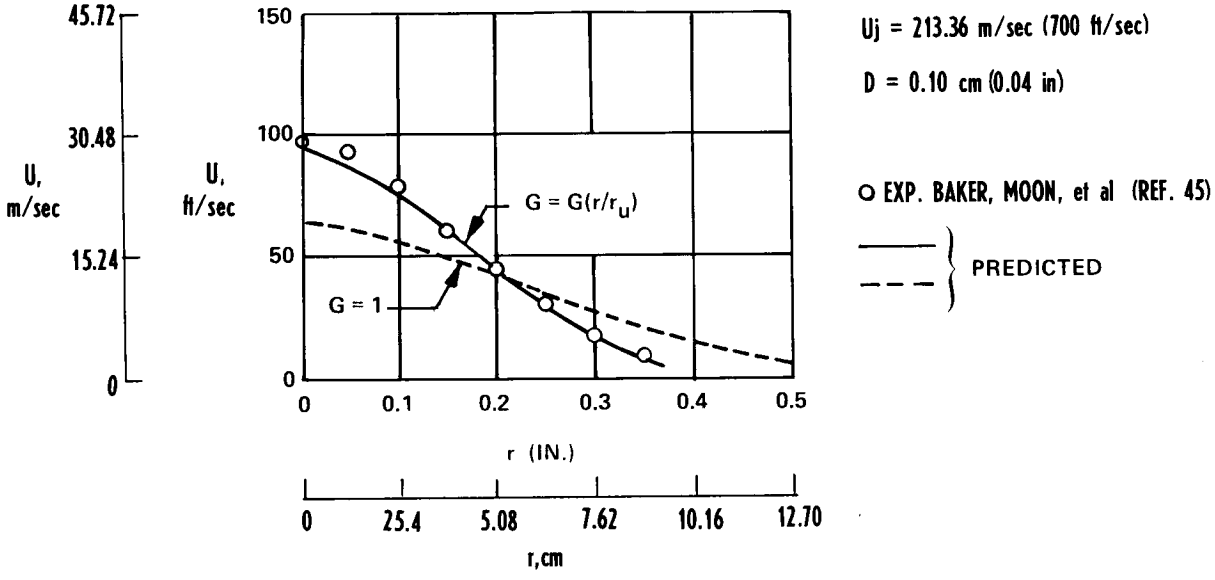

Figure 1.- Predicted velocity profiles at z/D = 50 showing effect of including radial variation in eddy viscosity model.

PREDICTION AND EVALUATION OF EDDY-VISCOSITY MODELS FOR FREE MIXING*

By V. Zakkay, R. Sinha, and S. Nomura
New York University

SUMMARY

Analysis for the turbulent mixing of free jets is presented in this paper and compared to recent experimental results. A turbulent mass diffusion model is presented and is based on the concentration potential core. The model yielded good results when compared with the experimental results except for low-speed flows where few experimental data are available.

A review of recent experimental results verifies again that the three diffusion processes in turbulent mixing are interrelated; however, no single diffusion model may be used for all three processes. This is especially true when pressure gradients are present in the flow field. It is shown that even though momentum diffusion is significantly affected by pressure gradients, mass diffusion is not.

It is further indicated that the mass diffusion model has been derived and is based on the accurate correlations of experimental results obtained for the concentration potential core. Similar techniques may be used in deriving an expression for the momentum and thermal diffusion coefficients. These expressions would be more complicated since they would have to take care of boundary layer at the start of the mixing region.

Finally, a comparison of the analyses, using this particular model and Ferri's model, with available experimental results is made.

INTRODUCTION

The problem of free turbulent mixing with large density gradients has been an area of considerable interest and ever increasing practical importance in the past decade. Problems of constant density mixing may be traced back as far as the 1930's. These types of problems have a wide variety of applications and have been used for wakes, rocket planes, supersonic combustion, nuclear core reactions, and so forth.

* This research was sponsored in part by the Aerospace Research Laboratories, Air Force Systems Command, United States Air Force, Wright-Patterson Air Force Base, Ohio, under Contract F-33615-68-C-1184 and in part by NASA International Fellowships.

In reference 1, the Prandtl eddy-viscosity model for constant density flow was extended to the variable density flow. However, as pointed out in reference 2, this model fails when the mass flux of each stream is equal. Ting and Libby (ref. 3) determined the compressibility factor for the Prandtl model using their transformation, while Donaldson and Gray (ref. 4) and Peters (ref. 5) obtained the compressibility factor empirically. These models, however, fail also when the velocity of each stream is equal, since the Prandtl model becomes zero. Zakkay, Krause, and Woo (ref. 6) developed the eddy-viscosity model in terms of the center-line velocity and velocity half-radius. Schetz (ref. 7) extended the Clauser model (ref. 8) to the axisymmetric wake which was expressed in terms of mass defect across the wake.

Each of all these models has a constant which is chosen such that the numerical solutions of wake equations agree with the experimental data by employing the proposed eddy viscosity and appropriate constant values for turbulent Prandtl number Pr_t and turbulent Schmidt number Sc_t. Therefore, it has been found in references 2, 9, and 10 and also in the present investigation that all these models provide good predictions for certain very restricted flow conditions, but none of them is valid for the general case.

In comparison with these numerous works for the eddy viscosity, only few extensive works have been done for other transport properties, namely Pr_t, Sc_t, and Le_t (turbulent Lewis number). In analytical and numerical investigations so far, constant values for Pr_t and Sc_t have been assumed, and several experimental studies seem to approve these assumptions of constant properties under the condition of zero pressure gradient in the mixing flow field.

In reference 11, Forstall and Shapiro determined $Le_t = 1.0$ and $Pr_t = Sc_t = 0.7$ using the data of air-to-air mixing measured at very low speed. Zakkay et al. (ref. 6) carried out extensive measurements for the turbulent mixing of high-speed coaxial jets comprised of several dissimilar gases. For hydrogen and air mixing, $Sc_t = 0.8$ to 2.0 and $Le_t = 0.9$ to 1.2 have been concluded. Chriss (ref. 12) measured very detailed profiles in mixing flows of high-speed coaxial air and hydrogen jets and obtained $Le_t = 1.0$. The accuracy of these experimental data has been checked by Zelazny, Morgenthaler, and Herendeen (ref. 9) and Harsha (ref. 10) by means of constant-momentum integral check and was found to be very good. Peters, Chriss, and Paulk (ref. 13) have shown for one case of hydrogen and air mixing measured by Chriss that $Pr_t = Sc_t = 0.85$ is approximately valid. Zelazny et al. (ref. 9) also calculated Sc_t for four cases of Chriss' data (ref. 12) and confirmed the result obtained by Peters et al. (ref. 13).

It is difficult at this time to generalize and to derive equations for a single application; however, some basic conclusions have been reached from past research efforts. For example, the authors have indicated previously that the mixing which occurs between two coaxial streams depends largely on their initial energy and their transfer phenomena

in the mixing region. Therefore, differentiation must be made between jets where momentum diffusion is the controlling mechanism and jets where mass diffusion, or thermal diffusion, is the controlling mechanism. Theoretical treatment of the problem is impossible since turbulent transport properties for the three diffusion processes are not yet available. Reference 6 has attempted to deduce such turbulent transport coefficients from mass diffusion experiments.

Similar attempts have been made in wakes to deduce momentum diffusion coefficients; however, no single model has been capable of analyzing the entire range of flow fields. In addition to the complications of the unknown transport properties, in several problems, the pressure field is not constant, and therefore complicates the analysis further. For instance, references 14 and 15 have indicated that pressure gradients do not affect mass diffusion; however, momentum diffusion is significantly affected. These regions of varying pressure gradients are present close to the exit of the jets and are directly responsible for the discrepancies among constant-pressure analyses. Results of mixing with pressure gradients, in reference 15, indicate a large discrepancy between theory and experiments for momentum diffusion, although good agreement exists for mass diffusion.

Therefore, since the topic under discussion is complex and cannot be described in terms of one single model, the present paper will concentrate on the mixing of coaxial jets with special emphasis on mass-diffusion processes. At first a description of the model used for mass diffusion will be derived (see fig. 1) and then the predictions of this model are compared with several of the test cases supplied by the organizers of the Langley working conference on free turbulent shear flows.

SYMBOLS

c_p specific heat at constant pressure

$\bar{c}_p$ normalized specific heat with respect to c_{p_e}

$\bar{c}_{p_k}$ normalized specific heat of kth gas; $k = 1$ corresponds to inner jet gas and $k = 2$ corresponds to outer jet gas

D_j inner jet nozzle diameter

D_t turbulent diffusion coefficient

H total enthalpy of gas

h_k static enthalpy of kth gas

Le_t turbulent Lewis number

M local Mach number

N total number of grid points in τ-direction

n concentration decay exponent along center line

p static pressure

Pr_t turbulent Prandtl number

R gas constant

Re Reynolds number

r radial coordinate

$\bar{r}$ normalized radial coordinate with respect to r_j

r_j radius of inner jet nozzle

r_{mc} concentration half-radius defined so that $Y_j = \frac{Y_{j_\ell}}{2}$ at $r = r_{mc}$

$\bar{r}_{mc}$ normalized half-radius with respect to r_j

r_{mu} velocity half-radius defined so that $u = \frac{u_\ell + u_e}{2}$ at $r = r_{mu}$

Sc_t turbulent Schmidt number

T temperature

$\bar{T}$ normalized temperature with respect to T_e

u axial component of velocity

$\bar{u}$ normalized axial velocity with respect to u_e

v	radial component of velocity
$\bar{v}$	nondimensional radial velocity
W	ratio of molecular weights, W_j/W_e
$\overline{W}$	normalized molecular weight with respect to W_e
x	axial coordinate
x_i	initial value of x to start computation
x_o	concentration potential core length
$\bar{x}$	normalized axial coordinate with respect to r_j
$\bar{x}_o$	normalized x_o with respect to r_j
$\tilde{x}$	normalized axial coordinate with respect to x_o
Y_j	mass concentration of inner jet gas
Y_k	mass concentration of kth gas; $k = 1$ corresponds to inner jet gas, and $k = 2$ corresponds to outer jet gas
ζ	transformed axial coordinate defined as $\frac{1}{4}\int_{\bar{x}_i}^{\bar{x}} Re^{-1}\, d\bar{x}$
ϵ	eddy viscosity
γ	specific-heat ratio
λ	mass-flow ratio defined as $\frac{\rho_j u_j}{\rho_e u_e}$
Ψ	modified stream function defined by equation (7)
ϕ_{u_ℓ}	normalized center-line velocity defined by $\frac{u_e - u_\ell}{u_e - u_j}$
ξ	transformed axial coordinate defined as $2\int_0^{\bar{x}} \overline{(\rho D_t)}\, d\bar{x}$

ρ density

$\bar{\rho}$ normalized density with respect to ρ_e

τ modified stream function defined as $\left(\int_0^{\bar{r}} \bar{\rho}\bar{u}\bar{r}\, d\bar{r}\right)^{0.5}$

τ_t turbulent shear stress

μ_t turbulent viscosity

$\overline{(\rho D_t)}$ normalized value of ρD_t with respect to $\rho_j u_j r_j$

$\overline{(\rho u)}$ normalized value of ρu with respect to $\rho_j u_j$

$\overline{(\rho v)}$ normalized value of ρv with respect to $\rho_e u_e$

Subscripts:

ℓ center-line values

e external conditions

i initial conditions

j inner jet conditions

THEORETICAL ANALYSIS

Basic Equations and Turbulent Diffusion Coefficient

The governing equations for the mean turbulent flow properties in coaxial mixing with axial pressure gradient can be described as follows:

Conservation of mass:

$$\frac{\partial}{\partial x}(\rho u) + \frac{1}{r}\frac{\partial}{\partial r}(\rho v r) = 0 \tag{1}$$

Conservation of momentum:

$$\rho u \frac{\partial u}{\partial x} + \rho v \frac{\partial u}{\partial r} = \frac{1}{r}\frac{\partial}{\partial r}\left(\rho \epsilon r \frac{\partial u}{\partial r}\right) - \frac{dp}{dx} \tag{2}$$

Conservation of energy:

$$\rho u \frac{\partial H}{\partial x} + \rho v \frac{\partial H}{\partial r} = u \frac{dp}{dx} + \frac{1}{r} \frac{\partial}{\partial r}\left(\frac{\rho \epsilon}{Pr_t} r \frac{\partial H}{\partial r} + \frac{Pr_t - 1}{Pr_t} \rho \epsilon r u \frac{\partial u}{\partial r} + \frac{Le_t - 1}{Pr_t} \rho \epsilon r \sum_k h_k \frac{\partial Y_k}{\partial r}\right) \tag{3}$$

Conservation of species:

$$\rho u \frac{\partial Y_j}{\partial x} + \rho v \frac{\partial Y_j}{\partial r} = \frac{1}{r}\left(\frac{\rho \epsilon}{Sc_t} r \frac{\partial Y_j}{\partial r}\right) \tag{4}$$

where the following conditions were assumed:

(1) The flow is chemically frozen.

(2) The radial pressure gradient is not existing.

(3) The streamwise pressure gradient is supposed to exist and therefore the external flow conditions could be variable.

In references 16 and 17, equations (1) to (4) are solved for the axisymmetric coaxial jet mixing with the assumptions of $dp/dx = 0$, $Pr_t = Sc_t = Le_t = 1.0$, and step initial profiles for velocity, enthalpy, and concentration. Obviously these assumptions reduce those equations to a single equation and the solution can be applicable for any flow properties. As for these assumptions, however, the transport coefficients Pr_t, Sc_t, and Le_t are generally not equal to unity, and the initial profiles are not always step profiles because of boundary layers developed on the jet nozzle wall. The exact application of this solution is possible only for the species equation involving the turbulent diffusion coefficient, for which the initial profile can be assumed correctly to be a step profile and in which other transport properties are not directly involved. Furthermore, even if the axial pressure gradients exist, the mass diffusion will not be affected significantly as shown experimentally in references 6, 14, and 15 and in the present experiment, since the pressure gradient affects the concentration indirectly through velocity and temperature field as seen in equation (4). Therefore, the solutions as obtained in references 16 and 17 can be employed exactly only for the species equation involving the turbulent diffusion coefficient in the mixing with axial pressure gradients.

The species equation with the diffusion coefficient is

$$\rho u \frac{\partial Y_j}{\partial x} + \rho v \frac{\partial Y_j}{\partial r} = \frac{1}{r} \frac{\partial}{\partial r}\left(\rho D_t r \frac{\partial Y_j}{\partial r}\right) \tag{5}$$

where the initial conditions at $x = 0$ are

$$Y_j = 1 \qquad \left(\text{for } 0 \leqq r \leqq r_j\right)$$

$$Y_j = 0 \qquad (\text{for} \quad r_j < r < \infty)$$

and the boundary conditions are

$$\frac{\partial Y_j}{\partial r} = 0 \qquad (\text{at} \quad r = 0)$$

$$Y_j = 0 \qquad (\text{at} \quad r \to \infty)$$

Applying the modified von Mises transformation, Kleinstein obtained the exact solution for the linearized boundary-layer equation in reference 17. Employing the same method, the species equation can be solved as follows:

Equation (5) is transformed to

$$\frac{\partial Y_j}{\partial x} = \frac{4}{\Psi}\frac{\partial}{\partial \Psi}\left[\overline{(\rho D_t)}\,\overline{(\rho u)}\bar{r}^2\left(\frac{1}{\Psi}\frac{\partial Y_j}{\partial \Psi}\right)\right] \tag{6}$$

by the transformation terms:

$$\left.\begin{aligned} \bar{x} &= \frac{x}{r_j} \\ \frac{\partial}{\partial \bar{r}}\left(\frac{\Psi}{2}\right)^2 &= \overline{(\rho u)}\bar{r} \\ \frac{\partial}{\partial x}\left(\frac{\Psi}{2}\right)^2 &= -\overline{(\rho v)}\bar{r} \end{aligned}\right\} \tag{7}$$

Neglecting the fourth-order term in the Taylor series expansion of

$$\left[\overline{(\rho D_t)}\,\overline{(\rho u)}\bar{r}^2\right]_{\bar{x},\Psi} = \left[\overline{(\rho D_t)}\right]_{\bar{x},0}\frac{\Psi^2}{2} + O\left(\Psi^4\right)$$

the species equation (6) reduces to the linear form in ξ,Ψ-plane as

$$\frac{\partial Y_j}{\partial \xi} = \frac{1}{\Psi}\frac{\partial}{\partial \Psi}\left(\Psi\frac{\partial Y_j}{\partial \Psi}\right)$$

where ξ is defined as $\xi = 2\int_0^{\bar{x}}\overline{(\rho D_t)}\,d\bar{x}$.

Assuming a step initial profile, the solution of this well-known heat-conduction equation can be expressed along the center line by

$$Y_{j_{\text{¢}}} = 1 - \exp\left(-\frac{\Psi_j^2}{4\xi}\right) \tag{8}$$

where Ψ_j is $\sqrt{2}$ by the definition given in equation (7). In the far wake region as $\xi \to \infty$, $Y_j/Y_{j_{\text{¢}}}$ approaches the Gaussian distribution (ref. 6) as

$$\frac{Y_j}{Y_{j_{\ell}}} = \exp\left(-\frac{\Psi^2}{4\xi}\right) \tag{9}$$

These solutions (eqs. (8) and (9)) can be used to introduce the diffusion model in a way similar to that developed in reference 6 where Zakkay et al. introduced the eddy-viscosity model.

Since $\overline{(\rho u)} \to \frac{1}{\lambda}$ in the far wake region as $\xi \to \infty$,

$$\Psi^2 = \frac{2\bar{r}^2}{\lambda}$$

and

$$\frac{Y_j}{Y_{j_{\ell}}} = \exp\left(-\frac{\bar{r}^2}{2\lambda\xi}\right) \tag{10}$$

Therefore, assuming the center-line concentration decay law to be $Y_{j_{\ell}} = \tilde{x}^{-n} = \left(\frac{x}{x_o}\right)^{-n}$, the concentration profile can be expressed in the physical plane by

$$Y_j = \tilde{x}^{-n}\left(1 - \tilde{x}^{-n}\right)^{\bar{r}^2/\lambda} \tag{11}$$

Then the asymptotic jet spread can be given by taking the limit of equation (11) as follows:

$$\lim_{\tilde{x}\to\infty} \frac{\partial \bar{r}}{\partial \tilde{x}} = \left(-\lambda \ln \frac{Y_j}{Y_{j_{\ell}}}\right)^{1/2} \frac{n}{2} \tilde{x}^{\left(\frac{n}{2}-1\right)}$$

Integrating this equation gives the half-radius for concentration r_{mc} in the far wake region as

$$r_{mc} = 0.833 r_j \left[\lambda\left(\frac{x}{x_o}\right)^n\right]^{1/2} \tag{12}$$

Equation (12) may provide an analytical prediction of the concentration half-radius. Once the concentration profile is expressed in the physical plane by equation (11), the turbulent diffusion coefficient can be derived from the species equation inversely.

The species equation (5) is described with the aid of the continuity equation by

$$\rho D_t r \frac{\partial Y_j}{\partial r} = \int_0^r \frac{\partial\left(\rho u Y_j\right)}{\partial x} r'\, dr' - Y_j \int_0^r r' \frac{\partial(\rho u)}{\partial x}\, dr'$$

Then the diffusion coefficient along the center line can be expressed as

$$\left(\rho D_t\right)_{\ell} = \left(\frac{\rho_u \frac{\partial Y_j}{\partial x}}{2\frac{\partial^2 Y_j}{\partial r^2}}\right)_{\ell} \tag{13}$$

Substituting equation (11) into equation (13) gives the turbulent diffusion coefficient on the center line as follows:

$$(\rho D_t)_{\text{¢}} = \frac{n r_j}{4\bar{x}_o}\left(\frac{\bar{r}_{mc}^2}{\ln 2}\right)^{\frac{n-1}{n}} \lambda^{1/n}(\rho u)_{\text{¢}} \tag{14}$$

In equation (14) there are two unknown parameters, namely $\bar{x}_o$ and n. The decay exponent n in $Y_{j_{\text{¢}}} = \tilde{x}^{-n}$ has been shown to be

$$n = 2 \tag{15}$$

for high-speed jet mixing in many experiments (for example, refs. 6, 14, and 15) and also will be shown to be $n = 2$ in the present experiment.

Now the potential core length $\bar{x}_o$ for concentration in high-speed mixing, where $n = 2$ is valid, should be formulated in terms of known values. The parametric investigation has shown the importance of momentum ratio at the initial exit plane on the potential core length for concentration. The typical correlation between the potential core length for concentration and the initial Mach number ratio can be seen obviously in figure 2. The Mach number ratio of two jets can be expressed by the momentum ratio as

$$\frac{\rho_j u_j^2}{\rho_e u_e^2} = \frac{\left(\frac{pu^2}{RT}\right)_j}{\left(\frac{pu^2}{RT}\right)_e} \approx \left(\frac{M_j}{M_e}\right)^2$$

since $p_j = p_e$. Therefore, figure 2 shows that when the momentum ratio becomes larger, the potential core length becomes longer.

These data are rearranged in figure 3, from which the correlation equation has been obtained as

$$\left(\frac{x_o}{D_j}\right)_{\text{concentration}} = 1 + 30\left(\frac{\rho_j}{\rho_e}\right)^{1/4} M_j^2 \left\{1 + M_j^2 \exp\left[-\frac{\left(1 - \frac{M_e}{M_j}\right)^2}{2}\right]\right\}^{-2} \tag{16}$$

From equation (16), when $M_j = 0$,

$$\left(\frac{x_o}{D_j}\right)_{\text{concentration}} = 1.0$$

which corresponds to the axisymmetric wake, and the result of $x_o/D_j = 1.0$ is supported by the data of the supersonic wake studies (refs. 18, 19, and 20). When $M_e = 0$, which corresponds to the jet injected into the quiescent atmosphere, the data of Keagy and Weller (ref. 21) and O'Connor (ref. 22) are fairly well correlated as seen in this figure.

Now the turbulent diffusion coefficient, assuming that it is only a function of x, can be described with the aid of equations (14) and (15) as

$$\rho D_t = (\rho D_t)_{\text{¢}} = 0.6 \frac{\lambda^{1/2}}{\bar{x}_o} r_{mc} (\rho u)_{\text{¢}} \tag{17}$$

It is noticeable that equation (17) does not include any adjustable constant to match the numerical solutions of wake equations with the experimental data. Such constants were included in all previous viscosity models suggested by Prandtl, Ferri, Schetz, and others.

As shown subsequently the diffusion model given by equation (17) provides good numerical predictions for the high-speed mixing of hydrogen and air, for which the decay exponent n satisfied equation (15) approximately. However, for the general case of arbitrary dissimilar gases, it has been found necessary (by means of numerical calculations) to include a molecular-weight factor given as $1 + 0.8(W_j/W_e)$ in the expression for turbulent diffusivity; thus,

$$\rho D_t = \frac{0.6}{1 + 0.8W} \frac{\lambda^{1/2}}{\bar{x}_o} r_{mc} (\rho u)_{\text{¢}} \tag{18}$$[1]

where

$$\bar{x}_o = 2 + 60\left(\frac{\rho_j}{\rho_e}\right)^{1/4} M_j^2 \left\{ 1 + M_j^2 \exp\left[-\frac{\left(1 - \frac{M_e}{M_j}\right)^2}{2} \right] \right\}^{-2}$$

Since the ratio of the molecular weights $W = W_j/W_e$ is very small for the mixing of light gas and heavy gas, equation (18) becomes of the same form as equation (17) as, for example, in the case of hydrogen-air mixing.

It is important to realize that the model chosen is based on the potential core derived from a step profile. Therefore, one cannot expect it to work if the initial profile consists of a boundary-layer profile. However, these difficulties could be avoided by always starting with an initial step profile, and calculating the length of the potential core for the step profile. This distance should be added to the calculations performed with the boundary-layer type profile. This procedure will result in a shift of the curve, which will indicate a slower mixing region. This fact will be evident in some of the results that will be given in the next section.

Application to the Numerical Solution of Wake Equations Without Pressure Gradients

In order to investigate the validity of the present diffusion model, the wake equations have been solved for the cases without pressure gradients. The wake equations

[1] For numerical calculation, the concentration half-radius r_{mc} should be determined by the numerical procedure instead of equation (12), which will provide the analytical prediction of the half-radius in the far wake region only.

in the general form are written in the modified von Mises plane as follows:

Momentum equation:

$$\frac{\partial \bar{u}}{\partial \zeta} = \frac{1}{\tau}\frac{\partial}{\partial \tau}\left(\frac{\bar{\rho}\bar{\mu}_t \bar{u}\bar{r}^2}{\tau}\frac{\partial \bar{u}}{\partial \tau}\right) - \frac{\bar{u}}{u_e}\frac{\partial u_e}{\partial \zeta}\left(1 - \frac{1}{\bar{\rho}\bar{u}^2}\right) \tag{19}$$

Energy equation:

$$\frac{\partial \overline{T}}{\partial \zeta} = \frac{1}{\tau \bar{c}_p}\frac{\partial}{\partial \tau}\left(\frac{\bar{\rho}\bar{\mu}_t \bar{c}_p \bar{u}\bar{r}^2}{Pr_t \tau}\frac{\partial \overline{T}}{\partial \tau}\right) + (\gamma_e - 1)M_e^2\left[\frac{\overline{T} - 1}{\bar{\rho}\bar{c}_p u_e}\frac{\partial u_e}{\partial \zeta} + \frac{\bar{\rho}\bar{\mu}_t \bar{r}^2 \bar{u}}{\bar{c}_p \tau^2}\left(\frac{\partial \bar{u}}{\partial \tau}\right)^2\right]$$

$$+ \frac{\bar{\rho}\bar{\mu}_t \bar{r}^2 \bar{u}}{Sc_t \bar{c}_p \tau^2}\frac{\partial \overline{T}}{\partial \tau}\sum_k \bar{c}_{p_k}\frac{\partial Y_k}{\partial \tau} \tag{20}$$

Species equation:

$$\frac{\partial Y_k}{\partial \zeta} = \frac{1}{\tau}\frac{\partial}{\partial \tau}\left(\frac{\bar{\rho}\bar{\mu}_t \bar{u}\bar{r}^2}{Sc_t \tau}\frac{\partial Y_k}{\partial \tau}\right) \qquad (k = 1, 2, \ldots) \tag{21}$$

where the modified von Mises transformation is defined by

$$\frac{\partial \tau^2}{\partial \bar{r}} = \bar{\rho}\bar{u}\bar{r}$$

$$\frac{\partial \tau^2}{\partial \bar{x}} = -\bar{\rho}\bar{v}\bar{r}$$

$$\zeta = \frac{1}{4}\int_{\bar{x}_i}^{\bar{x}} Re^{-1}\, d\bar{x}$$

and $\mu_t = Sc_t \rho D_t$ and $Pr_t = Le_t Sc_t$ are used.

The associated initial and boundary conditions are

$$\bar{u}(0,\tau) = \bar{u}_i(\tau)$$

$$\overline{T}(0,\tau) = \overline{T}_i(\tau)$$

$$Y_j(0,\tau) = Y_{ji}(\tau)$$

$$\frac{\partial}{\partial \tau}\bar{u}(\zeta,0) = \frac{\partial}{\partial \tau}\overline{T}(\zeta,0) = \frac{\partial}{\partial \tau}Y_j(\zeta,0) = 0$$

$$\lim_{\tau \to \infty} \bar{u}(\zeta,\tau) = \lim_{\tau \to \infty} T(\zeta,\tau) = 1.0$$

$$\lim_{\tau \to \infty} Y_j(\zeta,\tau) = 0$$

The numerical calculations for equations (19) to (21) were carried out by an implicit finite-difference scheme. The details of this numerical process have been reported in references 23 and 24. Also, some pertinent results relating to this program have been reported in references 25 to 27.

Once initial and boundary conditions are specified, equations (19) to (21) can be solved with the aid of equation (18) for diffusion coefficient and with the assumptions of appropriate constant values for Sc_t and Pr_t. In this present calculation, $Sc_t = Pr_t = 0.8$ and $Le_t = 1.0$ have been used.

The numerical calculations were carried out for the experimental data of Chriss (ref. 12) and Alpinieri (ref. 2). In figure 4, the numerical solutions for the data of Chriss are shown compared with the experimental data which were measured in hydrogen and air mixing. The accuracy of those experiments have been found to be very good by Zelazny et al. (ref. 9) and Harsha (ref. 10) (reportedly within 4 percent). Since the lateral profiles measured at several stations of x were reported in reference 12, the initial profiles for this numerical calculation were chosen at the position of $\bar{x}_i$ indicated in figures instead of the assumed profiles at the jet exit plane.

Figures 4(a), 4(c), and 4(f) show very good agreement of numerical solutions with the experiment for concentration decay on the center line and for the concentration half-radius. Figure 4(e) shows an example for the lateral concentration profiles which agree quite well with the experimental data. Also in figures 4(a), 4(c), and 4(f) the analytical predictions of concentration half-radius r_{mc} given by equation (12) are shown. The agreement with the experimental data is excellent, considering that equation (12) does not include any adjustable constant to match the solutions with data.

Concerning the velocity profiles for the data of Chriss (ref. 12), the center-line profile and the half-radius have been predicted well as seen in figures 4(b), 4(d), and 4(g). These results prove that if there is no pressure gradient in the flow field the assumptions of $Sc_t = Pr_t = 0.8$ and $Le_t = 1.0$ are valid for the high-speed mixing of hydrogen and air.

In figures 4(c) and 4(f), the numerical solutions obtained by employing the eddy-viscosity model of reference 1 are presented. The comparisons with the data show that the Ferri model provides fairly good predictions in the far wake region.

The numerical result for the data of Alpinieri (ref. 2), which are characterized by the very small momentum of the inner hydrogen jet, is shown in figure 5. The result given by the present diffusion model agrees fairly well with the data.

In figure 6, the results are shown for the case of CO_2 and air mixing measured by Alpinieri. In these cases numerical results agree fairly well with the data which have the decay exponent $n \approx 1.5$.

Throughout these numerical computations the momentum integral of the wake has been checked at each station of finite-difference calculation and found to be constant with a variation of less than ±1 percent.

COMPARISONS WITH SELECTED CASES

In addition to the cases presented in the previous section of this report, six cases (identified as 9, 10, 11, 12, 20, and 21) will be chosen for this section. Each of these cases will be discussed separately. An additional case was chosen in order to evaluate the numerical techniques used in the analysis. Table I presents initial conditions for all the above-mentioned cases.

Discussion of the Results of Selected Cases

Additional case.- For the additional case (see page 735 for explanation), a step profile has been given for the velocity as well as the concentration. The velocity did not present any problem; however, the concentration profile had to be rounded off slightly in order to start the calculation. For this case, the transformed $\bar{r}$ coordinate, which is indicated as τ, had a step size of $\Delta\tau$ equal to 0.009. The total number of grid points in the τ-direction was 60. The total time required for the calculation on the 6600 computer at NYU was 180 seconds. The results of this case are shown in figure 7.

Case 9.- In case 9, the analysis was carried out for the experimental conditions of Forstall and Shapiro (ref. 11). Initial profiles were given both for the velocity and concentration. However, one could hardly consider this case as the mixing of two dissimilar gases since the center jet contained $1\frac{1}{2}$ percent, by mass, of a helium tracer gas.

The momentum controls the mixing in this case, and therefore it dominates the mixing primarily. The results of the present analysis are presented in figure 8 and compared with the experimental results. It is noticed that the Ferri model, which essentially reduces to the Prandtl model for low speeds, has the best agreement with the experimental results.

Case 10.- In case 10 (see ref. 12) the initial profiles were given, and therefore no adjustments were needed. Figure 9 presents results of the Ferri model as well as the results of the present model. Both models seem to agree initially; however, the present model seems to give the correct trend of the experimental results. For this case, even though the flow is subsonic, the analysis still agrees excellently with the experimental results.

Case 11.- The results for case 11 are presented in figure 10. The center jet in this case is a subsonic air stream traveling at Mach 0.90 surrounded by an annular Mach 1.3 nozzle. In this case, a 1-percent ethylene tracer gas was mixed into the central stream. As far as the mixing is concerned, this was a predominantly momentum transfer, and

therefore the analysis which is presented herein and which has been derived from a concentration potential core would hardly be suitable. However, the analysis was still carried out for this model. Two different initial conditions were chosen for case 11:

(a) Assuming an initial step profile

(b) Assuming the initial profile provided

It is clearly seen that condition (a) provides the fastest mixing, and the boundary-layer type profile (condition (b)) results in a slower mixing region. In order to use this model for the potential core, the length required to reach the boundary-layer profile should be added as initial conditions, since the analysis here assumes a step profile. The results of such a correction are included in figure 10 and labeled "New model with correction." Even though the analysis of such a technique improves the agreement, it still falls short of the experimental results.

Case 12.- The results for case 12 are presented in figure 11. The center jet is entirely H_2 at a Mach number of 0.89. As seen in figure 11, the present analysis agrees fairly well with the experimental results; however, the Ferri model falls quite short of the experimental results.

Case 20.- In case 20, only a 2 percent by volume of H_2 was placed in the center jet, and therefore the mixing is dominated by momentum. The results for this case are presented in figure 12, which shows no agreement with the experimental results.

Case 21.- The center jet is entirely H_2 for case 21, and both inside and outside streams are subsonic. The results for this case are presented in figure 13, and the analysis, as expected, is in fair agreement with the experimental results.

Summary of Results of Selected Cases

The following general results were noted for the cases selected:

(1) For all the cases where a lighter molecular gas such as H_2 or He is placed in the center, the present analysis works very well (that is, $\lambda < 1$). This is independent of the conditions whether the flow is subsonic or supersonic.

(2) For low-speed flows, where $\lambda > 1$ (predominantly flows of air-to-air mixing), the Ferri model seems to work best.

(3) As noted previously, the decay such as exists for the flow described in result (1) is always proportional to x^{-2}.

CONCLUSIONS

A model has been presented for the prediction of the concentration decay for high-speed coaxial mixing. The model has been derived from accurate correlation of data

derived from the length of the concentration potential core. Comparisons of this model with available experimental results seem to indicate good agreement, except for cases where the mass-flow ratio is greater than 1 (mixing of gases having approximately the same molecular weight). For all the cases where the gas in the center was much lighter than the coflowing outer gas, the analyses predicted the concentration decays excellently. It is indicated in this paper that no single model could solve the problem of mixing, and attempts should be made to analyze each problem separately. In addition, differentiation should be made between momentum, mass, and thermal diffusion. These effects become much more important when pressure gradients are present in the flow field.

REFERENCES

1. Ferri, A.; Libby, P. A.; and Zakkay, V.: Theoretical and Experimental Investigation of Supersonic Combustion. High Temperatures in Aeronautics, Carlo Ferrari, ed., Pergamon Press, Inc., 1964, pp. 55-118.

2. Alpinieri, Louis J.: Turbulent Mixing of Coaxial Jets. AIAA J., vol. 2, no. 9, Sept. 1964, pp. 1560-1567.

3. Ting, Lu; and Libby, Paul A.: Remarks on the Eddy Viscosity in Compressible Mixing Flows. J. Aero/Space Sci., vol. 27, no. 10, Oct. 1960, pp. 797-798.

4. Donaldson, Coleman duP.; and Gray, K. Evan: Theoretical and Experimental Investigation of the Compressible Free Mixing of Two Dissimilar Gases. AIAA J., vol. 4, no. 11, Nov. 1966, pp. 2017-2025.

5. Peters, C. E.: Turbulent Mixing and Burning of Coaxial Streams Inside a Duct of Arbitrary Shape. AEDC-TR-68-270, U.S. Air Force, Jan. 1969. (Available from DDC as AD 680 397.)

6. Zakkay, Victor; Krause, Egon; and Woo, Stephen D. L.: Turbulent Transport Properties for Axisymmetric Heterogeneous Mixing. AIAA J., vol. 2, no. 11, Nov. 1964, pp. 1939-1947.

7. Schetz, Joseph A.: Turbulent Mixing of a Jet in a Coflowing Stream. AIAA J., vol. 6, no. 10, Oct. 1968, pp. 2008-2010.

8. Clauser, Francis H.: The Turbulent Boundary Layer. Vol. IV of Advances in Applied Mechanics, H. L. Dryden and Th. von Kármán, eds., Academic Press, Inc., 1956, pp. 1-51.

9. Zelazny, S. W.; Morgenthaler, J. H.; and Herendeen, D. L.: Reynolds Momentum and Mass Transport in Axisymmetric Coflowing Streams. Proceedings of the 1970 Heat Transfer and Fluid Mechanics Institute, Turgut Sarpkaya, ed., Stanford Univ. Press, c.1970, pp. 135-152.

10. Harsha, Philip Thomas: Free Turbulent Mixing: A Critical Evaluation of Theory and Experiment. AEDC-TR-71-36, U.S. Air Force, Feb. 1971. (Available from DDC as AD 718 956.)

11. Forstall, Walton, Jr.; and Shapiro, Ascher H.: Momentum and Mass Transfer in Coaxial Gas Jets. J. App. Mech., vol. 17, no. 4, Dec. 1950, pp. 399-408.

12. Chriss, D. E.: Experimental Study of the Turbulent Mixing of Subsonic Axisymmetric Gas Streams. AEDC-TR-68-133, U.S. Air Force, Aug. 1968. (Available from DDC as AD 672 975.)

13. Peters, C. E.; Chriss, D. E.; and Paulk, R. A.: Turbulent Transport Properties in Subsonic Coaxial Free Mixing Systems. AIAA Paper No. 69-681, June 1969.

14. Zakkay, Victor; and Krause, Egon: Mixing Problems With Chemical Reactions. Supersonic Flow Chemical Processes and Radiative Transfer, D. B. Olfe and V. Zakkay, eds., Pergamon Press, Inc., 1964, pp. 3-29.

15. Zakkay, V.; Sinha, R.; and Fox, H.: Some Remarks on Diffusion Processes in Turbulent Mixing. AIAA J., vol. 6, no. 7, July 1968, pp. 1425-1427.

16. Libby, Paul A.: Theoretical Analysis of Turbulent Mixing of Reacting Gases With Application to Supersonic Combustion of Hydrogen. ARS J., vol. 32, no. 3, Mar. 1962, pp. 388-396.

17. Kleinstein, Gdalia: Mixing in Turbulent Axially Symmetric Free Jets. J. Spacecraft & Rockets, vol. 1, no. 4, July-Aug. 1964, pp. 403-408.

18. Martellucci A.; Trucco, H.; Ranlet, J.; and Agnone, A.: Measurements of the Turbulent Near Wake of a Cone at Mach 6. AIAA Paper No. 66-54, Jan. 1966.

19. Sinha, Ram; and Zakkay, Victor: Experimental and Theoretical Investigation of the Near Wake in an Axisymmetric Supersonic Flow With and Without Base Injection. NYU-AA-68-26, New York Univ., May 1968. (Available from DDC as AD 683 528.)

20. Sinha, Ram P.: Experimental and Theoretical Investigation of the Near Wake in an Axisymmetric Supersonic Flow With and Without Base Injection. Ph. D. Thesis, New York Univ., 1968.

21. Keagy, W. R.; and Weller, A. E.: A Study of Freely Expanding Inhomogeneous Jets. 1949 Heat Transfer and Fluid Mechanics Institute, Amer. Soc. Mech. Eng., May 1949, pp. 89-98.

22. O'Connor, T. J.; Comfort, E. H.; and Cass, L. A.: Turbulent Mixing of an Axisymmetric Jet of Partially Dissociated Nitrogen With Ambient Air. AIAA J., vol. 4, no. 11, Nov. 1966, pp. 2026-2032.

23. Fox, Herbert; Sinha, Ram; and Weinberger, Lawrence: An Implicit Finite Difference Solution for Jet and Wake Problems. Pt. I: Analysis and Test Cases. ARL 70-0025, U.S. Air Force, Feb. 1970.

24. Sinha, Ram; Fox, Herbert; and Weinberger, Lawrence: An Implicit Finite Difference Solution for Jet and Wake Problems. Pt. II: Program Manual. ARL 70-0024, U.S. Air Force, Feb. 1970. (Available from DDC as AD 707 866.)

25. Fox, Herbert; Zakkay, Victor; and Sinha, Ram: A Review of Problems in the Nonreacting Turbulent Far Wake. Astronaut. Acta, vol. 14, no. 3, Mar. 1969, pp. 215-228.

26. Zakkay, V.; Sinha, R.; and Fox, H.: An Experimental Study of Some Base Injection Techniques and the Effect of Large Pressure Gradients on Turbulent Diffusion Processes. ARL 68-0160, U.S. Air Force, Aug. 1968. (Available from DDC as AD 679 218.)

27. Zakkay, V.; and Sinha, R.: An Experimental Investigation of the Near Wake in an Axisymmetric Supersonic Flow With and Without Base Injection. Israel J. Technol., vol. 7, nos. 1-2, 1969, pp. 43-53.

TABLE I.- INITIAL CONDITIONS FOR SELECTED CASES

Test case	Jet	x_i	u_j/u_e	$\Delta\tau$ (*)	N	Profile	λ	M_e
Additional	H_2	0.0	3.84	0.009	60	u-step α-step (modified)	0.262	0.681
9	He and air mixture	0.0	4.0	0.04	55	As given	3.68	0.0266
10	H_2	5.932	6.3	0.03	60	As given	0.508	0.422
11	Air	0.0	0.735	0.03	55	As given	0.634	1.312
12	H_2	0.0	2.726	0.03	70	As given	0.0439	1.32
20	H_2 and air mixture	0.4568	2.1926	0.03	55	As given	2.06	0.158
21	H_2	5.15	3.078	0.03	45	As given	0.398	0.497

* $\Delta\tau$ step size in τ-direction; τ transformed $\bar{r}$ coordinate as defined by $\tau = \left(\int_0^{\bar{r}} \bar{\rho}\bar{u}\bar{r}\, d\bar{r} \right)^{0.5}$.

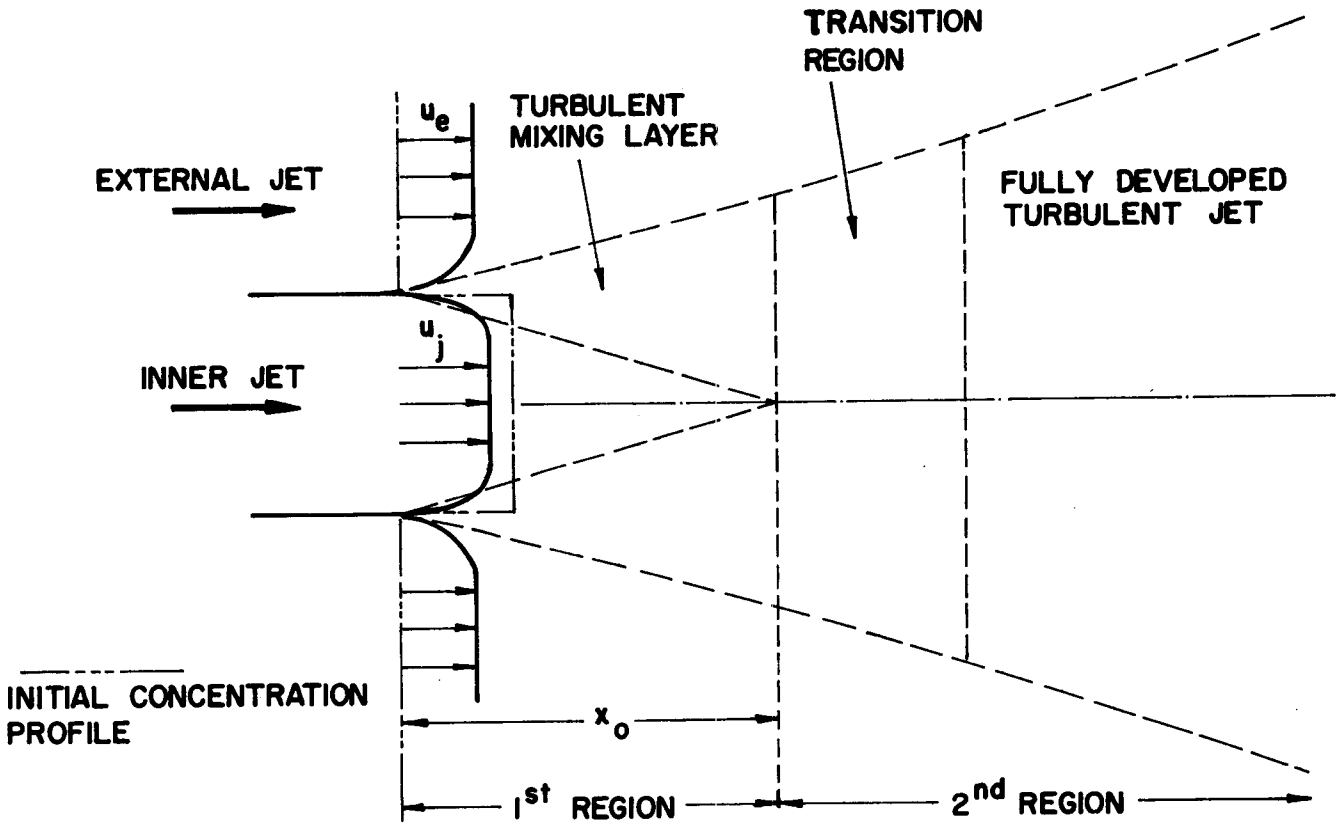

Figure 1.- Turbulent jet mixing flow model.

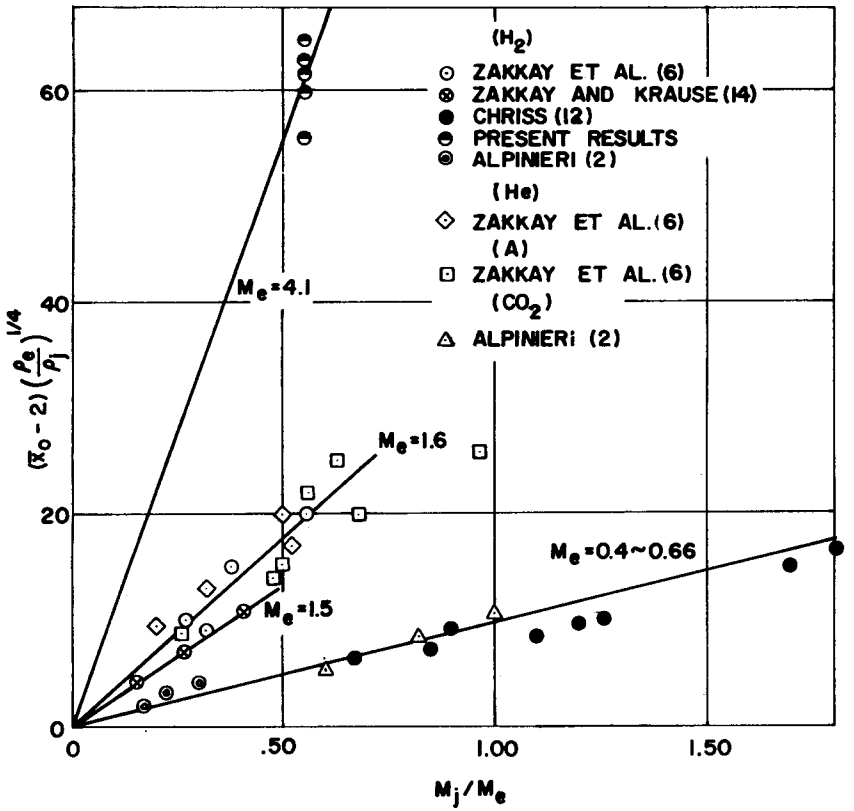

Figure 2.- Length of concentration potential core as a function of Mach number ratio.

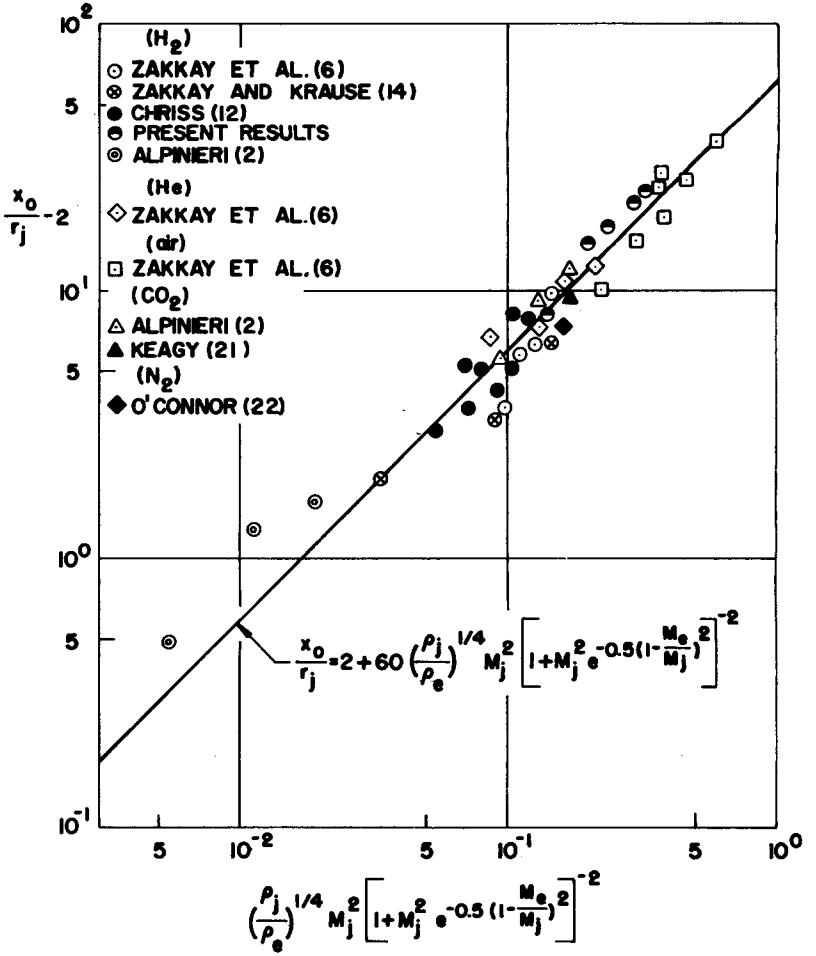

Figure 3.- Correlation for the length of concentration potential core.

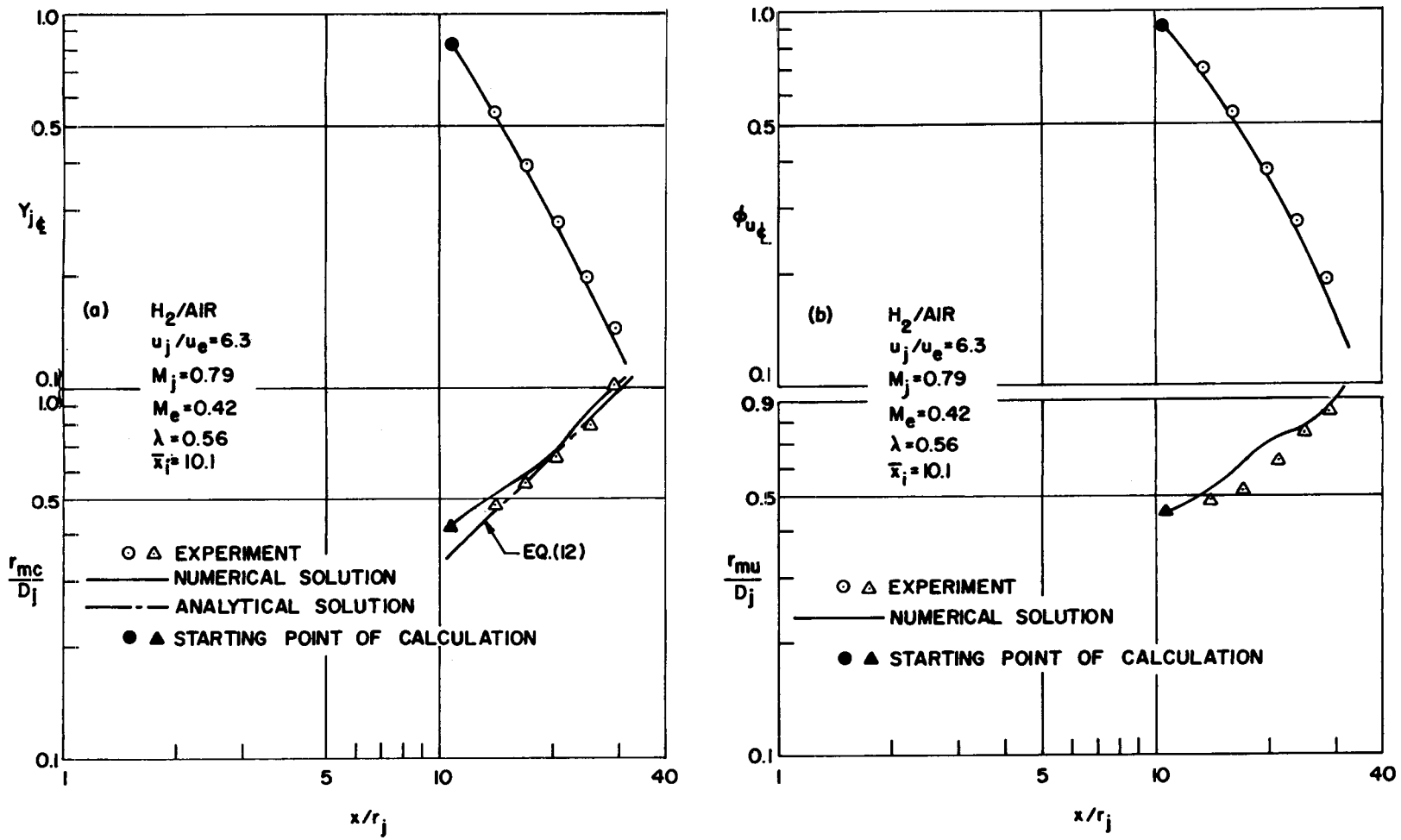

Figure 4.- Comparison of numerical results with the data of Chriss (ref. 12).

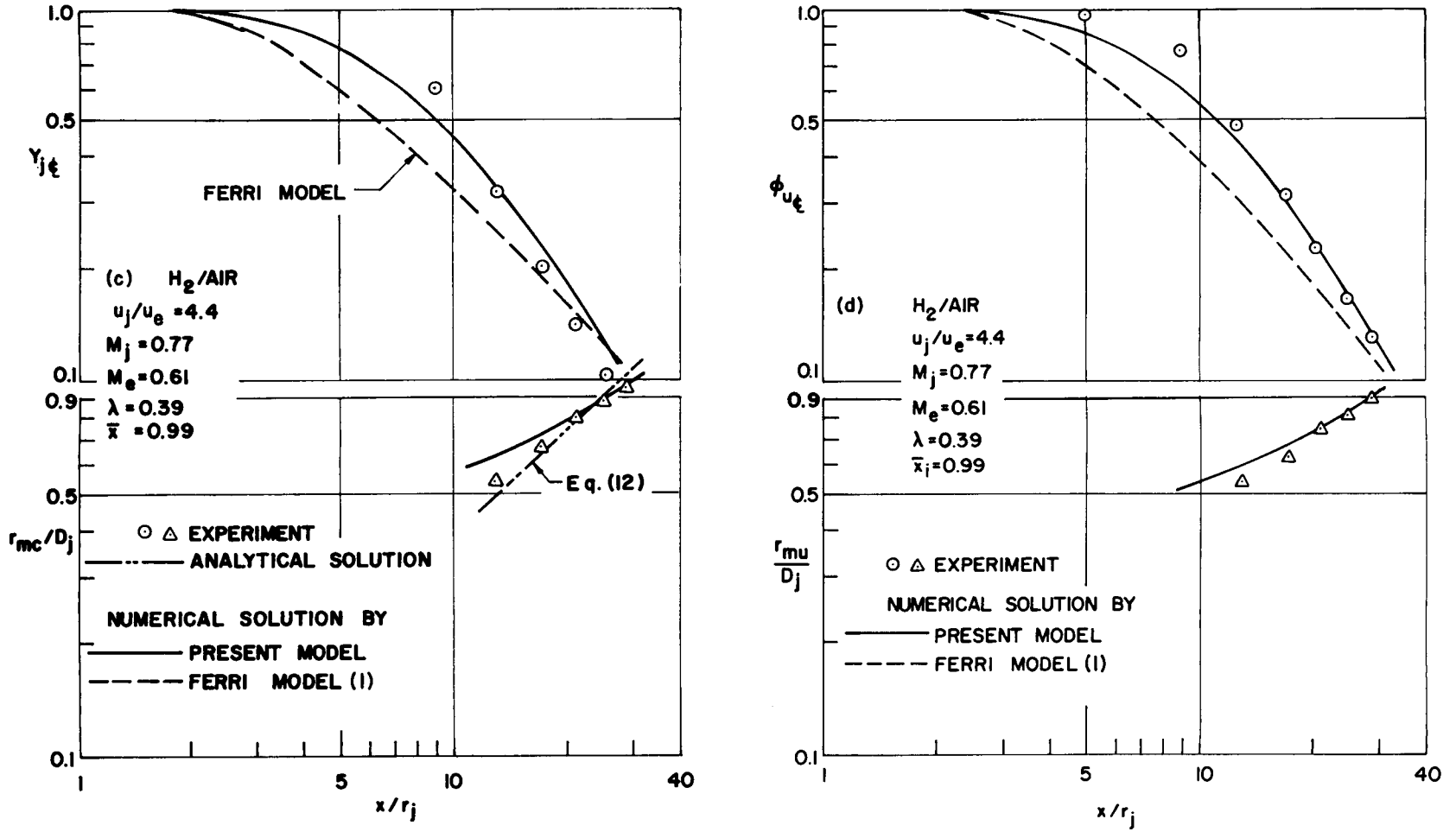

Figure 4.- Continued.

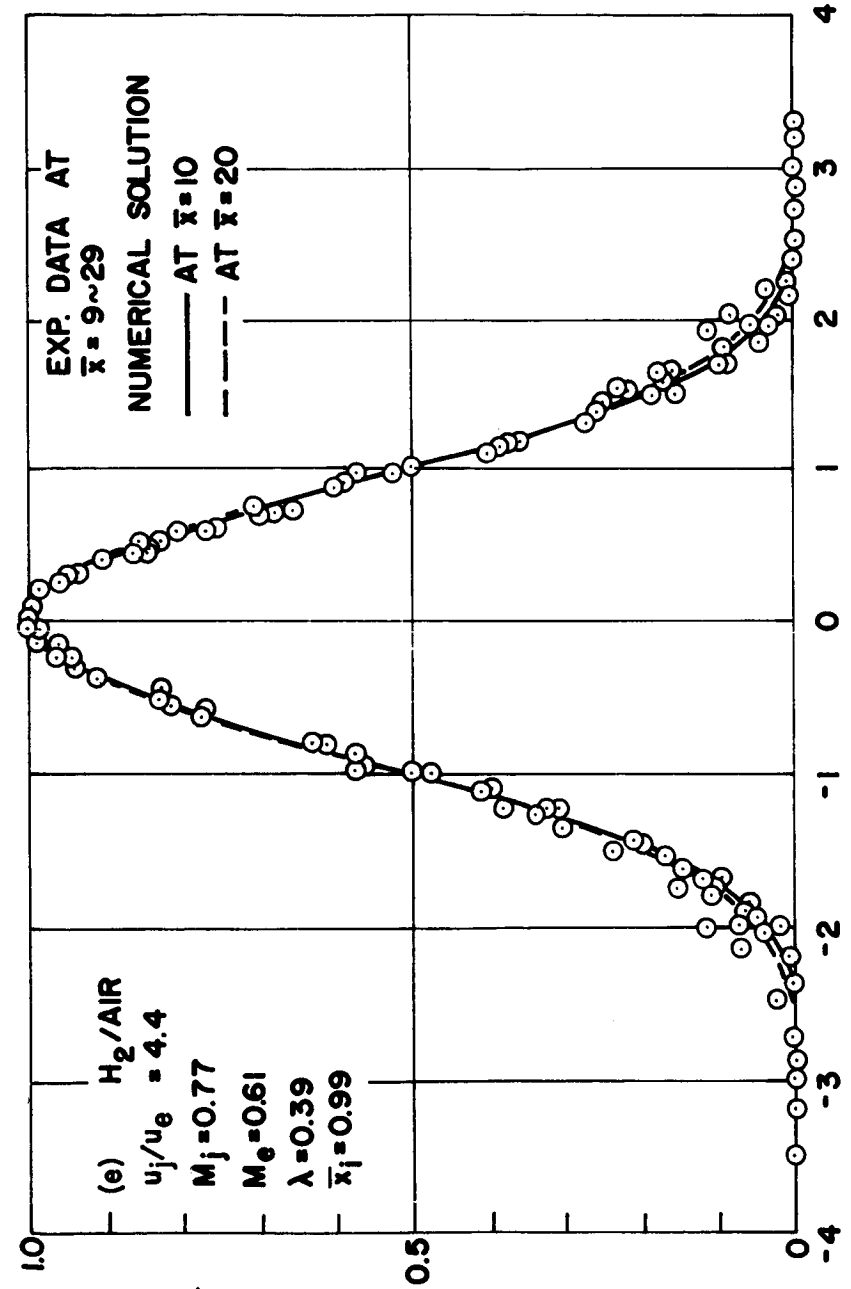

Figure 4.- Continued.

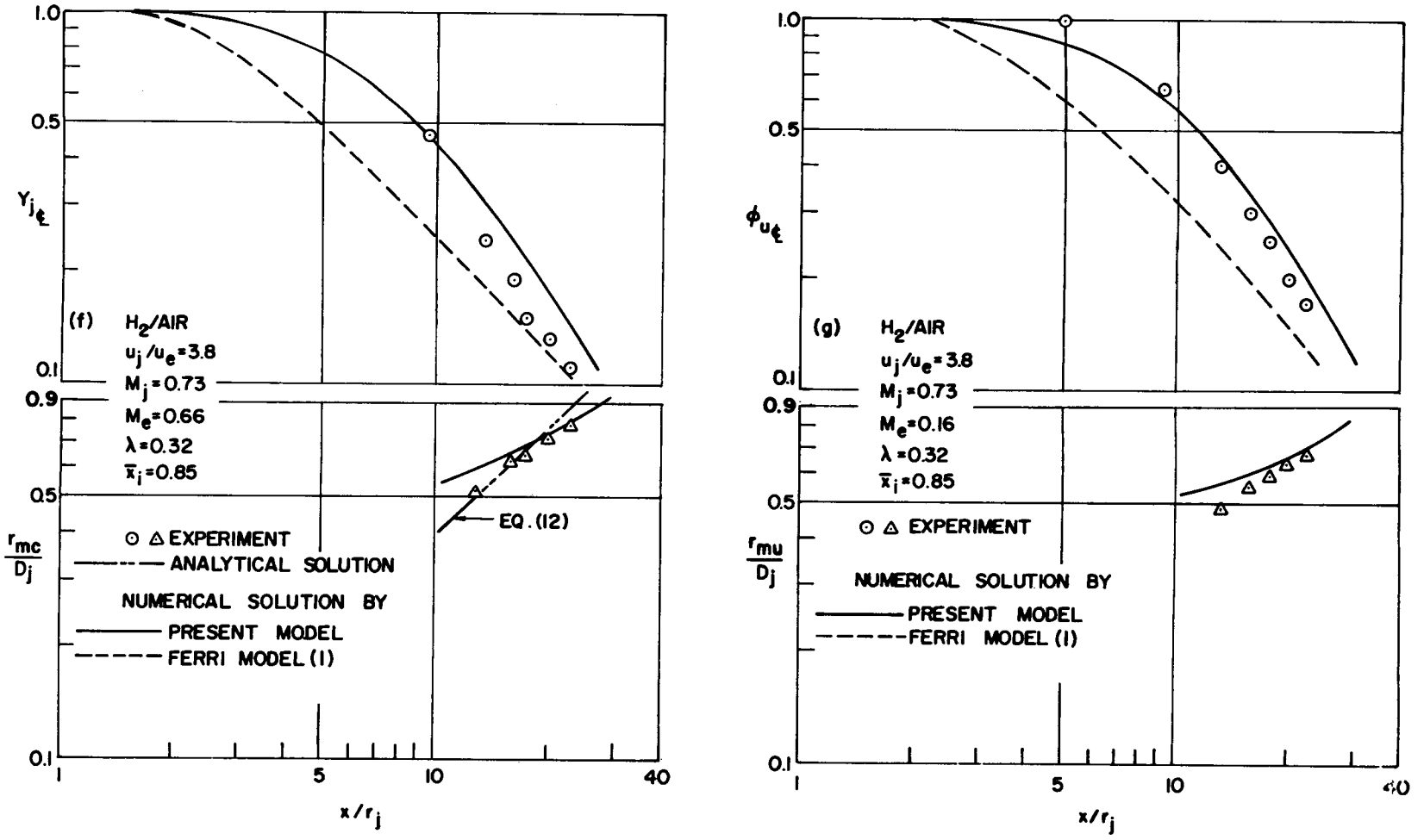

Figure 4.- Concluded.

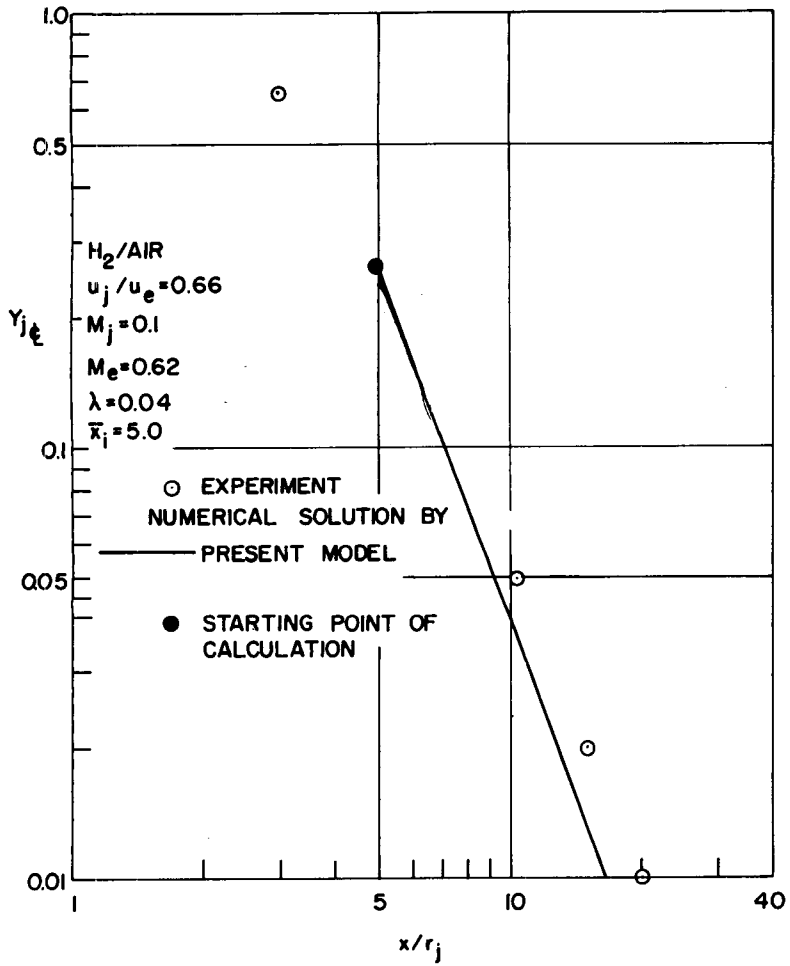

Figure 5.- Comparison of numerical results with the data of Alpinieri (ref. 2) for the mixing of hydrogen and air.

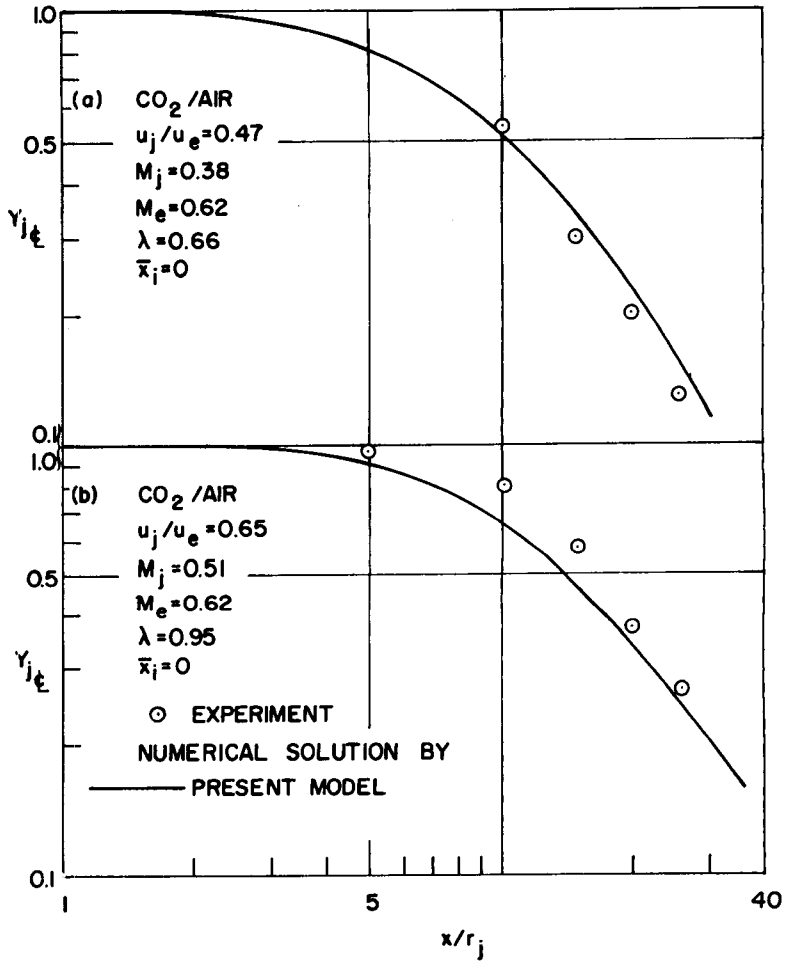

Figure 6.- Comparison of numerical results with the data of Alpinieri (ref. 2) for the mixing of carbon dioxide and air.

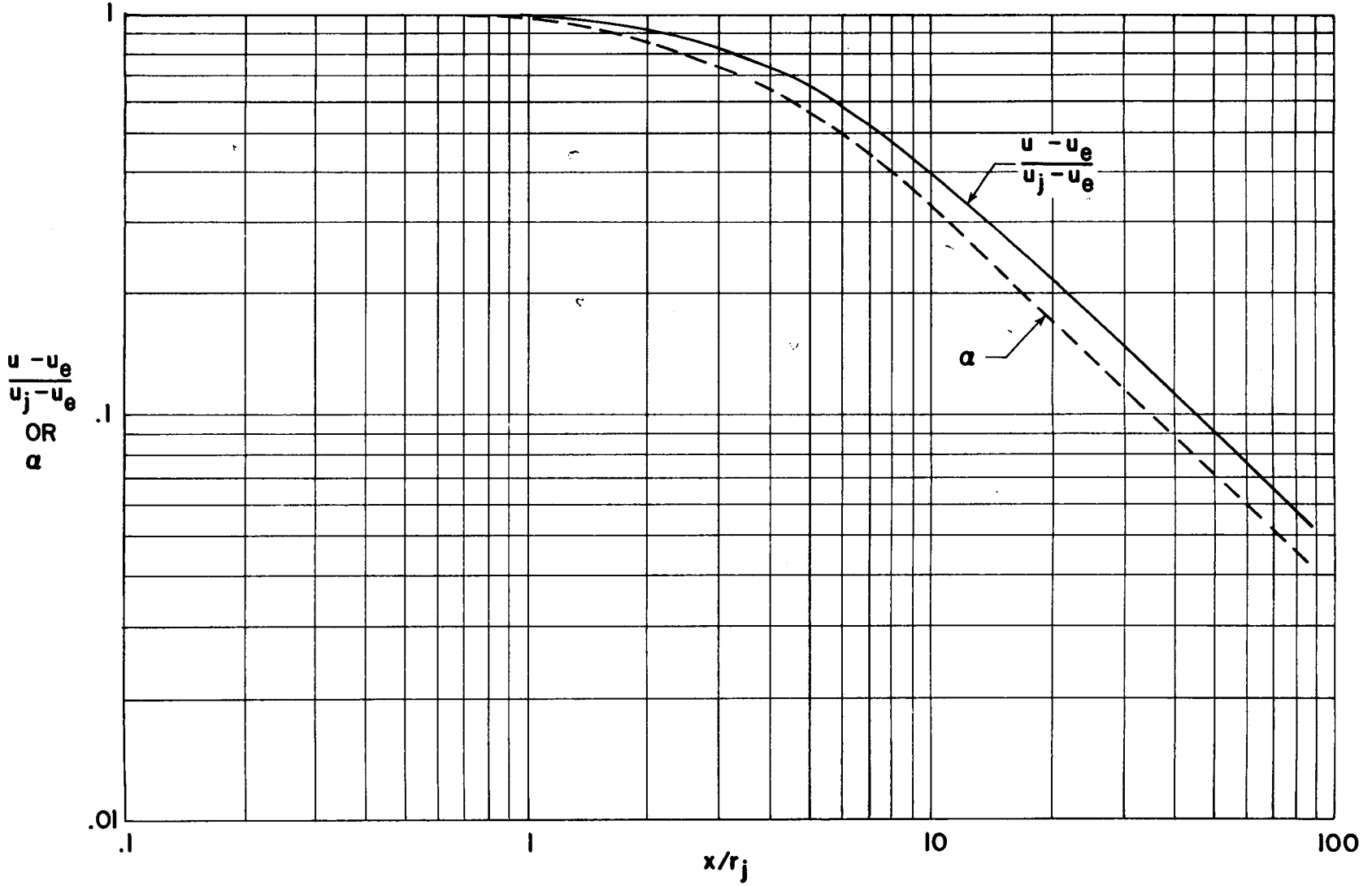

Figure 7.- Additional case.

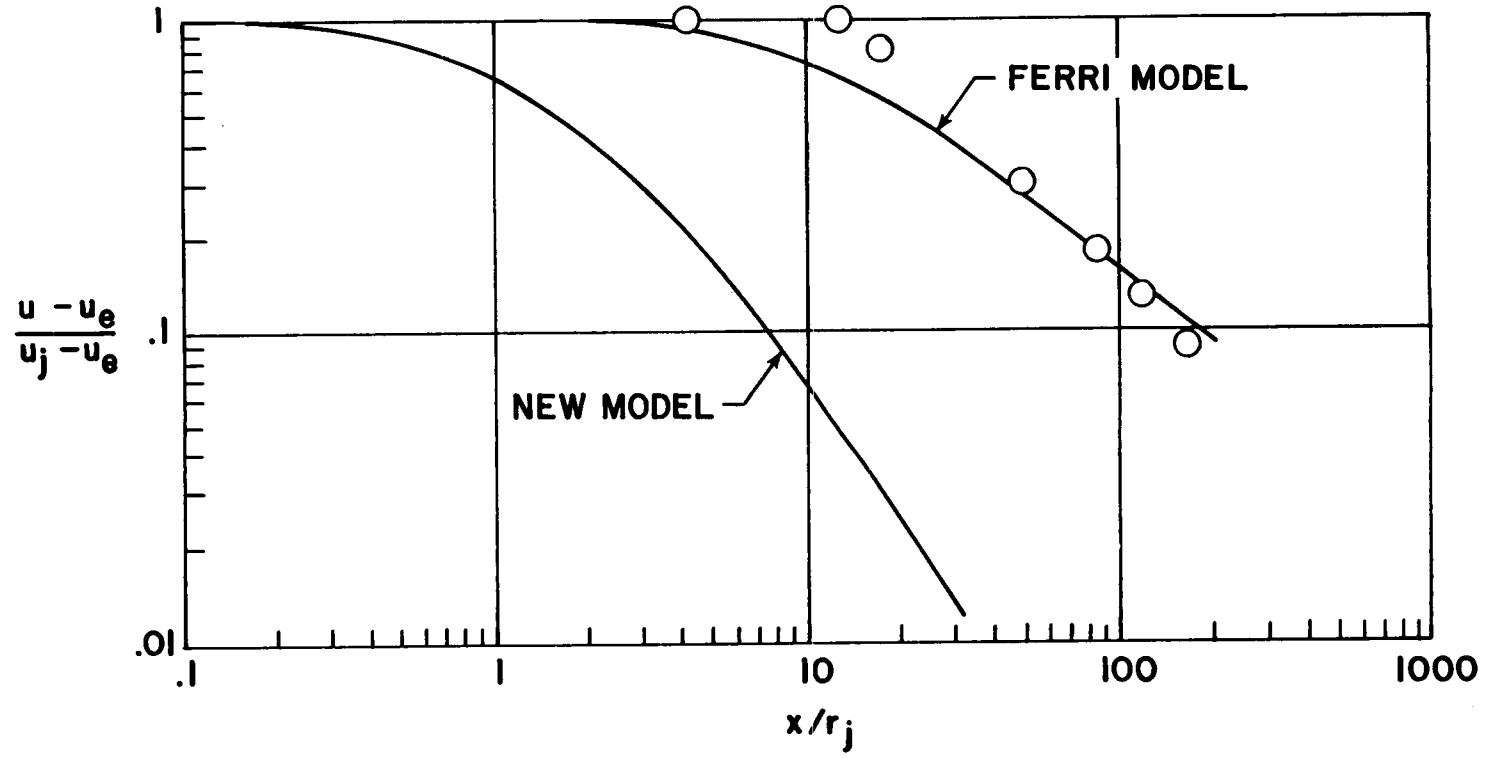

Figure 8.- Case 9.

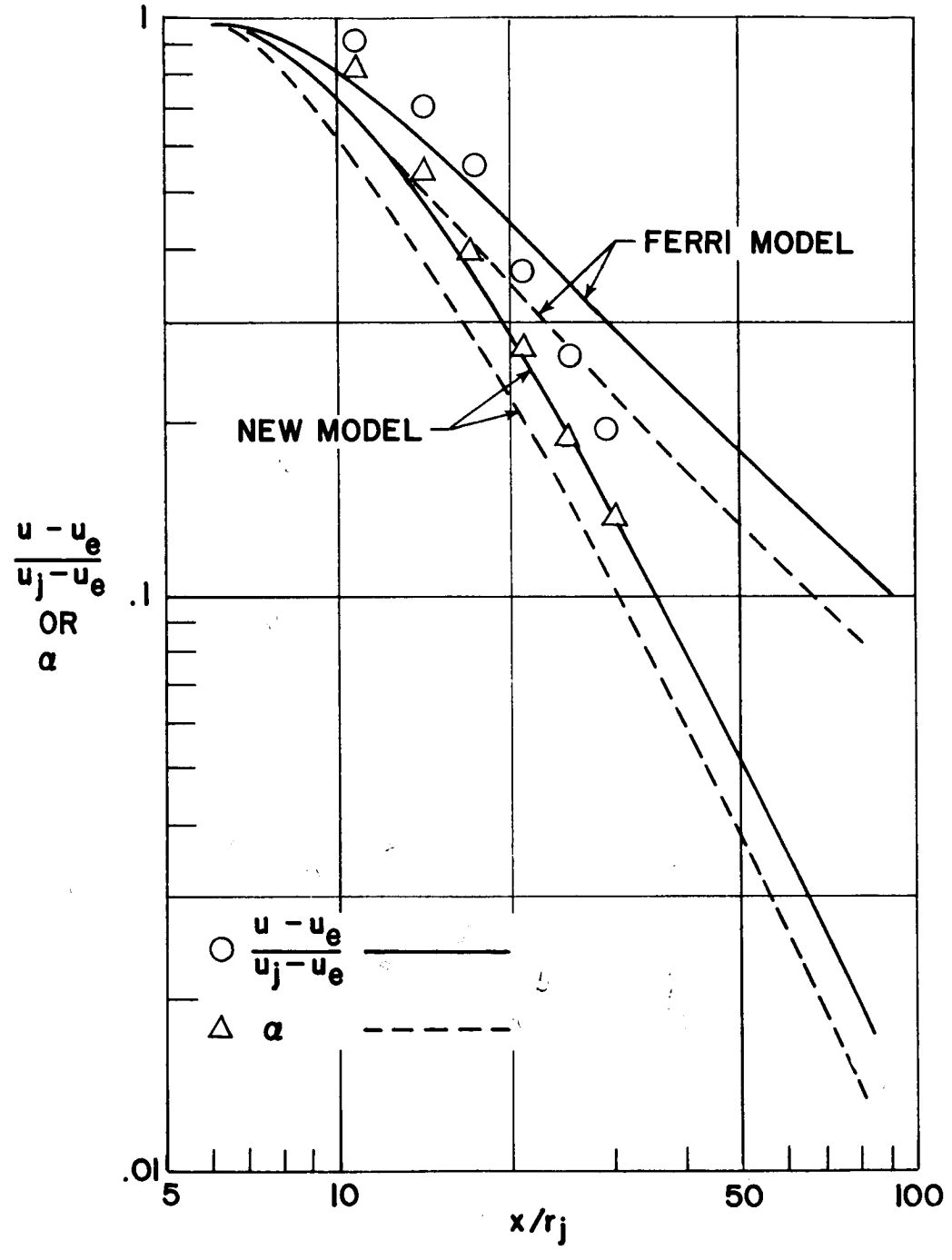

Figure 9.- Case 10.

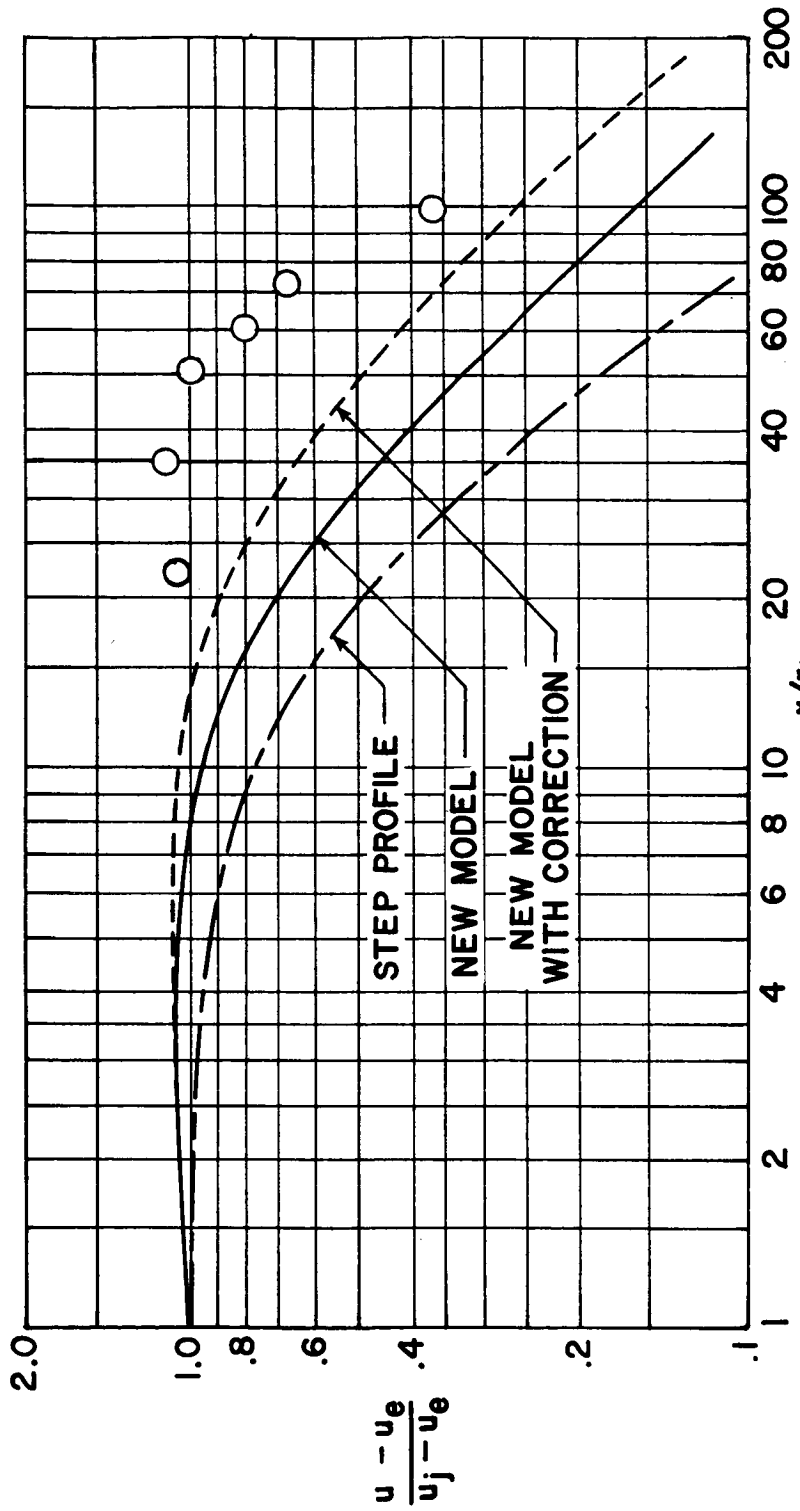

Figure 10.- Case 11.

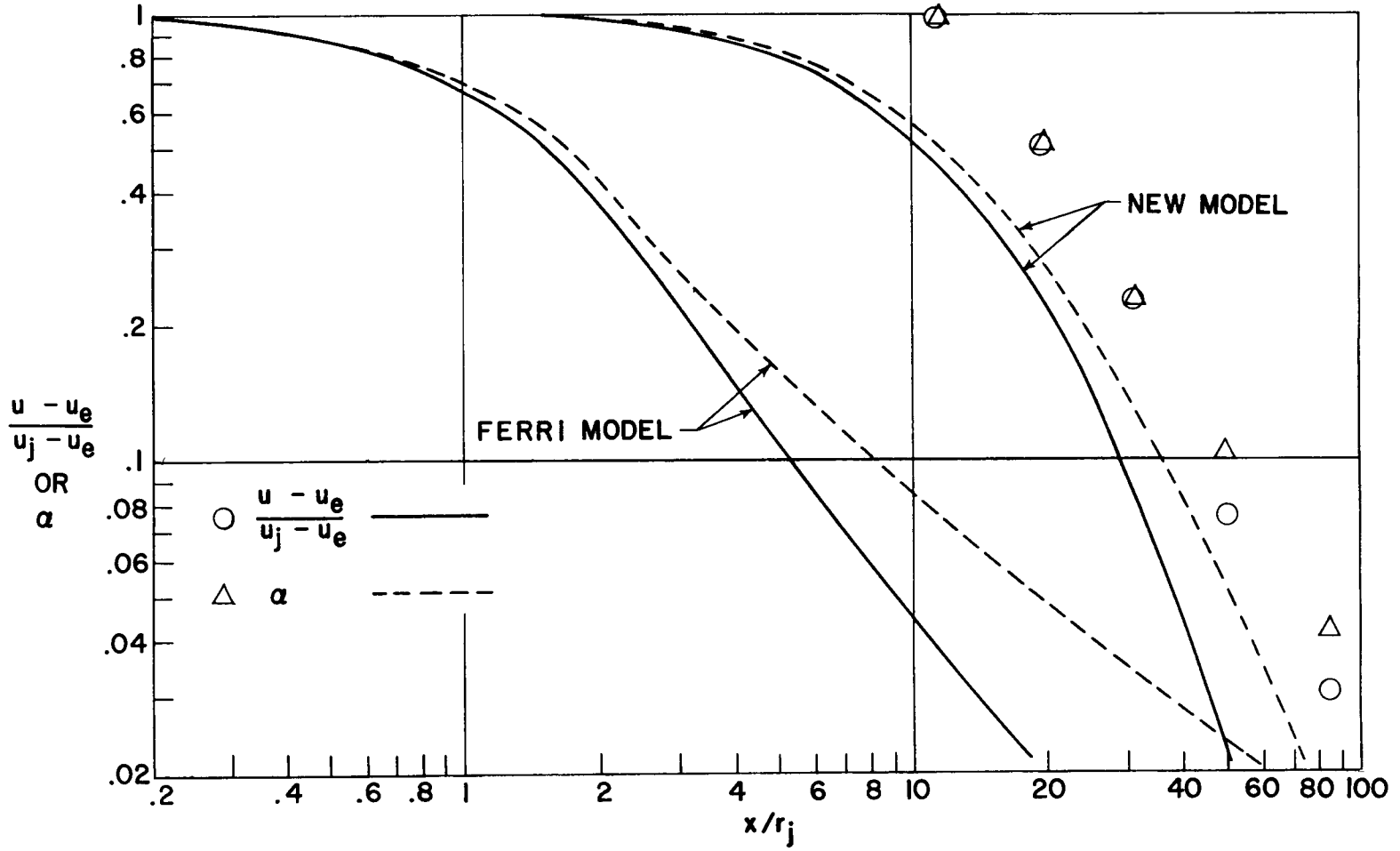

Figure 11.- Case 12.

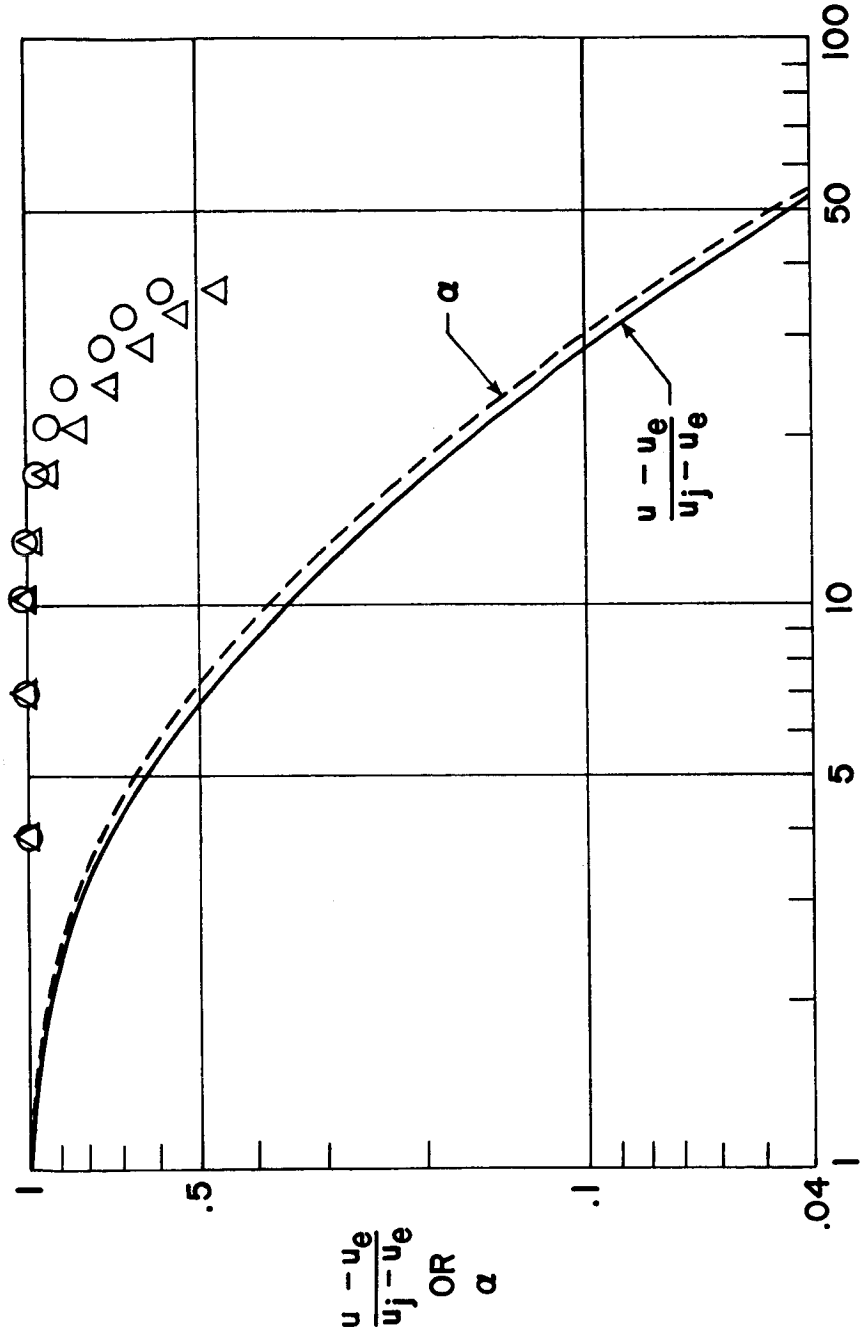

Figure 12.- Case 20.

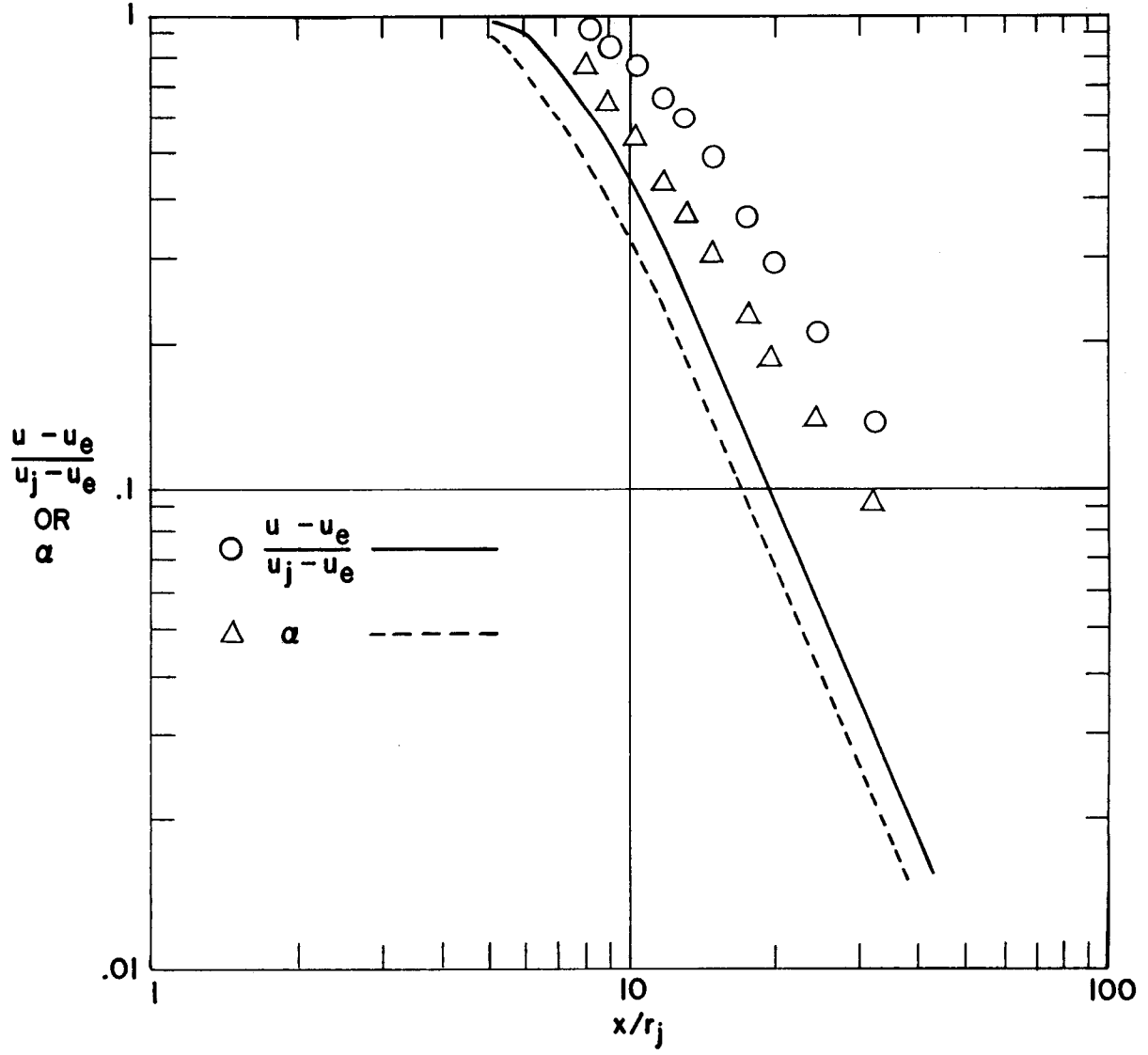

Figure 13.- Case 21.

PREDICTION OF FREE SHEAR FLOWS

A COMPARISON OF THE PERFORMANCE OF SIX TURBULENCE MODELS

By B. E. Launder, A. Morse, W. Rodi,
and D. B. Spalding
Imperial College of Science and Technology

SYMBOLS

C_s	constant prefixing diffusion term in $\overline{uv}k\epsilon$ and $\overline{u_iu_j}\epsilon$ models
C_ϵ	constant prefixing diffusion term in ϵ equation
$C_{\epsilon 1}, C_{\epsilon 2}$	constants appearing in transport equation for ϵ
C_μ	viscosity constant
$C_{\phi 1}$	constant appearing in first part of pressure-strain simulation
$C_{\phi 2}$	constant appearing in second part of pressure-strain simulation
D	diameter of jet or of wake-generating body
D_i	diameter of inner nozzle
D_o	diameter of outer nozzle
D_{ij}	net diffusion flux of $\overline{u_iu_j}$
g	a function of $\overline{P/\epsilon}$ (see table 4)
h	specific enthalpy of fluid
k	turbulence energy, $\left(\overline{u^2} + \overline{v^2} + \overline{w^2}\right)/2$
l	length scale of turbulence
l_m	mixing length

M	Mach number
m	mass fraction of chemical species
P	production rate of turbulence energy
P_{ij}	production rate of Reynolds stress $\overline{u_i u_j}$
r	radial coordinate
r_o	radius of nozzle exit
$\tilde{T}$	stagnation temperature
$\tilde{T}_o$	stagnation temperature at nozzle exit
t	time
U	mean velocity in streamwise direction
U_e	velocity of free stream
ΔU	change in mean velocity across shear flow
U_i, U_j	mean velocity components
U_{min}	minimum velocity
U_o	initial (uniform) value of streamwise mean velocity
u,v,w	fluctuating velocities in x,y,z directions
$\overline{uv}$	kinematic shear stress
$\overline{u_i u_j}$	kinematic Reynolds stresses
x	coordinate in streamwise direction
x_i, x_j	general Cartesian coordinates

y coordinate in cross-stream direction

y_G effective width of shear flow

y_1, y_2 values of y at which effective internal and external edges of the shear flow occur

y^j coordinate in cross-stream direction where j is 0 for plane flows and is 1 for axisymmetric flows

α normalized mass fraction

δ_{ij} Kronecker delta

ϵ turbulence energy dissipation rate

θ momentum deficit (or excess) thickness of wake (or jet)

λ constant in mixing length model

λ_s proportionality constant relating length scale ℓ to y_G in k model of turbulence

μ_t effective turbulent viscosity

ρ density

σ reciprocal of spreading rate of mixing layer

σ_o value of σ when one stream is at rest

σ_ϕ effective turbulent Prandtl/Schmidt number (where subscript ϕ stands for h, k, m, or ϵ and denotes the diffused quantity)

Φ_{ij} pressure strain term in equation for $\overline{u_i u_j}$

Subscripts:

$\mathfrak{L}$ value prevailing along center line of a symmetric flow

E external boundary of shear flow

I internal boundary of shear flow

1 high-velocity edge of shear layer

2 low-velocity edge of shear layer

Bar over symbol indicates time average of turbulence correlation.

THE TURBULENCE MODELS CONSIDERED

The authors' work for the NASA Conference on Free Shear Flows has led to the exploration of the performance of three distinct classes of turbulence model. These classes are

(1) turbulent-viscosity models [1] in which the length scale of turbulence is found by way of algebraic formulas

(2) turbulent-viscosity models in which the length scale of turbulence is found from a partial differential equation of transport

(3) models in which the shear stress itself is the dependent variable of a partial differential conservation equation

In the context of the group's work on this subject, these classes might equally be, respectively, labeled "yesterday's" models, "today's" models, and "tomorrow's" models. At the time of the AFOSR-IFP-Stanford Conference in 1968, detailed exploration had been confined to models of class (1). In the intervening years, the development and application of models of class (2) has commanded the major part of the group's attention and, although models of class (3) have been in use since 1969, they have not yet been refined sufficiently to achieve the level of universality of which they are believed to be capable.

Two models have been examined in each class; thus, six different models have been tested. A complete mathematical statement of these models is provided in tables 1 to 6; a brief commentary on the models now follows.

Tables 1 and 2 detail the group's versions of two of Prandtl's turbulence models (refs. 1 and 2), namely, his 1925 mixing-length hypothesis $(m\ell h)$ and his 1945 turbulence

[1] A turbulent-viscosity model is one in which the shear stress is taken to be proportional to the local gradient of time-average velocity. The proportionality factor may vary from point to point in the flow and is usually calculated by reference to local turbulence quantities. It is not implied that the effective viscosity of the fluid is uniform across the mixing region.

kinetic energy model (k). For each model, the length scale is taken as proportional to the width of the shear flow although a different constant of proportionality is adopted for plane and axisymmetric flows. Table 1 reveals how the width of flow is defined.

The models of class (2), described in tables 3 and 4, employ a differential equation for the decay rate of turbulence energy ϵ as well as one for the turbulence energy. By introduction of this second turbulence transport equation, the need to prescribe the length scale is removed. The same two turbulence variables have been used in similar models by Harlow and Nakayama (ref. 3) and by Jones and Launder (ref. 4); other models having just two differential equations have also been used and described by Rodi and Spalding (ref. 5), Ng and Spalding (ref. 6), and Spalding (ref. 7). In the $k\epsilon 1$ model set out in table 3, the viscosity constant C_μ differs according to whether the flow is plane or axisymmetric. The more elaborate $k\epsilon 2$ model, detailed in table 4, has been adapted from that presented by Rodi (ref. 8). Rodi found that C_μ did not, in fact, assume a constant value but varied significantly with the distortion rate of the turbulence; the local rate of turbulence production divided by the rate of dissipation may be taken as a dimensionless measure of this quantity. Figure 1 shows Rodi's proposal for the dependence of C_μ on the ratio of production to dissipation at any station; the same variation is adopted in the $k\epsilon 2$ model.

In the two-equation class, attention has been confined to models employing k and ϵ as variables because extensive research at Imperial College has shown that, for free turbulent flows, the models of references 5, 6, and 7 produce almost identical results. Indeed, it can be shown that the identity is exact whenever the length scale of turbulence is uniform across the mixing region, and this condition is very nearly fulfilled for all free shear flows. Further, ϵ is preferable to the second variables of the other models when walls are present, for the $k\epsilon$ model alone can dispense with a wall-effect correction of the empirical constants.

The models set out in tables 5 and 6 are ones which do not involve the effective-viscosity concept. Table 5 presents the model of Hanjalić and Launder (ref. 9), which has been applied by its originators to predict a number of boundary layers and free shear flows. Besides the differential equations for k and ϵ, it embodies one for the kinematic shear stress $\overline{uv}$ as well. Lastly, model 6 presented in table 6 is an orthodox Reynolds stress closure of the kind first proposed by Rotta (ref. 10); it provides transport equations for all the Reynolds stresses $\overline{u_i u_j}$ and for the energy dissipation rate. If the turbulence Reynolds number is assumed high enough for the dissipative motions to be isotropic, only two processes remain to be simulated in the Reynolds stress equations: those of diffusional transport and of energy redistribution, the latter arising from correlations between fluctuating pressures and instantaneous velocity gradients. Two approximations have been explored for the first process and three for the second. In the flows

considered for this conference, only four of the Reynolds stresses are nonzero; the model thus entails the solution of five transport equations for turbulence quantities.

DETAILS CONCERNING THE PREDICTIONS

Method of Solving the Equations

The systems of differential and auxiliary equations governing the development of the mean and turbulent flow field have been solved by means of the finite-difference procedure of Patankar and Spalding (ref. 11). The main features of the method – that is, the use of normalized stream function as cross-stream independent variable and the employment of a grid-control system to fit the width of the grid to that of the shear flow – are perhaps sufficiently well known not to require further elaboration here. For the readers who are unfamiliar with the procedure, reference 11 documents the method in full and provides a listing of the basic computer program, GENMIX, from which codes used in the present work have been adapted.

The number of cross-stream nodes employed has varied from 20 to 40 according to the complexity of the initial profiles; grid nodes have been concentrated in regions where velocity gradients were steepest. A Control Data 6600 computer system was used. Typically, with 25 cross-stream nodes, the programs executed 70 forward steps per second for calculations employing the mixing-length hypothesis, where differential equations were solved for the mean-flow field (x-momentum, species, and stagnation enthalpy); with the Reynolds stress turbulence model and with the same number of nodes, about 35 forward steps per second were taken for isothermal, single-species flows. This number could certainly have been increased substantially, for to save human time many redundant instructions were not removed. No attempt has been made to include the influence of normal-stress gradients in the mean momentum equation since, for the turbulent-viscosity models, retention of these terms would render the equations elliptic in character. Likewise, corresponding terms in the turbulence equations have been neglected.

Initial Profiles

For all models except the mixing-length hypothesis, the initial profiles supplied by the conference organizers were insufficient to prescribe fully the starting conditions. Therefore, some of the profiles of the turbulence energy, of the Reynolds stress, and of the energy-dissipation rate had always to be estimated. This section explains the group's practices for generating the profiles.

(1) When the initial shear-stress profile was not supplied, a number of trial calculations were made based on a constant effective viscosity. The value of the constant was adjusted until the predicted development in the vicinity of the starting point agreed with the measured; this value of the effective turbulent viscosity was then used to determine

the initial shear-stress profile from the given velocity profile. The values adopted for each test case are given in table 7; they have been normalized by the product of the density ρ, the velocity change across the shear flow ΔU, and the diameter of the jet (or the diameter of the obstacle giving rise to the wake) D. In some cases the local value of density has been used, in others the values prevailing in the external stream; the third column of the table contains 1 or e as appropriate to identify the practice.

(2) Where the initial turbulence energy was not available, it was estimated from the shear-stress profile (either measured or determined as in practice (1)) by use of the following relation:

$$k = \frac{|\overline{uv}|}{0.3}$$

Close to an axis of symmetry, this formula gives an unrealistically low value of energy; in this region the k profiles are adjusted to apparently reasonable values based on turbulence data of other similar flows.

(3) In none of the test cases is the profile of energy dissipation rate directly available. It is calculated by inverting the viscosity formula

$$\epsilon = \frac{C_\mu \rho k^2}{\mu_t}$$

where μ_t is taken as the value of effective viscosity found in practice (1) or, when shear-stress data are available, is calculated from

$$\mu_t = - \frac{\overline{uv}}{\partial U / \partial y}$$

(4) For the $k\epsilon 2$ model, the initial value of the function $g(\overline{P/\epsilon})$ must be specified. For this inquiry, the usual practice has been to take this ratio as unity; however, for two of the wakes values greater than 1 have been assumed, and for two mixing layers values less than unity have been adopted. These test cases are identified in the fourth column of table 7.

DISCUSSION OF THE PREDICTIONS

Preliminary Remarks

Predictions have been made with the four models of classes (1) and (2) of all the 24 test flows except test case 24. The last of the flows was omitted from this inquiry because over much of its development the flow appeared not to be fully turbulent and because these models have not yet been adapted to the prediction of low Reynolds num-

ber phenomena.[2] For the shear-stress models of class (3), predictions have been confined to the isothermal, single-species plane flows, that is, to test cases 1, 4, 13, and 14.

The results of the calculations are shown in the figures of the appendix, which provide standard comparisons of predictions with experimental data for the four models of classes (1) and (2), and in figures 2 to 7 which display further aspects of particular predictions referred to in this discussion section. Also included in this section are a discussion of the relative success of the models in predicting the test flows, an examination of the models in ascending order of complexity (beginning with the Prandtl energy model) to discover in what respects a particular model is superior to the immediately preceding one, and a discussion of those features of the measurements which are not well predicted by any of the models and the possible reasons for the discrepancies.

The Prandtl Kinetic Energy Model (k)

Our experience of predicting wall boundary layers had led us to believe that there were scarcely any advantages in using Prandtl's kinetic energy model rather than his earlier mixing-length hypothesis; Mellor and Herring (ref. 12) reported a similar conclusion. Therefore, it should be emphasized that for free shear flows, the k model performs consistently better than the $m\ell h$ hypothesis. This fact is well brought out by reference to the jet predictions of cases 8, 12, and 18 and the wake-flow predictions of cases 13 to 16.

In concept, the k model represents a substantial advance over the $m\ell h$ hypothesis. That it is also superior in practice may be attributed to the fact that, in free shear flows but not in wall boundary layers, the convective transport and diffusive transport of kinetic energy are usually important terms in the energy-balance equation.

The foregoing remarks, however, are nearly the only ones that can be made in favor of the k model, inasmuch as reference to the cases noted indicates that there are still large discrepancies between the measured and calculated development of the flow. Invariably, over the initial region of a jet, the predicted rate of decay is too rapid; whereas, far downstream, the decay rate is too slow. The behavior over the initial region could, of course, be improved by choosing the length scale to be a smaller fraction of the flow width, but such a move would make the far-region predictions worse than ever.

---

[2] Jones and Launder (ref. 4) have in fact provided a low Reynolds number version of the $k\epsilon 1$ model; however, at several points in its derivation, the assumption is made that the low Reynolds number region is adjacent to a rigid surface as in wall boundary-layer flows. The model is thus not immediately applicable to free-shear-flow transition phenomena.

The Energy-Dissipation Model of Turbulence ($k\epsilon 1$)

The introduction of a transport equation for the dissipation rate removes the need to prescribe the length scale and leads to a model of turbulence possessing a much greater degree of universality than Prandtl's energy model, inasmuch as the length scale of turbulence is by no means a universal fraction of the width of the shear flow. Specifically, it is noted that, for many of the jet flows, the correct behavior is predicted both in the vicinity of the nozzle and many diameters downstream (cases 6, 9, 11, and 12). The $k\epsilon 1$ predictions of cases 13, 14, 15, 16, and 17 are also in distinctly better agreement with the data than are the k predictions.

The Extended Energy-Dissipation Model ($k\epsilon 2$)

When there is just one significant component of the velocity-gradient tensor and when the energy production and dissipation rates are approximately in balance, the $k\epsilon 1$ model nearly always gives acceptable predictions. The second condition is always met in wall boundary layers, in mixing layers, and also in many jet-like flows. When, however, the shear flow is weak (that is, when the excess or defect of the shear flow is but a small fraction of the velocity of the external stream), the model predicts too slow a decay rate of the shear flow; this behavior is exemplified in the predictions for cases 13, 15, 16, and 17 (the data for case 13 and for other similar but currently unpublished flows measured by Bradbury are shown replotted in fig. 2 in the format that the organizers adopted for the other weak shear flows).

Reference to the same test cases shows that much better agreement with data is achieved with the $k\epsilon 2$ model. Distinct improvements may also be seen in the predictions of cases 11, 12, and 19. The result is particularly encouraging in that Rodi (ref. 8) determined the C_μ function without reference to the data considered at this conference.

The Stress Models of Turbulence ($\overline{u_i u_j}\epsilon$ and $\overline{uv}k\epsilon$)

Models of this class have been applied to only four of the flows so that inferences drawn must be more tentative than those for the models already discussed. Moreover, when this set of computations was made, little time remained before the conference deadline and, consequently, only a preliminary adjustment of the constants was possible.

Predictions for all models gave results for case 1 scarcely distinguishable from those obtained with the $k\epsilon$ viscosity models. For case 4 (standard comparisons shown in fig. 3), however, the stress models do give a small but definite improvement; the fact emerges clearly in figure 4 which shows the development of the minimum velocity with

distance downstream. The stress models[3] follow the measured development very closely, whereas the $k\epsilon 2$ predictions show initially too steep a rise and, later, a too gradual disappearance of the wake.

The other two sets of predictions are for flows which, superficially at any rate, are very similar; yet they would lead one to draw different conclusions about the relative correctness of the models. It is seen from figures 5 and 6 that the models which are best at predicting case 13 are worst for case 14 and vice versa.[4] The experimental data from both sets of investigations seem admirably consistent. Perhaps, therefore, the differences in the development of the two flows may be traced to the different initial shear flows from which they develop, namely, a mixing layer for case 13 and a wall boundary layer for case 14. Certainly it is known from parallel research at Imperial College that none of the pressure-strain approximations so far employed predict the normal-stress profiles well close to a wall; thus, possibly there is some residual influence of the wall in the initial region of case 14.

The profiles of the lateral and streamwise energy components for case 14 are compared with the experimental data in figure 7. Agreement with the data may be thought reasonably good. It is not believed possible, on the basis of the calculations made so far, to determine which of the approximations for the diffusion and pressure-strain correlations is the best. The proposal of Naot and coworkers (ref. 13) and Reynolds (ref. 14) for the pressure-strain correlation is simple and, for the four test cases examined, not discernibly worse than the other two. It seems likely, however, that a more elaborate form, akin to stress-model versions B and C, will be needed if the axisymmetric and plane flows are to be well predicted with a single set of constants.

Aspects of the Flows Which are Poorly Predicted

The most serious disagreements between the $k\epsilon 2$ predictions and measurements arise in flows where there are appreciable density gradients. Cases 5 and 7 both suggest that compressibility effects reduce, somewhat, the rate of spread of a mixing layer, whereas the $k\epsilon 2$ model indicates no significant variation with Mach number. This trend is not uniform over all the flows. However, the predictions of the jets of cases 19 and 12 both display reasonable agreement with the experimental data; whereas, the experiments of cases 10 and 21 exhibit a jet decay much faster than the predictions herein would indicate.

---

[3] The letter and number ascribed to the $\overline{u_i u_j}\epsilon$ models denote the versions of the diffusion and pressure-strain hypotheses which were employed. (See table 6.)

[4] The only reason that the $k\epsilon 2$ model gave good predictions for both flows was that the initial value of $g\left(\overline{P/\epsilon}\right)$ was raised to 1.2 for case 14.

At least some of these contradictions may be attributed to the difficulty of prescribing adequately the initial conditions, particularly for the hydrogen jets of cases 10 and 21 where calculations start nearly 3 diameters downstream from the exit. An additional prediction of these flows has been made, in which the initial values of k and μ_t across the jet have been doubled. The resultant predictions shown on the standard comparison are in much closer agreement with experimental data than those previously obtained with the $k\epsilon 2$ model. Moreover, if the turbulent Prandtl/Schmidt number had been taken as 0.5 rather than 0.7 (the former value was adopted with the k and $ml h$ models), the prediction of the velocity decay would have been further improved.

Apparently, little success has been had with any of Chriss and Paulk's data inasmuch as their air/air jet (case 20) also decays much faster than the $k\epsilon 2$ predictions herein show. Since computations are begun right at the jet lip, initial conditions have little effect on the flow for case 20. The rate of spread is, however, quite sensitive to the presence of turbulence in the core region. Included in the standard comparison for this flow is a prediction where the initial turbulence intensity $\left(\sqrt{\overline{u^2}}/U_o\right)$ was about 5 percent. It may be seen that this curve follows more closely the experimental data over the first 8 diameters or so.

Predictions are also in poor agreement with experimental data for the hydrogen jet of case 22. The flow is interesting because, through the presence of boundary layers on the nozzle walls, the "jet" actually has a momentum deficit. This discrepancy may be attributable to (1) the initial value of μ_t being too high (the effect of halving it is shown) and (2) the initial velocity profile having too small a momentum deficit.

For the uniform-density flows, disagreement between experiment and prediction is much less. The following discrepancies however are to be noted:

Case 4: The predicted shear stress at the downstream station is only half the measured. In view of the excellent predictions of the velocity profiles achieved by the stress models, it is difficult to accept that the predicted shear-stress profile can be much in error.

Case 14: It seems that the momentum deficit of the wake measured at $x = 1.5$ m may be rather more than that at the other stations.

Case 15: The near-wake behavior is not well predicted for this case, probably because of the pressure gradient across the boundary layer. In the calculations herein, zero cross-stream pressure variation is presumed.

Case 18: The predictions of the turbulence energy show a flatter top to the profile than do the standard data. It is seen that Rodi's (ref. 15) recent measurements, employing what is claimed to be a more accurate signal-processing technique, are in closer agreement with the prediction.

Case 23: For this case, the experimental data show a progressive loss of momentum as the flow develops downstream.

CONCLUSIONS

The following main conclusions can be drawn from this work:

1. Turbulence models which determine the length scale of turbulence from the transport equation for energy dissipation rate (or from some other length-scale-containing variable) can give correct predictions over a wider range of flows than is possible with models embodying algebraic prescriptions of l.

2. The $k\epsilon 2$ model, which incorporates the dependence of C_μ on $\left(\overline{P/\epsilon}\right)$, leads to reasonable predictions of both strong and weak free shear flows.

3. The versions of the Reynolds stress models which were tested already give, on the average, predictions for the four cases considered which are slightly superior to those of the $k\epsilon 1$ model. There is, however, evident need for further refinement, particularly with respect to the pressure-strain approximation.

4. More experiments are needed on flows with density variation in order to resolve the question of whether or not there is a systematic influence of density variation for which the present models do not account.

5. It is very desirable that experimenters should measure and report the distributions of turbulence quantities at the upstream boundaries of the flows, as well as just the time-mean velocities, temperatures, and compositions.

ACKNOWLEDGMENTS

The support of the Science Research Council is gratefully acknowledged through Research Grant B/RG/1863 and through the award of an SRC Research Studentship to A. Morse.

The computations were performed by means of digital computers under the control of the University of London Computer Centre.

Valuable assistance in the computations was provided by Mr. J. N. Loughhead; to him the authors offer their sincere thanks.

APPENDIX

PREDICTIONS OF TEST CASES 1 TO 23

This appendix contains, in order, predictions of test cases 1 to 23, obtained with the aid of the four turbulent-viscosity models. (See pages 697 and 698 for index to test cases.)

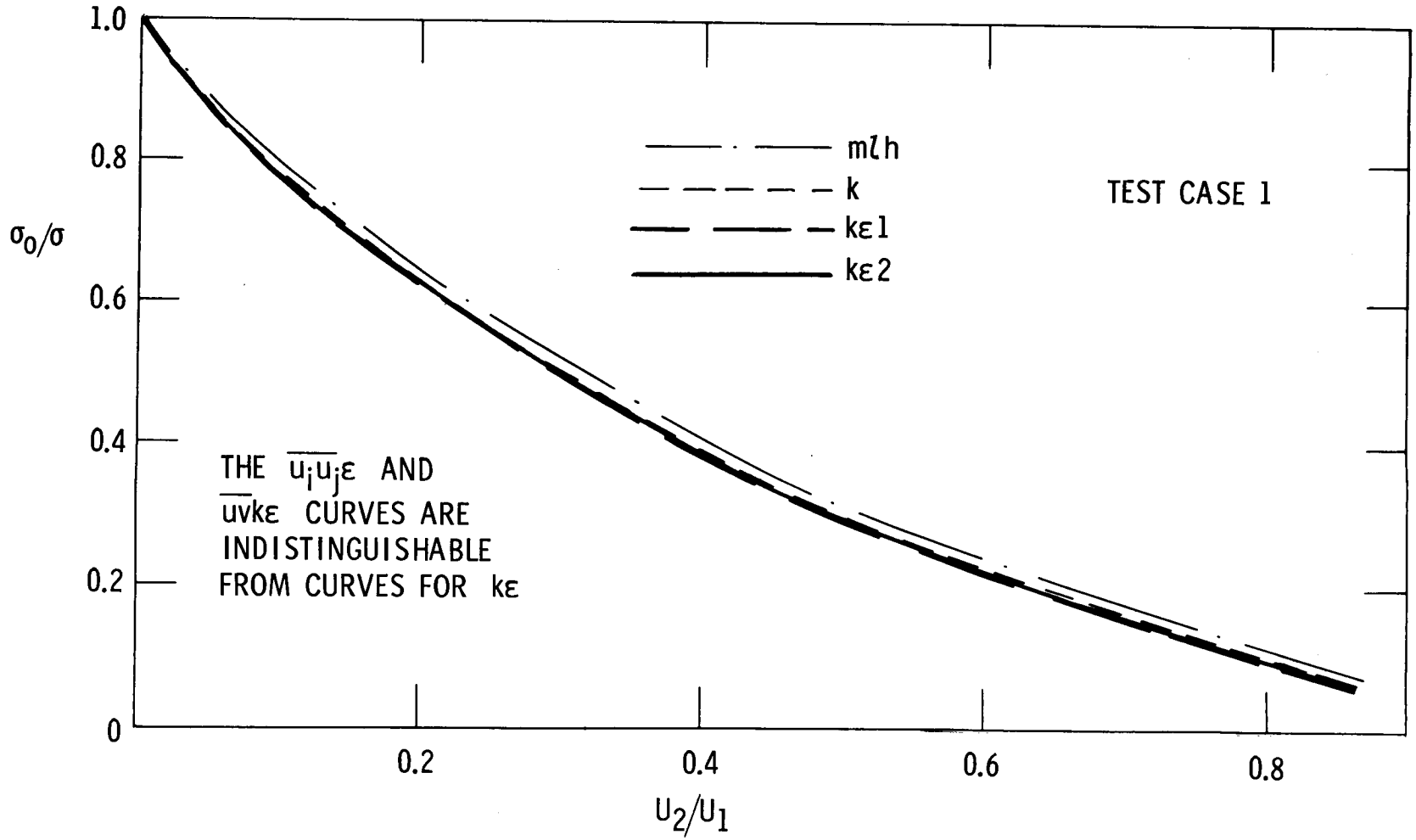
1.0
0.8
0.6
0.4
0.2
0
σ_0/σ
0.2
0.4
0.6
0.8
U_2/U_1
mlh
k
kε1
kε2
TEST CASE 1
THE $\overline{u_i u_j}\varepsilon$ AND
$\overline{uv}k\varepsilon$ CURVES ARE
INDISTINGUISHABLE
FROM CURVES FOR kε

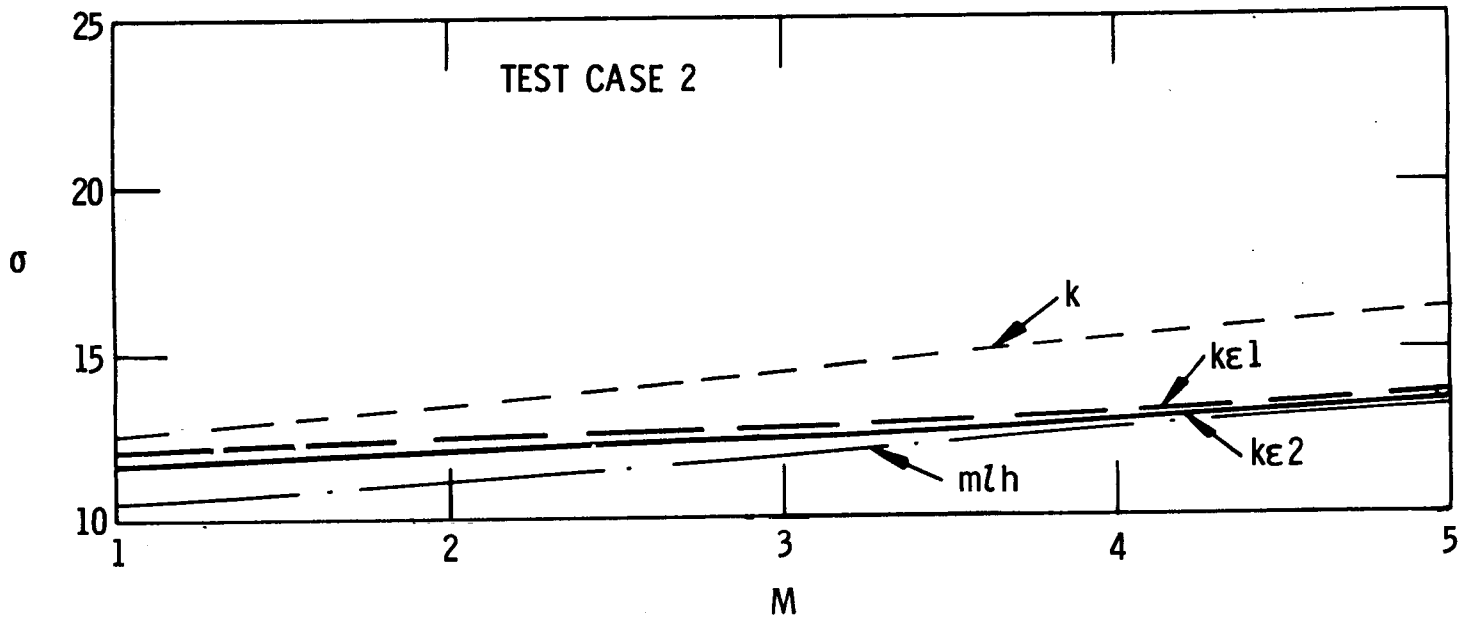
TEST CASE 2
25
20
15
10
σ
1
2
3
4
5
M
k
kε1
kε2
mℓh

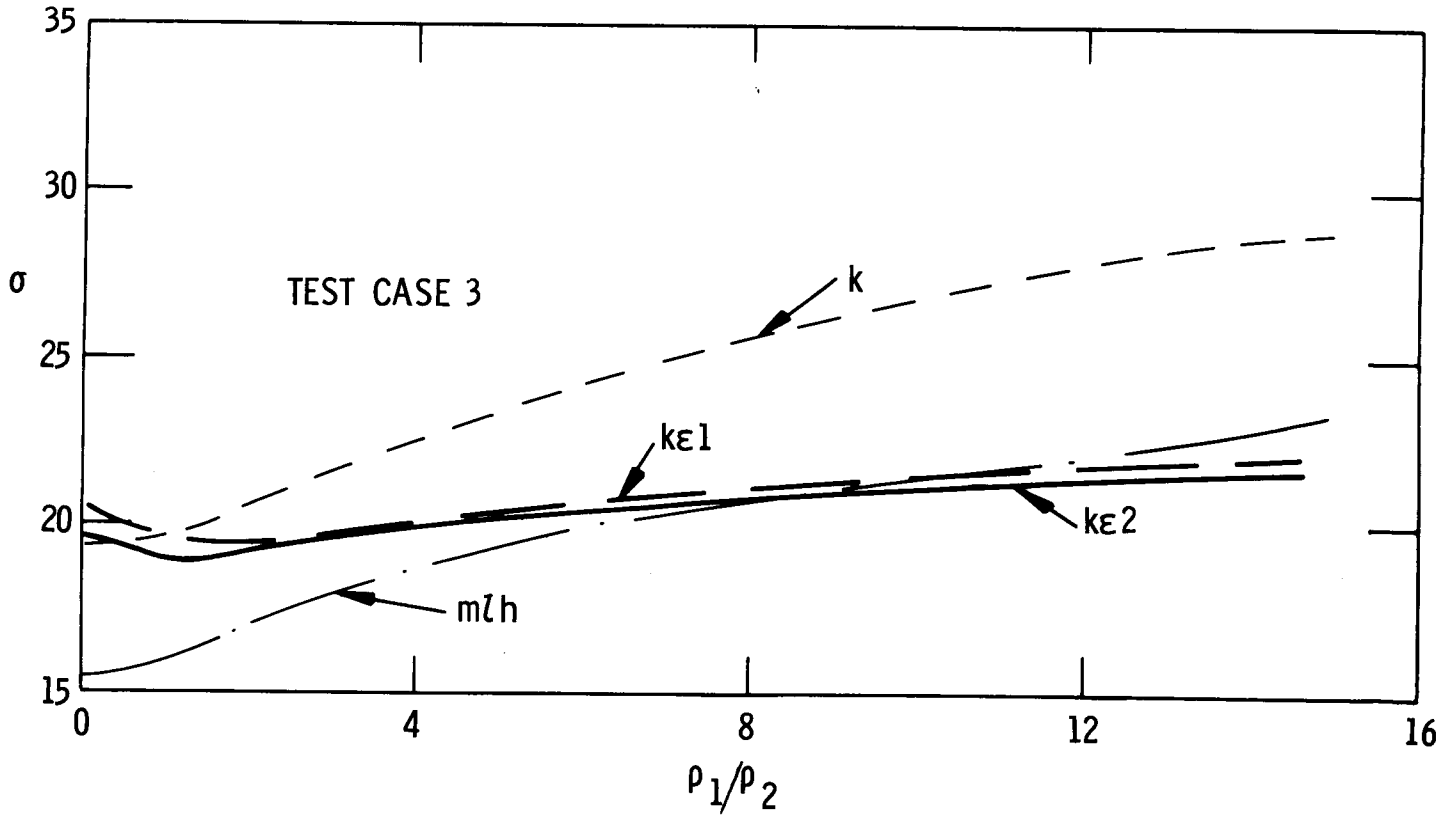
35
30
25
20
15
σ
TEST CASE 3
k
kε1
kε2
mℓh
0
4
8
12
16
ρ1/ρ2

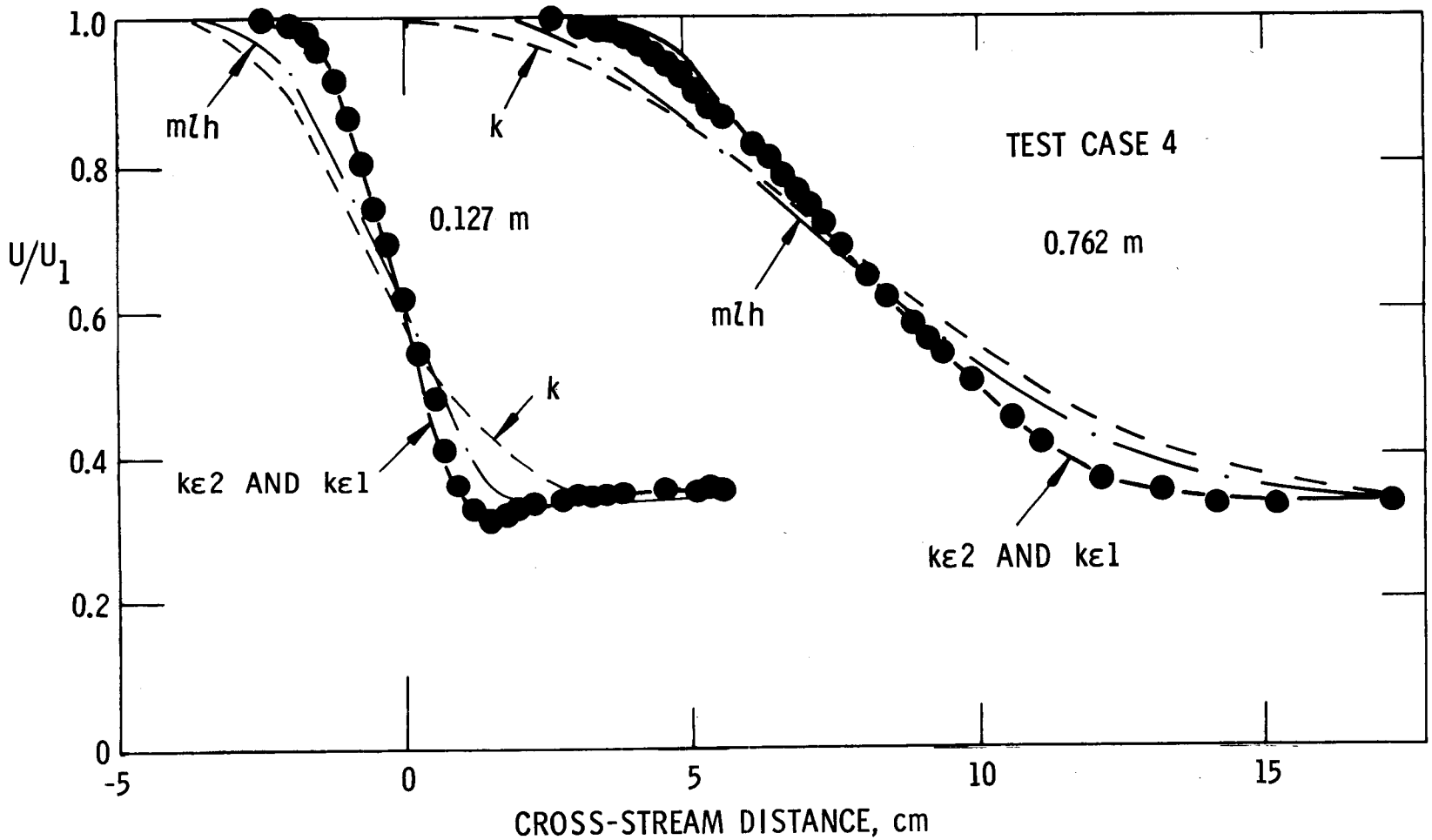
1.0
0.8
0.6
0.4
0.2
0
U/U1
mlh
k
0.127 m
kε2 AND kε1
k
TEST CASE 4
0.762 m
mlh
kε2 AND kε1
-5
0
5
10
15
CROSS-STREAM DISTANCE, cm

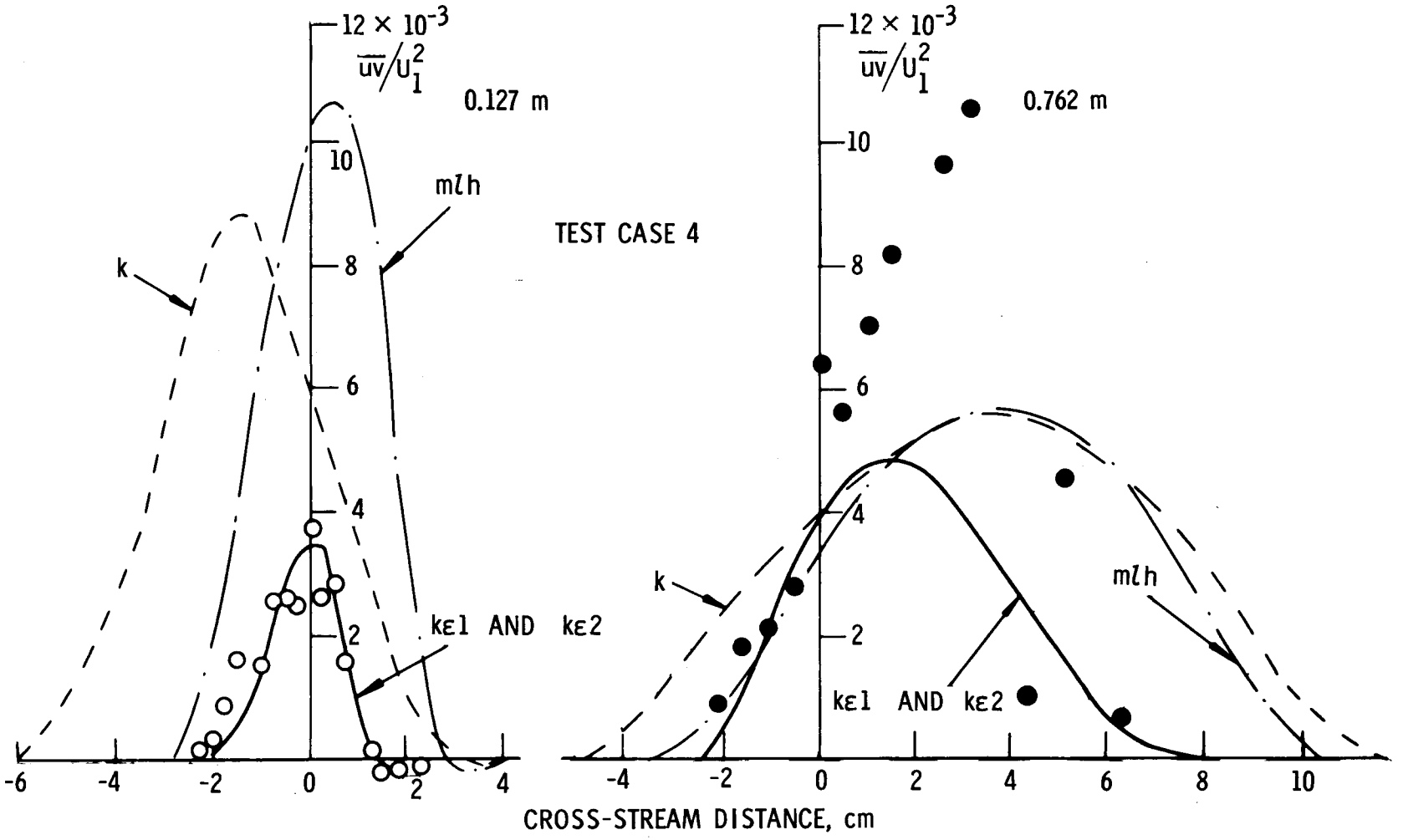
12×10^{-3}
$\overline{uv}/U_1^2$
0.127 m
10
8
6
4
2
mℓh
k
kε1 AND kε2
-6
-4
-2
0
2
4
TEST CASE 4
12×10^{-3}
$\overline{uv}/U_1^2$
0.762 m
10
8
6
4
2
k
mℓh
kε1 AND kε2
-4
-2
0
2
4
6
8
10
CROSS-STREAM DISTANCE, cm

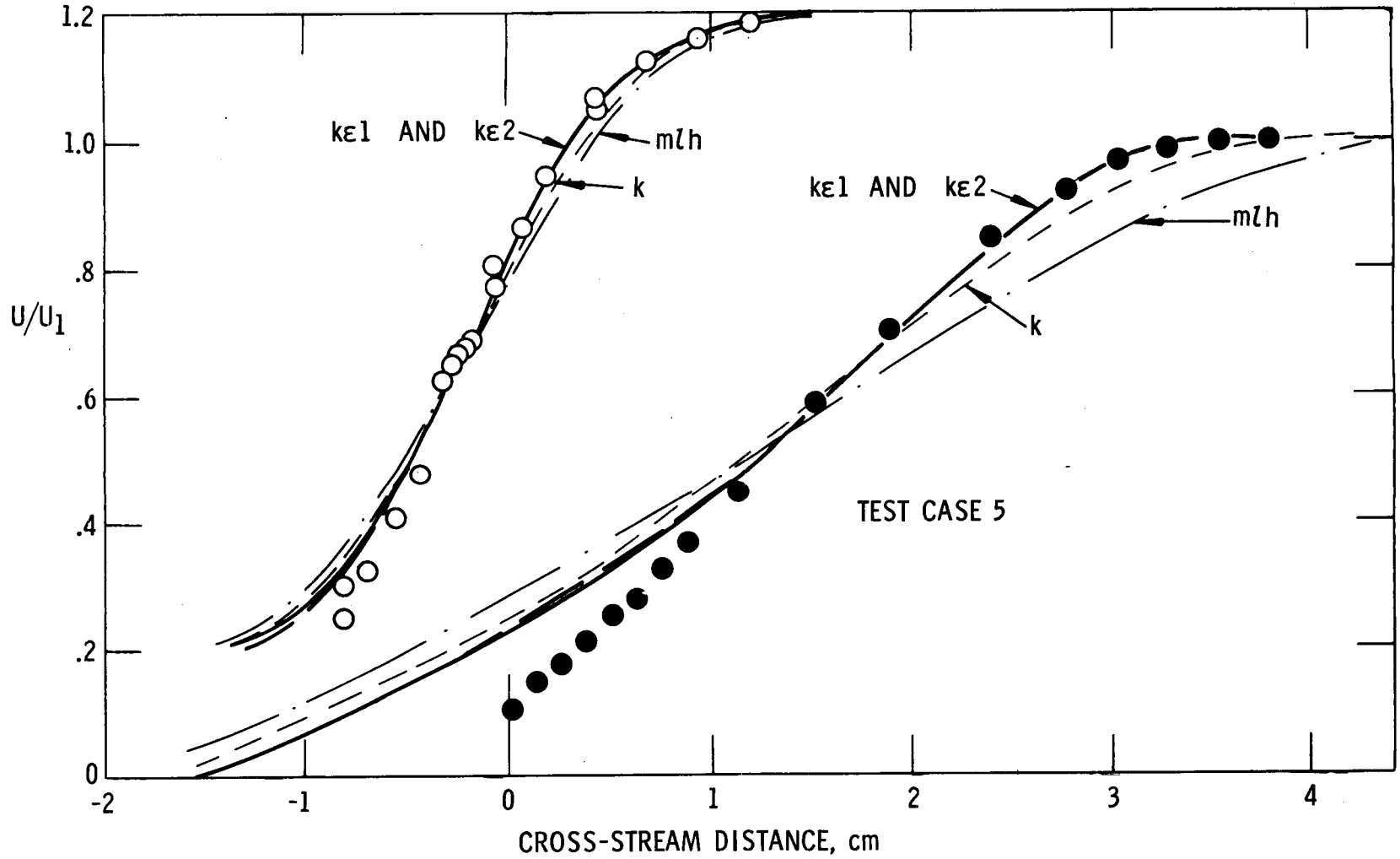
1.2
1.0
.8
.6
.4
.2
0
U/U1
kε1 AND kε2
mlh
k
kε1 AND kε2
mlh
k
TEST CASE 5
-2
-1
0
1
2
3
4
CROSS-STREAM DISTANCE, cm

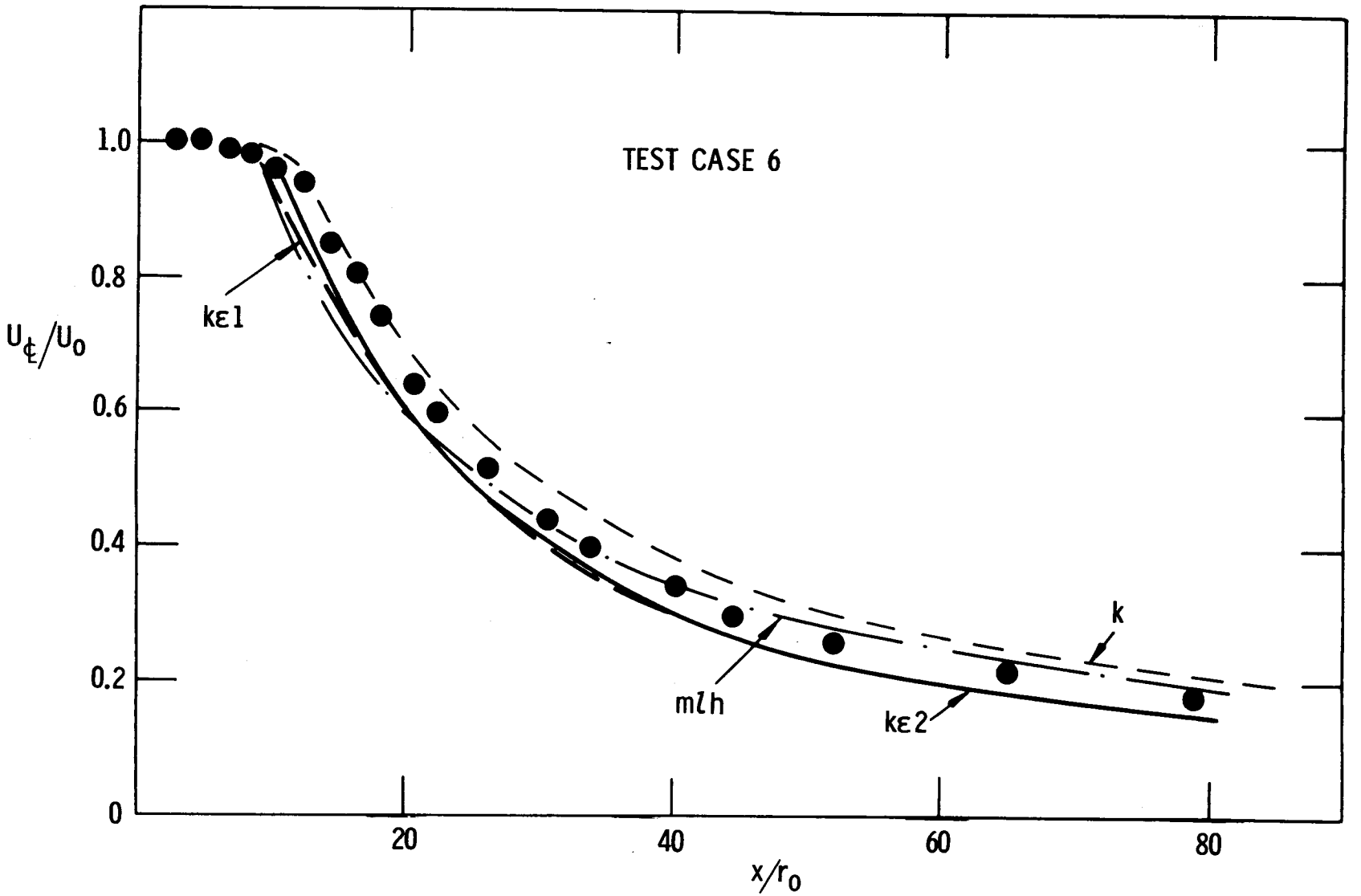
TEST CASE 6
1.0
0.8
0.6
0.4
0.2
0
U_{ℓ}/U_0
kε1
k
mℓh
kε2
20
40
60
80
x/r_0

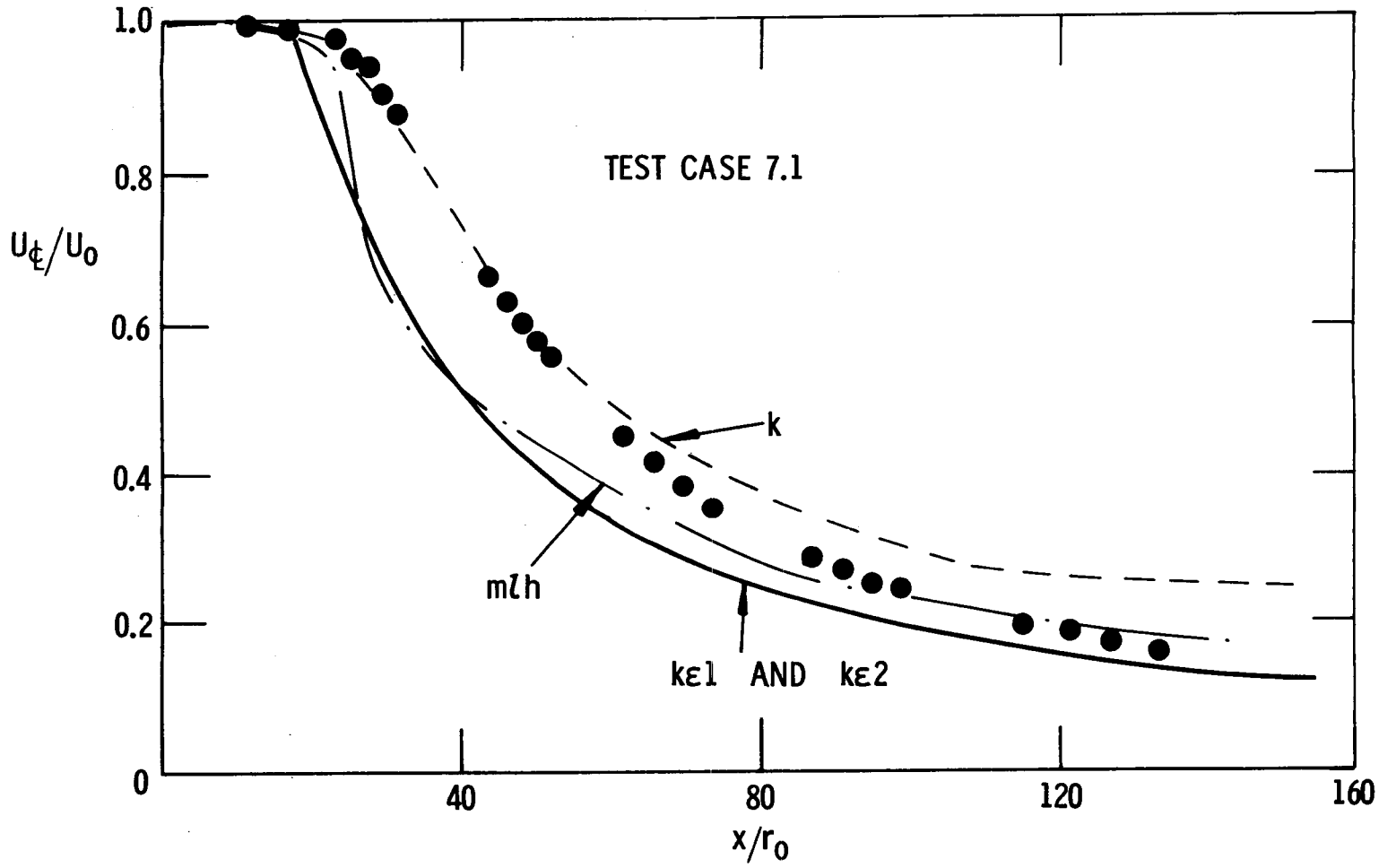
TEST CASE 7.1
U_{ℓ}/U_0
1.0
0.8
0.6
0.4
0.2
0
40
80
120
160
x/r_0
k
mlh
kε1 AND kε2

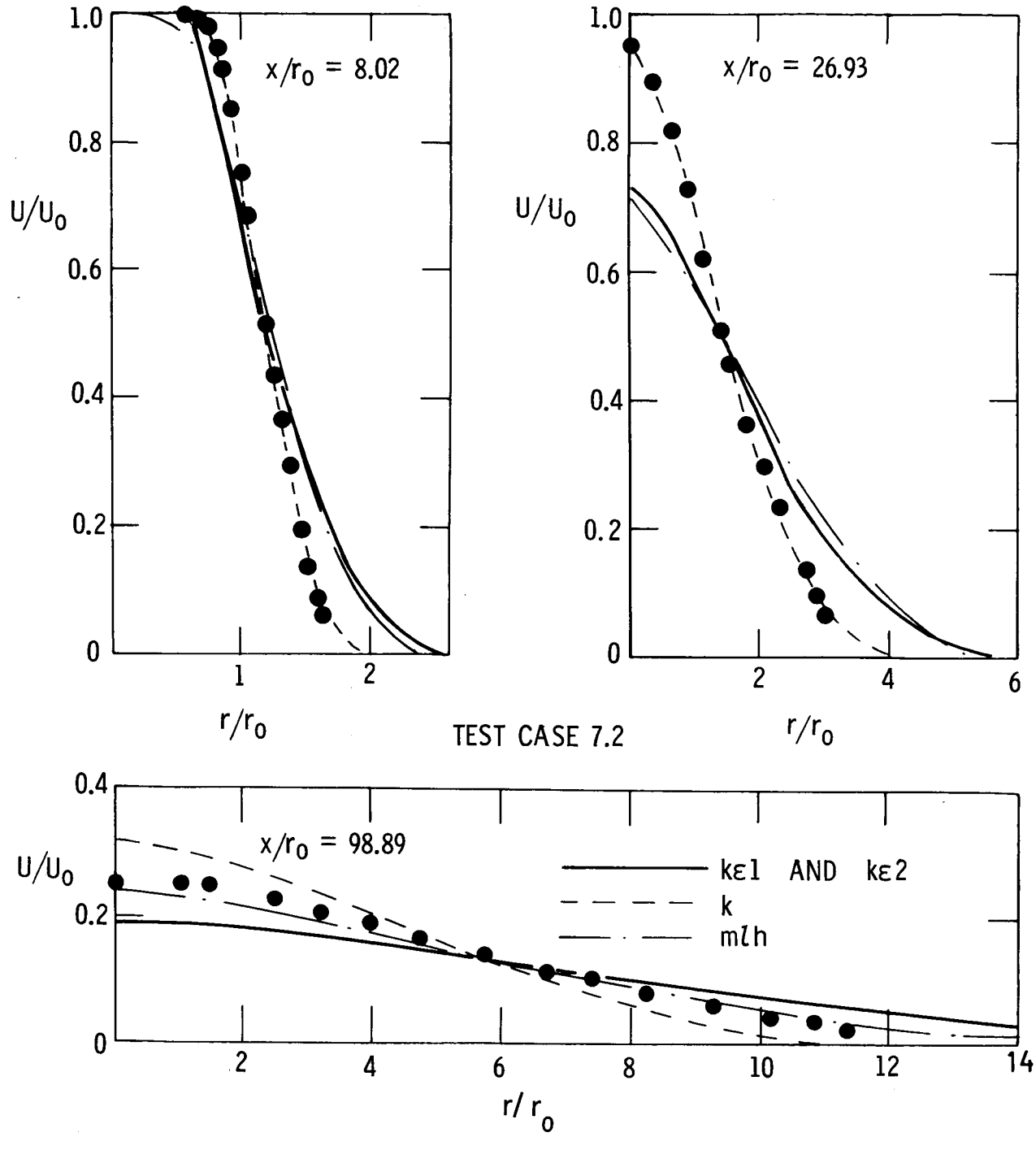
1.0
0.8
0.6
0.4
0.2
0
U/U0
x/r0 = 8.02
1
2
r/r0
x/r0 = 26.93
2
4
6
TEST CASE 7.2
0.4
x/r0 = 98.89
kε1 AND kε2
k
mlh
2
4
6
8
10
12
14
r/ r0

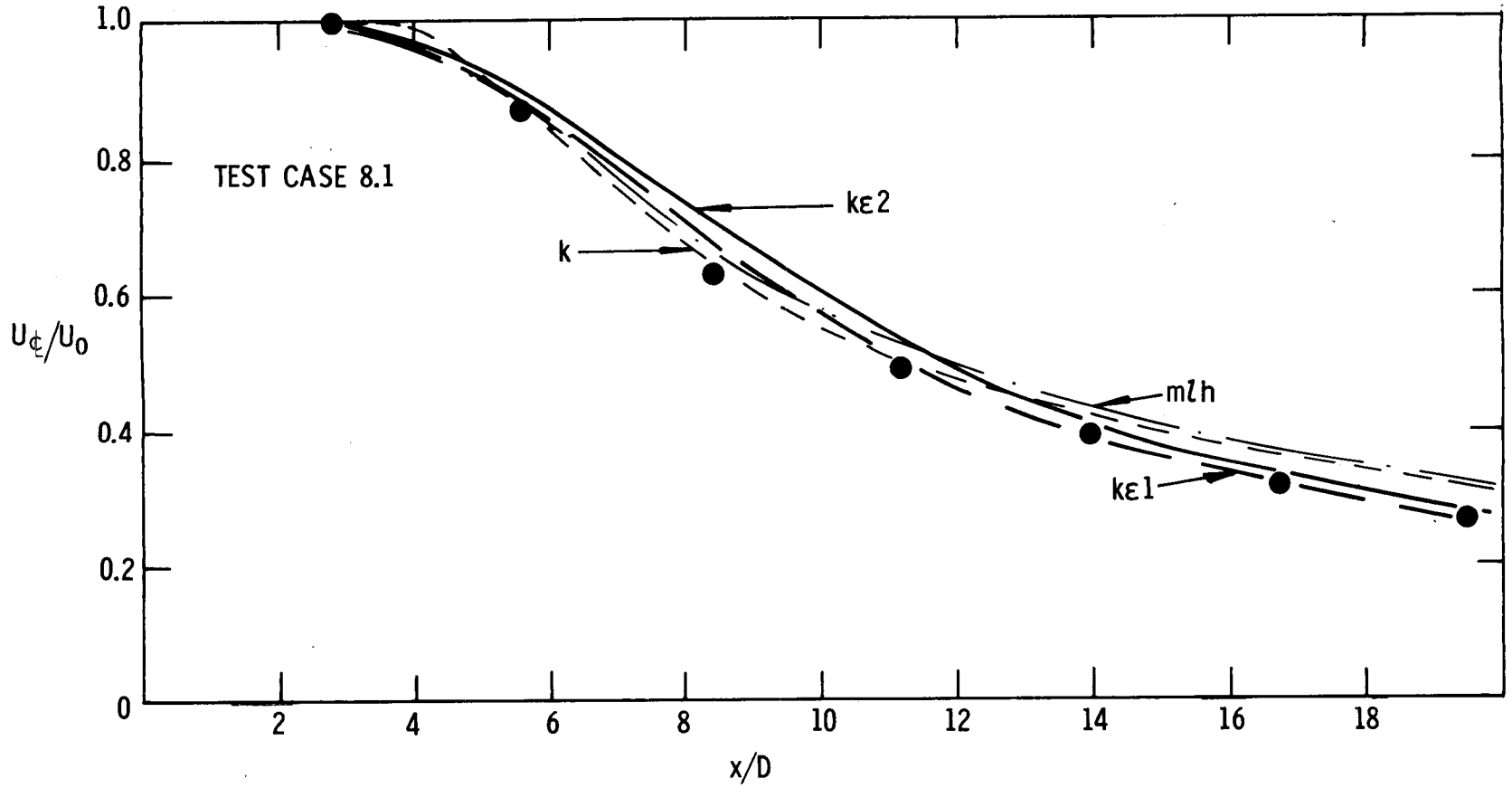
TEST CASE 8.1
kε2
k
mlh
kε1
U_{ℓ}/U_0
x/D
1.0
0.8
0.6
0.4
0.2
0
2
4
6
8
10
12
14
16
18

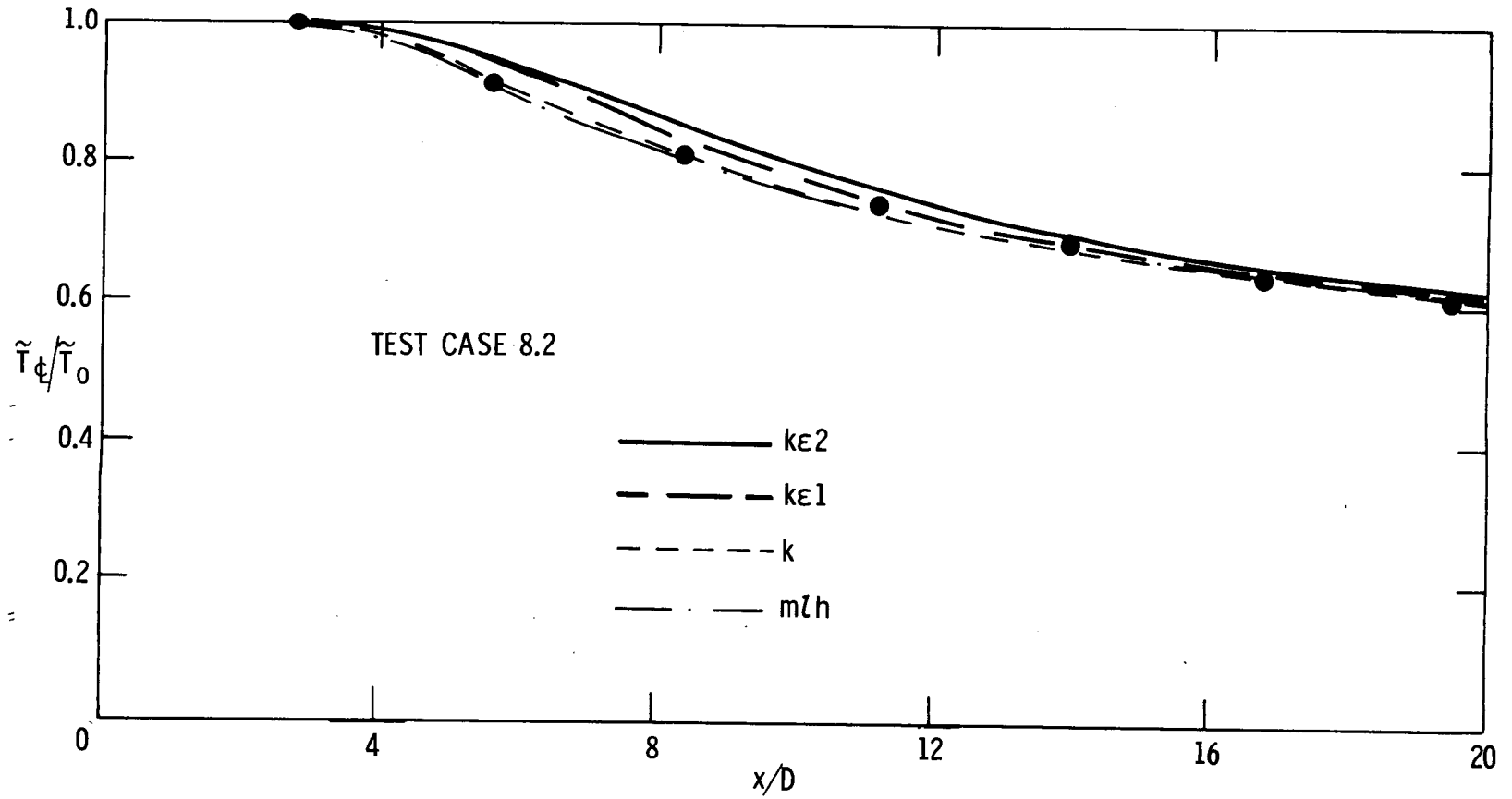
1.0
0.8
0.6
0.4
0.2
0
$\tilde{T}_{\ell}/\tilde{T}_0$
TEST CASE 8.2
kε2
kε1
k
mlh
4
8
12
16
20
x/D

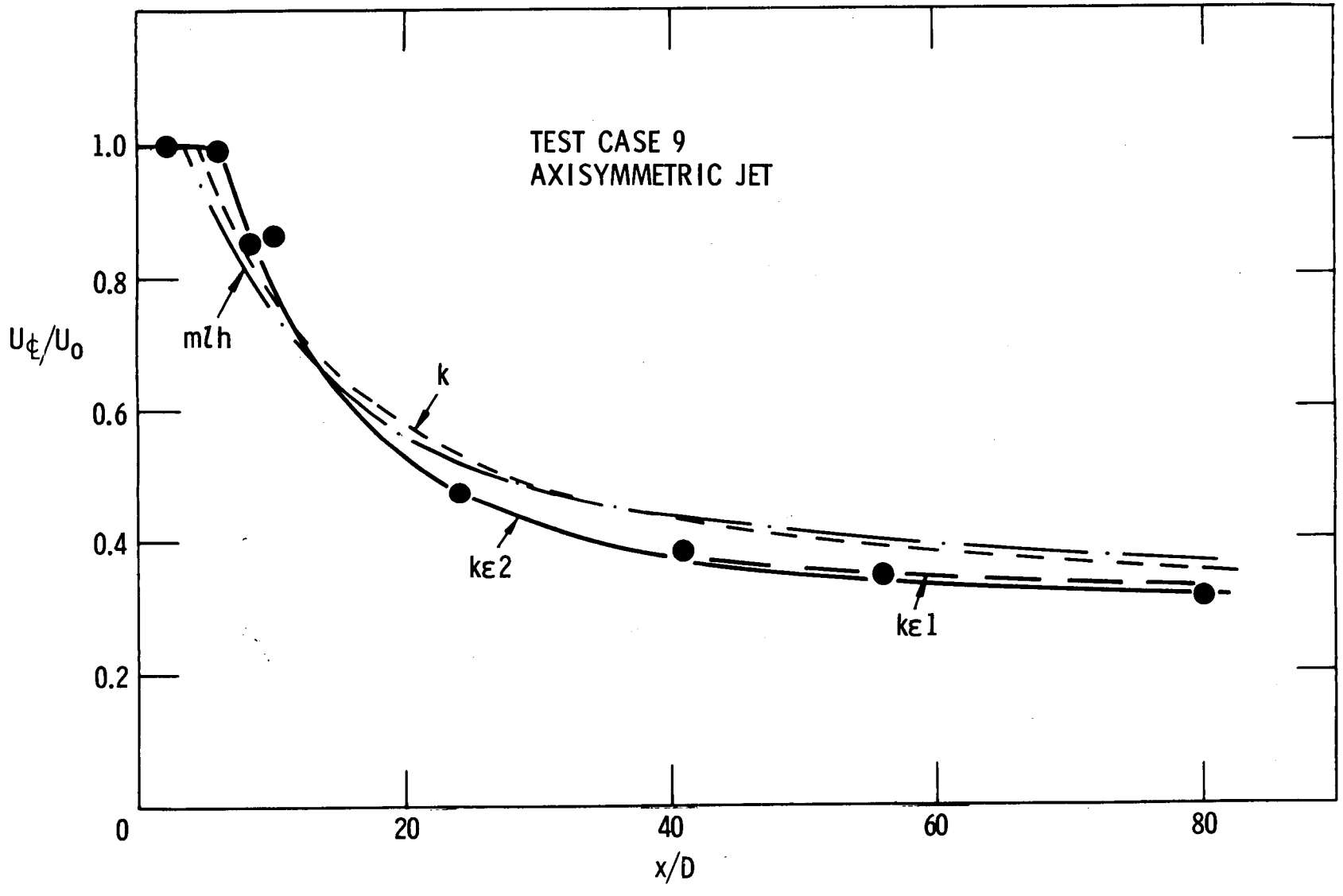
TEST CASE 9
AXISYMMETRIC JET
1.0
0.8
0.6
0.4
0.2
0
U_{ℓ}/U_0
mℓh
k
kε2
kε1
20
40
60
80
x/D

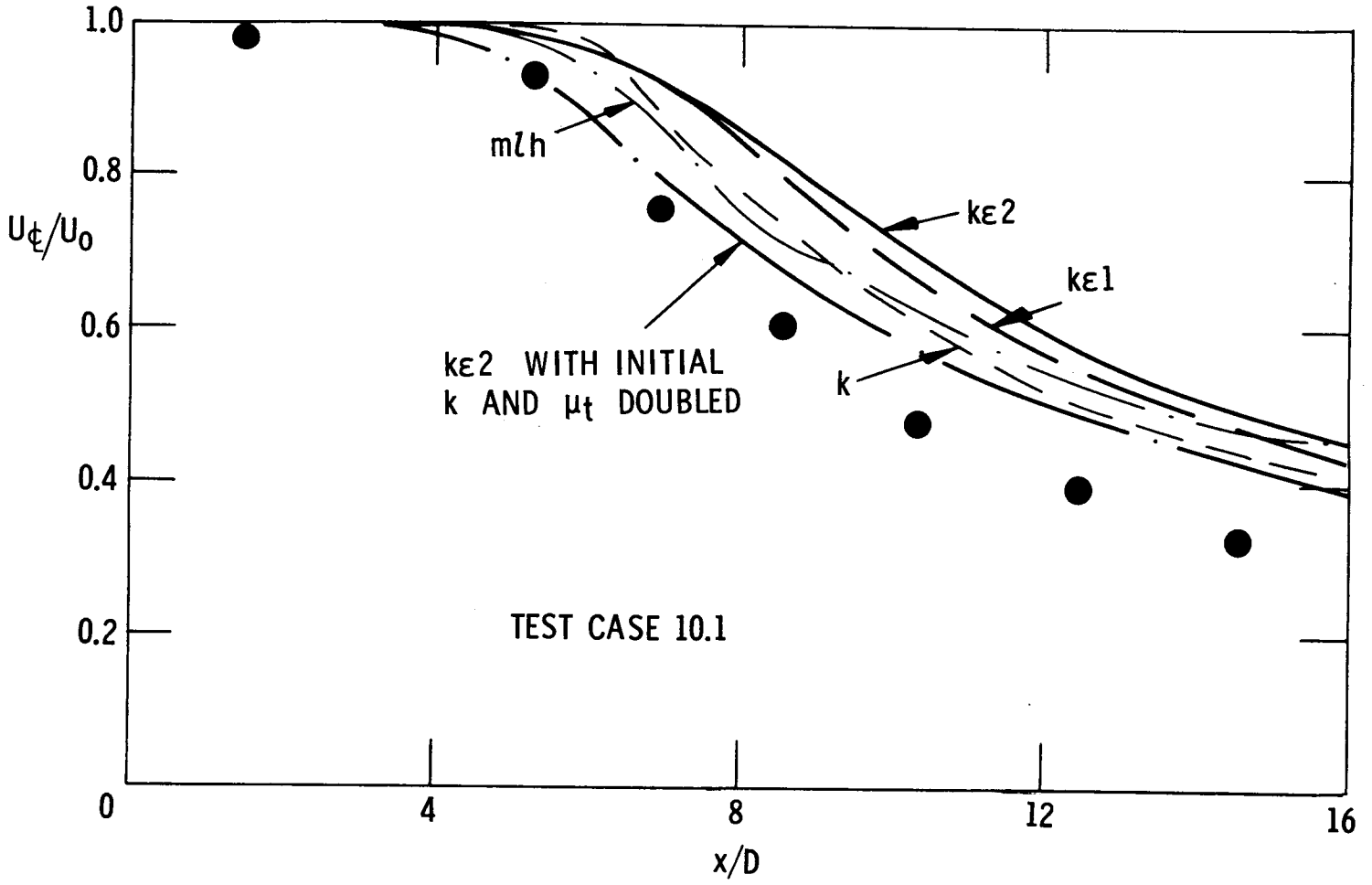
1.0
0.8
0.6
0.4
0.2
0
U_{ℓ}/U_0
4
8
12
16
x/D
mlh
kε2
kε1
k
kε2 WITH INITIAL
k AND μ_t DOUBLED
TEST CASE 10.1

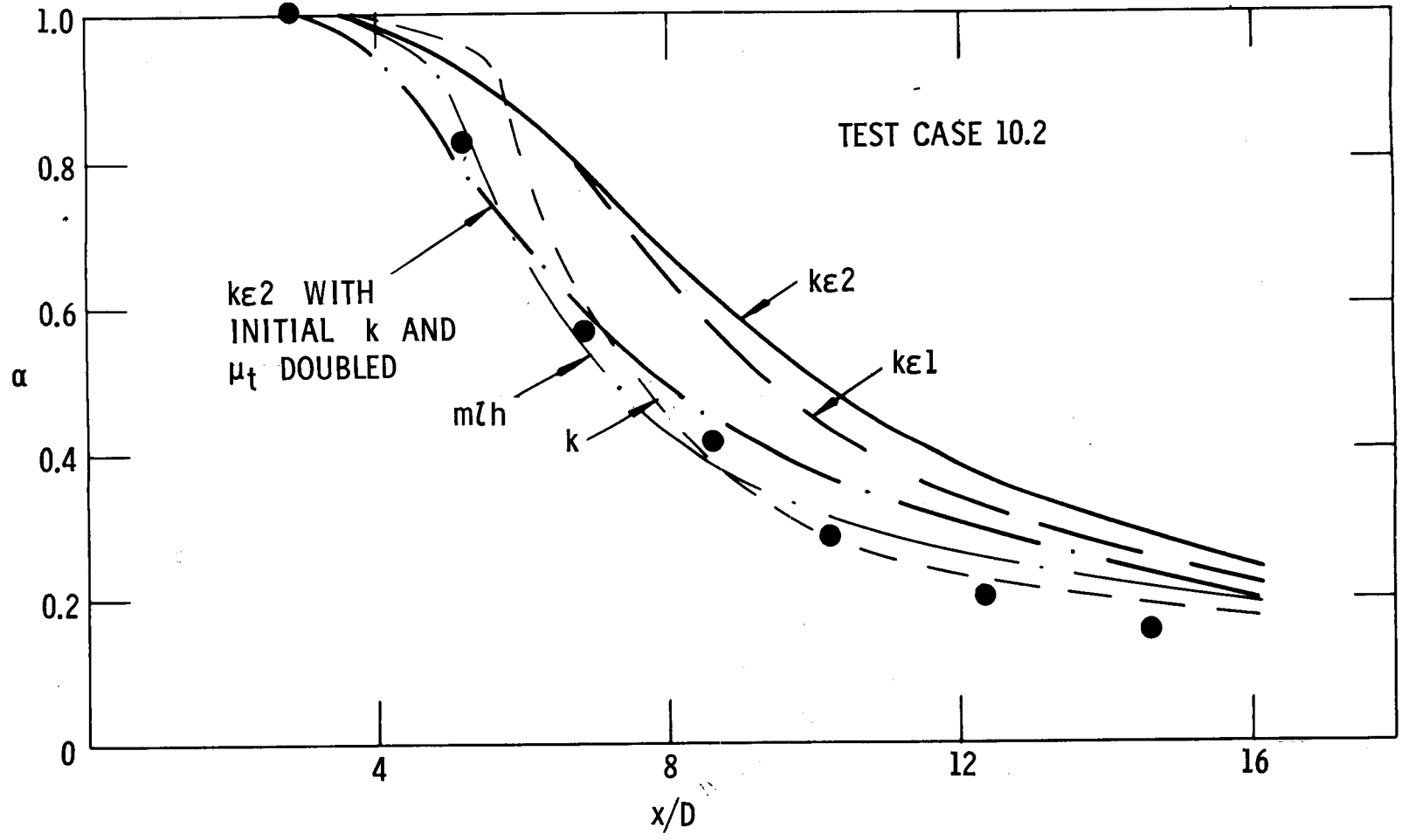
TEST CASE 10.2
kε2 WITH
INITIAL k AND
μ_t DOUBLED
kε2
kε1
mlh
k
α
x/D
1.0
0.8
0.6
0.4
0.2
0
4
8
12
16

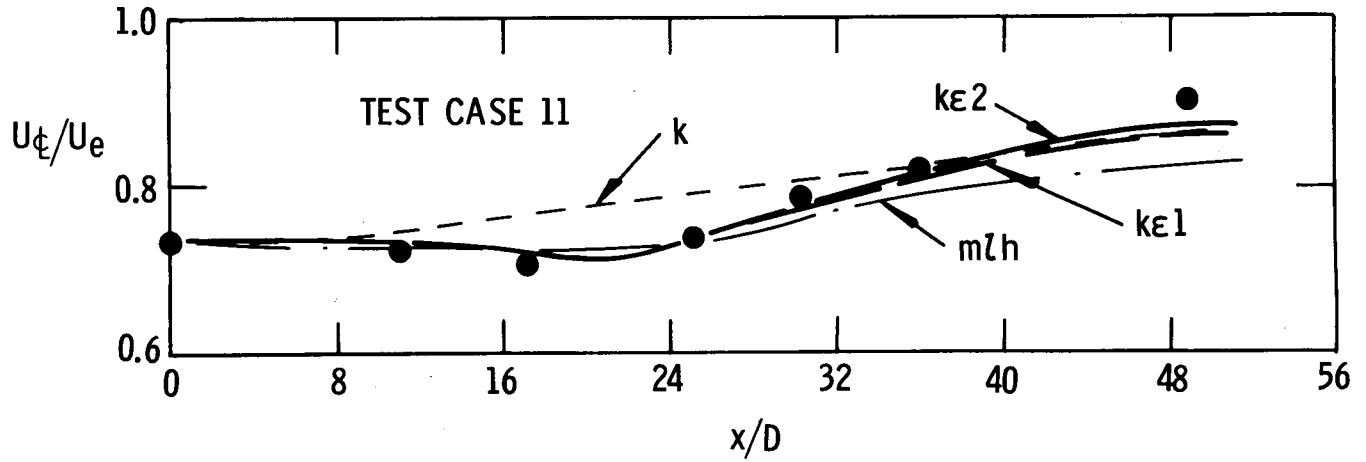
1.0
0.8
0.6
U_{ℓ}/U_e
TEST CASE 11
k
kε2
kε1
mlh
0
8
16
24
32
40
48
56
x/D

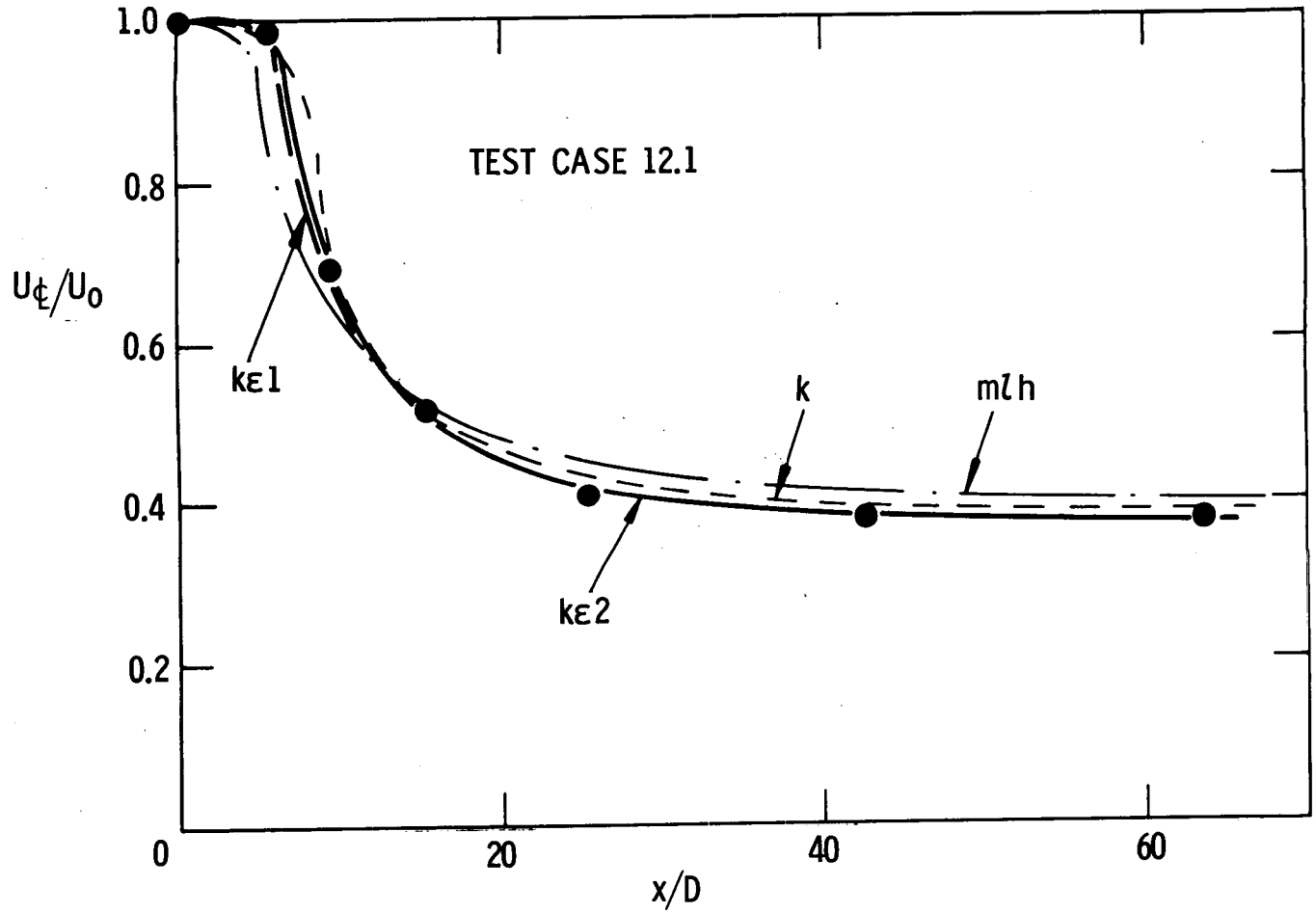
TEST CASE 12.1
U_{ℓ}/U_0
1.0
0.8
0.6
0.4
0.2
0
20
40
60
x/D
kε1
k
mℓh
kε2

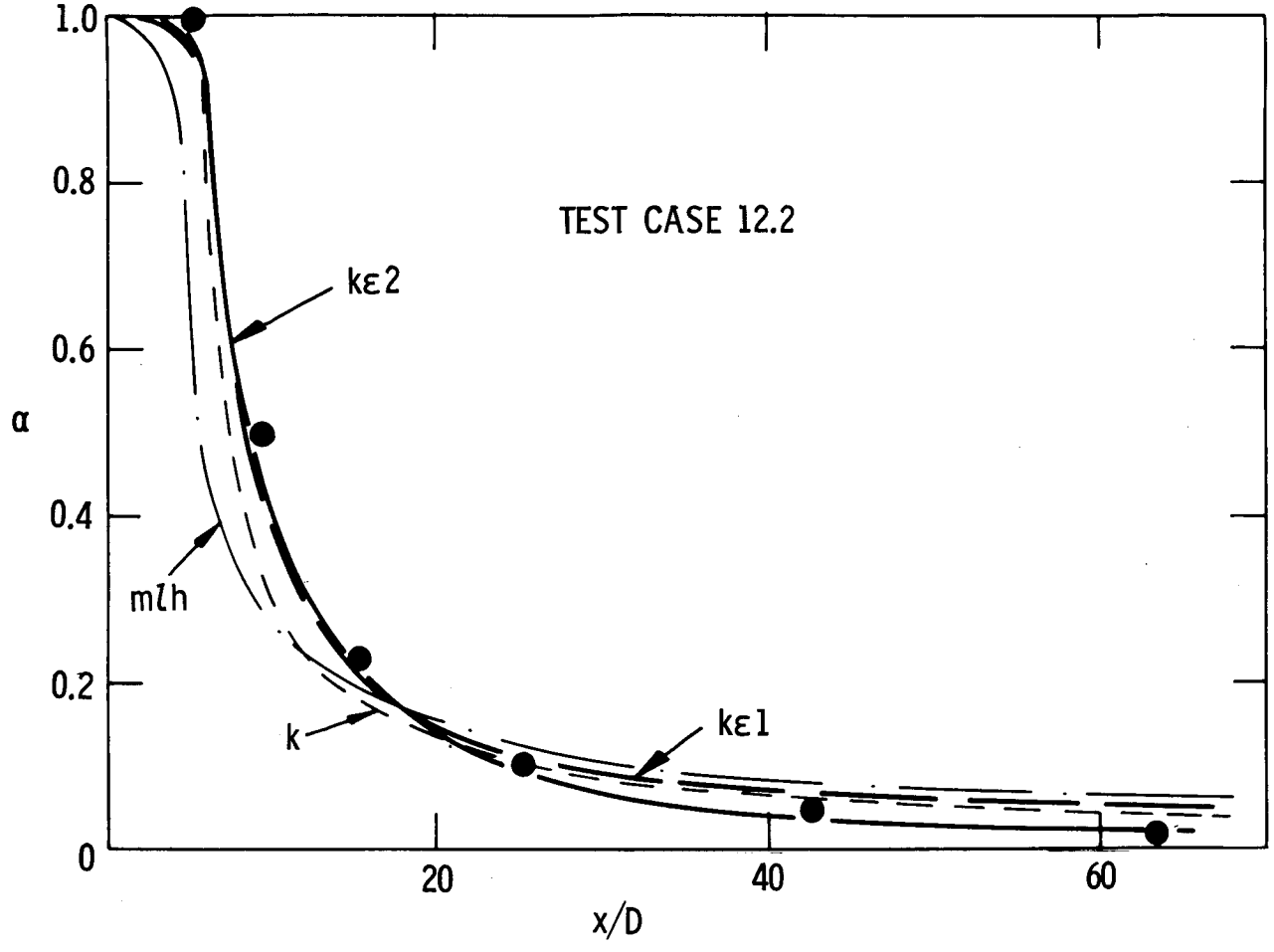
TEST CASE 12.2
kε2
mℓh
k
kε1
α
x/D
1.0
0.8
0.6
0.4
0.2
0
20
40
60

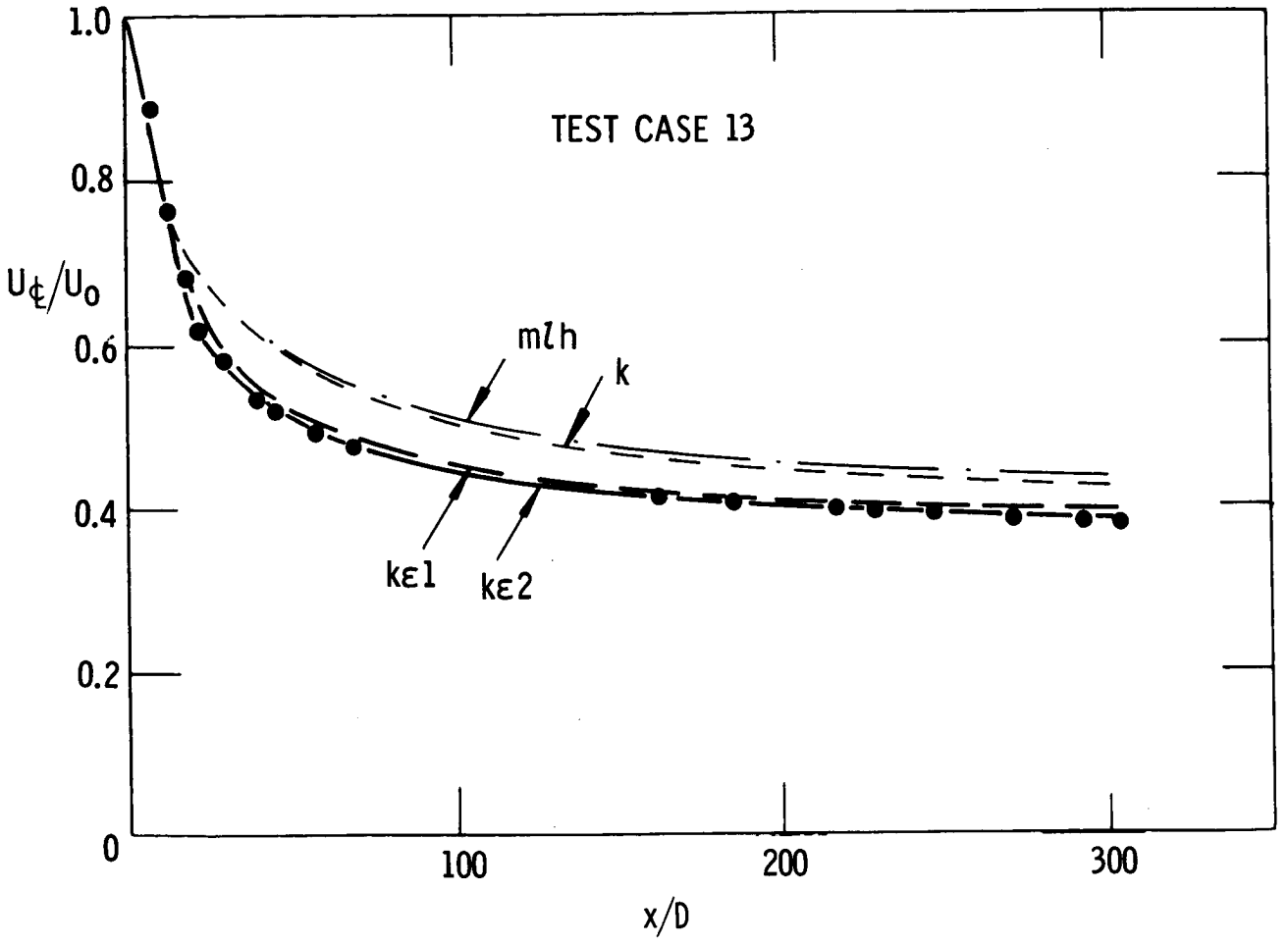
TEST CASE 13
1.0
0.8
0.6
0.4
0.2
0
U_{ℓ}/U_o
mlh
k
kε1
kε2
100
200
300
x/D

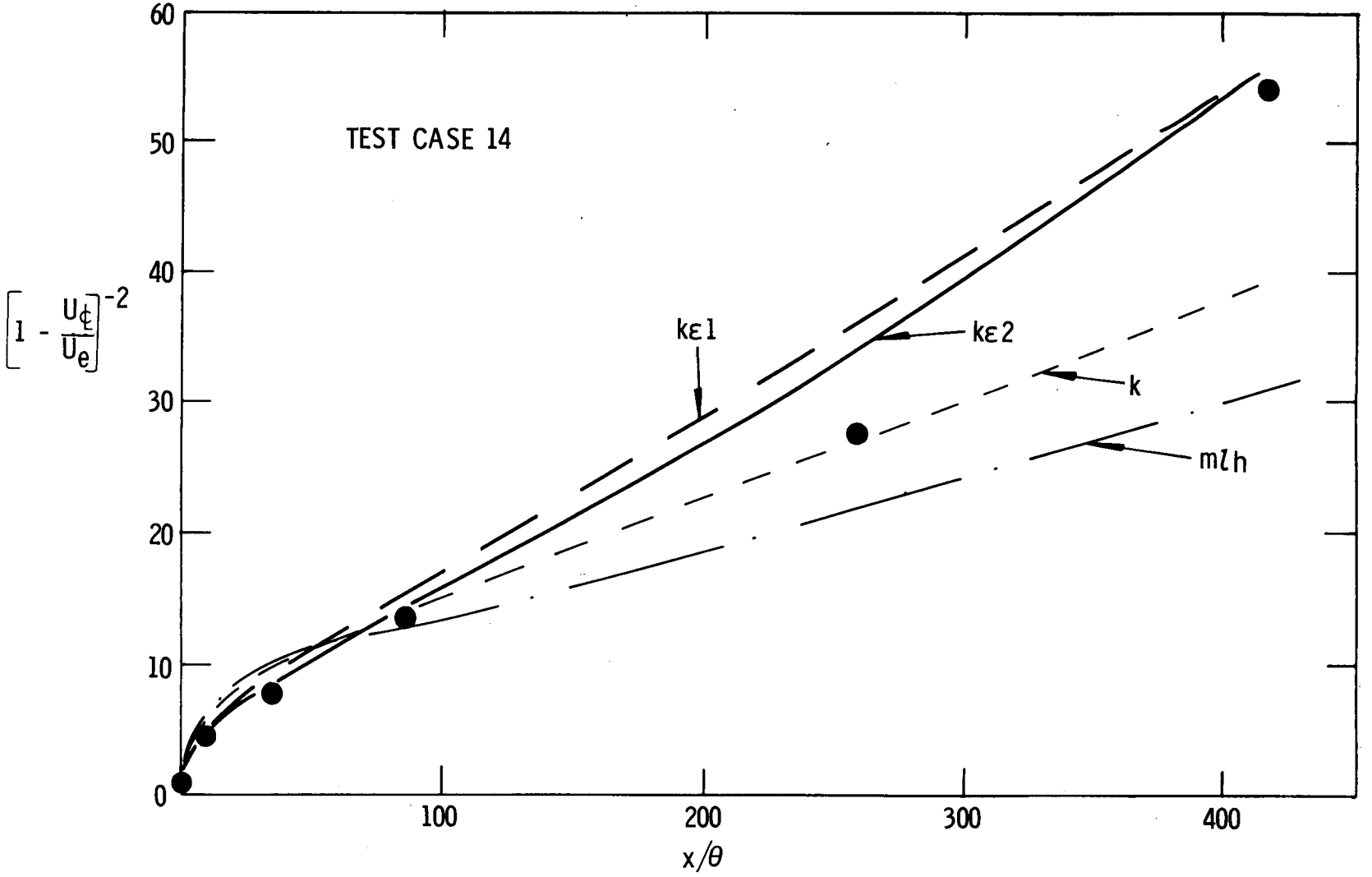
TEST CASE 14
$\left[1 - \frac{U_\ell}{U_e}\right]^{-2}$
60
50
40
30
20
10
0
100
200
300
400
x/θ
kε1
kε2
k
mlh

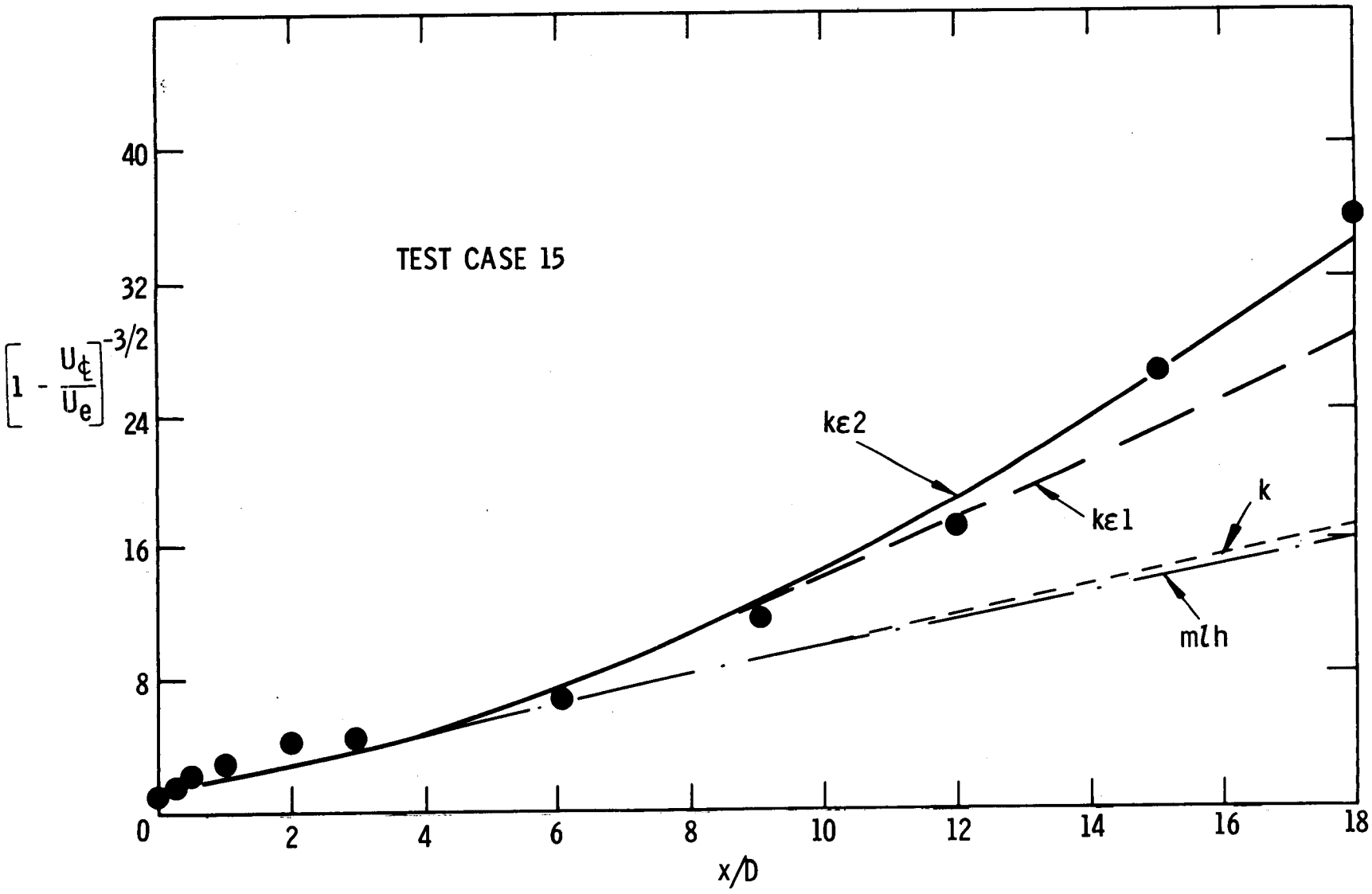
TEST CASE 15
$\left[1 - \frac{U_\ell}{U_e}\right]^{-3/2}$
40
32
24
16
8
0
2
4
6
8
10
12
14
16
18
x/D
kε2
kε1
k
mlh

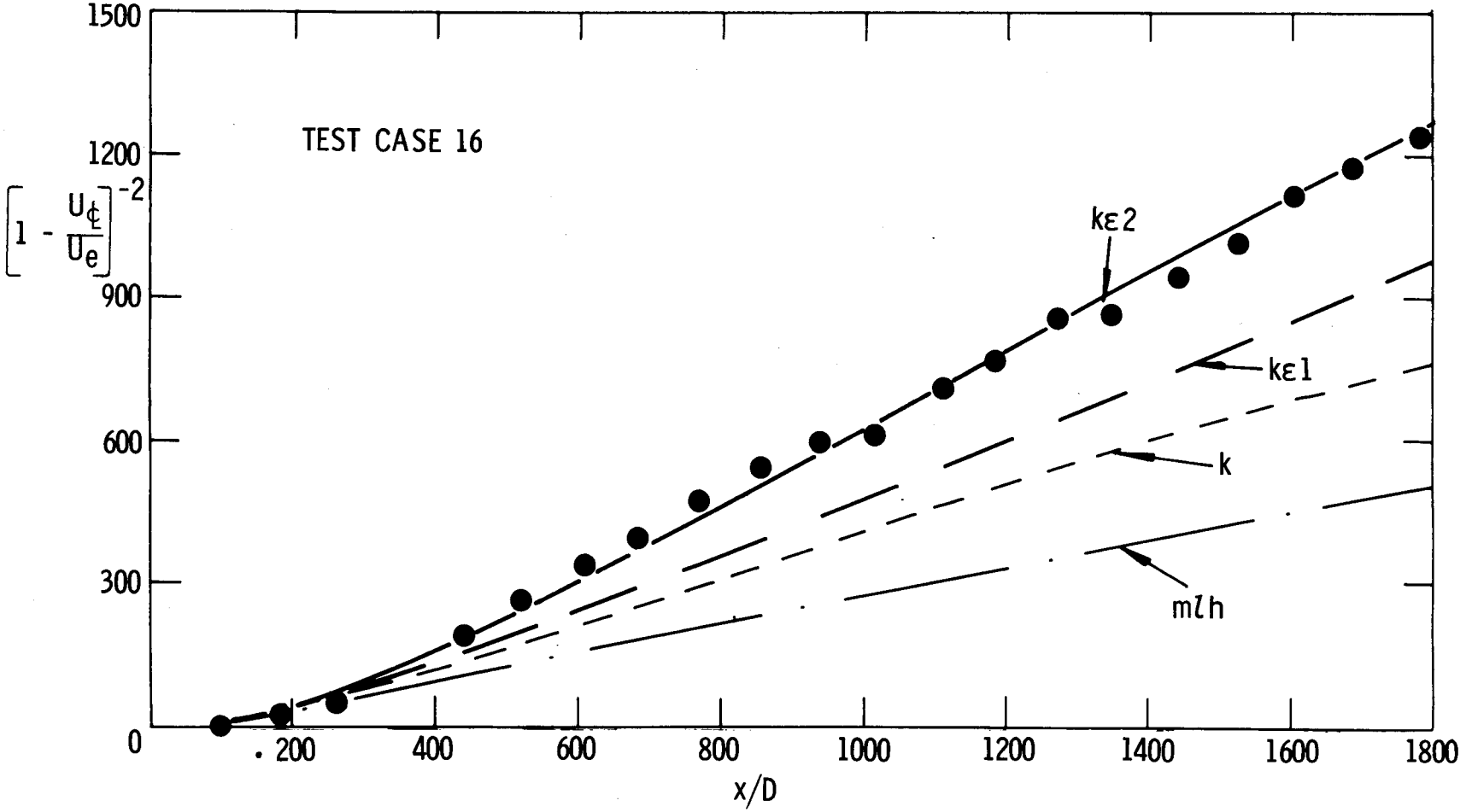
TEST CASE 16
$\left[1 - \frac{U_\phi}{U_e}\right]^{-2}$
1500
1200
900
600
300
0
200
400
600
800
1000
1200
1400
1600
1800
x/D
kε2
kε1
k
mlh

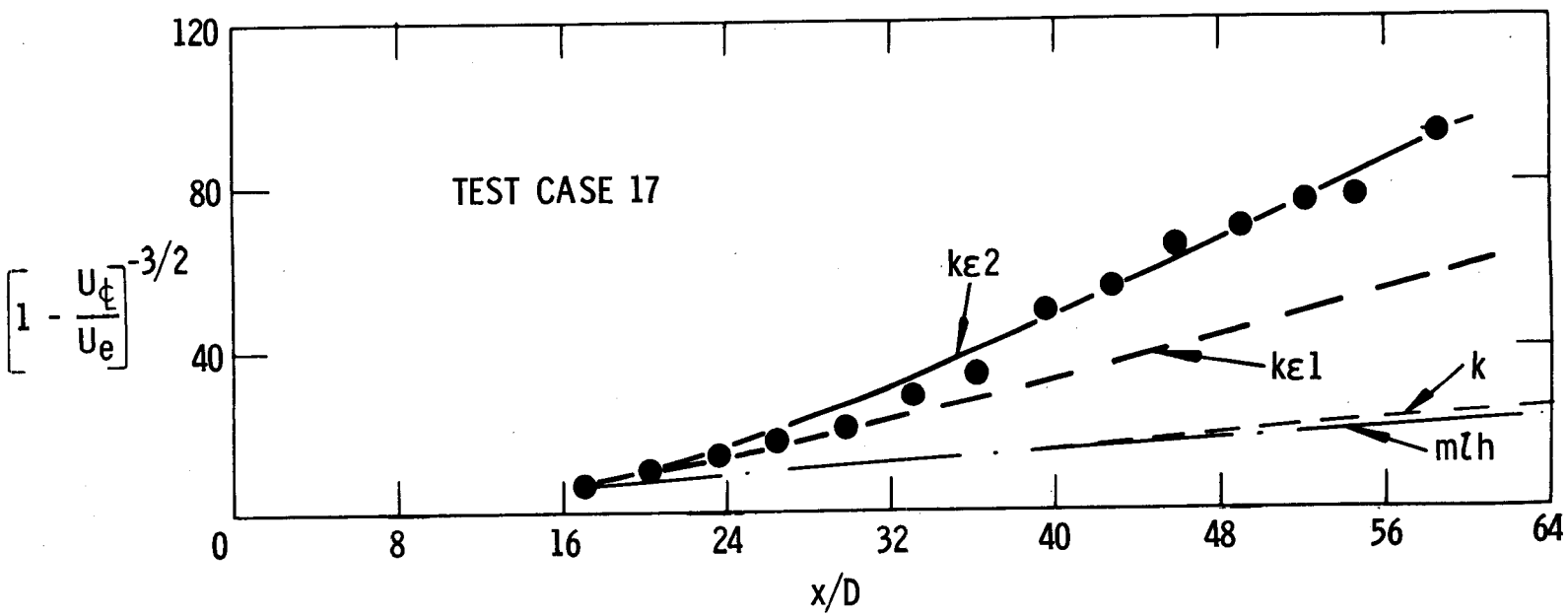
TEST CASE 17
$\left[1 - \frac{U_{\ell}}{U_e}\right]^{-3/2}$
120
80
40
0
8
16
24
32
40
48
56
64
x/D
kε2
kε1
k
mℓh

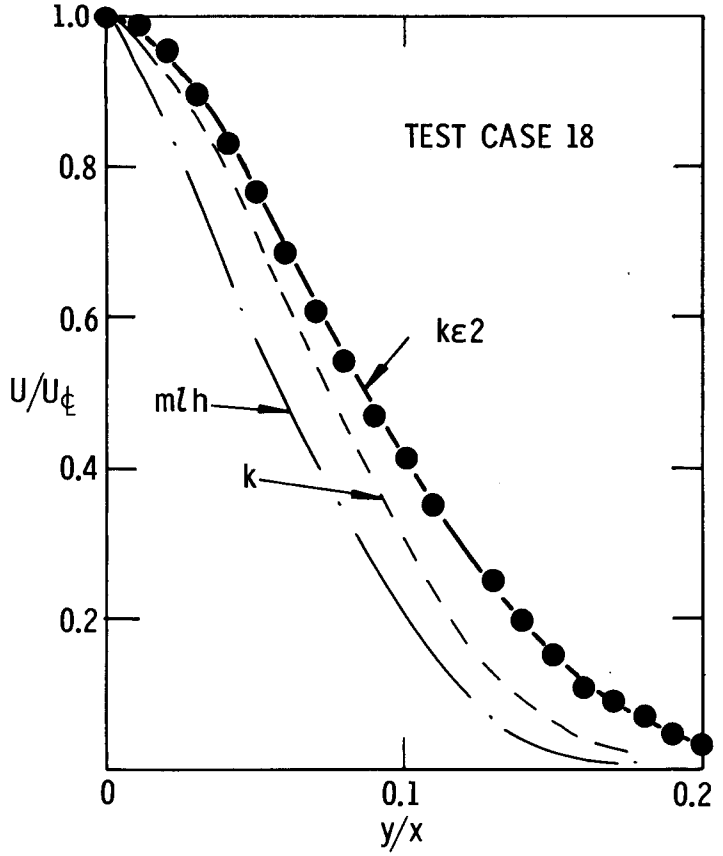
1.0
0.8
0.6
0.4
0.2
U/U℄
TEST CASE 18
kε2
mlh
k
0
0.1
0.2
y/x

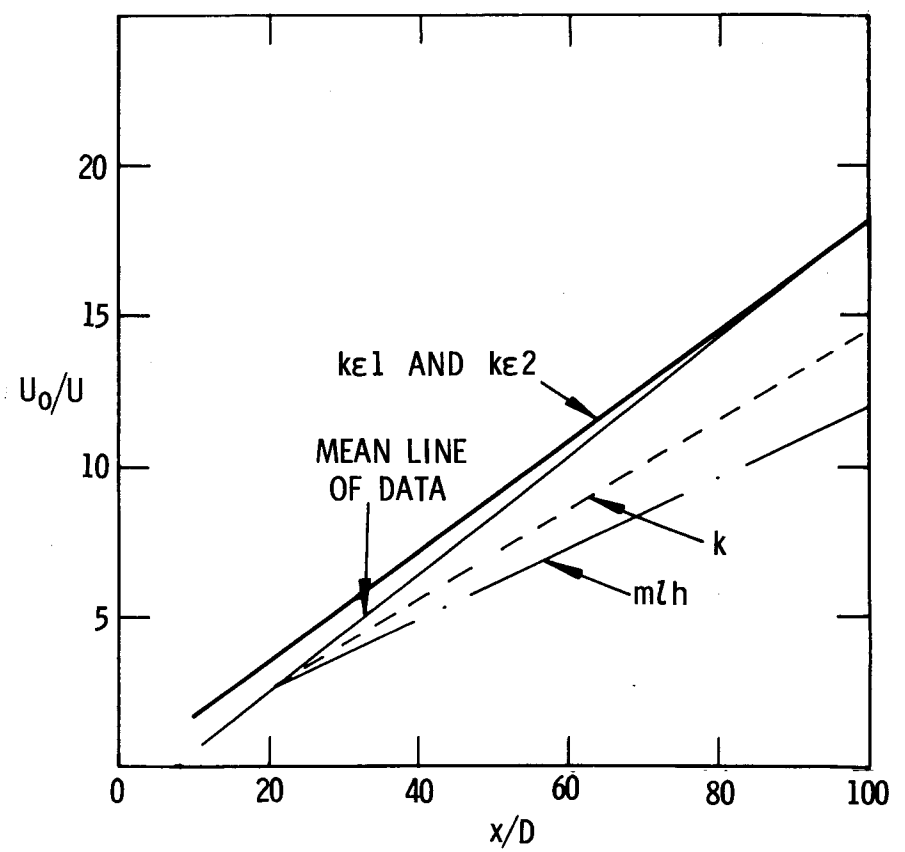
20
15
10
5
U0/U
kε1 AND kε2
MEAN LINE
OF DATA
k
mlh
0
20
40
60
80
100
x/D

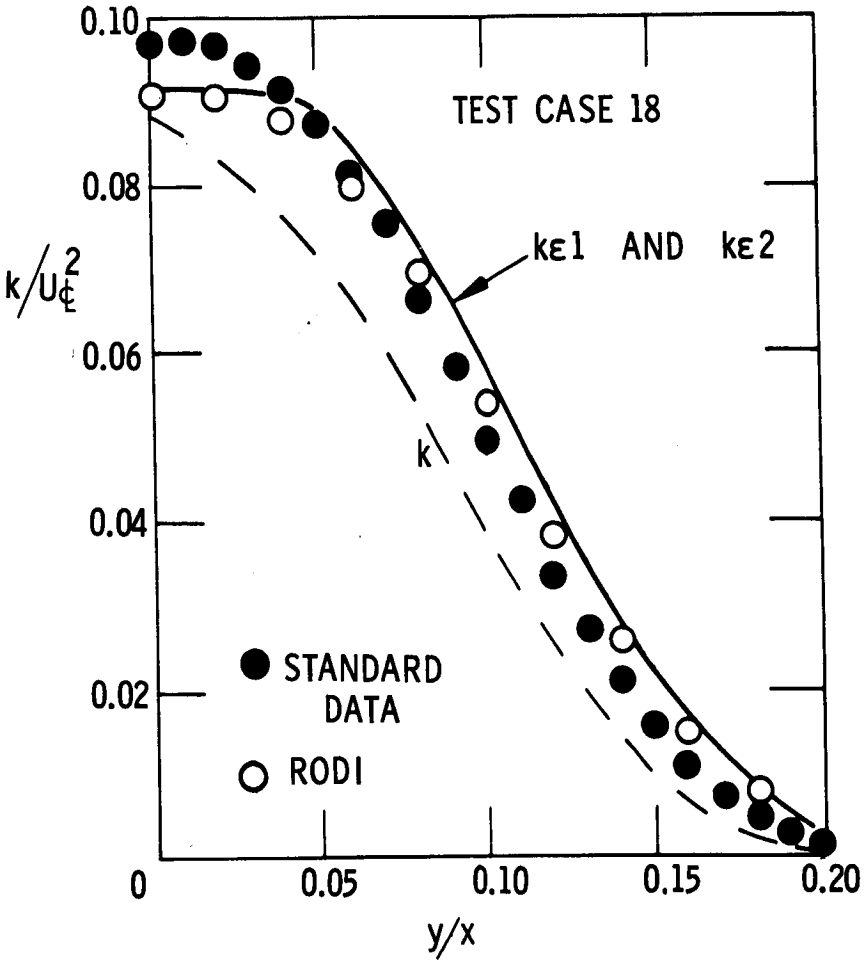
TEST CASE 18
kε1 AND kε2
k
STANDARD DATA
RODI
k/U_{ℓ}^2
y/x
0.10
0.08
0.06
0.04
0.02
0
0.05
0.10
0.15
0.20

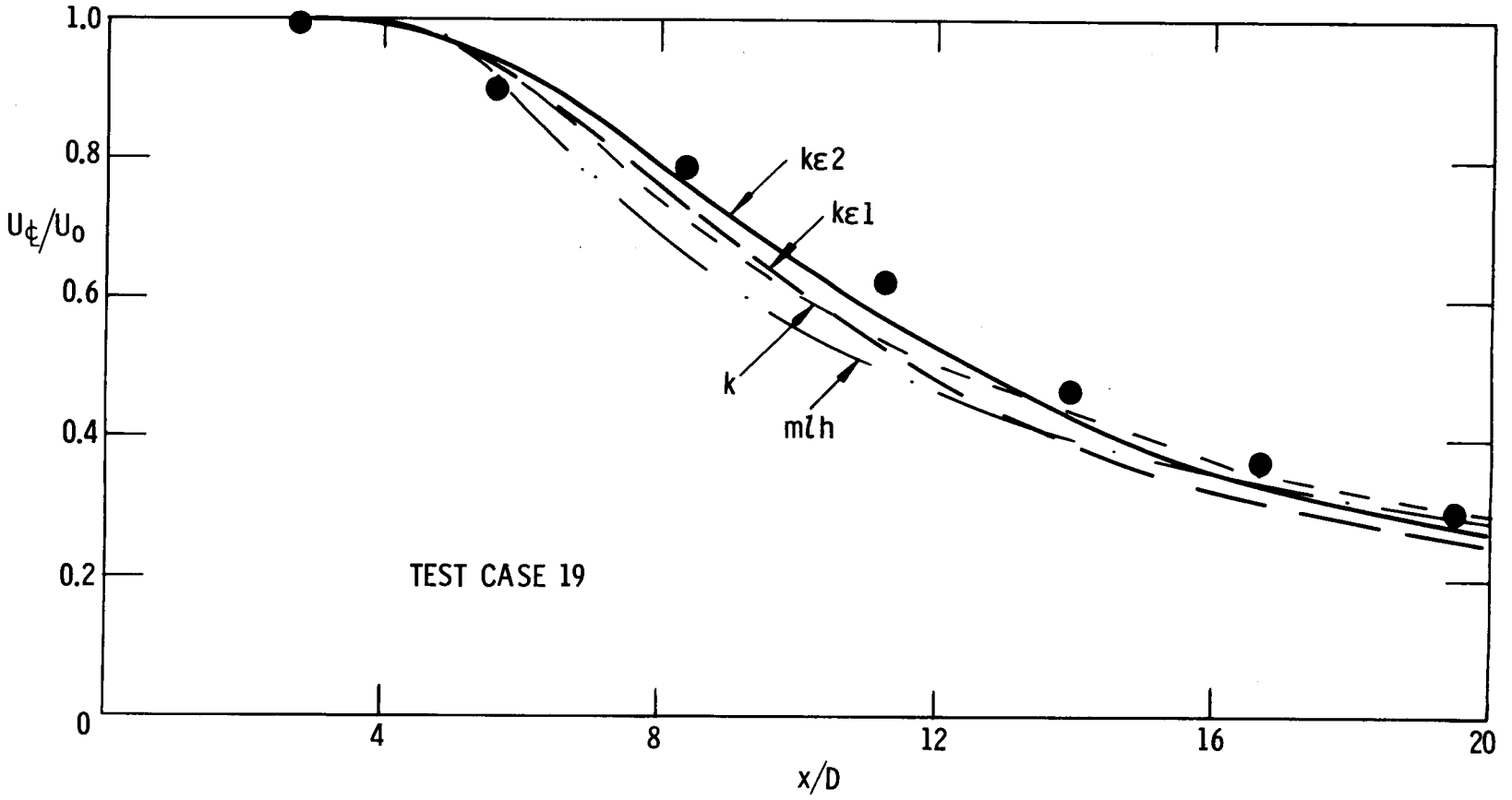
1.0
0.8
0.6
0.4
0.2
0
U_{ℓ}/U_0
kε2
kε1
k
mℓh
TEST CASE 19
4
8
12
16
20
x/D

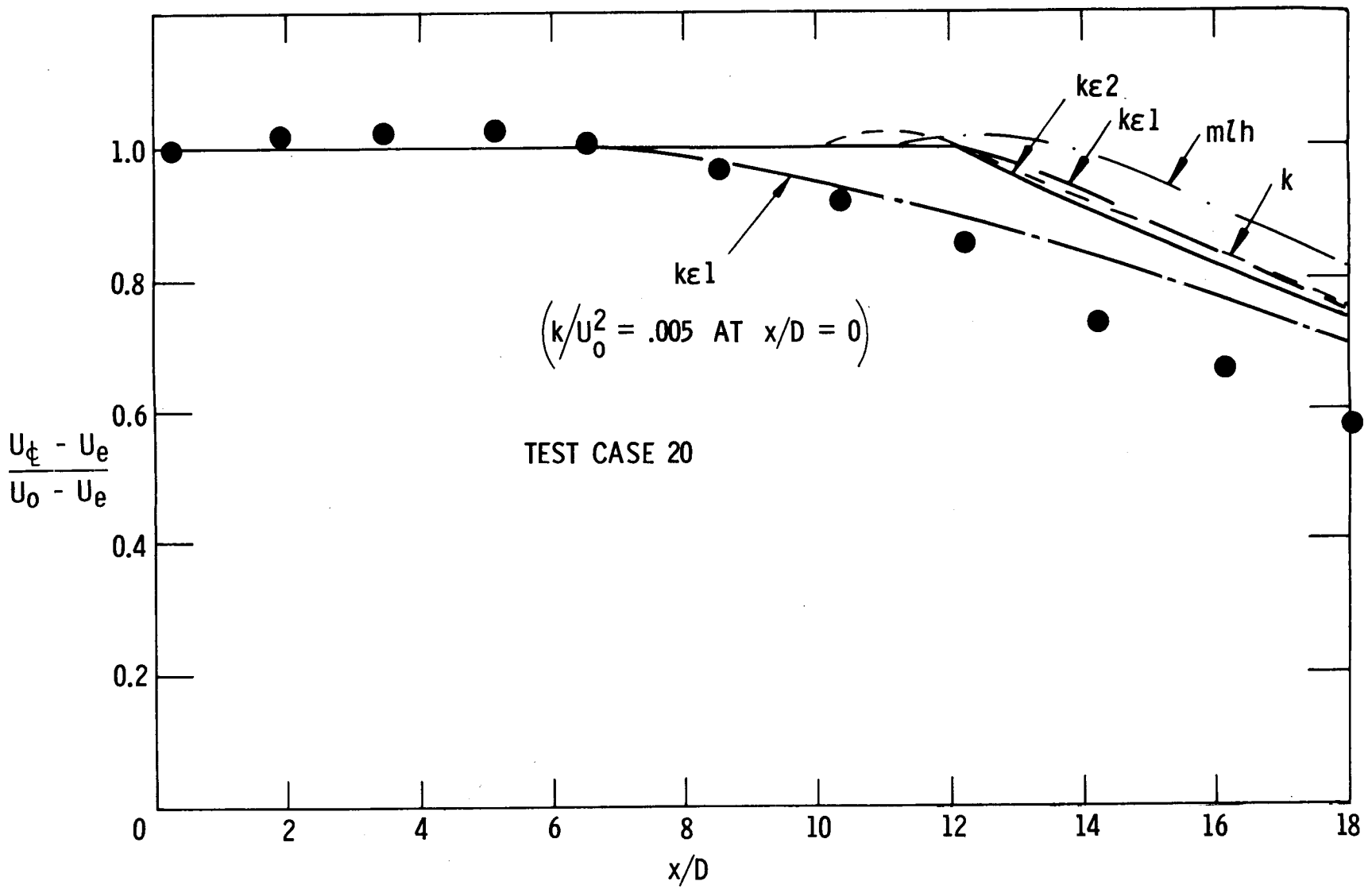
kε2
kε1
mlh
k
kε1
$\left(k/U_0^2 = .005 \text{ AT } x/D = 0\right)$
TEST CASE 20
$\frac{U_\ell - U_e}{U_0 - U_e}$
1.0
0.8
0.6
0.4
0.2
0
2
4
6
8
10
12
14
16
18
x/D

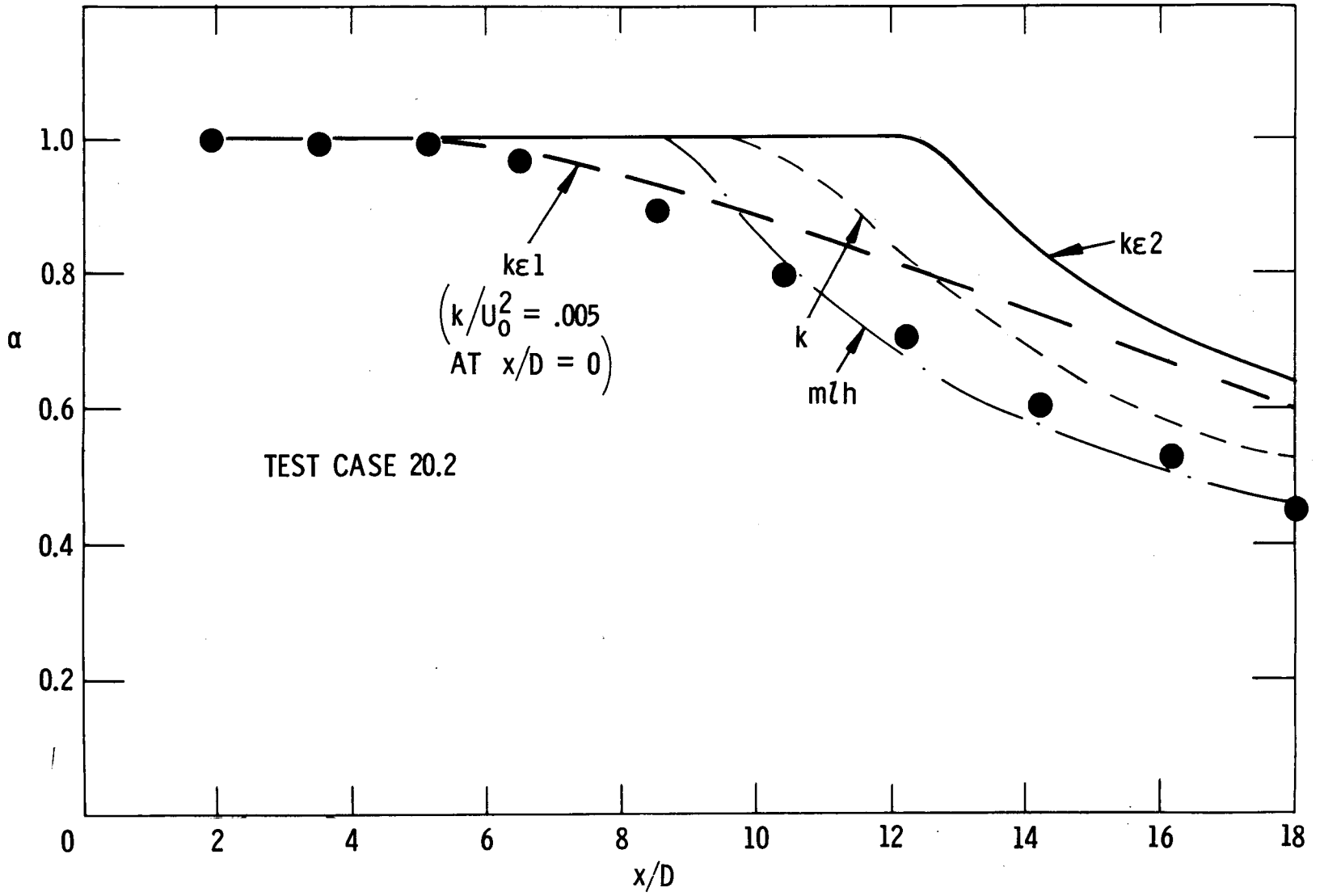
1.0
0.8
0.6
0.4
0.2
α
0
2
4
6
8
10
12
14
16
18
x/D
kε1
$(k/U_0^2 = .005$
AT x/D = 0)
kε2
k
mlh
TEST CASE 20.2

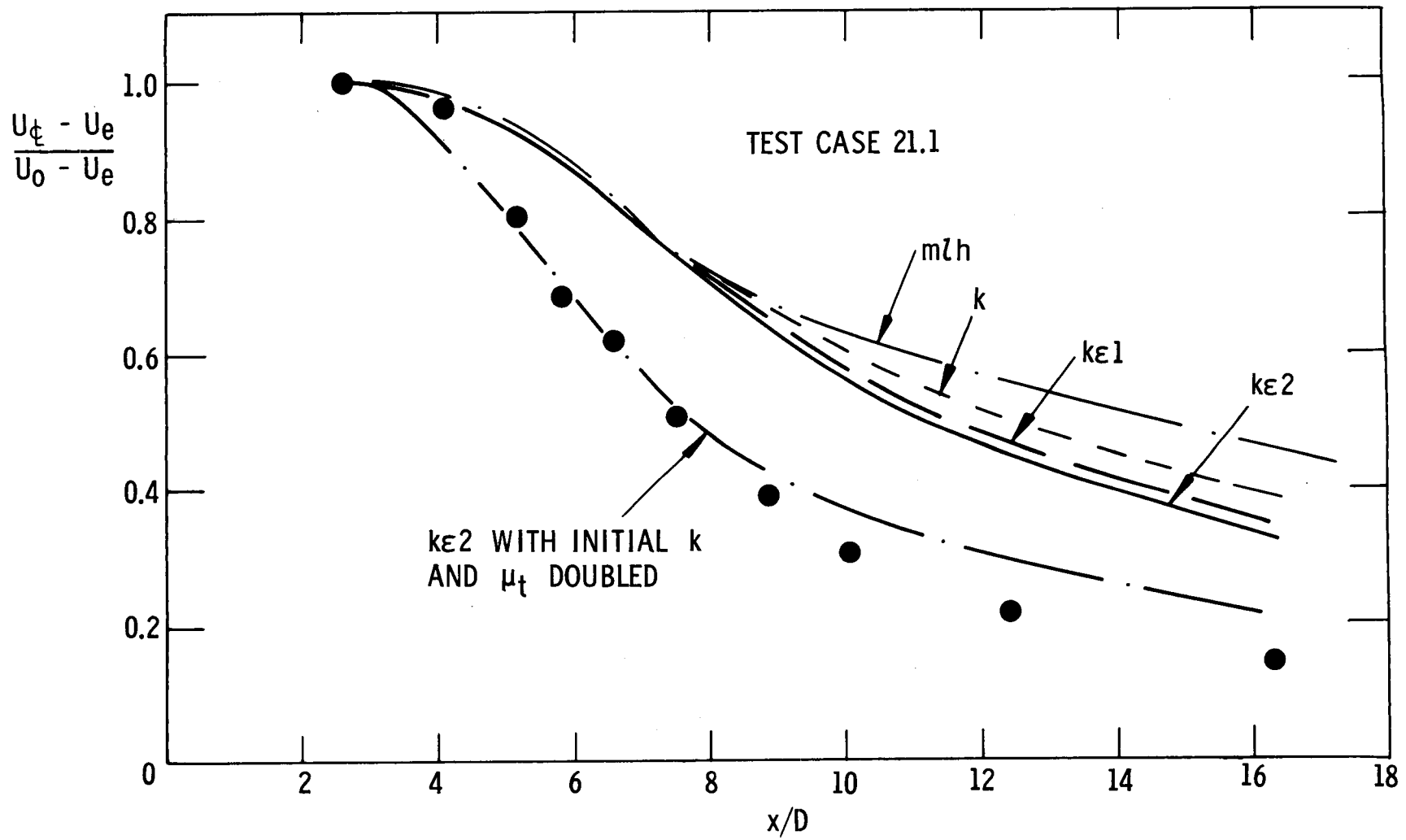
$\frac{U_{\ell} - U_e}{U_0 - U_e}$
1.0
0.8
0.6
0.4
0.2
0
2
4
6
8
10
12
14
16
18
x/D
TEST CASE 21.1
mℓh
k
kε1
kε2
kε2 WITH INITIAL k
AND μ_t DOUBLED

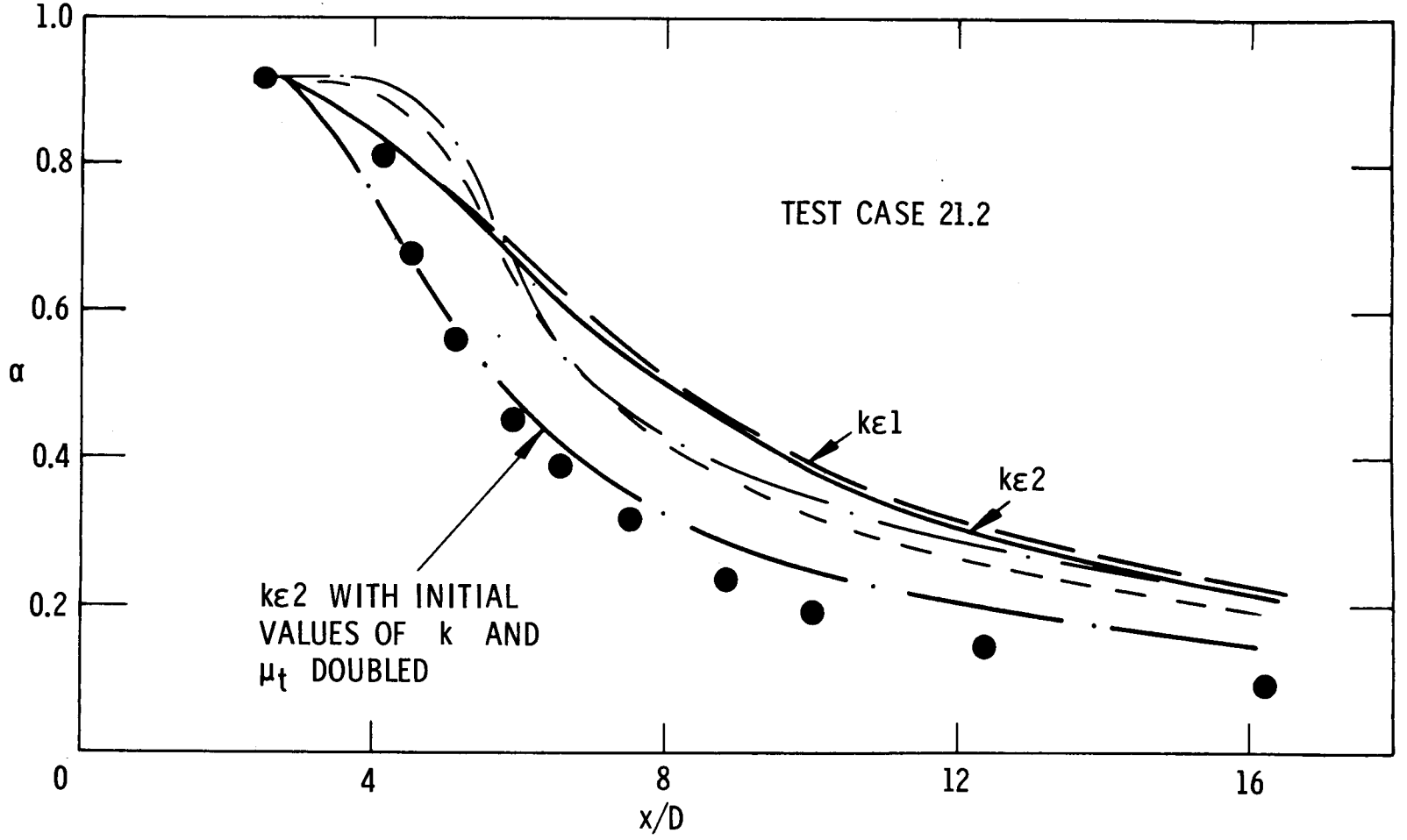
1.0
0.8
0.6
0.4
0.2
0
α
4
8
12
16
x/D
TEST CASE 21.2
kε1
kε2
kε2 WITH INITIAL VALUES OF k AND μt DOUBLED

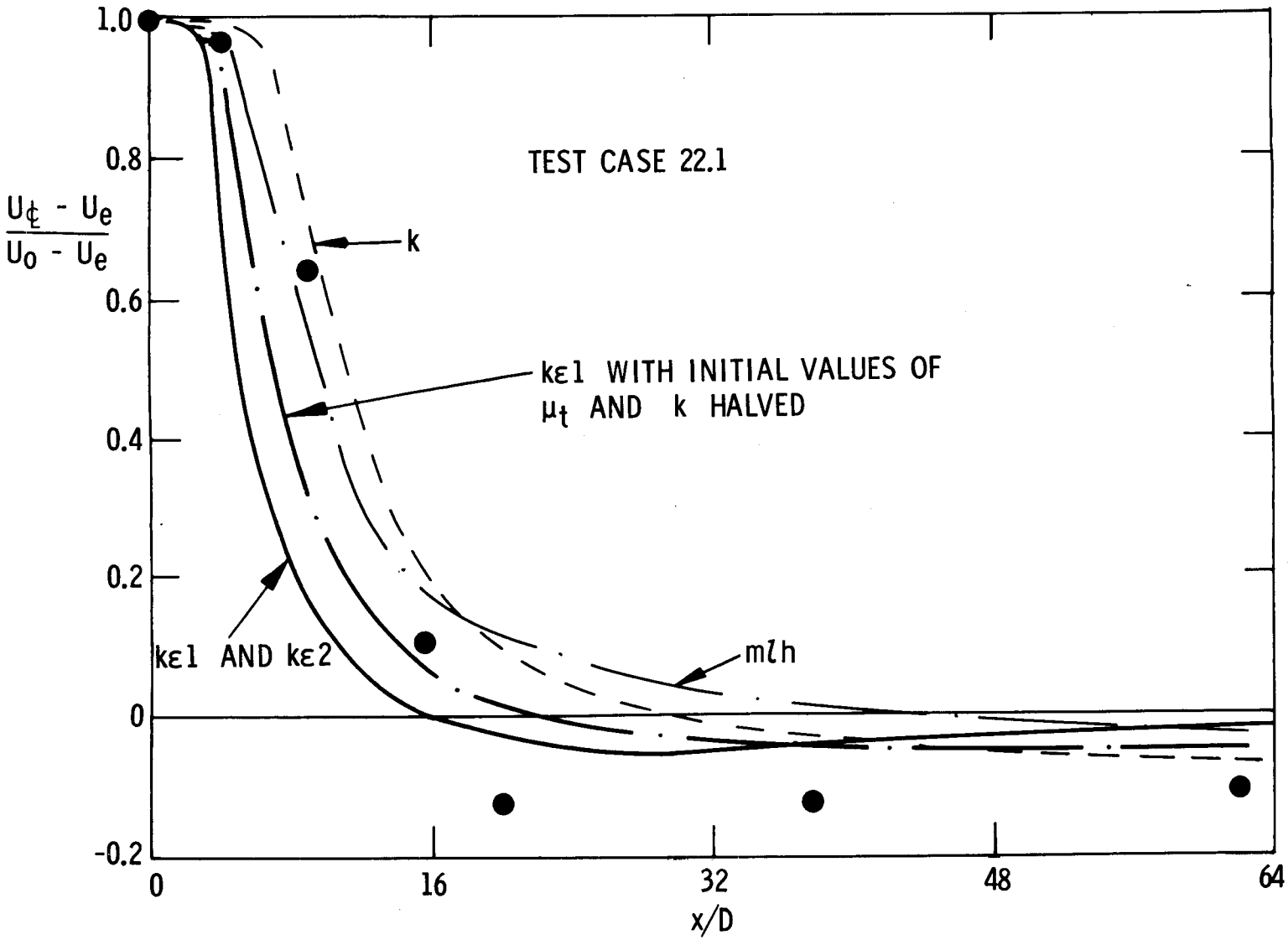
TEST CASE 22.1
$\frac{U_{\ell} - U_e}{U_0 - U_e}$
1.0
0.8
0.6
0.4
0.2
0
-0.2
0
16
32
48
64
x/D
k
kε1 WITH INITIAL VALUES OF
μ_t AND k HALVED
kε1 AND kε2
mlh

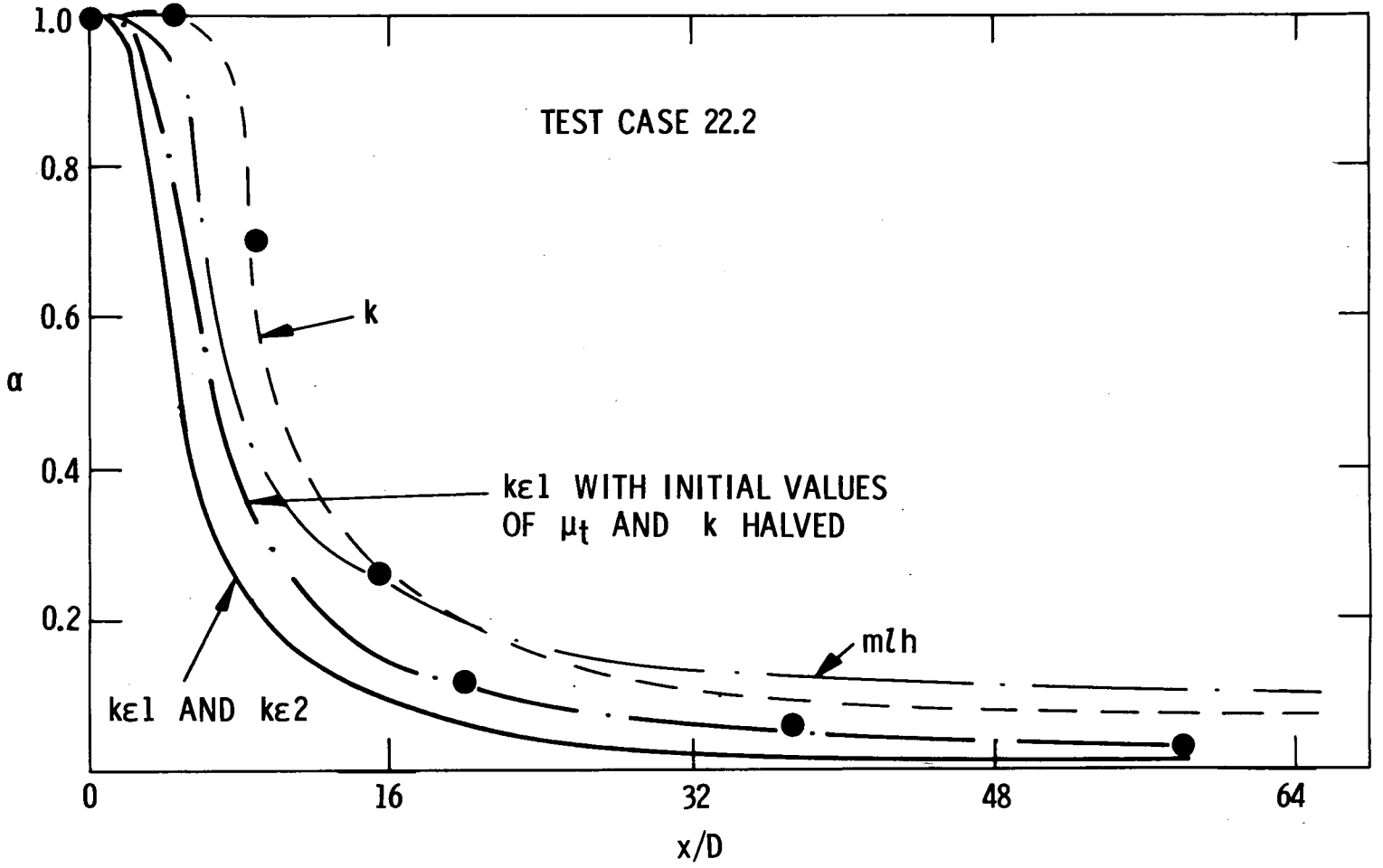
TEST CASE 22.2
1.0
0.8
0.6
0.4
0.2
α
k
kε1 WITH INITIAL VALUES
OF μt AND k HALVED
mlh
kε1 AND kε2
0
16
32
48
64
x/D

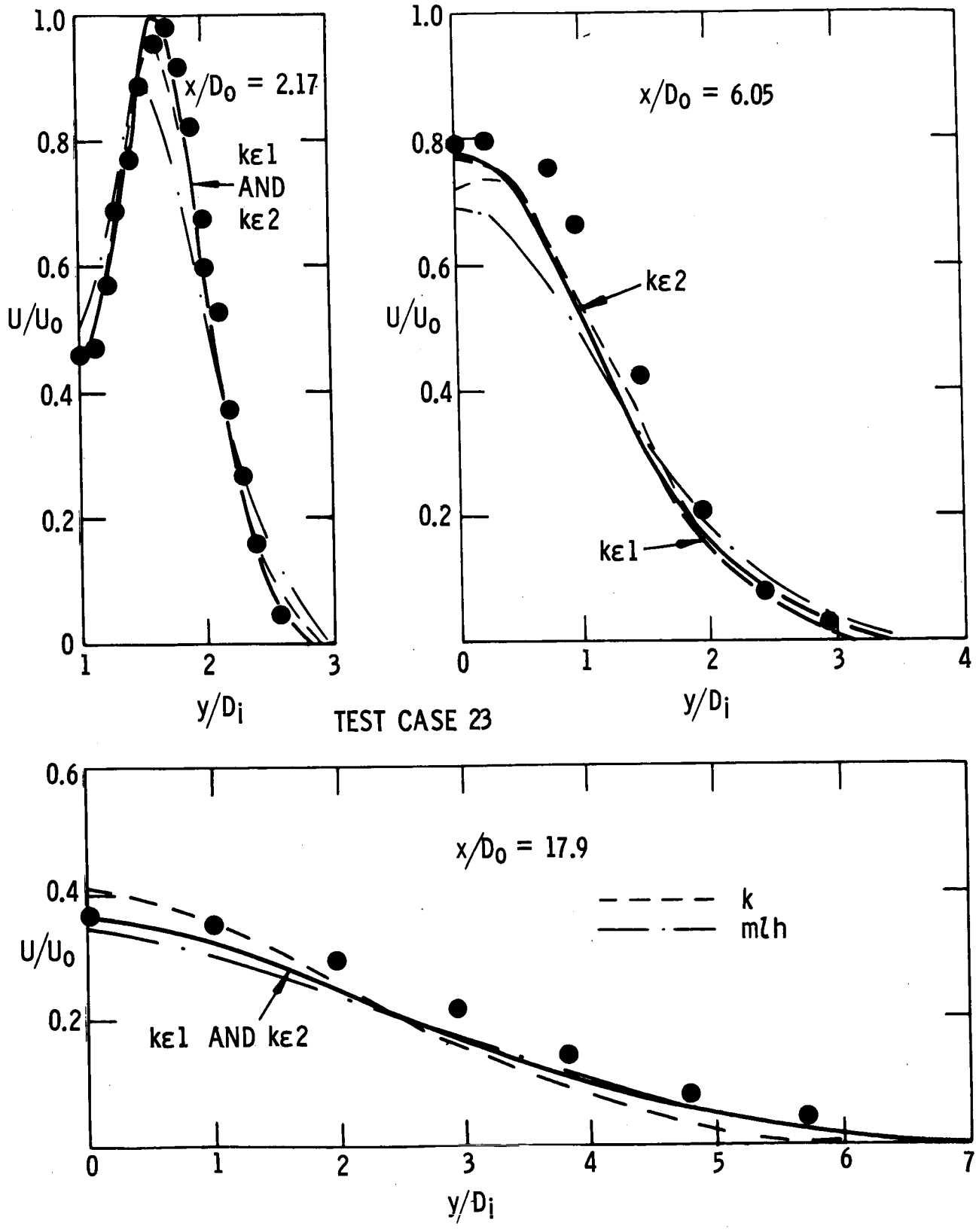
1.0
0.8
0.6
0.4
0.2
0
U/U0
x/D0 = 2.17
kε1
AND
kε2
1
2
3
y/Di
x/D0 = 6.05
kε2
kε1
0
1
2
3
4
y/Di
TEST CASE 23
0.6
0.4
0.2
U/U0
x/D0 = 17.9
k
mlh
kε1 AND kε2
0
1
2
3
4
5
6
7
y/Di

REFERENCES

1. Prandtl, L.: Bericht über Untersuchungen zur ausgebildeten Turbulenz. Z. Angew. Math. Mech., Bd. 5, Heft 2, Apr. 1925, pp. 136-139.

2. Prandtl, L.: Über ein neues Formelsystem für die ausgebildete Turbulenz. Nachr. Akad. Wiss. Göttingen. Math.-Physik. Kl., 1945, pp. 6-19.

3. Harlow, Francis H.; and Nakayama, Paul I.: Transport of Turbulence Energy Decay Rate. LA-3854 (Contract W-7405-ENG. 36), Los Alamos Sci. Lab., Univ. of California, Feb. 20, 1968.

4. Jones, W. P.; and Launder, B. E.: The Prediction of Laminarization With a Two-Equation Model of Turbulence. Int. J. Heat & Mass Transfer, vol. 15, no. 2, Feb. 1972, pp. 301-314.

5. Rodi, W.; and Spalding, D. B.: A Two-Parameter Model of Turbulence, and Its Application to Free Jets. Wärme- und Stoffübertragung, vol. 3, no. 2, 1970, pp. 85-95.

6. Ng, K. H.; and Spalding, D. B.: Turbulence Model for Boundary Layers Near Walls. Phys. Fluids, vol. 15, no. 1, Jan. 1972, pp. 20-30.

7. Spalding, D. B.: The kW Model of Turbulence. TM/TN/A/16, Dep. Mech. Eng., Imp. Coll. Sci. & Technol., Aug. 1971.

8. Rodi, Wolfgang: The Prediction of Free Turbulent Boundary Layers by Use of a Two-Equation Model of Turbulence. Ph. D. Thesis, Univ. of London, 1972.

9. Hanjalić, K.; and Launder, B. E.: A Reynolds Stress Model of Turbulence and Its Application to Thin Shear Flows. J. Fluid Mech., vol. 52, pt. 4, Apr. 25, 1972, pp. 609-638.

10. Rotta, J.: Statistical Theory of Nonhomogeneous Turbulence. Part I: Z. Physik, Bd. 129, 1951, pp. 547-572.

11. Patankar, S. V.; and Spalding, D. B.: Heat and Mass Transfer in Boundary Layers. Second ed., Int. Textbook Co. Ltd. (London), c.1970.

12. Mellor, George L.; and Herring, H. James: Two Methods of Calculating Turbulent Boundary Layer Behavior Based on Numerical Solutions of the Equations of Motion. Computation of Turbulent Boundary Layers – 1968 AFOSR-IFP-Stanford Conference, Vol. I, S. J. Kline, M. V. Morkovin, G. Sovran, and D. J. Cockrell, eds., Stanford Univ., c.1969, pp. 331-345.

13. Naot, D.; Shavit, A.; and Wolfshtein, M.: Interactions Between Components of the Turbulent Velocity Correlation Tensor Due to Pressure Fluctuations. Israel J. Technol., vol. 8, no. 3, 1970, pp. 259-269.

14. Reynolds, W. C.: Computation of Turbulent Flows – State-of-the-Art, 1970. Rep. MD-27 (Grants NSF-GK-10034 and NASA-NgR-05-020-420), Dep. Mech. Eng., Stanford Univ., Oct. 1970. (Available as NASA CR-128372.)

15. Rodi, W.: A New Method of Analysing Hot-Wire Signals in Highly Turbulent Flow, and Its Evaluation in a Round Jet. ET/TN/B/10, Dep. Mech. Eng., Imp. Coll. Sci. & Technol., Aug. 1971.

16. Bradshaw, P.; Ferriss, D. H.; and Johnson, R. F.: Turbulence in the Noise-Producing Region of a Circular Jet. J. Fluid Mech., vol. 19, pt. 4, Aug. 1964, pp. 591-624.

17. Bradbury, L. J. S.: The Structure of a Self-Preserving Turbulent Plane Jet. J. Fluid Mech., vol. 23, pt. 1, Sept. 1965, pp. 31-64.

18. Klebanoff, P. S.: Characteristics of Turbulence in a Boundary Layer With Zero Pressure Gradient. NACA Rep. 1247, 1955. (Supersedes NACA TN 3178.)

19. Champagne, F. H.; and Wygnanski, I. J.: An Experimental Investigation of Coaxial Turbulent Jets. Int. J. Heat & Mass Transfer, vol. 14, no. 9, Sept. 1971, pp. 1445-1464.

TABLE 1.- THE MIXING-LENGTH HYPOTHESIS ($m\ell h$)

$$-\overline{uv} = \ell_m^2 \left|\frac{\partial U}{\partial y}\right| \left(\frac{\partial U}{\partial y}\right)$$

where

$$\ell_m = \lambda y_G$$

and

$\lambda = 0.11$ (Axisymmetric flows)

$= 0.125$ (Plane flows)

For a monotonically increasing/decreasing velocity profile, the characteristic shear width of the flow is defined by

$$y_G = y_2 - y_1$$

where at y_1

$$\frac{U - U_I}{U_E - U_I} = 0.1$$

and at y_2

$$\frac{U - U_I}{U_E - U_I} = 0.9$$

(U_I = Axial velocity at internal boundary; U_E = Axial velocity at external boundary)

For velocity profiles without a maximum or minimum at either boundary:

At y_1

$$\frac{U - U_I}{\overline{U} - U_I} = 0.1$$

(For inner region of flow, i.e., between the internal boundary and the point of occurrence of the minimum/maximum velocity $\overline{U}$)

or at y_1

$$\frac{U - \overline{U}}{U_E - \overline{U}} = 0.9$$

(For outer region of flow)

At y_2

$$U = \overline{U}$$

For diffusion of enthalpy and species,

$$\sigma_h = \sigma_m = 0.5$$

TABLE 2.- THE PRANDTL ENERGY MODEL (k)

$$-\overline{uv} = C_\mu k^{1/2} l \left(\frac{\partial U}{\partial y}\right)$$

where

$$l = \lambda_s y_G \qquad \left(\text{With } y_G \text{ determined as in table 1}\right)$$

and

$\lambda_s = 0.625$ (Axisymmetric flows)

$= 0.875$ (Plane flows)

Equation solved for conservation of kinetic energy of turbulence is

$$\rho \frac{Dk}{Dt} = \frac{1}{y^j} \frac{\partial}{\partial y}\left(y^j \frac{\mu_t}{\sigma_k} \frac{\partial k}{\partial y}\right) + \mu_t \left(\frac{\partial U}{\partial y}\right)^2 - \frac{\rho k^{3/2}}{l}$$

where

$C_\mu = 0.08$

$\sigma_k = 0.7$

For diffusion of enthalpy and species,

$\sigma_h = \sigma_m = 0.5$

TABLE 3.- THE ENERGY-DISSIPATION MODEL (kϵ1)

$$-\rho\overline{uv} = \mu_t \frac{\partial U}{\partial y}$$

where

$$\mu_t = C_\mu \rho \frac{k^2}{\epsilon}$$

$$\rho \frac{Dk}{Dt} = \frac{1}{y^j} \frac{\partial}{\partial y}\left(y^j \frac{\mu_t}{\sigma_k} \frac{\partial k}{\partial y}\right) + \mu_t \left(\frac{\partial U}{\partial y}\right)^2 - \rho\epsilon$$

$$\rho \frac{D\epsilon}{Dt} = \frac{1}{y^j} \frac{\partial}{\partial y}\left(y^j \frac{\mu_t}{\sigma_\epsilon} \frac{\partial \epsilon}{\partial y}\right) + C_{\epsilon 1} \frac{\epsilon}{k} \mu_t \left(\frac{\partial U}{\partial y}\right)^2 - C_{\epsilon 2} \frac{\rho \epsilon^2}{k}$$

For plane flows:

C_μ	$C_{\epsilon 2}$	$C_{\epsilon 1}$	σ_k	σ_ϵ
0.09	1.92	1.43	1.0	1.3

For axisymmetric flows:

The same as plane flows except

$$C_\mu = 0.09 - 0.04f$$

$$C_{\epsilon 2} = 1.92 - 0.0667f$$

where

$$f \equiv \left| \frac{y_G}{2\,\Delta U}\left(\frac{dU_\mathcal{L}}{dx} - \left|\frac{dU_\mathcal{L}}{dx}\right|\right)\right|^{0.2}$$

For diffusion of enthalpy and species,

$$\sigma_m = \sigma_h = 0.7$$

TABLE 4.- THE EXTENDED ENERGY-DISSIPATION MODEL ($k\epsilon 2$)

The data are the same as in table 3 except as noted below.

For plane flows:

C_μ	$C_{\epsilon 2}$	$C_{\epsilon 1}$	σ_k	σ_ϵ
*	1.94	1.40	1.0	1.3

$$^{*}\, C_\mu = 0.09 g\left(\overline{P/\epsilon}\right)$$

where

$$\left(\overline{P/\epsilon}\right) \equiv \frac{\int_{y_1}^{y_2} \rho\overline{uv}\left(\frac{P}{\epsilon}\right) y^j dy}{\int_{y_2}^{y_1} \rho\overline{uv} y^j dy}$$

and the function $g\left(\overline{P/\epsilon}\right)$ is shown in figure 1

For axisymmetric flows:

The same as plane flows except

$$C_\mu = 0.09 g\left(\overline{P/\epsilon}\right) - 0.0534f$$

$$C_{\epsilon 2} = 1.94 - 0.1336f$$

TABLE 5.- THE HANJALIĆ-LAUNDER $\overline{uv}k\epsilon$ MODEL

The Reynolds shear stress $-\rho\overline{uv}$ is found from

$$\frac{D\overline{uv}}{Dt} = C_s \frac{\partial}{\partial y}\left(\frac{k^2}{\epsilon}\frac{\partial \overline{uv}}{\partial y}\right) - C_{\phi 1}\left(\frac{\overline{uv}\epsilon}{k} + C_\mu\, k \frac{\partial U}{\partial y}\right)$$

$$\frac{Dk}{Dt} = 0.9C_s \frac{\partial}{\partial y}\left(\frac{k^2}{\epsilon}\frac{\partial \overline{uv}}{\partial y}\right) - \overline{uv}\frac{\partial U}{\partial y} - \epsilon$$

$$\frac{D\epsilon}{Dt} = C_\epsilon \frac{\partial}{\partial y}\left(\frac{k^2}{\epsilon}\frac{\partial \epsilon}{\partial y}\right) - C_{\epsilon 1}\frac{\overline{uv}\epsilon}{k}\frac{\partial U}{\partial y} - C_{\epsilon 2}\frac{\epsilon^2}{k}$$

where

C_s	$C_{\phi 1}$	C_μ	C_ϵ	$C_{\epsilon 1}$	$C_{\epsilon 2}$
0.1	2.8	0.09	0.07	1.40	1.95

TABLE 6.- REYNOLDS STRESS MODELS $\left(\overline{u_i u_j}\epsilon\right)$

Reynolds stresses $-\rho\overline{u_i u_j}$ calculated from

$$\frac{D\overline{u_i u_j}}{Dt} = D_{ij} + \Phi_{ij} - \underbrace{\left(\overline{u_i u_\ell}\frac{\partial U_j}{\partial x_\ell} + \overline{u_j u_\ell}\frac{\partial U_i}{\partial x_\ell}\right)}_{P_{ij}} - \frac{2}{3}\epsilon\delta_{ij}$$

1. Simple version for D_{ij}

$$D_{ij} = C_s\frac{\partial}{\partial x_k}\left(\frac{k}{\epsilon}\overline{u_k u_\ell}\frac{\partial\overline{u_i u_j}}{\partial x_\ell}\right)$$

$C_s = 0.25$

2. Tensor invariant D_{ij}

$$D_{ij} = C_s\frac{\partial}{\partial x_k}\frac{k}{\epsilon}\left(\overline{u_i u_\ell}\frac{\partial\overline{u_j u_k}}{\partial x_\ell} + \overline{u_j u_\ell}\frac{\partial\overline{u_k u_i}}{\partial x_\ell} + \overline{u_k u_\ell}\frac{\partial\overline{u_i u_j}}{\partial x_\ell}\right)$$

$C_s = 0.10$

A. Rotta-Wolfshtein-Reynolds, Φ_{ij}

$$-C_{\phi1}\frac{\epsilon}{k}\left(\overline{u_i u_j} - \frac{2}{3}\delta_{ij}k\right) - C_{\phi2}\left(P_{ij} - \frac{2}{3}\delta_{ij}P\right)$$

$C_{\phi1} = 2.8$ $\quad C_{\phi2} = 0.4$ $\quad P$ = Total production rate of k

B. Rotta-Hanjalić-Launder, Φ_{ij}

$$-C_{\phi1}\frac{\epsilon}{k}\left(\overline{u_i u_j} - \frac{2}{3}\delta_{ij}k\right) + \left(\phi_{ij} + \phi_{ji}\right)$$

where

$$\phi_{ij} \equiv \frac{\partial U_l}{\partial x_m}a_{\ell j}^{mi}$$

$$a_{\ell j}^{mi} = \alpha\overline{u_m u_i}\delta_{ij} + \beta\left(\overline{u_m u_\ell}\delta_{ij} + \overline{u_m u_j}\delta_{\ell i} + \overline{u_i u_j}\delta_{m\ell} + \overline{u_i u_\ell}\delta_{mj}\right) + \left[\gamma\delta_{mi}\delta_{\ell j} + \eta\left(\delta_{m\ell}\delta_{ij} + \delta_{mj}\delta_{i\ell}\right)\right]k$$

$$+ \frac{\nu\left(\overline{u_m u_j u_i u_\ell} + \overline{u_m u_\ell u_i u_j}\right)}{k} + C_{\phi2}\frac{\left(\overline{u_m u_i u_\ell u_j}\right)}{k}$$

$\alpha = \dfrac{10 - 8C_{\phi2}}{11}$ $\quad \beta = \dfrac{-(2 - 6C_{\phi2})}{11}$ $\quad \gamma = \dfrac{-(4 - 12C_{\phi2})}{55}$ $\quad \eta = \dfrac{6 - 18C_{\phi2}}{55}$

$\nu = -C_{\phi2}$ $\quad C_{\phi1} = 2.5$ $\quad C_{\phi2} = 0.3$

C. Rotta-Launder, Φ_{ij} (present work)

$$-C_{\phi1}\frac{\epsilon}{k}\left(\overline{u_i u_j} - \frac{2}{3}\delta_{ij}k\right) + \left(\phi_{ij} + \phi_{ji}\right)$$

where

$$\phi_{ij} \equiv \frac{\partial U_l}{\partial x_m}a_{\ell j}^{mi}$$

$$a_{\ell j}^{mi} = \alpha\delta_{mi}\overline{u_\ell u_j} + \beta\left(\delta_{m\ell}\overline{u_i u_j} + \delta_{mj}\overline{u_i u_\ell} + \delta_{i\ell}\overline{u_m u_j} + \delta_{ij}\overline{u_m u_\ell}\right) + \gamma\delta_{\ell j}\overline{u_m u_i} + \left[\eta\delta_{mi}\delta_{\ell j} + \nu\left(\delta_{m\ell}\delta_{ij} + \delta_{mj}\delta_{i\ell}\right)\right]k$$

$\beta = \dfrac{-(2 + 3\alpha)}{11}$ $\quad \gamma = \dfrac{4\alpha + 10}{11}$ $\quad \eta = \dfrac{-(50\alpha + 4)}{55}$ $\quad \nu = \dfrac{20\alpha + 6}{55}$ $\quad \alpha = 0.3$ $\quad C_{\phi1} = 1.5$

$$\frac{D\epsilon}{Dt} = C_\epsilon\frac{\partial}{\partial x_k}\left(\frac{k}{\epsilon}\overline{u_k u_\ell}\frac{\partial\epsilon}{\partial x_\ell}\right) - C_{\epsilon1}\frac{\overline{u_i u_j}\epsilon}{k}\frac{\partial U_i}{\partial x_j} - C_{\epsilon2}\frac{\epsilon^2}{k}$$

$C_\epsilon = 0.2$ $\quad C_{\epsilon1} = 1.43$ $\quad C_{\epsilon2} = 1.92$ (Versions A and B for Φ_{ij})

$C_\epsilon = 0.16$ $\quad C_{\epsilon1} = 1.50$ $\quad C_{\epsilon2} = 1.95$ (Version C for Φ_{ij})

TABLE 7.- INITIAL CONDITIONS

Test case	$\frac{\mu_t}{\rho D \Delta U}$	ρ at –	Remarks
1, 2, 3			Arbitrary initial conditions
4			$\overline{uv}$ given; $k = \frac{\lvert\overline{uv}\rvert}{0.3}$; $\overline{u^2}/k$, $\overline{v^2}/k$, $\overline{w^2}/k$ as in test case 14
5	3.68×10^{-3}	e	D taken as 2.54 cm
6			$\overline{uv}$ and k taken from reference 16
7	3.3×10^{-3}	l	
8	6.6×10^{-3}	l	
9	1.6×10^{-3}	l	
10	0.72×10^{-3}	e	
11	1.25×10^{-3}	e	g = 0.8
12	5.5×10^{-3}	l	
13			$\overline{uv}$ and k from self-preserving plane jet (ref. 17); $\overline{u^2}/k$, $\overline{v^2}/k$, $\overline{w^2}/k$ assumed to be 2/3
14			$\overline{uv}$ given; $\overline{u^2}$ and $\overline{v^2}$ from reference paper for test case 14; $\overline{w^2}$ from reference 18; g = 1.2
15			$\overline{uv}$ given; k from reference paper for test case 15; computations begun at second station
16	0.19×10^{-3}	l	
17	12.9×10^{-3}		g = 1.3
18			A continuation of case 6
19	5×10^{-3}	l	
20	0.5×10^{-3}	e	
21	2.3×10^{-3}	e	
22	27×10^{-3}	l	
23			$\overline{u^2}$ and $\overline{v^2}$ given; $\overline{w^2} = \overline{v^2}$ assumed; $\overline{uv}$ from reference 19; g = 0.8; computations begun at second station

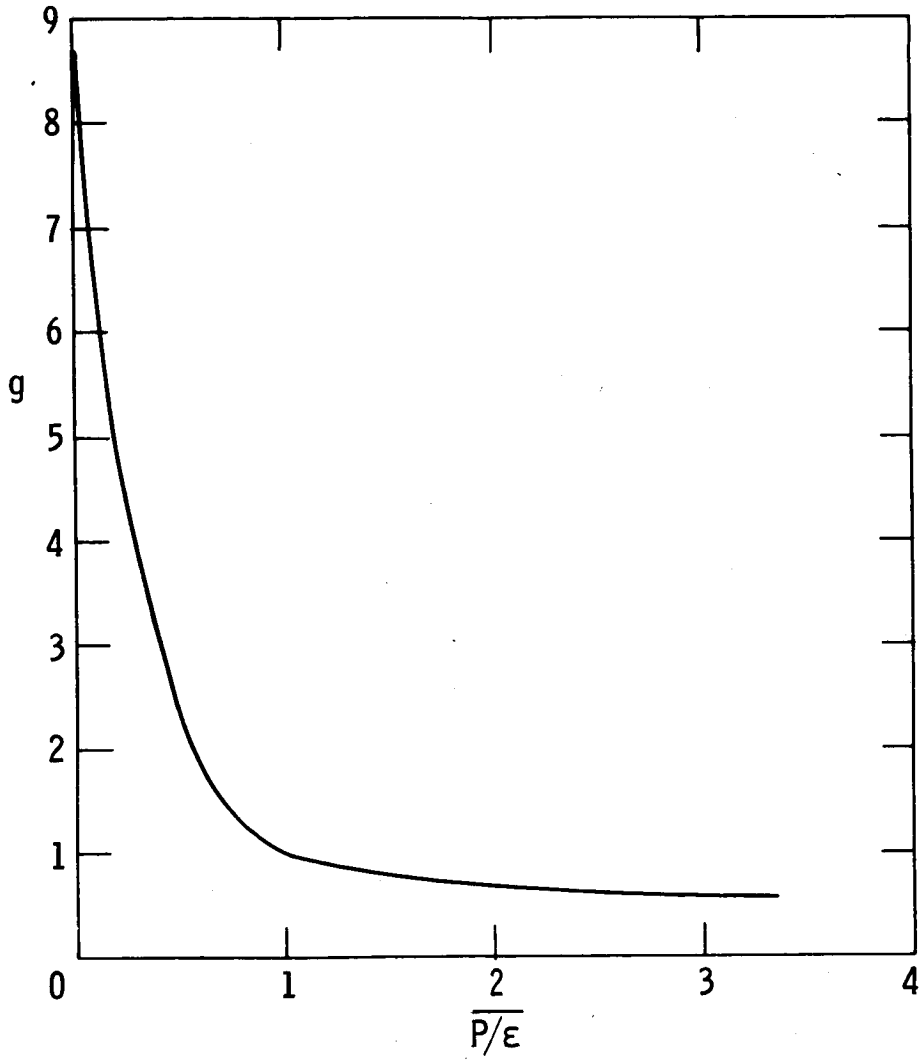

Figure 1.- Variation of g with $\overline{P/\epsilon}$ for kϵ2 model.

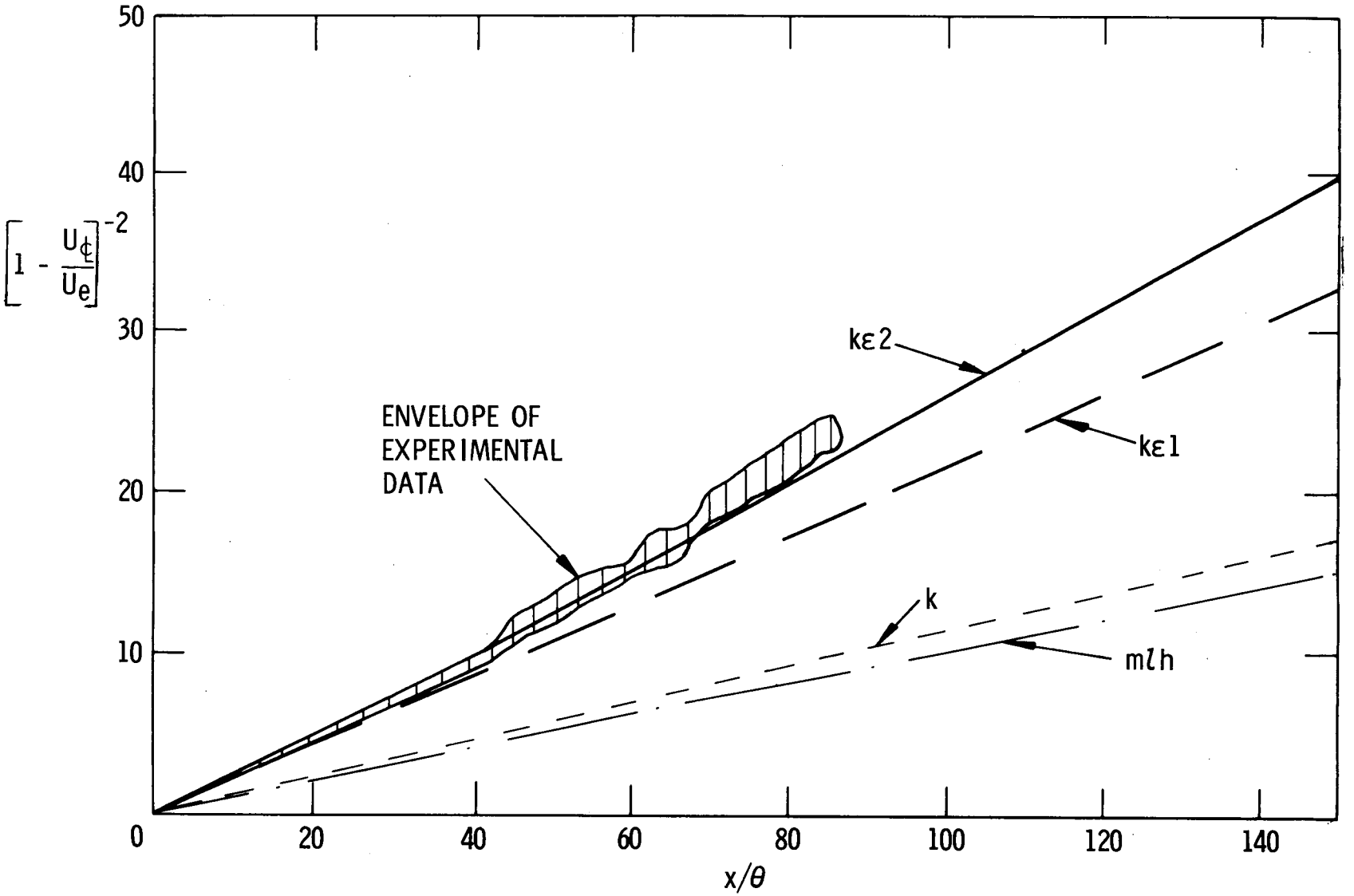

Figure 2.- Variation of $\left[1 - \frac{U_{C_L}}{U_e}\right]^{-2}$ with x/θ for case 13.

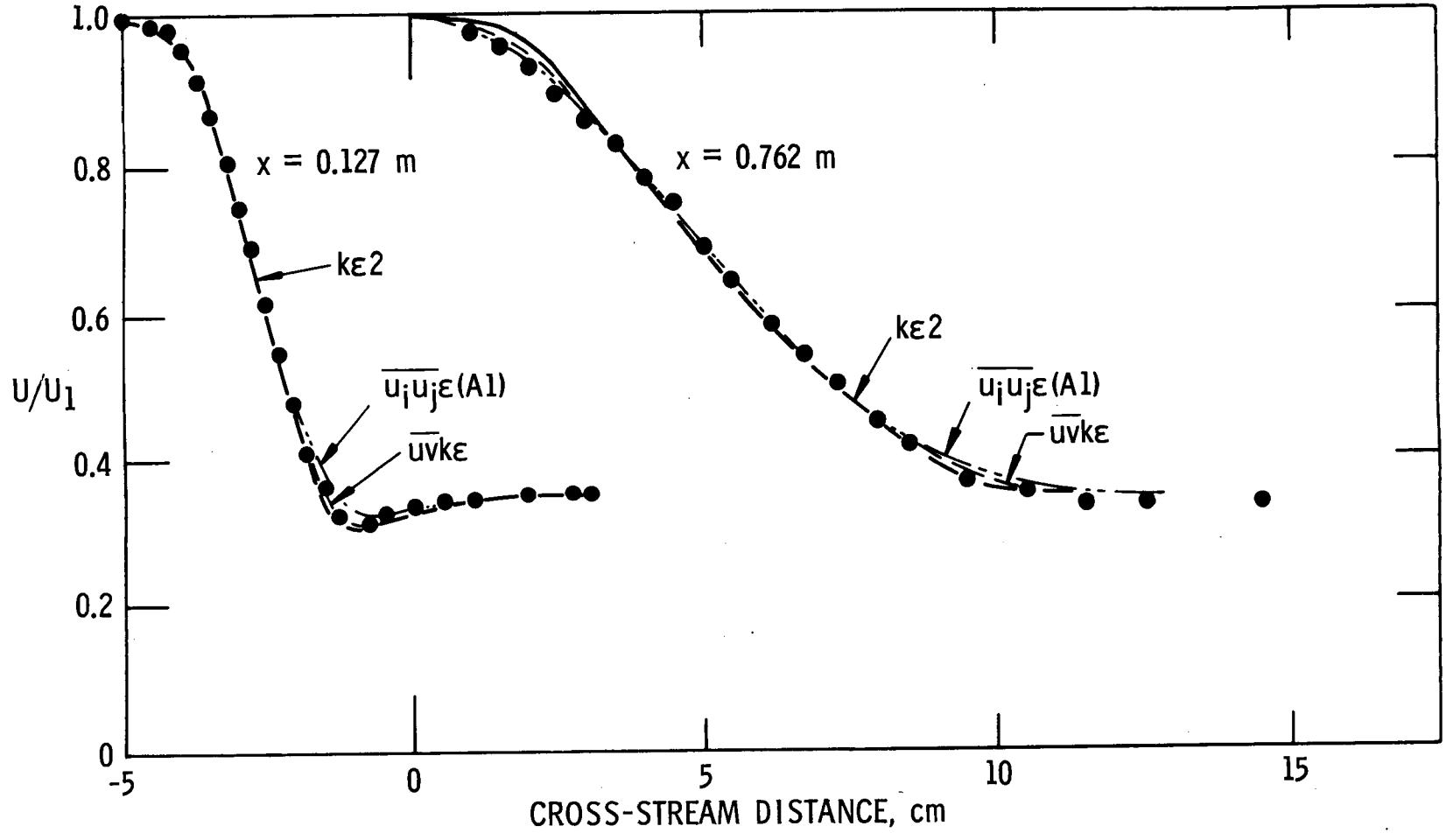

(a) Velocity profiles.

Figure 3.- Stress models, case 4. (Letter and number in parentheses denote modeling practice; see table 6.)

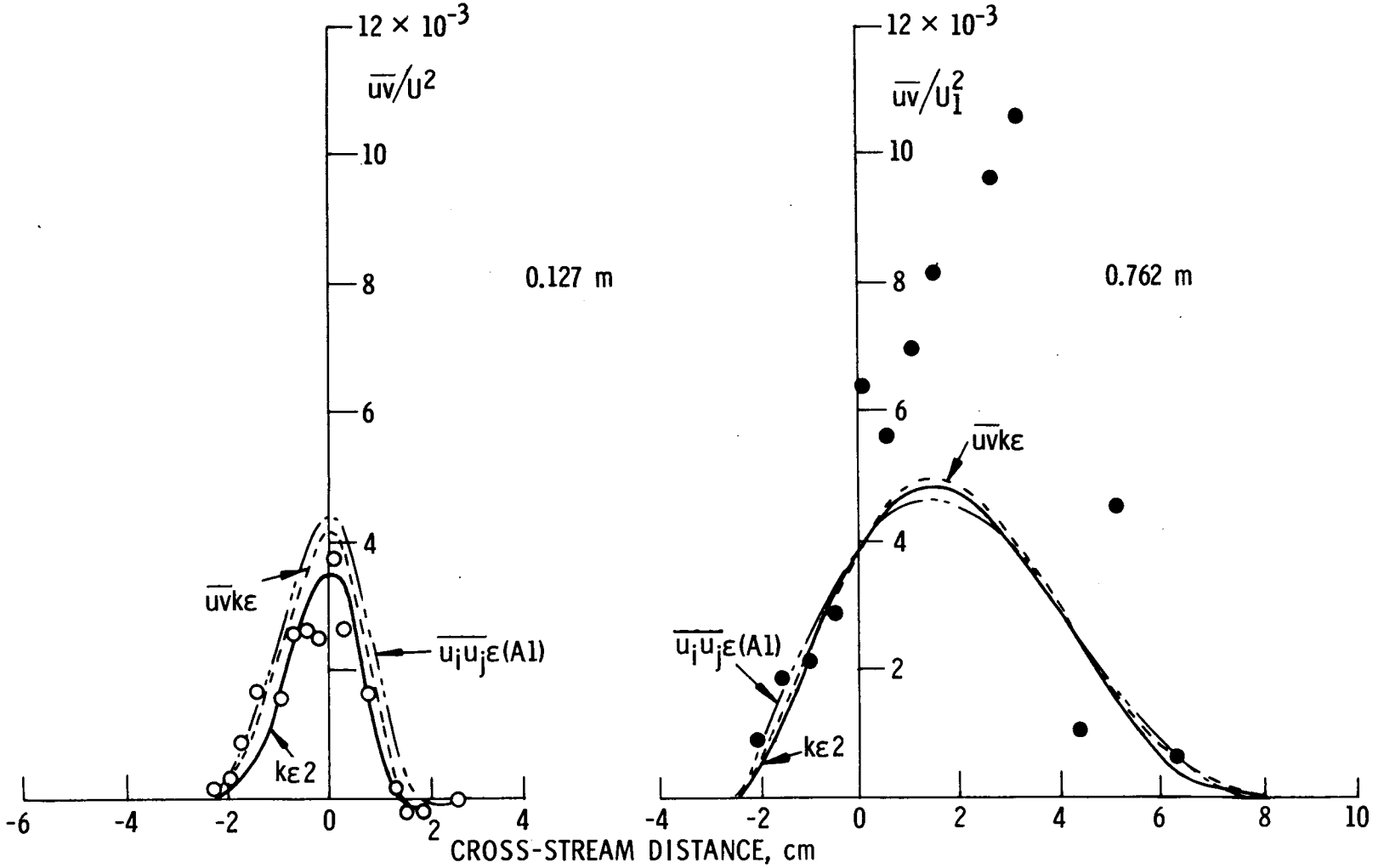

(b) Shear-stress profiles.

Figure 3.- Concluded.

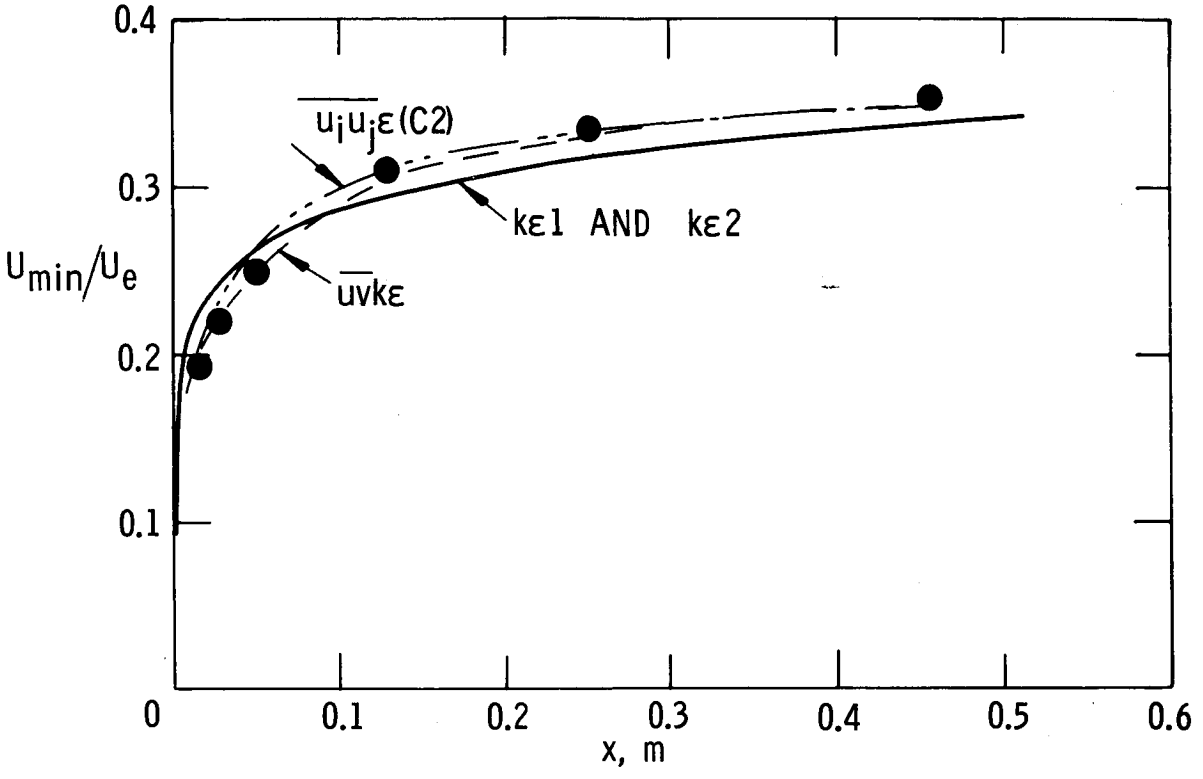

Figure 4.- Variation of minimum velocity for case 4.

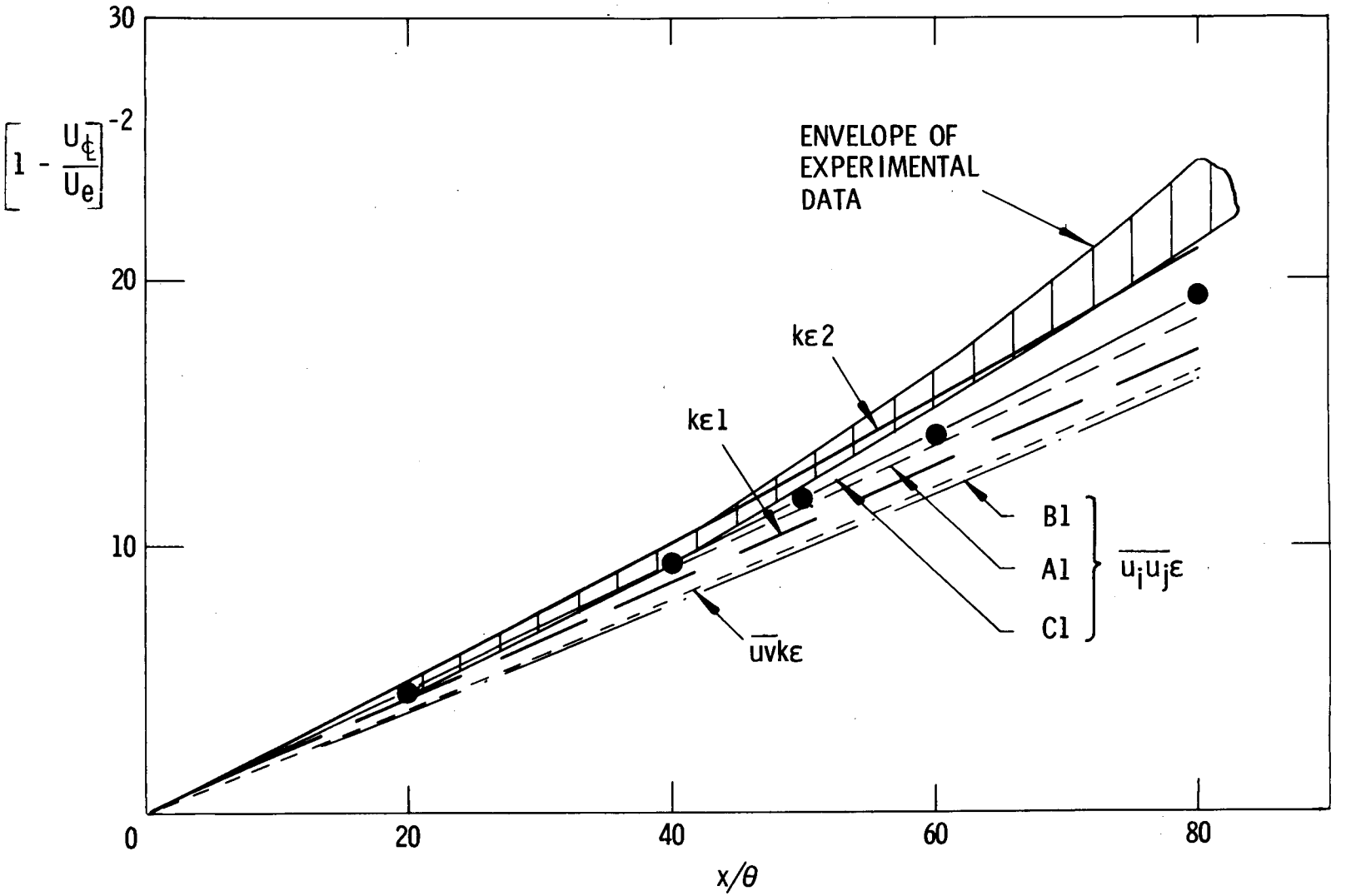

Figure 5.- Decay of plane jet in moving stream.

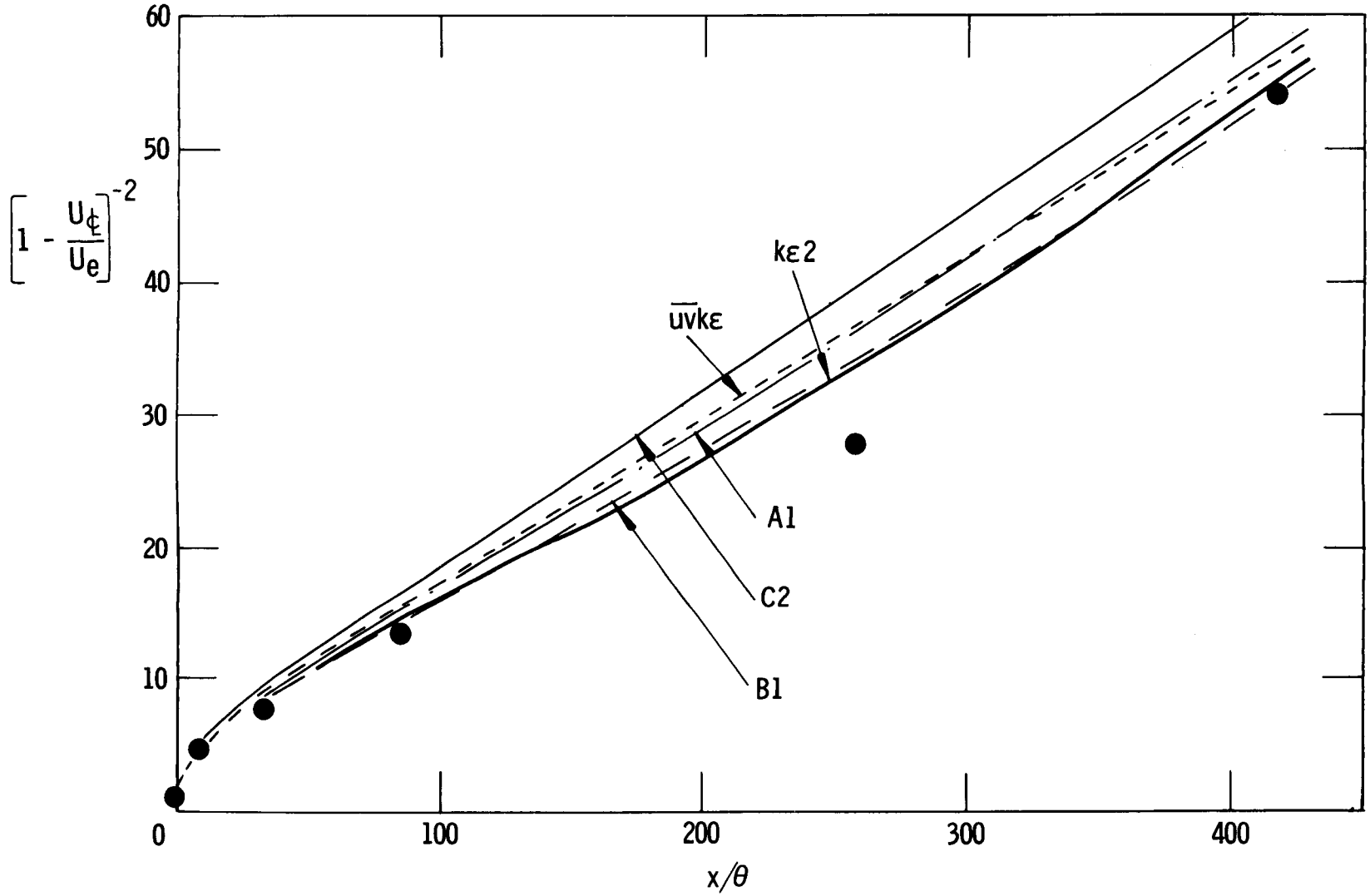

Figure 6.- Stress model predictions for case 14.

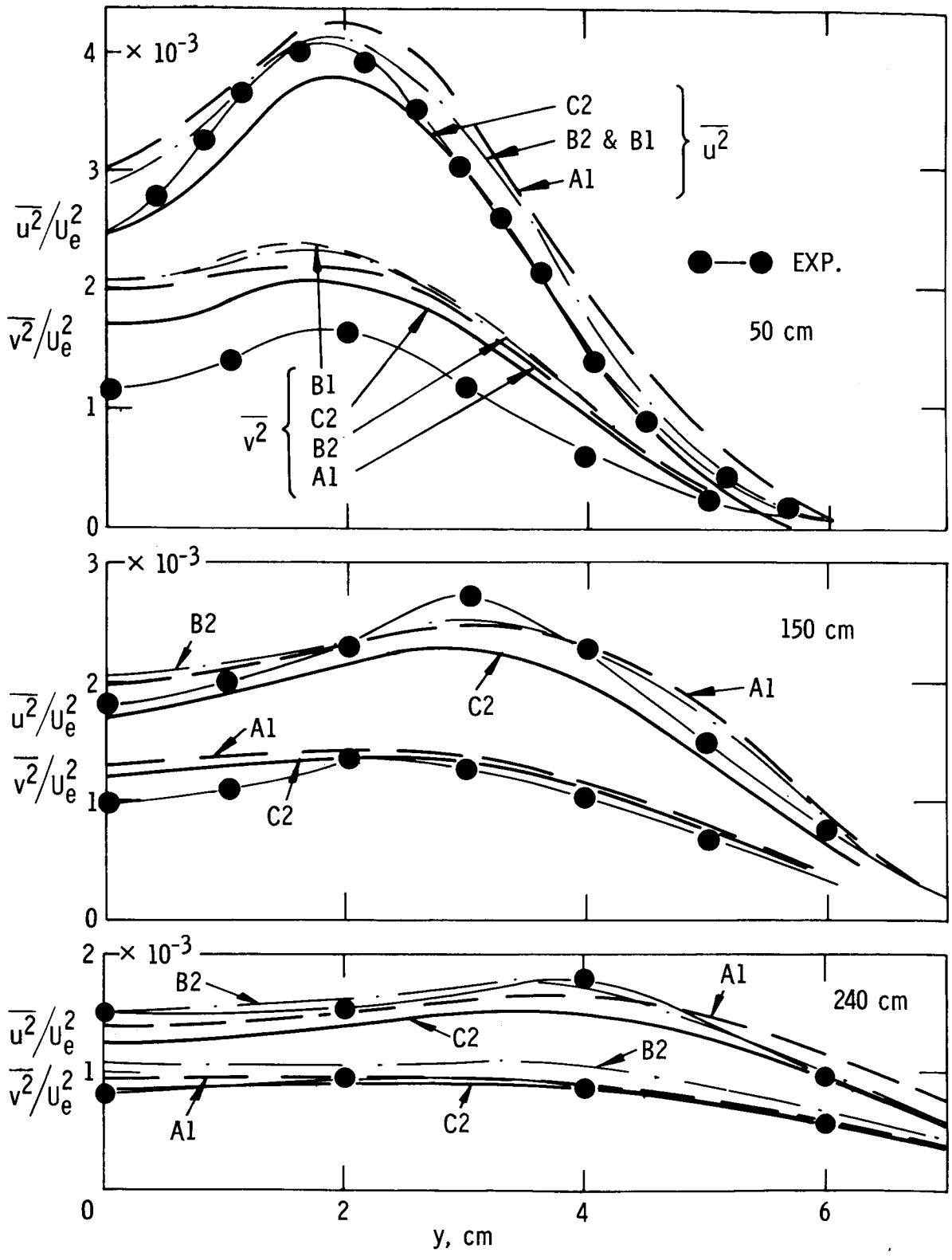

Figure 7.- Reynolds stress distributions for case 14.

DISCUSSION

D. M. Bushnell: I was wondering if you had any thoughts about the importance of the pressure-velocity correlations at compressible speeds, and how you presently handle them in your method.

D. B. Spalding: How they are handled at the present is that everything of that kind is lumped into the energy diffusion term. We simply see how well we can do by choosing the best constants, such as the effective Prandtl or Schmidt number, for turbulence diffusion, including in our review compressible or density-varying flow.

D. M. Bushnell: We have nothing to compare the diffusion model with at the compressible conditions. In other words, you are lumping a lot in there, and we are not sure how accurate the lump is.

D. B. Spalding: That is correct. All we see is the final result. We do not have enough detailed information. For incompressible flows, we can make detailed comparison; for compressible flows, we need corresponding detailed measurements and comparisons.

D. M. Bushnell: The only thing is, those terms look huge. That's my only comment.

I. E. Alber: With respect to the compressible calculations, I see that you get the results for the spreading rate for the two-dimensional mixing layer as a function of Mach number, which is quite similar to what other people have obtained; that is, there is very little variation of the spreading parameter with Mach number. However, the data, apparently the high Reynolds number data, indicate that there is a considerable increase in the spreading parameter with Mach number. Could you comment on what may be the cause of this discrepancy, and if the pressure velocity correlation effect at high speeds may come into the picture?

D. B. Spalding: I can't comment from any knowledge or any insight. I have noted the effect also, and so I wonder.

G. L. Mellor: Yes, I would like to be certain on one point that you made. Your length scale equation is a dissipation thing, which is energy to the 3/2 power over the length scale. And we know that Rotta has an equation for the transport of a velocity squared times the length scale. I think you said that you tried some of that too, and you said that it made no difference whatsoever? Is that my understanding?

D. B. Spalding: It makes little difference for the kind of flows considered in this conference, which are free turbulent flows. It is easy to explain. One can formally show that the transport equation for ϵ can be turned into the transport equation for the product of k times the length scale, except for an additional term involving the gradient across the layer of the length scale. There are many models in this family that differ only in

an additional length-scale-gradient term in the equation. That term is very small in all these flows. Flows near walls are different. There are some crucial experiments to be carried out which will enable us to distinguish between the models. But, at the practical level, the distinction between the models lies only in the different value given to the effective Prandtl number (or Schmidt) of the second turbulence quantity. There is just one good thing in favor of the ϵ models. You can have a constant value of the Schmidt number for the diffusion of this quantity, whether you are in a free turbulent flow or near a wall. All the other models, including the $k\ell$ model, require the Schmidt number to be varied, or they require something else to be done. So the $k\epsilon$ model has our favor for this quite small advantage connected with wall flows.

M. V. Morkovin: Could I ask for a comparison of your efforts and Donaldson's? In what respect are they similar and where do they depart?

B. E. Launder: Dr. Donaldson and our group at Imperial College are both developing turbulence models based on differential equations for the Reynolds stresses. We adopt in detail different approximations for the pressure-strain term; we use appreciably more elaborate closures than Dr. Donaldson. I think that he will find it necessary to use a more complicated closure when he comes to look at some of the shear flows that we have examined.

C. duP. Donaldson: We use a slightly different dissipation model. We have already started to put in more complicated pressure-strain terms that we came to from trying to use this method to study transition. This problem is similar to that of the wall region of a turbulent boundary layer. In this case, to be more complete, you do have to use mean gradients in the definition of pressure-strain and isotropy terms. I would like to make an additional comment while I've got the microphone and emphasize again what can be learned from these higher order models by setting the transport terms equal to zero and neglecting diffusion. It is really very interesting that you can see the difference between plain and axisymmetric jets and, in many cases of complicated flows with body forces or centrifugal forces, you can begin to see just where you don't want to use conventional methods.

C. E. Peters: I would like to address my question to either Professor Launder or Professor Spalding. These advanced methods depend greatly on the initial conditions, particularly in relatively weak shear flows. Your procedure of using either experimental initial conditions or an eddy viscosity which matches the initial region development only allows an after-the-fact correlation of an experiment. What is one to do in an engineering situation where the initial conditions are not well defined? Can you suggest procedures for approximately determining the initial conditions?

B. E. Launder: I would not entirely accept your assertion that our practices allow only "after-the-fact correlation." After all, if it were correct, we might expect nearly the same performance to be turned in by the various models; yet there are, in fact, large differences between predictions generated by the various models. However, I agree that when our procedures (or anyone else's for that matter) are used to predict engineering flows, insufficient experimental data will generally be available to describe the initial conditions with certainty. If the predictor has thorough acquaintance with experimental data of turbulent flows, he may well be able to assess with sufficient accuracy the initial profiles. Otherwise, the safest practice is to begin computations sufficiently far upstream for the (perhaps badly) guessed initial profiles to have negligible effect on the region of interest. For example, if one wants to predict a jet development, then computations might begin at the upstream end of the nozzle(s); or, if the flow is a wake, the calculations could start upstream of the obstacle generating the wake.

P. A. Libby: I am greatly impressed by the powers of the new methods developed by the Imperial College group and others when applied to flows with variable density, but I wonder whether we can expect the carefully selected constants in these methods to carry over without density effects to the variable density cases. My work in a simple flow shows that we must make these constants functions of the density.

B. E. Launder: Yes, it may be necessary to amend or extend our present models to provide consistently good predictions of variable density flows. The pressure-strain term would be the first term to be examined; others in the dissipation equation need to be looked at.

S. C. Lee: The turbulence kinetic energy equation consists of convection, diffusion, production, and dissipation terms. Why treat the dissipation term more favorably than the others? If we examine the figure of turbulence energy balance (shown by Professor Spalding with comparison of Bradbury's data), it appears that all terms are approximately the same order of magnitude.

B. E. Launder: In the models I have been talking about, based upon differential equations for the Reynolds stresses, the five processes of generation, dissipation, redistribution, diffusion, and convection interact to determine the local stress levels. Since we solve convective transport equations for the stress components, we may say that we account "exactly" for convection of the stresses. The generation term, too, is one that we treat without further approximation since it consists simply of the product of Reynolds stresses and mean velocity gradients. That leaves dissipation, diffusion, and redistribution to be accounted for; as you say, we solve a differential equation for the first of these but not for the other two. We could solve transport equations for the diffusion correlations as well as for the Reynolds stress and dissipation rate (Chou and a number of others have

suggested models of this kind). However, I regard this level of closure as unnecessarily elaborate since the diffusion terms are seldom decisively important in the Reynolds stress equations. I think therefore that the simpler gradient-diffusion approximation will suffice. Finally, there is the redistribution term to consider. Although this term does not appear in the turbulence energy equation (which was the equation you mentioned), it is of great influence in determining the magnitude of the individual stress components. The practice we adopt in simulating this term is, we think, suggested by the form of the exact correlation. Other practices are possible, however, and Kolovandin and Vatutin[1] describe a much more elaborate treatment involving the solution of three-dimensional elliptic differential equations. I do not believe such an approach is warranted since it seems that evaluation of the redistribution term would then absorb more computer time than all the rest of the calculation.

[1] Kolovandin, B. A.; and Vatutin, I. A.: Statistical Transfer Theory in Non-Homogeneous Turbulence. Int. J. Heat & Mass Transfer, vol. 15, no. 12, Dec. 1972, pp. 2371-2383.

A PROVISIONAL ANALYSIS OF TWO-DIMENSIONAL TURBULENT MIXING WITH VARIABLE DENSITY

By Paul A. Libby
University of California at San Diego

12

SUMMARY

A predictive method for the titled flows based on the Prandtl energy method is developed and assessed by comparing predicted results with experimental results. For constant-density flows, both gross properties such as spreading rate and maximum turbulent kinetic energy and detailed properties such as mean shear stress distributions are shown to be well predicted. For variable-density flows, considerable attention is devoted to the inclusion in the analysis of the added effect of pressure fluctuations and of the variation in the several extant empirical parameters on the turbulent kinetic energy. It is found that a variation with Mach number of the characteristic Reynolds number for turbulent transport is needed to account for the observed decrease in spreading rate. The predictions which result from these considerations are compared with the limited experimental data presently available for the two crucial cases: compressible adiabatic mixing and low-speed isothermal mixing of two dissimilar gases.

INTRODUCTION

There is considerable activity presently underway by several groups on the description of turbulent shear flows by methods which contain more of the physics of turbulence than do the well-known methods based on mixing length and the usual eddy-viscosity models. Bradshaw et al., Rodi and Spalding, Hanjalić and Launder, Donaldson, and Wilcox and Alber (refs. 1 to 5) provide recent entry points in this literature. Most of this activity has concerned turbulent flows with uniform properties, presumably because these new methods should first be assessed for this simpler case and because the amount of data for the case of variable density is limited. Concern here is with the simplest turbulent shear flow, the two-dimensional mixing of two different streams, but under circumstances involving variable density, either because of the high speed of one stream or because of different compositions of the two streams.

The two-dimensional mixing layer has the virtue that its description is given in terms of a similarity variable; thus, the numerical analysis associated with its study is modest. It has the further advantage that there are no solid walls present so that most effects of molecular transport are negligible and the modeling required to effect closure

in the describing equations is simplified. A disadvantage is that its study in the laboratory is relatively difficult when compared with other free mixing flows, for example, wakes and jets; therefore, experimental data suitable for purposes of comparison are limited, especially for the case of variable density.

Previous theoretical work on two-dimensional, turbulent mixing for constant fluid properties is extensive; the well-known references 6 and 7 may be examined. For the case of variable density due to either compressibility effects of high speed or to heterogeneous composition, the literature involving a serious effort to compare prediction and experimental data is sparse; most entries set up a model for the case of variable properties, validate it against the data for the constant-density case, and then use it to predict the effects of variable density. Typical thereof is reference 8.

This situation is perhaps due to the disarray in the experimental data presently existent in two crucial cases of two-dimensional mixing with variable density. The data have been recently reviewed by Birch and Eggers (paper no. 2 of this conference). With respect to the case of one high-speed stream mixing with a quiescent gas of the same composition under conditions such that the stagnation temperature is constant everywhere, that is, the case of so-called "compressible adiabatic flow," several sets of data indicate no effect of high speed (that is, of high Mach number) on the spreading angle. Other data indicate a significant increase in spreading parameter, that is, a decrease in spreading angle and mixing rate, as the Mach number of the high-speed stream increases.

The other crucial case of two-dimensional mixing with variable density involves the low-speed isothermal mixing of two gases of different molecular weights. Again, Birch et al. have pointed out the inconsistency of several sets of data related to the spreading parameter, in these cases to be considered a function of the velocity and density ratios of the two participating streams.

Given this situation, any theoretical analysis such as the present one must be treated as a provisional one until at least the experimental evidence related to these two crucial cases cited is considered to be well-established. In the present work, the Brown and Roshko data (ref. 9) for heterogeneous, low-speed mixing and the data shown by Brown and Roshko and by Birch and Eggers indicating significant effect of Mach number on the spreading parameter for compressible adiabatic flows have been accepted as correct. Accordingly, comparisons have been made of the present theoretical predictions against these data and the appropriate empirical constants have been adjusted to bring prediction and these experimental data into agreement insofar as possible. If future developments do not support these experimental data as correct, the present work should still provide a methodological framework of some value, but, of course, the adjustment of parameters would require some alteration.

A cursory examination of the new methods of analysis of turbulent shear flows indicates a wide variety of approaches, each of which can be extended to the case of variable density. One of the simpler ones, that is sometimes termed the "Prandtl energy method," is followed here. It is based on the idea of an eddy viscosity proportional to a length associated with the scale of the mixing layer and to the square root of the turbulent kinetic energy. It can be seen that the extension of this idea to flows with variable density is ambiguous and must be guided by comparison with data. Comparison is made by relying heavily on the data associated with the gross behavior of the mixing layer, as reviewed and codified recently by Brown and Roshko (ref. 9) and Birch and Eggers (paper no. 2).

The appropriate conservation equations are first developed and the terms as required for closure are modeled. One representation is then selected for the eddy viscosity for constant-density flows and the predictions based thereon are compared with various experimental results. The problem of incorporating the effects of variable density in such a fashion as to achieve agreement with experimental data relative to the two crucial cases cited is then discussed. Finally, a comparison with experimental data is made.

ANALYSIS

The idealized flow shown schematically in figure 1 is considered. Two streams with different composition, velocity, and energy but with the same uniform pressure undergo turbulent mixing at the end of a splitter plate which is the origin of a x_1,x_2 coordinate system. The symbols used in the analysis are defined in appendix A.

In developing the equations for the description of this flow, several assumptions are employed. The effect of molecular transport is neglected except for certain dissipation terms. Constant pressure in the two external flows, flow similarity, and no chemical reaction are assumed. Furthermore, work is done in terms of mass-averaged quantities after Favre (ref. 10). For clarity a tilde will be used for a mass-averaged temporal mean; a double prime, for the fluctuating part left over; and a conventional bar, for a regular temporal mean; thus, $u_i(x_1,x_2,x_3,t) = \frac{\overline{\rho u_i}}{\overline{\rho}} + u_i'' = \tilde{u}_i + u_i''$ with customary notation. Note that $\overline{u_i''} \neq 0$ whereas $\overline{\rho u_i''} = 0$.

Basic Equations

In terms of Cartesian tensor notation and in accord with these assumptions, it is readily established that the describing equations for the mean flow are

$$\left.\begin{aligned}
&\frac{\partial}{\partial x_k}\left(\bar{\rho}\tilde{u}_k\right) = 0 \\
&\frac{\partial}{\partial x_k}\left(\bar{\rho}\tilde{u}_k\tilde{u}_i + \overline{\rho u_k'' u_i''}\right) = -\frac{\partial \bar{p}}{\partial x_i} \qquad (i = 1, 2, \ldots, N) \\
&\frac{\partial}{\partial x_k}\left(\bar{\rho}\tilde{u}_k\tilde{h}_s + \overline{\rho u_k'' h_s''}\right) = 0 \\
&\frac{\partial}{\partial x_k}\left(\bar{\rho}\tilde{u}_k\tilde{Y}_i + \overline{\rho u_k'' Y_i''}\right) = 0 \qquad (i = 1, 2, \ldots, N)
\end{aligned}\right\} \tag{1}$$

where Y_i is the mass fraction of species i and where h_s is the stagnation enthalpy. In more detail

$$h_s \equiv \sum_{i=1}^{N} Y_i h_i + \frac{1}{2} u_k u_k = h + \frac{1}{2} u_k u_k \tag{2}$$

where h_i is the static enthalpy of species i. From equation (2),

$$\bar{\rho}\tilde{h}_s = \bar{\rho}\tilde{h} + \frac{1}{2}\left(\bar{\rho}\tilde{u}_k\tilde{u}_k + \overline{\rho u_k'' u_k''}\right) = \bar{\rho}\tilde{h} + \frac{1}{2}\bar{\rho}\left(\tilde{u}_k\tilde{u}_k + q^2\right)$$

where the mass-averaged turbulent kinetic energy is defined as

$$q^2 \equiv \frac{\overline{\rho u_k'' u_k''}}{\bar{\rho}} \tag{3}$$

Thus h_s contains all forms of energy of present interest.

For this particular closure scheme based on an eddy viscosity as discussed, a conservation equation for q^2 is needed; it is found to be

$$\frac{1}{2}\frac{\partial}{\partial x_k}\left(\bar{\rho}\tilde{u}_k q^2 + \overline{\rho u_k'' u_i'' u_i''}\right) + \overline{\rho u_i'' u_k''}\frac{\partial \tilde{u}_i}{\partial x_k} \approx \overline{-u_k''\frac{\partial p}{\partial x_k}} - \overline{\tau_{ik}\frac{\partial u_i''}{\partial x_k}} \tag{4}$$

where τ_{ik} is the viscous stress tensor.

Closure Assumptions

The closure of these equations as applicable to a thin shear layer wherein the boundary-layer approximations apply is next considered. First, in all the applications considered herein, it appears adequate to assume a single eddy transport coefficient essentially based on the mean velocity field. The generalization to a separate coefficient for each species, for the energy, and so forth is straightforward if an appropriate, separate length scale for each coefficient is introduced. Additional comments on this will be made. Thus for the present a single eddy transport coefficient is introduced and

$$\left.\begin{aligned}
\frac{\partial}{\partial x_k}\left(\overline{\rho u_k'' u_1''}\right) &\approx \frac{\partial}{\partial x_2}\left(\overline{\rho u_2'' u_1''}\right) \approx -\frac{\partial}{\partial x_2}\left(\bar{\rho}\epsilon \frac{\partial \tilde{u}_1}{\partial x_2}\right) \\
\frac{\partial}{\partial x_k}\left(\overline{\rho u_k'' h_s''}\right) &\approx \frac{\partial}{\partial x_2}\left(\overline{\rho u_2'' h_s''}\right) \approx -\frac{\partial}{\partial x_2}\left(\bar{\rho}\epsilon \frac{\partial \tilde{h}_s}{\partial x_2}\right) \\
\frac{\partial}{\partial x_k}\left(\overline{\rho u_k'' Y_i''}\right) &\approx \frac{\partial}{\partial x_2}\left(\overline{\rho u_2'' Y_i''}\right) \approx -\frac{\partial}{\partial x_2}\left(\bar{\rho}\epsilon \frac{\partial \tilde{Y}_i}{\partial x_2}\right)
\end{aligned}\right\} \tag{5}$$

The remaining terms to be modeled arise in the equation for the turbulent kinetic energy. Dependence rests heavily on previous work related to the new phenomenology of turbulent shear flows; previous ideas are adapted to the a priori and formal introduction of an eddy viscosity. Thus for the dissipation term,

$$\overline{\tau_{ik} \frac{\partial u_i''}{\partial x_k}} \approx \beta_1 \left(\frac{q}{\epsilon}\right) \bar{\rho} q^3 \tag{6}$$

where β_1 is a constant for flows with constant density but is considered provisionally a function of an appropriate density ratio for flows with variable density. Equation (6) may be compared with the usual form $\overline{\tau_{ik}\left(\partial u_i''/\partial x_k\right)} \propto \left(q^3/L\right)$ where L is a suitable length scale. Here dimensional arguments are used to let $L \propto \epsilon/q$ but a density ratio $\bar{\rho}/\rho_1$ raised to some power could be introduced without compromising dimensionality.

It is customary in previous work devoted principally to constant-density flows to group the triple correlation terms and the pressure-velocity correlation together. What remains is a pressure-strain correlation which for constant-density flows is zero. Here more care must be taken; in appendix B the maintenance of the customary grouping and the addition of several new terms to account for the pressure-strain correlation prevailing in variable-density flows are heuristically justified. There results (see eq. (B9))

$$\begin{aligned}
\frac{\partial}{\partial x_k}\left(\overline{\frac{1}{2} \rho u_k'' u_i'' u_i''}\right) + \overline{u_i'' \frac{\partial p}{\partial x_i}} \approx -\beta_2 \frac{\partial}{\partial x_2}\left(\bar{\rho}\epsilon \frac{\partial q^2}{\partial x_2}\right) \\
+ (1 - \varphi)\alpha \frac{\partial}{\partial x_k}\left(\bar{\rho}\tilde{u}_k q^2\right) - \alpha q^2 \bar{\rho}^2 \tilde{u}_k \frac{\partial}{\partial x_k}\left(\frac{1}{\bar{\rho}}\right)
\end{aligned} \tag{7}$$

where β_2 and α are at most functions of a density ratio, otherwise constants, and φ is a thermodynamic parameter. (See appendix B.) This procedure should be compared with the usual form for constant density, that is, $\frac{\partial}{\partial x_2}\left(qL \frac{\partial}{\partial x_2}\right)$. Here again L in terms of ϵ has been eliminated and the terms appropriate for variable density have been added.

The mean pressure $\bar{p}$ is now considered; the x_2-momentum equation with the pressure in the external flows set to zero yields $\bar{p} = \overline{-\rho u_2'' u_2''}$. Thus in the x_1-momentum equation,

$$\frac{\partial}{\partial x_1}\left(\bar{p} + \overline{\rho u_1'' u_2''}\right) = \frac{\partial}{\partial x_1}\left(\overline{\rho u_1'' u_1''} - \overline{\rho u_2'' u_2''}\right)$$

Although it is recognized that unless the turbulent kinetic energy is equally distributed among the three velocity components, this term is nonzero; it does not appear to contribute significantly and will be dropped.

Similarity Form

The describing equations are now transformed to similarity form and the nondimensional variables are introduced. It is considered to be convenient to include a density distortion of the x_2-coordinate since the resulting equations are formally simpler and since the inverse transformation back to the physical variables is readily performed once a similarity solution is obtained. Thus, let

$$\eta \equiv \frac{1}{x_1}\int_0^{x_2} \frac{\bar{\rho}}{\rho_1}\, dx_2' \tag{8}$$

and introduce

$$\left.\begin{aligned} f' &\equiv \frac{\tilde{u}_1}{U} \\ H &\equiv \frac{\tilde{h}_s}{h_{s1}} \\ Q^2 &\equiv \frac{q^2}{U^2} \\ \epsilon_0 &\equiv \left(\frac{\bar{\rho}}{\rho_1}\right)^2 \frac{\epsilon}{U x_1} \end{aligned}\right\} \tag{9}$$

where a prime denotes differentiation with respect to η. Thus,

$$\left.\begin{aligned} &\left(\epsilon_0 f''\right)' + f f'' = 0 \\ &\left(\epsilon_0 H'\right)' + f H' = 0 \\ &\beta_2\left[\epsilon_0 (Q^2)'\right] + \left[\frac{1}{2} + (1 - \varphi)\alpha\right] f (Q^2)' - \beta_1\left(\frac{\bar{\rho}}{\rho_1}\right)^2 \frac{Q^4}{\epsilon_0} + \epsilon_0 f''^2 - \alpha f Q^2 \frac{(\rho_1/\bar{\rho})'}{(\rho_1/\bar{\rho})} = 0 \end{aligned}\right\} \tag{10}$$

The first two of these equations imply a Crocco relation

$$H = 1 + \frac{H_2 - 1}{\gamma}(1 - f') \tag{11}$$

where $H_2 \equiv \left(h_{s2}/h_{s1}\right)$. Thus, equations (10) may be considered two equations for the two unknowns $f(\eta)$ and $Q(\eta)$, provided the density ratio $\left(\bar{\rho}/\rho_1\right)$ and the eddy-viscosity parameter ϵ_0 are appropriately given.

The boundary conditions are

$$\left.\begin{aligned} &f'(\infty) = 1, \quad f'(-\infty) = 1 - \gamma, \quad f(0) = 0 \\ &Q(\pm\infty) = 0 \end{aligned}\right\} \tag{12}$$

Several remarks as to the boundary conditions on $f(\eta)$ are perhaps indicated.

First, it is known from the work of Ting (ref. 11) that in applications of analyses of laminar or turbulent two-dimensional mixing of the sort considered here, the actual location of the dividing streamline $f = 0$ depends on details of the external flow, the presence of walls, and so forth. Thus, the coordinates x_1 and x_2 must be considered to be boundary-layer coordinates along the actual dividing streamline whose location in physical coordinates may be found for a particular flow situation by application of reference 11.

Second, in the presentation of experimental data relative to two-dimensional mixing it is customary to select as the origin of x_2 the line along which f' has a particular value, for example, $f'(0) = 1 - \frac{1}{2}\gamma$. The difference between these two means for selecting an origin is simply a translation in η so that comparison between the solutions and such data is readily possible.

Form for ϵ_0

Since the eddy transport parameter ϵ_0 clearly plays a central role in these equations, it is appropriate to make some remarks about it. In terms of an academic investigation, devoid of connection with the available data, a wide variety of relations for ϵ_0 can be assumed. Indeed, even if experimental results are conscientiously considered, there remain several such relations and in the course of this study several have been examined for flows with constant and variable density. Only those which involve coupling between the mean velocity and the turbulent kinetic energy, that is, those consistent with the spirit of the Prandtl energy method are reported.

Comparisons of prediction and experiment lean heavily on the gross property spreading rate, as specified by Brown and Roshko (ref. 9). Define a parameter σ such that

$$\sigma = \frac{1.32}{\left[\left(x_2/x_1\right)_1 + \left(-x_2/x_1\right)_2\right]}$$

where $\left(x_2/x_1\right)_i$, $i = 1, 2$ are defined by the velocity ratios

$$\left.\begin{aligned} \frac{\tilde{u}_1 - (1 - \gamma)U}{\gamma U} &= (0.9)^{1/2} \qquad (i = 1) \\ \frac{\tilde{u}_1 - (1 - \gamma)U}{\gamma U} &= (0.1)^{1/2} \qquad (i = 2) \end{aligned}\right\} \tag{13}$$

Note that in defining σ in terms of the mass-averaged velocity $\tilde{u}_1$ rather than in terms of the usual $\bar{u}_1$ which is implicitly assumed to be the mean velocity given by experimental data, the density-velocity correlations near the outer edges of the mixing layer are neglected since $\tilde{u}_1 = \bar{u}_1 + \left(\overline{\rho' u_1'}\right)\Big/\bar{\rho}$.

Note also that there are other possible definitions of quantities defining the spreading rate but equation (13) is convenient and according to Brown and Roshko (ref. 9) yields values of σ "very close to those obtained from the more elaborate . . ." definitions. Accordingly, in considering some experimental data not treated by Brown and Roshko, the values of σ given by the experimentalist have been taken and have been assumed to be equal to that which would be given by equations (13) if the detailed velocity profiles had been available. For the case $\gamma = 1$, the most often quoted value $\sigma \equiv \sigma_0 = 11.3$ is due to Liepmann and Laufer (ref. 12). However, Birch and Eggers (paper no. 2) have pointed out that many experimentalists assume that this value is the value they would measure if they, in fact, did so, and has provided a more rational means for estimating the value of σ_0 peculiar to their setup.

In the special case of constant density,

$$\epsilon_0 = \left(\frac{\epsilon}{\overline{U x_1}}\right) = \left(\frac{\epsilon}{q\Lambda}\right)\left(\frac{\Lambda}{x_1}\right)Q \tag{14}$$

where Λ is a scale length on the order of the mixing-layer thickness. Now in the spirit of the Prandtl energy method it is assumed that at least for constant density

$$\frac{q\Lambda}{\epsilon} \equiv R_q = \text{Constant} \tag{15}$$

that is, there is a characteristic Reynolds number whose exact value depends on how Λ is defined. In cases requiring several eddy transport coefficients, it would be hoped that R_q would be constant for each value, provided consistent definitions of Λ are applied to each property being mixed.

For the single eddy transport coefficient based on the velocity and for the two-dimensional mixing considered here, it is convenient to choose for Λ a thickness defined by

$$\Lambda = \left[U - U(1 - \gamma)\right]\left[\frac{\partial \tilde{u}_1}{\partial x_2}(x_1, 0)\right]^{-1} \tag{16}$$

This procedure is reminiscent of one means for defining the thickness of a shock wave and is readily generalized to other properties being mixed. Thus, the form of ϵ_0 examined for flows with constant density becomes

$$\epsilon_0 = \frac{\gamma}{R_q f''(0)} Q \tag{17}$$

The predictions of the analysis using equation (17) are compared with a variety of data for mixing having constant density and then ϵ_0 is reconsidered for the case of variable density.

In connection with the comparison of experiment and prediction, it is convenient to identify the similarity variable $\xi = \int_0^\eta \left(\frac{\rho_1}{\bar{\rho}}\right) d\eta' = \xi(\eta) = \frac{x_2}{x_1}$.

CONSTANT-DENSITY FLOWS

For constant-density flows with equation (17) taken to relate ϵ_0 to the dependent variables, a single parameter γ specifies the flow situation but R_q, β_1, and β_2 must be selected. The parameter $\varphi = 1$, and α is immaterial for these flows. For β_1 the following consideration is made: if in the last of equations (10), specialized to $\left(\bar{\rho}/\rho_1\right) \equiv 1$, it is assumed that production and dissipation of turbulent kinetic energy are roughly balanced, that is, that $\left(\beta_1 Q^4/\epsilon_0\right) \approx \epsilon_0 f''^2$, it is found that $\epsilon_0 f'' = (\beta_1)^{1/2} Q^2$. This result can be identified with the relation between the mean shear stress and the turbulent kinetic energy widely used in the new methods of analysis of turbulent shear flows. (See, for example, ref. 1.) The generally accepted constant in this relation suggests $\beta_1 = 0.024$, the value used.

Furthermore, for β_2, which appears not to be critical, it is found on the basis of numerical experimentation that an appropriate value is 0.5. Finally, again on the basis of numerical experimentation, $R_q = 22$ is taken.

Each of these three parameters has not been systematically varied to establish a set which is "optimum" in some sense but rather it has been determined on the basis of the comparisons of experiment and prediction that the cited set is adequate for many purposes. Also note that equations (10) have been solved by finite-difference methods and by iteration to handle their nonlinearity, the problem of the three-point boundary conditions, and the implicit appearance in the differential equations of $f''(0)$, a quantity obtained from the solution. No features of the numerical analysis appear to warrant special mention; in fact, the computer program was designed primarily to provide means for altering readily the several parameters and the various flow situations to be studied and not to provide efficient computation of any one case.

Now the predictions can be compared with experimental data. Solutions have been computed for a variety of values of γ and several parameters are shown in table I which are obtained from these solutions and which may have residual value. Note that $\sigma_0 = 11.4$ is predicted.

In accord with previous remarks, figure 2 shows the prediction for σ_0/σ as well as the analytic, empirical approximation due to Sabin (ref. 13), $\sigma_0/\sigma = \gamma/(2 - \gamma)$. This approximation was shown by Birch et al. to represent well a wide variety of data if σ_0 is appropriately estimated for those cases in which it is not directly measured. It is seen that the predictions for σ_0/σ are in good agreement with this empirical approximation and thus with experiment.

Next, consider a second gross property. Yule (ref. 14) has recently developed an empirical equation for the maximum turbulent kinetic energy as a function of γ. In terms of the variables used herein and with $\sigma_0 = 11.4$ for consistency, his equation becomes

$$Q^2(0) = 0.054(2 - \gamma)\gamma^2 \tag{18}$$

In figure 3 the predictions of this paper are compared with those of equation (18). Again, very reasonable agreement is obtained.

Because of the apparent high quality and completeness of the measured details of Spencer and Jones (ref. 15), they have been used to make comparisons with the predictions of this analysis. In figure 4 for $\gamma = 0.7$, the measured and predicted mean shear stresses in the form $-\epsilon_0 f'' = \left(\overline{u_1' u_2'}/U^2\right)$ are compared; in figure 5 a comparison is made for the turbulent kinetic energy in the form $Q^2 = \left(\overline{u_i' u_i'}/U^2\right)$. In both cases the agreement is good. It, of course, follows from the agreement in figure 4 that the measured and predicted mean velocity profiles $\left(\bar{u}_1/U\right)$ will also agree well. There seems little point in actually showing this comparison.

It is also perhaps of interest to compare the distribution of eddy viscosity inferred from the measurements of mean shear and mean velocity with that computed. Although the experimental results may be considered subject to possible error, the results of carrying out the comparison are shown in figure 6 for $x_1 = 23.5$ inches (59.69 cm) (distance from the virtual origin), and for $\gamma = 0.7$. The agreement must be considered highly satisfactory.

Thus on the basis of these comparisons, it is concluded that the analysis for two-dimensional mixing flows with constant density gives satisfactory agreement over the full span of velocity ratios with gross properties such as spreading rate and with some of the available detailed properties. Further refinements of the constants β_1, β_2, and R_q could presumably be made but to do so is not the main purpose of the present work.

VARIABLE-DENSITY FLOWS

In the case of variable-density flows the constants β_1, β_2, and R_q must be supplemented with the parameter α and the thermodynamic parameter φ. It is perhaps appropriate to make some general remarks about the approach used to incorporate the variable-density effects into the analysis.

Crucial Cases and Alterations of Analysis

As mentioned in "Introduction" there appear to be two crucial cases of variable-density, two-dimensional turbulent mixing. In the compressible adiabatic mixing, $\gamma = 1$ and to a good approximation

$$\frac{\rho_1}{\bar{\rho}} = 1 + \frac{\tilde{m}}{1 - \tilde{m}}\left(1 - f'^2\right) \tag{19}$$

where $\tilde{m} \equiv \left(U^2/2h_{s1}\right) = \frac{1}{2}(\gamma - 1)M_1^2\left[1 + \frac{1}{2}(\gamma - 1)M_1^2\right]^{-1}$ for the case of a calorically perfect gas, and where M_1 is the Mach number in the high speed stream.* Equation (19) gives the density ratio $\rho_1/\rho_2 = (1 - \tilde{m})^{-1}$.

The second crucial case is the low-speed isothermal mixing of two gases of different molecular weights, W_1 and W_2. In this case,

$$\frac{\rho_1}{\bar{\rho}} = 1 + \frac{w - 1}{\gamma}(1 - f') \tag{20}$$

where $w \equiv W_1/W_2$. In this case the density ratio for $\gamma = 1$ is $\rho_1/\rho_2 = w$.

The experimental data which apply to the first case, compressible adiabatic mixing, and which appears to be most reliable (see paper no. 2 by Birch and Eggers) indicate that a significant reduction in σ occurs as M_1 increases; in particular, $\sigma \approx 38$ for $\tilde{m} = 0.833$ $(M_1 = 5)$. On the contrary, the most reliable data for the second case seem to be that of Brown and Roshko (ref. 9) which indicate no significant change in σ with w over the range $0.143 \lessapprox w \lessapprox 7$. The essential data for $\gamma = 1$ are shown in figure 7 in terms of σ_0/σ plotted against ρ_1/ρ_2. On the basis of a comparison of equations (19) and (20), one would not expect such a disparate difference in mixing behavior.

---

*In this relation for $\tilde{m}$, γ is the ratio of specific heats; there should be no confusion with our other use of γ. In deriving equation (19), the contribution of turbulent kinetic energy to the stagnation enthalpy is essentially canceled by the variation of static pressure due to $\overline{\rho u_2'' u_2''}$. It is perhaps appropriate to observe here that $\tilde{m}$ is the proper similarity parameter for compressible adiabatic mixing of calorically perfect gases so that high-speed mixing of gases other than air, for example, high-speed helium with quiescent helium, should be correlated in terms of $\tilde{m}$.

In the interest of exposition it is indicated now that with the parameters β_1, β_2, and R_q equal to the values used for constant-density flows and with $\alpha = 0.25$ and φ appropriately selected, the analysis results in predictions in reasonable agreement with those of Brown and Roshko (ref. 9). However, it underpredicts very significantly the effect of high speed on the spreading parameter. Therefore, accepting the experimentally observed difference in the two crucial cases to be correct, that is, anticipating that it will be substantiated by further experimental results, the implications thereof are now discussed, that is, determination of the effect of Mach number through the parameter $\tilde{m}$. This apparent difference, accepted herein, in behavior of the two crucial cases rules out several possible means for incorporating the effects of variable density. Several means have been studied but have been abandoned, at least for the time being.

The most obvious candidate to account for the difference in the two cases is the pressure fluctuations which are expected to become more significant with Mach number. It is shown in appendix B that in the variable-density case, the pressure correlations introduce effects into the equation for the turbulent kinetic energy through the diffusion term, the convection term, and through an added term directly associated with the density gradient. However, this equation, and thus presumably the turbulent kinetic energy, is dominated by the production and dissipation terms, neither of which are directly influenced by the pressure fluctuations. Thus it is found by numerical experimentation that unreasonable values for β_2, treated as a function of $\tilde{m}$, must be assumed in order to achieve a significant alteration of σ with $\tilde{m}$. It thus appears that at least up to a Mach number of 5, pressure effects cannot account for a significant compressibility effect on two-dimensional turbulent mixing. This result is in accord with the finding of Laufer (ref. 16) for turbulent boundary layers.

If the changes in the empirical parameters with $\tilde{m}$ that might be rationalized to account for the observed effect on σ are considered, the parameter β_1 which accounts directly for dissipation and R_q appearing in ϵ_0 remain. Again by numerical experimentation, it is found that unreasonably large changes in β_1 with $\tilde{m}$ are required to bring prediction and experiment into agreement. Moreover, there appears to be no way to rationalize such changes; in this regard, note that such would imply a considerable deviation with $\tilde{m}$ of the coefficient in the frequently assumed relation between mean shear and turbulent kinetic energy. Although it is not certain that some alteration of this coefficient is not in fact indicated, the alteration associated with the required changes in β_1 is probably excessive.

Thus, alterations of R_q with Mach number, that is, of the only parameter at our disposal, are considered. As is seen in more detail subsequently, rather modest changes in R_q with $\tilde{m}$ can bring the predictions in agreement with the data for compressible adiabatic mixing. Consider here the possible physical explanation therefor, and keep in

mind a distinction between density and Mach number effects. With all the other parameters in ϵ_0 fixed, the value of R_q determines the rate of entrainment of external flow into the turbulent layer. This entrainment is known to be related to the detailed mechanisms connected with the superlayer at the interface between the potential and turbulent flows. Because of detailed experiments involving conditioned sampling (see Kovasznay et al. (ref. 17) and Kaplan and Laufer (ref. 18)), a great deal is known about these mechanisms for low-speed turbulent boundary layers, for example, about the relative speed of the large turbulent eddies and the external flow. Although the corresponding data for the high-speed mixing layer do not exist and will be extremely difficult to obtain, it appears intuitively clear that when the relative speed of the large-scale turbulent eddies and the external flow approaches a significant fraction of the local speed of sound, major changes in the detailed entrainment mechanisms could occur. The observed decrease in spreading angle and mixing rate with free-stream Mach number, for example, as implied by figure 7, supports this view. These effects are concluded to be attributed to R_q in the present analysis.

Accordingly, a strategy of seeking $R_q = R_q(\tilde{m})$ is adopted to bring the analysis into agreement with the case of compressible adiabatic mixing. Beyond the case of $\gamma = 1$, that is, of mixing with a quiescent gas, it is expected that R_q will depend on γ as well as on $\tilde{m}$ when the second stream becomes supersonic. Resolution of this effect awaits further experimental data.

Isothermal Binary Mixing

Consider now the low-speed isothermal mixing of two dissimilar gases and treat $w \equiv (W_1/W_2)$ and the velocity ratio by means of γ as parameters. The assumed values of w include helium-air cases with the molecular weight of air assumed to be 28. The value of φ is taken for simplicity to be three and represents its arithmetic mean for air and helium; these results are independent of any reasonable value for φ since it enters only in the convection term, that is, in one of the small terms, in the equation for the turbulent kinetic energy. Also $\alpha = 0.25$ is taken in all cases since it too does not enter importantly. Several of the combinations of w and γ are chosen to permit comparison with the experimental results of Brown and Roshko (ref. 9) for helium and air mixing.

Table II gives the principal gross results from this series of calculations. Several points are indicated there. For a given velocity ratio, that is, γ, the effect of the molecular weight ratio w on the spreading parameter σ is small. This result is in accord with the main conclusion of Brown and Roshko (ref. 9). Moreover, simple calculations using the results in table II show that for a given w, the effect of γ on σ is closely given by the equation of Sabin (ref. 13) developed for constant-density flows. This

prediction may be useful in determining σ_0 for binary mixing flows after the suggestion of Birch and Eggers (paper no. 2).

The results with respect to the spreading parameter σ for $\gamma = 1$ are shown in figure 7 in terms of σ_0/σ plotted against $\rho_1/\rho_2 = w$ in this case. The comparisons with the results deduced by Brown and Roshko (ref. 9) are seen to be good, as suggested earlier; that is, when no changes in the effective parameters β_1, β_2, and R_q are made, the spreading parameter is insensitive to density variations.

Attention is now turned to some of the detailed results of Brown and Roshko (ref. 9). In figure 8 a comparison is made of the predicted velocity and density profiles for one of their experiments corresponding to $\gamma = 0.622$, $w = 0.143$, that is, helium at a higher velocity mixing with slower air. It is seen that the velocity profile is well predicted but that the density profile reflects the single eddy transport coefficient assumed a priori in the analysis, whereas the experimental results indicate a considerably larger coefficient for the species. Contrast this result with another case shown in figure 9, $\gamma = 0.622$, $w = 7$, corresponding to faster moving air mixing with slower helium. Within the ability to read the plots in reference 9, it is not possible to distinguish the prediction from experiment so only the predicted results are shown. The reason for the difference in the predictability of the two cases is not clear.

It is of interest to consider the predicted alteration in the distribution of some mean quantities with molecular weight or density ratio. Accordingly, the velocity profiles for the constant density case ($w = 1$) and the hydrogen-air cases $w = 14$, $(1/14)$, each with zero velocity on one side of the mixing layer, are shown in figure 10. Although the spreading parameter is about the same in all three cases, it may be seen that the variation in mean density results in altered velocity profiles.

In figures 11 and 12 are shown the predicted distributions of production of turbulent kinetic energy in terms of $\epsilon_0 f''^2(\eta)$ and of dissipation in terms of $-\beta_1(\bar{\rho}/\rho_1)^2 Q^4 \epsilon_0^{-1}$ plotted against $\xi = x_2/x_1$ for these same three cases. There is a shift in the peaks of production and dissipation toward the low-density side of the dividing streamline and, as expected, the dissipation term is less than the production term in the central portion of the mixing layer. From the calculations it is found that the diffusion term provides most of the difference in the two main terms in the equation for the turbulent kinetic energy. It would be highly desirable if some measurements of the turbulent kinetic energy could be made in binary mixing flows to permit comparisons with predictions of the sort shown in figures 11 and 12 in order to establish whether the energy balances are as predicted or whether changes in the modeling are required.

It is thus concluded that the analysis for constant-density flows without essential change (the changes due to $\overline{p(\partial u_k''/\partial x_k)}$ are considered to be "unessential" here) largely

agrees with the results of Brown and Roshko (ref. 9) and shows little effect on the gross quantity, spreading parameter σ, although detailed distributions are as is to be expected altered by density variations.

Compressible Adiabatic Mixing

Attention is now turned to the case of compressible adiabatic mixing. Only $\gamma = 1$, that is, mixing with a quiescent gas, is considered and thus there is a single parameter, that associated with the Mach number in the moving stream, $\tilde{m}$. The previous values $\beta_1 = 0.024$, $\beta_2 = 0.5$, and $\alpha = 0.25$ are retained and $\varphi = 7/2$ is taken, corresponding to air. Again, the values of α and φ are unimportant. However, as discussed previously, R_q is adjusted to bring into agreement prediction and experiment with respect to the spreading parameter σ.

As a result of preliminary numerical experimentation, it is found that a simple variation of R_q with $\tilde{m}$ gives a variation of spreading parameter with $\rho_1/\rho_2 = (1 - \tilde{m})^{-1}$ in reasonable agreement with the data shown in figure 7; thus,

$$\left.\begin{aligned} R_q &= 22 + 5.2(1 - \tilde{m})^{-1} && (0 \leqq \tilde{m} \lessapprox 0.7) \\ R_q &= 39 && (0.7 \lessapprox \tilde{m} < 1) \end{aligned}\right\} \tag{21}$$

This variation of R_q is used for the calculations discussed here. The implication of this result in terms of the previous discussion of the possible physical explanation of a change in R_q with Mach number appears to be that at a Mach number of about 3 the large-scale eddies in the mixing layer readjust so that further effects of Mach number on the spreading parameter are small and so that the characteristic Reynolds number R_q may be taken as a constant at higher Mach numbers. This explanation is, of course, to be considered a conjecture based on a careful consideration of the present analysis and the experimental data presently considered definitive.

With the use of equations (21) a series of compressible adiabatic flows corresponding to a range of $\tilde{m}$ have been computed; the principal gross results are given in table III and the variation of the spreading parameter in terms of σ_0/σ with ρ_1/ρ_2 is shown in figure 7. It is seen that the simple variation of R_q with $\tilde{m}$ given by equations (21) results in increases in σ with $\tilde{m}$ in good agreement with the experimental data.

In figures 13 to 15 are shown the same distributions of mean quantities as in the case of binary mixing in order to provide some indication of the effect of high speed on turbulent mixing. From figure 13 it can be seen that a significant change in the velocity profile takes place when $\tilde{m}$ increases from 0 to 0.667 (M_1 from 0 to ≈ 3) but that little change seems to take place as $\tilde{m}$ increases further despite the doubling of the

density ratio ρ_1/ρ_2 as $\tilde{m}$ increases from 0.667 to 0.833. This behavior is also reflected in figures 14 and 15 which show that the distributions of production and dissipation of turbulent kinetic energy for $\tilde{m} = 0.667$ and $\tilde{m} = 0.833$ are alike but are very different from the low-speed case ($\tilde{m} = 0$).

It may also be noted from figures 14 and 15 that the peaks in production and dissipation shift toward the low-density side of the dividing streamline as in the case of binary mixing. Also to be noted is the close balance between production and dissipation which indicates, as suggested earlier, that the other terms in the equation for conservation of turbulent kinetic energy are dominated by these two terms.

The General Case

On the basis of the results for the two crucial cases of turbulent mixing studied in some detail, the present analysis could be used with the parameters β_1, β_2, and α fixed, with φ determined from thermodynamic considerations, and with $R_q(\tilde{m})$ as given by equations (21) to make predictions of the properties of a variety of mixing flows involving heterogeneous composition, high-speed effects, and nonadiabaticity. These have not been carried out in the present work because there appear to be no data with which to compare prediction and experiment. When such data are available, it would be of considerable interest to determine the extent of the agreement and/or disagreement.

Of considerable value in assessing the a priori assumption of a single transport coefficient and the overall accuracy of the present analysis for these fundamental flows, that is, for two-dimensional turbulent mixing, would be cases of heterogeneous mixing under nonisothermal conditions, for example, heated helium mixing with relatively cold air. The greater the statistical detail constituting the data the more valuable such experiments would be.

CONCLUDING REMARKS

A simple turbulent flow, the two-dimensional mixing layer, involving significant variations in density due either to heterogeneity in composition or to compressibility effects associated with the high speed of one flow has been analyzed in some detail. One of the simpler of the new methods of analysis of turbulent shear flows, that usually termed the "Prandtl energy method," has been used. It involves relating the eddy transport coefficient to the turbulent kinetic energy and to an appropriate length scale of the large-scale turbulent motion. Thus, one equation in the second level in the hierarchy of describing equations, that describing the conservation of turbulent kinetic energy, must be added to the usual set of equations describing the variables of the mean flow.

For two-dimensional mixing layers with constant density it is found that the analysis provides satisfactory predictions for gross properties of the flow over the entire range of velocity ratios of the two streams and for detailed properties for the one case, that is, one velocity ratio, examined.

With respect to flows involving variable density, there is discussed the existing experimental data for two crucial cases, the low-speed isothermal mixing of two dissimilar gases and the high-speed adiabatic mixing of air. It has been assumed provisionally that the results of Brown and Roshko, which show little alteration of the spreading rate with large density differences in the first case, and the results which show significant reduction in the spreading rate with Mach number in the second case are correct, and that they will be confirmed by further experiments. With this assumption fixing the strategy to be followed, it is found that an alteration with Mach number of the empirical parameters entering the analysis is required to bring prediction and experiment into agreement. The analysis suggests that neither the modeling of pressure rate of strain nor alterations in two parameters, those relating to diffusion and dissipation in the equation for the turbulent kinetic energy, can reasonably account for the observed Mach number effect. However, it is shown that a modest change in the Reynolds number characterizing the turbulence reduces the spreading rate in accord with experiment. A suggestion is made of how this required change is related to the physics of the turbulence.

It is emphasized that if further experiments do not support the assumed behavior of the two-dimensional mixing layer in the two crucial cases cited, the methodology of the present work may retain some value, but the strategy used to bring prediction and experiment into agreement would, of course, be altered. It is also emphasized that this study indicates the dangers of casually extending the new methods of analysis of turbulent shear flows to cases involving significant variations of density.

ACKNOWLEDGMENTS

This research was sponsored by the Office of Naval Research under Contract N00014-67-0226-0005 (Subcontract No. 4965-26) as part of Project SQUID. The author gratefully acknowledges the invaluable assistance of David Perlman of the Staff of the UCSD Computer Center in programing the equations. In the course of this work the author benefited from discussions with many colleagues and friends, particularly Professors C. H. Gibson, F. A. Williams, and John Laufer. Finally, the author notes that this version differs from one presented orally at the "Langley Working Conference on Free Turbulent Shear Flows" July 20-21, 1972; the changes were suggested by the presentation of Dr. Stanley Birch and by discussions with several participants.

APPENDIX A

SYMBOLS

c_p	coefficient of specific heat
c_{pi}	coefficient of specific heat of i species
f	stream function (see eq. (9))
H	stagnation enthalpy ratio (see eq. (9))
H_2	stagnation enthalpy ratio, h_{s2}/h_{s1}
h	static enthalpy
h_i	static enthalpy of i species
h_s	stagnation enthalpy (see eq. (2))
L	length scale
M_1	Mach number in stream 1
$\tilde{m}$	Mach number parameter (see eq. (19))
p	static pressure
Q	nondimensionalized turbulent kinetic energy
q	turbulent kinetic energy, $\frac{\overline{\rho u_i' u_i'}}{\bar{\rho}}$
R_0	universal gas constant
R_q	Reynolds number of turbulence
T	static temperature
t	time

U	x-component of velocity in stream 1
u_i	Cartesian velocity components, $i = 1, 2, 3$
W	molecular weight of mixture
W_i	molecular weight of i species
w	molecular weight ratio, W_2/W_1
x_i	Cartesian coordinates, $i = 1, 2, 3$
Y_i	mass fraction of i species
α	fraction of turbulent kinetic energy due to u_2
β_1, β_2	empirical constants
γ	parameter determining velocity of stream 2; ratio of coefficients of specific heat
ϵ	eddy viscosity
ϵ_0	nondimensionalized eddy viscosity
η	transformed similarity variable (see eq. (8))
Λ	length scale
ν	kinematic viscosity coefficient
ξ	similarity variable, x_2/x_1
ρ	density
ρ_1	density in stream 1
σ	spreading parameter

σ_0 spreading parameter when $u_i = 0$

τ_{ik} viscous stress tensor

φ thermodynamic parameter (see eq. (B7))

APPENDIX B

THE PRESSURE-STRAIN CORRELATION

Here the modeling of the velocity-pressure gradient correlation appearing in equation (4) is considered. The first step is to write

$$\overline{u_k'' \frac{\partial p}{\partial x_k}} = \frac{\partial}{\partial x_k}\left(\overline{p u_k''}\right) - \overline{p \frac{\partial u_k''}{\partial x_k}} \tag{B1}$$

For constant-density flows the second set of terms on the right-hand side is zero. Here the general case of a gas mixture described by a perfect gas law is considered. First

$$p = \rho \frac{R_0 T}{W} = \rho R_0 T \sum_{i=1}^{N} \frac{Y_i}{W_i} \tag{B2}$$

where R_0 is the universal gas constant and W is the mixture molecular weight. The conservation equations devoid of significant molecular effects are

$$\left.\begin{aligned}
&\frac{\partial}{\partial t}(\rho) + \frac{\partial}{\partial x_k}\left(\rho u_k\right) = 0 \\
&\frac{\partial}{\partial t}\left(\rho u_i\right) + \frac{\partial}{\partial x_k}\left(\rho u_k u_i\right) = -\frac{\partial p}{\partial x_i} \qquad (i = 1, 2, 3) \\
&\frac{\partial}{\partial t}\left(\rho h_s\right) + \frac{\partial}{\partial x_k}\left(\rho u_k h_s\right) = \frac{\partial p}{\partial t} \\
&\frac{\partial}{\partial t}\left(\rho Y_i\right) + \frac{\partial}{\partial x_k}\left(\rho u_k Y_i\right) = 0 \qquad (i = 1, 2, \ldots, N)
\end{aligned}\right\} \tag{B3}$$

The pressure relative to that in the two streams external to the mixing layer is measured so that $p\left(x_1, \pm\infty, x_3, t\right) \equiv 0$. In addition, the stagnation enthalpy is defined as

$$h_s \equiv h + \frac{1}{2} u_k u_k = \sum_{i=1}^{N} Y_i h_i(T) + \frac{1}{2} u_k u_k \tag{B4}$$

From mass conservation and the equation of state, it is easy to show that

$$\overline{p \frac{\partial u_k''}{\partial x_k}} = R_0 \left\{ \overline{\frac{\rho}{W}\left(\frac{\partial T}{\partial t} + u_k \frac{\partial T}{\partial x_k}\right)} + \overline{\rho T\left[\frac{\partial}{\partial t}\left(\frac{1}{W}\right) + u_k \frac{\partial}{\partial x_k}\left(\frac{1}{W}\right)\right]} \right\} - \overline{u_k \frac{\partial p}{\partial x_k}} - \bar{p} \frac{\partial \tilde{u}_k}{\partial x_k} \tag{B5}$$

Next from equations (B3) and (B4),

$$\overline{\frac{\rho}{W}\left(\frac{\partial T}{\partial t} + u_k \frac{\partial T}{\partial x_k}\right)} = \overline{\left(\frac{u_k}{c_p W}\right)\frac{\partial p}{\partial x_k}}$$

and

$$\overline{\rho T\left[\frac{\partial}{\partial t}\left(\frac{1}{W}\right) + u_k \frac{\partial}{\partial x_k}\left(\frac{1}{W}\right)\right]} = \sum_{i=1}^{N} \overline{T \frac{\rho}{W_i}\left(\frac{\partial Y_i}{\partial t} + u_k \frac{\partial Y_i}{\partial x_k}\right)} = 0$$

where

$$c_p = \sum_{i=1}^{N} c_{pi} Y_i$$

Thus

$$\overline{p \frac{\partial u_k''}{\partial x_k}} = \overline{\left(\frac{R_0}{c_p W} - 1\right) u_k \frac{\partial p}{\partial x_k}} - \bar{p} \frac{\partial \tilde{u}_k}{\partial x_k} \tag{B6}$$

Except for certain dissipation terms which would enter if molecular effects were included in equations (B3), equation (B6) is exact. Drastic simplifications are now made. It hardly seems reasonable to add to the result of the crude modeling usually associated with the first set of terms on the right-hand side of equation (B1) and complicated modeled terms arising from the second set. First note that $R_0/c_p W$ is to a good approximation constant because the model specific heat $c_{pi} W_i$ is roughly constant. Thus let

$$\overline{p \frac{\partial u_k''}{\partial x_k}} \approx \left(\overline{\frac{R_0}{c_p W}} - 1\right)\left(\tilde{u}_k \frac{\partial \bar{p}}{\partial x_k} + \overline{u_k'' \frac{\partial p}{\partial x_k}}\right) - \bar{p} \frac{\partial \tilde{u}_k}{\partial x_k}$$

Then by letting $\varphi^{-1} \equiv \left(\overline{R_0/c_p W}\right)$, it is found from equation (B1) that

$$\overline{u_k'' \frac{\partial p}{\partial x_k}} \approx \varphi \frac{\partial}{\partial x_k}\left(\overline{p u_k''}\right) - (1 - \varphi)\tilde{u}_k \frac{\partial \bar{p}}{\partial x_k} + \varphi \bar{p} \frac{\partial \tilde{u}_k}{\partial x_k} \tag{B7}$$

Note now that the x_2-momentum equation in the boundary-layer approximation and with the external pressure set equal to zero yields

$$\bar{p} = \overline{-\rho u_2'' u_2''} = -\alpha \bar{\rho} q^2 \tag{B8}$$

where α is a parameter (taken to be constant) representing the fraction of the total turbulent kinetic energy in the u_2-velocity fluctuations. Most low-speed data for turbulent

shear flows indicate $\alpha \approx 1/4$ but there does not appear to be any data related thereto for variable-density flows.

With equation (B8), equation (B7) can be rewritten to yield

$$\overline{u_k'' \frac{\partial p}{\partial x_k}} \approx \varphi \frac{\partial}{\partial x_k}\left(\overline{p u_k''}\right) + (1 - \varphi)\alpha \frac{\partial}{\partial x_k}\left(\bar{\rho}\tilde{u}_k q^2\right) - \alpha q^2 \bar{\rho}^2 \tilde{u}_k \frac{\partial}{\partial x_k}\left(\frac{1}{\bar{\rho}}\right) \tag{B9}$$

Several remarks about equation (B9) are appropriate. Equation (B9) reduces to that for constant density flows if $\varphi = 1$ so the usual model in this case is recovered. For compressible adiabatic flows, $\varphi = \gamma/(\gamma - 1)$ where γ is the ratio of specific heats. For binary isothermal flows, φ is really a function of concentration but an adequate approximation would appear to be an average value across the mixing layer. Finally, note that the inclusion of density effects in the velocity-pressure gradient correlation introduces two new terms (one directly related to the mean density gradient, and one to the convection of turbulent kinetic energy) and modifies the usual combination of the diffusion of turbulent kinetic energy and the pressure-velocity correlation.

REFERENCES

1. Bradshaw, P.; Ferriss, D. H.; and Atwell, N. P.: Calculation of Boundary-Layer Development Using the Turbulent Energy Equation. J. Fluid Mech., vol. 28, pt. 3, May 26, 1967, pp. 593-616.

2. Rodi, W.; and Spalding, D. B.: A Two-Parameter Model of Turbulence, and Its Application to Free Jets. Wärme- und Stoffübertragung, vol. 3, no. 2, 1970, pp. 85-95.

3. Hanjalić, K.; and Launder, B. E.: A Reynolds Stress Model of Turbulence and Its Application to Thin Shear Flows. J. Fluid Mech., vol. 52, pt. 4, Apr. 25, 1972, pp. 609-638.

4. Donaldson, Coleman duP.: Calculation of Turbulent Shear Flows for Atmospheric and Vortex Motions. AIAA J., vol. 10, no. 1, Jan. 1972, pp. 4-12.

5. Wilcox, D. C.; and Alber, I. E.: A Turbulence Model for High Speed Flows. Proceedings of 23rd Heat Transfer and Fluid Mechanics Institute, Stanford Univ. Press, June 1972, pp. 231-252.

6. Schlichting, Hermann (J. Kestin, transl.): Boundary Layer Theory. 5th ed., McGraw-Hill Book Co., Inc., 1965.

7. Townsend, A. A.: The Structure of Turbulent Shear Flow. Cambridge Univ. Press, 1956.

8. Baker, R. L.; Tao, L. N.; and Weinstein, H.: The Mixing of Two Parallel Streams of Dissimilar Fluids. Paper 70-WA/APM-37, Amer. Soc. Mech. Eng., Nov.-Dec. 1970.

9. Brown, Garry; and Roshko, Anatol: The Effect of Density Difference on the Turbulent Mixing Layer. Turbulent Shear Flows, AGARD-CP-93, Jan. 1972. pp. 23-1 – 23-12.

10. Favre, A.: Statistical Equations of Turbulent Gases. Problems of Hydrodynamics and Continuum Mechanics. Soc. Indust. & Appl. Math., 1969, pp. 231-266.

11. Ting, Lu: On the Mixing of Two Parallel Streams. J. Math. & Phys., vol. XXXVIII, no. 3, Oct. 1959, pp. 153-165.

12. Liepmann, Hans Wolfgang; and Laufer, John: Investigations of Free Turbulent Mixing. NACA TN 1257, 1947.

13. Sabin, C. M.: An Analytical and Experimental Study of the Plane, Incompressible, Turbulent Free Shear Layer With Arbitrary Velocity Ratio and Pressure Gradient. AFOSR-TN-5443, U.S. Air Force, Oct. 1963. (Available from DDC as AD 430 120.)

14. Yule, Andrew J.: Spreading of Turbulent Mixing Layers. AIAA J., vol. 10, no. 5, May 1972, pp. 686-687.

15. Spencer, B. W.; and Jones, B. G.: Statistical Investigation of Pressure and Velocity Fields in the Turbulent Two-Stream Mixing Layer. AIAA Paper No. 71-613, June 1971.

16. Laufer, John: Thoughts on Compressible Turbulent Boundary Layers. Memorandum RM-5946-PR (Contract F44620-67-C-0045) RAND Corp., Mar. 1969. (Available from DDC as AD 685 705.)

17. Kovasznay, Leslie S. G.; Kibens, Valdis; and Blackwelder, Ron F.: Large-Scale Motion in the Intermittent Region of a Turbulent Boundary Layer. J. Fluid Mech., vol. 41, pt. 2, Apr. 13, 1970, pp. 283-325.

18. Kaplan, R. E.; and Laufer, John: The Intermittently Turbulent Region of the Boundary Layer. Contract NONR-228(33), Univ. Southern California, Nov. 1968. (Available from DDC as AD 679 234.)

TABLE I.- NUMERICAL RESULTS FOR CONSTANT DENSITY FLOWS

γ	$f'(0)$	$f''(0)$	$Q^2(0)$	σ_0
1	0.578	6.07	6.42×10^{-2}	11.4
0.8	0.643	7.18	4.17	16.8
0.7	0.680	7.74	3.22	20.6
0.6	0.721	8.31	2.37	25.8
0.4	0.808	9.46	1.06	43.1
0.2	0.902	10.6	0.265	97.0

TABLE II.- NUMERICAL RESULTS FOR BINARY FLOWS

γ	w	$f'(\eta = 0)$	$f''(\eta = 0)$	$Q^2(0)$	$\frac{\rho_1}{\bar{\rho}(0)}$	σ_0
1	1	0.578	6.07	6.42×10^{-2}	1	11.4
	2	0.624	8.63	6.92	1.38	11.2
	4	0.664	13.0	6.88	2.01	11.6
	7	0.694	18.7	6.82	2.83	12.1
	14	0.729	30.7	6.70	4.53	13.2
	0.5	0.544	4.59	6.94	0.772	10.9
	0.25	0.505	3.68	6.92	0.629	11.1
	0.143	0.487	3.20	6.87	0.560	11.1
	0.0714	0.450	2.79	6.88	0.489	11.8
0.8	7	0.744	22.3	4.40	2.92	17.2
0.622		0.794	25.6	2.67	2.99	24.8
0.4		0.861	29.8	1.11	3.08	42.5
0.2		0.928	33.7	0.279	3.15	91.0
0.857	0.143	0.529	3.45	5.10	0.529	15.0
0.622		0.635	3.93	2.70	0.497	25.2
0.4		0.756	4.42	1.12	0.478	50.0
0.2		0.875	4.93	0.279	0.466	105

TABLE III.- NUMERICAL RESULTS FOR COMPRESSIBLE ADIABATIC MIXING

$[\gamma = 1]$

$\tilde{m}$	$f'(\eta = 0)$	$f''(\eta = 0)$	$Q^2(0)$	$\frac{\rho_1}{\bar{\rho}(0)}$	σ_0	R_q
0	0.578	6.07	6.42×10^{-2}	1	11.4	22
0.333	0.610	14.6	4.12	1.31	19.8	30
0.5	0.626	21.6	3.52	1.61	24.4	32
0.667	0.649	38.2	2.77	2.16	31.6	38
0.75	0.664	54.3	2.47	2.68	36.4	39
0.833	0.684	77.3	2.43	3.66	38.4	39
0.875	0.700	99.3	2.41	4.57	40.0	39

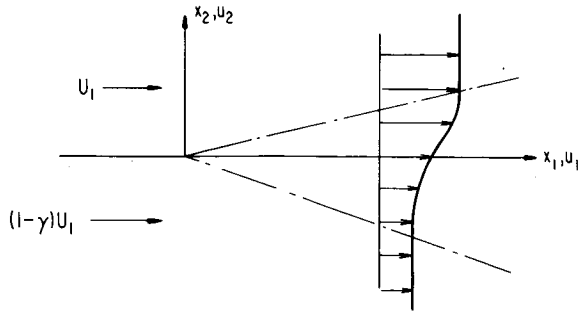

Figure 1.- Schematic representation of the flow.

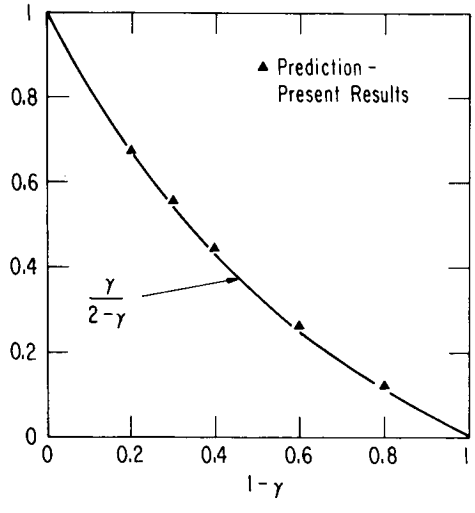

Figure 2.- Variation of spreading parameter with velocity ratio. Constant density flows.

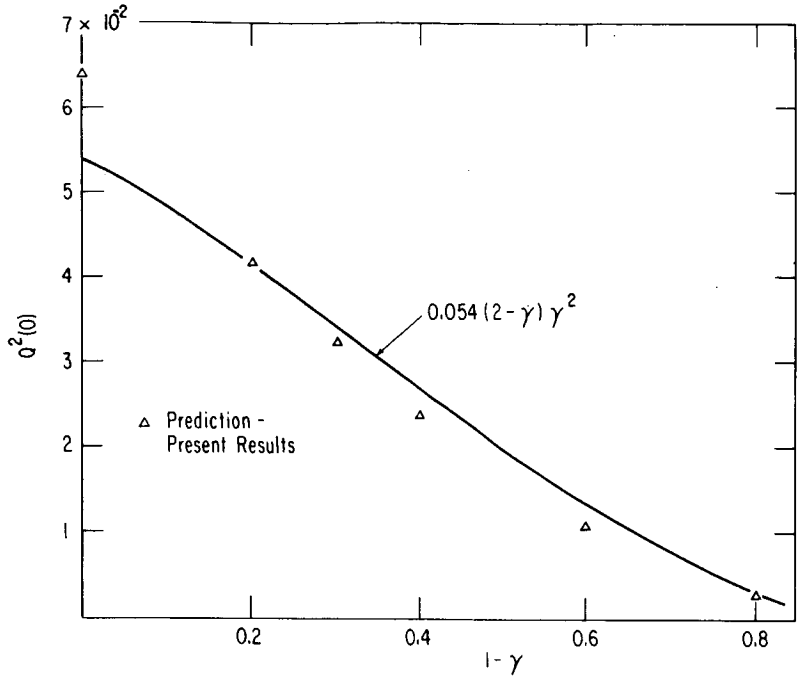

Figure 3.- Variation of turbulent kinetic energy on the dividing streamline with velocity ratio. Constant density flows.

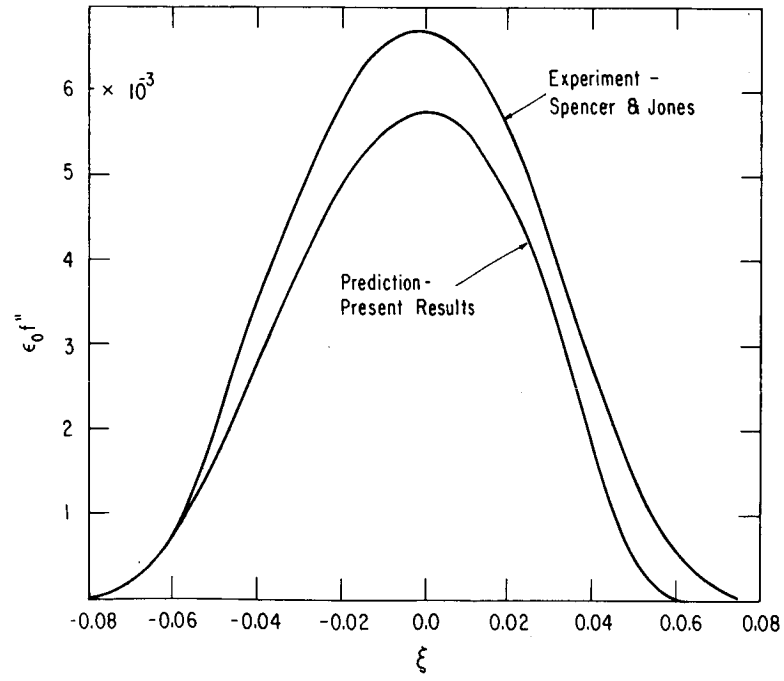

Figure 4.- Comparison of predicted and experimental mean shear stress. $\gamma = 0.7$; constant density flows.

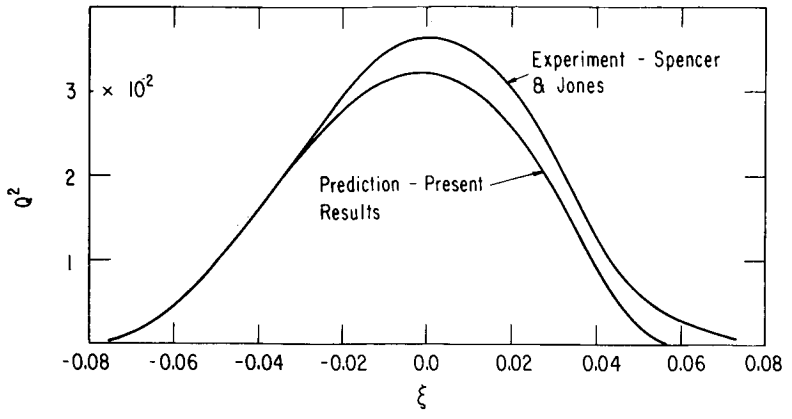

Figure 5.- Comparison of predicted and measured turbulent kinetic energy. $\gamma = 0.7$; constant density flows.

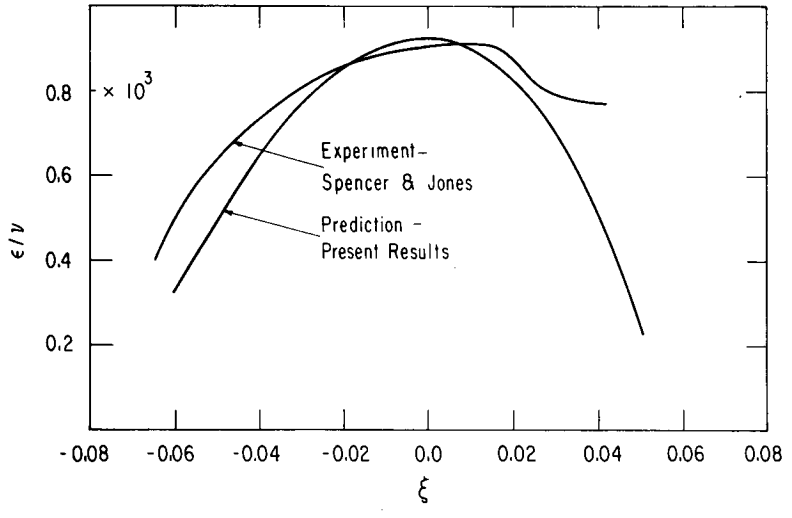

Figure 6.- Comparison of predicted and measured distributions of eddy viscosity. $\gamma = 0.7$; constant density flows; $x_1 = 23.5$ inches (59.69 cm).

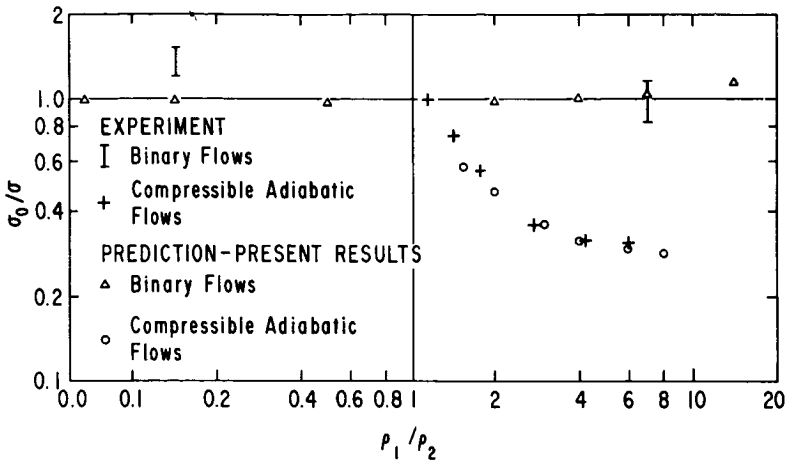

Figure 7.- Variation of spreading parameter in variable-density flows.

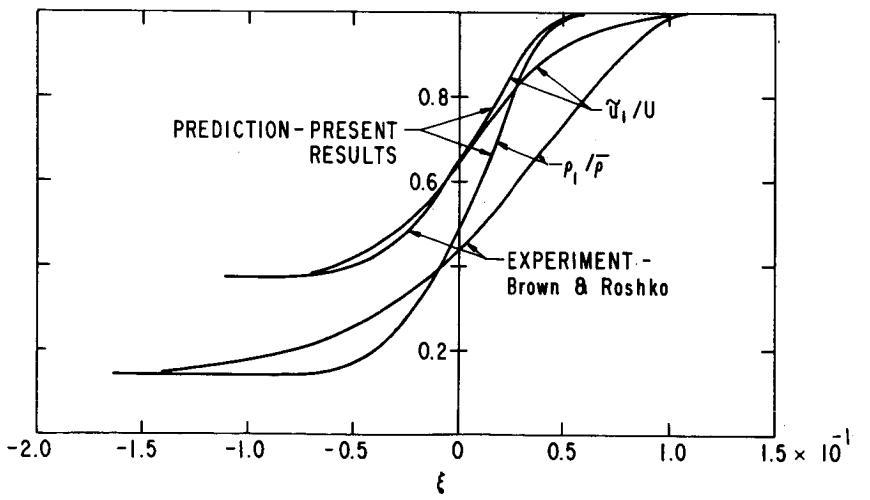

Figure 8.- Comparison of predicted and experimental mean velocity and mean density profiles. $\gamma = 0.622$; $w = 0.143$.

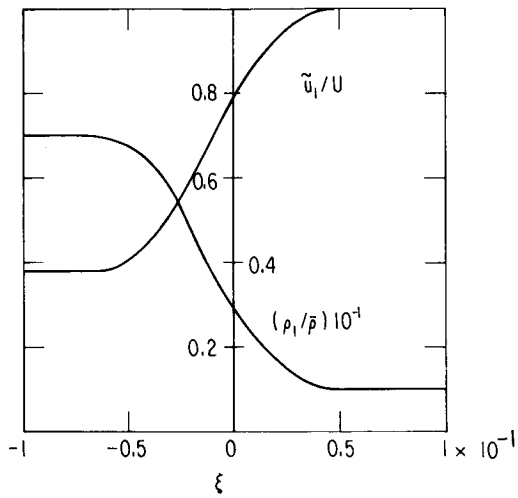

Figure 9.- Velocity and mean density profiles. $\gamma = 0.622$; $w = 7$.

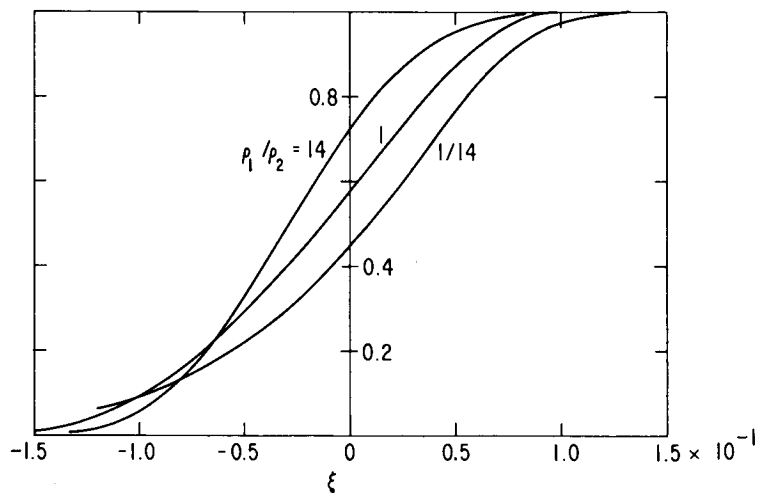

Figure 10.- Predicted velocity profiles for several density ratios. Binary mixing; $\gamma = 1$.

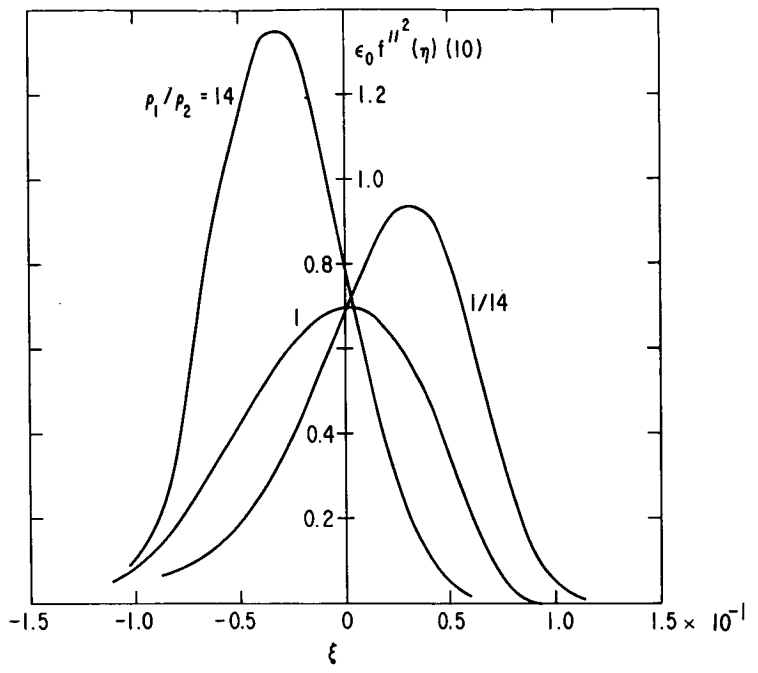

Figure 11.- Predicted distributions of production of turbulent kinetic energy for several density ratios. Binary mixing; $\gamma = 1$.

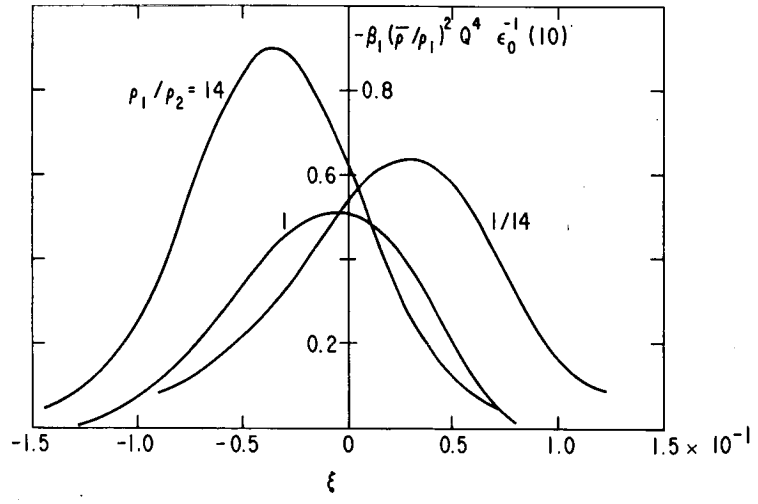

Figure 12.- Predicted distributions of dissipation of turbulent kinetic energy for several density ratios. Binary mixing; $\gamma = 1$.

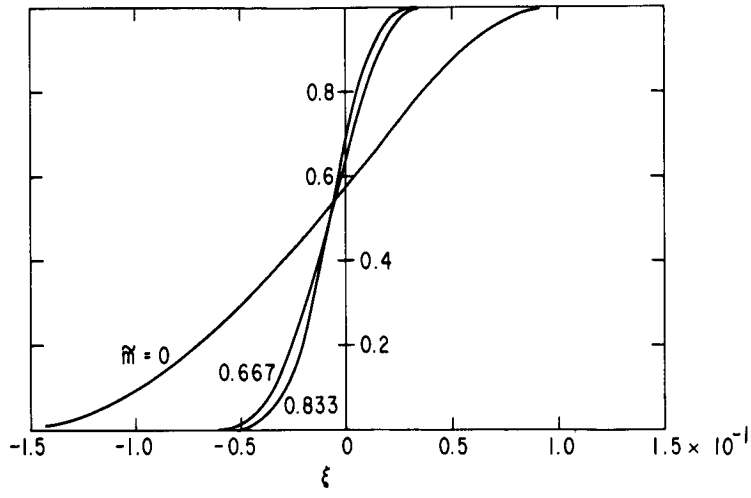

Figure 13.- Predicted velocity profiles for several values of the Mach number parameter. Compressible adiabatic mixing; $\gamma = 1$.

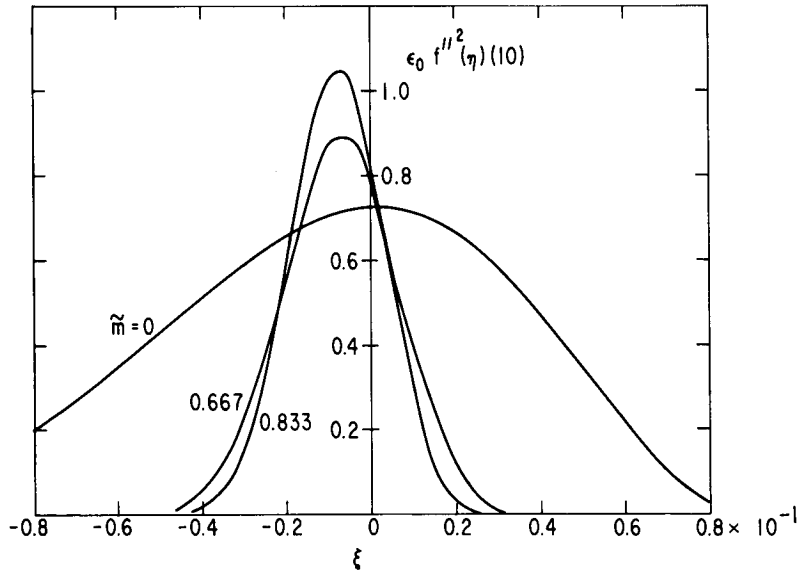

Figure 14.- Predicted distributions of production of turbulent kinetic energy for several values of the Mach number parameter. Compressible adiabatic mixing; $\gamma = 1$.

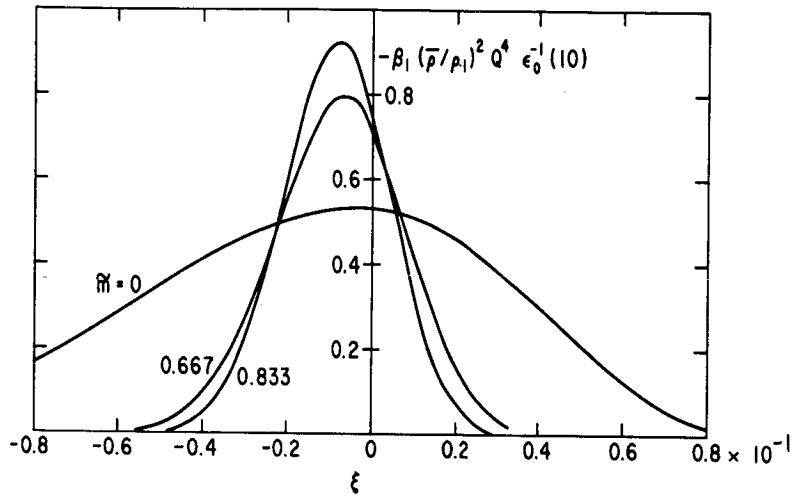

Figure 15.- Predicted distributions of dissipation of turbulent kinetic energy for several values of the Mach number parameter. Compressible adiabatic mixing; $\gamma = 1$.

DISCUSSION

J. Laufer: I think Libby showed us very well the extent of our ignorance as far as density fluctuations in the turbulent flow are concerned. At this stage I would like to just ask one question – and maybe that question should be more properly addressed to Professor Roshko. Dr. Libby pointed out the difference between the conventional average and mass average velocity. I suspect that in many cases, the experimentalist measures a mass average quantity with a pitot tube. Professor Roshko, could you tell us, is it a mass average or a mean velocity that you are measuring?

A. Roshko: Well, that is a little hard to say. The velocities are measured by getting a pitot tube reading for ρu^2, but there is a little question of what you are reading with a pitot tube because you have the turbulence part of the term. When we do have an accurate measurement of the average density, we simply divide one by the other. What that average means is hard to say. We estimate that it's perhaps within 10 percent.

J. Laufer: I would like to suggest just on the basis of the simple Bernoulli's equation that one uses in obtaining the velocity that that value is, in fact, a mass average and not a conventional average.

S. J. Kline: On the same point, we have some experiments going on in which we are trying to vary the fluctuations and see what happens in a pitot under some controlled conditions. I don't want to go into details, but perhaps we can shed some light on your question. One more comment, we are getting ready to measure time averages by using laser Doppler techniques that we are developing, and then you will have a little more information on this point.

P. A. Libby: John, that's exactly why I said, "if we take the experimenter's word for it that he is giving us the usual average," then we are, in fact, comparing two slightly different things. I understand, as we have talked before, about the fact that the experimenter may be wrong, but I do think that we have to take his word for it.

J. Ito: We have been working with heterogenous shear flows for applications to the gas-gas auxiliary propulsion on the space shuttle system. We have obtained quite a bit of data in the past 6 to 8 months with cold flow and chemical reactions. One of the things that we have determined empirically was that we can best correlate mixing rates with pressure-gradient-type terms when you look at heterogenous flows of variable densities. In our case, we used gaseous hydrogen and gaseous nitrogen to simulate our oxygen, and we found that our best correlating parameters were really $\frac{1}{2}\rho u^2$ of the two differing jets, and the ratios of them.

PREDICTION OF FREE TURBULENT MIXING USING A TURBULENT KINETIC ENERGY METHOD*

By Philip T. Harsha
ARO, Inc.

SUMMARY

Free turbulent mixing of two-dimensional and axisymmetric one- and two-stream flows is analyzed by a relatively simple turbulent kinetic energy method. This method incorporates a linear relationship between the turbulent shear stress and the turbulent kinetic energy and an algebraic relationship for the length scale appearing in the turbulent kinetic energy equation. Good results are obtained for a wide variety of flows. The technique is shown to be especially applicable to flows with heat and mass transfer, for which nonunity Prandtl and Schmidt numbers may be assumed.

INTRODUCTION

For some years a continuing research project has been underway at the Arnold Engineering Development Center (AEDC) aimed at the development of efficient and accurate techniques for the prediction of the entire range of free turbulent mixing phenomena. The goal of this project, sponsored by the Air Force Office of Scientific Research, has been the development of a method which will allow the accurate determination of the mean flow structure of free mixing flows. Although the requirements of accuracy and reliability have dictated the choice of a history-dependent model (i.e., one which takes into account some aspects of the turbulence structure), the prediction of turbulence structure per se has not been considered to be of great importance. In any event, it would seem to be unlikely that a model which predicted the mean flow field correctly for a variety of different flows, would be grossly in error in its prediction of the important features of the turbulence structure.

The model to be described in this paper is a development of the turbulent kinetic energy method originally reported by Lee and Harsha (ref. 1) and further

*This research was performed under the provisions of United States Air Force Contract No. F40600-72-C-0003 with ARO, Inc., the operating contractor of the Arnold Engineering Development Center (AEDC) for the Air Force Systems Command. Major financial support was provided by the Air Force Office of Scientific Research under Air Force Project 9711. Project Monitor was Dr. B. T. Wolfson.

described and extended to more complex flows in other publications (refs. 2 to 4). Even though the model includes flow history through its use of the turbulent kinetic energy equation, it is still an empirical model as are all current approaches to the prediction of free turbulent mixing. Indeed, the only basic difference between approaches is in the point at which empiricism enters. But although empirical information is used in this model, one restriction not commonly made is enforced: there must exist some systematic method for the application of the empiricisms to the calculation of any given flow. Put another way, the empiricisms must either be universal or have clearly defined limits of validity.

It is perhaps important to introduce the analytical model to be described in this paper with a summary of the features of the basic work described in references 1 to 4. In the first of these papers (ref. 1) a simple turbulent kinetic energy model was introduced, in which a linear relation between the turbulent kinetic energy and turbulent shear stress was employed to obtain the shear stress from the solution of the turbulent kinetic energy equation. Gradient diffusion of turbulent kinetic energy was assumed with a constant "kinetic energy Prandtl number," and the length scale required to evaluate the dissipation term in the kinetic energy equation was taken to be proportional to the local width scale of the mixing zone. In this context the model introduced and applied to two simple flows in reference 1 is a single-equation model, since compared to an eddy viscosity method, the only additional equation required is the turbulent kinetic energy equation. Universal constants were assumed for the kinetic energy Prandtl number, for the ratio between turbulent shear stress and turbulent kinetic energy, and in the dissipation term.

The work described in reference 2 (summarized in ref. 3) and the similar work described in reference 4 involved the application of the method to progressively more complex free mixing flows, including flows with heat and mass transfer. Throughout this work the universal constants defined in reference 1 were retained. In reference 2, which to some extent parallels the approach of this conference, the predictions of this single-equation turbulent kinetic energy method were compared with the predictions of a number of eddy viscosity models for a wide variety of flows, including several that are included as test cases for this conference. The conclusion drawn from this comparison was that, even though some serious difficulties remained, the predictions of the turbulent kinetic energy model with the universal constants were, in general, better than those of any eddy viscosity model tested when it was required that the constants appearing in the eddy viscosity models also be considered to be universal.

In particular, good agreement between kinetic energy theory and experiment was shown in reference 2 for coaxial air-air mixing, similar to test cases 9 and 20 of this conference, for hydrogen-air mixing, similar to test cases 10 and 21, and for wake flows such as test cases 14 and 15. Indeed, based on the work of reference 2, it is clear that the universal constant model would be capable of predicting at least 8 and probably 10 of

the 23 available test cases for this conference without change. However, reference 2 also showed that the universal-constant model was clearly in error for the important jet into still air flows. In addition, the asymptotic two-dimensional shear layer had not been attempted nor had initial conditions other than experimental shear stress profiles been used, except for one flow. Inevitably, the extension of the model described in references 1 to 4 to handle such problems led to the need for refinement of some features of the model.

As might be expected, the refinements incorporated in the model described in this paper involve the empirical functions that must be introduced to close the turbulent kinetic energy equation. The new functions have been developed primarily through a process of computer experimentation, in which the predictions made by turbulent kinetic energy theory have been compared both with experimental data and with the predictions of simple eddy viscosity models in those flows in which the simple models are known to be adequate. The integral turbulent kinetic energy theory developed by C. E. Peters at AEDC, which is briefly described in paper no. 17 of this compilation, has been very useful in the development of these improved functions. Such a theory allows a rapid investigation of the asymptotic behavior of a given turbulent kinetic energy model in certain relatively simple flows without the numerical complications that can develop with finite-difference techniques. In addition, integral techniques, in which the profiles of the dependent variables are specified a priori, eliminate the problem of specification of a diffusion function for turbulent kinetic energy (since the lateral diffusion integrated over a profile at a given x must be zero) and allow the production and dissipation terms to be evaluated in terms of integral quantities. This then simplifies the interpretation of the effects of changing the constants appearing in the turbulent kinetic energy equation for flows in which the profiles of the dependent variables can be adequately prescribed.

SYMBOLS

a_1 ratio of turbulent shear stress to turbulent kinetic energy, $\tau/\rho k$

a_2 dissipation parameter (see eq. (1))

b local width of mixing region

c jet species concentration

D diameter

k turbulent kinetic energy per unit mass, $1/2\left(\overline{u'^2 + v'^2 + w'^2}\right)$

k_p constant in Prandtl exchange coefficient model

l_k length scale, equal to distance between $0.90\Delta u$ and $0.10\Delta u$ in a shear layer, distance between $0.99\Delta u$ and $0.01\Delta u$ in the core region of a jet, and $2r_{1/2}$ in an axisymmetric flow

M Mach number

Pr_k kinetic energy Prandtl number

Pr_T turbulent Prandtl number

R_T "turbulent Reynolds number," equation (2)

r radius

Sc_T turbulent Schmidt number

T static temperature

u velocity

Δu characteristic velocity difference, $\left(u_{max} - u_{min}\right)$

$\overline{u'v'}$ turbulent shear stress correlation

v mean-flow lateral velocity component

$W = 1 - \frac{u_c}{u_e}$

x axial coordinate

y general lateral coordinate

α concentration

β parameter, 1 for axisymmetric flow and 0 for two-dimensional flow

δ_o initial boundary-layer thickness

ϵ turbulent eddy viscosity, $\frac{\tau/\rho}{\partial u/\partial y}$

θ momentum thickness

ρ density

σ_o reference value of spreading parameter σ

τ turbulent shear stress, $-\rho\overline{u'v'}$

Subscripts:

c center-line value

e free-stream value or maximum value in outer jet for coaxial mixing

max maximum value at cross section

min minimum value at cross section

o value at the nozzle

1 value on high velocity side of shear layer

2 value on low velocity side of shear layer

1/2 or mu value at point at which $u = 1/2(u_c + u_e)$

ANALYSIS

In addition to the continuity, momentum (mean flow), energy, and species equations necessary in any treatment of a general free turbulent mixing problem, the method described in this paper involves the solution of the turbulent kinetic energy equation. This equation can be written as described, for example, in reference 2: The parameter β is 0 for a two-dimensional flow and 1 for an axisymmetric flow.

$$\underbrace{\rho u \frac{\partial k}{\partial x} + \rho v \frac{\partial k}{\partial y}}_{\text{Convection}} = \underbrace{\frac{1}{y^\beta}\frac{\partial}{\partial y}\left(\frac{\rho \epsilon y^\beta}{Pr_k}\frac{\partial k}{\partial y}\right)}_{\text{Diffusion}} + \underbrace{\tau \frac{\partial u}{\partial y}}_{\text{Production}} - \underbrace{\frac{a_2 \rho k^{3/2}}{l_k}}_{\text{Dissipation}} \qquad (1)$$

In the development of this equation and its application along with the momentum equation to the solution of a given problem, empirical hypotheses have been invoked at three points. The first of these is in the definition of the appropriate form for the diffusion of turbulent kinetic energy. Equation (1) incorporates a gradient diffusion hypothesis; such a hypothesis, with a constant "kinetic energy Prandtl number" Pr_k equal to 0.70, was used in the model described in references 1 to 4, and is also used in this paper.

As written in equation (1), the form assumed for the dissipation term is unchanged from the earlier work. However, whereas a universal constant value for a_2, equal to 1.5, was assumed in the earlier work, constant a_2 fails to yield the proper asymptotic behavior in all flows, and an expression allowing axial variation of a_2 has been developed. No lateral variation of a_2 is allowed.

The third hypothesis is the relation between turbulent shear stress and turbulent kinetic energy. Again, the form of the relationship is the same as that used previously:

$$\tau = a_1 \rho k$$

In the earlier work, two expressions for the lateral variation of a_1 have been used. For two-dimensional flows (including the core region of an axisymmetric jet), a_1 has been taken to be essentially constant, with a value of 0.3 (and with its sign defined by the velocity gradient), whereas in axisymmetric flow, the expression

$$a_1 = \frac{0.3(\partial u/\partial r)}{\left|\partial u/\partial r\right|_{max}}$$

has been shown to apply (ref. 3). However, in the course of the work described in this paper, it became clear that a new function for the lateral variation of a_1 had to be developed for the two-dimensional shear layer. Such a function was devised and is described subsequently; the new function also has certain implications for the prediction of the core region of axisymmetric jets.

In addition, one of the often mentioned problems with turbulent kinetic energy methods is the fact that at the initial station, turbulent shear stress profiles are needed, and experimental profiles are seldom available. In the work described herein, two simple techniques have been used to start the calculations, the choice depending on the position of the start profile. Neither of these techniques involves a detailed knowledge of the initial shear stress profiles. Taken together, they effectively remove the "initial shear stress profile" objections.

The Dissipation Function

As mentioned previously, it quickly became evident during the development of the integral turbulent kinetic energy theory by C. E. Peters and W. J. Phares (paper no. 17) that a constant value of a_2 could not provide the proper asymptotic behavior for all flows considered in this conference. Although it is certainly arguable that the reason for this lies in the form of the term itself, it is less complicated to obtain the proper asymptotic behavior through variation of a_2, if this is at all possible. Thus, the basic $k^{3/2}/l_k$ proportionality has been formally retained, with a new expression describing the axial variation of a_2.

The a_2 function developed by Peters is based on a "turbulent Reynolds number" R_T defined as

$$R_T = \frac{\Delta u l_k}{\epsilon} \tag{2}$$

where Δu is a characteristic velocity difference across the mixing region, such as $u_{max} - u_{min}$; l_k is a characteristic length scale, for example, twice the half-velocity width $r_{1/2}$ in an axisymmetric flow; and ϵ is the local value of the effective (or eddy) viscosity. Because Peters evaluates the shear stress at only one point in a lateral profile $y_{1/2}$, R_T needs only one value at a given x; in the present work R_T varies across a profile, but in order to assign a characteristic value, the point of maximum turbulent energy is chosen as the point to evaluate R_T. With R_T defined as in equation (2), the appropriate values of this parameter can be immediately written down for some flows for which the Prandtl eddy viscosity model

$$\epsilon = k_p l_k \Delta u = \frac{1}{R_T} l_k \Delta u$$

is known to provide a good asymptotic prediction. Thus, for the incompressible two-dimensional shear layer, for which $k_p = 0.007$, R_T is 143, whereas for a circular jet in still surroundings, for which $k_p = 0.0125$, R_T is 80.

The relation between a_2 and R_T used in this work is one of a family of relations developed by Peters and is given by

$$a_2 = 3.89 - \frac{315}{R_T} \qquad (R_T > 143) \tag{3a}$$

$$a_2 = 1.69 \qquad (70 < R_T < 143) \tag{3b}$$

$$a_2 = 0.99 + 0.01R_T \qquad (R_T < 70) \qquad (3c)$$

The relationship expressed by equations (3) is not entirely optimum for the calculations described in this paper, primarily, because of differences in the point in a lateral profile at which R_T is calculated between the integral and the finite-difference methods. In particular, the point at which equation (3c) is applied in the finite-difference method probably should be at $R_T < 30$, and the break at $R_T = 143$ needs to be handled more gradually than equations (3) allow. However, as the results will show, equations (3) do allow the accurate calculation of a very wide variety of flows. Further development of the empirical functions represented by equations (3) is continuing; some of this development is described by Peters in paper no. 17.

Relation Between Shear Stress and Kinetic Energy

Although a_1, the ratio of the turbulent shear stress to the turbulent kinetic energy, is sensibly constant (at a value of 0.3) for a wide variety of flows (ref. 5), the necessity of allowing for some lateral variation of a_1 has always been understood. Thus, in previously reported work in axisymmetric flow, the expression

$$a_1 = \frac{0.3(\partial u/\partial r)}{|\partial u/\partial r|_{max}}$$

(where the subscript "max" refers to the point where $\partial u/\partial r$ attains its maximum value) has been used from the center line to the point at which

$$\frac{\partial u}{\partial r} = \left(\frac{\partial u}{\partial r}\right)_{max}$$

with the expression

$$a_1 = \frac{0.3(\partial u/\partial r)}{|\partial u/\partial r|}$$

being used for the rest of the profile to insure the proper algebraic sign for the shear stress. In two-dimensional flow, the expression

$$a_1 = \frac{0.3(\partial u/\partial y)}{|\partial u/\partial y|_{max}}$$

was used only in a small region around the point of maximum or minimum velocity gradient, primarily to avoid excessive steepening of this gradient.

However, in the course of the work carried out for this paper, it was found to be impossible to obtain an accurate prediction of the incompressible two-dimensional shear layer by using either of the two models described previously. Because the problem lay in the prediction of shear stress at the profile edge, it was not possible to determine the appropriate a_1 function from comparison with experimental data. Instead, use was made of the fact that the incompressible two-dimensional shear layer is one of the flows for which the Prandtl eddy viscosity model provides an accurate asymptotic prediction. A calculation was made with the Prandtl model to obtain the shear stress and the production term in the turbulent kinetic energy equation. The resulting shear stress and kinetic energy profiles were then used to obtain the lateral variation of the parameter a_1, as shown in figure 1. In this figure, the symbols represent different x-locations at which the calculated profiles were obtained, and the solid line represents the a_1 function derived from these results. Positive values of the abscissa represent the high-velocity edge of the shear layer. This variation was found to be reasonably universal for the incompressible shear layer, as can be seen from the figure, and has been used in all asymptotic shear layer calculations in this study.

The a_1 profile obtained for the two-dimensional shear layer may also be appropriate for the mixing layer in the core region of a jet. Because of time limitations it has not been possible to investigate the application of the a_1 function to these flows, but it is possible that use of a function such as that represented by figure 1 will reduce the fairly long transition region that is predicted in some of the flows described in the following section.

Initial Conditions

The most often-quoted major objection to the use of turbulent energy methods in the prediction of free turbulent mixing has been the apparent necessity of obtaining a turbulent shear stress (or turbulent kinetic energy) profile to start the calculation. In the calculations described, this problem has been in large part overcome; experimental shear stress profiles have not been used to start any of the calculations reported herein, and experimental estimates of the turbulent shear stress level have been used in only those few cases where other estimates could not properly be made.

To start these calculations, two techniques have been used. In all cases in which the initial profiles have been given at $x = 0$, the turbulent eddy viscosity profiles obtained for boundary-layer flows by Maise and McDonald (ref. 6) have been used to obtain the profiles of the turbulent shear stress. These profiles were also used for the boundary-layer portion of the initial velocity profile for the compressible two-dimensional shear layer (test case 5), although the start point for this case was not at $x = 0$. In all other computations, for which profiles have been given downstream of the origin of mixing (usually in the core region of a jet flow), constant eddy viscosity has been used to generate the initial shear stress profile. One exception is test case 24, for which the start point was in the laminar part of the flow. The eddy viscosity has in general been that appropriate for $R_T = 200$ (i.e., a Prandtl constant of 0.005), although in a few cases a more accurate estimate of the experimental R_T was necessary. As the results described in the next section show, it is not necessary to have detailed knowledge of the initial shear stress distribution for each case in order to get accurate predictions of the flow development.

Numerical Solution Technique

The finite-difference numerical technique used to make the calculations reported herein is identical to that reported in references 1 to 4. One of the features of this technique is that the constant-momentum-excess requirement applicable to free turbulent flows is satisfied at each station; that is,

$$\int_0^\infty \rho u(u - u_e)y^\beta dy = \text{Constant}$$

As a cross-check, the value of the product $\left(r_{1/2}/r_o\right)\left(u_c/u_o\right)$ was evaluated for the axisymmetric jet flow of test case 18. If momentum is conserved, this product should be constant for the similar profile region of the flow. Over the range $30 < x/D < 115$, the value of $\left(r_{1/2}/r_o\right)\left(u_c/u_o\right)$ varied within ±1.5 percent of its average for this calculation.

RESULTS

Successful computations were completed for 23 of the 24 test cases that were available. The only case not computed was test case 23, the compound coaxial jet, which would have required fairly complicated reprograming to account for the simultaneous development of two shear layers.

Because of the large number of cases to be covered, the discussion in this section is limited to the most significant aspects of each case computed. The comments to follow in the main emphasize the problems encountered in these computations. The overall

success of the method described in this paper will speak for itself. General details of the starting techniques and the dissipation function used are noted in table I, which also provides a guide to the appropriate figures.

Two-Dimensional Shear Layers

As might be inferred from the discussion of the a_1 function, the five shear layer cases required a relatively large development effort which is not yet complete. This development effort was particularly important for the three asymptotic cases, for which the new a_1 function was particularly necessary. For test cases 1 to 3, the calculations began with initial shear stress profiles obtained from the appropriate Maise and McDonald eddy viscosity profiles (ref. 6) and constant a_1, as is appropriate for boundary-layer flow. At an arbitrary distance downstream the a_1 profile indicated in figure 1 was introduced (approximated analytically by a series of straight-line segments). For test cases 1 to 3, since only the asymptotic behavior was required, the point at which the new a_1 function was applied could be truly arbitrary (it was taken to be 1 initial boundary-layer height), but as will be seen in test cases 4 and 5, the choice can be important for the preasymptotic shear layer. No transition function was used to change from a constant a_1 profile to the profile shown in figure 1.

Self-preservation was approached at relatively small axial distances for the incompressible shear layers, although with values of σ lower than are commonly reported. The calculation of σ was made by using the standard definition of σ for this conference

$$\sigma = 1.855 \frac{x_2 - x_1}{y_2 - y_1}$$

where y_1 and y_2 represent the lateral distance between the points at which $\frac{u - u_2}{u_1 - u_2} = 0.1$ and $\frac{u - u_2}{u_1 - u_2} = 0.9$ at x_1 and x_2, respectively. Figure 2 shows that the profile shape passes through a shape appropriate to the $\sigma = 11.8$ data of Liepmann and Laufer (ref. 7), but at these distances it is apparently still evolving with σ decreasing. Figure 3 shows that the predictions of σ are apparently uniformly low, since the classical behavior of σ with velocity ratio is recovered.

There is no evidence that the a_1 profile represented in figure 1 is invariant either with Mach number variation or density ratio variation. Indeed, there is some evidence that it is not, primarily from the differences between these calculations and those reported by Peters and Phares (paper no. 17). In the latter work, the shape of the turbulent kinetic energy profile is assumed to be invariant, which implies that the lateral variation of the

ratio of the turbulent shear stress to the turbulent kinetic energy (i.e., a_1) cannot be invariant with either Mach number or density ratio variation. In any event, the a_1 function shown in figure 1 was used for all shear layer calculations, and figure 4 shows the predicted variation of σ with Mach number. Note particularly the extremely great distances required to approach a self-preserving condition at the higher Mach number.

The variation of σ with density ratio predicted by using this model is shown in figures 5 and 6. As noted in figure 6, the density ratio was obtained by varying the temperature of the two streams. Within the framework of the commonly made unity turbulent Lewis number assumption, similar results would be obtained by varying the molecular weight of the two streams. However, the unity turbulent Lewis number assumption is not necessary in the analysis. The predicted variation of σ with density ratio is completely different from that predicted for a similar variation in density ratio caused by Mach number variation.

The asymptotic two-dimensional shear layer predictions are not meant to represent an adequate and correct theory of this particular flow. They do show the necessity for including a different sort of lateral variation of a_1 in such a flow from that which is necessary in other flows. This lateral variation may in turn be important in the prediction of the core region of axisymmetric jets. Further, these calculations indicate that, at least in some instances, self-preservation is only very slowly reached – an observation that raises obvious questions about the interpretation of experimental results.

Self-preservation, or the lack of it, is also a factor in the two remaining shear layer flows, test cases 4 and 5. In these calculations direct comparison with experimental profile data is made, and these comparisons indicate that both of these flows were preasymptotic.

Evidence for this statement in test case 4 is shown in figure 7, which shows that the "constant a_1" model provides a better prediction of the velocity profile at $x = 76$ cm than does the "shear layer a_1" model. For both test case 4 and test case 5, the predicted profiles were matched with the experimental ones at the half-velocity points. This technique was necessary because the calculation does not satisfy the proper lateral boundary condition at plus or minus infinity. As is well known, the effect of neglect of this boundary condition is to allow the calculated profiles to "float" in space.

The comparison of shear stress profiles for test case 4 shown in figure 8 shows that the constant a_1 model overpredicts the shear stress at $x = 12.7$ cm and strongly underpredicts it at $x = 76$ cm. However, analysis of the shear stress profiles given for test case 4 shows that the peak shear at $x = 76$ cm is considerably higher than the trend from the upstream data would indicate it should be. (The experimental peak shear stress is almost constant at $x = 25$ cm and $x = 46$ cm.) Furthermore, it is unlikely that an error in shear stress prediction of the magnitude shown in figure 8 at $x = 76$ cm would

be reflected by the small velocity profile deviations shown in figure 7 at this station. Therefore, the reported value of shear stress at $x = 76$ cm is, in the author's opinion, suspect.

Test case 5 is also evidently preasymptotic, as the comparison of the experimental and predicted velocity profiles in figure 9 shows. Again, the constant a_1 model provides the better prediction. This test case and test case 4 both raise the question of what is the proper point to begin to use the "asymptotic" a_1 profile represented by figure 1. The answer to this question clearly requires further research.

Axisymmetric Jets Into Still Air

Three test cases in the category of axisymmetric jets into still air were considered, test cases 6 to 8, and the results were good for all cases as figures 10 to 13 demonstrate. For all these calculations, the constant a_1 model was used in the mixing layer region (first regime) of the flow. Downstream of the end of the potential core, the model in which the constant value of a_1 is modified by the velocity gradient ratio was used as was used for all axisymmetric flows. The point at which the change of models takes place is arbitrarily assumed to be that at which the center-line velocity is 0.9 times the jet velocity. No transition function was used.

The prediction of the subsonic jet of test case 6 began at $x/r_o = 2$ with a Prandtl constant $k_p = 0.005$. As can be seen from figure 10, the prediction of this flow is quite good. The fact that the prediction is better if equation (3c) is not used, despite the fact that the predicted asymptotic value of the turbulent Reynolds number R_T is 35, indicates that for these predictions, the upper limit for the use of equation (3c) should be reduced.

One point of difference between this calculation and the integral technique reported by Peters is that the R_T value is in this analysis obtained at the point at which $k = k_{max}$ rather than the half-velocity point. This tends to lower the value of R_T somewhat compared with the value obtained by Peters. It would also have been possible in this analysis to evaluate R_T at the point at which $\tau = \tau_{max}$, which does not in general correspond to the point at which $k = k_{max}$. Had this been done, there would have been a 10-percent increase in R_T for the air-air flows, for which the eddy viscosity is essentially constant over the inner portion of the flow, and perhaps a 40-percent increase in R_T for hydrogen-air flows. Thus, the point at which R_T is evaluated is only a substantial factor in hydrogen-air flows for which the upper limit for equation (3c) is not a factor.

For test case 7, the length of the potential core is somewhat underpredicted, resulting in an overall overprediction of the velocity decay, as shown by figure 11. On the other hand, the profile prediction is quite good (fig. 12) if the underprediction of the center-line velocity is taken into account. The profile data are from reference 8.

Finally, the excellent center-line temperature and velocity agreement with the data of test case 8 (fig. 13) is obtained by using an assumed (and constant) value of 0.85 for the turbulent Prandtl number.

Jets in Moving Streams

The first of the coaxial jet cases, test case 9, represents the data of Forstall (ref. 9). For these calculations, the 10 percent by volume helium trace was included so that the initial jet to outer stream density ratio was 0.92. In table I it is noted that two initial profile offsets were used in the calculation for test case 9. One calculation was made by using the shifted profiles given by the data sheet for test case 9, and the others were made by using the unshifted profiles given in the data sheet. Figure 14 demonstrates that the most accurate prediction uses the latter start condition and further neglects the use of equation (3c). The initial radii reported in figure 14 represent the location of the inner edge of the viscous region. For test case 9, as for test case 6, the asymptotic value of R_T is of the order of 35, indicating again that the upper limit for equation (3c) should be of the order of $R_T = 30$ for this method. Profiles of velocity and concentration are shown in figure 15 (the data obtained from curves presented in ref. 9), and figure 16 shows excellent agreement with the data for the half-velocity width calculation. Both of these figures relate to the "unshifted" calculation shown by the dashed line in figure 14, for which equation (3c) is not used.

Perhaps the strongest feature of the method described in this paper is the relative ease and accuracy with which more complex flows involving heat and mass transfer are handled. Figures 17 and 18 show the excellent agreement between theory and experiment for the hydrogen-air mixing data of test case 10. The experimental profile data were obtained from reference 10.

For test case 10 (and the similar data of test case 21) a second regime start point was assumed for the calculations; that is, the initial viscous region was assumed to extend all the way to the center line. The profile data were obtained, as in all the calculations, from the appropriate data sheet. The start points for both test cases 10 and 21 are in the transition region between the first and second flow regimes, and such start points are among the most difficult to use with this method. For calculations which start at $x/D = 0$, the natural tendency is for the level of kinetic energy near the inside edge of the viscous region to increase fairly slowly but rapidly enough that the center-line kinetic energy is of the order of 70 percent of the maximum in a profile at the point at which the "second regime" a_1 profile is put into effect. In calculations starting in the transition region as this one does, the increase in kinetic energy near the inside edge of the viscous region does not occur, so that the kinetic energy (and hence the shear stress) is too low near the flow center line. The result is an excessively long transition region, with

6 diameters being required in this particular flow for the center-line velocity ratio to drop to 0.90.

However, this problem was overcome within the framework of a constant eddy viscosity start profile by using the second regime velocity gradient ratio throughout the flow. Since the initial shear stress is input, the initial kinetic energy was obtained by using the second regime velocity gradient ratio inverted; thus, the initial kinetic energy was maintained at a constant value from the center line to the maximum velocity gradient point, which is a reasonable approximation to the form that the kinetic energy profile would have had if the calculation started at $x = 0$. It must be stressed that this is only a problem if a transition region start is used and, thus, was only a problem for test cases 10 and 21. The hydrogen-air flows of test cases 12 and 22 did not require such treatment.

Incidentally, the value of the Prandtl constant implied by the shear stress used to start this calculation, which was obtained from the τ_{mu} data of reference 10, and the assumed width of the profile, is $k_p = 0.005$, the same as has been generally assumed for nonzero start points.

The data of test case 11 have some curious features, not the least of which is the fact that the value of the center-line velocity, initially lower than the free-stream velocity, drops still lower before beginning to rise. Nevertheless, the overall prediction still compares favorably with the data as shown in figure 19.

Comparison of the theoretical prediction of test case 12 with the experimental data (fig. 20) indicates that very good results can be obtained for hydrogen-air flow with a calculation starting at $x/D = 0$, with a Maise and McDonald eddy viscosity profile being used to obtain the initial shear stress. Profile comparison (fig. 21) also shows reasonably good agreement, if the difference between the predicted and actual center-line values at the axial station chosen is taken into account. The data are from reference 11.

The prediction of the two-dimensional jet in a moving stream, test case 13, is shown in figure 22. For this case, no initial boundary-layer data other than an initial momentum thickness for the two boundary layers together were available. Calculations were begun with 1/4 power-law initial boundary-layer profiles because the 1/7 power-law profile ordinarily used resulted in extremely thick initial boundary layers being necessary to equal the quoted momentum thickness. Maise and McDonald eddy viscosity profiles were used to obtain the initial shear stress level. The agreement between the experimental values of center-line velocity and the computed values is quite good as can be seen from figure 22.

Wakes

Accurate prediction of the two-dimensional wake flows required the use of a constant value of a_2 rather than the variation described by equations (3). The value 1.4 was considerably lower than equations (3) would predict at the R_T appropriate to the flow. For axisymmetric values, the function described by equations (3) seems to be adequate. However, the prediction of the axisymmetric wake flows is not sufficiently good for any strong conclusions to be drawn regarding the optimum a_2 for those flows.

The center-line velocity prediction for a preasymptotic two-dimensional wake, case 14, is shown in figure 23. Because the presentation method tends to emphasize the discrepancies between theory and experiment rather markedly, velocity profile shapes are compared in figure 24. The corresponding turbulent shear stress profiles are shown in figure 25, which indicate that the Maise and McDonald eddy viscosity profiles used to start these calculations may have significantly underpredicted the actual initial shear stress level.

Theory and experiment for an axisymmetric wake, test case 15, are compared in figure 26.

The asymptotic two-dimensional wake data of test case 16 were computed by using the initial R_T reported in reference 12 to obtain the initial shear stress. Prediction and experiment are compared in figure 27.

Again, an initial R_T reported in reference 12 was used to start the computation for test case 17, an axisymmetric wake; the comparison between theory and experiment is shown in figure 28.

Optional Test Cases

The first of the optional cases, test case 18, is the prediction of the asymptotic free jet. Unfortunately, the data given are not appropriate for an asymptotic jet. Figure 29 shows the center-line velocity decay for the data of reference 13 from which test case 18 was taken; it can be seen that the prediction for this case goes essentially through the data points. The start condition was taken from the data of Bradshaw, Ferriss, and Johnson (ref. 14) at $x/D = 1$. Also shown in figure 29 are the free jet center-line velocity results obtained by Albertson, Dai, Jensen, and Rouse (ref. 15), which follow the classical $(x/D)^{-1}$ decay law quite well. Clearly, the data of reference 13 do not satisfy this decay law, and, for $x = 100$, the center-line velocity recorded by Wygnanski and Fiedler (ref. 13) is considerably lower than that which would be obtained from an $(x/D)^{-1}$ decay from, say, $x/D = 40$. For a free jet, the excess momentum integral must be a constant. Thus, if two flows vary in center-line velocity with constant momentum excess in such a manner that the center-line decay curves cross, one would expect the flow with the lower center-line velocity to have the wider profile. Comparing the test case 18 data with data

from reference 15 (fig. 30) shows that this is not true. On the other hand, the theory does show a wider profile than either the reference 15 data or the test case 18 data. Therefore, the conclusion is made that the data for test case 18 were not, in fact, properly asymptotic.

Figure 31 demonstrates the good agreement of the present method with the data of test case 19. Three further coaxial mixing cases are presented in figures 32 to 36. Note especially the excellent profile agreement shown in figures 33 and 35, along with the good axial decay agreement shown in figures 32 and 34 for both test cases 20 and 21. Figure 36 demonstrates the quite acceptable prediction of the unusual hydrogen-air flow of test case 22 achieved with the present method. This method will, of course, not predict the negative velocity ratios measured experimentally, and the computation stopped at $x/D = 26$ where the velocity profile had all but flattened out.

The last case to be discussed is the interesting two-dimensional wake flow of test case 24. The start point for this case is in the laminar portion of the flow; there follows in the experimental data a fairly long transition region until behavior characteristic of a turbulent flow develops. In the computation of this flow, the viscosity term appearing in the momentum equation was taken to be made up of a laminar and a turbulent contribution. The laminar contribution was obtained from the experimental data of reference 12, and the turbulent contribution was obtained through the solution of the turbulent kinetic energy equation in the normal manner. A very low, uniform, initial turbulent kinetic energy profile was used to provide the initial condition for the solution of the turbulent kinetic energy equation, and the level of the energy was allowed to develop as described by the equation. Referring to the turbulent kinetic energy equation (eq. (1)), the production term was evaluated with only the turbulent contribution to the shear stress, whereas the viscosity appearing in the diffusion term was taken to be the total viscosity.

Results of several computations with this approach are shown in figure 37. The computations differ only in the initial turbulent kinetic energy level assumed. This level is described in the figure in terms of the associated turbulent intensity level based on an assumed isotropic condition – that is, $u' = v' = w'$. As can be seen from the figure, the effect of increasing the initial intensity level is to shorten the transition region, as would be expected. Note also that the level giving the best agreement with the data is 2 percent, which agrees well with the quoted intensity levels from reference 12, which, based on the outer stream mean velocity, ranged from 0.3 percent to 3 percent through the laminar and transition regions. Because the wake was heated, the turbulent Prandtl number for these calculations was taken to be 0.85.

Since it was not possible to completely establish a priori an appropriate start condition for this problem, the results shown herein should only be taken as a demonstration of the abilities of the method described in this report, using an admittedly crude start

technique. Transitioning flows such as test case 24 would appear to require more knowledge of the experimental initial conditions than fully turbulent flows.

CONCLUDING REMARKS

As was stated in the introduction, the work described in AEDC-TR-71-36 made it clear that the universal constant kinetic energy approach described in that reference was capable of handling a substantial number of the test cases for this conference without change. Indeed, ignoring the free shear layer cases for the moment, the only obvious area in which this method would have clearly failed was in the prediction of the circular jet, test cases 6, 7, 8, 18, and 19. On the other hand, it had not been developed to the point that calculations could be routinely initiated without detailed knowledge of the initial shear stress profiles.

The results described in this paper show that with a small increase in complexity – that is, the addition of a function describing the axial variation of the dissipation parameter a_2 – the kinetic energy method described in AEDC-TR-71-36 can be applied to a wide variety of flows of engineering interest. In particular, accurate predictions of jets with zero secondary flow and coaxial jets, including heat and mass transfer, can routinely be made without exact knowledge of the initial shear stress profiles and with a well-defined method of obtaining the necessary empirical constants which does not involve prior knowledge of the results desired.

Some work is still required to obtain the optimum function for the dissipation parameter a_2. The asymptotic free jet prediction does not seem proper, as the classical center-line velocity decay rate is not recovered. Also, the shear layer form for the lateral variation of the ratio of shear stress to turbulent kinetic energy, a_1, needs to be further investigated, with particular emphasis on the effects of Mach number and density variation. Further work is underway on this problem, as well as on the problem of integrating the shear layer a_1 model into an overall model for better prediction of the core region of axisymmetric jets.

REFERENCES

1. Lee, S. C.; and Harsha, P. T.: Use of Turbulent Kinetic Energy in Free Mixing Studies. AIAA J., vol. 8, no. 6, June 1970, pp. 1026-1032.

2. Harsha, Philip Thomas: Free Turbulent Mixing: A Critical Evaluation of Theory and Experiment. AEDC-TR-71-36, U.S. Air Force, Feb. 1971. (Available from DDC as AD 718 956.)

3. Harsha, Philip T.: Free Turbulent Mixing: A Critical Evaluation of Theory and Experiment. Turbulent Shear Flows, AGARD-CP-93, Jan. 1972, pp. 17-1 – 17-11.

4. Harsha, P. T.; and Lee, S. C.: Analysis of Coaxial Free Mixing Using the Turbulent Kinetic Energy Method. AIAA J., vol. 9, no. 10, Oct. 1971, pp. 2063-2066.

5. Harsha, P. T.; and Lee, S. C.: Correlation Between Turbulent Shear Stress and Turbulent Kinetic Energy. AIAA J., vol. 8, no. 8, Aug. 1970, pp. 1508-1510.

6. Maise, George; and McDonald, Henry: Mixing Length and Kinematic Eddy Viscosity in a Compressible Boundary Layer. AIAA J., vol. 6, no. 1, Jan. 1968, pp. 73-80.

7. Liepmann, Hans Wolfgang; and Laufer, John: Investigations of Free Turbulent Mixing. NACA TN 1257, 1947.

8. Eggers, James M.: Velocity Profiles and Eddy Viscosity Distributions Downstream of a Mach 2.22 Nozzle Exhausting to Quiescent Air. NASA TN D-3601, 1966.

9. Forstall, Walton, Jr.: Material and Momentum Transfer in Coaxial Gas Streams. Sc.D. Thesis, Massachusetts Inst. Technol., June 1949.

10. Chriss, D. E.; and Paulk, R. A.: An Experimental Investigation of Subsonic Coaxial Free Turbulent Mixing. AEDC-TR-71-236, AFOSR-72-0237TR, U.S. Air Force, Feb. 1972. (Available from DDC as AD 737 098.)

11. Eggers, James M.: Turbulent Mixing of Coaxial Compressible Hydrogen-Air Jets. NASA TN D-6487, 1971.

12. Demetriades, A.: Compilation of Numerical Data on the Mean Flow From Compressible Turbulent Wake Experiments. Publ. No. U-4970, Aeronutronic Div., Philco-Ford Corp., Oct. 1, 1971.

13. Wygnanski, I.; and Fiedler, H.: Some Measurements in the Self-Preserving Jet. J. Fluid Mech., vol. 38, pt. 3, Sept. 18, 1969, pp. 577-612.

14. Bradshaw, P.; Ferriss, D. H.; and Johnson, R. F.: Turbulence in the Noise-Producing Region of a Circular Jet. J. Fluid Mech., vol. 19, pt. 4, Aug. 1964, pp. 591-624.

15. Albertson, M. L.; Dai, Y. B.; Jensen, R. A.; and Rouse, Hunter: Diffusion of Submerged Jets. Paper No. 2409, Trans. Amer. Soc. Civil Eng., vol. 115, 1950, pp. 643-664.

TABLE I.- SUMMARY OF CALCULATION TECHNIQUES

Test case	Type	Start point	Start method	Dissipation parameter	Figure	Remarks
1	Incompressible 2D shear layer	x = 0 cm	Maise & McDonald eddy viscosity	$a_2 = 1.69$	3	Uses a_1 profile from fig. 1
2	Compressible 2D shear layer	x = 0 cm	As for case 1	Eqs. (3)	4	As for case 1
3	Variable density 2D shear layer	x = 0 cm	As for case 1	Eqs. (3)	5, 6	As for case 1
4	Incompressible 2D shear layer	x = 0 cm	As for case 1	$a_2 = 1.69$ Eqs. (3)	7, 8	As for case 1; also with a_1 = Constant
5	Compressible 2D shear layer	x = 2.5 cm	As for case 1[a]	Eqs. (3)	9	As for case 4
6	Circular jet	x/D = 1	Prandtl ϵ, $k_p = 0.005$	Eqs. (3)	10	$a_{2,min} = 1.69$ in one calculation
7	Supersonic circular jet	x = 0 cm	Maise & McDonald eddy viscosity	Eqs. (3)	11, 12	
8	Compressible circular jet	x/D = 2.8	Prandtl ϵ, $k_p = 0.005$	Eqs. (3)	13	
9	Coaxial air jets with He trace	x/D = 0	Maise & McDonald eddy viscosity	Eqs. (3a), (3b)	14, 15, 16	Two initial profile offsets
10	Coaxial H_2-air	x/D = 3	Constant eddy viscosity	Eqs. (3)	17, 18	ϵ obtained from extrapolation τ_{mu} plots of ref. 10
11	Compressible coaxial air-air	x/D = 0	Maise & McDonald eddy viscosity	Eqs. (3a), (3b)	19	
12	Compressible coaxial H_2-air	x/D = 0	As for case 11	Eqs. (3)	20, 21	Initial velocity profile from data of ref. 14
13	Plane jets	x = 0 cm	As for case 11	Eqs. (3)	22	
14	Incompressible plane wake	x = 0 cm	Maise & McDonald eddy viscosity	$a_2 = 1.4$ (constant)	23, 24, 25	
15	Incompressible axisymmetric wake	x/D = 0	Prandtl ϵ, $k_p = 0.005$	Eqs. (3)	26	
16	Compressible plane wake	x = 0.91 cm	Constant eddy viscosity	$a_2 = 1.4$ (constant)	27	ϵ obtained from extrapolation of R_T plots of ref. 12
17	Compressible axisymmetric wake	x = 6.74 cm	Constant eddy viscosity	Eqs. (3)	28	As for case 16
18	Circular jet	x/D = 1	Prandtl ϵ, $k_p = 0.005$	Eqs. (3a), (3b)	29, 30	Data not actually fully developed
19	Compressible circular jet	x/D = 2.8	Prandtl ϵ, $k_p = 0.005$	Eqs. (3)	31	
20	Coaxial air-air jets	x/D = 0.23	As for case 19	Eqs. (3)	32, 33	
21	Coaxial H_2-air jets	x/D = 2.6	Constant eddy viscosity	Eqs. (3)	34, 35	Eddy viscosity from extrapolated τ_{mu} of ref. 10
22	Coaxial compressible H_2-air jets	x/D = 0	Maise & McDonald eddy viscosity	Eqs. (3)	36	
23	Coaxial air-air jets	---	---	---	---	Not attempted
24	Compressible plane wake	x = 1.67 cm	Laminar viscosity + constant (low) turbulent intensity	$a_2 = 1.4$	37	Computed through transition to turbulent flow

[a]Maise and McDonald eddy viscosity profiles used for boundary-layer portion of initial profile with constant ϵ (equal to one-half the adjacent Maise and McDonald value) for remainder.

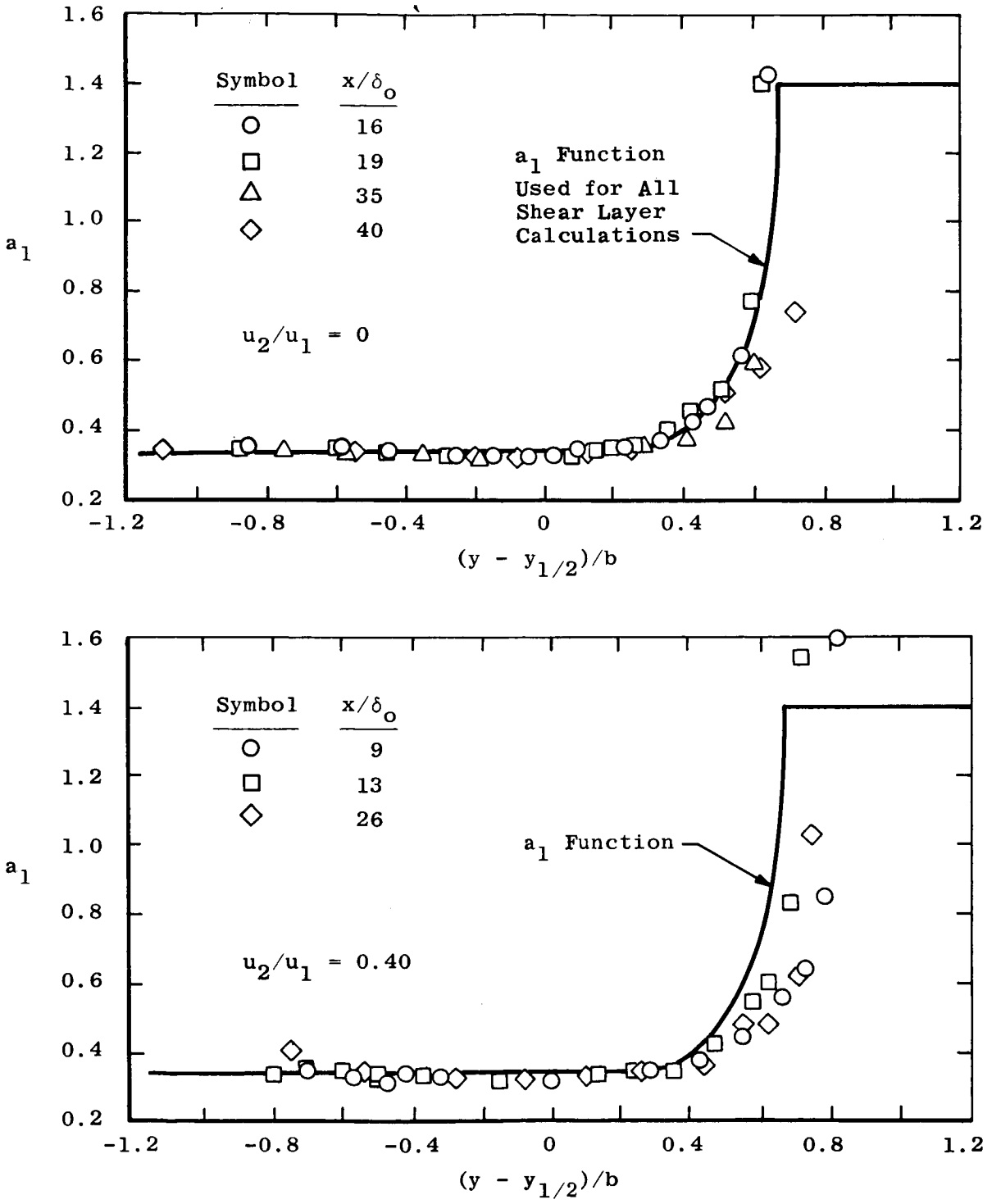

Figure 1.- Theoretical variation of parameter a_1 implied by Prandtl eddy viscosity model for two-dimensional shear layer.

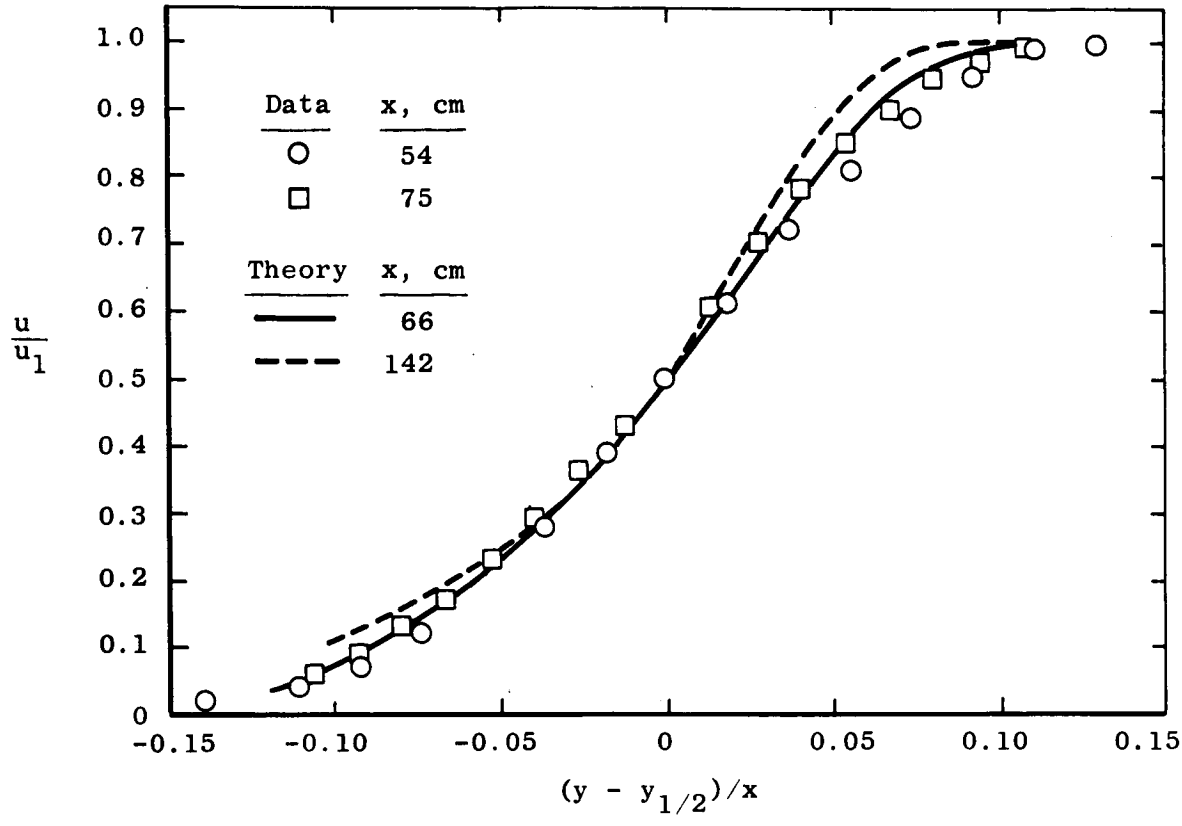

Figure 2.- Comparison of predicted shear layer velocity profile with data of Liepmann and Laufer (ref. 7) for test case 1.

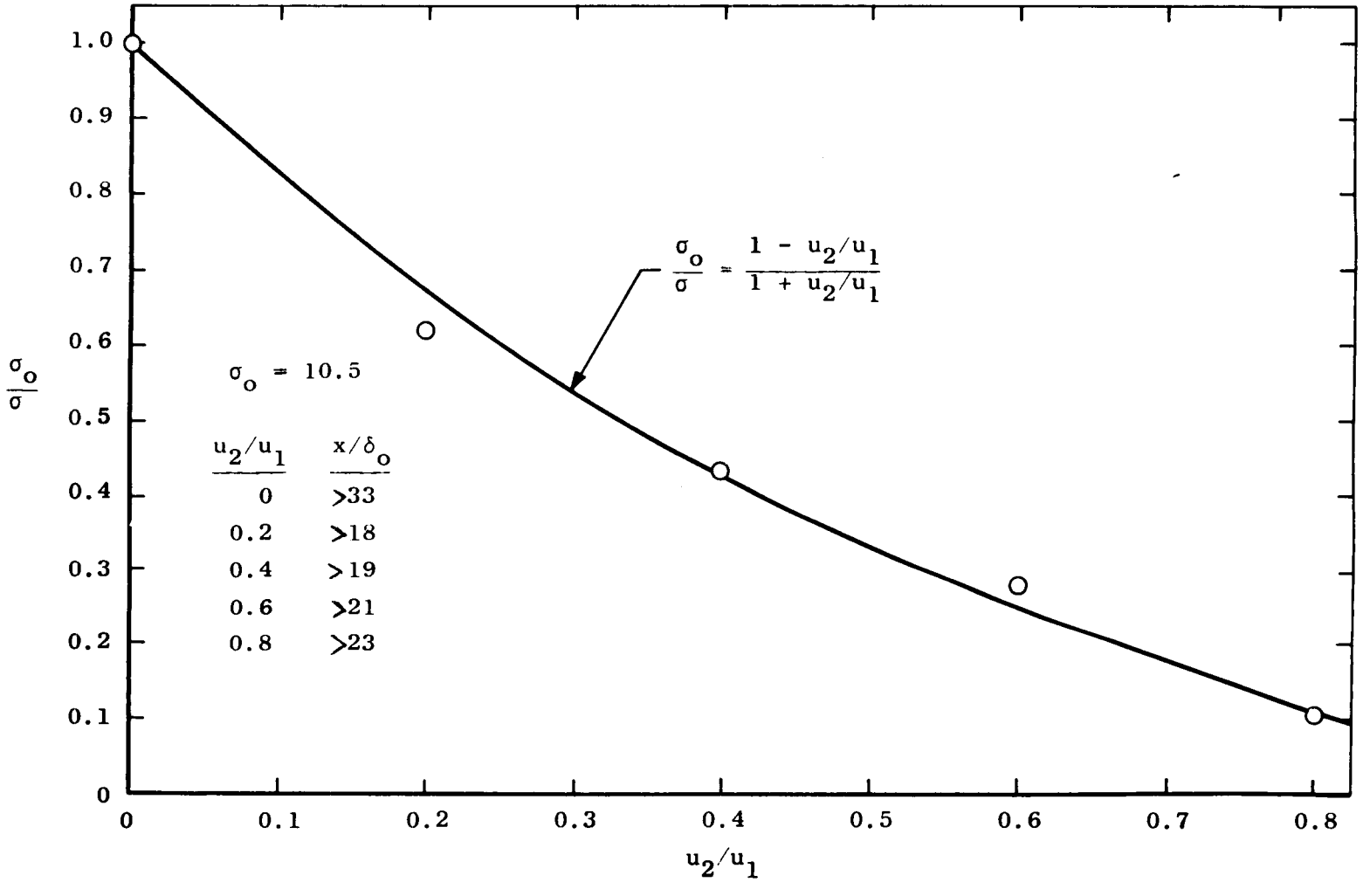

Figure 3.- Calculated variation of spreading parameter with velocity ratio for test case 1, two-dimensional shear layers.

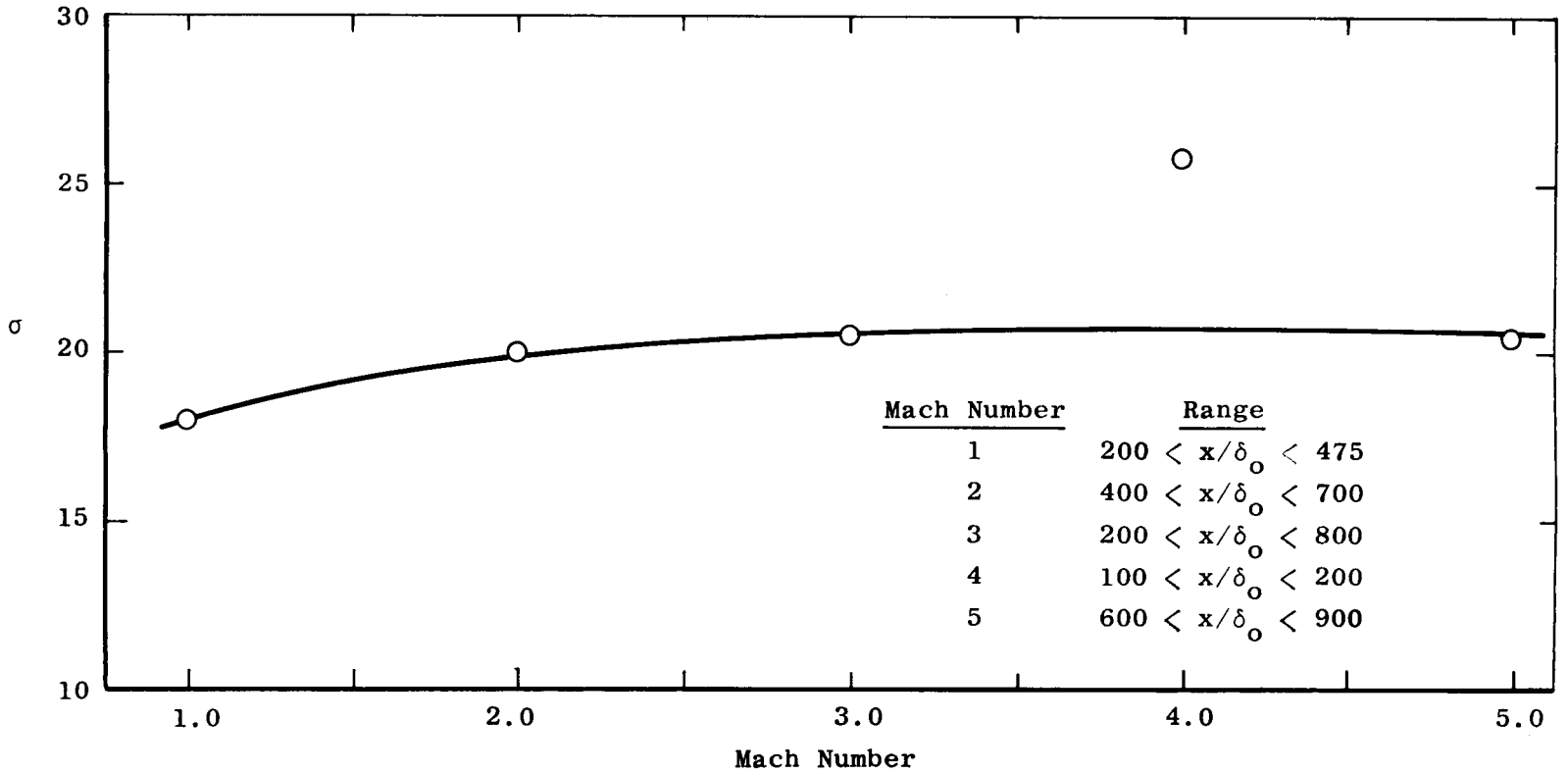

Figure 4.- Predicted variation in spreading parameter with Mach number.

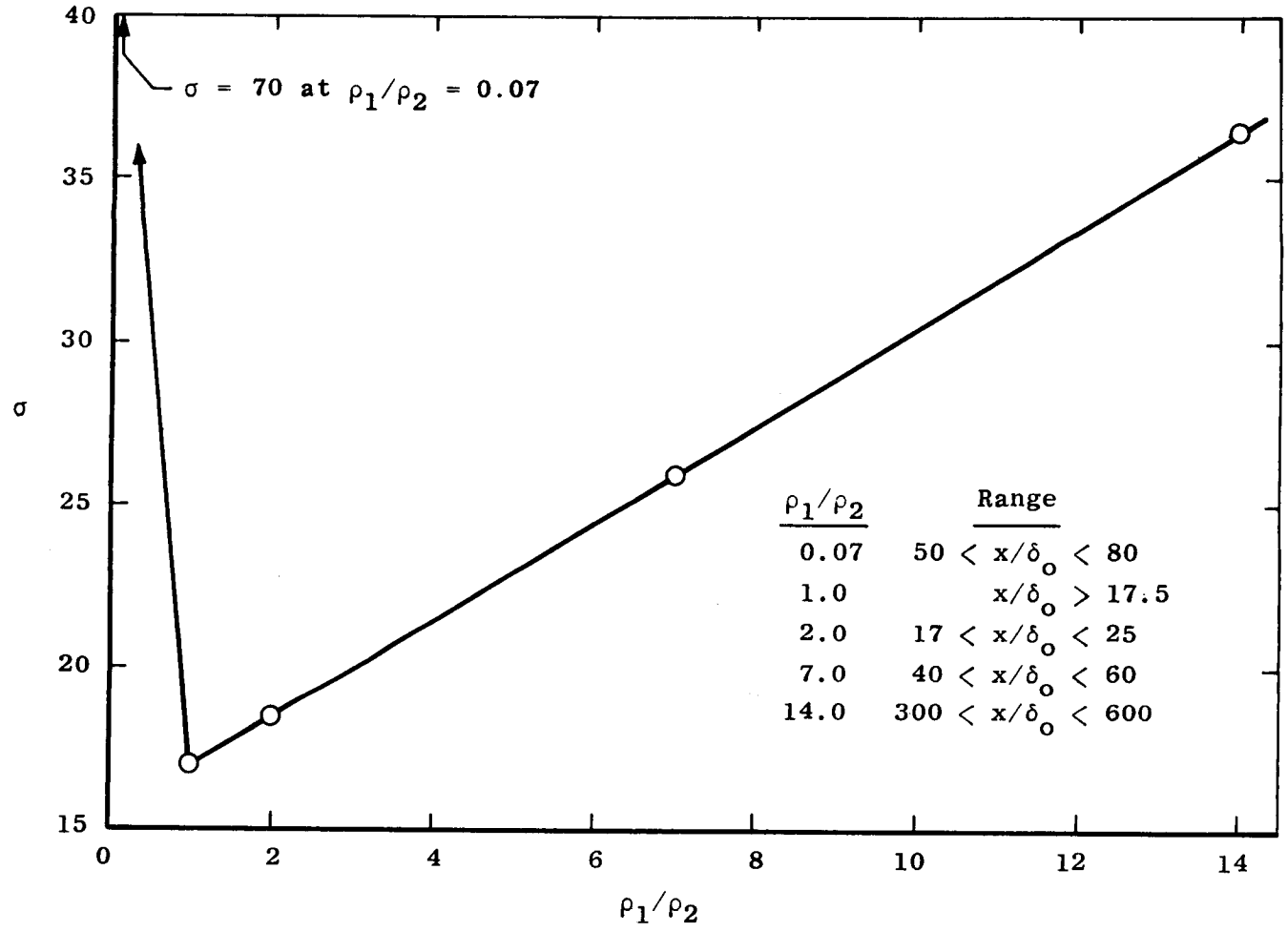

Figure 5.- Predicted variation of spreading parameter with density ratio for test case 3, two-dimensional shear layer with $u_2/u_1 = 0.2$.

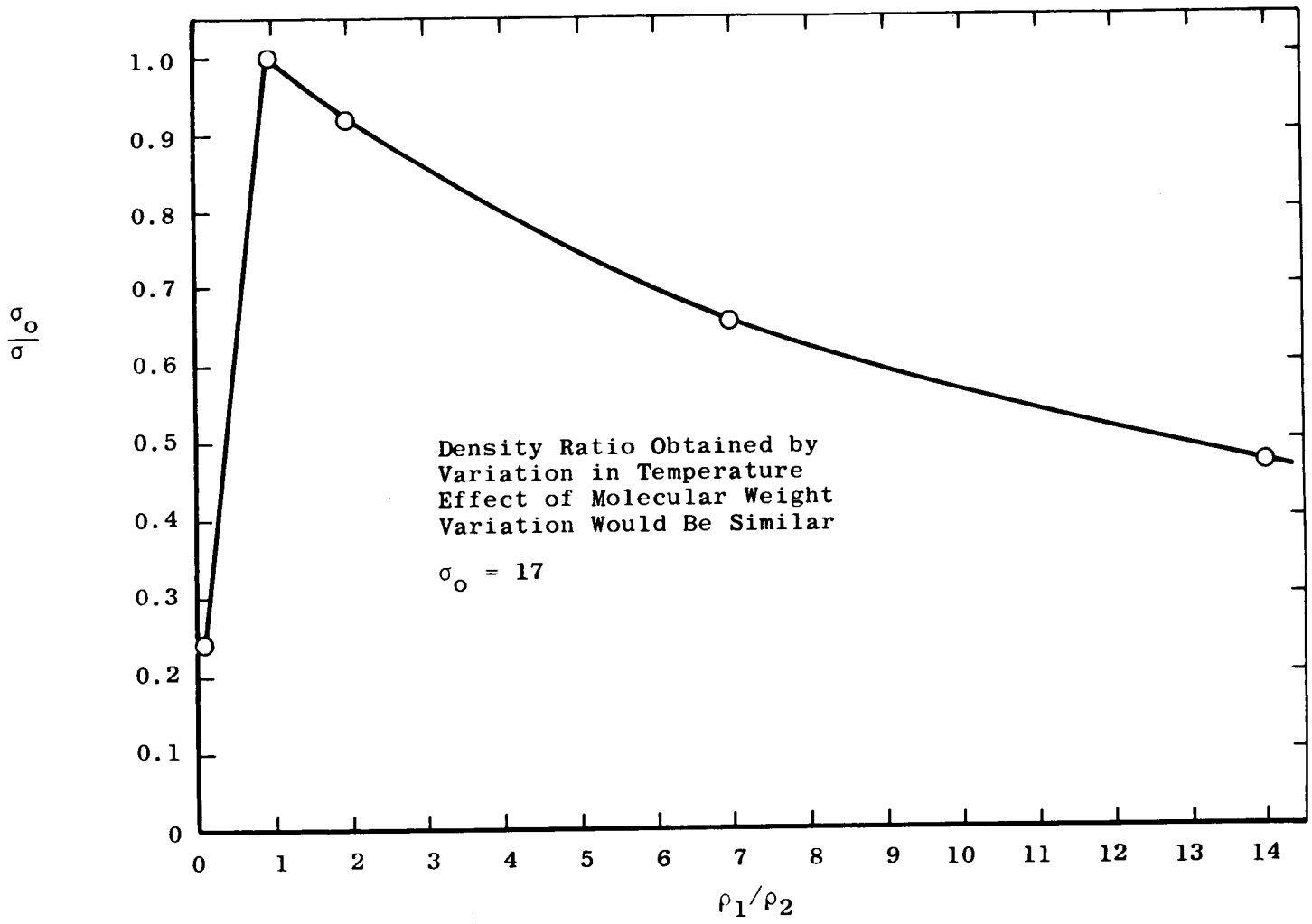

Figure 6.- Predicted variation of ratio of spread parameter to its constant-density value with density ratio for test case 3, two-dimensional shear layer with $u_2/u_1 = 0.2$.

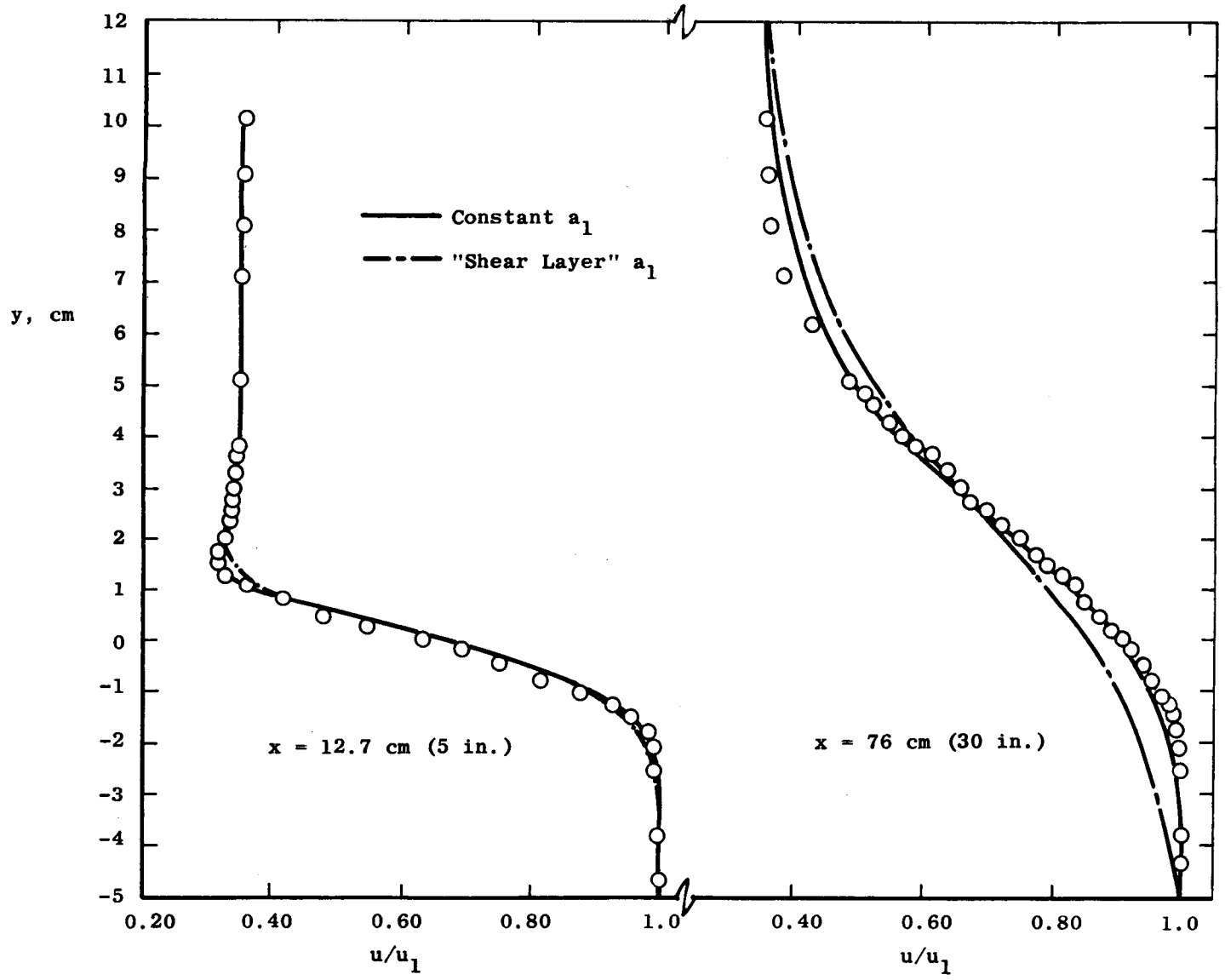

Figure 7.- Comparison of experimental and theoretical velocity profiles for test case 4, incompressible two-dimensional two-stream mixing with $u_2/u_1 = 0.357$.

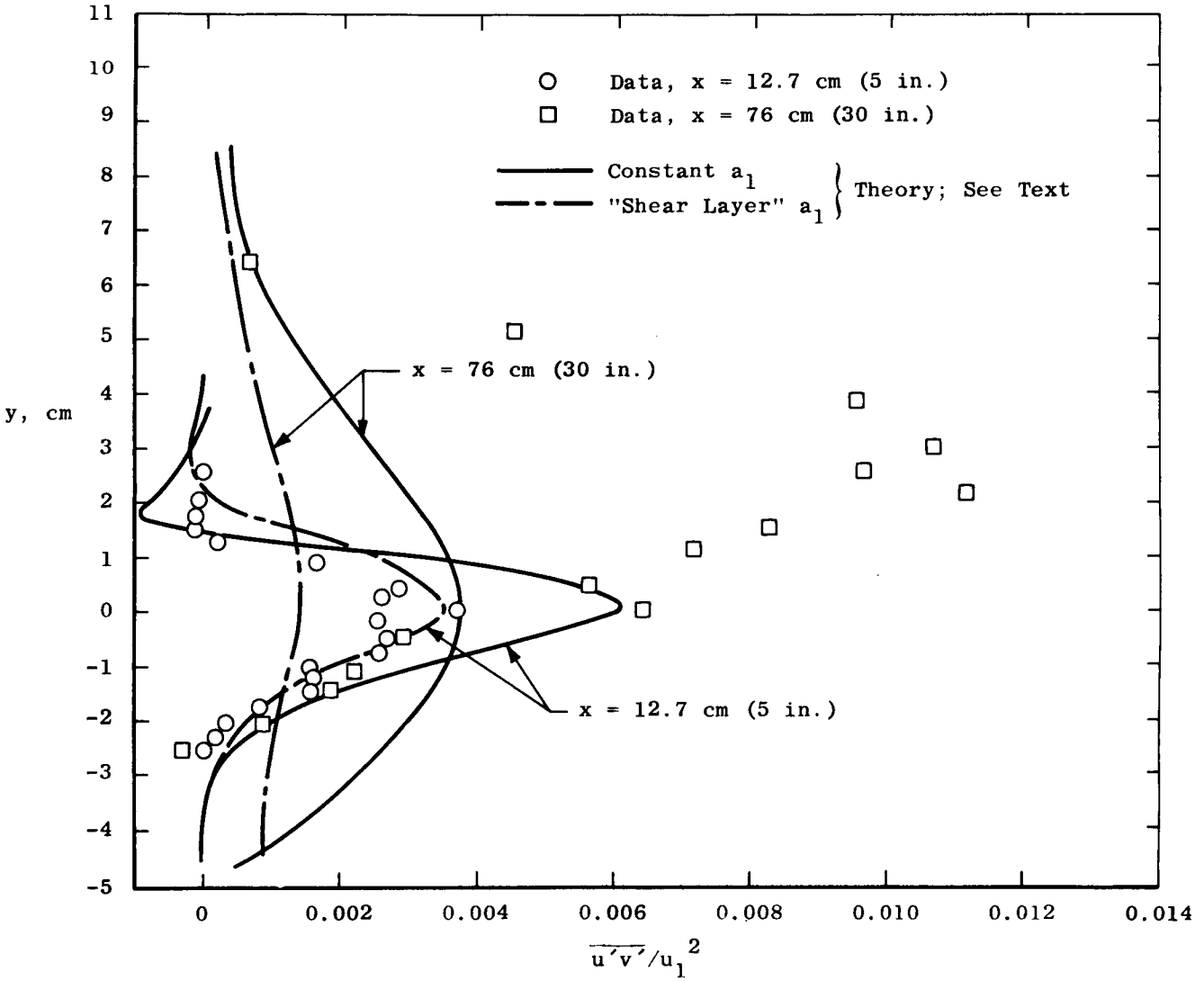

Figure 8.- Comparison of theoretical predictions of turbulent shear stress with experimental data for test case 4.

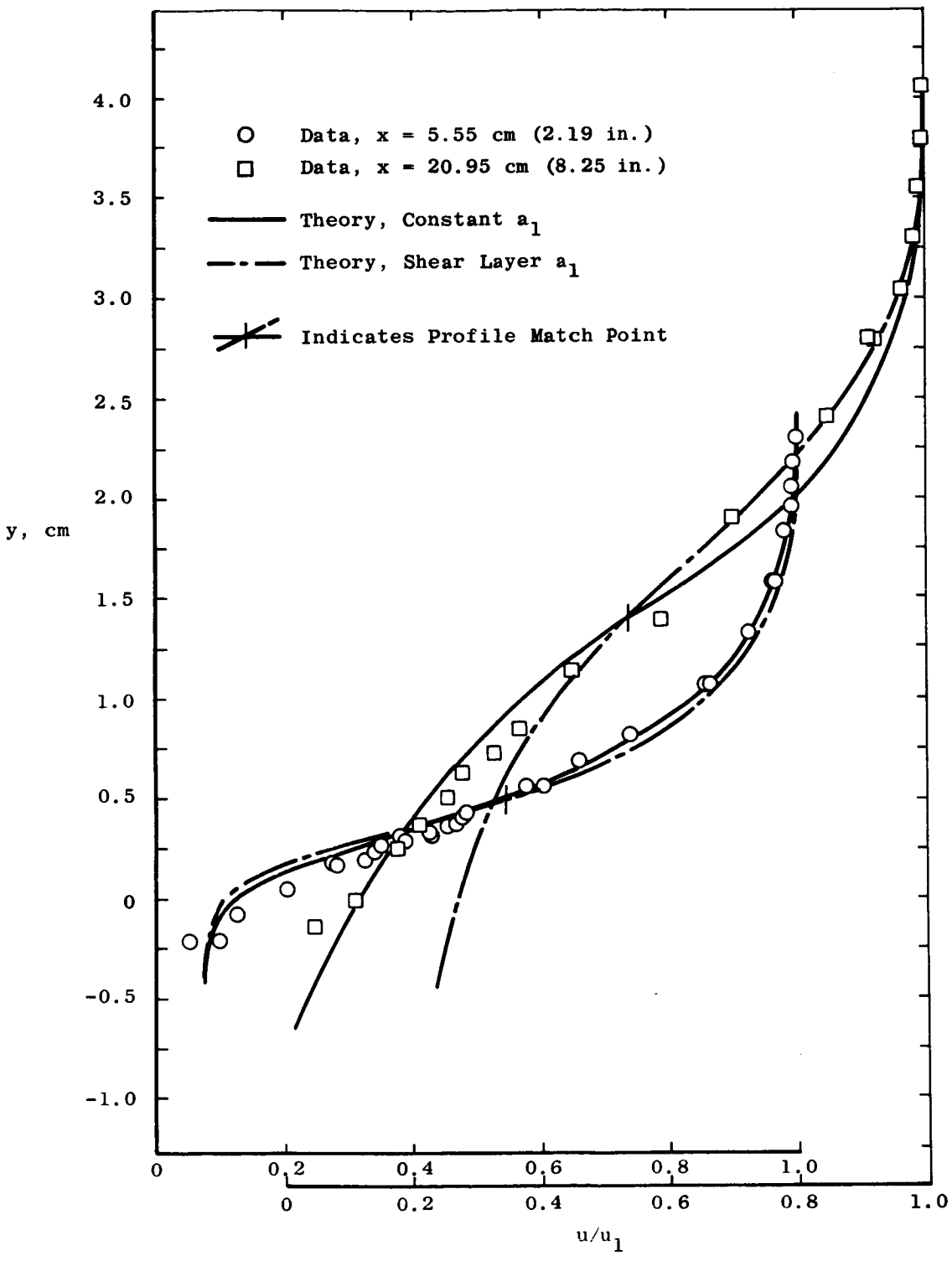

Figure 9.- Comparison of theoretical and experimental profiles for test case 5, compressible two-dimensional shear layer.

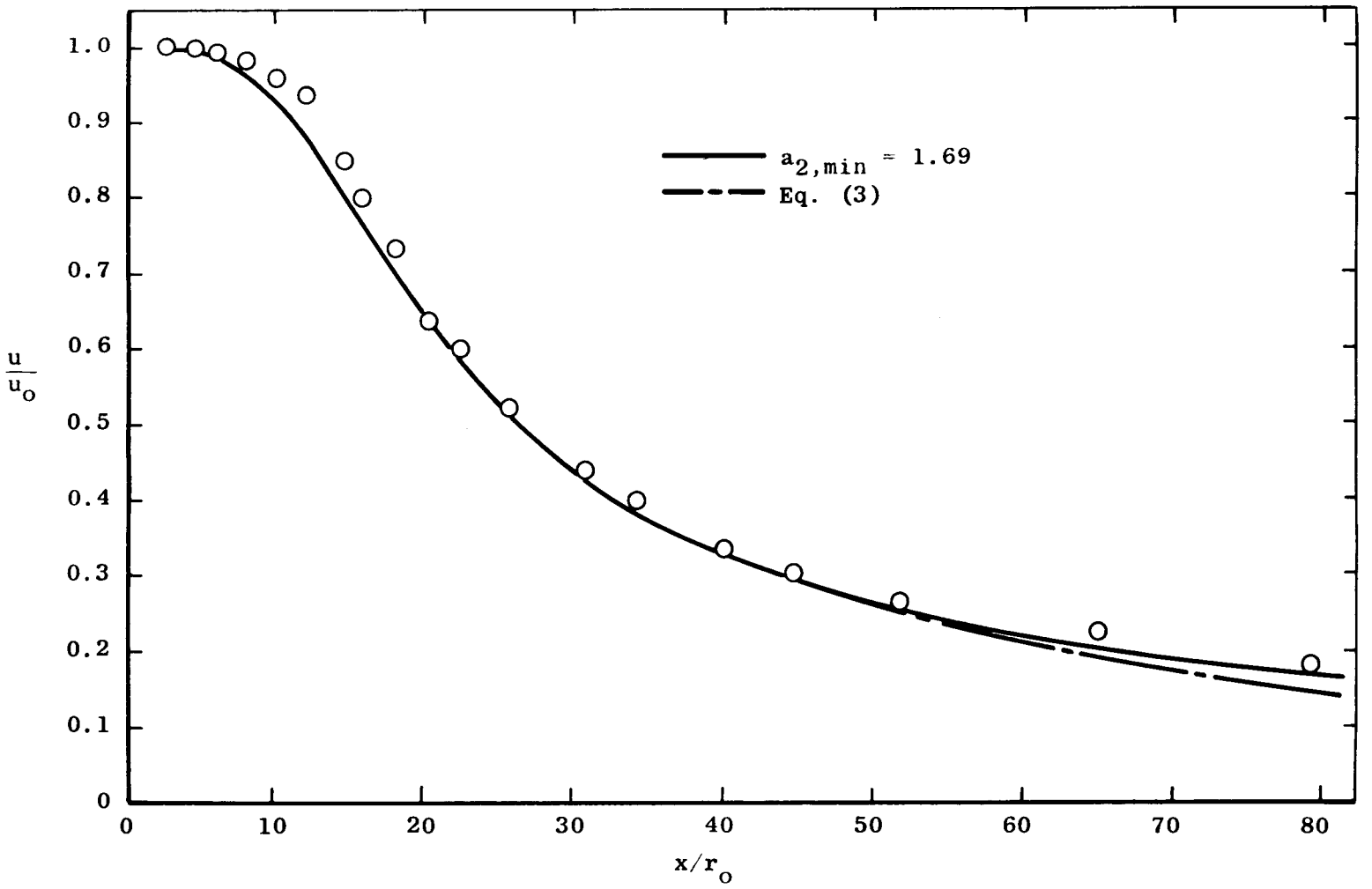

Figure 10.- Comparison of theoretical and experimental center-line velocity decay for test case 6, circular jet.

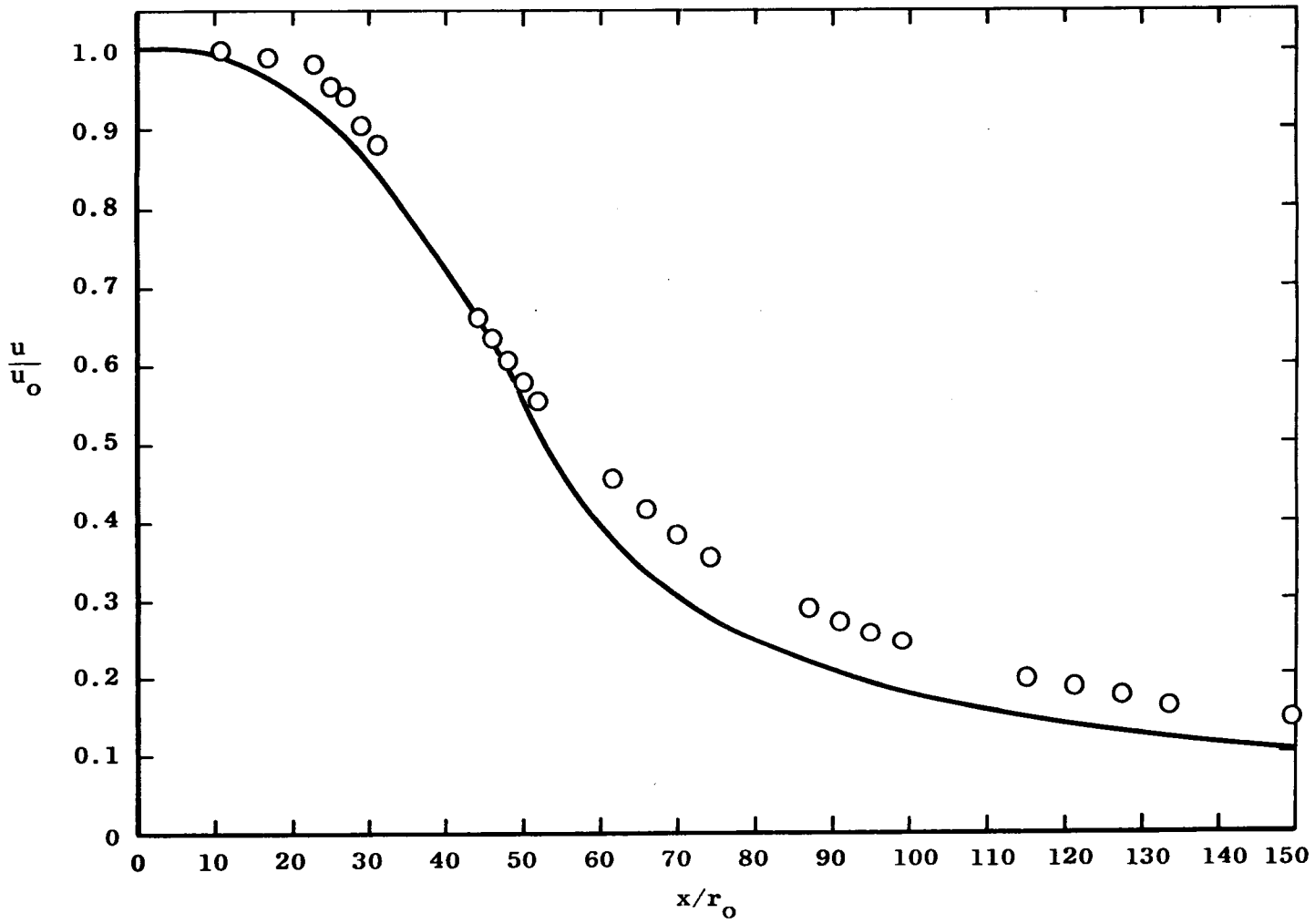

Figure 11.- Comparison of experimental and theoretical center-line velocity decay for test case 7, $M_o = 2.22$ circular jet.

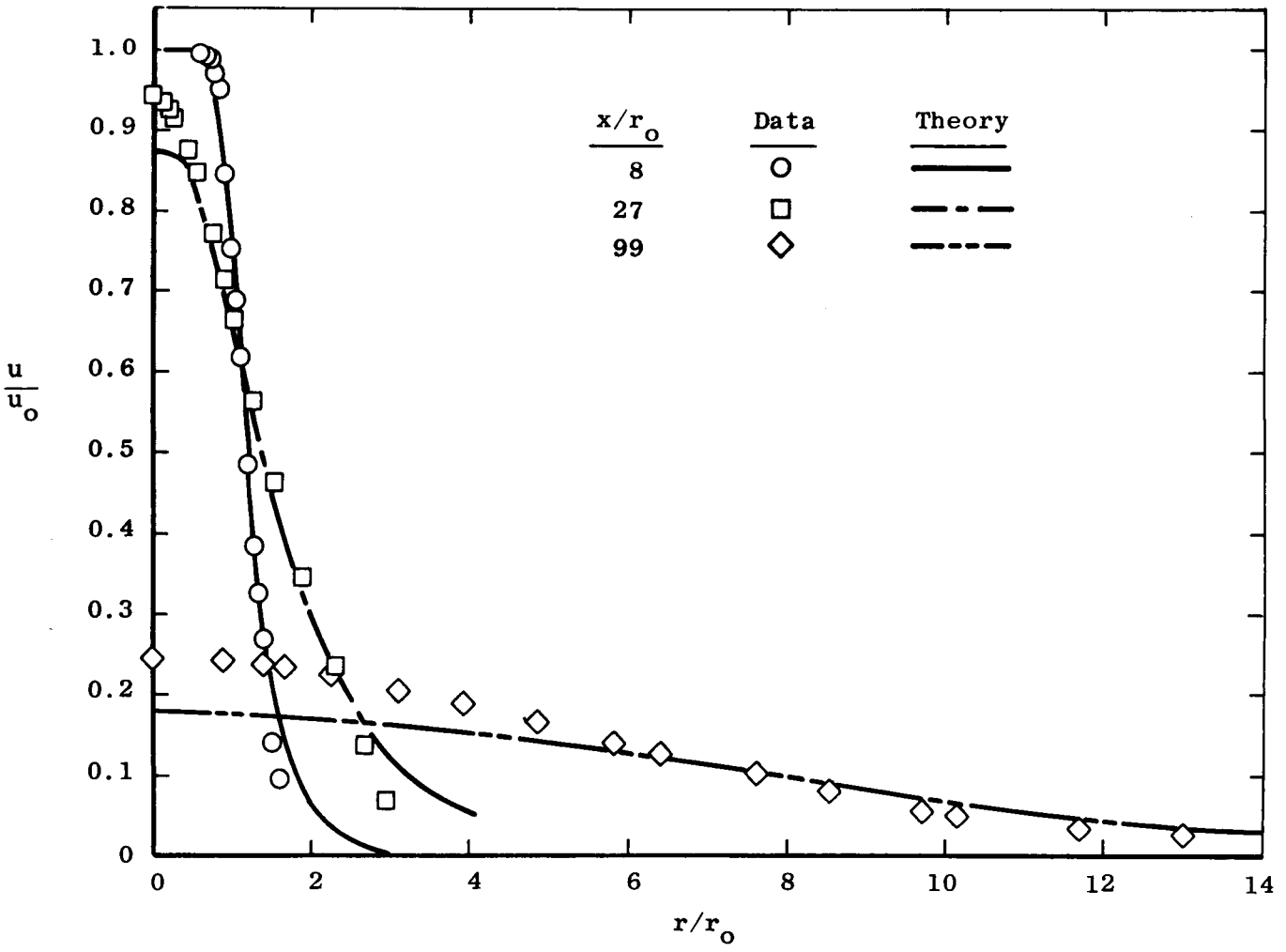

Figure 12.- Comparison of theoretical and experimental velocity profiles for test case 7, $M_o = 2.22$ circular jet. Data from reference 8.

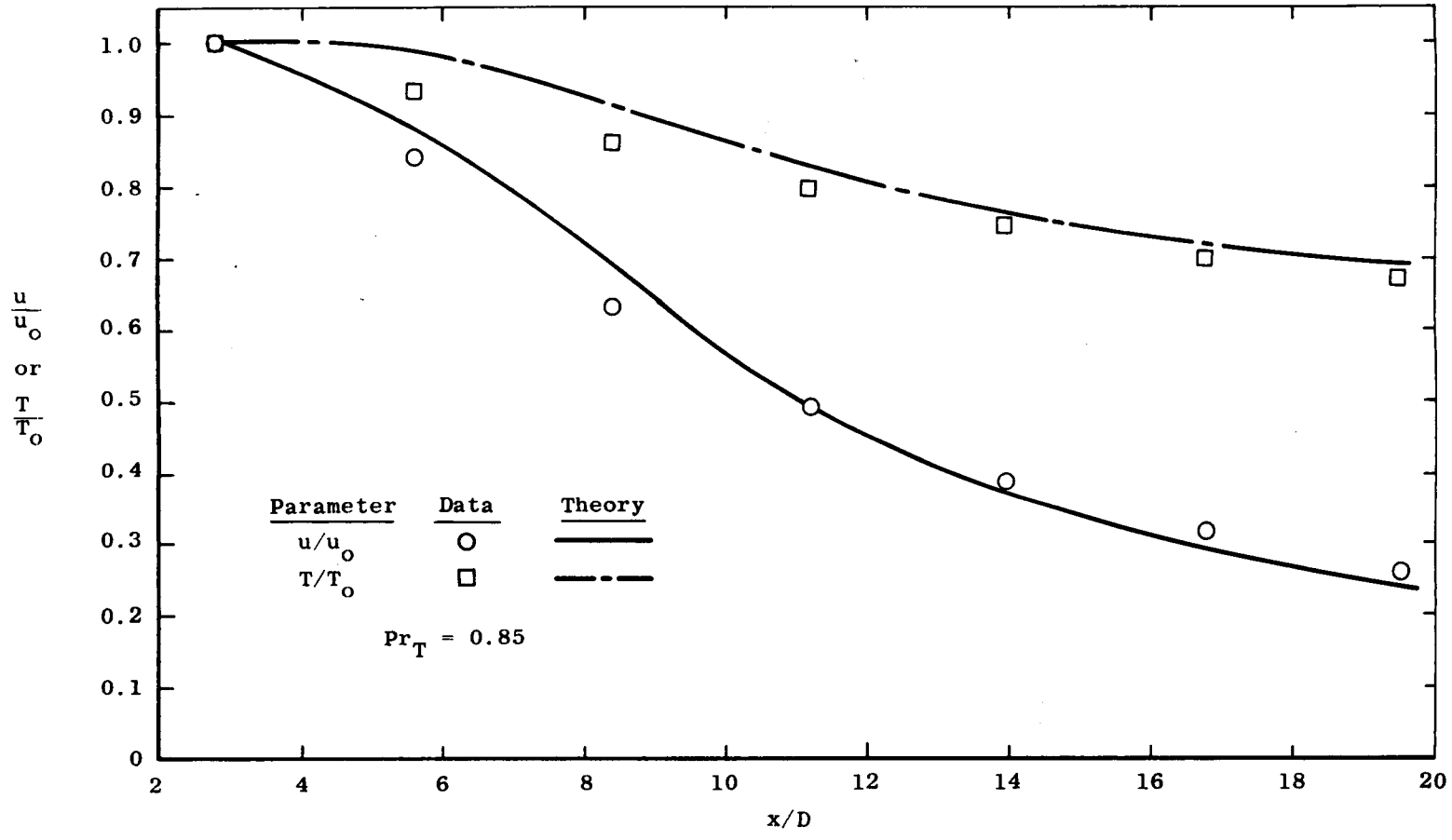

Figure 13.- Comparison of experimental and theoretical decay of center-line velocity and static temperature for test case 8, $M_o = 0.7$ circular jet.

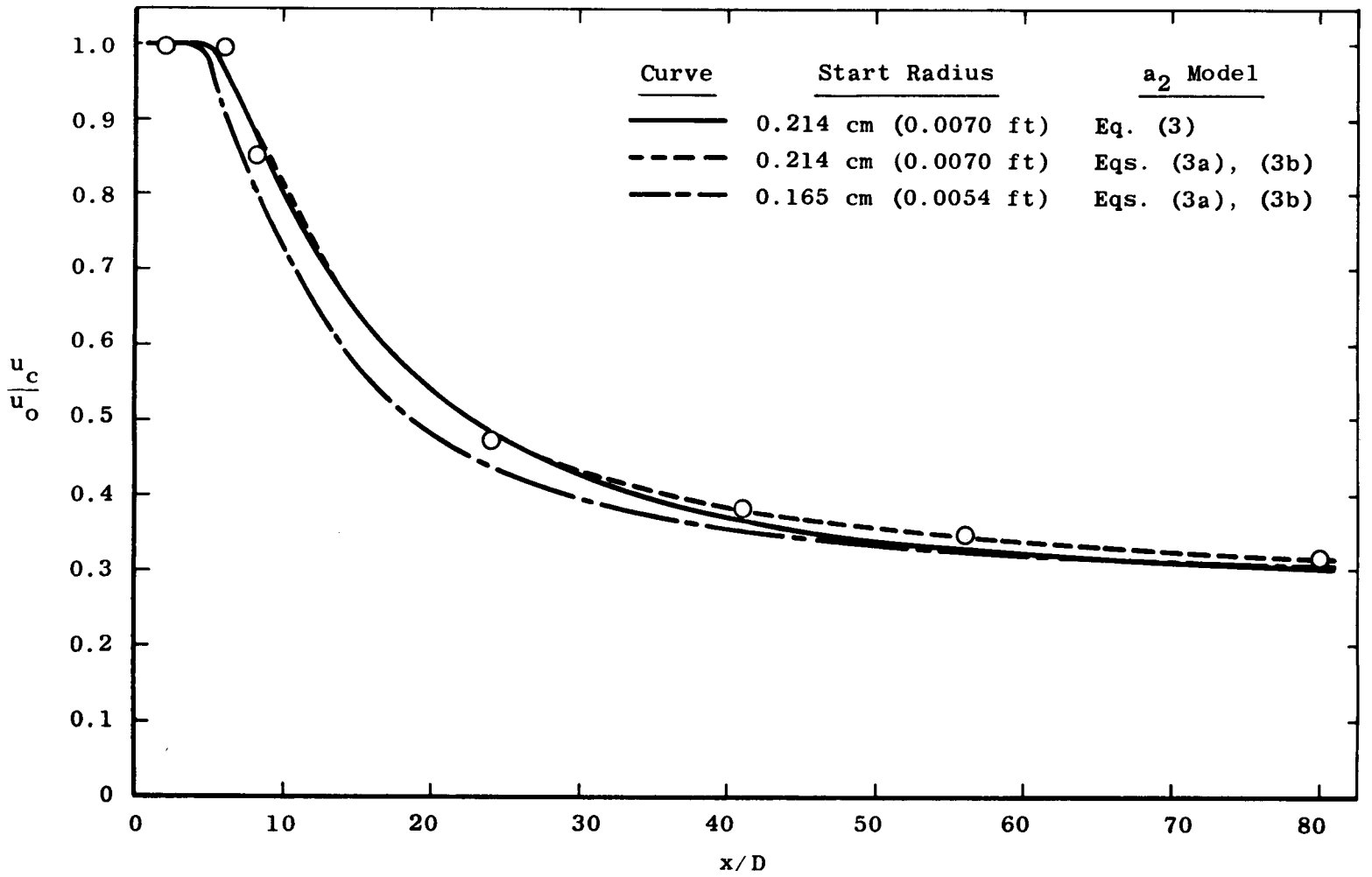

Figure 14.- Comparison of calculated center-line velocity with experiment for test case 9, coaxial air jets with He trace.

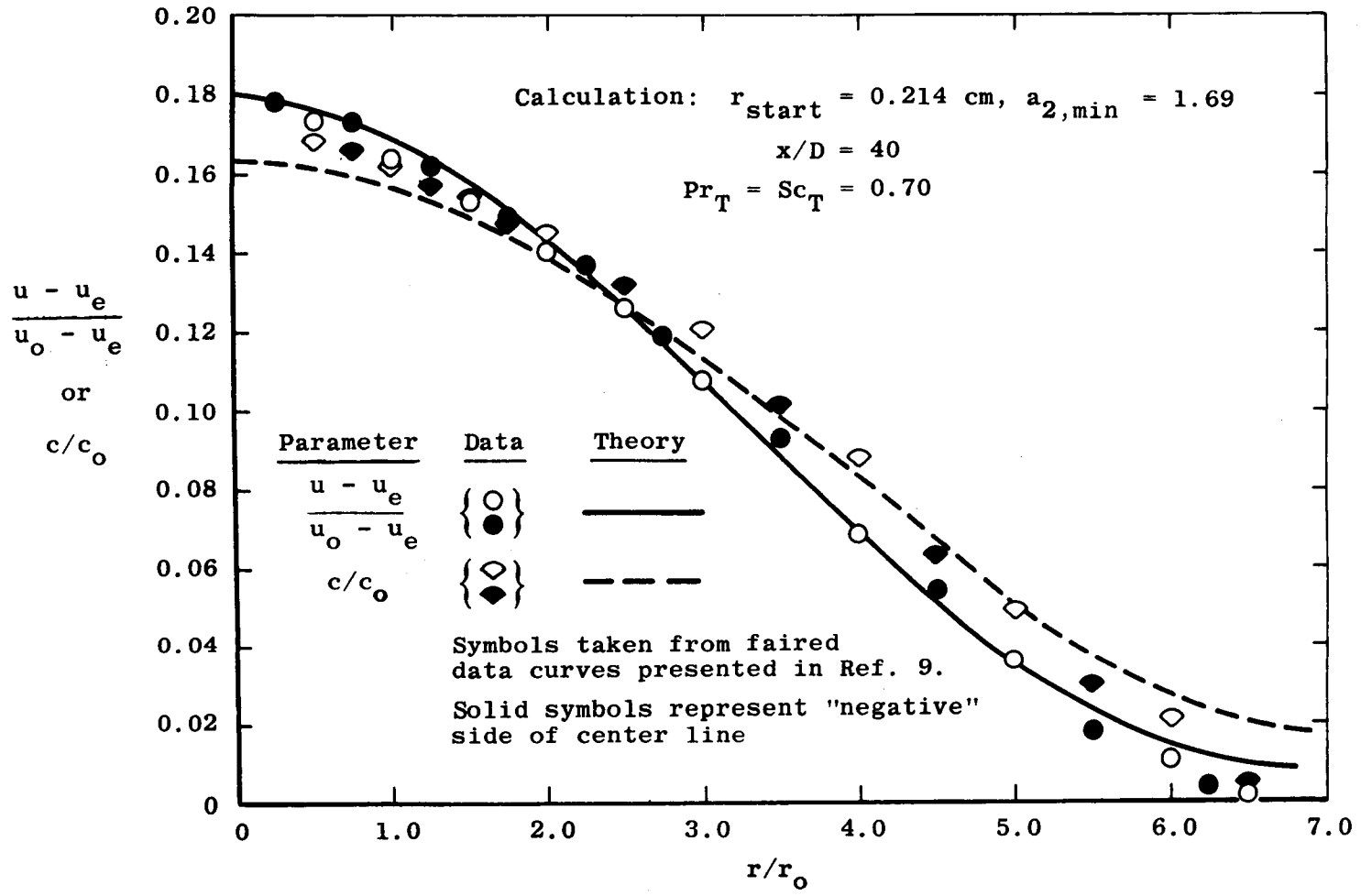

Figure 15.- Comparison of theoretical and experimental velocity and concentration profiles for test case 9.

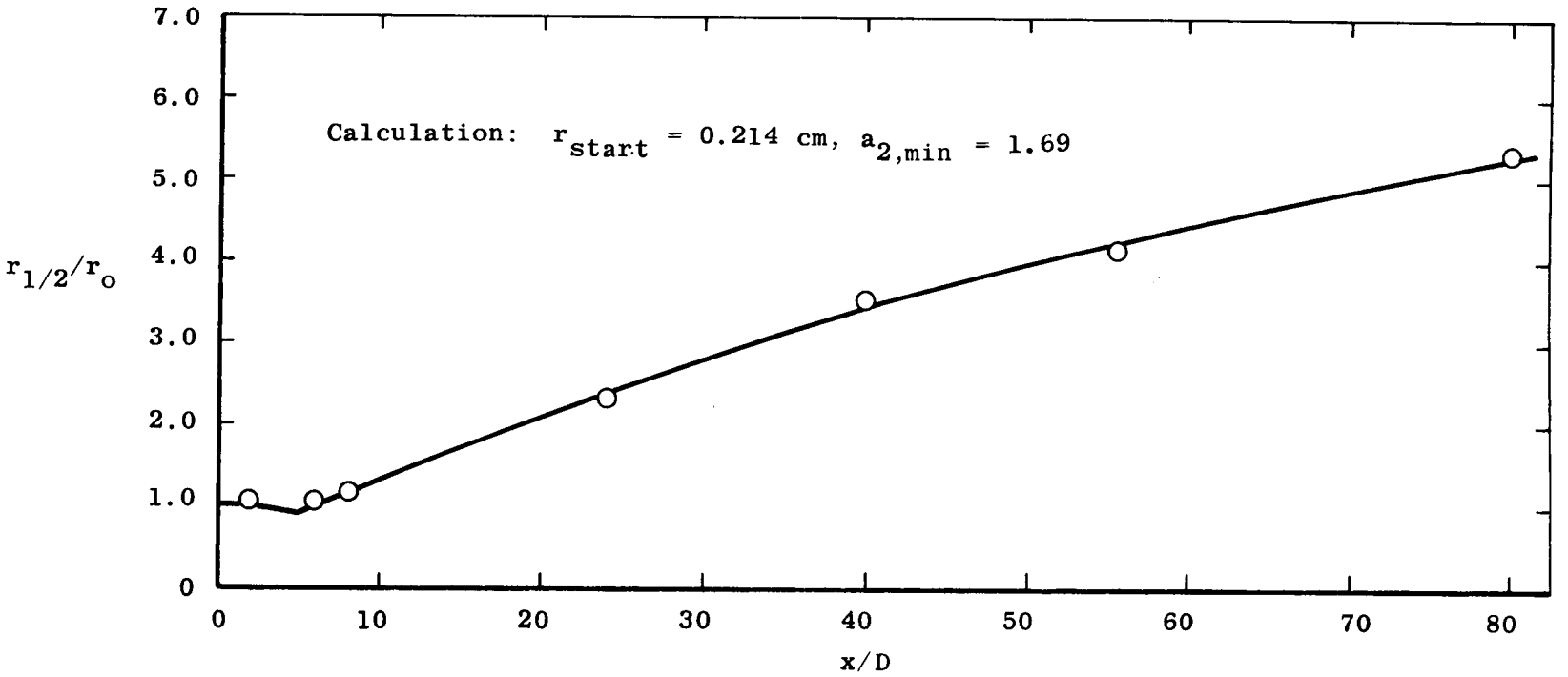

Figure 16.- Comparison of predicted and experimental half-velocity radius for test case 9.

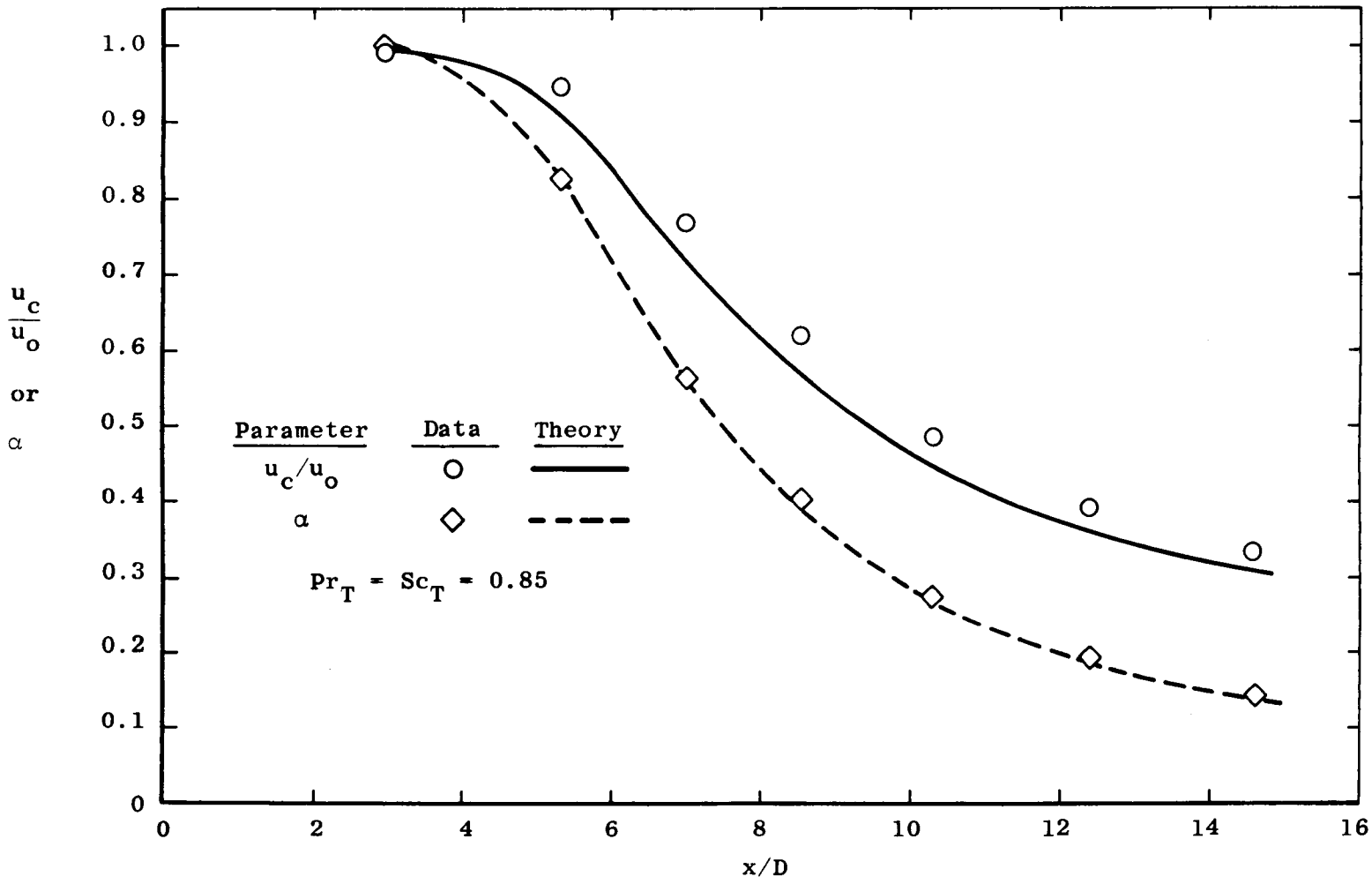

Figure 17.- Comparison of theoretical prediction of center-line decay with experimental data for test case 10, H_2-air jets.

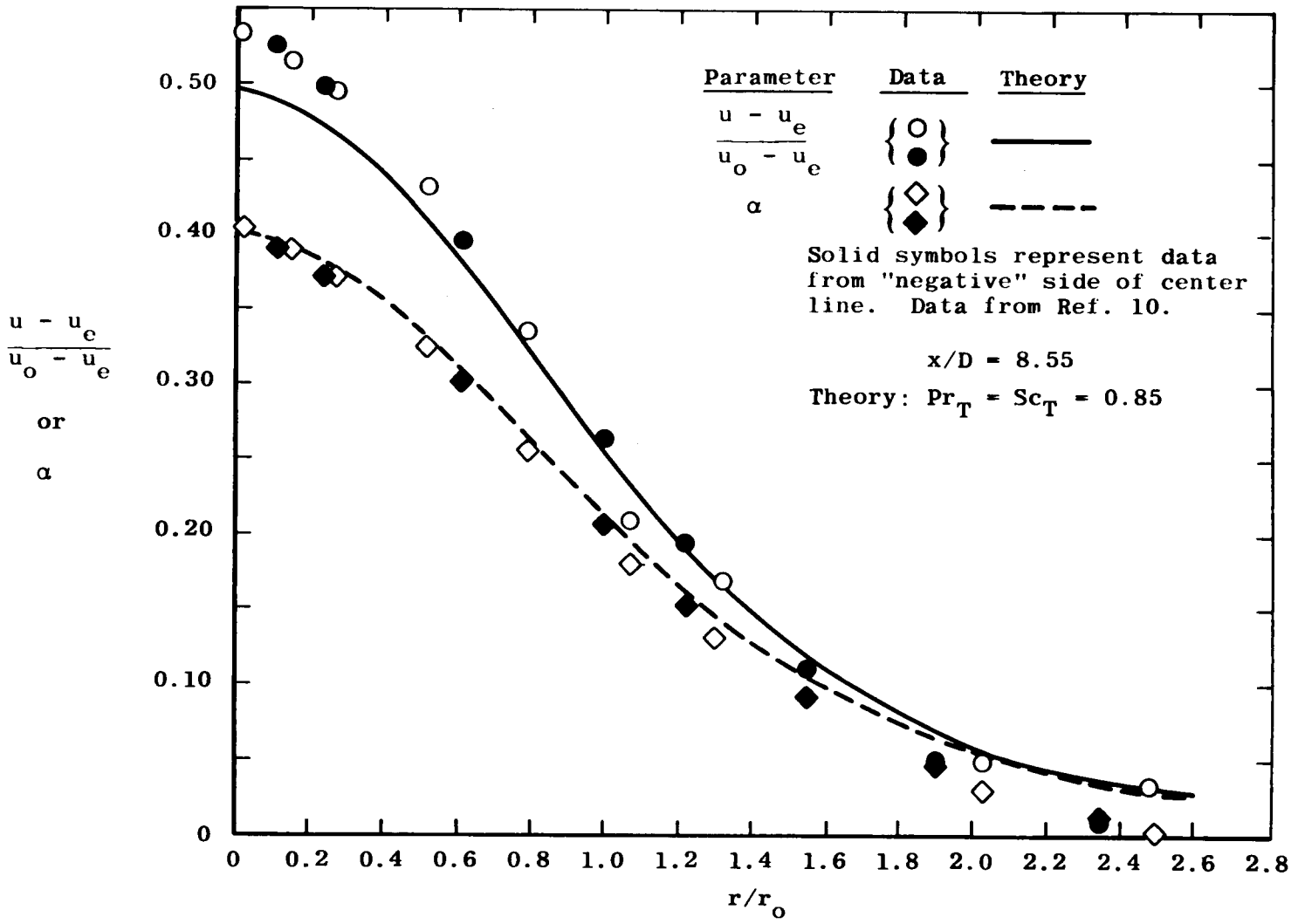

Figure 18.- Comparison of predicted and experimental radial profiles for test case 10, coaxial H_2-air.

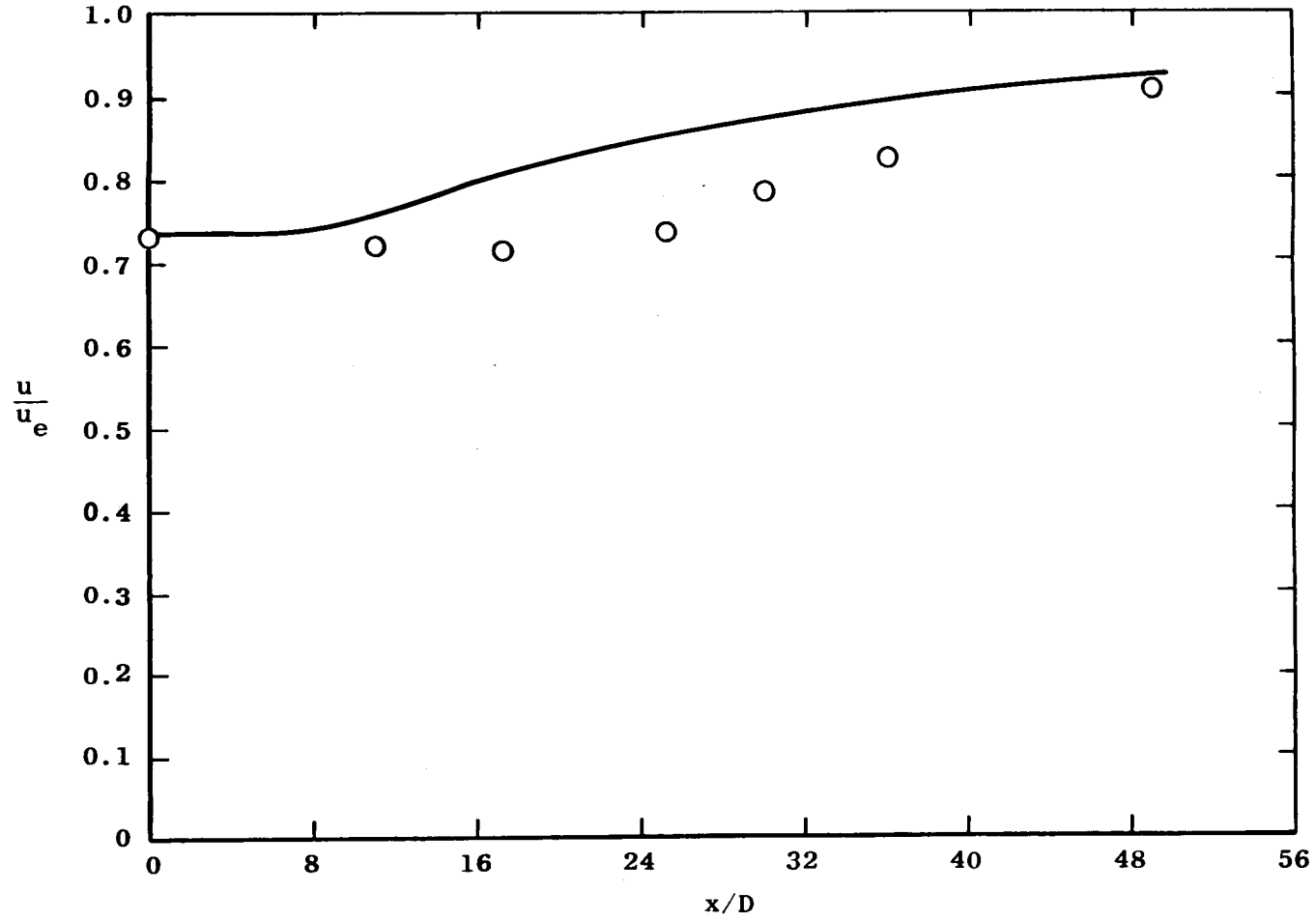

Figure 19.- Comparison of theoretical and experimental center-line velocity ratio for test case 11, axisymmetric jet in moving stream $M_o = 0.90$, $M_e = 1.30$.

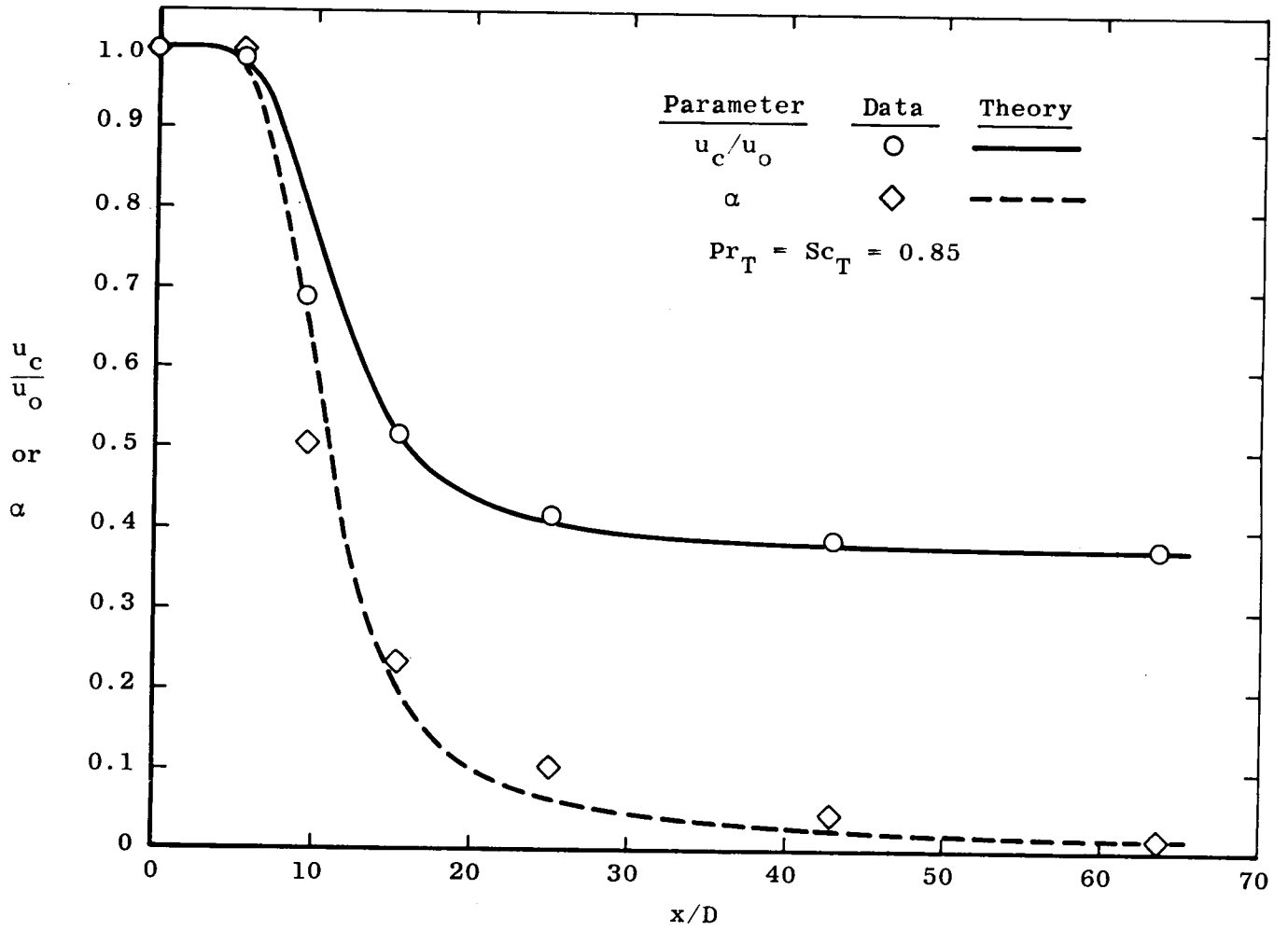

Figure 20.- Comparison of center-line velocity and jet species concentration decay predictions with experiment for test case 12, coaxial H_2-air jets.

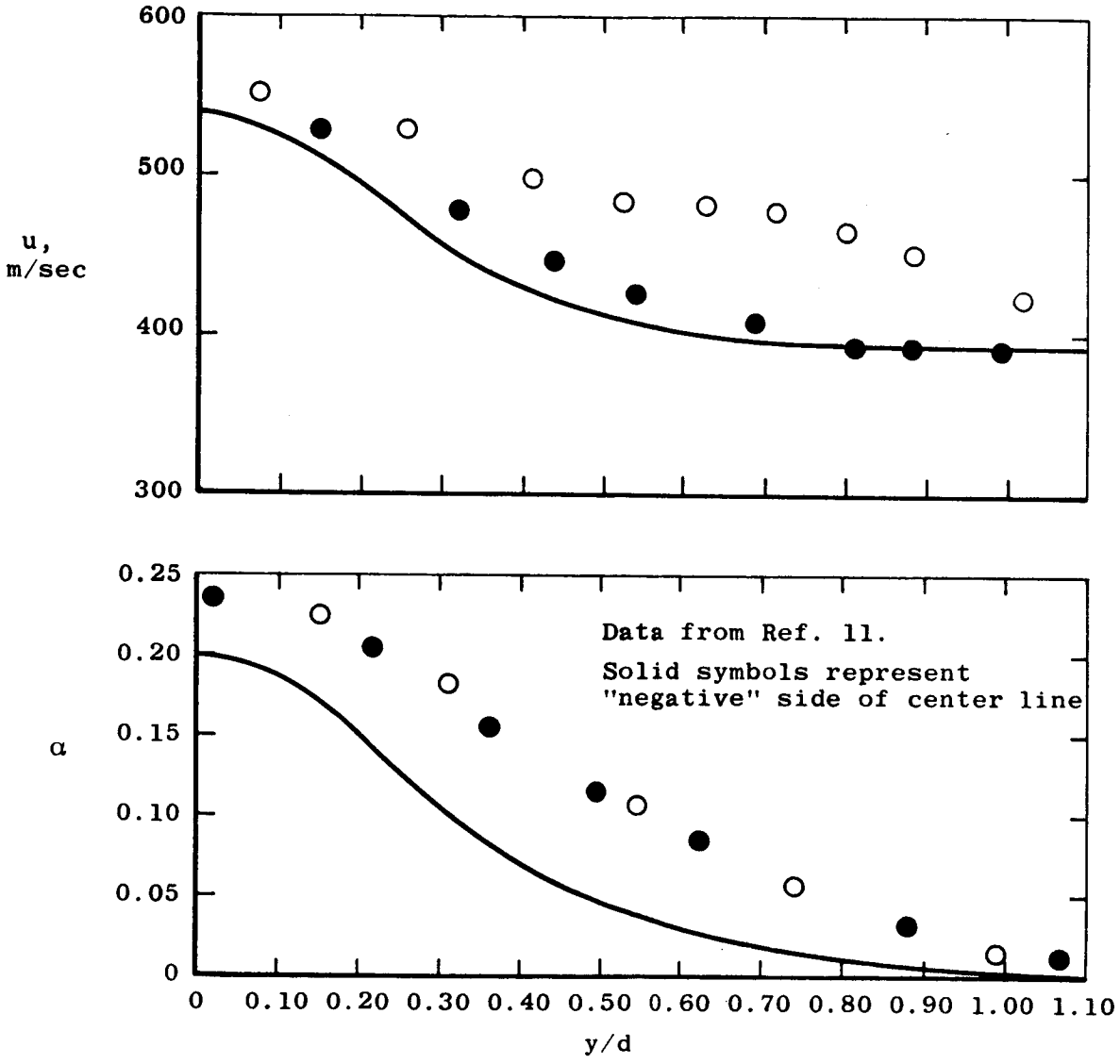

Figure 21.- Comparison of theoretical and experimental profiles for test case 12. x/D = 15.4.

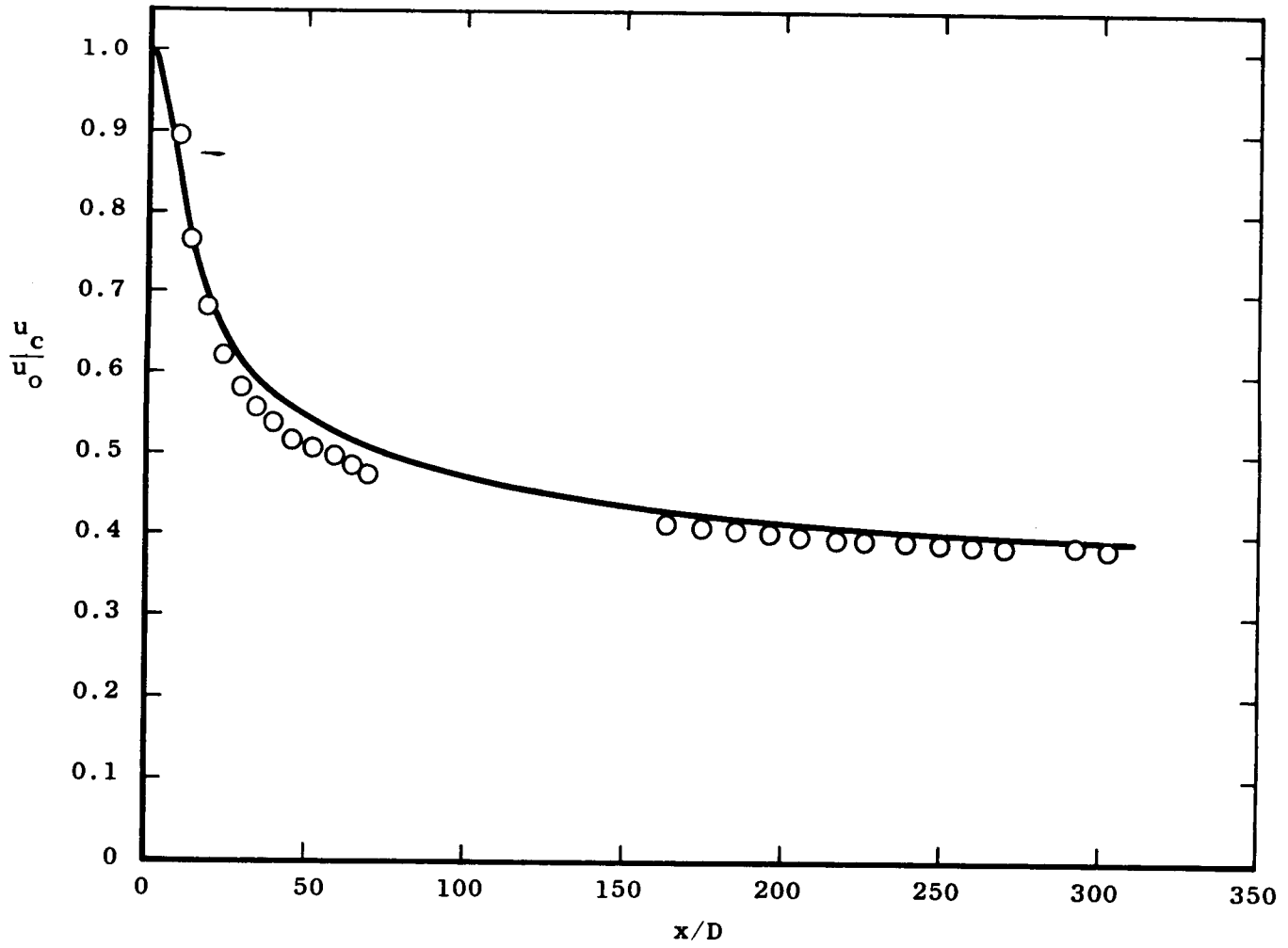

Figure 22.- Comparison of center-line velocity prediction with data for test case 13, two-dimensional jet with $u_o/u_e = 3.29$.

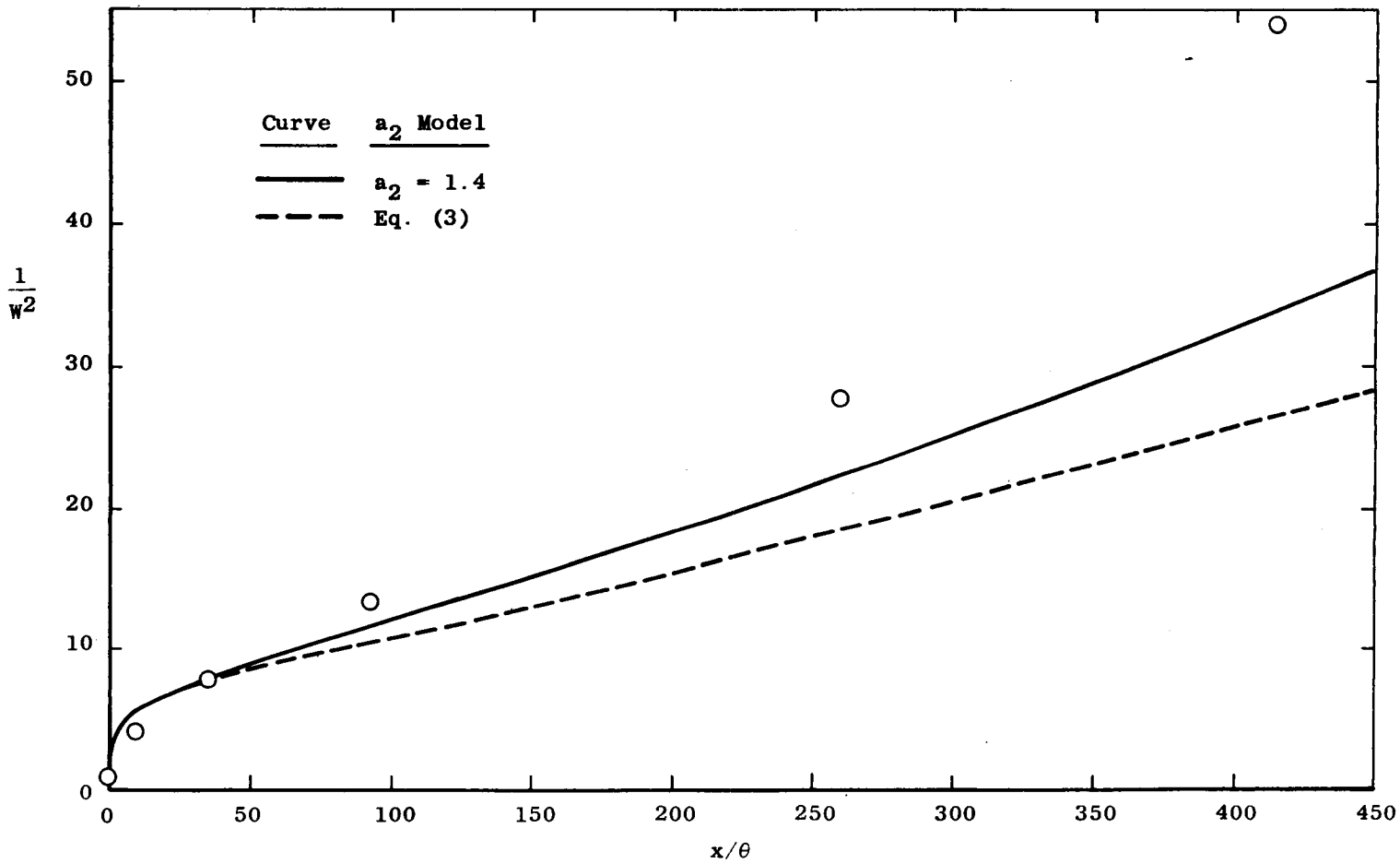

Figure 23.- Comparison of experimental center-line velocity increase with prediction for test case 14, two-dimensional wake.

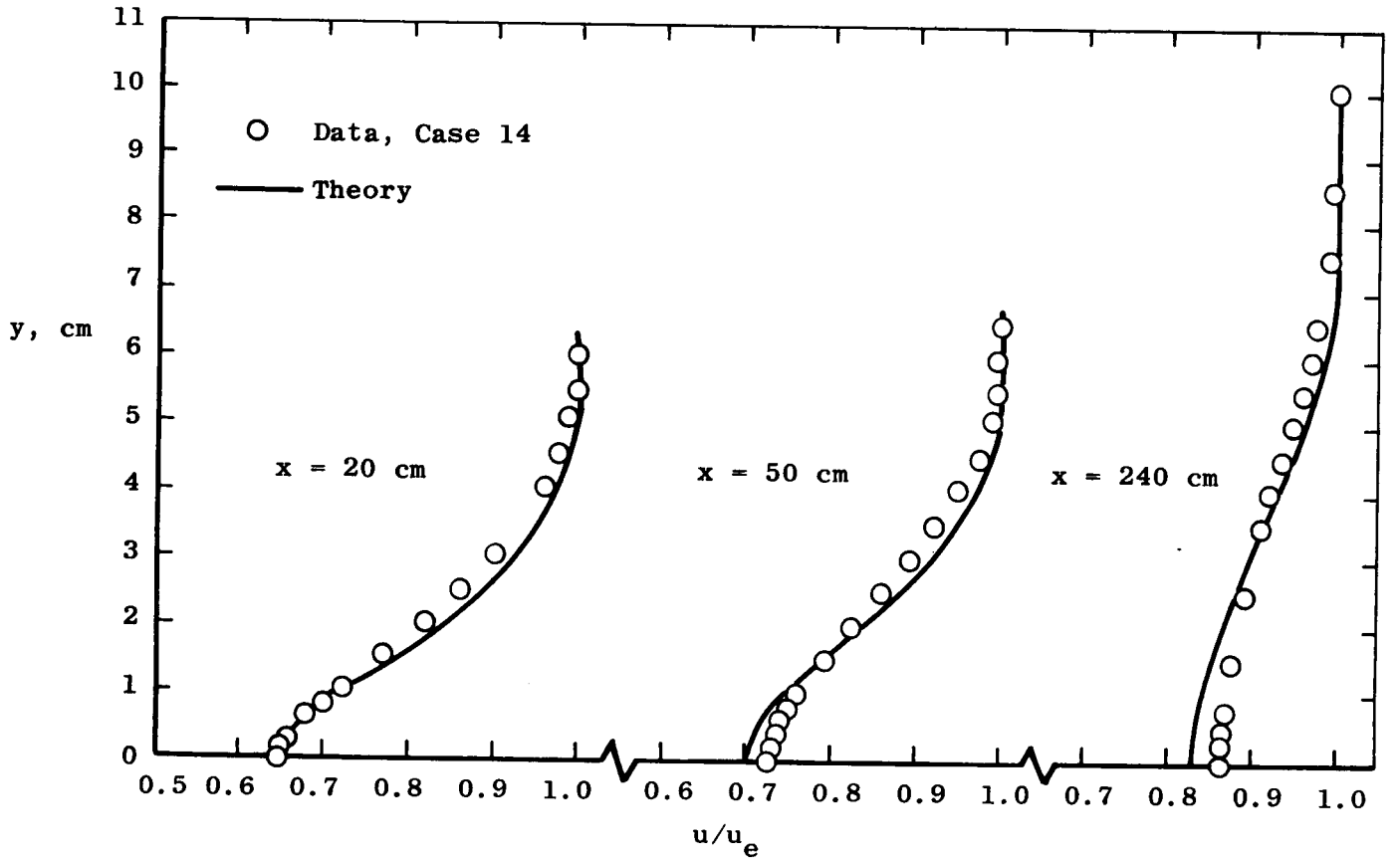

Figure 24.- Comparison of predicted velocity profiles with experimental data for test case 14, two-dimensional wake.

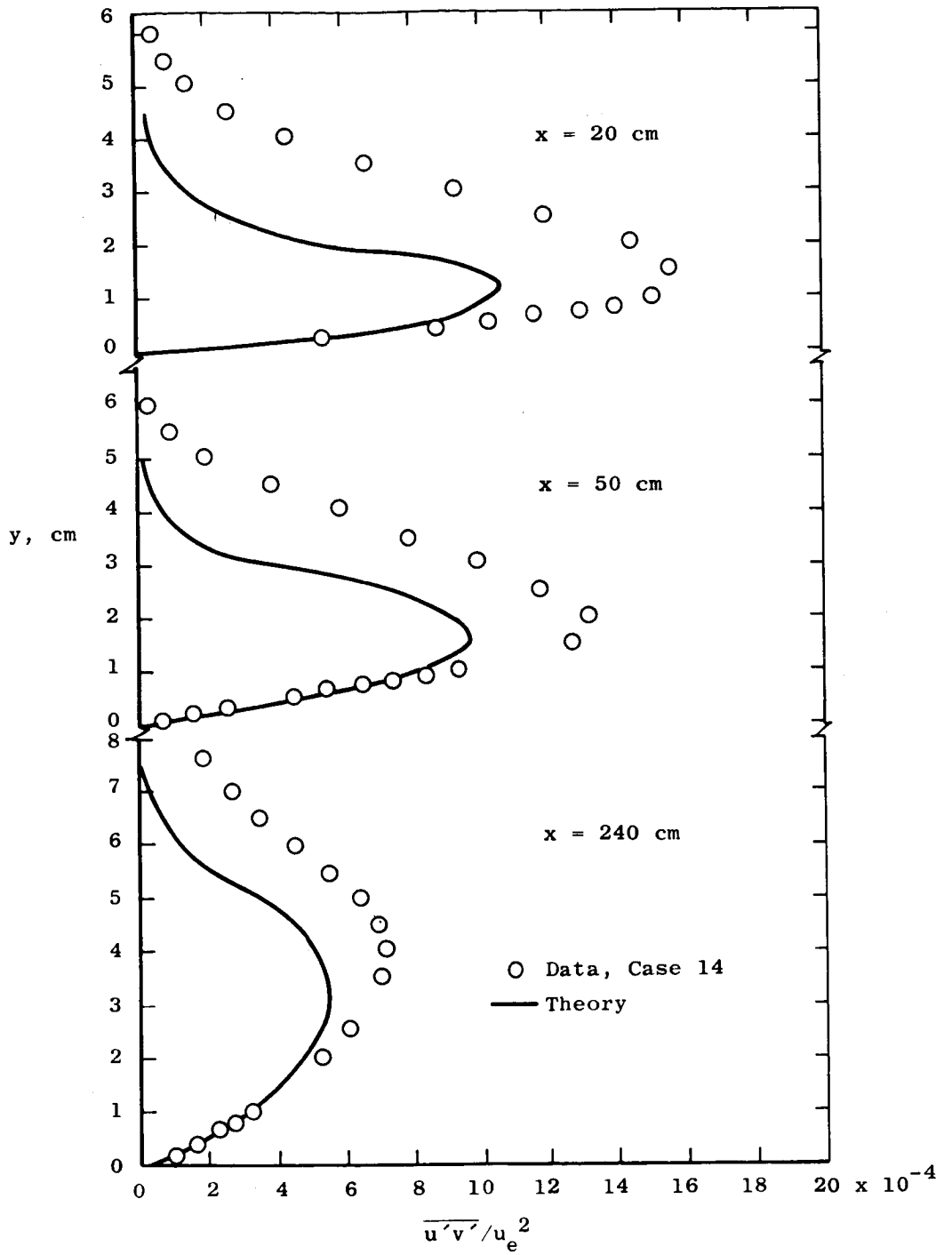

Figure 25.- Comparison of predicted turbulent shear stress with experimental data for test case 14.

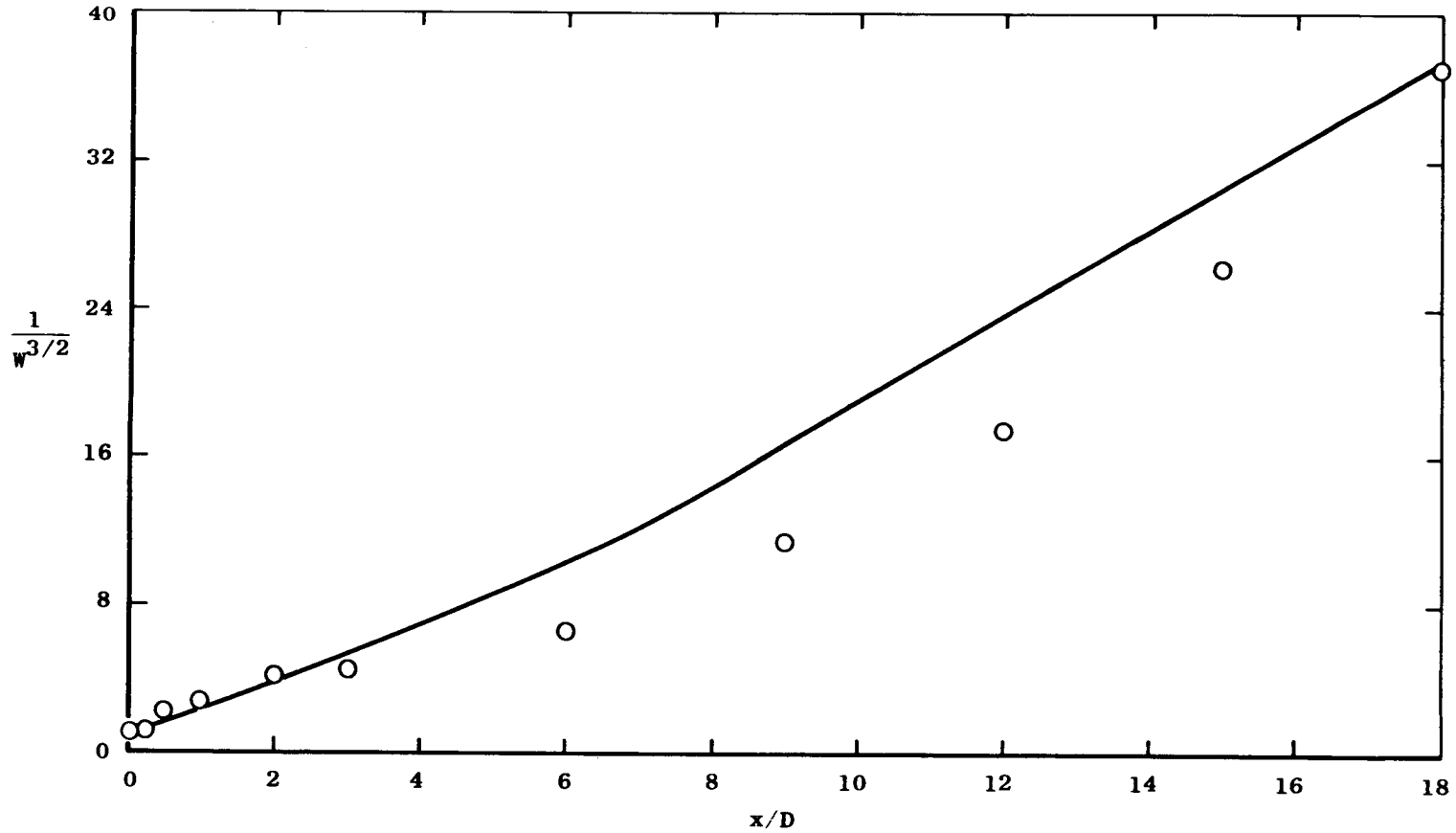

Figure 26.- Comparison of theoretical prediction of center-line velocity with experiment for test case 15, axisymmetric wake.

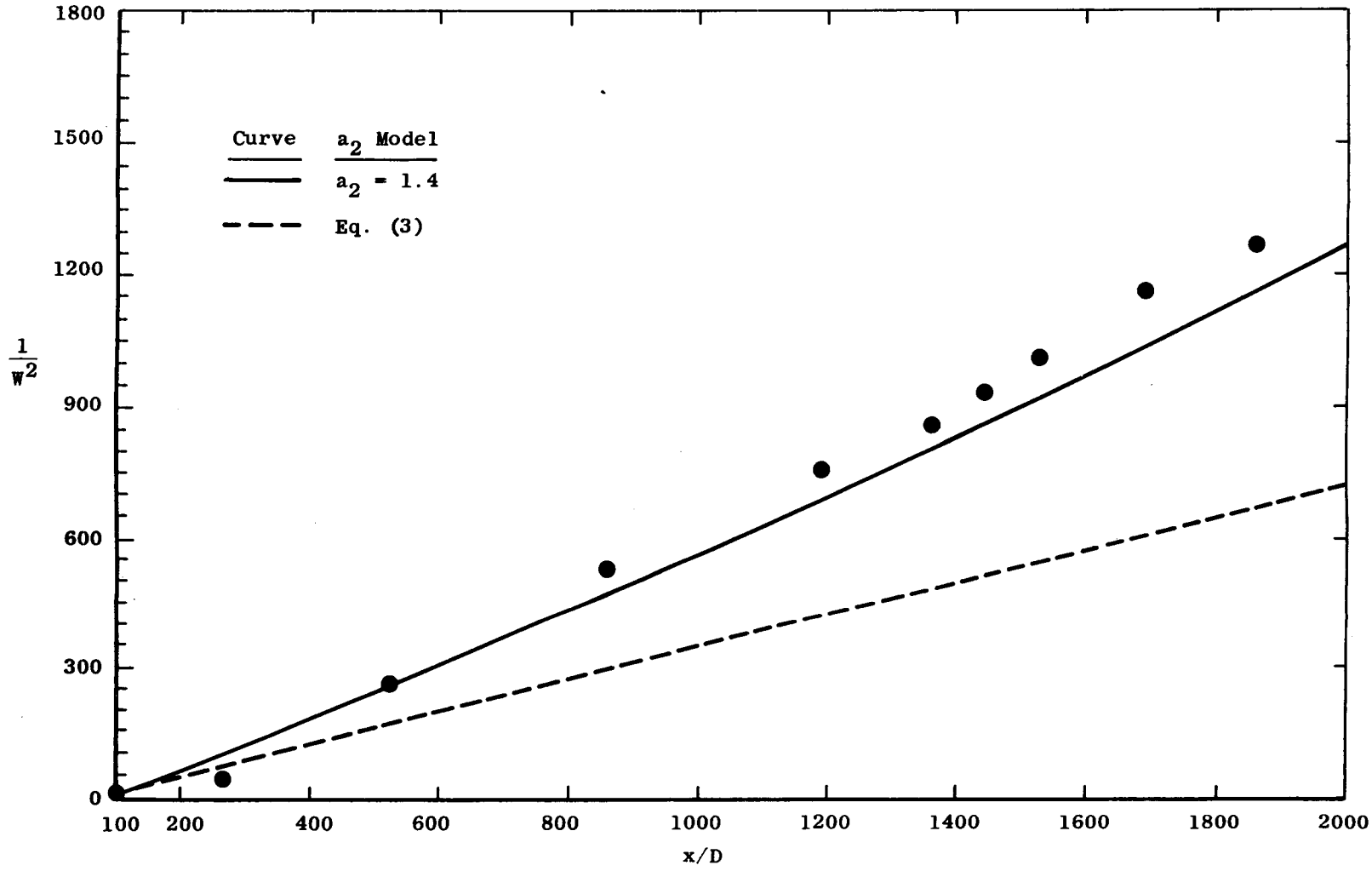

Figure 27.- Comparison of calculated and experimental center-line velocities for test case 16, compressible plane wake, D = 0.00909 cm.

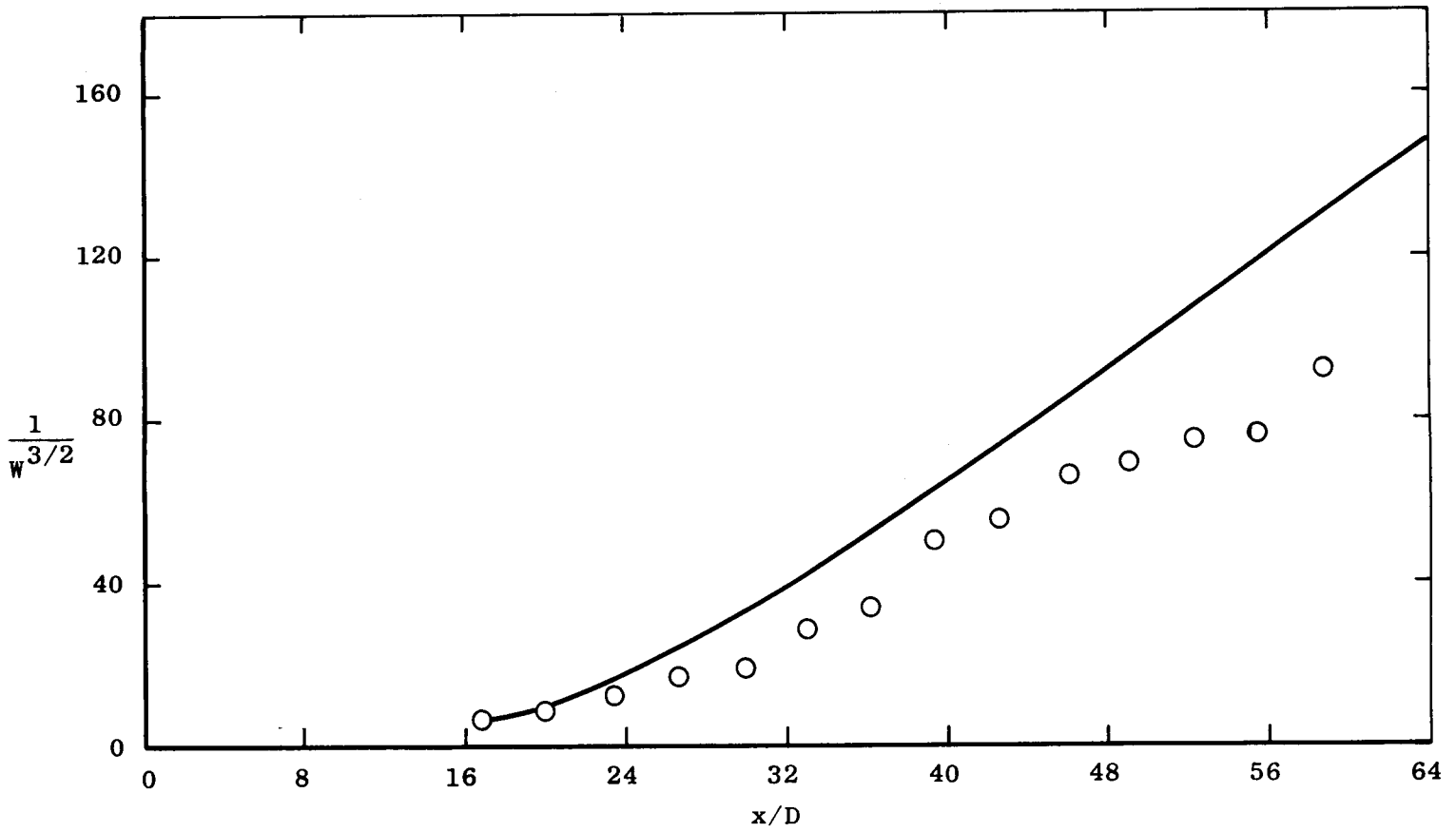

Figure 28.- Comparison of theoretical and experimental center-line velocity ratio for test case 17, compressible axisymmetric wake.

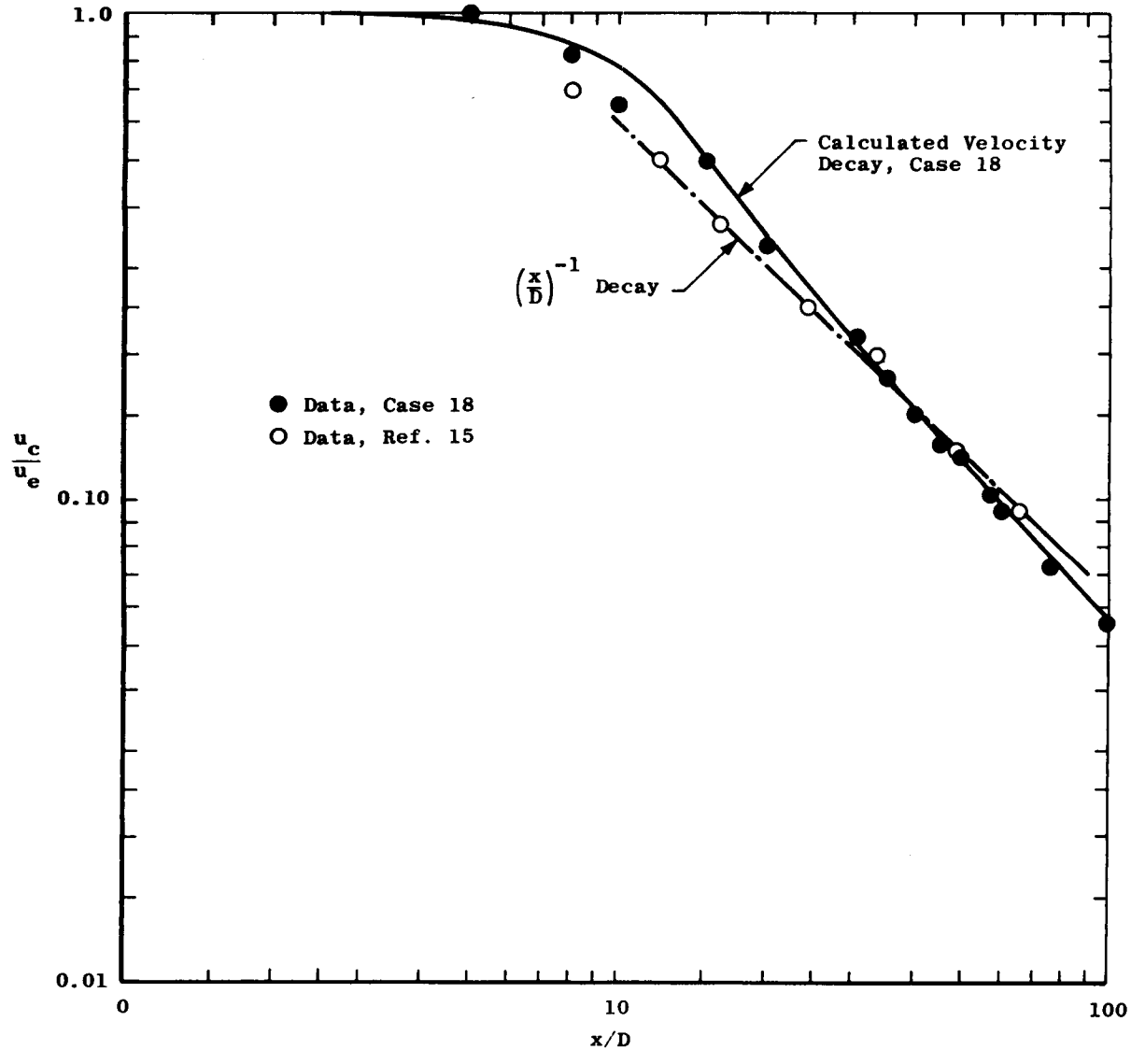

Figure 29.- Comparison of theoretical and experimental center-line velocity decay for test case 18, asymptotic jet.

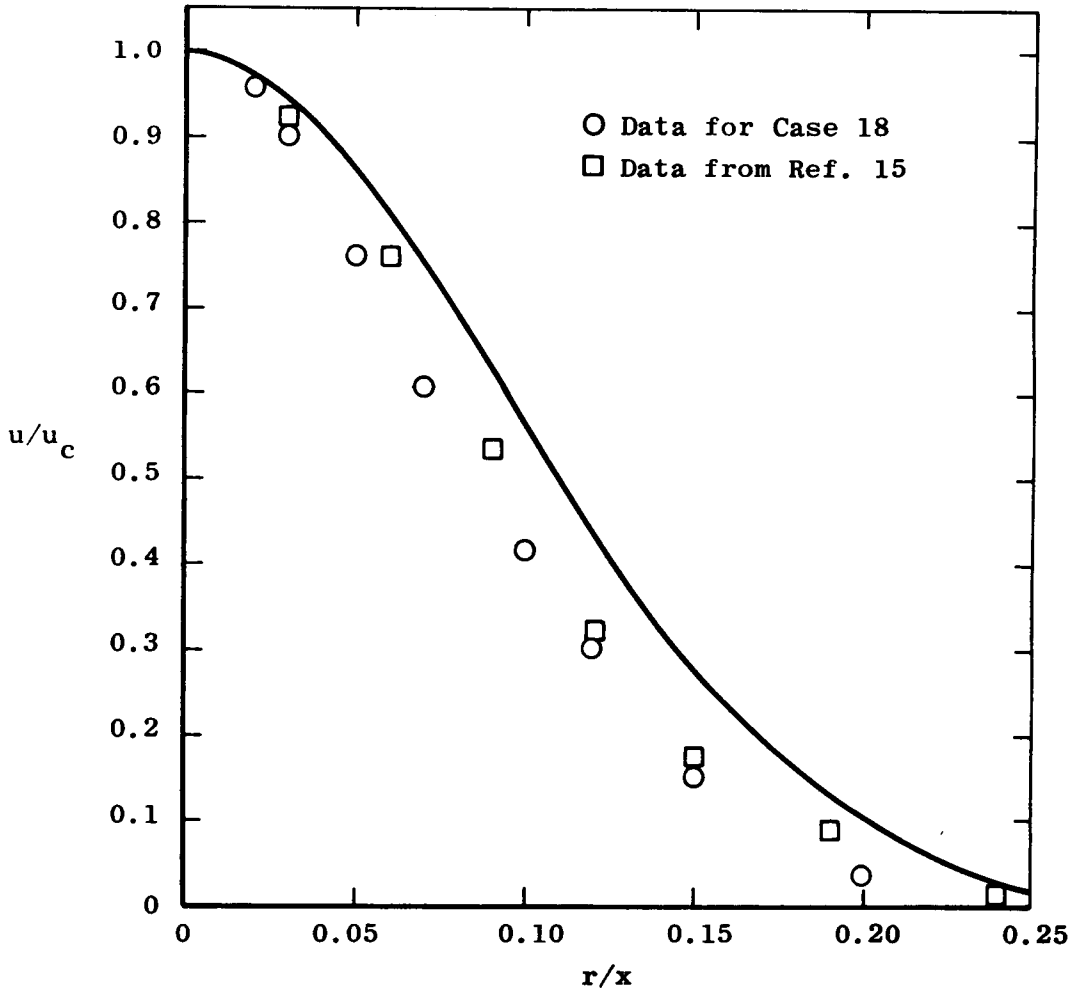

Figure 30.- Comparison of theoretical and experimental axial velocity profiles for test case 18, circular jet.

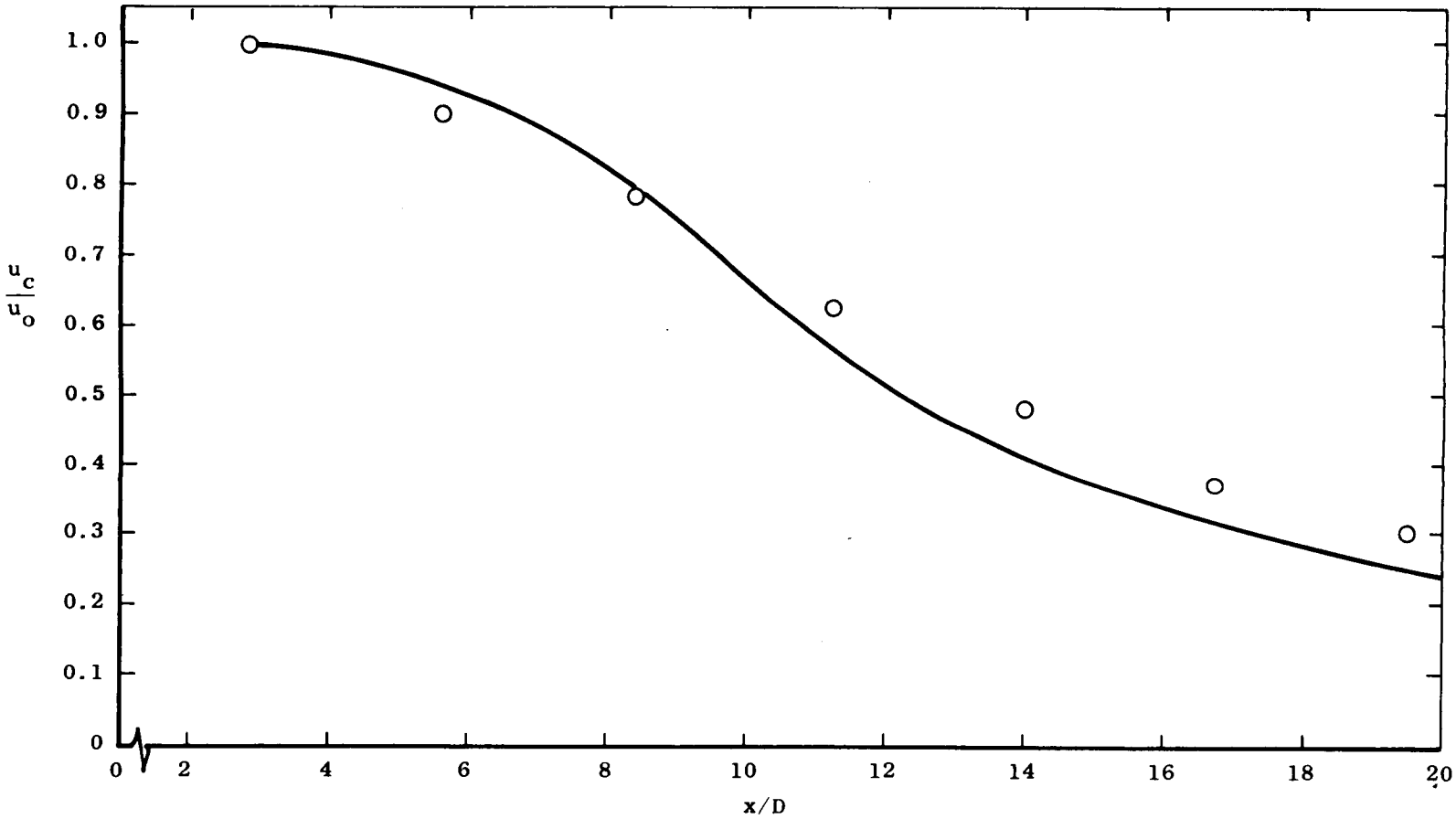

Figure 31.- Comparison of predicted center-line velocity decay with experiment for test case 19, $M_o = 1.4$ jet.

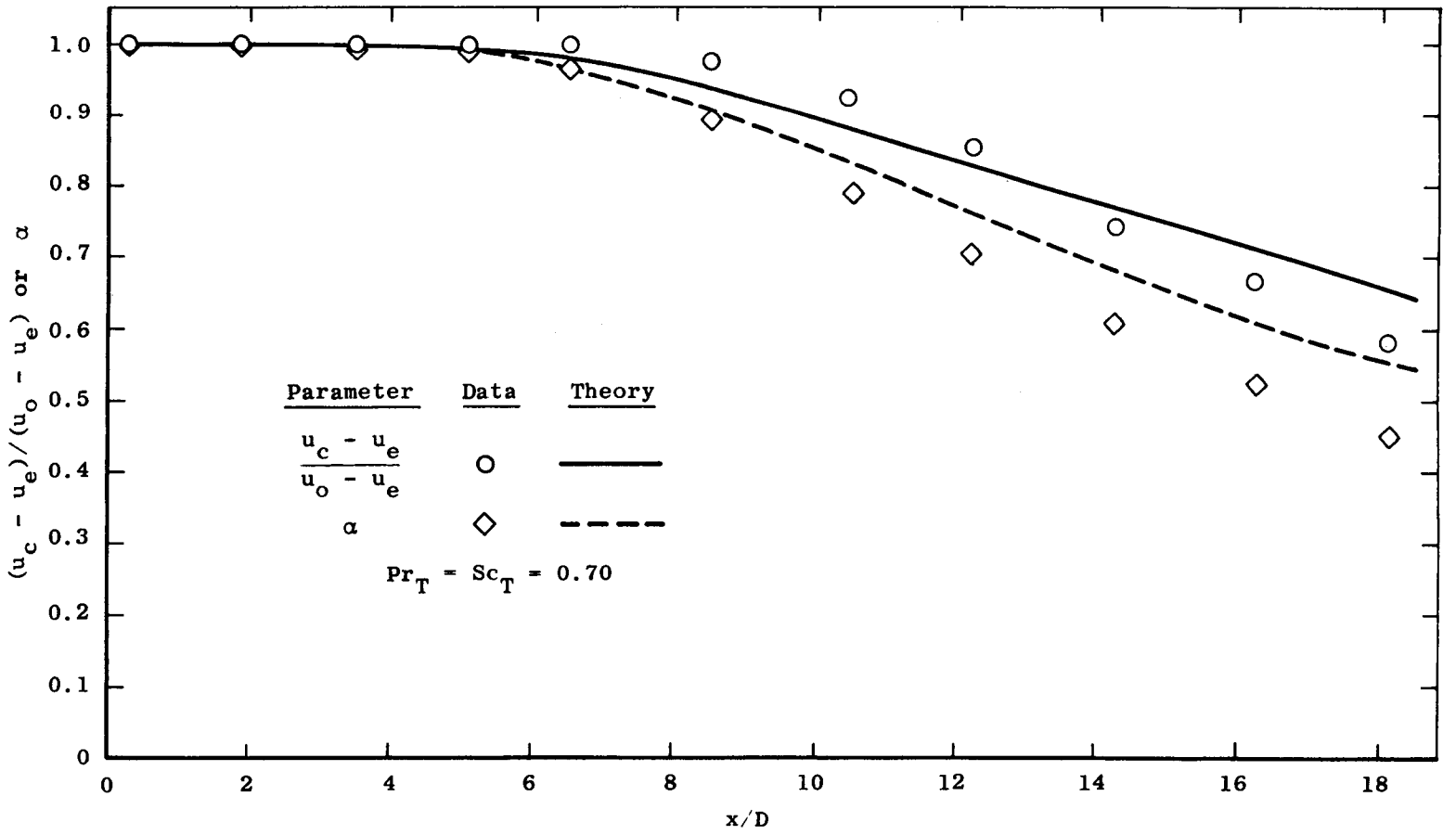

Figure 32.- Comparison of theoretical predictions of center-line velocity and jet species concentration with experimental data for test case 20, coaxial air jets.

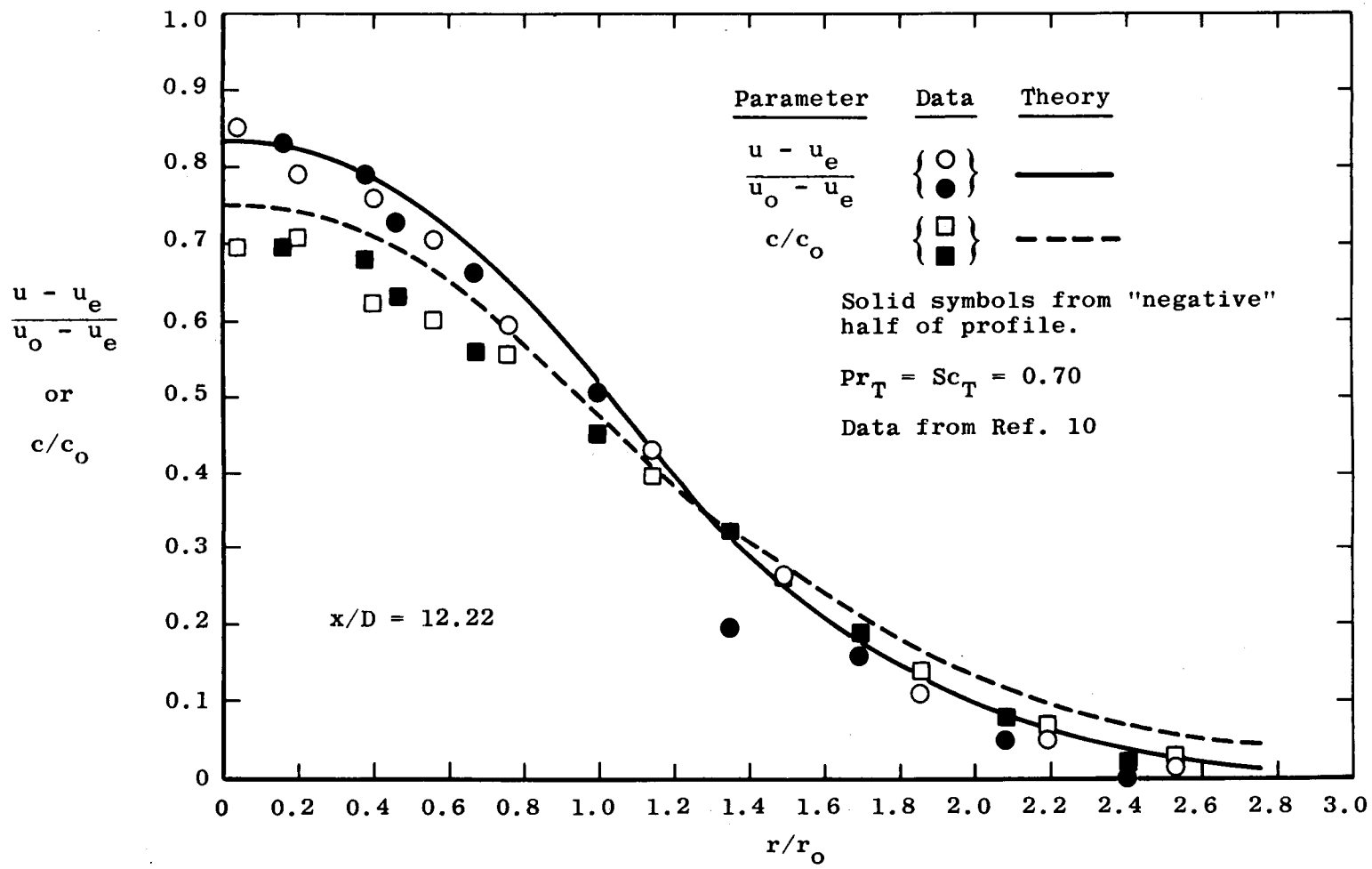

Figure 33.- Comparison of theoretical and experimental profiles for test case 20, coaxial air-air jets with H_2 trace.

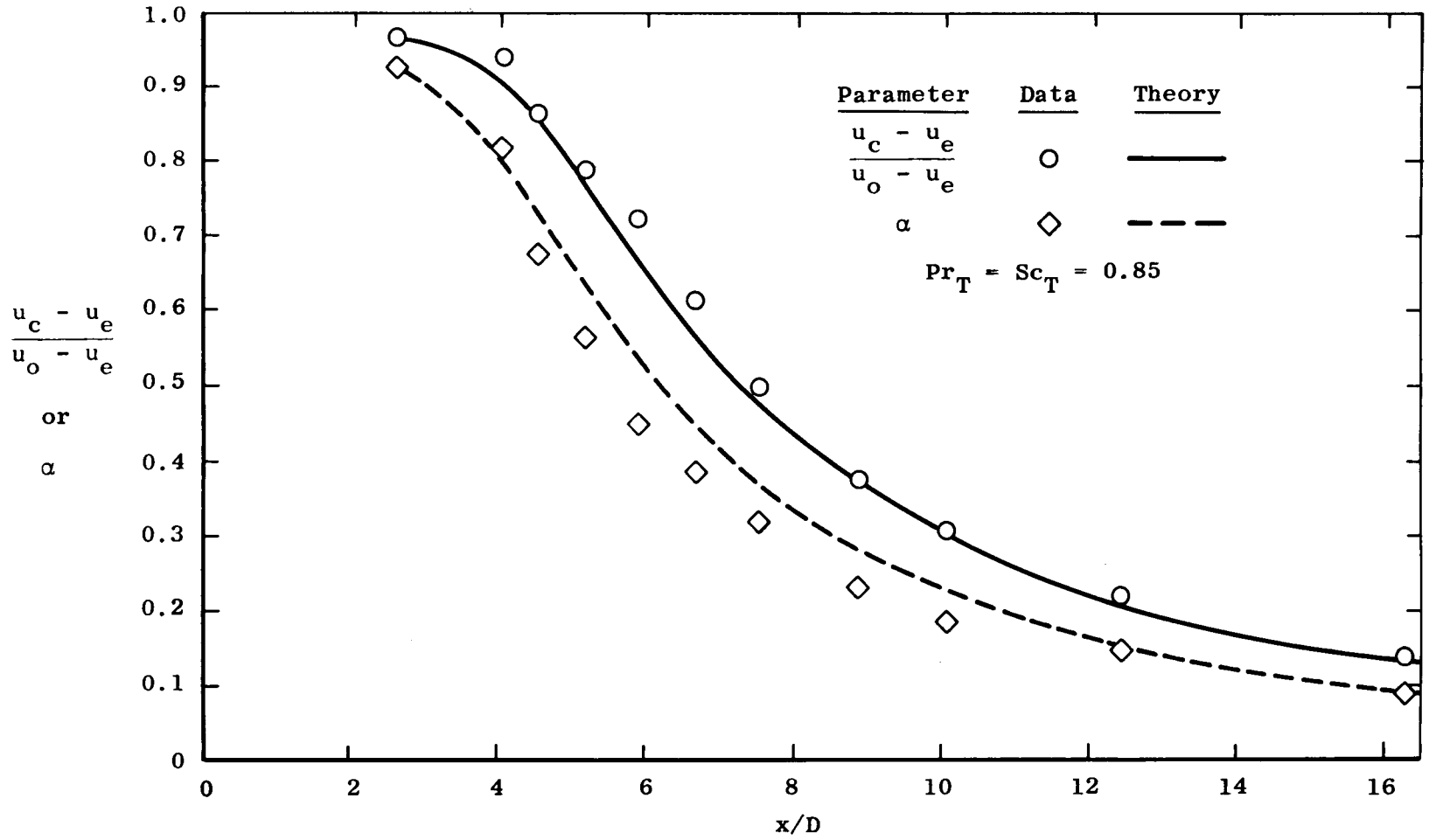

Figure 34.- Comparison of theoretical prediction of center-line velocity and composition decay with experimental data for test case 21, coaxial H_2-air mixing.

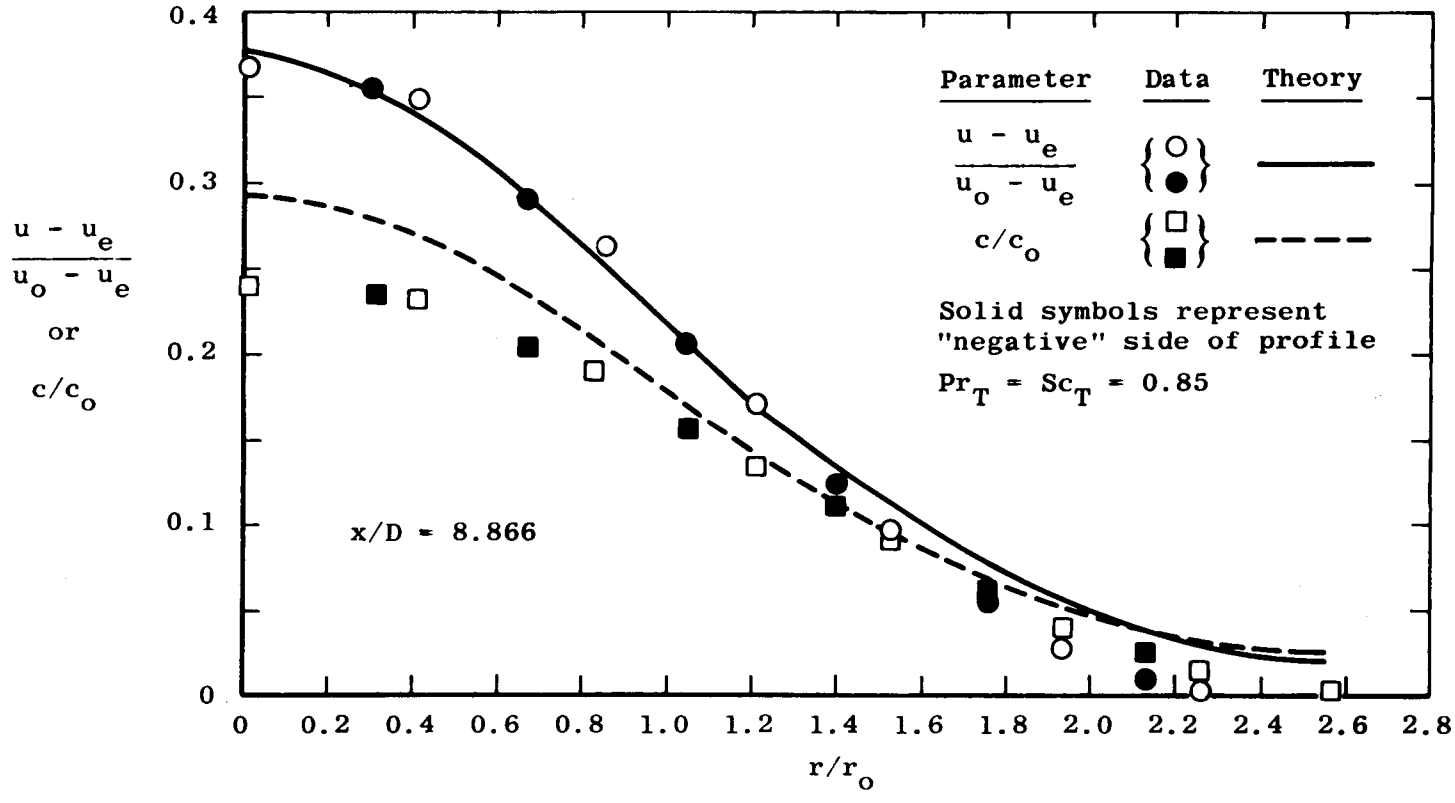

Figure 35.- Comparison of predicted and experimental profiles for test case 21, coaxial H_2-air mixing.

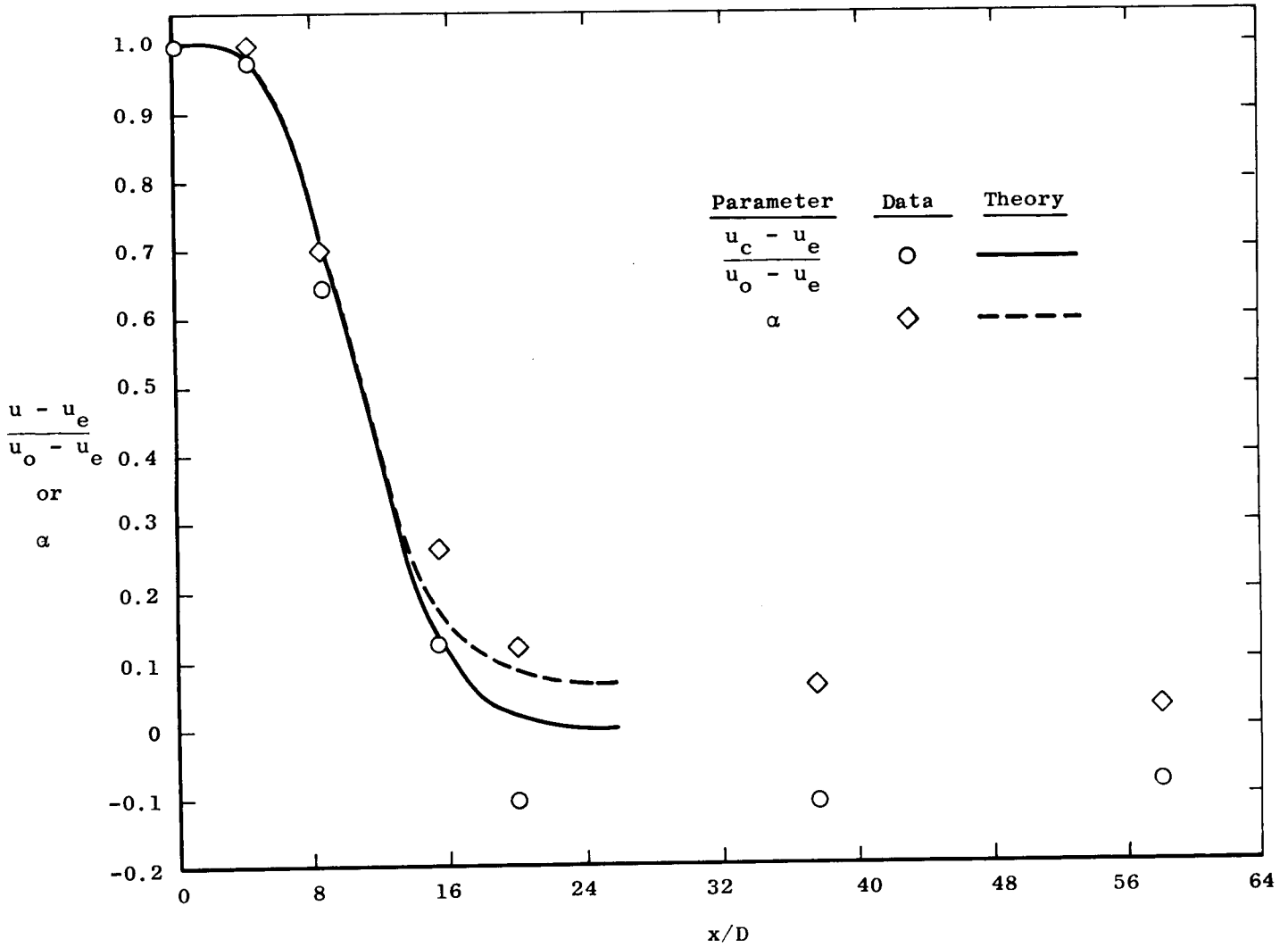

Figure 36.- Comparison of predicted center-line velocity and composition decay with experiment for test case 22, $M_O = 2.50$, H_2-air jets.

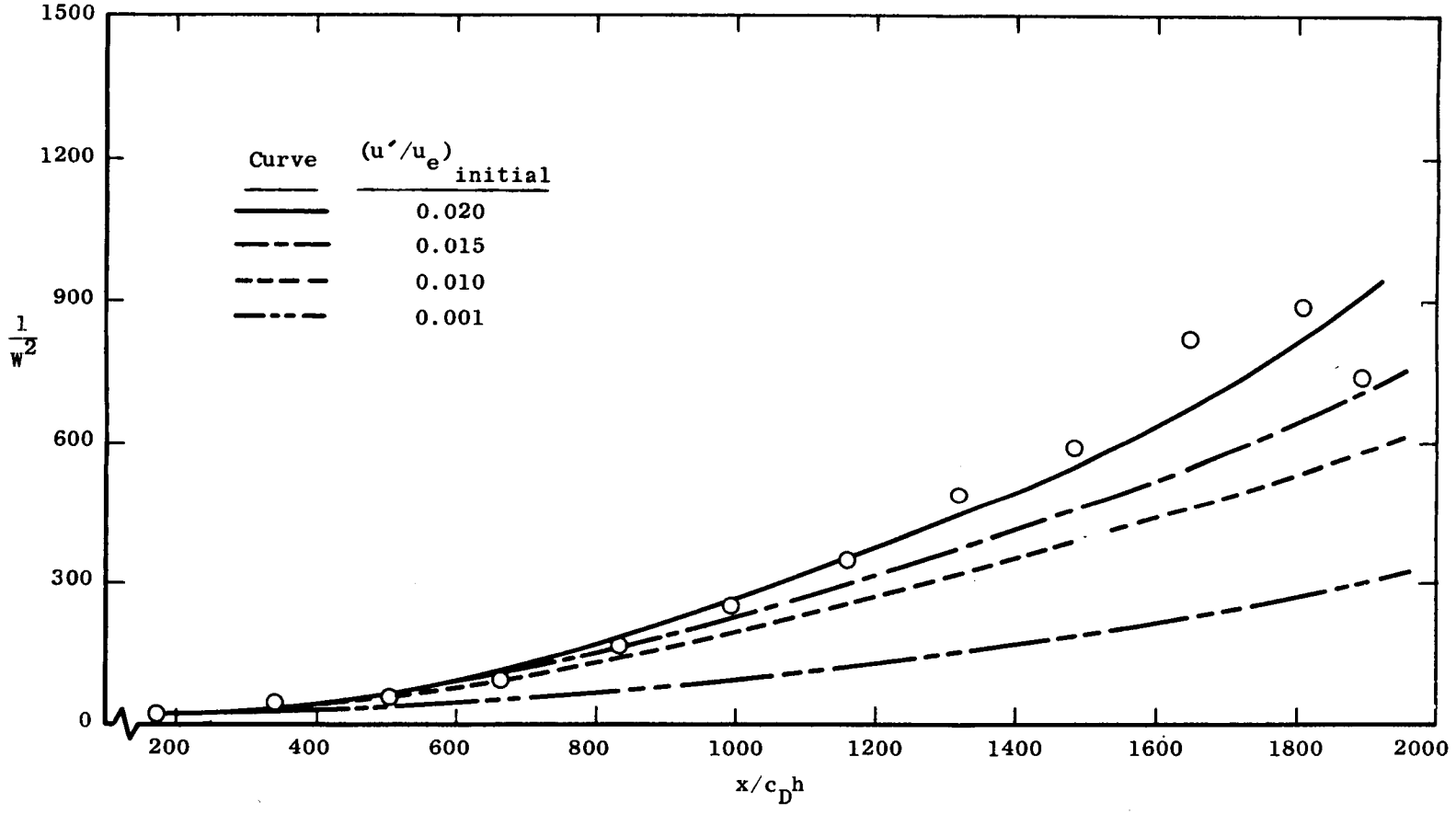

Figure 37.- Comparison of theoretical and experimental distribution of center-line velocity for test case 24, two-dimensional heated wake, $M_e = 2.9$, laminar start.

DISCUSSION

D. M. Bushnell: What has been your experience as far as predicting core length for heterogeneous mixing? You show results which indicate that you are picking up the right core length. I wonder, do you feel confident that this is a feature of your method and that you automatically get this?

P. T. Harsha: I feel confident that I get in the "right ballpark" with the core length. However, I am not overly confident that I can predict core length in every case. The results I show here, if I can use the Maise and McDonald type of start, seem to do quite well, however.

J. M. Eggers: Could you describe your experiences in applying this technique to the reacting flow field for which I understand you have performed at least some preliminary calculations.

P. T. Harsha: The problem with the reacting flow calculation is in general that the density field has an even larger density variation across the shear fields and this tends to create numerical difficulty for me. The results which we have reported using this have not used the a_1 and a_2 models I have described here, but that was only because we were attempting to reproduce some experimental results which were probably in error in any case. I think that the technique as described here can be used for calculations for reacting flows – the only problem being the amount of finesse required to handle large density ratios.

D. B. Spalding: I wonder if you could explain why you say you are using Bradshaw's model. I know that you start off by looking at the equation $\tau = a_1 \rho k$, but no sooner have you got it than you depart from it by saying a_1 must vary. The thing which is queer about the Bradshaw relationship is that it does require that the shear be proportional to the energy, and so you promptly change. Now your old method was to make a_1 proportional to the velocity gradient which immediately gives you an effective viscosity type of relationship. There is a direct proportionality between the shear stress and the velocity gradient. Later on you seem to have done more complicated things. But it seems to me that right from the start you just introduced Bradshaw's hypothesis and then threw it away while retaining the name.

P. T. Harsha: Your comment is well taken. I really meant to say that the hypothesis that I used was originally introduced by Bradshaw but it is necessary to put a lateral variation of a_1 in an axisymmetric flow. I don't believe that Bradshaw has attempted axisymmetric flows.

I. E. Alber: How do you obtain the length scale l_k in your formulation?

P. T. Harsha: The length scale is simply a geometric length scale. In the shear layer region, it is taken to be equal to the distance between the 99- and 1-percent velocity points and in the developed region of a jet it is taken to be twice the half-radius.

I. E. Alber: Also with respect to the two-dimensional mixing layer, I noticed that you find little variation with Mach number as other predictors have found, but with respect to the variation of the spreading parameter σ with the density ratio you find quite a considerable variation. Can you explain that?

P. T. Harsha: No. All I can say is that those were the results that I got. I simply ran the case to see what happened. I have no good explanation for it.

M. V. Morkovin: It seems to me that it would be desirable for you to take a good look at where it comes from because this is the central issue of the density stuff. If there is a clue in the thing it would be nice to know, and if it's a fluke, then it's a fluke, but it seems to me you want to follow up Alber's comment and see where it comes from.

P. T. Harsha: Well I fully agree, and I simply did not have time in preparing for this conference to look at it any more thoroughly than to just run the calculations. But I definitely agree that this is a major problem that must be faced.

Written Comment

S. C. Lee: Referring to the original paper I presented to an AIAA meeting in 1969,[1] I am very glad to see that Dr. Harsha has applied this method to supersonic free mixing problems. However, using several values for one empirical constant is exactly what I wish to eliminate by developing the turbulence kinetic energy method instead of using the simpler eddy viscosity approach. In Harsha's version, the coefficient a_2 (occurring in the dissipation term) is falling into this category. Professor Spalding introduces a dissipation rate equation which is one way to consider the dissipation term of the turbulence kinetic energy equation. I feel the direct approach is to measure the spatial correlations in addition to the Reynolds stresses to obtain a functional relationship of a_2 as I outlined in a paper presented at the 1972 Heat Transfer and Fluid Mechanics Institute.

[1]Lee, S. C.; and Harsha, P. T.: The Use of Turbulent Kinetic Energy in Free Mixing Studies. AIAA Paper No. 69-683, June 1969.

TURBULENT KINETIC ENERGY EQUATION AND FREE MIXING

By P. H. Heck and M. A. Smith
General Electric Company

14

Paper not available for publication

DISCUSSION

W. G. Hill, Jr.: Do you know of any measurements of the jet behind an actual aircraft in flight, where you have a lot of other things going on?

P. H. Heck: I know of tunnel data only, where they have used a scale model of an aircraft and tried to get behind it. Invariably the wake is highly distorted because of the lifting effect of the aircraft.

W. G. Hill: Yes, well that is part of the point. This question is primarily directed towards your comments about IR. In flight, you have a self-propelled body which has a net zero momentum wake. The place where most of the methods seem to have problems is with the wake, where those who do handle the wake use different constants than they do for the jets. Now, for the case where you have a wake and a jet that is essentially one and the same, what do you do?

P. H. Heck: That becomes a rather specialized problem in the IR area, and I don't think that I am able to answer it right here. For one thing, I have to admit that once you get into the particulars of IR, you have to stamp a security classification on everything, and I'll have to leave it out.

S. W. Zelazny: How did you get your initial turbulent energy profiles for cases where they weren't available?

P. H. Heck: We use a flat initial profile, and it has to be an estimate where we are not given information.

S. W. Zelazny: How do you determine the amplitude of the flat profile?

P. H. Heck: In our applications, we have enough data behind our combustion-type engines which give us an empirical model which we can use as a functional start. Otherwise, we have to look at the experiments and, in some cases, if we really want to fit data we have had to look at the experiment very critically and occasionally use trial and error to determine what the initial turbulence should have been. One of the characteristics we have found is that the experiments inherently have had low turbulence and, of course, the real applications have a turbulence of 10 to 20 percent initially.

D. M. Bushnell: I have two questions. First, I don't really understand how we can compute core length for these heterogenous compressible jets but we can't compute developed free shear layers. Is this because these near-field shear layers in the core are low Reynolds numbers or are we adjusting initial turbulence levels?

P. H. Heck: Adjusting initial turbulence levels to make them agree?

D. M. Bushnell: Yes, I just don't understand how we can compute these things and not developed shear layers.

P. H. Heck: The initial turbulence isn't adjusted there. We start with the given quantity and let the flow field develop, and in the parabolic sense we are moving down the axis.

D. M. Bushnell: Maybe it's the low Reynolds number thing catching up with us. The other question is, what about your length scale. You don't tell us what you use, especially in the transition region.

P. H. Heck: The length scale in the mixing layer follows an empirical work by Ollerhead [1] and in the fully developed region it becomes a constant; we have a transition between the two which is an exponential decay. It's empirical, of course.

M. V. Morkovin: Did I understand you correctly that you did use the Spalding model but with different constants?

P. H. Heck: Yes, we retained the constants in the dissipation term and the diffusion term that had been developed previously for boundary-layer work. They work quite well.

M. V. Morkovin: What I am driving at is whether a comparison of your results with those that Professor Spalding presented yesterday (for identical cases) would give us another clue of the sensitivity to changes in the coefficients. You apparently have differences between you, yet you are solving the same problems. Is the assumption correct that there would be some information coming from that?

P. H. Heck: I guess the comparisons of the details would be very valuable. But we have to sit down and see what the minute details are.

D. B. Spalding: It seems to me that what differences appear in the results must lie in the differences in the length scale distributions. That is what we really need to know about. That is where the differences stem from.

P. H. Heck: The length scale is the critical problem in these turbulent kinetic energy solutions.

B. E. Launder: In your presentation, you gave attention to the fact that you had included a correlation between density fluctuations and velocity fluctuation. I'm afraid I missed, however, how you actually approximated this in the model.

P. H. Heck: We used a definition of the turbulent kinetic energy and assumed local isotropy. I will admit that this assumption is going to be very loose in some of these flows with high gradients, both temperature and velocity.

B. E. Launder: I'm not sure that I quite understand what you said there. Are you implying that the correlation between density fluctuations and velocity fluctuations be presumed to be proportional to, say, a mean density gradient times a turbulent viscosity?

---

[1] Ollerhead, J. B.: On the Prediction of Near Field Noise of Supersonic Jets. NASA CR-857, 1967.

P. H. Heck: I'm sorry. In the solution technique, we use the Von Mises transformation. In using the transformation, the transverse momentum mass flux disappears and therefore is not left in the calculation scheme thereafter.

I. E. Alber: I understand, from hearing a talk at a previous AIAA meeting, that your length scale may be a function of the Mach number in some region of the flow. Is that correct?

P. H. Heck: In the initial shear region, the model of Ollerhead includes a term that is related to the jet exit Mach number squared.

I. E. Alber: I think that is quite important for determining that initial shear layer behavior. Also, I would like to comment on an earlier question about the in-flight problem – about the zero momentum wake. Typically, if you have engines mounted on the fuselage, the wakes do not get rolled up in the wing tip vortices, and so you do not have this direct cancellation of the momentum occurring earlier in the jet development. However, if you have the jet engines mounted outboard toward the wing tips, you can get the wakes entrained in the wing tip vortices which carry the induced drag of the aircraft. Then you can get some different momentum effects.

P. H. Heck: I agree.

S. Corrsin: You have assumed a form of the dissipation which is somewhat different from that which other people have assumed. Usually, I think, most of the previous speakers have assumed energy to the three-halves power over a characteristic scale, whereas you have energy over characteristic scale squared so that basically your characteristic length is the Taylor microscale, whereas the other people's characteristic length was basically the integral scale. And I think the shortcoming of this as an engineering technique is that the integral scale tends to be independent of Reynolds number for a given geometry, whereas the microscale tends to be quite sensitive to the Reynolds number for a given geometry. So this might be a more difficult thing to use.

P. H. Heck: We'll look into it.

S. C. Lee: I'm particularly interested in your correlation between acoustic and turbulence energy or turbulent intensity. One of the curves you showed was pressure fluctuations correlated with the intensity U'^2 divided by U^2.

P. H. Heck: The local pressure fluctuations correlated with turbulent intensity, yes.

S. C. Lee: Do you have those two relations directly related with each other? In other words, every time you measure turbulence intensity, can you say that it is also pressure fluctuations?

P. H. Heck: Maestrello's paper [2] showed a relation which included the equation showing the static pressure as a function of turbulence plus a constant times another turbulence term. The constant was arbitrary; not knowing the value of the constant (Maestrello didn't know it either), the assumption that we made at this point was that the constant was zero. Of course, we then took a look at the correlation and it did correlate.

S. C. Lee: So there is a relation but not necessarily a known invariant parameter?

P. H. Heck: Yes, the acoustic relations are much more involved, and that is where you get into the details.

[2] Maestrello, L.; and McDaid, E.: Acoustic Characteristics of a High-Subsonic Jet. AIAA J., vol. 9, no. 6, June 1971, pp. 1058-1066.

A LOCAL EDDY VISCOSITY MODEL FOR TURBULENT SHEAR FLOW

By Paul J. Ortwerth, Douglas C. Rabe,
and Donald P. McErlean
Air Force Aero Propulsion Laboratory
Wright-Patterson AFB, Ohio

INTRODUCTION

Turbulent flow fields are generated in shear flows of sufficiently high Reynolds number for which the laminar shear layer is unstable. Mean flow kinetic energy is transformed into a random turbulent kinetic energy and finally dissipated into random thermal energy. The present theoretical model attempts to make predictions of turbulent flow fields by using the historically popular eddy viscosity concept.

The eddy viscosity is assumed to be a fluid property dependent on the state of the fluid locally, namely the local density, turbulent kinetic energy, turbulence scale, and Mach number. An empirical law was found (ref. 1) which related eddy viscosity to these properties satisfactorily for free jets. This law is used without modification for the present set of test cases in free shear layers, free-jet decay, coaxial mixing, and wakes.

At present the scale of turbulence is taken as a constant at any axial location equal to the width of the shear layer.

By utilizing the boundary-layer order-of-magnitude analysis, a coupled set of fluid dynamic equations is formulated, which of necessity includes the equation for the production of turbulent kinetic energy.

SYMBOLS

$\bar{c}_p$ mean specific heat at constant pressure

d jet diameter

$\overrightarrow{\text{def}}\ \vec{U} = \vec{\nabla}\vec{U} + \left(\vec{\nabla}\vec{U}\right)^*$, where $\left(\vec{\nabla}\vec{U}\right)^*$ is the transpose of $\vec{\nabla}\vec{U}$

d_k rate of dissipation of turbulence kinetic energy into random thermal energy

$\bar{h}$ mean static enthalpy

$\bar{h}_i$	species enthalpy
$\bar{\bar{I}}$	identity tensor
k	turbulence kinetic energy, $\frac{1}{2}\left[\overline{(\rho U)'U'} + \overline{(\rho V)'V'} + \overline{(\rho W)'W'}\right]$
L_D	scale of large eddies
M	local Mach number
N_{Pr}	mean Prandtl number
$N_{Pr,T}$	turbulent Prandtl number, 0.75
N_{Sc}	Schmidt number, 0.75
$N_{Sc,T}$	turbulent Schmidt number
p_e	static pressure at edge of shear layer in the nonturbulent region
p_T	turbulence pressure
$\bar{p}$	mean static pressure
r	radial coordinate
r_o	jet radius
T_t	total temperature
$T_{t,o}$	initial total temperature
$\overline{T}$	mean static temperature
U	streamwise velocity
U_e	velocity at edge of shear layer
U_o	initial velocity

U_1 velocity on high-velocity side of shear layer

U_2 velocity on low-velocity side of shear layer

V normal velocity

$W = 1 - \frac{U}{U_e}$

x streamwise coordinate for two-dimensional shear layers

y coordinate normal to shear layer for two-dimensional shear layer

α_i mass fraction of species i

ϵ_k kinematic diffusivity for turbulent kinetic energy, $\rho\epsilon_k = \mu_T$

μ_T eddy viscosity

$\bar{\mu}$ mean molecular viscosity coefficient

ρ density

ρ_1 density on high-velocity side of shear layer

ρ_2 density on low-velocity side of shear layer

σ shear layer spreading parameter

σ_o incompressible spreading parameter for $\frac{U_2}{U_1} = 0$

$\bar{\bar{\tau}}_T$ Reynolds stress tensor, $\overline{(\rho\vec{U})'\vec{U}'}$

ψ stream function (subscripts r and x indicate derivatives with respect to radius and streamwise coordinate, respectively)

EQUATIONS

The equations are presented in cylindrical coordinates.

Reynolds stresses

The turbulence stresses are formulated in the following manner:

$$\bar{\bar{\tau}}_T = -p_T \bar{\bar{I}} + \mu_T \overrightarrow{\text{def}}\, \vec{U} \tag{1}$$

separating the turbulence stress tensor into static pressure and shear stress tensor. Turbulence pressure is by definition

$$p_T = \frac{2}{3} \rho k \tag{2}$$

Turbulent kinetic energy

The turbulent shear stress and pressure are coupled to the turbulent kinetic energy by the following equation:

$$\frac{1}{r} \frac{\partial}{\partial r}\left(r\overline{\rho V k}\right) + \frac{\partial}{\partial x}\left(\overline{\rho U k}\right) = -p_T \frac{\partial \overline{U}}{\partial x} + \mu_T \left(\frac{\partial \overline{U}}{\partial r}\right)^2 + \frac{1}{r} \frac{\partial}{\partial r}\left(r \bar{\rho} \epsilon_k \frac{\partial k}{\partial r}\right) - d_k \tag{3}$$

Eddy viscosity

Following reference 1, the equations for eddy viscosity, dissipation, and scale are

$$\mu_T = \bar{\rho} \frac{L_D}{16.5}\left(\frac{2}{3} k\right)^{1/2} \left(\frac{\epsilon}{\epsilon_o}\right) \tag{4}$$

$$L_D = \frac{\overline{U}_{max} - \overline{U}_{min}}{\left(\frac{\partial \overline{U}}{\partial r}\right)_{max}} \sqrt{2} \tag{5}$$

and

$$d_k = \frac{3}{2} \bar{\rho} \frac{\left(\frac{2}{3} k\right)^{3/2}}{L_D} \tag{6}$$

where

$$\frac{\epsilon}{\epsilon_o} = 1 - M^2 \qquad (0 \leqq M \leqq 0.6)$$

or

$$\frac{\epsilon}{\epsilon_o} = (1 + 0.25M)^{-2} \qquad (0.6 \leqq M < \infty) \tag{7}$$

Continuity

$$\frac{1}{r} \frac{\partial}{\partial r}\left(r\overline{\rho V}\right) + \frac{\partial}{\partial x}\left(\overline{\rho U}\right) = 0 \tag{8}$$

Radial momentum integral

$$\bar{p} + p_T = p_e \tag{9}$$

Streamwise momentum equation

$$\frac{1}{r}\frac{\partial}{\partial r}\left(r\overline{\rho V}\,\overline{U}\right) + \frac{\partial}{\partial x}\left(\overline{\rho U}\,\overline{U}\right) = -\frac{\partial p_e}{\partial x} + \frac{1}{r}\frac{\partial}{\partial r}\left[r\left(\bar{\mu} + \mu_T\right)\frac{\partial \overline{U}}{\partial r}\right] \tag{10}$$

Energy equation

$$\overline{\rho V}\frac{\partial \bar{h}}{\partial r} + \overline{\rho U}\frac{\partial \bar{h}}{\partial x} = \overline{U}\frac{\partial \bar{p}}{\partial x} + d_k + \bar{\mu}\left(\frac{\partial \overline{U}}{\partial r}\right)^2 + \frac{1}{r}\frac{\partial}{\partial r}\left[r\left(\frac{\bar{\mu}}{N_{Pr}} + \frac{\mu_T}{N_{Pr,T}}\right)\bar{c}_p\frac{\partial \overline{T}}{\partial r}\right]$$

$$+ \frac{1}{r}\frac{\partial}{\partial r}\left[r\left(\frac{\bar{\mu}}{N_{Sc}} + \frac{\mu_T}{N_{Sc,T}}\right)\sum \bar{h}_i\frac{\partial \alpha_i}{\partial r}\right] \tag{11}$$

Species continuity

$$\frac{1}{r}\frac{\partial}{\partial r}\left(r\overline{\rho V}\alpha_i\right) + \frac{\partial}{\partial x}\left(\overline{\rho U}\alpha_i\right) = \frac{1}{r}\frac{\partial}{\partial r}\left[r\left(\frac{\bar{\mu}}{N_{Sc}} + \frac{\mu_T}{N_{Sc,T}}\right)\frac{\partial \alpha_i}{\partial r}\right] \tag{12}$$

Numerical solution of these equations follows Edelman and Fortune (ref. 2).

The equations are transformed by the Von Mises transformation as

$$\left.\begin{aligned} X &= x \\ \psi\psi_r &= \overline{\rho U} r \\ \psi\psi_X &= -\overline{\rho V} r \\ a &= \frac{\mu\overline{\rho V} r}{\psi} \end{aligned}\right\} \tag{13}$$

Then the finite-difference equations are formed by using the following substitutions:

Partial derivative in the X-direction

$$\frac{\left(\phi_{n+1,m} - \phi_{n,m}\right)}{\Delta X} = \frac{\partial \phi}{\partial X} \tag{14}$$

Partial derivative in the ψ-direction

$$\frac{\left(\phi_{n,m+1} - \phi_{n,m-1}\right)}{2\,\Delta\psi} = \frac{\partial \phi}{\partial \psi} \tag{15}$$

Second derivative in the ψ-direction

$$\frac{a_{n,m}}{\Delta\psi^2}\left(\phi_{n,m+1} - 2\phi_{n,m} + \phi_{n,m-1}\right)$$

$$+\frac{1}{4}\frac{1}{\Delta\psi^2}\left(\phi_{n,m+1} - \phi_{n,m-1}\right)\left(a_{n,m+1} - a_{n,m-1}\right) = \frac{\partial}{\partial\psi}\left(a\frac{\partial\phi}{\partial\psi}\right) \tag{16}$$

Further discussion of these equations can be found in reference 1.

RESULTS

Numerical results have been obtained for each of the categories. For each problem an initial turbulence kinetic energy profile and scale are needed in addition to a velocity and temperature profile. These data on turbulence were not supplied and were estimated. This was not a serious problem for the test cases for free shear layers; however, initial turbulence level is important for the decay of free jets and coaxial jets, and free-stream turbulence is important to the decay of wakes. In the spirit of making predictions, no attempt was made to "fit" the solutions to the data by reinitializing those problems which did not work well. In fact, comparisons were not made until all cases were run.

Two-Dimensional Shear Layers

Test cases 1, 2, and 3.- Linear velocity profiles (figs. 1, 2, and 3) and a 1-percent turbulence intensity were used as input, and computations were started with 14 data points in ψ-direction. The initial shear layers were a few centimeters thick, and computations carried out 10 meters (30 ft) in the downstream direction.

Test cases 4 and 5.- The given profiles (figs. 4 to 8) and an initial turbulence intensity of 1 percent of U_1 were used to initialize the problems. The initial number of points in the ψ-direction were 16 and 19 for cases 4 and 5, respectively. For test case 4, the profiles were shifted so that a velocity ratio of 0.5 occurred at $y = 7$ cm (3 in.). For case 5, the 0.5 velocity ratio was shifted to $y = 2.5$ cm (1.0 in.).

Free Jets

Test case 7.- The given profile (figs. 9 and 10) was input with a 1-percent turbulence intensity by using 14 initial points in the ψ-direction. The theoretical points seem to have more scatter than the data points. This may be due to the nature of the ϵ/ϵ_o function used in equation (7).

Test case 8.- This problem was started downstream at $x/d = 2.79$ by using the given profile (fig. 11) and assuming a self-similar turbulence intensity in the shear layer and 15 initial points in the ψ-direction.

Coaxial Mixing

Test case 10.- The initial profiles (figs. 12 and 13) at $x/d = 2.966$ were used with a self-similar turbulence profile and 14 initial points in the ψ-direction. The potential core length is overpredicted in this problem, perhaps because of large initial turbulence levels in the jet and external stream. This problem is basically one of a free jet with an embedded coaxial jet. The outer shear layer may also have affected these data through acoustic radiation to the mixing zone.

Test case 11.- The initial profiles (fig. 14) and a 5-percent turbulence intensity were used as input. Thirty initial points were used in the ψ-direction to fit the profiles adequately. These initial profiles show that basically two shear layers are present – a feature not accounted for in the formulation of the theory where only one scale is used at a given axial location. The initial center-line behavior is adequately predicted but not the final or wakelike zone. The reason for this is not known.

Test case 12.- Fifteen points were used to describe the initial profiles (fig. 15) in the ψ-direction. An 8-percent turbulence intensity was used in the hydrogen boundary layer and a 3-percent initial turbulence intensity in the air boundary layer. Again the potential core length is overpredicted, and no definite reason can be offered to explain the discrepancy.

Wakes (Test Case 17)

Fourteen points were used to initialize the problem at the station $x/d = 17.0$. (See fig. 16.) An initial turbulence intensity of 6 percent on the center line varying to 1 percent in the free stream was used.

The prediction is an order of magnitude too low. The reason for such a large discrepancy between theory and data is not known. It appears that the physics employed in this model do not correspond to what occurred in the experiment or that some larger error exists in the programing.

RECOMMENDED EXPERIMENTATION

The achievement of rapid mixing is the goal of the propulsion engineer. Some ideas are proposed to achieve that goal. The instability of shear layers, be they laminar or turbulent, makes them capable of extracting power from various sources. The instability

of shear layers is not properly exploited by many devices except perhaps in whistles and musical instruments such as a flute or an organ.

Because of this instability, greatly enhanced mixing occurs, often leading to anomalous experimental results when not recognized. It is the authors' opinion that these exciting phenomena should be exploited more fully by the propulsion engineer. Figure 17 sketches some interesting examples of shear-layer instabilities producing enhanced mixing.

The addition of moving mechanical parts which act as triggers or amplifiers to shear layers is also possible. An example of this occurs when the vortex shedding frequency of a cylinder is equal to the frequency of cylinder oscillations.

REFERENCES

1. Ortwerth, Paul James: Mechanism of Mixing of Two Nonreacting Gases. AFAPL-TR-71-18, U.S. Air Force, Oct. 1971.

2. Edelman, R.; and Fortune, O.: An Analysis of Mixing and Combustion in Ducted Flows. AIAA Paper No. 68-114, Jan. 1968.

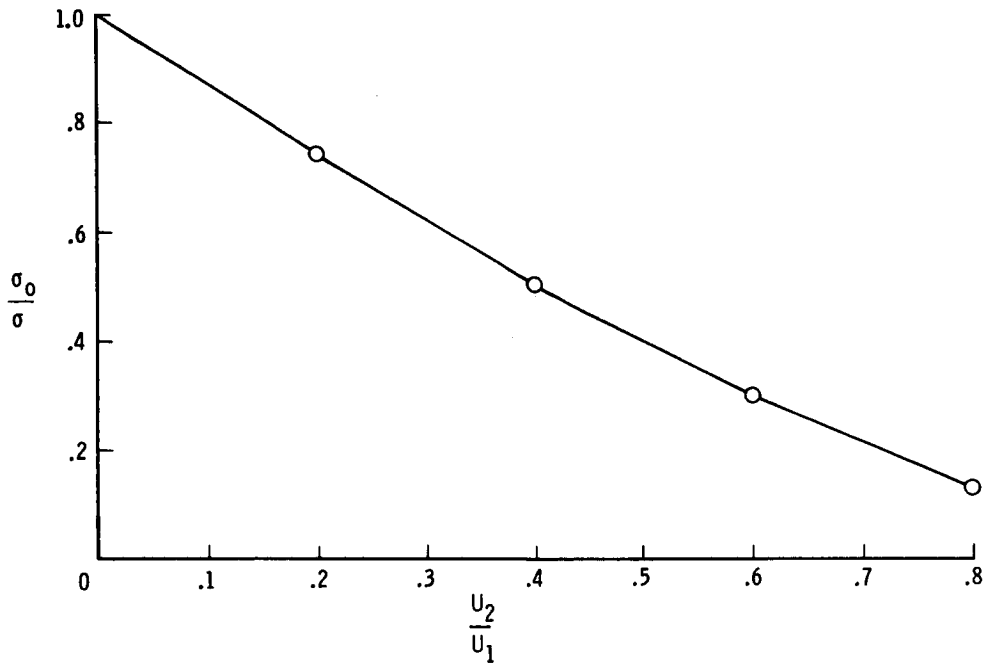

Figure 1.- Test case 1. M → 0.

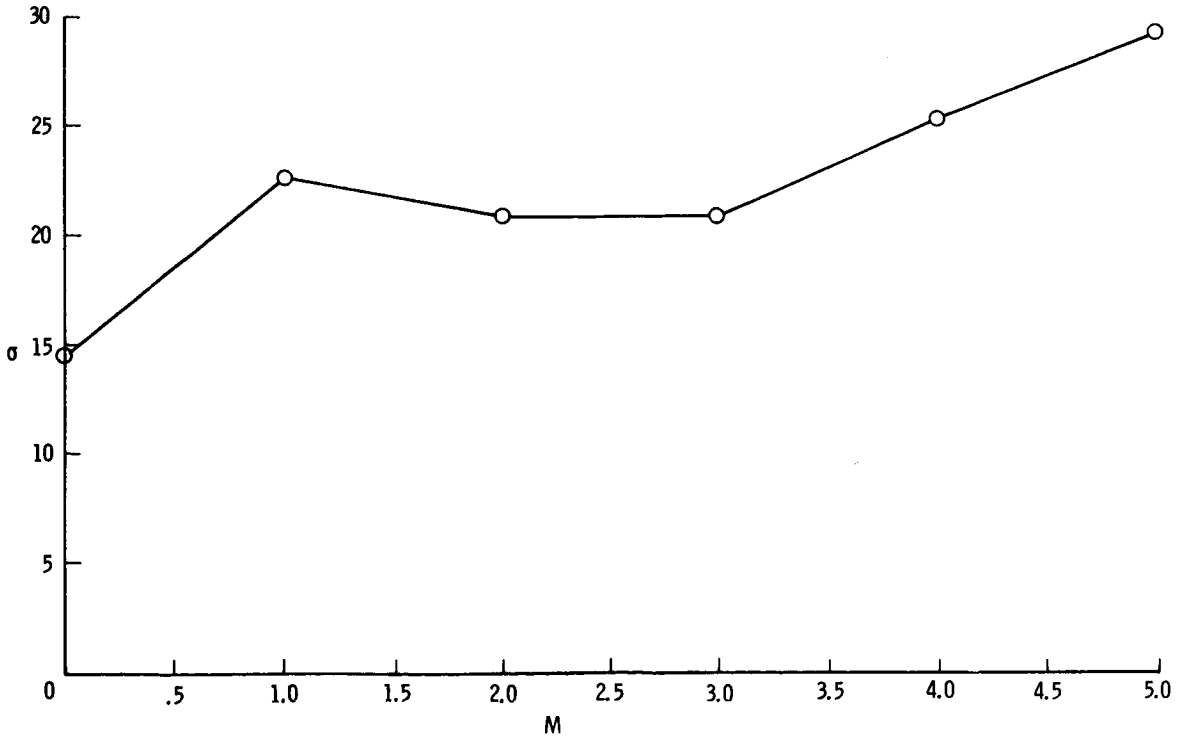

Figure 2.- Test case 2. $U_2/U_1 = 0.2$.

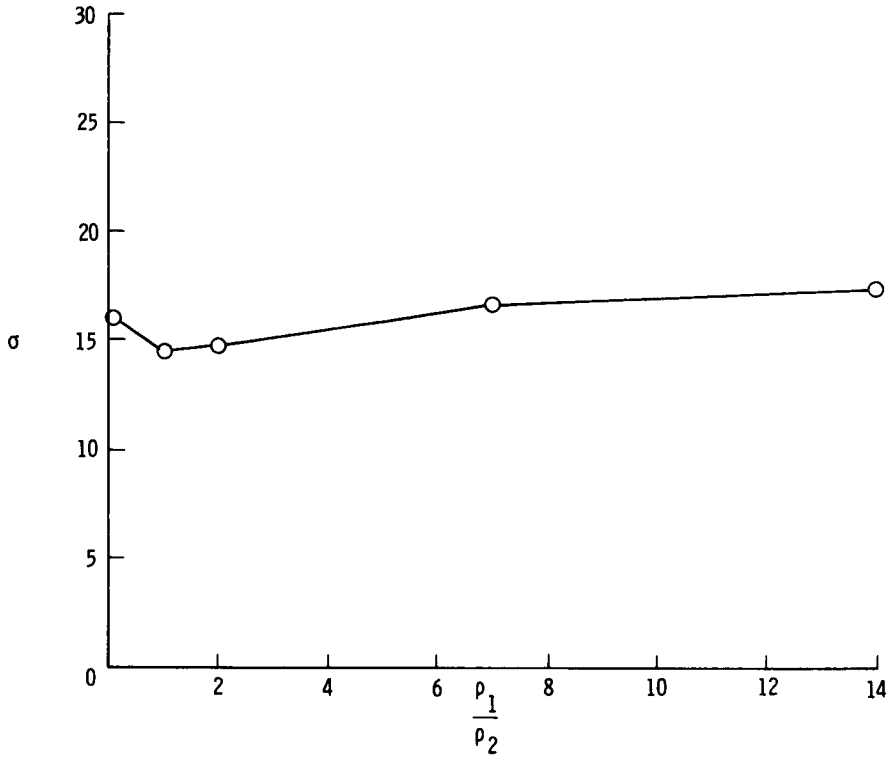

Figure 3.- Test case 3. $U_2/U_1 = 0.2$.

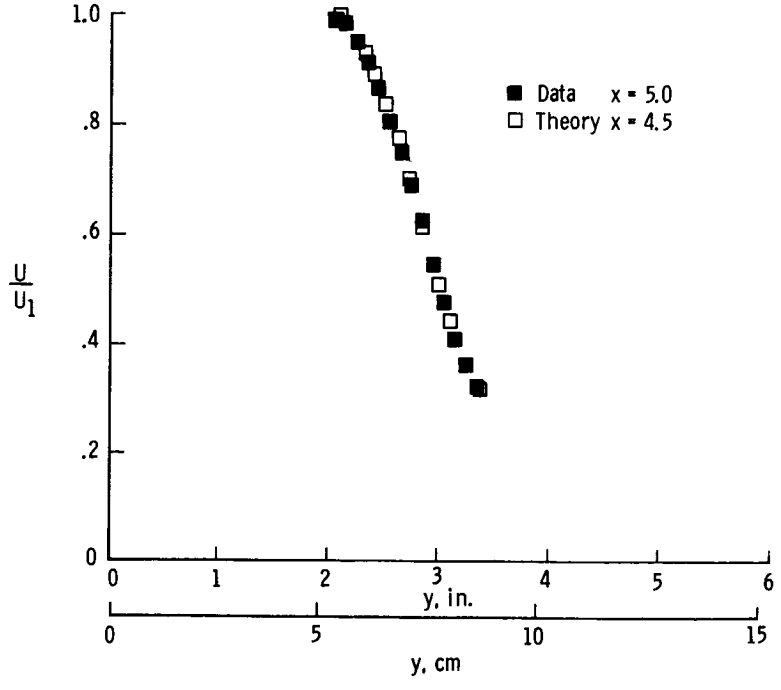

Figure 4.- Test case 4.

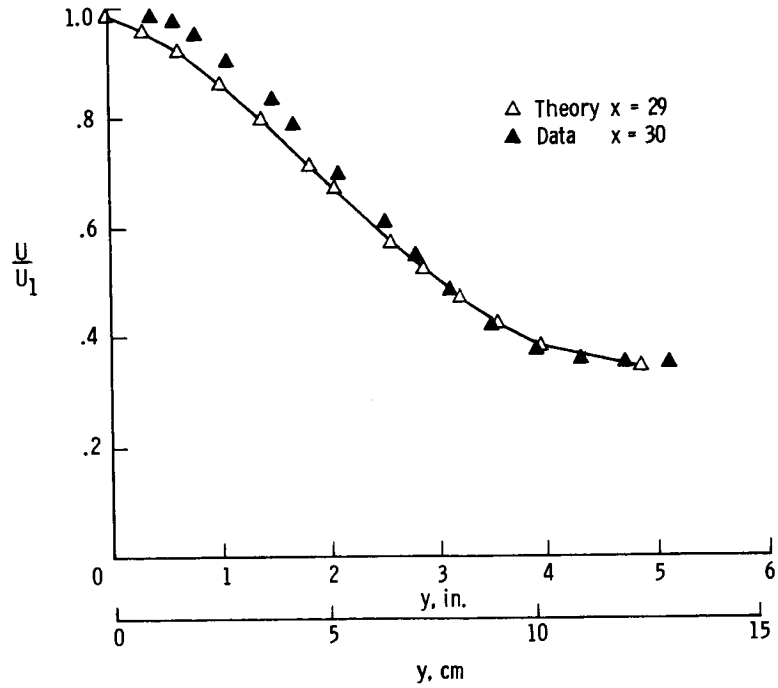

Figure 5.- Test case 4.

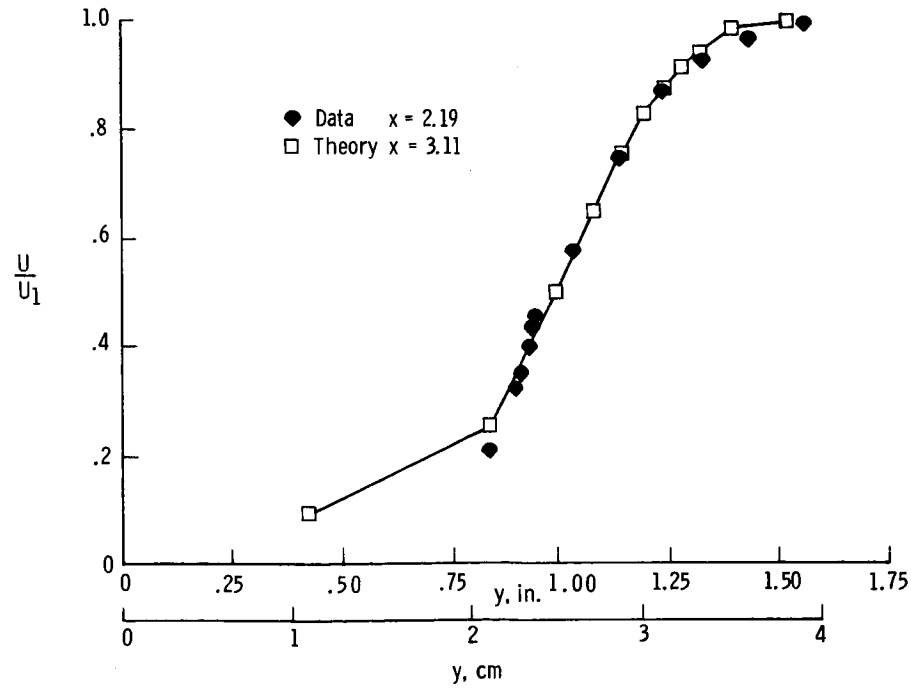

Figure 6.- Test case 5.

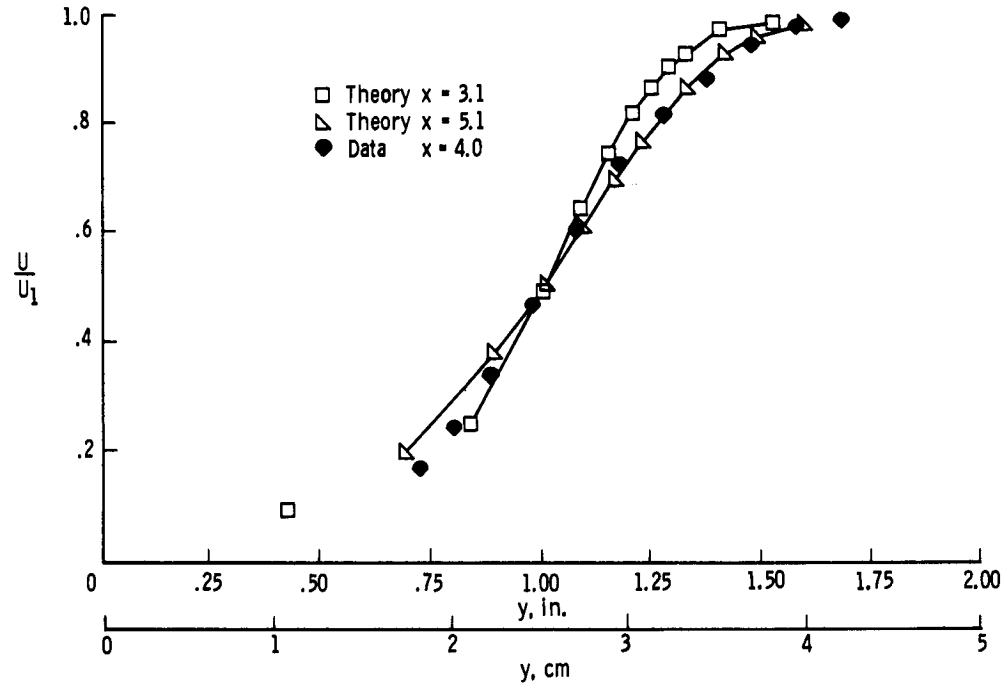

Figure 7.- Test case 5.

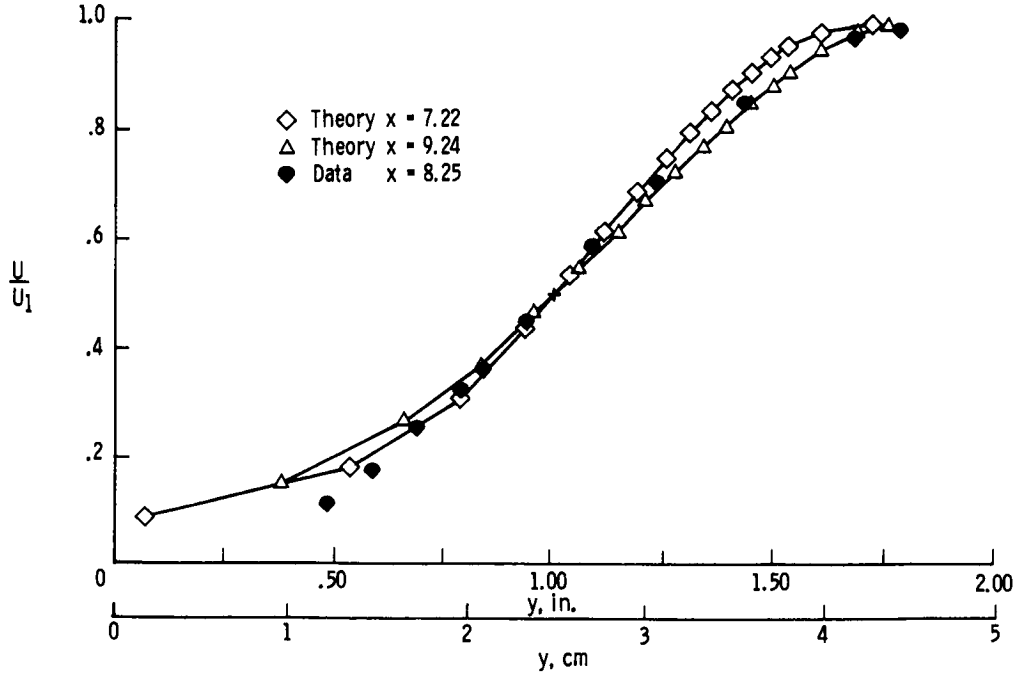

Figure 8.- Test case 5.

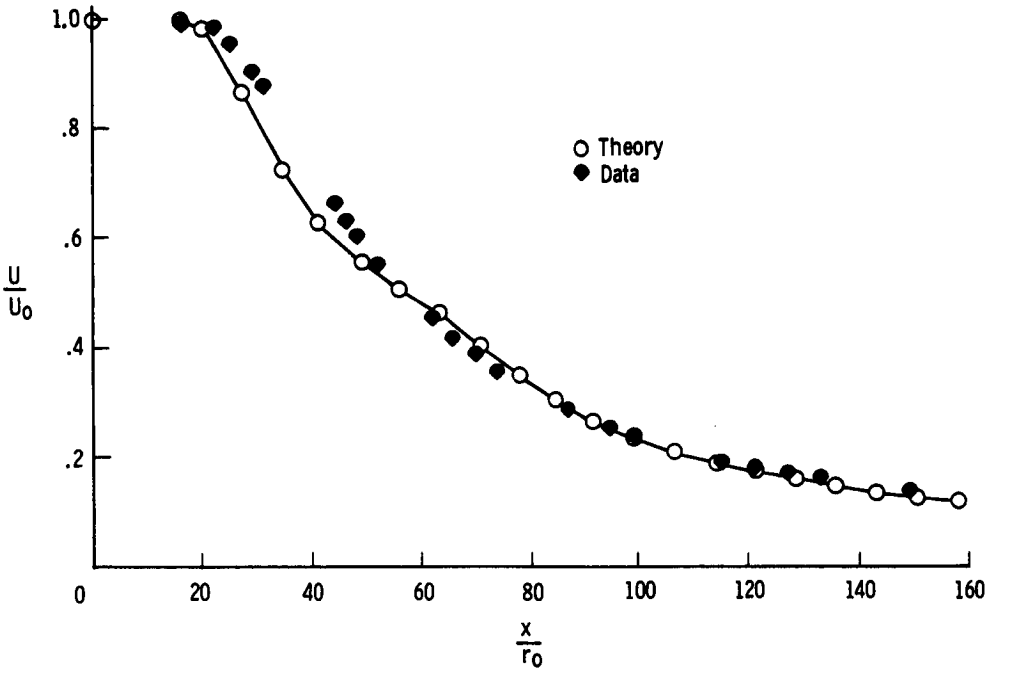

Figure 9.- Test case 7.

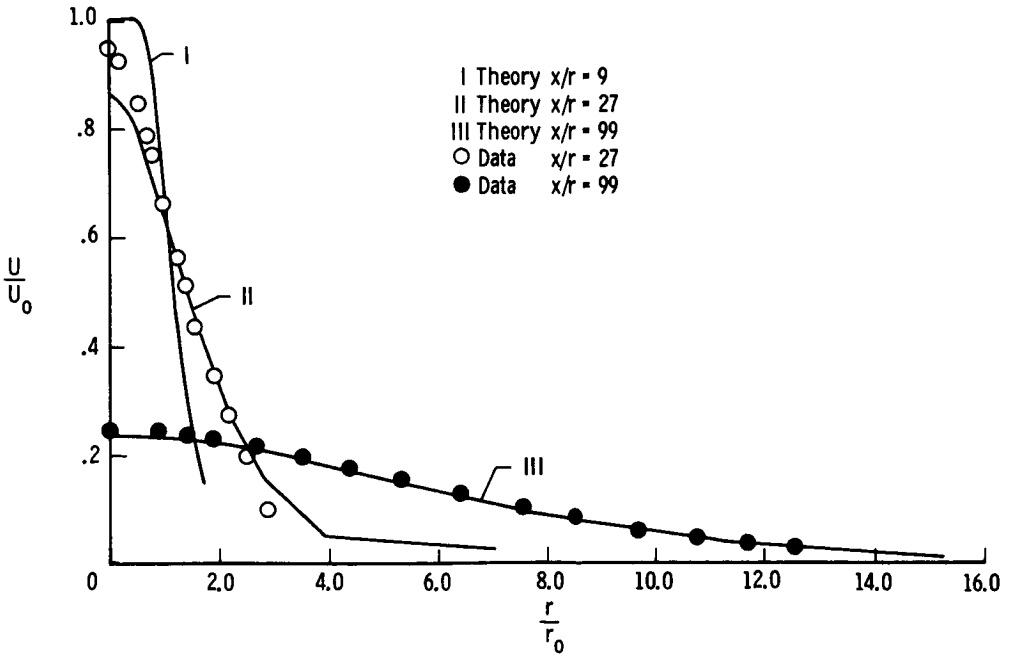

Figure 10.- Test case 7.

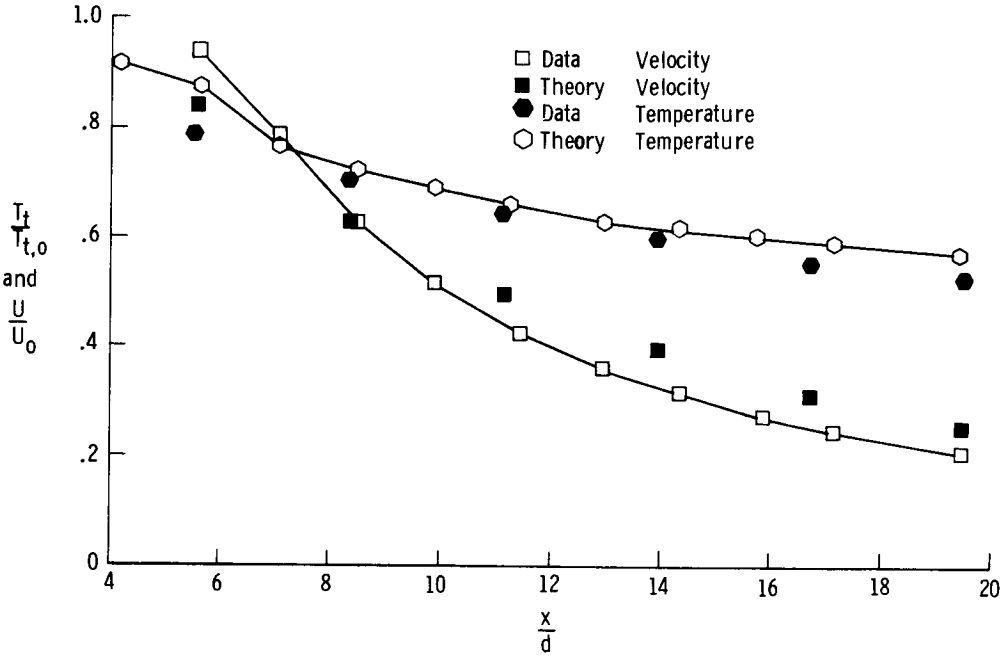

Figure 11.- Test case 8.

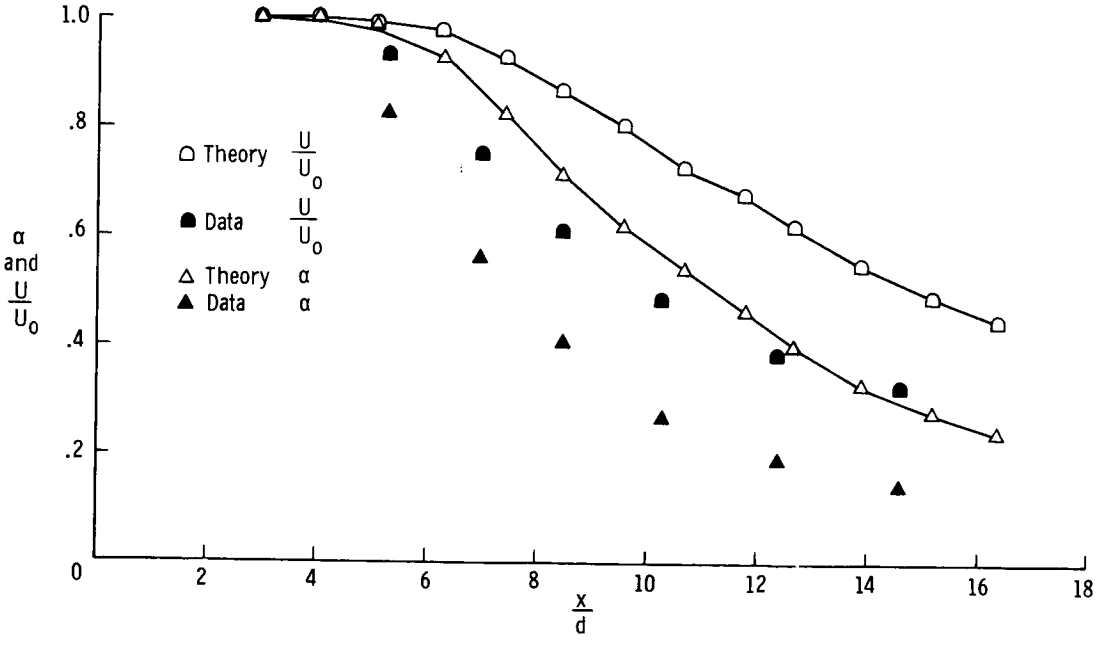

Figure 12.- Test case 10.

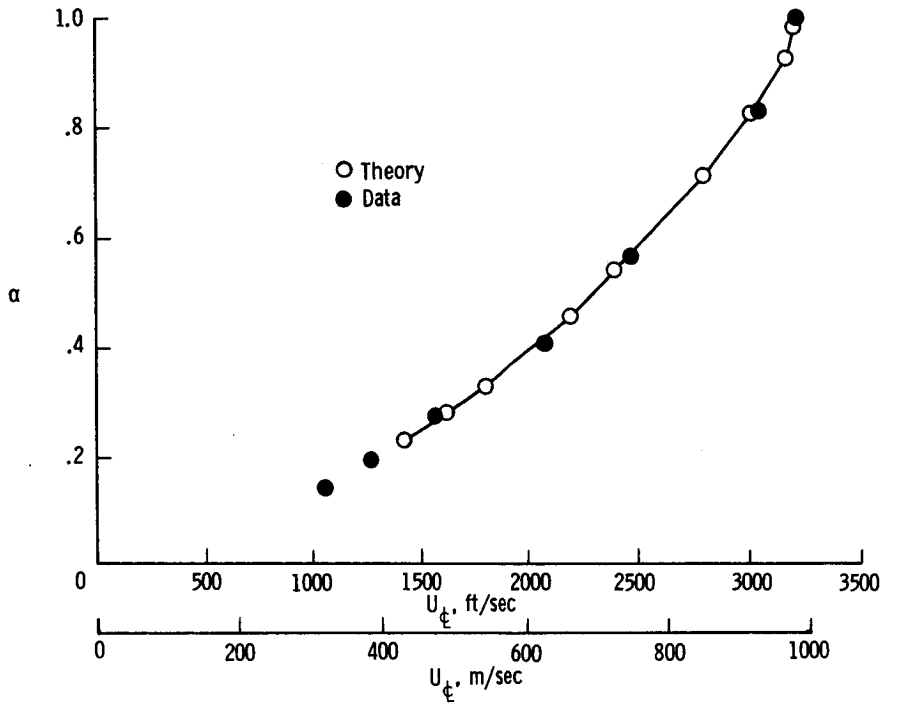

Figure 13.- Test case 10. Center-line variation of mass fraction and velocity.

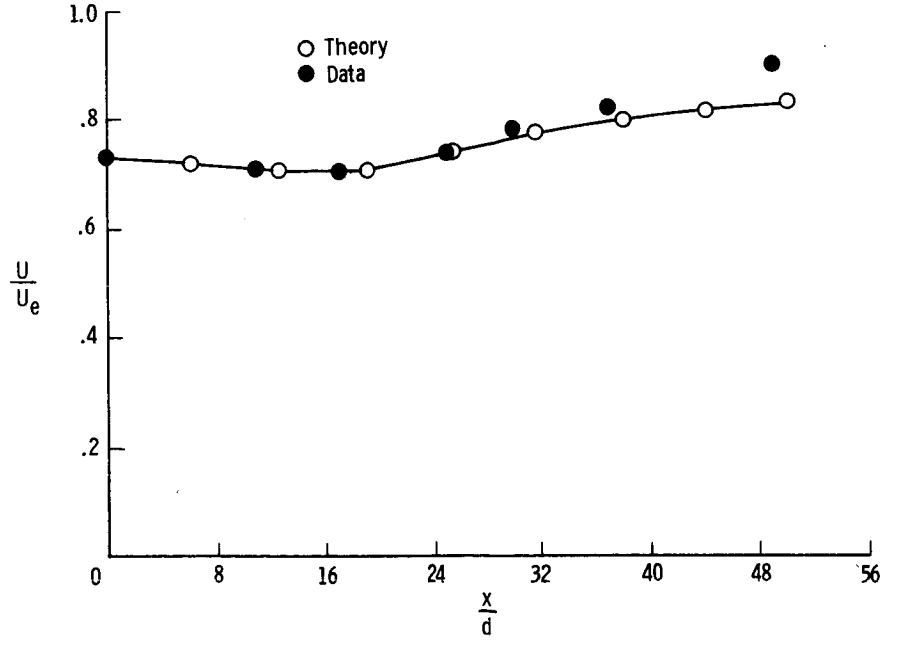

Figure 14.- Test case 11.

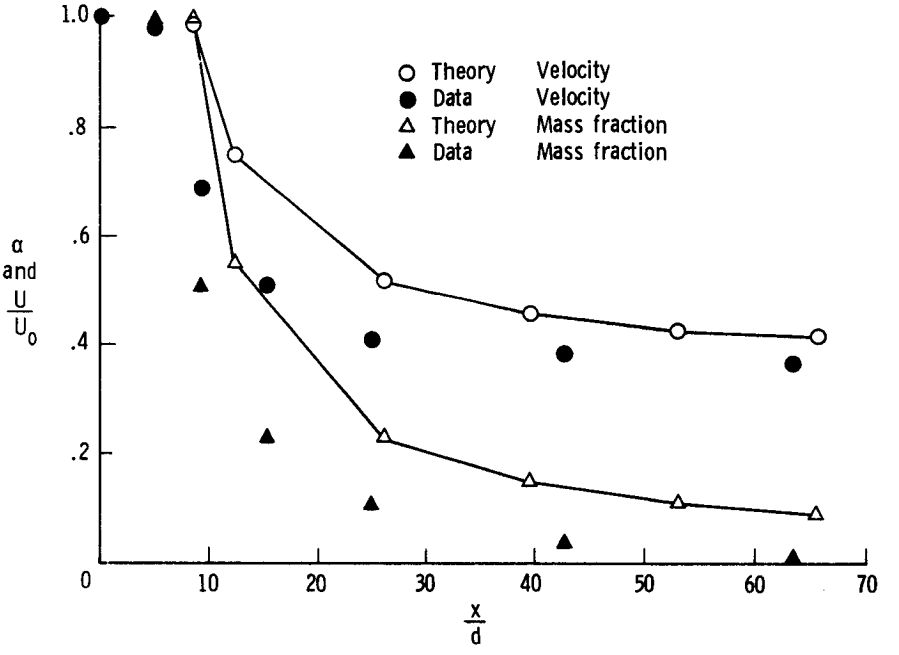

Figure 15.- Test case 12.

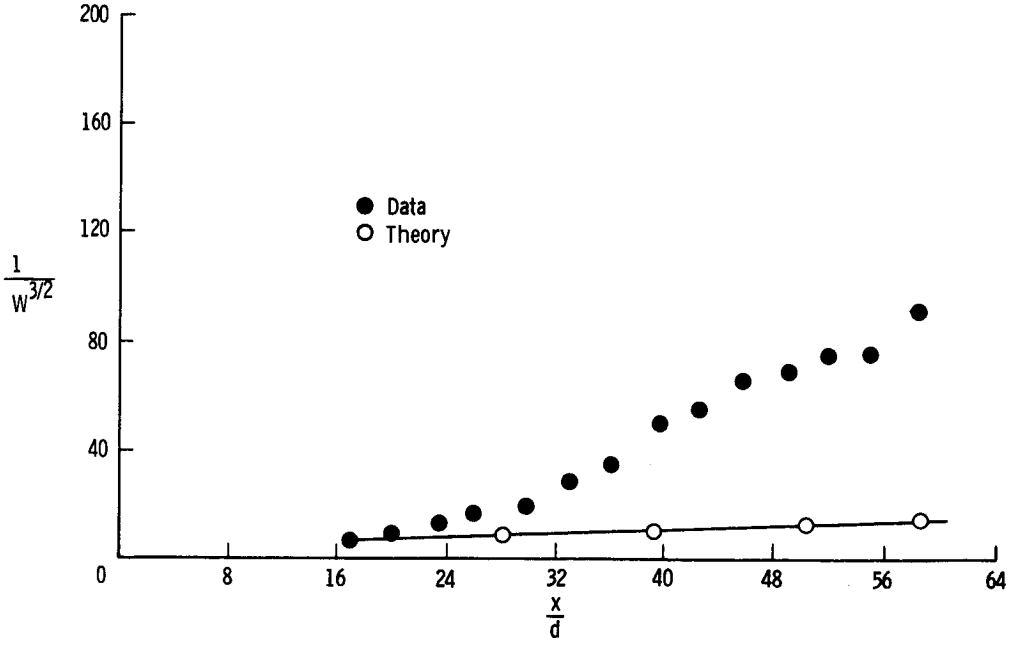

Figure 16.- Test case 17.

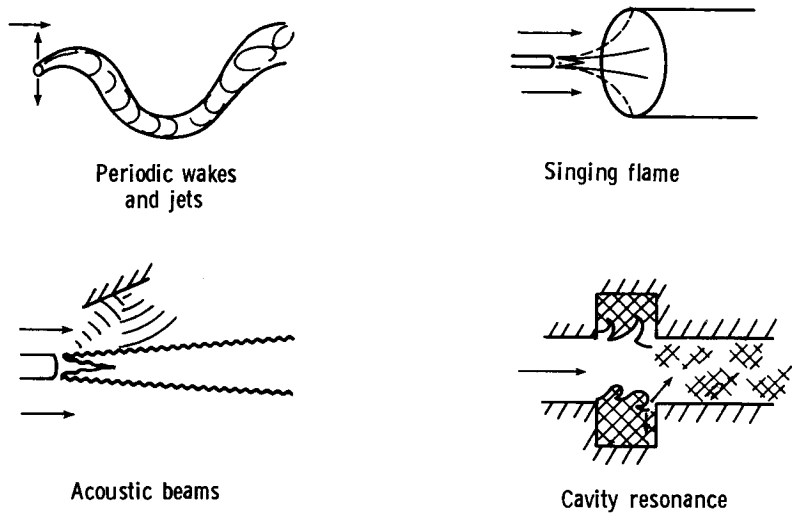

Figure 17.- Unsteady periodic mixing aids.

DISCUSSION

D. B. Spalding: Some of the plots of the axial concentration or axial velocity seem to show points which were rather far apart with straight lines drawn between them. Does that mean that you actually took very large forward steps in your computation?

P. J. Ortwerth: They were rather large but they weren't that large. That's how often the program printed out.

D. B. Spalding: What's your forward step size then as a fraction of width, for example?

P. J. Ortwerth: It's comparable to the step size in the radial direction. If you have 14 points, for example, across a shear layer, then you have to march forward with a little less than 1/14 of a shear layer in distance. So the curves are continuous; however, I really think that they are discontinuous enough that drawing straight lines between data points is not all that bad.

B. E. Launder: I noticed that when you showed your slide of the kinetic energy equation, that the first term on the right-hand side was, if memory serves me, something like, 2/3 Density × Turbulence energy × Mean velocity gradient. Could you explain briefly the origin of that term?

P. J. Ortwerth: I assume that's equal to the turbulence normal stresses if you break the turbulent stress tensor into a normal part and a shear part like you would for a normal molecular flow or laminar flow of gas; that is $p_T\left(\frac{2}{3}\rho k\right)$ by definition.

B. E. Launder: Well, certainly if we were concerned with the normal stresses, I would agree with you, but the production in the turbulence energy equation is associated with shear stresses.

P. J. Ortwerth: That is right. I tried to point that out. If you, for example, have a combustion chamber with a gas velocity in there of 8000 ft/sec (2400 m/sec), and you have a turbulence intensity of 20 percent, this will correspond to an amount of energy, translated into gas temperature so you can understand it, of several thousand degrees. Now when you expand that gas through a nozzle, of course, there's a pressure gradient and a velocity gradient, and the normal turbulence shear stresses are such a large part of the pressure in the flow, that the work done pushing the gas out of the nozzle is significant. I want to know how much that is so I can integrate that equation with that term in there. As far as you're concerned, maybe it doesn't make any difference. In the normal incompressible flow those terms are very small.

W. A. Rodi: In reference to test case 17 you mention a possible Reynolds number influence. We found very similar predictions with our model where we do not introduce a function of one of the constants. I believe the reason for your bad predictions is that you

use a constant. In this particular case, the production of kinetic energy is very low, and that's why we get a very different constant. I believe that differences occur because we introduce this function of production over dissipation.

P. J. Ortwerth: Where I would have difficulty with that comment is if the production of turbulent energy is low, I wind up with a lower viscosity and with poorer agreement with the data.

W. A. Rodi: But, we introduced a function where the new constant would increase by a factor of about 5, and that's why we get better agreement.

P. J. Ortwerth: If I change the constant by a factor of 5, it probably would agree.

TURBULENT KINETIC ENERGY EQUATION AND FREE MIXING*

By Thomas Morel, T. Paul Torda,
Illinois Institute of Technology

and Peter Bradshaw
Imperial College of Science and Technology, London

INTRODUCTION

The present work on calculation of free shear flows was carried out to investigate the usefulness of several concepts which were previously successfully applied to wall flows. The method belongs to the class of differential approaches. The turbulence is taken into account by the introduction of one additional partial differential equation, the transport equation for the turbulent shear stress. The structure of turbulence is modeled after Bradshaw et al. (ref. 1). This model has been used successfully in boundary layers and its applicability to other flows is demonstrated in this contribution. An earlier attempt to use this approach for calculation of free flows was made by Laster (ref. 2). The work reported here differs substantially from that of Laster in several ways. The most important difference is that the region around the center line is treated by invoking the interaction hypothesis (ref. 3) (concerning the structure of turbulence in the regions separated by the velocity extrema). The compressibility effects on shear layer spreading at low and moderate Mach numbers were investigated. In the absence of detailed experiments in free flows, the evidence from boundary layers that at low Mach numbers the structure of turbulence is unaffected by the compressibility was relied on. The present model was tested over a range of self-preserving and developing flows including pressure gradients using identical empirical input. The dependence of the structure of turbulence on the spreading rate of the shear layer $d\delta/dx$ was established.

16

SYMBOLS

a_1,G,L	defined by equations (2)
c_p	specific heat at constant pressure
L_o	width to the half velocity point on the profile
M	Mach number
p	mean pressure

*This research was supported in part by NASA Fellowship and partially by NASA Grant NGR-14-004-028.

$\overline{q^2} = \overline{u_i' u_i'}$

r recovery factor

T temperature

U,V mean velocity components

U_1, U_2 external velocities at edges of a mixing layer

ΔU maximum velocity difference across shear layer

u',v',w' fluctuating velocity components

$\tilde{V} = V + \frac{\overline{\rho' v'}}{\rho}$

$W = \frac{\Delta U}{U_1}$

X,Y coordinate axes

x,y distances along axes

α angle of characteristic

γ ratio of specific heats

δ shear layer thickness defined as distance between points where $\tau = 0.05\tau_m$

$\overline{\frac{d\delta}{dx}} = \frac{d\delta/dx}{(d\delta/dx)_{\text{still-air jet}}}$

ϵ dissipation rate

θ momentum thickness

ρ mean density

σ spreading parameter for free shear layers

$\tau = -\left(\overline{u'v'} + \frac{\overline{\rho' u' v'}}{\rho}\right)$

τ^+ and τ^- shear stress profiles of "simple" layers

Superscripts:

a exponent

' fluctuating quantities

Subscripts:

ℓ center-line value

i index

J initial jet value

m,max maximum value

1/2 half velocity point

ANALYSIS

Equations and the Model of Turbulence

The governing equations considered are the continuity, momentum, and turbulent kinetic energy equations:

$$\left.\begin{aligned} &\frac{\partial U}{\partial x} + \frac{\partial V}{\partial y} = 0 \\ &\left(U\frac{\partial}{\partial x} + V\frac{\partial}{\partial y}\right)U = -\frac{1}{\rho}\frac{dp}{dx} - \frac{\partial \overline{u'v'}}{\partial y} \\ &\left(U\frac{\partial}{\partial x} + V\frac{\partial}{\partial y}\right)\frac{\overline{q^2}}{2} = -\overline{u'v'}\frac{\partial U}{\partial y} - \frac{\partial}{\partial y}\left(\frac{\overline{p'v'}}{\rho} + \frac{1}{2}\overline{q^2 v'}\right) - \epsilon \end{aligned}\right\} \quad (1)$$

The turbulent kinetic energy equation contains three additional correlations not appearing in the other two equations. To close this system, assumptions about the structure of turbulence would have to be made, where by structure a given relation between the local values of two turbulent quantities is understood. As in Bradshaw et al. (ref. 1), three relations are used to define the structure:

$$\tau = a_1 \overline{q^2} \tag{2a}$$

$$\epsilon = \frac{\tau|\tau|^{1/2}}{L} \tag{2b}$$

$$\frac{\overline{p'v'}}{\rho} + \frac{1}{2}\overline{q^2 v'} = G\tau\left|\tau_{max}\right|^{1/2} \tag{2c}$$

The functions a_1, L, and G are specified by algebraic expressions and the local length and velocity scales of turbulence are assumed to be proportional, respectively, to δ and $\left|\tau_m\right|^{1/2}$.

By utilizing relations (2), the conservation equation for $\overline{q^2}$ may be converted into an empirical transport equation for τ

$$\left(U\frac{\partial}{\partial x} + V\frac{\partial}{\partial y}\right)\tau = 2a_1\left[\tau\frac{\partial U}{\partial y} - \frac{\partial}{\partial y}\left(G\tau\left|\tau_{max}\right|^{1/2}\right) - \frac{\tau|\tau|^{1/2}}{L}\right] + \tau\left(\frac{U}{a_1}\frac{\partial a_1}{\partial x} + \frac{V}{a_1}\frac{\partial a_1}{\partial y}\right) \tag{3}$$

The choice of convective type diffusion (eq. (2c)) over gradient type in free flows is supported by mixing layer experiments. (See refs. 4 and 5.) The positions of zero diffusion and maximum kinetic energy do not coincide, a fact for which gradient diffusion cannot account for. The two points are separated by a distance of the order of 5 percent of the shear layer thickness. Also, the free shear flows exhibit strong large-scale motions which made the convective diffusion important.

There is much experimental evidence to support the relation (2a). An examination of a wide range of experimental data showed that the value of a_1 varies within a small range depending on the flow considered. The only difficulty in this formulation occurs in the vicinity of a velocity extremum, as discussed in the next paragraph. Relation (2b) is a logical extension, based on equation (2a), of

$$\epsilon = \frac{\left(\overline{q^2}\right)^{3/2}}{L}$$

which is a commonly accepted model.

Flows With Velocity Extrema

The formulation presented was applied to free mixing layers with the simple choice of $a_1(y) = \text{Constant}$ as in boundary layers. In flows with velocity extrema, the shear

stress changes sign in the vicinity of the velocity extremum. The turbulent kinetic energy, by definition, does not change sign and this fact precludes the use of constant a_1. Also, the shear stress equation is singular at the point where $a_1 = 0$ (its solution being regular) and for this reason presents numerical difficulties. (See ref. 2.)

To avoid this problem, the suggestion of Bradshaw (ref. 3) is used and the flow with velocity extremum is regarded as two adjoining "simple" shear layers which interact only through the mean velocity profile. Each layer has its own shear profile and the algebraic sum of these profiles in the region of overlap gives the shear profile of the complete flow. One reason for looking at the flow from this viewpoint is that if the structure of turbulence in each layer is unaffected by the presence of the adjoining layer (does not actively participate in the interaction), then a simple tool for calculating more complex flows such as jets, wakes, and wall jets is obtained. There are two such simple or basic shear layer flows – the boundary layer and the mixing layer – and it is proposed to regard all other thin shear layer flows as combinations of these two. The empirical functions in each layer of a complex flow were to be the same, or nearly the same, as in the corresponding simple shear layer and, as a result, the task of determining them would be simplified. (The actual difference between jets and mixing layers can be seen in figures 1 and 2.) Another reason is that this point of view allows a simple explanation of the regions of "negative production" of turbulent kinetic energy which occur in asymmetric flows. The technique can be utilized for calculating these flows which otherwise require the a priori knowledge of the point of vanishing shear when the original formulation is used. The same shortcoming affects all models which involve the eddy-viscosity concept in one form or another.

The idea was applied to the duct flows (ref. 3) and very good results were obtained with the empirical functions which were developed for boundary layers. In this work the same approach is applied to jets and wakes.

Empirical Functions of the Structure

The empirical functions of the structure of turbulence in mixing layers $\left(\text{with } U_2/U_1 = 0\right)$ were derived from the experimental data (refs. 4 and 6) and then refined by comparison of the velocity and shear profiles with the experiments. (See fig. 1.) The simple choice of constant $a_1 = 0.15$ and $L/\delta = 0.09$ was found to be adequate for good results. The shape of the diffusion function G was obtained by integration of the diffusion in the turbulent kinetic energy balance. The proper values of the empirical functions for $U_2/U_1 \neq 0$ were deduced from calculations by comparison with the results of Spencer (ref. 7). The empirical functions were found to be dependent on the velocity ratio of the mixing layer. This dependence may be correlated with $d\delta/dx$, the spreading rate of the shear layer.

The same model was applied to jets and wakes as outlined. The two adjoining layers are calculated as two separate layers. They share joint U and V profiles but they have separate shear profiles. The only difference from the mixing-layer program appears in the momentum equation where the shear profiles are superposed to give the "true" shear profile in the region of overlap:

$$U \frac{\partial U}{\partial x} + V \frac{\partial U}{\partial y} = -\frac{1}{\rho} \frac{dp}{dx} + \frac{\partial \tau^+}{\partial y} + \left(\frac{\partial \tau^-}{\partial y}\right)_{\text{other layer}} \tag{4}$$

Beyond the velocity maximum, the layer experiences a negative production in the shear equation which limits the region of overlap.

The program is written, at the present time, for symmetric jets and wakes because of lack of experimental data. However, the concept is not restricted in any way to symmetric flows and its importance lies in its ability to treat and explain asymmetric flows.

The calculations show that in free flows the structure of the "simple" layer is affected by the interaction. The interaction tends to modify more the magnitude than the shape of the empirical functions. Thus, the a_1 and L/δ were retained constant and the shape of the diffusion function G was slightly altered. (See fig. 2.) The comparison with experiments indicates again the dependence of the structure on the spreading rate $d\delta/dx$. The limiting case for $d\delta/dx = 0$ is shown in broken lines in figure 2.

The results show the usefulness of the interaction concept for calculation of free shear flows. The required modifications of the empirical functions are not large and indicate that the flows with velocity extrema may be regarded as weakly interacting adjoining shear layers. There appears to be more interaction of turbulent structure in the free flows than in the ducts and the explanation may be sought in the behavior of the shear stress in the vicinity of the velocity extremum. (See fig. 3.) The shear stress profiles of free flows overlap significantly more and the value of the shear on the center line is typically $0.55\tau_{max}$, against $0.1\tau_{max}$ in the duct, and thus causes a stronger interaction.

All the results presented are calculated with the same input, the structure being a function of y/δ and $d\delta/dx$ alone.

Compressible Flow

The governing equations for the compressible flow are much more complicated than their incompressible counterpart. If the restriction is made to include only low and moderate Mach number flows, many of the new correlations appearing in the compressible equations may be neglected on the basis of order-of-magnitude arguments. (See ref. 8.) This neglect simplifies the equations which may then be written in boundary-layer form as follows:

$$\frac{\partial U}{\partial x} + \frac{\partial \tilde{V}}{\partial y} + \frac{U}{\rho}\frac{\partial \rho}{\partial x} + \frac{\tilde{V}}{\rho}\frac{\partial \rho}{\partial y} = 0$$

$$U\frac{\partial U}{\partial x} + \tilde{V}\frac{\partial U}{\partial y} = -\frac{1}{\rho}\frac{dp}{dx} + \frac{\partial \tau}{\partial y} + \frac{\tau}{\rho}\frac{\partial \rho}{\partial y}$$

$$U\frac{\partial \tau}{\partial x} + \left(\tilde{V} + 2a_1 G|\tau_m|^{1/2}\right)\frac{\partial \tau}{\partial y} = \tau\left[2a_1\left(\frac{\partial U}{\partial y} - |\tau_m|^{1/2}\frac{\partial G}{\partial y} - \frac{G|\tau_m|^{1/2}}{\rho}\frac{\partial \rho}{\partial y} - \frac{|\tau|^{1/2}}{L}\right) + \frac{U}{a_1}\frac{\partial a_1}{\partial x} + \frac{\tilde{V}}{a_1}\frac{\partial a_1}{\partial y}\right]$$

where

$$\tau = a_1\left(\overline{q^2} + \frac{\overline{\rho' q^2}}{\rho}\right)$$

$$L = \frac{\tau|\tau|^{1/2}}{\epsilon}$$

$$\frac{1}{2}\overline{p'v'} + \frac{1}{2}\overline{q^2 v'} + \frac{1}{2\rho}\overline{\rho' q^2 v'} = G\tau|\tau_m|^{1/2}$$

The inclusion of compressibility presents two additional tasks. The structure of turbulence in compressible flow and the density variation across the layer have to be determined.

For the values of the empirical functions in compressible flows, the suggestion (ref. 9) is relied on that the turbulence is convected passively by the mean flow as long as the local Mach number of the root-mean-square fluctuations $\left(\overline{\rho u'^2}/\gamma p\right)^{1/2}$ is much less than unity. The inference is that the structure of turbulence is Mach number independent and the "incompressible" values of the empirical functions may be used. This assumption is based on the analysis of experiments in boundary layers, where this condition is satisfied up to moderate Mach numbers ($M < 5$).

In the Mach number range to which the present approach is limited, a good approximation for the density profile can be obtained from the Crocco formula used in boundary layers:

$$c_pT + 0.5rU^2 = \text{Constant}$$

which together with the equation of state yields $\rho = \rho(U)$. It eliminates the need for an additional equation and may be incorporated into the incompressible version of the program with only small modifications.

Compressibility effects due to temperature or density differences were also incorporated by assuming, respectively, similarity between temperature and velocity profiles and between mass fractions and velocity profiles. That again yields a relation $\rho = \rho(U)$ which is useful for small compressibility effects. Large effects will require the solution of a separate equation.

METHOD OF SOLUTION

With the diffusion term in the kinetic energy equation modeled to be of the convective type, the set of equations becomes hyperbolic. There are two choices of solving this system, either by a procedure suitable for parabolic equations or to use the method of characteristics. The first approach is advantageous if it is intended to introduce additional equations, for example, for compressible flows or for a more involved model of turbulence. In the present work, it was decided to use the mathematically simpler method of characteristics used already in the boundary-layer calculations. (See ref. 1.) The model of turbulence and the empirical functions developed in the course of this work would be the same if an alternative method of solution of these equations is used.

The accuracy of the calculations is governed by the number of points on the profile and by the number of iterations used to improve the interpolation along the characteristics. However, even if several iterations are used, the momentum and mass balance are not preserved because of numerical inaccuracies and lead to a momentum thickness gain of the order of 0.1 percent per station. To avoid accumulation of error, the grid size is being readjusted by that very small amount after every step so that momentum is preserved. The mass balance is then very well preserved – to within 1 percent on a typical run. The largest inaccuracies occur for flows issuing into a small external stream. One of the characteristic angles near the edge tends to $\alpha = \arctan(V/U)$ and precludes calculation of mixing with still air unless some special numerical treatment for this boundary is introduced. The problem at the still-air edge affects other methods of solution as well. Calculation of mixing with small external stream has some practical limitations. The step size in the x-direction is inversely proportional to $\tan \alpha_{max}$ and, therefore, for economical calculation, it is necessary to maintain at least $U_1 = 0.05U_{max}$ which gives $\tan \alpha_{max} \approx 1$. The region of very small external stream also suffers from larger than average errors in mass balance.

COMPARISON WITH EXPERIMENTS

The model developed for the mixing layers can be used for all velocity ratios. Calculations for three ratios are compared with experiments below:

(a) Mixing into still air. (See Liepmann and Laufer (ref. 6) and Bradshaw and Ferriss (ref. 4) and also figure 4.) Note that the computed profile has a small external stream rather than still air on its edge; thus, the spreading rate is reduced somewhat.

(b) Mixing with a parallel moving stream. (See Spencer (ref. 7) and figures 5 and 6.)

The jet program is capable of handling both jets and wakes in the presence of pressure gradients by using the same empirical input. Some predictions compared with experiments are

(a) Jet mixing with still air. (See Bradbury (ref. 10) and figure 7.) Both the experiment and the calculations had actually a small external stream which does not affect the nondimensional profiles.

(b) Small deficit wake. (See Townsend (ref. 11).) The region in which Townsend made his measurements is far from complete self-preservation as documented by the difference between the measured shear profile and the profile required for self-preservation. (See fig. 8.) The calculations compare well in the region investigated by Townsend and show self-preservation far downstream. (See fig. 9.) The small excess jet tends toward the same results as the small deficit wake when $W \to 0$.

When the external flow varies as $U_1 \propto x^a$, there are ranges of the exponent a for which the momentum equation allows self-preservation of jets or wakes. The following two flows fall in that category:

(c) Wakes in a pressure gradient – investigated by Gartshore (ref. 12) who found them approximately self-preserving. The calculations show that, although the flow has the tendency to conform to the self-preservation, it drifts steadily away from it (fig. 10).

(d) Self-preserving jet in a pressure gradient. Value of the exponent $a = -\frac{1}{2.4}$ was used for the calculations. The results obtained are plausible, although there are no experiments to support them. (See fig. 11.)

APPENDIX

COMMENTS ON TEST CASES

This appendix presents comments on some of the test cases presented in figures 12 to 19.

Test Case 5 (Hill and Page)

The free shear layer was measured in the early stages of its development from a boundary layer separated over a cavity. At the separation the boundary layer was turbulent and had a momentum thickness of 0.0793 cm. The last measured station was at $x = 20.95$ cm or $x/\theta = 264$. The dimensions of the cavity and of the orientations of the axes X,Y are not clear in reference 13. Depending on the details of the geometry, significant backflow and transverse pressure gradient may have been present. In view of these uncertainties, it is difficult to comment on the disagreement of the calculations and of the experiment and also on the lack of spreading of the experimental profile on the low velocity side.

In any case, as the boundary layer was turbulent at the separation the shear layer was probably not in the self-preserving range even at the last station. (See Bradshaw, ref. 14.) In the calculations the maximum shear first increased above the "fully developed" value (overshoot). Its decrease toward the value far downstream was slow and monotonical. At $x = 20.95$ cm, its value was still higher by an amount on the order of 10 percent. Also the spreading rate $1/\sigma$ was still substantially higher at that station than far downstream.

Test Case 13 (Bradbury)

The calculations were not overly sensitive to the initial shear. An increase of the initial shear by 66 percent produced less than 1-percent difference in W at $x/D = 300$.

Test Case 14 (Chevray and Kovasznay)

In a wake very close to the trailing edge, the structure of turbulence may be expected to be that of a boundary layer rather than that of a free flow. The question remains how long does it take for the structure to undergo the change from one regime to another. The examination of the data of reference 15 showed that the mean velocity and turbulent quantities take on their wakelike shapes already by the distance $x = 20$ cm and possibly even earlier. It seems reasonable to expect that also the structure of turbulence came close to the wake type by that distance. This possibility was tested by starting the calculations at three different points $x_0 = 0$, 20, and 50 cm by using the experimental profiles as the

input. The results do confirm the expectation since although the latter two calculations differ from the first one they agree with each other. (See figs. 12(a) and 12(b).) It appears that the present model has difficulties near the trailing edge where the structure is still that of the boundary layer. The calculated and experimental profiles at $x = 240$ cm agree well when the calculations start at $x = 20$ cm (fig. 12(c)) or at $x = 50$ cm. From the figures it is also clear that the momentum thickness of the computed and measured profiles are not equal. A check on the momentum thickness at several stations revealed the following variation of θ and gives an idea about the general accuracy of the experiment:

x	0	20	50	240
θ	0.578	0.606	0.585	0.557

Test Case 16 (Demetriades (ref. 16))

The results of the calculations were found to be rather sensitive to the initial shear in contrast to the test case 13. A 20-percent change of the initial shear produced a substantial difference at $x/4\theta = 2000$ and this difference $\left(\text{as represented by the value of } \tau_m/\Delta U^2\right)$ still persisted very far downstream. This behavior was found both in compressible and incompressible flows. This lack of tendency "to forget" of small deficit wakes is very interesting and suggests that convection and diffusion of turbulence in these flows have a large influence on the flow development.

The presented results were obtained by using a recovery factor of 0.9.

REFERENCES

1. Bradshaw, P.; Ferriss, D. H.; and Atwell, N. P.: Calculation of Boundary-Layer Development Using the Turbulent Energy Equation. J. Fluid Mech., vol. 28, pt. 3, May 26, 1967, pp. 593-616.

2. Laster, M. L.: Inhomogeneous Two-Stream Turbulent Mixing Using the Turbulent Kinetic Energy Equation. AEDC-TR-70-134, U.S. Air Force, May 1970. (Available from DDC as AD 705 578.)

3. Bradshaw, P.; Dean, R. B.; and McEligot, D. M.: Calculation of Interacting Turbulent Shear Layers: Duct Flow. I. C. Rep. 71-14, Imperial College, Sci. & Technol., 1971.

4. Bradshaw, P.; and Ferriss, D. H.: The Spectral Energy Balance in a Turbulent Mixing Layer. C.P. No. 899, Brit. A.R.C., 1967.

5. Wygnanski, I.; and Fiedler, H. E.: The Two-Dimensional Mixing Region. J. Fluid Mech., vol. 41, pt. 2, Apr. 13, 1970, pp. 327-361.

6. Liepmann, Hans Wolfgang; and Laufer, John: Investigations of Free Turbulent Mixing. NACA TN 1257, 1947.

7. Spencer, Bruce Walton: Statistical Investigation of Turbulent Velocity and Pressure Fields in a Two-Stream Mixing Layer. Ph. D. Thesis, Univ. Illinois, 1970.

8. Bradshaw, P.; and Ferriss, D. H.: Calculation of Boundary-Layer Development Using the Turbulent Energy Equation: Compressible Flow on Adiabatic Walls. J. Fluid Mech., vol. 46, pt. 1, Mar. 15, 1971, pp. 83-110.

9. Morkovin, Mark V.: Effects of Compressibility on Turbulent Flows. The Mechanics of Turbulence, Gordon & Breach, Sci. Publ., Inc., c.1964.

10. Bradbury, L. J. S.: The Structure of a Self-Preserving Turbulent Plane Jet. J. Fluid Mech., vol. 23, pt. 1, Sept. 1965, pp. 31-64.

11. Townsend, A. A.: The Fully Developed Turbulent Wake of a Circular Cylinder. Aust. J. Sci. Res. A, vol. 2, Dec. 1949, pp. 451-468.

12. Gartshore, Ian S.: Two-Dimensional Turbulent Wakes. J. Fluid Mech., vol. 30, pt. 3, Nov. 29, 1967, pp. 547-560.

13. Hill, W. G., Jr.; and Page, R. H.: Initial Development of Turbulent, Compressible, Free Shear Layers. Trans. ASME, Ser. D: J. Basic Eng., vol. 91, no. 1, Mar. 1969, pp. 67-73.

14. Bradshaw, P.: The Effect of Initial Conditions on the Development of a Free Shear Layer. J. Fluid Mech., vol. 26, pt. 2, Oct. 1966, pp. 225-236.

15. Chevray, René; and Kovasznay, Leslie S. G.: Turbulence Measurements in the Wake of a Thin Flat Plate. AIAA J., vol. 7, no. 8, Aug. 1969, pp. 1641-1643.

16. Demetriades, Anthony: Turbulent Mean-Flow Measurements in a Two-Dimensional Supersonic Wake. Phys. Fluids, vol. 12, no. 1, Jan. 1969, pp. 24-32.

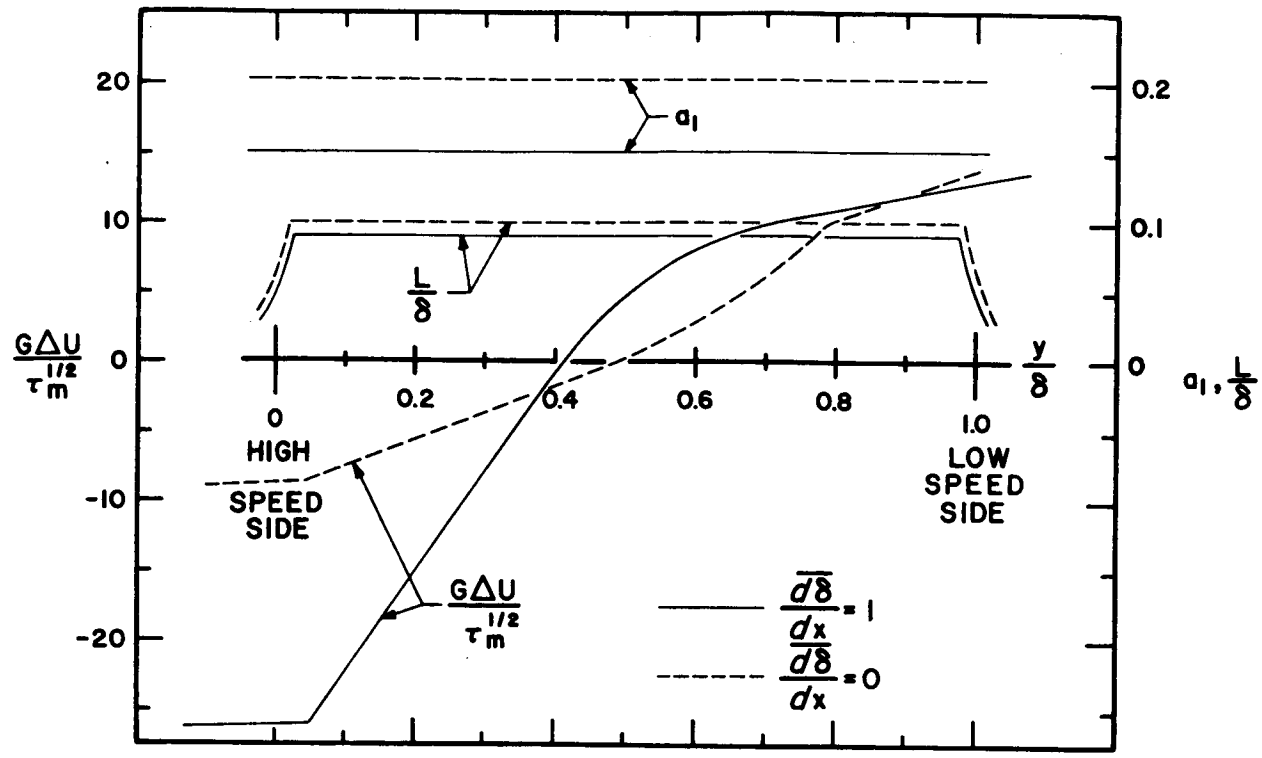

Figure 1.- Free shear layers – empirical functions (structure).

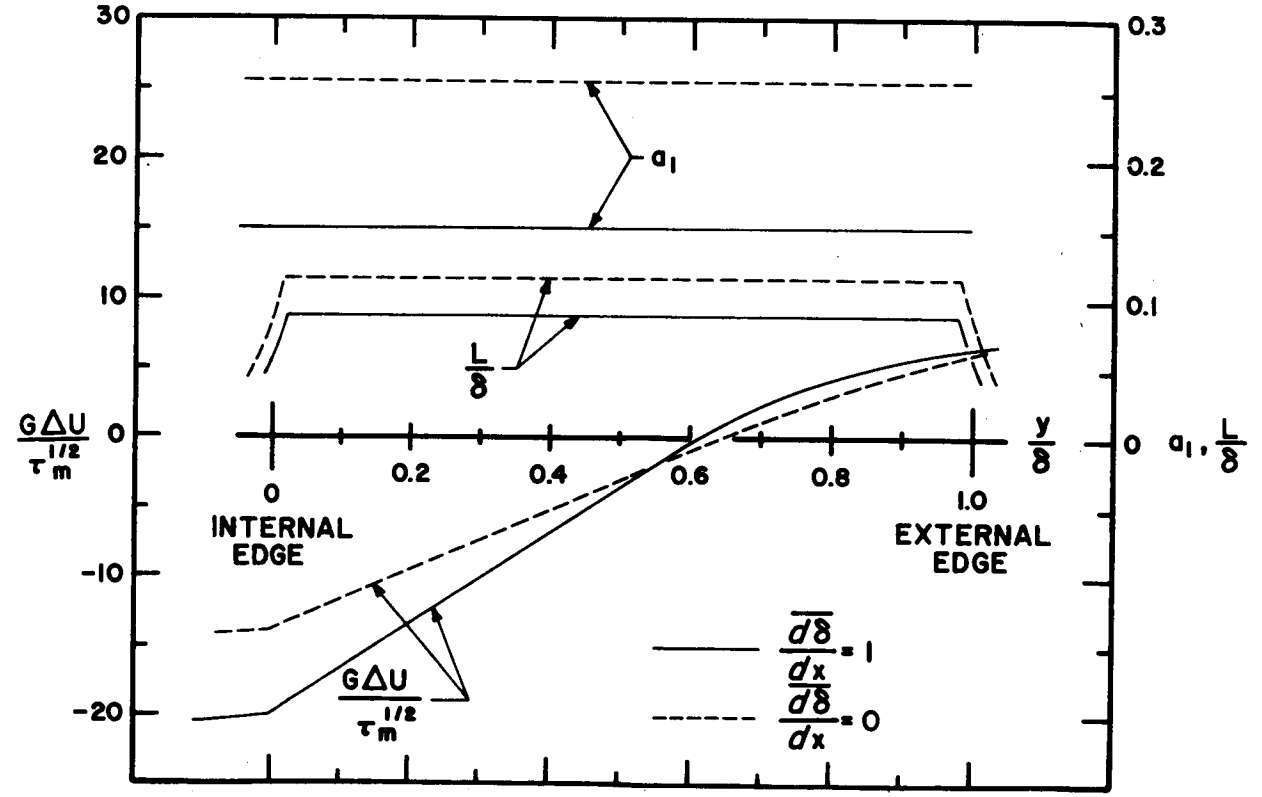

Figure 2.- Jets and wakes – empirical functions (structure).

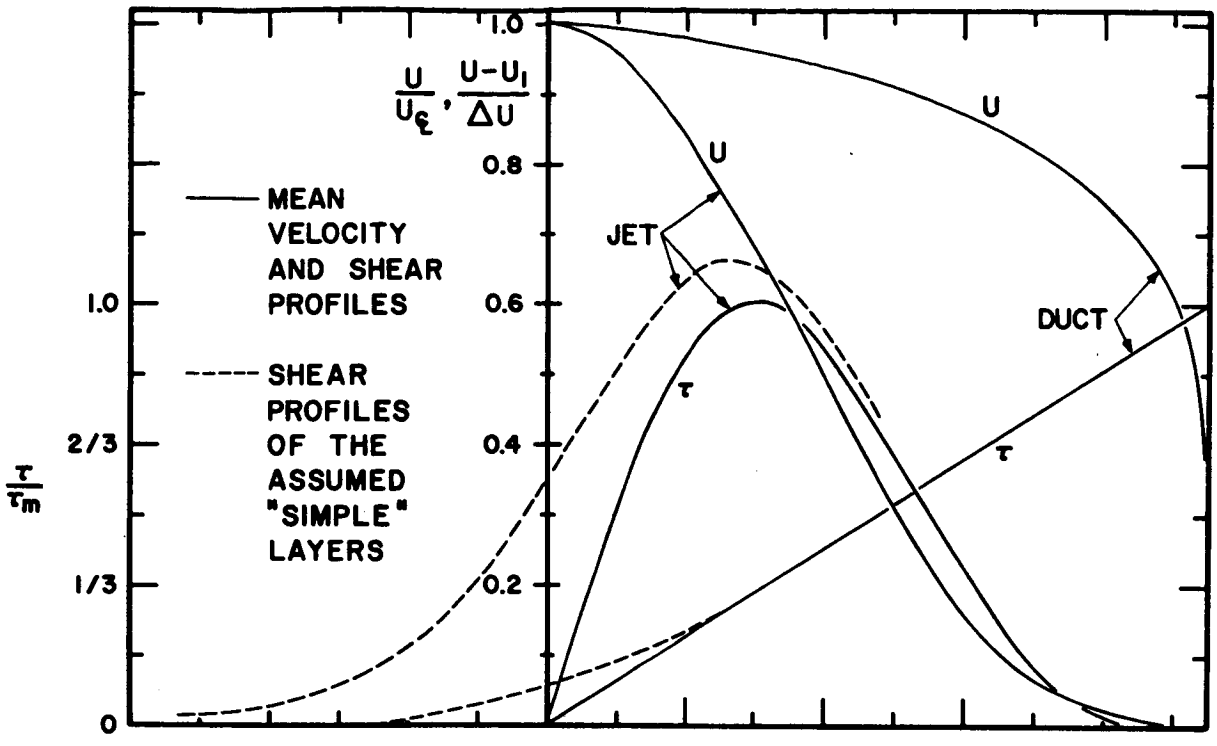

Figure 3.- Interaction approach – jets compared with ducts.

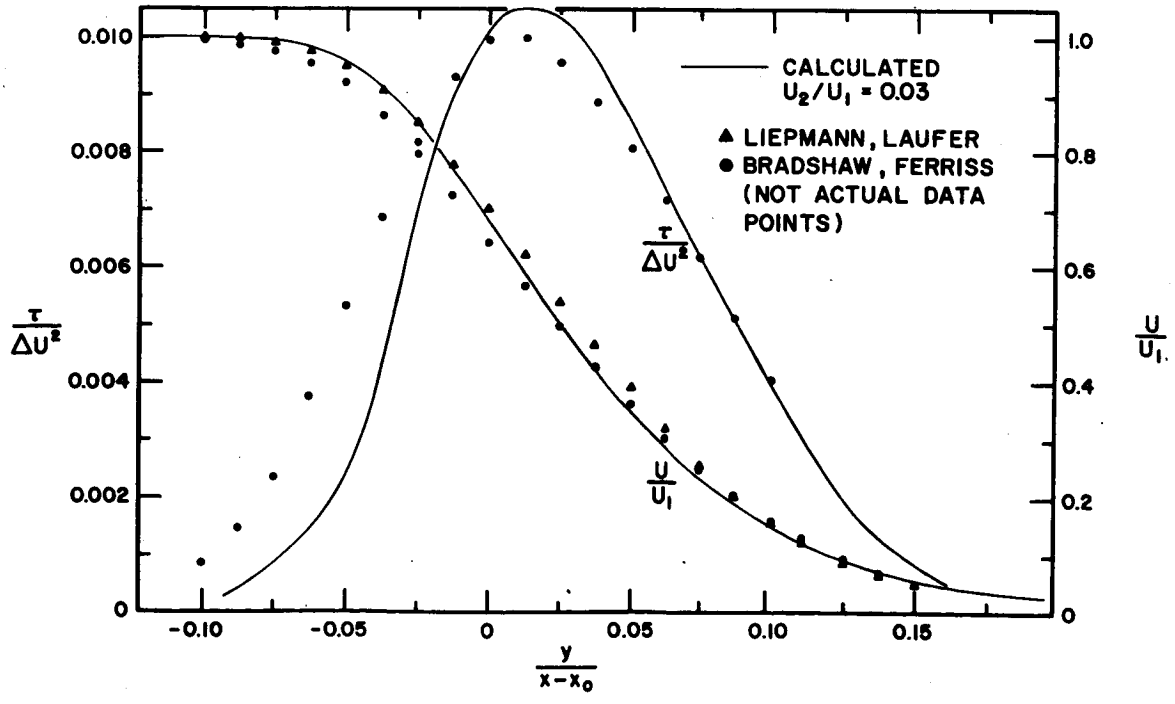

Figure 4.- Free shear layer; $U_2/U_1 = 0$.

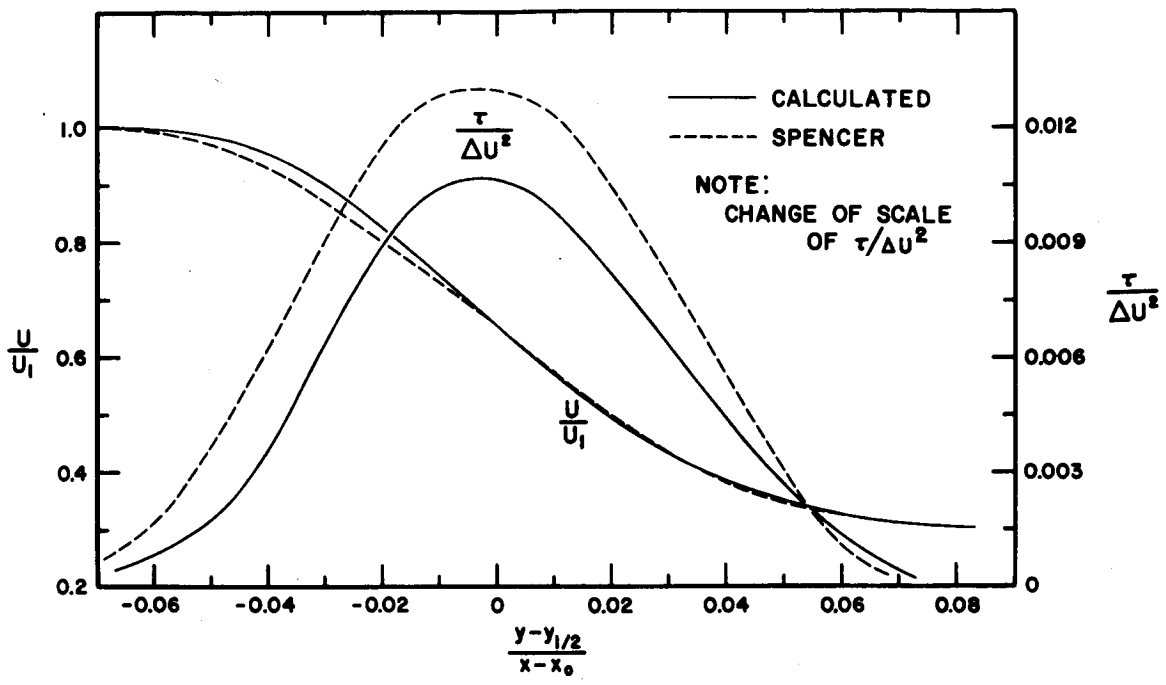

Figure 5.- Free shear layer; $U_2/U_1 = 0.3$.

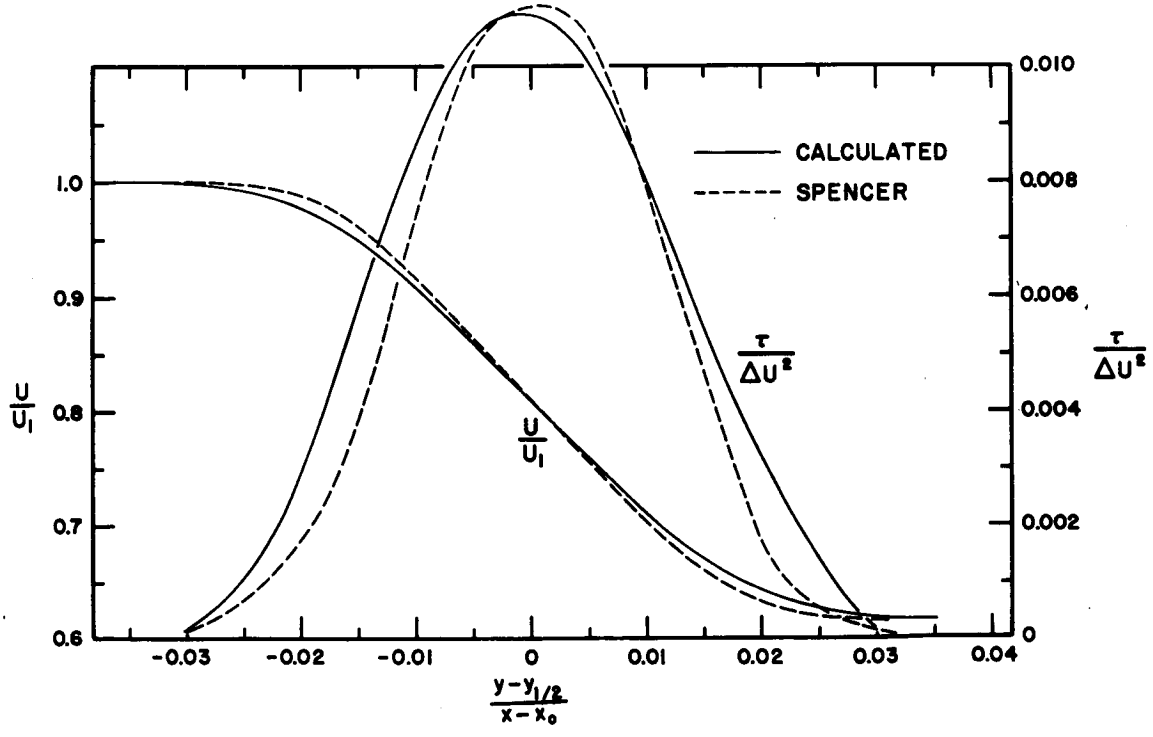

Figure 6.- Free shear layer; $U_2/U_1 = 0.61$.

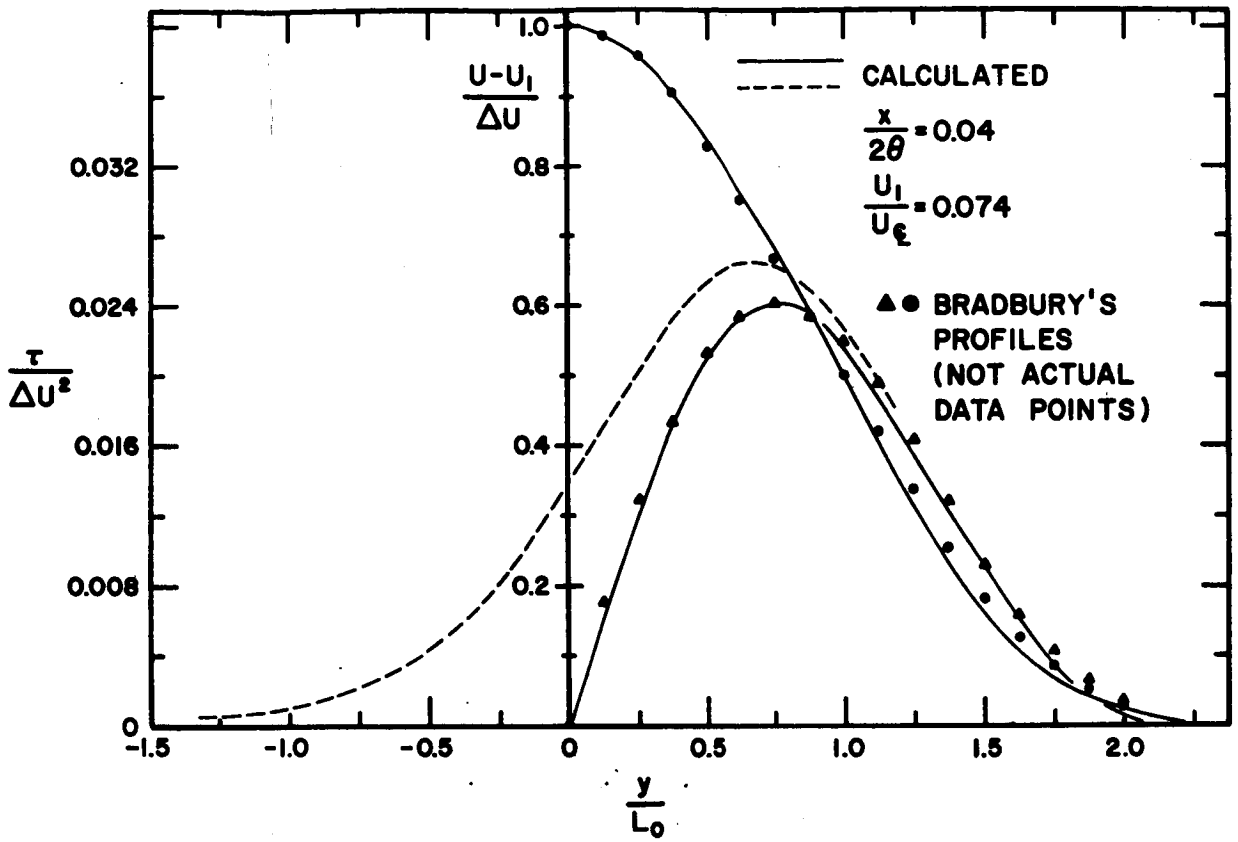

Figure 7.- Two-dimensional jet with small external flow.

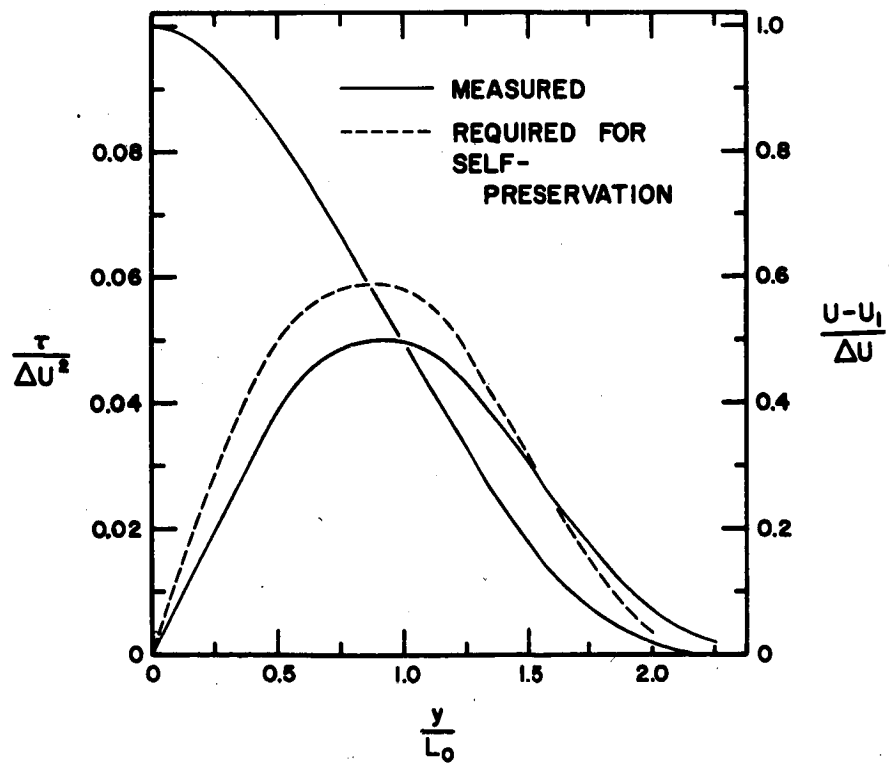

Figure 8.- Small-deficit two-dimensional wake – Townsend.

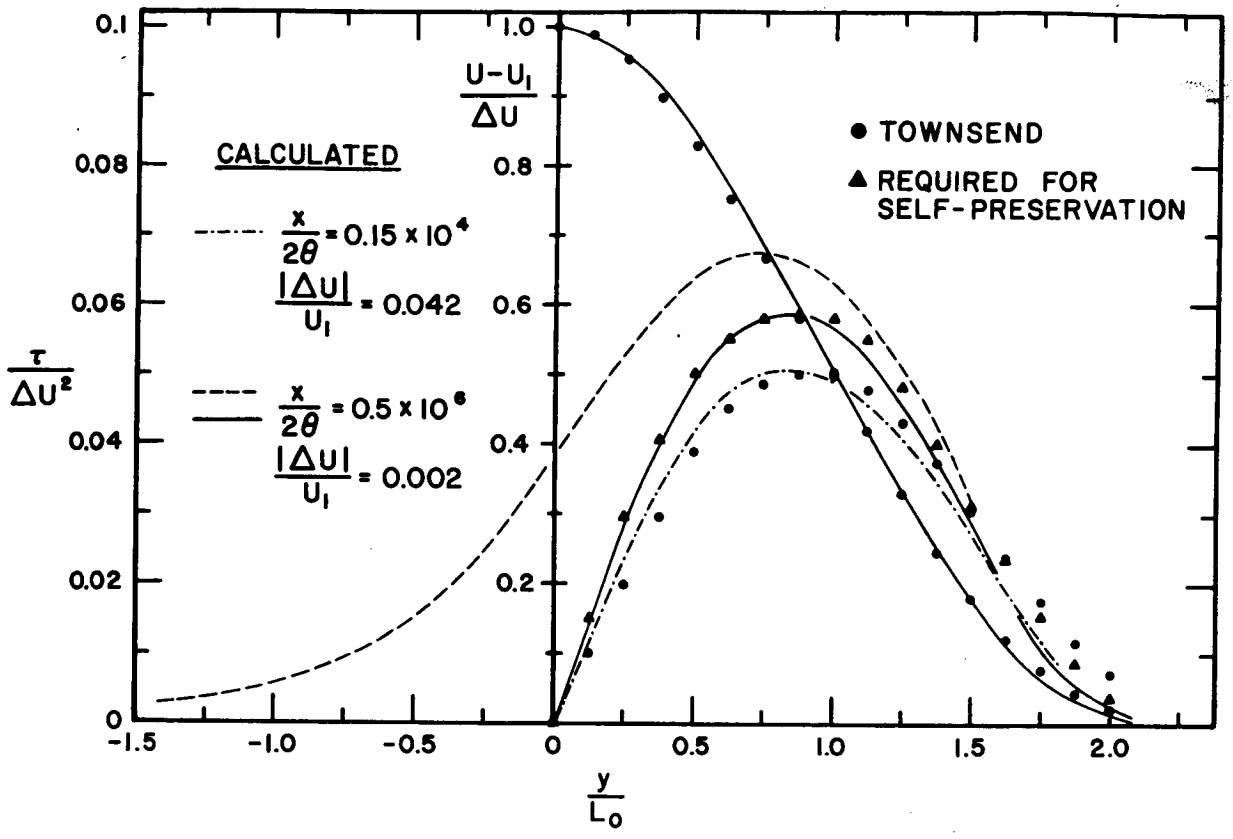

Figure 9.- Small-deficit two-dimensional wake – comparison with calculations.

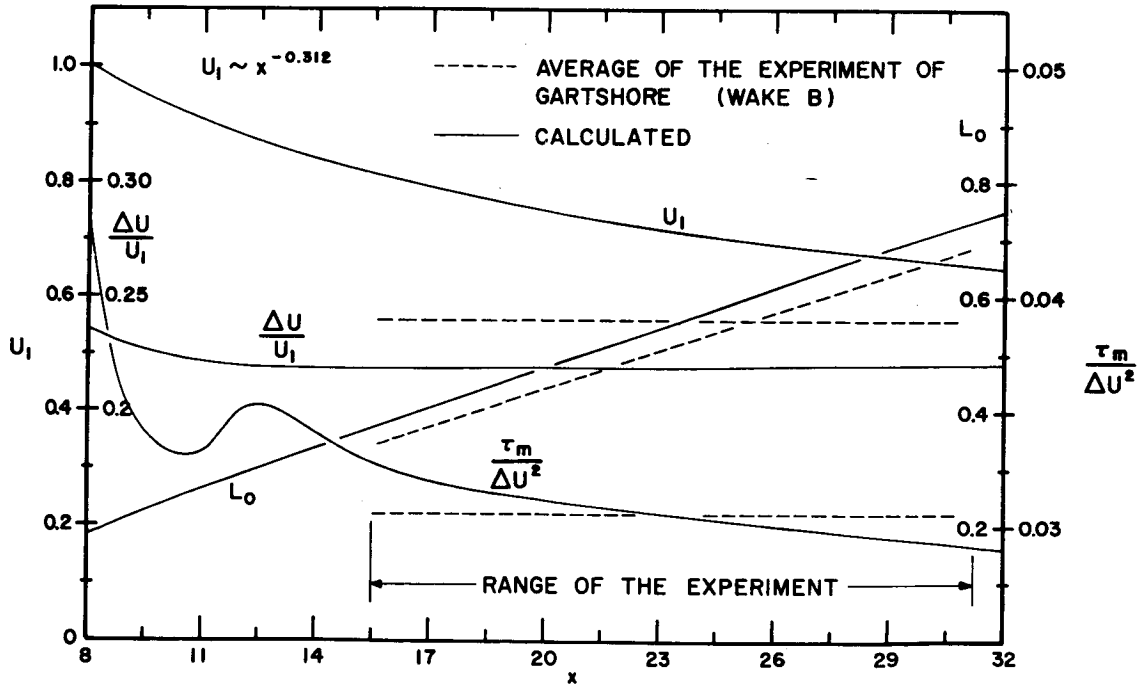

Figure 10.- Two-dimensional wake in "self-preserving" pressure gradient.

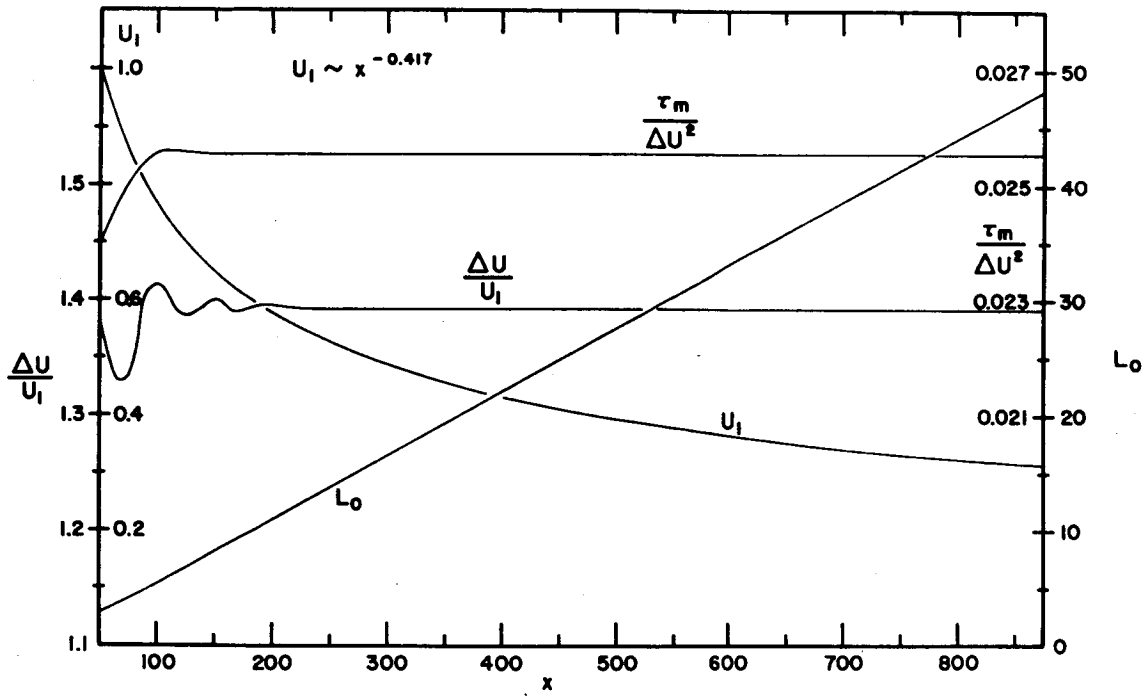

Figure 11.- Two-dimensional jet in "self-preserving" pressure gradient.

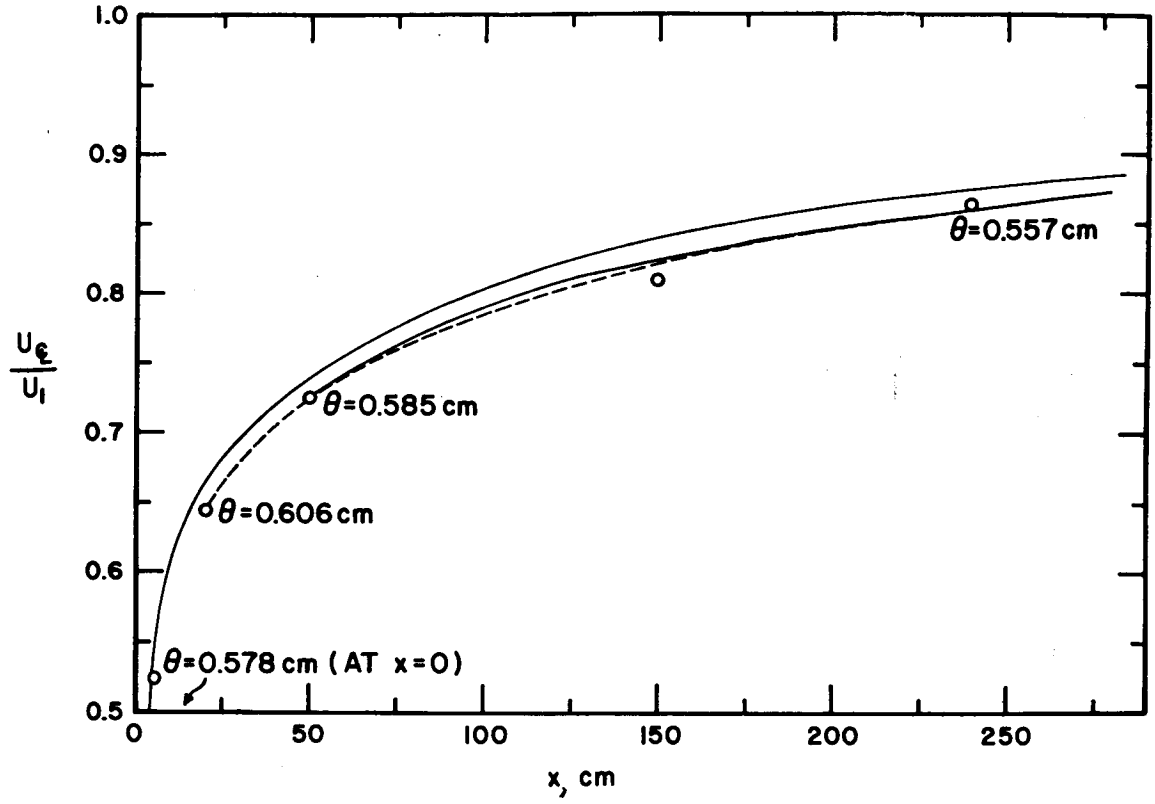

(a) Center-line velocity.

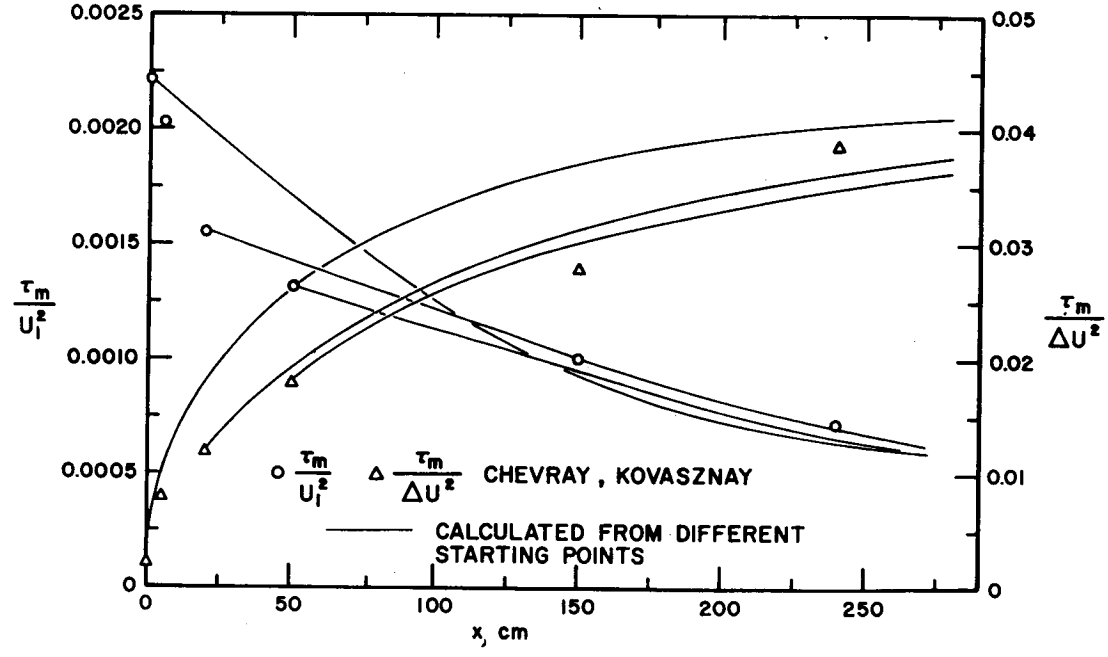

(b) Maximum shear.

Figure 12.- Two-dimensional wake of a thin flat plate.

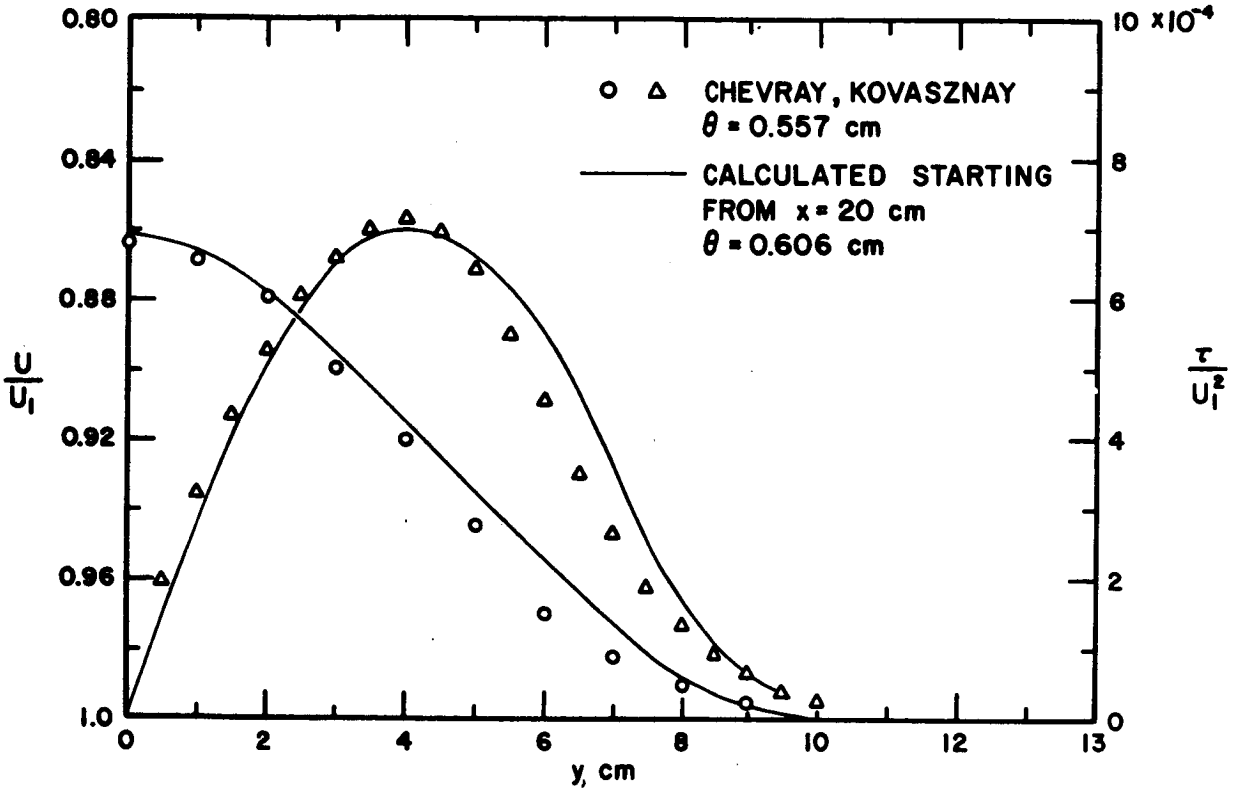

(c) Profiles at x = 240 cm.

Figure 12.- Concluded.

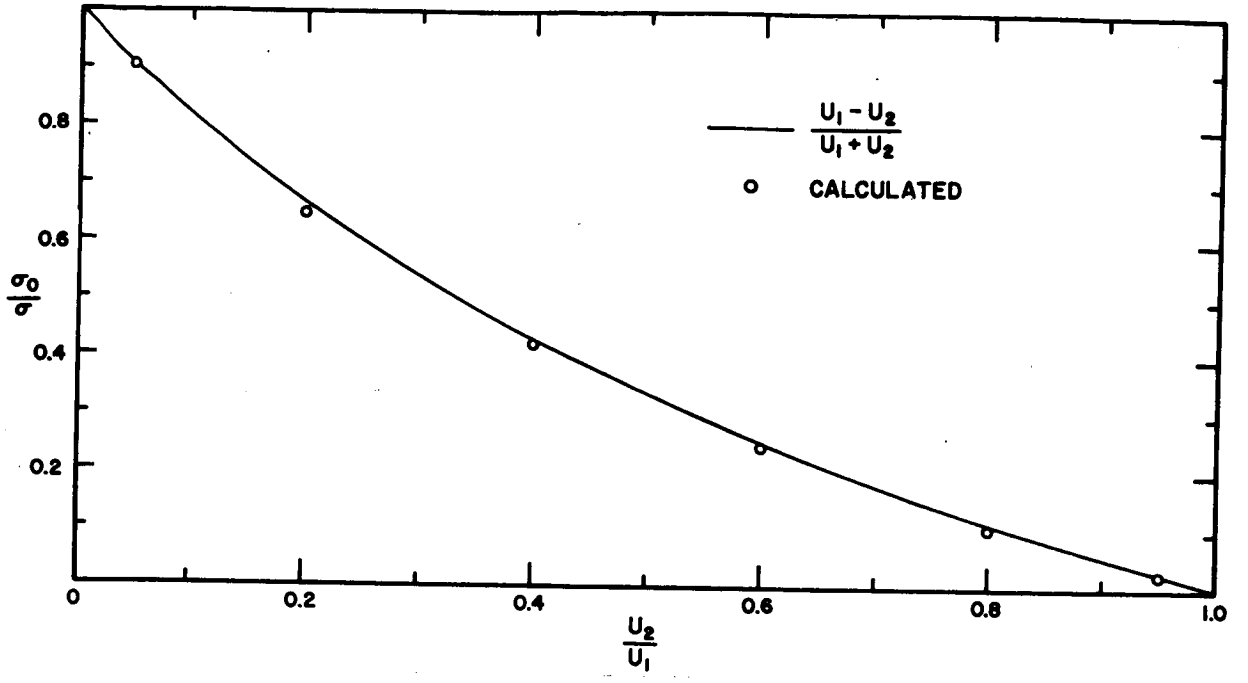

Figure 13.- Test case 1. Free shear layers – effect of the velocity ratio.

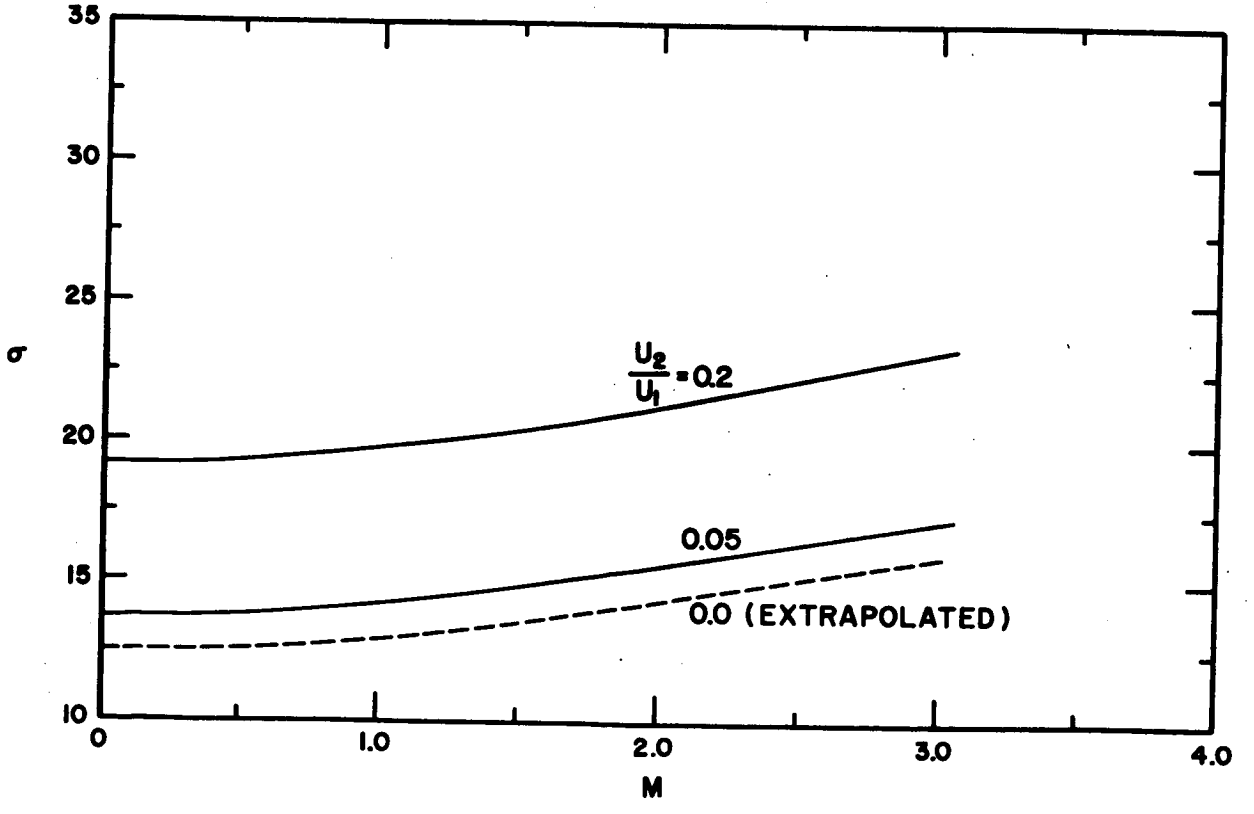

Figure 14.- Test case 2. Free shear layers – Mach number effect.

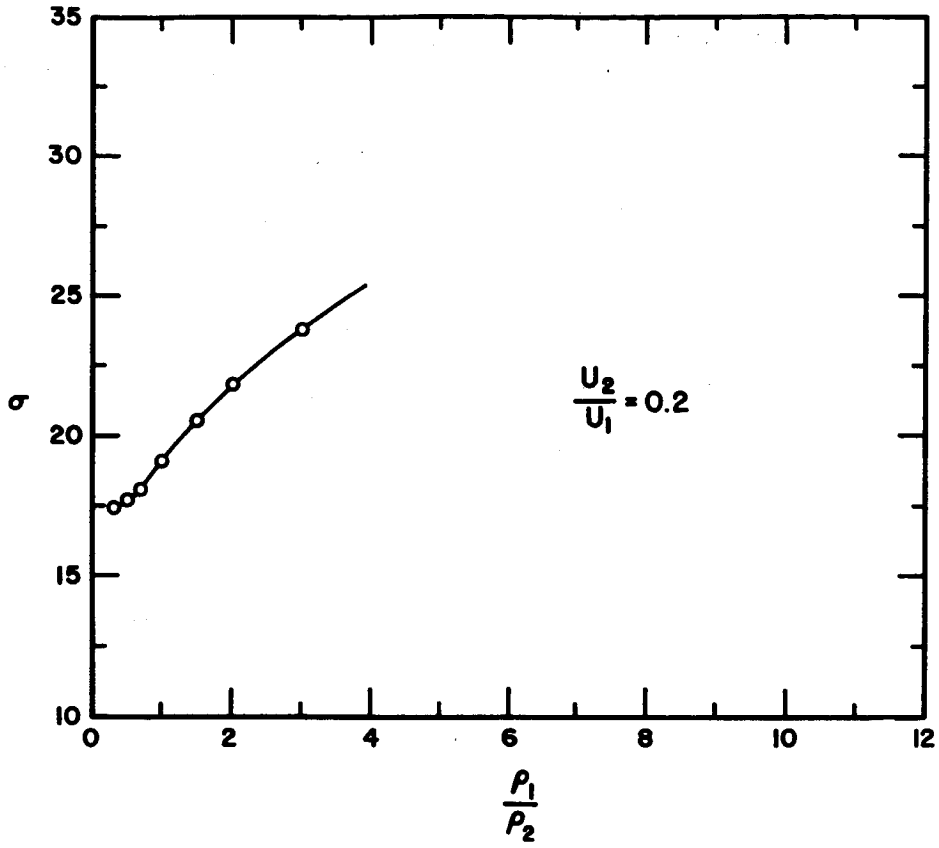

Figure 15.- Test case 3. Free shear layers -- effect of the density ratio.

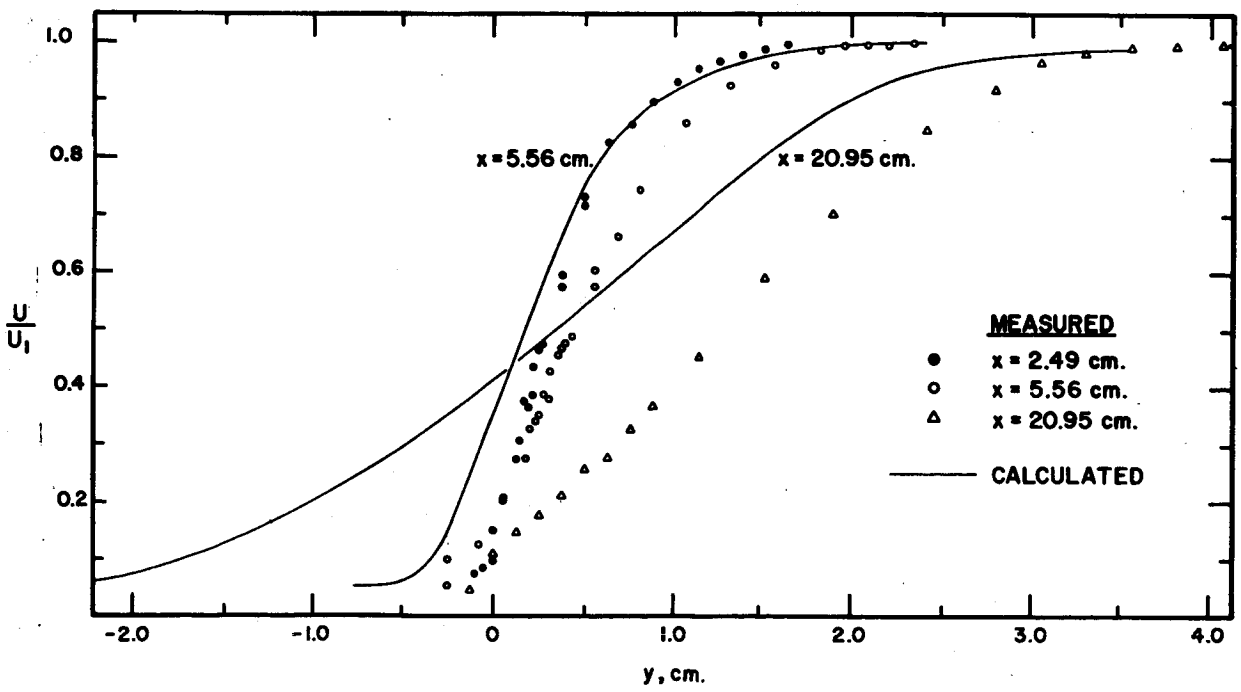

Figure 16.- Test case 5. Initial development of compressible free shear layer.

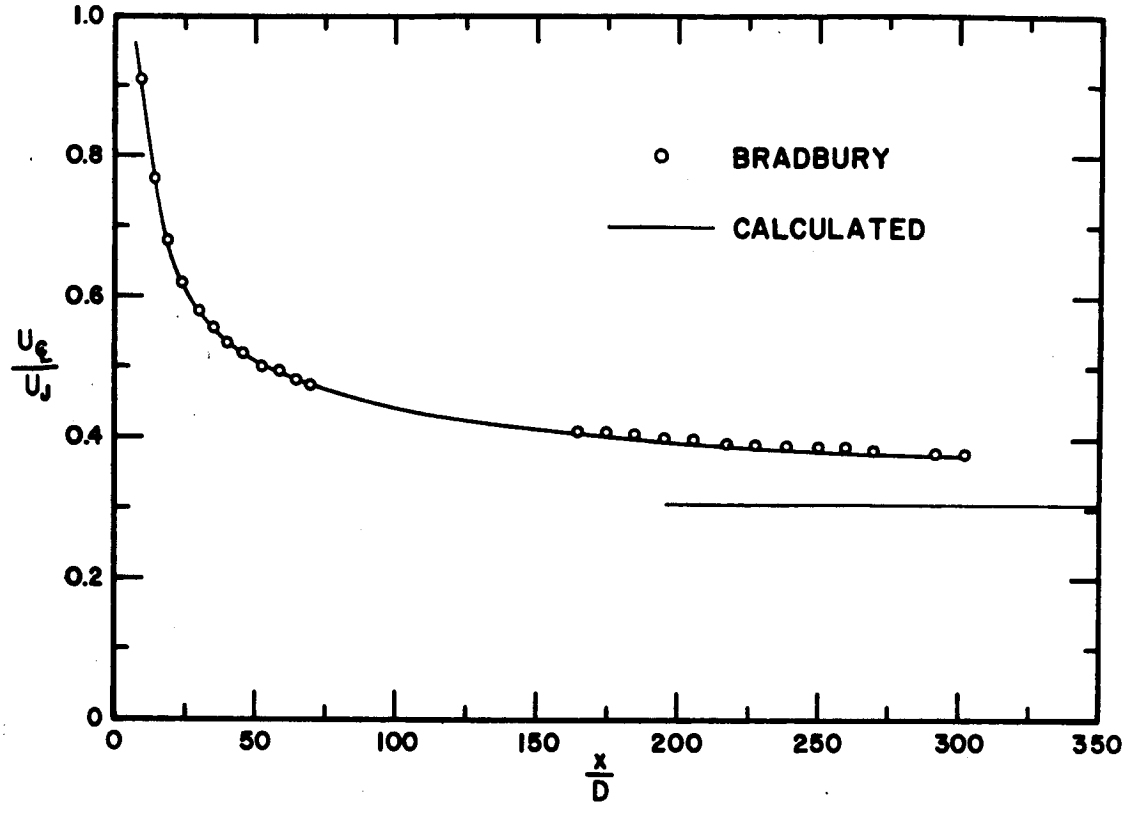

Figure 17.- Test case 13. Two-dimensional jet in a moving stream.

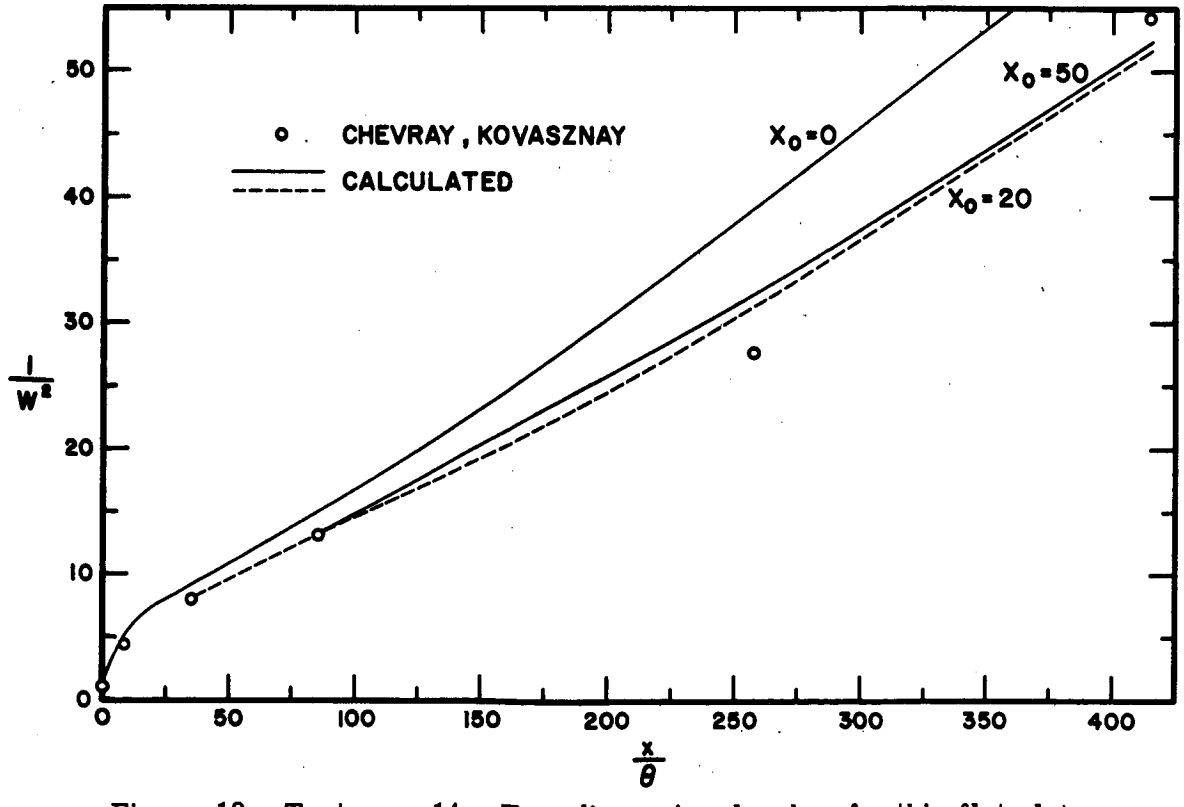

Figure 18.- Test case 14. Two-dimensional wake of a thin flat plate.

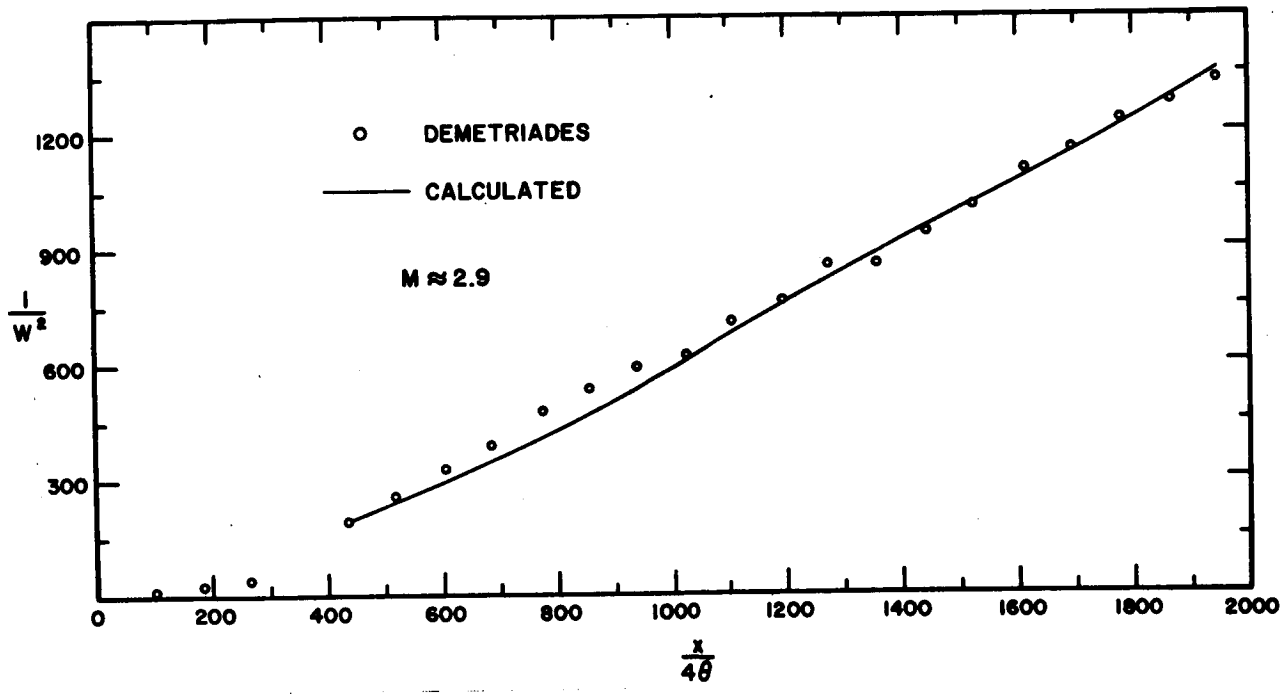

Figure 19.- Test case 16. Two-dimensional supersonic wake.

DISCUSSION

B. E. Launder: I would like to ask whether your method can be extended to cope with axisymmetric flows?

T. Morel: Presumably, one could certainly try to do that, and I would expect it would work. However, there we have to talk, strictly speaking, about an infinite number of interactions. That means we would lose the nice mental picture we were basing this on.

B. E. Launder: Doesn't it look then, that yours is a rather complicated way of doing something very simple? A more conventional simulation of the shear stress equation would permit one to treat both axisymmetric and plane shear flows.

T. Morel: The flows that we want to calculate are certainly not very simple and that is the reason we have all gathered here. We know so much more about the kinetic energy equation that we thought it worthwhile to pursue our work in this direction. Further, as I pointed out in the presentation, the interaction approach has a very important consequence. It allows us to use the kinetic energy equation to close the system without having to rely on the eddy viscosity to obtain the shear stress. This fact alone makes this work certainly worthwhile.

G. L. Mellor: One comment here – it looks like you are taking a perfectly good energy equation and turning it into a shear stress equation. And yet there closely exists a perfectly good shear stress equation. I think you get into trouble when you do that, as evidenced by qualitative argument required to avoid the jump in sign of a, when going from one sign at a channel to the other.

T. Morel: First, the exact shear stress equation is not necessarily a perfectly good equation. There are terms which we do not know enough about. The kinetic energy equation is very well documented; our results certainly seem to support that. Second, the pressure-rate-of-strain correlation in the exact shear stress equation is usually modeled as a sum of production and dissipation. When all the terms are modeled, that equation looks the same as our equation! You can ask Brian Launder about that. To your last question, if you view the flow from the point of view of separate layers, there is no jump of a_1 within either one of them. And that is precisely the point we are making.

A. Roshko: Yes, I would like to comment on Launder's comment. This question of whether what works for two-dimensional flow will work with axisymmetric flow is not so clear. For example, I have a feeling that these shear layers, in particular, have the large structure that has a lot of two-dimensionality in it. In fact our measurements show that. In a fully developed axisymmetric flow, I think that is going to have a very different structure. I think it is an instability structure. I don't think it will be axisymmetric. I

think it will be skewed, and random. Therefore I am sure that the physics will be the same for those two flows.

P. T. Harsha: Your figure 11 shows some pretty mystifying wiggles in your parameter $\Delta u/u_1$. Can you explain them?

T. Morel: Well they don't mean much. You start out with some initial conditions which are away from self-preservation and watch what happens. If it is a flow that likes the self-preservation, it will tend toward it. We started a bit off, and it had to adjust. It is just trying to adjust. That's explainable.

P. A. Libby: Tom, I would like to ask a question, not directly to you, but I think it does raise a question about some of these newer methods, and perhaps some of these other people will straighten me out. For example, in the method you described, if I look at the mathematical structure, I see a first-order differential of τ with respect to y. That raises the possibility of satisfying one boundary condition with respect to τ on some line of x. In a free shear problem, of course, you want to say that τ is 0 at two points, plus or minus infinity. I don't see how you do that. I've raised similar questions with other people; they say you've got to put in molecular viscosity which puts you back into a second-order equation. But of course, if you look at similar free-mixing flows, you cannot leave that molecular viscosity in, because it destroys the similarity. That term wants to vary as $\sqrt{x}$ and the purely turbulent problem wants to go like x itself. Now this, in my view, is just a manifestation of one of the problems that enter when you look at the newer methods of solving turbulent shear problems. I would like to hear what you and other people have to say about this matter. Would you like to comment?

T. Morel: No, I really didn't quite follow what you said. I would like to talk to you afterwards.

AN INTEGRAL TURBULENT KINETIC ENERGY ANALYSIS OF FREE SHEAR FLOWS[1]

By C. E. Peters and W. J. Phares
ARO, Inc.

SUMMARY

Mixing of coaxial streams is analyzed by application of integral techniques. An integrated turbulent kinetic energy (TKE) equation is solved simultaneously with the integral equations for the mean flow. Normalized TKE profile shapes are obtained from incompressible jet and shear layer experiments and are assumed to be applicable to all free turbulent flows. The shear stress at the midpoint of the mixing zone is assumed to be directly proportional to the local TKE, and dissipation is treated with a generalization of the model developed for isotropic turbulence. Although the analysis was developed for ducted flows, constant-pressure flows were approximated with the duct much larger than the jet. The axisymmetric flows under consideration have been predicted with reasonable accuracy. Fairly good results have also been obtained for the fully developed two-dimensional shear layers, which were computed as thin layers at the boundary of a large circular jet.

INTRODUCTION

An extensive integral analysis of ducted turbulent mixing processes (fig. 1) has been developed at the Arnold Engineering Development Center (AEDC) (refs. 1 and 2). As usual with such analyses, the shape of the velocity profile is assumed, and the integral form of the mean flow governing equations is used to compute the shear-layer growth rate and other dependent variables of the problem. In the integral analysis of references 1 and 2, the turbulent shear stress at the midpoint of the shear layer is computed by use of a model for the turbulent eddy viscosity. The integral analysis has been extended to flows with equilibrium chemical reactions, to flows which extend across the entire mixing duct, and to flows in which the inviscid portion of the jet flow must be treated with the method of characteristics. The method has also been applied to flows with embedded recirculation zones. The analytical framework has been developed for

[1] The research reported in this paper was sponsored by the Arnold Engineering Development Center, Air Force Systems Command, Arnold Air Force Station, Tennessee, under Contract No. F40600-72-0003 with ARO, Inc. Major financial support was provided by the Air Force Office of Scientific Research, under Program Element 61102F, Project 9711. Dr. B. T. Wolfson was the project monitor.

quite complex flow situations, but a serious deficiency has always been the model used for the turbulent eddy viscosity, the Prandtl incompressible model with a compressibility correction similar to that proposed by Donaldson and Gray (ref. 3). This eddy-viscosity model is not adequate when the secondary stream velocity exceeds about 0.2 times the primary stream velocity, or when large pressure gradients exist in the flow field. Other eddy-viscosity models have been proposed which would perhaps yield better results for certain flows, but based on the extensive evaluation by Harsha (ref. 4), it is not likely that any eddy-viscosity model will be applicable to the entire range of free turbulent flows of interest. A fundamental problem with eddy-viscosity models is that the turbulent shear stress is related only to the local mean flow properties (this local dependence is true only in simple limiting flow situations); most free turbulent flows are characterized by significant history effects on the turbulent transport.

Starting with the work of Bradshaw and associates (ref. 5) a few years ago, considerable effort has been devoted to development of the turbulent kinetic energy (TKE) methods for turbulent shear flows. In these methods, the turbulent shear stress is related to the kinetic energy of the turbulent motion, and the TKE governing equation is solved simultaneously with the mean flow governing equations; the TKE equation is, in effect, a governing equation for the turbulent shear stress. Two different methods have been used to relate the shear stress to the TKE in free shear flows. In the work at AEDC (refs. 4, 6, and 7), Bradshaw's direct relationship between shear stress and TKE has been used. Other investigators (refs. 8 to 11) have related shear stress to TKE by defining an eddy viscosity which is the product of a length scale and the square root of the TKE. Although there appears to be experimental evidence (ref. 12) for the Bradshaw approach, both approaches are great improvements over earlier eddy-viscosity models in that turbulent shear flows are recognized to be indeed turbulent, that is, to consist of both mean and fluctuating components. The current TKE methods are undoubtedly oversimplified for the whole spectrum of turbulent flows in nature; however, Harsha's work (ref. 4) has shown that the TKE approach is useful for a large class of shear flows which is commonly encountered in engineering applications.

In the present study, the earlier integral approach for ducted flows (refs. 1 and 2) has been extended to include an integrated TKE equation. Because the TKE equation has been integrated across the entire shear layer, no model for the lateral diffusion of TKE needs to be specified. In addition, the relation between the TKE and the shear stress is specified only at the midpoint of the shear layer. These simplifications are achieved with a penalty – the shape of the lateral TKE profiles in the shear layer must be specified. The TKE profile shapes have been obtained from incompressible experiments but have been used with reasonable success for flows with large density gradients.

The present integral method is limited to those flows in which the velocity profile shape is essentially fully developed (shape similar) throughout the flow field; that is, the initial boundary layers must be relatively thin. Deference must be made to the more powerful finite-difference TKE methods for those flows which have developing velocity profiles over a significant axial distance. In addition, the present integral method has been formulated for only axisymmetric flow, and the two-dimensional jet and wake flows have not been computed. However, the fully developed shear layers (test cases 1 to 3) have been computed as thin layers at the boundary of a very large axisymmetric jet.

SYMBOLS

a_1	constant in TKE shear-stress relation
a_2	coefficient in dissipation term
b	mixing zone width
c	correction factor for a_2
C	mass fraction of elements from primary stream
D	diameter of primary stream nozzle
H	stagnation enthalpy
k	turbulent kinetic energy
$\bar{k}$	normalized turbulent kinetic energy
K	exponent in velocity-concentration relation
M	Mach number
M_e	external stream Mach number
M_o	central stream Mach number
n	boundary-layer profile exponent

p	static pressure
r	radial coordinate
r_i	radius of inner mixing zone boundary
r_o	radius of primary stream nozzle
r_w	duct wall radius
R	gas constant
R_T	turbulent Reynolds number
T	static temperature
T_t	stagnation temperature
u	axial velocity component
u_e	outer stream velocity
u_o	initial primary stream velocity
$\overline{u'^2}$	square of turbulent velocity component in x-direction
v	radial or transverse velocity
$\overline{v'^2}$	square of turbulent velocity component in r-direction
w	TKE profile parameter (eq. (11))
$\overline{w'^2}$	square of turbulent velocity component in circumferential direction
W	wake center-line velocity defect, $\frac{1 - u_c}{u_e}$
x	axial coordinate
x_{core}	length of first regime

y	transverse coordinate
$\bar{y}$	mixing zone coordinate, $\frac{r - r_i}{b}$
α	mass fraction of primary stream species on center line
δ	boundary-layer thickness
ϵ	turbulent eddy viscosity
ρ	density
τ	turbulent shear stress
σ	spreading parameter for two-dimensional shear layer
σ_o	spreading parameter at a reference condition

Subscripts:

1	initial mixing station; high speed stream for two-dimensional shear layer
2	low-speed stream for two-dimensional shear layer
a	inviscid secondary flow
bl	boundary layer
c	center line
f	far field
j	inviscid primary flow
m	half-velocity control surface in mixing zone
n	near field

sl	shear layer
w	duct wall

DEVELOPMENT OF ANALYSIS

The first and second regimes of figure 1 will be considered in this paper. A region of inviscid secondary flow exists throughout the duct, and the turbulent mixing zone is free turbulent in nature; that is, the turbulent flow is not adjacent to the wall. The duct wall interacts with the turbulent shear layer only through the axial-pressure gradients which are imposed by its presence.

Fundamental Assumptions

The following principal assumptions have been used in developing the analysis:

(1) The flow is axisymmetric.

(2) All gases obey the perfect gas law.

(3) The usual boundary-layer assumptions are used; that is, negligible radial pressure gradients, and so forth.

(4) The inviscid portions of the primary and secondary flows are one-dimensional and isentropic.

(5) The mixing layer is completely turbulent, and the initial boundary-layer thicknesses at the initiation of mixing are very small compared with the length of the first regime (fig. 1).

(6) The thickness of the nozzle lip separating the primary and secondary flows is negligible.

(7) The viscous effects at the duct wall are negligible.

(8) The normalized velocity profiles in the mixing layer are similar in shape at all axial stations and are represented by a cosine function.

(9) The turbulent Prandtl and Lewis numbers are unity.

(10) The TKE profile shapes in the shear layer which have been obtained from constant-density experiments are unaffected by density gradients in the shear layer.

(11) The turbulent kinetic energy outside the shear layer boundaries is negligible.

Basic Integral Equations

Nomenclature for the analysis is illustrated in figure 1. In this section, the nomenclature is generally consistent with that of references 1 and 2; the results are described in terms of the recommended nomenclature for this conference.

By integrating the boundary-layer differential equations, five basic integral equations are obtained: (1) a continuity equation for the entire flow, (2) a momentum equation for the entire flow, (3) a momentum equation for the flow between the duct center line and a control surface arbitrarily located at the midpoint of the shear layer, (4) a jet species conservation equation for the entire flow, and (5) a turbulent kinetic energy equation for the shear layer.

Continuity equation:

$$\int_0^{r_w} \frac{\partial}{\partial x}(\rho u) r \, dr = -\rho_w v_w r_w = -\rho_a u_a r_w \frac{dr_w}{dx} \tag{1}$$

Overall momentum equation:

$$\int_0^{r_w} \frac{\partial}{\partial x}(\rho u^2) r \, dr = -\frac{r_w^2}{2}\frac{dp_w}{dx} - \rho_a u_a^2 r_w \frac{dr_w}{dx} \tag{2}$$

Half-radius momentum equation:

$$\int_0^{r_m} \frac{\partial}{\partial x}(\rho u^2) r \, dr - u_m \int_0^{r_m} \frac{\partial}{\partial x}(\rho u) r \, dr = \tau_m r_m - \frac{r_m^2}{2}\frac{dp_w}{dx} \tag{3}$$

Jet species conservation equation:

$$\int_0^{r_w} \frac{\partial}{\partial x}(\rho u C) r \, dr = 0 \tag{4}$$

The differential form of the TKE equation is

$$\rho u r \frac{\partial k}{\partial x} + \rho v r \frac{\partial k}{\partial r} = \tau r \frac{\partial u}{\partial r} + \text{Diffusion} - \text{Dissipation}$$

where

$$k = \frac{1}{2}\left(\overline{u'^2} + \overline{v'^2} + \overline{w'^2}\right)$$

By integrating the TKE equation across the entire shear layer, the lateral diffusion term disappears. The dissipation is given by the usual relation developed for isotropic turbulence (ref. 4):

$$\text{Dissipation} = \frac{a_2 \rho k^{3/2} r}{b}$$

Thus, the basic integral TKE equation is

$$\int_{r_i}^{r_i+b} \frac{\partial}{\partial x}(\rho u k) r \, dr = \int_{r_i}^{r_i+b} \tau \frac{\partial u}{\partial r} r \, dr - \frac{a_2}{b} \int_{r_i}^{r_i+b} \rho k^{3/2} r \, dr \tag{5}$$

Velocity Profile

The velocity profile is given by

$$\frac{u - u_a}{u_c - u_a} = \frac{1}{2} + \frac{1}{2} \cos(\pi \bar{y}) \tag{6}$$

where $\bar{y} = \frac{r - r_i}{b}$ and $u_c = u_j$ in the first regime. The cosine profile is shown in figure 2, along with the experimental results of Spencer (ref. 13) for a fully developed two-dimensional shear layer. At the control surface, $r_m \left(= r_i + \frac{b}{2}\right)$, the velocity is

$$u_m = \frac{1}{2}(u_c + u_a)$$

Concentration and Enthalpy Profiles

For unity Lewis number, the normalized total enthalpy and concentration profiles are essentially identical and are related to the velocity profile by

$$C = \frac{H - H_a}{H_j - H_a} = \left(\frac{u - u_a}{u_j - u_a}\right)^K \tag{7}$$

The parameter K has been introduced so that jet species can be conserved in variable pressure flows. For unity turbulent Prandtl number, equation (7) with $K = 1$ is identically true for constant-pressure flow; the pressure gradients in all the flows considered in this communication are negligible, and K remained unity for all computations. Therefore, equation (4) could have been deleted for these flows, since the assumption of $K = 1$ would have identically satisfied that equation.

Turbulent Kinetic Energy Profiles

As with the velocity profile, the shape of the TKE profiles must be specified. The near-field (first-regime) TKE profiles have been obtained from the experimental results of Spencer (ref. 13) and Liepmann and Laufer (ref. 14) for constant-density two-dimensional shear layers. The experimental results are shown in figure 3, along with the following analytical function which has been fitted to the data:

$$\bar{k}_n = \frac{k}{k_m} = 0.51 - 0.51 \cos \frac{\pi \bar{y}}{0.45} \qquad (0 \leq \bar{y} \leq 0.45) \tag{8a}$$

$$\bar{k}_n = 0.51 - 0.51 \cos\left[2\pi(0.0909 + 0.9091\bar{y})\right] \qquad (0.45 \leq \bar{y} \leq 1.0) \qquad (8b)$$

In fitting the data, the recent experiments of Spencer were given more weight than the Liepmann and Laufer experiments because of the improvement of hot-wire techniques in the past 20 years.

In the far field, well downstream of the end of the potential core, the experiments of Pindell (ref. 15) and Wygnanski and Fiedler (ref. 16) on the constant-density axisymmetric jet into still air were used. The experimental TKE profiles are shown in figure 4, along with the following analytical function which has been fitted to the data:

$$\bar{k}_f = 0.5 + \sin\frac{\pi}{2}\left(1 + \frac{4}{3}\bar{y}\right) \qquad (9)$$

Obviously, the shape of the TKE profile cannot change discontinuously from $\bar{k}_n$ to $\bar{k}_f$ at the end of the first regime. It has been hypothesized that a transition region exists in which the TKE profile evolves from $\bar{k}_n$ to $\bar{k}_f$. In this transition region, the TKE profile is assumed to be a linear combination of $\bar{k}_n$ and $\bar{k}_f$

$$\bar{k} = w\bar{k}_f + (1 - w)\bar{k}_n \qquad (10)$$

where w is an empirical function of x. The resulting family of TKE profiles is shown in figure 5. Because many features of jets scale with x/x_{core}, it has been hypothesized that w can also be related to x/x_{core}. The experiments of Pindell (ref. 15), Sami (refs. 17 and 18), and Bradshaw et al. (ref. 19) on the constant-density jet were used to develop the following empirical function for w:

$$w = 1 - \exp\left[-1.09\left(\frac{x}{x_{core}} - 1\right)\right] \qquad (11)$$

The center-line TKE, normalized with the value at r_m, is shown in figure 6 for the constant-density jet into still air. A value of $x_{core} = 4.66D$ was used in computing the curve shown in figure 6; this core length is predicted by the present theory for a jet with negligible initial boundary layer. The TKE profiles are seen to be essentially fully developed ($w \approx 1$) for x greater than $5x_{core}$. It should be noted that the value of x_{core} is not prescribed for a particular flow but is a result of the first-regime solution.

Even though the TKE profile shapes were obtained from relatively simple constant-density flows, the two-dimensional shear layer and the axisymmetric jet, it is assumed that these profile relationships apply to all flows. It should be noted that nothing has been stated about the level of TKE, but only that the TKE profiles, normalized with k_m, are given by equations (8) to (11).

Relation Between TKE and Shear Stress

As the present integral theory has been formulated, the relationship between τ and k must be specified only at the midpoint of the shear layer r_m. This method is

distinctly different from finite-difference TKE methods, in which it is necessary to specify the variation of τ with k across the entire mixing zone. The linear relationship

$$|\tau_m| = a_1 \rho_m k_m \tag{12}$$

is used, with $a_1 = 0.3$, the value found by Harsha and Lee (ref. 11) in the high shear region of a variety of constant-density free turbulent flows. This value of a_1 is also the same as that used by Bradshaw et al. (ref. 5) for turbulent boundary layers. In order to have the proper sign on τ_m, equation (12) is written as

$$\tau_m = \frac{a_1 \rho_m k_m (u_a - u_c)}{|u_a - u_c|} \tag{13}$$

The Dissipation Parameter a_2

In the extensive evaluation of his differential TKE method (ref. 4), Harsha used $a_2 = 1.5$. During the development of the present integral method, $a_2 = 1.69$ was found to give good results for constant-density two-dimensional shear layers and for the axisymmetric jet into still air. Other flows, however, were found to require significantly different values for a_2 if reasonably good mean flow predictions were to be achieved. Specifically, supersonic flows require a_2 to be larger than 1.69, and some flows with very high shear stress levels require a_2 to be less than 1.69. Finally, it was found that a_2 could be correlated with the turbulent Reynolds number R_T which is defined as

$$R_T = \frac{|u_c - u_a| b}{\epsilon_m}$$

where ϵ_m is the local eddy viscosity at r_m. Of course, the eddy viscosity is not specified but is computed from

$$\epsilon_m = \frac{\tau_m}{\rho_m \left.\frac{\partial u}{\partial r}\right|_m}$$

For the cosine profile,

$$\left.\frac{\partial u}{\partial r}\right|_m = \frac{\pi (u_a - u_c)}{2b}$$

and R_T may be written as

$$R_T = \frac{\pi (u_c - u_a)^2}{2 a_1 k_m} = 5.236 \frac{(u_c - u_a)^2}{k_m}$$

Thus, it has been found that the dissipation coefficient a_2 can be related to the ratio of the mean flow velocity difference across the shear layer to the turbulent velocity fluctua-

tion level (characterized by k_m) in the layer. The a_2 function which has been developed is shown in figure 7, along with the equations which describe the function.

The approach used in the development of the $a_2 - R_T$ function will be briefly described. For $R_T > 145$, the a_2 function was developed by computational experiments on the near field of unheated compressible air jets exhausting into still air. Warren's potential core length data (ref. 20) for experimental flows with thin initial boundary layers and $0.69 < M_j < 2.6$ were used to establish approximately a few desired a_2 values. A direct correlation of a_2 with a characteristic Mach number for the shear layer was abandoned because such a correlation fails for two-stream supersonic flows such as the combustion flows reported in reference 1. The turbulent Reynolds number was finally found to correlate consistently the a_2 values for the preceding flows. Because R_T is related to the local turbulence characteristics in the shear layer, it is more appropriate as a dissipation parameter than some other parameter which is related only to the mean flow in the layer. When it is considered that only the near-field results for a few experimental flows were used in developing the a_2 function for $R_T > 145$, the overall performance of this part of the $a_2 - R_T$ function (fig. 7) has been reasonably satisfactory for a variety of flows. The high R_T portion of the a_2 function is subject to further refinement, however, particularly for $R_T > 300$, that is, for fully developed single stream flows with $M_j > 2.7$.

Experience with far-field predictions of jets in moving streams indicated that a_2 should be somewhat less than 1.69 for $R_T < 70$. The function used for $R_T < 70$ (fig. 7) is the first one tried, and no attempt has been made to improve it.

The effects of density ratio caused by jet Mach number are adequately predicted by the $a_2 - R_T$ function; however, prediction of the entire range of flows of interest is improved if small additional corrections to a_2 are made as a function of density ratio. Tentatively, the following corrections have been developed and used:

$$a_2 = \frac{a_2(R_T)}{c}$$

where $a_2(R_T)$ is as shown in figure 7 and c is given by

$$c = 0.984 + 0.016 \frac{\rho_{a1}}{\rho_{j1}} \qquad (\rho_{a1} > \rho_{j1})$$

or

$$c = 0.95 + 0.05 \frac{R_a T_{ta}}{R_j T_{tj}} \qquad (\rho_{a1} < \rho_{j1})$$

These density corrections to the basic $a_2 - R_T$ function are perhaps required because the empirical TKE profiles are inadequate for flows with large density gradients; this

point will not be resolved until detailed turbulence structure data are available for flows with large density gradients.

The a_2 function as described has been used for all of the shear layer and jet computations presented in this paper. Experience has shown that wakes require somewhat different dissipation than jet flows, and the axisymmetric wake computations (test cases 15 and 17) were made with $a_2 = 1.40$.

Turbulence Production

The first term on the right-hand side of equation (5) represents the production of turbulence by the shear stress. For the boundary conditions of the shear layer, the production is equal but opposite in sign to the dissipation of mean flow mechanical energy:

$$\int_{r_i}^{r_i+b} \tau \frac{\partial u}{\partial r} r \, dr = -\int_{r_i}^{r_i+b} u \frac{\partial}{\partial r}(\tau r) \, dr = -\frac{1}{2}\int_0^{r_i+b} \frac{\partial}{\partial x}(\rho u^3) r \, dr$$

$$+ \frac{1}{2} u_a^2 \int_0^{r_i+b} \frac{\partial}{\partial x}(\rho u) r \, dr - \frac{dp_w}{dx}\int_0^{r_i+b} ur \, dr \qquad (14)$$

By substituting equation (14) into equation (5), the following form of the integral TKE equation is obtained:

$$\int_{r_i}^{r_i+b} \frac{\partial}{\partial x}(\rho u k) r \, dr = -\frac{1}{2}\int_0^{r_i+b} \frac{\partial}{\partial x}(\rho u^3) r \, dr + \frac{1}{2} u_a^2 \int_0^{r_i+b} \frac{\partial}{\partial x}(\rho u) r \, dr$$

$$- \frac{dp_w}{dx}\int_0^{r_i+b} ur \, dr - \frac{a_2}{b}\int_{r_i}^{r_i+b} \rho k^{3/2} r \, dr$$

By using the TKE equation in this form, the shape of the shear-stress profile need not be specified. The turbulence production is related only to the dissipation of mean flow mechanical energy, which, in turn, is related to the mean flow profiles and the rate of growth of the shear layer.

Solution Technique

Sufficient information is available to transform equations (1) to (5) into a system of ordinary differential equations which is linear in the derivatives of the dependent variables $(dp_w/dx$, etc.$)$. This transformation procedure is described in detail in reference 2. After the system of linear equations is solved for the derivatives, the resulting five differential equations are then numerically integrated with a modified Euler technique (variable step size). An IBM 370/155 digital computer was used to obtain the numerical solutions; a typical flow-field solution required a computation time of approximately 2 minutes.

In the first regime, the dependent variables are p_w, r_i, b, K, and k_m. In the second regime, the dependent variables are p_w, u_c, b, K, and k_m.

Initial Conditions

In order to integrate the system of differential equations, initial values must be specified for each of the dependent variables. The most critical of these initial values is that for k_m. As usual with TKE methods, the convective terms cause the initial condition for k_m (or τ_m) to be "remembered" for some distance downstream; the distance is dependent on the particular flow situation. Experience has shown that two stream flows with $u_a/u_j < 0.25$ can be started with a "fully developed" shear stress. This fully developed shear stress is obtained from the corresponding fully developed two-dimensional shear layer. Even though the present method is generally limited to flows with thin initial boundary layers, two stream jet flows with $u_a/u_j < 0.25$ and very thick initial boundary layers (jet nozzle boundary-layer thickness up to $0.4r_o$) have been successfully computed with the following procedure: (1) the initial boundary layer is assumed to be negligible, and (2) the inner shear layer radius r_i is adjusted to match the experimental value of the excess momentum.

Even for thin boundary layers, the influence of the initial conditions persists throughout the flow field when u_a/u_j exceeds about 0.3. Therefore, the concept of a negligible initial boundary layer and a fully developed initial shear stress is not usable for such flows. In order to treat these flows, a control volume analysis of the initial region has been developed.

Control Volume Analysis of Initial Region

A sketch of the initial region just downstream of the nozzle lip is shown in figure 8. The initial boundary layers are characterized by power law velocity profiles:

$$\frac{u}{u_a} = \left(\frac{r - r_o}{\delta_a}\right)^{n_a}$$

and

$$\frac{u}{u_j} = \left(\frac{r_o - r}{\delta_j}\right)^{n_j}$$

The nozzle wall is assumed to be adiabatic; therefore, the stagnation temperature is constant in each boundary layer. Specification of the wall skin-friction coefficients, c_{fa} and c_{fj}, and $a_1 = 0.3$ completely defines the mean flow and the turbulence quantities at the initial station $b\ell$. The wall skin-friction coefficients are determined with the method of Spalding and Chi (ref. 21).

At some downstream station, $s\ell$, the flow is assumed to have evolved to the fully developed shear layer profile shapes for velocity and near-field TKE. The following assumptions are made about the process between $b\ell$ and $s\ell$:

(1) There is no net entrainment into the shear layer.

(2) The process occurs at constant pressure.

(3) The excess momentum is conserved.

(4) The length scale of the process is sufficiently small to insure that the volume integral of turbulent dissipation is negligible.

The following equations are written between stations $b\ell$ and $s\ell$:

Momentum:

$$\int_0^{r_o+\delta_a} \rho u(u - u_a) r \, dr \Big|_{b\ell} = \int_0^{r_i+b} \rho u(u - u_a) r \, dr \Big|_{s\ell} \tag{15}$$

Continuity:

$$\int_{r_o-\delta_j}^{r_o+\delta_a} \rho u r \, dr \Big|_{b\ell} = \int_{r_i}^{r_i+b} \rho u r \, dr \Big|_{s\ell} \tag{16}$$

Turbulent kinetic energy:

$$\int_{r_o-\delta_j}^{r_o+\delta_a} \rho u k r \, dr \Big|_{b\ell} + \frac{1}{2} \int_{r_o-\delta_j}^{r_o+\delta_a} \rho u^3 r \, dr \Big|_{b\ell} + \frac{1}{4} \rho_j u_j \left(u_j^2 - u_a^2\right) \left[\left(r_o - \delta_j\right)^2 - r_i^2\right]$$

$$= \int_{r_i}^{r_i+b} \rho u k r \, dr \Big|_{s\ell} + \frac{1}{2} \int_{r_i}^{r_i+b} \rho u^3 r \, dr \Big|_{s\ell} \tag{17}$$

With δ_a, δ_j, n_a, n_j, c_{fa}, and c_{fj} specified, equations (15) to (17) are solved for r_i, b, and k_m. These values are then used as initial conditions for the integral TKE solution of the remainder of the flow field.

This control volume analysis is obviously not applicable as u_a/u_j approaches unity, since in such flows a very large distance is required to approach a fully developed profile shape. In addition, the initial region analysis as formulated is not applicable to mixing of streams with greatly different densities. The computations are made with $K = 1$ at station $s\ell$, and the solution does not, in general, conserve species or energy.

RESULTS AND DISCUSSION

Initial conditions for the computed experimental flows are presented in table I. The initial shear stress levels are characterized by the turbulent Reynolds number R_T. In addition to being used to specify the initial shear stress, the axial distribution of R_T throughout the flow field is very informative, and a number of such distributions is presented. For the cosine profile, the midpoint shear stress in the mixing layer is given by

$$\frac{|\tau_m|}{\rho_m(\Delta u)^2} = \frac{\pi}{2R_T}$$

where Δu is the local velocity difference across the layer. If self preservation is approached, then R_T must become constant in the flow field.

Most of the flows considered in this conference have a constant-pressure boundary condition, whereas the analysis was developed for a ducted system with a prescribed duct wall shape. The constant-pressure axisymmetric flows were computed in a very large cylindrical duct ($r_w = 1000r_o$) so that negligible axial pressure gradients were predicted. Integrated momentum in the duct is conserved to a high degree of accuracy in the computations, typically to within one part in 10^5. The degree to which the jet excess momentum is conserved in constant-pressure flows is illustrated by the fully developed axisymmetric jet (test case 18). For similar velocity profiles, the product of mixing zone width and center-line velocity should remain constant throughout the second regime. This product changed 1.5 percent from the value at the end of the core at $x/D = 50$, and 2.8 percent at $x/D = 100$. Even though the excess jet momentum is not exactly conserved in the calculations because of the ducted boundary condition, the results are considered to conserve excess momentum adequately when the inprecision of most experiments is taken into account.

Effect of Velocity Ratio on Growth of Fully Developed Two-Dimensional Shear Layer – Test Case 1

As presently formulated, the integral analysis cannot be used for zero secondary velocity. Therefore, all computations of flows with nominal zero secondary velocity were made with a secondary velocity 0.01 times the maximum velocity in the flow field (u_1 or u_o). The fully developed two-dimensional shear layers were computed as thin shear layers at the boundary of a large axisymmetric jet; the duct radius r_w was set equal to $100r_o$ for these cases. In no case did the predicted shear-layer thickness exceed 2 percent of the jet radius.

Computations for test case 1 were made for $u_2/u_1 = 0.01$, 0.2, 0.4, 0.6, and 0.8. The results, shown in figure 9 (test case 1), fall on the classic relationship

$$\frac{\sigma_o}{\sigma} = \frac{u_1 - u_2}{u_1 + u_2}$$

where $\sigma_o = 12.9$ for $u_2/u_1 = 0$. The standard relation for σ used in this computation becomes

$$\sigma = \frac{3.12}{db/dx}$$

for the cosine profile. It should be noted that $\sigma = 12.9$ by this definition corresponds to $\sigma = 12$ when the cosine profile midpoint slope is matched to the widely used error function profile. The fully developed R_T varied negligibly from 143 over the entire range of u_2/u_1.

Effect of Mach Number on Growth of Fully Developed Two-Dimensional Shear Layer – Test Case 2

Results for test case 2 are shown in figure 10(a). The computations were made with $u_2/u_1 = 0.01$; therefore, all σ values are about 2 percent too large. The ratio σ_o/σ, where σ_o is the value at $M_1 = 0$, is shown in figure 10(b), along with the value of fully developed R_T. Based on available experimental information on σ, the predicted σ_o/σ probably decreases too abruptly in the M_1 range of 0.5 to 1.5. The predicted σ values in this M_1 range can be altered by slight refinements of the a_2 function in the appropriate R_T range. The predicted σ values are considered to be good at $M_1 = 2$ and $M_1 = 3$.

Effect of Density Ratio on Growth of Fully Developed Two-Dimensional Shear Layer – Test Case 3

The computations for test case 3 were made for low-speed flow and $u_2/u_1 = 0.2$. Results for σ and R_T are shown in figure 11 as a function of ρ_1/ρ_2. Evaluation of the σ predictions at high ρ_1/ρ_2 is nearly impossible because of the lack of experiments in this range. The σ results for this case are not influenced by the factor which causes the density ratio, that is, temperature difference or molecular weight difference.

In general, very large axial distances were required to approach the fully developed condition in all these shear-layer computations. All the flows were computed for an axial distance of several hundred initial shear-layer thicknesses; such distances were required to approach closely the fully developed condition unless the initial shear stress was luckily chosen to be very close to the fully developed value. These results clarify the extreme difficulty in accomplishing a shear-layer experiment in which the flow truly approaches a fully developed condition.

Maestrello and McDaid Axisymmetric Jet – Test Case 6

The computations for test case 6 were made in two ways. In the first (curve a, fig. 12), the experimental profile at $x/r_o = 2$ was fitted with a cosine profile, and the computations were started with a fully developed shear stress. The predicted rate of mixing is too large; therefore, the shear stress does not yet approach the fully developed value at $x/r_o = 2$ but is somewhat lower. The computations were also started at $x = 0$, with negligible initial boundary layer, fully developed R_T and r_i corrected to achieve the excess momentum shown at $x = 2r_o$. This second computation (curve b, fig. 12) yields a first regime which is somewhat too long, but the results are better than those of the first computation.

The abrupt change in center-line velocity at the end of the first regime is characteristic of the integral method but is of little concern unless the main interest is in the transition region at the end of the potential core.

Eggers Supersonic Jet Into Still Air – Test Case 7

The prediction of this well-defined experimental flow (test case 7) is very satisfactory. (See fig. 13(a).) Computations were started by assuming a negligible initial boundary layer and fully developed R_T (from fig. 10(b)). The predicted potential core is slightly longer than that shown by the experiment, but the far-field agreement is excellent. The predicted velocity profiles at $x/r_o = 8$, 27, and 99 are also satisfactory. (See fig. 13(b).) These profiles illustrate that the cosine profile approaches zero at the outer edge of the layer more rapidly than does the experiment; the cosine profile is generally better for two stream flows.

The predicted axial variation of R_T (fig. 13(c)) shows a very large change in R_T for this flow (from 283 to 82). Thus, most of the $a_2 - R_T$ function (fig. 7) was used in this prediction.

G.E. Heated Subsonic Jet – Test Case 8

The experimental velocity profile at $x/D = 2.79$ was fitted with a cosine profile; the computations were started with this velocity profile and fully developed R_T. Predictions of both center-line velocity and center-line static temperature are very satisfactory for test case 8. (See fig. 14.)

Forstall Jet in Moving Stream – Test Case 9

This flow (test case 9) was computed by assuming a thin initial boundary layer and fully developed R_T; r_i was corrected to yield the experimental excess momentum and the actual duct radius $r_w/r_o = 16$ was used for the prediction. The predicted center-

line velocity agrees very well with the experiment at all axial locations. (See fig. 15(a).) The detailed far-field behavior of the excess center-line velocity is illustrated in the log plot (fig. 15(b)). Because of the assumption of unity Prandtl and Lewis numbers, the predicted α is identical to the excess velocity $(u_c - u_e)/(u_o - u_e)$. Predicted half-velocity width (fig. 15(c)) agrees well with the experiment for x/D up to 25, but falls about 10 percent under the experiment at $x/D = 80$.

Chriss Hydrogen Jet in Moving Air Stream – Test Case 10

This flow (test case 10) was computed in two ways. In the first, a cosine velocity profile was fitted to the data at $x/D = 2.97$. This profile, along with the experimental shear stress shown in reference 22 $(R_T = 98.3)$, was used to start the computations. Predicted results for the center-line velocity are fairly good (fig. 16(a)), but the predicted rate of decay of center-line concentration is too low. This type of concentration prediction is typical of the integral analysis, since it is limited to unity turbulent Prandtl and Lewis numbers.

The second computation was started at $x = 0$ with small initial shear layer thickness and fully developed shear stress $(R_T = 120)$. Predicted center-line velocities (fig. 16(b)) are somewhat better than those for the first computation, but, of course, the center-line concentration decay rate is again underpredicted.

Eggers and Torrence Axisymmetric Jet in Moving Air Stream – Test Case 11

This flow (test case 11) has wakelike behavior and it is unlikely that it can be properly predicted by a constant-pressure mixing analysis. In spite of the thick initial boundary layers and the velocity ratio $(u_e/u_j = 1.36)$, computations were started at $x = 0$ with thin initial shear layer and fully developed shear stress. The predicted center-line velocity distribution is surprisingly close to the experiment. (See fig. 17.) Wakelike jet flows, with jet momentum flux less than external stream momentum flux, tend to have relatively high relative shear levels (low R_T), and it is possible in such flows that the influence of the initial conditions does not persist very far downstream in the flow field. This aspect should certainly be further explored.

Eggers Hydrogen Jet in Moving Air Stream – Test Case 12

As with the preceding case, this flow (test case 12) has jet momentum flux less than external stream momentum flux. In this case, however, the jet momentum deficit is caused by density rather than by velocity $(u_e/u_j = 0.37)$. Again, the computations were started with a thin initial shear layer and fully developed R_T. Although the length of the

first regime is somewhat overpredicted (fig. 18), the downstream prediction for both center-line velocity and center-line concentration is very good. In view of the unity Schmidt number assumption, the good prediction of both velocity and concentration was unexpected; the results are undoubtedly caused in part by the neglect of the initial boundary layers.

Chevray Axisymmetric Wake – Test Case 15

Computation of this flow (test case 15) was started at $x = 0$ with an equivalent second regime cosine velocity profile; the cosine profile was selected to match the experimental momentum defect and mass flow in the shear layer. An initial value for R_T was established by equating the experimental TKE flux (ref. 23) with the TKE flux in the equivalent fully developed profile. The theory does not predict the initial rapid acceleration of the center-line velocity (fig. 19(a)) for $x/D < 2$. This rapid acceleration is caused in part by a favorable pressure gradient just downstream of the body; the axial pressure gradient was neglected in the calculations. For $x/D > 4$, the center-line velocity defect W is underpredicted; however, the log plot of W against x (fig. 19(b)) shows that the predicted decay rate at $x/D = 18$ is somewhat less than the experimental rate. The predicted axial distribution of W follows an x^{-1} decay from $x/D = 5$ to the maximum axial distance computed ($x/D = 200$). Better prediction of the decay rate at $x/D = 18$ would require less dissipation than that used in the calculations. On the other hand, achievement of the $x^{-2/3}$ decay rate for W, as predicted for self-preservation, would require much higher dissipation. One can only conclude that (1) the far-field dissipative mechanism is much different from the near-field mechanism, or (2) self-preserving axisymmetric wakes are never attained. The lack of far-field experiments on the axisymmetric wake makes it difficult to decide which of these conclusions is correct.

The predicted axial variation of R_T (fig. 19(c)) shows that R_T never approaches a constant value but continuously decreases in the axial direction.

Demetriades Supersonic Axisymmetric Wake – Test Case 17

This flow (test case 17) was computed by fitting a cosine profile to the experimental velocity data at $x/D = 17$, and by using the R_T value quoted by Demetriades (ref. 24) for $x/D = 17$. The plot of $\frac{1}{W^{3/2}}$ against x/D (fig. 20(a)) shows that the experimental center-line velocity defect is well predicted. A log plot (fig. 20(b)) shows that the predicted W decays even more rapidly than an x^{-1} decay. Again, this axisymmetric wake prediction is very different from the $x^{-2/3}$ decay of W which is required for self-preservation. The predicted axial variation of R_T (fig. 20(c)) is considerably different from that shown by Demetriades (ref. 24); he showed R_T to be nearly constant at 32 for x/D greater than about 30.

Fully Developed Axisymmetric Jet – Test Case 18

This important and fundamental flow (test case 18) was computed from $x = 0$ by assuming a thin initial shear layer and a fully developed near-field shear stress $(R_T = 143)$. The predicted center-line velocity (fig. 21(a)) follows an x^{-1} decay for x/D greater than 15. Although the predicted center-line velocity agrees well with the experiment of Albertson et al. (ref. 25) at all axial stations, the agreement with the Wygnanski and Fiedler experiment is fairly satisfactory only for $x/D > 40$. The Wygnanski and Fiedler flow apparently does not approach self-preservation as quickly as do other reported jet experiments; the terms "fully developed" or "self-preserving" are questionable when applied to the Wygnanski and Fiedler experiment.

The predicted velocity profile (fig. 21(b)) is based on the local mixing-zone growth rate at $x/D = 60$. Compared with the experimental profile of Wygnanski and Fiedler, the half-velocity radius is well predicted, but the predicted profile is fuller near the center line; the predicted profile is closer to the empirical profile of Albertson et al. (ref. 25) in the high-speed half of the shear layer. The theoretical profile approaches zero velocity in the outer part of the shear layer more rapidly than does the experimental profile. The predicted TKE level (fig. 21(c)) agrees well with the Wygnanski and Fiedler experiment in the outer half of the profile, but the predicted center-line TKE level is about 13 percent below the experiment. It should be noted that the predicted TKE level is satisfactory in the region of peak shear stress. Predicted axial variations of R_T and the TKE profile parameter w are shown in figure 21(d). Even though the center-line velocity closely follows the x^{-1} decay (required for self-preservation) downstream of $x/D = 15$, R_T and w do not become constant until considerably farther downstream.

G.E. Heated Supersonic Jet – Test Case 19

This flow (test case 19) was computed by fitting a cosine profile to the velocity data at $x/D = 2.79$, and by using a fully developed initial shear stress. Agreement between predicted and experimental center-line velocity (fig. 22) is fairly satisfactory.

Paulk Jet in Moving Stream – Test Case 20

Even though the initial boundary layers are fairly thin in this flow (test case 20), the velocity ratio $(u_e/u_o = 0.48)$ exceeds that where a fully developed initial shear stress can be used. A potential core length of approximately 12D is predicted with the assumption of a fully developed initial R_T. The control volume initial region analysis was applied with $\delta_a = 0.082r_o$ and $\delta_j = 0.063r_o$. The experimental boundary-layer shapes are not well defined in reference 22; therefore, the initial region computations were carried out for two values of the velocity profile exponent $(n_a = n_j = 1/4$ and $n_a = n_j = 1/7)$. The result-

ing values of b, r_i, and shear stress were then used to start (at $x = 0$) the computations for the entire flow field. Both computations are shown in figure 23; the predicted flow field is obviously not very sensitive to the initial boundary-layer shape. Both predictions agree fairly well with the experimental center-line velocity but, of course, the experimental center-line concentration decays more rapidly than predicted.

It should be noted that the experimental values of $(u_c - u_e)/(u_o - u_e)$ were computed with $u_o = 390$ ft/sec (119 m/sec) and $u_e = 187$ ft/sec (57 m/sec), the observed values of u_o and u_e downstream in the flow field.

Chriss Hydrogen Jet in Moving Air Stream – Test Case 21

As with test case 10, this flow (test case 21) was computed (1) with experimental initial conditions, and (2) with fully developed R_T at $x = 0$. The initial shear stress for the first computation was taken from reference 22 at the most upstream axial station for which a shear stress was measured in this flow. The predicted center-line velocity agrees well with experiment (fig. 24(a)) but, as usual, the center-line composition decay is underpredicted. The computations which were started at $x = 0$ are shown in figure 24(b); the agreement with experiment is poor. Therefore, it can be concluded that the velocity ratio of this flow ($u_e/u_o = 0.31$) exceeds that for successful use of a fully developed initial shear stress.

Eggers Hydrogen Jet in Moving Air Stream – Test Case 22

As with test cases 11 and 12, this flow (test case 22) is wakelike in that the jet momentum flux is less than the outer stream momentum flux. The flow also has very thick initial boundary layers. In spite of the thick boundary layers and the velocity ratio $(u_e/u_j = 0.54)$, computations were started at $x = 0$ with a thin initial shear layer and with fully developed R_T. The predictions (fig. 25) are not as bad as could be expected, but the analysis does not predict qualitatively the behavior of the center-line velocity. It is unlikely that this flow will ever be properly predicted with an analysis which ignores the significant pressure gradients in the flow field.

CONCLUDING REMARKS

When the rather small investment of empirical information on turbulence structure is considered, the quality of the mean flow predictions is surprisingly good. Experience in computing a variety of flows has not indicated that the assumption of universal TKE profile shapes is grossly incorrect. The utility of the admittedly oversimplified model for turbulent dissipation has been significantly increased by relating the dissipation coefficient a_2 to the local turbulent Reynolds number.

A persistent point of criticism about TKE methods for free shear flows has been that the required detailed information on initial conditions is not generally available for engineering flows. Experience has shown that a considerable number of practical flows can be computed without detailed information on the initial conditions. For u_e/u_o less than 0.25, specifying a fully developed initial shear stress works very well. Wakelike flows, such as test case 12, seem to be fairly insensitive to initial conditions. For jet flows with velocity ratio u_e/u_o greater than 0.25, the control volume initial region analysis shows promise. The very limited experience with this initial region analysis for constant density flows has indicated that the results are not overly sensitive to the initial boundary-layer characteristics; good guesses about the initial boundary layers seem to be sufficient.

Turbulent kinetic energy methods, of which this method is a simplified example, represent a fundamental improvement over eddy-viscosity models in that more of the physics of the turbulent motion is taken into account, albeit crudely. It appears that these methods have been developed to the point where they are routinely applicable to engineering calculations on a broad class of free turbulent flows.

REFERENCES

1. Peters, C. E.; Phares, W. J.; and Cunningham, T. H. M.: Theoretical and Experimental Studies of Ducted Mixing and Burning of Coaxial Streams. J. Spacecraft Rockets, vol. 6, no. 12, Dec. 1969, pp. 1435-1441.

2. Peters, C. E.: Turbulent Mixing and Burning of Coaxial Streams Inside a Duct of Arbitrary Shape. AEDC-TR-68-270, U.S. Air Force, Jan. 1969. (Available from DDC as AD 680 397.)

3. Donaldson, Coleman duP.; and Gray, K. Evan: Theoretical and Experimental Investigation of the Compressible Free Mixing of Two Dissimilar Gases. AIAA J., vol. 4, no. 11, Nov. 1966, pp. 2017-2025.

4. Harsha, Philip Thomas: Free Turbulent Mixing: A Critical Evaluation of Theory and Experiment. AEDC-TR-71-36, U.S. Air Force, Feb. 1971. (Available from DDC as AD 718 956.)

5. Bradshaw, P.; Ferriss, D. H.; and Atwell, N. P.: Calculation of Boundary-Layer Development Using the Turbulent Energy Equation. J. Fluid Mech., vol. 28, pt. 3, May 26, 1967, pp. 593-616.

6. Lee, S. C.; and Harsha, P. T.: Use of Turbulent Kinetic Energy in Free Mixing Studies. AIAA J., vol. 8, no. 6, June 1970, pp. 1026-1032.

7. Laster, M. L.: Inhomogeneous Two-Stream Turbulent Mixing Using the Turbulent Kinetic Energy Equation. AEDC-TR-70-134, U.S. Air Force, May 1970. (Available from DDC as AD 705 578.)

8. Patankar, S. V.; and Spalding, D. B.: A Finite-Difference Procedure for Solving the Equations of the Two-Dimensional Boundary Layer. Int. J. Heat Mass Transfer, vol. 10, no. 10, Oct. 1967, pp. 1389-1411.

9. Heck, P. H.; and Ferguson, D. R.: Analytical Solution for Free Turbulent Mixing in Compressible Flows. AIAA Paper No. 71-4, Jan. 1971.

10. Ortwerth, P. J.: Mechanism of Mixing of Two Nonreacting Gases. AFAPL-TR-71-18, U.S. Air Force, Oct. 1971.

11. Ortwerth, P. J.: Mechanism of Mixing of Two Nonreacting Gases. AIAA Paper No. 71-725, June 1971.

12. Harsha, P. T.; and Lee, S. C.: Correlation Between Turbulent Shear Stress and Turbulent Kinetic Energy. AIAA J., vol. 8, no. 8, Aug. 1970, pp. 1508-1510.

13. Spencer, Bruce Walton: Statistical Investigation of Turbulent Velocity and Pressure Fields in a Two-Stream Mixing Layer. Ph. D. Thesis, Univ. of Illinois, 1970.

14. Liepmann, Hans Wolfgang; and Laufer, John: Investigation of Free Turbulent Mixing. NACA TN 1257, 1947.

15. Pindell, Robert George: An Experimental Study of the Coaxial Turbulent Jet. Ph. D. Dissertation, North Carolina State Univ., 1970.

16. Wygnanski, I.; and Fiedler, H.: Some Measurements in the Self-Preserving Jet. J. Fluid Mech., vol. 38, pt. 3, Sept. 18, 1969, pp. 577-612.

17. Sami, Sedat: Velocity and Pressure Fields of a Diffusing Jet. Ph. D. Dissertation, Univ. of Iowa, 1966.

18. Sami, S.; Carmody, Thomas; and Rouse, Hunter: Jet Diffusion in the Region of Flow Establishment. J. Fluid Mech., vol. 27, pt. 2, Feb. 2, 1967, pp. 231-252.

19. Bradshaw, P.; Ferriss, D. H.; and Johnson, R. F.: Turbulence in the Noise-Producing Region of a Circular Jet. J. Fluid Mech., vol. 19, pt. 4, Aug. 1964, pp. 591-624.

20. Warren, Walter R.: An Analytical and Experimental Study of Compressible Free Jets. Ph. D. Dissertation, Princeton Univ., 1957.

21. Spalding, D. B.; and Chi, S. W.: The Drag of a Compressible Turbulent Boundary Layer on a Smooth Flat Plate With and Without Heat Transfer. J. Fluid Mech., vol. 18, pt. 1, Jan. 1964, pp. 117-143.

22. Chriss, D. E.; and Paulk, R. A.: An Experimental Investigation of Subsonic Coaxial Free Turbulent Mixing. AEDC-TR-71-236, AFOSR-72-0237 TR, U.S. Air Force, Feb. 1972. (Available from DDC as AD 737 098.)

23. Chevray, R.: The Turbulent Wake of a Body of Revolution. Trans. ASME, Ser. D: J. Basic Eng., vol. 90, no. 2, June 1968, pp. 275-284.

24. Demetriades, Anthony: Mean-Flow Measurements in an Axisymmetric Compressible Turbulent Wake. AIAA J., vol. 6, no. 3, Mar. 1968, pp. 432-439.

25. Albertson, M. L.; Dai, Y. B.; Jensen, R. A.; and Rouse, Hunter: Diffusion of Submerged Jets. Paper No. 2409, Transactions Amer. Soc. Civil Eng., vol. 115, 1950, pp. 639-664.

TABLE I.- INITIAL CONDITIONS FOR THE EXPERIMENTAL FLOWS

Test case	Flow	x_1	b_1	r_{i1}	$R_{T,1}$	Notes
6	Maestrello and McDaid axisymmetric jet, $M_o = 0.64$	$2r_o$	$0.87r_o$	$0.52r_o$	190	Experimental profile, fully developed R_T
		0	$.01r_o$	$.86r_o$	190	r_o corrected for momentum
						Fully developed R_T
7	Eggers supersonic jet, $M_o = 2.22$	0	$.01r_o$	r_o	283	Fully developed R_T
8	G.E. heated jet, $M_o = 0.7$	$5.58r_o$	$1.70r_o$	$.18r_o$	212	Experimental profile, fully developed R_T
9	Forstall jet in moving stream, $u_e/u_o = 0.25$	0	$.01r_o$	$.88r_o$	143	r_o corrected for momentum
						Fully developed R_T
10	Chriss H_2 jet in air stream, $u_e/u_o = 0.16$	$5.94r_o$	$1.132r_o$	$.412r_o$	98.3	Experimental profile and R_T
		0	$.01r_o$	r_o	120	Fully developed R_T
11	Eggers and Torrence jet in moving stream	0	$.01r_o$	r_o	130	Fully developed R_T
12	Eggers H_2 jet in air stream, $M_e = 1.33$	0	$.01r_o$	r_o	125	Fully developed R_T
15	Chevray axisymmetric wake	0	.0257D	0	1930	Equivalent cosine profile, $u_c = 0.083u_e$
17	Demetriades axisymmetric wake, $M_e = 3$	17D	1.00D	0	48	Experimental profile. R_T quoted by Demetriades
18	Fully developed axisymmetric jet	0	$.01r_o$	r_o	143	Fully developed R_T
19	G.E. heated jet, $M_o = 1.36$	$5.58r_o$	$1.30r_o$	$.46r_o$	238	Experimental profile, fully developed R_T
20	Paulk jet in moving stream, $u_e/u_o = 0.48$	0	$.113r_o$	$.916r_o$	36.8	Initial condition analysis, $n_a = n_j = 1/4$
		0	$.122r_o$	$.923r_o$	42.9	Initial condition analysis, $n_a = n_j = 1/7$
21	Chriss H_2 jet in air stream, $u_e/u_o = 0.31$	$5.15r_o$	$1.17r_o$	$.464r_o$	48.2	Experimental profile and R_T
		0	$.01r_o$	r_o	130	Fully developed R_T
22	Eggers H_2 jet in air stream, $M_e = 2.5$	0	$.01r_o$	r_o	110	Fully developed R_T

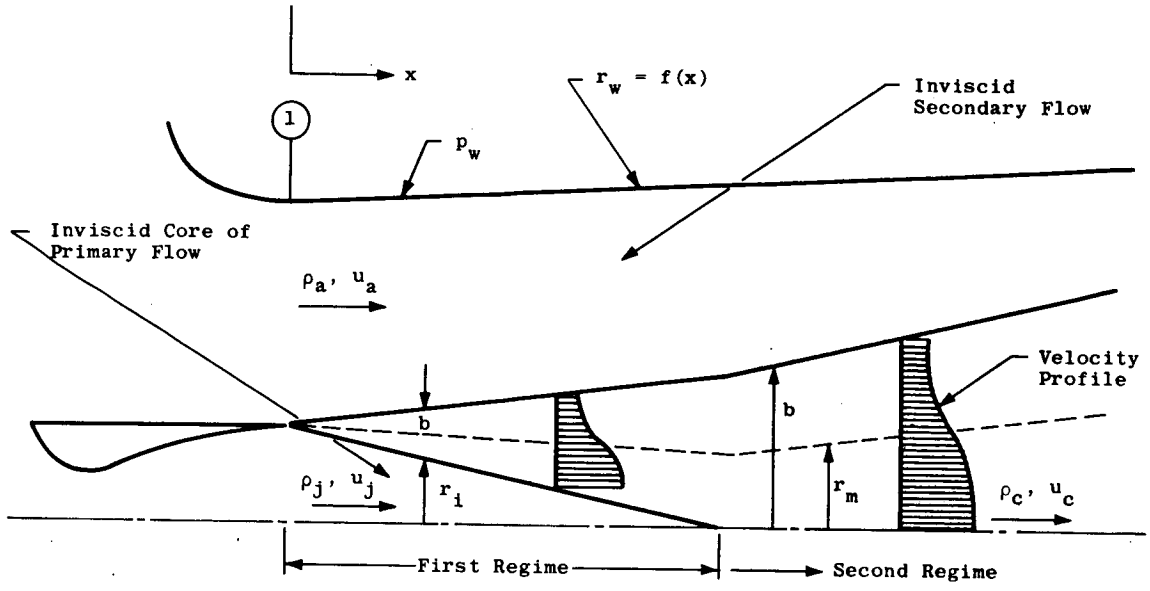

Figure 1.- Nomenclature for integral analysis.

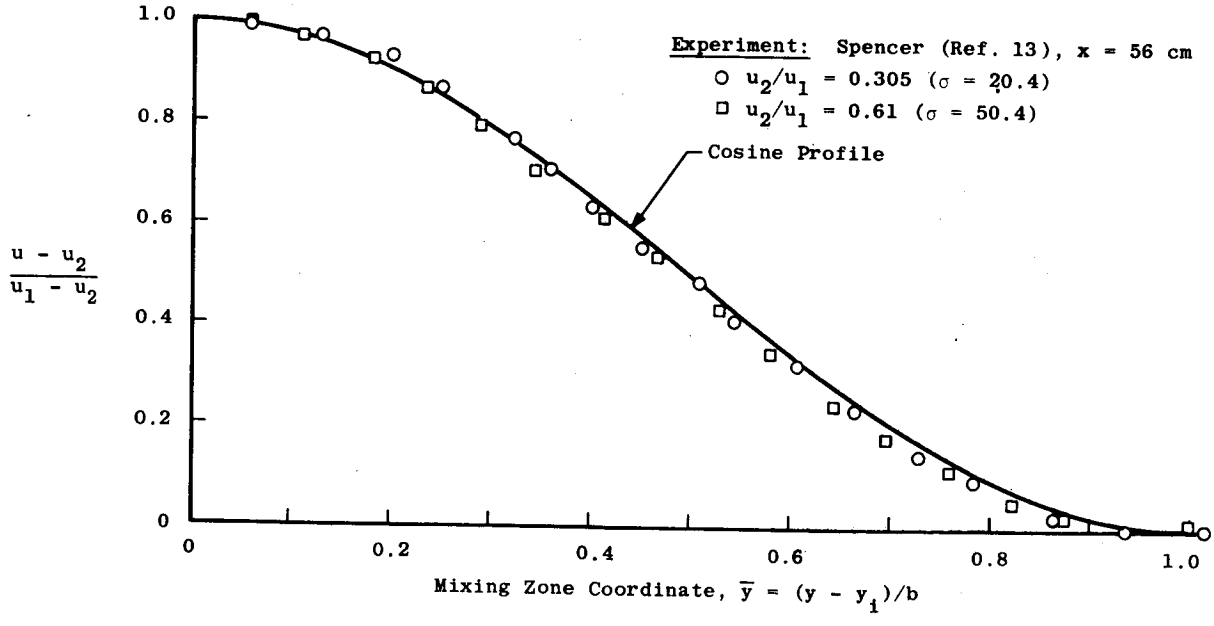

Figure 2.- Near-field velocity profile.

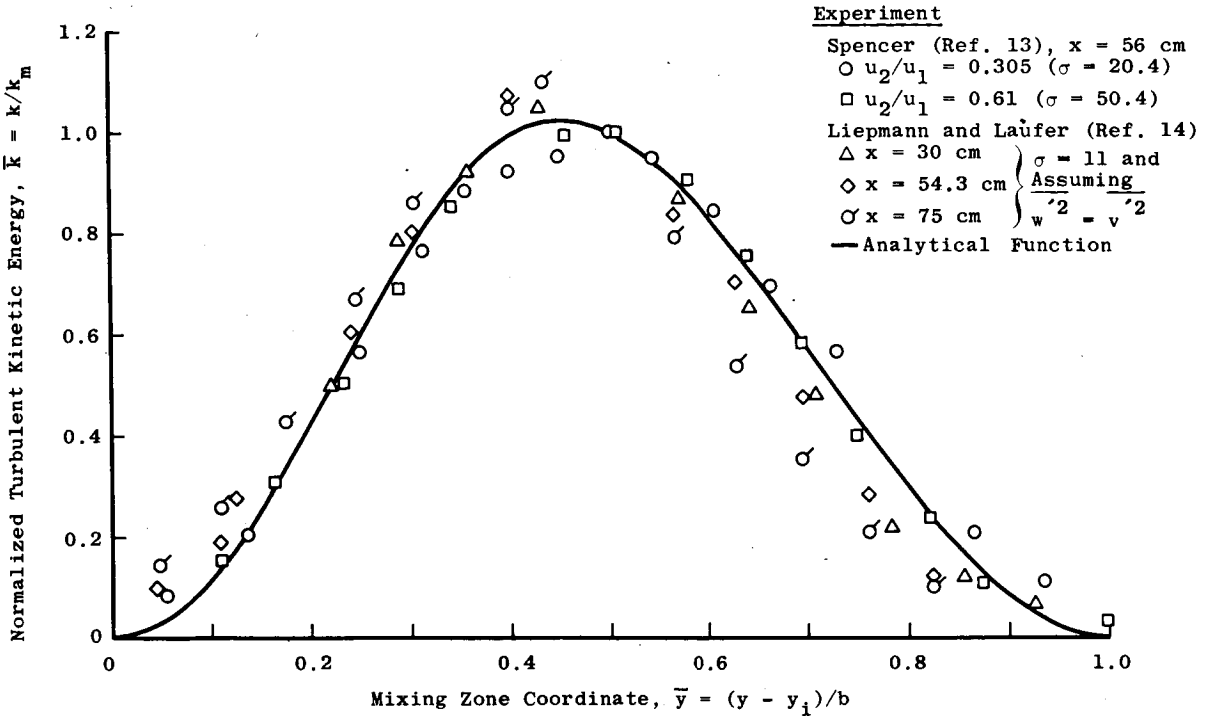

Figure 3.- Near-field turbulent kinetic energy profile.

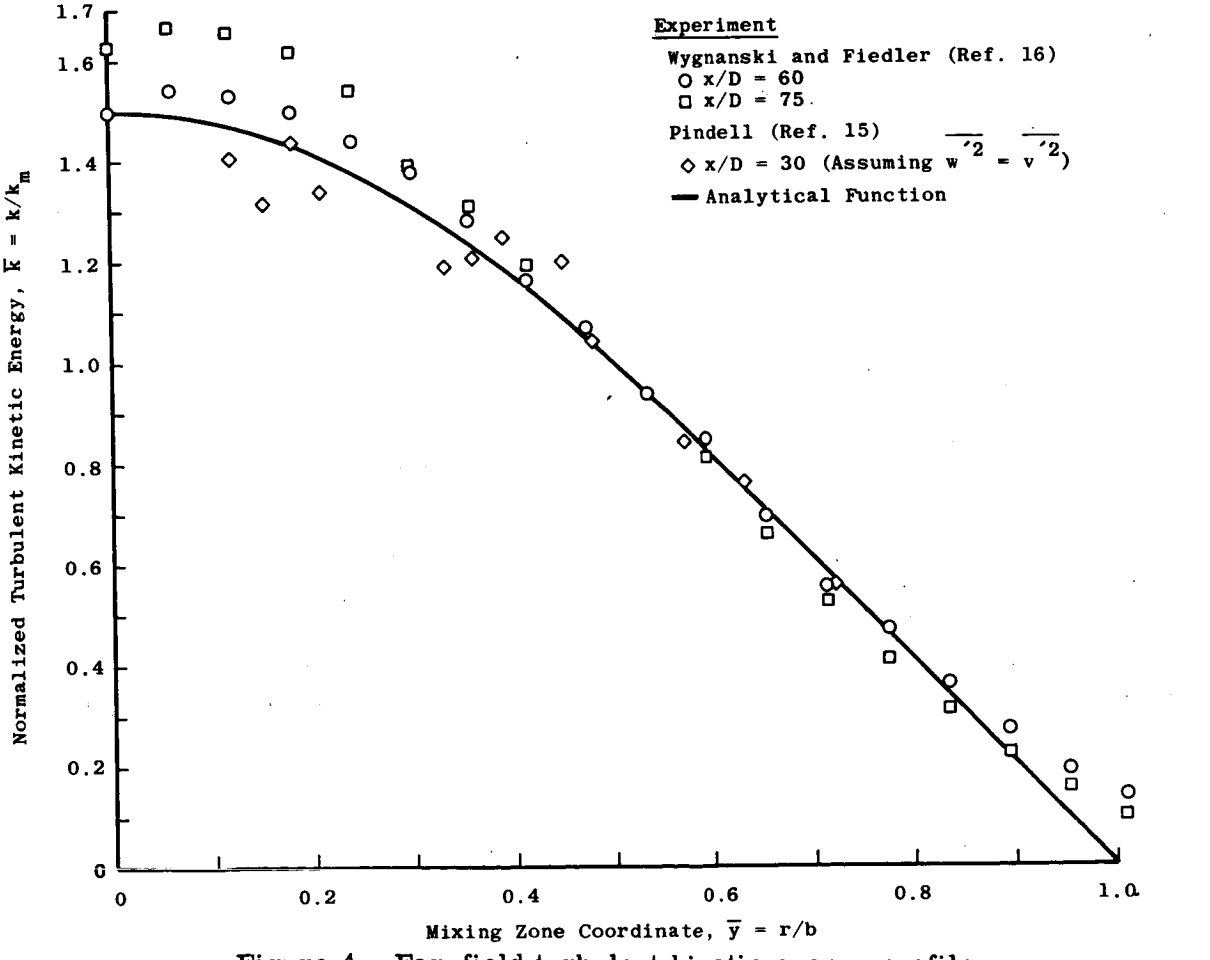

Figure 4.- Far-field turbulent kinetic energy profile.

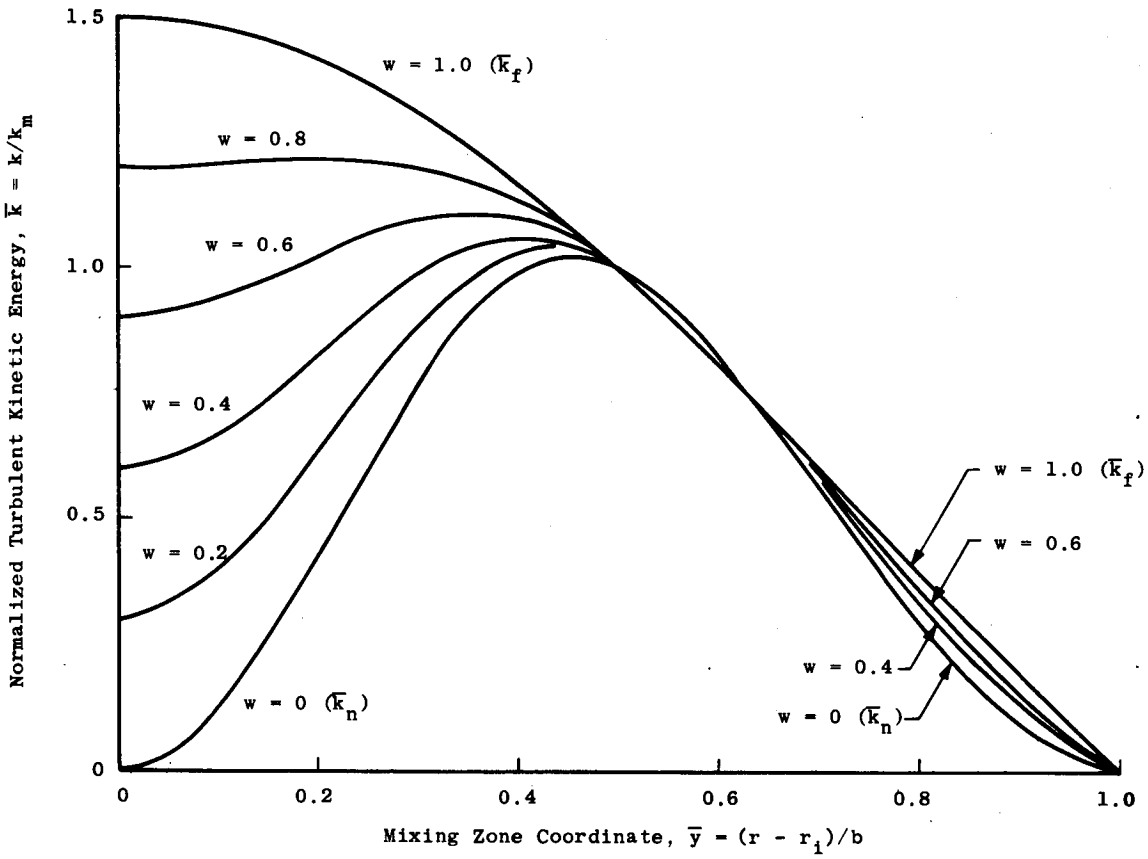

Figure 5.- Family of turbulent kinetic energy profiles.

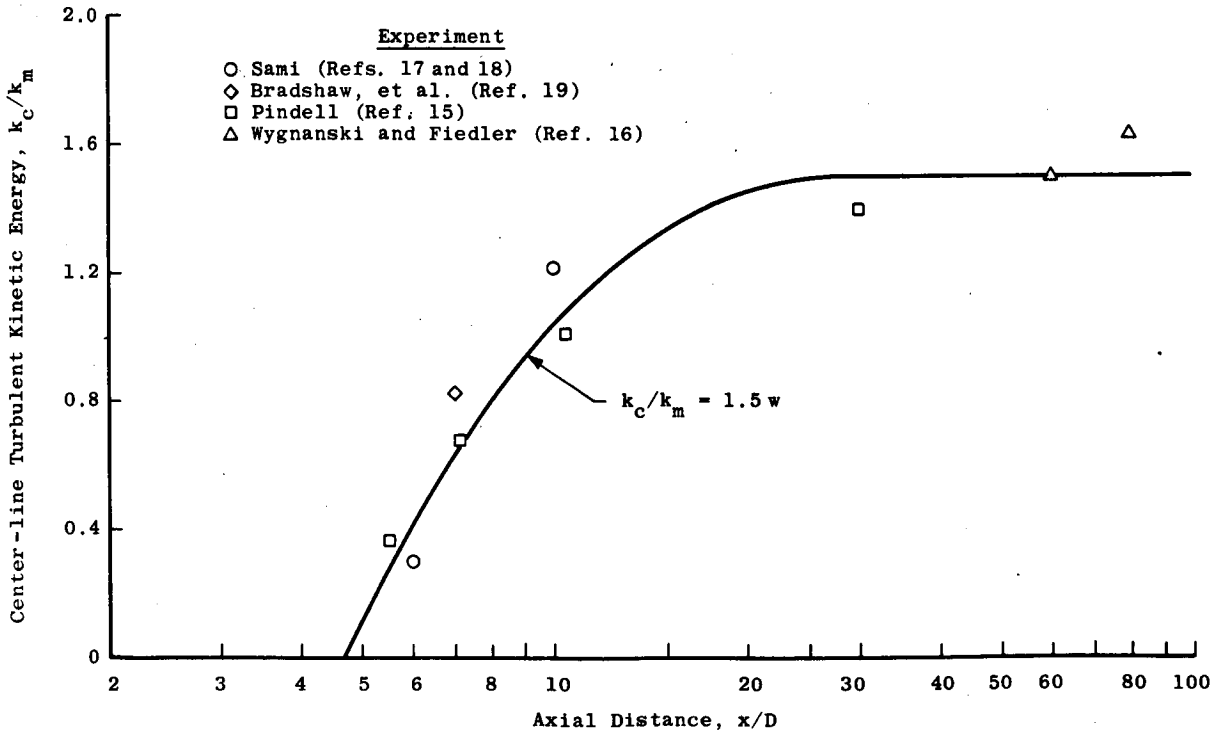

Figure 6.- Center-line turbulent kinetic energy for axisymmetric jet into still air.

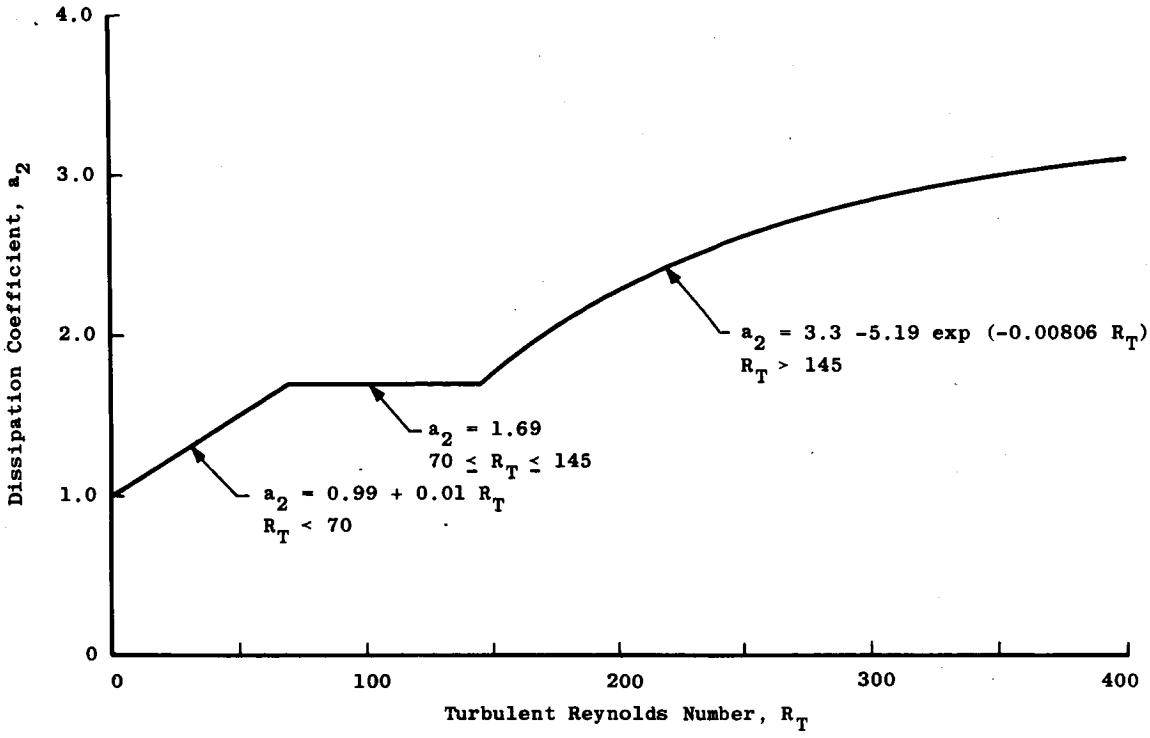

Figure 7.- Dissipation coefficient as a function of turbulent Reynolds number.

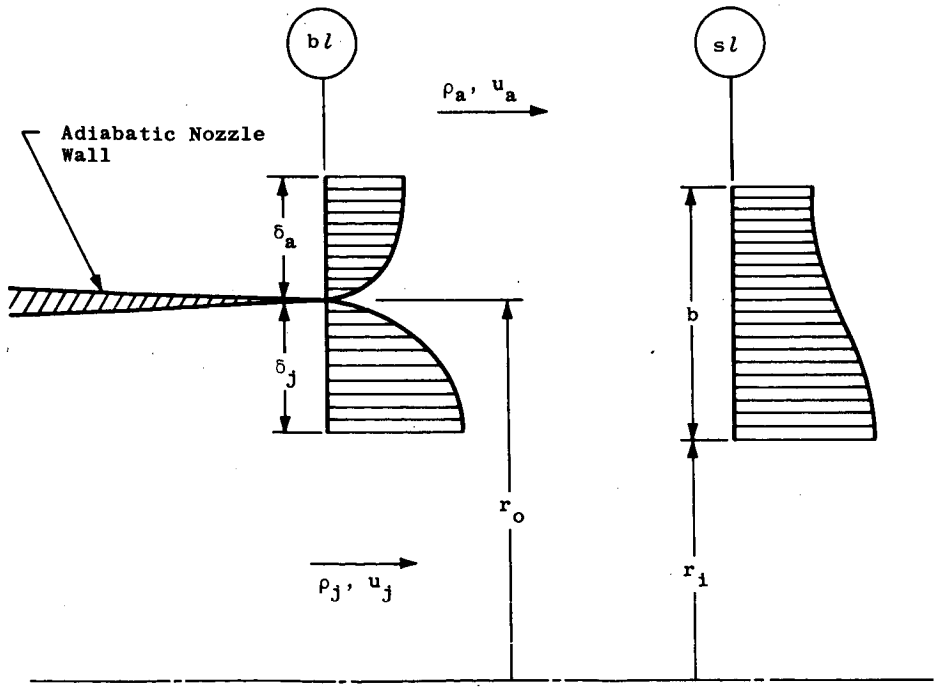

Figure 8.- Nomenclature for initial region analysis. *sl* and *bl* denote shear layer and boundary layer.

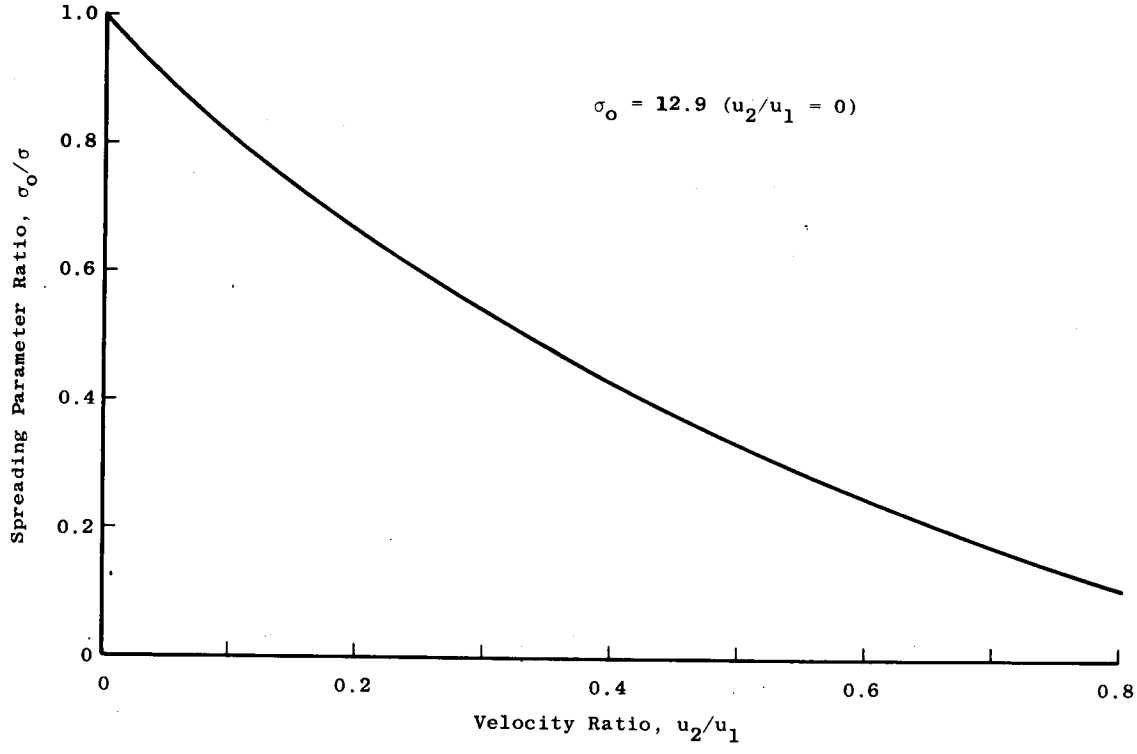

Figure 9.- Test case 1 – Effect of velocity ratio on growth of constant-density two-dimensional fully developed shear layer.

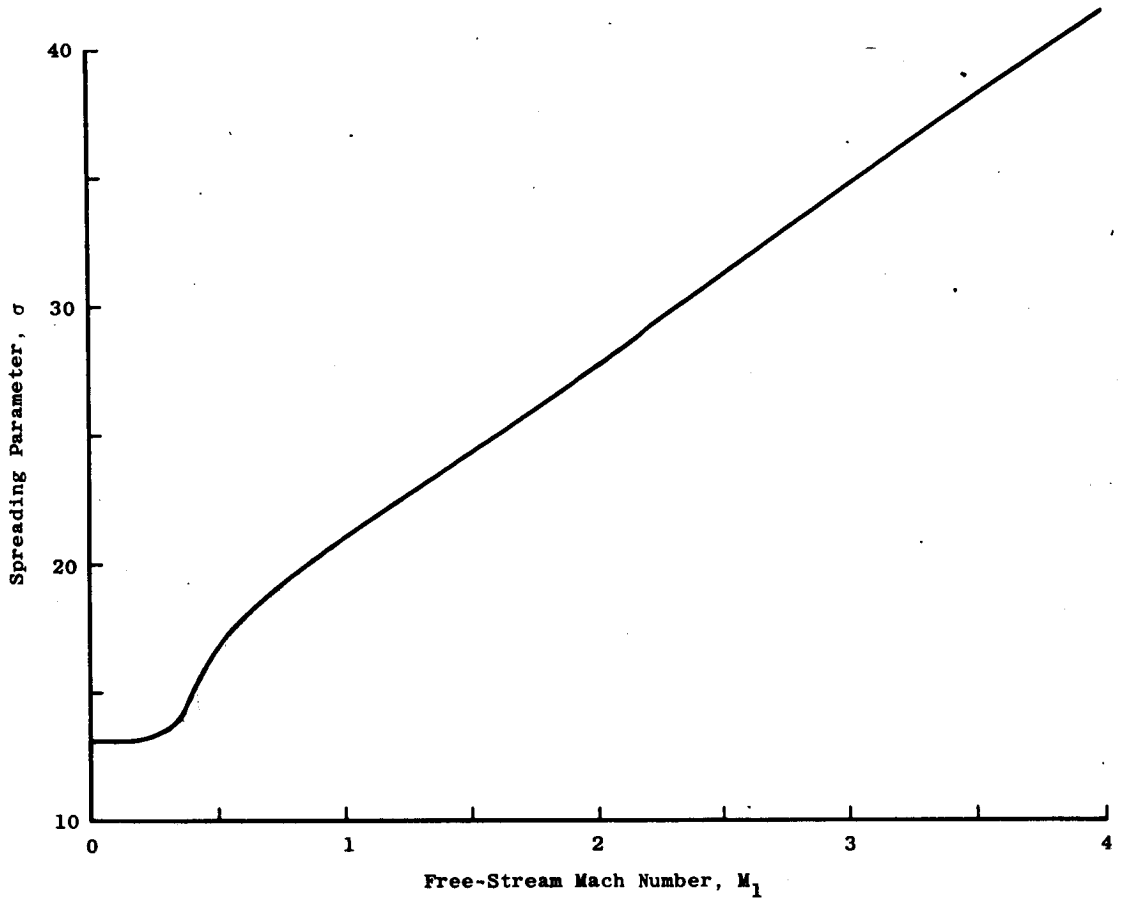

(a) Variation of σ with Mach number.

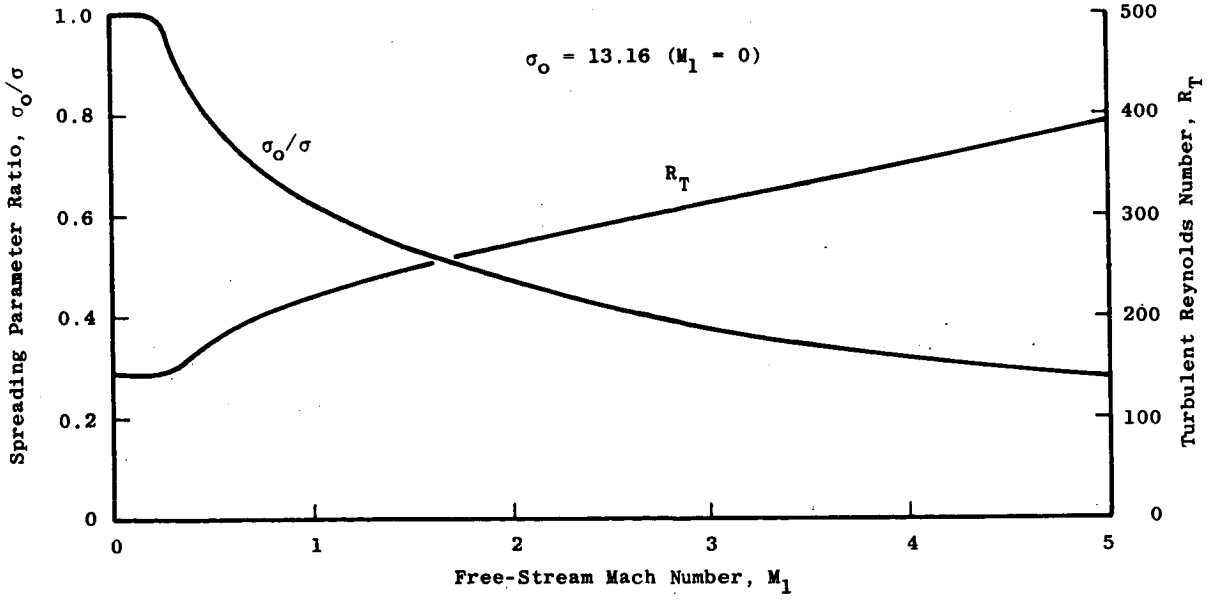

(b) Variation of σ_o/σ and R_T with Mach number.

Figure 10.- Test case 2 – Effect of Mach number on fully developed spreading parameter.

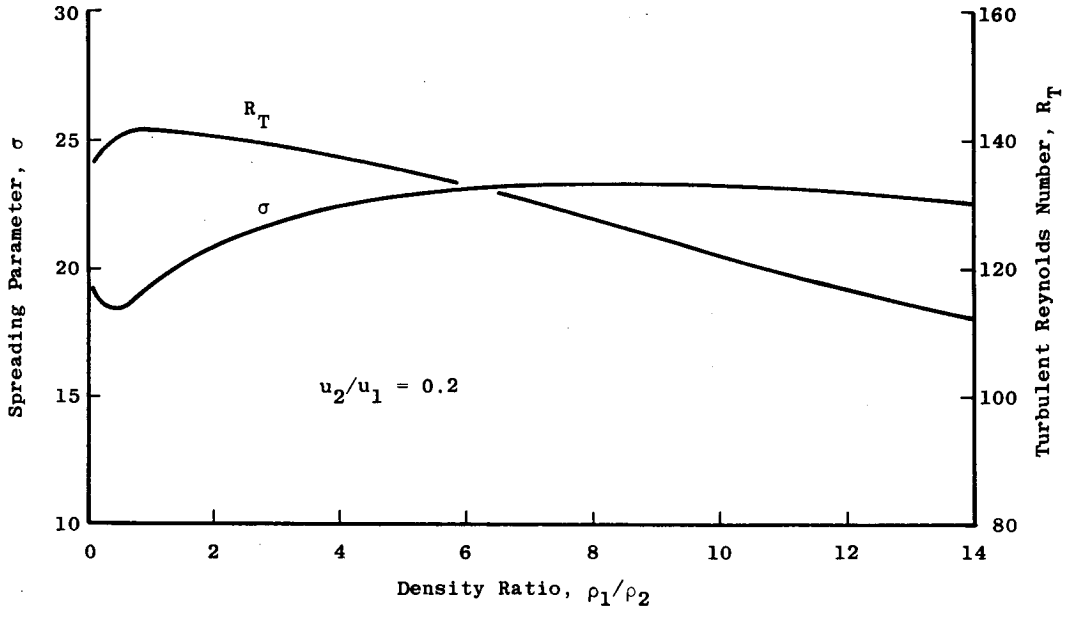

Figure 11.- Test case 3 – Effect of density ratio on growth rate of fully developed two-dimensional shear layer.

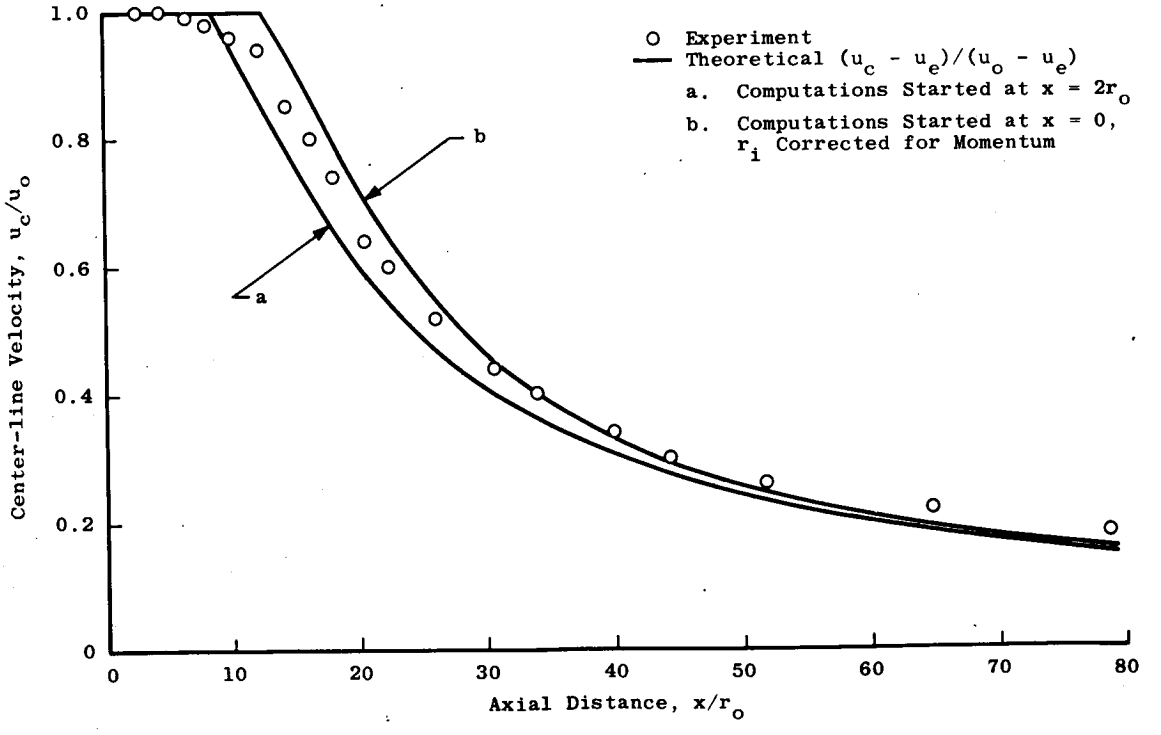

Figure 12.- Test case 6 – Maestrello and McDaid axisymmetric jet into still air. $M_o = 0.64$.

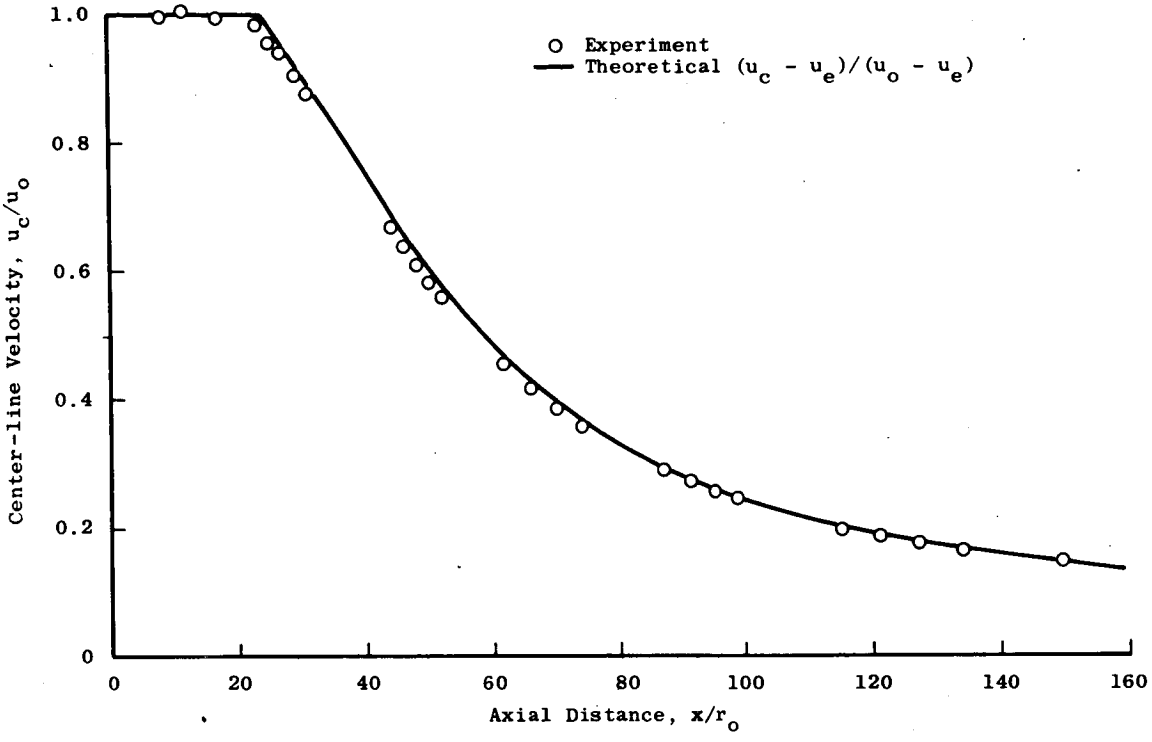

(a) Center-line velocity decay.

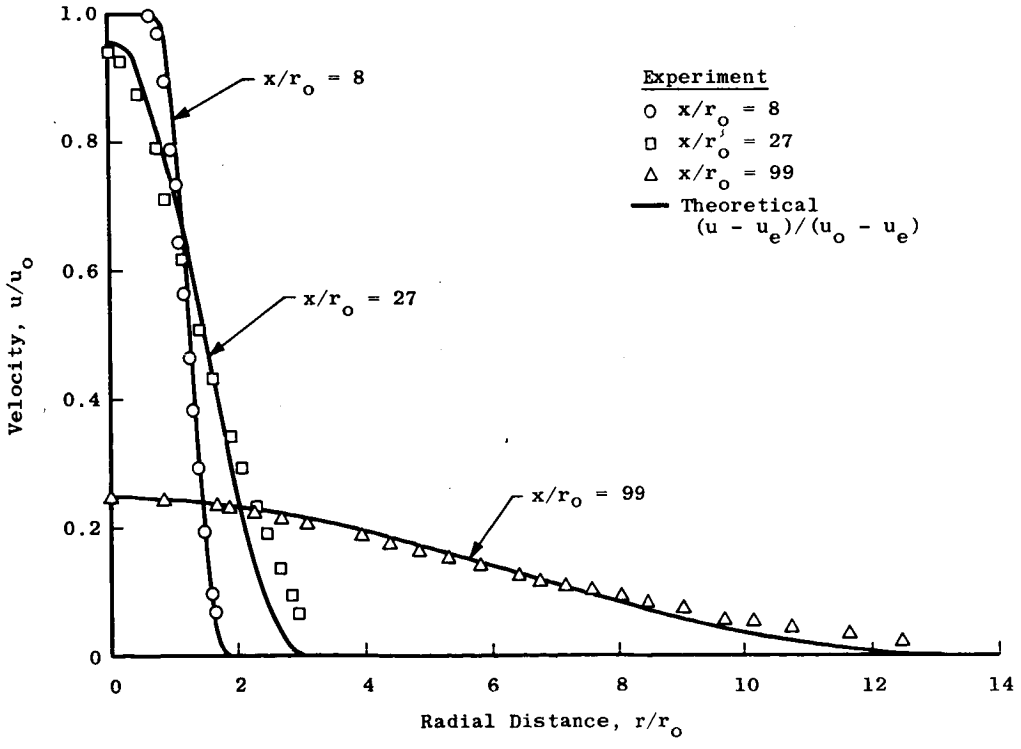

(b) Radial velocity profiles.

Figure 13.- Test case 7 – Eggers axisymmetric jet into still air. M_O = 2.22.

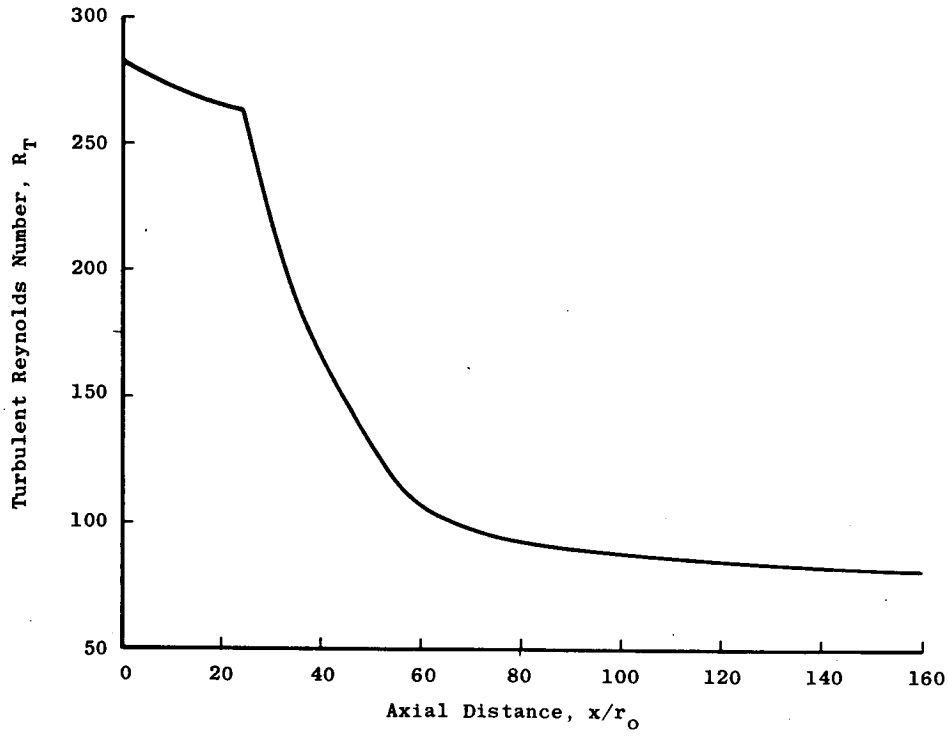

(c) Variation of R_T with x/r_o.

Figure 13.- Concluded.

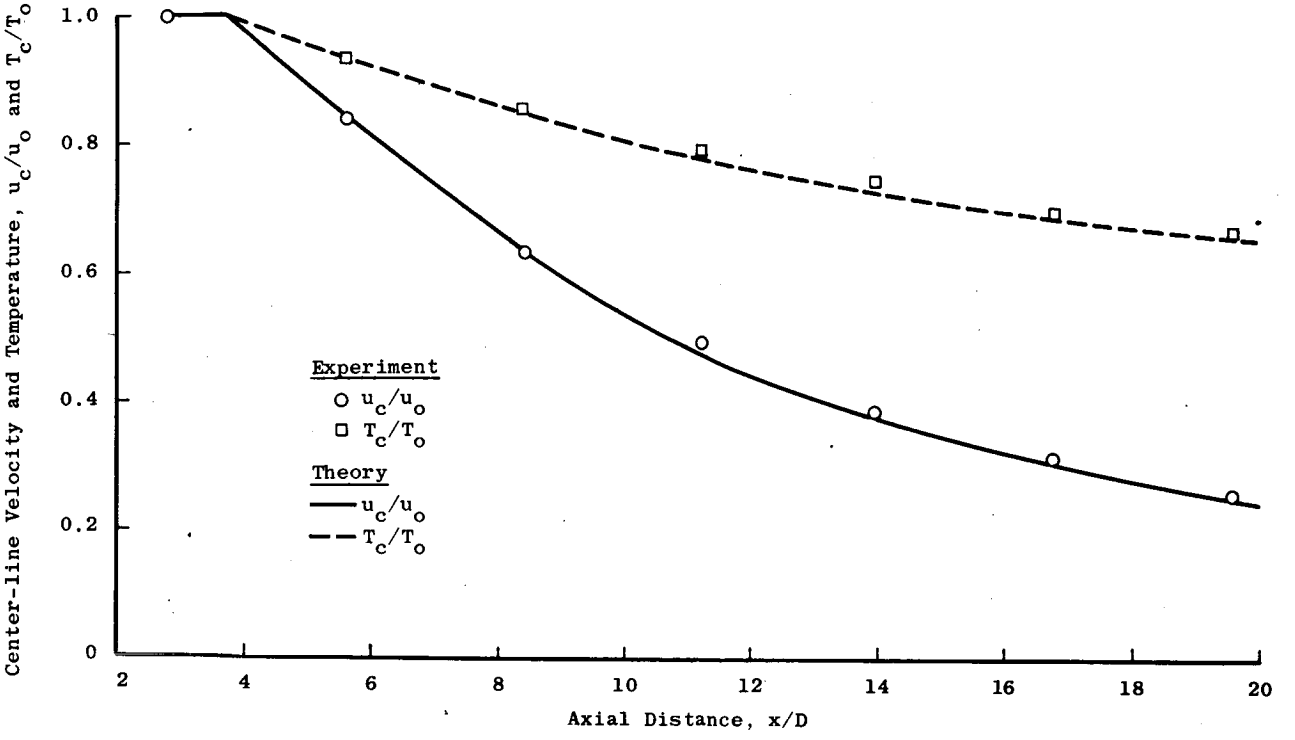

Figure-14.- Test case 8 – Heated axisymmetric jet. $M_o = 0.7$.

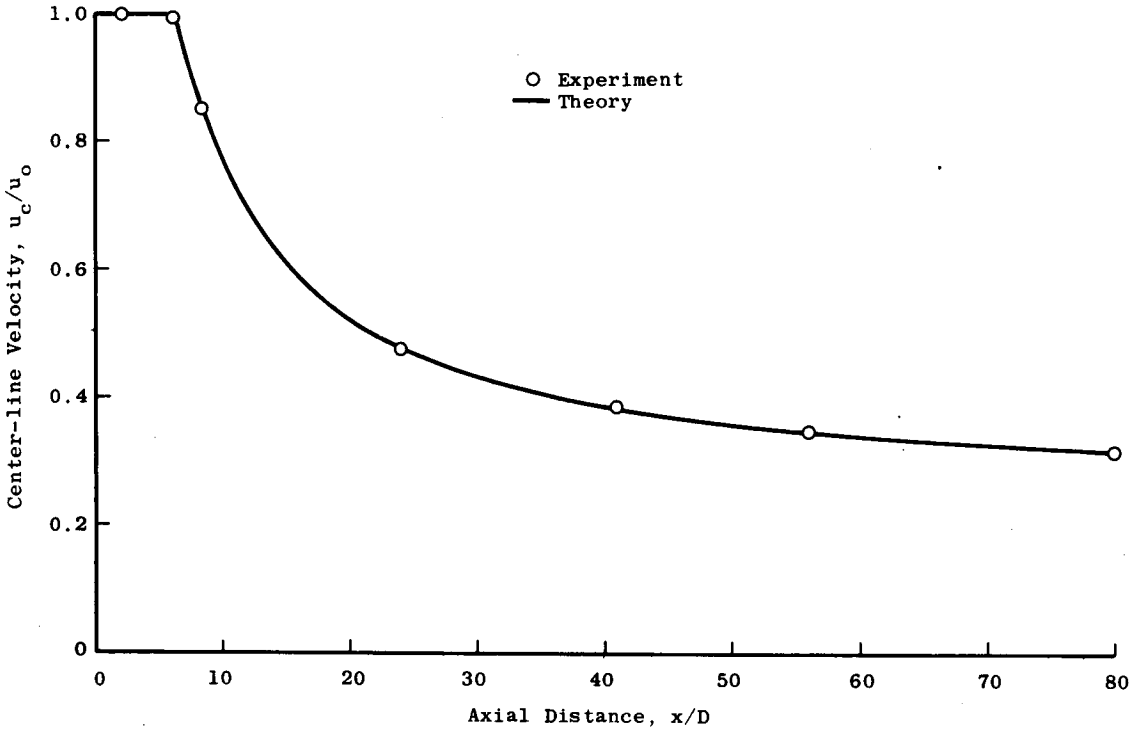

(a) Center-line velocity.

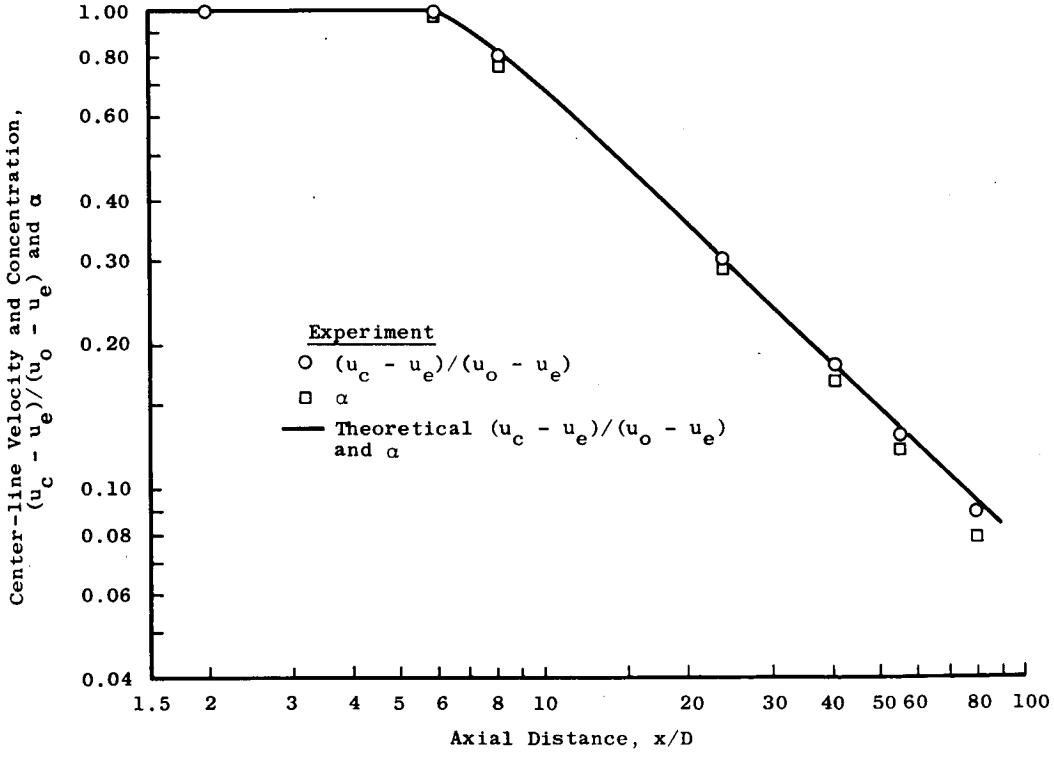

(b) Log plot of center-line velocity and concentration.

Figure 15.- Test case 9 – Forstall axisymmetric jet in moving stream. $u_e/u_o = 0.25$.

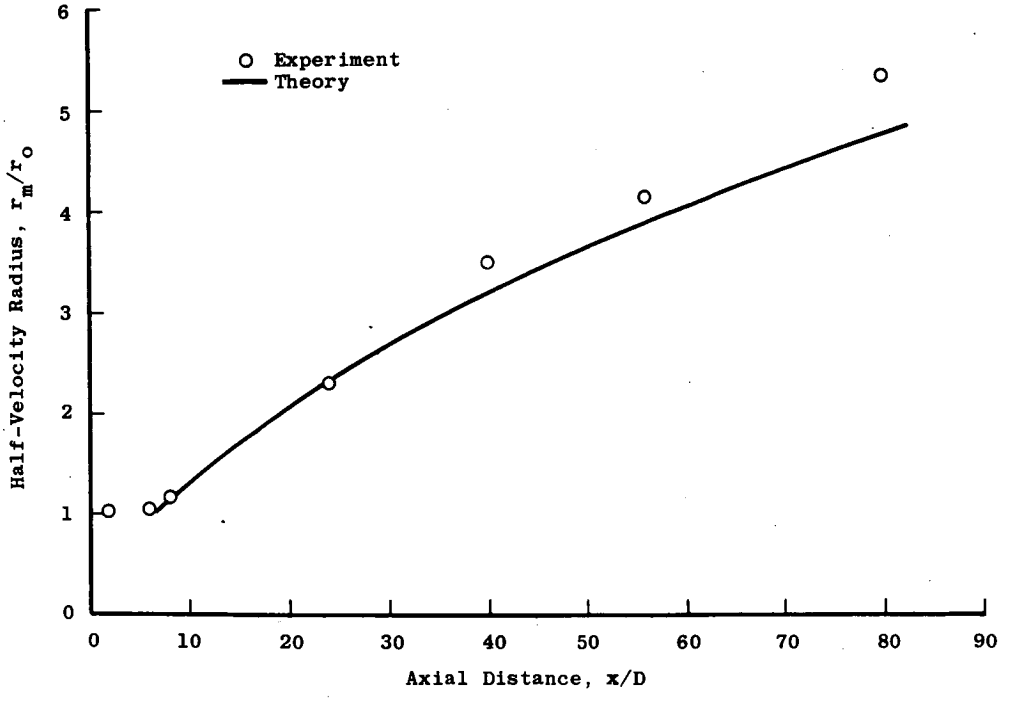

(c) Half-velocity radius.

Figure 15.- Concluded.

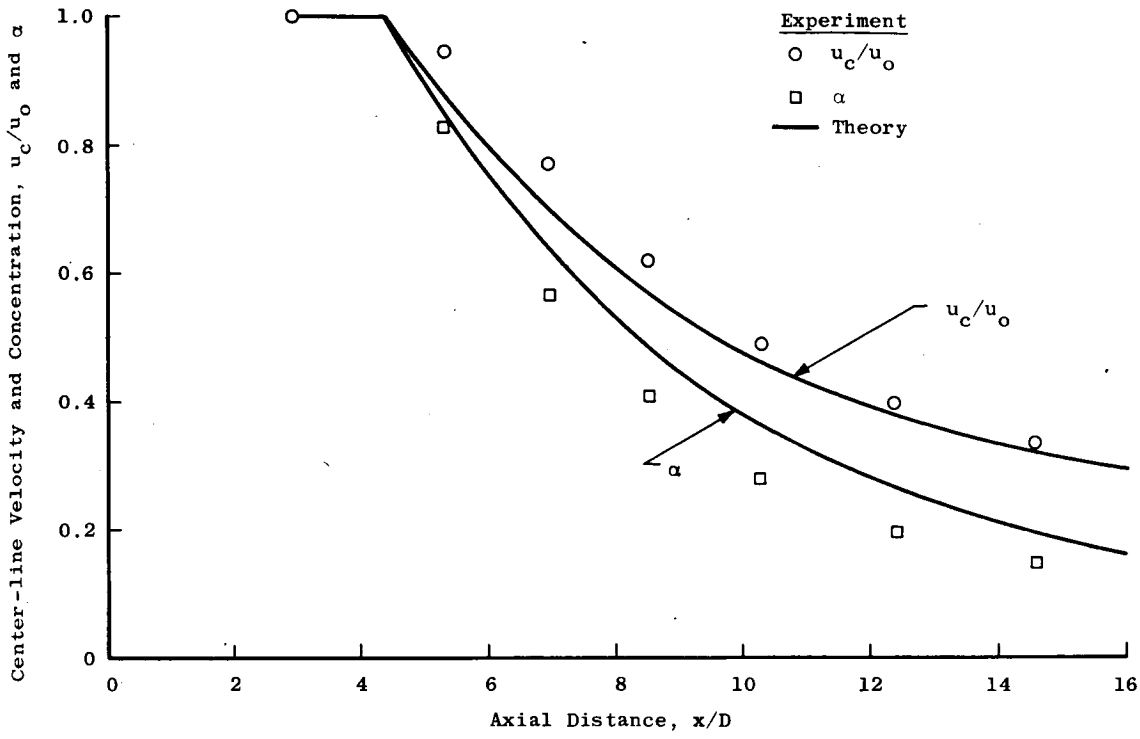

(a) Computations started at x/D = 2.97.

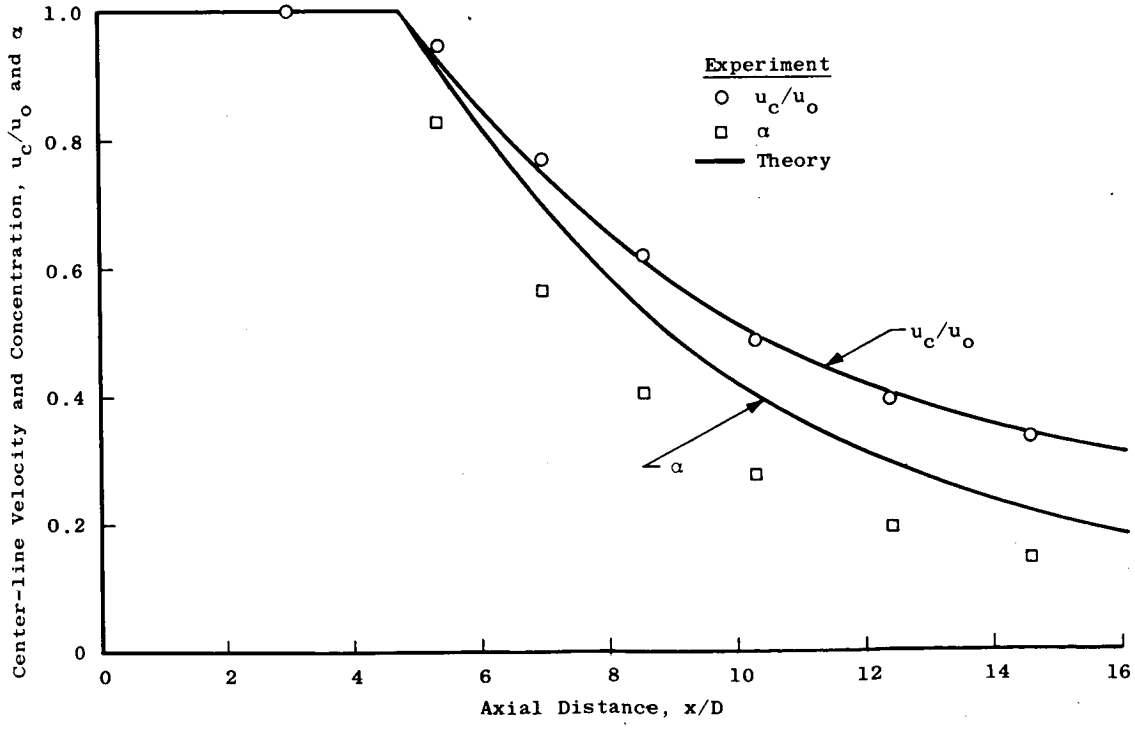

(b) Computations started at x = 0.

Figure 16.- Test case 10 – Chriss H_2 jet in moving stream. $u_e/u_o = 0.16$.

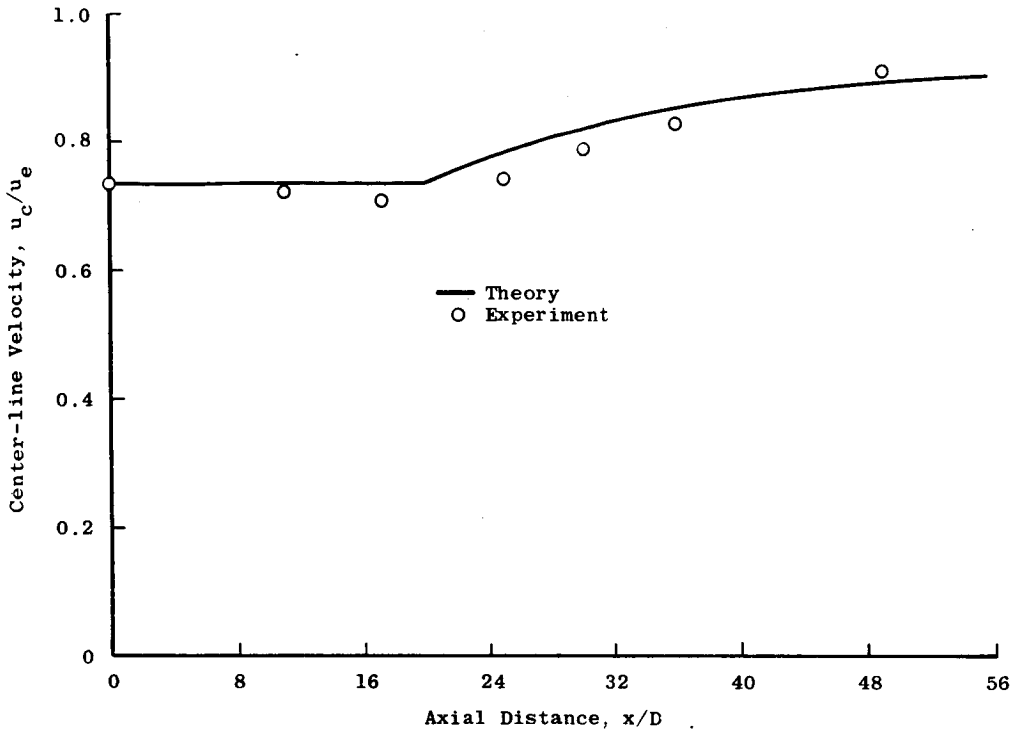

Figure 17.- Test case 11 – Eggers and Torrence axisymmetric jet in a moving stream.

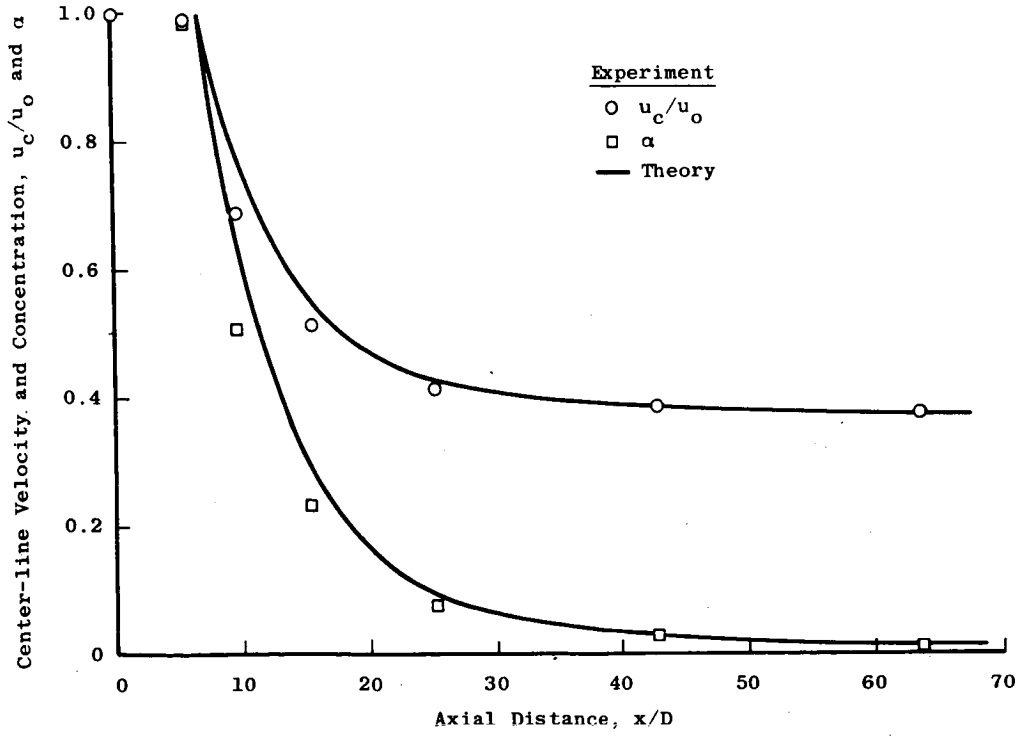

Figure 18.- Test case 12 – Eggers H_2 jet in moving stream. $M_e = 1.33$.

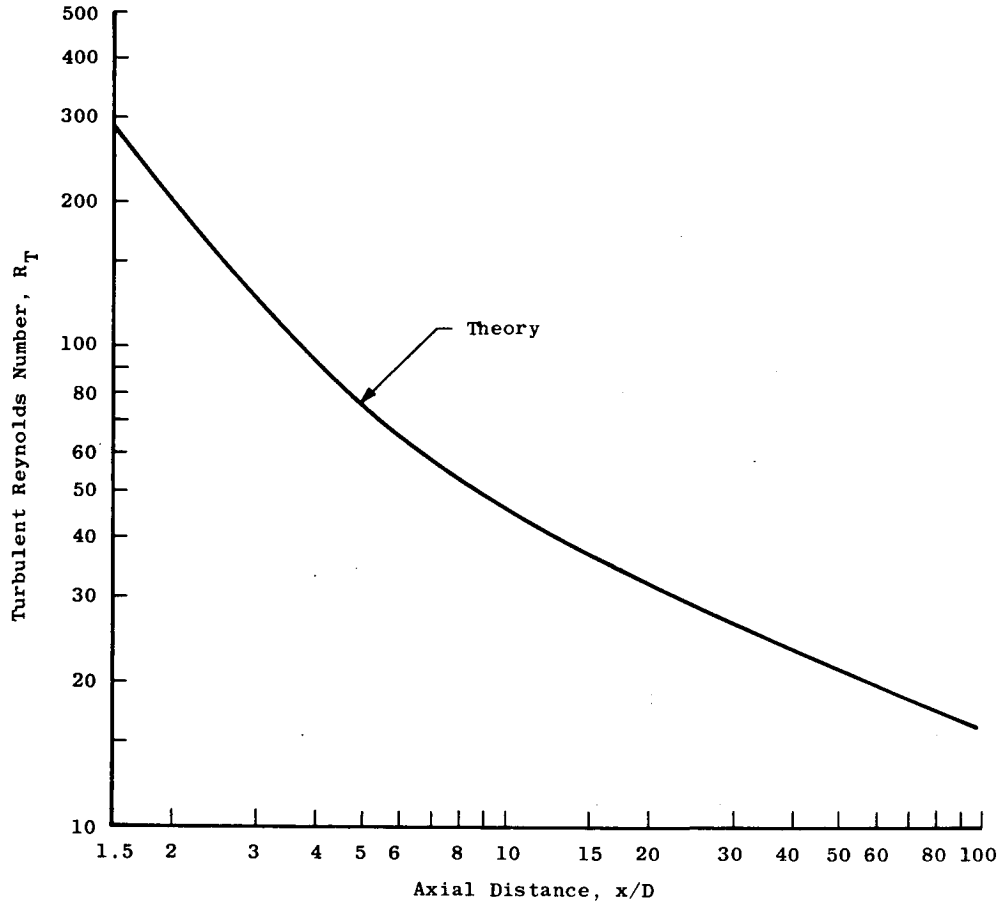

(c) Variation of R_T with x/D.

Figure 19.- Concluded.

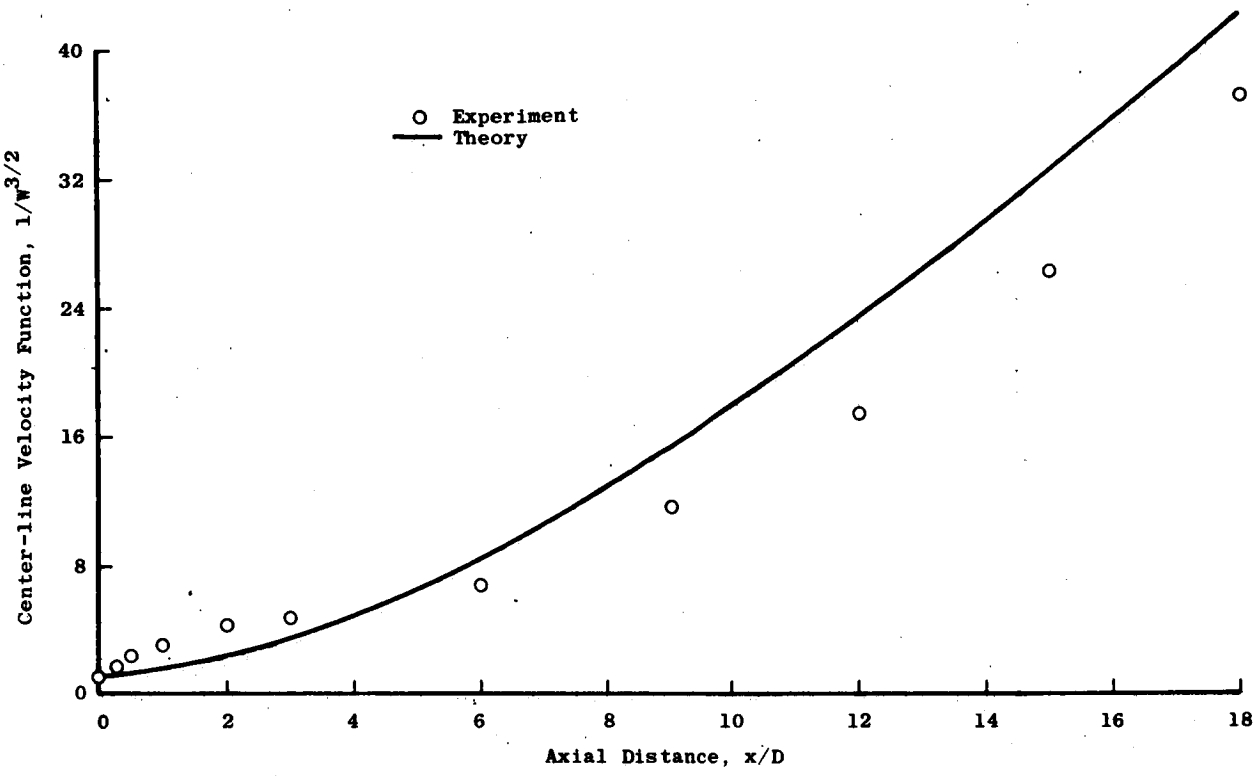

(a) Variation of $1/W^{3/2}$ with x/D.

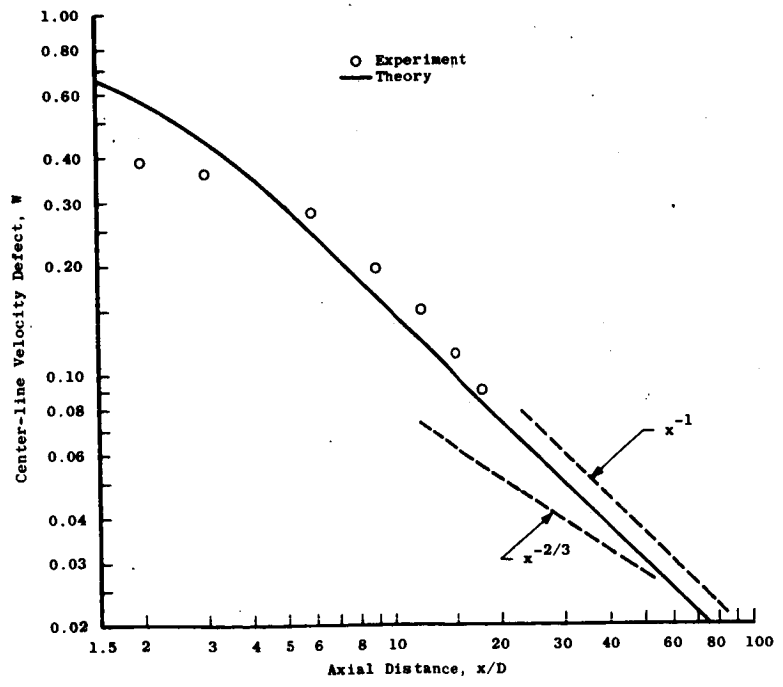

(b) Log plot of W against x/D.

Figure 19.- Test case 15 – Chevray axisymmetric wake.

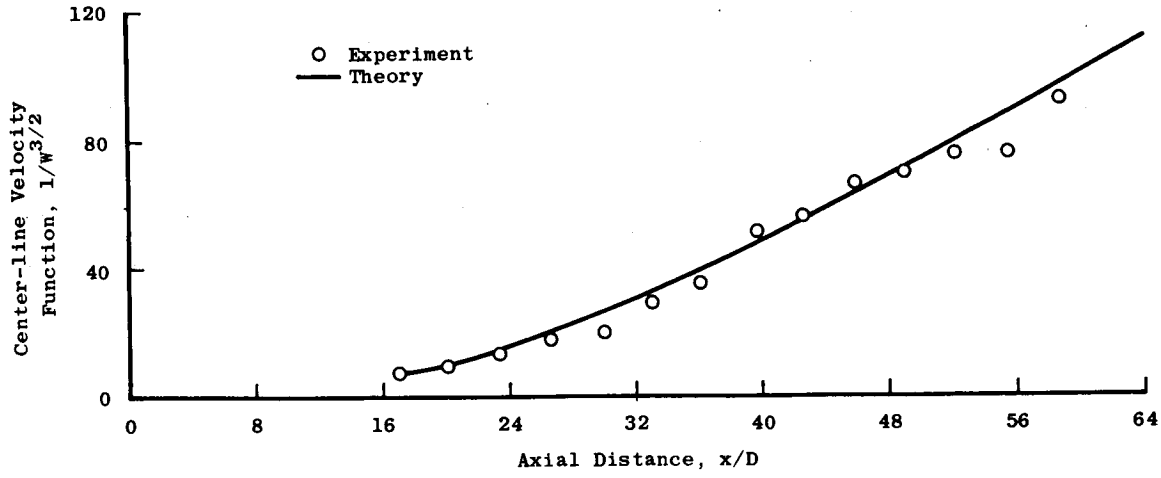

(a) Variation of $1/W^{3/2}$ with x/D.

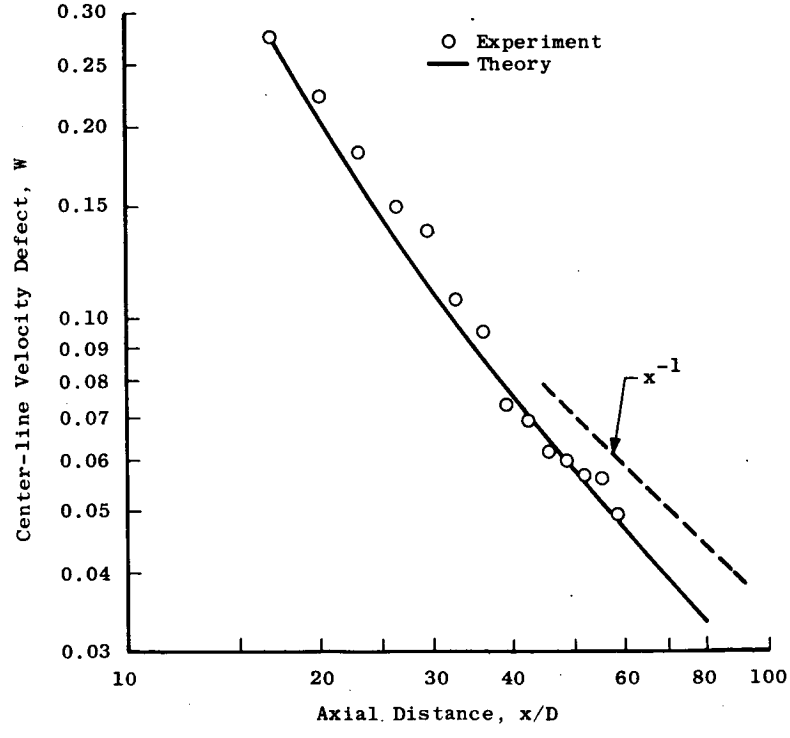

(b) Log plot of W against x/D.

Figure 20.- Test case 17 – Demetriades axisymmetric wake. $M_e = 3$.

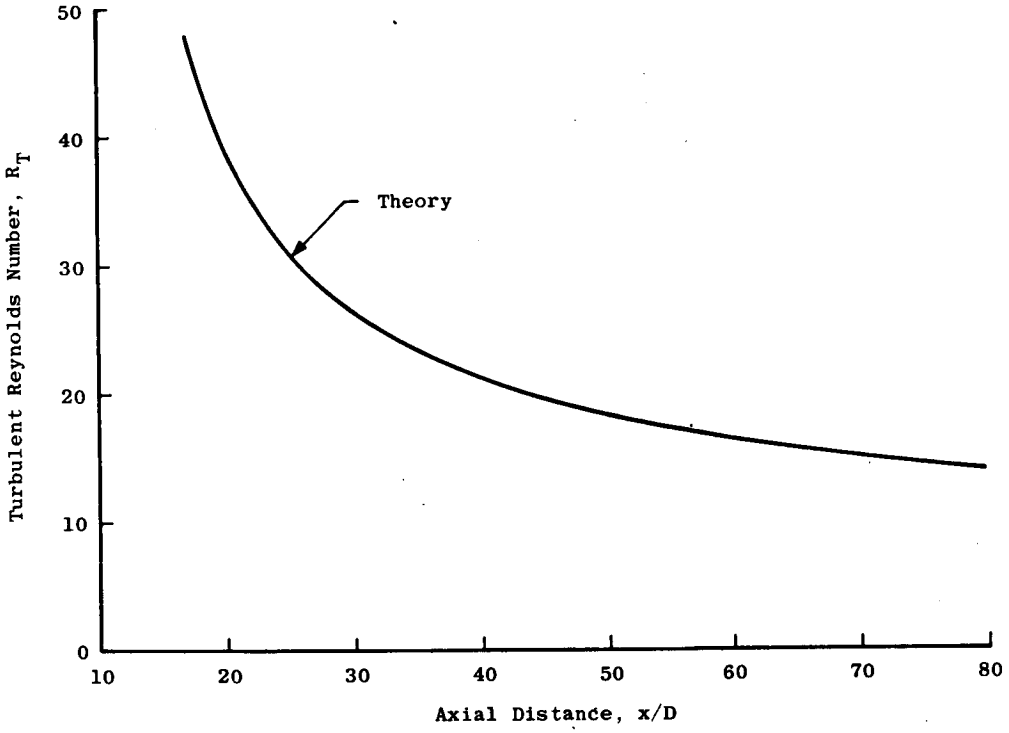

(c) Variation of R_T with x/D.

Figure 20.- Concluded.

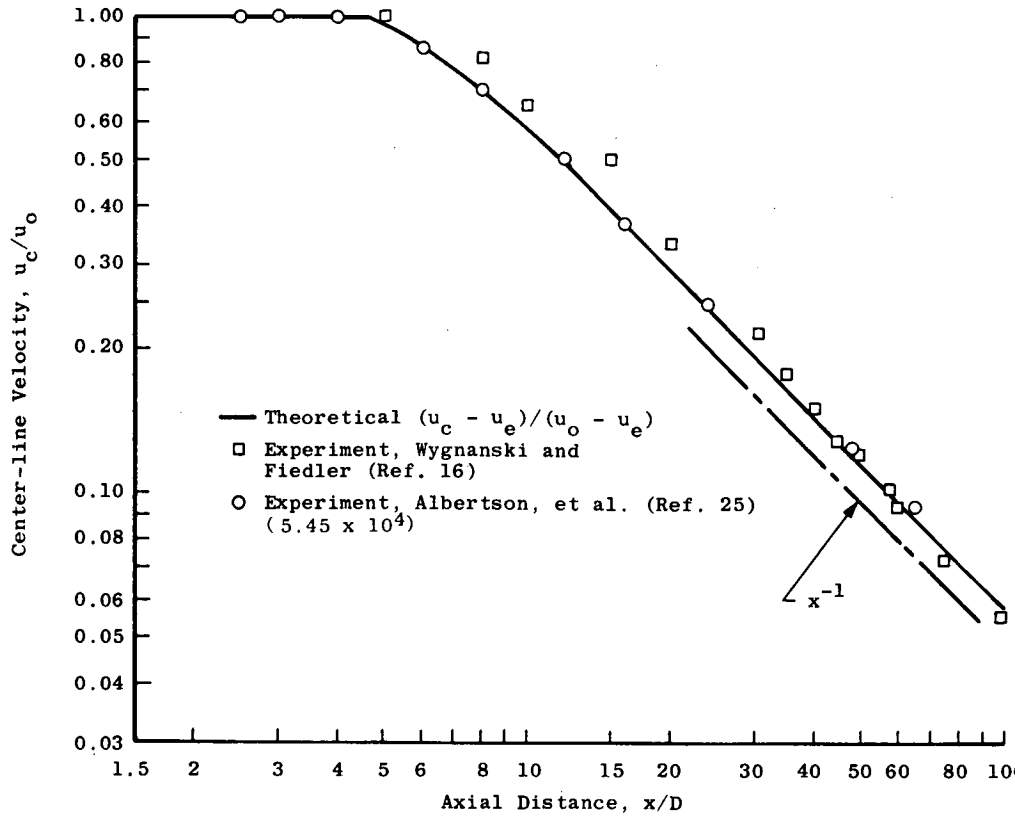

(a) Variation of u_c/u_o with x/D.

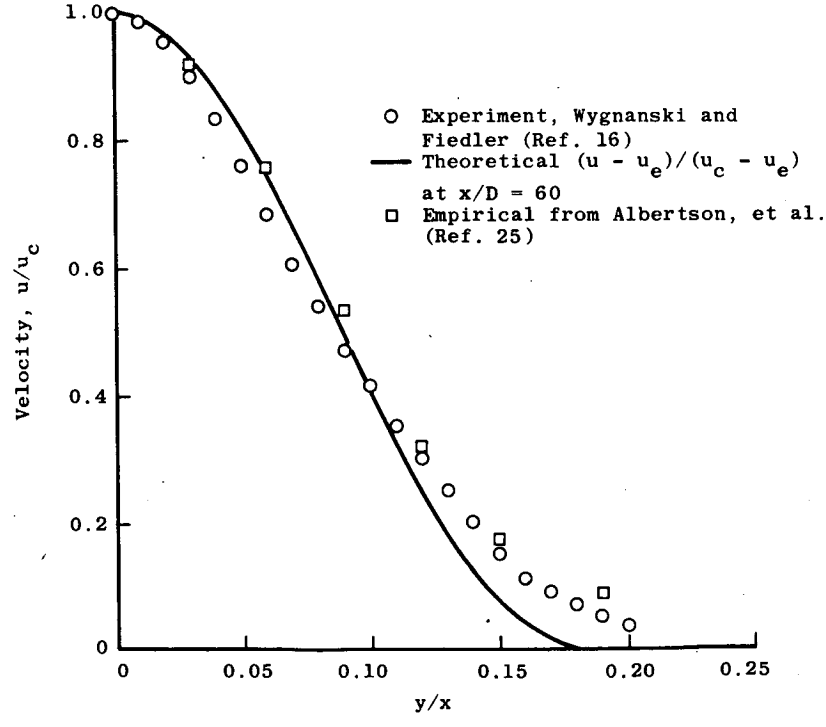

(b) Velocity profile.

Figure 21.- Test case 18 – Fully developed axisymmetric jet into still air.

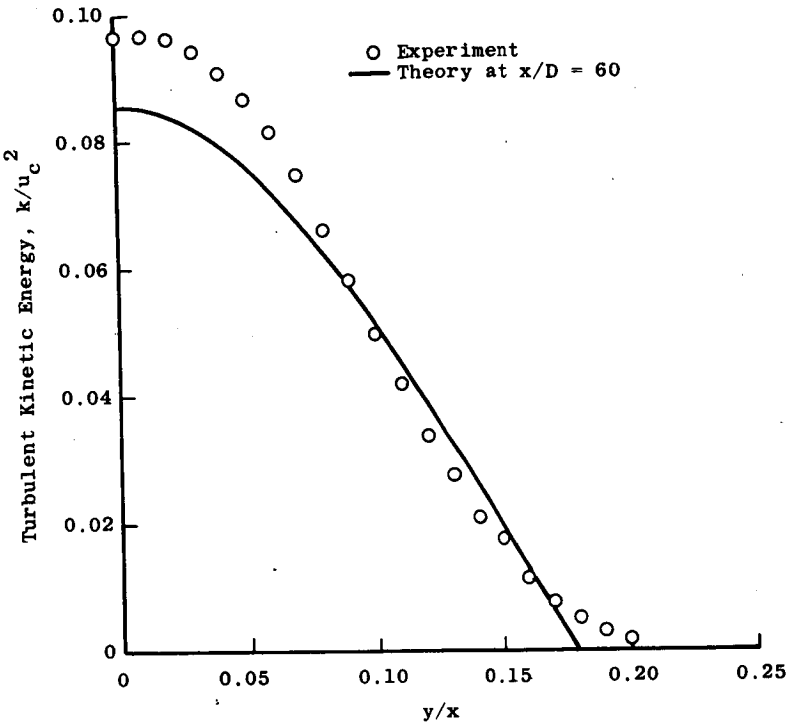

(c) Turbulent kinetic energy profile.

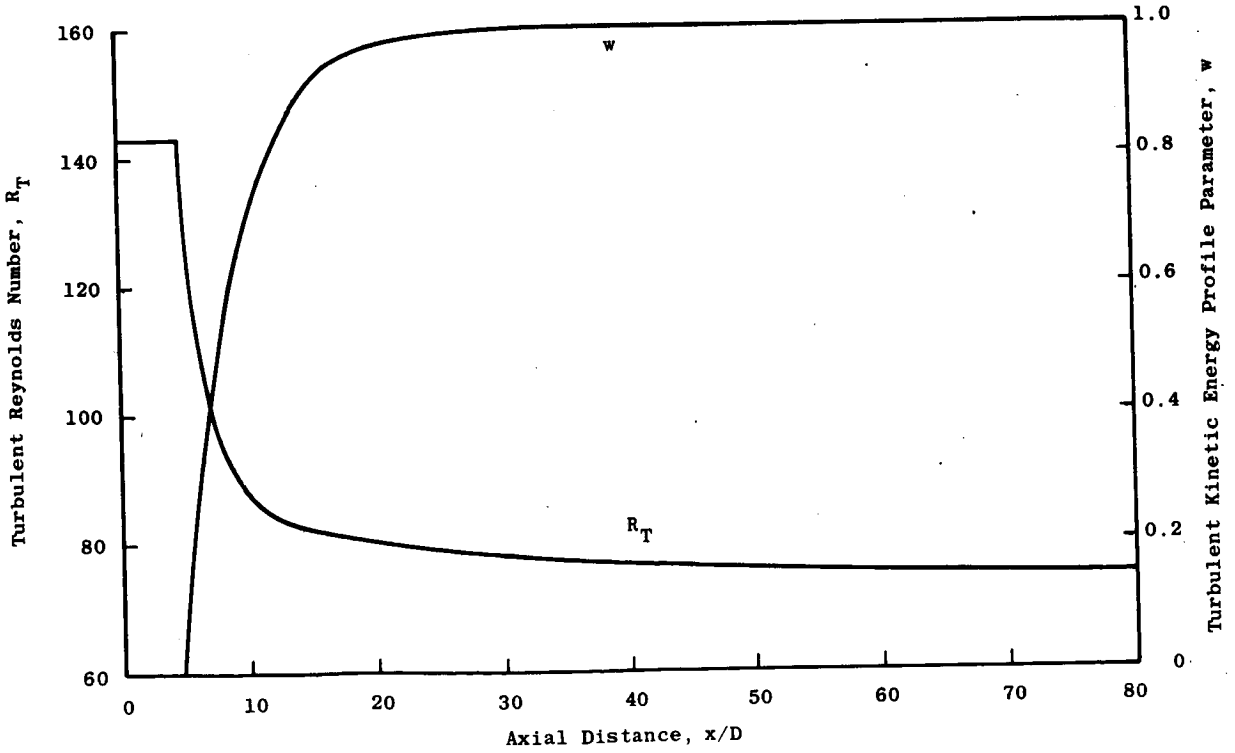

(d) Variation of R_T and w with x/D.

Figure 21.- Concluded.

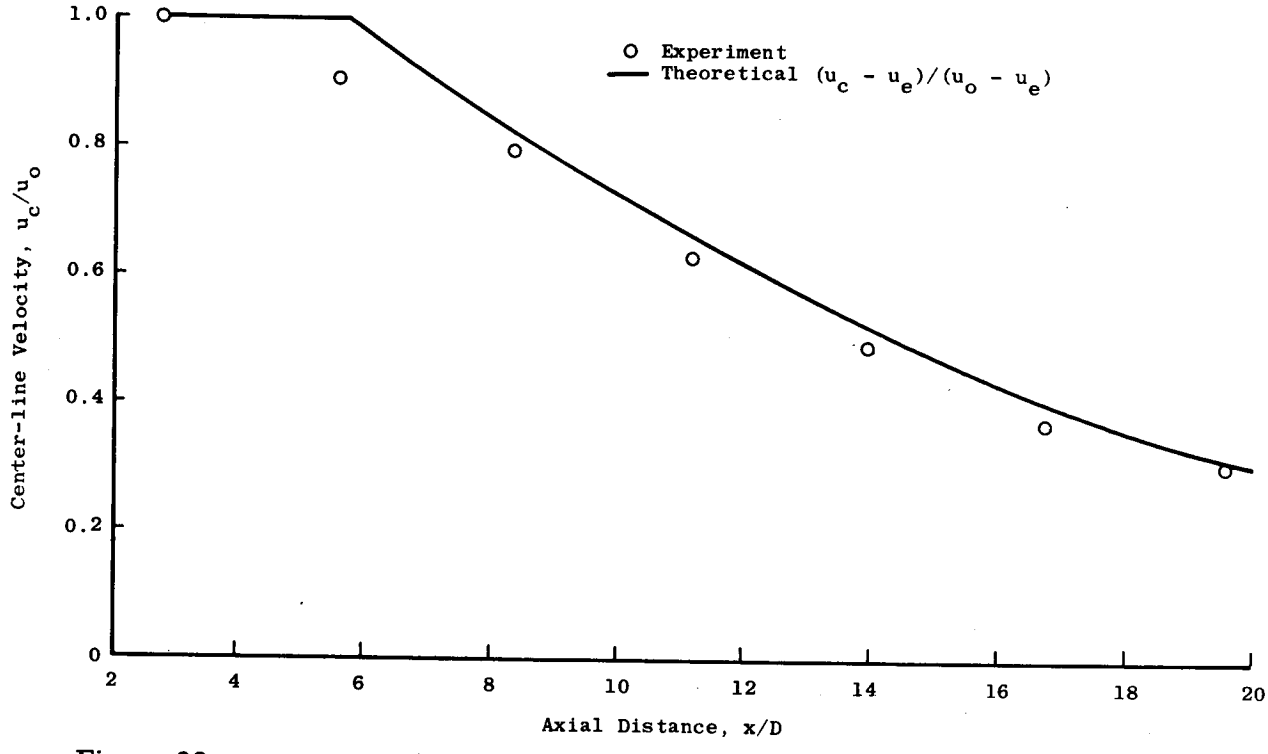

Figure 22.- Test case 19 – Heated axisymmetric jet into still air. $M_o = 1.36$.

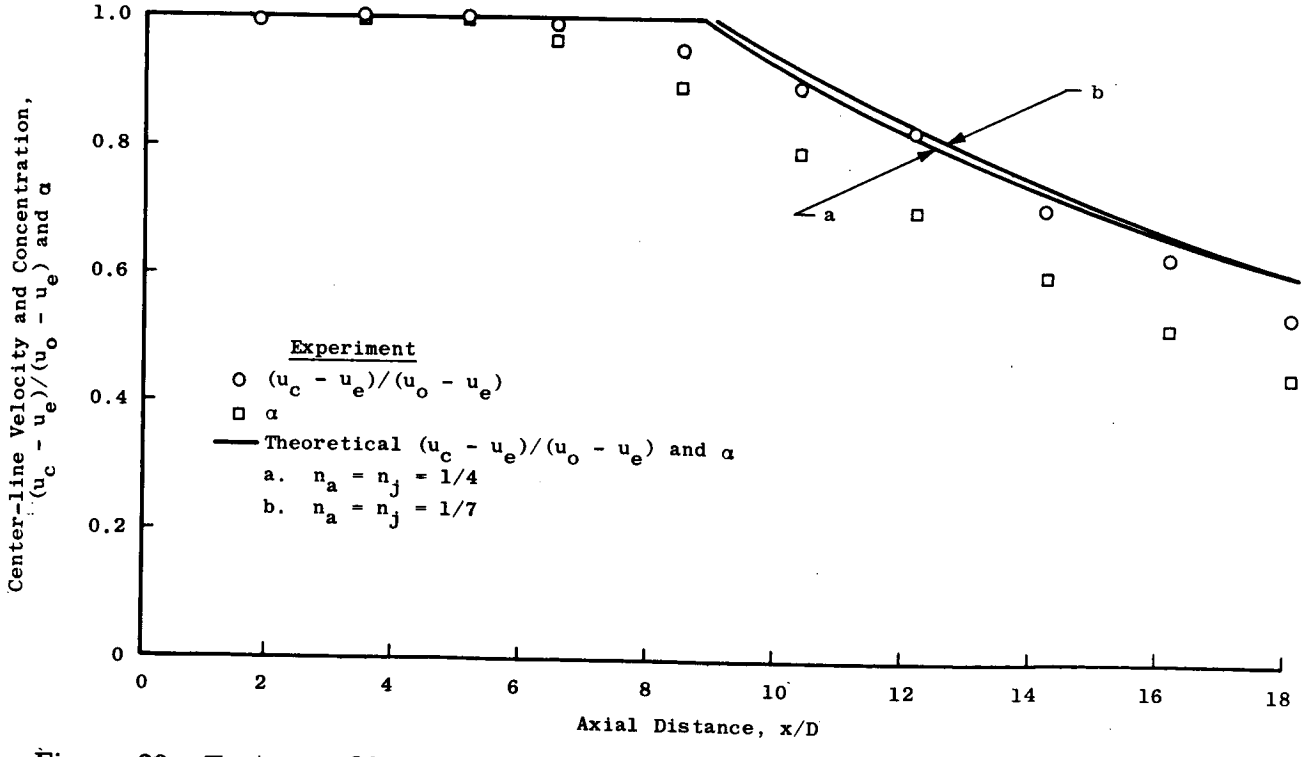

Figure 23.- Test case 20 – Paulk axisymmetric jet in moving stream. $u_e/u_o = 0.48$.

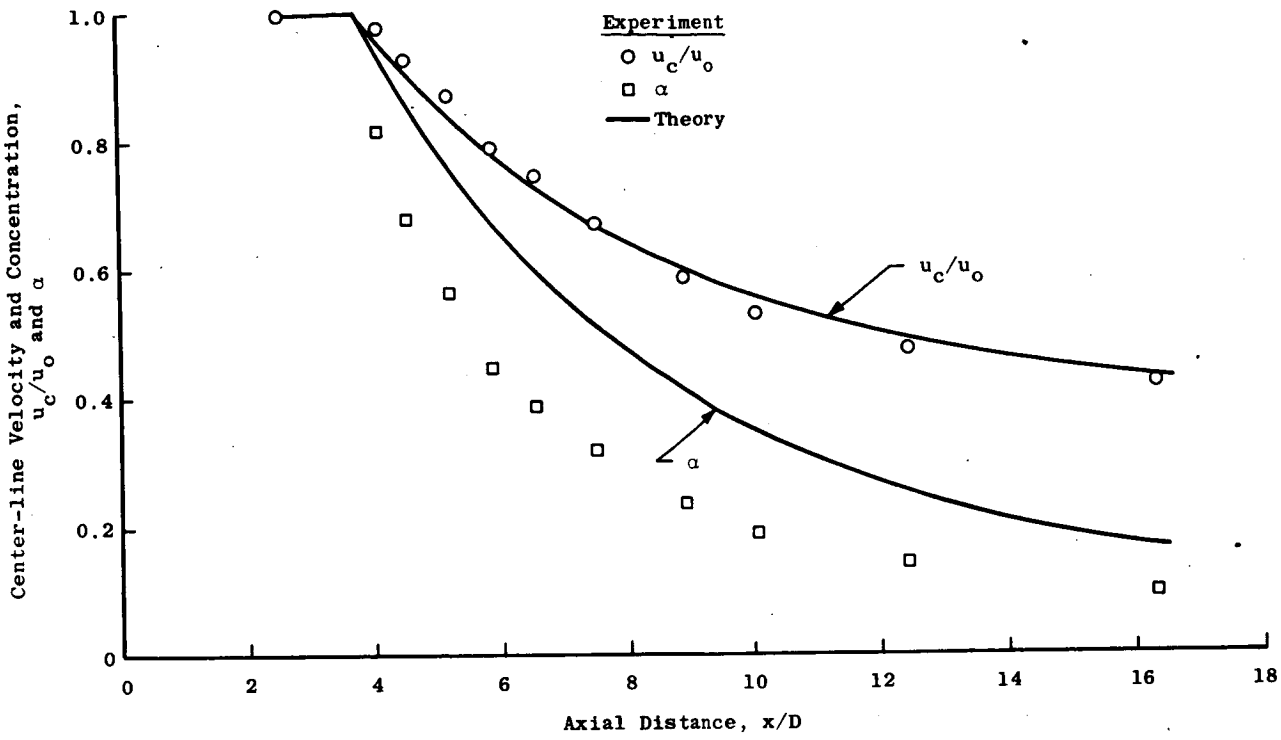

(a) Computations started at x/D = 2.575.

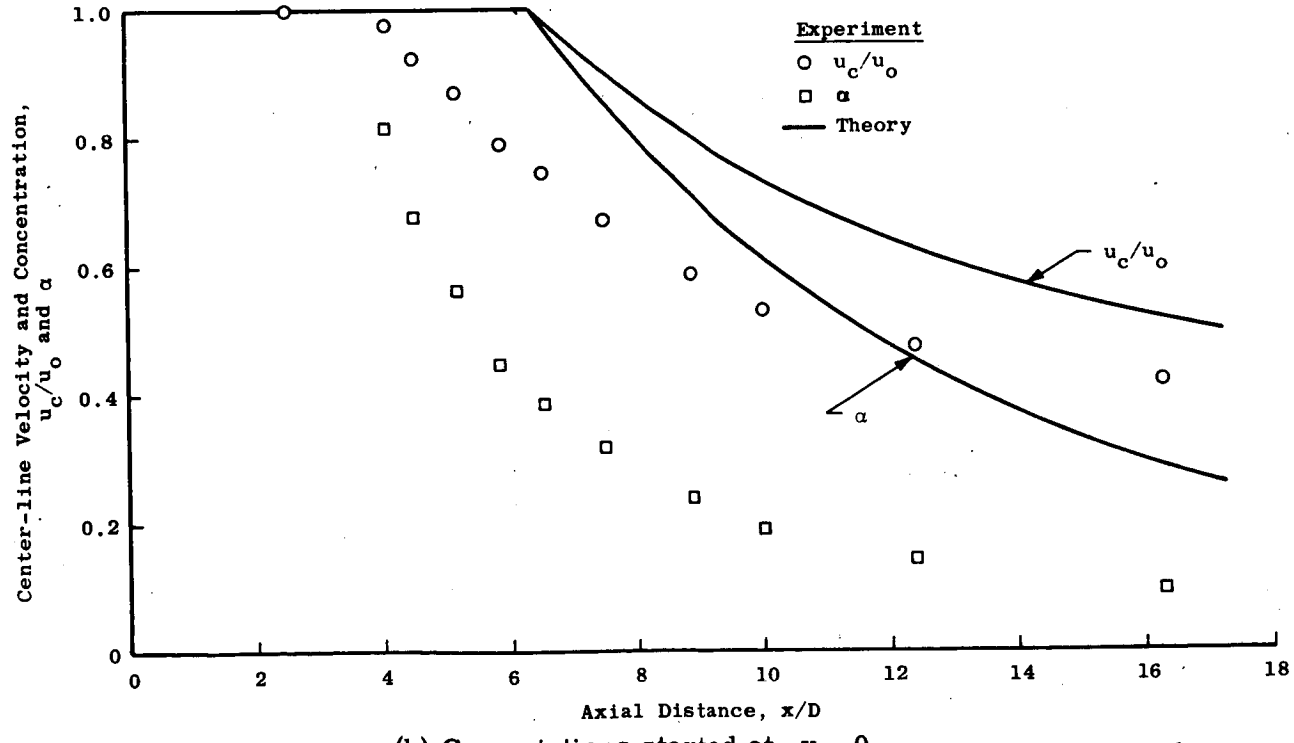

(b) Computations started at x = 0.

Figure 24.- Test case 21 – Chriss H_2 jet in moving stream. $u_e/u_o = 0.31$.

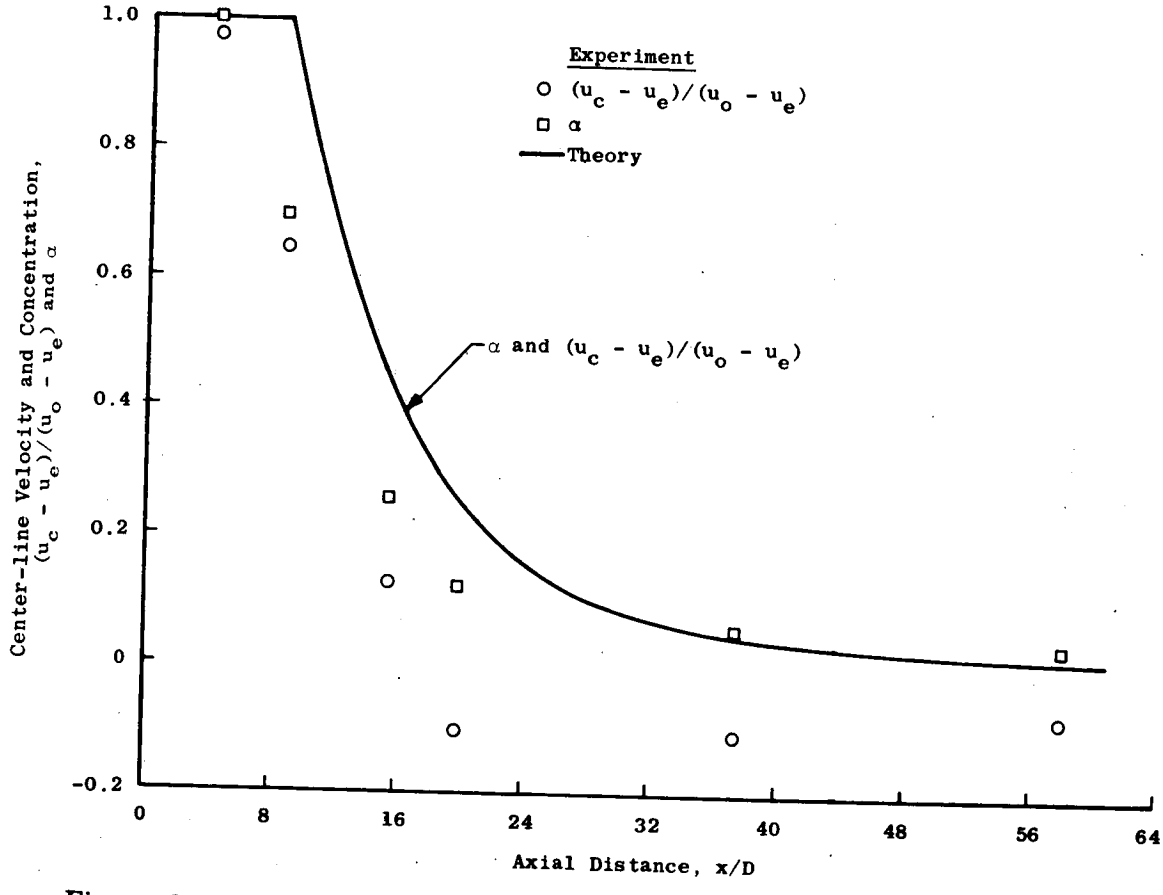

Figure 25.- Test case 22 – Eggers H_2 jet in moving stream. $M_e = 2.5$.

DISCUSSION

S. W. Zelazny: You assume that the Schmidt number was unity in your analysis. Wouldn't it be a simple exercise to remove that restriction by introducing an additional equation?

C.E. Peters: Yes sir, we plan to do that. It's a little frustrating because obviously I have access to Tom Harsha, who sits 15 feet away, and for those flows where I'm interested in a nonfully developed case or nonunity Schmidt number I can always use the finite-difference results. But there are certain flows that I can handle with the integral method we can't handle yet with the finite-difference method. So I will probably go ahead and try to do something to approximately handle nonunity Schmidt number.

S. C. Lee: You mentioned this method you have has some advantage over finite-difference schemes.

C. E. Peters: I didn't refer to it as an advantage, I called it a difference. It's a different set of approximations. Instead of assuming an a_1 function we just assume that the turbulent kinetic energy profile shapes are invariant as a different approach.

S. C. Lee: Perhaps you could summarize for us what would be the difference between this method and the finite-difference method as Harsha presented it.

C. E. Peters: The point is that my kinetic-energy profiles are universal in the given position in terms x/x_{core}. Because of the variable-density and variable-velocity ratio, the shear profile varies from flow to flow; that is, the normalized shape of the shear profile. Therefore, a_1 varies in shape from flow to flow, a condition implied through the whole analysis. I backed it out for some flows, and it does vary from flow to flow. So it's an alternate approximation to saying something about a_1. That's the only fundamental difference. Tom and I are using essentially the same dissipation, and, of course, in return for my specifying the profile shape of kinetic energy, I don't have to say anything about diffusion.

M. V. Morkovin: I think this is another case where we can benefit from the comparisons of different methods. Could you tell us something about your general experience, when you prefer to use Harsha's method to yours and how much more complex it is. I gather you do have some problems in sensitivity to initial conditions. If you could give us a little bit of briefing on that, I think it would be highly valuable.

C. E. Peters: I'll give you my experience first and Tom can comment on it if he likes. The implication of my being able to use a fully developed initial shear stress up to a velocity ratio of 0.25 merely says that these flows are strong shear flows, and they wipe out any small inaccuracies in the initial condition fairly quickly. So that seems to be a viable procedure. When the flows become wake-like in nature, of course, the initial conditions persist indefinitely; in that case my analysis is not applicable at all. For example,

if the hole never fills up, it's not useful. So I limit it to a velocity ratio of maybe 0.7 or 0.8 as the upper limit. I haven't tried to define carefully an upper limit here. Certainly, the finite-difference method is much more powerful in a sense of handling nonsimilar initial conditions and so forth. It's interesting to note the sort of generalized information one can back out with an alternate set of assumptions. For example, about a_1 profiles. So in addition to the practical requirement that we have a better transport model for our "nuts and bolts" engineering calculation schemes, we are also interested in some of the implications in general.

Anon.: Which costs more?

C. E. Peters: This is embarrassing for me because Harsha's program runs faster. But one of the reasons is that this program is a mess; it does lots of different things. This regime is far beyond what we were talking about in this particular calculation. We even do circulating flows with them by using patched up techniques. So the program is not optimized for this kind of flow. If we build a constant-pressure version, I am sure we can get our run time down perhaps an order of magnitude.

I. E. Alber: Your calculation of the spreading parameter variation with Mach number for the two-dimensional shear layer shows quite an increase in the variation of sigma with M. That is your figure 10. Now in this same calculation by Harsha, which I believe is a very similar model to yours, he shows hardly any variation at all.

C. E. Peters: We can't explain that – it's different. Tom, would you care to comment?

P. T. Harsha: Well, the only comment I could make really is that with shear layers I was forced to use an almost patently ridiculous a_1 model which Peters does not have to use because his a_1 comes out of shear stress profile and kinetic energy profiles. I would suspect that the problem is that the a_1 model that I used is simply inappropriate for the shear layer.

J. M. Eggers: I was wondering if you or anyone else here could comment on what we could do to improve the modeling in the transition region to get rid of this somewhat atrocious inflection point at the end of the core region.

C. E. Peters: The sharp corner on the center-line velocity distribution is characteristic of integral methods, at least as we have put them together. It doesn't bother me very much because most of the required information is not centered in that particular region, but the finite difference smooths it out. That's the idea of patching together two regimes discontinuously. It's bound to give a sharp corner with an integral method without some relaxation of profile shapes locally or something.

D. B. Spalding: I have a question and a comment about R_T. The question is a simple one – in the paper R_T seems to be defined twice, once it has the difference between

u_c and u_a on the top and in the second it has the square of those. Which of those was actually used?

C. E. Peters: I think the difference comes because when you plug in the midpoint velocity profile slopes, it is in terms of delta u over width and I think that's where it comes from.

D. B. Spalding: The other remark I want to make is that this quantity appears to be related to the ratio of the production term to the dissipation term which Rodi found also to be significant, and it will be interesting when we have time just to compare whether there was a quantitative connection between your function of R_T and our function of production over dissipation.

C. E. Peters: Yes, I certainly agree. We haven't had time to give much thought as to what this R_T function means in terms of structure, but it would be nice if we could at least rationalize, in terms of energy spectrum or whatever, why the length scale changes or the R_T changes the effective dissipation.

D. B. Spalding: At least you can see that with your definition, when u_c equals u_a, there will be no shear stress, so production is zero. And so R_T is zero; it's the same as $R_{p/\epsilon}$ is equal to zero. Even closer quantitative connections are being worked out.

C. E. Peters: It was also interesting for me to read in Joe Schetz's written version that the constant in his eddy-viscosity model perhaps should be related to a similar parameter to this – the ratio of U prime over delta U. So, this parameter is obviously developed by mean flow correlations during the near field of the wire and jet series, and I just stumbled across it. I think it is better than a mean flow parameter, such as Mach number or some density parameter, and I think it is related to the turbulent structure.

S. Corrsin: I was interested in R_T because the numbers look so much larger than the ones I computed 15 years ago.* Did you compute it for a wake also?

C. E. Peters: Yes, it was shown in the paper I think on the Chevray case. Remember my length scale is the full width of the shear layer; that is, from the centerline out to the outer edge.

S. Corrsin: Well, I was just looking at my paper from 1957 in which is used the half-width and the full-velocity difference. I got a value of 12 for Townsend's wake.

C. E. Peters: I didn't do the two-dimensional wake.

S. Corrsin: And for the round jet, I defined it in terms of the momentum diameter and it came out to be 15.

---

*Corrsin, S.: Some Current Problems in Turbulent Shear Flows. Symposium on Naval Hydrodynamics (Washington, D.C.), Sept. 24-28, 1956, pp. 373-400.

C.E. Peters: My number of 75 for the asymptotic value for the fully developed jet is consistent, considering the difference in length scale definition, with the number tabulated experimentally by B. G. Newman.

S. Corrsin: By whom?

C. E. Peters: Newman, in his survey paper a few years ago. So I think it is consistent with other quoted information.

S. Corrsin: I can make a physical comment about this concept. I first heard it suggested back in the early 1940's by Hans Liepmann, who proposed the idea that perhaps turbulent shear flows tend to keep themselves in a state of lower critical Reynolds number based on the turbulent viscosity, and it's a sort of self-destroying system that always disturbs itself violently. That was sort of the reason that I computed these. For bounded flows, they seem to vary more, but the general idea was that for shear flows without boundaries there are probably universal constants for each geometry.

OPEN FORUM

A. Roshko: I'd like to tell you about some experiments on turbulent free shear layers in pressure gradients that we've been able to do. I know that Stan Birch said yesterday that effects of pressure gradient are not included in this conference, but maybe it will give us something to think about for the next conference. Actually I probably ought to be talking about the older results (with no pressure gradient) since many of you probably haven't seen them or did not hear Garry Brown's talk[1] in London last fall. Furthermore, I realize that there is considerable skepticism about them, particularly about the large vortex structures which we see (fig. 1). We were a little startled ourselves when we saw them in our first pictures but are now convinced that they are quite real and are basically two dimensional, with a scale that increases on the average with x. One thing I'd like to mention is that in the recent measurements of Spencer and Jones,[2] they find a definite spectral peak in their turbulent shear layers (in homogeneous flow). Using the average vortex spacing at any point from our pictures (actually movies) and assuming that they are convected with average speed $\frac{1}{2}(U_1 + U_2)$, we calculate a dimensionless frequency $n_o x/U_1 = 1.7$ as compared with 2.1 from the Spencer and Jones data at $U_2/U_1 = 0.3$. (Our case is for $U_2/U_1 = 0.38$ and $\rho_2/\rho_1 = 7$.) Thus, we feel that the spectral peak measured by Spencer and Jones corresponds to the passage of the vortex structures we see in our pictures.

Another thing that has worried people about the experiments is the effect of the channel walls. These are used to set the pressure gradient and, for the case we are discussing right now, they were set for uniform pressure along the flow. Now we also wondered about the effect of the fairly close proximity of the walls, and so we made some measurements on turbulent shear layers in homogeneous flow. The results agreed fairly well with those of other investigators on homogeneous flows.

Now, for the case of a mixing layer in pressure gradient, here's the setup (fig. 2). ρ_1 and ρ_2 do not vary with x. Similarly U_1 and U_2 are constants in the case of zero pressure gradient. But if the pressure gradient is not zero then U_1 and U_2 are functions of x. Bernoulli's equation shows that if we try to maintain U_2/U_1 the

---

[1]Brown, Garry; and Roshko, Anatol: The Effect of Density Difference on the Turbulent Mixing Layer. Turbulent Shear Flows, AGARD-CP-93, Jan. 1972, pp. 23-1 – 23-12.

[2]Spencer, Bruce Walton: Statistical Investigation of Turbulent Velocity and Pressure Fields in a Two-Stream Mixing Layer. Ph. D. Thesis, Univ. of Illinois, 1970.

Spencer, B. W.; and Jones, B. G.: Statistical Investigation of Pressure and Velocity Fields in the Turbulent Two-Stream Mixing Layer. AIAA Paper No. 71-613, June 1971.

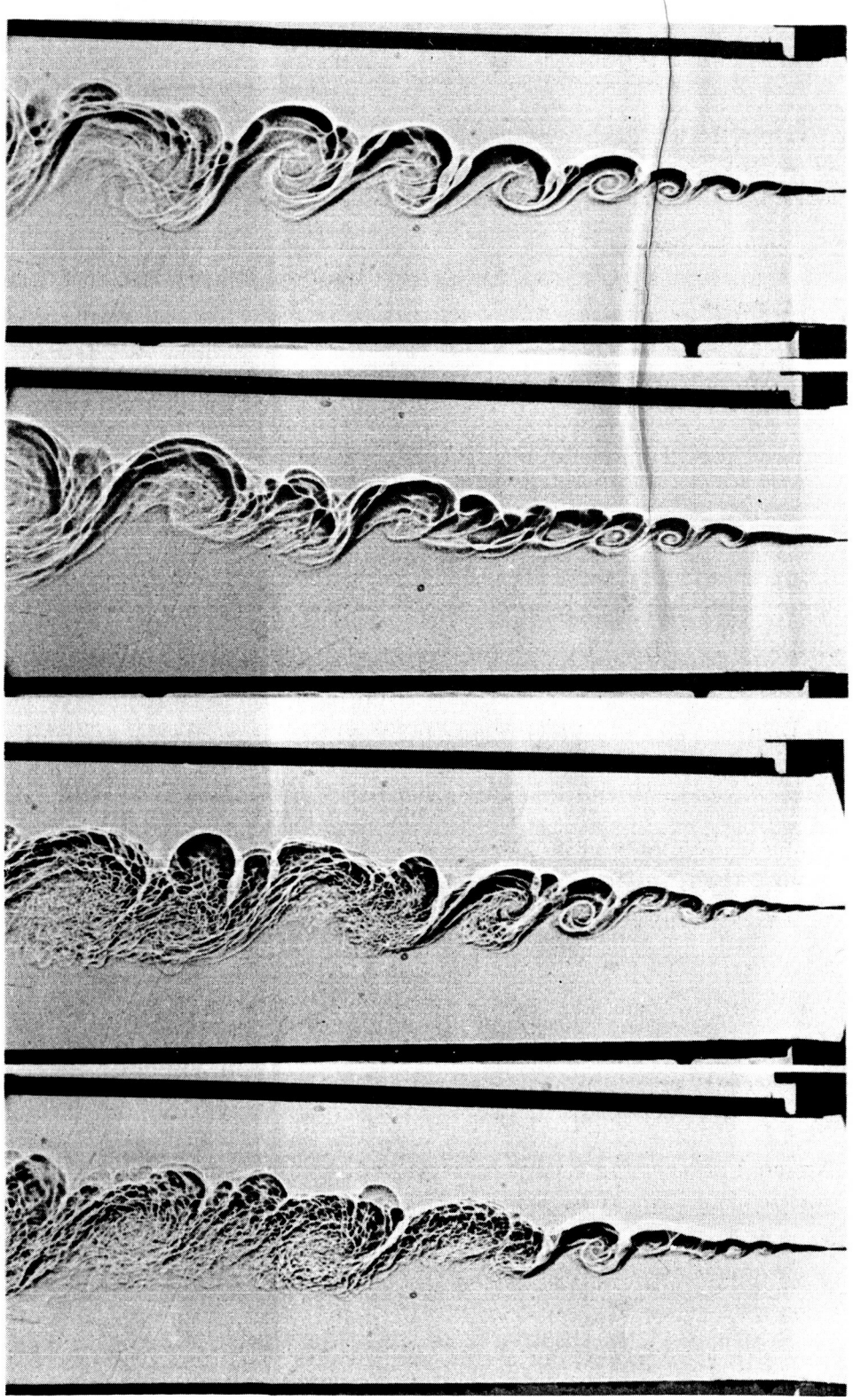

Figure 1

Effect of dU_1/dx

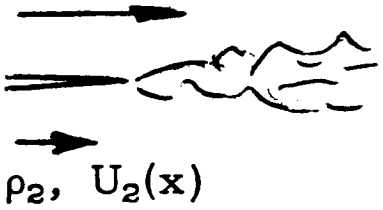

Similarity in y/x if

(a) $\rho_1 U_1^2 = \rho_2 U_2^2$

(b) $\frac{x}{U_1}\frac{dU_1}{dx} = \frac{x}{U_2}\frac{dU_2}{dx} \equiv \alpha = \text{const.}$

Experiment for $\alpha = -0.18$

Figure 2

same at all x, then, in general, the pressure will not develop the same way on both sides of the layer. But, for one particular case, namely $\rho_2 U_2^2 = \rho_1 U_1^2$, the pressure p(x) will be the same on both sides. For that one particular case, you might hope to get an equilibrium or similarity shear layer even in a pressure gradient.

Well, if you play with this idea, you find that, if the parameter $\alpha = \frac{x}{U_1}\frac{dU_1}{dx} = \frac{x}{U_2}\frac{dU_2}{dx}$, the Falkner Skan parameter, is a constant, then you would expect to have an equilibrium shear layer. It will still spread linearly but not necessarily at the same rate as for $\alpha = 0$ where y/x is still the similarity coordinate.

To set up these flows in our apparatus we had to diverge the walls (for adverse pressure gradients) and put slots in them to allow outflow helped by some resistance added at the channel exit. One of our graduate students, M. Rebollo, did the experiments. It took some adjusting and playing around but we think we produced an equilibrium flow and I'd like to show you those results.

Figure 3 shows, for comparison, a profile of dynamic pressure for the case $\rho_2 U_2^2 = \rho_1 U_1^2$ and with $\alpha = 0$. Here similarity is shown by the fact that the points all fall on one curve when plotted against $\eta = y/(x - x_o)$. Values of x were 2 to 3 inches and x_o was about -0.20 inch. This is a stronger test of similarity than one can get from velocity profiles or density profiles, since here we have points of maximum and minimum that all have to be the same for every value of x. Keep in mind the horizontal scale; it is a measure of the spreading angle; you see that the layer extends over a width of about 0.2 in y/x. Also noted is the location of the dividing streamline η_o.

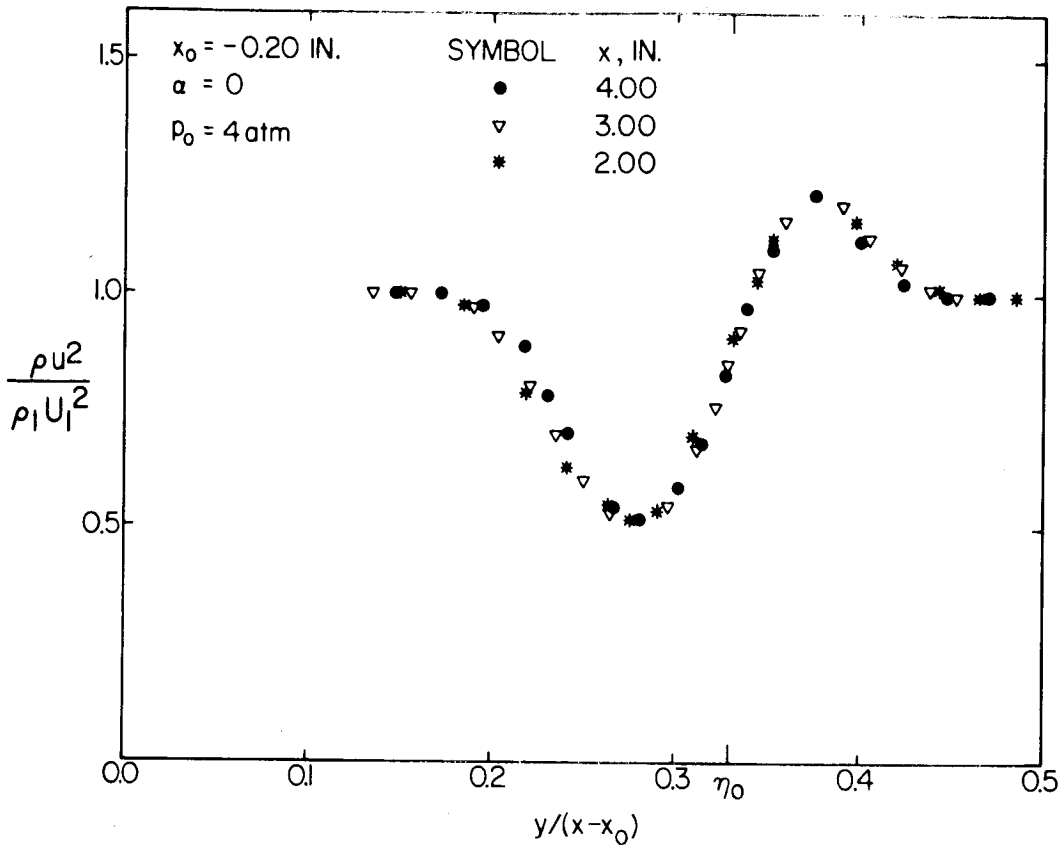

Figure 3

The next figure (fig. 4) shows the corresponding result for an adverse pressure gradient with $\alpha = -0.18$. First of all, you see that there's a tremendous effect on the spreading angle – it's just about doubled (the scale is the same as before). There's also a larger dip at the minimum. If you had a more adverse pressure gradient, you'd reach zero velocity at the minimum and would be tending to flow reversal in this part of the shear layer.

One of the better tests for existence of similarity or equilibrium is that the turbulence structure shows similarity, and we've recently begun to make measurements of this. We are able to measure the fluctuating density, or concentration, in the flow, using the probe developed by Brown and Rebollo.[3] The root mean square of the concentration fluctuation does tend to fall on one similarity curve, indicating equilibrium. Shown in figure 5 is the case for $\alpha = -0.18$ compared with that for $\alpha = 0$. Again you see the large change in the width of the layer.

---

[3]Brown, G. L.; and Rebollo, M. R.: A Small, Fast-Response Probe To Measure Composition of a Binary Gas Mixture. AIAA J., vol. 10, no. 5, May 1972, pp. 649-652.

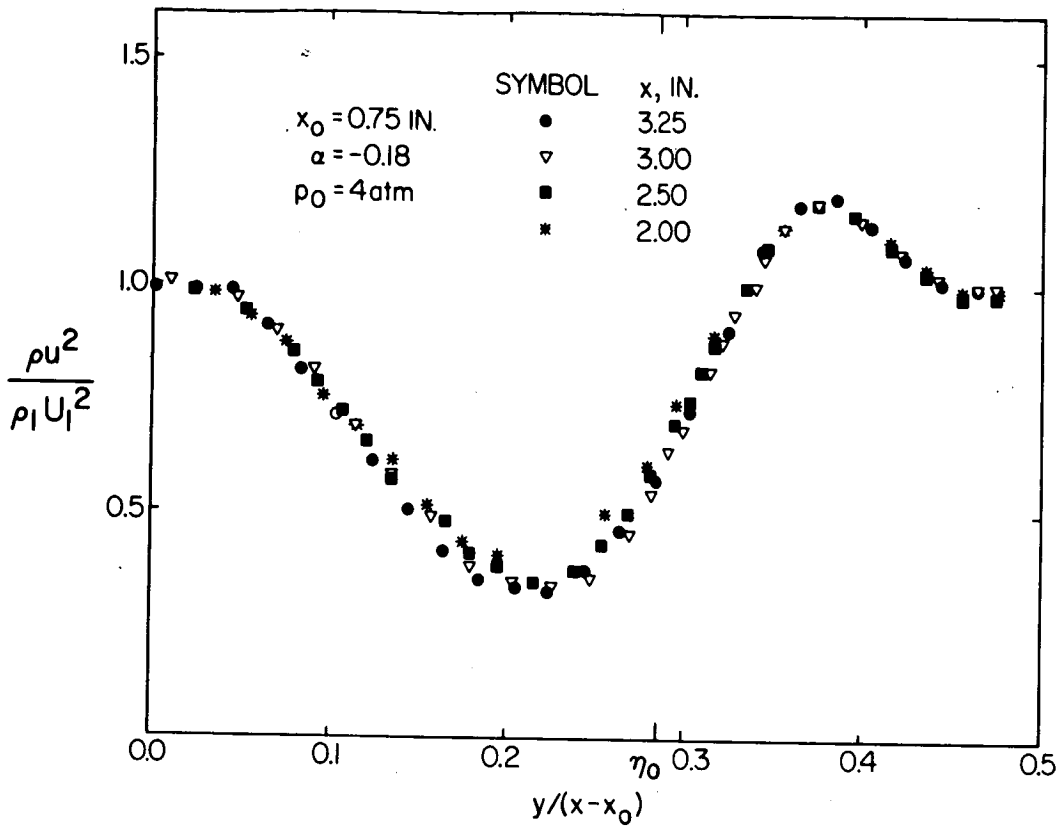

Figure 4

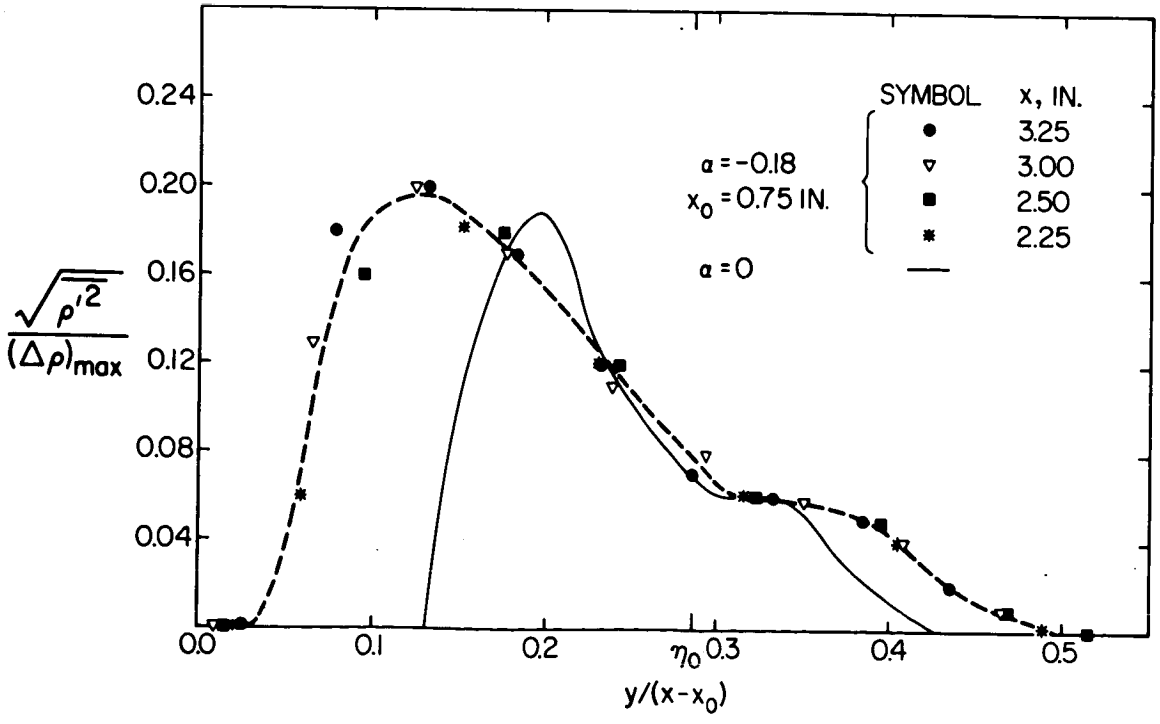

Figure 5

From the measurements of the mean density profile and the mean velocity profile, you can compute the shearing stress distribution; in figure 6 is a comparison of this for $\alpha = 0$ and $\alpha = -0.18$. There is quite a difference in the maximum shear stress.

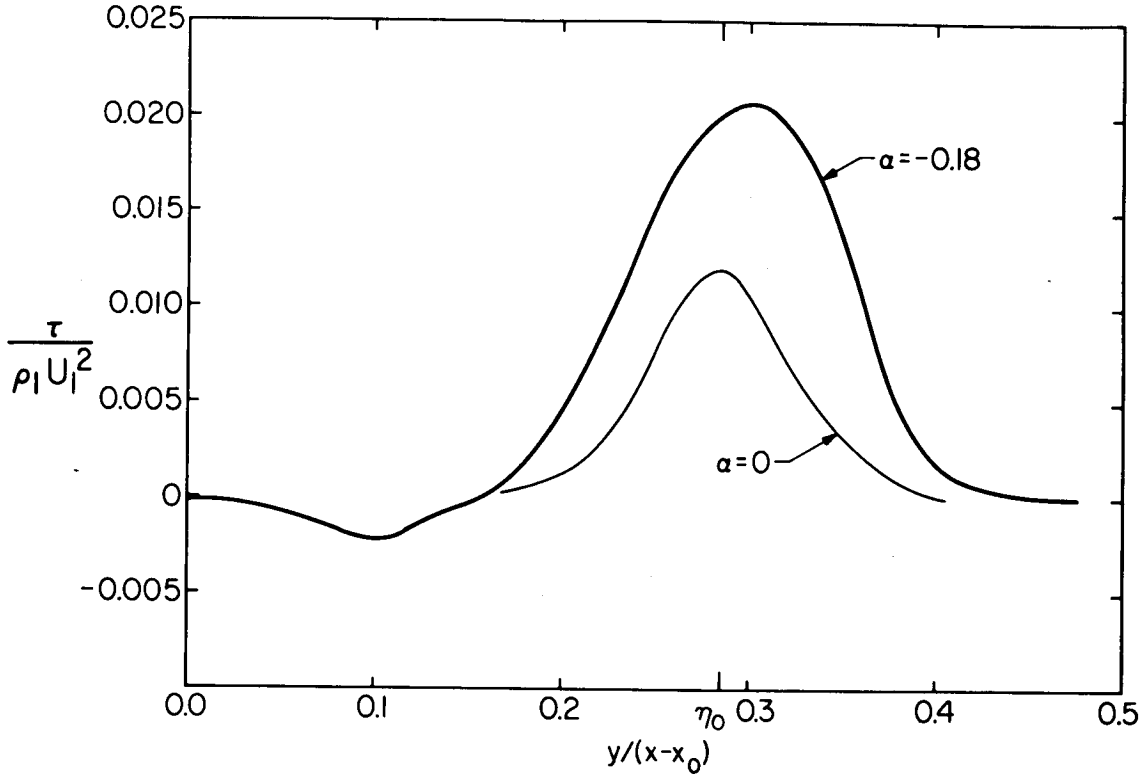

Figure 6

The next figure (fig. 7) shows the same comparison for the turbulent mass diffusion $\overline{\rho' v'}$. There is not a great difference in the maximum for the two cases.

The last figure (fig. 8 on p. 636) is a summary of some of the parameters that can be computed from the mean profiles. For example, the maximum shear stresses and mass diffusions are shown. If you use the measured and computed profiles to infer eddy viscosities and diffusivities you find the results shown here. (The asterisk indicates values on the dividing streamline.) The eddy viscosity, normalized with x, is much larger for the case $\alpha = -0.18$. Even if normalized with δ (which itself is larger in the adverse gradient), it still is about 50 percent larger than for $\alpha = 0$. The eddy diffusivity normalized with x is not much changed. But, most interesting, the turbulent Schmidt numbers here are nothing like what we've been hearing about today or at any other time that I know about. They are down at around 0.2 and 0.3 rather than about 0.8 to 1.

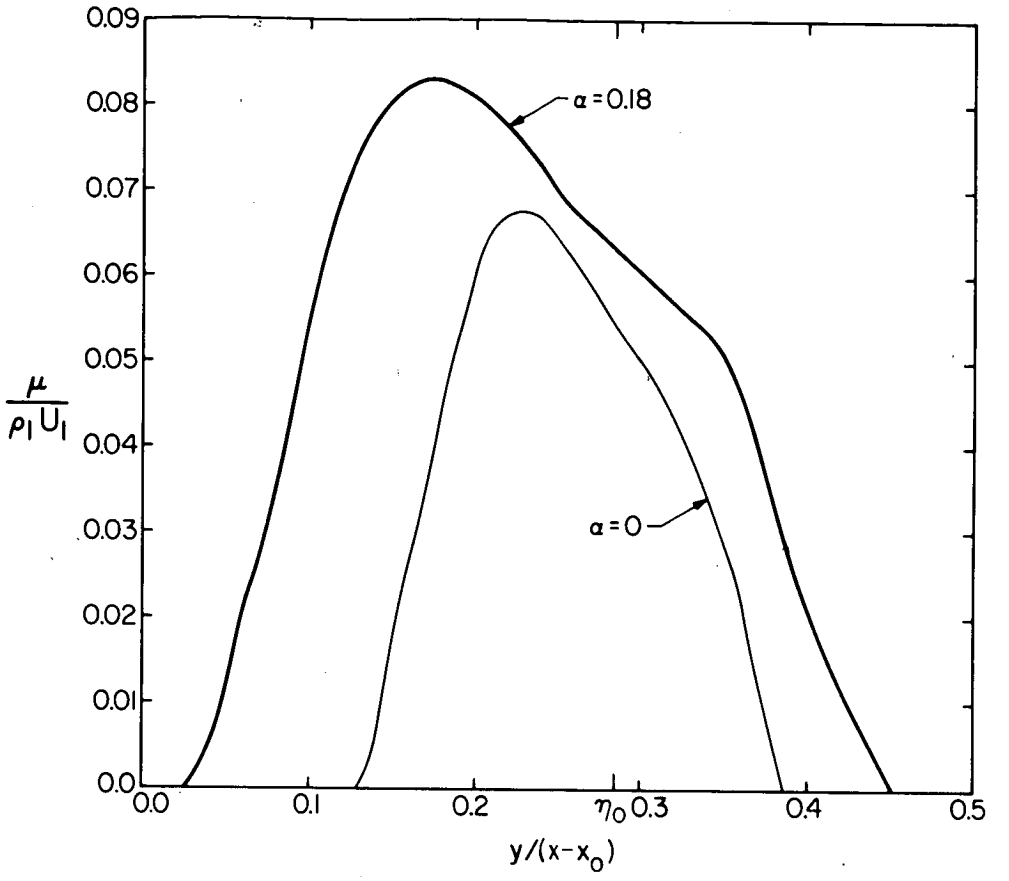

Figure 7

In closing, I'd like to say that Dr. Garry Brown was very much involved in this work until he left for Australia a year ago, Mr. Manuel Rebollo made most of the measurements you have seen today, and the research is sponsored by the Office of Naval Research.

P. A. Libby: Does that mean that the concentration profiles and the velocity profiles are not related according to the Crocco relation?

A. Roshko: Yes, I think so. I think that when you have this tremendous density difference which is continually maintained, the physics is rather different from where you have a small concentration that is passively floating around. I think all the ideas about Schmidt numbers near 1 come from cases where the contamination is rather small – that is, that there is not a large density difference or concentration difference.

I. E. Alber: I'll just ask you the question that I asked you before in private for the whole audience to comment on. Do you expect that you would get the same structure in the shear layer if you had an initial turbulent boundary layer ahead of the separation point, compared with the case which you ran where you had laminar initial boundary layer?

	$U_1/U_2 = \sqrt{7}$	$\rho_1/\rho_2 = 1/7$
$\frac{x}{U_1}\frac{dU_1}{dx} = \alpha$	0	- 0.18
u^*/U_1	.70	.59
ρ^*/ρ_1	1.78	1.70
$(\rho u^2/\rho_1 U_1^2)_{min}$	0.52	0.32
$(\rho u^2/\rho_1 U_1^2)_{max}$	1.22	1.20
$\sqrt{\overline{\rho'^2_m}}/(\rho_2 - \rho_1)$	0.19	0.20
$\tau_m/\rho_1 U_1^2$	0.012	0.021
$\mu_m/\rho_1 U_1$	0.068	0.082
$\frac{\nu_{t*}}{(U_1 - U_2)x}$	0.0016	0.0040
$\frac{\delta_{t*}}{(U_1 - U_2)x}$	0.010	0.012
Sc_t	0.16	0.33

Figure 8

A. Roshko: Well, I really don't know the answer, but I don't think so. Again, my feelings about this relate to some of my ideas that were kicked around here in regard to the stability – that this is really an instability phenomenon. For example, I think that instability in the supersonic layer would be rather different from the instability in the subsonic layer. I think, in fact, it accounts for the difference between the σ in the supersonic and the subsonic cases. I think that supersonic layers are stiffer in some sense than the subsonic ones.

I. E. Alber: But the instability mode would be different depending on the shape of the initial profile. Then you would have a much fuller profile in the turbulent case than the laminar case. You may expect a different response.

A. Roshko: It's not the initial profile that matters, it's the average profile at any point in the developed layer, which has a universal shape. In other words, the instability from any point in the shear layer is determined by the profile at that time. So I don't think that, if I understand you correctly, the initial profiles of the separation points should matter if there is any validity at all to these ideas about mean flow similarity.

V. W. Goldschmidt: There are three things I want to refer to. These are measurements taken related to the problems of (a) upstream effects, (b) similarity, and (c) stability. Figure 1 (from unpublished data) relates to upstream effects. It shows the widening rates of plane free jets (the inverse of σ) on the ordinate. Along the abscissa is shown the turbulence intensity at the mouth of the different jets. These values may be in slight absolute but not relative error. As you see there is an increase in widening rate with upstream turbulence intensity. Shown, just for reference, is where $\sigma = 9$ and 11 would be located.

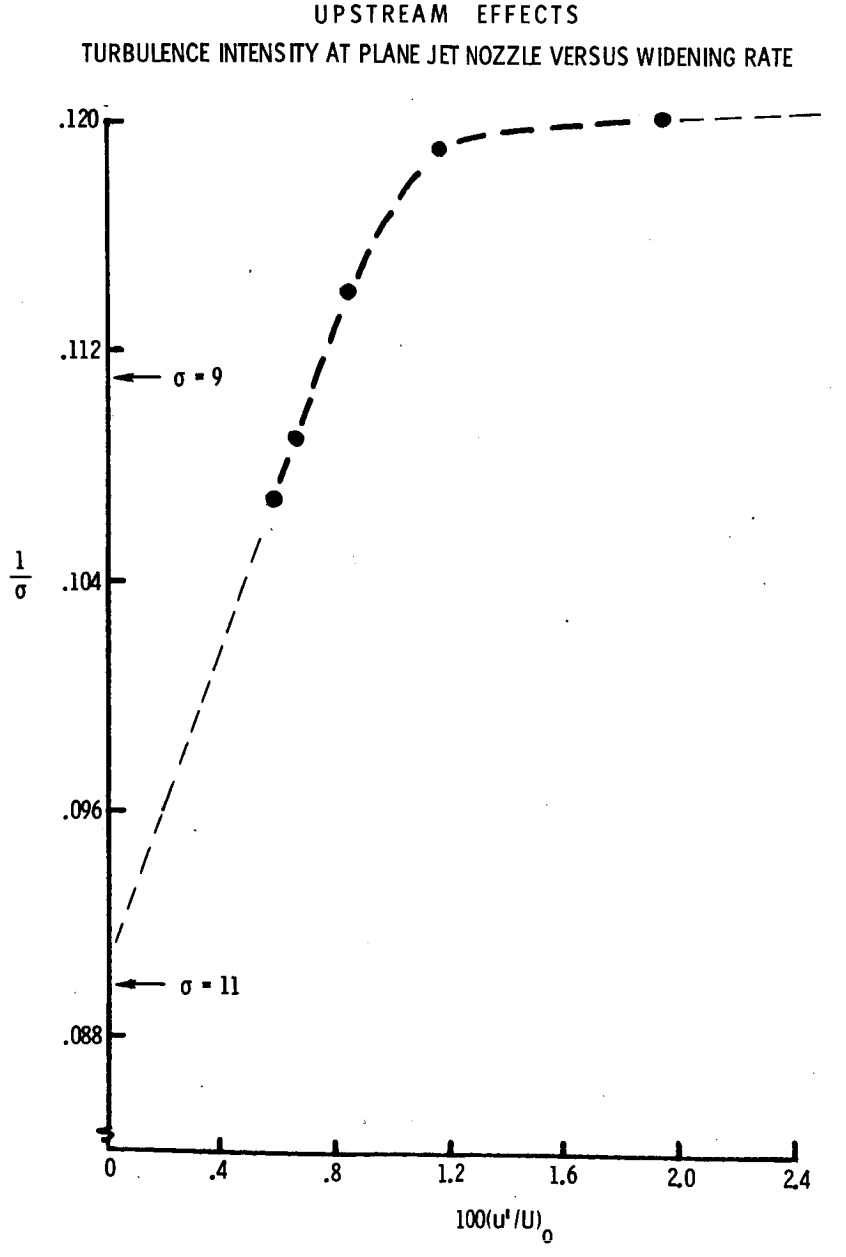

Figure 1

Figure 2 considers the macroscale downstream of a circular jet. The macroscale is on the ordinate, a dimensionless radial coordinate on the abscissa. The three curves are for three different x/d stations. Never do we get them to scale with anything. Although the velocity profiles look similar, the turbulence intensity looks similar, and the Reynolds stresses seem to reach similarity, the macroscales do not. These results were published in the Trans. ASME, Ser. D: J. Basic Eng.[4] Similar results (still unpublished) were

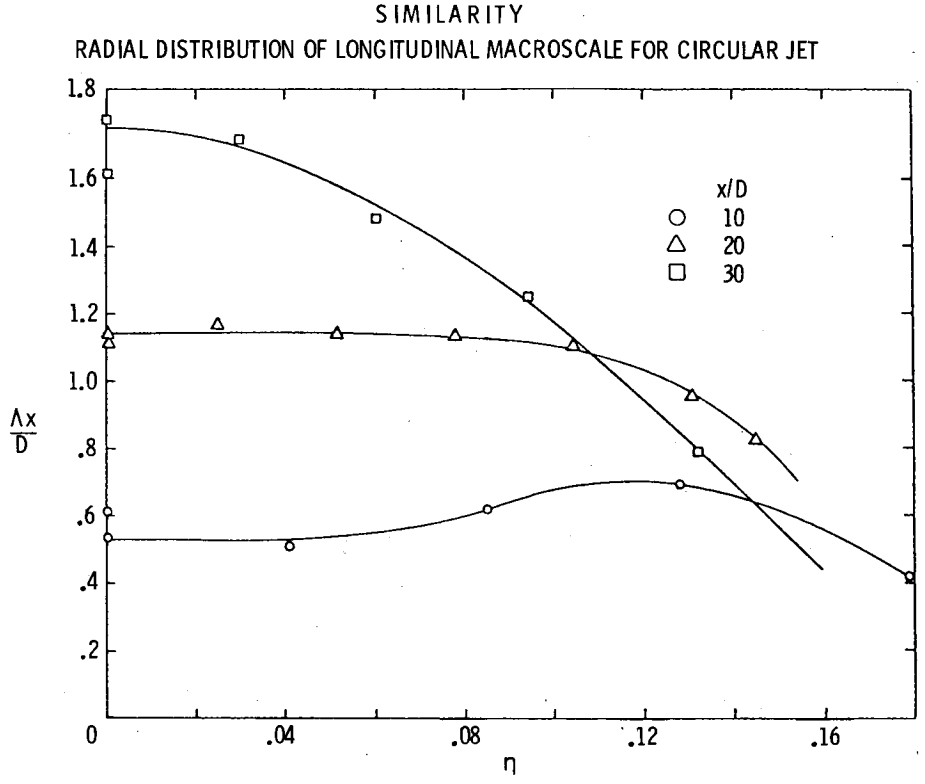

Figure 2

[4]Goldschmidt, V. W.; and Chuang, S. C.: Energy Spectrum and Turbulent Scales in a Circular Water Jet. Trans. ASME, Ser. D: J. Basic Eng., vol. 94, no. 1, Mar. 1972, pp. 22-26.

noted for a plane jet. The problem of some kind of periodicity or stability or something coming in is alluded to in figure 3.[5] Trying to answer the question, "Do jets flap?," two-hot-wire probes were placed on opposite sides of the center of a plane jet. The time cross correlation of these two is shown in the figure. A negative correlation for no time delay on either of the signals ($\tau = 0$) would imply or suggest flapping. The figure shows that there is flapping, and what is interesting is that there is a certain periodicity to this flapping.

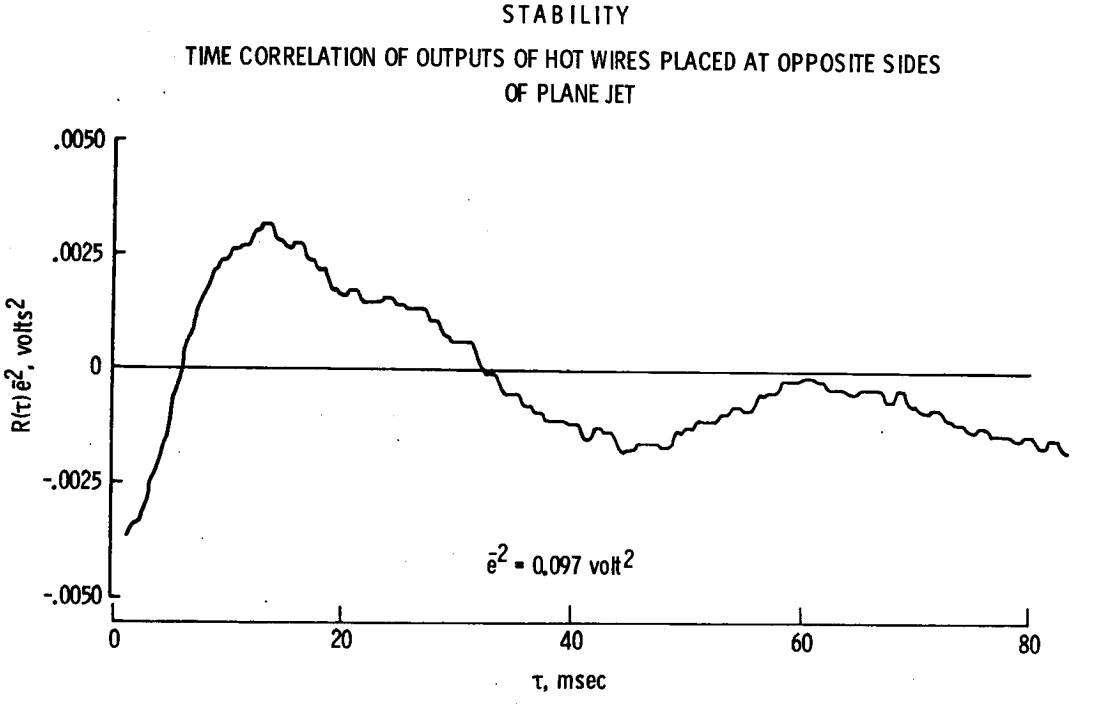

Figure 3

[5]Goldschmidt, V. W.; and Bradshaw, P.: Flapping of a Plane Jet. Phys. Fluids, vol. 16, no. 3, Mar. 1973, pp. 354-355.

V. W. Goldschmidt: I have a question for Jack Herring that we discussed after his presentation, but I think it would be worthwhile to bring it to the group as a whole. My question was whether, as you recall in the model proposed, there was a need for what you call a random force or a random wave mix that regenerates and brings energy back into the flow. The distribution of this random input was made random throughout all wave numbers. My question to him was can this input be made selective over wave numbers and, hence, try to simulate how the turbulent flow gains energy from the mean flow and how dependent would his results be on the distribution of this random input. Did I make this question correct?

J. R. Herring: Yes. It is the same question you asked yesterday. Perhaps I wasn't very clear on this point. What I meant yesterday was that you start by modeling the turbulence "force," the $(V \cdot \Delta V)$ term (the nonlinear terms in the Navier-Stokes equations), as if they were normally distributed multipoint Gaussian. In having made the assumption that the turbulence force could be so modeled, you need no information about the spectral shape because you are going to compute that in a self-consistent way after you have finished constructing the theory. Next, having made the Gaussian assumption, you immediately discover that along with such a random stirring force, in modeling turbulence, you will need an eddy viscosity because random stirring always increases the energy of systems to which it is applied. This eddy viscosity (really a generalized eddy viscosity) is determined by the spectrum of the random stirring force representing the "turbulence force" through the condition of energy conservation. In that case you have a model with no empirical constants and this is Kraichnan's direct interaction approximation.[6] Of course, the discussion here was not a derivation but rather a description of the ingredients of the theory. However, a derivation along these lines has been developed by Phythian.[7]

V. W. Goldschmidt: If I could elaborate on that, the reason for the question is that we found that when we use different distributions for this random stirring force we could generate different macroscales on the resulting flow, although the microscales remained basically unchanged.

M. V. Morkovin: Could you elaborate on your critique of this subgrid-scale closure? As I understood you, because of a mismatch of the statistical behavior on one side of the large wave numbers and the actual computed nonstatistical values on the other side of the wave-number interface, you do have propagation of errors into the larger scales. You made some very definite statements about the amount of spoiling that this error propagation would do to your original results.

---

[6]Kraichnan, Robert H.: Direct-Interaction Approximation for Shear and Thermally Driven Turbulence. Phys. Fluids, vol. 7, no. 7, July 1964, pp. 1048-1062.

[7]Phythian, R.: Self-Consistent Perturbation Series for Stationary Homogeneous Turbulence. J. Phys. A: Gen. Phys., vol. 2, no. 2, Mar. 1969, pp. 181-192.

J. R. Herring: Yes, this is a very topical subject now because it limits the ultimate predictability of equations that you are using. If you make small error perturbations on the small-scale structures, these feed back and contaminate the large scales. Hence, any deterministic aspects that these large scales may originally have can be ruined. I believe that the figure quoted now is that within about three eddy circulation times a given scale will be contaminated with the error originally residing at very small scales. As to how this affects the large scales in a real problem depends upon the geometry of the flow, whether the flow has boundaries and so on. The defenders of the subgrid-scale theory argue that the method is to be used to forecast "typical" flows, and as such, the theory need not tie back to any particular initial conditions.

M. V. Morkovin: Isn't there a difference between behavior in three-dimensional turbulence and two-dimensional turbulence? Two-dimensional turbulence, as long as we are away from the small viscous scales, should have circulation preservation, vorticity preservation. And so automatically you do have a chance of cascade upstream, I mean up to the larger scale. Is this the problem that you are talking about? Wouldn't the same thing be true for three-dimensional turbulence?

J. R. Herring: Errors initially in the small scales work their way back to larger scales in both two and three dimensions. Their penetration into the large-scale regime is aided – in two dimensions – by the energy cascade to larger scales that you mentioned. However, the "error cascade" to larger scales occurs in three-dimensional turbulence, despite the fact that here the energy cascade is dominantly to smaller scales.

P. A. Libby: I think it would be very valuable for the evaluation committee if Dr. Herring could make some conjectures about the future prospects of these more deterministic methods of calculation. He has seen, in the last day or so, some of the complexities which the engineers have to deal with. I think the answer we would like to hear from him really is what he thinks in the next 10 years perhaps, when computers become even more powerful, as to whether or not all the methods that he has heard today would be simply passé, and we would all be doing, even for relatively simple calculations, these more advanced methods based on direct integration of Navier-Stokes, direct interaction, or the subscale closure and things of that sort. I think it would be very valuable for us to have his notions in that regard for the sort of flows that we have been dealing with here not boxes.

J. R. Herring: I tried, in the talk to limit myself to simple geometries to get some insight into whether the parameterizations make sense in terms of a more deductive theory. When it comes to doing problems with complicated geometries you have in mind in this conference and at large Reynolds numbers, a direct application of the statistical theories seems to me out of the question. At best, one can hope for solutions to problems with simple geometries, such as parallel plate shear flow or cylindrical pipe flow. It

seems to me that the future value of such statistical methods may lie in their ability to shed light on simpler closures by way of either generalizing them or determining their constants. For example, I think that the proposals of Hanjalić and Launder's model[8] are in some sense suggested by the direct interaction kinds of equations, although the latter are certainly more complicated and laborious to solve. Possibly one should try to extract information from the direct interaction theory to get a theory at the level of Hanjalić and Launder by assuming shapes for the various spectra – energy spectra and so on. Some work has been done along this line already by Leslie.[9] That may be a good avenue along which to attack the problem and I have tried to give some indication of how such a calculation would go at the end of the printed version of my talk. To summarize, then, it would appear that the future rule at statistical turbulence theory in the type problems discussed here would be in improving and generalizing existing second-order, single-point moment closures.

As for the other two approaches, the subgrid-scale closure and the spectral method, these appear to have a better chance of being used directly on complicated problems discussed here. The subgrid-scale method has already been used for shear flows and thermal convection by Deardorff.[10] Of course, this method is a model of turbulence and hence is open to doubts on this account. However, as I pointed out in my talk, it is a method which can be progressively improved (at the expense of more computer time), and so hopefully one can avoid the disquieting doubts of other procedures, where errors are less easy to assess. This method could be applied, now, to the problems dealt with at this conference. No one has done so, principally I guess because of the additional programing needed to treat the complicated geometries you have. Of course, the method cannot, at present, deal with the boundary layer itself. It seems to me that such a calculation would be very valuable, because, it would predict so much flow structure, that it would be easy to tell whether the method is sensible or not. You cannot do this with the "global-averaged" procedures described here by, say, Launder and Donaldson, because of the averaging over the turbulent structure.

With reguard to the spectral technique, one must be more guarded. This method deals with all scales, so its principal contribution is at low Reynolds numbers, where there aren't many. It may serve (and is now serving) as a useful tool in assessing other

---

[8]Hanjalić, K.; and Launder, B. E.: A Reynolds Stress Model of Turbulence and Its Application to Thin Shear Flows. J. Fluid Mech., vol. 52, pt. 4, Apr. 25, 1972, pp. 609-638.

[9]Leslie, D. C.: Simplification of the Direct Interaction Equations for Turbulent Shear Flow. J. Phys. A: Gen. Phys., vol. 3, no. 3, May 1970, pp. L16-L18.

[10]Deardorff, J. W.: A Three-Dimensional Numerical Investigation of the Idealized Planetary Boundary Layer. Geophys. Fluid Dyn., vol. I, no. 4, Nov. 1970, pp. 377-410.

methods, such as the subgrid-scale method. For example, for some of the two-dimensional calculations carried out at The National Center for Atmospheric Research (NCAR) by Orszag, the behavior of the large scales seem to be relatively insensitive to the detailed phases of the small scales. All that's apparently required is for the magnitude of the small scales to be approximately correct. Such calculations tend, in this case, to bolster one's confidence in the subgrid-scale method.

S. J. Kline: Something bothers me about that, and I'm not quite sure of all of what you are saying. Let me try to explain myself. If you try to do what Professor Launder and Professor Spalding were doing where they were dealing with the ratios of production and dissipation, then this implies that you are saying something about the production. I am not at all persuaded from the physical evidence that the nature of production is the same as the nature of the cascade process in the statistics of decay, which is the box problem. If that is true, then there is a fundamental gap between the box problem and the kinds of things that we are doing here. Can you comment on that?

J. R. Herring: I'm not sure that I understand the question.

S. J. Kline: What I am saying, is that those models which seem to fit, for example, the two-point space-time correlations for shear flows (the only ones that we know that work at all, and also the visual data, the data that Gupta has taken with Laufer, and so forth) suggest that what one sees during the peak periods of production, which is intermittent, is of a qualitatively different nature from the processes that lead from there to decay. Now if that is true, then it seems to me that there is a fundamental gap between doing problems of statistics in which you are dealing with the decay process and cases where there is strong shear and high turbulence production.

J. R. Herring: Well, maybe I can answer part of that. Let me say as a general comment that the theories are capable of treating any kind of flow with mean fields (production) present or not. In my talk, I stressed the decay problem because it is simplest and because we have more numerical experience with it than with problems having production terms. I would agree that the physics of turbulent production is fundamentally different from that of decay; but I think the statistical theory may be flexible enough to handle both production and "decay." The issue you raised about the intermittency is, however, a problem with statistical moment theories, and it is not clear to me that they can handle correctly highly intermittent flows.

J. Laufer: I think that is a very fundamental question that Professor Kline brought up. And maybe it might be worthwhile to argue about this a little further. The sort of modeling that we have seen today and yesterday really tried to model some average equations, primarily Reynolds equations and some higher order equations of the turbulent quantities. We have not yet tried to – certainly not in this conference – make some physical model of turbulence itself. There is a great deal of skepticism about the formulation of the

turbulence problem, a lá Reynolds, in several people's mind working with turbulence. I think many of us are convinced that a great deal of information, especially phase information, is lacking in that. And the obvious consequence of that is that we cannot close the problem. So when we are talking about the production term in the Reynolds equation, to me it is really just a nomenclature – I have no physical picture of it. Certainly not until the first suggestions as to how this production might take place (made in Professor Kline's group) did I begin to get a physical picture. That was really the first notion that suggested some actual physical process that this is the way the flow might break down and produce turbulence. So the question is, how far can we go by trying to do the modeling according to these equations. Might it not be better to go back more into the physical work and the modeling? And this actually has been done – any of you who have tried to get into the details of Townsend's book[11] – he actually had a very physical picture in mind when he tried to come up with a value for turbulent Reynolds number. That I consider to be a sort of modeling – physical modeling. Clearly this is a much more difficult task, and I certainly don't have any obvious suggestions of how we can do that. But I think that it would be worthwhile for people who work in this area to think in terms of other possible modeling processes besides the ones that we have heard in the past 2 days.

A. Roshko: I'd like to pick up the idea that Paul Libby started and has been continued here – and that is, the question that has also come to my mind occasionally, one of these days will computers be able to calculate the flow directly without putting in any physical models let alone Reynolds equations. I think that there is some possibilities that this might occur. I'm thinking of some examples that I know of where you try to model a vortex shedding, for example, behind a circular cylinder by just letting vortices peel off from the cylinder into the wake and do a time calculation. This reproduces these flows at least qualitatively fairly well. Just this year in the Physics of Fluids, there was a short paper by a couple of Russians, Kadomtsev and Kostomarov,[12] in which they try to model the mixing layers that we have been talking about here so much. They simply feed vortices off the splitter plate and let it go. This is really just solving the Euler equation on a computer, leaving out the viscous terms. We do think that these free turbulent flows are viscous independent, and it is really quite remarkable that you get mean velocity profiles which look quite reasonable. My objection is that this is a two-dimensional calculation; these are all line vortices. However, for some flows like these mixing layers and vortex shedding down a cylinder, I think the large structure is to some extent two dimensional. I think there might be some progress in that direction. There has been really little work of this kind done.

---

[11]Townsend, A. A.: The Structure of Turbulent Shear Flow. Cambridge Univ. Press, 1956.

[12]Kadomtsev, B. B.; and Kostomarov, D. P.: Turbulent Layer in an Ideal Two-Dimensional Fluid. Phys. Fluids, vol. 15, no. 1, Jan. 1972, pp. 1-3.

D. B. Spalding: On this particular point of whether it will be practical in the near future to compute turbulent flows by a time-dependent solution of the Navier-Stokes equations, there is a simple computation that one can do about the number of grid points that one will need. Undoubtedly, if we are to proceed in that way, we must have grid points sufficiently close together so that we can accurately describe the behavior in the smallest eddies where energy is being dissipated. Now these are very small indeed. And so we can compute just how many grid points we will need, and thus see by how many orders of magnitude our current computers are away from being able to compute a turbulent pipe flow. I think it is quite a long way.

J. R. Herring: If I can make one comment along those lines. Some of those calculations done at NCAR on decaying turbulence suggest that it is not really so – that if you wish to calculate the large-scale structures accurately, you don't have to do a clean job of calculating the tiniest dissipation scales present. The examples I'm referring to here are two-dimensional calculations; it may be that in three dimensions there is a difference.

M. V. Morkovin: I was hoping that Dr. Spalding would share with us some of the early experience of Imperial College with three-dimensional flows. As I understand it you are computing things that have streamwise vorticity. How much of a complication, how much for instance, do you have to increase the number of grids to get something decent. Those are pioneering, rather smeared numerical experiments as yet, but they must be giving you some feeling of what the future potentials are. Isn't that right?

D. B. Spalding: I think that my answer must follow the lines of what I was saying just now. We are doing three-dimensional time-dependent computations, and we are doing them for turbulent flows. But we are doing them only by the use of turbulent models. They are still the quite simple two-equation turbulent models. We do not have higher level ones for three-dimensional flows. But we are struggling with computer storage at that level. And I think that we should have to have computers of many orders of magnitude greater capacity before we could approach the task of solving for turbulent flows by any other means than by way of turbulent models. But once that is said, there are no special problems about three-dimensional flows. If you've got a computer program that solves the three-dimensional equations and the continuity equation, and then an equation that will solve for any other scalar, like the energy or the dissipation rate or like concentration, then you just go ahead and solve. We have seen that there is still much comparison to be done between predictions and measurements for two-dimensional free turbulent boundary layers. For two-dimensional recirculating flows, there is much work to be done, and after that there is a comparison to be done with three-dimensional turbulent flows. So there is an immense amount of utilization of these techniques. And we are just at the very beginning of this.

S. J. Kline: I agree with Professor Spalding. You will recall that a number of people have made this calculation that he suggests. Howard Emmons has made it, Bill Reynolds has made it, and I think a number of other people have made it. And it is not just a small jump from present computers. I think you will recall that if you want to do a complete solution to the smallest scales as he suggested, then there is a graph in the 1968 Conference proceedings, I think Emmons[13] did that particular one, which shows that you have to run about 30 years on a computer that is slightly larger than anything that exists to get out one point for a fairly simple flow. That is pretty hard to imagine. So unless we get really a very big jump in computer power, one has to do something other than simply putting the Navier-Stokes equations into the computer and letting it run. Now the next question that immediately comes beyond that is what approximations do you make. Jack Herring suggested one kind of approximation, which may in fact be a very good one – that is, you model the small scales and try to do the larger scales. But that still is a modeling. And it still involves all these problems. I think that that really is the situation. I think it is naive to say that you are going to put all this in the computer and it is simply going to run. I wanted to revert also to the exchange between Jack Herring and me earlier and add one other remark – it may be helpful, I don't know. And that is, if you look at Lahey's model[14] of the two-point space-time correlation which does seem to fit all of them remarkably well, it is a two-part model which is the sum of the Markov noise and a traveling wave which has a stochastic jitter on the wave number and a stochastic phase coefficient. The situation is analogous in some simple sense to a simple harmonic oscillator which is underdamped or overdamped. If you work out the spectra using that model, it is essentially overdamped. But the constants are such that, if you just do long-term averaging, you don't see any peak at all. If you do the short-term stuff, there is a marked peak for certain kinds of events. If you take a long-term average, which is equivalent mathematically to Reynolds stress averaging, then this simply washes out. Experimentally, this would be the same as trying to find the critical frequency or resonant frequency of a simple harmonic oscillator by perturbing an overdamped system – you don't get anything. This is quite disturbing in terms of understanding the basic physics, as John Laufer said, from measurements based on the normal kinds of long-term averages.

D. R. Chapman: I would like to say a few words on behalf of the large computers as one who looks at their possibilities rather optimistically. The trends over the last decade or 15 years are such that computer speed is increasing by a factor of 10 approximately every

---

[13]See Comments by H. W. Emmons on page 651 for his present views.

[14]Lahey, Richard Thomas, Jr.; and Kline, Stephen J.: Stochastic Wave Model Interpretation of Correlation Functions for Turbulent Shear Flows. Rep. MD-26, Stanford Univ., Mar. 1971.

3 years, and the cost to do a given number of calculations is going down by a factor of 10 about every 5 years. So if you make a computation of how long it would take you to compute a hundred million grid points, which I did, by the present numerical methods of solving the unsteady Navier-Stokes equations that Bob McCormick uses at Ames and extrapolate these past trends as they have been going on out in the future, you come to a situation, where I estimate about 1982 or 1985, that the computers will be able to do such calculations in a practical amount of time and at a practical cost. Now a hundred million grid points is quite a few. I would like to make a comment about Howard Emmons' calculation also. I think that he was unduly pessimistic. He picked a grid size and assumed that you had to maintain that grid size throughout the flow. He picked a size that was probably necessary to maintain only in the sublayer. Because of that, he computed that it would take very much longer to do on the computer the unsteady Navier-Stokes equation for pipe flow of say a Reynolds number of 10^7 than it would for 10^5. His grid scale was roughly 100 different and in three dimensions, that means a factor of a million. If you only have to use the smaller grid scales in the sublayer the amount of computation time to do a Reynolds number of 10^7 is the same as to do 10^5. In my judgment, it is going to be more nearly independent of Reynolds number. After all, the velocity profiles in a pipe when plotted in terms of the right variables (shear stress, etc.) are independent of Reynolds number, surface roughness, and so forth. So I think that Emmons' paper has been quite misleading to many people about the ultimate prospects of what the large computers will do.

S. C. Lee: I just want to make the same kind of comment on this large computer. With our experiments recently we have calculated a flow around a sphere using NCAR's CDC 7600. We start with rotational symmetry, solving the entire Navier-Stokes equation. With a Reynolds number equal to 20, it only takes 5 minutes to get the results. By the time the Reynolds number reached 130, the flow began to oscillate. The time for the CDC 7600 to calculate to a Reynolds number of 300 is more than 10 hours. So we decided that that was enough, and we stopped. If we are going to calculate as far as we are talking about, in the neighborhood of Reynolds numbers of 100 000, I really don't know how long it would take.

T. Morel: I think that there is some limitation to this. We can't expect to increase it indefinitely. We are limited by the physical side of the computers, since the speed of light is just the speed of light.

D. R. Chapman: This point has been raised a number of times before, but the computer people that I have talked to are not concerned about this limitation for quite a while yet. The size of the computers keeps going down, and the idea of putting the computers in parallel gets around this to a large degree. Whether or not the trends of the last 15 or 20 years or so keep on going, we really won't know until another 10 years have gone by.

But the trends on log paper are not linear, they are accelerating. In other words, 10 years ago, the average time it would take a computer to increase its speed by a factor of 10 was longer than 3 years – it was 4 years or so. At least I haven't heard anyone in the computer business identify a foreseeable limit on the trends.

D. B. Spalding: There is another subject that I would like to raise. I would like to refer to a remark that Dr. Corrsin made yesterday in the Discussion for Donaldson's paper (paper no. 7), which I think is a very important one. He cast some doubts on the gradient-diffusion type of approximations for transport. I think that it is very important and that we ought to think about it. It came to my mind when he spoke about the book by Bosworth[15] in which there is a connection made between this problem and that of radiated transfer. In radiated transfer, one of the important parameters is the ratio of the mean free paths of the radiation to the dimensions of the apparatus. In turbulence transport we have the problem that the mean free path of the turbulence eddies is not small compared with the dimensions of the apparatus; the mixing length is one-tenth of the width. It is for this reason that we are in an area where the gradient type of approximation isn't quite good enough. That connection with radiation theory has a useful aspect to it. There are, coming from the astrophysicists, quite simple theories for radiative transport which do better than the conduction – the gradient type of approximation. I want to say that it is possible, it has been done, to work out the corresponding transport equations in turbulence also. One can write a correlation, for example, the temperature-prime—velocity-prime correlation, for the transport of heat. Write that in terms of a random velocity and a temperature of the outward moving and a temperature of the inward moving fluid. Following the exact pattern which is used in radiation theory, we find ourselves with an equation saying that the flux is proportional not to the gradient of the average temperature but to the gradient of the sum of the temperatures of the outward going and the inward coming balls of fluid. And then only in the limit of small mean free path, or whatever the appropriate parameter is in turbulence, do we reduce to the gradient type of approximation. I think I have said enough. I think that remark of Professor Corrsin is important and that we can follow up its implications by turning to radiation theory to get a practical improvement by that means.

M. V. Morkovin: The diffusion-gradient problem and the diffusion terms in general, those that involve pressure-velocity correlations, are indeed one of those things that may be used as a constraint on the mathematics which may not correspond to the physics. One of the things I would like to raise is the general trend that one sees in the observations, more detailed observations of turbulence, disclosing increasingly more some aspects of instability of the field. I was wondering to what extent the computable budgets of energy

---

[15]Bosworth, Richard Charles Leslie: Heat Transfer Phenomena – The Flow of Heat in Physical Systems. John Wiley & Sons, Inc., [1952].

which do have exact solutions for the pressure-velocity correlations in linearized stabilities can guide us in trying to reformulate some of the questions on these terms. There are really two questions. Is it true that we really see more and more instability behavior in turbulence, and, then, whether one can learn something from stability theories for it?

C. duP. Donaldson: I agree with Mark. I think that any way you can use an exact known solution and look at the physics of it to see if you can get a handle on how you can model something better is precisely the way to go. I don't think that we have made enough use of exact solutions in making these models initially.

J. Laufer: I think that we get back to the comment I made earlier on physical modeling. In response to Professor Morkovin's question, I think that we can say yes we see now, by making more visual observations, more and more instances where some type of instability process does take place, even in regions where we think that the flow is completely turbulent. One good example is the type of instability that the Stanford group discovered and we studied further in the sublayer of a turbulent boundary layer. We are now taking almost instantaneous measurements of the profiles, velocity profiles, in the sublayer. When we compare those profiles with the well-known figure in Schlichting's book, showing the eigenvalue distribution of a Tollmien-Schlichting wave in a laminar boundary layer, the resemblance is quite striking. This is one example of getting back to the geometry that we are concerned with at this meeting in the case of the free shear layer, the mixing layer. You have seen in Professor Roshko's pictures and again here that we are dealing with a completely well-developed turbulent flow with very definite large-scale motion in that flow that seem to indicate some type of instability origin. In fact, we are looking at the same type of problem in a water flow, where we can very nicely see how these large-scale motions generate from some interface instability originating right at the $x = 0$ station.

Written Comments

P. A. Libby and C. duP. Donaldson: We wish to call attention to the need for consideration of the proper specification of initial and boundary data when the newer methods of closure of the system of equations describing turbulent shear flows are employed. We do so because we are so familiar with the initial and boundary data appropriate for the well-known eddy viscosity and/or mixing length formulations for such flows that we may casually carry over these ideas to the newer methods, some of which lead to different orders in the normal derivative than are customary and to other differences in the mathematical nature of the describing equations.

Caution seems to be especially called for in the case of the free mixing flows under consideration at this conference. This is because in these flows we usually make the

assumption that the shear stress due to molecular transport is negligible in the streamwise momentum equation and, thus, that we can drop the $\bar{u}_{yy}$ term in that equation; but in some formulations this leads to a loss in our ability to specify two boundary conditions on $\bar{u}$! Contrast this with boundary-layer flows in which we must retain molecular effects near the solid boundary because of the laminar sublayer.

It should also be recognized that in some of the new, higher order closure schemes for turbulent shear flows the mean shear stress $\bar{\tau}$ is an explicit, dependent variable, which usually appears differentiated once with respect to the normal coordinate. However, again in free-mixing flows we wish to specify $\bar{\tau} = 0$ at $y \to \pm\infty$!

Since we are dealing with parabolic equations and their solutions in either a quarter- or half-plane, we recognize that there is an interrelation between initial data (at $x = 0$ or $x = x_0$) and the boundary conditions at $y \to \infty$, or $y \to \pm\infty$. It may well be that the initial data plus some benign conditions of "boundedness" are sufficient to get us around apparent difficulties, such as those indicated previously, of not having the ability to specify all the boundary conditions we desire. However, mathematicians can usually help us on these questions only for highly idealized models of our problems.

Finally, we note that in one class of free-mixing flows, i.e., two-dimensional mixing, we have always had the problem of determining the orientation of the "zero" streamline in space. The proper treatment of the boundary conditions in this case has been provided some years ago by Ting.[16] As a result we now recognize that the theoretician may legitimately formulate his boundary conditions so as to make his analytic or numerical problem "well posed," but that when he compares his predictions with experiment or when an experimentalist employs that theory, the predictions must be properly reoriented in space so as to be consistent with the environment of the experiment, i.e., so that the zero streamlines are consistent.

These remarks should be sufficient to call attention to the need for careful consideration of the appropriate and proper specification of initial and boundary data for a set of describing equations, especially a set based on the new, higher order methods. The ease with which such equations can be "put on the computer" should not be allowed to disguise our ignorance of what constitutes a "well-posed" problem. We may well learn some important aspects of the phenomenology of turbulent space flows by considering the formalism before hasty computation.

---

[16]Ting, Lu: On the Mixing of Two Parallel Streams. J. Math. & Phys., vol. XXXVIII, no. 3, Oct. 1959, pp. 153-165.

Comments on the Place of the Computer in Turbulence Research and Application*

H. W. Emmons
Harvard University

The current lack of understanding of the basic nature of turbulence prevents the prediction of just what approach can ultimately be successful. It is not now known whether turbulent flow is an initial instability followed by a complex, nonlinear, transfer of macroscopic kinetic energy through random interaction down through a chain of ever smaller scale motions to end as molecular chaos or whether each scale of motion develops ever more intense until it in turn becomes unstable and thus passes its energy down with various wave number and phase control or whether in these processes significant information can be fed up from the microscopic "chaos" (turbulent, molecular, or both) to control some significant aspects of the macroscopic motions.

The most pessimistic view of this situation would require a quantum statistical mechanical kinetic theory. Essentially no questions of current interest require this level of description. Furthermore it will be a long time, if ever, that 10^{25} particles could be followed in detail. Finally for turbulence research now of interest, there are many reasons to reject this view.

The most important simplification is the replacement of the effect of the molecular chaos by a laminar viscosity based upon the observation that the smallest "significant" eddy is large compared with intermolecular dimensions and the supposition that no significant control of the turbulent motions can be exerted by the details of the microscopic molecular processes. A test of this supposition is now being made in the Doctoral Thesis study by Carol Russo who is measuring the details of grid turbulence in methyl alcohol. The expected agreement with air grid turbulence will confirm that the total effect of the molecular chaos is subsumed under the Reynolds number (through ν) and that no other dimensionless variables are required and, therefore, the Navier-Stokes equations are adequate for the description of turbulent flow.

The present conference is devoted to a discussion of the varying ideas, methods, and results available to describe the essentially four dimensional $(\vec{r},t)$ turbulent flows. A wide ranging variety of ideas is being tried as is necessary because of the failure of the obvious replacement of the turbulent motions by a constant "turbulent viscosity" inspired by the molecular chaos replacement.

---

*In view of the current interest in the role of the computer in turbulence studies, the editors invited Professor Howard Emmons to submit his present views on the subject.

The direct numerical solution of the Navier-Stokes equations must be carried out on such a scale that the smallest eddies with significant macroscopic effect are properly described. A very fine scale is clearly needed at high Reynolds numbers in the turbulent energy creation regions near walls and internal shear layers. I believe they will also be needed in the high dissipation regions if a complete description of the turbulent flow is desired. Thus, while computation net grading may save a few orders of magnitude of points, I do not believe that direct solution of the Navier-Stokes equations will be possible for general turbulent flows for a very long time (if ever).

Again the growth in computer speed, a factor of 10 every 3 years, will no doubt continue for awhile. However there are only about four orders of magnitude available before a speed-of-light limitation and a like increase by further size reduction. Before these limits are reached, thermal fluctuations will have to be reduced by cryogenic computer elements. Finally, parallel computation can further increase computer speed by a couple of orders of magnitude. Thus I can expect something like 10^{14} computation to be over the horizon (present machines are about 10^{7}) but not 10^{20}.

Eventually a few of the simpler, lower Reynolds numbers, turbulent flows will be directly computable and these will prove invaluable for checking out the various simplifying assumptions. However, complex turbulent flows, like flow around and in the wake of a building – or even a sphere – are not in my view likely to be directly computable for a very long time – if ever.

On the other hand, I fully expect work of the kind reported at this conference to lead to approximate methods of calculation of general turbulent flows. The successful method will incorporate both a phenomenologically and mathematically justifiable procedure which provides for the computation of the growth and decay of the appropriate turbulent transport of momentum, energy, and specie. There will eventually be a hierarchy of such methods which permit the computation of any turbulent flow with any desired precision, the decision being a compromise of need and pocketbook.

OPENING REMARKS

By H. H. Korst
University of Illinois at Urbana-Champaign

We are now approaching the summarizing portion of our conference which will consist of formal panel presentations and subsequent discussions of their reports on the floor.

The first panel, the Committee To Recommend Critical Experiments, chaired by Professor S. J. Kline from Stanford, will attempt to draw conclusions as to the present status of, and the continuing need for, both supporting and exploring experimentation to gain a better understanding of the physical phenomena underlying jet mixing.

The second panel, the Conference Evaluation Committee, chaired by Professor Mark V. Morkovin, will address itself to the efforts made by the predictors to utilize various physical models and mathematical procedures to arrive at solutions for test cases submitted to them earlier upon the recommendations of the Data Selection Committee.

EXPERIMENTS IN FREE SHEAR FLOWS –

STATUS AND NEEDS FOR THE FUTURE

By Committee To Recommend Critical Experiments:
S. J. Kline (Chairman), Stanford University
D. E. Coles, California Institute of Technology
J. M. Eggers, NASA Langley Research Center
P. T. Harsha, ARO, Inc.

CLASSES OF PROBLEMS

Experiments on free turbulent shear flows have two primary objectives:

(1) Accumulation of experience with simple classical flows as a basis for evaluating constants in closure models of predictive theories

(2) Applied work on flows of technological significance

Unfortunately, requirements for objectives 1 and 2 tend not to coincide in the case of free shear flows. This condition can be seen by considering the typical case of a low-speed axisymmetric jet of air flowing into still air. The flow field is usually considered to contain three zones: (a) the near field, (b) the transition (or intermediate) field, and (c) the far field.

In the near field, a gaggle of initial conditions arises from the presence of flow-control devices and upstream solid surfaces. In real flows, as contrasted to ideal models, these initial conditions often involve one or more sets of back-to-back boundary layers trailing from solid surfaces. In the transition region, the potential core has disappeared, but the mean velocity has not yet reached a state of self-similarity. In the far field, by definition, self-similarity is characteristic of the mean-velocity field and at least the second-order correlations of the velocity perturbations.

Simple scaling laws have been established only for the far field, and the properties of this zone tend to be the best established and the most used for construction of predictive theories. The vast bulk of applications, on the other hand, depend on flow characteristics in the near field. Typical cases include jet ejectors, wake signatures, base-pressure control, combustors, flow over steps and cut-outs, jet noise, jet interactions, etc.

Since the variety of applications of technological significance is so great, and since increased fundamental understanding will aid in all of them, this report is concerned primarily with classical flows to augment understanding and for model building.

THE ROLE OF CLASSICAL EXPERIMENTS

Test data for five well-known types of classical, free turbulent shear flow are included in this conference:

(1) Mixing layer (half jet)

(2) Round jet

(3) Plane jet

(4) Round wake

(5) Plane wake

Other potentially classical flows of lesser importance include

Radial jet

Zero-momentum wake

Round plume*

Plane plume*

Each of these classical flows, by definition, has the property of self-similarity. A key assumption, which is noncontroversial in the limit of large Reynolds number, is that effects of molecular transport can be neglected. What remains then is usually a simple problem in dimensional analysis with very little physical content. Given a rather vague notion of what constitutes a boundary-layer approximation for turbulent flow, an elementary argument leads in each case to simple and well-known similarity laws of a power-law type.

An instructive conclusion from these analyses, at least for purposes of planning experiments, is that as the flow proceeds downstream, the Reynolds number based on local length scale and mean-velocity scale can increase (mixing layer, plane jet), remain constant (round jet, radial jet, plane wake), or decrease (round wake).

A second conclusion is that in the absence of a pressure gradient, the plane mixing layer, in particular, has self-similar properties (corresponding to linear growth) regardless of velocity ratio and presumably also regardless of density ratio, Mach number, or whatever. This plane flow therefore provides an opportunity to study a variety of special effects, singly or in combination, under relatively clean conditions. In view of present confusion about the effect of density ratio and to a lesser degree about the effect of initial conditions, much more might well be done with this particular flow configuration. Substitution of an axisymmetric geometry for the plane geometry is a little hazardous, as long

*Plume here refers to a free convective flow and not to a jet engine or rocket flow.

as effects of lateral curvature are no better understood than they are at present. However, studies of the axisymmetric configuration should continue because of the technical importance, particularly of the near fields in this geometry. Flow in the far field of a jet (plane or axisymmetric) is especially unsuitable as a model for investigating effects of density variations on turbulent mixing, because most of the jet fluid (eventually, all of it) is characteristic of the ambient fluid rather than the fluid used as the original momentum source. The flow is therefore a relaxation or transition problem and is best approached from this point of view.

The committee believes that other classical or near-classical experiments, if possible with known similarity properties, need to be sought and experimentally documented. Examples include (1) curved plane jets, such as are encountered in jet flaps and thrust augmenters; (2) cross- or counter-flowing streams; and (3) vortex flows, flows with large coriolis forces, or other flows which contain regions having large mean rate of strain but small turbulence production. No recommendation is being made of a single class of experiments, but rather careful consideration of what experiments are worth extensive documentation to aid model building for turbulent flows.

The description in the section "Classes of Problems" of the near, intermediate, and far fields also provides the basis for a classification of levels of difficulty, and hence levels of confidence, regarding the agreement between predictive output of a given theory and available data. At the lowest level, any theory which does not reproduce the well-established limiting similarity forms for shear and spreading rate as x approaches ∞ should be rejected, unless overriding practical considerations force its use.

At a second level, a predictive theory should provide some information about the transition region where the conditions are essentially now initial conditions for calculation of the far field.

At a third (and possibly fourth) level, predictive theories might be able to cope with the evolution of the near field and to specify the total distance required for evolution of the downstream regions.

In each case, as in boundary-layer flows, predictions for integral quantities, local mean-field quantities, and correlations of fluctuating quantities form a second hierarchy of successively more difficult checks on the power and accuracy of predictions.

Most technological applications entail added complications, such as curved layers, recirculating flows, chemical reactions, species diffusion, pressure gradients, and gross unsteadiness. Although such experiments are essential, it is difficult, if not impossible, to obtain reliable experimental data for purposes of model building from these more complex flows. It may be possible to use them to check the output of theoretical models, but it must be recognized that in most cases, substantial differences in behavior may occur between the more complex cases and the simpler classical cases.

CRITICAL EXPERIMENTS

Five classes of experiments appear to the committee to be particularly significant for the near future.

(1) Additional experiments clarifying the effect of density variation owing to use of different gases, with and without the additional effect of density variation owing to high Mach number or other effects. Whenever possible, a density ratio of unity should be run as a base line for variable-density data. One configuration which may be valuable for study of both subsonic and supersonic plane mixing layers is flow over a two-dimensional downstream-facing step. The bottom wall downstream of the step should be porous, uniform injection of an arbitrary gas being in a direction normal to the main flow. The natural entrainment rate is presumably matched when pressure disturbances in the free stream are minimized.

(2) Experiments clarifying the role and importance of various parameters which determine the behavior of the near field as well as the conditions under which any of these parameters can be neglected.

(3) Experiments determining the cumulative effect of initial conditions in terms of the distance to fully established flow. Experiments relating these results to those of the second class. Note that similarity seems to be reached significantly earlier for mean-velocity profiles than for second-order correlations of velocity fluctuations. The distance to similarity for higher order correlations is probably still greater.

(4) There exist few documented cases of coflowing turbulent layers, that is, cases where two layers of distinctly different initial turbulence structure flow side by side at the same mean speed. Data on such flows should increase our understanding of free turbulent shear flows and aid in model building.

(5) Experiments using contemporary experimental techniques (computer-assisted instrumentation, conditional sampling, and averaging) should be carried out to study structure in free turbulent shear flows in order to complement and support contemporary work on boundary layers. The emphasis among predictors at this conference has been on turbulent field methods based on conventional long-time averaging. However, there is a growing conviction among many experimenters that long-time averaging (Reynolds stresses, higher correlations, spectra) may not be the most productive way to describe turbulent flows. An alternative approach is implicit in recent work on large-eddy (or wave) structure in turbulent boundary layers by Kovasznay, Offen, and others (refs. 1 to 3). If a large eddy can eventually be described experimentally with sufficient credibility for a given flow, then averaging over a moving pattern of such eddies can serve the same purpose as conventional averaging while avoiding some of the present disadvantages (such as trying to cope with the phenomenon of intermittency). With few exceptions, research

in free turbulent flows has so far not used conditional averaging techniques or attempted to exploit the contemporary point of view.

DESIRABLE MEASUREMENTS FOR VARIOUS CASES

The committee believes that improved and extended data are needed both for construction of models and for tests of specific applications of these models. Many of the existing data fail to report significant experimental parameters and are also deficient in reporting cross-checks and in estimating uncertainties. In only a handful of cases have the effects of systematic variation of initial conditions been reported. Parameters estimated from complex flows have often been mixed indiscriminately with parameters estimated from nearly classical flows in model building.

The committee believes that rapid advancement of predictive capability requires more complete reporting of experimental data and also requires arrangements for storage of complete original data in suitable archives (not merely on small published figures).

Because of existing difficulties (see paper no. 2 by Birch and Eggers) in establishing a value for the spreading parameter σ for the plane mixing layer, the committee suggests that the dependence of σ on χ be reported. Different workers have employed different definitions for σ; the specific definition employed should always be explained. In the plane mixing layer and other flows with similarity, there is usually some confidence in the exponents for the similarity laws. Therefore, more can be learned about the effect of initial conditions on apparent origin, about rate of approach to similarity, and about effects of scatter in difficult measurements far downstream, by abandoning the usual log-log scales in favor of plotting dependent variables to the appropriate limiting power against a linear scale for the independent variable x.

Various permutations of laminar and turbulent boundary layers can occur on the solid surfaces which are involved in the generation of a free shear flow. Documentation of these boundary layers just before separation should be an inherent part of near-field studies and should also be recorded whenever persistence of effects of initial conditions into the intermediate and far field is of concern.

For the case of laminar initial boundary layers, two kinds of instabilities have been observed; sinuous oscillations of the entire layer (ref. 4) and vortex roll-up of the individual layers (ref. 5). Sinuous instability is also reported by Brown and Roshko (paper no. 18 of this compilation) for the turbulent case. The presence of such instabilities should be suspected and reported if found.

In confined jets the committee urges that static pressure, including at least wall pressure, be measured and reported. In closed regions of separation (with recirculation), both curvature of the dividing mean streamlines and lateral constraints on the flow

(for example, end conditions and wall proximities) should be reported. There may be a tendency for cellular three-dimensionality to develop, often with unsteady elements; this possibility should be carefully examined.

The round jet involves relaxation of one classical flow in the near field toward another classical flow in the far field. Our belief is that such flows should be studied extensively for the sake of the relaxation property, with particular attention to the rate of approach to the final equilibrium state. From the predictor's point of view, such relaxing flows involve a change in local length scale. Examples of relaxing flow studies are the Chevray and Kovasznay experiment (ref. 6) where a symmetric pair of turbulent boundary layers relaxes toward a plane wake; the Knystautas experiment (ref. 7) where a row of round jets relaxes toward a plane jet; and the productive study by Prabhu and Narasimha (ref. 8) of a plane wake relaxing after being perturbed. The relaxing of a jet or wake with significant density variation toward a constant-density flow has previously been mentioned. Note that initially rectangular or elliptical wakes or jets are known to interchange their major and minor axis of symmetry (at least once) during their approach to equilibrium. In all cases, it should be expected that the relaxation process may be extremely slow.

More work directly on instrument development is needed, for example,

(a) for means to measure static pressure fluctuations in a moving fluid

(b) for use in high temperature fluids, and

(c) for more accurate sampling techniques for measurement of species concentration

EXPERIMENTAL PRECAUTIONS AND PITFALLS

Considerable caution is required regarding three-dimensionality in nominally plane flows. End-wall boundary-layer effects which modify the entrainment process, and other obstacles which block or otherwise displace the flow, can give seriously distorted results. Note specifically that comparison of $\overline{u}(y)$ profiles at various lateral stations is not a sufficient guarantee of two-dimensionality. Streamwise invariance of momentum flux is a much better check. Specific calculations and experiments are needed to ascertain when three-dimensional effects are negligible.

In axisymmetric (or three-dimensional nonround) flows, traverses should be made in more than one direction both as a cross-check and because transformation of major to minor dimension by action of turbulent shear stresses can occur.

A key property in the growth of any free turbulent shear layer is entrainment of nonturbulent flow from the surroundings. Jets, in particular, have an equivalent sink effect (ref. 9), and this effect needs to be studied and understood by the experimenter.

Because of entrainment, the surrounding fluid is not really at rest, and the presence of walls (as in flow over a step or a cavity) can seriously affect the value of the spreading parameter. It follows that any aspect of an apparatus which can affect entrainment (for example, closed versus open test sections, walls close to separated flows, downstream obstacles, etc.) can introduce scatter in any correlation of results. Even for a flow as simple as the round jet out of a wall, the presence and size of the wall may modify the pressure field and the spreading rate. Although no single prescription can be given, it is recommended that specific consideration of the entrainment process be incorporated in planning and designing any realization of a classical experiment in the sense used herein.

In supersonic cases, caution is necessary to avoid (or at least document) the effects of lip shocks and other pressure perturbations. Observations of static pressure for supersonic regimes are also essential for clear interpretation.

Direct calibration of hot wires for compressible flows (Mach number greater than 0.3) is essential in order to separate effects of velocity from those of temperature and density. (See, for example, ref. 10.)

REFERENCES

1. Kovasznay, L. S. G.: Summary of Remarks. Proceedings Computation of Turbulent Boundary Layers – 1968 AFOSR-IFP-Stanford Conference, Vol. I, S. J. Kline, M. V. Morkovin, G. Sovran, and D. J. Cockrell, eds., Stanford Univ., c.1969, p. 404.

2. Kline, S. J.; Offen, G. R.; and Reynolds, W. C.: Current Investigations of Turbulent Shear. 1971 Proceedings of Symposium on Turbulence and Liquids, J. L. Zakin and G. K. Patterson, eds., Univ. of Missouri at Rolla, 1972, pp. 61-68.

3. Gupta, A. K.; Laufer, J.; and Kaplan, R. E.: Spatial Structure in the Viscous Sublayer. J. Fluid Mech., vol. 50, pt. 3, 1971, pp. 493-512.

4. Sato, Hiroshi; and Kuriki, Kyoichi: The Mechanism of Transition in the Wake of a Thin Flat Plate Placed Parallel to a Uniform Flow. J. Fluid Mech., vol. 11, pt. 3, Nov. 1961, pp. 321-352.

5. Oseberg, Öyvind K.; and Kline, S. J.: The Near Field of a Plane Jet With Several Initial Conditions. Rep. MD-28 (NSF Grant GK-10034 and Contracts AF 49(638-1278 and AF-F44620-69-C-0010), Stanford Univ., May 1971.

6. Chevray, Renè; and Kovasznay, Leslie S. G.: Turbulence Measurements in the Wake of a Thin Flat Plate. AIAA J., vol. 7, no. 8, Aug. 1969, pp. 1641-1643.

7. Knystautas, R.: The Turbulent Jet From a Series of Holes in Line. Aeronaut. Quart., vol. XV, pt. 1, Feb. 1964, pp. 1-28.

8. Narasimha, R.; and Prabhu, A.: Equilibrium and Relaxation in Turbulent Wakes. J. Fluid Mech., vol. 54, pt. 1, July 1972, pp. 1-17.

9. Taylor, Geoffrey: Flow Induced by Jets. J. Aero/Space Sci., vol. 25, no. 7, July 1958, pp. 464-465.

10. Morkovin, Mark V.: Turbulence in Small Air Jets at Exit Velocities Up to 705 Feet Per Second. J. Appl. Mech., vol. 25, no. 2, June 1958, pp. 314-315.

DISCUSSION

R. B. Edelman: I will address this question to the panel in general: Have you given any consideration to the type of instrumentation that should be used for the types of quantities that one might be interested in, in turbulent flow; for example, mean flow properties, the turbulence quantities, and then finally concentration measurements. And perhaps I should generalize this to include reacting flows as well, which is an area that is of ultimate interest to many of us.

D. E. Coles: Well, I will think out loud a little bit, I would like to be excused from talking about reacting flows. I do not have any experience with those and perhaps I do not want any. I think the most promising instrument these days is the laser Doppler anemometer and I think very rapid developments will occur. We even have hopes of being able to measure vorticity with one of those things, if we can figure out how to do it. It is not so much a matter of instrumentation as it is a matter of attitude toward these flows, I think. One of the points that Kline made and that I would like to underline is that there is a significant body of experimenters, mostly working in the boundary-layer field, who are not going in the same direction as everybody else. They are aiming at substituting some other kind of formulation for these turbulent problems than the classical one which began with Osborne Reynolds about 100 years ago. Laufer made the point that you clearly throw away all phase information in the problem as soon as you draw bars over things, and experience has shown that clever kinds of conditional sampling and conditional averaging can reveal highly unexpected properties of these turbulent flows. I think the first of these was intermittency, but there are many others; the bursting phenomenon, the sublayer structure in boundary layers, and large-scale structure in shear layers. All these things suggest that what is going to happen or what may happen is that the eddy chasers will succeed in catching an eddy and assigning some properties to it, a shape, and an intrinsic velocity field. The kind of averaging we will come to, maybe 10 years from now, will be an average over a moving pattern of these eddies treated as operators. I like the word operators; others do not agree with me. This is virtually a complete rejection of the traditional schemes of thinking in terms of correlations, auto- or cross-correlations, Reynolds stresses, spectral operators, etc.; and I would like to see more work done in the free shear flow business along these lines. I think Wygnanski has been the only man who has tried to apply these ideas in the sense that the boundary-layer people are doing, although I think the Brown and Roshko experiments[1] will certainly have to be continued with this point of view. You have to explain those pictures. You have to know about those pictures and if you know about those pictures you should be nervous about Reynolds stress.

[1] Brown, Garry; and Roshko, Anatol: The Effect of Density Difference on the Turbulent Mixing Layer. Turbulent Shear Flows, AGARD-CP-93, Jan. 1972, pp. 23-1 – 23-12.

S. J. Kline: I think there is a general dearth of experimental work in relation to the level of theoretical work. Some of the big hangs-ups are in the data and there is not enough data taking and even less effort on instrumentation. There is even no really good text-book on the subject of how measurements are made in moving fluid fields. There are very few schools that give courses in this subject. I can advertise a little bit here, we are one of the very few that do. I think that more effort on both of those problems is needed and that there is really an enormous amount of work to be done.

H. H. Korst: Considering myself now as a spokesman for those who contributed to this conference as predictors, I wish to direct attention to the lack of concise and needed information concerning initial conditions in some of the selected test cases. This, in particular, refers to the specification of the microstructure for the starting profile.

If a well-defined attached boundary layer precedes the mixing process, one may assume that the work of Maise and McDonald[2] provides some guidance; yet, there seems to be evidence that such a structure does not carry over smoothly into the developing free shear layer but may actually be subjected to a rapid and rather catastrophic breakdown as a consequence of large-scale instabilities as has been shown so dramatically in the work of Brown and Roshko.[3]

So I would like to ask the panel to suggest what instrumentation and observations may be needed to cope with, and extract information on, boundary-layer breakdown which may have a large influence on the structure and initial development of near wakes.

S. J. Kline: Yes, I wanted to say one think about that and I wanted to show some pictures that I brought with me. Mr. Oseberg,[4] in my laboratory a couple of years ago did study a plane jet in water using a kind of visualization technique which is well-known to you. He studied three different velocity ratios and three different sets of initial conditions. He did find instabilities for the laminar separating layer very much like those in the pictures that Professor Roshko showed. When one has a turbulent boundary layer leaving the surface, one still gets quite a lot of instability but it is not as clean and as pronounced. I had hoped to show those pictures but the projectionist tells me that the motion-picture copy that I brought with me has no holes in it – so we will not see those, but they do appear in Oseberg's thesis.[4] As far as instrumentation goes, I think there are lots of ways of measuring that – a simple visual technique which Roshko has already shown you will get beginning measurements. Cross-correlation measurements, which

---

[2] Maise, George; and McDonald, Henry: Mixing Length and Kinematic Eddy Viscosity in a Compressible Boundary Layer. AIAA J., vol. 6, no. 1, Jan. 1968, pp. 73-80.

[3] Brown, Garry; and Roshko, Anatol: The Effect of Density Difference on the Turbulent Mixing Layer. Turbulent Shear Flows, AGARD-CP-93, Jan. 1972, pp. 23-1 – 23-12.

[4] Oseberg, Öyvind K.; and Kline, S. J.: The Near Field of a Plane Jet With Several Initial Conditions. Rep. MD-28 (NSF Grant GK-10034 and Contracts AF 49(638)-1278 and AF-F44620-69-C-0010), Stanford Univ., May 1971.

Vic Goldschmidt has already suggested, should certainly be very adequate to measure that kind of phenomena at least in the beginning. I would suggest that one wants to document whether the layer at separation at the back of the solid surface is laminar or turbulent because this does make a qualitative difference.

P. A. Libby: I was rather disappointed that our distinguished panel did not use the leverage of their prestige when they called for very careful and detailed experiments to point out to those in the audience who have money to disburse in this direction that they must be patient when they disburse that money. They must expect to fund that sort of work over years, not a 6-month affair. I assume that our panel agrees on that and is very embarrassed by its omission.

V. W. Goldschmidt: I cannot answer Paul's point – I would like to speak about the eddy chasers a little bit. I think Val Kibens[5] is looking at the wake of a flat plate right now and I think he is also heating it. Renè Chevray[6] at Stonybrook is looking at a circular jet; Fiedler[7] in Berlin is also looking at a heated circular jet and our group at Purdue University is also looking at a plane heated jet. However, I would like to direct a question to the panel. You made reference to a need for documenting information that is available and I think this is a crucial point. We cannot pass the buck to NASA. I think we can start accusing ourselves in the shortcomings of previous work. For instance, to be more direct, the selection committee for experiments forgot to include Gunnar Heskestad's[8] work which I think is the best around on plane, circular, and radial jets. But coming to the point on hand, how can we be more cautious and how would you suggest creating these archives of data that you refer to.

S. Corrsin: I am not volunteering but I would like to remind everybody that there is still no generally accepted way of measuring static-pressure fluctuations in a turbulent flow. It would be nice if somebody would go to all the trouble of developing appropriate instrumentation. I guess there are probably half a dozen places in the world where people are allegedly working on such instruments and I think that no two of them agree that anybody else is doing it right. So, if someone could set aside his interest in detailed hydrodynamics for awhile and develop such a device it would be very useful. In terms of the

---

[5] Oswald, L. J.; and Kibens, V.: Measurements in the Wake of a Disk. Paper EA1, 1970 Annual Meeting of Division of Fluid Dynamics, Amer. Phys. Soc. (Charlottesville, Va.), Nov. 1970.
Oswald, Lawrence James: Turbulent Flow in the Wake of a Disk. Ph. D. Diss., Univ. of Michigan, 1971.

[6] Dr. Renè Chevray: Department of Mechanics, State University of New York at Stonybrook, Stonybrook, Long Island, New York 11790.

[7] H. Fiedler: Hermann Scöttinger Institute, Flür Strömungstechnik, Technische Universität, Berlin, Germany.

[8] Heskestad, Gunnar: Two Turbulent Shear Flows: I. A Plane Jet. II. A Radial Jet. Ph. D. Diss., Johns Hopkins Univ., 1963.

applicability of gradient transport models, one of the things that I pointed out a long time ago is that they have greater success in free shear flows than in wall shear flows. This is coincident with the fact that the principal axes of the mean strain rate tensor and the stress tensor happen to coincide for reasons which are unknown in free shear flows and they definitely do not coincide in wall flows. If we move one order higher in the moment hierarchy and use the Reynolds shear stress equations and the energy equations, then we move to the question of whether the gradient transport model might be appropriate for the transport of shear stress or energy. Therefore, it would be worthwhile finding out whether the principal axes of those things happen to coincide with the corresponding transport quantities and this information could be found very easily with existing instrumentation. We just have not done it for some reason which I do not know.

B. G. Jones: Professor Corrsin has commented on the current status of static-pressure information and I wish to add a further comment concerning some experimental observations which we have made at the University of Illinois. Our initial results were reported in Spencer's thesis[9] with some root-mean-square static-pressure measurements in a plane mixing layer included in the AIAA paper.[10] We did not stop our studies at that point although we realized these early measurements were severely contaminated because of velocity fluctuation sensitivity. We cannot say exactly how severe, but it was substantial and was caused primarily from the sensor tip configuration and its orientation. We have continued the studies with the same basic sensor in terms of its internal structure, using bleed type anemometer sensing, but we have modified the tip configuration to make it less sensitive to velocity contamination. Examining this new configuration (which resembles a pitot static tube) far downstream in the self-preserving region of a circular jet, we have been able to estimate the contamination to the pressure signal caused by the transverse and axial velocity field components. The axial component effect is reduced to approximately 2 percent, whereas the transverse component effect is less than 10 percent. With these levels of contamination we are able to make some estimates of corrections to be applied to both root-mean-square pressure levels and velocity-pressure results.

We are now in the process of applying these results to our aerodynamic noise generation program, which was mentioned briefly in our session this morning. We are examining the two-point spatial pressure correlations in the initial mixing and in the developing regions of the circular jet. We expect to continue this work in the plane mixing layer as a means of examining in more detail the initial shear layer in circular and

---

[9] Spencer, Bruce Walton: Statistical Investigation of Turbulent Velocity and Pressure Fields in a Two-Stream Mixing Layer. Ph. D. Thesis, Univ. of Illinois, 1970.

[10] Spencer, B. W.; and Jones, B. G.: Statistical Investigation of Pressure and Velocity Fields in the Turbulent Two-Stream Mixing Layer. AIAA Paper No. 71-613, June 1971.

plane jets. This will also enable a reexamination of the original study of the energy budget across the plane mixing layer and allow improved estimates, particularly with respect to pressure-velocity transport terms.

H. H. Korst: Coming back to the problem of preserving information: We have here a reservoir of people and minds. Having assembled, processed or produced stockpiles of data, is it safe to assume that NASA will, for the time between now and the publication of the Proceedings, act as a guardian of this information?

Furthermore, are there any plans whether this information will be kept beyond that time at a selected central location, preferably at NASA Langley Research Center? Shall we leave this question open or shall we try to exert some gentle pressure on potentially willing individuals or organizations?

D. M. Bushnell: We will publish as Volume II the data that we sent out to the predictors. This is fairly complete data, at least as far as the mean flow is concerned. The problem is not stockpiling the reports that are available, the problem is getting the details on the experiments, that is, the details that Professor Kline has called for and which have often not been included. When one gets an AIAA paper, there is no guarantee that you will get the detail you need to check out the more sophisticated numerical programs. The theses we see coming out of Georgia Tech now that are 3 and 4 inches thick may well have the detail that is necessary. But I do not know where you would store these things and how you would insure that the details are put in.

H. H. Korst: Mr. Bushnell, will you collect and make available such information, if it should be sent to you, and can we write to you at Langley for it?

D. M. Bushnell: I very regretfully decline your invitation – we pay COSMIC [11] to stockpile computer programs and there is a possibility through NASA Headquarters that they could be prevailed upon to fund other sources of storage for this type of information (the experimental data). I think this is the only hope if you want it done on a Government basis.

H. H. Korst: Is there a hope that some organization will take the responsibility at least for the time being? This information is now hoarded and collected by you. Can some responsibility be established, say through a committee, to keep this body of information available?

D. M. Bushnell: Stan Birch really is the one who has collected this stuff. Stan started working in the area about $1\frac{1}{2}$ to 2 years ago and he has an immense pile of information in this area. He was the source for most of the initial data for this conference. The other people I have are regular NASA employees and we are being pushed projectwise just like

[11] Computer Software Management and Information Center, Barrow Hall, University of Georgia, Athens, Ga. 30601.

everybody else is in the Government, and after Stan goes (he is an NRC associate with us), we just do not have anyone who can spend their time cataloging this stuff and storing it.

S. J. Kline: Could I make one comment on this? I quite agree with Mr. Bushnell that our problem is not simply to get the stuff sent to the Ann Arbor microfilm library[12] or something like that. One of the reasons that we were able to do some of the things we did do in the 1968 Conference[13] was that Don Coles had been an archivist on boundary layers for quite a long time. It does take somebody who has some knowledge about which questions to ask and what to compare with what in order to get the right kind of information. It is not just a function of sending it in and putting it on disks. It does need somebody (we appear to have no volunteers just at the moment), but we thought that – I am not volunteering – this freeway should be in somebody else's backyard. That is the problem. If someone would do that it would help a great deal.

M. V. Morkovin: I think we are putting too much emphasis on past data. I believe that the panel actually decided that an awful lot of that data was not that good. I think the emphasis is on new data (new data with better instruments) that is just going to make the other stuff obsolete. Now we do not have any institution short of ASME, Division of Fluid Mechanics, to do something like that. I think that what we can do is to assure that in the future we have sufficiently viable data that can be preserved. I think our emphasis is on the future; I think we have spent too much time on the past.

S. J. Kline: I am sorry if I did not make myself clear. There was no intention to talk about restockpiling past data, but the intention was to have someone look at the data as it came in. We have some questions about data taken 20 years ago which we cannot answer because the people do not remember. If someone could collect the future data, look at it critically and ask those questions, you would get better documented data and it would be available. I am talking about looking toward the future, not looking at the past.

C. E. Peters: It seems to me that all of us have more than one kind of document that we can disseminate. Papers are not the place to present the details of experiments. Most of us have access to some reporting technique, for example, a technical report of some sort, and if it has not been brought up before I strongly suggest that you summarize your results in papers but go to the trouble of writing reports, like Jim Eggers'[14] report or

---

[12] University Microfilms, Inc., Ann Arbor, Michigan.

[13] Kline, S. J.; Morkovin, M. V.; Sovran, G.; and Cockrell, D. J., eds.: Computation of Turbulent Boundary Layers – 1968 AFOSR-IFP-Stanford Conference. Vol. I – Methods, Predictions, Evaluation and Flow Structure. Stanford Univ., c.1969.

[14] Eggers, James M.: Velocity Profiles and Eddy Viscosity Distributions Downstream of a Mach 2.22 Nozzle Exhausting to Quiescent Air. NASA TN D-3601, 1966.

Don Chriss'[15] report from our laboratory, in that kind of detail so that you do not need a central repository for data. It is then recoverable, particularly for those people who have different interests in the experiment than the original experimenter. I picked these two examples because they have relatively good tabulations of the mean flow results, which is one thing that is overlooked so often.

S. Corrsin: I want to make a comment about Dr. Peters' suggestion that published papers could be essentially summaries and that internal reports of some kind could be the repositories of all knowledge. One of the greatest tragedies in public science and engineering in the world has been the growth of the shadow literature of reports which are not generally referenced and which are generally inaccesible to anyone who does not have a Government contract. There is nothing more distressing to a graduate student who does not have a contract than to see a bibliography in someplace like the AIAA Journal where two-thirds of the things referred to are inaccessible to him. I think this is exactly the wrong way to go.

C. duP. Donaldson: Maybe the thing that really should be done, since it is going to be very difficult to get somebody to do this archival job, would be for the people here at NASA to prepare a report which listed what they considered to be the minimum standards for a decent job of reporting a turbulence experiment.

D. M. Bushnell: I think that Professor Kline is much more able to do that especially in regard to the committee activity.

S. J. Kline: We have not dealt with the details of whether one should measure particular kinds of correlations because that is so dependent upon which model you are looking at and also because we are aware of the difficulties that Professor Corrsin just mentioned. There is no point in recommending that somebody measure static pressure correlated with something else if you cannot measure static pressure. I will agree that we should say something about the need to be able to measure static pressure. But I would like to emphasize again what I said in the beginning of this talk that we would like to hear all the ideas from this audience on exactly the point that Dr. Donaldson mentioned. We did include remarks about the need for a variety of flows to be documented, that is, flows where there are large mean strain but not much production as being the kind of thing people ought to think about and investigate.

D. E. Coles: I want to add some detail to some things Steve Kline said in the summary. I am not myself a practitioner of the delicate art of mobilizing armies of rate equations to calculate the development of turbulent flows. I would leave that to the people who are now doing it and others who may wish to join them. I would stop with something much

[15] Chriss, D. E.; and Paulk, R. A.: An Experimental Investigation of Subsonic Coaxial Free Turbulent Mixing. AEDC-TR-71-236; AFOSR-TR-72-0237, U.S. Air Force, Feb. 1972. (Available from DDC as AD 737 098.)

simpler. But, regardless of the use that is to be made of the data, I think it would be refreshing to see a number of experiments done with the attitude that they are dealing with relaxation problems involving some kind of perhaps, linear system relaxing toward an equilibrium state. One of the flows in this conference, the Chevray and Kovasznay flow with a plane wake developing from a boundary layer, is the kind of flow I have in mind. You understand the starting condition for that flow; the boundary layer has been documented to death by now. You understand the wake of that flow. What you do not understand is what happens in between and the defect in those particular measurements is that they do not give enough detail. They do not give enough detail both in kinds of measurements and in the resolutions of the measurements. The exciting things in that relaxation process all happen in about the first two boundary-layer thicknesses behind the trailing edge.

One of the reasons I mentioned this is that we have what I consider to be a very beautiful piece of work by Prabhu and Narasimha,[16] who produced a plane wake with a body which they tinkered around with until the wake was in equilibrium somewhat sooner than it would be behind a cylinder, for example. Then this wake was run through a pressure gradient and the test was to define some measure of the departure from the equilibrium state in the new constant-pressure field and how fast this flow recovered. It turned out that it approached the asymptotic state exponentially. That is a very nice thing to know if you could figure out what the exponent is or how to calculate it. The departure was measured in terms of the difference in the amplitude of the shearing stress distribution compared with the amplitude that went with the velocity profile in the equilibrium state. Given the velocity profile, there are two stress distributions, the equilibrium one and the one you measure. These are different and that difference is the measure of the departure from the equilibrium in this approximation. I have mentioned some other flows that I think are examples of relaxation problems. One of these has to do with the wake behind a body which is not round, for example, rectangular or elliptical. There has been a little work done on this wake, mostly at Colorado State University. These wakes are a little rubbery; the axes downstream in the wake are inverted with respect to the major and minor axes of the body itself.

Jets do the same thing. It would be nice to know something about these flows. Sooner or later somebody will have an idea. I do not claim that I know what should be done with information like this; but I do claim that the more of this that there is the sooner the ideas will appear. Most of these flows (except for the mixing layer which is in a class by itself) flow with variable densities, heated wakes or jets with either density

---

[16] Narasimha, R.; and Prabhu, A.: Equilibrium and Relaxation in Turbulent Wakes. J. Fluid Mech., vol. 54, pt. 1, July 1972, pp. 1-17.
Prabhu, A.; and Narasimha, R.: Turbulent Non-Equilibrium Wakes. J. Fluid Mech., vol. 54, pt. 1, July 1972, pp. 19-38.

differences due to Mach number, or density differences due to composition, are also relaxing flows. There is a significant region of the flow where, if you only looked at the velocity, you would think of it as being in equilibrium, but if you look at the density, there are significant density differences, which are wiped out eventually by entrainment. I am saying that I think that this is a simple corner of the shear flow problem that I would like to see somebody spend some time in. I mention even the experiment by Knystautas.[17] I do not know how many of you are familiar with it but I thought that this was a well-conceived experiment. It was a series of round jets at the trailing edge of an airfoil spaced a couple of diameters apart. Presently what you saw far downstream looked like a plane jet as it obviously would have to, except that I think that if you look carefully enough at it, it might not look like a plane jet – the scale might be haywire.

The reason for this statement is the experience people have had with grid turbulence. As we know the characteristic velocity in a plane wake decreases like $x^{-1/2}$, and therefore if you produce turbulence with an array of plane wakes you would expect the square of that velocity or the turbulence intensity to decrease like x^{-1}, which is about what it does. If you make a grid out of spheres we know that the characteristic velocity downstream of a sphere decays like $x^{-2/3}$. Therefore, the energy in that kind of isotropic turbulence should decay like $x^{-4/3}$ which is a different rule, although the tendency is to think that isotropic turbulence is just that no matter where you find it. Well, the experiment was done by Kistler (unpublished) some years ago at our place. I never saw the results, but my impression was that the decay rates were different.

S. Corrsin: Geneviève Comte-Bellot[18] conducted experiments with a silver dollar grid made out of aluminum at our place and the decay was the same as behind square rods and round rods.

D. E. Coles (speaking from a sketch on the blackboard): I am not sure this is original, but it is a representation of something a student named Ikawa[19] is doing at our place; he is somewhere in the depths of Guggenheim and we see him infrequently. He is interested in the mixing layer in which the external stream is supersonic. The scheme is simply to inject, I believe air, but it obviously does not have to be air, through a porous wall and to adjust the injection rate until the pressure disturbances are a minimum in the external flow. That means you have the entrainment tailored right, the entrainment on the low-speed side. All sorts of nasty things happen to you when you try to do this, like secondary

---

[17] Knystautas, R.: The Turbulent Jet From a Series of Holes in Line. Aeronaut. Quart., vol. XV, pt. 1, Feb. 1964, pp. 1-28.

[18] Comte-Bellot, Geneviève; and Corrsin, Stanley: The Use of a Contraction To Improve the Isotropy of Grid-Generated Turbulence. J. Fluid Mech., vol. 25, pt. 4, Aug. 1966, pp. 657-682.

[19] Hideo Ikawa is a student of Dr. Toshi Kubota, Professor of Aeronautics at California Institute of Technology. The Ph. D. thesis of Ikawa is to be published in June 1973.

flows in the cavity and so on. They also found that they had to put a thing downstream to steer the flow out of the cavity and to minimize the pressure disturbances; otherwise, there is liable to be a separated region there and some shocks and so forth. But this is a geometry that I think might be very useful in looking at what I consider to be the deepest mystery in the subject right now – the effect of density on the mixing layer. As far as I can tell, that is a mess! Certainly, if no other experiments get done, I would like to see that subject cleared up.

REPORT OF CONFERENCE EVALUATION COMMITTEE

By Mark V. Morkovin (Chairman), Illinois Institute of Technology;
Dennis M. Bushnell, NASA Langley Research Center;
R. B. Edelman, General Applied Science Laboratories, Inc.;
and Paul A. Libby, University of California at San Diego

INTRODUCTION

For the past 2 days we have been exposed to the concentrated comparison of screened data with the results of months and months of effort on the part of our best predictors. Apparently some honing of the methods took place even before the conference as the predictors generally confronted a broader range of flows than those which conditioned the original choices of their empirical constants or functions. Thus, part of the objectives of the conference were accomplished before its start.

To the working engineer the proliferation of the methods appearing helter-skelter in the journals has presented a confusing picture. We believe that the codification of these methods and their exposure to the same broad set of data should go a long way in clarifying the limits of validity and the areas of usefulness of the different classes of methods.

As the reader can judge, the presentations were uneven and the results do not lend themselves to easy evaluation. It would indeed be presumptuous and unscientific to render any definitive judgments on the performance of the 13 heterogeneous predictive methods in the conference; we could do more damage than good. This situation is, in part, brought about by the less satisfactory state of experimental information for free shear layers than for attached boundary layers.

Rather, we shall report on our strongest impressions of the issues pertinent to the modeling of turbulent flows primarily for applied objectives, as conveyed by comparison figures[1] (pp. 699 to 737), and by the lively discussions during the conference sessions (which many participants continued late into the night). An engineer interested in free turbulent shear flows will find these figures a gold mine of information. In fact, the experimental data with the many theoretical predictions provide him with a zeroth-order tool for his own quick engineering estimates. He is also referred to the correlation of Stanley F. Birch and James M. Eggers (paper no. 2) for the spreading rate of simple mixing layers which is useful on the same level.

[1]Only a small part of these comparisons was available to the Conference Evaluation Committee. Thus, we could not pinpoint several of the methods which leave a lot to be desired.

Before we proceed to the predictive methods themselves, we need to consider the potential uses of these methods and relate them to the distinguishing characteristics of the methods. Advances in technology usually involve the development of more efficient systems out of existing concepts. Examples include reductions in system size and weight through optimization of cooling requirements and reaction volumes in (1) power generating equipment, (2) propulsion and vehicle systems, (3) varieties of chemical process plants, and (4) specialty hardware such as in gas dynamics and chemical laser systems. In many of these systems public concern over the questions of thermal, chemical, and noise pollution must also be considered in present and future designs. Achieving high performance, as well as controlling pollutant emissions (where appropriate), requires the development of highly accurate predictive techniques. Such systems usually contain turbulent free shear layers and mixing zones (including jets and wakes). The understanding and description of these turbulent shear flows should enable us to predict the structure of the flow field and determine relationships among design parameters. Due to the intractable nature of turbulent flows, approximate mathematical models must be formulated to describe these turbulent processes.

Many problems require definition of the mean flow only. Quantities of interest include the spreading rate, penetration, and degree of nonuniformity in the mean-flow properties downstream of the origin of the mixing zone. The aerodynamic influence of a shear layer on its environment and the effectiveness of momentum exchange and fuel distribution in a combustor are typical examples of problems requiring primarily a definition of mean-flow properties. For these problems a simple representation may be employed for the turbulent exchanges. However, these models must account accurately for the effects of velocity, temperature and density differences, and pressure gradients.

Another class of problems requires more detailed descriptions and computations of the turbulent structure. These problems include (1) the propagation of disturbances through turbulent layers, (2) the generation of noise, (3) dynamic loads on aircraft, and (4) flows involving kinetic processes where the reactants are not intimately mixed and rates of reaction cannot be defined in terms of mean-flow properties only. For example, predictions of ignition and pollutant emission are crucially sensitive to trace amounts of free radicals and these, in turn, depend upon the local turbulent spectrum. It is therefore apparent that the complexity required in turbulence modeling depends on the problem. That is, the selection of a method should depend upon a careful determination of the information required to resolve the particular needs of the user. It would be unreasonable to employ a highly complex method where only gross quantities are needed. Conversely, low-order techniques cannot be expected to provide answers to problems requiring detailed information on turbulent structure.

CLASSIFICATION OF METHODS OF INCORPORATING TURBULENCE EFFECTS

As indicated by the wide variety of methods presented at this conference, there are a number of approaches to the prediction of turbulent shear flows. It seems worthwhile to make a general classification of these approaches in order that minor differences between two methods should not obscure their commonality and that we may see where the various contributions to the conference fit into a broad methodological structure. This classification will pertain to the means by which the physics of turbulence is incorporated into the describing equations, not to the means by which the resulting equations are solved.[2] To emphasize the distinction, the equations developed for a sophisticated closure scheme could conceivably be solved by an integral method, although to do so would not be reasonable.

The basic problem in the description of turbulent flows (as usually treated in terms of the time average of the dynamical variables and their correlations) is that an open-ended hierarchy of equations results from the systematic treatment of the original, time-dependent conservation equations. This is the so-called closure problem. To illustrate, for constant-density flows the momentum equation corresponding to direction x_i involves the mean velocity components $\bar{u}_i$ $(i = 1, 2, 3)$, the mean pressure $\bar{p}$, and the six correlations $\overline{u_i'u_k'}$ $(i,k = 1, 2, 3)$. In many flows of applied interest, boundary-layer approximations and other simplifications apply so that these six reduce to one, namely, $\overline{u_1'u_2'}$.

Until recent years this problem was overcome, in most engineering problems, by introducing a closure model at the first level in hierarchy, e.g., by formally introducing an eddy viscosity ϵ, so that $-\overline{u_1'u_2'} = \epsilon\left(\partial u_1/\partial x_2\right)$ and by then relating ϵ to specified flow properties and to the dependent variables. Today this approach provides only one class of methods for turbulent free mixing flows. The variations on the eddy-viscosity approach involve introduction of mixing length concepts, turbulent Prandtl and Schmidt numbers, and sophisticated correlations for ϵ involving a variety of effects – for example, variable density. In view of the minimal content of the physics of turbulence in this class of methods, it is somewhat surprising that in many problems of applied interest entirely adequate answers are provided. This can be seen for several of the contributions to this conference, especially where empirically determined constants are grafted on the correct dimensional constraints of the procedure. Thus, if the problem relates to the spreading rates and diffusion – either of a coaxial jet in a moving stream or of the wake of a reentry body – the customary and generally adequate approach for its solution would involve utilization of some appropriate model for ϵ, preferably one which has been verified by comparison with experiment in a closely related flow. This situation concerning

[2] The reader would benefit greatly at this stage by referring to reference 1 and to sections 4 and 5 of reference 2. Longer discussions can be found in references 3 and 4.

the utility of eddy-viscosity methods is likely to continue; that is, such methods will be entirely adequate for many problems. In this conference the contributions of David H. Rudy and Dennis M. Bushnell (paper no. 4); L. S. Cohen (paper no. 5); H. H. Korst, W. L. Chow, R. F. Hurt, R. A. White, and A. L. Addy (paper no. 6); Joseph A. Schetz (paper no. 8); J. H. Morgenthaler and S. W. Zelazny (paper no. 9); and V. Zakkay, R. Sinha, and S. Nomura (paper no. 10) fall within this first classification.

As mentioned previously, there do arise in engineering applications problems which involve more of the physics of turbulence than is contained in eddy-viscosity approaches. In addition, there are cases in which the eddy-viscosity approaches are inadequate for the prediction of mean properties. For example, flows which involve abrupt changes in the character of the main stream, with the so-called nonequilibrium effects and relaxation to a new dynamical state, are not well predicted by methods employing eddy-viscosity concepts because of their local nature.[3] Because of this situation and because of the advent of high-speed computers which make feasible the numerical treatment of complex systems of partial differential equations, new approaches have been developed in recent years which incorporate more of the physics of turbulence into the describing equations. These approaches possess greater variety and flexibility. At this conference the contribution of B. E. Launder, A. Morse, W. Rodi, and D. B. Spalding (paper no. 11) provides an excellent review of several of these new methods; an earlier paper by W. Rodi and D. B. Spalding (ref. 5) gives a somewhat broader perspective.

These new methods may be characterized according to whether they introduce the turbulent kinetic energy alone or other velocity correlations as well, and according to whether the one or more length scales which arise in the analysis are specified algebraically in terms of computed quantities such as the thickness of the mixing layer, or are defined by partial differential equations. For clarity, consider one of the early types of these new methods. (See ref. 6 and paper no. 16 by Thomas Morel, T. Paul Torda, and Peter Bradshaw.) It has been observed that in a wide variety of flows the mean turbulent shear is related algebraically to the turbulent kinetic energy; that is, $\overline{u'v'} = a\overline{q^2}$, where a is a semiempirical function. Thus, one adds to the usual set of mean equations, the equation for the conservation of $\overline{q^2}$, an equation which is on the second level of the hierarchy of describing equations. However, this equation involves certain correlations, for example, the triple correlation $\overline{u_2'u_i'u_i'}$. These must be described in terms of the principal dependent variables by what is usually called "structure" or "modeling"; the modeling process introduces at least one length scale. In applications of this early method, only one length scale appears and is taken to be an algebraic function of the thickness of the shear layer.

---

[3]The method presented by David H. Rudy and Dennis M. Bushnell (paper no. 4) attempts by appropriate phenomenology to extend the mixing length concept to some of these problems.

A closely related method is termed the "Prandtl energy method" wherein the eddy viscosity is expressed in terms of $\overline{q^2}$ so that

$$-\overline{u_1'u_2'} \propto q\Lambda \frac{d\bar{u}_1}{dx_2}$$

where Λ is a suitable length scale. Again an equation for Λ must be established.

Further developments involve use of the conservation equations for velocity correlations other than those associated collectively with $\overline{q^2}$. Each of these equations are entries in the second level of the hierarchy of describing equations and involve modeling to close the set of equations. Indeed, a separate equation for the mean shear $\overline{u_1'u_2'}$ can be included. It will be recognized that these methods provide, as part of the solution procedure, predictions for some of the physical aspects of turbulence. For example, in the method outlined above, the turbulent kinetic energy is found in the course of the solution and this may be of interest by itself. Furthermore, the mean shear depends on the turbulent kinetic energy which involves convection, diffusion, and dissipation and therefore involves an upstream history. Accordingly, the shortcomings listed previously regarding nonequilibrium effects may be more readily overcome.

In applications of these methods involving well-defined length scales, the assumption of relatively simple relations for these lengths is justified. However, in problems involving more than one scale (e.g., when two shear layers with different characteristic dimensions interact or when a turbulent boundary layer expands around a downstream facing step), these simple relations are not convincing and more complicated means of describing the length scale (e.g., by partial differential equations) are probably needed. There are at least three means for deriving appropriate length-scale equations; each generally involves a high degree of modeling with attendant possibilities for error.

The many feasible combinations of correlations and length scales make possible a wide variety of methods and have led to a proliferation of publications on these methods in recent years – a mixed blessing. These new methods are under rapid development; some will become obsolete through further refinement. Their utilization should be undertaken only if the nature of the flow and of the desired information warrants dissatisfaction with the less sophisticated methods. It should be emphasized that the incorporation of the elusive effect of variable density into these methods has only been tentative and that much improvement is in order in this regard.

The new methods require specifications of initial data – for example, the distribution of turbulent kinetic energy or other correlations at some initial station. Thus exploitation of these more powerful methods for more accurate predictions, in fact, requires more detailed a priori knowledge of the initial features of the flows than is generally

available.[4] Scattered evidence suggests that downstream developments of free shear flows are more sensitive to such details of initial turbulent structure than are developments in wall boundary layers, both experimentally and numerically. Adequate assessment of the new methods involving turbulence characteristics will naturally place additional demands on the experimentalists. As additional correlation terms which are explicitly modeled in the theories become accessible to direct, accurate measurements, the credibility of the methods could increase convincingly beyond that based on present comparisons of gross quantities and mean profiles. In this connection reference is made to the report of the Committee To Recommend Critical Experiments, and to the open forum discussion disclosing scepticism as to the relevance of the Reynolds' type of averaging to the important physical mechanisms governing the flows.

At this conference in addition to the contributions of B. E. Launder et al. (paper no. 11), those of Paul A. Libby (paper no. 12), P. T. Harsha (paper no. 13), P. M. Heck and M. A. Smith (paper no. 14), P. J. Ortwerth (paper no. 15), Thomas Morel et al. (paper no. 16), and C. E. Peters and W. J. Phares (paper no. 17) involve these newer techniques.

IMPRESSIONS

When the reader embarks upon his own study of the results in the comparison figures (pp. 699 to 737), he would do well to refer constantly to the classification sheets (pp. 739 to 761) for the concise description of the methods as well as for an appreciation of the costs.

– Substantial progress has been made in sharpening the predictive capability for both mean and turbulent quantities in several basic flow configurations. Yet no single technique appears sufficiently general to warrant classification above all others.

– The cross-checked and related group of methods reported by the team at the Imperial College of Science and Technology represents a broad approach which promises a systematic development toward a practical degree of generality.

– The one integral technique presented is adequate for mean properties but while more flexible than other integral methods, it cannot provide the details of the flow offered by finite difference methods.

– The selection of a method by a user should be based upon the requirements of the problem and the cost of computations.

– Information concerning computational costs can be determined from the data given on the program descriptions in the classification sheets (pp. 739 to 761).

---

[4]See also comments on the "near field" in the report of the Committee To Recommend Critical Experiments.

– Many methods have been oversold. It is most important to specify limitations of regions of applicability of the methods; this has rarely been done in the past.

– One wonders what the agreements would be if the answers were not known.

– Methods in the same formal category may be quite different in their effectiveness. It apparently depends, in part, on who is using the procedure and on the details of the modeling or fitting of empirical constants. When an author's method is employed by a competitor for comparison purposes, the author invariably complains that his method was not used to the best advantage by hands unfamiliar with the fine points.

SPECIFIC PROBLEMS

Variable Density

In many important turbulent flows, the density varies in space and time due to variations (a) in temperature or (b) in composition, or both. To describe these flows the various predictive methods for turbulent flows with constant density must be extended or reformulated to take into account satisfactorily the effects of variable mean and fluctuating density for both cases (a) and (b). This is one of the central problems in applied turbulence research. However, the physics of such flows must be better understood before their analytic description can make substantive progress. The report of the Committee To Recommend Critical Experiments has emphasized the role of high-quality experimentation in developing this understanding.

The equations describing the mean flow field and the various correlations, in cases involving variable density, can be written in a variety of ways depending on how the decomposition into mean and fluctuating quantities is performed. For free shear flows of interest here, the consideration of mass-averaged quantities after Favre (ref. 7) leads to equations which are more compact. But if the quantities which are desired either for comparisons with experiment or for purely predictive purposes involve conventional time averages, then some estimates of the correlations involving density must be made a posteriori. On the other hand, if all dynamical quantities are decomposed in the straightforward manner into a mean-plus fluctuation, the resulting equations are cluttered and various a priori approximations must be considered.[5] No matter which approach is used for describing equations and/or method of solution, the means for incorporating the effects of variable density are generally unclear.[6]

---

[5]In the conference, J. Laufer cautioned that in some cases the experimenter may be measuring a mass-averaged quantity without being aware of it.

[6]As a revealing exercise the reader is urged to decide on a consistent mean equation of state for a perfect gas by perturbing the instantaneous forms $p = R\rho T$ and $RT = p/\rho$ (where p is pressure, R is gas constant, T is temperature, and ρ is density).

One should keep in mind that in many flows of applied interest large variations of density do not persist over extended downstream regions. For example, in the case of an axisymmetric jet of hydrogen injected coaxially into an airstream, the mean concentration of hydrogen on the axis decreases rapidly, so that within several orifice diameters on the order of 10, the mean-density difference from the axis to the external flow becomes relatively small. Such insensitive flows do not provide crucial tests of predictive methods, although for the practicing engineer agreement between prediction and experiment may be all he requires.

One class of turbulent shear flows appears crucial for the careful assessment of the effects of variable density. These are the two-dimensional mixing layers wherein the variable density arises from differences in velocity, temperature, or composition in the two mixing streams. In these flows the density differences persist indefinitely in the downstream direction. In addition, the corresponding equations have self-similar solutions so that their numerical analysis can be greatly simplified and the effects of variable density clearly exposed.

Unfortunately, two-dimensional mixing flows exhibiting unequivocal self-similarity are difficult to establish in the laboratory. The effects of initial boundary layers, of transition, and of adjacent walls in both directions (in the XY- and XZ-planes in the usual notation) appear to alter even gross but essential properties of the mixing such as the spreading parameter σ. To illustrate, we consider a special case of two-dimensional mixing, involving a high-speed airstream mixing with quiescent air under conditions such that the stagnation temperature of the moving stream equals the static temperature of the quiescent gas. This is the so-called compressible adiabatic case for which the Mach number M_1 in the high-speed flow provides the only parameter. (More generally $(1/2)(\gamma - 1)M_1^2$ should be considered the parameter (where γ is the ratio of specific tests), but since air is the only gas considered in such flows to date, we confine our attention to M_1.) The effect of M_1 on σ is at present obscure; some data indicate no effect of M_1 on σ whereas other data indicate a significant effect. Similar discrepancies exist for the low-speed mixing of dissimilar gases, e.g., helium and air. These points were brought out and emphasized at the conference in the contribution of Stanley F. Birch and James M. Eggers (paper no. 2).

It thus appears crucial to the development of accurate predictive methods for turbulent shear flows with variable density that high-quality, experimental data be obtained on a few examples of two-dimensional mixing layers with large density differences in the two streams. (For further insight and problems of implementation see the report of the Committee To Recommend Critical Experiments.) Before these are available, the various extensions to include variable density of existing predictive methods for turbulent shear flows must be considered provisional, and they cannot be used with confidence in many flows of applied interest.

Sensitivity of Prediction Methods to Parameter Values and Initial Data

We feel that many of the current methodologies cannot be fully relied upon for general application until their sensitivities to (a) selection of "empirical" coefficients and (b) specification of initial conditions has been documented. Although this type of study was not provided for at the conference, the generality and practical utility of each technique depend largely upon the implications of these sensitivities. We believe that such studies should be performed so that both the theoretical implications and the practical requirements for initial conditions can be defined.

Pressure Fluctuation Terms

Operationally, we view the predictive methods as sophisticated interpolation schemes subject to basic physical constraints, which connect functionally the past empirical data. Whenever we add another algebraic or differential equation to account for the development of another feature of turbulence, we increase the capacity of the scheme to fit better various selected characteristics of the exceedingly complex turbulent fields. It is not surprising that the extra mathematical flexibility (bought at a price which should be properly weighed by the user) leads to better predictions – within the confines of past empirical information. As the predictor works with his program, the terms in his equations tend to acquire a reality of their own which should not be confused with physical reality. Time and again this distinction is brought home with a shock as the predictor applies his machinery to regimes beyond the original empirical foundations, such as we witnessed here in connection with large density changes and higher Mach numbers.

We foresee steady progress in the refinements of the differential field methods commensurate with the need for answers to more refined technological problems, for example, for flows with reactions. The progress, however, could be more apparent than real if the modeling of the turbulence terms do not mirror physical reality accurately. The currently most suspect group of terms describes the effect of the fluctuating pressure, namely, $\overline{u \frac{\partial p}{\partial x}}$ and $\overline{v \frac{\partial p}{\partial y}}$. These terms are usually transformed (utilizing incompressible continuity $\frac{\partial u}{\partial x} + \frac{\partial v}{\partial x} = 0$) and lumped together with "convective diffusion terms," which are distinctly different in physical nature. In compressible flow, continuity involves density derivatives and the difference in the terms is thereby underscored. Since these terms grow with M^2, their careful treatment at supersonic speeds is desirable. We commend to you the remarks of J. Laufer (pp. 687 and 688) on their possible important role in compressible turbulence. These pressure fluctuation terms may well hold the key to the understanding of the changes in free turbulence at supersonic speeds, including the appar-

ent decrease in the spreading rate. The compressible turbulence experts conjecture that these effects would be felt in free turbulent flows at lower Mach numbers than in attached turbulent boundary layers (primarily because of the low-speed wall constraint). Thus the free-shear-layer workers have an extra task as well as an extra opportunity for research.

Gradient Diffusion

In almost all closure schemes including the basic eddy-viscosity models it is assumed that the mean flux of some quantity is proportional to the gradient of an appropriate quantity, for example,

$$\overline{u_1' u_2'} \propto \frac{\partial \bar{u}_1}{\partial x_2}$$

Such assumptions are made at several stages in the analysis in the new closure schemes. Although such models have been used extensively for a long period of time and are repeatedly employed in a casual, uncritical manner, it was emphasized at the conference that gradient diffusion, in principle, applies only when the length scale associated with the large eddies is small in comparison with a length characterizing the gradient. Since this is generally not the case in shear flows of applied interest, it is clear that the use of gradient diffusion must be considered risky.

Alternatives include a bulk diffusion expression and combined bulk and gradient diffusion. (See ref. 8.) In Bradshaw's method for turbulent shear flow (ref. 6 and paper no. 16), the turbulent kinetic energy equation is closed with a bulk diffusion model. However, the general preference for gradient diffusion persists among developers of predictive methods. With improved measuring and computing capabilities, renewed attention should be given to careful assessments of alternative modeling of the various diffusion terms.

Low Reynolds Number

There is evidence that many of the research experiments – and for that matter the intended applications – show Reynolds number sensitivity. For the simple mixing layers the energy supply from the two cocurrent streams is infinite in principle, and we expect an asymptotic approach to a Reynolds-number-independent, self-similar shear layer if we only march far enough downstream. However, the jet and wake flows may be conditioned by low Reynolds number effects throughout their lifetimes. The turbulence structure then may not be "universal," and the measurement and adequate predictions of these flows may present special problems.

We believe that insufficient attention has been paid to understanding of the implications of a larger, active role of viscosity in turbulent shear flows either experimentally or theoretically and to developing modified techniques for computation of flows at lower Reynolds numbers. Some of the apparent experimental scatter may well be a reflection of the unavoidable nonuniversality.

What appears to be needed are simple rules for the experimentalist to use in order to suppress Reynolds number as a parameter. Some years ago, Corrsin provided a lower bound for the Reynolds number of a low-speed circular jet discharging into quiescent air. Bradshaw has done something similar for the two-dimensional, low-speed mixing layer (see paper no. 2). How their rules are affected by high speed and by variable density is not known.

Influence of Geometry

We agree with A. Roshko's remark (during discussion of paper no. 16) about the possibility of real difference in the turbulence structure of two-dimensional and axisymmetric turbulent flows. Although the impact may not be large on our present methods – mostly changes of coefficients – the potentially different structure of the large energetic eddies should entail consequences for the more detailed properties of the flows.

NON-BOUNDARY-LAYER ANALYSES

One of the essential features of all the prediction techniques presented at this conference is the use of the boundary-layer approximation. Evidence of non-boundary-layer effects appeared in some flows used in the conference, such as in wakelike jet flows and mixing regions involving large entrainment rates. Flow situations of this type raise doubts concerning the approximation that $\bar{v}/\bar{u} \ll 1$. In addition, there are flows in which displacement effects and longitudinal curvature alter the streamwise and normal pressure gradients, respectively.

In the case of laminar flow the method of matched asymptotic expansions provides a systematic method for accounting in part for these effects which may be associated with non-boundary-layer phenomena inasmuch as they are not included in the classical boundary-layer theory. In view of the considerable phenomenology we must introduce in order to describe turbulent thin shear layers, it appears inappropriate to use the machinery developed for laminar flow on our turbulent cases. However, some of the physical ideas which evolve from the treatment of laminar flows – for example, in accounting for the effects of large entrainment rates (suspiciously large $v^{(1)}(x,\infty)$ in the usual notation of "inner solutions") and for displacement and curvature effects – may well provide the basis for handling their counterparts in turbulent flows in a rational but nonformalistic way.

In this matter of non-boundary-layer effects, attention might well be called to a contribution of Bradshaw (ref. 9) which shows that many of the complex turbulent flows that are important in engineering are recognizable as perturbations of the classical thin shear layers. The point here is that we should carefully assess the nonclassical, non-boundary-layer effects at hand because, as Bradshaw points out, we may be able to treat these effects as perturbations to our familiar methodology rather than to plunge into an unwarranted formalism.

Behind all the activity related to flows of the boundary-layer type such as dominated this conference looms the specter of many flows which arise in practical applications and which have none of the features required for application of the boundary-layer approximation. Frequently, such flows are turbulent and are amenable only to experimental analysis. Even here our knowledge of turbulence should prove useful with respect to development of the appropriate scaling and similarity laws.

THE ROLE OF THE COMPUTER IN TURBULENCE STUDIES

One of the pregnant questions which arose in the discussion during the conference concerns the role of the high-speed computer in turbulence studies of interest to engineers and engineering scientists. There are already underway at various centers (e.g., ref. 10) studies of elementary flows – for example, flow in a cavity – in which the time-dependent Navier-Stokes equations are solved with random initial conditions. After sufficient computing time, statistics of the flow, such as the various correlations of interest, can be computed and the turbulence characteristics determined.

In this conference, J. R. Herring of the National Center for Atmospheric Research (paper no. 3) discussed several current attempts to utilize the high-speed computer in turbulence research. For a given Reynolds number, such methods attempt to reduce the computing time and increase the accuracy from that required by a brute-force attack on the Navier-Stokes equations. The rapid expansion of the power and speed of the digital computer and the steadily decreasing cost per operation raise the prospect that in the foreseeable future such techniques can be employed on problems of interest to engineers, e.g., turbulent shear flows of great complexity. It is clear from the discussion of this prospect (see the remarks of J. R. Herring, D. R. Chapman, D. B. Spalding, and S. C. Lee in the Open Forum) that there is no unanimity on this matter. It does seem certain that these new methods will continue to be developed as the capacity of digital computers grows and that certain idealized numerical experiments will be carried out with them. The results thereof may be analogous to the fundamental, high-quality experiments which presently play such a central role in the development of turbulence theories and methods. What is not clear is the impact of these developments on the engineering methods which evolve from those presented at this conference.

REFERENCES

1. Reynolds, W. C.: A Morphology of the Prediction Methods. Computation of Turbulent Boundary Layers – 1968 AFOSR-IFP-Stanford Conference, Vol. I, S. J. Kline, M. V. Morkovin, G. Sovran, and D. J. Cockrell, eds., Stanford Univ., c.1969, pp. 1-15.

2. Bradshaw, P.: The Understanding and Prediction of Turbulent Flow. J. Roy. Aeronaut. Soc., vol. 76, no. 739, July 1972, pp. 403-418.

3. Reynolds, W. C.: Computation of Turbulent Flows – State-of-the-Art, 1970. Rep. MD-27 (Grants NSF-GK-10034 and NASA-NgR-05-020-420), Dep. Mech. Eng., Stanford Univ., Oct. 1970. (Available as NASA CR-128372.)

4. Rotta, Julius C.: Turbulente Strömungen – Eine Einführung in die Theorie und ihre Anwendung. B. G. Teubner Stuttgart, 1972.

5. Rodi, W.; and Spalding, D. B.: A Two-Parameter Model of Turbulence, and its Application to Free Jets. Wärme- und Stoffübertragung, vol. 3, no. 2, 1970, pp. 85-95.

6. Bradshaw, P.; and Ferriss, D. H.: Derivation of a Shear-Stress Transport Equation From the Turbulent Energy Equation. Computation of Turbulent Boundary Layers – 1968 AFOSR-IFP-Stanford Conference, Vol. I, S. J. Kline, M. V. Morkovin, G. Sovran, and D. J. Cockrell, eds., Stanford Univ., c.1969, pp. 264-274.

7. Favre, A.: Statistical Equations of Turbulent Gases. Problems of Hydrodynamics and Continuum Mechanics. Soc. Induct. & Appl. Math., 1969, pp. 231-266.

8. Townsend, A. A.: The Structure of Turbulent Shear Flow. Cambridge Univ. Press, 1956, pp. 107-110.

9. Bradshaw, Peter: Variation on a Theme of Prandtl. Turbulent Shear Flows, AGARD-CP-93, Jan. 1972, pp. C-1 – C-10.

10. Fox, Douglas G.; and Lilly, Douglas K.: Numerical Simulation of Turbulent Flows. Rev. Geophys. & Space Phys., vol. 10, no. 1, Feb. 1972, pp. 51-72.

DISCUSSION

R. B. Edelman: As a member of the industrial community, I would like to add some comments to help put certain aspects of the proceedings into perspective. Some of us have some very relevant practical problems to cope with, and, each day, these are becoming very much more complicated. We are the first to realize and appreciate the need for a better understanding of turbulence. Although this need is apparent, we cannot lose sight of the realities of complex models which would serve to discourage potential users from applying them, simply because the theoretical model developers have not concerned themselves with aiding in how these models should be applied. For example, in classes of problems which may require the higher order methods, the specification of initial conditions becomes more demanding. This must be the concern of both the theoretician as well as the user. If this isn't the case, then I think that we are both going to lose. Secondly, although this conference has focused on the free shear layer, and specifically the fluid mechanics aspects of the mixing process, there are numerous problems of practical relevance which even though fundamentally more complicated are in current need of solution. Specifically, I am referring to problems involving mixing inside ducts (combustion chamber problems, for example, which embody a wide variety of applications), turbojet engines, rocket engines, and furnaces. Then one must include the problems of kinetic processes, multiphase flows. There has been no mention of these aspects which are not problems that can wait until the simpler yet very instructive free-shear-layer unbounded flows are fully understood before we move on and tackle these more practical aspects. I refer to them as more practical, but they are simply problems that are in current need of a solution. What I would like to see is how these current systems of equations work now. This will help to determine the paths that should be followed to provide current stopgaps and to provide some direction for continued research. I think we should do this concurrently while we are looking at the more simple flows where it has been made quite clear, during the past 2 days, that there are many things that we don't understand. If we don't do this, and we try to work in series, instead of in parallel, I think that some valuable information and insight will just not be available on a timely basis.

D. M Bushnell: I have one very simple comment: I have been playing for a number of years in the sandbox of very high Mach number turbulent boundary layers. If one looks at the equations, there are some very interesting p' and ρ' terms, the type of terms that at Mach numbers less than 5 are usually dropped but now should be included. We have obtained data at very high Mach numbers where we have density changes across these boundary layers on the order of 100. When we look at these data and try to compute them, I for one have been disappointed because when we put in low Reynolds number effects, we can compute them. We have no right being able to compute them. At this conference, at long last, it looks as if the free shear layer is a flow which may exhibit

some Mach number effects. Finally, we have a flow where we can start seeing if the p' and ρ' terms are important. I hope that this is the case. I hope we aren't just missing something in the experiments, such as secondary flows in the apparatus, which are tending to change the entrainment rate. Several years ago I heard Donaldson cite the example of an open jet in a hangar, and when the hangar door was opened, the entrainment rate changed. This sort of a thing bothers me. I just hope that we have a nice juicy problem here, which will tax us, rather than just something that is going to eventually degenerate into some very simple answer in terms of some inviscid effects, or some quirk in the experimental data.

J. Laufer: The question, of course, has concerned us for a number of years: In what way do compressibility effects alter a turbulent flow?

Purely from a formalistic approach, one may get a first indication for an answer if one follows Lagerstrom's arguments used on laminar flows[1] and applies them to the mean equations of motion describing turbulent flows. If the equations are put into a proper non-dimensional form, one can see right away that the Mach number appears explicitly in the equation for the mean static enthalpy as the coefficient $(\gamma - 1)M^2$ in the work term $\overline{u_i \frac{\partial p}{\partial x_i}}$ and as $\frac{M^2}{Re}$ in the dissipation term. For high Reynolds number flows of particular significance is the work term containing the pressure fluctuations. This may be seen further by considering the equations for the turbulent kinetic energy and for the mean static enthalpy:

$$\frac{\partial}{\partial x_j}\left(\overline{\frac{1}{2}\rho u_i' u_i' \tilde{u}_j}\right) = \overline{-\rho u_i' u_j'}\frac{\partial \tilde{u}_i}{\partial x_j} \boxed{\overline{-u_j'\frac{\partial p}{\partial x_i}}} + \frac{\partial}{\partial x_j}\boxed{\overline{u_i'\left(\tau_{ij} - \frac{1}{2}\rho u_i' u_j'\right)}} \boxed{\overline{-\tau_{ij}\frac{\partial u_i'}{\partial x_j}}}$$

$$\frac{\partial}{\partial x_j}\left(\bar{\rho}\tilde{h}\tilde{u}_j\right) = \tilde{u}_j\frac{\partial \bar{p}}{\partial x_j} \boxed{+\overline{u_j'\frac{\partial p}{\partial x_i}}} + \frac{\partial}{\partial x_j}\left(\bar{q}_j - \overline{\rho h' u_j'}\right) \boxed{+\overline{\tau_{ij}\frac{\partial u_i'}{\partial x_j}}} + \overline{\tau_{ij}}\frac{\partial \tilde{u}_i}{\partial x_j}$$

The terms that explicitly show an energy interchange between the mean and turbulent flow (terms that occur in both equations but with opposite signs) are shown in the dashed boxes. Now since the interaction due to viscosity usually occurs at high frequencies where the energy level is low, it is primarily the term containing the pressure that indicates the important new sources (or sinks) for the production of turbulent energy in addition to the well-known production term involving the Reynolds stresses.

[1] Lagerstrom, P. A.: Laminar Flow Theory. Theory of Laminar Flows, F. K. Moore, ed., Princeton Univ. Press, 1964, pp. 20-285.

Let us now try to speculate about the physical process through which such an interchange might come about. The term in question can be rewritten as follows:

$$\overline{u_i' \frac{\partial p}{\partial x_i}} = \frac{\partial}{\partial x_i} \overline{u_i' p} - \overline{p \frac{\partial u_i'}{\partial x_i}}$$

where the first term on the right-hand side of the equation represents a spatial gradient transport of energy and our attention should be concentrated primarily on the second term that represents interchange between internal and kinetic energy. In incompressible flows this term is usually referred to as the "tendency toward isotropy" term since it expresses the action of the pressure due to which the u component of the turbulent kinetic energy (generated by the $\overline{\rho u'v'}$ stress) is partially transformed into the v and w energy components making the net value of this term vanish; that is,

$$-\overline{p \frac{\partial u'}{\partial x}} = \overline{p \frac{\partial v'}{\partial y}} + \overline{p \frac{\partial w'}{\partial z}}$$

It is conjectured that in a compressible flow such a balance does not take place. Using a somewhat descriptive rather than exact terminology, one may say the flow is stiffer and more resistive to changes in the direction of large Mach number gradients; consequently, less energy is transferred into the v component. This fact has then the important consequence that the Reynolds stress $\overline{\rho u'v'}$ becomes smaller and, therefore, the turbulent transport process becomes less efficient. Furthermore, the nonzero value of the dilatation $\frac{\partial u_i'}{\partial x_i}$ brings about changes in the density. These density changes can be seen in a most dramatic fashion on a holograph picture of the outer edge of a turbulent jet. It is known that at the outer edge the occasionally outward moving (with v velocity) "turbulent bumps" interact with the ambient field producing pressure fluctuations. At low speeds these fluctuations are clearly incompressible. As the jet velocity is increased, the spreading angle decreases and clearly distinguishable density variations appear around the turbulent bumps. It is conjectured that these density fluctuations arise due to the dilatation effect of the compressibility which inhibits motion in the radial direction.

I have to emphasize that the above discussion is quite speculative; it is given mainly with the hope that it will stimulate more thorough studies on this question.

M. V. Morkovin: I would like to thank Dr. Laufer. Obviously, I asked him to comment on the modeling of the pressure-velocity correlation terms, especially at higher Mach numbers. Remember, it is with respect to the spreading that all of our methods were having

difficulties. The high Mach number spreading was really the one thing that was most off, and the possibility that we are not modeling right in that direction is why we are talking about it now.

J. A. Schetz: I would like to make two comments – one technical and one a formalism about the evaluation. If we are going to tabulate the comparisons of all the predictors with the data, I think it would be worthwhile to make some unified scoreboard of other features of the method. After all, their relative accuracy of prediction is not the only evaluation that a potential user might make. Other factors might be types of problems that can't be treated (some of the eddy-viscosity models will obviously fall into this category) and typical time for computation. There are a lot of other measures of the usefulness of procedure which perhaps should be tabulated in this publication.

H. H. Korst: Is it your feeling that the questionnaire that has been passed out to the predictors at this conference may have been incomplete or composed in haste and should it be revised and made more complete, or do you have any other suggestions?

J. A. Schetz: Well, I think that most people put down approximate times. Perhaps we should be asked how long it took us to do a couple of representative cases. I mean, most people guessed at the time it took them or estimated the time.

D. M. Bushnell: We will be corresponding with the authors anyway and we will send along another sheet which they can fill out or, if they wish, we will use the original.

J. A. Schetz: I would like to mention again that we have measured rather substantial static pressure gradients in situations which are perhaps surprising, in line with Dennis Bushnell's comments. We have measured large static pressure gradients in the wake behind a circular cylinder, for example, up to 25 to 30 percent of the free-stream static pressure. We have also done the same thing at supersonic speeds where it is perhaps not so surprising. This is an area which requires some attention, even if we are using the simplest type of approach, and where I think further experiments and some analytical work is needed.

M. V. Morkovin: Where does this static pressure gradient come from? I mean, is it part of the model? We all know that on the backside of a cylinder we have low pressure. We have the drag, right?

J. A. Schetz: We have observed that this static-pressure variation persists for surprisingly long distances downstream (20 or 30 diameters). If in the same wind tunnel you take a cylinder of a certain size and measure the normal pressure gradient and then you take a sphere of exactly the same size and put it in the same wind tunnel, you will find a very much smaller static pressure gradient. So it is not as simple as that.

H. H. Korst: Yes, but you address yourself to the wake problem in a more general sens than just mixing when you say that the wake problem may involve nonconstant pressure mixing.

M. V. Morkovin: I'm trying to pursue this thing. Is this divorced from entrainment? Do you have entrainment without such a gradient? How does entrainment come about? Isn't a static-pressure field concomitant with the entrainment?

J. A. Schetz: My only comment is that you can have entrainment without such a big static pressure gradient. We get entrainment in a jet. You get entrainment in the wake behind a sphere and we don't measure anything like these large pressure gradients. We found out that this is not a new discovery on our part. If you examine Schlichting's thesis (1930), you will find he measured similar large static pressure gradients. It may have something to do with the rate of entrainment. It is surprising that when you go from a cylinder to a sphere you find such a big difference.

M. V. Morkovin: As you know, in laminar boundary layers and in other laminar flows (jets or otherwise), you can proceed by iteration and compute your displacement thickness to get a pressure gradient. I think Van Dyke[2] has shown, at least for laminar boundary layers, that even in complex situations like laminar entry into a duct (which is much more tricky because the displacement accelerates the flow), the simple next approximation $\left(\text{the } 1\frac{1}{2} \text{ approximation}\right)$ is a relatively good one. When I was referring to the ellipticity, I was not being party to the predictors, I was still thinking that perhaps with the marching techniques there is a possibility of putting a $1\frac{1}{2}$ type of step into the calculation.

J. Ito: I guess Dennis Bushnell more or less intimidated me right at the very beginning in that he said that this conference will not account for mixing with static pressure gradients and it will not account for mixing with chemical reaction effects. Now in industry, as has been pointed out before, we can't necessarily solve ideal problems or classical problems. We have to solve problems as they occur and we do have a model which I have mentioned to Dennis Bushnell and to Dr. Birch, which does take these factors into account and is based on physical insight. It's not a model which is based on mathematical derivations. Now the reason I didn't speak up earlier in this conference is that I didn't want to disrupt the tone of this conference by bringing up additional factors which were beyond the scope of this present conference. If anyone is interested in some of the details of this, I would be willing to discuss it with them privately.

---

[2]Van Dyke, Milton: A Survey of Higher-Order Boundary-Layer Theory. SUDAAR No. 326 (Contract No. AF 49(638)-1274), Dep. Aeronaut. & Astronaut., Stanford Univ., Sept. 1967.

H. H. Korst: I think that was a self-imposed restriction of the conference. I am quite sure that not only in industry but also at other places, of maybe less practicality, these problems have found considerable interest and are worked upon and you may find here interested partners to discuss it right away.

S. F. Birch: I would like to invite comments from some of the predictors on the modeling of length scale. In many of the papers details of the other terms and constants have been elaborated upon considerably. The question I am asking is as follows: In these complex flows where initially you have boundary layers with different length scales for different regions of the flow, where the length scales are in some cases defined differently and where differences in length scales that have cropped up between planar and axisymmetric flows, do you feel that these differences represent real physical differences between these regions of the flow? Also, how do you feel they should be dealt with?

D. B. Spalding: I would just like to say that it is our opinion that if one is interested in flows of any generality at all, one can forget about formally describing the length scale. The only practical way forward (the only economical way forward) is to deduce the length scale by solving an appropriate differential equation. We need to think of only simple separated flows like the flow downstream of a sudden enlargement in a pipe and we immediately see that the length scale just downstream of the enlargement and in the neighborhood of it must be similar to that in a mixing layer, because there is a mixing layer there. Far downstream the length-scale distribution of a pipe flow must be approached. Then, in the eddy region, there is some kind of length scale which perhaps close to the wall is proportional to the distance. You can see some of the limits but you can't at all tell how to propose the length-scale distribution. I think it is not worthwhile. If you can solve any differential equations at all, you can solve those two extra ones – one for the energy and the other for an equation which will lead to the length scale. I would argue that's what all engineers ought to do.

D. M. Bushnell: I would like to ask the Imperial college people if they have ever presented the results of their length-scale calculations. I've seen quite a few predictions of mean profiles. I've never seen plots of your computed length-scale developments in various flows. It might be of some interest to see just what these things are doing.

D. B. Spalding: I cannot be absolutely certain about the papers, but I can recall length-scale distribution for that sudden enlargement flow and also for certain film cooling flows, film cooling downstream of a slot. Certainly we have presented there a length-scale distribution in the form of profiles.

D. M. Bushnell: Are these the length scales which you have computed from your $k\epsilon 1$ and $k\epsilon 2$ models?

D. B. Spalding: Correct.

M. L. Finson: I agree with Professor Spalding's points about the importance of solving for the length scale in many situations. I gave a paper[3] at the recent AIAA meeting, which Stan Birch alluded to briefly, having to do with the near wake behind hypersonic bodies with turbulent boundary layers. In that case, the near-wake turbulence is apparently residual boundary-layer turbulence and can have a scale size that will be off by an order of magnitude from a normal wake scale size. This can have a very large effect on the development of the wake. When you have scale sizes that are far from similarity, things like dissipation rates will be far from similarity, and it can take a very long time to recover.

H. H. Korst: I have one observation which I would like to share. While the appearance of similarity solutions was recognized and observed by many of the predictors, I was wondering why no reference was made to the levels of modified Reynolds numbers involving the virtual kinematic viscosity as published many years ago by Schlichting[4] for two-dimensional and axisymmetric wakes which could be compared with the turbulent Reynolds number defined in Dr. Peters' paper. Is there anyone who would like to comment on that?

M. L. Finson: I would like to amplify on your question because I wondered many of the same things. For instance, Professor Spalding, in analyzing the wake flows with the various models, showed that as one went downstream the lower level models diverged from the data and from the higher order models. I found this rather surprising. I would have thought that the one thing any model could reproduce would be similarity; the asymptotic self-preserving behavior. I would think that would be the first thing one would check with the models to make sure that you get the right asymptotic solution, presuming, of course, that the Reynolds number is high enough that you do have that behavior. Perhaps those particular cases did not go far enough downstream, but I was shocked by that.

D. B. Spalding: The first thing that we did do when we began all this work, long before the conference, was to look at those self-similar flows. You saw one slide, I showed it, it is one of Mr. Rodi's slides, for four or five different self-similar layers and I quite agree, one must at least be able to make predictions for self-similar layers. This is why I argued that the $k\epsilon 2$ is the one which we have to prefer, because only it can handle those well-known plane and axisymmetrical wake flows which appear in Schlichting.[4] That is why we must have a model of that kind. Now in this conference we weren't asked to compare our predictions with those data we were asked to compare them with developing flows and you saw what the results were. I entirely agree with what the speaker has just said, and we've done it.

---

[3]Finson, Michael L.: Hypersonic Wake Aerodynamics at High Reynolds Numbers. AIAA Paper No. 72-701, June 1972.

[4]Schlichting, Hermann (J. Kestin, transl.): Boundary-Layer Theory. Sixth ed., McGraw-Hill Book Co., Inc., 1968, ch. 24.

H. H. Korst: I was particularly interested in whether Dr. Peters would be able to correlate his terminal and universal Reynolds number to such a value. Did you give some thought to that?

C. E. Peters: Are you referring to the value of the fully developed terminal Reynolds number R_T in a wake?

H. H. Korst: That is right.

C. E. Peters: The one thing we commented on in the written version of the paper is that the axisymmetric incompressible wake, the Chevray wake, was a situation where the length scale of the experiment, which was far from fully developed, did not go to the ultimate $x^{-2/3}$ decay or whatever is proper; it varies as x^{-1} all the way. Personally, I have never seen any incompressible axisymmetrical wake data behind a streamlined body which go to the $x^{-2/3}$ decay. Perhaps I am not aware of it. There may be a question of whether or not self-preservation exists in that case, within practical distances.

H. H. Korst: Steve Kline has mentioned and given due weight to this. The fact that we do not reach similarity does not mean that we cannot anticipate its approach as we plot consecutive data and see an asymptotic narrowing down of the gap.

C. E. Peters: In the particular flow that I mentioned before, we maintained an x^{-1} center-line velocity distribution (that is, the defect distribution) to x/D of 200 or so, far beyond where the experimental data stopped. We commented on this in the written paper.

M. V. Morkovin: I would like to have some advice on my own philosophy. On the panel, we strongly came out for motherhood; that is, there was a need for simple solutions as well as a need for more complex solutions. Maybe that wasn't right if I understand what the industrial members are saying. For one thing, Peters says his simple solution is really consuming an awful lot of time too and that no solution is really simple. If I understood Professor Spalding, the extra differential equation isn't really that much more difficult. We have made that statement partly because we felt that the computer technology is sucking us into a method pollution just like technology is sucking us into general pollution. Perhaps, that's wrong and we should use the most up-to-date method and recommend it to everybody; I don't know. I'm not in a position to judge and I'd be very happy to be corrected in terms of a yearning for the simple old days.

C. E. Peters: May I clarify one point about our computation times. Our program is at least an order of magnitude slower than it needs to be for these particular flows because, as I mentioned during my presentation, it is full of extraneous information going much beyond the requirements for the flows considered in this conference; therefore, I think it is faulty to say that it is extremely slow. The point is that it is still a monumental computation task even as an integral method. I mean it is not something one can do on the

back of an envelope as classical integral methods have been, unless one has an awfully big envelope and an awful lot of time.

M. V. Morkovin: It has been said that the Stanford conference did one piece of damage; that is, it pushed in the direction of the proliferation of the extra complex things. Is that a correct criticism? Is the idea to use the best tool that you have because it is not really that complicated?

S. J. Kline: It seems to me that what Dr. Morkovin is saying is that we no longer need motherhood but we need population control, for one thing. With regard to the Stanford conference,[5] I remember the recommendations were that we need some simple methods. We said, in fact, that one couldn't differentiate between the integral methods and the differential methods, as some of each were good. But since then, in looking at the actual figures, critical readers of the proceedings have observed that the center of gravity of the population of the differential methods is certainly at a better place than the center of gravity of the integral methods. If you are going to go to a computer, as Peters has said, then certainly you are going to use more sophisticated methods. And in another comment, I tend to agree with Professor Spalding. It seems to me that what progress has been made toward improved calculations of turbulent boundary layers and of the class of problems we have been discussing here – I think there is some progress – is due more to the computer than to any other single factor in the last 20 years.

C. duP. Donaldson: I would like to make a suggestion in regard to when you use more sophisticated methods and when you don't. I found it is enormously instructive to do what I did or do what Professor Spalding did. If you wish to use a simpler method, you don't use all these additional equations. But really the essence of a lot of the physics, but not all of the physics, of eddy-viscosity methods comes from looking at the super equilibrium form of those equations. In particular, what is the effect of heat release by chemical reactions on eddy viscosity? You can get that effect – the first-order effect – by taking an equilibrium nondiffusive limit. This is a very helpful thing to do and it also helps tell you, when you look at the problem, whether that's the kind of problem you can do that way with any degree of confidence. If you don't feel you can, then you will have to use one of these more elaborate methods.

C. E. Peters: I would like to add one bit of clarification about integral methods. Classically, integral methods have been, I think, of two types, and we should differentiate between them, not mathematically but grammatically. The classic integral method is one where you may not input information on the intergrand but you input information on the integral quantities from empirical information and this does not give you back a detailed

---

[5]Kline, S. J.; Morkovin, M. V.; Sovran, G.; and Cockrell, D. J., eds.: Computation of Turbulent Boundary Layers – 1968 AFOSR-IFP-Stanford Conference. Vol. I – Methods, Predictions, Evaluation and Flow Structure. Stanford Univ., c.1969.

flow-field description from the integral method. That's one approach. What we have done is a bit different: We have input information on the integrand – that is, the shape of things – and this means that we get back not just the distribution of net quantities (the solution variables, wall pressure in the case of our ducted flow) but also spatial distributions. We get back just as much information qualitatively as we would get from a differential method. We get spatial distributions of kinetic energy, of shear stress, of velocity, and so forth. So the output is not quite the same as in some simpler integral methods.

H. H. Korst: The different complexity of the problems on one side and in methods of solution on the other side can be illustrated rather simply. As topics for this conference, we have excluded certain problem types entirely by definition. That doesn't mean that we as individuals haven't been concerned with such practical problems as hydrogen burning in wakes (and have found solutions experimentally verified by simple flame sheet methods) or that we haven't utilized such things as virtual origin shift and equivalent bleed to attack problems of base bleed in rather complicated configurations. We have here concentrated on the better founded ways – not seeking simple solutions like saying what do I care for σ if I'm only interested in the dividing streamline because the dividing streamline without any bleed in its asymptotic behavior doesn't care about σ. It is just a simple similarity solution which does not require any empirical information. Therefore, I think we have gone quite a bit into more details. We always find that some people will continue to make contributions to a better physical understanding and other people, such as in industry, will be more or less forced to utilize whatever simple and maybe nonsophisticated methods that have become available and can be readily compared to and applied to problems expecting a certain degree of ball-park type accuracy for their solutions.

S. C. Lee: Any method selection should be based on what we want to calculate. If we are interested in design parameters such as a drag force or aerodynamic heating, I think the so-called integral methods would be quite sufficient for giving us this information. However, if we are interested in the fuel-air mixing for a hypersonic jet, I think the integral method would not be sufficient to give you the mixing in proper details. If we are interested in problems of meteorology, and we would like to see how the air masses move, we have to go to more sophisticated methods like those Professor Spalding proposed – maybe going even further, like analyzing the diffusion terms as well as the production and dissipation terms.

INDEX TO TEST CASES

Two-Dimensional Shear Layers:

1. Spreading parameter for a fully developed free turbulent shear layer for velocity ratios u_2/u_1 of 0, 0.2, 0.4, 0.6, and 0.8.
2. Spreading parameter for a fully developed free turbulent shear layer with a velocity ratio u_2/u_1 of 0 for Mach numbers of 1.0, 2.0, 3.0, 4.0, and 5.0.
3. Spreading parameter for a fully developed free turbulent shear layer with a velocity ratio u_2/u_1 of 0.2 and density ratios ρ_2/ρ_1 of 14, 1/2, 1/7, and 1/14.
4. Lee, Shen Ching: A Study of the Two-Dimensional Free Turbulent Mixing Between Converging Streams With Initial Boundary Layers. Ph. D. Diss., Univ. of Washington, 1966.
5. Hill, W. G., Jr.; and Page, R. H.: Initial Development of Turbulent, Compressible, Free Shear Layers. Trans. ASME, Ser. D: J. Basic Eng., vol. 91, no. 1, Mar. 1969, pp. 67-73.

Axisymmetric Jets Into Still Air:

6. Maestrello, L.; and McDaid, E.: Acoustic Characteristics of a High-Subsonic Jet. AIAA J., vol. 9, no. 6, June 1971, pp. 1058-1066.
7. Eggers, James M.: Velocity Profiles and Eddy Viscosity Distributions Downstream of a Mach 2.22 Nozzle Exhausting to Quiescent Air. NASA TN D-3601, 1966.
8. Heck, P. H.: Jet Plume Characteristics of 72-Tube and 72-Hole Primary Suppressor Nozzles. T.M. No. 69-457 (FAA Contract FA-SS-67-7), Flight Propulsion Div., Gen. Elec. Co., July 1969.

Jets in Moving Stream:

9. Forstall, Walton, Jr.; and Shapiro, Ascher H.: Momentum and Mass Transfer in Coaxial Gas Jets. J. Appl. Mech., vol. 17, no. 4, Dec. 1950, pp. 399-408.
10. Chriss, D. E.: Experimental Study of the Turbulent Mixing of Subsonic Axisymmetric Gas Streams. AEDC-TR-68-133, U.S. Air Force, Aug. 1968. (Available from DDC as AD 672 975.)
11. Eggers, James M.; and Torrence, Marvin G.: An Experimental Investigation of the Mixing of Compressible-Air Jets in a Coaxial Configuration. NASA TN D-5315, 1969.
12. Eggers, James M.: Turbulent Mixing of Coaxial Compressible Hydrogen-Air Jets. NASA TN D-6487, 1971.
13. Bradbury, L. J. S.: The Structure of a Self-Preserving Turbulent Plane Jet. J. Fluid Mech., vol. 23, pt. 1, Sept. 1965, pp. 31-64.

Wakes:

14. Chevray, René; and Kovasznay, Leslie S. G.: Turbulence Measurements in the Wake of a Thin Flat Plate. AIAA J., vol. 7, no. 8, Aug. 1969, pp. 1641-1643.

15. Chevray, R.: The Turbulent Wake of a Body of Revolution. Trans. ASME, Ser. D: J. Basic Eng., vol. 90, no. 2, June 1968, pp. 275-284.

16. Demetriades, Anthony: Turbulent Mean-Flow Measurements in a Two-Dimensional Supersonic Wake. Phys. Fluids, vol. 12, no. 1, Jan. 1969, pp. 24-32.

17. Demetriades, Anthony: Mean-Flow Measurements in an Axisymmetric Compressible Turbulent Wake. AIAA J., vol. 6, no. 3, Mar. 1968, pp. 432-439.

Optional Test Cases:

18. Wygnanski, I.; and Fiedler, H.: Some Measurements in the Self-Preserving Jet. J. Fluid Mech., vol. 38, pt. 3, Sept. 18, 1969, pp. 577-612.

19. Heck, P. H.: Jet Plume Characteristics of 72-Tube and 72-Hole Primary Suppressor Nozzles. T.M. No. 69-457 (FAA Contract FA-SS-67-7), Flight Propulsion Div., Gen. Elec. Co., July 1969.

20. Chriss, D. E.; and Paulk, R. A.: An Experimental Investigation of Subsonic Coaxial Free Turbulent Mixing. AEDC-TR-71-236, AFOSR-72-0237TR, U.S. Air Force, Feb. 1972. (Available from DDC as AD 737 098.)

21. Chriss, D. E.: Experimental Study of the Turbulent Mixing of Subsonic Axisymmetric Gas Streams. AEDC-TR-68-133, U.S. Air Force, Aug. 1968. (Available from DDC as AD 672 975.)

22. Eggers, James M.: Turbulent Mixing of Coaxial Compressible Hydrogen-Air Jets. NASA TN D-6487, 1971.

23. Champagne, F. H.; and Wygnanski, I. J.: Coaxial Turbulent Jets. D1-82-0958, Flight Sci. Lab., Boeing Sci. Res. Lab., Feb. 1970. (Available from DDC as AD 707 282.)

24. Demetriades, Anthony: Observations on the Transition Process of Two-Dimensional Supersonic Wakes. AIAA J., vol. 9, no. 11, Nov. 1971, pp. 2128-2134.

COMPOSITE PLOTS

The composite plots of the predictions for each test case were prepared by using the figures in the original predictors' papers. They are intended only to facilitate an overall comparison between the predictions and the experimental data. For a detailed study of the success or failure of a particular method and an explanation of the symbols used, the reader should refer to the original paper.

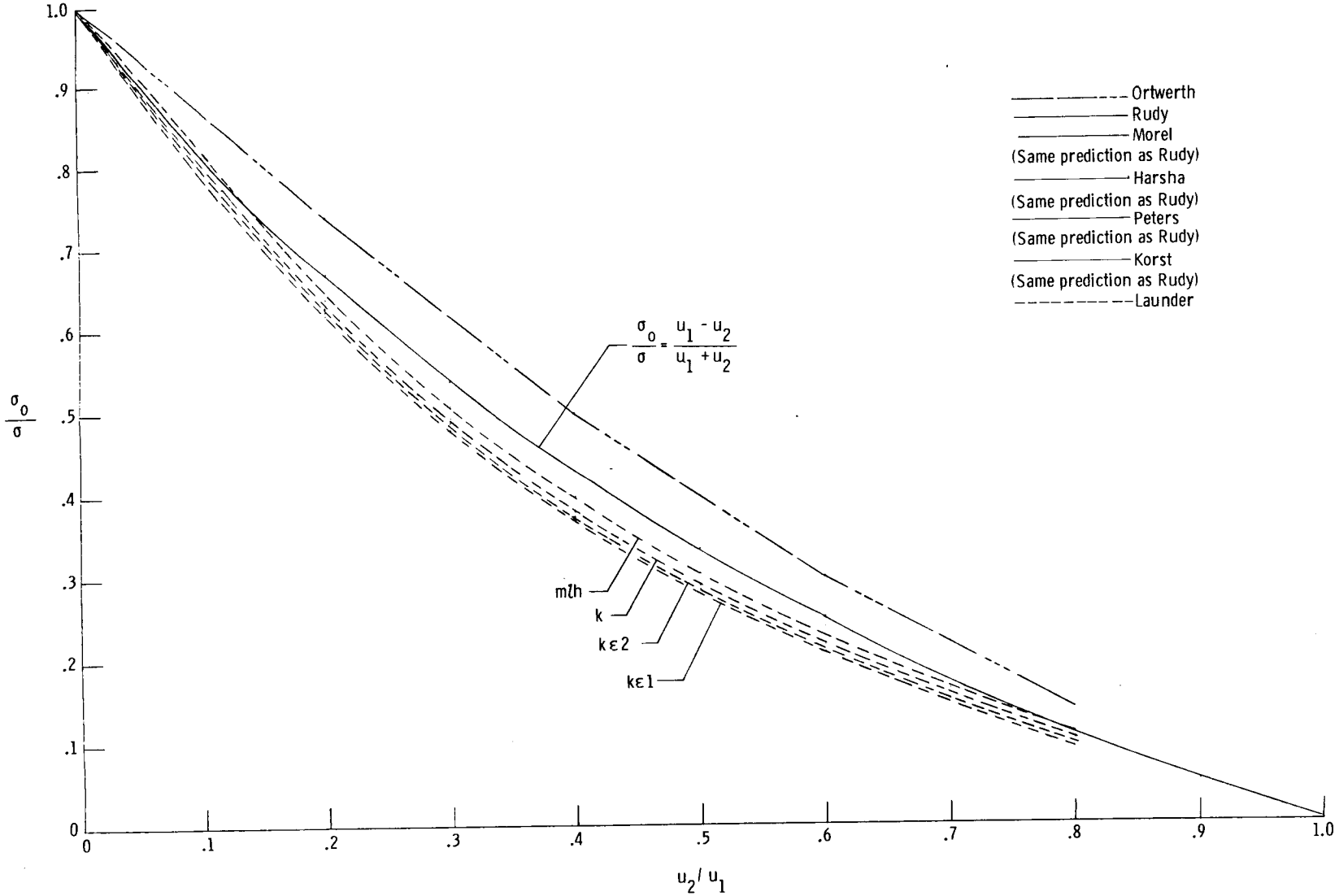
1.0
.9
.8
.7
.6
.5
.4
.3
.2
.1
0
$\frac{\sigma_0}{\sigma}$
0
.1
.2
.3
.4
.5
.6
.7
.8
.9
1.0
u_2/u_1
$\frac{\sigma_0}{\sigma} = \frac{u_1 - u_2}{u_1 + u_2}$
mℓh
k
kε2
kε1
Ortwerth
Rudy
Morel
(Same prediction as Rudy)
Harsha
(Same prediction as Rudy)
Peters
(Same prediction as Rudy)
Korst
(Same prediction as Rudy)
Launder

Test case 1

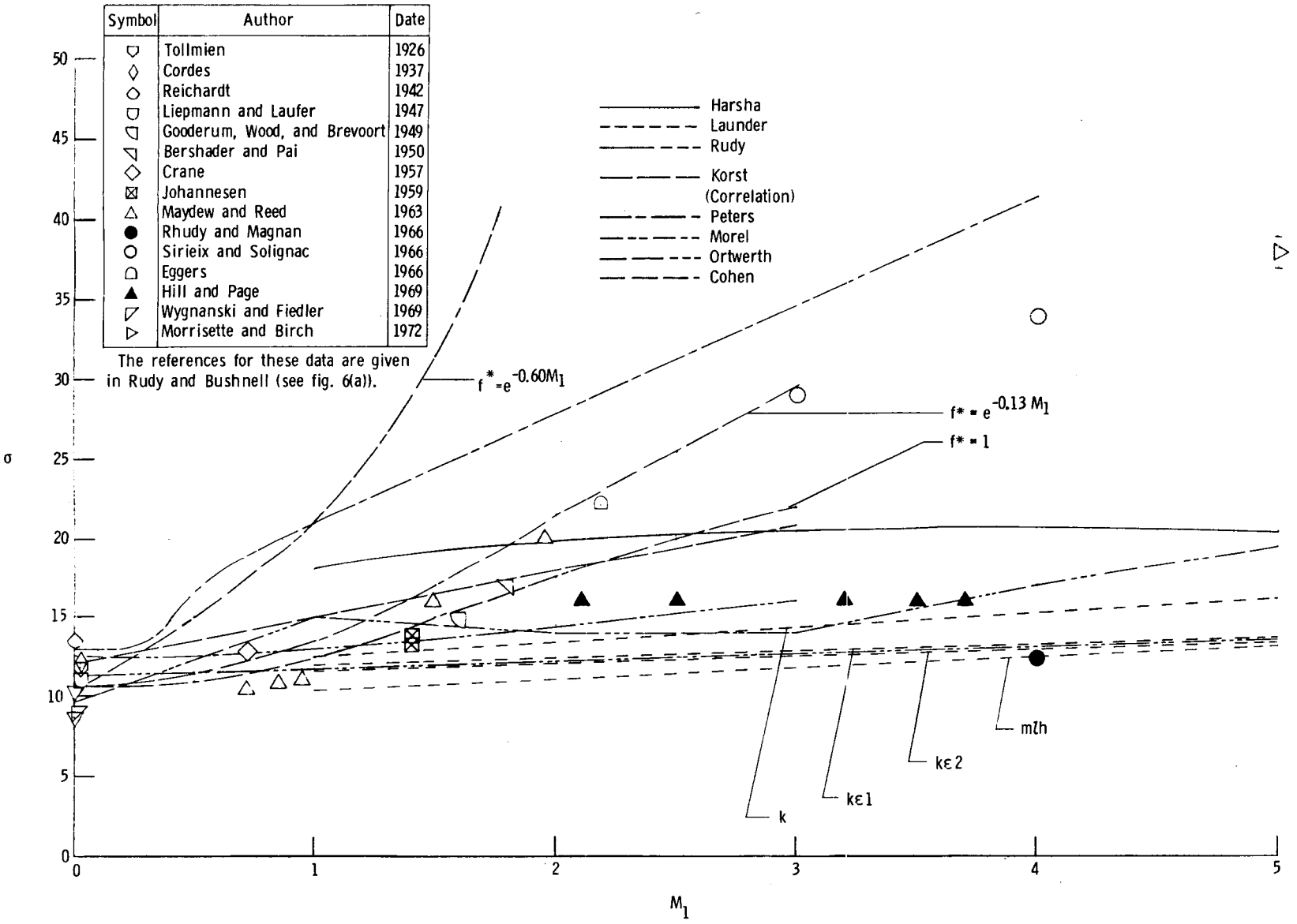
Symbol
Author
Date
Tollmien 1926
Cordes 1937
Reichardt 1942
Liepmann and Laufer 1947
Gooderum, Wood, and Brevoort 1949
Bershader and Pai 1950
Crane 1957
Johannesen 1959
Maydew and Reed 1963
Rhudy and Magnan 1966
Sirieix and Solignac 1966
Eggers 1966
Hill and Page 1969
Wygnanski and Fiedler 1969
Morrisette and Birch 1972
The references for these data are given in Rudy and Bushnell (see fig. 6(a)).
Harsha
Launder
Rudy
Korst (Correlation)
Peters
Morel
Ortwerth
Cohen
f* = e^-0.60M1
f* = e^-0.13 M1
f* = 1
σ
M1
k
kε1
kε2
mℓh
0
5
10
15
20
25
30
35
40
45
50
0
1
2
3
4
5

Test case 2

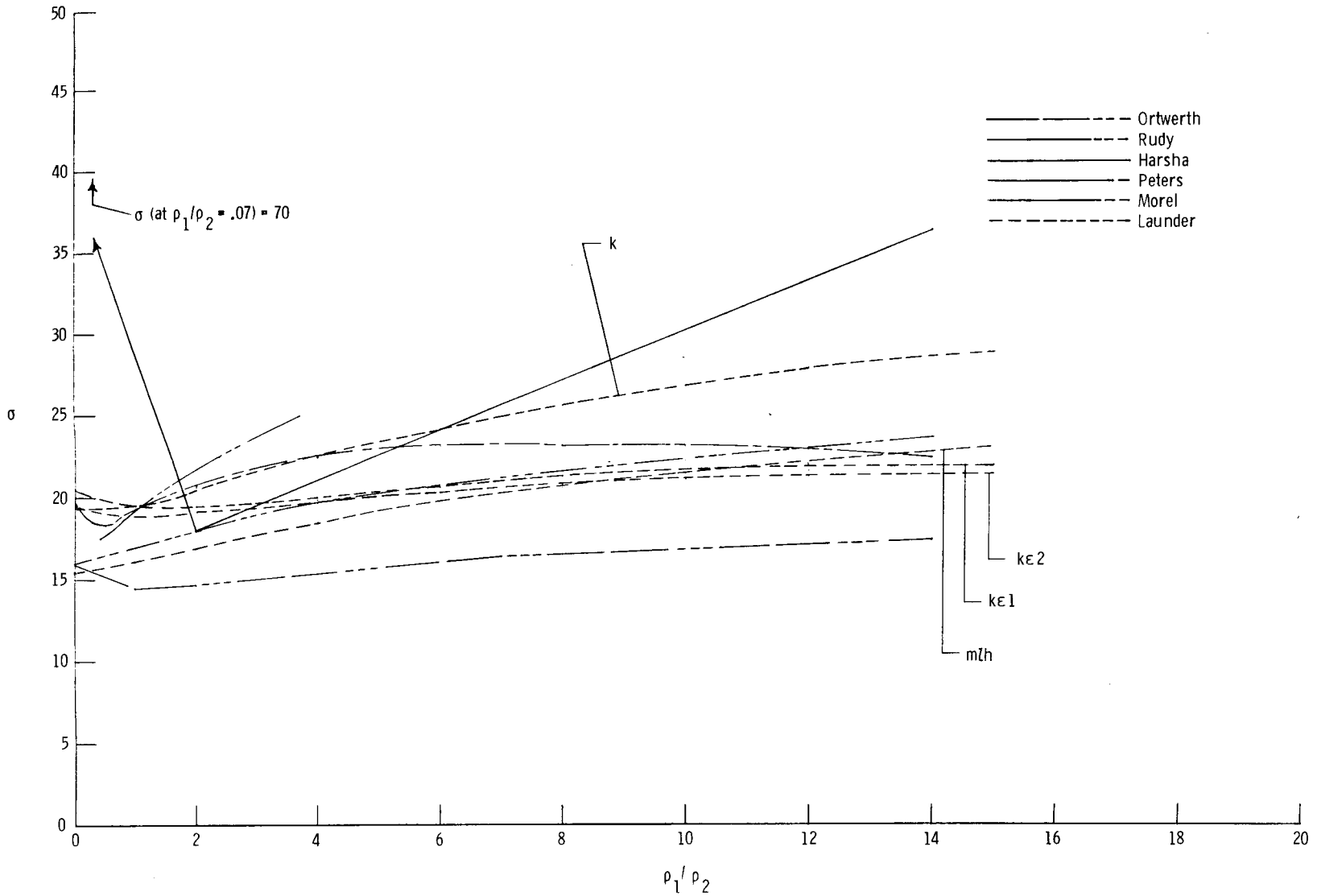
Ortwerth
Rudy
Harsha
Peters
Morel
Launder
σ (at ρ1/ρ2 = .07) = 70
k
kε2
kε1
mℓh
σ
ρ1/ρ2
0
5
10
15
20
25
30
35
40
45
50
0
2
4
6
8
10
12
14
16
18
20

Test case 3

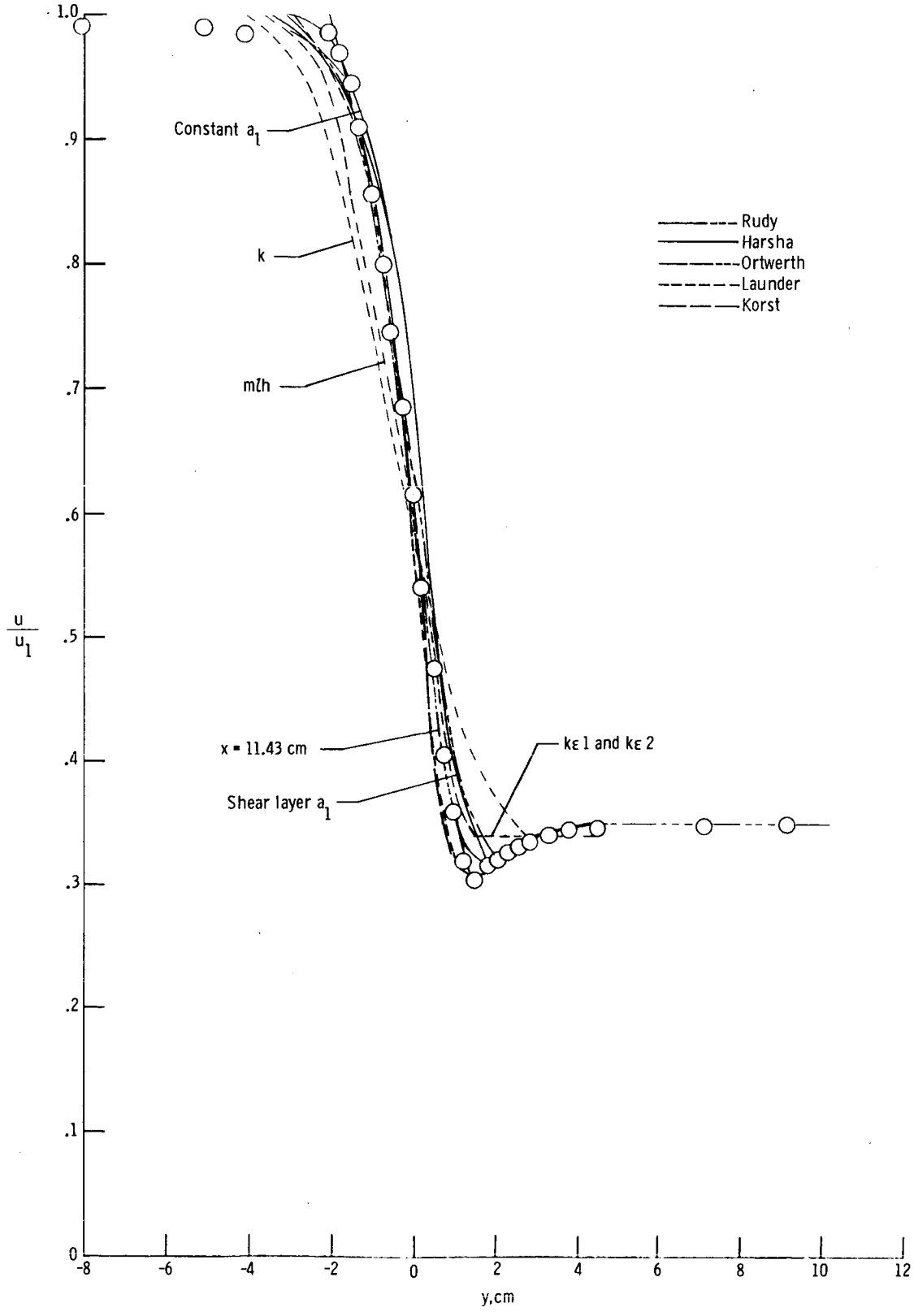

Test case 4 (x = 12.7 cm)

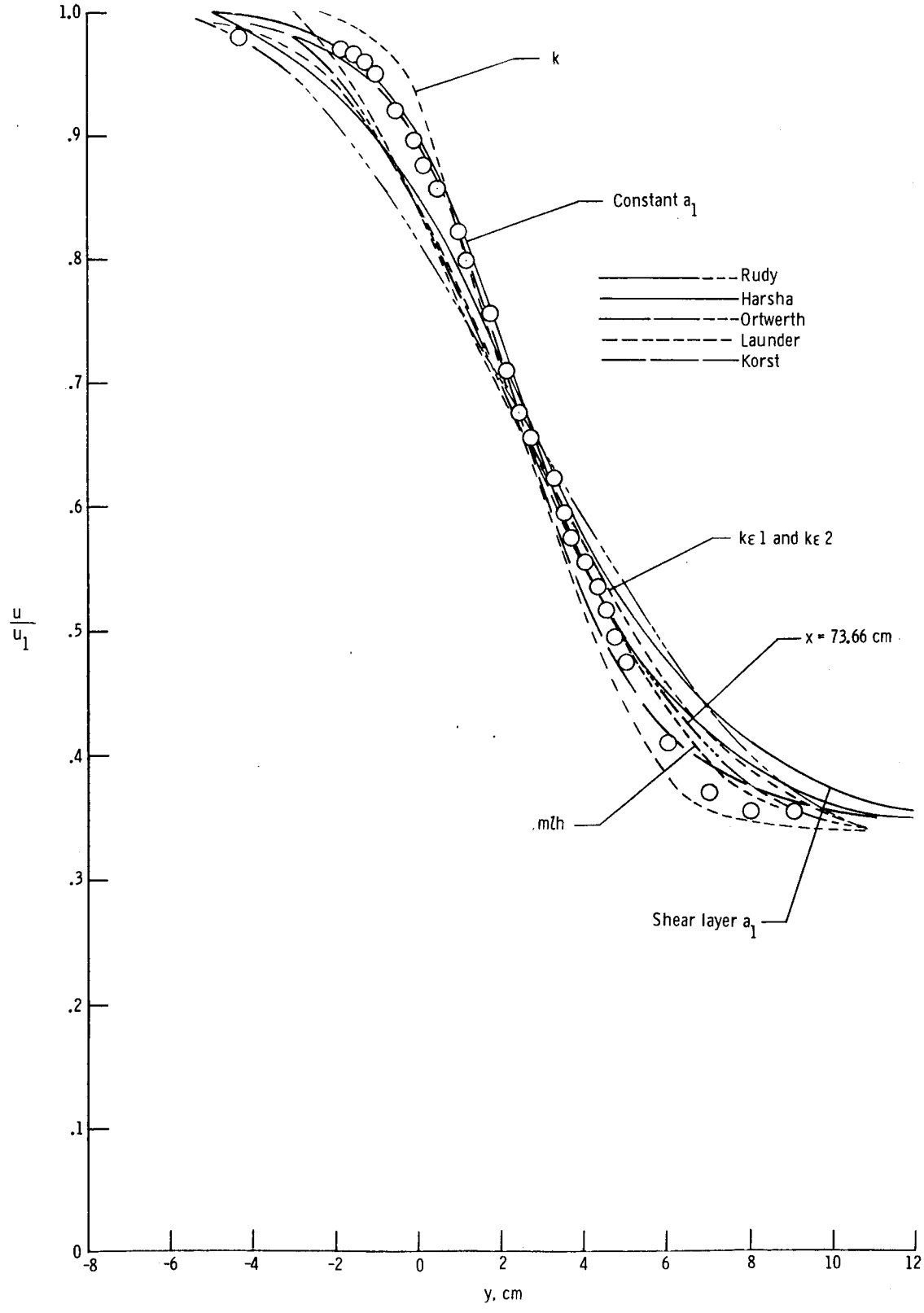

Test case 4 (x = 76 cm)

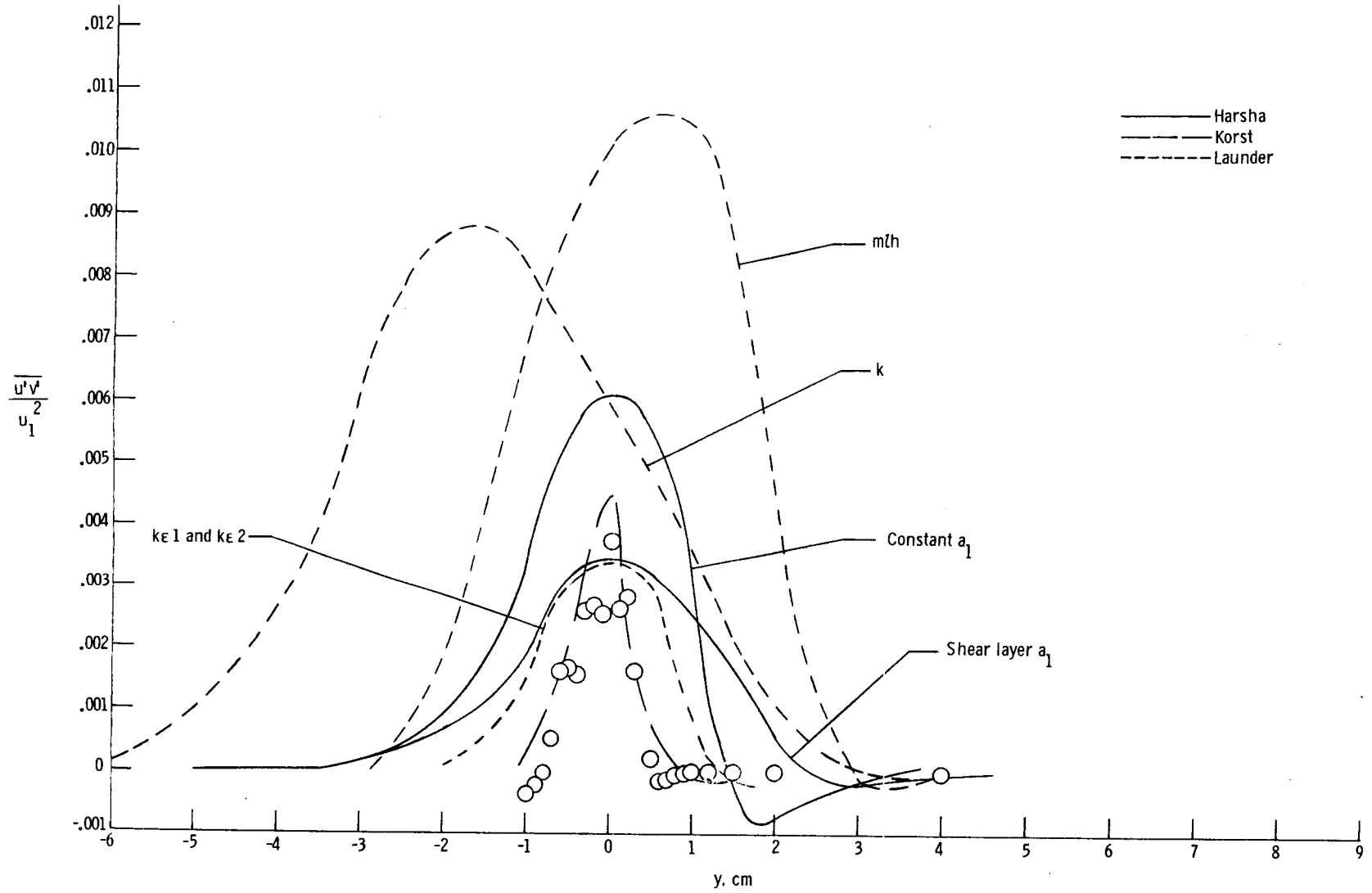

Test case 4 (x = 12.7 cm)

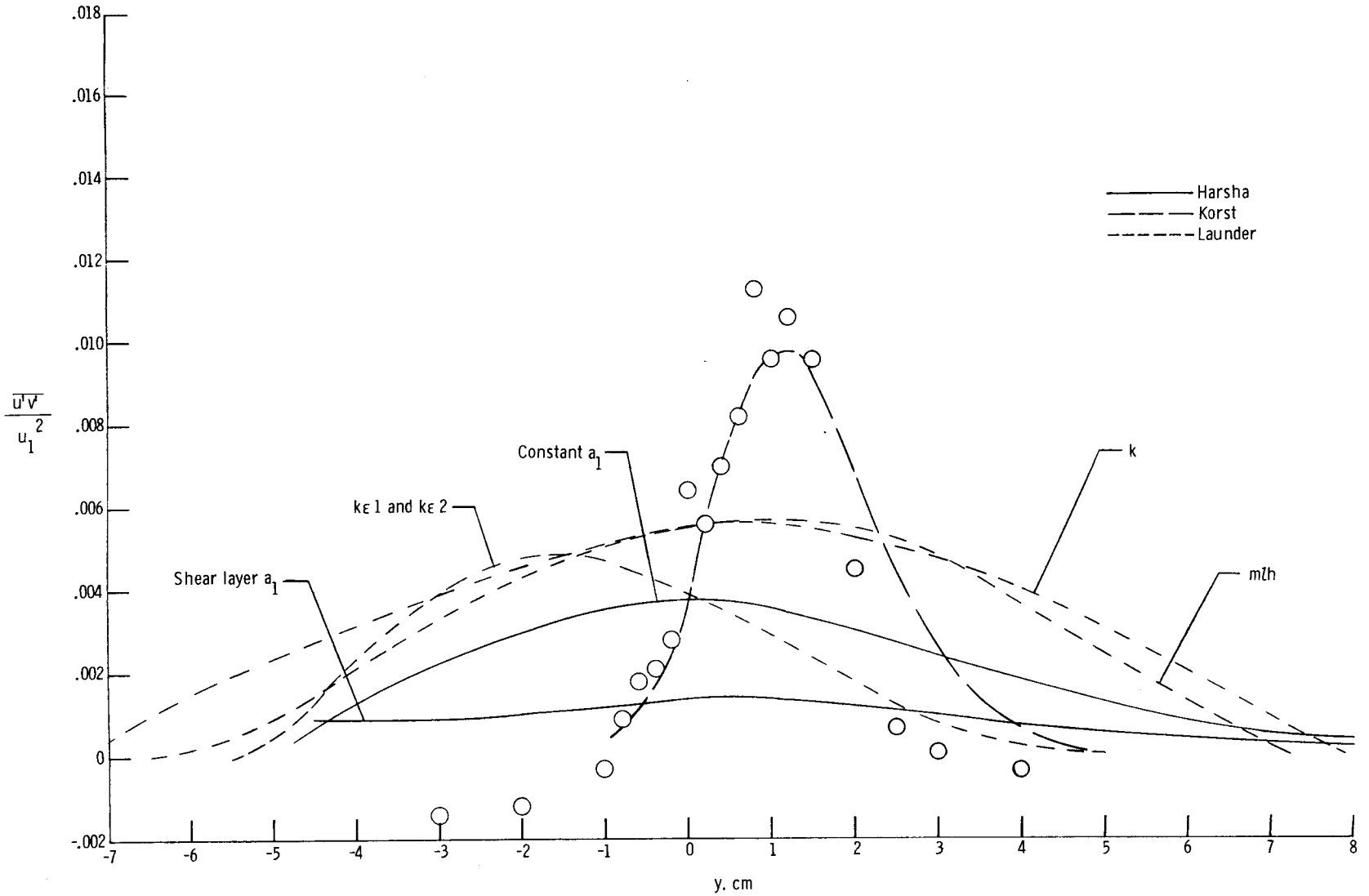

Test case 4 (x = 76 cm)

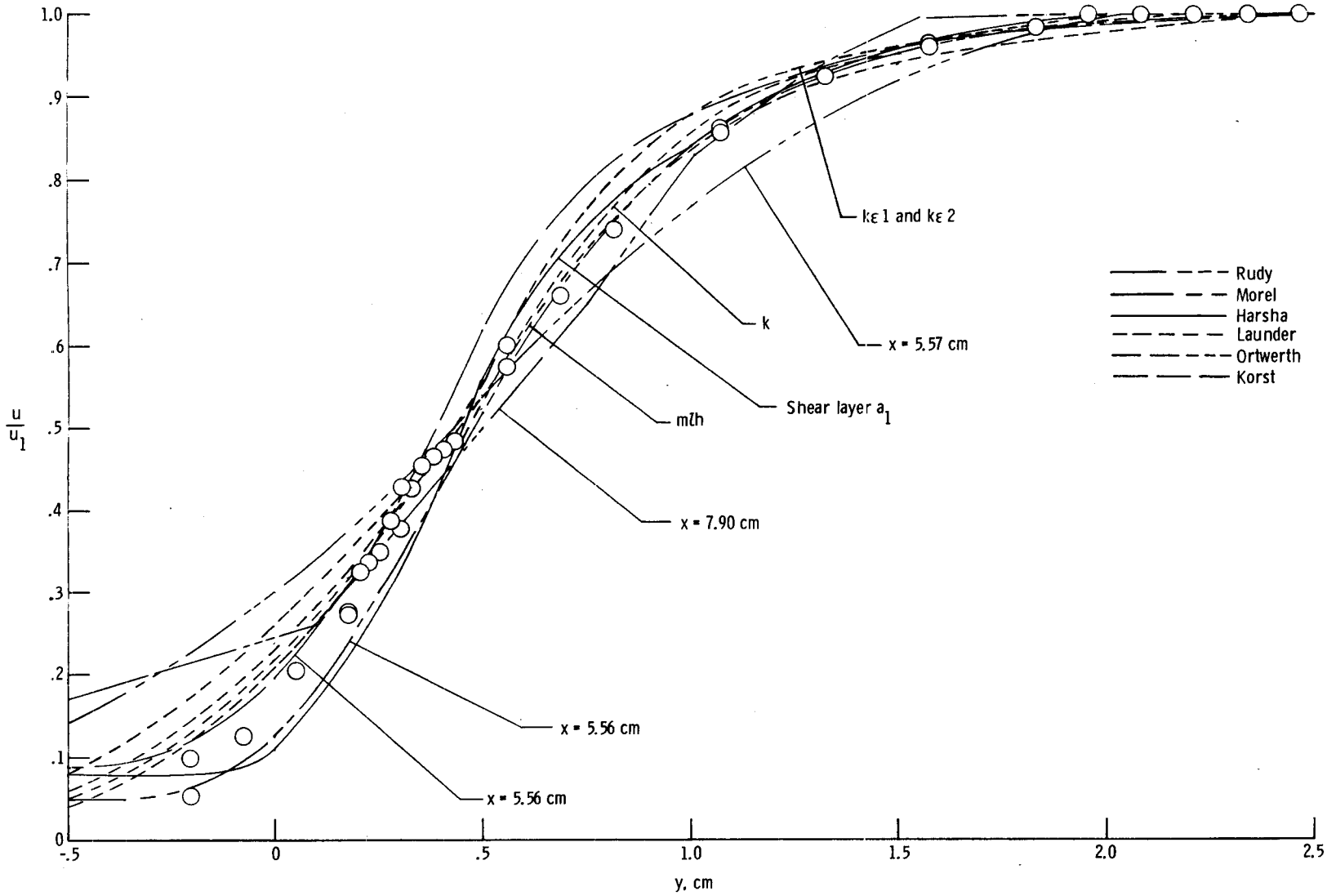

Test case 5 (x = 5.56 cm)

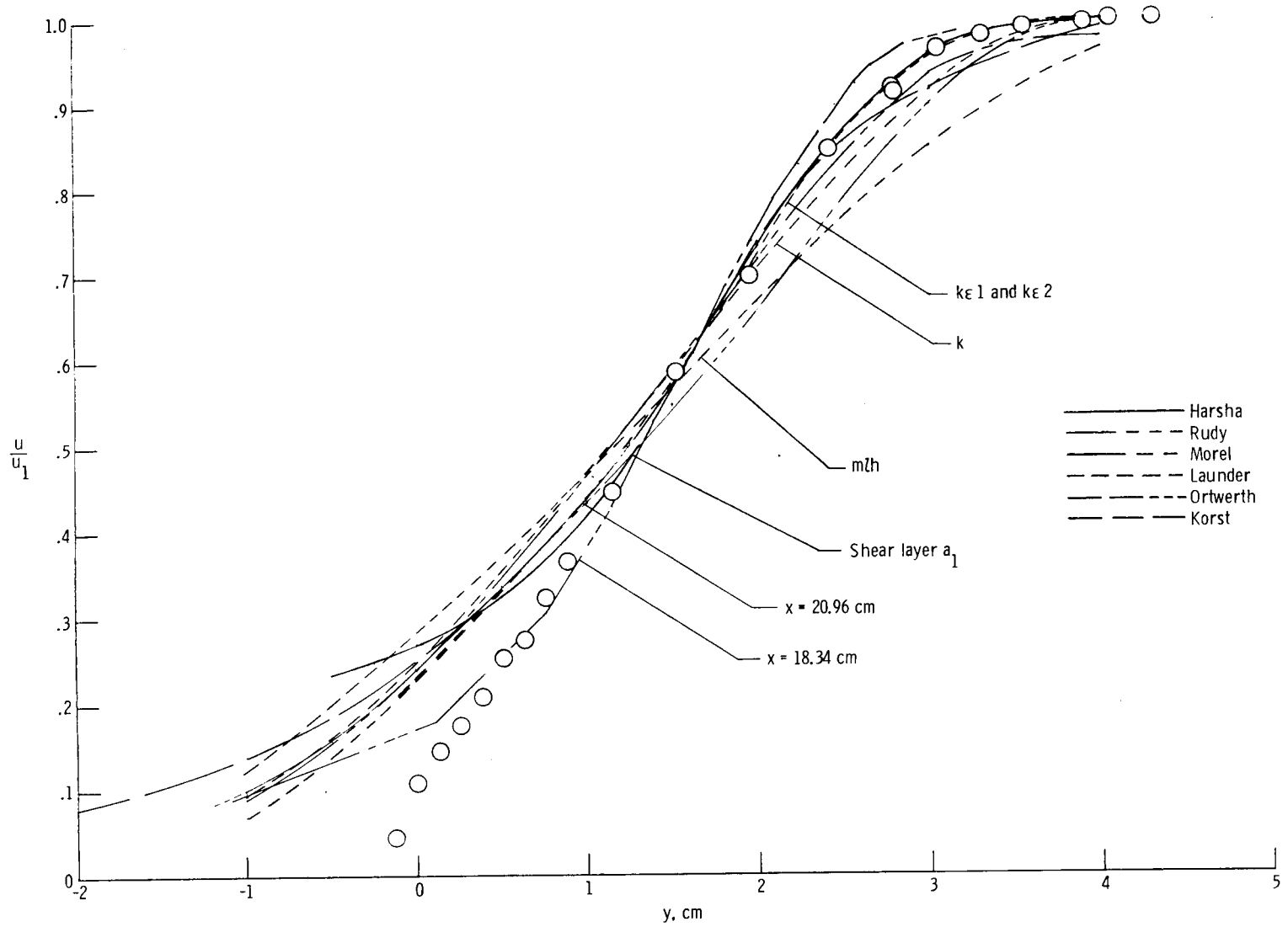

Test case 5 (x = 20.96 cm)

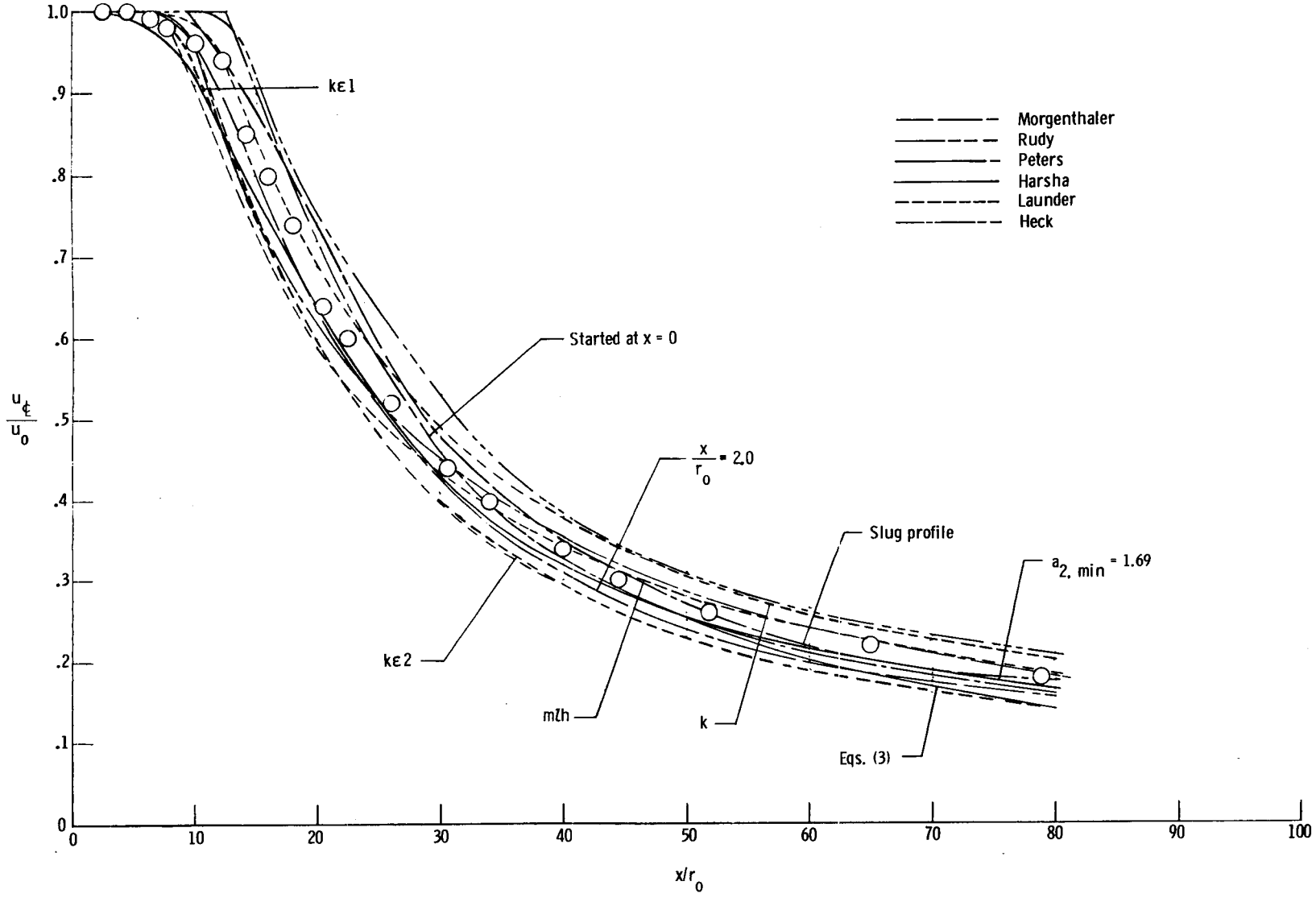
1.0
.9
.8
.7
.6
.5
.4
.3
.2
.1
0
$\frac{u_\ell}{u_0}$
kε1
Started at x = 0
$\frac{x}{r_0}$ = 2.0
Slug profile
$a_{2,\,min}$ = 1.69
kε2
mℓh
k
Eqs. (3)
Morgenthaler
Rudy
Peters
Harsha
Launder
Heck
0
10
20
30
40
50
60
70
80
90
100
x/r_0

Test case 6

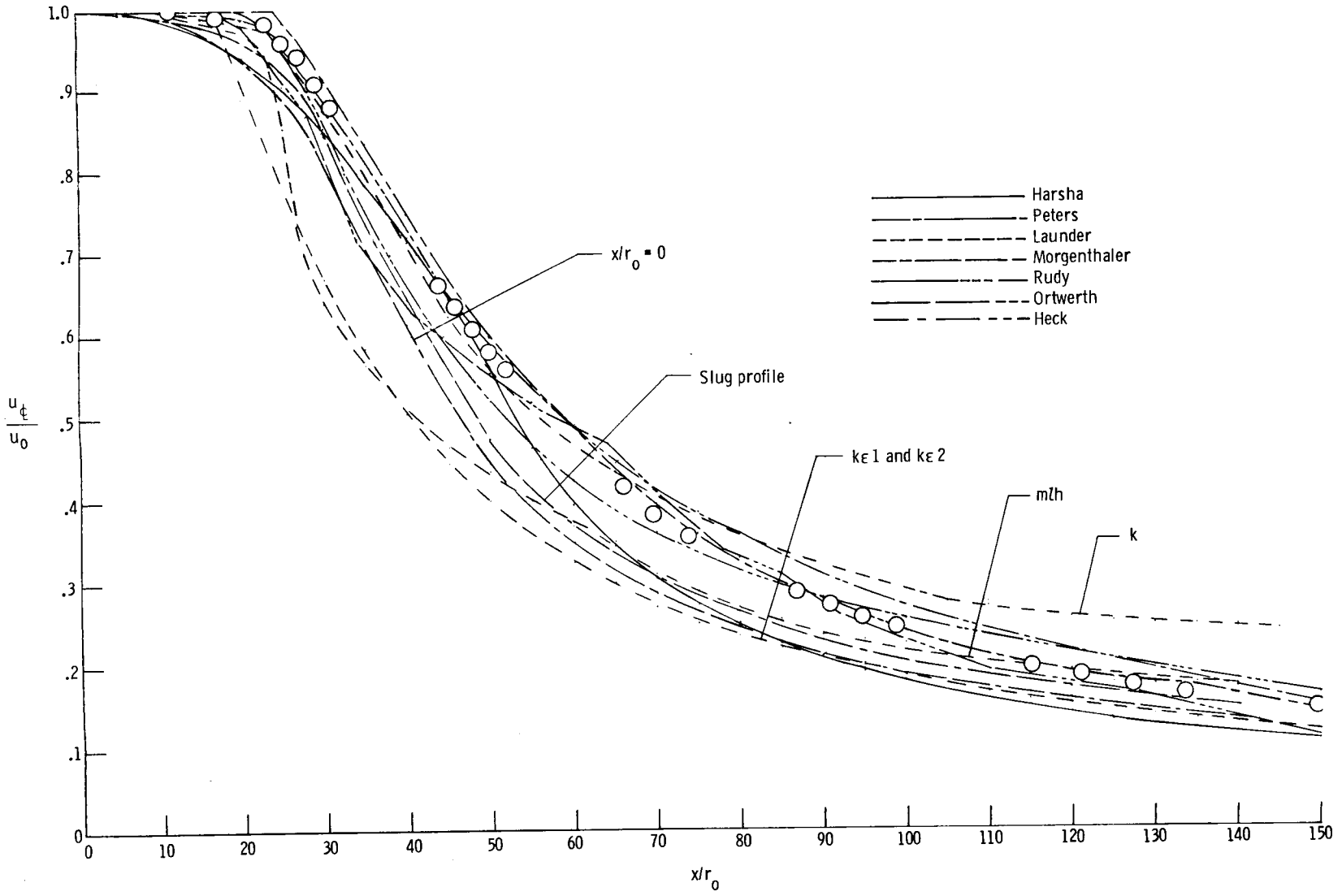
1.0
.9
.8
.7
.6
.5
.4
.3
.2
.1
0
$\frac{u_\ell}{u_0}$
0
10
20
30
40
50
60
70
80
90
100
110
120
130
140
150
x/r_0
Harsha
Peters
Launder
Morgenthaler
Rudy
Ortwerth
Heck
$x/r_0 = 0$
Slug profile
kε 1 and kε 2
mlh
k

Test case 7

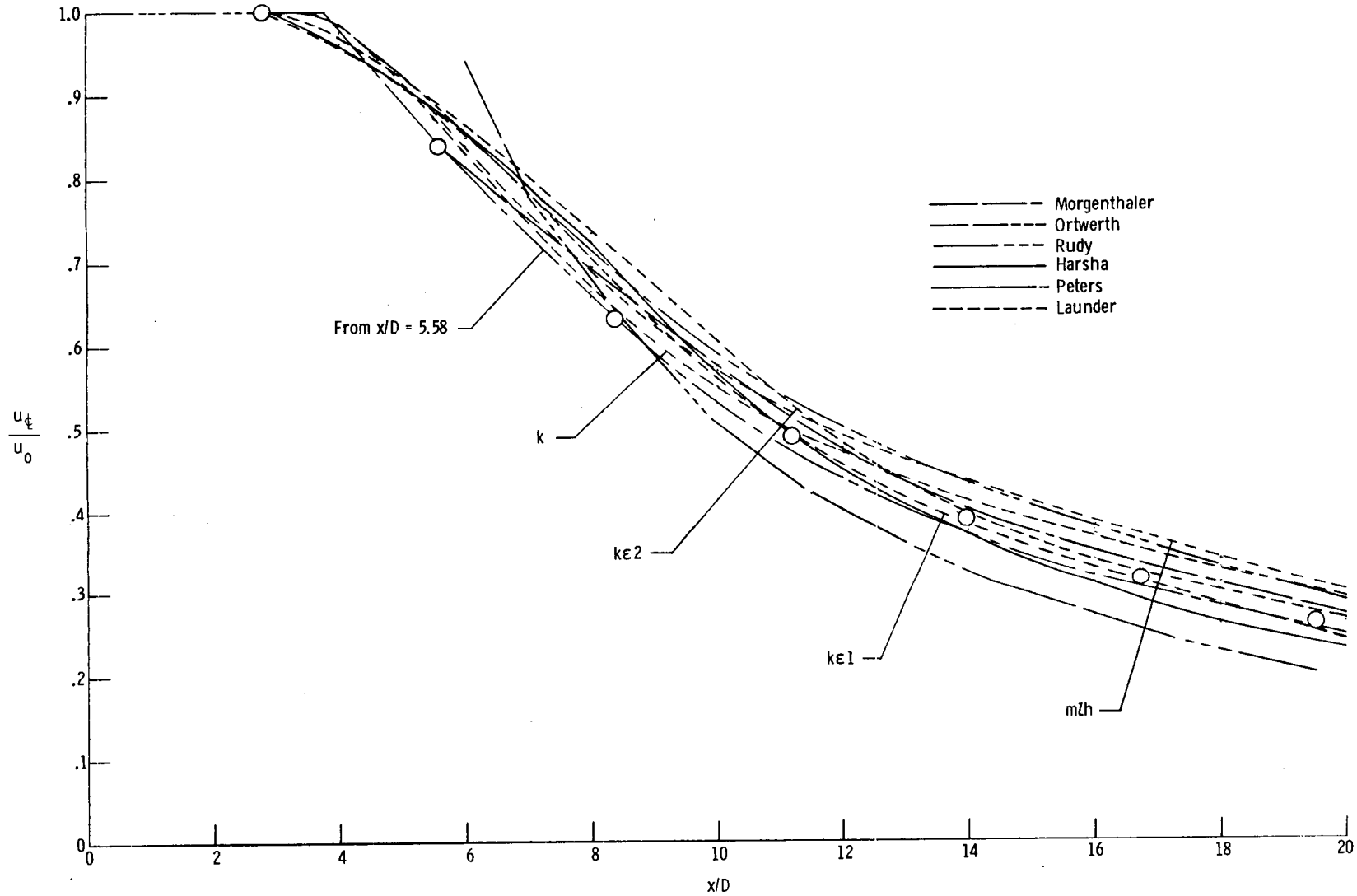
1.0
.9
.8
.7
.6
.5
.4
.3
.2
.1
0
$\frac{u_\ell}{u_0}$
0
2
4
6
8
10
12
14
16
18
20
x/D
Morgenthaler
Ortwerth
Rudy
Harsha
Peters
Launder
From x/D = 5.58
k
kε2
kε1
mℓh

Test case 8

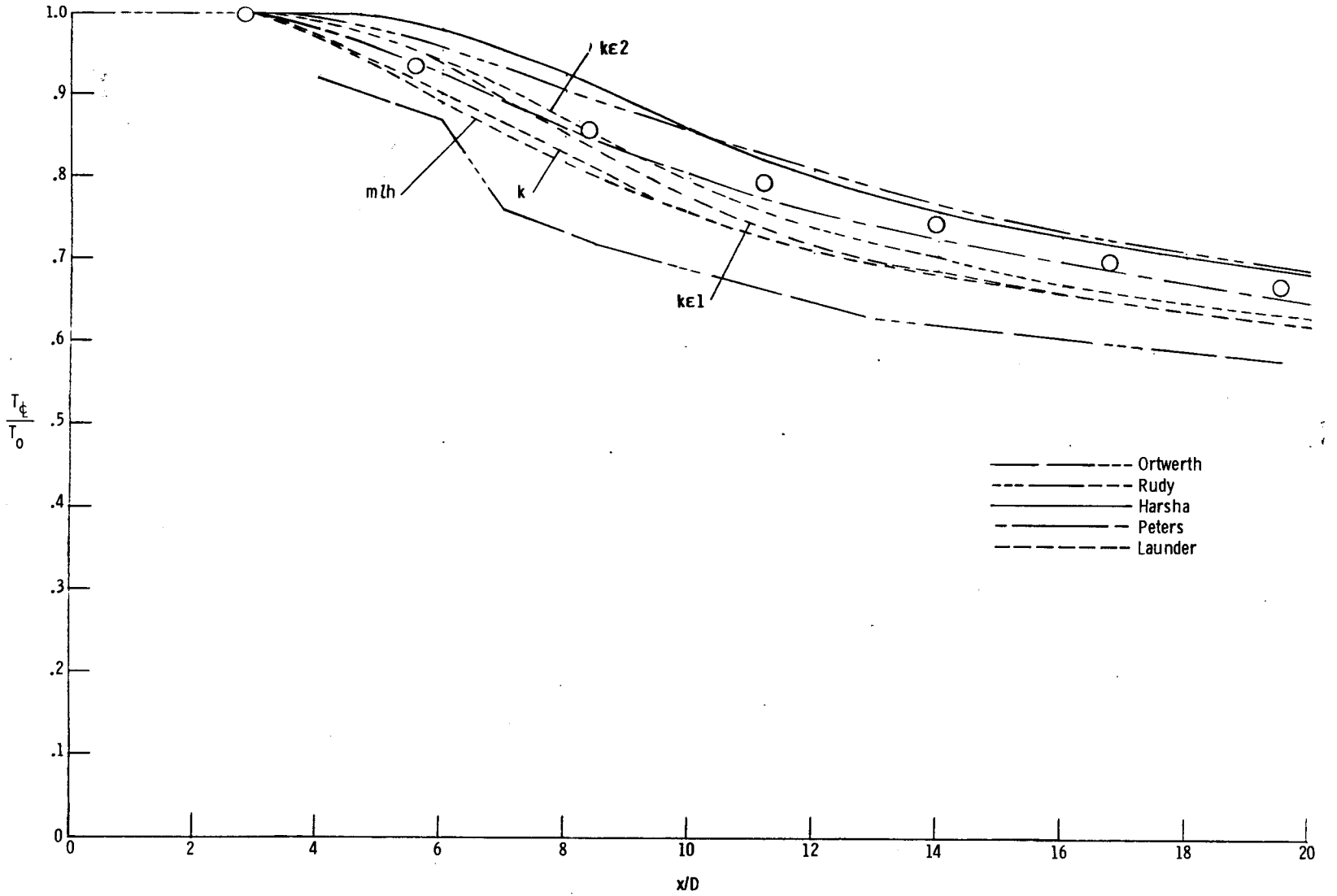
1.0
.9
.8
.7
.6
.5
.4
.3
.2
.1
0
$\frac{T_\ell}{T_0}$
kε2
mℓh
k
kε1
Ortwerth
Rudy
Harsha
Peters
Launder
0
2
4
6
8
10
12
14
16
18
20
x/D

Test case 8

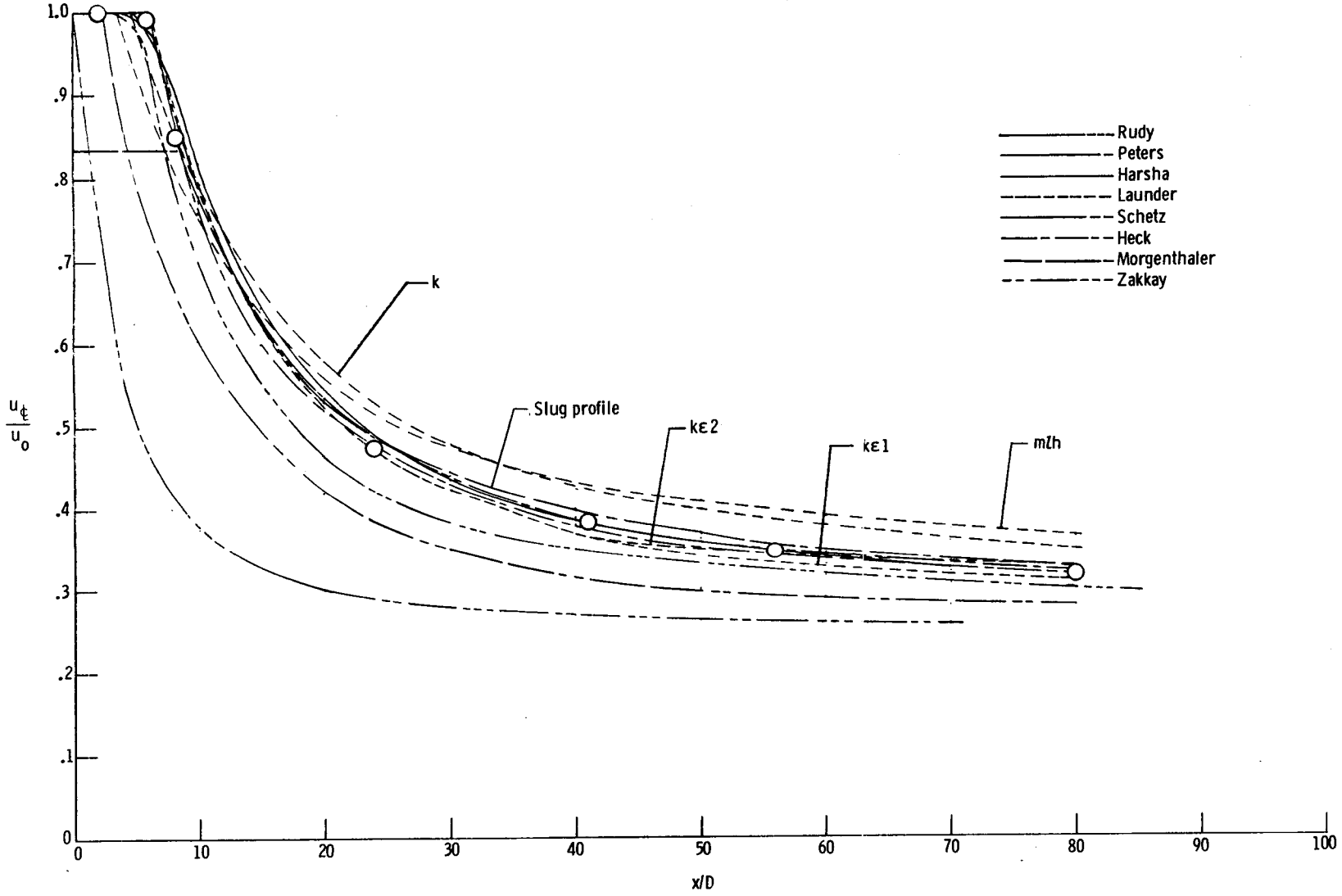
1.0
.9
.8
.7
.6
.5
.4
.3
.2
.1
0
$\frac{u_\ell}{u_o}$
0
10
20
30
40
50
60
70
80
90
100
x/D
Rudy
Peters
Harsha
Launder
Schetz
Heck
Morgenthaler
Zakkay
k
Slug profile
kε2
kε1
mℓh

Test case 9

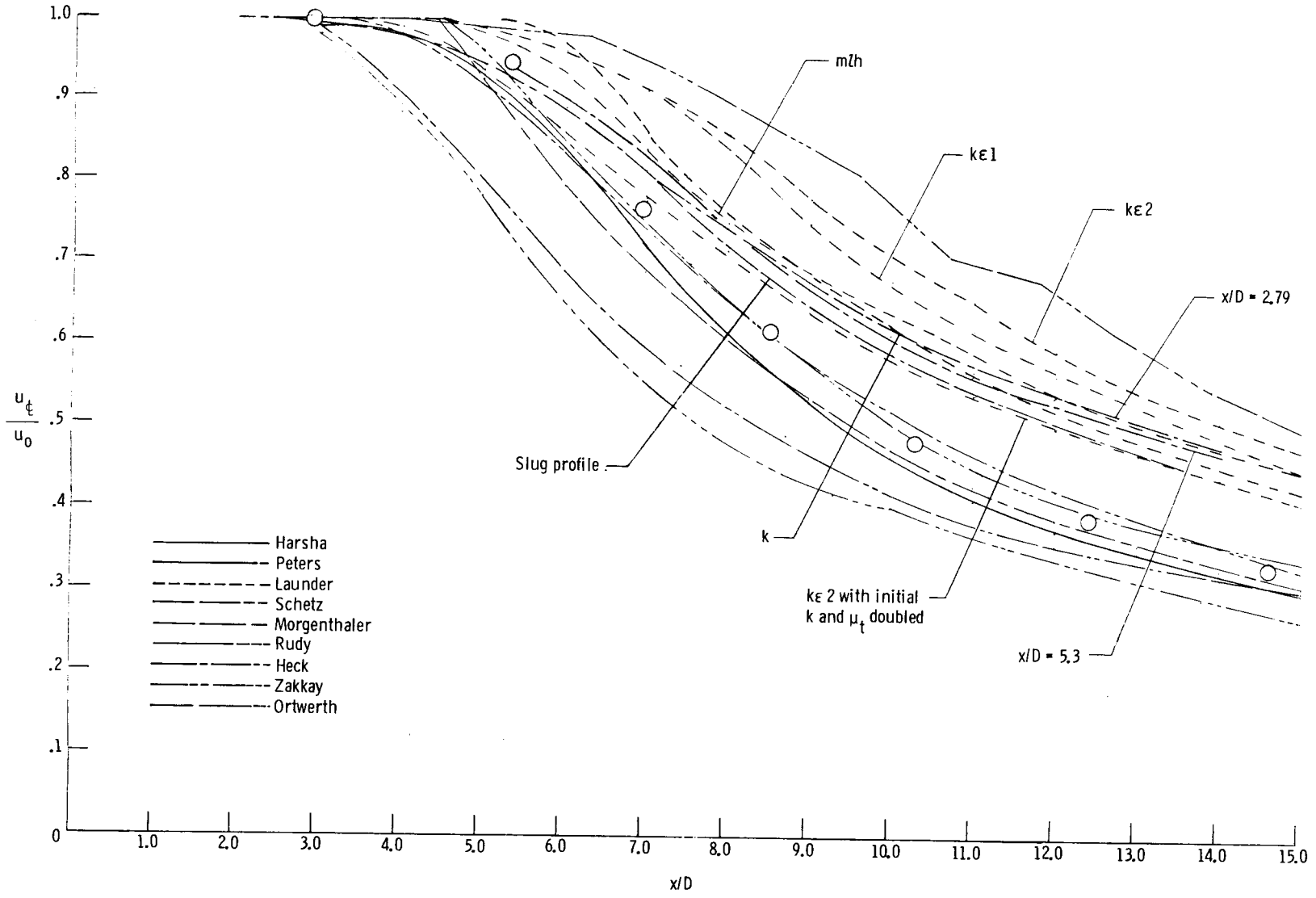
1.0
.9
.8
.7
.6
.5
.4
.3
.2
.1
0
$\frac{u_\ell}{u_0}$
1.0
2.0
3.0
4.0
5.0
6.0
7.0
8.0
9.0
10.0
11.0
12.0
13.0
14.0
15.0
x/D
mlh
kε1
kε2
x/D = 2.79
x/D = 5.3
Slug profile
k
kε 2 with initial
k and μ_t doubled
Harsha
Peters
Launder
Schetz
Morgenthaler
Rudy
Heck
Zakkay
Ortwerth

Test case 10

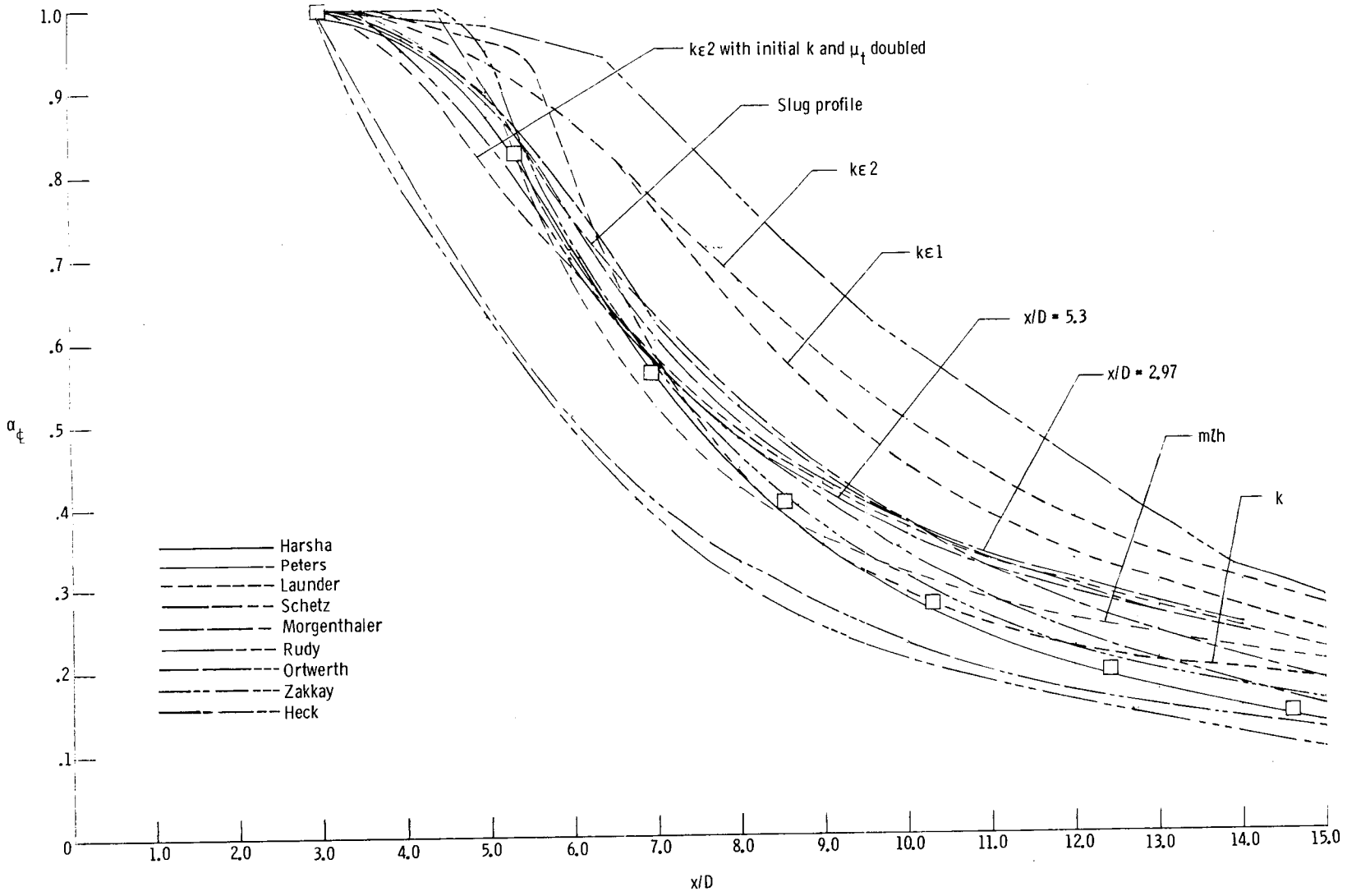
kε2 with initial k and μ_t doubled
Slug profile
kε2
kε1
x/D = 5.3
x/D = 2.97
mℓh
k
Harsha
Peters
Launder
Schetz
Morgenthaler
Rudy
Ortwerth
Zakkay
Heck
α_t
1.0
.9
.8
.7
.6
.5
.4
.3
.2
.1
0
1.0
2.0
3.0
4.0
5.0
6.0
7.0
8.0
9.0
10.0
11.0
12.0
13.0
14.0
15.0
x/D

Test case 10

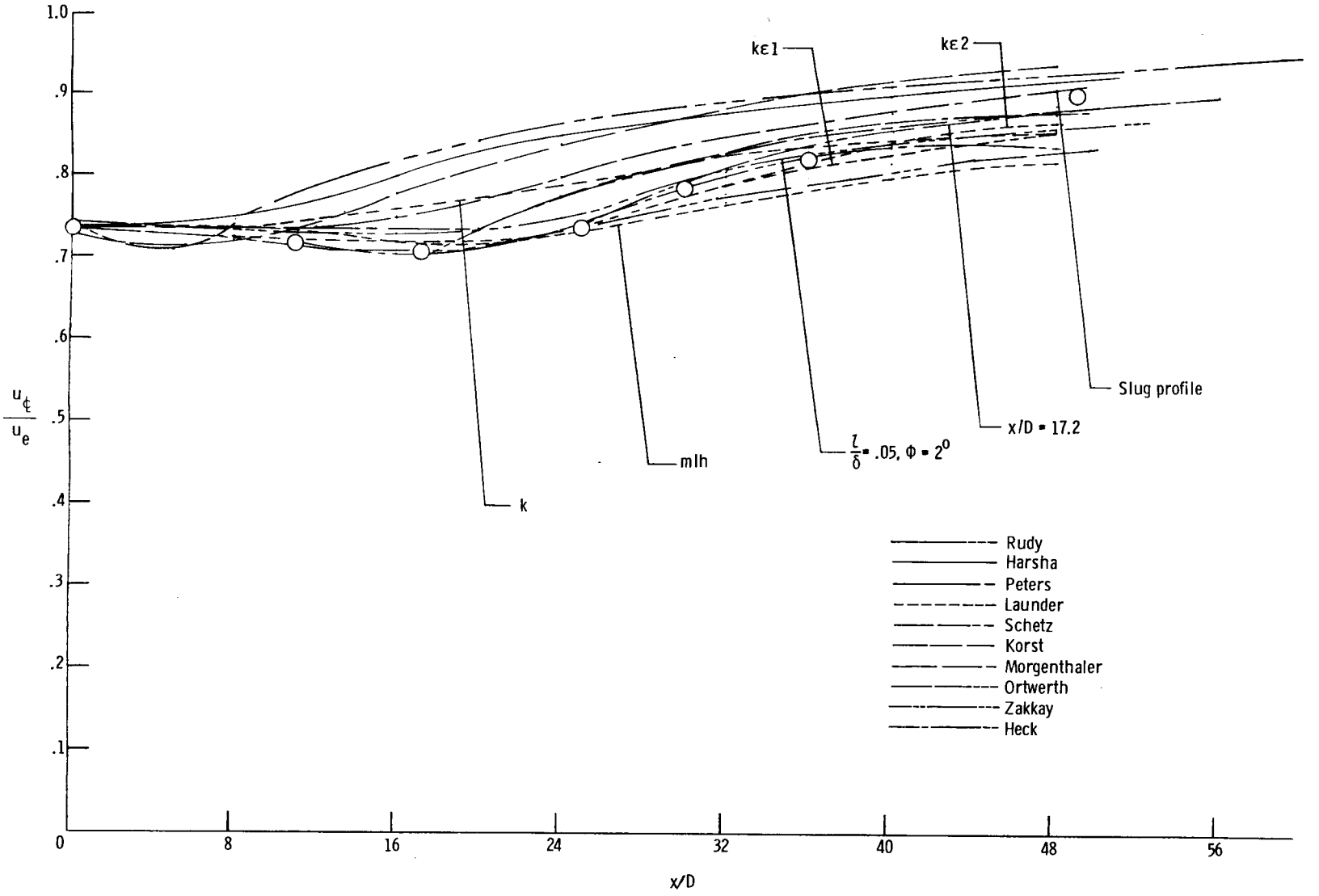
1.0
.9
.8
.7
.6
.5
.4
.3
.2
.1
0
8
16
24
32
40
48
56
x/D
$\frac{u_\ell}{u_e}$
kε1
kε2
k
mlh
$\frac{l}{\delta}$ = .05, Φ = 2°
x/D = 17.2
Slug profile
Rudy
Harsha
Peters
Launder
Schetz
Korst
Morgenthaler
Ortwerth
Zakkay
Heck

Test case 11

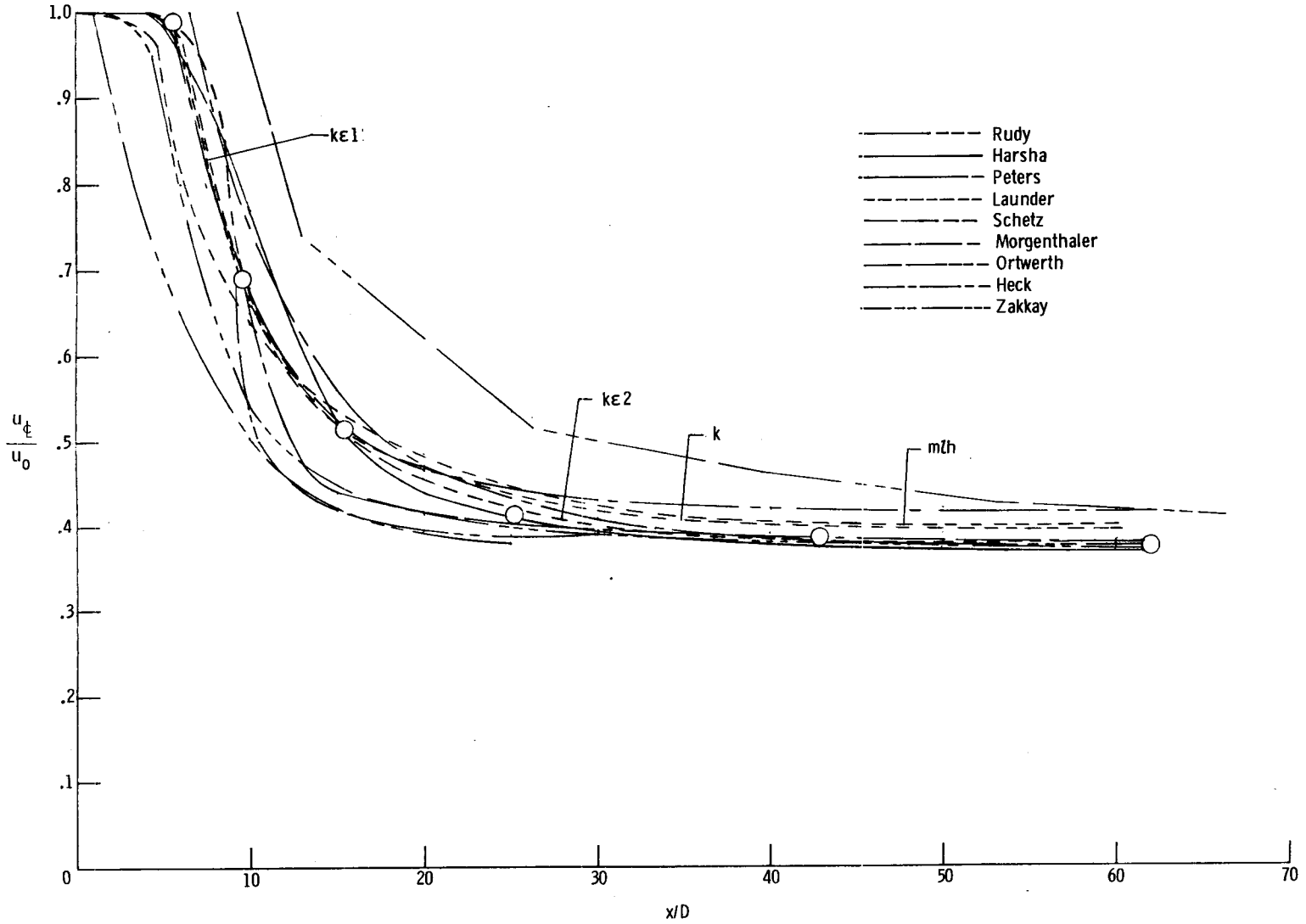
1.0
.9
.8
.7
.6
.5
.4
.3
.2
.1
0
$\frac{u_{\ell}}{u_0}$
kε1
kε2
k
mℓh
Rudy
Harsha
Peters
Launder
Schetz
Morgenthaler
Ortwerth
Heck
Zakkay
10
20
30
40
50
60
70
x/D

Test case 12

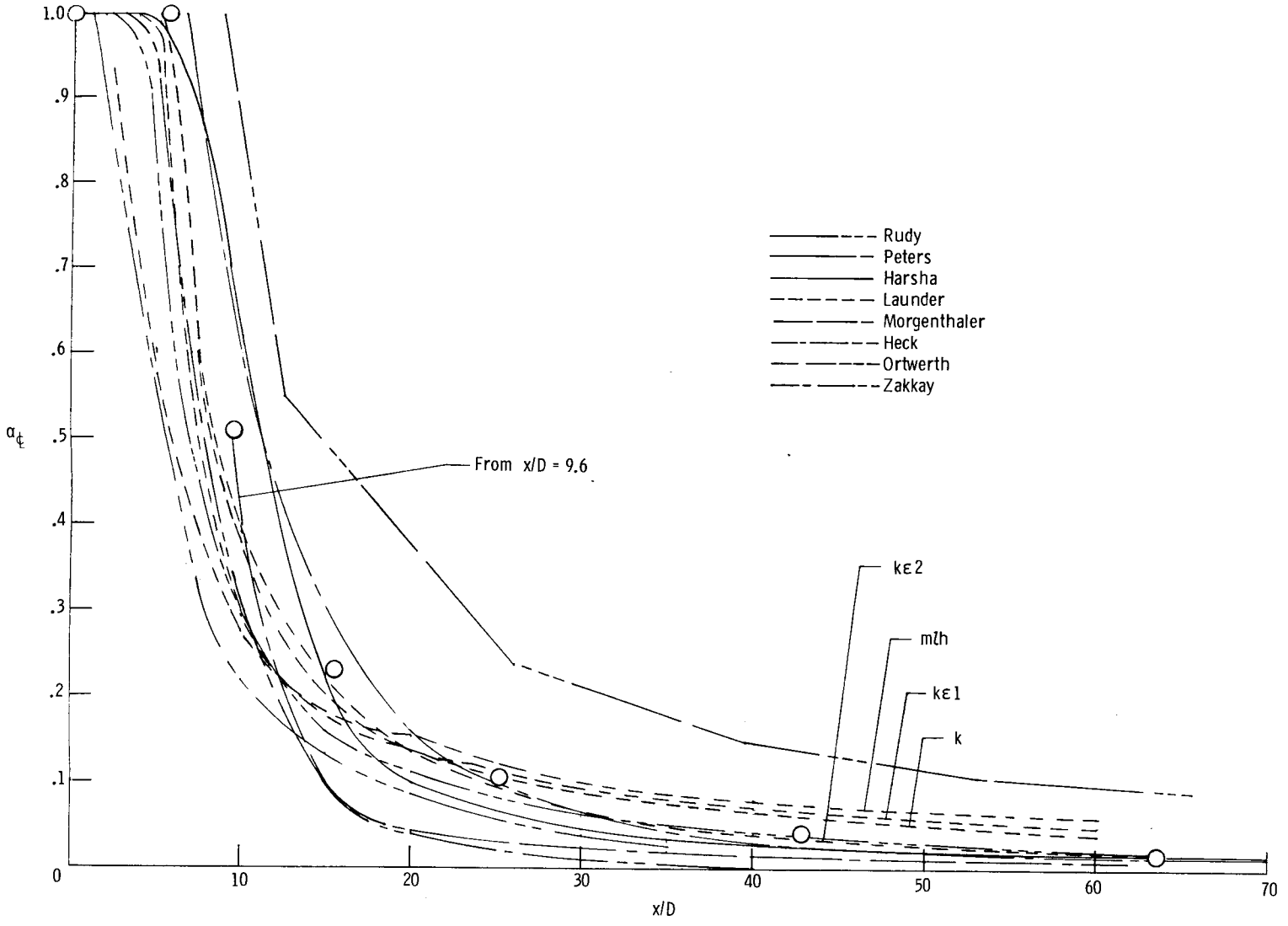
1.0
.9
.8
.7
.6
.5
.4
.3
.2
.1
0
α_ϕ
10
20
30
40
50
60
70
x/D
Rudy
Peters
Harsha
Launder
Morgenthaler
Heck
Ortwerth
Zakkay
From x/D = 9.6
kε2
mlh
kε1
k

Test case 12

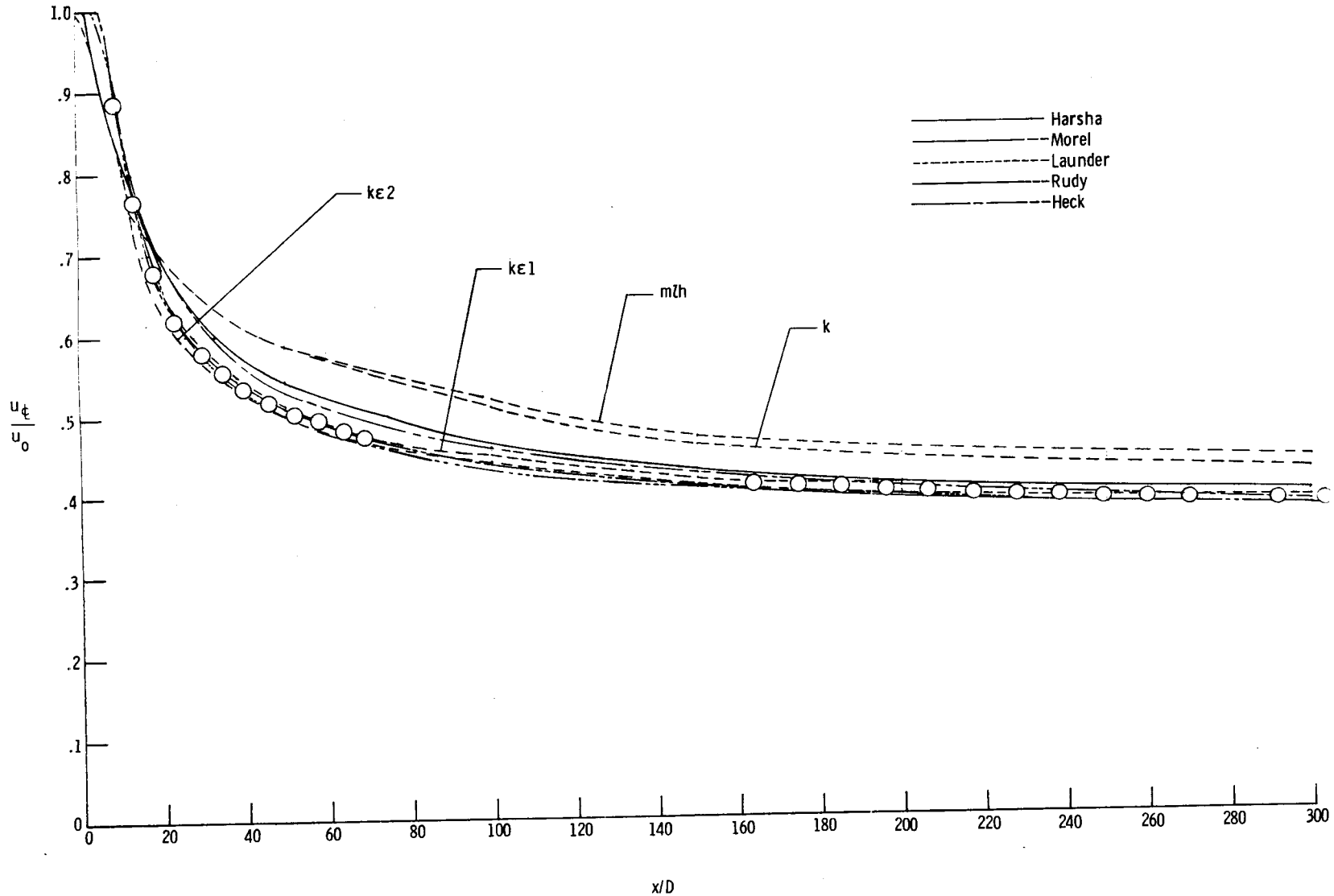
1.0
.9
.8
.7
.6
.5
.4
.3
.2
.1
0
$\frac{u_\phi}{u_0}$
kε2
kε1
mZh
k
Harsha
Morel
Launder
Rudy
Heck
0
20
40
60
80
100
120
140
160
180
200
220
240
260
280
300
x/D

Test case 13

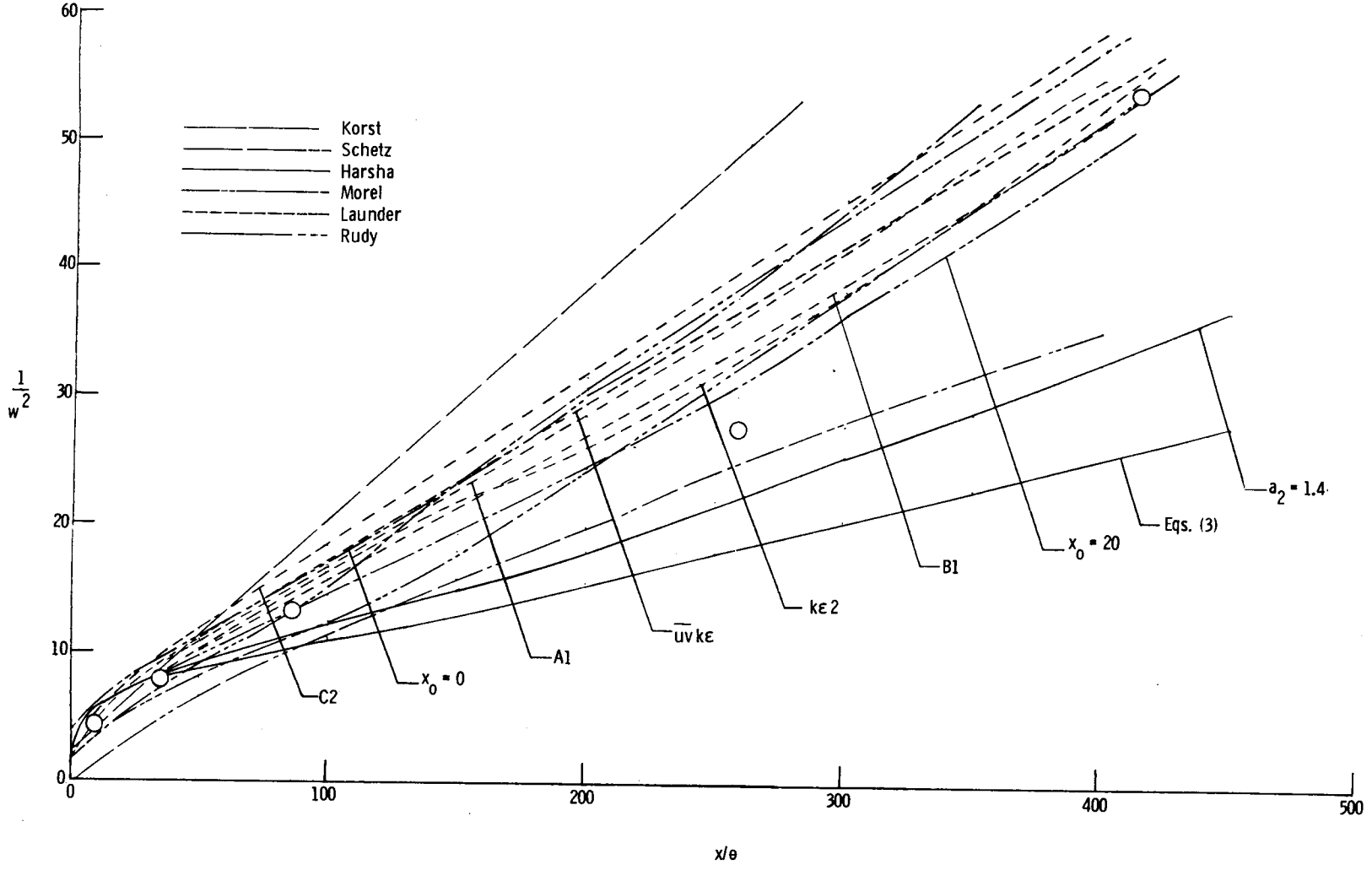
Korst
Schetz
Harsha
Morel
Launder
Rudy
$\frac{1}{w^2}$
x/θ
C2
$x_0 = 0$
A1
$\overline{uv}k\varepsilon$
$k\varepsilon 2$
B1
$x_0 = 20$
Eqs. (3)
$a_2 = 1.4$

Test case 14

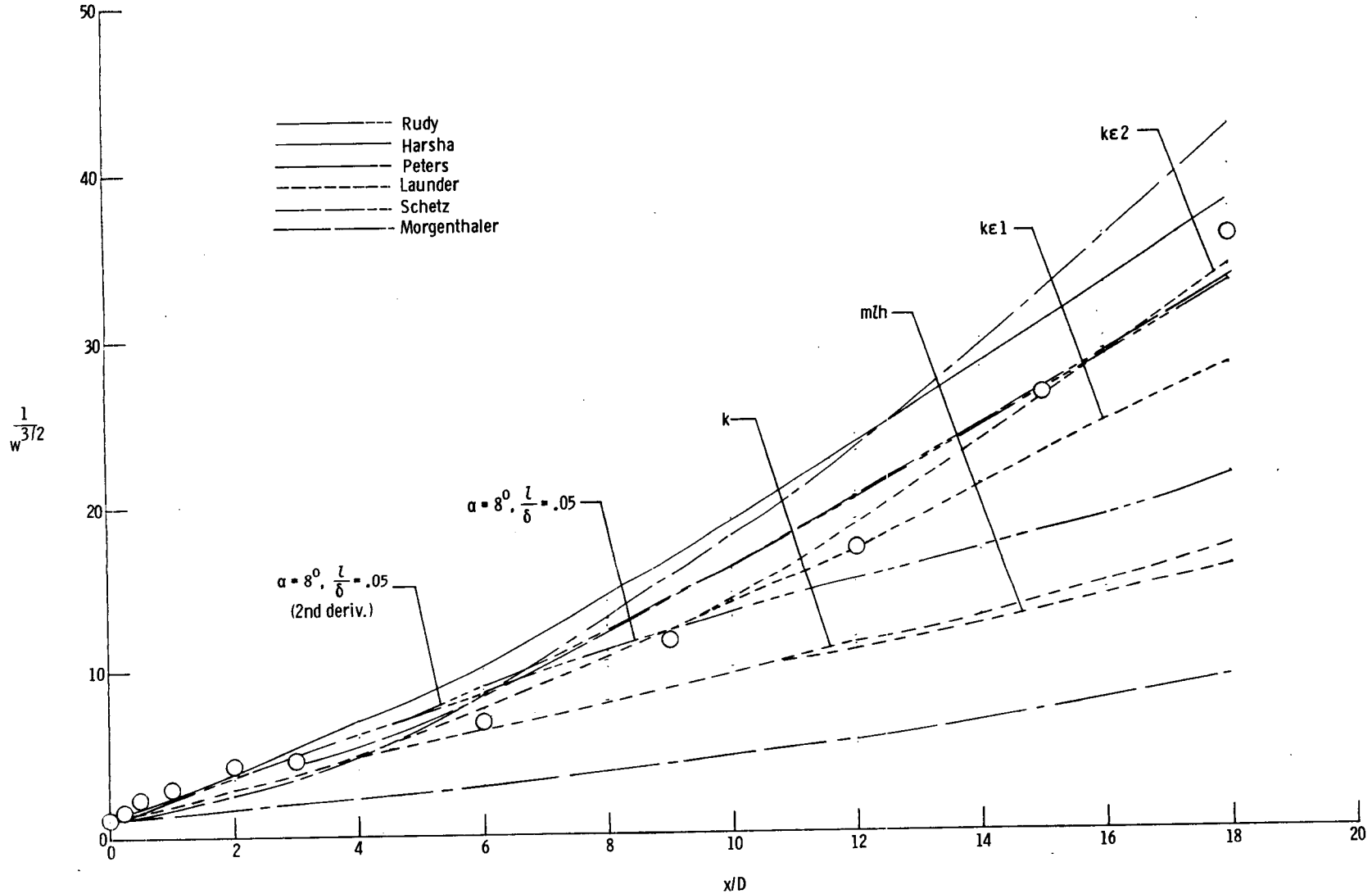
Rudy
Harsha
Peters
Launder
Schetz
Morgenthaler
kε2
kε1
mℓh
k
α = 8°, l/δ = .05
α = 8°, l/δ = .05
(2nd deriv.)
l/w^3/2
x/D
0
10
20
30
40
50
0
2
4
6
8
10
12
14
16
18
20

Test case 15

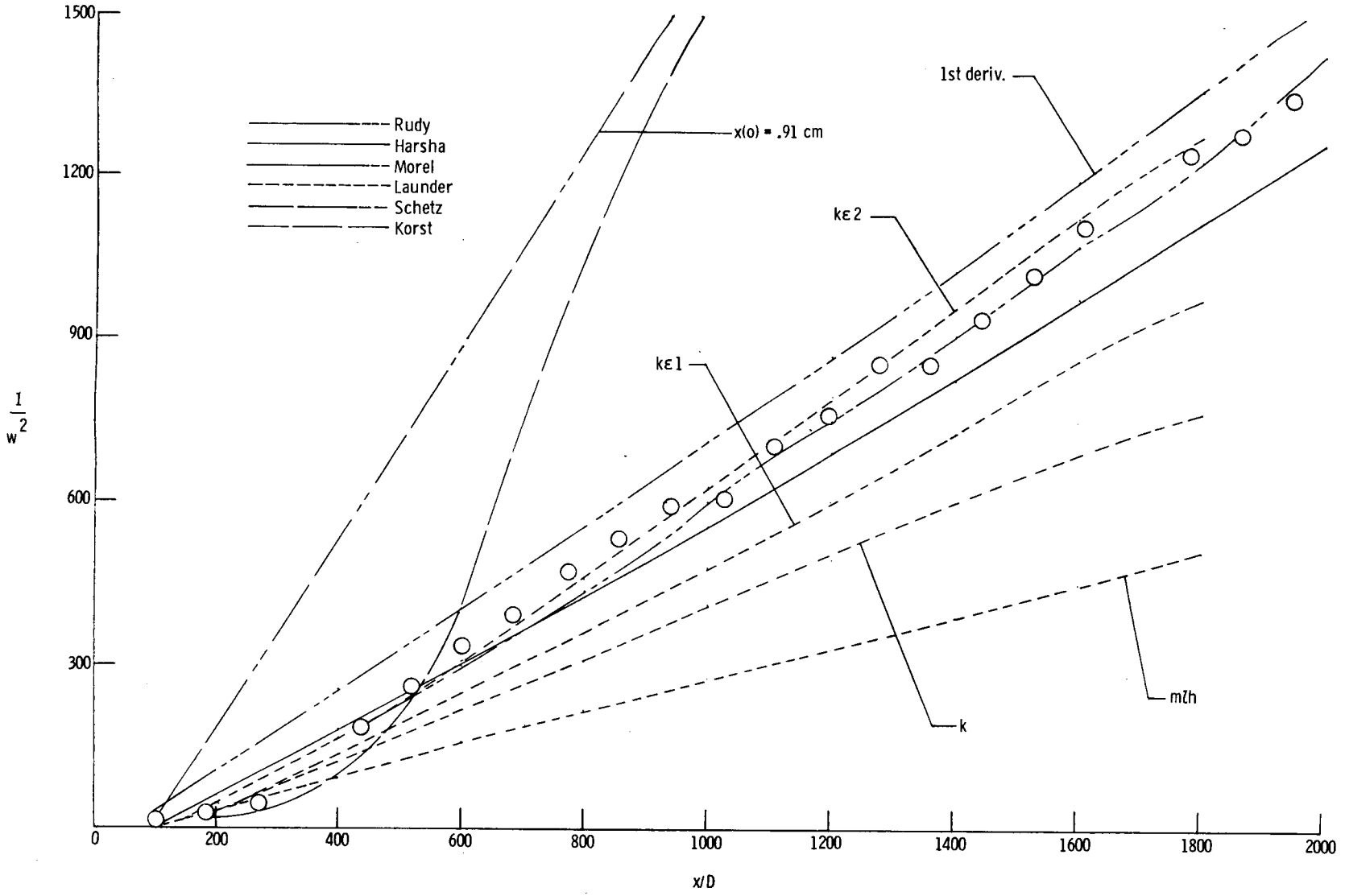
1500
1200
900
600
300
0
200
400
600
800
1000
1200
1400
1600
1800
2000
x/D
$\frac{1}{w^2}$
Rudy
Harsha
Morel
Launder
Schetz
Korst
x(o) = .91 cm
1st deriv.
kε2
kε1
k
mℓh

Test case 16

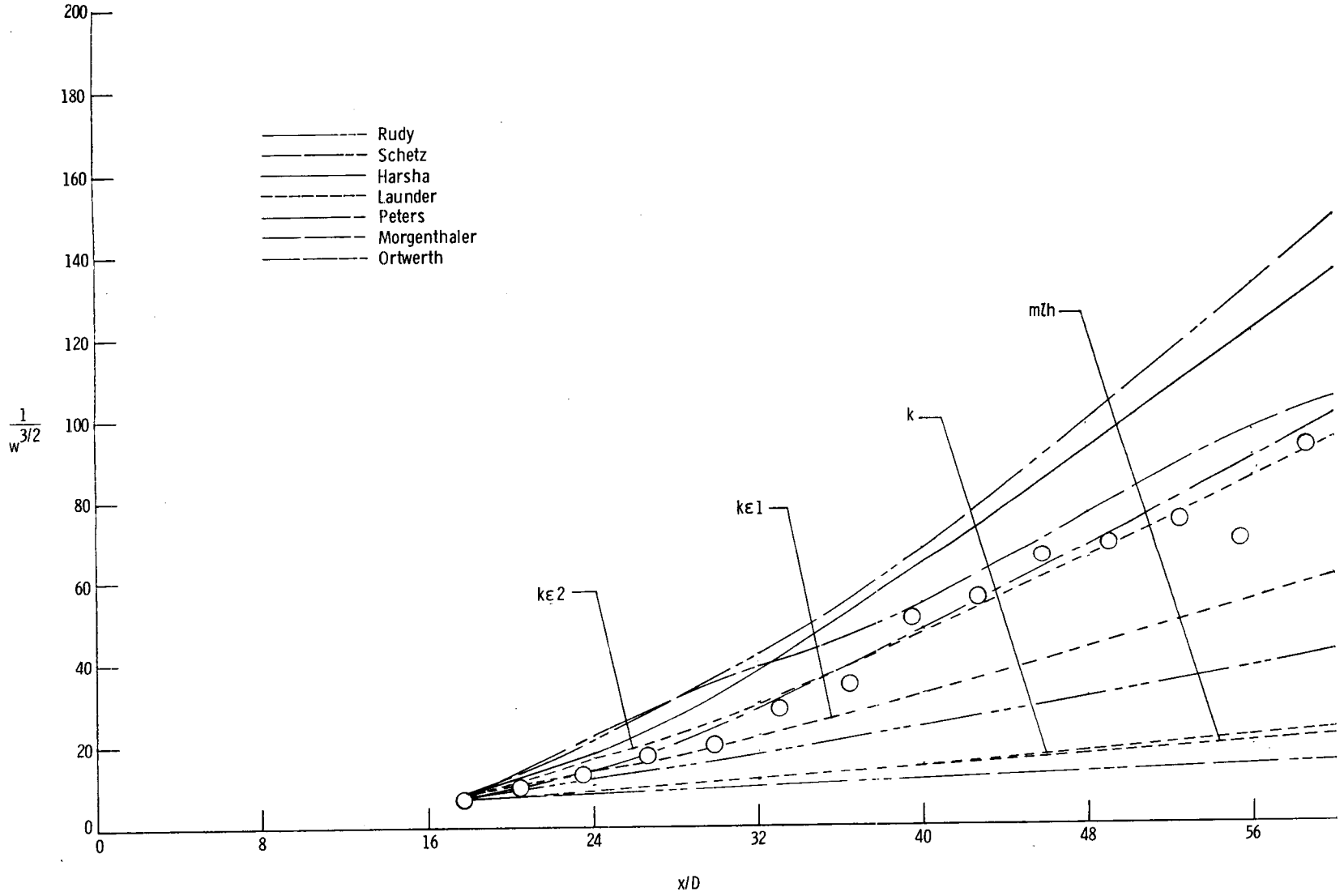
Rudy
Schetz
Harsha
Launder
Peters
Morgenthaler
Ortwerth
mℓh
k
kε1
kε2
$\frac{1}{w^{3/2}}$
x/D
0
20
40
60
80
100
120
140
160
180
200
0
8
16
24
32
40
48
56

Test case 17

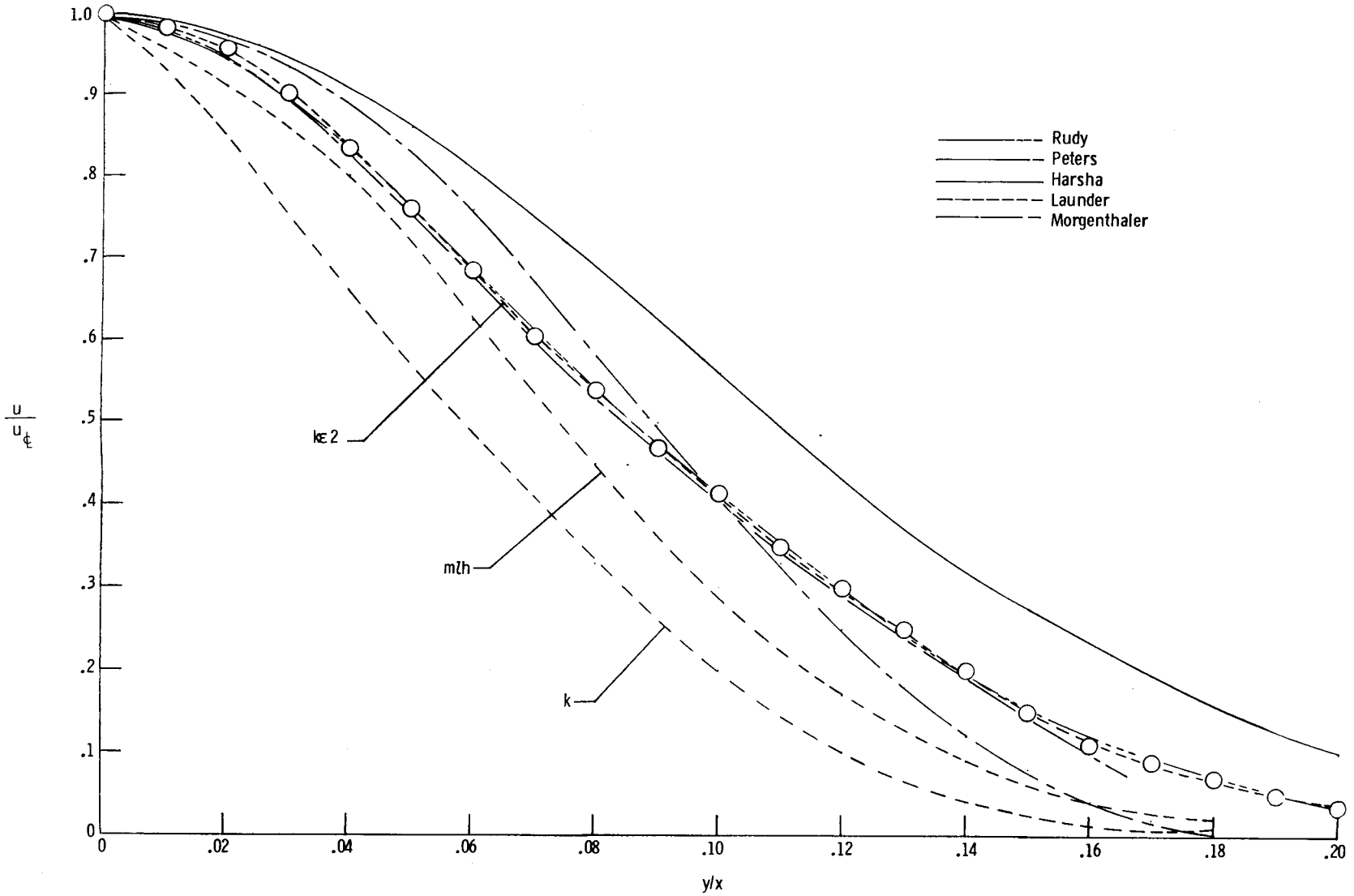
Rudy
Peters
Harsha
Launder
Morgenthaler
kε2
mℓh
k
u/u_e
y/x
1.0
.9
.8
.7
.6
.5
.4
.3
.2
.1
0
0
.02
.04
.06
.08
.10
.12
.14
.16
.18
.20

Test case 18

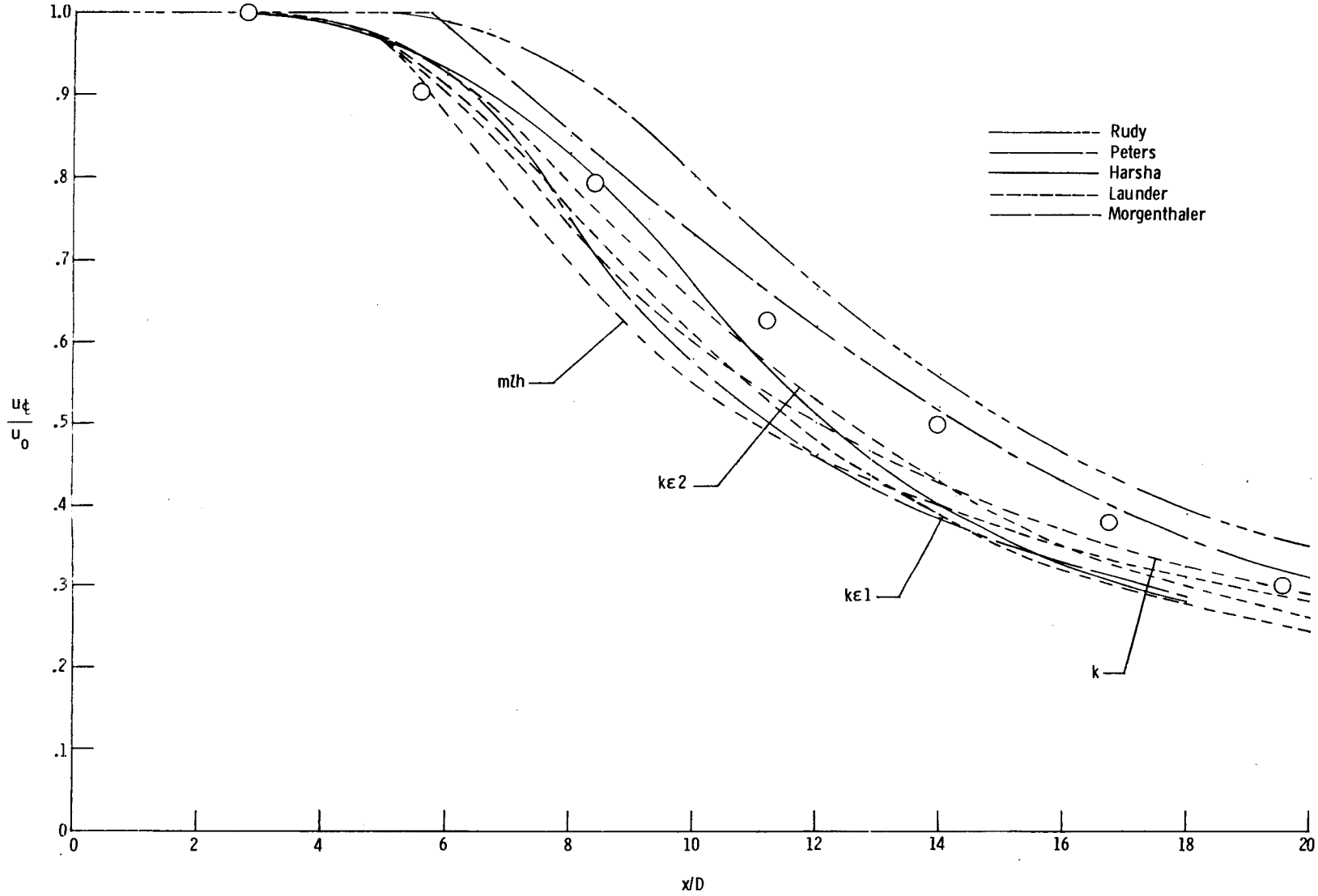
Rudy
Peters
Harsha
Launder
Morgenthaler
mℓh
kε2
kε1
k
$\frac{u_\ell}{u_0}$
x/D
1.0
.9
.8
.7
.6
.5
.4
.3
.2
.1
0
0
2
4
6
8
10
12
14
16
18
20

Test case 19

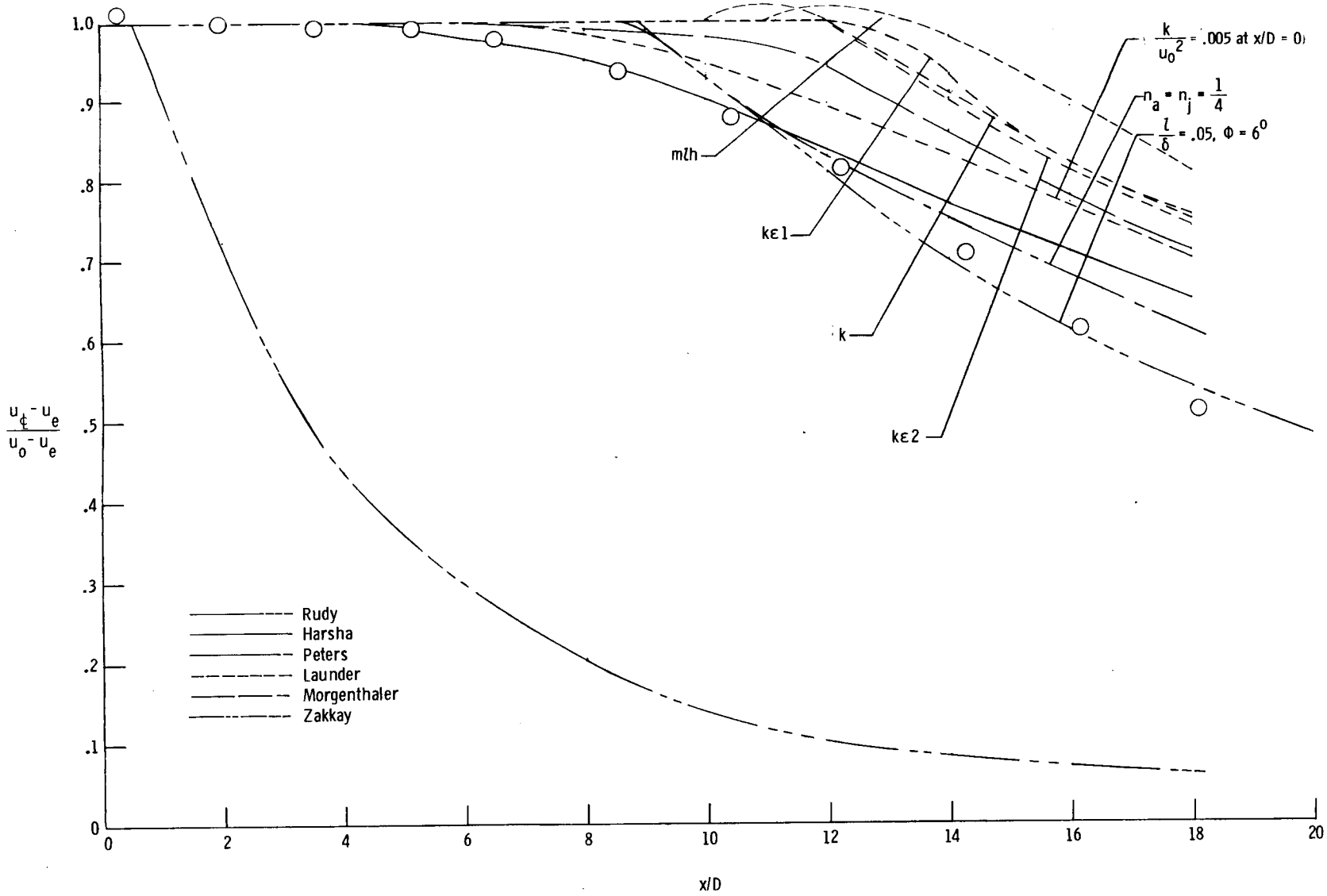
$\frac{k}{u_0^2}$ = .005 at x/D = 0
$n_a = n_j = \frac{1}{4}$
$\frac{l}{\delta}$ = .05, Φ = 6°
mℓh
kε1
k
kε2
Rudy
Harsha
Peters
Launder
Morgenthaler
Zakkay
$\frac{u_\ell - u_e}{u_0 - u_e}$
x/D
1.0
.9
.8
.7
.6
.5
.4
.3
.2
.1
0
0
2
4
6
8
10
12
14
16
18
20

Test case 20

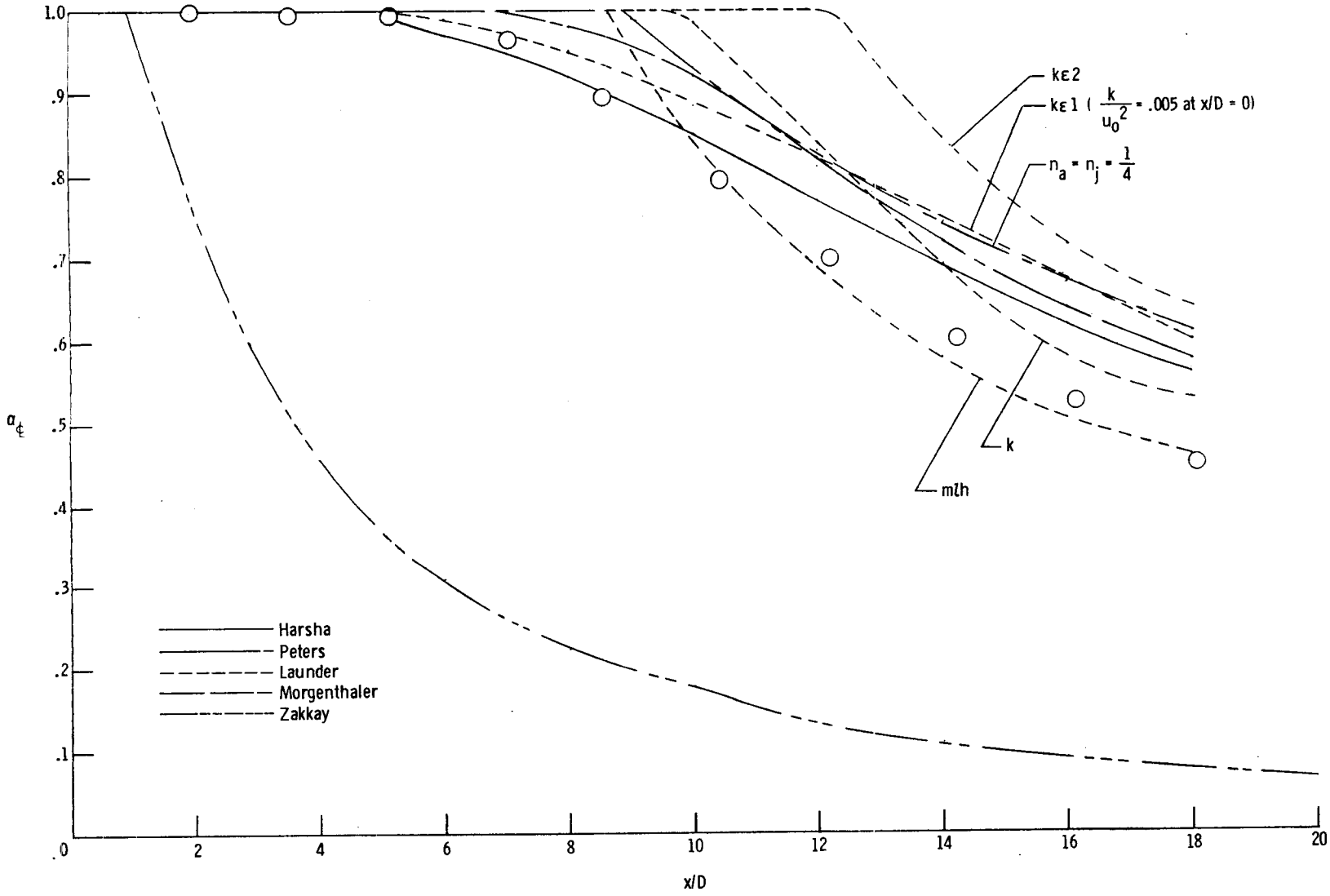
1.0
.9
.8
.7
.6
.5
.4
.3
.2
.1
0
a_ℓ
2
4
6
8
10
12
14
16
18
20
x/D
kε2
kε1 ($\frac{k}{u_0^2}$ = .005 at x/D = 0)
$n_a = n_j = \frac{1}{4}$
k
mℓh
Harsha
Peters
Launder
Morgenthaler
Zakkay

Test case 20

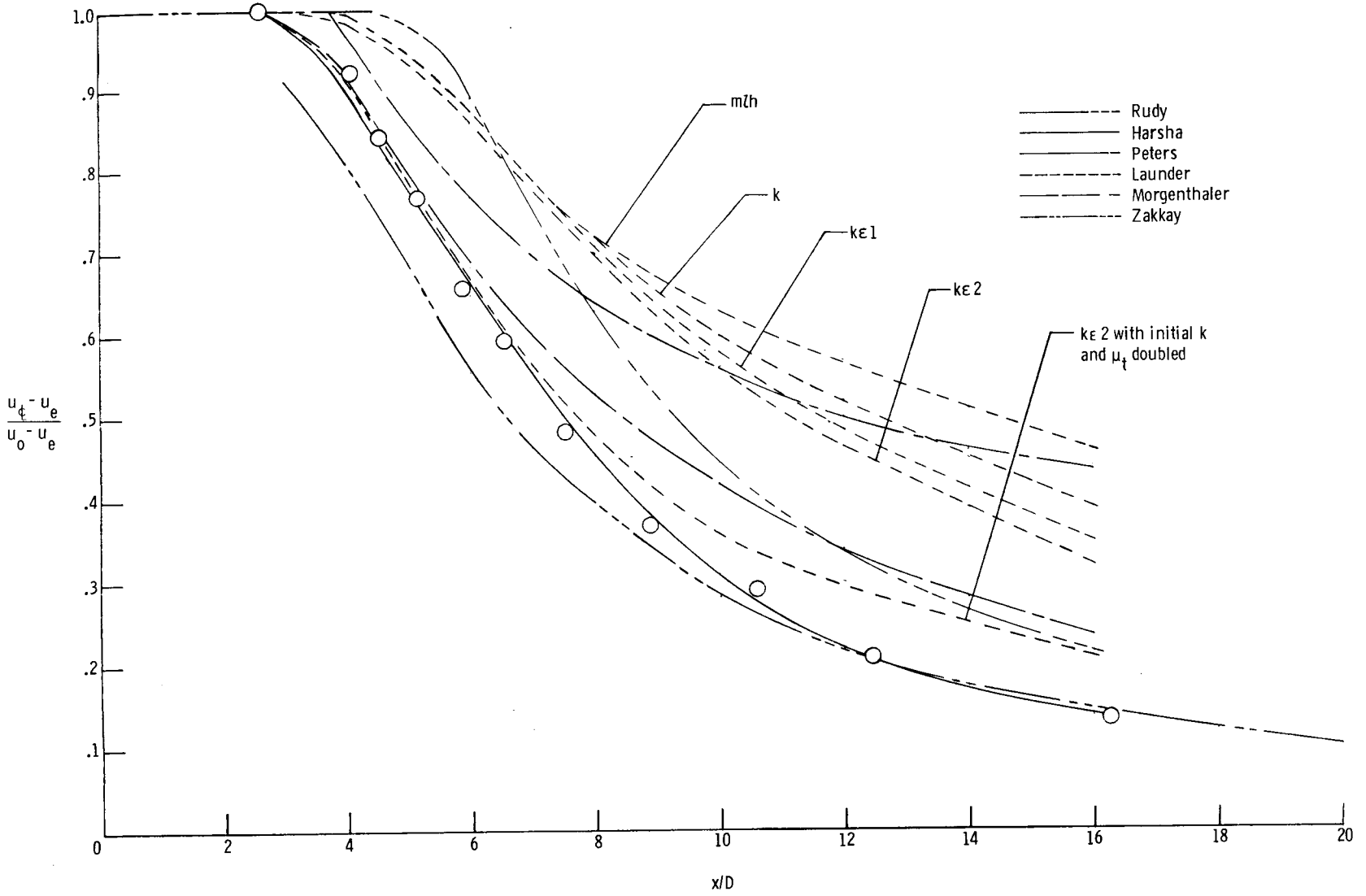
1.0
.9
.8
.7
.6
.5
.4
.3
.2
.1
0
2
4
6
8
10
12
14
16
18
20
x/D
$\frac{u_\ell - u_e}{u_o - u_e}$
mℓh
k
kε1
kε2
kε2 with initial k and μ_t doubled
Rudy
Harsha
Peters
Launder
Morgenthaler
Zakkay

Test case 21

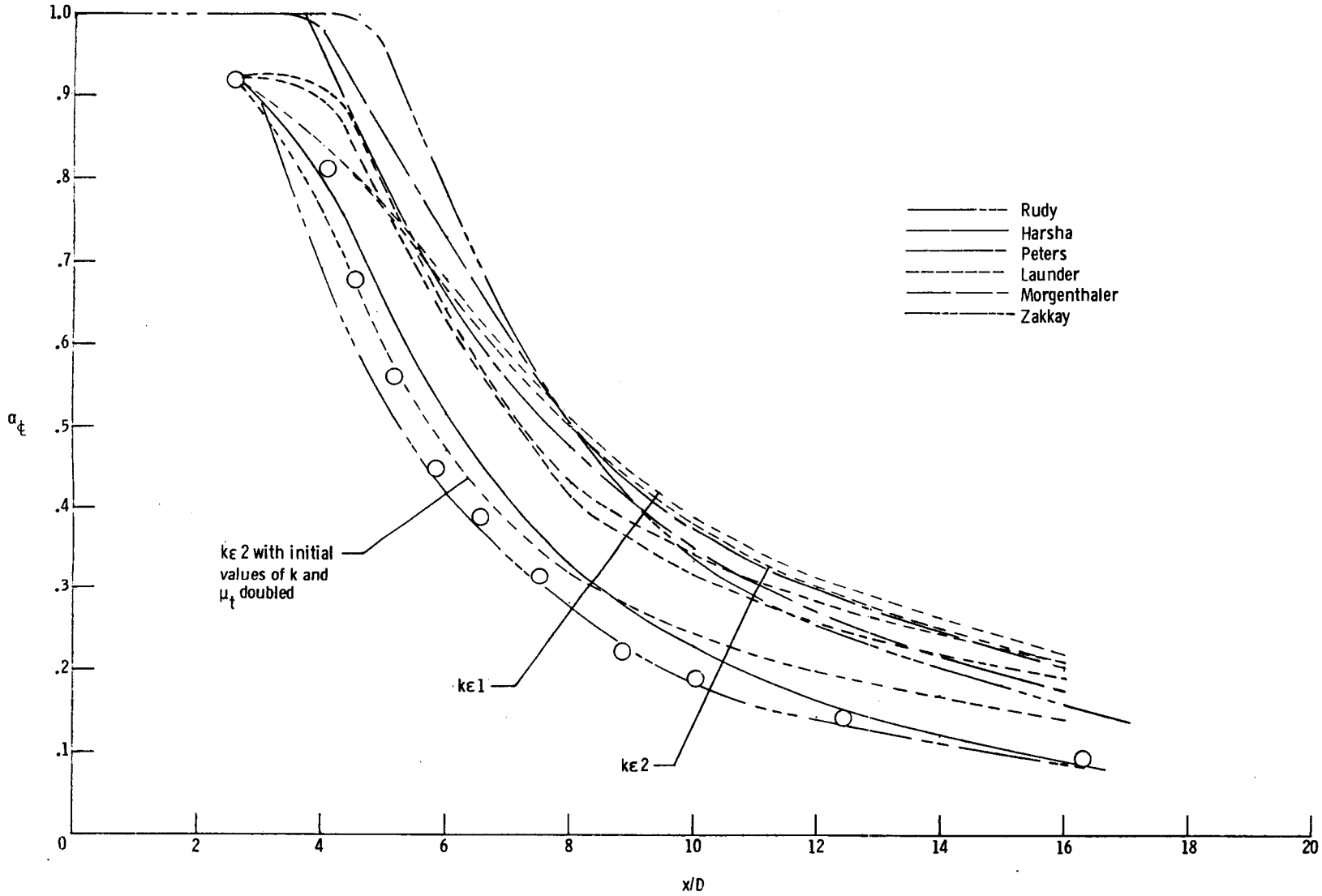
1.0
.9
.8
.7
.6
.5
.4
.3
.2
.1
0
α_ℓ
2
4
6
8
10
12
14
16
18
20
x/D
Rudy
Harsha
Peters
Launder
Morgenthaler
Zakkay
kε 2 with initial values of k and μ_t doubled
kε 1
kε 2

Test case 21

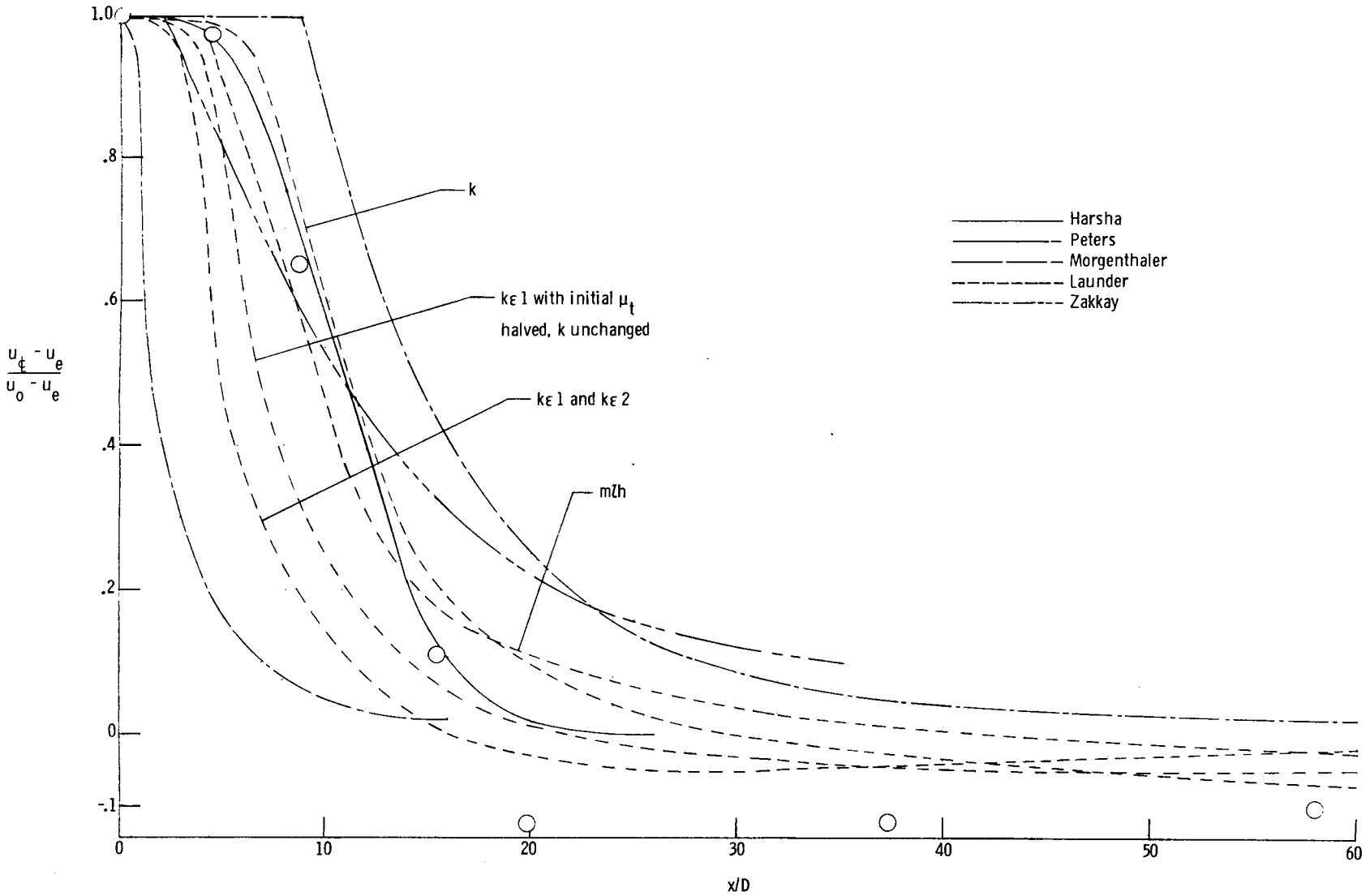
1.0
.8
.6
.4
.2
0
-.1
$\frac{u_\ell - u_e}{u_o - u_e}$
k
kε 1 with initial μ_t halved, k unchanged
kε 1 and kε 2
mžh
Harsha
Peters
Morgenthaler
Launder
Zakkay
0
10
20
30
40
50
60
x/D

Test case 22

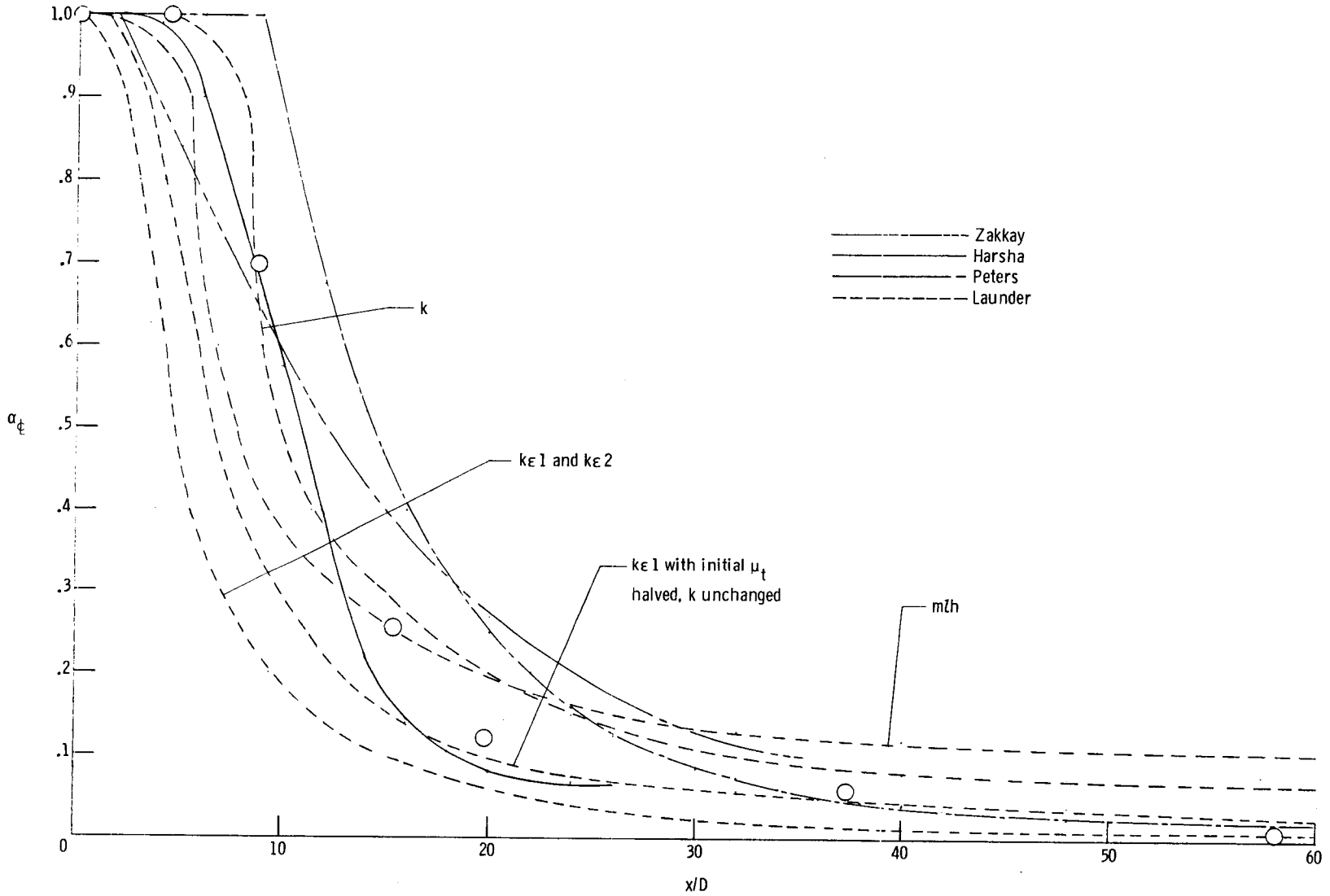
1.0
.9
.8
.7
.6
.5
.4
.3
.2
.1
0
α_{ℓ}
10
20
30
40
50
60
x/D
Zakkay
Harsha
Peters
Launder
k
kε1 and kε2
kε1 with initial μ_t
halved, k unchanged
mlh

Test case 22

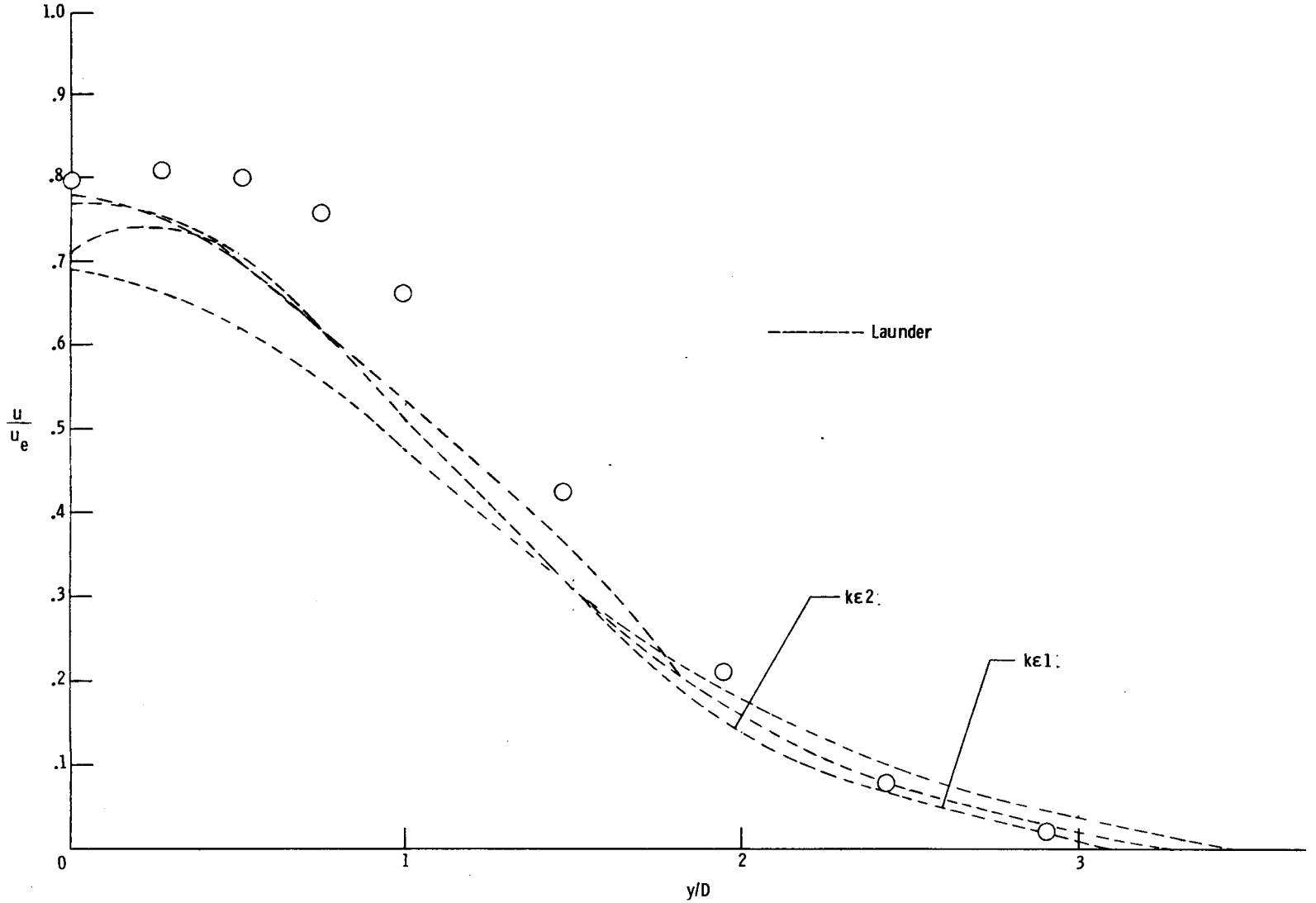

Test case 23 (x/D = 6.05)

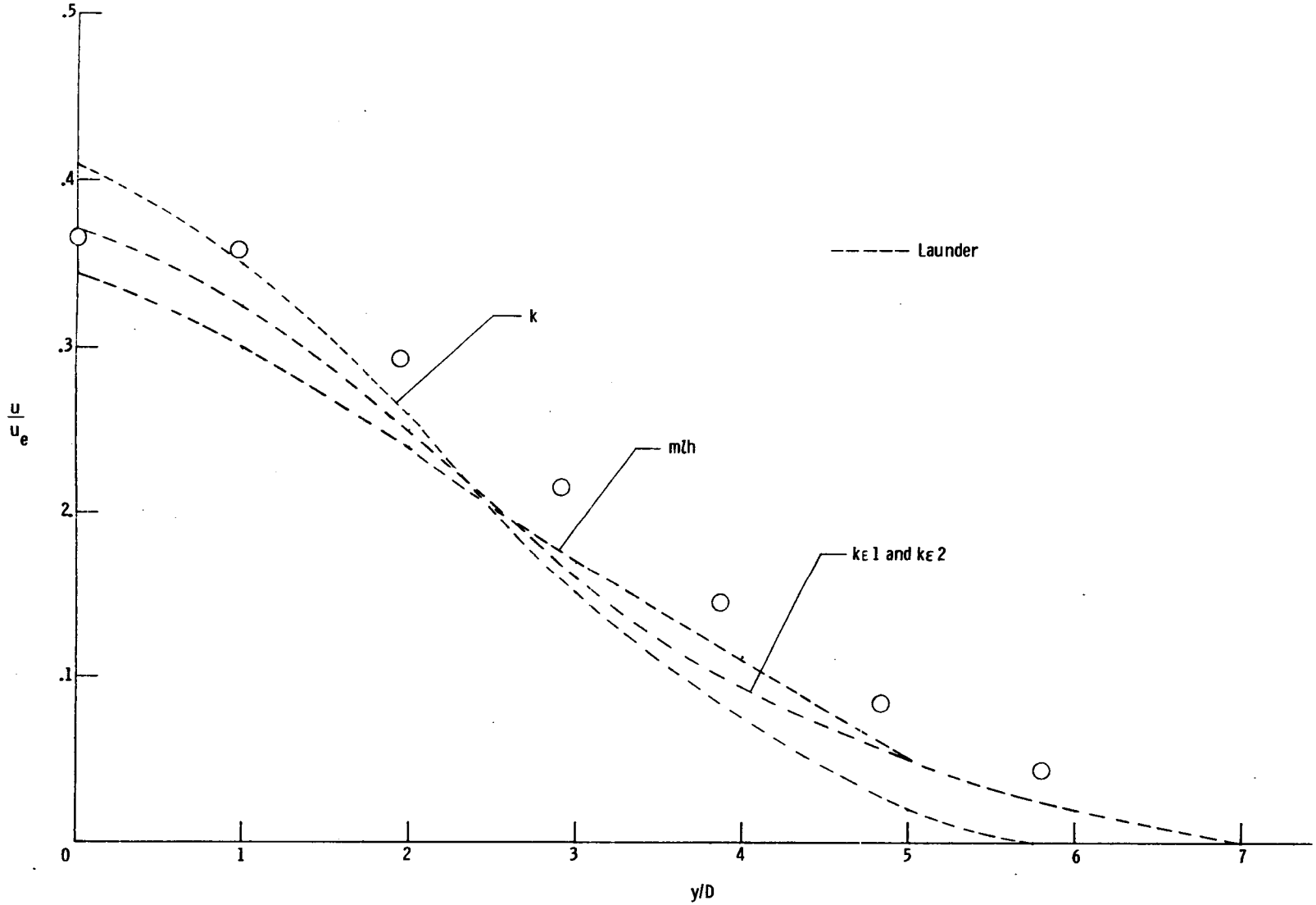

Test case 23 (x/D = 17.9)

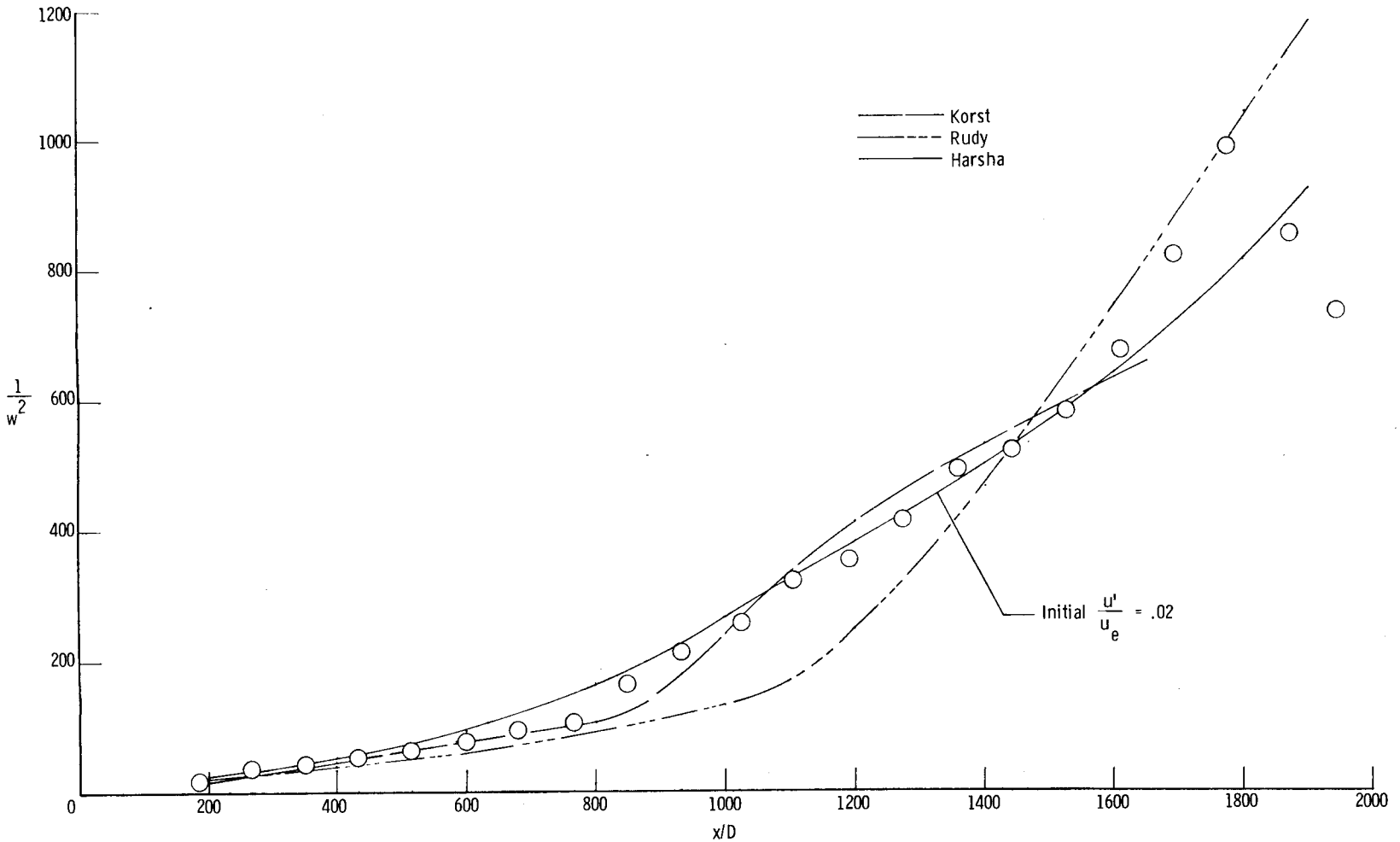
1200
1000
800
600
400
200
0
$\frac{1}{w^2}$
200
400
600
800
1000
1200
1400
1600
1800
2000
x/D
Korst
Rudy
Harsha
Initial $\frac{u'}{u_e}$ = .02

Test case 24

Results of the Additional Test Case to Compare Computer Codes

In the comparison of turbulent free mixing predictions from different authors the possibility exists that variation between the predictions may be due in part to differences in numerical computing procedures. To investigate this possibility the predictors were asked to run an additional test case using a prescribed eddy viscosity model with given initial conditions. This additional test case was considered optional since some predictors could not run the case without substantial changes in their computer programs.

The geometry of the additional test case flow was chosen to be coaxial with flow conditions typical of a hydrogen-air mixing experiment as follows:

$u_e/u_o = 0.26$

$u_o = 1000$ m/sec

$T_o = T_e = 650^o$ R

Turbulent Prandtl number = 0.7

Turbulent Schmidt number = 0.8

Primary stream: pure H_2

Secondary stream: air

Nozzle radius: $r_o = 2.0$ cm

The initial profiles were to be uniform with discontinuous changes in u, ρ, and α_{H_2} at $r/r_o = 1.0$.

The following eddy viscosity model (which was not being used in the conference by any of the predictors) was specified:

$$\mu_t = 0.02\left|\rho_e u_e - \rho_{\ell} u_{\ell}\right| r_{1/2}$$

where $r_{1/2}$ is the value of r where

$$u = \frac{1}{2}\left|u_{\ell} + u_e\right|$$

The objective of this additional test case was to compare computing procedures rather than turbulence modeling. Six of the predictors (Rudy, Harsha, Launder, Schetz, Morgenthaler, and Zakkay) ran the case. The resulting center-line velocity distributions are shown in the first figure and center-line values of mass fraction of H_2 are shown in the second figure. The resulting spread in the predictions corresponds to approximately a 10-percent variation in the value of the constant in the eddy viscosity model.

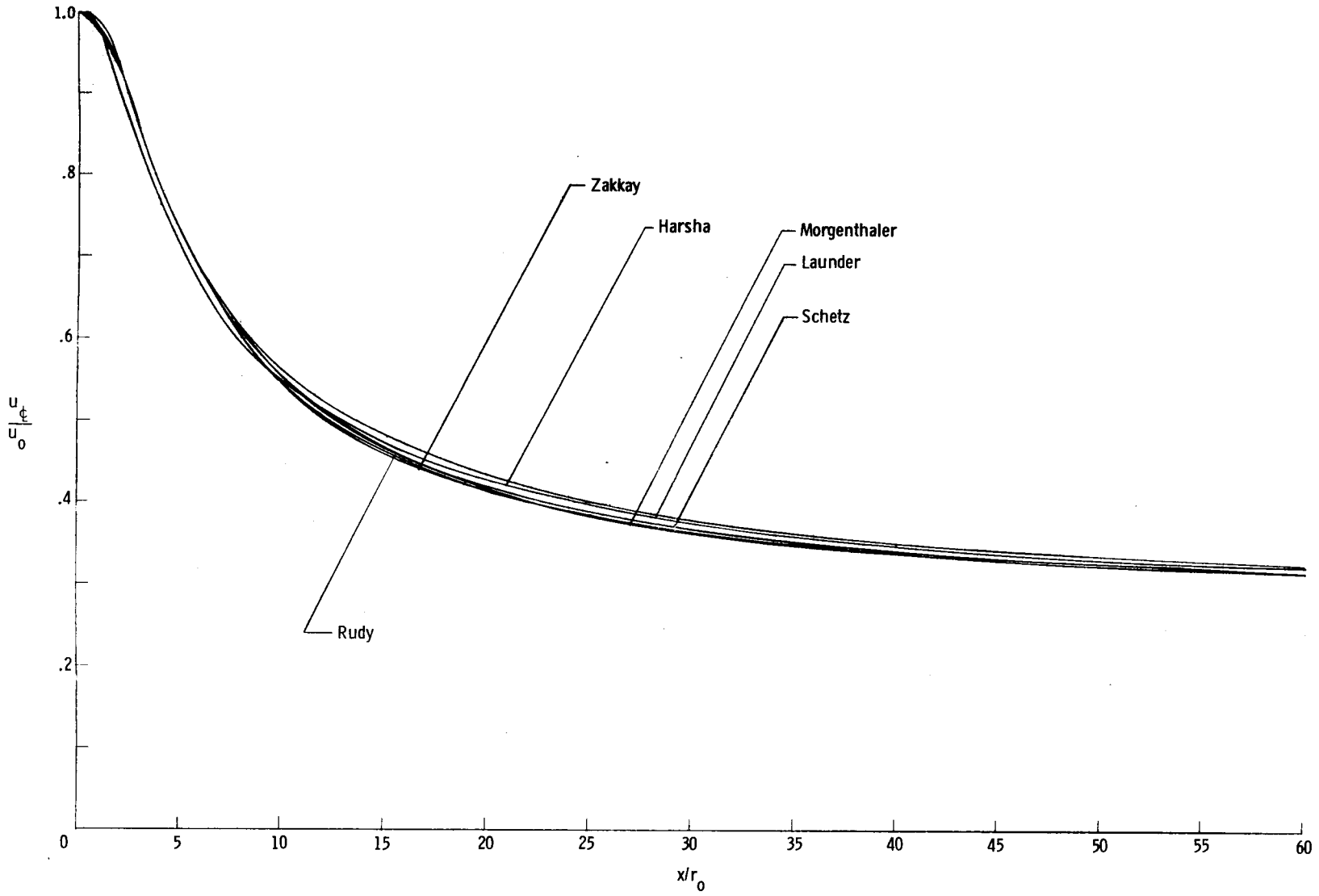

Additional test case

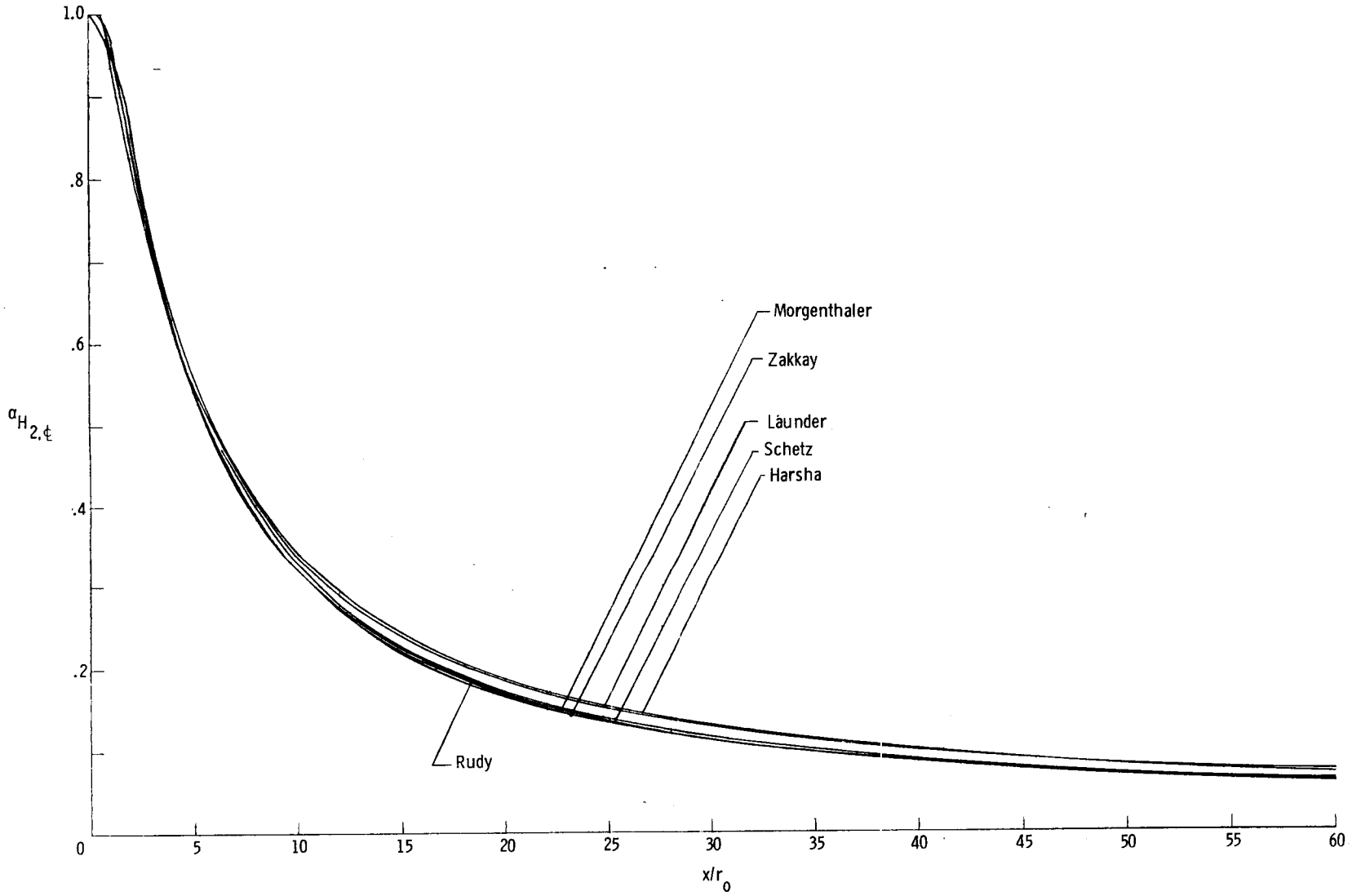

Additional test case

CLASSIFICATION SHEETS

The classification sheets were completed by the predictors and are intended to give the reader a concise description of the various prediction methods.

Authors: David H. Rudy and Dennis M. Bushnell

Class of method: Eddy viscosity method with algebraic length scale equation

Number of empirical constants or functions: Two (l/δ, ϕ or β)

Were the same ones used for all cases? No

Reason (numerical, physical) for any changes?

Two values for l/δ { 0.05 axisym. / 0.07 2-dim. } (δ defined differently in each region of jet and wake flows)

If needed in your method, how is initial shear profile generated? Are the initial $\tau_{max}/\rho(u_2 - u_1)^2$ values different for the four different classes of flows? Not needed

Time for running of method on typical cases on what computer: CDC 6600

Shear layers:	
Subsonic, constant density	100 to 200 sec
Supersonic $(u_2/u_1 = 0.05)$	1200 sec
Jets into still air:	
Test case 7 (supersonic)	2000 sec
Test cases 6, 18 (subsonic)	1200 sec
Coaxial jets:	
Typical case	200 to 300 sec
Wakes:	
Subsonic (test cases 14, 15)	600 to 1200 sec
Supersonic (test cases 16, 17, 24)	70 sec

Cost estimate: $40/1000 sec

Availability of the deck: From authors – unlimited distribution

Precautions for potential industrial user: Equations solved in Von Mises plane (see paper) with constant step size in normal direction

Special assumptions for compressible flows: None

Test cases tried (please circle):

S: (1) (2) (3) (4) (5)

J: (6) (7) (8) (18) (19)

JJ: (9) (10) (11) (12) (13) (20) (21) 22 23

W: (14) (15) (16) (17) (24)

Key definitions to remember:

δ width of mixing region (see details in paper no. 4)

Authors: Leonard S. Cohen

Class of method: Boundary layer form of conservation equations with kinematic eddy viscosity

Number of empirical constants or functions: Two

Were the same ones used for all cases? No

Reason (numerical, physical) for any changes? One "constant" takes on different values for two-dimensional and axisymmetric flows. The other depends on initial turbulence level.

If needed in your method, how is initial shear profile generated? Are the initial $\tau_{max}/\rho(u_2 - u_1)^2$ values different for the four different classes of flows? Not applicable

Time for running of method on typical cases on what computer: 10 min on UNIVAC 1108

Cost estimate: $30/case

Availability of the deck: Available to Government contractors through Contract Officer

Precautions for potential industrial user: (1) No transverse pressure gradient,
(2) Momentum flux ratio between outer and inner jet should not much exceed 4, and
(3) Initial boundary layer requires special treatment in search for mixing layer height.

Special assumptions for compressible flows: None

Test cases tried (please circle):

S: (1) (2) 3 4 5

J: 6 (7) 8 18 19

JJ: 9 10 11 12 13 20 21 22 23

W: 14 15 16 17 24

Key definitions to remember:

m is the external to centerline velocity ratio

n is the external to centerline density ratio

m_1 is the external to centerline velocity ratio at which the preturbulence mechanism achieves dominance.

Authors: H. H. Korst, W. L. Chow, R. F. Hurt, R. A. White, and A. L. Addy

Class of method: Numerical method with average eddy diffusivity

Number of empirical constants or functions: One

Were the same ones used for all cases? Yes (two-dimensional flow cases only)

Reason (numerical, physical) for any changes?

If needed in your method, how is initial shear profile generated? Are the initial $\tau_{max}/\rho(u_2 - u_1)^2$ values different for the four different classes of flows?

Initial shear stress is matched with the wall boundary layer flow

Time for running of method on typical cases on what computer: ≈1 min on IBM 7094

Cost estimate: $5

Availability of the deck: Yes

Precautions for potential industrial user:

Special assumptions for compressible flows: None

Test cases tried (please circle):

S: (1) (2) (3) (4) (5)

J: 6 7 8 18 19

JJ: 9 10 11 12 13 20 21 22 23

W: (14) 15 (16) 17 (24)

Key definitions to remember:

$$\frac{\epsilon_t}{\theta^{2-d}} = f(\xi)$$

Eddy viscosity models for jet mixing and wake flows

Authors: Joseph A. Schetz

Class of method: Differential mean field

Number of empirical constants or functions: One (each for planar and axisymmetric)

Were the same ones used for all cases? Yes

Reason (numerical, physical) for any changes?

If needed in your method, how is initial shear profile generated? Are the initial $\tau_{max}/\rho(u_2 - u_1)^2$ values different for the four different classes of flows?

Time for running of method on typical cases on what computer:

68 sec for test case 16 on IBM 370/155

Cost estimate:

Availability of the deck: Original code obtained from Gen. Appl. Sci. Lab. through Navy

Precautions for potential industrial user:

Avoid $\rho_j U_j/\rho_e U_e$ greater than 3.0 or less than 0.4

Special assumptions for compressible flows: None

Test cases tried (please circle):

S: 1 2 3 4 5

J: 6 7 8 18 19

JJ: (9) (10) (11) (12) 13 20 21 22 23

W: (14) (15) (16) (17) 24

Key definitions to remember:

Authors: J. H. Morgenthaler and S. W. Zelazny

Class of method: Differential mean field with eddy viscosity model

Number of empirical constants or functions: One constant and three functions

Were the same ones used for all cases? Yes

Reason (numerical, physical) for any changes?

If needed in your method, how is initial shear profile generated? Are the initial $\tau_{max}/\rho(u_2 - u_1)^2$ values different for the four different classes of flows?

Time for running of method on typical cases on what computer: 4.5 min on IBM 360/65

Cost estimate: $36/typical case

Availability of the deck: Developed on internal research and development program

Precautions for potential industrial user:

Special assumptions for compressible flows: None

Test cases tried (please circle):

S: 1 2 3 4 5

J: (6) (7) (8) (18) (19)

JJ: (9) (10) (11) (12) 13 (20) (21) (22) 23

W: 14 (15) 16 (17) 24

Key definitions to remember: Eddy viscosity proportional to the mass defect and inversely proportional to a characteristic length which reduces to the velocity half width downstream of the core. Models of axial and transverse turbulence intensity are obtained through a derived relationship with eddy viscosity. Radial variation of these models is included.

Authors: V. Zakkay, R. Sinha, and S. Nomura

Class of method: Numerical: Von Mises transformation

Number of empirical constants or functions: One

Were the same ones used for all cases? Yes

Reason (numerical, physical) for any changes?

If needed in your method, how is initial shear profile generated? Are the initial $\tau_{max}/\rho(u_2 - u_1)^2$ values different for the four different classes of flows?

Time for running of method on typical cases on what computer: 3 min on CDC 6600

Cost estimate: University cost: $20

Availability of the deck:

Precautions for potential industrial user: Special precautions to be used for step profile

Special assumptions for compressible flows: None

Test cases tried (please circle):

S: 1 2 3 4 5

J: 6 7 8 18 19

JJ: (9) (10) (11) (12) 13 (20) (21) (22) 23

W: 14 15 16 17 24

Key definitions to remember:

Authors: B. E. Launder, A. Morse, W. Rodi, and D. B. Spalding

Class of method: 2-equation turbulent-viscosity model (kϵ2)

Number of empirical constants or functions: 4 constants, 1 function (2 functions for axisymmetric flows)

Were the same ones used for all cases? No. See table 4 on page 411.

Reason (numerical, physical) for any changes?

If needed in your method, how is initial shear profile generated? Are the initial $\tau_{max}/\rho(u_2 - u_1)^2$ values different for the four different classes of flows?

See pages 366 and 367.

Time for running of method on typical cases on what computer: 20 sec on CDC 6600

Cost estimate:

Availability of the deck: Negotiable

Precautions for potential industrial user: ϵ equation occasionally produces numerical instability; eliminated by adjustment to grid distribution in outer region and to forward step.

Special assumptions for compressible flows: None

Test cases tried (please circle):

S: (1) (2) (3) (4) (5)
J: (6) (7) (8) (18) (19)
JJ: (9) (10) (11) (12) (13) (20) (21) (22) (23)
W: (14) (15) (16) (17) 24

Key definitions to remember:

Authors: B. E. Launder, A. Morse, W. Rodi, and D. B. Spalding

Class of method: 2-equation turbulent-viscosity model (kϵ1)

Number of empirical constants or functions: 5[†] constants + (for axisymmetric flows) 1 function

Were the same ones used for all cases? No, small differences for axisymmetric and plane flows. See table 3 on page 410.

Reason (numerical, physical) for any changes?

If needed in your method, how is initial shear profile generated? Are the intial $\tau_{max}/\rho(u_2 - u_1)^2$ values different for the four different classes of flows?

See pages 366 and 367.

Time for running of method on typical cases on what computer: 20 sec on CDC 6600

Cost estimate:

Availability of the deck: Negotiable

Precautions for potential industrial user:

Special assumptions for compressible flows: None

Test cases tried (please circle):

S: (1) (2) (3) (4) (5)
J: (6) (7) (8) (18) (19)
JJ: (9) (10) (11) (12) (13) (20) (21) (22) (23)
W: (14) (15) (16) (17) 24

Key definitions to remember:

[†] One extra constant if species and/or stagnation enthalpy equation solved.

Authors: B. E. Launder, A. Morse, W. Rodi, and D. B. Spalding

Class of method: Shear-stress transport + dissipation rate transport equation

Number of empirical constants or functions: 6 constants (See table 6 on p. 413.)

Were the same ones used for all cases? Yes

Reason (numerical, physical) for any changes?

If needed in your method, how is initial shear profile generated? Are the initial $\tau_{max}/\rho(u_2 - u_1)^2$ values different for the four different classes of flows?

See pages 366 and 367.

Time for running of method on typical cases on what computer: 25 sec on CDC 6600

Cost estimate:

Availability of the deck: Negotiable

Precautions for potential industrial user: As kϵ2 model

Special assumptions for compressible flows: No compressible flows considered

Test cases tried (please circle):

S: (1) 2 3 (4) 5

J: 6 7 8 18 19

JJ: 9 10 11 12 (13) 20 21 22 23

W: (14) 15 16 17 24

Key definitions to remember:

Authors: B. E. Launder, A. Morse, W. Rodi, and D. B. Spalding

Class of method: Reynolds stress transport model + dissipation-rate transport equation

Number of empirical constants or functions: 6 constants

Were the same ones used for all cases? Yes

Reason (numerical, physical) for any changes?

If needed in your method, how is initial shear profile generated? Are the initial $\tau_{max}/\rho(u_2 - u_1)^2$ values different for the four different classes of flows?

See pages 366 and 367 and table 7 on page 414.

Time for running of method on typical cases on what computer: 30 sec on CDC 6600

Cost estimate:

Availability of the deck: Negotiable

Precautions for potential industrial user: None especially; but he would be advised to gain some practice with a simpler model first.

Special assumptions for compressible flows: None considered

Test cases tried (please circle):

S: (1) 2 3 (4) 5

J: 6 7 8 18 19

JJ: 9 10 11 12 (13) 20 21 22 23

W: (14) 15 16 17 24

Key definitions to remember:

Authors: B. E. Launder, A. Morse, W. Rodi, and D. B. Spalding

Class of method: Prandtl energy model

Number of empirical constants or functions: 3 constants for isothermal 1-species flow; otherwise 4 constants

Were the same ones used for all cases? No. See table 2 on page 409.

Reason (numerical, physical) for any changes? To provide better overall predictions, a different value of one of constants was adopted in plane and axisymmetric flows.

If needed in your method, how is initial shear profile generated? Are the initial $\tau_{max}/\rho(u_2 - u_1)^2$ values different for the four different classes of flows?

See pages 366 and 367.

Time for running of method on typical cases on what computer: 15 sec on CDC 6600

Cost estimate:

Availability of the deck:

Precautions for potential industrial user: As for mixing-length hypothesis

Special assumptions for compressible flows: None

Test cases tried (please circle):

S: (1) (2) (3) (4) (5)
J: (6) (7) (8) (18) (19)
JJ: (9) (10) (11) (12) (13) (20) (21) (22) (23)
W: (14) (15) (16) (17) 24

Key definitions to remember:

Authors: B. E. Launder, A. Morse, W. Rodi, and D. B. Spalding

Class of method: Mixing-length hypothesis

Number of empirical constants or functions: 1 constant for uniform density flows; otherwise 2 constants

Were the same ones used for all cases? No. See table 1 on page 408.

Reason (numerical, physical) for any changes? A different mixing-length constant was used for axisymmetric and plane flows to improve agreement with data.

If needed in your method, how is initial shear profile generated? Are the initial $\tau_{max}/\rho(u_2 - u_1)^2$ values different for the four different classes of flows?

Time for running of method on typical cases on what computer: 10 sec on CDC 6600

Cost estimate:

Availability of the deck: Basic listing of GENMIX published in reference 11 of paper

Precautions for potential industrial user: The user must be prepared to alter the mixing-length constant according to the kind of shear flow considered.

Special assumptions for compressible flows: None

Test cases tried (please circle):

S: (1) (2) (3) (4) (5)
J: (6) (7) (8) (18) (19)
JJ: (9) (10) (11) (12) (13) (20) (21) (22) (23)
W: (14) (15) (16) (17) 24

Key definitions to remember:

Authors: Philip T. Harsha

Class of method: Parabolic turbulent kinetic energy with algebraic length scale

Number of empirical constants or functions: Three: a_1 ($= \tau/\rho k$), a_2 (dissipation), Pr_k (TKE Prandtl no.)

Were the same ones used for all cases? All except 2D shear layer for a_1, all except 2D wake for a_2

Reason (numerical, physical) for any changes? Lateral function for a_1 used in asymptotic shear layer is not recommended (physically implausible); a_1 function used for axisymmetric flows is supported by experiment.

If needed in your method, how is initial shear profile generated? Are the initial $\tau_{max}/\rho(u_2 - u_1)^2$ values different for the four different classes of flows?

(1) If flow starts from initial boundary layers, Maise and McDonald eddy viscosity profiles used to establish initial τ.

(2) If flow starts downstream, either (a) constant ϵ from $\epsilon = kpb\Delta u$, $kp = 0.005$ or (b) constant ϵ estimated from experimental maximum shear.

Time for running of method on typical cases on what computer: 1 min on IBM 370/155 (time varies with number of equations; H_2-air (test case 12) involves 4 equations and takes 1 min 45 sec)

Cost estimate: \$5-\$10 at \$300/hr

Availability of the deck: Available on request

Precautions for potential industrial user: $\frac{\rho_o}{\rho_e} \leqq \frac{1}{14}$ causes numerical difficulties with grid spacing and requires careful handling. Zero pressure gradient; needs definition of initial boundary layers to start.

Special assumptions for compressible flows: No differences in formulation, which implies neglect of $\overline{\rho' u'}$ etc. terms in TKE equation for these cases.

Test cases tried (please circle):

S: (1) (2) (3) (4) (5)

J: (6) (7) (8) (18) (19)

JJ: (9) (10) (11) (12) (13) (20) (21) (22) 23

W: (14) (15) (16) (17) (24)

Key definitions to remember:

$$a_1 = \frac{\tau}{\rho k} = 0.3 \times f\left(\frac{r}{b}\right)$$

$$\text{Dissipation} = \frac{a_2 \rho k^{3/2}}{l_k}$$

$l_k = \left| y_{99} - y_{01} \right|$ for 2D flow, near field of jets

$l_k = 2y_{1/2}$ for axisymmetric jets

$y_{1/2} = y$ at which $u = \frac{1}{2}(u_c + u_e)$

TKE diffusion constant = $Pr_k = 0.7$

Authors: P. H. Heck and M. A. Smith

Class of method: Turbulent kinetic energy

Number of empirical constants or functions: 4 + 3 constants in length scale

Were the same ones used for all cases? Yes, except in length scale model

Reason (numerical, physical) for any changes? Physical

If needed in your method, how is initial shear profile generated? Are the initial $\tau_{max}/\rho(u_2 - u_1)^2$ values different for the four different classes of flows?

Uniform initial profile

Time for running of method on typical cases on what computer: 4 to 6 min on GE635
4 min on GE635 = 1 min on CDC 6600

Cost estimate: $25-$35

Availability of the deck: Under Air Force contract – CDC deck

Precautions for potential industrial user: None

Special assumptions for compressible flows: None

Test cases tried (please circle):

S: 1 2 3 4 5

J: (6) (7) 8 18 19

JJ: (9) (10) (11) (12) (13) 20 21 22 23

W: 14 15 16 17 24

Key definitions to remember:

Authors: Paul J. Ortwerth, Douglas C. Rabe, and Donald P. McErlean

Class of method: Turbulent kinetic energy (eddy viscosity)

Numer of empirical constants: Three: (1) large eddy scale for dissipation, (2) small scale for mixing, (3) compressibility

Were the same ones used for all cases? Yes

Reason (numerical, physical) for any changes? Not any

If needed in your method, how is initial shear profile generated? Are the initial $\tau_{max}/\rho(u_2 - u_1)^2$ values different for the four different classes of flows?

An initial turbulence intensity profile is needed. When not available it must be estimated from data on pipe flows or boundary layers. Self-similar profile data can also be used.

Time for running of method on typical cases on what computer: 20 sec on CDC 6600, 2-3 min on IBM 7094

Cost estimate: I don't know

Availability of the deck: Unlimited

Precautions for potential industrial user: Works well for high Reynolds number flows but not for flows with instabilities, such as wakes, only one scale is used at each downstream station, not correct for two or more shear layers.

Special assumptions for compressible flows: Empirical relation for the variation of eddy viscosity with local Mach number.

Test cases tried (please circle):

S: (1) (2) (3) (4) (5)

J: 6 (7) (8) 18 19

JJ: 9 (10) (11) (12) 13 20 21 22 23

W: 14 15 16 (17) 24

Key definitions to remember:

Authors: Thomas Morel, T. Paul Torda, and Peter Bradshaw

Class of method: Differential, solving continuity momentum and kinetic energy equations

Number of empirical constants or functions: Three

Were the same ones used for all cases? Two sets: Mixing layers; jets and wakes

Reason (numerical, physical) for any changes? Physical – basic differences in structure of the two flows

If needed in your method, how is initial shear profile generated? Are the initial $\tau_{max}/\rho(u_2 - u_1)^2$ values different for the four different classes of flows?

Shear stress profile is not generated, must be input. The level of initial shear stress may be estimated using an eddy viscosity formula. Yes (to the last question)

Time for running of method on typical cases on what computer: 20 to 30 sec on UNIVAC 1108

Cost estimate: $3 – (at IIT)

Availability of the deck: From the first author

Precautions for potential industrial user: No known bugs, requires small external flow (cannot handle still-air); details are in the paper.

Special assumptions for compressible flows: Density profiles obtained from $c_pT + \frac{1}{2} rU^2 = \text{Constant}$ (Crocco relation)

Test cases tried (please circle):

S: (1) (2) (3) 4 (5)

J: 6 7 8 18 19

JJ: 9 10 11 12 (13) 20 21 22 23

W: (14) 15 (16) 17 24

Key definitions to remember:

$$a_1 = \frac{\tau}{\overline{g^2}}$$

$$G = \frac{\overline{\frac{pv}{\rho}} + \frac{1}{2}\overline{vq^2}}{\tau|\tau|^{1/2}}$$

$$L = \frac{\tau|\tau|^{1/2}}{\epsilon}$$

Authors: C. E. Peters and W. J. Phares

Class of method: (1) Integral method, and (2) Turbulent kinetic energy method

Number of empirical constants or functions: Three: (1) a_1 to relate τ to TKE, (2) universal TKE profile shapes, (3) dissipation coefficient a_2 – related to turbulent Reynolds number and density ratio.

Were the same ones used for all cases? Yes, except $a_2 = 1.4$ (constant) was used for the two axisymmetric wakes.

Reason (numerical, physical) for any changes? Wakes seem to have somewhat different dissipation than jets and shear layers. A single constant a_2 was used and no attempt was made to refine the dissipation function for wakes.

If needed in your method, how is initial shear profile generated? Are the initial $\tau_{max}/\rho(u_2 - u_1)^2$ values different for the four different classes of flows?

Starting conditions defined in text and in table II. Strong shear flows $(u_e/u_o \leq 0.25)$ can be reliably started with fully developed τ_m. This also seems true of wake-like flows $(u_e > u_o)$. Note that only one initial value of $\tau(\tau_m)$ must be specified.

Time for running of method on typical cases on what computer: 3 min on IBM 370/155 (3.3 min for test case 7 from $x = 0$ to $x = 150r_o$) program not yet optimized for run time.

Cost estimate:

Availability of the deck: Available. Note that program has been developed for more complex flows than covered in this conference.

Precautions for potential industrial user: Except for strong shear flows, more work is needed on establishment of initial conditions. Method is limited to fully developed velocity profile shape and to unity turbulent Prandtl and Schmidt numbers.

Special assumptions for compressible flows: None. a_2 function developed to account for compressibility effects.

Test cases tried (please circle):

S: (1) (2) (3) 4 5

J: (6) (7) (8) (18) (19)

JJ: (9) (10) (11) (12) 13 (20) (21) (22) 23

W: 14 (15) 16 (17) 24

Key definitions to remember:

(1) Fundamental assumption is universal shapes for TKE profiles. Shapes obtained from incompressible experiments.

(2) At midpoint of shear layer (r_m), τ is directly proportional to TKE: $\tau_m = a_1 \rho_m k_m$

(3) Important point of analysis is relating dissipation coefficient (a_2) to relative turbulence level (R_T) and to density ratio.

ATTENDEES

Alber, Irwin E.	TRW Systems Group
Anderson, Griffin Y.	NASA Langley Research Center
Audeh, Beverly J.	Lockheed Missiles and Space Co.
Bangert, Louis H.	Georgia Institute of Technology
Becker, John V.	NASA Langley Research Center
Beckwith, Ivan E.	NASA Langley Research Center
* Birch, Stanley F.	NASA Langley Research Center
Brink, Donald F.	Old Dominion University
Buckingham, Alfred C.	Physics International Company
Bushnell, Dennis M.	NASA Langley Research Center
Carter, James E.	NASA Langley Research Center
Cary, Aubrey M., Jr.	NASA Langley Research Center
Cebeci, Tuncer	Douglas Aircraft Company
Chapman, Dean R.	NASA Ames Research Center
Chow, W. L.	University of Illinois at Urbana-Champaign
Cohen, Leonard S.	United Aircraft Research Laboratories
Coles, Donald	California Institute of Technology
Corrsin, Stanley	Johns Hopkins University
Donaldson, Coleman duP.	Aeronautical Research Associates of Princeton, Inc.
Drewry, James E.	Aerospace Research Laboratories, Wright-Patterson Air Force Base
Dvorak, Frank A.	Flow Research, Inc.
Edelman, Raymond B.	General Applied Science Laboratories, Inc.
Eggers, James M.	NASA Langley Research Center
Ellis, Macon C.	NASA Langley Research Center
Evans, John S.	NASA Langley Research Center
Fejer, Andrew	Illinois Institute of Technology
Feller, William V.	NASA Langley Research Center
Finson, Michael L.	Avco-Everett Research Laboratory
Fischer, Michael C.	NASA Langley Research Center
Foss, John F.	Michigan State University
Goldschmidt, Victor W.	Purdue University
Grose, William L.	NASA Langley Research Center
* Gupta, Roop Narayan	NASA Langley Research Center

* NRC-NASA Resident Research Associate.

Hamilton, Harris H., II	NASA Langley Research Center
Harris, Julius E.	NASA Langley Research Center
Harsha, Philip T.	ARO, Inc., Arnold Engineering Development Center
Harvey, William D.	NASA Langley Research Center
Heck, P. H.	Aircraft Engine Group, General Electric Company
Herring, J. R.	National Center for Atmospheric Research
Hill, William G., Jr.	Grumman Aerospace Corporation
Hirsh, Richard S.	NASA Langley Research Center
Holdeman, James D.	NASA Lewis Research Center
Holden, Michael S.	Cornell Aeronautical Laboratory, Inc.
Ito, Jackson	Aerojet Liquid Rocket Company
Jones, Barclay G.	University of Illinois at Urbana-Champaign
Kaiser, John E., Jr.	Virginia Polytechnic Institute and State University
Keyes, J. Wayne	NASA Langley Research Center
Kline, Stephen J.	Stanford University
Korst, H. H.	University of Illinois at Urbana-Champaign
Kurkov, Anatole P.	NASA Lewis Research Center
Lamb, J. Parker	University of Texas at Austin
Laufer, John	University of Southern California
Launder, Brian E.	Imperial College of Science and Technology
Lea, George K.	National Science Foundation
Lee, Shen C.	University of Missouri at Rolla
Legner, Hartmut	Avco-Everett Research Laboratory
Levine, Robert S.	NASA Langley Research Center
Libby, Paul A.	University of California at San Diego
Maestrello, Lucio	NASA Langley Research Center
Marvin, Joseph G.	NASA Ames Research Center
Mathis, Joe J., Jr.	NASA Langley Research Center
McClinton, Charles R.	NASA Langley Research Center
McDonald, Henry	United Aircraft Research Laboratories
Mellor, George L.	Princeton University
Moore, Jeffrey A.	McDonnell Douglas Astronautics Company
Morel, Thomas	Illinois Institute of Technology
Morgenthaler, J. H.	Bell Aerosystems Company
Morkovin, Mark V.	Illinois Institute of Technology
Morris, Dana J.	NASA Langley Research Center
Morrisette, E. Leon	NASA Langley Research Center
Muir, James F.	Sandia Laboratories

Nicks, Oran W.	NASA Langley Research Center
* Oh, Youn Hwan	NASA Langley Research Center
Ortwerth, Paul J.	Air Force Aero Propulsion Laboratory, Wright-Patterson Air Force Base
Pai, Shih-I.	University of Maryland
Peters, C. E.	ARO, Inc., Arnold Engineering Development Center
Phares, W. J.	ARO, Inc., Arnold Engineering Development Center
* Reda, Daniel C.	NASA Ames Research Center
Reihman, Thomas C.	Virginia Polytechnic Institute and State University
Rodi, W. A.	Imperial College of Science and Technology
Rogers, R. Clayton	NASA Langley Research Center
Roshko, Anatol	California Institute of Technology
Rubesin, Morris W.	NASA Ames Research Center
Rudy, David H.	NASA Langley Research Center
Schetz, Joseph A.	Virginia Polytechnic Institute and State University
Sebacher, Daniel I.	NASA Langley Research Center
Sforza, Pasquale M.	Polytechnic Institute of Brooklyn
Smith, Westcott H.	Air Force Office of Scientific Research
Spalding, D. B.	Imperial College of Science and Technology
Stallings, Robert E., Jr.	NASA Langley Research Center
Sterrett, James R.	NASA Langley Research Center
Torda, T. Paul	Illinois Institute of Technology
Torrence, Marvin G.	NASA Langley Research Center
Trimpi, Robert L.	NASA Langley Research Center
Wagner, Richard D.	NASA Langley Research Center
Whitehead, Allen H., Jr.	NASA Langley Research Center
Zelazny, Stephen W.	Bell Aerosystems Company
Zumwalt, Glen W.	Wichita State University

* NRC-NASA Resident Research Associate.

*U.S. GOVERNMENT PRINTING OFFICE: 1973-739-028/42